

P. V. Mohanan
Sudha Kappalli *Editors*

Biomedical Applications and Toxicity of Nanomaterials

 Springer

Biomedical Applications and Toxicity of Nanomaterials

P. V. Mohanan • Sudha Kappalli
Editors

Biomedical Applications and Toxicity of Nanomaterials

 Springer

Editors

P. V. Mohanan
Toxicology Division, Biomedical
Technology Wing
Sree Chitra Tirunal Institute for Medical
Sciences and Technology (Govt. of India)
Poojapura, Trivandrum, Kerala, India

Sudha Kappalli
Department of Zoology
Central University of Kerala
Kasaragod, Kerala, India

ISBN 978-981-19-7833-3

ISBN 978-981-19-7834-0 (eBook)

<https://doi.org/10.1007/978-981-19-7834-0>

© The Editor(s) (if applicable) and The Author(s), under exclusive license to Springer Nature Singapore Pte Ltd. 2023

This work is subject to copyright. All rights are solely and exclusively licensed by the Publisher, whether the whole or part of the material is concerned, specifically the rights of translation, reprinting, reuse of illustrations, recitation, broadcasting, reproduction on microfilms or in any other physical way, and transmission or information storage and retrieval, electronic adaptation, computer software, or by similar or dissimilar methodology now known or hereafter developed.

The use of general descriptive names, registered names, trademarks, service marks, etc. in this publication does not imply, even in the absence of a specific statement, that such names are exempt from the relevant protective laws and regulations and therefore free for general use.

The publisher, the authors, and the editors are safe to assume that the advice and information in this book are believed to be true and accurate at the date of publication. Neither the publisher nor the authors or the editors give a warranty, expressed or implied, with respect to the material contained herein or for any errors or omissions that may have been made. The publisher remains neutral with regard to jurisdictional claims in published maps and institutional affiliations.

This Springer imprint is published by the registered company Springer Nature Singapore Pte Ltd. The registered company address is: 152 Beach Road, #21-01/04 Gateway East, Singapore 189721, Singapore

Preface

Nanotechnology has been one of the rapid evolution fields of science during the past decade. Being a field of applied science, nanotechnology unlocked many technological advancements in the pharmaceutical/biomedical, agricultural/aquacultural, environmental, electronic, textile, and energy sectors. As the nanotech-designed materials infiltrate almost every industry, research into the toxicity properties of the chemical components used as nano-sized materials on the health and environment must be updated. Considering the situation of the covid pandemic, a 2-day webinar event on ‘Food, chemical, and nanomaterials toxicity’ was jointly conducted by Sree Chitra Thirunal Institute for Medical Sciences and Technology, Trivandrum (Govt. of India), Central University of Kerala, Kasaragod (CUK), and Kerala Academy of Sciences (KAS) at an international level. The webinar series provided an excellent opportunity for interactive sessions across a virtual online platform to exchange information among directors, scientists, and researchers from national and international organizations and research institutions across India, the UK, the USA, and Japan. This book has emerged as an innovation based on the international webinar on ‘food, chemical and nanomaterials toxicity’, which cover the progress of nanotechnology in food and healthcare sectors.

The emerging field of nanotoxicity is the theme of this book and will definitely help the readers to assess the quality of nanomaterials used in biomedical, agricultural and environmental applications. This book is written in a clear and lively language and is divided into 28 chapters authored by internationally renowned experts. The chapters serve as a practical introduction to the principles of nanomaterials and particularize the chemical components and their unique properties. The opening chapters introduce the readers to the scope of the book. Starting from a brush-up of the nanoparticle-based applications in environmental management and clinical applications. The book helps to build up an understanding of the prospects of nanomaterials in biomedical applications, nano-drug delivery and nanomaterials in cancer and cardiovascular diseases. It also covers the toxicity assessment of nanomaterials in the medical/food industry and advancement of nanochemicals in agriculture and animal husbandry.

The Editors are delighted to publish this book with Cambridge scholar’s publications. The data presented in the book will be highly useful for the companies, product developers, scholars, researchers, academicians and practitioners as well.

This will also be important for government agencies, regulators, policy and lawmakers, biomedical industries, technocrats, etc. Also the book may be a part of course curriculum for graduate and post-graduate biomedical engineering students, biotechnology research students, etc.

It has been a great pleasure to work with multidisciplinary contributors, who have several years of experience in their chosen areas. Without their cooperation, it would not have been possible to bring out this book, focusing on Safety and Applications of Chemicals and Nanoparticles. Furthermore, we wish to express our sincere gratitude to Director and Head, Biomedical Technology Wing, Sree Chitra Thirunal Institute for Medical Sciences and Technology (Govt. of India), Trivandrum, Kerala and Vice Chancellor, Central University of Kerala, Kasargod, India, for their phenomenal support and advice throughout this work. The support and encouragement from family and friends is greatly acknowledged.

Thiruvananthapuram, Kerala, India
Kasaragod, Kerala, India

P. V. Mohanan
Sudha Kappalli

Contents

1	Macroporous Cryogel-Based Systems for Water Treatment Applications and Safety: Nanocomposite-Based Cryogels and Bacteria-Based Bioreactors	1
	Irina N. Savina, Lila Otero-Gonzalez, and Dmitriy Berillo	
2	One-Dimensional Semiconducting Nanomaterials: Toxicity and Clinical Applications	51
	Ashtami Jayakumar, Chandra Mohan, and Oomman K. Varghese	
3	Prospects of Safe Use of Nanomaterials in Biomedical Applications	83
	Damini Verma and Pratima R. Solanki	
4	Hyaluronic Acid-Based Nanotechnologies for Delivery and Treatment	103
	Alice Spadea, Ponpawee Pingrajai, and Annalisa Tirella	
5	Theranostics Nanomaterials for Safe Cancer Treatment	129
	Sindhu C. Pillai, Athira Anirudhan, and D. Sakthi Kumar	
6	Cardiovascular Safety Assessment of New Chemical Entities: Current Perspective and Emerging Technologies	155
	Richa Tyagi and Shyam S. Sharma	
7	Toxicology of Pharmaceutical Products During Drug Development	187
	Mishra Abhishek, Singla Rubal, Joshi Rupa, and Medhi Bikash	
8	Safety and Risk Assessment of Food Items	203
	Suradeep Basak, Joseph Lewis, Sudershan Rao Vemula, and Prathapkumar Shetty Halady	
9	Nontoxic Natural Products as Regulators of Tumor Suppressor Gene Function	229
	Dibya Ranjan Jalli and Debasmita Pankaj Alone	

10	Advancements in the Safety of Plant Medicine: Back to Nature . . .	257
	Ankita Misra, Bhanu Kumar, Deepali Tripathi, and Sharad Srivastava	
11	Chemicals and Their Interaction in the Aquaculture System	277
	T. A. Jose Priya and Sudha Kappalli	
12	Zebrafish as a Biomedical Model to Define Developmental Origins of Chemical Toxicity	299
	Jennifer L. Freeman	
13	Green Synthesis of Nontoxic Nanoparticles	319
	K. B. Megha, X. Joseph, and P. V. Mohanan	
14	Synthesis, Characterization and Applications of Titanium Dioxide Nanoparticles	339
	Remya Rajan Renuka, Narenkumar Jayaraman, Angeline Julius, Velmurugan Palanivel, Vasudevan Ramachandran, Rajesh Pandian, Umesh Luthra, and Suresh Kumar Subbiah	
15	Characterization of Nontoxic Nanomaterials for Biological Applications	363
	Ashna Poullose, T. Shibina, T. Sreejith, Anitta Sha Mercy, Drisya Das, K. Haritha, A. K. Sijo, George Mathew, and Pramod K. S.	
16	Toxicity Assessment of Nanoparticle	401
	X. Joseph, Akhil, Arathi, K. B. Megha, U. Vandana, and P. V. Mohanan	
17	Safety of Nanoparticles: Emphasis on Antimicrobial Properties . . .	425
	Kuljit Singh, Shimona Ahlawat, Diksha Kumari, Uma Matlani, Meenakshi, Tejinder Kaur, and Alka Rao	
18	Quantum Dots for Imaging and Its Safety	459
	Akhil, Arathi, K. B. Megha, X. Joseph, V. P. Sangeetha, and P. V. Mohanan	
19	Genotoxicity Evaluation of Nanosized Materials	477
	V. P. Sangeetha, Vandana Arun, and P. V. Mohanan	
20	Scaffold Materials and Toxicity	535
	S. Ajikumaran Nair and V. Gayathri	
21	Biological Safety and Cellular Interactions of Nanoparticles	559
	Arathi, K. B. Megha, X. Joseph, and P. V. Mohanan	
22	Role of Artificial Intelligence in the Toxicity Prediction of Drugs . . .	589
	Manisha Malani, Anirudh Kasturi, Md. Moinul, Shovanlal Gayen, Chittaranjan Hota, and Jayabalan Nirmal	
23	Chemicals and Rodent Models for the Safety Study of Alzheimer's Disease	637
	Nimmi Varghese and Viji Vijayan	

24	Mitochondria-Targeted Liposomal Delivery in Parkinson's Disease	657
	Bipul Ray, Arehally M. Mahalakshmi, Mahendran Bhaskaran, Sunanda Tuladhar, A. H. Tousif, Musthafa Mohamed Essa, Byoung-Joon Song, and Saravana Babu Chidambaram	
25	Routes of Nano-drug Administration and Nano-based Drug Delivery System and Toxicity	671
	Boobalan Gopu, Ramajayan Pandian, Angayarkanni Sevel, and Sanket Shukla	
26	Green Synthesized Silver Nanoparticles Phytotoxicity and Applications in Agriculture: An Overview	703
	R. Santhoshkumar, A. Hima Parvathy, and E. V. Soniya	
27	Status of Safety Concerns of Microplastic Detection Strategies	727
	Deepika Sharma, Virender Sharma, and Gurjot Kaur	
28	Impact of Insecticides on Man and Environment	751
	C. A. Jayaprakas, Joseph Tom, and S. Sreejith	

Editors and Contributors

About the Editors

P. V. Mohanan is a Fellow of National Academy of Science and Royal Society of Biologists, UK. He was a JSPS Post-doctoral Fellow at the University of Tsukuba, Japan, in the field of Neurotoxicity. He joined Sree Chitra Tirunal Institute for Medical Sciences and Technology (SCTIMST), Govt. of India, in 1989 and has spent 33 years of professional life here. As a toxicologist, he has been intimately associated with all the medical devices/technologies developed at SCTIMST. Currently, he heads the Division of Toxicology. He is a Visiting Professor and Visiting Researcher at Toyo University, Japan, and a Certified Biological Safety Specialist. He received lifetime achievement award from the Society of Toxicology India, for the outstanding contribution in the field of toxicology. Mohanan has been teaching toxicology to postgraduates and guiding research scholars. Development of Human-on-a-chip is a new mega project, apart from several other externally funded research projects. Patented an ELISA kit for the measurement of pyrogenicity. Mohanan made significant contributions to the development of medical device regulations in India. He received certificate of appreciation from the Hon. Minister of Science and Technology, Govt. of India, for the contribution to India getting full adherent status on GLP from OECD. He has authored 265 publications and edited 6 books. Presently, he is the Secretary General of Society of Toxicology, India.

Sudha Kappalli is Professor at the Department of Zoology, School of Biological Science, Central University of Kerala. Her research areas include Crustacean Growth-Reproduction interaction and its endocrine regulation, biodiversity of parasitic isopods and copepods and host-parasite interaction. She obtained PhD from the University of Calicut in 1993. She has 27 years of teaching experience at PG level. Dr. Sudha is recipient of CAS-PIFI Visiting Scientist Fellowship (2015), CAS-TWAS Visiting Scholar Fellowship (2009 and 2011), Commonwealth Academic Staff Fellowship (2007), INSA Visiting Scientist Fellowship (2007) IAS Summer Teacher Fellowship (2005) and University Post-Doctoral Fellowship (1994). She has completed four major research projects funded by International Foundation for Science (Stockholm, Sweden), BRNS, UGC, KSCSTE and SERB as Principal Investigator. Currently, she is PI of three research projects funded by

KSCSTE, DST-RFBR and DST-JSPS. She has published 40 research papers in the peer-reviewed journals and 6 papers in conference proceedings with one book chapter. She has presented 18 papers in the conferences held in India and abroad. She has guided four PhD students. She has been the reviewer of many reputed international journals. Dr. Sudha serves as a member for several professional and academic bodies of universities and government agencies. Holding honour for excellence in teaching, Dr. Sudha was chosen for Dr. P.K. Rajan Memorial Excellent Award (2012), Prof. Sivaprasad Memorial Award (2013), and St. Berchmans Award (2013) for Best College Teacher in Kerala. She organized one national level Lecture-Workshop in Molecular Endocrinology in 2006 and eight DST-INSPIRE Internship Science Camps. She served as Co-convenor of the national level workshop on Aquacultural Biotechnology (2005), also served as NSS Programme Officer during 2009–2012 and Co-ordinator of DST-INSPIRE Science Camp (2011–2019).

Contributors

Mishra Abhishek Department of Pharmacology, PGIMER, Chandigarh, India

Shimona Ahlawat CSIR-Institute of Microbial Technology, Chandigarh, India

Akhil Toxicology Division, Biomedical Technology Wing, Sree Chitra Tirunal Institute for Medical Sciences and Technology (Govt. of India), Trivandrum, Kerala, India

Debasmita Pankaj Alone School of Biological Sciences, National Institute of Science Education and Research (NISER), HBNI, Khurda, Odisha, India

Athira Anirudhan Department of Nephrology, All India Institute of Medical Sciences, Bhopal, Madhya Pradesh, India

Arathi Toxicology Division, Biomedical Technology Wing, Sree Chitra Tirunal Institute for Medical Sciences and Technology (Govt. of India), Poojapura, Trivandrum, Kerala, India

Vandana Arun Toxicology Division, Biomedical Technology Wing, Sree Chitra Tirunal Institute for Medical Sciences and Technology (Govt. of India), Trivandrum, Kerala, India

Suradeep Basak Department of Food Science and Technology, Pondicherry University, Pondicherry, India

Dmitriy Berillo Department of Pharmaceutical and Toxicological Chemistry, Pharmacognosy and Botany School of Pharmacy at Asfendiyarov Kazakh National Medical University, Almaty, Kazakhstan

Mahendran Bhaskaran Department of Pharmaceutics, JSS College of Pharmacy, JSS Academy of Higher Education and Research, Mysuru, India

Medhi Bikash Department of Pharmacology, PGIMER, Chandigarh, India

Saravana Babu Chidambaram Department of Pharmacology, JSS College of Pharmacy, JSS Academy of Higher Education and Research, Mysuru, India
Centre for Experimental Pharmacology and Toxicology, Central Animal Facility, JSS Academy of Higher Education and Research, Mysuru, India

Drisya Das Department of Physics, St. Mary's College, Sulthan Bathery, Kerala, India

Musthafa Mohamed Essa Department of Food Science and Nutrition, CAMS, Sultan Qaboos University, Muscat, Oman
Aging and Dementia Research Group, Sultan Qaboos University, Muscat, Oman
Biomedical Sciences Department, University of Pacific, Sacramento, CA, USA

Jennifer L. Freeman School of Health Sciences, Purdue University, West Lafayette, IN, USA

V. Gayathri Phytochemistry and Phytopharmacology Division, KSCSTE-Jawaharlal Nehru Tropical Botanic Garden and Research Institute (KSCSTE-JNTBGRI), Palode, Thiruvananthapuram, Kerala, India

Shovanlal Gayen Laboratory of Drug Design and Discovery, Department of Pharmaceutical Technology, Jadavpur University, Kolkata, West Bengal, India

Boobalan Gopu Pharmacology Division, CSIR-Indian Institute of Integrative Medicine, Jammu, India

Prathapkumar Shetty Halady Department of Food Science and Technology, Pondicherry University, Pondicherry, India

K. Haritha Department of Physics, St. Mary's College, Sulthan Bathery, Kerala, India

A. Hima Parvathy Transdisciplinary Biology, Rajiv Gandhi Centre for Biotechnology, Thiruvananthapuram, Kerala, India

Chittaranjan Hota Department of Computer Science and Information Systems (CSIS), Birla Institute of Technology and Science-Pilani, Hyderabad Campus, Hyderabad, Telangana, India

Dibya Ranjan Jalli School of Biological Sciences, National Institute of Science Education and Research (NISER), HBNI, Khurda, Odisha, India

Ashtami Jayakumar Department of Biomedical Engineering, University of Houston, Houston, TX, USA
Nanomaterials and Devices Laboratory, Department of Physics, University of Houston, Houston, TX, USA

C. A. Jayaprakas Biopesticide Laboratory, Division of Crop Protection, ICAR-Central Tuber Crops Research Institute, Thiruvananthapuram, Kerala, India

T. A. Jose Priya Department of Zoology, School of Biological Sciences, Central University of Kerala, Kasaragod, Kerala, India

X. Joseph Toxicology Division, Biomedical Technology Wing, Sree Chitra Tirunal Institute for Medical Sciences and Technology (Govt. of India), Poojapura, Trivandrum, Kerala, India

Angeline Julius Centre for Materials Engineering and Regenerative Medicine, Bharath Institute of Higher Education and Research, Chennai, Tamil Nadu, India

Sudha Kappalli Department of Zoology, School of Biological Sciences, Central University of Kerala, Kasaragod, Kerala, India

Anirudh Kasturi Department of Computer Science and Information Systems (CSIS), Birla Institute of Technology and Science-Pilani, Hyderabad Campus, Hyderabad, Telangana, India

Gurjot Kaur School of Pharmaceutical Sciences, Shoolini University, Solan, India

Tejinder Kaur CSIR-Institute of Microbial Technology, Chandigarh, India

Bhanu Kumar Pharmacognosy Division, CSIR-National Botanical Research Institute, Lucknow, Uttar Pradesh, India

Diksha Kumari Infectious Diseases Division, CSIR-Indian Institute of Integrative Medicine, Jammu, India

Joseph Lewis National Institute of Nutrition-ICMR, Hyderabad, India

Umesh Luthra Centre for Materials Engineering and Regenerative Medicine, Bharath Institute of Higher Education and Research, Chennai, Tamil Nadu, India

Arehally M. Mahalakshmi Department of Pharmacology, JSS College of Pharmacy, JSS Academy of Higher Education and Research, Mysuru, India

Manisha Malani Translational Pharmaceutics Research Laboratory (TPRL), Department of Pharmacy, Birla Institute of Technology and Science-Pilani, Hyderabad Campus, Hyderabad, Telangana, India

George Mathew Department of Physics, St. Mary's College, Sulthan Bathery, Kerala, India

Uma Matlani CSIR-Institute of Microbial Technology, Chandigarh, India

Meenakshi Academy of Scientific and Innovation Research (AcSIR), Ghaziabad, India

K. B. Megha Toxicology Division, Biomedical Technology Wing, Sree Chitra Tirunal Institute for Medical Sciences and Technology (Govt. of India), Poojapura, Trivandrum, Kerala, India

Anitta Sha Mercy Department of Physics, St. Mary's College, Sulthan Bathery, Kerala, India

Ankita Misra Pharmacognosy Division, CSIR-National Botanical Research Institute, Lucknow, Uttar Pradesh, India

Chandra Mohan Department of Biomedical Engineering, University of Houston, Houston, TX, USA

P. V. Mohanan Toxicology Division, Biomedical Technology Wing, Sree Chitra Tirunal Institute for Medical Sciences and Technology (Govt. of India), Poojapura, Trivandrum, Kerala, India

Md. Moinul Department of Pharmaceutical Sciences, Dr. Harisingh Gour University, Sagar, Madhya Pradesh, India

S. Aji Kumaran Nair Phytochemistry and Phytopharmacology Division, KSCSTE-Jawaharlal Nehru Tropical Botanic Garden and Research Institute (KSCSTE-JNTBGR), Palode, Thiruvananthapuram, Kerala, India

J. Narenkumar Centre for Materials Engineering and Regenerative Medicine, Bharath Institute of Higher Education and Research, Chennai, Tamil Nadu, India

Jayabalan Nirmal Translational Pharmaceutics Research Laboratory (TPRL), Department of Pharmacy, Birla Institute of Technology and Science-Pilani, Hyderabad Campus, Hyderabad, Telangana, India

Lila Otero-Gonzalez IDENER, La Rinconada, Seville, Spain

Rajesh Pandian Centre for Materials Engineering and Regenerative Medicine, Bharath Institute of Higher Education and Research, Chennai, Tamil Nadu, India

Ramajayan Pandian Pharmacology Division, CSIR-Indian Institute of Integrative Medicine, Jammu, India

Sindhu C. Pillai Bio Nano Electronics Research Center, Graduate School of Interdisciplinary New Science, Toyo University, Kawagoe Campus, Saitama, Japan

Ponpawee Pingrajai Division of Pharmacy and Optometry, Faculty of Biology, Medicine and Health, University of Manchester, Manchester, UK

Ashna Poullose Department of Physics, St. Mary's College, Sulthan Bathery, Kerala, India

K. S. Pramod Department of Physics, St. Mary's College, Sulthan Bathery, Kerala, India

Alka Rao Academy of Scientific and Innovation Research (AcSIR), Ghaziabad, India
CSIR-Institute of Microbial Technology, Chandigarh, India

Bipul Ray Department of Pharmacology, JSS College of Pharmacy, JSS Academy of Higher Education and Research, Mysuru, India
Centre for Experimental Pharmacology and Toxicology, Central Animal Facility, JSS Academy of Higher Education and Research, Mysuru, India

R. R. Remya Centre for Materials Engineering and Regenerative Medicine, Bharath Institute of Higher Education and Research, Chennai, Tamil Nadu, India

Singla Rubal Department of Pharmacology, PGIMER, Chandigarh, India

Joshi Rupa Department of Pharmacology, PGIMER, Chandigarh, India

D. Sakthi Kumar Bio Nano Electronics Research Center, Graduate School of Interdisciplinary New Science, Toyo University, Kawagoe Campus, Saitama, Japan

V. P. Sangeetha Toxicology Division, Biomedical Technology Wing, Sree Chitra Tirunal Institute for Medical Sciences and Technology (Govt. of India), Trivandrum, Kerala, India

R. Santhoshkumar Transdisciplinary Biology, Rajiv Gandhi Centre for Biotechnology, Thiruvananthapuram, Kerala, India

Irina N. Savina School of Applied Sciences, University of Brighton, Brighton, UK

Angayarkanni Sevvel National Institute of Siddha, Chennai, India

Deepika Sharma School of Pharmaceutical Sciences, Shoolini University, Solan, India

Shyam S. Sharma Department of Pharmacology and Toxicology, National Institute of Pharmaceutical Education and Research (NIPER), Mohali, Punjab, India

Virender Sharma School of Pharmaceutical Sciences, Shoolini University, Solan, India

T. Shibina Department of Physics, St. Mary's College, Sulthan Bathery, Kerala, India

Sanket Shukla Pharmacology Division, CSIR-Indian Institute of Integrative Medicine, Jammu, India

A. K. Sijo Department of Physics, St. Mary's College, Sulthan Bathery, Kerala, India

Kuljit Singh Infectious Diseases Division, CSIR-Indian Institute of Integrative Medicine, Jammu, India
Academy of Scientific and Innovation Research (AcSIR), Ghaziabad, India

Pratima R. Solanki Special Centre for Nanoscience, Jawaharlal Nehru University, New Delhi, India

Byoung-Joon Song Section of Molecular Pharmacology and Toxicology, Laboratory of Membrane Biochemistry and Biophysics, National Institute on Alcohol Abuse and Alcoholism, Bethesda, MD, USA

E. V. Soniya Transdisciplinary Biology, Rajiv Gandhi Centre for Biotechnology, Thiruvananthapuram, Kerala, India

Alice Spadea Division of Pharmacy and Optometry, Faculty of Biology, Medicine and Health, University of Manchester, Manchester, UK
NorthWest Centre for Advanced Drug Delivery (NoWCADD), School of Health Sciences, University of Manchester, Manchester, UK

S. Sreejith Biopesticide Laboratory, Division of Crop Protection, ICAR-Central Tuber Crops Research Institute, Thiruvananthapuram, Kerala, India

T. Sreejith Department of Physics, St. Mary's College, Sulthan Bathery, Kerala, India

Sharad Srivastava Pharmacognosy Division, CSIR-National Botanical Research Institute, Lucknow, Uttar Pradesh, India

S. Suresh Kumar Centre for Materials Engineering and Regenerative Medicine, Bharath Institute of Higher Education and Research, Chennai, Tamil Nadu, India

Annalisa Tirella Division of Pharmacy and Optometry, Faculty of Biology, Medicine and Health, University of Manchester, Manchester, UK

Joseph Tom Biopesticide Laboratory, Division of Crop Protection, ICAR-Central Tuber Crops Research Institute, Thiruvananthapuram, Kerala, India

A. H. Tousif Department of Pharmacology, JSS College of Pharmacy, JSS Academy of Higher Education and Research, Mysuru, India
Centre for Experimental Pharmacology and Toxicology, Central Animal Facility, JSS Academy of Higher Education and Research, Mysuru, India

Deepali Tripathi Pharmacognosy Division, CSIR-National Botanical Research Institute, Lucknow, Uttar Pradesh, India

Sunanda Tuladhar Department of Pharmacology, JSS College of Pharmacy, JSS Academy of Higher Education and Research, Mysuru, India
Centre for Experimental Pharmacology and Toxicology, Central Animal Facility, JSS Academy of Higher Education and Research, Mysuru, India

Richa Tyagi Department of Pharmacology and Toxicology, National Institute of Pharmaceutical Education and Research (NIPER), Mohali, Punjab, India

U. Vandana Toxicology Division, Biomedical Technology Wing, Sree Chitra Tirunal Institute for Medical Sciences and Technology (Govt. of India), Trivandrum, Kerala, India

Nimmi Varghese Department of Biochemistry, University of Kerala, Kariavattom Campus, Thiruvananthapuram, Kerala, India

Oomman K. Varghese Nanomaterials and Devices Laboratory, Department of Physics, University of Houston, Houston, TX, USA
Texas Center for Superconductivity, University of Houston, Houston, TX, USA

R. Vasudevan Centre for Materials Engineering and Regenerative Medicine, Bharath Institute of Higher Education and Research, Chennai, Tamil Nadu, India

P. Velmurugan Centre for Materials Engineering and Regenerative Medicine, Bharath Institute of Higher Education and Research, Chennai, Tamil Nadu, India

Sudershan Rao Vemula Regulatory Affairs, PFNDAI, Mumbai, India

Damini Verma Special Centre for Nanoscience, Jawaharlal Nehru University, New Delhi, India

Viji Vijayan Department of Biochemistry, University of Kerala, Kariavattom Campus, Thiruvananthapuram, Kerala, India



Macroporous Cryogel-Based Systems for Water Treatment Applications and Safety: Nanocomposite-Based Cryogels and Bacteria-Based Bioreactors

Irina N. Savina, Lila Otero-Gonzalez, and Dmitriy Berillo

Abbreviations

AA	Allylamine
AAM	Acrylamide
AAS	Atomic absorption spectroscopy
AMPS	2-Acrylamido-2-methyl-1-propanesulfonic acid
APTES	3-Aminopropyltriethoxysilane
DABA	Dimethyl-amino-benzaldehyde
DLS	Dynamic light scattering
DMAAm	N,N-dimethylacrylamide
DTT	DL-dithiotreitol
GA	Glutaraldehyde
GO	Graphene oxide
HEMA	2-Hydroxyethyl methacrylate
ICP-MS	Inductively-coupled plasma mass spectroscopy
ICP-OES	Inductively-coupled plasma optical emission spectroscopy
MAAc	Methacrylic acid

I. N. Savina (✉)

School of Applied Sciences, University of Brighton, Brighton, UK

e-mail: i.n.savina@brighton.ac.uk

L. Otero-Gonzalez

IDENER, La Rinconada, Seville, Spain

D. Berillo

Department of Pharmaceutical and Toxicological Chemistry, Pharmacognosy and Botany School of Pharmacy at Asfendiyarov Kazakh National Medical University, Almaty, Kazakhstan

MTT	3-(4,5-Dimethylthiazol-2-yl)-2,5-diphenyl-tetrazolium bromide
NP	Nanoparticles
NTA	Nanoparticle tracking analysis
p(4-VP)	Poly(4-vinylpyridine)
p(AAc),	Poly(acrylic acid)
p(AMPS)	Poly(2-acrylamido-2-methyl-1-propansulfonic acid)
p(APTMA)	Poly((3-acrylamidopropyl)trimethylammonium chloride)
p(DMAEM-co-MAA)	N,N-dimethylaminoethylmethacrylate and methacrylic acid
p(HEMA)	Poly(2-hydroxyethyl methacrylate)
p(SPM)	Poly(3-sulfopropyl methacrylate)
p(VI)	Poly(vinyl imidazole)
PEI-al	Aldehyde-modified polyethyleneimine
PEO	Poly(ethylene oxide)
p-NBA	p-Nitrobenzoic acid
p-NP	p-Nitrophenol
PVA	Polyvinyl alcohol
PVA-al	Aldehyde-modified polyvinyl alcohol
SEM	Scanning electron microscopy
sp-ICP-MS	Single-particle inductively-coupled plasma mass spectrometry
TEM	Transmission electron microscopy
TMP	1,1,3,3-Tetramethoxypropane
TOF	Turnover frequency
TON	Turnover number
VP	N-vinyl pyrrolidone
XTT	2,3-Bis-(2-methoxy-4-nitro-5-sulfophenyl)-2h-tetrazolium-5-carboxanilide

1.1 Introduction

One of the global challenges is to provide everyone with clean water (Anonymous 2015). The expansion of industry, agriculture, and population growth are increasing water consumption, which continues to grow. According to a 2017 United Nations report, about 80% of all wastewater is discharged into the environment without treatment (UN 2017). Thus, polluted water discharged into rivers and lakes ends up in the oceans, negatively impacting the environment and public health. Industrial wastewaters, landfill leaches, mining wastes, municipal wastewater, and urban runoff are the main sources of contamination by heavy metals, solvents, phenolic, and pharmaceutical compounds. Some of them are poisonous and particularly difficult to remove. Current methods of water purification cannot always meet

existing needs. Many of the procedures in use today, including precipitation, filtration, chemical methods, and reverse osmosis, were developed in the early twentieth century and do not meet many of the requirements of today's pollution problems. New and innovative methods and solutions are required for the management and treatment of water.

Recent studies have shown that engineered nanoparticles could provide cost-effective solutions to many challenging environmental remediation problems due to their large surface area, which is available for interaction with contaminants, and high surface reactivity (Sadegh et al. 2017; Palani et al. 2021; Westerhoff et al. 2016). They have been tested for adsorption and decomposition of the range of inorganic and organic contaminants (Palani et al. 2021; Khin et al. 2012). Direct use of free nanoparticles can bring various inconveniences to traditional water purification technologies. This can cause column clogging or blockage of flow, resulting in high backflow resistance when used in a column setup. The recovery and reuse of nanoparticles from an aqueous solution are extremely difficult, and the loss of mobile nanoparticles in purified water can cause new environmental problems. Various polymer-carriers such as beads, filters, and fibers are used to immobilize nanoparticles, which prevents them from entering the environment, leading to safer water treatment methods (Ghadimi et al. 2020).

Besides the immobilization of nanoparticles, there is interest in the immobilization of enzymes and whole bacterial cells to develop bioreactors for the degradation of pollutants. Bacterial cells have already been used in bioremediation as an effective and safe way to remove contaminants from soil, water, and other environments. Immobilizing them on polymer support offers several advantages, such as protecting bacteria from aggressive and toxic environments, increasing bioremediation efficiency, recovering and reusing bacteria-based devices. The polymer support for the immobilization of bacteria must be nontoxic and support the metabolic activity of the cells. Porous substrates are the best choice because they provide a large surface area for bacteria growth, an unlimited supply of nutrients and the removal of metabolic by-products.

Cryogels are a promising carrier for the immobilization of both nanoparticles and bacterial cells. Cryogels are macroporous hydrogels with a well-developed system of large interconnected pores (Gun'ko et al. 2017). Cryogels are obtained by cryotropic treatment of a gel precursor solution (Savina et al. 2016a, 2021; Gun'ko et al. 2013; Savina and Galaev 2016). When the initial reagent solution freezes, ice crystals form, displacing all reagents and any other additives into small, unfrozen liquid zones where gelation occurs (Fig. 1.1). After thawing, voids (pores filled with water) form in place of the ice crystals. Due to the concentration of reagents during cryogel formation, mechanically strong elastic cryogels are formed, which can withstand significant deformation without damaging their structure (Savina et al. 2009; Gun'ko et al. 2013). In addition, the system of interconnected pores provides high permeability and passage of aqueous solutions through cryogel matrices, which makes them promising materials for creating filters and flow-through devices (Lozinsky et al. 2003; Savina et al. 2011). Cryogels have been studied for several applications

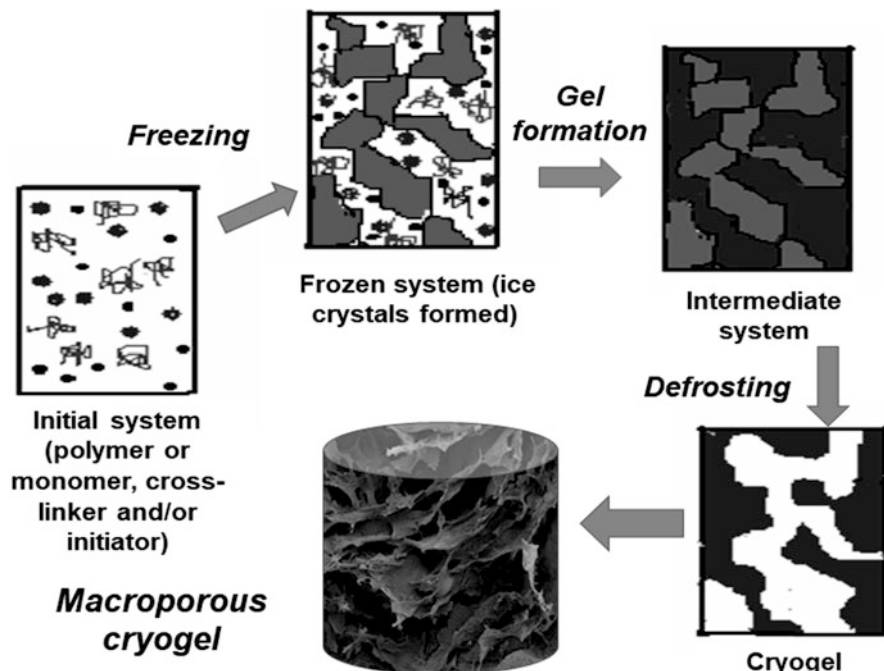


Fig. 1.1 Scheme of preparation of cryogels: (i) initial system (the gel precursor solution is cooled down to a temperature below freezing point); (ii) frozen system (the ice crystals formed and solutes are concentrated in nonfrozen zones); (iii) intermediate system (gel is formed in the nonfrozen liquid around ice crystals); (iv) cryogel is formed upon defrosting. The figure is reprinted from Savina, I.N.; Zoughaib, M.; Yergeshov, A.A. Design and Assessment of Biodegradable Macroporous Cryogels as Advanced Tissue Engineering and Drug Carrying Materials. *Gels* 2021, 7, 79. <https://doi.org/10.3390/gels7030079> (Savina et al. 2021) under the Creative Commons Attribution License

in the biomedical, biotechnology, and environmental fields (Savina et al. 2021, 2016b; Shiekh et al. 2021; Lozinsky 2020; Kudaibergenov 2019).

In this chapter, the preparation of cryogel-based nanocomposites is discussed, with particular emphasis on the methods of nanoparticle immobilization in cryogels. The effect of immobilization of nanoparticles on their reactivity and use in the water clean-up is discussed. Examples of adsorption and catalytic removals of pollutants such as heavy metals, dyes, and phenolic compounds from water by nanocomposite cryogels are reviewed. The assessment of the safety of nanocomposites: the needs, currently used methods, and regulation, is critically reviewed. In addition, methods of immobilizing bacterial cells in cryogels and preparing bioreactors based on bacteria are discussed with examples of their use for removing phenolic and other compounds.

1.2 Nanocomposite-Based Cryogels

Cryogel nanocomposites are cryogels containing nanoparticles within their structure. IUPAC defines a nanoparticle as “a particle of any shape with at least two dimensions below 100 nm.” Thus, composite cryogels that contain bigger particles, such as carbon beads of several micrometer sizes (Busquets et al. 2016), will be excluded from the discussion.

1.2.1 Nanocomposite Cryogel Preparation

Nanocomposites can be prepared using three approaches: (i) by mixing a suspension of nanoparticles with a reagent solution, which leads to the formation of composites, a direct method, (ii) by immobilizing nanoparticles on the surface of cryogels (through ice-mediated coating, deposition, or covalent bond formation), and (iii) in situ preparation where nanoparticles are formed inside the preformed cryogel (Fig. 1.2). All of these approaches have their advantages and disadvantages (Table 1.1).

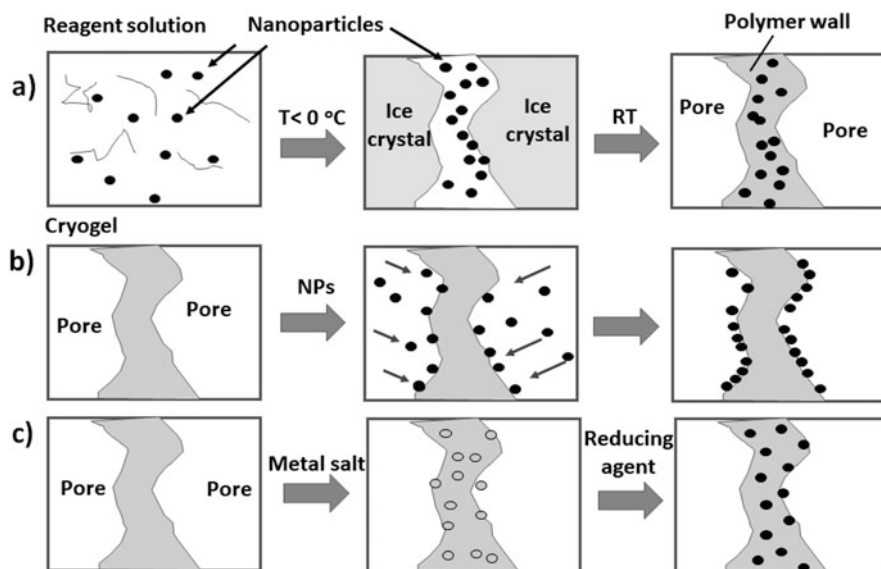


Fig. 1.2 Schematic illustration of three approaches for the preparation of cryogel nanocomposites: (a) by mixing a suspension of nanoparticles with a reagent solution, a direct method, (b) by immobilizing nanoparticles on the surface of cryogels (through ice-mediated coating, deposition, or covalent bond formation), and (c) in situ preparation; nanoparticles are formed by reduction of metal salt absorbed by preformed cryogel

Table 1.1 Methods for preparing nanocomposite cryogels

Methods	Advantages	Disadvantages	Examples	Ref.
Direct method, by adding nanoparticles to reaction solution before cryogel preparation	<ul style="list-style-type: none"> • simple, as it involves one step (cryogelation of reagents with NP added); • low wastage due to high efficiency of NP incorporation in cryogel; • commercial nanoparticles can be used; • the synthesis of nanoparticles with desirable properties could be better controlled; • particles can be analyzed using standard techniques for particles analysis; • forms stronger cryogel composites; 	<ul style="list-style-type: none"> • deposition of nanoparticles during the gel formation and uneven distribution in the final material; • agglomeration of nanoparticles in the reaction solution; • presence of nanoparticles could affect cryogelation and properties of cryogel formed, so need reoptimization; • nanoparticles embedded inside the polymer matrix and are less exposed to the surface; 	HEMA-Fe ₃ O ₄ , pAAm-iron oxide hydrogel, pAAm-TiO ₂ , pAAm-γ-Al ₂ O ₃	Otero-Gonzalez et al. (2020) Savina et al. (2011) Önnby et al. (2015) Önnby et al. (2014)
Immobilizing nanoparticles on the surface of cryogels	<ul style="list-style-type: none"> • can use the cryogel with optimized porosity, mechanical and swelling properties • nanoparticles are immobilized at the surface of pore walls 	<ul style="list-style-type: none"> • high wastage of the NP due to lower incorporation efficiency • low NP content due to dispersion problems; 	ZnO-pHEMA cryogel ZnO-pAAm Ag-	Ussia et al. (2018) Inal et al. (2021) Loo (2016)
In situ preparation (nanoparticles prepared inside of the cryogel)	<ul style="list-style-type: none"> • can use the cryogel with optimized porosity, mechanical and swelling 	<ul style="list-style-type: none"> • the reaction condition needs to be optimized to obtain the nanoparticles of the desired 	p(VI) with Co, Ni, and Cu NPs; Chitosan-AuNPs Chitosan-	Tercan et al. (2020) Berillo (2020), Berillo and Cundy (2018), Kudaibergenov

(continued)

Table 1.1 (continued)

Methods	Advantages	Disadvantages	Examples	Ref.
	properties <ul style="list-style-type: none"> • even distribution of nanoparticles in the cryogel; • no effect on the cryogelation process; • no particles agglomeration; 	amount, size, and shape; <ul style="list-style-type: none"> • a limited number of methods suitable for analysis of nanoparticles inside the polymer; • low NPs load, and it is necessary to repeat the loading steps to get more NPs 	PdNPs; DMAEM-co-MAA-AuNPs	et al. (2018) Atta et al. (2018)

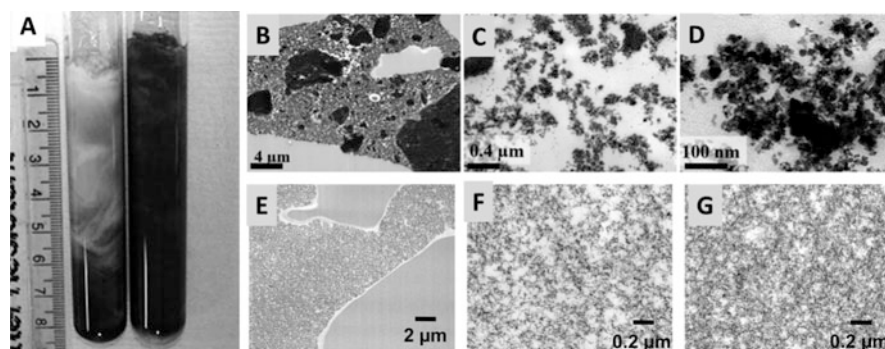


Fig. 1.3 (a) Sedimentation of nanoparticles in pAAm solution during freezing (sample on the left) and even distribution applying prefreezing method (sample on the right) (Savina et al. 2016a), (b–d) TEM images of a transverse section through Fe_3O_4 -HEMA cryogels with the iron oxide nanoparticles randomly distributed inside the polymer wall. High-magnification TEM image reveals agglomerated nanoparticles (Savina et al. 2011). (e–g) TEM image of a cross-section of the iron oxide-HEMA cryogel with a 33% of iron oxide hydrogel content (E and F) and with a 100% iron oxide hydrogel content (g) (Otero-Gonzalez et al. 2020)

1.2.1.1 Direct method

The direct method involves a one-step preparation of nanocomposites by mixing nanoparticles with reagent solution before making the cryogel. Better control of the size and shape of nanoparticles can be achieved by pre-preparing the nanoparticles first (Önnby et al. 2015) or simply using commercially available nanoparticles (Savina et al. 2011). Nanoparticles are easier to analyze in suspension than inside a polymer matrix using dynamic light scattering (DLS), transmission electron microscopy (TEM), scanning electron microscopy (SEM), UV-vis spectrometry, and nitrogen adsorption. Thus, a comprehensive analysis of the nanoparticles

could be carried out before the preparation of the composite. However, nanoparticles tend to aggregate during synthesis (Fig. 1.3b–d) (Önnby et al. 2015; Savina et al. 2011), so mixing and stabilizing the nanoparticles in the reaction solution is critical. Sonication is often used to better disperse nanoparticles in the reaction solution prior to polymerization (Önnby et al. 2015). Often it is difficult to achieve a uniform distribution of nanoparticles throughout the cryogel volume due to their higher density compared to the reaction solution. As a result, the nanoparticles will tend to precipitate (settle) in the cryogel sample before the gel formation is complete and form a concentration gradient with a low content of nanoparticles in the upper part of the sample compared to the lower one (Fig. 1.3a) (Savina et al. 2011, 2016a; Otero-Gonzalez et al. 2020). To avoid this, the researchers used more viscous reaction solutions, for example, using PEGDA as a cross-linking agent instead of MBA, to obtain a more viscous solution and slow down the precipitation (Savina et al. 2011). In the work (Kumar et al. 2013), to minimize the sedimentation of Fe-Al hydroxide particles, test tubes with samples were pre-cooled for 15 min. Before adding the sample solution, several crystals of silver iodide were added to each tube. Silver iodide is insoluble and acts as a seed to promote ice formation. All these measures help to increase the freezing rate of the reagent solution and reduce the deposition of NPs. Shu et al selected polyacrylamide as the main polymer as a dispersing agent for the preparation of cryogel composites with TiO₂ uniformly loaded into cryogels (Shu et al. 2017). In addition, reducing the size of the sample and then creating an adsorption column by stacking several pieces of cryogels together can be a way to overcome the uneven distribution of NPs in the purification device (Savina et al. 2016a). Savina et al. (Savina et al. 2016a) proposed a new method for the production of cryogels by prefreezing the reaction solution with constant stirring before starting polymerization. This shortens the time for complete freezing of the sample but also creates mechanical obstacles to the separation of nanoparticles, since ice crystals stop the deposition of nanoparticles in a large volume. In another approach, a hydrated nanostructured iron oxide hydrogel was used instead of dried nanoparticles (Otero-Gonzalez et al. 2020). Iron oxide hydrogel disperses better in the reagent solution. This made it possible to obtain cryogels with increased content of iron oxide nanoparticles, which were well distributed over the entire volume of the cryogel (Fig. 1.3e–g).

After the formation of the cryogel, nanoparticles are captured inside the polymer matrix and are less exposed to the surface of the cryogel wall, which affects the kinetic and adsorption capacity of cryogels. Thus, the researchers were looking for immobilizing NP on the surface of polymer walls.

1.2.1.2 Immobilizing Nanoparticles on the Surface of Cryogels

Nanoparticles could be directly immobilized on the surface of the cryogel by deposition or chemical attachment. This method has several advantages. First, the properties of the cryogel and nanoparticles can be well controlled, and there is no need to optimize the porosity further, mechanical properties, and swelling properties of the cryogel. The particles will be immobilized mainly on the surface of the polymer walls and thus will be exposed to an aqueous solution that facilitates

interaction with the contaminant, be it chemicals or bacterial cells. There are different methods reported on immobilization. Loo et al. used ice-mediated coating, which involves swelling of cryogel in preformed stabilized NPs solution followed by freezing and keeping it in a frozen state (Loo 2016). The ice formed in the cryogel expels the nanoparticles towards the pore wall surface, making them attached. Inal et al. (Inal et al. 2021) chemically cross-linked ZnO nanorods with polyacrylamide (pAAm) cryogels. The first pAAm cryogels were modified by the introduction of amino groups followed by glutaraldehyde (GA) treatment, and the ZnO nanorods were activated with 3-aminopropyltriethoxysilane (APTES) before being attached to the cryogel surface. SEM analysis shows that this approach does not provide a good distribution of ZnO nanorods, which appeared as clusters of nanoparticles sitting inside the cryogel pores. This was probably the result of pure dispersion of nanorods in solution and inside the cryogel. This is also a more complicated method since it requires additional modification of the cryogel and nanoparticles before attaching NPs to the cryogel. In another work (Ussia et al. 2018), ZnO was deposited on poly (2-hydroxyethyl methacrylate) (pHEMA) cryogel and its composite with GO by atomic layer deposition. ZnO, which appeared as small grains on SEM images, was uniformly distributed on the surface, showing a regular shape and sizes coating.

1.2.1.3 In Situ Preparation

In situ preparation involves the formation of nanoparticles directly inside the polymer matrix of cryogel. In the literature, it is also sometimes called intermatrix synthesis (Jia et al. 2018). For in situ nanoparticles preparation, cryogels with ionizable groups will be synthesized first using polymers having ionizable groups, such as 2-acrylamido-2-methylpropane sulfonate (AMPS) (Al-Hussain et al. 2018), poly(vinyl imidazole) (p(VI)) (Sahiner et al. 2015b), chitosan (Berillo and Cundy 2018), and others. In general, hydrophilic and strongly ionizable groups such as $-\text{SO}_3\text{H}$, $-\text{OH}$, $-\text{COOH}$, $-\text{SH}$ and $-\text{NH}_2$ have been reported as functional groups responsible for capturing metal ions (Kudaibergenov 2019; Seven and Sahiner 2014a). After the adsorption of metal ions by the cryogel matrix, the excess will be washed away (Sahiner et al. 2015b), and then metal ions will be reduced to metal nanoparticles using NaBH_4 , NH_4OH , and others as reducing agents (Jia et al. 2018). p(AAm) cryogel was synthesized and chemically modified with hydroxylamine hydrochloride for metal ion absorption (Seven and Sahiner 2014a). In situ reduction to obtain metallic nanoparticles using NaBH_4 was performed. To obtain p(VI) cryogel with Co, Ni, and Cu, the cryogel amino groups were first protonated, and then the gel was loaded with Co, Ni, and Cu chloride salts (Tercan et al. 2020; Sahiner et al. 2015b). The metal ions were reduced with NaBH_4 . Co, Ni, and Cu NPs were successfully prepared within p(VI) cryogels in the size range of 20–100 nm, depending on the nature of the corresponding metal salts. The amount of Co, Ni, and Cu NP in p(VI) cryogels was calculated as 48.4 ± 2.5 , 37.5 ± 3.2 , and 128.2 ± 6.3 mg of nanoparticle per gram of cryogel, respectively (Tercan et al. 2020). The difference in the amounts of metal ions in cryogels can be explained by the affinity of imidazole groups for metal ions. The loading of metal ions into p(VI) cryogel occurred through nitrogen atoms in the imidazole ring. The lone pair of

nitrogen is weakly bound, and Cu(II) ions interact easier and more efficiently than other ions.

The amount of nanoparticles prepared inside the cryogel depends on the number of metal ions retained by the cryogel, which will depend on the number of ionic groups present and may be limited. It can be increased by repeating the process of loading-reduction of metal ions. The content of Co in p(AAm) cryogels after the first loading was 121.6 ± 1.5 mg/g and increased significantly; after the second and third cycles of loading-reduction, p(AAm) cryogel composites had 135.1 ± 1.0 and 278.5 ± 1.1 mg of Co per gram of cryogel (Seven and Sahiner 2014a). The sponge-like property has been utilized to saturate the cryogel with a metal ion (Kurozumi et al. 2015). The cryogel was first saturated with the metal ions, and then the excess of the solution was squeezed out before adding the reduction solution. Another approach to retaining metal ions inside a cryogel is to swell the cryogel in a solution of metal ions followed by drying before immersion in a reducing solution (Al-Hussain et al. 2018). This keeps all of the ions inside the dried sample, which are then reduced to NPs.

Another approach was to add metal ions during the formation of the cryogel and use their ability to form complexes with the ionic polymer to crosslink simultaneously. Metal ions were reduced to nanoparticles after the formation of cryogels. Berillo et al. produced chitosan-based cryogels by complexation of chitosan with metal ions such as $[\text{PdCl}_4]^{2-}$, $[\text{PtBr}_4]^{2-}$, or $[\text{PtCl}_4]^{2-}$ under subzero temperatures (Berillo et al. 2014; Berillo and Cundy 2018). The reduction of noble metal complexes with chitosan was performed after cryogel formation using glutaraldehyde (GA) (Berillo and Cundy 2018). In another work, 1,1,3,3-tetramethoxypropane (TMP) has been used for one-step preparation of covalently cross-linked cryogel with in situ formed gold nanoparticles (Berillo 2020). The chitosan, TMP, and different concentrations of $\text{H}[\text{AuCl}_4]$ have been mixed and subjected to cryogenic treatment. TMP performs as a cross-linker and reducing agent for gold salt, which co-occurs during the cryogelation process. Increased concentration of gold salt leads to an increased number of AuNPs formed in the cryogel, as can be seen in Fig. 1.4a. Increased AuNPs concentration led to a higher intensity of red, which appeared grey in these images. AuNPs had mostly spherical morphology confirmed by TEM and were evenly distributed in the polymer walls (Fig. 1.4b). The particle content depends on the concentration of metal salt used. An increase in the concentration of $\text{H}[\text{AuCl}_4]$ in the reaction solution led to the formation of cryogels with 98.5, 196.9, 393.9, and 787.8 mg/L of AuNPs (Fig. 1.4).

Loo et al. compared all three synthesis routes for the production of AgNPs in PSA cryogel: (i) incorporation of pre-synthesized AgNPs during cryogelation, (ii) ice-mediated coating of pre-synthesized AgNPs on preformed PSA cryogels, and (iii) in situ reductions of PSA cryogels loaded with Ag^+ (Loo 2016; Loo et al. 2015b). The PSA-AgNPs cryogels prepared via the different methods have varying AgNP size, pore morphology, and mechanical behavior (Table 1.2).

The presence of AgNP in the solution for gel formation affected the cryogelation process, as a result of which the yield of the gel fraction was significantly reduced (30% versus 95% without AgNP) when using the direct method. The direct method

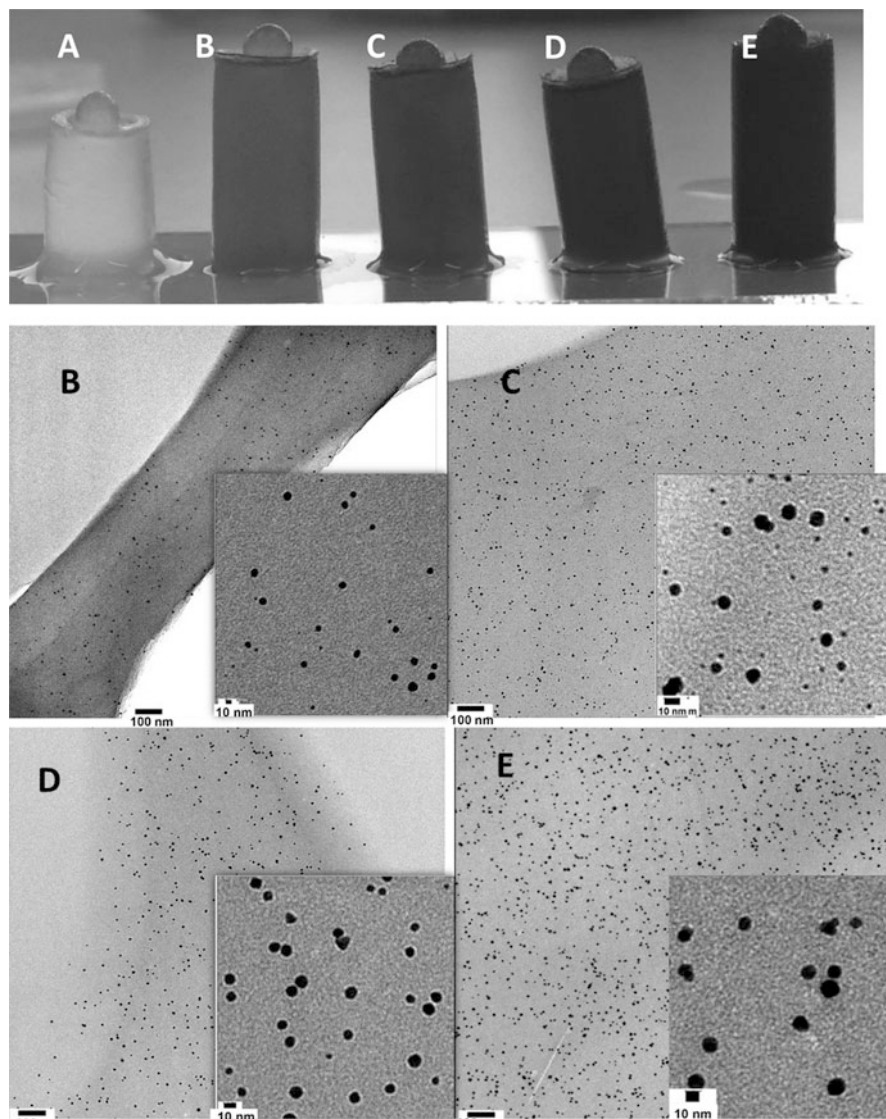


Fig. 1.4 Chitosan cryogels with different AuNP content: above photographs of cryogels swollen in water at RT and below TEM images of chitosan cryogels with no AuNP (a) and with 98.5 (b), 196.9 (c), 393.9 (d), and (e) 787.8 mg/L of AuNPs. Adapted from (Berillo 2020)

provides higher efficiency of AgNP incorporation; most of them (>99%) were embedded into the cryogel. This also resulted in a stronger cryogel with higher Young's moduli than the original PSA cryogel. Nevertheless, due to the very low (<5 $\mu\text{g/L}$) concentration of AgNP used, the AgNP content in the final material was the lowest compared to other cryogels obtained by another method (Table 1.2). The

Table 1.2 Properties of the PSA-AgNP cryogels were prepared via different methods (Loo 2016)

Sample	AgNP content (mg/g)	Efficiency of AgNP incorporation, w/w%	Mean AgNP size ^a (nm)	Young's modulus, kPa
PSA plain cryogel	NA	NA	NA	2.5 ± 0.8
PSA-AgNP				
• direct method	0.8 ± 0.3	>99	25.1 ± 13.4	6.0 ± 0.1
• ice-mediated precipitation	1.4 ± 0.2	26.0 ± 3.8	12.2 ± 8.5	2.3 ± 0.5
• in situ formation	4.0 ± 0.2	74.8 ± 2.7	5.1 ± 2.1	3.5 ± 0.7

^aDetermined from TEM images

content of AgNP in the reaction solution can be increased, as it was done in another study, but this can have a more negative effect on polymerization, as well as lead to higher agglomeration of nanoparticles before they are incorporated into the polymer matrix. On the other hand, for the ice-assisted and in situ formation methods, cryogels were prepared without AgNPs (with a gel yield of 95%), which allows better control of the cryogel properties as well as NP incorporation. It was found that second freezing significantly improved the incorporation efficiency of AgNPs. Compared to PSA-AgNP cryogels prepared without the post-freezing step, the Ag incorporation efficiency increased from $4.6 \pm 0.6\%$ to $26.0 \pm 3.8\%$ with the additional freezing step. Without the additional freezing step, most of the AgNPs absorbed were released back into the solution during washing. TEM images also show some agglomeration of nanoparticles for both direct and ice-mediated approaches, which is reflected in NP size. The in situ method was chosen by the authors as the most reliable and straightforward to perform with good reproducibility. This allows for a high and predictable AgNP content in cryogels.

As has been discussed, all methods for the preparation of nanocomposites have their advantages and disadvantages, which need to be considered during the preparation of novel materials. Nanoparticle content and distribution have a significant effect on the application. For catalytic applications, it is not necessary to have a very high nanoparticle content, while for adsorption applications, it is essential to have the highest possible adsorbent concentration for the best performance. The distribution of nanoparticles within the cryogel matrix, polymer walls is also critical. NPs activity depends on their surface area and their availability for interaction with a pollutant. NPs on the surface of polymer walls will be more accessible than those located inside a polymer or coated with a polymer (Kumar et al. 2013, 2014). In any case, the macroporous structure of cryogels with polymer walls several micrometers in size provides a small diffusion passage compared to conventional hydrogels, and the interconnected pore system provides good mass transfer within cryogel materials supporting the adsorption or catalytic process.

1.2.2 Application of Cryogel Nanocomposites for Water Treatment

Cryogel nanocomposites were used in two water purification processes: adsorption and catalysis. In this section, we discuss recent research on the removal of organic and inorganic contaminants with cryogel nanocomposites.

1.2.2.1 Adsorption

The adsorption process is a surface phenomenon in which the adsorbate is concentrated or deposited on the adsorbent surface. The adsorption process is usually classified as physisorption (adsorbate bound to a surface by weak van der Waals forces) and chemisorption (adsorbate bound by a covalent bond or due to electrostatic attraction). Adsorption methods are widely used in water purification as one of the most feasible, efficient, and inexpensive approaches. An effective adsorbent must have several properties, for example, it must be nontoxic, resistant to mechanical stress, and have a high adsorption capacity for efficient waste removal. Adsorbents based on metals or metal oxides are widely used to remove heavy metal ions and dyes. Nanosized metals or metal oxides including Fe_3O_4 , TiO_2 , and ZnO provide a large number of active adsorption sites, large surface area, and specific affinity, which provides excellent adsorption capacity for removing organic pollutants and heavy metals. Inside the composition of cryogel, they have been used to remove metalloids and heavy metal ions such as As(III) (Kumar et al. 2016, 2013; Savina et al. 2011, 2016a; Otero-Gonzalez et al. 2020), Cr(VI) (Andrabi et al. 2016; Jia et al. 2018), Cd(II) (Önnby et al. 2015), Pb(II) (Shu et al. 2017), and dyes, such as methyl blue (Al-Hussain et al. 2018; Ussia et al. 2018; Atta et al. 2018) and orange G (Inal et al. 2021) (Table 1.3).

The adsorption capacity depended on the amount of adsorbent loaded into the cryogel, the size of nanoparticles and surface area, as well as their accessibility for contact with the adsorbate. When NPs are embedded in a cryogel, adsorption will take place along short diffusion paths through the polymer. The incorporation of nanoparticles into cryogels affected the kinetics of adsorption, slowing it down, but the overall adsorption capacity will be close to naked nanoparticles used in suspension (Önnby et al. 2015, 2012; Savina et al. 2011; Shu et al. 2017). Thus, analysis of the adsorption of As(III) by nanostructured iron oxide hydrogel in solution and when it was embedded inside pAAm cryogel showed similar maximum adsorption values (q_{max}), 625 and 588 mg As(III) per g of Fe for the iron hydrogel and pAAm-iron oxide-cryogel (Otero-Gonzalez et al. 2020). The As(III) adsorption was very fast on the iron oxide hydrogel, and about 90% As(III) removal was achieved after only 15 min. On the other hand, adsorption kinetics was slower on the pAAm-iron oxide-cryogel, and it required about 24 h to achieve the same adsorption capacity. Only 55% As(III) removal was attained after 15 min (Otero-Gonzalez et al. 2020). During the adsorption of Cd^{2+} by TiO_2 nanotubes in suspension, adsorption equilibrium was reached within less than 50 min, whereas the two pAAm- TiO_2 cryogel composites with an adsorbent concentration of 0.5 and 1 g/L required more than 200 min to reach saturation (Önnby et al. 2015). Higher loading of nanoparticles will initially increase adsorption, as increasing nanoparticle mass increases surface area and

Table 1.3 Examples of application of cryogel nanocomposites for removal of dyes and metal ions by adsorption

Pollutant (adsorbate)	Nanoparticles	Cryogel	Initial aqueous phase concentration of pollutant, mg/L	Adsorption capacity, mg/g,	pH	Reference
Metal(loid) ions						
As(III)	Fe ₃ O ₄	Chitosan-co-DMAEMA	0.25	11.5	–	Andrabi et al. (2016)
	Fe ₂ O ₃	p(HEMA)	2	2.7	7	Savina et al. (2011)
	Fe ₃ O ₄	p(HEMA)	4	3.1	7	Savina et al. (2011)
	Fe(OH) ₃ - Al(OH) ₃	p(AAm)	5–200	24.6	7	Kumar et al. (2013)
	Fe(OH) ₃ - Al(OH) ₃	p(AAm)	5–200	82.3	7	Kumar et al. (2016)
	α-Fe ₂ O ₃	P(HEMA)	2	3.1	7	Savina et al. (2011)
	Fe ₃ O ₄	P(HEMA)	2	2.7	7	Savina et al. (2011)
	Fe-oxide	p(AAm)	9.5	118	7.5	Otero-Gonzalez et al. (2020)
	Fe-oxide	pHEMA	9.5	35.7	7.5	Otero-Gonzalez et al. (2020)
	As(V)	Fe(OH) ₃ - Al(OH) ₃	p(AAm)	5–200	49.6	7
Cd(II)	FeO(OH)	p(AAm)	100	20	7	Kurozumi et al. (2015)
	Al ₂ O ₃	p(AAm)	5	6	7	Önby et al. (2014)
	Fe ₃ O ₄	p(APTMA)	400	118	9.3	Sahiner et al. (2015a)
	TiO ₂ nanotubes	pAAm	10	10.8	7.2	Önby et al. (2015)
Cr(III)	Fe ₃ O ₄	p(APTMA)		30		Sahiner et al. (2016)
Cr(VI)	Fe ₃ O ₄	Chitosan-co-DMAEMA	0.25	14.22	–	Andrabi et al. (2016)

	nZVI	PSA	50	138.80	5.6	Jia et al. (2018)
I ⁻	Fe ₃ O ₄	p(APTMA)	–	40		Sahiner et al. (2016)
	Ag/Ag ₂ O	AA-MAAc-DMAAm	100	117.2	–	Baimenov et al. (2020)
	Ag/Ag ₂ O	AA-AMPS-DMAAm	100	96.8	–	Baimenov et al. (2020)
Pb(II)	TiO ₂	A.Arm	100	23.3	6	Shu et al. (2017)
Dyes						
MB	Fe ₃ O ₄	AMPS	–	1428.57	–	Al-Hussain et al. (2018)
	Fe ₃ O ₄	AMPS/NP	–	1428.57	–	Al-Hussain et al. (2018)
	Fe ₃ O ₄	AMPS/HEMA	–	1428.57	–	Al-Hussain et al. (2018)
	GO	pHEMA	4.8	0.97	pH 7.0	Ussia et al. (2018)
	ZnO	pHEMA	4.8	0.82	pH 7.0	Ussia et al. (2018)
Orange G	ZnO + GO	pHEMA	4.8	0.94	pH 7.0	Ussia et al. (2018)
	ZnO nanorods	A.Arm	400	142.79	–	Inal et al. (2021)

provides more adsorption sites. However, an increase in the concentration of NPs in the reaction solution will likely lead to aggregation of NPs and, in this case, will not lead to an increase in the surface area and adsorption centers (Önnby et al. 2015). Önnby et al. observed an 18% reduction in the adsorption of Cd^{2+} by pAAm-TiO₂ cryogels at 2% of the adsorbent concentration in the cryogel (Önnby et al. 2015). In another work, higher As(V) removal was obtained at higher loads of gamma-Al₂O₃-NPs up to 4%, with a slight drop observed at 5% and more loads (Önnby et al. 2014).

Agglomeration, one of the reasons for the lower adsorption capacity, could be avoided by using a stabilizing agent in a suspension of NPs or by using another method of introducing NPs into the cryogel, as discussed in the section above. More uniform and finer particle dispersions will improve the available surface area and improve adsorption performance. Otero-Gonzalez et al. produce iron oxide cryogels by adding hydrated nanostructured iron oxide hydrogel instead of dried NPs (Otero-Gonzalez et al. 2020). As a result, the adsorption efficiency was significantly improved by adding more nanoparticles and their better distribution in the cryogel matrix. In this case, the content of Fe oxide increased from 0.08 to 2.5 wt%, and the adsorption capacity for As(III) increased seven times from 0.21 to 1.5 mg/g of swollen pHEMA cryogel (Otero-Gonzalez et al. 2020).

Adsorption depends on pH, temperature, the concentration of contaminants and other ions, adsorption time, cryogel size, as well as the physical and chemical nature of the adsorbate and adsorbent. For example, pH can affect the adsorption capacity by changing the surface groups present on the adsorbent and the charge/speciation of the contaminant (Savina et al. 2011; Kumar et al. 2013, 2016; Shu et al. 2017). Extreme pH can also lead to the dissolution of the adsorbent itself (Kumar et al. 2013). An increase in temperature can improve the adsorption capacity in endothermic reactions. The presence of other ions and organic compounds can interfere with the adsorption process by competing for adsorption sites (Kumar et al. 2013, 2016). All these factors are essential to consider, especially for understanding the characteristics of the adsorbent in real wastewater. pAAm-TiO₂ cryogel was assessed for adsorption of Cd^{2+} from real nutrient-rich process water generated from hydrolysis of seaweed, pollutant-rich biomass (Önnby et al. 2015). Optimal conditions were found for high removal of Cd^{2+} (about 94%), despite the molar excess (from 100 to 500) of co-present ions (for example, Mg^{2+} , Ca^{2+} , Na^+ , K^+) and while maintaining the total phosphorus content. As(III) adsorption by pAAm cryogel with Al-Fe hydrous oxide dropped from 95% to 83% in the presence of the prevailing competing ions present in municipal wastewater (Kumar et al. 2013). pH plays a significant role in the adsorption of Pb(II) on the TiO₂-cryogel composite (Shu et al. 2017). Cryogel adsorbents had low adsorption of Pb(II) at pH 2, and then the adsorption capacity rapidly increased from pH 2 to 5.

Most of the experiments were carried out in batch mode, when the cryogel was immersed in a solution of contaminants and then removed after the adsorption process (Kumar et al. 2013; Savina et al. 2011; Shu et al. 2017; Al-Hussain et al. 2018). However, of great interest is adsorption in a continuous mode, when a cryogel is placed inside the column, and the solution flows through (Önnby et al. 2015, 2014;

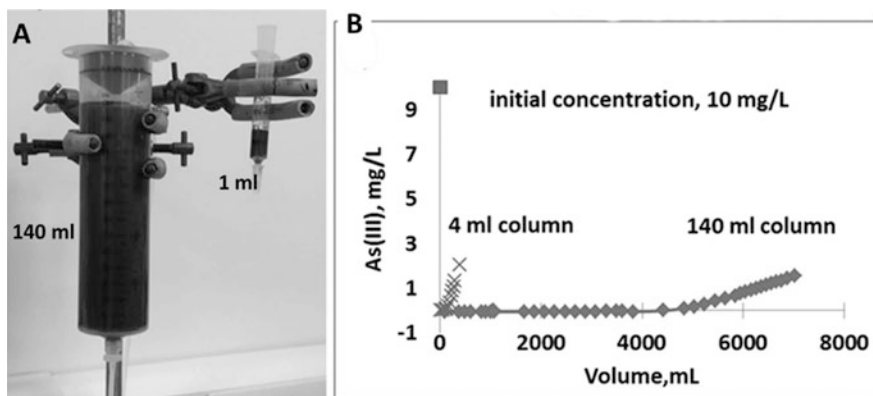


Fig. 1.5 (a) pAAm- α -Fe₂O₃-cryogel column produced by the pre-freezing method (140 mL volume) and conventional method (1 mL volume); (b) adsorption of As(III) by 4 and 140 mL α -Fe₂O₃-pAAm cryogel column (Savina et al. 2016a)

Savina et al. 2016a). Column experiments showed that the pAAm-Al-Fe hydroxide cryogel composite could treat higher volumes of As(III) solutions when compared with a commercially available adsorbent based on granular ferric hydroxide (Kumar et al. 2016). This application was limited to composites of smaller size; a small column (bed height 20 mm and inner diameter 7 mm) was tested.

In the work (Savina et al. 2011), a 4 mL column was made by stacking four separate gel pieces together. Savina et al. have been able to upscale the cryogels further and prepared a pAAm- α -Fe₂O₃ composite cryogel column of a total volume of 140 mL (Fig. 1.5) (Savina et al. 2016a). A solution of 10 mg/L As (III) was pumped through the 4 and 140 mL columns at a flow rate of 4 and 10 mL/min, respectively. The breakthrough profiles (Fig. 1.5b) clearly demonstrate efficient scaling up of the adsorption process using a large column and higher efficiency in As(III) removal. The breakthrough was observed at about 100 and 5000 mL for columns 4 and 140 mL, respectively.

Adsorption has its limitation. When the adsorbent is saturated, the adsorption of pollutants is not possible. The adsorbent does not entirely eliminate the pollutant but pre-concentrates it on the adsorbent. The adsorbent must be utilized (Kumar et al. 2013) or recovered (Al-Hussain et al. 2018), which is associated with additional costs and can lead to the appearance of secondary pollutants in the ecosystem. Thus, techniques that can completely eliminate contaminants, such as catalysis, are the preferred choice for some applications.

Ussia et al. combined adsorption and catalysis in a single process by preparing pHEMA cryogel composites with graphene oxide (GO) and ZnO (Ussia et al. 2018). The amount of methylene blue (MB) adsorbed at equilibrium was 0.73, 0.97, 0.82, and 0.94 mg/g for cryogels pHEMA, pHEMA-GO, pHEMA-ZnO, and pHEMA-GO-ZnO, respectively, which indicates that GO plays a vital role during adsorption. However, although pHEMA and pHEMA-GO lost their adsorption capacity after

several cycles, the ZnO-coated samples were able to retain it after being regenerated by UV light (Ussia et al. 2018).

1.2.2.2 Catalysis

Significant research efforts are directed towards the development of a highly active, selective, stable, easy to handle, and reusable catalytic system. Nanocatalysis systems are attracting attention as an efficient way to eliminate pollutants. One of the major barriers to the wide use of nanocatalytic systems is their recovery after water treatment. The separation of nanoparticles is not an easy process, and if they enter the ecosystem, they can cause severe toxicity to aquatic organisms and humans. Thus, immobilization of nanoparticles inside a polymer is a safe approach to creating a nanoparticle-based catalytic system. The main advantage of the macroporous structure of the cryogel as a carrier for nanoparticle catalyst is the large contact area between the catalyst and the substrate, the possibility of multiple uses, the ease of separating the catalyst from the reaction medium, and the ability to perform catalysis in flow-through mode. Examples of nanocomposite-based catalysts for degradation of organic compounds, catalytic efficiency, TOF, and TON values are summarized in Table 1.4.

Sahiner et al. have used various polymers as templates for preparing nanoparticles. Poly(3-sulfopropyl methacrylate), pHEMA, poly(acrylic acid) (pAAc), poly(4-vinylpyridine) (p(4-VP)), and poly(2-acrylamido-2-methyl-1-propansulfonic acid) cryogels have been prepared with Ni, Cu, and Co nanoparticles (Sahiner et al. 2015d; Sahiner and Seven 2014; Seven and Sahiner 2014b; Sahiner and Yildiz 2014). These cryogels were used in hydrogen generation from the hydrolysis of NaBH₄. The hydrogen generation rate and turnover frequency (TOF) were temperature-dependent and increased with increasing temperature (Sahiner et al. 2015d).

P(4-VP) and p(VI) cryogels containing Ni and Cu nanoparticles were used as the catalysts for the continuous reduction of p-nitrophenol (Sahiner and Demirci 2019). p(AAm) cryogel modified by amidoximation to bind metal ions and prepare metal nanoparticles of Cu, Ni, and Co were used for the catalytic reduction of 2- and 4-nitrophenol (2- and 4-NP) and some dyes, MB and Eosin Y (EY) (Sahiner et al. 2015c). The higher total TOF and low activation energy (E_a) values of 2.46 (mole 2-NP) (mole Cu. min)⁻¹ and 20.2 kJmol⁻¹ were observed for catalytic reduction of 2-NP by pAAM-CuNP composite (Sahiner et al. 2015c).

N,N-dimethylaminoethylmethacrylate and methacrylic acid (p(DMAEM-co-MAA)) cryogel composites with AuNPs and PdNPs have been tested for the catalytic reduction of 4-NP by NaBH₄ (Kudaibergenov et al. 2018) and oxidation of DL-dithiotreitol (DTT) by hydrogen peroxide (Tatykhanova et al. 2016). The kinetic parameters, turnover number (TON), TOF, and activation energy of hydrogenation of 4-NP have been calculated (Tatykhanova et al. 2016). The reaction was performed in a flow-through reactor, and 95% conversion was reached 4 min after 5 times repeated passing of 10 mL mixture of 4-NP and NaBH₄ through the catalytic reactor. Similar catalytic activity was observed after the passing of 100 mL of 4-NP and NaBH₄ mixture (Tatykhanova et al. 2016). The AuNPs immobilized

Table 1.4 Examples of catalysis using cryogel nanocomposites

Cryogels	Nanoparticles	Pollutant	Reaction conditions	Efficiency/ Conversion, %	TON	TOF (h ⁻¹)	References
Chitosan	AuNPs	4-NP	49 µg AuNPs, 0.6 × 10 ⁻⁴ mol L ⁻¹ of 4-NP, 1.5 × 10 ⁻³ mol L ⁻¹ NaBH ₄ , pH 10, tested for 14 cycles	86–92.4%	18.3	0.619	Berillo (2020)
Chitosan	PdNPs	4-NP	2.66 µg PdNPs, 7 mL 50 mM carbonate buffer at +0.15 mL of 50 mM of 4NP 0.15 mL of 0.2 M NaBH ₄ pH 10, tested for 9 cycles	85–98%	10.3	0.53	Berillo and Cundy (2018)
Chitosan	AuNPs	dimethyl-amino-benzaldehyde (DABA)	15 mL of 0.04 mM DABA, cryogels volume 0.5 mL containing 10 ⁻⁶ mol L ⁻¹ AuNPs flow rate 0.5 mL/min reactant dissolved air	80%	–	–	Berillo et al. (2014)
Chitosan	AuNPs	4-NP	0.6 × 10 ⁻⁴ mol L ⁻¹ of 4-NP, 1.5 × 10 ⁻³ mol L ⁻¹ NaBH ₄ , pH 10	86–92.4%	18.3	0.619	Berillo (2020)
p (DMAEM- co-MAA)	AuNPs	p-NBA	5 × 10 ⁻⁵ mol L ⁻¹ of p-NBA NaBH ₄ varied from 1 × 10 ⁻² to 2.5 × 10 ⁻³ mol L ⁻¹ .	58–62.6%	–	–	Kudaibergenov et al. (2018)
	PdNPs	p-NBA	5 × 10 ⁻⁵ mol L ⁻¹ of p-NBA NaBH ₄ varied from 1 × 10 ⁻² to 2.5 × 10 ⁻³ mol L ⁻¹ .	58–62.6%	–	–	Kudaibergenov et al. (2018)
p(VI)	AuNPs	4-NP	0.5 × 10 ⁻⁴ mol L ⁻¹ of 4-NP, 0.5 mL 0.5 × 10 ⁻³ mol L ⁻¹ of NaBH ₄ , flow-through mode	95%	38.17	21.56	Tatykhanova et al. (2016)
	Co Ni	MB	0.02 mmol Co, Ni, and Cu NP, 5.0 mmol NaBH ₄ .	Catalytic activity	–	292 ± 3.3	Tercan et al. (2020)

(continued)

Table 1.4 (continued)

Cryogels	Nanoparticles	Pollutant	Reaction conditions	Efficiency/ Conversion, %	TON	TOF (h ⁻¹)	References
	Cu Co, Ni, and Cu calculated as 48.4 ± 2.5, 37.5 ± 3.2, and 128.2 ± 6.3 mg nanoparticle per g cryogel,			Co > Cu > Ni for MB, Conversion % 97.1 ± 1.2 62.0 ± 1.6 79.4 ± 6.1		186 ± 4.8 239.2 ± 9.75	
	Co Ni Cu	EY	0.02 mmol Co, Ni and Cu NP, 5.0 mmol NaBH ₄ .	Co > Ni > Cu 78.4 ± 1.1 52.0 ± 1.7 13.7 ± 3.6		234.2 ± 3.3 156.0 ± 5.1 41.1 ± 10.8	Tercan et al. (2020)
	Co Ni Cu	4-NP	0.02 mmol Co, Ni, and Cu NP, 5.0 mmol NaBH ₄	Ni = Co > Cu for 4-NP 96.3 ± 3.1 98.3 ± 0.4 66.1 ± 4.2		288.9 ± 9.3 294.9 ± 1.2 198.3 ± 12.6	Tercan et al. (2020)
	Co	p-NP	0.4 M NaBH ₄ , 0.01 M p-NP, flow-through mode	–	–	1.37	Sahiner and Demirci (2019)
p(4-VP)	Co	p-NP	0.4 M NaBH ₄ , 0.01 M p-NP, flow-through mode	–	–	2.19	Sahiner and Demirci (2019)

Table 1.5 TON and TOF parameters of chitosan-AuNP composite cryogel catalysts for the reduction of 4-NP ($n = 2$) (Berillo 2020)

Sample	Weight of AuNP, μg per sample	The average size of AuNP, nm	Number of tested cycles	[4-NP], μmol	TON	TOF, h^{-1}
1	49.0	5.9 ± 2.1	14	60	18.3	0.619
2	197	8.0 ± 2.0	12	60	5.14	0.255
3	394	9.6 ± 2.5	10	50	1.40	0.066

cryogel catalyst sustained over 50 cycles without substantial loss of the catalytic activity. DTT oxidation was more efficient than 4-NP reduction. The p(DMAEM-co-MAA)-AuNPs cryogel catalyst showed high catalytic activity in the oxidation of DTT and sustained cyclic oxidation of the substrate with a conversion of 97–98%. The TON and TOF values after 10 DTT oxidation cycles were 985.2 and 412.2 h^{-1} , respectively (Tatykhanova et al. 2016).

The embedding of a high concentration of NP does not always lead to better catalyst performance. Thus, the apparent TON and TOF values for the reduction of 4-NP by chitosan–AuNP cryogels depended on the total AuNP mass and NP size and decreased with an increase in the AuNP weight and size and a number of tested cycles (Table 1.5) (Berillo 2020). This could be associated with the change in the catalyst surface area available for the substrate due to a change in the NP size. The apparent TON means that it is based on the number of cycles tested if the catalytic reaction rate does not decrease over time. The higher the number of cycles, the higher the TON number.

Organic pollutants do not exist alone, and it is desirable that a single catalyst can handle multiple pollutants as this provides a cost-effective solution. P(VI) cryogels with Co, Ni, and Cu NPs were prepared and assessed for degradation of dyes: MB and EY, and 4-nitrophenol (4-NP) reduction in the presence of NaBH_4 in aqueous media (Tercan et al. 2020). It was found that catalytic efficiency varies as $\text{Co} > \text{Cu} > \text{Ni}$ for MB, $\text{Co} > \text{Ni} > \text{Cu}$ for EY, and $\text{Ni} \approx \text{Co} > \text{Cu}$ for 4-NP. Cryogel composites can be successfully used in the simultaneous degradation/reduction of a solution containing two or three contaminants, such as MB and EY, EY and 4-NP, and MB and 4-NP mixtures, and even a mixture of MB, EY, and 4-NP (Table 1.6) (Tercan et al. 2020). The degradation efficiencies of MB, EY, and 4-NP vary for all mixtures depending on the catalyst used with the highest values for p(VI)-CoNPs cryogel.

Loo et al. have prepared PSA-AgNPs cryogel composites for point-of-use water treatment (Loo et al. 2015a, 2013; Loo 2016). The proposed treatment includes the swelling of cryogels in contaminated water, followed by removal by squeezing the water out of the cryogel. PSA-AgNP cryogels could achieve over a 2-log reduction of viable bacteria with minimal Ag release ($<100 \mu\text{g/L}$). They were reusable as there was no significant difference in disinfection efficiency over five working cycles, and they could be compressed multiple times for over 1000 cycles (Loo 2016). It is a compact and easily deployable emergency water treatment technology with simple

Table 1.6 Conversion percentage and TOF values for catalytic degradation/reduction reactions of dyes and 4-NP catalyzed by p(VI)-cryogel composite with Co, Ni, and Cu NPs catalysts (Tercan et al. 2020)

Substrate mixtures	Pollutant	P(VI)-CoNPs		P(VI)-NiNPs		P(VI)-CuNPs	
		Conversion, %	TOF (h ⁻¹)	Conversion, %	TOF (h ⁻¹)	Conversion, %	TOF (h ⁻¹)
MB and EY	MB	91.9	275.7	31.8	95.4	67.2	201.6
	EY	22.9	68.7	20.3	60.9	14.3	42.9
	EY	21.6	64.8	46.1	138.3	17.4	52.2
MB and 4-NP	4-NP	94.7	284.1	93.0	279.0	80.3	240.9
	MB	96.2	288.6	71.4	214.2	87.7	263.1
	4-NP	89.4	268.2	80.6	241.8	24.6	73.8
MB, EY, and 4-NP	MB	94.6	283.8	53.8	161.4	85.3	255.9
	EY	25.4	76.2	45.9	137.7	13.0	39.0
	4-NP	87.6	262.8	83.2	249.6	21.9	65.7

and low-energy operation. A similar treatment can be designed to remove other contaminants.

1.2.3 Assessment of the Safety of Nanocomposite Devices

Nanocomposites facilitate the application of nanoparticles in water and wastewater treatment by creating an external 3D structure that retains the nanoparticles without losing their reactivity. Nevertheless, unintentional leaching of nanoparticles from the nanocomposite structure could cause a secondary pollution problem. Many nanoparticles have shown potential toxic effects on humans, animals, plants, and microbes (Albanese et al. 2012; Sharifi et al. 2012). The release of nanoparticles from nanocomposites during, for example, drinking water treatment could pose a risk to users. Likewise, the accidental release of nanoparticles during wastewater treatment could harm the aquatic life of the water bodies receiving the treated stream (Bundschuh et al. 2018). Therefore, the development of nanocomposites intended for water and wastewater treatment should be accompanied by a thorough assessment of their health and environmental safety. Surprisingly, the risk assessment of such nanocomposite devices is usually overlooked in the scientific literature.

The concern about the risk of nanotechnology has driven the parallel development of reliable methodologies for the evaluation of the health and environmental risk of nanomaterials (Yang et al. 2017; Savage et al. 2019; Schwirn et al. 2020). Moreover, during the last years, several initiatives from international organizations have aimed for the standardization of terminology, methodologies, and data analysis in the toxicological testing of nanomaterials. For example, the OECD recently published a guidance document on aquatic and sediment toxicological testing of nanomaterials (OECD 2020), and the European Commission adopted a regulation that modifies various REACH annexes, introducing nano-specific clarifications and new provisions in the chemical safety assessment, registration information requirements, and downstream user obligations (European 2018). However, the evaluation of the health and environmental risk of nanomaterials in research settings is a matter that remains largely unstandardized due to rapid developments in technologies used for the identification and characterization of nanomaterials and in nanocomposites with new properties and functionalities.

In general, two main characteristics determine the health and environmental risk of nanoparticles: their toxicity and their mobility or fate (Bundschuh et al. 2018). Both characteristics are relevant for the assessment of the safety of newly developed nanocomposites.

1.2.3.1 Assessment of Nanoparticle Leaching from Nanocomposites

The leaching of nanoparticles from nanocomposites into the treated effluent is a primary concern for water treatment applications. The release of bound nanoparticles—either as particles or as dissolved ions—may not only lead to health and environmental risks but also affect the nanocomposite structure, proper functioning, efficiency, and service life. Moreover, for metallic nanoparticles, the release

of particles or dissolved ions could be restricted by specific regulations limiting the concentration of heavy metals in drinking water or discharge effluent. These values vary depending on the location and may be imposed by local, regional, national, or supranational authorities (e.g., US EPA's National Primary Drinking Water Regulations or UE's Drinking Water Directive). However, the lack of standardized leaching tests for devices intended for water and wastewater treatment applications presents some challenges for a reliable risk assessment. Firstly, the leaching of nanoparticles may be affected by pH, temperature, water composition, time, etc. Secondly, the detection of nanoparticles in complex matrices is complicated due to analytical artifacts caused by sample preparation, nanoparticle characteristics (size, aggregation, solubility, etc.), and background compounds.

Multiple techniques have been developed and optimized in the last decades for the identification, measurement, and characterization of natural and engineered nanoparticles in aqueous complex matrices (Tiede et al. 2008; Park et al. 2017). These are either based on the identification particles, dissolved ions, or both. Techniques such as TEM, SEM, DLS, nanoparticle tracking analysis (NTA), or single-particle inductively coupled plasma mass spectrometry (sp-ICP-MS) have been applied for the detection of nanoparticles in wastewater (Westerhoff et al. 2011), sewage effluent (Johnson et al. 2014), surface water (Hadioui et al. 2015), or drinking water (Donovan et al. 2016). However, these techniques are usually time-consuming, relatively expensive, and prone to measurement artifacts (which translates into the need for a rigorous preliminary optimization of measurement protocols tailored for the specific particle and matrix). Although some of these techniques are frequently used for the characterization of nanocomposites (e.g., TEM, SEM, DLS), the drawbacks make them almost absent from the evaluation of nanoparticles released from nanocomposites. Instead, most works base the detection of leached nanoparticles on the measurement of the metals that form those nanoparticles. This is an easy alternative that relies upon the metal analysis through conventional techniques, such as atomic absorption spectroscopy (AAS), inductively coupled plasma optical emission spectroscopy (ICP-OES), or inductively coupled plasma mass spectrometry (ICP-MS), and by which researchers can obtain a quick picture of the potential risk of the nanocomposite. Moreover, metal detection can be complemented with simple size fractionation techniques (e.g., membrane filtration) for discrimination between dissolved ions and particles of different sizes. Table 1.7 shows a summary of research works that included the evaluation of the nanoparticles released from the developed nanocomposites, mainly by measurement of metal ions.

The conditions in which the potential for nanoparticle leaching from the nanocomposite devices is assessed should be representative of the solution chemistry expected during application. Many researchers choose to assess the nanoparticle leaching simultaneously with the experiments of the nanocomposite performance assessment. In this way, both the performance and the risk can be evaluated at the same time. This approach has been used to evaluate the release of Fe from pAAm-based and pHEMA-based macroporous monolithic cryogels with embedded Fe oxide nanoparticles used for As adsorption, proving that the cryogel matrices

Table 1.7 Summary of publications in which the release of nanoparticles from nanocomposites was evaluated. The leaching assessment is described with the highlights of the preparation of the extract, sample pretreatment (if any), and the analytical technique used for elemental measurement

Nanocomposite type and matrix component	Nanoparticle	Application	Nanoparticle/Ion leaching assessment	Reference
<i>Beads</i>				
Polystyrene	$\alpha\text{-Fe}_2\text{O}_3$	As adsorption	<ul style="list-style-type: none"> pH-dependent incubation for 48 h Fe analysis with AAS 	Pan et al. (2017)
Chitosan	Fe_3O_4	As adsorption	<ul style="list-style-type: none"> Beads were shaken in deionized water for 24 h Fe analysis with AAS 	Ayub et al. (2020)
<i>Membranes</i>				
Thiolated poly (vinylidene fluoride)	Ag	Biocidal	<ul style="list-style-type: none"> Membrane pieces incubated for 3 h in deionized water Ag analysis with ICP-OES 	Sharma et al. (2016)
Polyethersulfone	Fe-Ag, MWCNT	Removal of Cr (VI)	<ul style="list-style-type: none"> Membrane pieces sonicated in deionized water Fe, Ag analysis with ICP-OES 	Masheane et al. (2017)
Polyetherimide nanofiber	TiO_2	Water disinfection; photocatalytic degradation of dye	<ul style="list-style-type: none"> Membrane pieces stirred in ultrapure water for 5 days Ti analysis with ICP-MS 	Al-Ghafri et al. (2019)
Poly(lactic-co-glycolic) acid and chitosan nanofiber	TiO_2 , reduced graphene oxide	As photocatalytic oxidation	<ul style="list-style-type: none"> Simultaneously with arsenic oxidation experiments Leaching evaluated over six oxidative cycles Samples diluted with nitric acid and hydrogen peroxide Ti analysis with ICP-MS 	Fausey et al. (2019)
Polyethersulfone	Fe-Cu, MWCNT	Catalytic degradation of 2,4,6-trichlorophenol	<ul style="list-style-type: none"> Simultaneously with dechlorination experiments Permeate 	Dube et al. (2020)

(continued)

Table 1.7 (continued)

Nanocomposite type and matrix component	Nanoparticle	Application	Nanoparticle/Ion leaching assessment	Reference
			<p>samples preconcentrated using nitric acid</p> <ul style="list-style-type: none"> • Cu analysis with ICP-OES 	
Polysulfone	Fe–Ni oxide	Removal of heavy metals and proteins	<ul style="list-style-type: none"> • Membrane pieces stirred in deionized water for 3 days • Fe, Ni analysis with ICP-MS 	Raviya et al. (2020)
Polyethersulfone	Ag, cellulose nanocrystals	Biocidal	<ul style="list-style-type: none"> • Membrane pieces shook in deionized water for ten days • Ag analysis with ICP-OES 	Xu et al. (2020)
<i>Aerogels/Cryogels</i>				
Polyacrylamide and poly(2-hydroxyethyl methacrylate)	α -Fe ₂ O ₃ , Fe ₃ O ₄	As adsorption	<ul style="list-style-type: none"> • Simultaneously with As adsorption experiments • Fe analysis with ICP-OES 	Savina et al. (2011)
Poly(sodium acrylate)	Ag	Biocidal	<ul style="list-style-type: none"> • Immersion in ultrapure water for 24 h • Sample filtered through 0.45 μm • Digestion of total sample • Ag analysis with ICP-OES or ICP-MS 	Loo et al. (2013)
Polyacrylamide	γ -Al ₂ O ₃	As adsorption	<ul style="list-style-type: none"> • Leaching evaluated through a weight loss of the cryogel in the flow-through experiments 	Önnby et al. (2014)
Polyacrylamide	TiO ₂	Pb(II) removal	<ul style="list-style-type: none"> • Leaching evaluated through a weight loss of the cryogel in the flow-through experiments 	Shu et al. (2017)
Chitosan-glutaraldehyde cryogel	In situ formed Pd, Pt	Nitrophenol removal	<ul style="list-style-type: none"> • Leaching of metal nanoparticles from the cryogel • Pd analysis with AAS 	Berillo and Cundy (2018)

(continued)

Table 1.7 (continued)

Nanocomposite type and matrix component	Nanoparticle	Application	Nanoparticle/Ion leaching assessment	Reference
Poly(sodium acrylate)	Zero-valent Fe	Cr removal	<ul style="list-style-type: none"> • Simultaneously with Cr removal experiments • Samples filtered through a 0.45 μm filter • Fe analysis with AAS 	Jia et al. (2018)
Co-allylamine-methacrylic acid and co-allylamine-2-acrylamido-2-methyl-1-propansulfonic acid	Ag_2O , Ag^0	Iodide removal	<ul style="list-style-type: none"> • Shaking for ten days at pH 7 • Ag analysis with AAS 	Baimenov et al. (2020)
Chitosan-tetrametoxypuran cryogel	Au	Nitrophenol removal	<ul style="list-style-type: none"> • Leaching of metal nanoparticles from the cryogel • Au analysis with AAS 	Berillo (2020)
Graphene aerogel	$\alpha\text{-Fe}_2\text{O}_3$	Electro-Fenton organic matter elimination	<ul style="list-style-type: none"> • Simultaneously with Electro-Fenton experiments • Fe analysis with colorimetric method 	Cao et al. (2020)
Polyacrylamide and poly(2-hydroxyethyl methacrylate)	Fe oxides	As adsorption	<ul style="list-style-type: none"> • Simultaneously with As adsorption experiments • Sample acidified • Fe analysis with ICP-OES 	Otero-Gonzalez et al. (2020)

efficiently held the Fe oxide nanoparticles within the 3D structure (Otero-Gonzalez et al. 2020; Savina et al. 2011). Likewise, the release of Ti from a TiO_2 -containing nanofibrous mat was evaluated while testing the nanocomposite for As photocatalytic oxidation, resulting in a significant 2–4% leaching in the first four cycles and decreasing to <1% afterwards (Fausey et al. 2019).

The evaluation of nanoparticle leaching over a range of solution chemistries may be relevant to obtain more information about the potential mechanisms of leaching and improve the nanocomposite properties to avoid leaching. Typically, pH dramatically affects the amount of nanoparticles released from the nanocomposite structure. Low pH values (2.0–4.0) have been proven to increase the dissolution of Fe from a

PSA macroporous cryogel embedded with zero-valent Fe nanoparticles (Jia et al. 2018), which is expected due to the higher dissolution rates of metals in acidic conditions. In contrast, α -Fe₂O₃-polystyrene beads and α -Fe₂O₃-graphene aerogels showed a greater holding capacity of Fe₂O₃ nanoparticles within the nanocomposite structure, as evidenced by low dissolution rates even at acidic pH (Pan et al. 2017; Cao et al. 2020).

Besides the solution chemistry, the properties of the nanocomposite may affect the leaching rate. Among these, the nanoparticle loading in the nanocomposite may significantly affect the risk of nanoparticle leaching. For example, an increment from 0.2% to 0.6% in the loading of TiO₂ nanoparticles into a polyetherimide nanofiber membrane increased the leaching of Ti into solution from an almost undetectable concentration of 0.0002 ppm to 9.7282 ppm (Al-Ghafri et al. 2019). The authors hypothesized that at higher loading rates, the particles agglomerate on the fiber surface rather than integrating into the nanofiber matrix, making them prone to escape when an external force is applied. Moreover, the nanocomposite membranes with higher TiO₂ loading showed poorer mechanical properties, evidenced by lower tensile strength and elongation at break (Al-Ghafri et al. 2019). This example illustrates how the increased risk of nanoparticle leaching may correlate with the inferior performance of the nanocomposite, further supporting the importance of proper characterization during nanocomposite development.

1.2.3.2 Assessment of Nanocomposite Toxicity

The measurements of the released nanoparticles or metal ions are an indication of the potential health and environmental risk of the nanocomposite device. However, a more exhaustive risk assessment should consider the actual toxicity that could derive from the leached particles. The toxicity assessment of nanocomposites should be approached differently depending on the size of the nanocomposite. Two groups of nanocomposites can be differentiated based on their overall size: (i) nanocomposites with size in the nanometer scale; (ii) nanocomposites with a larger size. The first group of nanocomposites is those formed by the structuring of two or more (nano)-materials and a polymeric matrix within the nanometer scale. The small size allows the dispersion of these materials in aqueous media. Therefore, the toxicity evaluation of these nanocomposites can be done analogously as bare nanoparticles (Su 2017). In case that the physicochemical characteristics (e.g., isoelectric point) of the nanocomposite prevent the efficient dispersion under the conditions of interest, the techniques typically used for nanoparticles (such as, sonication, mixing, supplementation of dispersants, and others) may be applied well to enhance the nanocomposite dispersion (Horst et al. 2012; Hartmann et al. 2015).

Classical toxicity assessment methods have been developed and optimized for the evaluation of toxicity of soluble compounds. During the last years, much effort has been put into reliable adaptation for the evaluation of toxicity of nanoparticles (Yang et al. 2017; Savage et al. 2019), which allows their application for nanocomposites that can be efficiently dispersed. However, these methods have limitations to assess the toxicity risk of larger nanocomposites such as beads, membranes, or monolithic hydrogels and cryogels. For obvious reasons, these materials cannot be

Table 1.8 Summary of advantages and disadvantages of the most common approaches used for the assessment of toxicity of nanocomposite devices intended for water treatment

Approach	Advantages	Disadvantages	References
<i>Biofouling/cell attachment</i>	<ul style="list-style-type: none"> • Relevant to test antifouling of membranes <ul style="list-style-type: none"> • The target cell/microorganism directly interacts with the material as a whole • Relevant to test biocompatibility and bactericidal power 	<ul style="list-style-type: none"> • Not all cells are suitable for attached growth <ul style="list-style-type: none"> • Not all composites are suitable for cell attachment 	Sharma et al. (2016)
<i>Toxicity assessment of aqueous leachates/extracts</i>	<ul style="list-style-type: none"> • Relevant for water treatment • Any compound that may be released is taken into account 	<ul style="list-style-type: none"> • Do not test the toxicity of the material itself 	Önnby et al. (2014), Otero-Gonzalez et al. (2020), Busquets et al. (2016)

homogeneously dispersed in aqueous media, preventing an efficient and controllable contact pattern with the target cell.

A few publications have dealt with these limitations in different ways depending on the intended application of the nanodevice (Table 1.8). For example, nanocomposites developed for the reduction of biofouling of filtration membranes are commonly assessed for their biocidal effect by testing the attachment and growth of bacteria on the composite membrane surface. Either a batch or a continuous flow-through approach can be used (Sharma et al. 2016). In the first case, a suspension of bacteria, such as the model *Escherichia coli*, of known concentration (using cell count, or optical density) is incubated with a representative piece of the nanocomposite membrane for a period of time. Alternatively, in a flow-through approach, a bacteria suspension is pumped through the membrane. After a proper period of time, the surface of the membrane is analyzed for bacterial attachment and growth (Sharma et al. 2016). Techniques such as optical, fluorescence, or electron microscopy can be used for the estimation of biofouling on the membrane surface. The flow-through approach is a more realistic representation of the operational conditions that these nanocomposites would endure during their service life. However, cell attachment on the nanocomposites is not always a relevant characteristic for the evaluation of the toxicity risk, for example, when the risk derives from the release of toxic nanoparticles. Additionally, not all cells (either prokaryotic or eukaryotic) are able to attach and grow on surfaces and not all nanocomposite surfaces are suitable to promote cell attachment.

For devices intended for water and wastewater treatment, the main concern is the release of toxic nanoparticles (or ions) into the treated effluent. Therefore, some researchers tested the toxicity of extracts of the nanocomposite as a proxy of the nanodevice toxicity. This approach complements the evaluation of the risk of nanoparticle release from the nanocomposite, as described in the previous section. Additionally, this approach may also indicate if compounds other than nanoparticles

of their ions are released from the device, for example, potentially toxic organic chemicals. The nanocomposite extract can be prepared by passing water through a bed of nanocomposite to simulate the flow-through conditions that the device would encounter in a real application (Önnby et al. 2014; Busquets et al. 2016). This approach has been used to test the safety risk of γ -Al₂O₃-polyacrylamide-based nanocomposite cryogels for arsenic adsorption (Önnby et al. 2014) as well as carbon-poly(vinyl alcohol) cryogel composites for removal of trace organic pollutants (Busquets et al. 2016). In both studies, the effluent percolating through the nanocomposite column was collected and freeze-dried. Then, the lyophilized extract was reconstituted in the cell growth medium and used to dose the target cells for toxicity assessment (human colorectal adenocarcinoma cells Caco-2) (Önnby et al. 2014; Busquets et al. 2016). By performing the pre-lyophilization of the extract samples, the researchers avoided dosing the aqueous extract directly to the cells, which would result in the dilution of both the extract itself and the biological growth medium. However, it is unclear whether the lyophilization may affect other characteristics of the extracts, for example, chemical changes of other organic compounds that may be present or the aggregation of the potentially leached nanoparticles, which could affect their toxicity. Alternatively, the nanocomposite extract can be prepared directly in the biological growth medium (Otero-Gonzalez et al. 2020). In this way, laborious and potentially altering pretreatment of the sample is avoided. However, this approach is less representative of the actual nanodevice operating conditions and may affect the propensity for nanoparticle leaching from the material. Moreover, the nanocomposite may interact with components of the biological medium (for example, by adsorption of medium essential components), which could affect the later toxicity evaluation. In a composite cryogel based on chitosan with AuNP, developed for the accelerated oxidation of aromatic aldehydes to less toxic corresponding aromatic acids in a flow mode, no release of free AuNPs was observed, which was indirectly confirmed by a constant reaction rate over several cycles (Berillo et al. 2014).

The evaluation of toxicity of extracts resembles an increasingly common trend used for the assessment of the efficiency of water remediation. As the chemical complexity of pollutants and their transformation intermediates increases, some researchers tend to evaluate how effective the remediation treatment is in reducing the toxicity of the initial solution. This approach is very relevant to test the efficiency of (photo)catalytic nanodevices for the degradation of complex pollutants such as dyes (Liu et al. 2017) or antibiotics (Wang et al. 2019; Dong et al. 2021; Puga et al. 2020). The (photo)catalytic treatment of such complex chemicals may lead to the formation of toxic degradation intermediates or products. Therefore, many studies evaluate the toxicity of the solution of interest before and after treatment to ensure that reduced toxicity is achieved. While the goal is to evaluate the toxicity of a solution, the results can also indicate whether toxic chemicals may be released from the nanocomposite during treatment.

Despite the great interest in the use of nanocomposite devices for water and wastewater treatment, their safety assessment is usually overlooked. To bring these devices closer to real applications, the following issues should be addressed: (i) more

data on the toxicity of nanocomposites needed as a whole; (ii) more reliable protocols for toxicity evaluation of nanocomposite devices should be developed and validated; and (iii) different conditions of the nanocomposite operation should be considered during risk assessment, including end of life. In fact, regulatory authorities are acknowledging some of these gaps. For example, the recently enacted revised EU Drinking Water Directive recognizes the obligation of national authorities to ensure that materials intended for use in contact with drinking water do not compromise the protection of human health; affect the color, odor, or taste of water; increase the growth of microbes, or leach contaminants into the water (The European Parliament and the Council of the European Union 2020). While such regulations do not specifically apply to nanocomposites, they can be a step forward in the safe development and use of nanocomposites for water and wastewater treatment.

1.3 Bacteria-Based Bioreactors

Bioremediation is the process of purifying water or soils using viable organisms, including fungi, bacteria, plants, warmers, and others that use contaminants as a source of food and energy. Water bodies are natural, efficient bioremediation systems. The bioremediation process is widely used for water treatment in wastewater treatment plants. In most cases, a wastewater treatment plant uses a combination of steps to improve the removal efficiency of pollutants and reduce the cost of treatment. For example, immobilized on a substrate or free suspension of bacteria utilizes toxic contaminants in water or partially metabolizes them to less harmful derivatives that are consumed by other bacteria or microorganisms as a carbon source, so in many cases a consortium of various species is used. This is followed by the stage of removing bacteria from purified water, which can be carried out by physical or biological approaches. The physical approach involves membrane filtration, while the biological approaches use plankton and other organisms that consume bacteria, and then this water is discharged into a body of water with other inhabitants, such as worms or fish that consume plankton. It can be planted with a variety of grasses or other plants that have the unique ability to accumulate heavy metals, harmful and toxic pollutants that have not been entirely removed by bacteria or fungi. Each type of bioremediation process has some limitations due to the extremely high persistence of anthropogenic pollutants or unfavorable bioremediation conditions. It is known that the rate of consumption of a pollutant decreases with a decrease in its concentration; at some limit concentrations, bioaccumulation and metabolism by bacteria are considered to be ineffective from a cost point of view. Therefore, the use of a combination of different plants and wetlands is necessary at the final stage of water purification.

Bioremediation can be carried out both *in situ* and *ex situ*. *In situ* bioremediation is based on the removal of a contaminant without removing contaminated water from the affected area, such as in the event of an oil spill or a chemical plant accident. Since it does not require soil or water movement, it is cheaper, less dusty, and

releases less volatile pollutants compared to ex situ methods. However, it requires the usage of highly resistant and robust immobilized microorganisms for controlled treatment. The most crucial factor in in situ bioremediation is the introduction of oxygen into contaminated soil and water using special equipment for enhanced stimulation of the growth of microorganisms and aerobic digestion of pollutants. In addition, bioremediation can be enhanced by the addition of nutrients (nitrogen and phosphorus fertilizers) to water and soil to stimulate the growth and metabolism of microbes that utilize pollutants.

Ex situ bioremediation is based on removing a layer of contaminated water or soil and recovering it from contaminants outside the affected area. This approach is significantly more expensive as compared to in situ bioremediation. However, this method has several advantages: it provides greater control over the purification process in bioreactors and is less time-consuming. Carrying out ex situ remediation allows creating optimal conditions for activated sludge or other immobilized microorganisms in the bioreactor for more efficient water purification from pollutants. After completion of the remediation process, the water is returned to the environment.

Despite the fact that biological treatment is environmentally friendly and economical in comparison with physicochemical treatment, it does not always work satisfactorily at high or too low concentrations of pollutants. At high concentrations of toxic substances, enzymatic treatment is recognized as a suitable strategy for treatment in mild conditions. However, this requires preliminary sterilization of purified water with chlorine or ozone to remove microorganisms that can destroy many enzymes. Enzymes are unstable in suspension in a free state and therefore must be incorporated into the support to increase the lifetime. To facilitate enzymatic remediation, a process using whole cells as an enzymatic system can be applied, which significantly reduces costs. The immobilized bacteria can be used for a number of technological cycles without loss of activity, which makes it easy to recover and reuse (Dedov et al. 2017). Immobilization in most cases increases the operational stability of bacteria, protecting them from the harmful effects of extreme pH, high concentrations of toxic derivatives, temperature fluctuations, and turbulent flow of the reaction mixture during the bioremediation process (Villegas et al. 2016). As a result, immobilized bacteria are preferred over free, planktonic bacterial cells (Hailei et al. 2016; Partovinia and Rasekh 2018). For example, immobilization of sulfate-reducing bacteria in the filter improved the biological reduction of sulfate to sulfide (Kuo and Shu 2004). Sulfide toxicity in the systems fed with glucose displayed that sulfide starts to inhibit methanogens at 276.4 ppm. The immobilized cells were found to be protected in the filter and therefore withstand high concentrations of dissolved sulfide (448 ppm) and total sulfide (940 ppm), resulting in significantly higher biomass concentrations (13.2–13.5 g VSS/L) to be achieved (Kuo and Shu 2004).

Immobilized cells have shown tremendous potential for purifying a wide range of contaminants, including phenolic compounds, hydrocarbons, propionitrile, organic and inorganic dyes, N,N-dimethylformamide, pyridine, and unwanted nutrients such as nitrogen and phosphorus from wastewater (Alessandrello et al. 2018;

Serebrennikova et al. 2017). The integrated process of assimilation, sorption, and bioremediation is the only responsible mechanism for wastewater treatment using immobilized microorganisms. More research is still required in this area to develop more carefully integrated technologies and make purification efficiency cost-effective (Das and Adholeya 2015).

The bacteria were immobilized on several chemically activated substrates (epoxy, copolymer dimethylacrylamide-acroleine, dextran dialdehyde, carbodiimide activated alginate, pectin, carboxymethylcellulose) (Zaushitsyna et al. 2014); and inert supports such as activated carbon, inorganic metal oxides (clays, aluminosilicates, zeolites, silica gel, ceramics, vermiculite), membranes or porous polymers (Lim et al. 2018). The density of bacteria on a material depends on the structure, pore size, and surface area of the carrier, as well as the nature of the material (hydrophobicity, charge, etc.) and environmental conditions such as ionic strength, the presence of certain trace elements that enhance hydrogen bonds, pH, and temperature. The major difference between cryogels and other porous materials (aerogel, inorganic, and polyurethane foams) of similar pore size is that the former show tissue-like elasticity and flexibility and, in some cases, can withstand deformation without being destroyed or damaged (Plieva and Mattiasson 2008). Below we discuss methods of bacteria immobilization in cryogels and give examples of their application for water clean-up.

1.3.1 Methods for Bacteria Immobilization

Immobilization techniques can be classified as follows: (a) cell attachment and biofilm formation on the substrate (natural, spontaneous, and slow process) (Kuyukina et al. 2009); (b) the immobilization of cells in the bulk of the polymer material during the formation of the carrier (artificially accelerated process) (Choi et al. 2020; Magri et al. 2012), and (c) direct cross-linking of bacterial cells with formation of the porous substrate (Berillo et al. 2019; Al-Jwaid et al. 2018). All three approaches are illustrated in Fig. 1.6.

Using porous support for immobilizing bacteria is beneficial as it provides a large surface area available for the attachment of cells and formation of biofilm (Fig. 1.6a). For example, porous poly(ethylene oxide) (PEO) cryogels were used for the formation of biofilm of KCM R₅ and KCM RG₅ bacteria cultured from xenobiotics polluted environments and tested for phenol biodegrading capability (Satchanska et al. 2009). PEO cryogels provide a nontoxic environment for bacteria and have excellent mechanical properties. Biofilms remained compact on porous and elastic PEO cryogel after aggressive phenol treatment. However, biofilm formation often takes a long time, which is the reason for the main costs and is one of the key limitations of many biotechnological processes using immobilized bacteria (van Wolferen et al. 2018).

Capturing bacteria directly into the bulk of polymeric materials makes it possible to obtain materials with immobilized bacteria in one step (Fig. 1.6b). However, the number of cells, as well as their viability, can be low. It can also create restrictions on

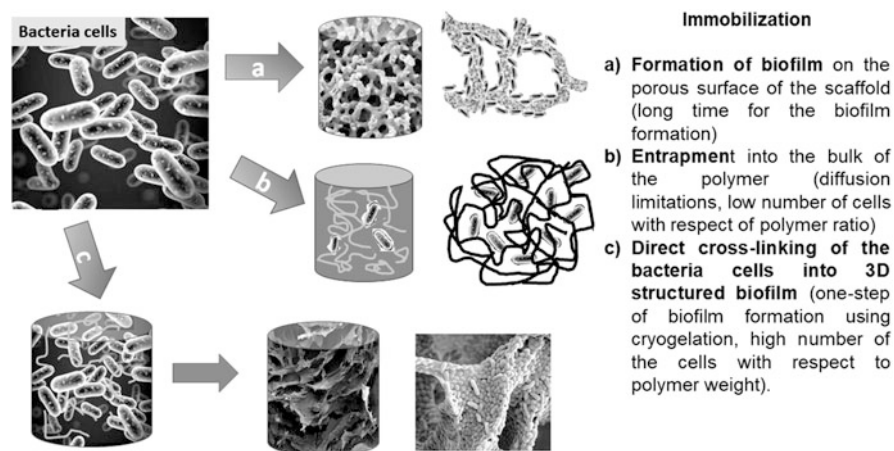


Fig. 1.6 Strategies for bacterial cell immobilization onto scaffold/polymer supports and their benefits and limitations. Figures are adapted from (Al-Jwaied et al. 2018)

the internal diffusion of reagent molecules inside the polymer network and affect cells' activity. The entrapment of bacteria within macromolecules of polyvinyl alcohol (PVA) cryogels was one of the first applications in microbiology for the preparation of biocatalytic systems (Lozinsky and Plieva 1998; Choi et al. 2018). Cryogels with bacterial cells from activated sludge and pre-enriched anammox bacteria were prepared by adding cells to the PVA reaction mixture (Choi et al. 2020). Cryogels were made in the form of a film since it improves the access of microorganisms to physiologically important substrates inside the cryogels, which was significantly limited in cubic or bead type cryogels, the thickness of which (>1.5 mm) is more difficult to control. The viability of microorganisms within the PVA cryogel and the effect of temperature stress was estimated via the activity of immobilized photobacteria (Aleskerova et al. 2017). It was shown that the intensity of bioluminescence of microorganisms significantly depends on the pH of the incubation medium. It was shown that a shift in pH towards acidic values during prolonged incubation of immobilized cells is one of the factors for quenching bioluminescence. The temperature effect was insignificant, and a decrease in the rate of reduction of the flavin substrate of luciferase could be the reason for the quenching of bioluminescence. The consortium of bacteria strains (*Rhodococcus*, *Bacillus*, *Pseudomonas taiwanensis* and *Acinetobacter baumannii*, *Rhodococcus opacus* IEGM 263 or *Rhodococcus Ruber* IEGM 263) entrapped in PVA was applied to widen options of pollutant biodegradation and their concentration range. Additionally, other methods of immobilization for effective purification of industrial waters from polyaromatic hydrocarbons and oil-polluted waters have been investigated (Alessandrello et al. 2018; Serebrennikova et al. 2017).

The most exciting approach of cells immobilization is the formation of cryogels with a minimum of polymer, which is used as a cross-linking agent ("glue") to form three-dimensional structured materials (Fig. 1.6c) (Berillo et al. 2019; Al-Jwaied et al.

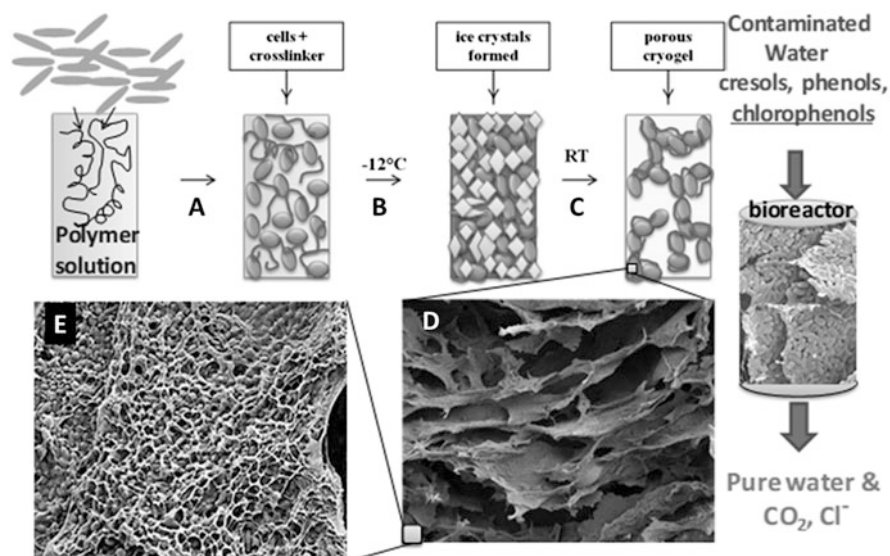


Fig. 1.7 Scheme of preparation of cryogels (a–c), SEM images of bacterial cryogels (d, e), and schematic representation of bioreactor for phenols degradation (on the right). The figure is modified from (Berillo et al. 2019)

2018). This technique allows obtaining a 3D porous scaffold in one step with a high number of immobilized bacteria within 2–3 days and polymer content of 1–2%.

The concept of cryogel preparation based on cells is illustrated in Fig. 1.7 (Berillo et al. 2019). Cryostructuring allows the production of elastic cryogels with a wide range of porosity, morphology, and the ability to adjust mechanical properties of final material (Lozinsky 2018; Lozinsky et al. 2003).

The cell suspension is mixed with activated polymers and frozen to a temperature below the freezing point of the solvent. This leads to freezing of up to 90% of the solvent, while polymers and cells remain in an unfrozen liquid state where bonds between activated polymer and cells are formed (Fig. 1.7). Scanning electron microscopy confirms that cells are bound to each other, forming a thick cell film (walls of the cryogel) which are separated by large pores (Fig. 1.7d, e) (Al-Jwaid et al. 2018). Cryogels with immobilized whole cells of non-viable bacteria were first obtained by linking bacterial cells with GA (Kirsebom et al. 2009). The disadvantage of using GA as a cross-linking agent is that GA can negatively affect the growth and viability of bacterial cells. GA is a small molecule and penetrates cell membranes, which leads to the disruption of cellular metabolism (Zaushitsyna et al. 2014; Al-Jwaid et al. 2018). Therefore, the concentration of GA and other low molecular weight aldehydes or highly reactive precursors used as cross-linking agents requires careful adjustment to achieve a balance between the elasticity and stiffness of the cryogel and the viability of bacterial cells. High molecular weight aldehydes, such as oxidized dextran 40–500 kDa, have been found to be less harmful to microorganisms

(Zaushitsyna et al. 2014; de Alteriis and Scardi 1990; Börner et al. 2014). Thus, in order to reduce damage to bacterial cells during the freezing process, the toxic cross-linker must be replaced with less toxic high molecular weight cross-linkers such as dextran dialdehyde, aldehyde-modified synthetic polymers of PVA (PVA-al), and polyethyleneimine (PEI-al). These polymers were used for crosslinking *Clostridium acetobutylicum* DSM 792 cells. The resulting cryogels were used to produce acetone, ethanol, and butanol, indicating a 2.7-fold increase in production compared to planktonic cells (Börner et al. 2014). The resulting solid elastic cryogel had high porosity with good mass transfer in the butanol production process. The possibility of reusing cryogels 3–5 times in a partially or completely fresh medium confirms the prospects of using cryogels for anaerobic wastewater treatment using related bacterial strains. Conditions of usage of PVA-al and PEI-al in terms of elasticity and water permeability have been optimized using *E. coli* strain with b-Glucosidase activity. Among the tested variants of the two components, it was found that using final concentrations of PEI-al and PVA-al of 0.55% and 0.35%, respectively, resulted in a self-supporting gel with a water permeability of 0.5 ± 0.17 mL/min. The combination of PVA-al and PEI-al resulted in cryogels with 90% β -glucuronidase activity in *Escherichia coli* (*E. coli*) cells, while *E. coli* cross-linked only with GA showed a complete loss of activity (Zaushitsyna et al. 2014).

The toxicity of polymers for various bacterial strains, as well as the effect of freezing conditions on cell viability, can be assessed using the spectrophotometric analysis of MTT (3-(4,5-dimethylthiazol-2-yl)-2,5-diphenyl-tetrazolium bromide) and XTT (2,3-bis-(2-methoxy-4-nitro-5-sulfophenyl)-2H-tetrazolium-5-carboxanilide), a colorimetric assay for the non-radioactive quantification of cellular proliferation, viability, and cytotoxicity (Berillo et al. 2019). Petroff-Hausser Counting Chamber is not applicable for cross-linked cells and counting the number of viable cells. The MTT and XTT tests are based on the cleavage of the yellow tetrazolium ring salt of MTT or XTT to form the violet dye derivative formazan (Fig. 1.8). A decrease in the number of living cells leads to a decrease in the metabolic activity of the test culture. This decrease directly correlates with the amount of violet formazan formed, which is monitored by optical density (Xu et al. 2016; Moss et al. 2008).

For example, the toxicity rating of PVA-al revealed a relatively low level based on MTT assay data, whereas the toxicity of PEI-al was comparable to the baseline positively charged PEI with 25% viable cells (Berillo et al. 2019). The high toxicity of PEI and PEI-al is due to their positive charge and, consequently, high electrostatic adsorption on the negatively charged cell membrane. The mixing of bacterial suspension with the PEI-al solution results in immediate aggregation due to a large number of aldehyde groups. To overcome the toxic effect of PEI-al on bacteria, a combination of PVA-al and PEI-al and a lower concentration of PEI-al can be used. It was found that a high density of cell suspensions does not lead to the formation of cryogels with small pores, and, therefore, does not affect liquid permeability inside the cryogel (Al-Jwaid et al. 2018; Berillo et al. 2019).

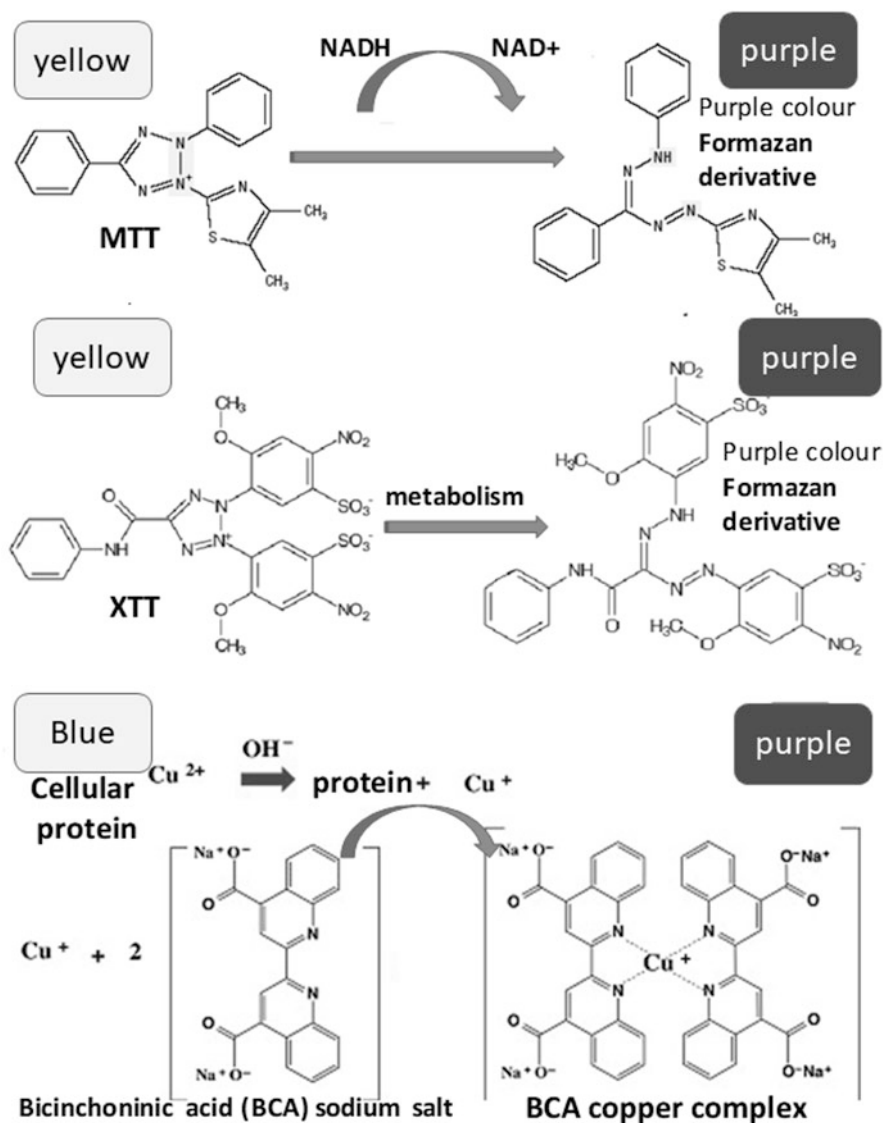


Fig. 1.8 Spectrophotometric assays used for estimation viability of cells and total concentration of proteins

The industrial scale of bioremediation plants requires the purification of large volumes of water, which can be achieved by intensive mechanical stirring or using gas. In most cases, conventional cryogels are fragile during long-term use. To make the cryogels resistant to shear forces during stirring in a bioreactor, they were fabricated inside a protective plastic core (Plieva and Mattiasson 2008). The cores, known as Kaldnes carriers, were initially used as supports for bacterial biofilms for



Fig. 1.9 Kaldnes carriers (at the top) and cryogels with immobilized bacteria prepared in Kaldnes carriers in the syringe (at the bottom)

use in moving bed biofilm reactors used for biological wastewater treatment and have been adapted to enhance the mechanical stability of cryogels (Fig. 1.9) (Rusten et al. 2006; Berillo et al. 2019).

The use of cryogels prepared in plastic carriers is beneficial for conventional water treatment approaches such as activated sludge (Önnby et al. 2012). For example, in the case of bioremediation of the marine environment from oil spills, which requires mainly the management of surface waters, the use of floating materials with low density and high porosity is required, and cryogels can be adapted to that (Al-Jwaid et al. 2018; Berillo et al. 2019).

The immobilization method can affect the productivity of cells as well as the population of viable cells and, as a consequence, the productivity of the biocatalytic or bioremediation process (Berillo et al. 2019). Until recently, the number of viable cells was not quantified by biochemical assays (MTT, XTT, and others), and therefore it is difficult to conduct a proper comparative analysis of different methods of immobilization reported in the literature.

1.3.2 Environmental Applications of Cryogels with Immobilized Bacteria

Cryogels with immobilized bacteria were used to remove several contaminants from water. The first examples include the production of a biocatalyst based mainly on PVA cryogels with immobilized enzymes and whole bacterial cells (Lozinsky et al. 2003). Bioremediation of petroleum-contaminated water was performed in a fluidized-bed bioreactor of *Rhodococcus* bacteria immobilized in PVA and pAAm cryogels and sawdust carrier (Kuyukina et al. 2009). Before the immobilization of cells, the cryogels were hydrophobized to increase contact between the immobilization matrices and *Rhodococcus* cells, which are characterized by a relatively high hydrophobicity of the cell surface. Sawdust showed better catalytic activity and PAH oxidation, which was associated with a large number of immobilized cells. Nitrate removal was demonstrated by using *Thiobacillus denitrificans* (*T. denitrificans*) embedded in PVA cryogel (Zhang et al. 2009). The denitrification efficiency of

free *T. denitrificans* cells and cells immobilized on PVA carriers was compared in batch reactors, demonstrating higher efficiency for PVA carriers. *T. denitrificans* immobilized on a PVA support could remove 75% NO_3^- -N after 12 days of operation, when an initial NO_3^- -N concentration of 700 mg/L was used, and the average denitrification rate of NO_3^- -N was 44 mg (NO_3^- -N)/L day. Bioremediation of o-cresol was studied using acclimatized biomass immobilized in alginate PVA hydrogel and cryogel beads. PVA hydrogel showed a higher removal efficiency of o-cresol compared to PVA cryogel, probably due to cell damage during freezing. However, the cryogel beads had better stability and reusability. The efficiency of PVA biomass cryogel in o-cresol depletion was improved by adding 0.5% powdered activated carbon to the cryogel. The combination of biomass with activated carbon allows the cryogel to run for nine cycles, showing a removal yield of 82% per cycle. No biomass leakage was observed as a result of treatment with 300 ppm o-cresol (See et al. 2015). PVA cryogels were used to encapsulate slow-growing anammox bacteria for deammonification treatment of wastewater (Magri et al. 2012). The cryogels were tested with synthetic and partially nitrified swine wastewater using continuous stirred-tank reactors packed at 20% (w/v). Anammox activity was retained after immobilization of cells and maintained for about 5 months under nonsterile conditions. An ammonium removal efficiency was 95%.

PEO cryogels with immobilized xenobiotics degrading KCM R₅ and KCM RG₅ bacterial strains were evaluated for their ability to remove phenol at concentrations of 300, 400, 600, and 1000 mg/L for 28 days (Satchanska et al. 2009). The PEO-KCM RG₅ cryogel utilized phenol up to 600 mg L⁻¹ for 24 h while the PEO-KCM R₅ was able to utilize phenol at a large concentration, 1000 mg L⁻¹ for 24 h. Long-term treatment with phenol does not affect the compactness and mechanical strength of the created PEO biofilms (Satchanska et al. 2009).

Natural negatively charged polysaccharide alginate cross-linked by Ca²⁺ cryogels illustrated the different performances of cryogel beads with respect to the rate of 4-nitrophenol remediation and beads breakdown (Sam et al. 2021). Such parameters as alginate concentration, number of freezing-thawing cycle effects cells viability. Extreme 4-nitrophenol biodegradation degree of 7.4 mg/L per hour and minimum fracture of 0% was achieved using 8% of PVA, 1.4% of alginate, 3% of calcium chloride, having bead dimensions of 3.6 mm and three cycles for freezing-thawing. At a low initial pollutant concentration of 100 mg/L, the PVA/alginate-activated sludge cryogel beads were reusable without a decline biodegradation rate for 20 consecutive cycles (Sam et al. 2021).

The kinetics of degradation of phenol and its chlorine derivatives using specific phenol-degrading bacterial strains (*Pseudomonas mendocina*, *Rhodococcus koreensis*, and *Acinetobacter radioresistens*) in cryogels were studied (Berillo et al. 2019; Al-Jwaid et al. 2018). The use of bare carbonate buffer allows to degrade of up to 50 ppm of phenol, whereas the usage of minimum salt media buffer allowed to carry out bioremediation of at least up to 300 mg/L. Cryogel can be reused for at least ten cycles of phenol bioremediation in a minimal saline environment without reducing activity. As can be seen from Fig. 1.10, cells multiply over time, reaching 2–7 times the initial concentration (Berillo et al. 2019). Cell activity was retained

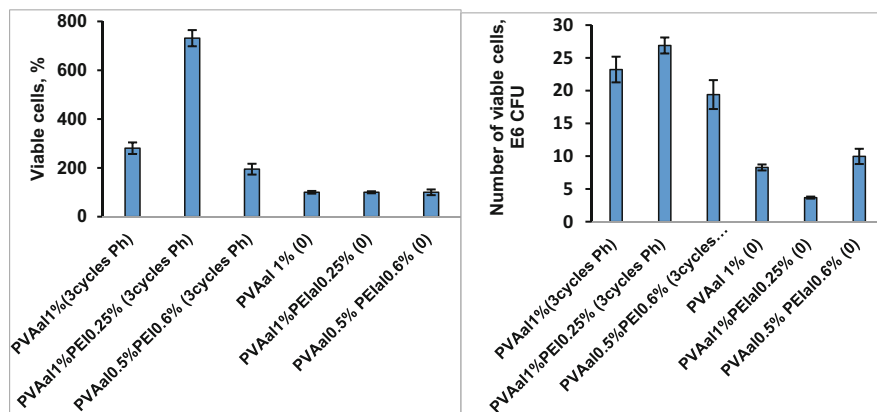


Fig. 1.10 Comparison of the number of cells *Acinetobacter radioresistance* in plastic carriers before/just prepared and after three cycles of bioremediation of phenol (Ph) 50 mg/L with minimal salt medium 40 mL at pH7.1. The viability of cells was studied using MTT assay and is shown in % (on the left) and CFU (on the right)

even after long-term storage at -80°C for 4–6 weeks, demonstrating the possibility of long-term storage of prepared materials and activation on demand, which is very important for transport and industrial applications (Al-Jwaid et al. 2018).

1.3.3 Sensors for Monitoring Water Quality

Online monitoring of water quality for bacteria and heavy metals is an important task. It is known that such organic compounds as phenol, nitrophenol, resorcinol, 1,4-dioxane, nitriles of carboxylic acids and benzotriazole, and methylbenzene, vinyl benzene, cyclohexane, xylene, and benzene can significantly inhibit the bioremediation process by activated sludge. Polar compounds had a more strong inhibitory effect, although nonpolar hydrocarbons had less effect or insignificant inhibition of activated sludge activity only in large concentrations (Inglezakis et al. 2017). Taking into account these circumstances, the quality of wastewater at the plant's entrance should be monitored by the use of whole-cell immobilized biosensors for toxicity assessment of wastewater for phenol and 3-chlorophenol (Philp et al. 2003). Recently, reusable fluorescent ion-sensing cryogels (pAAm-Pyrene) have been reported. This sensor can detect low concentrations of Hg^{2+} (2 $\mu\text{g/L}$) in solutions as well as illustrate an extraordinary selectivity for mercury in the mixture of competitive ions in water (Sahin et al. 2017).

1.4 Concluding Remarks

This chapter demonstrated the potential of cryogel nanocomposites and bacteria-based reactors for removing or breaking down a range of contaminants. The three-dimensional macroporous structure of cryogels provides good support for the immobilization of nanoparticles and bacterial cells, which are easier to handle and remove from the water after treatment. Cryogels come in a variety of shapes and sizes and can be produced in a variety of end-use configurations: particles, monolithic blocks, polymer sheets, discs or columns for through-flow (or flow-over) applications, and within robust plastic carriers for more aggressive physical settings, for example, in settlement tanks. This provides significant flexibility in terms of device configuration. The ability to purify water in a continuous flow mode provides additional benefits for continuous purification and the development of portable water purification devices. However, there are certain areas that need to be addressed before applying cryogels in real conditions. It is necessary to evaluate the effectiveness of cryogel-based devices in comparison with existing technologies. It is important to evaluate the efficiency of removing pollutants, as well as the cost and feasibility of using it on a large scale. Until now, most of the research has been done in a laboratory setting. Fewer reports investigate the performance of cryogel devices in real water and when handling wastewater samples. To fill the gap between basic research and practical applications, it is necessary to focus on the potential practical applications of cryogels in potable reuse water systems.

The production of cryogels is associated with additional costs: materials (polymer and nanoparticles) and the cost of synthesis (creation and maintenance of cryogenic conditions). While the cost of using cryogel for biomedical applications can be justified by the cost of current treatment and the lower amount of materials required for it, this is not the case for environmental applications. For environmental applications, we are looking for a cost-effective approach that will compete with the current one, where activated carbon or other cheap material is used. The additional cost of using cryogel-based devices can be justified by improved water treatment, such as the ability to deal with particularly persistent pollutants and harmful chemicals that cannot be removed with existing approaches. Based on current research and assessment of small volume cryogels, they can be used in a tap or small-scale treatment plants application, as the wastewater treatment plant requires a larger volume and very high flow rates. Scaling techniques to match industrial levels will be required.

To ensure water safety, the use of nanocomposite cryogel devices requires an understanding of environmental and health standards. Thus, to be able to use new technology, it must undergo a risk assessment and a health and safety assessment to reduce the potential risks of the technology itself. More assessment of use on nanoparticle-based devices needs to be done. In addition, the toxicity and health risks of decomposition by-products must be assessed appropriately. Overall, cryogels represent a promising alternative to existing materials for developing new approaches to purifying water from new emerging pollutants, and we believe that

cryogel-based devices will enter the market in the future to provide clean water to the public.

Acknowledgments Dr Savina acknowledges the Royal Society International Exchanges 2019 Cost Share scheme (grant IECR2\192043) for support and Prof E. S. Lokteva for valuable discussion of the current persistent organic pollutants (POPs) problem and the use of NPs as a potential solution.

References

- Albanese A, Tang PS, Chan WCW (2012) The effect of nanoparticle size, shape, and surface chemistry on biological systems. In: Yarmush ML (ed) *Annual Review of Biomedical Engineering*, vol 14. Annual Reviews, Palo Alto, pp 1–16
- Aleskerova LE, Alenina KA, Efremenko EN, Ismailov AD (2017) The factor stabilizing the bioluminescence of PVA-immobilized photobacteria. *Microbiology* 86(2):218–224. <https://doi.org/10.1134/s0026261717020047>
- Alessandro MJ, Tomás MSJ, Isaac P, Vullo DL, Ferrero A (2018) Use of immobilized biomass as low-cost technology for bioremediation of pahs contaminated sites. In: Fuentes MS, Colin VL, Saez JM (eds) *Strategies for bioremediation of organic and inorganic pollutants*. CRC Press, pp 67–81
- Al-Ghafri B, Lau WJ, Al-Abri M, Goh PS, Ismail AF (2019) Titanium dioxide-modified polyetherimide nanofiber membrane for water treatment. *J Water Process Eng* 32:9. <https://doi.org/10.1016/j.jwpe.2019.100970>
- Al-Hussain SA, Ezzat AO, Gaffer AK, Atta AM (2018) Removal of organic water pollutant using magnetite nanomaterials embedded with ionic copolymers of 2-acrylamido-2-methylpropane sodium sulfonate cryogels. *Polymer Int* 67(2):166–177. <https://doi.org/10.1002/pi.5492>
- Al-Jwaid AK, Berillo D, Savina IN, Cundy AB, Caplin JL (2018) One-step formation of three-dimensional macroporous bacterial sponges as a novel approach for the preparation of bioreactors for bioremediation and green treatment of water. *RSC Adv* 8(54):30,813–30,824
- de Alteriis E, Scardi V (1990) Oxidized starch as a hardening agent in the gelatin-immobilization of living yeast-cells. *Starch-Starke* 42(2):57–60. <https://doi.org/10.1002/star.19900420208>
- Andrabi SM, Tiwari J, Singh S, Sarkar J, Verma N, Kumar A (2016) Supermacroporous hybrid polymeric cryogels for efficient removal of metallic contaminants and microbes from water. *Int J Polym Mater Polym Biomater* 65(12):636–645. <https://doi.org/10.1080/00914037.2016.1157795>
- Atta AM, Al-Lohedan HA, Tawfeek AM, Ahmed MA (2018) In situ preparation of magnetic Fe₃O₄.Cu₂O.Fe₃O₄/cryogel nanocomposite powder via a reduction-coprecipitation method as adsorbent for methylene blue water pollutant. *Polymer Int* 67(7):925–935. <https://doi.org/10.1002/pi.5582>
- Ayub A, Raza ZA, Majeed MI, Tariq MR, Irfan A (2020) Development of sustainable magnetic chitosan biosorbent beads for kinetic remediation of arsenic contaminated water. *Int J Biol Macromol* 163:603–617. <https://doi.org/10.1016/j.ijbiomac.2020.06.287>
- Baimenov AZ, Berillo DA, Inglezakis VJ (2020) Cryogel-based Ag degrees/Ag₂O nanocomposites for iodide removal from water. *J Mol Liq* 299:13. <https://doi.org/10.1016/j.molliq.2019.112134>
- Berillo D (2020) Gold nanoparticles incorporated into cryogel walls for efficient nitrophenol conversion. *J Clean Prod* 247:12. <https://doi.org/10.1016/j.jclepro.2019.119089>
- Berillo D, Cundy A (2018) 3D-macroporous chitosan-based scaffolds with in situ formed Pd and Pt nanoparticles for nitrophenol reduction. *Carbohydr Polym* 192:166–175. <https://doi.org/10.1016/j.carbpol.2018.03.038>

- Berillo D, Mattiasson B, Kirsebom H (2014) Cryogelation of chitosan using noble-metal ions: in situ formation of nanoparticles. *Biomacromolecules* 15(6):2246–2255. <https://doi.org/10.1021/bm5003834>
- Berillo DA, Caplin JL, Cundy AB, Savina IN (2019) A cryogel-based bioreactor for water treatment applications. *Water Res* 153:324–334
- Börner RA, Zaushitsyna O, Berillo D, Scaccia N, Mattiasson B, Kirsebom H (2014) Immobilization of *Clostridium acetobutylicum* DSM 792 as macroporous aggregates through cryogelation for butanol production. *Process Biochem* 49(1):10–18. <https://doi.org/10.1016/j.procbio.2013.09.027>
- Bundschuh M, Filser J, Luderwald S, McKee MS, Metreveli G, Schaumann GE, Schulz R, Wagner S (2018) Nanoparticles in the environment: where do we come from, where do we go to? *Environ Sci Eu* 30:17. <https://doi.org/10.1186/s12302-018-0132-6>
- Busquets R, Ivanov AE, Mbundi L, Horberg S, Kozynchenko OP, Cragg PJ, Savina IN, Whitby RLD, Mikhalovsky SV, Tennison SR, Jungvid H, Cundy AB (2016) Carbon-cryogel hierarchical composites as effective and scalable filters for removal of trace organic pollutants from water. *J Environ Manage* 182:141–148. <https://doi.org/10.1016/j.jenvman.2016.07.061>
- Cao XL, Jiang DM, Huang MY, Pan J, Lin JJ, Chan W (2020) Iron oxide nanoparticles wrapped in graphene aerogel composite: Fabrication and application in electro-fenton at a Wide pH. *Colloids Surf A Physicochem Eng Aspects* 587:12. <https://doi.org/10.1016/j.colsurfa.2019.124269>
- Choi M, Cho K, Lee S, Chung YC, Park J, Bae H (2018) Effective seeding strategy using flat type poly (vinyl alcohol) cryogel for anammox enrichment. *Chemosphere* 205:88–97. <https://doi.org/10.1016/j.chemosphere.2018.04.055>
- Choi, M., R. Chaudhary, M. Lee, J. Kim, K. Cho, Y. C. Chung, H. Bae, and J. Park. 2020. "Enhanced selective enrichment of partial nitrification and anammox bacteria in a novel two-stage continuous flow system using flat-type poly (vinylalcohol) cryogel films." *Bioresour Technol* 300:9. doi: <https://doi.org/10.1016/j.biortech.2019.122546>.
- Das M, Adholeya A (2015) Potential uses of immobilized bacteria, fungi, algae, and their aggregates for treatment of organic and inorganic pollutants in wastewater. In: Ahuja S, DeAndrade JB, Dionysiou DD, Hristovski KD, Loganathan BG (eds) *Water Challenges and Solutions on a Global Scale*. Amer Chemical Soc, Washington, pp 319–337
- Dedov AG, Ivanova EA, Sandzhieva DA, Lobakova ES, Kashcheeva PB, Kirpichnikov MP, Ishkov AG, Buznik VM (2017) New materials and ecology: biocomposites for aquatic remediation. *Theor Foundations Chem Eng* 51(4):617–630. <https://doi.org/10.1134/S0040579517040042>
- Dong SY, Xia LJ, Chen XY, Cui LF, Zhu W, Lu ZS, Sun JH, Fan MH (2021) Interfacial and electronic band structure optimization for the adsorption and visible-light photocatalytic activity of macroscopic ZnSnO₃/ graphene aerogel. *Composites Part B Eng* 215:11. <https://doi.org/10.1016/j.compositesb.2021.108765>
- Donovan AR, Adams CD, Ma YF, Stephan C, Eichholz T, Shi HL (2016) Single particle ICP-MS characterization of titanium dioxide, silver, and gold nanoparticles during drinking water treatment. *Chemosphere* 144:148–153. <https://doi.org/10.1016/j.chemosphere.2015.07.081>
- Dube ST, Moutloali RM, Malinga SP (2020) Hyperbranched polyethyleneimine/multi-walled carbon nanotubes polyethersulfone membrane incorporated with Fe-Cu bimetallic nanoparticles for water treatment. *J Environ Chem Eng* 8(4):17. <https://doi.org/10.1016/j.jece.2020.103962>
- European (2018) Commission. Commission Regulation (EU) 2018/1881 of 3 December 2018 Amending Regulation (EC) No 1907/2006 of the European Parliament and of the Council on the Registration, Evaluation, Authorisation, and Restriction of Chemicals (REACH) as Regards Annexes I, III, VI, V
- Fausey CL, Zucker I, Shaulsky E, Zimmerman JB, Elimelech M (2019) Removal of arsenic with reduced graphene oxide-TiO₂-enabled nanofibrous mats. *Chem Eng J* 375:11. <https://doi.org/10.1016/j.cej.2019.122040>

- General Assembly of United Nation A/70/L.1 (2015) Transforming our world: the 2030 agenda for sustainable development. United Nations. <https://sdgs.un.org/publications/transforming-our-world-2030-agenda-sustainable-development-17981>
- Ghadimi M, Zangenehtabar S, Homaeigohar S (2020) An overview of the water remediation potential of nanomaterials and their ecotoxicological impacts. *Water* 12(4):23. <https://doi.org/10.3390/w12041150>
- Gun'ko VM, Savina IN, Mikhailovsky SV (2013) Cryogels: morphological, structural and adsorption characterisation. *Adv Colloid Interface Sci* 187:1–46
- Gun'ko VM, Savina IN, Mikhailovsky SV (2017) Properties of water bound in hydrogels. *Gels* 3(4): 30. <https://doi.org/10.3390/gels3040037>
- Hadioui M, Merdzan V, Wilkinson KJ (2015) Detection and characterization of ZnO nanoparticles in surface and waste waters using single particle ICPMS. *Environ Sci Technol* 49(10): 6141–6148. <https://doi.org/10.1021/acs.est.5b00681>
- Hailei W, Ping L, Qin Y, Hui Y (2016) Removal of phenol in phenolic resin wastewater by a novel biomaterial: the *Phanerochaete chrysosporium* pellet containing chlamydo-spore-like cells. *Appl Microbiol Biotechnol* 100(11):5153–5164. <https://doi.org/10.1007/s00253-016-7353-7>
- Hartmann NB, Jensen KA, Baun A, Rasmussen K, Rauscher H, Tantra R, Cupi D, Gilliland D, Pianella F, Sintes JMR (2015) Techniques and protocols for dispersing nanoparticle powders in aqueous media-is there a rationale for harmonization? *J Toxicol Environ Health Part B Crit Rev* 18(6):299–326. <https://doi.org/10.1080/10937404.2015.1074969>
- Horst AM, Ji ZX, Holden PA (2012) Nanoparticle dispersion in environmentally relevant culture media: a TiO₂ case study and considerations for a general approach. *J Nanopart Res* 14(8):14. <https://doi.org/10.1007/s11051-012-1014-2>
- Inal M, Erduran N, Gokgoz M (2021) The dye adsorption and antibacterial properties of composite polyacrylamide cryogels modified with ZnO. *J Industrial Eng Chem* 98:200–210. <https://doi.org/10.1016/j.jiec.2021.04.001>
- Inglezakis VJ, Kudarova A, Tarassov D, Jetybayeva A, Myngtay Y, Zhalmuratova D, Nurmukhambetov D (2017) Inhibitory effects of polar and non-polar organic substances on activated sludge activity. *Desalination Water Treatment* 91:185–191. <https://doi.org/10.5004/dwt.2017.20783>
- Jia ZZ, Shu YH, Huang RL, Liu JG, Liu LL (2018) Enhanced reactivity of nZVI embedded into supermacroporous cryogels for highly efficient Cr(VI) and total Cr removal from aqueous solution. *Chemosphere* 199:232–242. <https://doi.org/10.1016/j.chemosphere.2018.02.021>
- Johnson AC, Jurgens MD, Lawlor AJ, Cisowska I, Williams RJ (2014) Particulate and colloidal silver in sewage effluent and sludge discharged from British wastewater treatment plants. *Chemosphere* 112:49–55. <https://doi.org/10.1016/j.chemosphere.2014.03.039>
- Khin MM, Nair AS, Babu VJ, Murugan R, Ramakrishna S (2012) A review on nanomaterials for environmental remediation. *Energ Environ Sci* 5(8):8075–8109. <https://doi.org/10.1039/c2ee21818f>
- Kirsebom H, Mattiasson B, Galaev IY (2009) Building macroporous materials from microgels and microbes via one-step cryogelation. *Langmuir* 25(15):8462–8465. <https://doi.org/10.1021/la9006857>
- Kudaibergenov SE (2019) Physicochemical, complexation and catalytic properties of polyampholyte cryogels. *Gels* 5(1):22. <https://doi.org/10.3390/gels5010008>
- Kudaibergenov S, Daultbekova M, Toletay G, Kabdrakhmanova S, Seilkhanov T, Abdullin K (2018) Hydrogenation of p-nitrobenzoic acid by gold and palladium nanoparticles immobilized within macroporous amphoteric cryogels in aqueous solution. *J Inorg Organometallic Polymers Mater* 28(6):2427–2438. <https://doi.org/10.1007/s10904-018-0930-8>
- Kumar PS, Önnby L, Kirsebom H (2013) Arsenite adsorption on cryogels embedded with iron-aluminium double hydrous oxides: possible polishing step for smelting wastewater? *J Hazard Mater* 250:469–476. <https://doi.org/10.1016/j.jhazmat.2013.02.022>

- Kumar PS, Önnby L, Kirsebom H (2014) Reversible in situ precipitation: a flow-through approach for coating macroporous supports with metal hydroxides. *J Mater Chem A* 2(4):1076–1084. <https://doi.org/10.1039/c3ta13307a>
- Kumar PS, Flores RQ, Sjøstedt C, Önnby L (2016) Arsenic adsorption by iron-aluminium hydroxide coated onto macroporous supports: Insights from X-ray absorption spectroscopy and comparison with granular ferric hydroxides. *J Hazard Mater* 302:166–174. <https://doi.org/10.1016/j.jhazmat.2015.09.065>
- Kuo WC, Shu TY (2004) Biological pre-treatment of wastewater containing sulfate using anaerobic immobilized cells. *J Hazard Mater* 113(1-3):147–155. <https://doi.org/10.1016/j.jhazmat.2004.05.033>
- Kurozumi M, Yano Y, Kiyoyama S, Kumar A, Shiomori K (2015) Adsorption properties of arsenic (V) by polyacrylamide cryogel containing iron hydroxide oxide particles prepared by 'in situ' method. *Resour Process* 62(1):17–23. <https://doi.org/10.4144/rpsj.62.17>
- Kuyukina MS, Ivshina IB, Serebrennikova MK, Krivorutchko AB, Podorozhko EA, Ivanov RV, Lozinsky VI (2009) Petroleum-contaminated water treatment in a fluidized-bed bioreactor with immobilized *Rhodococcus* cells. *Int Biodeter Biodegr* 63(4):427–432. <https://doi.org/10.1016/j.ibiod.2008.12.001>
- Lim J-W, Zaid HFM, Isa MH, Wen-Da O, Adnan R, Bashir MJK, Kiatkittipong W, Wang DK (2018) Shielding immobilized biomass cryogel beads with powdered activated carbon for the simultaneous adsorption and biodegradation of 4-chlorophenol. *J Clean Prod* 205:828–835. <https://doi.org/10.1016/j.jclepro.2018.09.153>
- Liu YY, Liu XM, Zhao YP, Dionysiou DD (2017) Aligned alpha-FeOOH nanorods anchored on a graphene oxide-carbon nanotubes aerogel can serve as an effective Fenton-like oxidation catalyst. *Appl Catal B Environ* 213:74–86. <https://doi.org/10.1016/j.apcatb.2017.05.019>
- Loo, Siew Leng. 2016. "Superabsorbent cryogels decorated with silver nanoparticles as a novel technology for emergency point-of-use water treatment."
- Loo SL, Fane AG, Lim TT, Krantz WB, Liang YN, Liu X, Hu X (2013) Superabsorbent cryogels decorated with silver nanoparticles as a novel water technology for point-of-use disinfection. *Environ Sci Technol* 47(16):9363–9371. <https://doi.org/10.1021/es401219s>
- Loo SL, Krantz WB, Fane AG, Gao YB, Lim TT, Hu X (2015a) Bactericidal mechanisms revealed for rapid water disinfection by superabsorbent cryogels decorated with silver nanoparticles. *Environ Sci Technol* 49(4):2310–2318. <https://doi.org/10.1021/es5048667>
- Loo SL, Krantz WB, Fane AG, Hu X, Lim TT (2015b) Effect of synthesis routes on the properties and bactericidal activity of cryogels incorporated with silver nanoparticles. *RSC Adv* 5(55):44626–44635. <https://doi.org/10.1039/c5ra08449k>
- Lozinsky VI (2018) Cryostructuring of polymeric systems. 50.† Cryogels and cryotropic gel-formation: terms and definitions. *Gels* 4(3):77
- Lozinsky VI (2020) Cryostructuring of polymeric systems. 55. Retrospective view on the more than 40 years of studies performed in the annesmeyanov institute of organoelement compounds with respect of the cryostructuring processes in polymeric systems. *Gels* 6(3):59. <https://doi.org/10.3390/gels6030029>
- Lozinsky VI, Plieva FM (1998) Poly(vinyl alcohol) cryogels employed as matrices for cell immobilization. 3. Overview of recent research and developments. *Enzyme Microb Technol* 23(3-4):227–242. [https://doi.org/10.1016/s0141-0229\(98\)00036-2](https://doi.org/10.1016/s0141-0229(98)00036-2)
- Lozinsky VI, Galaev IY, Plieva FM, Savina IN, Jungvid H, Mattiasson B (2003) Polymeric cryogels as promising materials of biotechnological interest. *Trends Biotechnol* 21(10):445–451
- Magri A, Vanotti MB, Szogi AA (2012) Anammox sludge immobilized in polyvinyl alcohol (PVA) cryogel carriers. *Bioresour Technol* 114:231–240. <https://doi.org/10.1016/j.biortech.2012.03.077>
- Masheane ML, Nthunya LN, Malinga SP, Nxumalo EN, Mamba BB, Mhlanga SD (2017) Synthesis of Fe-Ag/f-MWCNT/PES nanostructured-hybrid membranes for removal of Cr(VI) from water. *Sep Purif Technol* 184:79–87. <https://doi.org/10.1016/j.seppur.2017.04.018>

- Moss BJ, Kim Y, Nandakumar MP, Marten MR (2008) Quantifying metabolic activity of filamentous fungi using a colorimetric XTT assay. *Biotechnol Prog* 24(3):780–783. <https://doi.org/10.1021/bp070334t>
- OECD (2020) Guidance document on aquatic and sediment toxicological testing of nanomaterials. Series on testing and assessment.
- Önnby L, Pakade V, Mattiasson B, Kirsebom H (2012) Polymer composite adsorbents using particles of molecularly imprinted polymers or aluminium oxide nanoparticles for treatment of arsenic contaminated waters. *Water Res* 46(13):4111–4120. <https://doi.org/10.1016/j.watres.2012.05.028>
- Önnby L, Svensson C, Mbundi L, Busquets R, Cundy A, Kirsebom H (2014) gamma-Al₂O₃-based nanocomposite adsorbents for arsenic(V) removal: Assessing performance, toxicity and particle leakage. *Sci Total Environ* 473:207–214. <https://doi.org/10.1016/j.scitotenv.2013.12.020>
- Önnby L, Harald K, Nges IA (2015) Cryogel-supported titanate nanotubes for waste treatment: Impact on methane production and bio-fertilizer quality. *J Biotechnol* 207:58–66. <https://doi.org/10.1016/j.jbiotec.2015.05.014>
- Otero-Gonzalez L, Mikhalevsky SV, Vaclavikova M, Trenikhin MV, Cundy AB, Savina IN (2020) Novel nanostructured iron oxide cryogels for arsenic (As(III)) removal. *J Hazard Mater* 381:10. <https://doi.org/10.1016/j.jhazmat.2019.120996>
- Palani G, Arputhalatha A, Kannan K, Lakkaboyana SK, Hanafiah MM, Kumar V, Marella RK (2021) Current trends in the application of nanomaterials for the removal of pollutants from industrial wastewater treatment-a review. *Molecules* 26(9):16. <https://doi.org/10.3390/molecules26092799>
- Pan SY, Zhang X, Qian JS, Lu Z, Hua M, Cheng C, Pan BC (2017) A new strategy to address the challenges of nanoparticles in practical water treatment: mesoporous nanocomposite beads via flash freezing. *Nanoscale* 9(48):19154–19161. <https://doi.org/10.1039/c7nr06980d>
- Park CM, Chu KH, Her N, Jang M, Baalousha M, Heo J, Yoon Y (2017) Occurrence and removal of engineered nanoparticles in drinking water treatment and wastewater treatment processes. *Separation Purification Rev* 46(3):255–272. <https://doi.org/10.1080/15422119.2016.1260588>
- Partovinia A, Rasekh B (2018) Review of the immobilized microbial cell systems for bioremediation of petroleum hydrocarbons polluted environments. *Crit Rev Environ Sci Technol* 48(1): 1–38. <https://doi.org/10.1080/10643389.2018.1439652>
- Philp JC, Balmand S, Hajto E, Bailey MJ, Wiles S, Whiteley AS, Lilley AK, Hajto J, Dunbar SA (2003) Whole cell immobilised biosensors for toxicity assessment of a wastewater treatment plant treating phenolics-containing waste. *Anal Chim Acta* 487(1):61–74. [https://doi.org/10.1016/s0003-2670\(03\)00358-1](https://doi.org/10.1016/s0003-2670(03)00358-1)
- Plieva FM, Mattiasson B (2008) Macroporous gel particles as novel sorbent materials: rational design. *Indust Eng Chem Research* 47(12):4131–4141. <https://doi.org/10.1021/ie071406o>
- Puga A, Rosales E, Pazos M, Sanroman MA (2020) Prompt removal of antibiotic by adsorption/electro-Fenton degradation using an iron-doped perlite as heterogeneous catalyst. *Process Saf Environ Protect* 144:100–110. <https://doi.org/10.1016/j.psep.2020.07.021>
- Raviya MR, Gauswami MV, Raval HD (2020) A novel Polysulfone/Iron-Nickel oxide nanocomposite membrane for removal of heavy metal and protein from water. *Water Environ Res* 92(11):1990–1998. <https://doi.org/10.1002/wer.1356>
- Rusten B, Eikebrokk B, Ulgenes Y, Lygren E (2006) Design and operations of the Kaldnes moving bed biofilm reactors. *Aquacult Eng* 34(3):322–331. <https://doi.org/10.1016/j.aquaeng.2005.04.002>
- Sadegh H, Ali GAM, Gupta VK, Makhlof ASH, Shahyari-Ghoshekandi R, Nadagouda MN, Sillanpaa M, Megiel E (2017) The role of nanomaterials as effective adsorbents and their applications in wastewater treatment. *J Nanostruct Chem* 7(1):1–14. <https://doi.org/10.1007/s40097-017-0219-4>
- Sahin ZM, Alimli D, Tonta MM, Kose ME, Yilmaz F (2017) Highly sensitive and reusable mercury (II) sensor based on fluorescence quenching of pyrene moiety in polyacrylamide-based cryogel. *Sens Actuators B* 242(C):362–368. <https://doi.org/10.1016/j.snb.2016.11.048>

- Sahiner N, Demirci S (2019) The use of M@p(4-VP) and M@p (VI) (M:Co, Ni, Cu) cryogel catalysts as reactor in a glass column in the reduction of p-nitrophenol to p-aminophenol under gravity. *Asia Pacific J Chem Eng* 14(3):12. <https://doi.org/10.1002/apj.2305>
- Sahiner N, Seven F (2014) The use of superporous p(AAc (acrylic acid)) cryogels as support for Co and Ni nanoparticle preparation and as reactor in H-2 production from sodium borohydride hydrolysis. *Energy* 71:170–179. <https://doi.org/10.1016/j.energy.2014.04.031>
- Sahiner N, Yildiz S (2014) Preparation of superporous poly(4-vinyl pyridine) cryogel and their templated metal nanoparticle composites for H-2 production via hydrolysis reactions. *Fuel Process Technol* 126:324–331. <https://doi.org/10.1016/j.fuproc.2014.05.025>
- Sahiner N, Demirci S, Sahiner M, Yilmaz S, Al-Lohedan H (2015a) The use of superporous p (3-acrylamidopropyl)trimethyl ammonium chloride cryogels for removal of toxic arsenate anions. *J Environ Manage* 152:66–74. <https://doi.org/10.1016/j.jenvman.2015.01.023>
- Sahiner N, Yildiz S, Sahiner M, Issa ZA, Al-Lohedan H (2015b) Macroporous cryogel metal nanoparticle composites for H-2 generation from NaBH₄ hydrolysis in seawater. *Appl Surf Sci* 354:388–396. <https://doi.org/10.1016/j.apsusc.2015.04.183>
- Sahiner N, Seven F, Al-Lohedan H (2015c) Super-fast hydrogen generation via super porous Q-P (VI)-M cryogel catalyst systems from hydrolysis of NaBH₄. *Int J Hydrogen Energy* 40(13): 4605–4616. <https://doi.org/10.1016/j.ijhydene.2015.02.049>
- Sahiner N, Seven F, Al-lohedan H (2015d) Superporous cryogel-M (Cu, Ni, and Co) composites in catalytic reduction of toxic phenolic compounds and dyes from wastewaters. *Water Air Soil Pollut* 226(4):12. <https://doi.org/10.1007/s11270-014-2247-8>
- Sahiner N, Demirci S, Sahiner M, Yilmaz S (2016) Application of superporous magnetic cationic cryogels for persistent chromate (toxic chromate and dichromate) uptake from aqueous environments. *J Appl Polym Sci* 133(20):10. <https://doi.org/10.1002/app.43438>
- Sam SP, Adnan R, Ng SL (2021) Statistical optimization of immobilization of activated sludge in PVA/alginate cryogel beads using response surface methodology for p-nitrophenol biodegradation. *J Water Process Eng* 39:13. <https://doi.org/10.1016/j.jwpe.2020.101725>
- Satchanska G, Topalova Y, Dimkov R, Petrov P, Tsvetanov C, Selenska-Pobell S, Gorbovskaya A, Bogdanov V, Golovinsky E (2009) Phenol biodegradation by two xenobiotics-tolerant bacteria immobilized in polyethylene oxide cryogels. *Comptes Rendus De L Academie Bulgare Des Sciences* 62(8):957–964
- Savage DT, Hilt JZ, Dziubla TD (2019) In vitro methods for assessing nanoparticle toxicity. *Methods Mol Biol* (Clifton, NJ) 1894:1–29. https://doi.org/10.1007/978-1-4939-8916-4_1
- Savina, I, and I Galaev. 2016. "3 Production of Synthetic Cryogels and the Study of Porosity Thereof." *Supermacroporous Cryogels: Biomedical and Biotechnological Applications*:91.
- Savina IN, Tomlins PE, Mikhailovsky SV, Galaev IY (2009) Characterization of macroporous gels. In: *Macroporous Polymers: Production Properties and Biotechnological/Biomedical Applications*. CRC Press Boca Raton, FL, pp 211–235
- Savina IN, English CJ, Whitby RLD, Zheng Y, Leistner A, Mikhailovsky SV, Cundy AB (2011) High efficiency removal of dissolved As (III) using iron nanoparticle-embedded macroporous polymer composites. *J Hazard Mater* 192(3):1002–1008
- Savina IN, Shevchenko RV, Allan IU, Illsley M, Mikhailovsky SV (2016a) 6 Cryogels in Regenerative Medicine. *Supermacroporous Cryogels Biomed Biotechnol Appl*:177
- Savina IN, Ingavle GC, Cundy AB, Mikhailovsky SV (2016b) A simple method for the production of large volume 3D macroporous hydrogels for advanced biotechnological, medical and environmental applications. *Sci Rep* 6:21154. <https://doi.org/10.1038/srep21154>
- Savina IN, Zoughaib M, Yergeshov AA (2021) Design and assessment of biodegradable macroporous cryogels as advanced tissue engineering and drug carrying materials. *Gels* 7(3). <https://doi.org/10.3390/gels7030079>
- Schwirn K, Voelker D, Galert W, Quik J, Tietjen L (2020) Environmental Risk Assessment of Nanomaterials in the Light of New Obligations Under the REACH Regulation: Which Challenges Remain and How to Approach Them? *Integr Environ Assess Manag* 16(5): 706–717. <https://doi.org/10.1002/ieam.4267>

- See S, Lim PE, Lim JW, Seng CE, Adnan R (2015) Evaluation of o-cresol removal using PVA-cryogel-immobilised biomass enhanced by PAC. *Water SA* 41(1):55–60. <https://doi.org/10.4314/wsa.v41i1.8>
- Serebrennikova MK, Golovina EE, Kuyukina MS, Ivshina IB (2017) A Consortium of Immobilized Rhodococci for Oilfield Wastewater Treatment in a Column Bioreactor. *Appl Biochem Microbiol* 53(4):435–440. <https://doi.org/10.1134/s0003683817040123>
- Seven F, Sahiner N (2014a) Enhanced catalytic performance in hydrogen generation from NaBH₄ hydrolysis by super porous cryogel supported Co and Ni catalysts. *J Power Sources* 272:128–136. <https://doi.org/10.1016/j.jpowsour.2014.08.047>
- Seven F, Sahiner N (2014b) Superporous P(2-hydroxyethyl methacrylate) cryogel-M (M:Co, Ni, Cu) composites as highly effective catalysts in H₂ generation from hydrolysis of NaBH₄ and NH₃BH₃. *Int J Hydrogen Energy* 39(28):15455–15463. <https://doi.org/10.1016/j.ijhydene.2014.07.093>
- Sharifi S, Behzadi S, Laurent S, Forrest ML, Stroeve P, Mahmoudi M (2012) Toxicity of nanomaterials. *Chem Soc Rev* 41(6):2323–2343. <https://doi.org/10.1039/c1cs15188f>
- Sharma M, Padmavathy N, Remanan S, Madras G, Bose S (2016) Facile one-pot scalable strategy to engineer biocidal silver nanocluster assembly on thiolated PVDF membranes for water purification. *RSC Adv* 6(45):38972–38983. <https://doi.org/10.1039/c6ra03143a>
- Shiekh PA, Andrabi SM, Singh A, Majumder S, Kumar A (2021) Designing cryogels through cryostructuring of polymeric matrices for biomedical applications. *Eur Polym J* 144. <https://doi.org/10.1016/j.eurpolymj.2020.110234>
- Shu YH, Huang RL, Wei XY, Liu LL, Jia ZZ (2017) Pb(II) removal using TiO₂-embedded monolith composite cryogel as an alternative wastewater treatment method. *Water Air Soil Pollut* 228(9):16. <https://doi.org/10.1007/s11270-017-3559-2>
- Su CM (2017) Environmental implications and applications of engineered nanoscale magnetite and its hybrid nanocomposites: a review of recent literature. *J Hazard Mater* 322:48–84. <https://doi.org/10.1016/j.jhazmat.2016.06.060>
- Tatykhanova GS, Klivenko AN, Kudaibergenova GM, Kudaibergenov SE (2016) Flow-through catalytic reactor based on macroporous amphoteric cryogels and gold nanoparticles. *Macromol Symposia* 363(1):49–56. <https://doi.org/10.1002/masy.201500137>
- Tercan M, Demirci S, Dayan O, Sahiner N (2020) Simultaneous degradation and reduction of multiple organic compounds by poly(vinyl imidazole) cryogel-templated Co, Ni, and Cu metal nanoparticles. *New J Chem* 44(11):4417–4425. <https://doi.org/10.1039/d0nj00148a>
- Tiede K, Boxall ABA, Tear SP, Lewis J, David H, Hasselov M (2008) Detection and characterization of engineered nanoparticles in food and the environment. *Food Additives Contaminants Part A-Chem Anal Control Exposure Risk Assessment* 25(7):795–821. <https://doi.org/10.1080/02652030802007553>
- UN (2017) World water development report
- Ussia M, Di Mauro A, Mecca T, Cunsolo F, Nicotra G, Spinella C, Cerruti P, Impellizzeri G, Privitera V, Carroccio SC (2018) ZnO-pHEMA nanocomposites: an ecofriendly and reusable material for water remediation. *ACS Appl Mater Interfaces* 10(46):40100–40110. <https://doi.org/10.1021/acsami.8b13029>
- Villegas LGC, Mashhadi N, Chen M, Mukherjee D, Taylor KE, Biswas N (2016) A short review of techniques for phenol removal from wastewater. *Curr Pollut Reports* 2(3):157–167. <https://doi.org/10.1007/s40726-016-0035-3>
- Wang YZ, Zhang HM, Li BK, Yu MC, Zhao R, Xu XT, Cai L (2019) gamma-FeOOH graphene polyacrylamide carbonized aerogel as air-cathode in electro-Fenton process for enhanced degradation of sulfamethoxazole. *Chem Eng J* 359:914–923. <https://doi.org/10.1016/j.cej.2018.11.096>
- Westerhoff P, Song GX, Hristovski K, Kiser MA (2011) Occurrence and removal of titanium at full scale wastewater treatment plants: implications for TiO₂ nanomaterials. *J Environ Monit* 13(5): 1195–1203. <https://doi.org/10.1039/c1em10017c>

- Westerhoff P, Alvarez P, Li QL, Gardea-Torresdey J, Zimmerman J (2016) Overcoming implementation barriers for nanotechnology in drinking water treatment. *Environ Sci Nano* 3(6): 1241–1253. <https://doi.org/10.1039/c6en00183a>
- van Wolferen M, Orell A, Albers SV (2018) Archaeal biofilm formation. *Nat Rev Microbiol* 16(11): 699–713. <https://doi.org/10.1038/s41579-018-0058-4>
- Xu ZB, Liang YR, Lin SQ, Chen DQ, Li B, Li L, Deng Y (2016) Crystal violet and XTT assays on staphylococcus aureus biofilm quantification. *Curr Microbiol* 73(4):474–482. <https://doi.org/10.1007/s00284-016-1081-1>
- Xu CY, Chen WS, Gao HP, Xie X, Chen YS (2020) Cellulose nanocrystal/silver (CNC/Ag) thin-film nanocomposite nanofiltration membranes with multifunctional properties. *Environ Sci Nano* 7(3):803–816. <https://doi.org/10.1039/c9en01367a>
- Yang Y, Qina Z, Zeng W, Yang T, Cao YB, Mei CR, Kuang Y (2017) Toxicity assessment of nanoparticles in various systems and organs. *Nanotechnol Rev* 6(3):279–289. <https://doi.org/10.1515/ntrev-2016-0047>
- Zaushitsyna O, Berillo D, Kirsebom H, Mattiasson B (2014) Cryostructured and crosslinked viable cells forming monoliths suitable for bioreactor applications. *Top Catalysis* 57(5):339–348. <https://doi.org/10.1007/s11244-013-0189-9>
- Zhang ZY, Lei ZF, He XY, Zhang ZY, Yang YN, Sugiura N (2009) Nitrate removal by *Thiobacillus denitrificans* immobilized on poly(vinyl alcohol) carriers. *J Hazard Mater* 163(2-3):1090–1095. <https://doi.org/10.1016/j.jhazmat.2008.07.062>



One-Dimensional Semiconducting Nanomaterials: Toxicity and Clinical Applications

2

Ashtami Jayakumar, Chandra Mohan, and Oomman K. Varghese

2.1 Introduction

Low-dimensional materials have dimensions restricted to nanometer-scale along at least one of the three axes. In one-dimensional (1D) materials, one of the dimensions (say, along the z -axis) is unrestricted, and the other two (in the x and y directions) are limited to less than 100 nm, typically (Barth et al. 2010). 1D materials exist in a wide range of morphologies. While shapes such as a tube, rod, wire, fiber, filament, ribbon, and belt are commonly explored (Devan et al. 2012), the geometry can deviate from standard to hollow, porous, core-shell, or branched forms (Huo et al. 2019). Labeling the nanoscale materials in terms of physical dimensions is often subjective and strict guidelines in this direction have not yet evolved. For 1D materials, the ratio of length to diameter, called aspect ratio, is usually used as a defining term (Huo et al. 2019). By adopting bottom-up or top-down building strategies, these materials can be fabricated either as a coating on a substrate or in dispersed form. The array architecture formed by the vertical orientation of the 1D building blocks on a substrate is a unique feature of these materials. 1D structures

A. Jayakumar

Department of Biomedical Engineering, University of Houston, Houston, TX, USA

Nanomaterials and Devices Laboratory, Department of Physics, University of Houston, Houston, TX, USA

C. Mohan

Department of Biomedical Engineering, University of Houston, Houston, TX, USA

O. K. Varghese (✉)

Nanomaterials and Devices Laboratory, Department of Physics, University of Houston, Houston, TX, USA

Texas Center for Superconductivity, University of Houston, Houston, TX, USA

e-mail: okvarghese@uh.edu

can be fabricated into extremely thin and weightless nanostructures over a large area at the minimum expense (Sattler 2020).

1D nanostructures exhibit exceptional properties due to the availability of a large fraction of atoms at the surface of the solid, ultrahigh surface area, and the constraints imposed in two dimensions by the geometry on the behavior of electrical charge carriers and phonons. Such properties are highly pronounced in the case of 1D semiconductors due to the strong influence of nanoscale dimensions on the energy band structure and electron and hole transport. While holes and electrons can travel along the length, they always remain in the vicinity of the surface, and this is a unique feature of 1D semiconductors. In structures like quantum wires, the confinement of electrons in two dimensions approaching de Broglie wavelength of electrons provides distinct size-dependent electronic and optoelectronic properties. For example, the demonstration of ultraviolet lasing in 1D zinc oxide (ZnO) dates back to 2001 (Huang et al. 2001; Li et al. 2019). As a result of the intriguing properties of 1D semiconductors, elemental semiconductors, as well as binary and multinary compound semiconductors in the form of oxides, nitrides, chalcogenides, and carbides (Barth et al. 2010), have been explored for diverse applications in the areas such as optoelectronics (Choudhary et al. 2020), electronics (Jin et al. 2018), supercapacitors (Zheng et al. 2019), sensors (Li et al. 2018), solar fuels (Qin et al. 2015) and medicine (Fahmi et al. 2010).

Dimensions, morphology, arrangement, and geometric surface area are critical parameters influencing the electrical and optical properties of a 1D semiconductor (Devan et al. 2012). For example, a coating of ordered vertically aligned wide bandgap titanium dioxide nanotubes (the array structure) was shown to increase the optical transmittance of transparent conducting oxide-coated glass by reducing the reflectance (Varghese et al. 2009; Ong et al. 2007). Highly ordered 1D structures can also improve electron transport through the material and reduce electron-hole recombination (Ong et al. 2007; Xiao et al. 2020). For specific applications, morphology also is a critical factor. For instance, the TiO₂ nanotube scaffold was demonstrated to have the ability to protect organic-inorganic perovskite light absorbers from environmental interaction and enhance solar cell stability (Qin et al. 2015). High roughness factor (ratio of geometric surface area to the horizontal area occupied) enables the 1D semiconductors to have specific applications related to light absorption and environmental interaction. In a photoelectrochemical water-splitting process, the 1D geometry of the photoelectrodes enhances the light-harvesting ability and charge transfer between the semiconductor and the electrolyte leading to improved solar energy to hydrogen conversion efficiency (Hsu et al. 2009; Shankar et al. 2007; Varghese et al. 2005; Balan et al. 2018). The nanoscale dimensions, together with the high roughness factor, make the 1D semiconductor interesting for applications such as chemical sensing. The semiconductors can change the electrical resistance remarkably in a chemical analyte environment when their lateral dimensions approach the Debye length (Paulose et al. 2005). Furthermore, the fast transfer of electrons/holes between bulk and surface facilitated by the low lateral dimensions could positively influence the adsorption/desorption

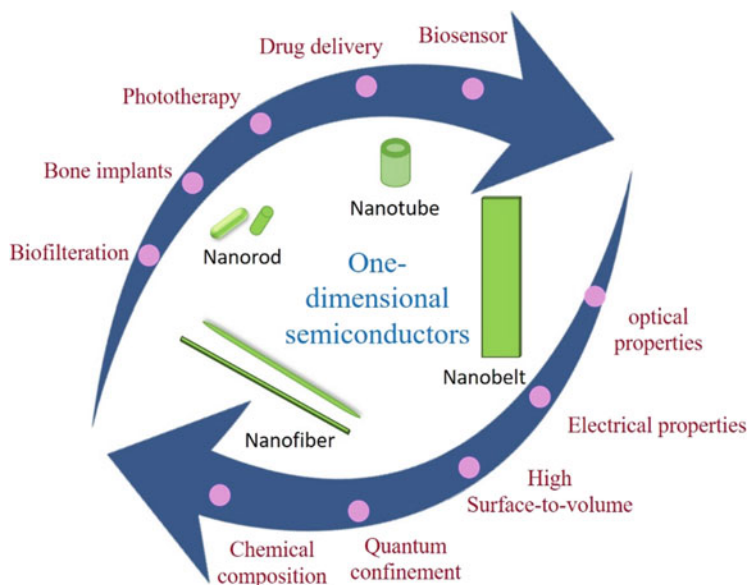


Fig. 2.1 Properties and clinical scope of 1D semiconductors

kinetics responsible for the fast sensor response and complete recovery during the cycling of the atmosphere (Kolmakov and Moskovits 2004).

Because of these unusual electro-optic properties and surface chemistry, 1D semiconductors have become highly sought after for unconventional applications in areas such as medicine and biotechnology. 1D semiconducting type functional materials have been rigorously investigated for applications like targeted drug delivery, proteomics, biosensing, bone implants, biofiltration, clinical diagnosis, and disease treatment (e.g., phototherapy). Some of the relevant properties of 1D architectures of semiconductors and heterostructures in relation to their biomedical applications are schematically illustrated in Fig. 2.1. The ease of fabrication, a wide choice of morphology, the possibility of controlling the morphology and dimensions precisely, ability to form dispersed as well as monolithic structures on substrates and options to add multimode functionalities make 1D functional materials appealing (Zhang et al. 2011; Yan et al. 2012). There has been a dramatic increase in the application range of structures showing quantum confinement effects. The possibility of using electrical and optical stimulation at the cellular interface with the aid of 1D semiconductors is being explored for next-generation drug development and screening. The unique optical and electrical properties of 1D semiconductors make them ideal nano-electronic platforms for detecting electrical signals from neurons (Patolsky et al. 2006).

Biocompatibility is a critical criterion to be verified in any material used for in vivo applications. While many nanostructures have poor biocompatibility, some of the 1D semiconductors were reported to have high compatibility with live cells. A

study by Kin et al. showed positive results for the use of silicon nanowires as a compatible interface for cellular growth (Kim et al. 2007). Conjugating 1D nanostructures with biomolecules is a strategy to ameliorate the allied toxicity in some materials (Wang 2009). Another limiting factor in the clinical translation of 1D nanostructures is the poor dispersion in water, which is necessary to administer the formulation into a biosystem for any in vivo healthcare applications. Chemical modification, either specific or nonspecific depending on the surface affinity of the surface, is an approach to solve the issue.

This chapter presents 1D semiconductors as future clinical platforms for effective theragnostics. Here we give an overview of some of the biomedical applications in which 1D semiconductors exhibited significant potential for practical implementation. We will begin with a brief discussion of the fabrication techniques. The biocompatibility and the strategies adopted to ameliorate the toxic potential of 1D semiconductors form a part of the discussion.

2.2 Fabrication of 1D Semiconductors

For a low-dimensional material to be useful for commercial applications, the fabrication technique should be scalable, and it should provide control over parameters influencing the morphology, structure, and chemical and electrical properties. In the case of 1D semiconductors, a wide range of fabrication techniques have emerged in recent decades, and some of them satisfy the above criteria. Some methods directly yield crystalline, either single or polycrystalline, 1D materials, while the others produce amorphous. Irrespective of the crystalline nature, the growth should be restricted to a single direction.

1D semiconductors are synthesized either by bottom-up or top-down methods. In a top-down approach, macro/bulk structures are broken down via etching or other chemical means to form the desired nanostructure. While bottom-up methods are of various types involving different principles, a typical bottom-up method involves the aggregation of atoms at supersaturation to form nuclei, followed by the growth of nuclei into seeds and eventually into the 1D nanostructure. The bottom-up growth can be template-assisted or template-free. The 1D structures can be grown on a substrate or without a substrate. The fast growth on a substrate generally leads to amorphous or polycrystalline structures. Some methods require a catalyst for preferential 1D growth. Based on the phase at which the catalyst-assisted growth occurs, the method is again classified into vapor-liquid-solid (VLS), solid-liquid-solid (SLS), vapor-solid-solid (VSS), and vapor solid (VS) (Zhang et al. 2012). Other methods transform liquid to solids and solids to solids. The top-down method and some of the commonly employed bottom-up methods are indicated in Fig. 2.2 and are briefly discussed below (Xia et al. 2003; Law et al. 2004).

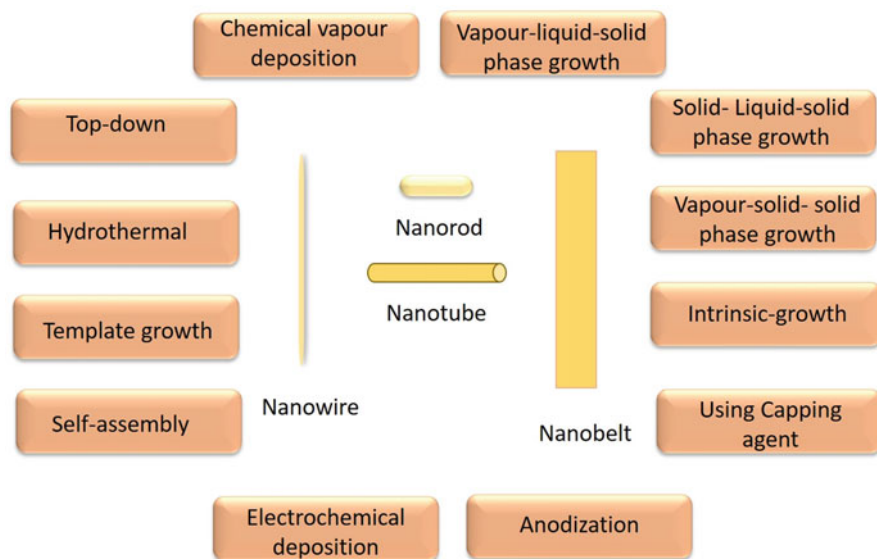


Fig. 2.2 Commonly used routes for 1D semiconductor growth

2.2.1 Top-Down Fabrication

The top-down approach, in simple terms, involves breaking down the higher dimensional counterparts into 1D materials. A top-down approach provides appropriate options to impart desired functionalities onto 1D nanostructures and assures better control of the dimensionality, crystalline nature, doping levels, and other attributes than many bottom-up methods. Chemical etching is a widely chosen technique to obtain desired 1D nanostructures. Gallium arsenide (GaAs) and indium phosphide (InP) nanowires were fabricated from their respective bulk wafers using a combinational technique of photolithography followed by chemical etching (Sun et al. 2005). GaAs and InP are broad bandgap III–V semiconductors with high carrier mobility that are used in a range of practical applications where reliable production of high-quality single-crystalline nanowires was required. The combinational top-down approach provides not only high quality and crystallinity but also facilitates fine-tuning of the morphology and dimensions. InP nanowires were reported to be obtained in a metal-aided chemical etching method (Soopy et al. 2021). Metal-aided etching strategy is applicable to semiconductors capable of having variation in etching rate on metal-covered and non-metal-covered surfaces. Another option for the top-down approach to obtain 1D semiconductors is the reactive ion etching method, a much sought after option for GaN nanowires (Lohani et al. 2019). By reactive ion etching technique, reactive ions are utilized for etching a heterostructure or a 2D layer leading to the formation of the nanowire.

2.2.2 Vapor-Liquid-Solid (VLS) Phase Growth

VLS growth (VLS) is one of the most commonly relied-on bottom-up synthesis methods for 1D semiconductors, especially for nanorods and nanowires. In VLS growth, a liquid droplet on a solid surface acts as a catalyst for the restricted lateral growth of discrete 1D nanostructures (Chun and Lee 2010). The gaseous reactants dissolve into the catalyst facilitating 1D nanostructure formation. VLS is advantageous for getting a highly anisotropic single crystal structure with desired size, length, and diameter. The method involves metal alloying and nucleation followed by axial growth. The 1D nanostructure formation is in strict correlation with supersaturation. The dissolution of the gaseous reactant onto the metal catalyst results in a rise in the amount of target material, causing supersaturation. On attaining supersaturation, nuclei formation at the liquid-solid interface is triggered, which further promotes the preferential axial growth.

Recently, Sutter et al. demonstrated that the morphology of the 1D semiconductors could be tuned by modulating the VLS reaction conditions (Sutter et al. 2021). In their research, the introduction of tin sulfide (SnS) in the silver catalyzed synthesis of germanium sulfide (GeS) via the VLS method caused a change in morphology of the 1D nanostructure from chiral ribbon to angled nanoribbon and tilted-layered nanoribbon. The results established that better control over the morphology of the resultant structure could be achieved by the precise choice of additives in the VLS method. The VLS methods became attractive because of their ability to yield high-quality wires with better morphology and crystal-phase control and the availability of a wide range of options for liquid catalysts. Nonetheless, the high-temperature requisite that puts constraints on scaling up and difficulty in obtaining wires of diameter below about 10 nm lower its prominence (Güniat et al. 2019). The high-temperature requirement also causes chances of metal catalyst contamination onto the semiconductor nanostructures. The catalyst metal impurity in the final fabricated nanostructure reduces the acceptance of the VLS method.

2.2.3 Solution-Liquid-Solid (SLS) Method

SLS method is analogous to the VLS growth (Wang et al. 2016a). SLS growth of 1D semiconductors however does not require temperatures as high as those used in VLS growth. In the SLS method, the growth occurs typically in solution. Colloidal nanoparticles capable of melting into the nanodroplets form are used as catalysts in SLS. The size of the nanoparticles plays a crucial role in determining the resulting 1D nanostructure diameter. The merits of SLS lie in the opportunity it opens up to yield lower diameter, dispersible, and surface-controlled 1D structures. Nanoparticles that melt at lower temperatures are selected as catalysts for SLS. The solution dispersible reactant adsorbs onto nanodrops formed upon nanoparticle melting. The factors that influence SLS methods are the nature of the solvating agent, melting point, and reaction conditions; however, fine-tuning these factors to yield the desired structure is an art that has not yet been fully mastered (Wang et al. 2006).

SLS technique is opted for obtaining colloidal solutions of nanowires and nanorods (Wang et al. 2016a). SLS is scalable. While VLS yields nanowires of diameter above ~10 nm, the SLS technique makes it possible to produce nanowires of diameter less than 10 nm. Nevertheless, the need for low-melting point catalysts imposes restrictions on the SLS method, and, therefore, the method is not as generalizable as VLS (Güniat et al. 2019).

2.2.4 Vapor-Solid-Solid (VSS) Method

VSS is also a derivative version of VLS in which instead of a liquid catalyst, a solid catalyst is used. The advantage of the VSS method is that it can produce sharper heterostructures with a single-layer precision. Similar to SLS, catalyst availability is one limiting factor here also. The method also has constraints per scalability, as in the case of VLS (Güniat et al. 2019). The slow growth rate in the case of VSS is another drawback. Maliakkal et al. studied the dynamics in the growth of GaAs nanowires via both VLS and VSS methods and came up with some exciting findings (Maliakkal et al. 2021). It was found that the VLS growth occurred preferably by single-layer growth at a time, while VSS showed the possibility of two-layer nucleation and growth concurrently. No significantly large difference in growth rate was observed under similar growth conditions. Therefore, it was concluded that the lower growth rate in the VSS method compared to VLS was possibly arising from the thermal history, catalyst shape, growth conditions, and material system. Better insights about the growth dynamics of VSS-based methods would help in overcoming its low growth rate and improving feasibility.

2.2.5 Vapor-Solid (VS) Method

In VS method, no catalyst is required. The 1D semiconductors are grown directly on solid particles as substrate. The quality determining factors are supersaturation step, growth temperature, and time. The method is used commonly for the synthesis of 1D semiconductor nanowires and nanobelts. The high-temperature reaction condition on metal oxides causes the formation of liquid droplets and evaporation of the metal oxides to grow nanobelts. The process is considered self-catalytic (Zhang and Senz 2013). The high-temperature requirement and high cost are major drawbacks of the VS technique. Moreover, supersaturation increases the potential for 2D growth than 1D growth leading to unwanted sheet structures (Lu et al. 2018).

2.2.6 Electrospinning

The electrospinning technique is a synthesis route preferred for nanofibers of semiconductors. In this technique, the precursor solution is charged under an applied electrical field and ejected from a needle to form a fibrous structure on the collector.

The ruling principle is that the applied voltage between the needle and the collector causes the electrostatic repulsive force to be higher than the surface tension of the precursor droplet at the needle point (Yang et al. 2021a). 1D semiconductor synthesis involves the preparation of spinning solution in polymer matrix for ejection under electric field and then calcination in order to remove the polymer. The calcination conditions decide the morphology and structure of prepared 1D semiconductors and determine whether the 1D structure adopts an amorphous or a crystalline structure or a nanotube or a nanowire morphology (Smok and Tański 2021). This technique yields a large area of ordered fibers with high specific surface area opening up the potential scope in sensor applications. For instance, In_2O_3 nanofiber formed via electrospinning was reported to possess a high specific area for triethylamine detection (Ma et al. 2020). Also, the electrospinning technique is the top pick for the synthesis of core-shell 1D semiconductors owing to the ease of fabricating the inner core and outer coating. 1D pristine CuO and multijunction $\text{In}_2\text{O}_3@\text{CuO}$ nanofibers synthesized by single-step electrospinning followed by calcination at 600 °C were reported to have excellent sensing properties towards hydrogen sulfide and ammonia (Zhou et al. 2018).

2.2.7 Electrochemical Deposition

Electrochemical deposition can be either template aided or without using any surface to grow on (She et al. 2009a). In substrate-assisted electrochemical deposition, the template serves as a support for one-dimensional growth of the deposited material. The template can be either hard as a metal surface or soft like surfactants or liquid crystals. One of the hard templates used for electrodeposition is aluminum oxide. The factors influencing the morphology and growth of 1D semiconductors produced from this technique are precursor solution, the voltage applied, temperature, and time of deposition. In fact, in a study of electrochemical deposition of free-standing manganese oxide on porous alumina, increasing the deposition time caused a change in morphology from nanotube to nanowire (Xia et al. 2010). In the case of non-template-assisted electrodeposition, 1D growth is triggered by the intrinsic property of the material rather than external aid. Non-template-based electrodeposition has opted in cases where the material has an inherent tendency to grow in one dimension favorably. Tellurium nanowires fabrication by intrinsic electrodeposition route was reported by She et al. (She et al. 2009b).

2.2.8 Hydrothermal Synthesis

The hydrothermal route is preferred for single crystal formation. It uses an aqueous precursor solution subjected to high pressure and elevated temperature to grow the 1D semiconductors (Sattler 2020). The process is called solvothermal when the solution is not aqueous. The method involves two steps: nucleation at supersaturation and growth. The precursor, under high temperature and pressure, forms nuclei,

which can grow to form desired nanostructures. The morphology and size of the nanostructure fabricated using the hydrothermal route are dependent on the hydrothermal temperature, vapor pressure, time, pH, and chemical nature of the solvent. This method provides an easier and cost-effective pathway for 1D semiconductor fabrication; however, the precise control of the growth kinetics is a bit tricky. This method is commonly used for the growth of 1D metal oxide semiconductor nanowires and nanotubes on substrates as well as in dispersed form (Sattler 2020; Li et al. 2011; Wang et al. 2004; Feng et al. 2008). TiO₂ nanowires with a large surface area prepared using these techniques were successfully used as anode in Li-ion batteries to improve the speed of charging and discharging (Li et al. 2011).

2.2.9 Chemical Vapor Deposition (CVD)

In CVD, the precursor is allowed to enter the reaction chamber with the help of vapor as carriers (Ye et al. 2021). The solid precursor from the vapor is made to deposit on or near a heated surface based on the chemical reaction occurring there (Carlsson and Martin 2010). The growth of the deposited solid depends on various factors influencing the CVD techniques including precursor type, growth time, carrier gas flow rate, as well as the temperature of the chamber, gas carriers, and deposition surface. It is widely used for the preparation of nanofibers and nanowires of appreciably high crystal quality. 1D structures of many semiconductors, including silicon, were synthesised via CVD (Puglisi et al. 2019; Shi and Wang 2011; Choi and Park 2004).

2.2.10 Intrinsic Growth

Some materials display preferential growth as 1D structures owing to their intrinsic anisotropic nature. For materials that exhibit a high anisotropic effect, there are high chances of preferential unidirectional growth along the c-axis alone during the crystallization leading to 1D structure formation. Single-crystalline copper telluride nanoribbon was synthesized in aqueous conditions at low temperatures due to its inherent anisotropic character that facilitates preferential 1D growth without using a template or capping agent (She et al. 2008). Recently, template-free electrodeposition of trigonal tellurium in ribbon morphology was achieved without any high-temperature treatment requirements (She et al. 2009b). Tellurium owing to its interesting optical and electrical properties turned out to be a highly preferred multifunctional material. The highly anisotropic crystalline nature of tellurium enabled its growth into a 1D ribbon with minimum defects. This mode of 1D growth is beneficial due to the elimination of requirements such as high-temperature conditions, growth template, and capping agents.

2.2.11 Manipulating the Growth Using Capping Agents

In some instances, the help of capping agents is sought to fine-tune the growth of 1D nanostructures. Agents that are capable of tuning the surface energies of the synthesized nanostructures are used to attain the desired morphology. A study of the effect of capping agents on the 1D growth of ZnO nanostructure revealed that the presence of capping agent-induced low-sized ZnO nanorods with screw-like ends. In contrast, nonuniform irregular ZnO nanorods with spherical ends and larger sizes were formed in a capping agent-free situation. Ethylene glycol as a capping agent successfully capped Zn²⁺ ions causing nucleation with lower surface tension, eventually reducing agglomeration of the formed nanostructures and reduction of crystalline size (Lefatshe et al. 2021). Precise selection of capping agent helps to get control over the size, morphology, and associated properties of the desired nanostructure.

2.2.12 Self-Assembly

Self-assembly of nanoparticles is a conventional bottom-up approach opted for 1D semiconductor synthesis. It occurs by dipole-dipole interactions between the nanoparticle crystals that fuse together during the crystallization process. Basically, nanoparticle crystals act as building blocks and, due to their highly anisotropic nature, get aligned unidirectionally to form a 1D structure. The diameter of the initial nanoparticle is a decisive factor for the diameter of the formed 1D nanostructure. Tang et al. reported that cadmium telluride (CdTe) nanoparticles could self-assemble to form high-quality uniform CdTe nanowires having appreciably high quantum yield. The option for selecting the starting nanoparticle provides the luxury of fine-tuning the diameter, aspect ratio, and morphology of the final structure (Tang et al. 2002). Similarly, ZnO nanorods were prepared from the self-assembly of ZnO nanodots. The ZnO nanodots of diameter ~3 nm were found to preferentially orient along the *c*-axis to form single-crystalline 1D ZnO nanowires (Pacholski et al. 2002).

2.2.13 Template-Assisted

Template-assisted growth is a broad class of 1D semiconductor synthesis approach. It can be used in many techniques, including, but not limited to, VLS, SLS, VSS, electrochemical deposition, chemical polymerization, CVD, sol-gel process, anodization, and hydrothermal synthesis. The desired SC material is deposited on to a template by different techniques, and the template is removed later by posttreatment, such as calcination or etching to form 1D nanostructures (Xia et al. 2003). Template-assisted growth utilizes a soft, hard, or porous template that could serve the purpose of a scaffold for facilitating the growth of 1D semiconductors. For example, Wang et al. used Cu(OH)₂ nanowires as a soft template for growing copper

oxide nanowires (Wang et al. 2003). Ordered porous alumina grown by anodic oxidation is a commonly used hard template for growing semiconductor nanowires and nanotubes (Ahmadzadeh et al. 2021). In some cases, the precursor crystallizing on the substrate can act as a seed crystal (Zhang and Senz 2013). The orientation follows that of the substrate. The template-based method provides ways to tune the structure and morphology. High growth rates can be achieved and harsh reaction settings can be avoided (Huczko 2000).

2.2.14 Electrochemical Anodization

Anodization stands for a technique for introducing an oxide layer on a positively charged metal surface. Electrochemical anodization is carried generally in an electrolyte under an electric field applied between two electrodes. The metal where oxide growth is desired is used as the anode.

Electrochemical anodization is one of the oldest commercially used techniques for oxide growth. It has been traditionally viewed as a low-cost scalable technique for protective coatings on metals, especially aluminum and titanium, and different metal alloys. The most remarkable feature of this technique is its ability to facilitate highly ordered nanotube growth on metal surfaces. The growth of compact and porous films had been the focus in the field till the 1990s. Apparently, the first report on the growth of ordered semiconductor nanotubes came out in the 1980s; however, the potential of the method was realized when the anodically grown titania nanotube arrays became extremely useful for various applications at the beginning of this millennium (Gong et al. 2001; Varghese et al. 2003a; Mor et al. 2003a, 2006, 2005; Wu et al. 2005).

Choice of electrolyte, applied voltage, temperature, and time of anodization have pivotal roles in determining the morphological characteristics of the nanostructures grown (Rao et al. 2016; Cai et al. 2005). The mechanism of oxide formation via anodization involves the metal oxidation and growth of the oxide layer accompanied by the dissolution of the oxide chemically as well as by a process assisted by the applied electric field. The separation of walls to form nanotube structures is a distinct phenomenon that is not yet clearly understood (Mor et al. 2003b). In general, the process involves three steps: (1) metal oxide formation, (2) pore formation as a result of barrier dissolution, or (3) pore separation and nanotube growth with time. The physical parameters like length, pore diameter, wall thickness, and distance between the tubes are greatly influenced by the selection of electrolytes. For instance, an electrolyte based on ethylene glycol yielded TiO_2 nanotube closely packed into highly ordered structures that could find applications in sensors, biofiltration, etc. (Prakasam et al. 2007). On the other hand, DMSO and diethylene glycol electrolytes would yield well-spaced TiO_2 nanotubes in the array (Yoriya et al. 2007; Ruan et al. 2005; Wu et al. 2005). By changing the electrolyte from aqueous to organic type, maximum attainable nanotube length could be increased from a few hundred nanometres to hundreds of micrometers with the potential to yield any desired length

limited by the substrate thickness (Shankar et al. 2007; Yang et al. 2021a; Gong et al. 2001; Cai et al. 2005; Prakasam et al. 2007; Wu et al. 2005).

Anodization is a proven technique for fabricating the nanotubes and other 1D architectures of various other semiconductors also. Fabrication of copper (II) oxide (Mukherjee et al. 2003), iron oxide (Prakasam et al. 2006; Jang and Park 2014), niobium pentoxide (Wei et al. 2012), tantalum oxide (Jin et al. 2021), vanadium oxide (Lee et al. 2021), and zinc oxide (Katwal et al. 2016) was reported (Rao et al. 2016). ZnO nanorods, nanowire/nanotube architecture and other structures were fabricated by Miles et al. (Miles et al. 2015) and Katwal et al. (Katwal et al. 2016). Nevertheless, the growth mechanism of these structures does not involve the conventional processes responsible for the nanotube formation.

2.3 Biocompatibility

A prerequisite for testing any material for biomedical applications is the assessment of its toxicity and compatibility with cellular structure. The toxicity is decided not by the chemical composition alone; it could vary dramatically with dimensions and morphology (Tong et al. 2013). A material that is benign on the microscale can be toxic when it takes nanoscale dimensions (Ma et al. 2019) and vice versa (Rajput et al. 2021). The high surface area available for the interaction with the biological environment and the unique surface chemistry provided by the nanoscale dimensions and morphology can make an otherwise biocompatible material toxic in low dimensions. 1D semiconductors are no exception.

A recent study on the cell viability and toxicity of titania (TiO₂) nanotubes fabricated by electrochemical anodization showed interesting results (Mohamed et al. 2017). The TiO₂ nanotubes were grown on titanium foil and detached and dispersed for toxicity studies using human dermal fibroblast cells. The nanotubes exhibited toxicity at lower concentrations and high cell viability, similar to control samples at higher concentrations. The aggregating tendency of these nanotubes at higher concentrations was believed to trigger the formation of large clusters that could not be efficiently endocytosed by the cells. As a result, the toxicity was ameliorated at elevated concentrations. Further investigations on the mechanism leading to cell death indicated an apoptotic pathway rather than a necrotic pathway. Even in the presence of low-concentration nanotubes, the cytoskeletal components of the cell that are responsible for the structural integrity and cell-cell/cell-matrix interactions remained intact. On the other hand, the reactive oxygen species (ROS) level was elevated in the nuclear compartment; however, the mitochondrial apparatus was not damaged by the ROS. The H2AX staining was indicative of damages to the DNA (deoxyribonucleic acid). Apparently, the increased ROS in the nuclear region attacked the nuclear components by inducing nuclear condensation and chromosomal distortion leading to genotoxicity. While the toxicity of this 1D material at lower concentrations (~0.1 mg/mL) could be alarming, the study revealed the potential of the material in destroying cancer cells without the involvement of chemotherapeutic agents. The apoptotic pathway of cell death was also reported in

ZnO nanorod-based *in vitro* toxicity profiling experiments on human alveolar adenocarcinoma (A549) cells (Ahamed et al. 2011). The nanorod was found to induce ROS production and cause oxidative stress. The apoptotic route of cell death became evident from the overexpression of cell damage proteins. Apparently, in another study, the biocompatibility of ZnO nanorod-silver nanostructure on multiple cell lines was scrutinised (Zhang et al. 2008). The prepared ZnO-nanorod-silver nanostructures were found to be compatible with Chinese Hamster cells and HeLa cells.

In light of dental and osteo applications, it is indispensable to check the biocompatibility of TiO₂ nanotubes. On this account, the compatibility of TiO₂ nanotubes with osteoblast cells was evaluated using SaSO2 cells (Wang et al. 2014). According to the study, TiO₂ nanotubes achieved better cellular attachment, proliferation, and compatibility compared to bare titania. Also, in comparison between TiO₂ nanotubes with and without porous surface layer, the one short of the porous surface turned out to show better cellular interaction. TiO₂ nanotubes are modified with other elements to improve their performance as implants (Indira et al. 2014). For example, TiO₂ nanotubes were modified using strontium for orthopedic applications. Evaluation of the toxicity profile of TiO₂ nanotubes containing strontium revealed better wettability and cellular compatibility.

In vivo toxicity studies provide a better understanding of the biocompatibility of a material as it involves more dynamic interaction of the material with the animal model compared to a two-dimensional micro-environment that mimics the biological interactions in *in vitro* studies. In the *in vivo* study conducted by Ahmed et al., ZnO nanorods were exposed to Swiss Albino Mice, and the results showed elevated blood platelets count, suggesting poor blood compatibility of the material (Ahamed et al. 2011). The shoot in serum enzymes also suggested material-induced oxidative stress. The histopathology data validated potent organ toxicity induced by ZnO nanorods. Liu et al. compared the toxicity of cadmium sulfide nanorods with nanodots using the mice model. According to the study, nanorods showed a lower accumulation tendency in exposed mice and lesser toxicity compared to the nanodots (Liu et al. 2014).

Although many 1D semiconductors are not sufficiently biocompatible in pristine form, they can be made benign by functionalizing the surface. This strategy helps the investigation of 1D materials for diverse biomedical applications. For example, Hou et al. used PEGylation to make ammonium tungstate [(NH₄)_xWO₃] nanorods, a functional photothermal agent, biocompatible with photothermal therapy (Hou et al. 2019). In treatment methods such as photothermal therapy (discussed later), the photoresponsive material should cause no toxicity in the absence of light and induce cell death in the presence of light. This is vital for the material to be selective and induce tumor cell death without affecting the normal cells. They found PEGylated tungsten oxide biocompatible unless triggered by near-infrared (NIR) light when it destroys the tumor cells in its proximity.

There have been many conflicting reports about the toxicity of 1D materials. The evaluation protocols have not yet been finely defined for low-dimensional materials, and, therefore, the variations in the methodologies and analyses make it hard to

arrive at reliable conclusions. As of now, the concerns over the toxicity of 1D semiconductors are mitigated by the surface functionalization approach.

2.4 Biomedical Applications

2.4.1 Sensors for Medical Diagnosis

Semiconductors can change their electrical and optical properties upon interaction with chemical species on the surface. The interaction involves the transfer of charge carriers to or from the semiconductor directly via adsorption of the analyte on the semiconductor surface or indirectly through other functional groups on the surface. While semiconductor-based sensors are known for their small size and low cost, the sensors based on bulk materials generally suffer from insufficient response to low-concentration chemical species and poor specificity (ability to discriminate different analytes). 1D semiconductors have a tremendous surface area that could provide a better room for analyte adsorption and surface redox reactions, and, therefore, they could detect analyte concentrations in the parts per million (ppm) to parts per billion levels (ppb) (Yang et al. 2021a; Varghese and Grimes 2003). The nanoscale lateral dimensions could improve the speed of operation and influence the nature and density of the surface states formed during fabrication that decide the selectivity (specificity). The 1D geometry facilitates the fabrication of microsensors using a single 1D building block (say, single nanowire or nanotube). Furthermore, the availability of a wide range of scalable methods to grow 1D semiconductors easily in the isolated form or as films, especially in the vertical array geometry, on various substrate types and shapes makes these materials more interesting than 0D and 2D materials for device development. Because of these unique properties, 1D semiconductors were recognized as highly promising for developing low-cost point-of-care devices for medical applications.

One of the most attractive emerging applications of chemical sensors based on nanoscale semiconductors is the detection of exhaled gases and volatile organic compounds (VOCs) that are disease-specific (Varghese 2016; Liyanage et al. 2020). It has been known since the time of Greek physician Hippocrates that the aroma of exhaled gas and urine could provide indications about the disease state of the human body. Systematic studies to correlate exhaled gases with diseases began in the second half of the twentieth century (Henderson et al. 1952). The realization that dogs could sniff out cancer and the early-stage detection of diseases such as cancer and lethal infectious diseases would improve the effectiveness of treatment and reduce mortality rate made the research in this area rigorous in the recent couple of decades (Williams and Pembroke 1989). It is now known that concentrations of VOCs and various gases including NO, H₂, and CH₄ in the exhaled gas can be used to differentiate the healthy functioning of the human body from abnormal states caused by cancer, digestive problems, airway diseases like allergic asthma, cardiovascular diseases, diabetes, tuberculosis, and a number of other diseases including novel coronavirus disease (COVID-19) (Haick et al. 2014; Ignarro et al. 1987;

Amann et al. 2014; Tormo et al. 2001; Grassin-Delyle et al. 2021). Gases and VOCs are created in tissues due to oxidative stress or other pathogenic processes and released to the bloodstream and then to exhaled breath through the lungs and airways. A few thousand distinct VOCs, most of them at very low concentrations, have been detected so far from breath samples. Nevertheless, some of them are disease or pathogen-specific, and these are generated at the early stages of disease development and propagation.

The endogenous VOC/gas profiling and disease correlation studies are primarily performed using expensive analytical tools such as Gas Chromatography-Mass Spectrometry (GCMS). Chemiresistive sensors based on 1D semiconductors are quick in giving a response, potentially affordable, and portable for point-of-care testing/monitoring. These sensors relate the electrical resistance change in semiconductors in the presence of a chemical species with its concentration. Although these are not analytical devices, they can be operated by experts or non-experts to get indications about the onset of diseases.

Katwal et al. demonstrated that 1D ZnO could be used for sensing breast cancer VOCs (Katwal et al. 2016). A ZnO nanotube-nanowire hybrid architecture was fabricated using electrochemical anodization. The anodization of zinc was carried out using an aqueous electrolyte consisting of washing soda and baking soda-produced zinc oxide nanowire at the initial stages of the process. A large fraction of these nanowires turned into nanotubes subsequently. Heat treatment transformed the amorphous pristine samples to crystalline ZnO. The walls of the nanotubes and nanowires became porous after annealing that enhancing the surface area further. As a result, the material kept at 250 °C became highly sensitive to ppm level acetophenone, isopropyl alcohol, and heptanal and ppb level isopropyl myristate while showing negligible response to species such as H₂, CH₄, CO₂, and water vapor. Mechanistic studies showed that the VOCs interacted primarily through chemisorbed oxygen species on the surface of the material. Oxygen chemisorption on the ZnO surface makes the material highly resistive, and its removal by VOCs increases the conductance. Wang et al. converted 2D SnS₂ nanotubes to SnO₂ nanotubes via thermal oxidation and found the material to be sensitive to ppm level acetone (Wang et al. 2019).

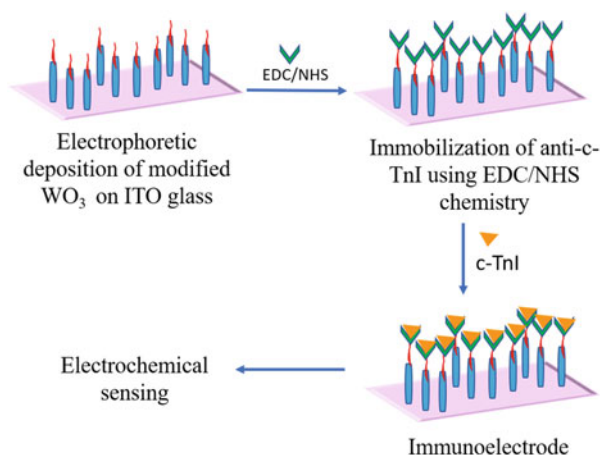
Highly ordered 1D semiconductors with interconnected 1D building blocks were reported to have immense potential for chemiresistive medical sensor development. TiO₂ nanotube fabricated by anodic oxidation array was found to outperform any other hydrogen sensor with astonishing sensitivity (Paulose et al. 2005). The material possesses incredible surface area facilitating active chemisorption of hydrogen gas that manifests in the form of a large increase in electrical conductance. A remarkable feature of this material is the control over the sensitivity, specificity, and sensor operating temperature by nanoscale feature size (Varghese et al. 2003b, 2004). Nanotubes of lower diameter and more contact points exhibited higher sensitivity to hydrogen. Nanotubes with pore diameter ~30 nm and an optimized length ~1 μm detected 1000 ppm hydrogen at room temperature, giving a remarkable response of about 8.7 orders of magnitude variation in the electrical resistance. Lower length nanotubes showed high sensitivity at elevated temperatures (Paulose

et al. 2005; Varghese et al. 2003a). The potential of TiO₂ nanotube array-based portable detectors was explored by detecting hydrogen for lactose intolerance diagnosis (Varghese et al. 2006). Bacterial fermentation of undigested lactose generates hydrogen and other gases. The study conducted on lactose intolerant patients showed a strong association between breath level hydrogen measured using a gas chromatograph and transcutaneous hydrogen detected using the nanotube sensor. Such transcutaneous sensors are also useful in monitoring the health of preterm infants with life-threatening diseases, such as necrotizing enterocolitis, where breath collection is not an option.

1D semiconductors have a strong ability to discriminate different VOCs and gases, and the specificity is still not sufficient in distinguishing low-concentration biomarkers from breath samples that possess a complex environment. Sensor arrays consisting of individual sensor elements with distinct functions are used in conjunction with machine learning algorithms such as principal component analysis to classify the biomarkers and identify the diseases. For example, Yang et al. developed a breath test using electronic nose Cyranose[®] 320, which is a commercial device, to predict breast cancer with high accuracy (Yang et al. 2021b). They enrolled 899 subjects for the study. Cyranose[®] 320 consists of an array of 32 sensors with individual sensors made of chemically modified single-wall carbon nanotubes, nanocomposites, or other materials. By analyzing the sensor output using the random forest technique, they could predict breast cancer with an accuracy of 91%, sensitivity of 86%, and specificity of 97%.

Field-effect transistor (FET) sensor configuration is also commonly explored and is suitable for employing isolated 1D semiconductors as sensing elements (Sadighbayan et al. 2020). FET biosensors are developed to achieve quick biological analyte detection based on charge transfer or electrostatic grating (Yan et al. 2012) thereby eliminating the stipulation for labeling. The electronic properties of 1D semiconductors make them respond quickly to analyte binding onto the highly active surface states so that fast, highly responsive, reliable FET biosensors with low detection limits can be fabricated. The leeway for functionalizing the surface of 1D semiconductors further simplifies the specificity and recognition for biomolecules or biomarkers. For instance, ZnO nanowires with biotin surface modification, when fabricated as FET sensor, displayed a detection limit as low as 2.3 nM for streptavidin concentrations, a biomolecule involved in tumor diagnosis and treatment (Choi et al. 2010). The ZnO nanowires for the study were prepared by VLS growth on a gold-coated aluminum oxide substrate. In another recent study, In₂O₃ nanoribbons fabricated by top-down strategy performed as an excellent sensor for ions, small molecules, and notably oligonucleotides. The photolithographic process used for the nanoribbon fabrication would provide better control over morphology and structural uniformity compared to the bottom-up method. Also, 350 nm wide In₂O₃ nanoribbons-based FET sensor showed remarkable sensitivity in detecting complementary DNA outperforming 20 μm wide nanoribbons of the same composition and under similar conditions, validating the fact that materials with a higher surface-to-volume ratio ensures higher sensitivity. Furthermore, functionalizing In₂O₃ nanoribbons with serotonin-recognizing aptamer enabled

Fig. 2.3 Fabrication of functionalized WO_3 nanorod as immunoelectrode for an electrochemical biosensor. Abbreviations: (EDC-NHS: [1-(3-(dimethylamino)-propyl)-3-ethylcarbodiimide hydrochloride and N-hydroxysulfosuccinimide], (cTnI):cardiac troponin I



complementary DNA strand detection (Zhao et al. 2020). FET sensors could be used for breath VOC detection also. Shehada et al. developed silicon nanowire FET sensors and linked their responses to exhaled gas with pattern recognition algorithms to diagnose several diseases, including lung cancer, gastric cancer, and asthma (Shehada et al. 2016).

Another type of sensor exploiting the unique properties of 1D semiconductors is an electrochemical biosensor (Li et al. 2017). In electrochemical biosensors, the presence of any biomolecule is detected from biological reactions like antigen-antibody interaction or enzyme-substrate binding, etc., which are converted into electrical signals like current, voltage, or impedance. Electrochemical sensor comprises of (1) an analyte, which is the biomolecule to be sensed, (2) bio-interface that exhibits specificity towards the analyte, (3) transducer which detects the change in ion flow between the analyte and bio-interface upon binding and converts to electrical signals, (4) metal oxide semiconductors are primarily explored for this application. For instance, tungsten oxide nanorods (WO_3) that are n-type semiconductors with an electronically active surface, and an ability to accomplish fast electron transfer have their electrical conductivity remarkably sensitive towards analyte/biomolecule presence. This functional behavior of the material was utilized in the development of electrochemical sensors for biomarkers of health conditions such as acute myocardial infarction, which is a serious cardiac dysfunction occurring commonly (Sandil et al. 2019). Developing affordable biosensors capable of detecting cardiac markers accurately is considered a great leap towards achieving disease diagnosis. WO_3 nanorods-based biosensor fabricated on indium-doped tin oxide glass was reported to be functional as a reliable immunosensor for cardiac biomarkers like cardiac troponin I (cTnI) with an impressive detection limit of 0.01–10 ng/mL (see Fig. 2.3).

The exceptional optical properties of 1D semiconductors make them suitable transducers for optical biosensors. For example, a ZnO semiconductor with a direct bandgap, favorable near-UV emission properties, and high exciton binding energy is

a useful material for biosensors working on optical principles (Tereshchenko et al. 2016). Additionally, restricting the lateral dimensions further improves surface reactivity, which is vital for analyte biomarker detection for disease diagnosis.

2.4.2 Bone Applications

Bone fractures remain a primary medical condition accounting for 15 million cases/year (Gómez et al. 2016). Bone ranks second as the most transplanted tissue after blood (Oryan et al. 2014). Autografts and allografts are two major options for bone repair. The problems associated with currently available options raise the need to develop new materials that can mimic the microstructure of natural bone.

1D semiconductors, especially metal oxides like TiO_2 (Alves-Rezende et al. 2020) and ZnO (Kong et al. 2019), are intensively researched as bone-regenerating materials. TiO_2 has been explored as a bone implant for decades (Rajh et al. 2014), and now TiO_2 nanotubes are extensively researched for their potential application as a bone implant material. Studies reveal that the negatively charged TiO_2 surface becomes an ideal platform for osteoblast cell adhesion and proliferation by absorbing positively charged cell adhesion proteins, which in turn attract osteoblast cells (Wang et al. 2014).

It has been shown that the surface charge plays a pivotal role in inducing the bioactivity of TiO_2 as a bone-regeneration material, while morphological parameters influence their performance. On examining the effect of the tube diameter of TiO_2 nanotube on cell adhesion and osteogenesis, it was found that the functionality was greatly influenced by the diameter. Smaller diameters (30 nm) induced more osteoblast cell adhesion compared to 100 nm diameter TiO_2 nanotubes. However, the 100 nm diameter TiO_2 nanotubes showed elongated cellular and nuclear morphology with alkaline phosphatase activity, beneficial for bone regeneration. As per their analysis, higher diameter TiO_2 nanotubes had better functionality as bone-regeneration materials, suitable for bone implant (Brammer et al. 2009).

Another oxide, zirconium dioxide (ZrO_2), is reported to have better mechanical strength and biocompatibility compared to TiO_2 , and this finding urged researchers to explore their potential use in bone implant applications. ZrO_2 nanotubes grown on ZnO nanorod were found to be a better host platform for fibroblast adhesion and growth compared to titania surfaces. Additionally, cells adhered to ZrO_2 nanotubes were found to develop elongated filopodia, a clear sign of close and strong interaction between the cells and the interface, further validating their potential as biocompatible and bioactive implant materials (Lu et al. 2014).

2.4.3 Phototherapy

Phototherapy utilizes the energy from the electromagnetic radiation in the UV-Vis-NIR region for therapeutic purposes. The photon energy is converted to other forms with the help of nanomaterials. Photothermal and photodynamic therapies (PTT and

PDT, respectively) are the most widely investigated phototherapies for treating diseases such as cancer.

In photothermal therapy, low-dimensional metals or semiconductors dispersed near the cancer cells absorb light and convert the photon energy to heat to destroy tumor cells. Noble metals such as gold convert the photon energy to thermal energy via localized surface plasmon resonance. In semiconductors, the electrons excited using the photons de-excite with the release of thermal energy (called non-radiative relaxation) and heat the surrounding tumor cells. Metal-semiconductor heterostructures are also used as photosensitizers for synergistic effects (discussed below). The kinetic energy gained by the atoms in the cells with the increase of temperature causes lipid peroxidation, DNA damage, or protein destruction leading to tumor cell death through necrosis, apoptosis, or necroptosis. A temperature in the range of 40–47 °C creates a hypothermic condition in the cellular environment causing apoptosis, and a temperature in the range of 50 °C or above causes necrosis (Khot et al. 2019). While UV and visible sources are used in studies, the NIR radiation can travel the maximum distance (typically up to ~5 cm) through tissues. Therefore, lasers operating with output in the NIR wavelength range are commonly explored for this therapy.

PDT also requires a photosensitizer that is activated upon UV or NIR irradiation to excited singlet states. The mechanism involves a system transition from excited singlet to triplet states, where electron transfer reactions with the oxygen result in the formation of ROS, causing cell death. The ideal selection of photosensitive material is a decisive step in bringing about treatment success. The potential of PDT to induce immune cell death has facilitated immune cancer therapy. Phototherapy and immunotherapy go hand in hand to provide a much versatile treatment method.

Functional nanomaterials with remarkable photo-absorption and thermal properties form an essential part of phototherapy for anti-tumor treatments. Recently, one-dimensional materials have been explored and found promising. While conventional 1D semiconductors and plasmonic metal nanoparticles with the ability to absorb NIR radiations were the most investigated, 1D metal/semiconductor heterostructures were demonstrated to have synergistic effects (Kalluru et al. 2013). 1D metal particles, especially gold, could exhibit surface plasmon resonance, and by altering their aspect ratio, the localized surface plasmon resonance (LSPR) could be changed from visible to NIR region (Huo et al. 2019).

The oxides of tungsten and related compounds were proven to be beneficial for both PTT and PDT. Hou et al. synthesized $(\text{NH}_4)_x\text{WO}_3$ nanorods via solvothermal route by treating peroxide tungstic acid under the hydrothermal condition at 400 °C for 6 h. The obtained nanorods of length 0.5–1 μm and diameter 100 nm showed a remarkable potential for phototherapy (Huo et al. 2019). $(\text{NH}_4)_x\text{WO}_3$ nanorods with larger sizes were favorable for better tumor accumulation compared to smaller nanorods, which could enter normal cells from capillaries as well. PEG functionalization was done on the synthesized nanorod to increase the biocompatibility, which was later found to have the added advantage of facilitating the macrophage escape. The $(\text{NH}_4)_x\text{WO}_3$ nanorods possessed a negative charge that risked its macrophage uptake and clearance leading to treatment failure. But

PEGylation neutralized the surface charge helping in lower recognition and uptake by macrophage and enhancing bioavailability for photoresponse. The $(\text{NH}_4)_x\text{WO}_3$ nanorods showed enhanced photothermal conversion efficiency of 32.7% when irradiated with 808 nm laser and appreciable photostability up to four cycles. The synthesized nanorods achieved a temperature of 60 °C with 3 min irradiation and caused hyperthermia-mediated tumor cell death. When nanorod-dispersed cancer cells were exposed to NIR radiation, the nanorods successfully killed about 80% of cells within 10 min—extending the exposure time to 20 min eradicated the tumor cells via necrosis. Earlier, Macharia et al. reported that $(\text{NH}_4)\text{WO}_3$ rods of length several hundreds of nm and diameter about 30 nm synthesized by solvothermal process, were capable of PTT while serving as an X-ray computed topography agent. $(\text{NH}_4)_x\text{WO}_3$ -PEG showed six-fold X-ray attenuation compared to contrast agent Iopromide, already used clinically for tumor imaging and detection. The PEGylated tungsten oxide nanorods used in this study induced tumor cell death when exposed to 920 nm irradiation. A temperature rise of 42.9 °C when irradiated for 1 min and 45.3 °C after 2 min of irradiation was detected. The material also showed appreciable photostability (upto seven cycles).

LSPR, the property of which is the collective oscillation of free charge carriers confined in nanoparticles on exposure to light depending upon the polarizability/dielectric function, is favorable from a photoresponse point of view. For a long time, LSPR was exhibited in metals alone, now LSPR property is attained in semiconductors, particularly transition metal oxides as well by doping, making stoichiometric changes, creating oxygen deficiency, etc. (Agrawal et al. 2018; Manthiram and Paul Alivisatos 2012; Li et al. 2020). The LSPR exhibited by the semiconductors are in the THz (microwave) to near-infrared region. There are reports that the LSPR in the case of 1D semiconductors can be fine-tuned by focussing on the diameter and composition (Min et al. 2018; Milla et al. 2016).

$\text{W}_{18}\text{O}_{49}$ possesses flexible LSPR that could be exploited for simultaneous PTT and PDT treatments. The slightly higher LSPR band gap of this material than singlet oxygen at 980 nm makes it an ideal material as a photosensitizer for PDT treatment with high singlet oxygen generation. $\text{W}_{18}\text{O}_{49}$ has an extinction coefficient much higher than the conventionally available photosensitizers and organic dyes. In a study conducted by Kalluru et al., 1D $\text{W}_{18}\text{O}_{49}$ of length 50 nm and thickness 1 nm, and width of 4 nm were functionalized using polyethylene glycol (Kalluru et al. 2013). The molar extinction coefficient for the synthesized PEGylated tungsten oxide is $0.5 \times 10^7 \text{ M}^{-1} \text{ cm}^{-1}$. The PEGylated $\text{W}_{18}\text{O}_{49}$ induced higher cell death (almost 2.3 times) when exposed to 909 nm (55%) compared to 808 nm laser (22%) at 37 °C. Interestingly, when the temperature was lowered from 37 °C to 4 °C, there was an evident change in cell death in the case of 808 nm laser condition (only 11% cell death), whereas not much reduction in cell death for 909 nm laser exposed cases (53%). The variation depicts a change in the cell-killing mechanism involved via using different lasers. The mechanism of cell death occurring when exposed to 909 nm was confirmed to be via PDT from the presence of a high level of reactive oxygen species. On the other hand, cells exposed to 808 nm laser showcased the presence of heat shock proteins, confirming that cell death is induced as a result of

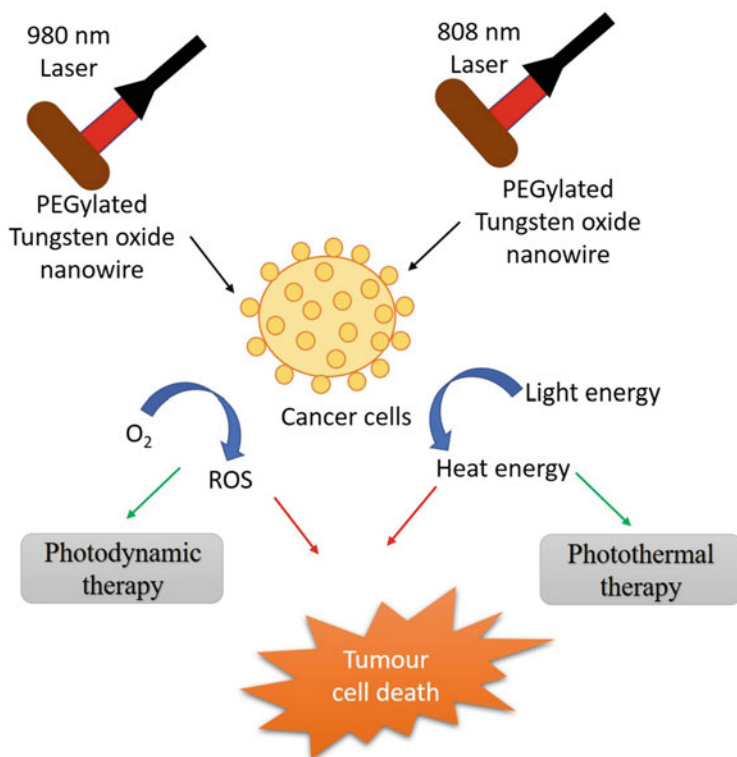


Fig. 2.4 Combinational phototherapy using tungsten oxide nanowire

the PTT pathway. While the relatively lower influence on cell death with a drop in temperature at 980 nm suggests PDT action (Fig. 2.4).

Similarly, TiO₂ nanotubes are also explored for photothermal applications. TiO₂ nanotubes in the presence of NIR were found effective in cancer cell killing (Hong et al. 2010). Above 96% cell viability was observed in TiO₂ nanotubes alone or NIR irradiation alone exposed cases. On the other hand, the combination of TiO₂ nanotubes and NIR condition caused complete cell destruction in TiO₂ nanotubes concentration-dependent manner. TiO₂ nanotubes are functionalized or chemically modified to enhance their efficiency in phototherapy. Flak et al. reported a study on the applicability of TiO₂ nanotubes for photodynamic therapy (Flak et al. 2015). For the study, TiO₂ nanotubes and iron-doped TiO₂ nanotubes were synthesized under hydrothermal conditions via the sol-gel route. The doped TiO₂ nanotubes showed better killing efficiency on irradiation on to HeLa cells compared to bare TiO₂ nanotubes. The organelle staining of exposed HeLa cells depicts mitochondrial damage, and the authors point out to be involved in apoptosis. According to the study, iron doping improved the photosensitivity of TiO₂ nanotubes, a vital factor for PDT, and resulted in enhanced ROS generation leading to PDT-mediated cell death via apoptosis. On similar grounds, the modification of TiO₂ nanotubes using silver

nanocrystals improved the photosensitizing power of TiO₂ nanotubes (Yang et al. 2017) and enhanced its applicability as a PDT agent.

Even though much attention has been devoted to stretching out the capacity of cancer treatment methods by including phototherapy, the technique is still in its outset, and there is much to go before making clinical confirmations. The limiting factors predominating the clinical success of phototherapy are uncontrolled hyperthermia affecting normal cells, ineffective penetration, and futile life span. All these call for spotting an efficient photosensitive material capable of covering all the existing inadequacies of the present treatment style.

2.4.4 Drug Delivery

1D semiconductors have been investigated heavily for their potential usage as delivery agents for drugs, biomolecules, or other interesting molecules of choice (Wang et al. 2016b). The one-dimensional morphology provides 1D semiconductors with a high surface area for drug loading and favorable surface chemistry for conjugating drugs. The possibility to fine-tune the release kinetics of loaded drugs from TiO₂ nanotubes makes them highly sought-after for drug delivery. The morphology of TiO₂ nanotubes also facilitates the possibility of loading the drugs onto the inside of the nanotube apart from surface loading (Wang et al. 2016b).

Light-responsive drug release has been reported on TiO₂ nanotube-based drug vesicles (Xu et al. 2016). TiO₂ nanotubes were fabricated with a cap containing gold nanoparticles, which are responsive to incident light and initiate the release of loaded drug molecules present in the interior of the TiO₂ nanotubes. The highlight of the report is the success of the fabricated system for the controlled release of the drug in response to light without any light-induced damage.

On similar grounds, You et al. reported the feasibility of utilizing functionalized silica nanorods for targeted drug delivery specifically to tumor cells (Xu et al. 2016). Nanorods with a higher aspect ratio cross the cell membrane faster than the low aspect ratio ones. This could be evidently detected by the enhanced accumulation of nanorods in comparison to nanospheres. Also, nanorod morphology facilitated significantly higher drug loading capacity in comparison to sphere-shaped nanoparticles. The authors reported that efficient cancer cell death was achieved by triggering apoptosis at the tumor site without producing a toxic response to normal cells (Fig. 2.5).

2.4.5 Other Applications

Stem cell therapy is a state-of-the-art approach for achieving effective cures for several challenging diseases. But various factors limit the feasibility of stem cell therapy. The loss of pluripotency on continuous differentiation over time or, in simple terms, “loss of stemness” is one of the restricting issues associated with stem therapy. Recently, Kong et al. reported that ZnO nanorod array fabricated onto

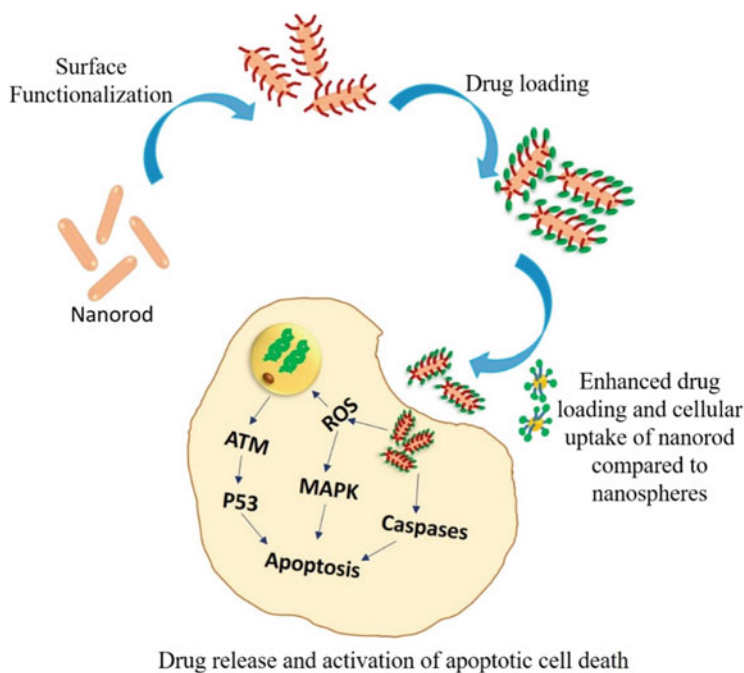


Fig. 2.5 Schematic representation of functionalized TiO_2 nanorods used for enhanced drug loading and release

ITO glass served as an ideal platform for human adipose-derived stem cell growth and proliferation without affecting their inherent cellular properties of stemness over time (Kong et al. 2019). The study showed satisfying results that validated the efficacy of these ZnO nanorod arrays in maintaining the pluripotency as well as enzyme activity of the attached human adipose-derived stem cells in comparison to cells grown over glass slides and ZnO film.

Hemorrhage is a critical concern in trauma patients, and there is a need for effective blood-clotting agents. On that account, TiO_2 nanotubes synthesized by anodization in an electrolyte consisting of HF and DMSO were evaluated for their efficacy in modulating clotting kinetics. TiO_2 nanotubes dispersed into the blood or, when added onto the surface of band-aids, induced 75% higher strength in formed blood clots in 10% lesser time (Roy et al. 2007).

Nanotube array membranes prepared by detaching the anodized nanotube array from the substrate were explored for their efficiency as a biofiltration unit. Polymer membranes are used commonly for biofiltration, but the wide pore size compromises filtration efficiency. On the other hand, the TiO_2 nanotube array membranes with controllable pore diameter prepared by fine-tuning the fabrication conditions facilitated controlled diffusion of the model molecule, phenol red, used for the study (Paulose et al. 2007). This seminal study revealed the potential of TiO_2 nanotube arrays for biofiltration application.

Another important application for 1D semiconductor nanostructures is its proficiency in separating phosphorylated proteins from non-phosphorylated ones (Wijeratne et al. 2015). In comparison to commercially used agents for protein separation, namely, Titansphere™ beads, TiO₂ nanotube radially arranged over titanium wire performed equally well in separating out the phosphorylated proteins. According to the authors, the orderly aligned TiO₂ nanotube turned out to be a low-cost alternative to those currently available in the market.

2.5 Conclusion and Outlook

1D semiconductors have shown remarkable clinical application potential primarily owing to the advantageous properties arising from their restricted lateral dimensions and unrestricted third dimension. Many morphological variations of 1D semiconductors, including nanotubes, nanorods, nanowires, nanobelts, and nanofibers, can easily be fabricated with different growth techniques. The 1D semiconductors fabricated in different morphologies have been researched for therapeutic performance. Advanced fabrication techniques have made it possible to fine-tune dimensional features thus facilitating the rational design of 1D semiconductors for targeted applications. The electrical, optical, as well as chemical properties, could be finely manipulated to incorporate the desired functionality. The tunable surface chemistry and scope of functionalization of the 1D surface helped to achieve better specificity and compatibility for the targeted applications.

1D semiconductors have the potential to serve as multifunctional materials for future biomedical applications. Most importantly, these systems have dimensional or morphological boon and exhibit excellent performance as cost-effective substitutes for various clinical applications encompassing rapid diagnosis, enhanced detection, and effective treatment options. Completed research in this arena authenticates the scope of using this class of materials for sensing, biofiltration, photoresponsiveness, drug delivery, and tissue engineering. Recent research findings also confirm the possibility of using 1D semiconductors for hybrid therapies by exploring their efficacy for biomolecule loading, light responsiveness, sensing potential, and so on. While exploring the potency of these materials for healthcare applications, it is equally important to monitor their potential toxicity. Thus far, most of the biocompatibility studies involve response analysis over short exposure times. However, with clinical translation being the ultimate target, a more profound scrutinization of the material is required.

Successful translation of 1D semiconductors from a bench research material to an actual clinical substitute still remains a lofty target. But with intense interdisciplinary research, 1D semiconductors could morph into next-generation multimodal materials for a broad spectrum of clinical applications, ranging from point-of-care diagnostics to novel treatment modalities.

References

- Agrawal A, Cho SH, Zandi O, Ghosh S, Johns RW, Milliron DJ (2018) Localised surface plasmon resonance in semiconductor nanocrystals. *Chem Rev* 118(6):3121–3207
- Ahamed M, Akhtar MJ, Raja M, Ahmad I, Siddiqui MKJ, AlSalhi MS, Alrokayan SA (2011) ZnO nanorod-induced apoptosis in human alveolar adenocarcinoma cells via p53, survivin and bax/bcl-2 pathways: role of oxidative stress. *Nanomedicine* 7(6):904–913
- Ahmadzadeh M, Kashi MA, Noormohammadi M, Ramazani A (2021) Small-diameter magnetic and metallic nanowire arrays grown in anodic porous alumina templates anodised in selenic acid. *Appl Phys A* 127(6):1–12
- Alves-Rezende MCR, Capalbo LC, Limírio JPJDO, Capalbo BC, Limírio PHJO, Rosa JL (2020) The role of TiO₂ nanotube surface on osseointegration of titanium implants: biomechanical and histological study in rats. *Microsc Res Tech* 83(7):817–823
- Amann A, Miekisch W, Schubert J, Buszewski B, Ligor T, Jezierski T, Pleil J, Risby T (2014) Analysis of exhaled breath for disease detection. *Annu Rev Anal Chem* 7:455–482
- Balan AP, Radhakrishnan S, Woellner CF, Sinha SK, Deng L, Reyes CDL, Rao BM et al (2018) Exfoliation of a non-van der Waals material from iron ore hematite. *Nat Nanotechnol* 13(7):602–609
- Barth S, Hernandez-Ramirez F, Holmes JD, Romano-Rodriguez A (2010) Synthesis and applications of one-dimensional semiconductors. *Prog Mater Sci* 55(6):563–627
- Brammer KS, Seunghan O, Cobb CJ, Bjursten LM, van der Heyde H, Jin S (2009) Improved bone-forming functionality on diameter-controlled TiO₂ nanotube surface. *Acta Biomater* 5(8):3215–3223
- Cai Q, Paulose M, Varghese OK, Grimes CA (2005) The effect of electrolyte composition on the fabrication of self-organised titanium oxide nanotube arrays by anodic oxidation. *J Mater Res* 20(1):230–236
- Carlsson JO, Martin PM (2010) Chapter 7. Chemical vapor deposition. In: Martin PM (ed) *Handbook of deposition technologies for films and coatings*, 3rd edn. William Andrew Publishing, Boston, pp 314–363
- Choi H, Park S-H (2004) Seedless growth of free-standing copper nanowires by chemical vapor deposition. *J Am Chem Soc* 126(20):6248–6249
- Choi A, Kim K, Jung H-I, Lee SY (2010) ZnO nanowire biosensors for detection of biomolecular interactions in enhancement mode. *Sensors Actuators B Chem* 148(2):577–582
- Choudhary M, Shukla SK, Kumar V, Govender PP, Wang R, Hussain CM, Mangla B (2020) 1D nanomaterials and their optoelectronic applications. In: *Nanomaterials for optoelectronic applications*. Apple Academic Press, pp 105–123
- Chun J, Lee J (2010) Various synthetic methods for one-dimensional semiconductor nanowires/nanorods and their applications in photovoltaic devices. *Eur J Inorg Chem* 2010(27):4251–4263
- Devan RS, Patil RA, Lin J-H, Ma Y-R (2012) One-dimensional metal-oxide nanostructures: recent developments in synthesis, characterisation, and applications. *Adv Funct Mater* 22(16):3326–3370
- Fahmi A, Pietsch T, Bryszewska M, Rodríguez-Cabello JC, Koceva-Chyla A, Arias FJ, Rodrigo MA, Gindy N (2010) Fabrication of CdSe-nanofibers with potential for biomedical applications. *Adv Funct Mater* 20(6):1011–1018
- Feng X, Shankar K, Varghese OK, Paulose M, Latempa TJ, Grimes CA (2008) Vertically aligned single crystal TiO₂ nanowire arrays grown directly on transparent conducting oxide coated glass: synthesis details and applications. *Nano Lett* 8(11):3781–3786
- Flak D, Coy E, Nowaczyk G, Yate L, Jurga S (2015) Tuning the photodynamic efficiency of TiO₂ nanotubes against HeLa cancer cells by Fe-doping. *RSC Adv* 5(103):85,139–85,152
- Gómez S, Vlad MD, López J, Fernández E (2016) Design and properties of 3D scaffolds for bone tissue engineering. *Acta Biomater* 42:341–350
- Gong D, Grimes CA, Varghese OK, Wenchong H, Singh RS, Chen Z, Dickey EC (2001) Titanium oxide nanotube arrays prepared by anodic oxidation. *J Mater Res* 16(12):3331–3334

- Grassin-Delyle S, Roquencourt C, Moine P, Saffroy G, Carn S, Heming N, Fleuriet J et al (2021) Metabolomics of exhaled breath in critically ill COVID-19 patients: a pilot study. *EBioMedicine* 63:103154
- Güniat L, Caroff P, Fontcuberta A, i Morral. (2019) Vapor phase growth of semiconductor nanowires: key developments and open questions. *Chem Rev* 119(15):8958–8971
- Haick H, Broza YY, Mochalski P, Ruzsanyi V, Amann A (2014) Assessment, origin, and implementation of breath volatile cancer markers. *Chem Soc Rev* 43(5):1423–1449
- Henderson MJ, Karger BA, Wrenshall GAW (1952) Acetone in the breath. *Diabetes* 1, No. HS-039 615
- Hong C, Kang J, Lee J, Zheng H, Hong S, Lee D, Lee C (2010) Photothermal therapy using TiO₂ nanotubes in combination with near-infrared laser. *J Cancer Ther* 1:52–58
- Hou J, Yong D, Zhang T, Mohan C, Varghese OK (2019) PEGylated (NH₄)_xWO₃ nanorod mediated rapid photonecrosis of breast cancer cells. *Nanoscale* 11(21):10,209–10,219
- Hsu L-C, Kuo Y-P, Li Y-Y (2009) On-chip fabrication of an individual α -Fe₂O₃ nanobridge and application of ultrawide wavelength visible-infrared photodetector/optical switching. *Appl Phys Lett* 94(13):133108
- Huang MH, Mao S, Feick H, Yan H, Yiying W, Kind H, Weber E, Russo R, Yang P (2001) Room-temperature ultraviolet nanowire nanolasers. *Science* 292(5523):1897–1899
- Huczko A (2000) Template-based synthesis of nanomaterials. *Appl Phys A* 70(4):365–376
- Huo D, Kim MJ, Lyu Z, Shi Y, Wiley BJ, Xia Y (2019) One-dimensional metal nanostructures: from colloidal syntheses to applications. *Chem Rev* 119(15):8972–9073
- Ignarro LJ, Buga GM, Wood KS, Byrns RE, Chaudhuri G (1987) Endothelium-derived relaxing factor produced and released from artery and vein is nitric oxide. *Proc Natl Acad Sci* 84(24): 9265–9269
- Indira K, Kamachi Mudali U, Rajendran N (2014) In-vitro biocompatibility and corrosion resistance of strontium incorporated TiO₂ nanotube arrays for orthopaedic applications. *J Biomater Appl* 29(1):113–129
- Jang J-W, Park J-W (2014) Iron oxide nanotube layer fabricated with electrostatic anodisation for heterogeneous Fenton like reaction. *J Hazard Mater* 273:1–6
- Jin T, Han Q, Wang Y, Jiao L (2018) 1D nanomaterials: design, synthesis, and applications in sodium-ion batteries. *Small* 14(2):1703086
- Jin B, Hejazi S, Chu H, Cha G, Altomare M, Yang M, Schmuki P (2021) A long-term stable aqueous aluminum battery electrode based on one-dimensional molybdenum–tantalum oxide nanotube arrays. *Nanoscale* 13(12):6087–6095
- Kalluru P, Vankayala R, Chiang C-S, Hwang KC (2013) Photosensitisation of singlet oxygen and in vivo photodynamic therapeutic effects mediated by PEGylated W18O₄₉ nanowires. *Angew Chem Int Ed* 52(47):12,332–12,336
- Katwal G, Paulose M, Rusakova IA, Martinez JE, Varghese OK (2016) Rapid growth of zinc oxide nanotube–nanowire hybrid architectures and their use in breast cancer-related volatile organics detection. *Nano Lett* 16(5):3014–3021
- Khot MI, Andrew H, Svavarsdottir HS, Armstrong G, Quyn AJ, Jayne DG (2019) A review on the scope of photothermal therapy–based nanomedicines in preclinical models of colorectal cancer. *Clin Colorectal Cancer* 18(2):e200–e209
- Kim W, Ng JK, Kunitake ME, Conklin BR, Yang P (2007) Interfacing silicon nanowires with mammalian cells. *J Am Chem Soc* 129(23):7228–7229
- Kolmakov A, Moskovits M (2004) Chemical sensing and catalysis by one-dimensional metal-oxide nanostructures. *Annu Rev Mater Res* 34:151–180
- Kong Y, Ma B, Liu F, Chen D, Zhang S, Duan J, Huang Y et al (2019) Cellular stemness maintenance of human adipose-derived stem cells on ZnO nanorod arrays. *Small* 15(51): 1904099
- Law M, Goldberger J, Yang P (2004) Semiconductor nanowires and nanotubes. *Annu Rev Mater Res* 34:83–122

- Lee H, Jung M, Hyunchul O, Lee K (2021) Electrochemical anodic formation of VO₂ nanotubes and hydrogen sorption property. *J Electrochem Sci Technol* 12(2):212–216
- Lefatshe K, Dube P, Sebuso D, Madhuku M, Muiva C (2021) Optical dispersion analysis of template assisted 1D-ZnO nanorods for optoelectronic applications. *Ceram Int* 47(6): 7407–7415
- Li J, Wan W, Zhou H, Li J, Dongsheng X (2011) Hydrothermal synthesis of TiO₂ (B) nanowires with ultrahigh surface area and their fast charging and discharging properties in Li-ion batteries. *Chem Commun* 47(12):3439–3441
- Li H, Liu X, Li L, Xiaoyi M, Genov R, Mason AJ (2017) CMOS electrochemical instrumentation for biosensor microsystems: a review. *Sensors* 17(1):74
- Li Q, Na L, Wang L, Fan C (2018) Advances in nanowire transistor-based biosensors. *Small Methods* 2(4):1700263
- Li H, Tang J, Lin F, Wang D, Fang D, Fang X, Liu W, Chen R, Wei Z (2019) Improved optical property and lasing of ZnO nanowires by Ar plasma treatment. *Nanoscale Res Lett* 14(1):1–8
- Li X, Wang D, Zhang Y, Liu L, Wang W (2020) Surface-ligand protected reduction on plasmonic tuning of one-dimensional MoO_{3-x} nanobelts for solar steam generation. *Nano Res* 13(11): 3025–3032
- Liu L, Sun M, Li Q, Zhang H, Alvarez PJJ, Liu H, Chen W (2014) Genotoxicity and cytotoxicity of cadmium sulfide nanomaterials to mice: comparison between nanorods and nanodots. *Environ Eng Sci* 31(7):373–380
- Liyanage T, Qamar AZ, Slaughter G (2020) Application of nanomaterials for chemical and biological sensors: a review. *IEEE Sensors J*
- Lohani J, Varshney S, Rawal DS, Tyagi R (2019) Vertically aligned nanowires comprising AlGaN/GaN axial heterostructure by convenient maskless reactive ion etching. *Mater Res Exp* 6(10): 105001
- Lu Z, Zhu Z, Liu J, Weihua H, Li CM (2014) ZnO nanorod-templated well-aligned ZrO₂ nanotube arrays for fibroblast adhesion and proliferation. *Nanotechnology* 25(21):215102
- Lu J, Liu H, Zhang X, Sow CH (2018) One-dimensional nanostructures of II–VI ternary alloys: synthesis, optical properties, and applications. *Nanoscale* 10(37):17,456–17,476
- Ma H, Lenz KA, Gao X, Li S, Wallis LK (2019) Comparative toxicity of a food additive TiO₂, a bulk TiO₂, and a nano-sized P25 to a model organism the nematode *C. elegans*. *Environ Sci Pollut Res* 26(4):3556–3568
- Ma Q, Li H, Shushu Chu Y, Liu ML, Xinghua F, Li H, Guo J (2020) In₂O₃ hierarchical structures of one-dimensional electrospun fibers with in situ growth of octahedron-like particles with superior sensitivity for triethylamine at near room temperature. *ACS Sustain Chem Eng* 8(13): 5240–5250
- Maliakkal CB, Tornberg M, Jacobsson D, Lehmann S, Dick KA (2021) Vapor-solid-solid growth dynamics in GaAs nanowires. *Nanoscale Adv* 3:5928–5940
- Manthiram K, Paul Alivisatos A (2012) Tunable localised surface plasmon resonances in tungsten oxide nanocrystals. *J Am Chem Soc* 134(9):3995–3998
- Miles DO, Cameron PJ, Mattia D (2015) Hierarchical 3D ZnO nanowire structures via fast anodisation of zinc. *J Mater Chem A* 3(34):17,569–17,577
- Milla MJ, Barho F, González-Posada F, Cerutti L, Bomers M, Rodriguez JB, Tournié E, Taliercio T (2016) Localised surface plasmon resonance frequency tuning in highly doped InAsSb/GaSb one-dimensional nanostructures. *Nanotechnology* 27(42):425201
- Min Y, Seo HJ, Choi J-J, Hahn B-D, Moon GD (2018) Dimensional and compositional change of 1D chalcogen nanostructures leading to tunable localised surface plasmon resonances. *Nanotechnology* 29(34):345603
- Mohamed MS, Torabi A, Paulose M, Kumar DS, Varghese OK (2017) Anodically grown titania nanotube induced cytotoxicity has genotoxic origins. *Sci Rep* 7(1):1–11
- Mor GK, Varghese OK, Paulose M, Grimes CA (2003a) A self-cleaning, room-temperature titania-nanotube hydrogen gas sensor. *Sens Lett* 1(1):42–46

- Mor GK, Varghese OK, Paulose M, Mukherjee N, Grimes CA (2003b) Fabrication of tapered, conical-shaped titania nanotubes. *J Mater Res* 18(11):2588–2593
- Mor GK, Shankar K, Paulose M, Varghese OK, Grimes CA (2005) Enhanced photocleavage of water using titania nanotube arrays. *Nano Lett* 5(1):191–195
- Mor GK, Shankar K, Paulose M, Varghese OK, Grimes CA (2006) Use of highly-ordered TiO₂ nanotube arrays in dye-sensitised solar cells. *Nano Lett* 6(2):215–218
- Mukherjee N, Paulose M, Varghese OK, Mor GK, Grimes CA (2003) Fabrication of nanoporous tungsten oxide by galvanostatic anodisation. *J Mater Res* 18(10):2296–2299
- Ong KG, Varghese OK, Mor GK, Shankar K, Grimes CA (2007) Application of finite-difference time domain to dye-sensitised solar cells: the effect of nanotube-array negative electrode dimensions on light absorption. *Sol Energy Mater Sol Cells* 91(4):250–257
- Oryan A, Alidadi S, Moshiri A, Maffulli N (2014) Bone regenerative medicine: classic options, novel strategies, and future directions. *J Orthop Surg Res* 9(1):1–27
- Pacholski C, Kornowski A, Weller H (2002) Self-assembly of ZnO: from nanodots to nanorods. *Angew Chem Int Ed* 41(7):1188–1191
- Patolsky F, Timko BP, Guihua Y, Fang Y, Greytak AB, Zheng G, Lieber CM (2006) Detection, stimulation, and inhibition of neuronal signals with high-density nanowire transistor arrays. *Science* 313(5790):1100–1104
- Paulose M, Varghese OK, Mor GK, Grimes CA, Ong KG (2005) Unprecedented ultra-high hydrogen gas sensitivity in undoped titania nanotubes. *Nanotechnology* 17(2):398
- Paulose M, Prakasam HE, Varghese OK, Peng L, Popat KC, Mor GK, Desai TA, Grimes CA (2007) TiO₂ nanotube arrays of 1000 μm length by anodisation of titanium foil: phenol red diffusion. *J Phys Chem C* 111(41):14,992–14,997
- Prakasam HE, Varghese OK, Paulose M, Mor GK, Grimes CA (2006) Synthesis and photoelectrochemical properties of nanoporous iron (III) oxide by potentiostatic anodisation. *Nanotechnology* 17(17):4285
- Prakasam HE, Shankar K, Paulose M, Varghese OK, Grimes CA (2007) A new benchmark for TiO₂ nanotube array growth by anodisation. *J Phys Chem C* 111(20):7235–7241
- Puglisi RA, Bongiorno C, Caccamo S, Fazio E, Mannino G, Neri F, Scalese S, Spucches D, La Magna A (2019) Chemical vapor deposition growth of silicon nanowires with diameter smaller than 5 nm. *ACS Omega* 4(19):17,967–17,971
- Qin P, Maggie Paulose M, Dar I, Moehl T, Arora N, Gao P, Varghese OK, Grätzel M, Nazeeruddin MK (2015) Stable and efficient perovskite solar cells based on titania nanotube arrays. *Small* 11(41):5533–5539
- Rajh T, Dimitrijevic NM, Bissonnette M, Koritarov T, Konda V (2014) Titanium dioxide in the service of the biomedical revolution. *Chem Rev* 114(19):10,177–10,216
- Rajput V, Chaplygin V, Gorovtsov A, Fedorenko A, Azarov A, Chernikova N, Barakhov A et al (2021) Assessing the toxicity and accumulation of bulk-and nano-CuO in *Hordeum sativum* L. *Environ Geochem Health* 43(6):2443–2454
- Rao BM, Torabi A, Varghese OK (2016) Anodically grown functional oxide nanotubes and applications. *MRS Commun* 6(4):375–396
- Roy SC, Paulose M, Grimes CA (2007) The effect of TiO₂ nanotubes in the enhancement of blood clotting for the control of hemorrhage. *Biomaterials* 28(31):4667–4672
- Ruan C, Paulose M, Varghese OK, Mor GK, Grimes CA (2005) Fabrication of highly ordered TiO₂ nanotube arrays using an organic electrolyte. *J Phys Chem B* 109(33):15,754–15,759
- Sadighbayan D, Hasanzadeh M, Ghafar-Zadeh E (2020) Biosensing based on field-effect transistors (FET): recent progress and challenges. *TrAC Trends Anal Chem*:116067
- Sandil D, Sharma SC, Puri NK (2019) Protein-functionalised WO₃ nanorods–based impedimetric platform for sensitive and label-free detection of a cardiac biomarker. *J Mater Res* 34(8):1331–1340
- Sattler KD (ed) (2020) 21st century nanoscience—a handbook: low-dimensional materials and morphologies (volume four). CRC Press

- Shankar K, Mor GK, Prakasam HE, Yoriya S, Paulose M, Varghese OK, Grimes CA (2007) Highly-ordered TiO₂ nanotube arrays up to 220 μm in length: use in water photoelectrolysis and dye-sensitised solar cells. *Nanotechnology* 18(6):065707
- She G, Zhang X, Shi W, Cai Y, Wang N, Liu P, Chen D (2008) Template-free electrochemical synthesis of single-crystal CuTe nanoribbons. *Crystal Growth Design* 8(6):1789–1791
- She G, Lixuan M, Shi W (2009a) Electrodeposition of one-dimensional nanostructures. *Recent Pat Nanotechnol* 3(3):182–191
- She G, Shi W, Zhang X, Wong T, Cai Y, Wang N (2009b) Template-free electrodeposition of one-dimensional nanostructures of tellurium. *Crystal Growth Design* 9(2):663–666
- Shehada N, Cancilla JC, Torrecilla JS, Pariente ES, Brønstrup G, Christiansen S, Johnson DW et al (2016) Silicon nanowire sensors enable diagnosis of patients via exhaled breath. *ACS Nano* 10(7):7047–7057
- Shi J, Wang X (2011) Growth of rutile titanium dioxide nanowires by pulsed chemical vapor deposition. *Cryst Growth Des* 11(4):949–954
- Smok W, Tański T (2021) A short review on various engineering applications of electrospun one-dimensional metal oxides. *Materials* 14(18):5139
- Soopy AKK, Najjar A, Ravau F, Anjum DH (2021) Facile development of InP nanowires via metal-assisted chemical etching and their optical properties. In 2021 6th International conference on renewable energy: generation and applications (ICREGA), pp 25–28. IEEE
- Sun Y, Khang D-Y, Hua F, Hurley K, Nuzzo RG, Rogers JA (2005) Photolithographic route to the fabrication of micro/nanowires of III–V semiconductors. *Adv Funct Mater* 15(1):30–40
- Sutter E, French JS, Sutter P (2021) Tunable layer orientation and morphology in vapor–liquid–solid growth of one-dimensional GeS van der Waals nanostructures. *Chem Mater*
- Tang Z, Kotov NA, Giersig M (2002) Spontaneous organisation of single CdTe nanoparticles into luminescent nanowires. *Science* 297(5579):237–240
- Tereshchenko A, Bechelany M, Viter R, Khranovskyy V, Smyntyna V, Starodub N, Yakimova R (2016) Optical biosensors based on ZnO nanostructures: advantages and perspectives. A review. *Sensors Actuators B Chem* 229:664–677
- Tong T, Shereef A, Jinsong W, Binh CTT, Kelly JJ, Gaillard J-F, Gray KA (2013) Effects of material morphology on the phototoxicity of nano-TiO₂ to bacteria. *Environ Sci Technol* 47(21):12,486–12,495
- Tormo R, Bertaccini A, Conde M, Infante D, Cura I (2001) Methane and hydrogen exhalation in normal children and in lactose malabsorption. *Early Hum Dev* 65:S165–S172
- Varghese O (2016) Exhaled gas detection for medical diagnosis: can it be made a tool for self-screening. *J Nanomed Res* 3(3)
- Varghese OK, Grimes CA (2003) Metal oxide nanoarchitectures for environmental sensing. *J Nanosci Nanotechnol* 3(4):277–293
- Varghese OK, Gong D, Paulose M, Ong KG, Grimes CA (2003a) Hydrogen sensing using titania nanotubes. *Sensors Actuators B Chem* 93(1–3):338–344
- Varghese OK, Gong D, Paulose M, Ong KG, Dickey EC, Grimes CA (2003b) Extreme changes in the electrical resistance of titania nanotubes with hydrogen exposure. *Adv Mater* 15(7–8):624–627
- Varghese OK, Mor GK, Grimes CA, Paulose M, Mukherjeeb N (2004) A titania nanotube-array room-temperature sensor for selective detection of hydrogen at low concentrations. *J Nanosci Nanotechnol* 4(7):733–737
- Varghese OK, Paulose M, Shankar K, Mor GK, Grimes CA (2005) Water-photolysis properties of micron-length highly-ordered titania nanotube-arrays. *J Nanosci Nanotechnol* 5(7):1158–1165
- Varghese OK, Yang X, Kendig J, Paulose M, Zeng K, Palmer C, Ong KG, Grimes CA (2006) A transcutaneous hydrogen sensor: from design to application. *Sens Lett* 4(2):120–128
- Varghese OK, Paulose M, Grimes CA (2009) Long vertically aligned titania nanotubes on transparent conducting oxide for highly efficient solar cells. *Nat Nanotechnol* 4(9):592–597
- Wang J (2009) Biomolecule-functionalised nanowires: from nanosensors to nanocarriers. *ChemPhysChem* 10(11):1748–1755

- Wang W, Varghese OK, Ruan C, Paulose M, Grimes CA (2003) Synthesis of CuO and Cu₂O crystalline nanowires using Cu(OH)₂ nanowire templates. *J Mater Res* 18(12):2756–2759
- Wang W, Varghese OK, Paulose M, Grimes CA, Wang Q, Dickey EC (2004) A study on the growth and structure of titania nanotubes. *J Mater Res* 19(2):417–422
- Wang F, Dong A, Sun J, Tang R, Heng Y, Buhro WE (2006) Solution–liquid–solid growth of semiconductor nanowires. *Inorg Chem* 45(19):7511–7521
- Wang Y, Wen C, Hodgson P, Li Y (2014) Biocompatibility of TiO₂ nanotubes with different topographies. *J Biomed Mater Res A* 102(3):743–751
- Wang F, Dong A, Buhro WE (2016a) Solution–liquid–solid synthesis, properties, and applications of one-dimensional colloidal semiconductor nanorods and nanowires. *Chem Rev* 116(18):10,888–10,933
- Wang Q, Huang J-Y, Li H-Q, Chen Z, Zhao AZ-J, Wang Y, Zhang K-Q, Sun H-T, Al-Deyab SS, Lai Y-K (2016b) TiO₂ nanotube platforms for smart drug delivery: a review. *Int J Nanomedicine* 11:4819
- Wang L, Hao F, Jin Q, Jin H, Haick H, Wang S, Kefu Y, Deng S, Wang Y (2019) Directly transforming SnS₂ nanosheets to hierarchical SnO₂ nanotubes: towards sensitive and selective sensing of acetone at relatively low operating temperatures. *Sensors Actuators B Chem* 292:148–155
- Wei W, Lee K, Shaw S, Schmuki P (2012) Anodic formation of high aspect ratio, self-ordered Nb₂O₅ nanotubes. *Chem Commun* 48(35):4244–4246
- Wijeratne AB, Wijesundera DN, Paulose M, Ahiabu IB, Chu WK, Varghese OK, Greis KD (2015) Phosphopeptide separation using radially aligned titania nanotubes on titanium wire. *ACS Appl Mater Interfaces* 7(21):11,155–11,164
- Williams H, Pembroke A (1989) Sniffer dogs in the melanoma clinic? *Lancet* 333(8640):734
- Wu X, Bai H, Zhang J, Chen F'e, Shi G (2005) Copper hydroxide nanoneedle and nanotube arrays fabricated by anodisation of copper. *J Phys Chem B* 109(48):22,836–22,842
- Xia Y, Yang P, Sun Y, Yiying W, Mayers B, Gates B, Yin Y, Kim F, Yan H (2003) One-dimensional nanostructures: synthesis, characterisation, and applications. *Adv Mater* 15(5):353–389
- Xia H, Feng J, Wang H, Lai MO, Li L (2010) MnO₂ nanotube and nanowire arrays by electrochemical deposition for supercapacitors. *J Power Sources* 195(13):4410–4413
- Xiao L, Yanan Y, Schultz EL, Stach EA, Mallouk TE (2020) Electron transport in dye-sensitized TiO₂ nanowire arrays in contact with aqueous electrolytes. *J Phys Chem C* 124(40):22,003–22,010
- Xu J, Zhou X, Gao Z, Song Y-Y, Schmuki P (2016) Visible-light-triggered drug release from TiO₂ nanotube arrays: a controllable antibacterial platform. *Angew Chem* 128(2):603–607
- Yan S, Shi Y, Xiao Z, Zhou M, Yan W, Shen H, Dong H (2012) Development of biosensors based on the one-dimensional semiconductor nanomaterials. *J Nanosci Nanotechnol* 12(9):6873–6879
- Yang D, Gulzar A, Yang G, Gai S, He F, Dai Y, Zhong C, Yang P (2017) Au nanoclusters sensitized black TiO₂-x nanotubes for enhanced photodynamic therapy driven by near-infrared light. *Small* 13(48):1703007
- Yang B, Myung NV, Tran T-T (2021a) 1D metal oxide semiconductor materials for Chemiresistive gas sensors: a review. *Adv Electron Mater*:2100271
- Yang H-Y, Wang Y-C, Peng H-Y, Huang C-H (2021b) Breath biopsy of breast cancer using sensor array signals and machine learning analysis. *Sci Rep* 11(1):1–9
- Ye K, Wang B, Nie A, Zhai K, Wen F, Congpu M, Zhao Z, Xiang J, Tian Y, Liu Z (2021) Broadband photodetector of high quality Sb₂S₃ nanowire grown by chemical vapor deposition. *J Mater Sci Technol* 75:14–20
- Yoriya S, Paulose M, Varghese OK, Mor GK, Grimes CA (2007) Fabrication of vertically oriented TiO₂ nanotube arrays using dimethyl sulfoxide electrolytes. *J Phys Chem C* 111(37):13,770–13,776

- Zhang Z, Senz S (2013) One-dimensional semiconductor nanostructure growth with templates. In: Zhai T, Yao J (eds) *One-dimensional nanostructures: principles and applications*. John Wiley & Sons, Inc., pp 1–18
- Zhang W-Q, Yang L, Zhang T-K, Weiping X, Zhang M, Shu-Hong Y (2008) Controlled synthesis and biocompatibility of water-soluble ZnO nanorods/au nanocomposites with tunable UV and visible emission intensity. *J Phys Chem C* 112(50):19,872–19,877
- Zhang Z, Zou R, Li Y, Junqing H (2011) Recent research on one-dimensional silicon-based semiconductor nanomaterials: synthesis, structures, properties and applications. *Crit Rev Solid State Mater Sci* 36(3):148–173
- Zhang J, Jian W, Xiong Q (2012) One-dimensional semiconductor nanowires: synthesis and Raman scattering. In: Zhai T, Yao J (eds) *One-dimensional nanostructures: principles and applications*. Wiley, pp 145–166
- Zhao C, Liu Q, Cheung KM, Liu W, Yang Q, Xiaobin X, Man T, Weiss PS, Zhou C, Andrews AM (2020) Narrower nanoribbon biosensors fabricated by chemical lift-off lithography show higher sensitivity. *ACS Nano* 15(1):904–915
- Zheng F, Xi C, Jiahe X, Yi Y, Yang W, Pengfei H, Li Y, Zhen Q, Bashir S, Liu JL (2019) Facile preparation of WO₃ nanofibers with super large aspect ratio for high performance supercapacitor. *J Alloys Compd* 772:933–942
- Zhou J, Ikram M, Rehman AU, Wang J, Zhao Y, Kan K, Zhang W, Raziq F, Li L, Shi K (2018) Highly selective detection of NH₃ and H₂S using the pristine CuO and mesoporous In₂O₃@CuO multijunctions nanofibers at room temperature. *Sensors Actuators B Chem* 255:1819–1830



Prospects of Safe Use of Nanomaterials in Biomedical Applications

3

Damini Verma and Pratima R. Solanki

3.1 Introduction

Nanotechnology is a novel scientific methodology that includes equipment and materials capable of influencing the substance's chemical and physical properties at molecular stages. It has possibly removed the apparent boundaries among chemistry, physics, and biology to a great level and improved the present understanding and ideas. It has been revealed helpful to many specialties, including data management, water purification, drug delivery, and formation of nanomaterials for industrial, healthcare, and other biomedical applications (Mabrouk et al. 2021). At present, various applications like molecular imaging, target-specific drug delivery (Sahoo and Labhasetwar 2003), sensing (Verma et al. 2021a,b), and disease diagnosis (Sri et al. 2019) are laboriously explored. For carrying out these applications, nanomaterials fabrication has got top-priority research aim to develop particular usage in biomedical. In the past years, numerous analyses have been made in nanotechnology applications such as biomedical research (Fig. 3.1), which includes fabrication, manipulation, and visualization of nanomaterials in a range of 1–100 nm scales. These materials have made a remarkable impact on the health of humans as they are continuously used in therapeutic and diagnostic applications, having the potential to revolutionize biomedicine (Samal and Manohara 2019).

The field of biomedicine has made many advancements. However, there are still numerous significant challenges that continue to create problems in translating a biomedical understanding of disease markers into clinically significant devices that could be utilized for monitoring or diagnostic tools for disease management. Developing adequate analytical methods for detecting biomarkers and others is vital, and,

D. Verma · P. R. Solanki (✉)

Special Centre for Nanoscience, Jawaharlal Nehru University, New Delhi, India

e-mail: partima@mail.jnu.ac.in

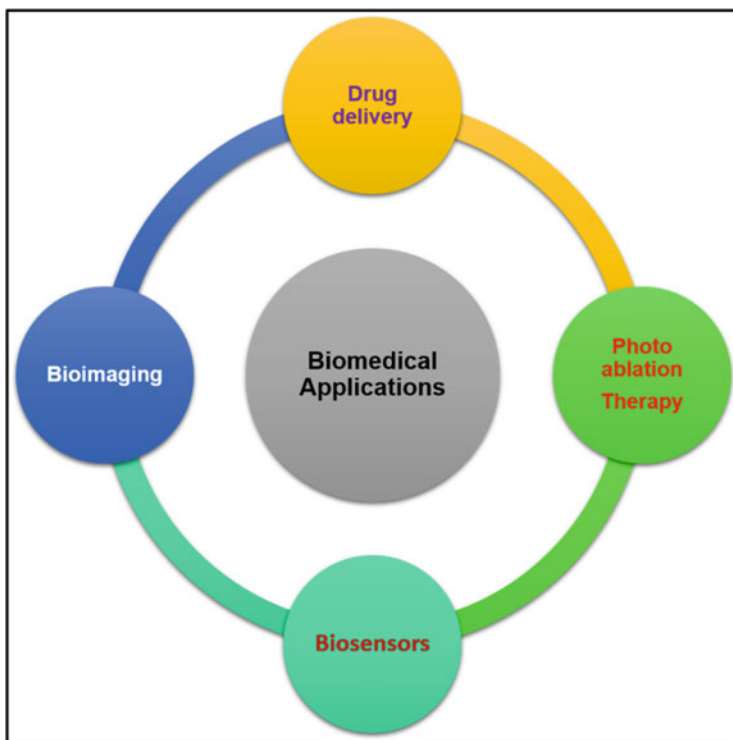


Fig. 3.1 The biomedical applications arising from nanotechnology

therefore, challenging. Though many conventional analytical techniques are employed for the detection of numerous biomarkers due to expensive, lengthy-time procedures, more human resources, and lack of onsite detection, it has restricted its use (Kolch et al. 2005; Mateos et al. 2005; Collier et al. 2011; Dalle-Donne et al. 2003; Chen et al. 2008b). On the other hand, biosensors have emerged to be excellent techniques as they offer many benefits over the traditional methods like direct and real-time detection, cost-effectiveness, small size, sensitivity, portability, and high specificity (Chauhan et al. 2021; Yadav et al. 2020, 2021; Lakshmi et al. 2021). These biosensors having the biological recognition component are essential for monitoring and detecting the biomarkers concerned with biochemical or physiological processes attached to the physiochemical transducer, converting the recognition signal to a detectable output signal. Recently, the fast development of biosensors based on novel nanomaterials in the biomedical field has been designed for sensitive detection of the target analyses and for determining the non-target molecules. It is well-known that nanomaterials display remarkable physical properties in the nano range that differentiate them from bulk and molecular scales, opening innovative biomedical applications and research prospects. Nowadays, the rapid detection of disease biomarkers has become a need to provide information regarding the primary

mechanism of disease initiation that provides a potent tool for defining the exact state of disease for early treatment (Swierczewska et al. 2012; Stern et al. 2010). Hence, developing a biosensor for disease biomarkers has become essential for detecting abnormal proteins or genes at deficient levels, as numerous biomarkers exist at trace levels at initial disease phases. In addition, biosensors have proved to be more scalable and handy for point-of-care (POC) sample studies and real-time analysis. We believe that this chapter highlights the advancement of biosensors for their applications in the biomedical field based on nanomaterials to detect cancer biomarkers such as cytokeratin fragment-21-1 (Cyfra-21-1), interleukin (IL-8), and vitamin D₃. Also, this chapter describes the use of carbon quantum dots for bioimaging of cancerous cells, along with a briefing about the biosensors, nanomaterials, and functionalization of nanomaterials.

3.2 Biosensors

These days, biosensors have become universal for biomedical diagnosis and other broad areas like biomedical and forensics research, drug discovery, food control, environmental monitoring, disease progression, and endpoint-of-care monitoring. Many techniques are being employed for biosensor development utilizing nanomaterials. Typically, the biosensors consist of three parts: the bio part recognizes the analyte; the transducer transforms this analyte detection into output. The output system amplifies and shows the result in a suitable format as shown in Fig. 3.2 (Collings and Caruso 1997). Several types of transducers depend upon the various ways of sending signals, i.e., the conversion of biological sensing analyte to a measurable signal, like mass or thermal, photonic, and electronic signal. (Wu et al. 2013; Gao et al. 2013).

Moreover, this could be divided into thermal, surface acoustic wave, piezoelectric, mechanical, optical, field-effect transistor (FET), electrochemical (Higgins and Weetall 1998; Jain 2007), and so on. Furthermore, there are three divisions of

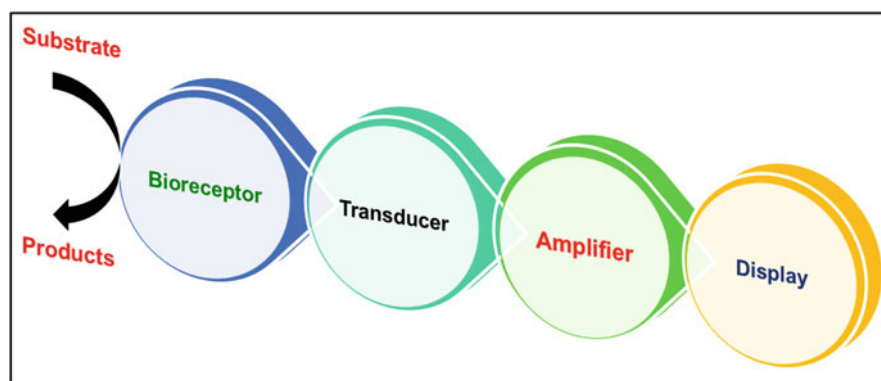


Fig. 3.2 Components of biosensors

biosensors based on the recognition elements: tissue, cellular, and molecular biosensors (such as ion or enzyme channels, nucleic acids, and antibodies.) (Jiang and Wang 2012; Chang et al. 2011). The first two bioreceptor elements depend on the organisms. At the same time, the latter is immobilized biological constituents whose coupling using high-affinity biomolecules permits the selective and sensitive determination of many analytes. Among the various biosensors, electrochemical biosensors are analytical devices that convert the biochemical signals like the reaction between enzyme-substrate and interaction among the antigen-antibody into the electrical signals (like impedance, voltage, current, etc.) (Li et al. 2017a; Zheng et al. 2013). Since Clark established the first variety of electrochemical biosensors to detect blood glucose, numerous biosensors have been sequentially introduced and marketed for different applications (Clark Jr and Lyons 1962). For the electrochemical biosensor, the electrode is an essential element utilized as a solid substrate for immobilizing the biomolecules such as nucleic acid, antibody, and enzyme for transferring electrons. Numerous methods are being used for chemical modification that is based on the chemical groups present on electrode surface having the existence or non-existence of supporting materials through thiol (maleimide), aldehyde (hydrazide), carboxyl, and amine (1-ethyl-3-(3-dimethylaminopropyl) carbodiimide: EDC), etc. (Wang and Dai 2015; Krishnan et al. 2019; Kafi and Crossley 2013). As unsuitable immobilization might result in low biocompatibility, less specificity, and loss of activity, it is essential to adequately immobilize the biomolecule, not only for maintaining the biological activity but also for the appropriate orientation of the biomolecules.

Moreover, selecting suitable functional material is vital for the electrode to achieve high biosensor performance. Recently, numerous biosensing approaches have been used to get miniaturized and simple analytical devices for onsite examination that substitute the profitable laboratory instruments made for well-known *in vitro* studies. In addition, the working principle of electrochemical biosensors depends upon the transducer element, which is enclosed by biorecognition elements. This biorecognition element on interaction with the target analyte produces a chemical signal. Later, the electrochemical transducer converts the chemical signal into the electrical one linked with the quantity of the target analyte. Depending upon the nature of electrochemical methods such as amperometric, voltammetric, and potentiometric, the transducer is then utilized finally to detect target analytes.

3.3 Nanomaterials

Nanomaterials are those materials whose at least one dimension falls in the range of 1–100 nm. They have significantly smaller sizes, mostly their constituent-like molecules or atoms are placed on their surface, providing remarkable difference from the same bulk materials in their basic physicochemical properties. Another aspect is the quantum effects that result in remarkable differences in the features of nanomaterials that arise from irregular performance due to the quantum confinement of moving electrons (Baig et al. 2021). Depending on the chemical constitution,

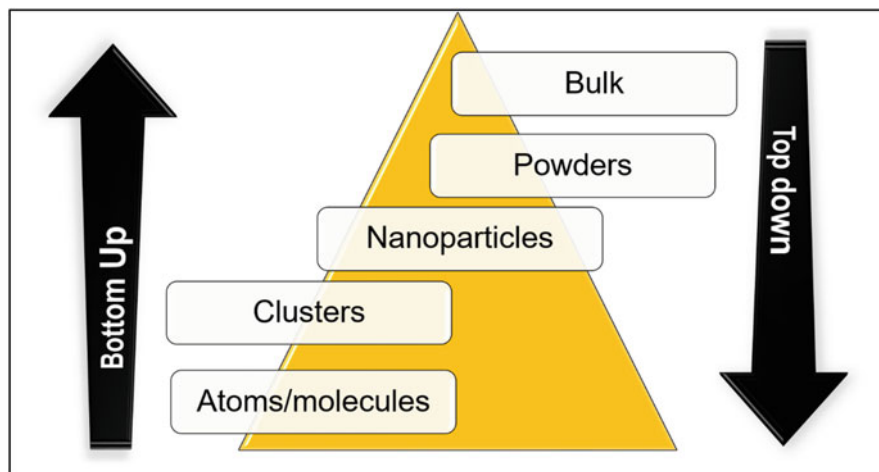


Fig. 3.3 Synthesis of nanomaterials by two chief approaches: bottom-up and top-down

nanomaterials can be possibly classified into various categories such as (i) Carbon allotrope-based nanomaterials (comprising of carbon atoms only), (ii) inorganic nanomaterials like metallic/nonmetallic elements, and (iii) organic nanomaterials (including majorly polymeric nanomaterials like cellulose). The nanostructured materials are essential for a biosensor as they have several advantages associated with it like high specific surface area, negligible enlargement in both nonaqueous and aqueous solutions in comparison to organic polymers, high electron communication, high adsorption capability, electrochemical activity, high chemical stability, and biocompatibility. The fabrication of nanomaterials could be done by employing two chief approaches, i.e., bottom-up and top-down approaches, as presented in Fig. 3.3 (Kolahalam et al. 2019). In the latter approach, smaller nanoparticles are formed using a macroscale machine designed to control the fabrication of an exact copy with a smaller dimension. This small structure again underwent the same process to form an even smaller composition, and this procedure is subsequently repeated until the structure of nanoscale sizes is attained. In the former approach, large structures are made by assemblage of individual molecules or atoms through supramolecular chemistry, scanning probes, or biotechnology. However, both of the methodologies mentioned above show a significant part in nanomaterial synthesis utilized for biosensors; the bottom-up approach discovers more importance in the application.

3.3.1 Surface Functionalization of Nanoparticles

The biological interaction occurs at the electrode surface in the case of all the electrochemical biosensors to detect the analyte. The cost, specificity, reusability, stability, and sensitivity of the biosensor could be affected by the biorecognition

element and its availability or reactivity. Provided the efficient mechanism for electrochemical biosensors, suitable modification at the electrode surface is vital for its performance. The surface modifications at the electrode not merely aid unsuitable bio-receptor immobilization but also provide high sensitivity and control noise. The surface functionalization aids in removing the unwanted or nonspecific attachment of the analyte or other constituents on the electrode surface.

Furthermore, the alignment of biomolecules on the electrode surface has a crucial role in describing the selectivity and sensitivity of a biosensor. This shows that biosensors' performance relies on various materials utilized for functionalizing the surfaces and the modification approach or the surface chemistry employed for immobilizing the bio-receptors. Numerous nanomaterials have been used for the electrode in the electrochemical biosensors, such as nanocomposites, polymers, cerium oxide, graphene, carbon nanotubes, lanthanum, reduced graphene oxide, etc. Many modification techniques are reported and assessable from previous literature, using various nanomaterials showing distinct performance of biosensors. The selection of immobilizing methods for the nanomaterials is based on the substrate used.

The surface modification of nanostructured materials is necessary due to their limited behavior in various solvents thereby improving the solubility in aqueous solution; hence, its surface functionalization becomes vital for nanomaterials. It is usually done to attain anticorrosive, conductive, hydrophobic, or hydrophilic properties of nanoparticles. The functionalization has even proven to help reduce toxicity and make eco-friendly nanomaterials. Moreover, surface modification improves the multiple attachment sites for enhanced capacity of adsorption.

Over the past decades, much curiosity has been developed for functionalizing the inorganic nanoparticles with hydroxyl, carboxylic, and amine groups showing their promising application for clinical and drug delivery diagnosis. The surface of nanomaterials is modified with these functional groups, which requires additional modification with other preferred biomolecules, providing an enhanced platform for biosensing as electrochemical and lab-on-chip devices. The chemicals that are found to be used for the *ex situ* functionalization of nanomaterials are olylamine, citric acid, oleic acid, polyethylene glycol, 3-aminopropyl triethoxysilane (APTES), 3-mercaptopropyl trimethoxysilane, etc. (Chen and Chatterjee 2013; Hsiao et al. 2007; Kumar et al. 2016a; Kaushik et al. 2009; Xu and Sun 2007). However, these chemical reagents have an adverse impact indirectly or directly on human health and also the *ex situ* functionalization need and additional stage in the procedure, leading to aggregation (Vashist et al. 2014). For avoiding these problems, biomolecules such as amino acids, which are nontoxic and enable the improvement of nanomaterials functionalization and immobilization of preferred biomolecules, have stood quite promising to be used for the fabrication of biosensor and its application. Amino acids are organic composites with amine carboxylic acid ($-\text{COOH}$) and ($-\text{NH}_2$) as functional groups accompanied by specific side chains. For example, L-Cysteine (Cys) is one of the proteinogenic amino acids that occurs naturally and nontoxic, having $-\text{NH}_2$, $-\text{COOH}$ functional groups with sulfur ($-\text{S}$) groups in the side chain, making it a promising binder for achieving a stable functionalization in case of metal

oxide, especially along with the preferred biomolecules (nucleic acid, antibodies, and so on) (White et al. 1959). It has been employed as a stabilizing agent for nanomaterials by several researchers, majorly for biomedical research and the environmental field. Similarly, some more instances of functionalized nanomaterials for biosensor application and others are described here: L-cysteine functionalized carbon dots for bioimaging in cancerous cell lines (Sri et al. 2018), L-cysteine functionalized lanthanum hydroxide-based electrochemical biosensor for detection Of Cyfra-21-1 (Tiwari et al. 2017), L-cysteine functionalized magnetite nanoparticles ($\text{Fe}_3\text{O}_4\text{Nps}$) for absorption of lead and chromium from water (Bagbi et al. 2017), oxalic acid coated with iron oxide nanorods was employed as a sensing platform for detection of *V. cholerae* (Sharma et al. 2015), so on.

3.4 Cancer Biomarkers

The initial diagnosis of biomarkers has become the preliminary and preferred approach to analyze or determine the disease state in the human body as the change in concentration of biomarkers has a straight connection with the disease. The early analysis of the disease environment could aid in timely medical treatment and a rise in survival rate (Tiwari and Solanki 2015). The biomarkers are discharged into the body fluids with different measurable levels, i.e., Fg to $\mu\text{g mL}^{-1}$. Mostly, these biomarkers are found in less quantity in the case of a healthy individual; however, these amounts are enhanced accordingly with disease advancement in a diseased person. The initial disease development could be examined with the help of a specific biomarker approximation (Soper et al. 2006; Wang 2006).

On the other hand, the minor traces of biomarkers needs a highly sensitive and more accurate method that could deliver a user-friendly, cost-effective, and easy way, resulting in minimal invasive or noninvasive sample collection procedure in body fluids. As stated previously, numerous researchers have put much effort into developing many biosensors for fulfilling the needs like non-invasive, reliable, user-friendly, fast, and accurate biosensors for detecting cancer (Kumar et al. 2016b; Li and Yang 2011; Malhotra et al. 2010; Nagler et al. 2006). The presence of many cancer biomarkers in saliva, tears, sweat, and urine can be utilized as an analytical sample for non-invasive determination. Few oral cancer biomarkers like Cyfra-21-1, endothelien 1 (ET-1), IL-1, IL-6, IL-8, vascular endothelial growth factor, and epidermal growth factor receptor are secreted into patients' saliva suffering from oral cancer (Bano et al. 2015). Out of these, Cyfra-21-1 fragments of 40 KD cytokeratin 19, which is an acidic protein biomarker with a cut-off range of 3.8 ng mL^{-1} found in oral cancer. However, in oral cancer patients, its quantity reaches $17.46 \pm 1.46 \text{ ng mL}^{-1}$. Numerous research has reported its specific cut-off level, i.e., 3.8 ng mL^{-1} , that can be utilized to identify cancerous conditions (Jose et al. 2013; Kumar et al. 2016a).

3.4.1 Lanthanum Hydroxide Nanoparticles (La(OH)₃) Based Electrochemical Biosensor for Detection of Cyfra-21-1 Cancer Biomarker

Recently, the biomedical uses of rare-earth hydroxide and metal oxide have attained considerable interest in researches owing to their electrochemical properties, excellent electrocatalytic, oxygen ion mobility, and negligible toxicity (Singh et al. 2013; Wang et al. 2009). Among the various rare-earth metal hydroxides, lanthanum hydroxide (La(OH)₃) consists of lanthanum ions [La (III)] that displays the unique chemical coordination capability, electrochemical inertia, high surface area-to-volume ratio, chemical and physical properties (Liu et al. 2008; Wang et al. 2009). The electrochemical properties of La(OH)₃ are predominately owing to the transition of electrons within the 4f shell. The electrocatalytic behavior, surface basicity, and electron transfer mobility provide a favorable environment for these materials to be used in biosensing applications (Liu et al. 2008). Moreover, La(OH)₃ offers additional free adsorption or binding locations (Zhang et al. 2012) for molecules such as L-Cysteine (Cys) that result in better biomolecules (antibodies) attachment with high shelf-life of biosensing electrode.

Considering this, Tiwari et al. (Tiwari et al. 2017) prepared L-cysteine capped lanthanum hydroxide nanoparticles [Cys-La(OH)₃NPs] through a one-step, simple method for fabricating a label-free and highly sensitive biosensor for detection of oral cancer biomarker, i.e., Cyfra-21-1 found in the saliva of oral cancer patients. For this, an amino acid such as Cys was employed as a linker molecule to cap the La(OH)₃NPs. The thin films of Cys-La(OH)₃NPs were deposited electrophoretically on indium tin oxide (ITO) glass substrate by using the technique of electrophoretic deposition (EPD) for 2 min at 30 V. Then functionalization of anti-Cyfra-21-1 with N-ethyl-N-(3-dimethyl aminopropyl) carbodiimide hydrochloride and N-hydroxysuccinimide (EDC-NHS) was done subsequently. Also, bovine serum albumin (BSA) was taken as a blocking agent for covering the matrix area of the electrode surface. The BSA/anti-Cyfra-21-1/Cys-La(OH)₃/ITO immunoelectrode showed enhanced electrochemical response against Cyfra-21-1 concentration having linearity in the range of 0.001–10.2 ng mL⁻¹, the limit of detection of 0.001 ng mL⁻¹ and high sensitivity of 12.044 μA (ng per mL cm⁻²)⁻¹, in comparison with earlier reported biosensors as well as commercially existing ELISA kit (Kinesis DX). The specificity of the biosensor was performed in the presence of the analytical species found in saliva having different concentrations such as glucose (7 mg mL⁻¹), potassium chloride (8.38 mM), sodium carboxymethyl cellulose (10 mg mL⁻¹), sodium chloride (20 mM), CA125 (5 ng mL⁻¹), and IL-8 (13 pg mL⁻¹) and have the stability of 17 weeks. Thus, this Cys functionalized La(OH)₃ presented a new route for developing highly sensitive biocompatible, ex situ, and in situ biochips and biosensors devices.

3.4.2 Detection of Cyfra-21-1 Cancer Biomarker Using Cubic Cerium Oxide–Reduced Graphene Oxide (CeO₂–RGO) Nanocomposite–Based Electrochemical Biosensor

The nanocomposite of Cerium Oxide–Reduced Graphene Oxide (CeO₂–RGO) has been considered a promising electrochemical platform because of its conducting nature of RGO and highly exposed surface area that leads to rapid transfer of electrons between the electrolyte and electrode, causing improved catalytic efficacy (Srivastava et al. 2013; Solanki et al. 2008; Strobel et al. 2014; Khan et al. 2017; Saha et al. 2009; Cheng et al. 2011; Jiang et al. 2012). The rise in oxygen (O₂) moieties of CeO₂–RGO nanocomposite is amplified due to the restacked RGO, leading to improved stability of nanocomposite. Moreover, the benefits of both RGO sheets and CeO₂ have led to enhanced oxygen vacancy in CeO₂ and RGO conductivity due to the synergistic effect that could be fully used by employing this nanocomposite (Jiang et al. 2012; Huang et al. 2014). Apart from this, the CeO₂ fixed RGO matrix was also used for other applications such as energy storage (Yang et al. 2013), photocatalysis (Liang et al. 2010), electro-catalysis (Wu et al. 2012), high affinity (Cheng et al. 2012), and electrochemical studies (Li et al. 2012b).

Pachauri et al. developed an electrochemical sensing platform consisting of a novel nanocomposite of cerium oxide nanocubes (ncCeO₂)–reduced graphene oxide (RGO) for Cyfra-21-1 detection, i.e., the biomarker of oral cancer (Shaloo and Sakshi 2020). The nanocomposite of CeO₂–RGO was synthesized by reducing the graphene oxide (GO) in situ through hydrazine hydrate in the presence of ncCeO₂. The thin and smooth films of ncCeO₂–RGO nanocomposite were deposited onto the ITO-coated glass using the spin coating technique and further utilized to co-immobilize the particular antibody of Cyfra-21-1 through the EDC–NHS coupling agents. This BSA/anti-Cyfra-21-1/ncCeO₂–RGO/ITO immunosensor after experimental optimization has displayed enhanced parameters of sensing like high sensitivity (14.5 mA ng¹ mL cm²), low LOD (0.625 pg mL¹), and broad linear range from 0.625 pg mL¹ to 15 ng mL¹ for detection of Cyfra-21-1. This biosensor showed good selectivity against Cyfra-21-1 in the presence of IL-8, mucin 16 (MUC-16), sodium chloride (NaCl), and glucose. Therefore, the nanocomposite of CeO₂–RGO could be considered a potential medium for application in electrochemical biosensors.

3.4.3 RGO Modified Mediator Paper-Based Electrochemical Biosensor for IL-8 Cancer Biomarker Detection

Over the years, paper-based techniques have been well-known and followed by large-scale to small industries to commercialize the devices as paper-based point-of-care (POC) devices have disposable, environment-friendly, low cost, and accessible synthesis properties. Numerous researchers have presented paper-based tools for POC analysis, comprising biosensors (Hu et al. 2009, 2010; Chen et al. 2008a; Compton et al. 2010) to detect multiple analytes using electrochemical or

microfluidic methods (Silveira et al. 2016; Cinti and Arduini 2017). Diverse materials like carbon-based materials, metal, polymers, or conductive ink (Gonçalves et al. 2017) have been brought into usage for paper substrate employing highly sophisticated tools that include conductive inkjet printing (Hu et al. 2009; Lesch et al. 2017) as well as screen printing (Abellán-Llobregat et al. 2017), making it an appropriate substrate for electrochemical devices. Therefore, there seems to be a wide area to discover new strategies for making paper-based substrates more conductive for their use in electrochemical devices.

Dave et al. (Dave et al. 2019) developed a cost-effective, convenient, simple, and novel synthesis approach for fabricating a conductive RGO paper-based electrochemical immunosensor against cancer biomarker IL-8 detection. The conductivity of RGO paper was estimated to be 0.86 S cm^{-1} and the sensing platform was made onto the ivory paper through in situ GO reduction. This conductive paper was then utilized for depositing the cysteine-capped gold nanoparticles (Cys-AuNPs) through EPD at 60 V for its further use in biosensors. The BSA-Ab-CysAuNPs-RGO immunosensor was based on the chronoamperometry technique, transferring the electrons directly deprived of any mediator. This Cys-AuNPs-RGO paper offers suitable sites for the attachment of monoclonal antibody (Ab) which is particular to IL-8. The paper-based electrode provides a remarkable linearity range from 1 to 12 pg mL^{-1} , the sensitivity of $10.93 \text{ } \mu\text{A mL pg}^{-1} \text{ cm}^{-2}$ with a low LOD of 0.589 pg mL^{-1} . Thus, this platform can replace commercially existing electrodes such as fluorine-doped tin oxide (FTO), gold, glassy carbon, and ITO-coated glass substrates for its use in electrochemical and electronic applications, comprising POC devices.

3.5 Vitamin-D₃ Biomarker

Vitamin-D₃ (Vit-D) deficiency is a universal health problem in humans, almost found in persons of any age group. It plays an essential part in bone metabolism. However, its shortage leads to many severe health problems such as osteomalacia, rickets, and bone-related disease in the case of adults and children, respectively. Recently, the research reports of low Vit-D levels have shown an association with neuropsychiatric disorders (Ozbakir et al. 2015) (Alzheimer's, Parkinson's, and depression disease), cardiovascular disease (Judd and Tangpricha 2009), cancer risks, and diabetes type-2 (Dalgård et al. 2011). Among the various forms of Vit-D, i.e., Vit-D₂, Vit-D₃ (Fig. 3.4), the most desirable form is Vit-D₃, measured in serum samples (Armas et al. 2004). Also, among the different metabolites of Vit-D, only 1,25(OH)₂D and 25-hydroxy vitamin-D₃ (25-OHD₃) gain importance in measuring levels of Vit-D in samples of serum, and the deficiency of Vit-D is completed utilizing assays for 25-OHD₃ (Yin et al. 2019; Ozbakir et al. 2015). Thus, a broad possibility arises for making a simple, disposable, and economic biosensing platform to detect 25-OHD₃.

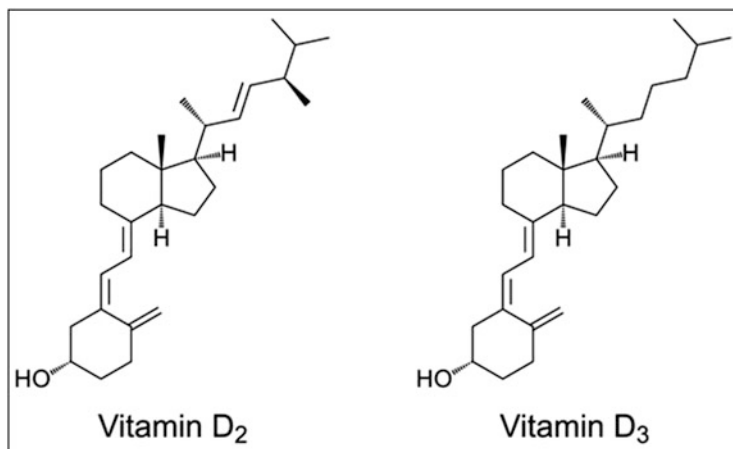


Fig. 3.4 Two different forms of Vitamin D, i.e., Vitamin D₂ and D₃

3.5.1 Insoluble and Hydrophilic Electro Spun Cellulose Acetate Fiber-Based Electrochemical Biosensor for 25-OHD₃ Biomarker Detection

The demand for cellulose acetate (CA) is increasing for its use in industries as it is a biodegradable organic polymer with promising properties such as chemical and thermal stability, high binding affinity with other substances, cheap, and biocompatibility. The cellulose acetate fibers (CAEFs) at the nanoscale also have several benefits like higher interconnectivity, unique one-dimensional configuration, and high surface area (Balasubramanian 2010; Sun et al. 2015). These features of CAEFs assure different biomedical applications that include tissue engineering, antimicrobial membranes, wound dressing, drug delivery, biosensors, and affinity membrane to immobilize the biomolecule (Awal et al. 2011, 2009; Bhardwaj and Kundu 2010; Lee et al. 2009). The fibers offer an interconnected 3D structure with more capturing and binding sites than commercially existing membranes (Thavasi et al. 2008; Mertz et al. 2011), providing better biomolecule immobilization for enzymes, DNA, and antibodies. The oxygen moieties and functional groups present on CAEFs are highly likely to attach with hydrogen-containing molecules (biomolecules) through intermolecular hydrogen bonding to detect the analyte, comprising Vit-D. For fabricating the fibers, many techniques are being used (Fang et al. 2008); however, electrospinning is the most versatile and suitable tool as it provides benefits of being synthesized at a large scale, having a low cost, relatively fast, and easy process. Considering this, Chauhan et al. have developed a disposable, eco-friendly, low cost simple conducting paper (RCP) which is decorated with electrospun cellulose acetate fibers (CAEFs) for its use in a biosensor to detect 25-OHD₃ (Chauhan and Solanki 2019). The electrospinning technique was used to fabricate CAEFs collected on RCP directly having a tip-to-collector distance of

15 cm, a flow rate of 0.2 mL h^{-1} , at a voltage of 16 kV. The AB concentration (AB-25OHD₃) was estimated after optimization as $50 \text{ } \mu\text{g mL}^{-1}$ for 25OHD₃ bio-marker, and then modification of CAEF/RCP electrode was done with AB-25OHD₃ followed by BSA (blocking agent for matrix) to fabricate BSA/AB-25OHD₃/CAEF/RCP immunoelectrode for determine 25-OHD₃. The chronoamperometry response study was carried out for immunoelectrode against the detection of 25-OHD₃ that displays the linear range of $10\text{--}100 \text{ ng mL}^{-1}$, the sensitivity of $0.16 \text{ } \mu\text{A ng}^{-1} \text{ mL cm}^{-2}$, and lowest LOD of 10.0 ng mL^{-1} . Also, the immunoelectrode showed no interference while detecting 25-OHD₃ and presented satisfactory results of validation studies, carried out using the ELISA kit. Therefore, the CAEFs showed the potential to detect 25-OHD₃ successfully and could be further utilized for monitoring the delivery/release system of biomedical uses.

3.6 Carbon Dots (CDs) for Bioimaging Applications in Cancerous Cells

Carbon Dots (CDs) are new family members of the carbon group that have attained massive interest due to their biocompatibility, excellent photo-stability, and ultra-small size, along with their fluorescent properties. They are highly biocompatible and zero-dimensional compared to metal-based quantum dots (QDs) (Li et al. 2012a; Wolfbeis 2015). Also, the CDs display non-blinking photoluminescence that makes them valuable over the organic dyes. Though several methods are reported for synthesizing the CDs, utilization of green precursors gains importance owing to its easy availability. For example, mango leaf (Kumawat et al. 2017), corn flour (Wei et al. 2014), ginkgo fruits (Li et al. 2017b), watermelon, sesame oil, aloe vera, garlic, coriander leaf, eggshell membrane, orange, honey juice, meat, hair fibers, saffron, apple juice, pulp, are being used to synthesize CDs (Wu et al. 2017; Sharma et al. 2017). However, CDs need rigorous steps of purification and also have low fluorescence in comparison to CDs manufactured via organic precursors (Lim et al. 2015). Thus, organic precursors become the top choice for the preparation of CDs having high purity and yields.

Moreover, it is well recognized that the zwitterionic surface of CDs delivers a superior platform compared to its equivalents for bioconjugation to take place in the presence of numerous analytes devoid of any accumulation (Jung et al. 2015; Cheng et al. 2014). The CDs bearing negative charges are associated with a low fluorescent quantum yield of neutral or positive species. Also, the CDs carrying the positive charge are found to be less biocompatible. Thus, these zwitterionic properties of the CDs improve the biocompatibility and fluorescent quantum yield. These zwitterionic particles adsorb proteins on their surface, less specifically, so that they can rapidly be taken into cytosol without any agglomeration problem (Verma and Stellacci 2010). In addition, due to rich carboxylic moieties on CD surface, these can bioconjugate easily with different biomolecules like enzymes, aptamers, antibodies, etc. (Motaghi et al. 2017; Li et al. 2010; Posthuma-Trumpie et al. 2012; Bu et al. 2014). On the interaction of zwitterionic particles with the microenvironment of cancer cells, they

discard its anionic element, creating a positive charge on its surface and thereby improving its entrance into the cells (Behzadi et al. 2017). Hence, the CDs, due to their beneficial property, could be used for various biomedical applications.

It is usually reported without a doubt that cancer is the deadliest disease that occurs in humans in their lifetime. Identifying cancer in the initial stage for its diagnosis remains a significant challenge. Surplus studies have been dedicatedly done to diagnose the initial stage that targets anti-cancerous drugs. The sixth most commonly found cancer is oral cancer (Chiou et al. 2008), which generally occurs in Asian countries, mainly South Asia, due to the high consumption of oral tobacco like smoking, cigarette, quid, and beetle (Rao et al. 2013). Mostly, 90% of oral cancer occurs from the epithelial lining of the oral cavity, known as Oral Squamous Cell Carcinoma (OSCC). Thus, there arises a need to diagnose initially for improving the OSCC prognosis. Imaging intracellular tissues, cells, and compartments permit them to treat and diagnose the disease accurately. Therefore, fluorescent imaging techniques can be utilized for real-time monitoring of tissue samples in patients cells suffering from cancer.

Since their unexpected finding, CDs have predominantly been utilized for photocatalysis, therapeutic vehicle, biosensing, and bioimaging. CDs have been extensively explored for bioimaging in different cell lines (cancerous and noncancerous) and bacteria (Song et al. 2014). Sri et al. have synthesized excellently photostable, highly biocompatible sulfur and nitrogen comprising novel zwitterionic carbon dots (CDs) via microwave-assisted procedure (Sri et al. 2018). The estimated size of CDs was in the range of 2–5 nm (having an average size, i.e., 2.61 ± 0.7 nm). These CDs displayed a highly fluorescent nature in UV light at even lower concentrations along with an excitation-independent photoluminescence behavior. In addition to its fluorescent nature, it even showed a quantum yield of as high as 80%, i.e., equivalent to the organic dyes.

Further, these CDs were utilized for imaging two distinct cell lines of oral cancer like Cal-27 (Human Tongue Carcinoma) and FaDu (Human Pharyngeal Carcinoma). The high biocompatibility of CDs displayed by the cell viability assay was further proved through side scattering analysis as no other alteration was seen even at the maximum concentration (1600 $\mu\text{g/mL}$) in the granularity. The production of Reactive Oxygen Species (ROS) was also studied, and insignificant generation of ROS was noticed. Furthermore, the uptake phenomenon, the analysis of exocytosis, cell cycle, and cellular uptake in the presence of ATP inhibitor at 4 °C have also been examined. These results showed that CDs could simply move across the plasma membrane without damaging the integrity of the cell. Thus, highly biocompatible, fluorescent, and novel CDs were made to diffuse very quickly passively out and into the cytoplasm, providing a fast and reliable assay for monitoring cancer in the initial stages.

3.7 Conclusion

The recent advancement of biosensors based on nanotechnology has emerged and displayed a promising approach for monitoring, analyzing, and detecting the analytes concerned with biochemical or physiological processes in the biomedical field. A rise in the number of researches has shown that biosensors predominantly have many benefits like being highly sensitive, cheap, and portable for monitoring or diagnosis of diseases and other biomedical applications. These nanomaterials, by the combination of high surface area and small size, provide many fascinating piezoelectric, optical, and electromagnetic properties having massive potential for its use in the field of biosensing, healthcare diagnostics, bioimaging, and medical diagnostics. This chapter highlighted the highly specific and sensitive biosensors using nanomaterials employed for rapid detection of biomarker levels and discriminated among the unfavorable and favorable results of diseases (particularly cancers, Vitamin D₃), guiding its further treatment. In addition, CQDs, on the other hand, have been described for bioimaging the cancerous cells synthesized via microwave-assisted technique.

Though the existing sensitivities of biosensors have been found under the optimized situations of the laboratory, their utilization at a commercial scale remains a challenge for researchers. Furthermore, a vital need arises to see the interaction processes occurring between the biomarkers and nanomaterials in diverse biological microenvironments. At last, huge emphasis needs to be given to the approach utilized for improving the performance of biosensors currently for its application in the biomedicine field. The challenges and trends should be predicted for the upcoming time.

Acknowledgments These works were financially supported by the DBT Indo-Russia project (DBT/IC-2/Indo-Russia/2017-19/02), Department of Biotechnology (Project BT/PR10638/PFN/20/826/2013), DST purse project, Nanomission project (SR/NM/NS-1144/2013 (G)) and Department of Science and Technology, Government of India.

References

- Abellán-Llobregat A, Jeerapan I, Bandodkar A, Vidal L, Canals A, Wang J, Morallon E (2017) A stretchable and screen-printed electrochemical sensor for glucose determination in human perspiration. *Biosens Bioelectron* 91:885–891
- Armas LAG, Hollis BW, Heaney RP (2004) Vitamin D₂ is much less effective than vitamin D₃ in humans. *J Clin Endocrinol Metab* 89(11):5387–5391
- Awal A, Ghosh SB, Sain M (2009) Development and morphological characterization of wood pulp reinforced biocomposite fibers. *J Mater Sci* 44(11):2876–2881
- Awal A, Sain M, Chowdhury M (2011) Preparation of cellulose-based nanocomposite fibers by electrospinning and understanding the effect of processing parameters. *Composites B Eng* 42(5):1220–1225
- Bagbi Y, Sarswat A, Mohan D, Pandey A, Solanki PR (2017) Lead and chromium adsorption from water using L-cysteine functionalized magnetite (Fe₃O₄) nanoparticles. *Sci Rep* 7(1):1–15

- Baig N, Kammakam I, Falath W (2021) Nanomaterials: a review of synthesis methods, properties, recent progress, and challenges. *Mater Adv* 2(6):1821–1871
- Balasubramanian K (2010) Challenges in the use of 1D nanostructures for on-chip biosensing and diagnostics: a review. *Biosens Bioelectron* 26(4):1195–1204
- Bano S, David MP, Indira AP (2015) Salivary biomarkers for oral squamous cell carcinoma: an overview. *IJSS Case Rep Rev* 1(8):39–45
- Behzadi S, Serpooshan V, Tao W, Hamaly MA, Alkawareek MY, Dreaden EC, Brown D, Alkilany AM, Farokhzad OC, Mahmoudi M (2017) Cellular uptake of nanoparticles: journey inside the cell. *Chem Soc Rev* 46(14):4218–4244
- Bhardwaj N, Kundu SC (2010) Electrospinning: a fascinating fiber fabrication technique. *Biotechnol Adv* 28(3):325–347
- Bu D, Zhuang H, Yang G, Ping X (2014) An immunosensor designed for polybrominated biphenyl detection based on fluorescence resonance energy transfer (FRET) between carbon dots and gold nanoparticles. *Sens Actuators B Chem* 195:540–548
- Chang H, Wu X, Wu C, Yu C, Jiang H, Wang X (2011) Catalytic oxidation and determination of β -NADH using self-assembly hybrid of gold nanoparticles and graphene. *Analyst* 136(13):2735–2740
- Chauhan D, Solanki PR (2019) Hydrophilic and insoluble electrospun cellulose acetate fiber-based biosensing platform for 25-hydroxy vitamin-D₃ detection. *ACS Appl Polym Mater* 1(7):1613–1623
- Chauhan D, Yadav AK, Solanki PR (2021) Carbon cloth-based immunosensor for detection of 25-hydroxy vitamin D₃. *Microchim Acta* 188(4):1–11
- Chen A, Chatterjee S (2013) Nanomaterials based electrochemical sensors for biomedical applications. *Chem Soc Rev* 42(12):5425–5438
- Chen H, Müller MB, Gilmore KJ, Wallace GG, Li D (2008a) Mechanically strong, electrically conductive, and biocompatible graphene paper. *Adv Mater* 20(18):3557–3561
- Chen X, Ba Y, Ma L, Cai X, Yin Y, Wang K, Guo J, Zhang Y, Chen J, Guo X (2008b) Characterization of microRNAs in serum: a novel class of biomarkers for diagnosis of cancer and other diseases. *Cell Res* 18(10):997–1006
- Cheng G, Zhang J-L, Liu Y-L, Sun D-H, Ni J-Z (2011) Synthesis of novel Fe₃O₄@ SiO₂@ CeO₂ microspheres with mesoporous shell for phosphopeptide capturing and labeling. *Chem Commun* 47(20):5732–5734
- Cheng G, Liu Y-L, Wang Z-G, Zhang J-L, Sun D-H, Ni J-Z (2012) The GO/rGO-Fe₃O₄ composites with good water-dispersibility and fast magnetic response for effective immobilization and enrichment of biomolecules. *J Mater Chem* 22(41):21,998–22,004
- Cheng L, Li Y, Zhai X, Bing X, Cao Z, Liu W (2014) Polycation-b-polyzwitterion copolymer grafted luminescent carbon dots as a multifunctional platform for serum-resistant gene delivery and bioimaging. *ACS Appl Mater Interf* 6(22):20,487–20,497
- Chiou S-H, Yu C-C, Huang C-Y, Lin S-C, Liu C-J, Tsai T-H, Chou S-H, Chien C-S, Hung-Hai K, Lo J-F (2008) Positive correlations of Oct-4 and Nanog in oral cancer stem-like cells and high-grade oral squamous cell carcinoma. *Clin Cancer Res* 14(13):4085–4095
- Cinti S, Arduini F (2017) Graphene-based screen-printed electrochemical (bio) sensors and their applications: efforts and criticisms. *Biosens Bioelectron* 89:107–122
- Clark LC Jr, Lyons C (1962) Electrode systems for continuous monitoring in cardiovascular surgery. *Ann New York Academy of sciences* 102(1):29–45
- Collier P, Watson CJ, Voon V, Phelan D, Jan A, Mak G, Martos R, Baugh JA, Ledwidge MT, McDonald KM (2011) Can emerging biomarkers of myocardial remodelling identify asymptomatic hypertensive patients at risk for diastolic dysfunction and diastolic heart failure? *Eur J Heart Failure* 13(10):1087–1095
- Collings AF, Caruso F (1997) Biosensors: recent advances. *Rep Progr Phys* 60(11):1397
- Compton OC, Dikin DA, Putz KW, Brinson LC, Nguyen SBT (2010) Electrically conductive “alkylated” graphene paper via chemical reduction of amine-functionalized graphene oxide paper. *Adv Mater* 22(8):892–896

- Dalgård C, Petersen MS, Weihe P, Grandjean P (2011) Vitamin D status in relation to glucose metabolism and type 2 diabetes in septuagenarians. *Diabetes Care* 34(6):1284–1288
- Dalle-Donne I, Rossi R, Giustarini D, Milzani A, Colombo R (2003) Protein carbonyl groups as biomarkers of oxidative stress. *Clin Chim Acta* 329(1–2):23–38
- Dave K, Pachauri N, Dinda A, Solanki PR (2019) RGO modified mediator free paper for electrochemical biosensing platform. *Appl Surf Sci* 463:587–595
- Fang J, Niu HT, Lin T, Wang XG (2008) Applications of electrospun nanofibers. *Chin Sci Bull* 53(15):2265–2286
- Gao A, Tang C-X, He X-W, Yin X-B (2013) Electrochemiluminescent lead biosensor based on GR-5 lead-dependent DNAzyme for Ru(phen)₃²⁺ intercalation and lead recognition. *Analyst* 138(1):263–268
- Gonçalves BF, Oliveira J, Costa P, Correia V, Martins P, Botelho G, Lanceros-Mendez S (2017) Development of water-based printable piezoresistive sensors for large strain applications. *Compos Part B* 112:344–352
- Higgins BR, Weetall HH (1998) Biosensors: an introduction. *Appl Biochem Biotechnol* 73(1):79
- Hsiao VKS, Waldeisen JR, Zheng Y, Lloyd PF, Bunning TJ, Huang TJ (2007) Aminopropyltriethoxysilane (APTES)-functionalized nanoporous polymeric gratings: fabrication and application in biosensing. *J Mater Chem* 17(46):4896–4901
- Hu L, Choi JW, Yang Y, Jeong S, La Mantia F, Cui L-F, Cui Y (2009) Highly conductive paper for energy-storage devices. *Proc Natl Acad Sci* 106(51):21,490–21,494
- Hu W, Cheng P, Luo W, Lv M, Li X, Li D, Huang Q, Fan C (2010) Graphene-based antibacterial paper. *ACS Nano* 4(7):4317–4323
- Huang K, Li YH, Lin S, Liang C, Xu X, Zhou YF, Fan DY, Yang HJ, Lang PL, Zhang R (2014) One-step synthesis of reduced graphene oxide–CeO₂ nanocubes composites with enhanced photocatalytic activity. *Mater Lett* 124:223–226
- Jain KK (2007) Applications of nanobiotechnology in clinical diagnostics. *Clin Chem* 53(11):2002–2009
- Jiang, Hui, and Xuemei Wang. 2012. “Time-dependent nanogel aggregation for naked-eye assays of α -amylase activity.” *Analyst* 137 (11):2582–2587
- Jiang L, Yao M, Liu B, Li Q, Liu R, Lv H, Shuangchen L, Gong C, Zou B, Cui T (2012) Controlled synthesis of CeO₂/graphene nanocomposites with highly enhanced optical and catalytic properties. *J Phys Chem C* 116(21):11,741–11,745
- Jose J, Sunil PM, Madhavan Nirmal R, Varghese SS (2013) CYFRA 21-1: an overview. *Oral Maxillofac Pathol J* 4(2)
- Judd, Suzanne E, and Vin Tangpricha. 2009. “Vitamin D deficiency and risk for cardiovascular disease.” *Am J Med Sci* 338 (1):40–44
- Jung YK, Shin E, Kim B-S (2015) Cell nucleus-targeting zwitterionic carbon dots. *Sci Rep* 5(1):1–9
- Kafi AKM, Crossley MJ (2013) Synthesis of a conductive network of crosslinked carbon nanotube/hemoglobin on a thiol-modified Au surface and its application to biosensing. *Biosens Bioelectron* 42:273–279
- Kaushik A, Solanki PR, Pandey MK, Ahmad S, Malhotra BD (2009) Cerium oxide-chitosan based nanobiocomposite for food borne mycotoxin detection. *Appl Phys Lett* 95(17):173,703
- Khan S, Ansari AA, Rolfo C, Coelho A, Abdulla M, Al-Khayal K, Ahmad R (2017) Evaluation of in vitro cytotoxicity, biocompatibility, and changes in the expression of apoptosis regulatory proteins induced by cerium oxide nanocrystals. *Sci Technol Adv Mater* 18(1):364–373
- Kolahalam LA, Kasi Viswanath IV, Diwakar BS, Govindh B, Reddy V, Murthy YLN (2019) Review on nanomaterials: synthesis and applications. *Mater Today Proc* 18:2182–2190
- Kolch W, Neusüß C, Pelzing M, Mischak H (2005) Capillary electrophoresis–mass spectrometry as a powerful tool in clinical diagnosis and biomarker discovery. *Mass Spectrom Rev* 24(6):959–977
- Krishnan SK, Singh E, Singh P, Meyyappan M, Nalwa HS (2019) A review on graphene-based nanocomposites for electrochemical and fluorescent biosensors. *RSC Adv* 9(16):8778–8881

- Kumar S, Kumar S, Tiwari S, Augustine S, Srivastava S, Yadav BK, Malhotra BD (2016a) Highly sensitive protein functionalized nanostructured hafnium oxide based biosensing platform for non-invasive oral cancer detection. *Sens Actuators B Chem* 235:1–10
- Kumar S, Sharma JG, Maji S, Malhotra BD (2016b) Nanostructured zirconia decorated reduced graphene oxide based efficient biosensing platform for non-invasive oral cancer detection. *Biosens Bioelectron* 78:497–504
- Kumawat MK, Thakur M, Gurung RB, Srivastava R (2017) Graphene quantum dots from mangifera indica: application in near-infrared bioimaging and intracellular nanothermometry. *ACS Sustain Chem Eng* 5(2):1382–1391
- Lakshmi GBVS, Yadav AK, Mehlawat N, Jalandra R, Solanki PR, Kumar A (2021) Gut microbiota derived trimethylamine N-oxide (TMAO) detection through molecularly imprinted polymer based sensor. *Sci Rep* 11(1):1–14
- Lee KY, Jeong L, Kang YO, Lee SJ, Park WH (2009) Electrospinning of polysaccharides for regenerative medicine. *Adv Drug Deliv Rev* 61(12):1020–1032
- Lesch A, Jović M, Baudoz M, Zhu Y, Tacchini P, Gummy F, Girault HH (2017) Point-of-care diagnostics with inkjet-printed microchips. *ECS Trans* 77(7):73
- Li T, Yang M (2011) Electrochemical sensor utilizing ferrocene loaded porous polyelectrolyte nanoparticles as label for the detection of protein biomarker IL-6. *Sens Actuators B Chem* 158(1):361–365
- Li Q, Ohulchanskyy TY, Liu R, Koynov K, Dongqing W, Best A, Kumar R, Bonoiu A, Prasad PN (2010) Photoluminescent carbon dots as biocompatible nanoprobe for targeting cancer cells in vitro. *J Phys Chem C* 114(28):12,062–12,068
- Li H, Kang Z, Yang L, Lee S-T (2012a) Carbon nanodots: synthesis, properties and applications. *J Mater Chem* 22(46):24,230–24,253
- Li J, Kuang D, Feng Y, Zhang F, Zhifeng X, Liu M (2012b) A graphene oxide-based electrochemical sensor for sensitive determination of 4-nitrophenol. *J Hazard Mater* 201:250–259
- Li H, Liu X, Lin L, Xiaoyi M, Genov R, Mason AJ (2017a) CMOS electrochemical instrumentation for biosensor microsystems: a review. *Sensors* 17(1):74
- Li L, Li L, Chen C-P, Cui F (2017b) Green synthesis of nitrogen-doped carbon dots from ginkgo fruits and the application in cell imaging. *Inorg Chem Commun* 86:227–231
- Liang Y, Wang H, Casalongue HS, Chen Z, Dai H (2010) TiO₂ nanocrystals grown on graphene as advanced photocatalytic hybrid materials. *Nano Res* 3(10):701–705
- Lim SY, Shen W, Gao Z (2015) Carbon quantum dots and their applications. *Chem Soc Rev* 44 (1): 362–381
- Liu L, Song J-F, Yu P-F, Cui B (2008) Enhancement action of lanthanum hydroxide nanowire towards voltammetric response of Dobesilate and its application. *Chin J Chem* 26(1):220–224
- Mabrouk M, Das DB, Salem ZA, Beherei HH (2021) Nanomaterials for biomedical applications: production, characterisations, recent trends and difficulties. *Molecules* 26(4):1077
- Malhotra R, Patel V, Vaqué JP, Silvio Gutkind J, Rusling JF (2010) Ultrasensitive electrochemical immunosensor for oral cancer biomarker IL-6 using carbon nanotube forest electrodes and multilabel amplification. *Anal Chem* 82(8):3118–3123
- Mateos R, Lecumberri E, Ramos S, Goya L, Bravo L (2005) Determination of malondialdehyde (MDA) by high-performance liquid chromatography in serum and liver as a biomarker for oxidative stress: application to a rat model for hypercholesterolemia and evaluation of the effect of diets rich in phenolic antioxidants from fruits. *J Chromatogr B* 827(1):76–82
- Mertz TO, Kunduru V, Patra PK, Vattipalli K, Prasad S (2011) Patterned polymer nanofibers based biosensors. *MRS Online Proceedings Library (OPL)*, p 1358
- Motaghi H, Mehrgardi MA, Bouvet P (2017) Carbon dots-AS1411 aptamer nanoconjugate for ultrasensitive spectrofluorometric detection of cancer cells. *Sci Rep* 7(1):1–8
- Nagler, Rafael, Gideon Bahar, Thomas Shpitzer, and Raphael Feinmesser. 2006. “Concomitant analysis of salivary tumor markers—a new diagnostic tool for oral cancer.” *Clin Cancer Res* 12 (13):3979–3984

- Ozbakir HF, Sambade D, Majumdar S, Linday L, Banta S, West AC (2015) Detection of 25-hydroxyvitamin D3 with an enzyme modified electrode. *J Biosens Bioelectron* 7:193
- Posthuma-Trumpie GA, Wichers JH, Koets M, Berendsen LBJM, van Amerongen A (2012) Amorphous carbon nanoparticles: a versatile label for rapid diagnostic (immuno) assays. *Anal Bioanal Chem* 402(2):593–600
- Rao SVK, Mejia G, Roberts-Thomson K, Logan R (2013) Epidemiology of oral cancer in Asia in the past decade—an update (2000–2012). *Asian Pac J Cancer Prevent* 14(10):5567–5577
- Saha S, Arya SK, Singh SP, Sreenivas K, Malhotra BD, Gupta V (2009) Nanoporous cerium oxide thin film for glucose biosensor. *Biosens Bioelectron* 24(7):2040–2045
- Sahoo SK, Labhasetwar V (2003) Nanotech approaches to drug delivery and imaging. *Drug Discov Today* 8(24):1112–1120
- Samal SS, Manohara SR (2019) Nanoscience and nanotechnology in india: a broad perspective. *MaterToday Proc* 10:151–158
- Shaloo V, Sakshi SD (2020) Graphene and its composites used in research of dental and oral infection. *Int J Sci Res Chem Sci* 7(3)
- Sharma A, Baral D, Bohidar HB, Solanki PR (2015) Oxalic acid capped iron oxide nanorods as a sensing platform. *Chem Biol Interact* 238:129–137
- Sharma V, Tiwari P, Mobin SM (2017) Sustainable carbon-dots: recent advances in green carbon dots for sensing and bioimaging. *J Mater Chem B* 5(45):8904–8924
- Silveira CM, Monteiro T, Almeida MG (2016) Biosensing with paper-based miniaturized printed electrodes—a modern trend. *Biosensors* 6(4):51
- Singh J, Roychoudhury A, Srivastava M, Solanki PR, Lee DW, Lee SH, Malhotra BD (2013) A highly efficient rare earth metal oxide nanorods based platform for aflatoxin detection. *J Mater Chem B* 1(35):4493–4503
- Solanki PR, Kaushik A, Ansari AA, Sumana G, Malhotra BD (2008) Zinc oxide-chitosan nanobiocomposite for urea sensor. *Appl Phys Lett* 93(16):163903
- Song Y, Zhu S, Yang B (2014) Bioimaging based on fluorescent carbon dots. *RSC Adv* 4(52):27184–27200
- Soper SA, Brown K, Ellington A, Frazier B, Garcia-Manero G, Gau V, Gutman SI, Hayes DF, Korte B, Landers JL (2006) Point-of-care biosensor systems for cancer diagnostics/prognostics. *Biosens Bioelectron* 21(10):1932–1942
- Sri S, Kumar R, Panda AK, Solanki PR (2018) Highly biocompatible, fluorescence, and zwitterionic carbon dots as a novel approach for bioimaging applications in cancerous cells. *ACS Appl Mater Interf* 10(44):37,835–37,845
- Sri S, Dhand C, Rathee J, Ramakrishna S, Solanki PR (2019) Microfluidic based biosensors as point of care devices for infectious diseases management. *Sensor Lett* 17(1):4–16
- Srivastava M, Das AK, Khanra P, Uddin ME, Kim NH, Lee JH (2013) Characterizations of in situ grown ceria nanoparticles on reduced graphene oxide as a catalyst for the electrooxidation of hydrazine. *J Mater Chem A* 1(34):9792–9801
- Stern E, Vacic A, Rajan NK, Criscione JM, Park J (2010) BR Llic, DJ Mooney, MA Reed and TM Fahmy. *Nat Nanotechnol* 5:138–142
- Strobel C, Förster M, Hilger I (2014) Biocompatibility of cerium dioxide and silicon dioxide nanoparticles with endothelial cells. *Beilstein J Nanotechnol* 5(1):1795–1807
- Sun H, Deng J, Qiu L, Fang X, Peng H (2015) Recent progress in solar cells based on one-dimensional nanomaterials. *Energy Environ Sci* 8(4):1139–1159
- Swierczewska M, Liu G, Lee S, Chen X (2012) High-sensitivity nanosensors for biomarker detection. *Chem Soc Rev* 41(7):2641–2655
- Thavasi V, Singh G, Ramakrishna S (2008) Electrospun nanofibers in energy and environmental applications. *Energy Environ Sci* 1(2):205–221
- Tiwari S, Solanki PR (2015) Emerging aid in oral cancer diagnosi. *J Mol Biomarkers Diagn* 6(6):1
- Tiwari S, Gupta PK, Bagbi Y, Sarkar T, Solanki PR (2017) L-cysteine capped lanthanum hydroxide nanostructures for non-invasive detection of oral cancer biomarker. *Biosens Bioelectron* 89:1042–1052

- Vashist SK, Lam E, Hrapovic S, Male KB, Luong JHT (2014) Immobilization of antibodies and enzymes on 3-aminopropyltriethoxysilane-functionalized bioanalytical platforms for biosensors and diagnostics. *Chem Rev* 114(21):11,083–11,130
- Verma A, Stellacci F (2010) Effect of surface properties on nanoparticle–cell interactions. *Small* 6 (1):12–21
- Verma D, Chauhan D, Mukherjee MD, Ranjan KR, Yadav AK, Solanki PR (2021a) Development of MWCNT decorated with green synthesized AgNps-based electrochemical sensor for highly sensitive detection of BPA. *J Appl Electrochem* 51(3):447–462
- Verma D, Yadav AK, Mukherjee MD, Solanki PR (2021b) Fabrication of a sensitive electrochemical sensor platform using reduced graphene oxide-molybdenum trioxide nanocomposite for BPA detection: an endocrine disruptor. *J Environ Chem Eng* 9(4):105504
- Wang J (2006) Electrochemical biosensors: towards point-of-care cancer diagnostics. *Biosens Bioelectron* 21(10):1887–1892
- Wang Z, Dai Z (2015) Carbon nanomaterial-based electrochemical biosensors: an overview. *Nanoscale* 7(15):6420–6431
- Wang P-p, Bai B, Hu S, Zhuang J, Wang X (2009) Family of multifunctional layered-lanthanum crystalline nanowires with hierarchical pores: hydrothermal synthesis and applications. *J Am Chem Soc* 131(46):16,953–16,960
- Wei J, Zhang X, Sheng Y, Shen J, Huang P, Guo S, Pan J, Feng B (2014) Dual functional carbon dots derived from cornflour via a simple one-pot hydrothermal route. *Mater Lett* 123:107–111
- White, Abraham, Philip Handler, Emil Smith, DeWitt Stetten Jr (1959) Principles of biochemistry. In Principles of biochemistry. 2nd ed
- Wolfbeis OS (2015) An overview of nanoparticles commonly used in fluorescent bioimaging. *Chem Soc Rev* 44(14):4743–4768
- Wu Z-S, Yang S, Sun Y, Parvez K, Feng X, Müllen K (2012) 3D nitrogen-doped graphene aerogel-supported Fe₃O₄ nanoparticles as efficient electrocatalysts for the oxygen reduction reaction. *J Am Chem Soc* 134(22):9082–9085
- Wu X, Chai Y, Yuan R, Huilan S, Han J (2013) A novel label-free electrochemical microRNA biosensor using Pd nanoparticles as enhancer and linker. *Analyst* 138(4):1060–1066
- Wu ZL, Liu ZX, Yuan YH (2017) Carbon dots: materials, synthesis, properties and approaches to long-wavelength and multicolor emission. *J Mater Chem B* 5(21):3794–3809
- Xu C, Sun S (2007) Monodisperse magnetic nanoparticles for biomedical applications. *Polym Int* 56(7):821–826
- Yadav AK, Dhiman TK, Lakshmi GBVS, Berlina AN, Solanki PR (2020) A highly sensitive label-free amperometric biosensor for norfloxacin detection based on chitosan-γ-tria nanocomposite. *Int J Biol Macromol* 151:566–575
- Yadav AK, Lakshmi GBVS, Eremin S, Solanki PR (2021) Fabrication of label-free and ultrasensitive electrochemical immunosensor based on molybdenum disulfide nanoparticles modified disposable ITO: an analytical platform for antibiotic detection in food samples. *Food Chem*:130245
- Yang X, Cheng C, Wang Y, Qiu L, Li D (2013) Liquid-mediated dense integration of graphene materials for compact capacitive energy storage. *Science* 341(6145):534–537
- Yin S, Yang Y, Ling W, Li Y, Sun C (2019) Recent advances in sample preparation and analysis methods for vitamin D and its analogues in different matrices. *TrAC Trends Anal Chem* 110: 204–220
- Zhang L, Zhou Q, Liu J, Chang N, Wan L, Chen J (2012) Phosphate adsorption on lanthanum hydroxide-doped activated carbon fiber. *Chem Eng J* 185:160–167
- Zheng H, Ma X, Chen L, Lin Z, Guo L, Qiu B, Chen G (2013) Label-free electrochemical impedance biosensor for sequence-specific recognition of double-stranded DNA. *Anal Methods* 5(19):5005–5009



Hyaluronic Acid-Based Nanotechnologies for Delivery and Treatment

4

Alice Spadea, Ponpawee Pingrajai, and Annalisa Tirella

4.1 Introduction: CD44 and Hyaluronic Acid Interaction

4.1.1 CD44

CD44 is a cell membrane glycoprotein that is involved in many physiological cellular processes, including regulation of cell-cell and cell-matrix interactions, cell growth, survival, differentiation, and motility; in fact, CD44 can complex with other molecules present in the inner side of the plasma membrane, which is involved in signaling processes (Misra et al. 2015). A single gene encodes CD44

Alice Spadea and Pompawee Pingrajai are co-first authors, providing equal contribution to this work.

A. Spadea

Division of Pharmacy and Optometry, Faculty of Biology, Medicine and Health, University of Manchester, Manchester, UK

NorthWest Centre for Advanced Drug Delivery (NoWCADD), School of Health Sciences, University of Manchester, Manchester, UK

P. Pingrajai

Division of Pharmacy and Optometry, Faculty of Biology, Medicine and Health, University of Manchester, Manchester, UK

A. Tirella (✉)

Division of Pharmacy and Optometry, Faculty of Biology, Medicine and Health, University of Manchester, Manchester, UK

BIOTech Center for Biomedical Technologies, Department of Industrial Engineering, University of Trento, Trento, Italy

e-mail: annalisa.tirella@manchester.ac.uk

glycoproteins; however, CD44 isoforms differ in size (from ~85 to ~250 kDa) due to N- and O-glycosylations and alternative splicing of specific exons in the extracellular domains of the receptor. In the smallest of standard isoforms (CD44s), the exons 1–5 and 16–20 are spliced together, and the protein includes seven extracellular domains: a transmembrane domain and a cytoplasmic domain. The inclusion of variant exons 6–15 (also known as v1–10) may depend on mitogenic signals that regulate alternative splicing. Not surprisingly, cancer cells frequently express larger variants (CD44v) (Hu et al. 2017; Wang et al. 2007). CD44s consist of 363 amino acids (aa) which form a protein with three regions: a 270 aa extracellular domain, a 21 aa transmembrane domain, and a 72 aa C-terminal cytoplasmic domain. The N-terminal domain contains two binding domains, the “link domain” (aa 32–132), where there are binding sites for collagen, laminin, fibronectin, and for other receptors, such as E-selectin and L-selectin. Within the “link domain,” there is a basic motif (aa 150–158) where hyaluronic acid (HA) specifically binds. The N-terminal domain also contains other two regions (aa 21–45 and 144–167) rich in conserved basic residues, which are considered important in HA binding (Peach et al. 1993). The molecular weight (MW) of the CD44s protein is about 85 kDa; CD44v, when containing peptides from all variant exons, is larger and reaches MW over 250 kDa, which is much greater than the expected value. This increase in MW is due to the substantial posttranslational modifications of CD44 isoforms. Regardless of post-translational modifications, there are at least five conserved N-glycosylation sites in the N-terminal external domain and two chondroitin sulfate attachment sites on the exon 5 product. Several potential O-glycosylation sites are situated in the region proximal to the membrane, and also variant exons can contain specific posttranslational modification sites (Bartolazzi et al. 1996; English et al. 1998).

4.1.2 CD44 Role in Physiological Condition vs Cancer

Pathological conditions or specific stimuli can trigger alternative splicing and post-translational modifications thereby leading to the production of different CD44 proteins. Such CD44v may present altered HA binding affinity, as well as increased tumorigenicity (Wang et al. 2018). A typical fingerprint of cancer cells is the abnormal CD44 expression or the disrupted CD44-ligand interaction, and both can directly or indirectly affect the signal transduction causing chemo- and/or radio-resistance, resistance to oxidative stress, adhesion, extracellular matrix interaction, tumor matrix formation, or modulation of cancer stem cells (CSCs) niche (Birzele et al. 2015). Among all the CD44 variants, there are some of particular interests in cancer, and these are CD44v3, CD44v6, and CD44v10. CD44v3, for example, contains a site for heparan sulfate, which in turn binds proteins such as basic fibroblast growth factor (bFGF) (Bennett et al. 1995). CD44v6 contains a binding site for a hepatocyte growth factor (HGF), VEGF and osteopontin (OPN), and CD44v10 also contains a binding site for OPN (Zöller 2011; Tremmel et al. 2009). Over the past years, many clinical data demonstrated that CD44v expression

is crucial for malignancy and could be correlated with higher metastatic potential and mortality in many tumors (Hu et al. 2017, Li et al. 2014, Ivan Stamenkovic et al. 1989). In particular, CD44v6 has been associated with increased tumor progression and metastatic potential in colon, lung, and breast cancer (Ma et al. 2019; Afify et al. 2011; Qiao et al. 2018). In general, it is possible to conclude that the overexpression of CD44 has unfavorable effects on cancer progression and prognosis, as well as predicts any therapeutic outcome.

4.1.3 CD44 expression in normal, inflamed, and cancer tissues

Immune cells, and many other cells, express CD44. Inactivated cells typically express the standard isoform, CD44s; whereas, immune cells subsets or activated cells are known to express CD44v, as summarized in Table 4.1. When cells are activated by inflammatory stimuli and other changes in the microenvironment, immune cells change their fingerprint, switch expression of CD44 isoforms, and migrate to the inflammatory (or tumorigenic) sites. In fact, in inflammatory or pathophysiological states, the homeostasis of the microenvironment changes and the resulting composition is characterized by the presence of HA with different MWs; in this case, HA may act itself on immune cells to activate inflammation (Gupta et al. 2019). The effects of HA with different MWs on immune cells are reported in Table 4.2. Alternatively, when immune cells such as monocytes and lymphocytes are activated by invading pathogens or inflammatory stimuli, the CD44 variant isoforms expressed on their membrane can strongly interact and bind to HA (Lesley et al. 1995). A similar change in the expression of CD44 variants is described in the presence of inflammation in the vascular system, where endothelial cells activated by inflammatory stimuli express a higher level of CD44, with more HA detected on the cell membrane as bound to CD44 receptors (Mohamadzadeh et al. 1998; Nandi et al. 2000). Such presence of CD44v and HA in immune and endothelial cells promotes the rolling of immune cells and endothelial cells to the inflammation sites.

4.1.4 Hyaluronic Acid and Its physiological Role

HA is a negatively charged non-sulfated linear polysaccharide constituted of disaccharides of N-acetyl-D-glucosamine and D-glucuronic acid linked via

Table 4.1 Expression of CD44 isoforms expressed by immune cells adapted from Lesley et al. (1993) and Naor et al. (1997)

Types of cells	Isoforms of CD44
Inactivated cells	CD44s
Lymphocytes (Activated)	CD44v3, CD44v6, CD44v10
T cells (Inactivated)	CD44v3, CD44v6, CD44v10
T cells (Memory, Activated)	CD44v6, CD44v9
B cells (Activated)	CD44v6, CD44v6,7, CD44v10

Table 4.2 The link between inflammatory effects and hyaluronic acid with different molecular weights on immune cells

HA MW	Cell type	Reported effects	References
4–1700 kDa	Murine macrophages	Decrease pro-inflammatory cytokine	Baeva et al. (2014)
5 kDa	Murine macrophages	Increase pro-inflammatory cytokine	Rayahin et al. (2015)
50 kDa	Murine chondrocytes	Increase pro-inflammatory cytokine and gene	Campo et al. (2009)
100–150 kDa	Human peripheral blood mononuclear cells	Increase pro-inflammatory cytokine	Yamawaki et al. (2009)
200 kDa	Murine macrophages	Increase pro-inflammatory genes	McKee et al. (1996) Scheibner et al. (2006)
500–730 kDa	Murine macrophages	No effects	Yamawaki et al. (2009)
1000 kDa	Murine chondrocytes	No effects	Campo et al. (2009)
1200 kDa	Murine macrophages	Decrease pro-inflammatory gene	Neumann et al. (1999)
1900 kDa	Human peripheral blood mononuclear cells	Decrease pro-inflammatory cytokine	Yamawaki et al. (2009)
3000 kDa	Murine macrophages	Decrease pro-inflammatory gene and cytokine	Rayahin et al. (2015)
5000 kDa	Murine chondrocytes	Increase pro-inflammatory cytokine and gene	Campo et al. (2009)

alternating β -1,4 and β -1,3 glycosidic bonds. HA is synthesized on the cell membrane by HA synthases (HAS1, HAS2, HAS3 in humans and mice), a family of integral membrane proteins (Agarwal et al. 2019). Polymers of HA are present in the body in a wide size range, with MW varying from 5 to 20,000 kDa in vivo; typically, high molecular weight (HMW) HA can be digested into low molecular weight (LMW) polymers by hyaluronidase 2 (Hyal 2) present on the cell membrane (Cyphert et al. 2015). HA is the main component of the extracellular matrix (ECM), and it can also be internalized by cells. Figure 4.1; every 24 h, about 30% of HA present in the human body is replaced by a newly synthesized polymer to guarantee tissue and microenvironment homeostasis (Fraser et al. 1997). In the case of inflammation, homeostasis is disrupted with HA undergoing uncontrolled degradation; as a result, the MW of the HA present in the microenvironment changes from the composition of normal tissues, with specific MW having been recognized to cause-effect on immune cells.

4.1.4.1 Role of Hyaluronic Acid in inflammation

As introduced in the previous paragraph, HA with different MW can be present in normal, inflamed, and pathological microenvironments. In inflammation, HA can

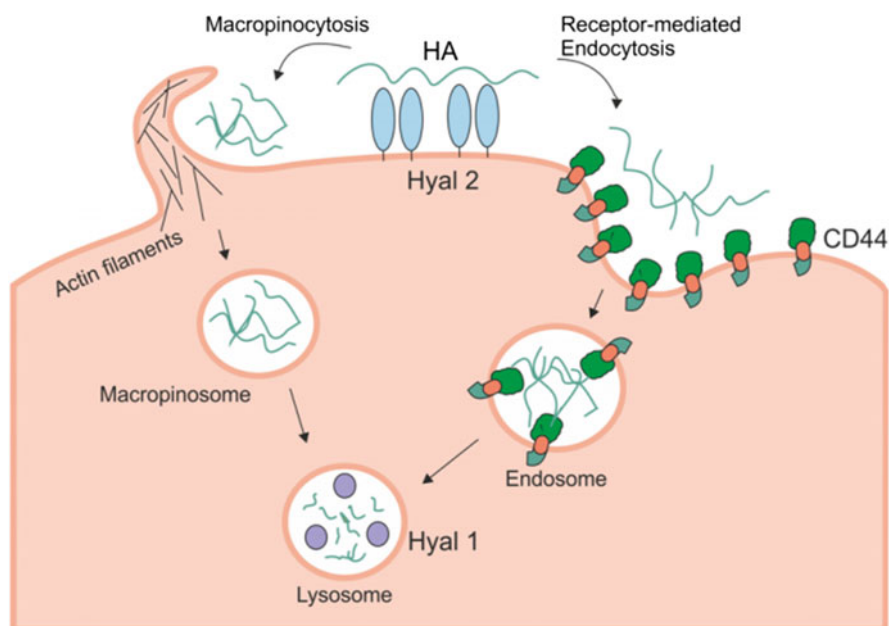


Fig. 4.1 Schematic of HA metabolism. HMW HA is first degraded by Hyal 2 into smaller fragments that can be internalized by the cell through receptor-mediated endocytosis or macropinocytosis. Once internalized, HA is directed to the lysosome, which contains Hyal 1 that degrades HA into small fragments

induce distinctive inflammatory responses, and it is hypothesized that HA MW is crucial in regulating them: HA with high MW (>1000 kDa) is reported to induce anti-inflammatory signals, whereas HA with low MW (<500 kDa) is associated with pro-inflammatory signals. In general, and when homeostasis is preserved, HA in the body has a molecular weight of 1000 kDa (or higher MW); the MW varies depending on the tissue and interaction with other extracellular matrix components. In synovial fluids, HA has MW in the range of 6000–7000 kDa, while the skin is reported to be ~ 2000 kDa (Cowman et al. 2015). The effects associated with specific MW of HA on immune cells are reported in Table 4.2.

In the inflamed environment, HA is cleaved into smaller polymers by reactive oxygen species (ROS) and hyaluronidases, both highly expressed at the inflammation site (Monzón et al. 2008; Monzon et al. 2010). Moreover, Monzon and coworkers reported that in inflammatory microenvironments, HA is degraded, hypothesizing a correlation between the increased concentrations of low MW HA and induced inflammatory responses (Monzón et al. 2008, Monzon et al. 2010). Table 4.3 summarizes the inflammation-related effects caused by low MW HA. Of note, the effects caused by HA with different MW in inflammation are still quite contradictory. For example, Baeva et al. reported that low molecular weight HA (<500 kDa) was found to have anti-inflammatory effects on murine macrophages

Table 4.3 Role of hyaluronic acid on macrophages in regulating inflammatory processes, with specific reference to the molecular weight of hyaluronic acid

Effects of HA	Size of HA	Markers	Reference
Pro-inflammatory response	4–6 kDa	Pro-inflammatory cytokine (IL-1 β \uparrow)	Baeva et al. (2014)
	5 kDa	Pro-inflammatory cytokine (TNF- α \uparrow)	Rayahin et al. (2015)
	200 kDa	Chemokines (CCL3 \uparrow CCL4 \uparrow)	McKee et al. (1996)
		Chemokine (CCL3 \uparrow)	Scheibner et al. (2006)
Anti-inflammatory response	1200 kDa	Pro-inflammatory cytokines (IL-6 \downarrow IL-1 α \downarrow TNF- α \downarrow)	Neumann et al. (1999)
	1500–1700 kDa	Pro-inflammatory cytokines (IL-1 β \downarrow TNF- α \downarrow)	Shi et al. (2019)
		Anti-inflammatory cytokine (IL-10 \uparrow)	
	3000 kDa HA	Pro-inflammatory cytokine (TNF- α \downarrow)	Rayahin et al. (2015)

(Baeva et al. 2014). Consequently, there are still some open questions on the mechanisms by which HA can induce inflammation-related effects.

When trying to decipher the role of HA (and its MW) in inflammatory processes, many studies have shown that the CD44 receptor and its interaction with HA, not only is important to regulate inflammation-related effects of HA (Fitzgerald et al. 2000) but also its expression on immune cells may change when they get activated in inflamed microenvironments (Guan et al. 2011; Liang et al. 2007). Moreover, other researchers have reported a close link between CD44 and toll-like receptors (TLRs), which are the receptors that induce inflammatory signals in cells (Jiang et al. 2005).

In inflammatory processes, and when the homeostasis of the microenvironment is disrupted, macrophages are the very first cells to respond (Mosser and Edwards 2008); the release of cytokines triggers specific signaling pathways that may be linked to the variation in the composition of the extracellular matrix and the different MW of HA present in such matrix (Bonnans et al. 2014). As a consequence of inflammation and the presence of soluble HA, macrophages change their inflammatory profiles. Again, high and low MW HA is responsible for inducing pro- and anti-inflammatory signals in macrophages (Table 4.3). Soluble low MW HA induces the higher expression of pro-inflammatory genes, chemokines, and cytokines such as TNF- α , IL-1 β , and IL-6 by macrophages; whereas, the expression of pro-inflammatory genes and cytokines are reduced in the presence of high MW HA, also resulting in a higher expression of anti-inflammatory cytokines (Table 4.3).

4.1.4.2 Role of Hyaluronic Acid in Cancer

HA possesses different cellular functions depending on the environment and its MW; where the MW can confer different binding modes on specific cell signal-transducing receptors (Heldin et al. 2013). For example, small fragments of HA (2–10 disaccharides) are proven to induce angiogenesis and endothelial cell differentiation (Slevin et al. 2007; Takahashi et al. 2005). Generally, HA is accumulated whenever tissues undergo rapid turnover and repair, as during embryogenesis,

wound healing, inflammation, and cancer. Homeostasis then kick-off and regulates the composition of the extracellular matrix, including concentration and MW of HA. Accumulation of HA has been reported in a few tumors when the extracellular composition is compared to the corresponding healthy epithelium, like in the breast (Auvinen et al. 2000; Wu et al. 2020), prostate, ovarian, and pancreatic cancer (Sato et al. 2016). In such a scenario, a correlation between poor prognosis and resistance to therapies emerged (Anttila et al. 2000). The accumulation of HA is hypothesized to result from aberrant expression of HA synthases, hyaluronidases, presence of ROS, and altered CD44-mediated internalization (Passi et al. 2019). Besides cancer cells, HA can also be produced by stromal cells in response to factors released by cells present in the tumor microenvironment (Asplund et al. 1993).

4.1.5 Internalization of Soluble Hyaluronic Acid

Two main mechanisms of internalization have been described for HA: receptor-mediated endocytosis and micropinocytosis. Receptor-mediated endocytosis of HA seems to be correlated with the expression level of its receptors on the cellular membrane. CD44 is the HA main receptor and other HA receptors, such as RHAMM, LYVE-1, and HARE, are also found on cell membrane and can be partially responsible for HA binding and uptake. Even though all CD44 isoforms contain the basic motif where the HA binds, not all the cells expressing CD44 are capable of binding/internalizing HA constitutively (Spadea et al. 2019). HA binding and internalization are two separate events, and they depend on the activation state of the receptor, which can be regulated by external stimuli (DeGrendele et al. 1997; Guo et al. 2021). Since they are ubiquitous molecules, this mechanism is in place to avoid unnecessary responses. Post-transcriptional or post-translational modifications can affect the affinity of CD44 for HA. However, it is still not completely clear whether they influence this affinity directly or if the structure of certain variants is responsible for favoring oligomerization of the receptor hence conferring an increased affinity (Chen et al. 2018; Yang et al. 2012). For example, it has been reported that clustering of CD44, which can, in turn, be regulated by the expression of variant exons glycosylations and phosphorylation of specific serine in the intracellular domain, can enhance HA binding (Lesley et al. 1995; Sleeman et al. 1996). In particular, CD44 glycosylations were reported to have both stimulatory and inhibitory effects on HA affinity, and they can vary between cell lines (Skelton et al. 1998). Desialylation of CD44 instead may increase HA affinity, possibly due to a reduction of negative charges in the receptor (Faller and Guvench 2014).

Recently, we screened the expression of CD44 in a wide panel of cancer cell lines and human dermal fibroblasts, *in vitro* reporting that in certain cancer cell lines, the expression of CD44 variants (CD44v) can negatively influence HA. At the same time, high levels of CD44s promoted uptake. Despite expressing high CD44s, healthy normal cells were less efficient in taking up HA compared to cancer cells, proving that factors other than the amount of CD44 receptor itself can affect the interaction with HA, including its activation state (Spadea et al. 2019).

The other HA receptors (i.e., RHAMM, LYVE-1, and HARE) are only marginally involved in HA uptake (Cai et al. 2014). There is still a gap in knowledge about RHAMM-mediated HA internalization, and, whereas it was reported that anti-RHAMM antibodies were not able to block HA uptake in mesenchymal cells, it was also seen that RHAMM overexpression led to an increased HA uptake in the same cells, although this was CD44-dependent. This links well to the fact that RHAMM was found to regulate CD44 expression (Veisoh et al. 2015). LYVE-1 is mainly expressed on endothelial cells of lymphatic vessels. When it binds to HA, this is recognized and bound by the CD44 receptor expressed on leukocyte cells. Leukocyte cells use this connection to endothelial cells via LYVE-1/HA/CD44 to migrate into lymphatic vessels. The HA internalization mechanism is not very well known but is similar to the CD44-mediated one (Racine and Mark 2012). HARE is mainly involved in systemic HA turnover, and it is localized mainly in the liver, spleen, and lymph nodes (Harris et al. 2007).

HA was also reported to enter the cells in a non-CD44-dependent manner (Greyner et al. 2010): macropinocytosis is an action-driven HA internalization mechanism that occurs through plasma membrane ruffled extensions and the formation of macropinosomes, which can internalize extracellular entities and fluid (Fig. 4.1).

4.1.6 Hyaluronic Acid and Current Treatments

4.1.6.1 Role of Hyaluronic Acid as Therapeutic

In 1934, Karl Meyer and John Palmer first isolated HA from cow's eyes. The first use of HA for a clinical application was only in the 1950s when HA, isolated from the umbilical cord and rooster comb back, was used as a vitreous substitute during eye surgery (Fakhari and Berklund 2013). Since then, HA has been used widely as health product, spanning from biomedical to cosmetic applications, because of its biocompatibility and hydrating capacity, allowing HA to maintain high water-content in a given environment/tissue. There are two main purposes of the treatment of HA: one is to use HA as a biopolymer for its main characteristic to retain water, the other is to replace the degraded HA within tissues extracellular matrix. Many cosmetic and therapeutic products containing HA as a principal and active component are approved by the FDA and are available in the market, some of which are described in the next paragraphs.

4.1.6.2 Ophthalmic and Injectable Hyaluronic Acid Treatments

There are many products based on HA that have been developed to be used in ophthalmology. For example, HA is used in many eye-drop products to keep the eyes lubricated and prevent dry eyes, because of its property to retain water. Some FDA-approved examples include Bluyal, Blugel, Hyabak, Artelac, and Splash (Salzillo et al. 2016). The MW of the HA and their concentration in these products may vary: most of the products contain HA with an MW in the range 500–1000 kDa, although there are also products with HA MW <500 kDa or >1000 kDa (Aragona

et al. 2019). Regarding the concentration of HA in eye-drop formulations, this is usually in the range of 0.1–0.4%wt (Salzillo et al. 2016). The use of different MW and concentrations of HA results in products with different viscosity. Products with higher viscosity are used to treat the damaged ocular surface, whereas products with lower viscosity are used to maintain tear film stability (Aragona et al. 2019).

Besides eye-related products, HA is often used for the treatment of joint-related pathologies, such as osteoarthritis. In fact, the HA present in the extracellular matrix of osteoarthritic joints is degraded in the case of injury, or inflammation: this cause a reduction of MW, leading to impaired lubricant activity in patients (Altman et al. 2015). Therefore, high MW HA can be injected to better lubricate the joints and to replace the degraded extracellular matrix. However, this is not a long-term treatment. Many injectable-HA products are available as osteoarthritis treatments, including Hyalgan, Supartz, E Monovisc, Orthovisc, Euflexxa, Gel-One, Synvisc, and Synvisc-One (Nicholls et al. 2018). The MW of HA in most of these products is >1000 kDa, and few of the products contain HA with a MW between 500 and 1000 kDa (Bhadra et al. 2017).

4.1.6.3 Hyaluronic Acid Conjugates

Most of the products available on the market and mentioned above are used because of the intrinsic property of HA to retain water. However, beyond the HA water-retention property, HA has other functions. The most important is that HA can be internalized into the cells through CD44 receptors because of the difference in CD44 expression of different types of cells (Fig. 4.1). Thanks to its capacity of being internalized by CD44-expressing cells, many scientists have attempted to use HA and a drug-conjugate to target cancer cells that express a high level of CD44 receptors, proving high receptor-binding affinity of HA to CD44 both in vitro and in vivo (Choi et al. 2010). Some HA-conjugated chemotherapy drugs are studied at the preclinical stage, while some are in the clinical stages. The summary of these conjugated drugs is presented in Table 4.4.

4.2 Hyaluronic Acid-Based Nanotechnologies to Target CD44

HA is an attractive component for the formulation of anti-cancer therapeutics as it can specifically bind to various cancer cells that overexpress CD44, as anticipated in previous sections. Several studies report HA-nanotechnologies developed for cancer

Table 4.4 Summary of available HA-conjugated therapeutics and their related function

Conjugations/Function	Drug names
Chemotherapy	Paclitaxel (Clinical I) 5-fluorouracil Camptothecin
Anti-inflammatory drugs	Hydrocortisone Methotrexate Diclofenac
Analgesics and Opioid drugs	Bupivacaine Morphine

treatments, such as HA-drug conjugates and drug-loaded HA-based nanoparticles (NPs). These formulations were proven to have enhanced targeting ability to CD44 expressing cells, as well as higher therapeutic efficacy when compared to soluble anti-cancer agents (e.g. doxorubicin, paclitaxel, siRNA) (Eliaz and Szoka 2001; Thomas et al. 2015; Choi et al. 2010; Lee et al. 2007).

4.2.1 Current Strategies to Manufacture Hyaluronic Acid-Based Nanotechnologies

Many HA-based NPs have been developed over the past years. Across all reported processes to manufacture HA-based technologies, there is a lack of consensus on the formulation and its characteristic properties, as well as the fabrication methods used. Therefore, each described process reports different manufacturing variables tested. A more systematic approach on the main manufacturing processes may be more useful to translate findings for the development of HA-based NPs for the delivery of anti-cancer therapeutics, as well as provide higher control over NPs manufacturing processes and characteristics (e.g. size, surface properties, stability, and storage). Between all the reported fabrication processes, a shared fact is that HA NPs are prepared through emulsification or nanoprecipitation in discontinuous processes. Yun et al. produced sodium hyaluronate NPs by emulsifying the aqueous phase in mineral oil (W/O), showing that the emulsifying technique produced polydisperse particles (size range 2–23 μm) (Yun et al. 2004). However, this process highlighted one major disadvantage: removing oil and surfactants used in the process. Consequently, more recent processes for the production of free surfactant and oil HA NPs have been developed.

Nanoprecipitation is a one-step manufacturing process used for the production of HA NPs. This requires the use of two miscible solvents, with HA to be soluble in one solvent only. Hence, as the solvent diffuses into the miscible nonsolvent, the polymer precipitates rapidly, enabling the formation of NPs (100–300 nm) with a narrow unimodal distribution (Fessi et al. 1989; Bilati et al. 2005).

Emerging technologies (e.g. microfluidics) have been used to fabricate NPs within a continuous process, providing a higher degree of control over the manufacturing variables (Xu et al. 2009). Moreover, such a continuous process provides dynamic control of flow and mixing that can be manipulated to produce particles for specific applications (Jahn et al. 2004; Zhao et al. 2011). Microfluidics was firstly reported to gain control over the spontaneous self-aggregation of liposomes from a dispersion of phospholipids (Jahn et al. 2004). Different configurations of microfluidic devices (and in specific reference to chip geometry/junction and organic solvents used) were reported for the fabrication of lipid nanoparticles (Maeki et al. 2018), polymeric NPs such as poly(lactic-co-glycolic acid) and polyethylene glycol NPs (Li et al. 2021), and biopolymers, including HA (Bicudo and Santana 2012). Table 4.5 summarizes the variable, advantages, and disadvantages of these processes for the fabrication of HA-based nanoparticles.

Table 4.5 Summary of variables currently used to control the manufacturing of Hyaluronic Acid nanoparticles, with specific reference to emulsification, nanoprecipitation, and microfluidics

Process	Variables	Advantages	Disadvantages
Emulsification	<ul style="list-style-type: none"> – Aqueous drug phase with HA; – A drug in organic phase with HA in aqueous phase; – Physical variables: mixing energy, time, temperature; 	<ul style="list-style-type: none"> – Control over size distribution; – Good EE (%) for the drug in the organic phase. 	<ul style="list-style-type: none"> – Poor EE% for the drug in water phase; – Multiple-step process; – Removal of organic phase solvent (s).
Nanoprecipitation	<ul style="list-style-type: none"> – HA: MW, concentration; – Therapeutic: concentration; – Mixing: device, stirring speed, time, temperature. 	<ul style="list-style-type: none"> – One-step process; – Water-based phases; – Low-energy mixing device. 	<ul style="list-style-type: none"> – Low concentration of HA in the dispersed phase; – Water-soluble drug; – Low DL(%); – Nanoparticles may aggregate.
Microfluidics	<ul style="list-style-type: none"> – HA: MW, concentration; – Therapeutic: concentration, dissolution phase; – Microfluidic chip: geometry, channel size, mixing junction. – Mixing process: TFR, FRR, time, temperature. 	<ul style="list-style-type: none"> – One-step process; – Control formation processes precisely; – Desired EE%; – Multiple drugs loading capacities; – Low-energy mixing device. 	<ul style="list-style-type: none"> – Low viscosity phases (low concentration HA); – Possible limitation for scaling-up the process.

4.2.2 Hyaluronic Acid-Based Nanoparticles and Design of Experiments

The design of experiments (DOE) offers a better understanding of the role of manufacturing parameters on the formation of drug delivery systems (e.g. NPs). By using this approach, critical parameters that control the NP size can be identified (Sedighi et al. 2019), as well as predicting the factors influencing the loading of the therapeutic of interest (e.g. siRNA) (Cun et al. 2011). This strategy could be particularly useful to predict the presence of HA on NPs' surface, offering the possibility to increase further the interaction/adhesion of HA with biological components and its internalization.

As previously mentioned, the MW of HA can determine its physiological function, regulating cell migration, proliferation, internalization via receptors, and many other processes (Misra et al. 2015; Rios de la Rosa et al. 2018). In the case of HA-based NPs, the MW and functionalization of HA are known to impact targeting ability and internalization (Zhong et al. 2019), as well as the size of nanoparticles

(Choi et al. 2010). Moreover, the nanoparticles' characteristics and "availability" of HA on their surface can be further controlled by using different electrostatic interactions (Carton et al. 2019; Lallana et al. 2017). Among all the cationic polymers, chitosan (CS) is possibly the most-used polymer for the formulation of HA NPs. Both CS and HA offer good biocompatibility, bioadhesion, and the possibility to release therapeutics. In particular, we have evaluated the possibility to use CS for the delivery of nucleic acids as it could facilitate their release in the cytoplasm (Almalik et al. 2013; Gennari et al. 2019; Lallana et al. 2017; Rios de la Rosa et al. 2019a; Tirella et al. 2019). Typical manufacturing variables for CS/HA nanoparticles preparation to directly impact on size and surface composition were identified as: the pH of the polymeric solution, the concentration of polymers, ratio of CS/HA. Many are the parameters that impact CS/HA nanoparticles properties: pH and mixing have been identified as the most critical ones to determine the size and size distribution. Nazeri et al. investigated the impact of stirring time while preparing ultra-low MW CS/HA NPs, reporting that higher stirring speed reduced the size of particles (Nazeri et al. 2013). Furthermore, parameters such as pH and CS to HA ratio were also critical to forming nanoparticles with a low polydispersity index (PDI), suggesting optimal values for the formulation of CS/HA nanoparticles for drug and gene delivery.

The composition of nanoparticles surface affects their uptake when interacting with CD44+ cells, with cell-specific factors determining binding vs internalization efficiency. The properties of the polycation used (e.g. CS MW) are hypothesized to influence the representation of HA on nanoparticles surface hence promoting (or not) internalization of HA-based NPs by CD44 receptors on the cell membrane. Apaolaza et al. reported on the preparation of cationic solid lipid NPs coated with HA to deliver DNA using nonviral vectors. Nanoparticles with a size range of 240–340 nm were internalized via CD44 in epithelial cells. HA of three MW (150 kDa, 500 kDa, 1630 kDa) was evaluated in the study to decorate the surface of solid lipid nanoparticles, and no direct impact of MW in transfection was observed (Apaolaza et al. 2014). Lu et al. also studied the relationship between HA MW and active targeting efficiency for delivering doxorubicin in CD44-expressing cancer cells (Zhong et al. 2019). Results indicated that HA MW could tune the active targeting capacity of HA-based NPs, with HA conjugates (MW 63 kDa) having a better efficacy in delivering doxorubicin to cancer cells.

4.2.3 Formulation of Nanoparticles for Delivery of Nucleic Acid to Cancer Cells

In recent years, the loading of Nucleic Acid (NA) in nonviral (nano) vectors has been widely investigated. HA-coated NPs constitute a large representative not only for their intrinsic characteristic of targeting CD44-expressing cells but also for their high binding and internalization profiles. Polycations caught much interest for the delivery of NAs, with MW and physicochemical characteristics impacting the properties of formed complexes, their ability to protect/release NA intracellularly, and their

therapeutic potential (Begines et al. 2020). The affinity between the NA and the polycation influence the drug loading (DL) and the encapsulation efficiency (EE) in NPs (Lallana et al. 2017). Optimizing the drug loading of NAs in NPs is of utmost importance to determine the ultimate therapeutic potential. In this perspective, DOE offers an efficient method to identify the process parameters for the preparation of nanoparticles able to release NAs in the required therapeutic interval. Such challenges will be discussed more in detail in the next section.

4.2.3.1 Chitosan Hyaluronic Acid Nanoparticles and Impact of Formulation and Preparation Processes on Their Characteristics

Between many polycations, CS is a safe and efficient carrier for delivering negatively charged therapeutics, such as NAs. The size of CS/NAs complexes is typically characterized by measuring the hydrodynamic mean diameter, polydispersity index (PDI), and zeta potential. However, common techniques used, such as dynamic light scattering, produce bare estimations of the size of particles, assuming them as having rigid, non-interacting, spherical conformations (Alatorre-Meda et al. 2009). Scanning electron microscopy could be used to elucidate better NPs morphology (size and shape) and interaction with cells in the physiological environment (Chithrani and Chan 2007; Kim et al. 2007).

Ionotropic gelation and polyelectrolyte complexation are commonly used processes to form CS/NAs NPs. Ionotropic gelation uses multivalent polyanions to form inter- and intra-molecular crosslinks between the selected polyanions and CS. Tripolyphosphate (TPP) is possibly the most popular polyanion used with CS in drug delivery applications because of its nontoxic property, as well as fast electrostatic gelation with CS (Shu and Zhu 2000; Katas and Alpar 2006; Wu et al. 2017; Deng et al. 2014). NPs' properties, such as particle size, the density of surface charge, and loading of NAs, can be predicted knowing process parameters such as CS MW, CS concentration, CS degree of deacetylation (DD), CS to TPP weight ratio, and solution pH value (Gan et al. 2005). CS can be modified to enhance the transfection efficiency of NAs, to tune their size and morphology hence interaction with cells. Fabrication processes are typically performed at RT, with constant TPP concentration (0.5–1.0 mg/mL); whereas the types of CS used have a typical range of values of MW (30–700 kDa), concentration (0.5–4% w/v, pH ~4.5), DD (50–85%), and CS to TPP weight ratio (3:1–7:1). The mixing process is also known to impact particle size and size distribution, with mixing speed and time adjusted for each specific study. However, ionotropic gelation is a multistep process requiring additional purification steps before CS NPs can be used. Polyelectrolyte complexation instead offers the advantage of being a single-step process and uses negatively charged polymers, such as HA, to form CS-nanoparticles (de la Fuente et al. 2008; Lallana et al. 2017; Tirella et al. 2019). In polyelectrolyte complexation, fabrication process parameters are CS MW, CS DD, HA MW, and CS to HA ratio; typically, mixing speed, mixing time, and temperature are kept constant during the process. Obtained CS/HA NPs are in the size range of 100–400 nm, with narrow size distribution and relatively high NAs loading.

4.2.3.2 Design Criteria for the Formulation of Nanoparticles to Deliver Nucleic Acids to Target CD44+ Cells

Polycation Molecular weight. NPs have to be stable enough to protect the siRNA before cellular internalization, and de-complex once internalized to release the cargo. The MW of the CS has been shown to affect the carrier stability, and therefore can be considered as a tunable characteristic to improve its activity: siRNA binding efficiency and NPs size were both found to increase with the increase of CS MW (Mao et al. 2010; Liu et al. 2007; Ragelle et al. 2013). Almalik et al. showed that 25 kDa CS complexed with triphosphate (TPP) and HA formed NPs with a crown of loosely bound HA, probably because HA was unable to penetrate the compact CS core. In comparison, 684 kDa CS formed a more porous structure where the HA can accommodate better, giving no apparent external crown (Almalik et al. 2013).

Degree of deacetylation (DD). The deacetylation degree (DD) can be defined as the percentage of deacetylated amine groups, which at the end reflects the CS charge density in acidic conditions. Therefore, it also affects the complexation ability of siRNA. It has been reported that a high DD (>80%) is required to efficiently form siRNA-loaded NPs (Lallana et al. 2017; Rios de la Rosa et al. 2019a). A Higher N/P ratio (amine—positive charges—of CS vs phosphate—negative charges—of siRNA) was reported to improve carrier stability. However, this ratio should not be too high; otherwise, it would limit the release of siRNA intracellularly.

CS to HA weight ratio. When CS and HA are mixed, polyelectrolyte complexation occurs. The impact of intrinsic parameters (e.g., HA, MW, CS MW, CS DD) was discussed, mainly influencing the size and representation of HA on nanoparticle surfaces. Extrinsic parameters such as the charge mixing ratio, the concentration of both polymers, and the pH of polyelectrolyte solutions also impact particle sizes and polydispersity (Duceppe and Tabrizian 2009; Al-Qadi et al. 2013; Wu and Delair 2015). Although all these parameters are directly linked one to the other, the first factor that is typically considered to impact the charge mixing ratio is the pH of CS solution (typical pH range of 4.0–5.5). The pH of the solution determines the dispersion of the polycation in the aqueous phase and the protonation of the polymer. CS and HA concentrations are also critical, typically 1:2 to 1:4 CS to HA weight ratio are used to form nanoparticles, with a higher ratio returning higher concentration of HA on nanoparticles surface hence lower ζ -potential (Tirella et al. 2019).

Hyaluronic Acid Molecular Weight and modifications. Modification of HA with hydrophobic groups/therapeutic biomolecules can be used to obtain amphiphilic derivatives. Control over the degree substitution (DS) of amphiphilic HA-conjugate and the manufacturing process (e.g. sonication as reported by Choi et al. (Choi et al. 2010)) were reported to influence the particle's physical properties, with a typical size range of 200–400 nm.

Mixing process. The mixing (or stirring) speed, the temperature, and the mixing time also impact the size and size distribution of formed nanoparticles. Typically, processes are performed at room temperature, with a mixing speed of 500–2000 rpm. The geometry of the container, or the junction of the microchip, is critical to guarantee the mixing of both phases.

Therapeutic/Cargo properties. Solubility, charge, MW, and stability of the therapeutic of interest are critical formulation parameters. These determine the amount of therapeutic loaded in the nanoparticles (drug loading), as well as its release at the site of interest. Of all the parameters, this is of utmost importance as not only does it drive the complexation of the nanoparticle, but it also determines whether a formulation may achieve the required therapeutic index hence being eventually used clinically.

4.2.4 Considerations on the Single-Step Fabrication of Hyaluronic Acid Nanoparticles

The formulation of NPs, the preparation processes, and the characterization of the final products are all equally critical for both efficacy and safety aspects. For translatability to clinical applications, the selection of materials and technologies should focus on the properties/biocompatibility and the regulatory status to ensure their safety profiles in further preclinical and clinical studies. In the vast majority of the reported studies, NPs preparation processes are optimized for the production of small batches and further used for in vitro or small-scale in vivo studies. However, this is a limiting factor when larger quantities are required.

Emerging technologies have been previously discussed and offer a favorable approach for the fabrication of NPs in continuous processes. In this, microfluidics offers a high degree of control over operational parameters; moreover, when combined with DOE, microfluidics can have an easy and fast validation of NP formulations, as well as facilitate the scaling-up of monodispersed NPs with required features. However, many processes designed for microfluidics may use toxic compounds and solvents, requiring additional purification and sterilization steps prior to the use of NPs. Souza Bicudo et al. reported the fabrication of HA-based NPs by precipitation using a microfluidic system (Bicudo and Santana 2012). In the study, different organic solvents were used, allowing the precipitation of HA NPs using a T-junction chip. The influence of the type of organic solvent, the flow rates (i.e. FRR, TFR), and the HA concentration on mean diameter, PDI, and zeta potential of HA NPs were studied.

On the one hand, the study looked at organic phase-type (i.e. ethanol, isopropyl alcohol, acetone) and flow rates (40–140 μ L/min) as the process variables, keeping constant flow rate of aqueous phase (70 μ L/min) and concentration of HA (1 mg/mL). NPs with a size range of 100–450 nm were obtained. The concentration of HA in the aqueous solution was further evaluated (0.25–1 mg/mL) using a constant flow rate of 40 μ L/min, and with isopropyl alcohol as an organic phase with the flow rate set to 70 μ L/min was found the optimal process parameters to fabricate HA NPs, with minimal impact of HA concentration on particle size and size distribution (PDI \sim 0.1). NPs were further crosslinked with adipic hydrazide by a reaction mediated by chloride carbodiimide, obtaining oil and surfactant-free products.

Continuous processes typically require the presence of organic solvents, whereas simple mixing processes using aqueous solutions offer shorter preparation times and

allow for easier implementation of aseptic manufacturing conditions. The latter processes may be more convenient for immediate use, preventing the potential degradation of therapeutic agents. Several mixing methods have been described in the literature for the preparation of HA-based NPs loading NAs. As previously discussed, ionotropic gelation and polyelectrolyte complexation have been widely explored for the preparation of HA-based NPs, both characterized by a simple mixing procedure of aqueous solutions and absence of purification steps and producing HA-based nanoparticles with sizes <500 nm, HA on their surface, negligible toxicity *in vitro*, and effective encapsulation and protection of NAs. Lallana et al. evaluated the impact of CS MW and CS DD on the encapsulation of mRNA and siRNA, as well as their intracellular release after CD44-mediated internalization, finding that CS with higher MW and higher DD returned the higher transfection efficiency in CD44 expressing cancer cells *in vitro* (Lallana et al. 2017; Tirella et al. 2019).

4.3 Manufacturing of Chitosan/Hyaluronic Acid Nanoparticles for the Delivery of Nucleic Acids

4.3.1 Current Challenges to Deliver siRNA

Over the past decade, NPs have gained attention as gene delivery vehicles as many drawbacks were associated with viral vectors, including safety concerns, their limited payload capacity, and difficulty of large-scale production. NPs have various advantages, such as economic stability, potential to be manufactured at a large scale, safety profile, and capacity for the payload of larger NAs (Liu and Zhang 2011; Ediriwickrema and Saltzman 2015). In the previous paragraphs, several processes for the fabrication of HA-based NPs were discussed, with many encapsulating NAs for gene delivery and as anti-cancer agents.

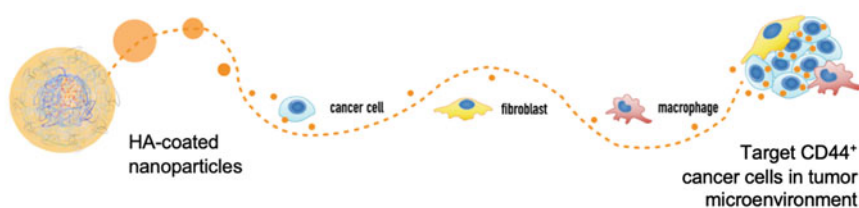
Briefly, positively charged polymers (typically referred to as polycations) and liposomes are the most-used nonviral vectors for gene therapy, mainly because of the lack of immunogenicity. For many polycations polymers such as PEI, poly (L-lysine), and CS (Moghimi et al. 2005), the *in vitro* transfection potential is quite high. However, some of such polymers are cytotoxic or may trigger an immune response. CS is particularly attractive for gene delivery because of its biodegradability, biocompatibility, and mucoadhesive (Jain and Jain 2016). Additionally, CS offers a high density of positive charges along its polymeric chain, particularly attractive to complex with the negatively charged siRNA into compact structures, giving it protection during blood trafficking and promoting cellular uptake (Lallana et al. 2017; Rudzinski and Aminabhavi 2010).

Protection of loaded NAs is also important. Naked siRNAs cannot be delivered systemically because of their inherent limitations (negative charge and immunogenicity) and instability (easily degraded by serum endonucleases, rapid elimination by renal excretion). Polycations encapsulate/complex with NAs and form stable NPs can also protect and deliver siRNAs to target cells. The ideal polycation should

preferably be nontoxic, biodegradable, non-immunogenic, and able to de-complex and release the loaded NAs intracellularly.

Another important criterion to consider in the formulation of NPs for the delivery of NAs is their functionalization. NPs should facilitate intracellular uptake (e.g. via CD44/HA interaction) and promote endosome release/escape of the payload/therapeutic into the cytoplasm. Most of HA-based NPs are proven effective for siRNA delivery with low toxicity levels and limited safety concerns for clinical applications. The presence of HA on the surface of NPs reduces non-specific interactions with serum proteins, as well as promotes internalization into cells expressing HA receptors (e.g. CD44, RHAMM). Figure 4.2 summarized the fate of CS-HA NPs in the tumor microenvironment (Rios De La Rosa et al. 2019b), also sketching the

A | Delivery of HA-coated nanoparticles to CD44⁺ cancer cells



B | Internalization pathways in cancer cells

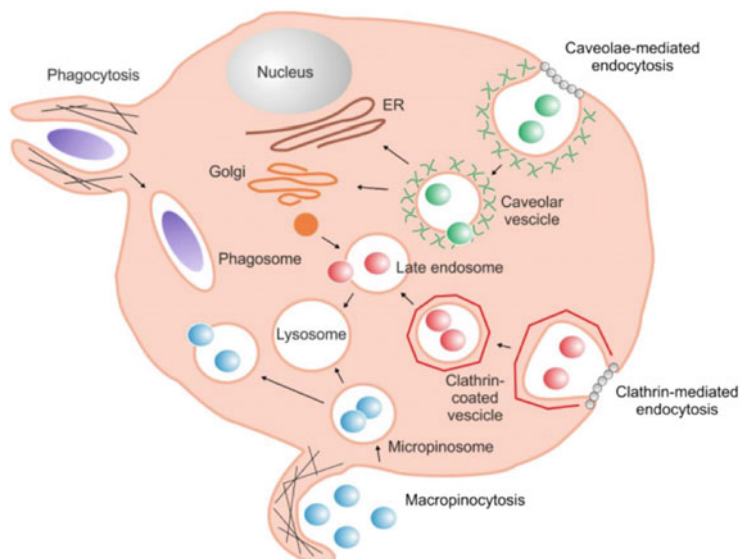


Fig. 4.2 Delivery of HA-coated nanoparticles to CD44-expressing cancer cells: (a) Targeting of CD44-expressing cancer cells, hijacking the immune response and fibroblasts, to release payloads with therapeutic dose; (b) Internalization pathways and intracellular trafficking of nanoparticles in cancer cells, adapted from (Khalil et al. 2006)

release of NAs upon internalization in CD44-expressing cancer cells after escaping vesicular compartments with further accumulation in the perinuclear region and cell nuclei.

Modification of HA with different macromolecules was successfully reported to deliver siRNA in cancer cells (Ganesh et al. 2013). Ganesh et al. described a series of CD44 targeting HA self-assembling nanotechnologies delivering a therapeutic dose of siRNA showing gene knock-down both in vitro and in vivo. Low MW HA (20kDa) was selected to target CD44 and promote internalization. In contrast, the efficacy of bifunctional fatty amines and several polyamines linked to PEGylated-HA was evaluated for the delivery of loaded siRNA. In this study, results evidenced a minimal effect of HA MW on the delivery of NAs.

Recently, our group investigated CS/HA NPs for cancer cell targeting, demonstrating a correlation between CD44 expression and NPs uptake and that cancer cell targeting was favored compared to healthy cells (macrophages, fibroblasts) (Rios de la Rosa et al. 2019a). Moreover, the effect of CS MW was investigated. HMW CS showed high avidity for RNA, which led to higher polyplex stability but, unexpectedly, higher transfection efficiency, suggesting that perhaps HMW CS can also boost endosomal escape or the RNA (Lallana et al. 2017).

4.3.2 Models to Validate Delivery Via CD44: Internalization Mechanisms of Hyaluronic Acid Modified Chitosan Nanoparticles

NPs internalization into cells is affected by many factors, including size, shape, charge, and surface modification. Typically, since the surface area to volume ratio increases with the decrease in NPs size and smaller particles have a greater surface area to interact with the cell membrane, the smaller the size of NPs, the better they are internalized (Salatin and Yari Khosroushahi 2017). NPs shape also can affect their internalization and biodistribution. In fact, for the same reasons as above, elongated NPs were found to interact more efficiently with cell membranes than spherical NPs (Salatin et al. 2015). Positively charged NPs are also known to interact better with the plasma membrane, which contains negatively charged phospholipids. However, they have been related to higher cell toxicity and aggregation with plasma proteins compared to negatively charged NPs. Protein corona formation around NPs in a coat can affect their stability, biodistribution, and interaction with receptors on the cell surface (Monopoli et al. 2012). Modifying the NPs surface with cell-targeting peptides or ligands has been reported to improve their stability and cellular uptake and reduce immunogenicity (Almalik et al. 2017). HA-modified CS NPs (HA/CS NPs) showed better targeting and nucleic acid delivery into osteoarthritic chondrocytes (which express high levels of CD44) compared to non-modified CS NPs (Lu et al. 2011). In another work, it was reported that HA/CS NPs uptake in corneal and conjunctival cells was partially inhibited by preincubation with anti-CD44 Hermes-1 antibody, excess HA (that saturates all the HA receptors), and filipin (that inhibits caveolin-mediated endocytosis) (Contreras-Ruiz et al. 2011).

These results may suggest that the uptake of HA/CS NPs begins with the interaction with CD44 followed by internalization through caveolae. Yamada et al. recently demonstrated that CD44-mediated uptake is an important route for transgene expression. The modification with HA of a novel gene nanovector (plasmid DNA core contained in a lipid bilayer modified with octaarginine) favored the CD44-mediated internalization (24% of total uptake) and improved transfection efficiency in the CD44-positive cancer cell line HCT-116. However, it caused a reduction in transfection of CD44-negative cells, NIH3T3, mouse embryonic fibroblasts, where the HA-modified nanovector did not penetrate through CD44. About 50% of the nanovector uptake (independently if HA-modified or non-modified) was performed by micropinocytosis in both cell lines (Yamada et al. 2015). These results demonstrate that the preferential pathway that cells use for internalization of nanotechnologies is affected by the type of carrier and cell line used, that cells usually do not rely only on one pathway, but on a combination of them and that undoubtedly HA modification confer some cell-specific targeting ability to the carrier.

4.4 Conclusion

HA is a natural polymer used for the treatment of many pathophysiological conditions, being also widely used as an anti-aging agent in many health products. Thanks to its biocompatibility, bioactivity, safety and interaction with specific receptors expressed by human cells, HA is the ideal component to target certain cell types involved in inflammation and tumorigenic processes. Evidence suggests that, when delivered to inflamed tissues, HA may reduce inflammatory processes. HA-based nanotechnologies have been designed to deliver therapeutics to target cells/tissues with proven safety and efficacy in the past years. Considering the importance of HA NPs for drug delivery applications, and the need of more controlled fabrication steps, emerging technologies have been used to improve manufacturing with a single-step process. In this direction, more studies on the use of DOE are required to optimize the concentration of therapeutics loaded in HA-based nanotechnologies hence increasing efficacy and still keeping their safety aspect while improving their fabrication. This approach will offer advantages for the safe and efficacious delivery of therapeutics in target inflamed and/or diseased tissues.

Acknowledgments Dr E Lallana, Dr J Rios de La Rosa, Dr M Pelliccia, Dr A Gennari, Prof IJ Stratford, and Prof N Tirelli are gratefully acknowledged by all the authors for discussions on nanoparticle formulation and delivery. Dr Alice Spadea gratefully acknowledge financial support by the NorthWest Centre of Advanced Drug Delivery (NoWCADD) established at the University of Manchester. The authors thank Prof J Lawrence (University of Manchester), Dr M Ashford (AstraZeneca) and NoWCADD for support and discussions on nanoparticles formulation and intracellular delivery.

References

- Afify AM, Tate S, Durbin-Johnson B, Rocke DM, Konia T (2011) Expression of CD44s and CD44v6 in lung cancer and their correlation with prognostic factors. *Int J Biol Markers* 26:50–57
- Agarwal G, Krishnan KV, Prasad SB, Bhaduri A, Jayaraman G (2019) Biosynthesis of hyaluronic acid polymer: dissecting the role of sub structural elements of hyaluronan synthase. *Sci Rep* 9: 12510
- Alatorre-Meda M, Taboada P, Sabín J, Krajewska B, Varela LM, Rodríguez JR (2009) DNA–chitosan complexation: a dynamic light scattering study. *Colloids Surf A Physicochem Eng Aspects* 339:145–152
- Almalik A, Karimi S, Ouasti S, Donno R, Wandrey C, Day PJ, Tirelli N (2013) Hyaluronic acid (HA) presentation as a tool to modulate and control the receptor-mediated uptake of HA-coated nanoparticles. *Biomaterials* 34:5369–5380
- Almalik A, Benabdelkamel H, Masood A, Alanazi IO, Alradwan I, Majrashi MA, Alfadda AA, Alghamdi WM, Alrabiah H, Tirelli N, Alhasan AH (2017) Hyaluronic acid coated chitosan nanoparticles reduced the immunogenicity of the formed protein corona. *Sci Rep* 7:10,542
- Al-Qadi S, Alatorre-Meda M, Zaghoul EM, Taboada P, Remunán-López C (2013) Chitosan-hyaluronic acid nanoparticles for gene silencing: the role of hyaluronic acid on the nanoparticles' formation and activity. *Colloids Surf B Biointerfaces* 103:615–623
- Altman RD, Manjoo A, Fierlinger A, Niazi F, Nicholls M (2015) The mechanism of action for hyaluronic acid treatment in the osteoarthritic knee: a systematic review. *BMC Musculoskeletal Disord* 16:321
- Anttila MA, Tammi RH, Tammi MI, Syrjänen KJ, Saarikoski SV, Kosma VM (2000) High levels of stromal hyaluronan predict poor disease outcome in epithelial ovarian cancer. *Cancer Res* 60: 150–155
- Apaolaza PS, Delgado D, del Pozo-Rodríguez A, Gascón AR, Solinís M (2014) A novel gene therapy vector based on hyaluronic acid and solid lipid nanoparticles for ocular diseases. *Int J Pharm* 465:413–426
- Aragona P, Simmons PA, Wang H, Wang T (2019) Physicochemical properties of hyaluronic acid-based lubricant eye drops. *Transl Vis Sci Technol* 8:2
- Asplund T, Versnel MA, Laurent TC, Heldin P (1993) Human mesothelioma cells produce factors that stimulate the production of hyaluronan by mesothelial cells and fibroblasts. *Cancer Res* 53: 388–392
- Auvinen P, Tammi R, Parkkinen J, Tammi M, Agren U, Johansson R, Hirvikoski P, Eskelinen M, Kosma VM (2000) Hyaluronan in peritumoral stroma and malignant cells associates with breast cancer spreading and predicts survival. *Am J Pathol* 156:529–536
- Baeva LF, Lyle DB, Rios M, Langone JJ, Lightfoote MM (2014) Different molecular weight hyaluronic acid effects on human macrophage interleukin 1 β production. *J Biomed Mater Res A* 102:305–314
- Bartolazzi A, Nocks A, Aruffo A, Spring F, Stamenkovic I (1996) Glycosylation of CD44 is implicated in CD44-mediated cell adhesion to hyaluronan. *J Cell Biol* 132:1199–1208
- Begines B, Ortiz T, Pérez-Aranda M, Martínez G, Merinero M, Argüelles-Arias F, Alcludia A (2020) Polymeric nanoparticles for drug delivery: recent developments and future prospects. *Nanomaterials* 10
- Bennett KL, Jackson DG, Simon JC, Tanczos E, Peach R, Modrell B, Stamenkovic I, Plowman G, Aruffo A (1995) CD44 isoforms containing exon V3 are responsible for the presentation of heparin-binding growth factor. *J Cell Biol* 128:687–698
- Bhadra AK, Altman R, Dasa V, Myrick K, Rosen J, Vad V, Vitanzo P, Bruno M, Kleiner H, Just C (2017) Appropriate use criteria for hyaluronic acid in the treatment of knee osteoarthritis in the United States. *Cartilage* 8:234–254

- Bicudo RCS, Santana MHA (2012) Production of hyaluronic acid (HA) nanoparticles by a continuous process inside microchannels: effects of non-solvents, organic phase flow rate, and HA concentration. *Chem Eng Sci* 84:134–141
- Bilati U, Allémann E, Doelker E (2005) Development of a nanoprecipitation method intended for the entrapment of hydrophilic drugs into nanoparticles. *Eur J Pharm Sci* 24:67–75
- Birzele F, Voss E, Nopora A, Honold K, Heil F, Lohmann S, Verheul H, Le Tourneau C, Delord JP, van Herpen C, Mahalingam D, Coveler AL, Meresse V, Weigand S, Runza V, Cannarile M (2015) CD44 Isoform Status Predicts Response to Treatment with Anti-CD44 Antibody in Cancer Patients. *Clin Cancer Res* 21:2753–2762
- Bonnans C, Chou J, Werb Z (2014) Remodelling the extracellular matrix in development and disease. *Nat Rev Mol Cell Biol* 15:786–801
- Cai S, Alhowsyan AA, Yang Q, Forrest WC, Shnyder Y, Forrest ML (2014) Cellular uptake and internalization of hyaluronan-based doxorubicin and cisplatin conjugates. *J Drug Target* 22: 648–657
- Campo GM, Avenoso A, Campo S, D’Ascola A, Traina P, Calatroni A (2009) Differential effect of molecular size HA in mouse chondrocytes stimulated with PMA. *Biochim Biophys Acta* 1790: 1353–1367
- Carton F, Chevalier Y, Nicoletti L, Tarnowska M, Stella B, Arpicco S, Malatesta M, Jordheim LP, Briançon S, Lollo G (2019) Rationally designed hyaluronic acid-based nano-complexes for pentamidine delivery. *Int J Pharm* 568:118526
- Chen C, Zhao S, Karnad A, Freeman JW (2018) The biology and role of CD44 in cancer progression: therapeutic implications. *J Hematol Oncol* 11:64
- Chithrani BD, Chan WC (2007) Elucidating the mechanism of cellular uptake and removal of protein-coated gold nanoparticles of different sizes and shapes. *Nano Lett* 7:1542–1550
- Choi KY, Chung H, Min KH, Yoon HY, Kim K, Park JH, Kwon IC, Jeong SY (2010) Self-assembled hyaluronic acid nanoparticles for active tumor targeting. *Biomaterials* 31:106–114
- Contreras-Ruiz L, de la Fuente M, Párraga JE, López-García A, Fernández I, Seijo B, Sánchez A, Calonge M, Diebold Y (2011) Intracellular trafficking of hyaluronic acid-chitosan oligomer-based nanoparticles in cultured human ocular surface cells. *Mol Vis* 17:279–290
- Cowman MK, Lee HG, Schwertfeger KL, McCarthy JB, Turley EA (2015) The content and size of hyaluronan in biological fluids and tissues. *Front Immunol* 6:261
- Cun D, Jensen DK, Maltesen MJ, Bunker M, Whiteside P, Scurr D, Foged C, Nielsen HM (2011) High loading efficiency and sustained release of siRNA encapsulated in PLGA nanoparticles: quality by design optimization and characterization. *Eur J Pharm Biopharm* 77:26–35
- Cyphert JM, Trempus CS, Garantzis S (2015) Size matters: molecular weight specificity of hyaluronan effects in cell biology. *Int J Cell Biol* 2015:563818
- DeGrendele HC, Kosfiszter M, Estess P, Siegelman MH (1997) CD44 activation and associated primary adhesion is inducible via T cell receptor stimulation. *J Immunol* 159:2549–2553
- Deng X, Cao M, Zhang J, Hu K, Yin Z, Zhou Z, Xiao X, Yang Y, Sheng W, Wu Y, Zeng Y (2014) Hyaluronic acid-chitosan nanoparticles for co-delivery of MiR-34a and doxorubicin in therapy against triple negative breast cancer. *Biomaterials* 35:4333–4344
- Duceppe N, Tabrizian M (2009) Factors influencing the transfection efficiency of ultra low molecular weight chitosan/hyaluronic acid nanoparticles. *Biomaterials* 30:2625–2631
- Ediriwickrema A, Saltzman WM (2015) Nanotherapy for cancer: targeting and multifunctionality in the future of cancer therapies. *ACS Biomater Sci Eng* 1:64–78
- Eliasz RE, Szoka FC (2001) Liposome-encapsulated doxorubicin targeted to CD44: a strategy to kill CD44-overexpressing tumor cells. *Cancer Res* 61:2592–2601
- English NM, Lesley JF, Hyman R (1998) Site-specific de-N-glycosylation of CD44 can activate hyaluronan binding, and CD44 activation states show distinct threshold densities for hyaluronan binding. *Cancer Res* 58:3736–3742
- Fakhari A, Berkland C (2013) Applications and emerging trends of hyaluronic acid in tissue engineering, as a dermal filler and in osteoarthritis treatment. *Acta Biomater* 9:7081–7092

- Faller CE, Guvench O (2014) Terminal sialic acids on CD44 N-glycans can block hyaluronan binding by forming competing intramolecular contacts with arginine sidechains. *Proteins* 82: 3079–3089
- Fessi H, Puisieux F, Devissaguet JP, Ammoury N, Benita S (1989) Nanocapsule formation by interfacial polymer deposition following solvent displacement. *Int J Pharm* 55:R1–R4
- Fitzgerald KA, Bowie AG, Skeffington BS, O'Neill LA (2000) Ras, protein kinase C zeta, and I kappa B kinases 1 and 2 are downstream effectors of CD44 during the activation of NF-kappa B by hyaluronic acid fragments in T-24 carcinoma cells. *J Immunol* 164:2053–2063
- Fraser JR, Laurent TC, Laurent UB (1997) Hyaluronan: its nature, distribution, functions and turnover. *J Intern Med* 242:27–33
- de la Fuente M, Seijo B, Alonso MJ (2008) Bioadhesive hyaluronan-chitosan nanoparticles can transport genes across the ocular mucosa and transfect ocular tissue. *Gene Ther* 15:668–676
- Gan Q, Wang T, Cochrane C, McCarron P (2005) Modulation of surface charge, particle size and morphological properties of chitosan-TPP nanoparticles intended for gene delivery. *Colloids Surf B Biointerfaces* 44:65–73
- Ganesh S, Iyer AK, Morrissey DV, Amiji MM (2013) Hyaluronic Acid based self-assembling nanosystems for CD44 target mediated siRNA delivery to solid tumors. *Biomaterials* 34:3489–3502
- Gennari A, Rios de la Rosa JM, Hohn E, Pelliccia M, Lallana E, Donno R, Tirella A, Tirelli N (2019) The different ways to chitosan/hyaluronic acid nanoparticles: templated vs direct complexation. Influence of particle preparation on morphology, cell uptake and silencing efficiency. *Beilstein J Nanotechnol* 10:2594–2608
- Greyner HJ, Wiraszka T, Zhang LS, Petroll WM, Mummert ME (2010) Inducible macropinocytosis of hyaluronan in B16-F10 melanoma cells. *Matrix Biol* 29:503–510
- Guan H, Nagarkatti PS, Nagarkatti M (2011) CD44 Reciprocally regulates the differentiation of encephalitogenic Th1/Th17 and Th2/regulatory T cells through epigenetic modulation involving DNA methylation of cytokine gene promoters, thereby controlling the development of experimental autoimmune encephalomyelitis. *J Immunol* 186:6955–6964
- Guo Q, Liu Y, He Y, Du Y, Zhang G, Yang C, Gao F (2021) CD44 activation state regulated by the CD44v10 isoform determines breast cancer proliferation. *Oncol Rep* 45
- Gupta RC, Lall R, Srivastava A, Sinha A (2019) Hyaluronic acid: molecular mechanisms and therapeutic trajectory. *Front Vet Sci* 6:192
- Harris EN, Kyoosseva SV, Weigel JA, Weigel PH (2007) Expression, processing, and glycosaminoglycan binding activity of the recombinant human 315-kDa hyaluronic acid receptor for endocytosis (HARE). *J Biol Chem* 282:2785–2797
- Heldin P, Basu K, Olofsson B, Porsch H, Kozlova I, Kahata K (2013) Deregulation of hyaluronan synthesis, degradation and binding promotes breast cancer. *J Biochem* 154:395–408
- Hu J, Li G, Zhang P, Zhuang X, Hu G (2017) A CD44v. *Cell Death Dis* 8:e2679
- Jahn A, Vreeland WN, Gaitan M, Locascio LE (2004) Controlled vesicle self-assembly in microfluidic channels with hydrodynamic focusing. *J Am Chem Soc* 126:2674–2675
- Jain A, Jain SK (2016) Optimization of chitosan nanoparticles for colon tumors using experimental design methodology. *Artif Cells Nanomed Biotechnol* 44:1917–1926
- Jiang D, Liang J, Fan J, Yu S, Chen S, Luo Y, Prestwich GD, Mascarenhas MM, Garg HG, Quinn DA, Homer RJ, Goldstein DR, Bucala R, Lee PJ, Medzhitov R, Noble PW (2005) Regulation of lung injury and repair by Toll-like receptors and hyaluronan. *Nat Med* 11:1173–1179
- Katas H, Alpar HO (2006) Development and characterisation of chitosan nanoparticles for siRNA delivery. *J Control Release* 115:216–225
- Khalil IA, Kogure K, Akita H, Harashima H (2006) Uptake pathways and subsequent intracellular trafficking in nonviral gene delivery. *Pharmacol Rev* 58:32–45
- Kim TH, Jiang HL, Nah JW, Cho MH, Akaike T, Cho CS (2007) Receptor-mediated gene delivery using chemically modified chitosan. *Biomed Mater* 2:S95–S100

- Lallana E, Rios de la Rosa JM, Tirella A, Pelliccia M, Gennari A, Stratford IJ, Puri S, Ashford M, Tirelli N (2017) Chitosan/hyaluronic acid nanoparticles: rational design revisited for RNA delivery. *Mol Pharm* 14:2422–2436
- Lee H, Mok H, Lee S, Oh YK, Park TG (2007) Target-specific intracellular delivery of siRNA using degradable hyaluronic acid nanogels. *J Control Release* 119:245–252
- Lesley J, Hyman R, Kincade PW (1993) CD44 and its interaction with extracellular matrix. *Adv Immunol* 54:271–335
- Lesley J, English N, Perschl A, Gregoroff J, Hyman R (1995) Variant cell lines selected for alterations in the function of the hyaluronan receptor CD44 show differences in glycosylation. *J Exp Med* 182:431–437
- Li Z, Chen K, Jiang P, Zhang X, Li X (2014) CD44v/CD44s expression patterns are associated with the survival of pancreatic carcinoma patients. *Diagn Pathol* 9:79
- Li W, Chen Q, Baby T, Jin S, Liu Y, Yang G, Zhao C-X (2021) Insight into drug encapsulation in polymeric nanoparticles using microfluidic nanoprecipitation. *Chem Eng Sci* 235:116468
- Liang J, Jiang D, Griffith J, Yu S, Fan J, Zhao X, Bucala R, Noble PW (2007) CD44 is a negative regulator of acute pulmonary inflammation and lipopolysaccharide-TLR signaling in mouse macrophages. *J Immunol* 178:2469–2475
- Liu C, Zhang N (2011) Nanoparticles in gene therapy principles, prospects, and challenges. *Prog Mol Biol Transl Sci* 104:509–562
- Liu X, Howard KA, Dong M, Andersen M, Rahbek UL, Johnsen MG, Hansen OC, Besenbacher F, Kjems J (2007) The influence of polymeric properties on chitosan/siRNA nanoparticle formulation and gene silencing. *Biomaterials* 28:1280–1288
- Lu HD, Zhao HQ, Wang K, Lv LL (2011) Novel hyaluronic acid-chitosan nanoparticles as nonviral gene delivery vectors targeting osteoarthritis. *Int J Pharm* 420:358–365
- Ma L, Dong L, Chang P (2019) CD44v6 engages in colorectal cancer progression. *Cell Death Dis* 10:30
- Maeki M, Kimura N, Sato Y, Harashima H, Tokeshi M (2018) Advances in microfluidics for lipid nanoparticles and extracellular vesicles and applications in drug delivery systems. *Adv Drug Deliv Rev* 128:84–100
- Mao S, Sun W, Kissel T (2010) Chitosan-based formulations for delivery of DNA and siRNA. *Adv Drug Deliv Rev* 62:12–27
- McKee CM, Penno MB, Cowman M, Burdick MD, Strieter RM, Bao C, Noble PW (1996) Hyaluronan (HA) fragments induce chemokine gene expression in alveolar macrophages. The role of HA size and CD44. *J Clin Invest* 98:2403–2413
- Misra S, Hascall VC, Markwald RR, Ghatak S (2015) Interactions between hyaluronan and its receptors (CD44, RHAMM) regulate the activities of inflammation and cancer. *Front Immunol* 6:201
- Moghimi SM, Symonds P, Murray JC, Hunter AC, Debska G, Szweczyk A (2005) A two-stage poly(ethylenimine)-mediated cytotoxicity: implications for gene transfer/therapy. *Mol Ther* 11:990–995
- Mohamadzadeh M, DeGrendele H, Arizpe H, Estess P, Siegelman M (1998) Pro-inflammatory stimuli regulate endothelial hyaluronan expression and CD44/HA-dependent primary adhesion. *J Clin Invest* 101:97–108
- Monopoli MP, Aberg C, Salvati A, Dawson KA (2012) Biomolecular coronas provide the biological identity of nanosized materials. *Nat Nanotechnol* 7:779–786
- Monzón ME, Manzanares D, Schmid N, Casalino-Matsuda SM, Forteza RM (2008) Hyaluronidase expression and activity is regulated by pro-inflammatory cytokines in human airway epithelial cells. *Am J Respir Cell Mol Biol* 39:289–295
- Monzon ME, Fregien N, Schmid N, Falcon NS, Campos M, Casalino-Matsuda SM, Forteza RM (2010) Reactive oxygen species and hyaluronidase 2 regulate airway epithelial hyaluronan fragmentation. *J Biol Chem* 285:26126–26134
- Mosser DM, Edwards JP (2008) Exploring the full spectrum of macrophage activation. *Nat Rev Immunol* 8:958–969

- Nandi A, Estess P, Siegelman MH (2000) Hyaluronan anchoring and regulation on the surface of vascular endothelial cells is mediated through the functionally active form of CD44. *J Biol Chem* 275:14939–14948
- Naor D, Sionov RV, Ish-Shalom D (1997) CD44: structure, function, and association with the malignant process. *Adv Cancer Res* 71:241–319
- Nazeri N, Avadi MR, Faramarzi MA, Safarian S, Tavosoidana G, Khoshayand MR, Amani A (2013) Effect of preparation parameters on ultra low molecular weight chitosan/hyaluronic acid nanoparticles. *Int J Biol Macromol* 62:642–646
- Neumann A, Schinzel R, Palm D, Riederer P, Münch G (1999) High molecular weight hyaluronic acid inhibits advanced glycation endproduct-induced NF-kappaB activation and cytokine expression. *FEBS Lett* 453:283–287
- Nicholls M, Manjoo A, Shaw P, Niazi F, Rosen J (2018) Rheological properties of commercially available hyaluronic acid products in the United States for the treatment of osteoarthritis knee pain. *Clin Med Insights Arthritis Musculoskelet Disord* 11:1179544117751622
- Passi A, Vigetti D, Buraschi S, Iozzo RV (2019) Dissecting the role of hyaluronan synthases in the tumor microenvironment. *FEBS J* 286:2937–2949
- Peach RJ, Hollenbaugh D, Stamenkovic I, Aruffo A (1993) Identification of hyaluronic acid binding sites in the extracellular domain of CD44. *J Cell Biol* 122:257–264
- Qiao GL, Song LN, Deng ZF, Chen Y, Ma LJ (2018) Prognostic value of CD44v6 expression in breast cancer: a meta-analysis. *Onco Targets Ther* 11:5451–5457
- Racine RM, Mark E (2012) Hyaluronan endocytosis: mechanisms of uptake and biological functions. In: *Molecular Regulation of Endocytosis* (ed) B. Ceresa
- Ragelle H, Vandermeulen G, Pr at V (2013) Chitosan-based siRNA delivery systems. *J Control Release* 172:207–218
- Rayahin JE, Buhrman JS, Zhang Y, Koh TJ, Gemeinhart RA (2015) High and low molecular weight hyaluronic acid differentially influence macrophage activation. *ACS Biomater Sci Eng* 1:481–493
- Rios de la Rosa JM, Tirella A, Tirelli N (2018) Receptor-targeted drug delivery and the (many) problems we know of: the case of CD44 and hyaluronic acid. *Adv Biosyst* 2:1800049
- Rios de la Rosa JM, Pingrajai P, Pelliccia M, Spadea A, Lallana E, Gennari A, Stratford IJ, Rocchia W, Tirella A, Tirelli N (2019a) Binding and internalization in receptor-targeted carriers: the complex role of CD44 in the uptake of hyaluronic acid-based nanoparticles (siRNA delivery). *Adv Healthc Mater* 8:e1901182
- Rios De La Rosa JM, Tirelli N, Tirella A (2019b) Hyaluronic acid carrier-cell interactions: a tri-culture model of the tumour microenvironment to study siRNA delivery under flow conditions. *Int J Nano Biomater* 8:106–117
- Rudzinski WE, Aminabhavi TM (2010) Chitosan as a carrier for targeted delivery of small interfering RNA. *Int J Pharm* 399:1–11
- Salatin S, Yari Khosroushahi A (2017) Overviews on the cellular uptake mechanism of polysaccharide colloidal nanoparticles. *J Cell Mol Med* 21:1668–1686
- Salatin S, Maleki Dizaj S, Yari Khosroushahi A (2015) Effect of the surface modification, size, and shape on cellular uptake of nanoparticles. *Cell Biol Int* 39:881–890
- Salzillo R, Schiraldi C, Corsuto L, D’Agostino A, Filosa R, De Rosa M, La Gatta A (2016) Optimization of hyaluronan-based eye drop formulations. *Carbohydr Polym* 153:275–283
- Sato N, Kohi S, Hirata K, Goggins M (2016) Role of hyaluronan in pancreatic cancer biology and therapy: Once again in the spotlight. *Cancer Sci* 107:569–575
- Scheibner KA, Lutz MA, Boodoo S, Fenton MJ, Powell JD, Horton MR (2006) Hyaluronan fragments act as an endogenous danger signal by engaging TLR2. *J Immunol* 177:1272–1281
- Sedighi M, Sieber S, Rahimi F, Shahbazi MA, Rezayan AH, Huwyler J, Witzigmann D (2019) Rapid optimization of liposome characteristics using a combined microfluidics and design-of-experiment approach. *Drug Deliv Transl Res* 9:404–413
- Shi Q, Zhao L, Xu C, Zhang L, Zhao H (2019) High molecular weight hyaluronan suppresses macrophage M1 polarization and enhances IL-10 production in PM. *Molecules* 24

- Shu XZ, Zhu KJ (2000) A novel approach to prepare tripolyphosphate/chitosan complex beads for controlled release drug delivery. *Int J Pharm* 201:51–58
- Skelton TP, Zeng C, Nocks A, Stamenkovic I (1998) Glycosylation provides both stimulatory and inhibitory effects on cell surface and soluble CD44 binding to hyaluronan. *J Cell Biol* 140:431–446
- Sleeman J, Rudy W, Hofmann M, Moll J, Herrlich P, Ponta H (1996) Regulated clustering of variant CD44 proteins increases their hyaluronate binding capacity. *J Cell Biol* 135:1139–1150
- Slevin M, Krupinski J, Gaffney J, Matou S, West D, Delisser H, Savani RC, Kumar S (2007) Hyaluronan-mediated angiogenesis in vascular disease: uncovering RHAMM and CD44 receptor signaling pathways. *Matrix Biol* 26:58–68
- Spadea A, Rios de la Rosa JM, Tirella A, Ashford MB, Williams KJ, Stratford IJ, Tirelli N, Mehibel M (2019) Evaluating the efficiency of hyaluronic acid for tumor targeting via CD44. *Mol Pharm* 16:2481–2493
- Stamenkovic I, Amiot M, John MPABS (1989) A lymphocyte molecule implicated in lymph node homing is a member of the cartilage link protein family. *Cell* 56:1057–1062
- Takahashi Y, Li L, Kamiryo M, Asteriou T, Moustakas A, Yamashita H, Heldin P (2005) Hyaluronan fragments induce endothelial cell differentiation in a CD44- and CXCL1/GRO1-dependent manner. *J Biol Chem* 280:24195–24204
- Thomas RG, Moon M, Lee S, Jeong YY (2015) Paclitaxel loaded hyaluronic acid nanoparticles for targeted cancer therapy: in vitro and in vivo analysis. *Int J Biol Macromol* 72:510–518
- Tirella A, Kloc-Muniak K, Good L, Ridden J, Ashford M, Puri S, Tirelli N (2019) CD44 targeted delivery of siRNA by using HA-decorated nanotechnologies for KRAS silencing in cancer treatment. *Int J Pharm* 561:114–123
- Tremmel M, Matzke A, Albrecht I, Laib AM, Olaku V, Ballmer-Hofer K, Christofori G, Héroult M, Augustin HG, Ponta H, Orian-Rousseau V (2009) A CD44v6 peptide reveals a role of CD44 in VEGFR-2 signaling and angiogenesis. *Blood* 114:5236–5244
- Veisoh M, Leith SJ, Tolg C, Elhayek SS, Bahrami SB, Collis L, Hamilton S, McCarthy JB, Bissell MJ, Turley E (2015) Uncovering the dual role of RHAMM as an HA receptor and a regulator of CD44 expression in RHAMM-expressing mesenchymal progenitor cells. *Front Cell Dev Biol* 3:63
- Wang SJ, Wreesmann VB, Bourguignon LY (2007) Association of CD44 V3-containing isoforms with tumor cell growth, migration, matrix metalloproteinase expression, and lymph node metastasis in head and neck cancer. *Head Neck* 29:550–558
- Wang Z, Zhao K, Hackert T, Zöller M (2018) CD44/CD44v6 a reliable companion in cancer-initiating cell maintenance and tumor progression. *Front Cell Dev Biol* 6:97
- Wu D, Delair T (2015) Stabilization of chitosan/hyaluronan colloidal polyelectrolyte complexes in physiological conditions. *Carbohydr Polym* 119:149–158
- Wu J, Wang Y, Yang H, Liu X, Lu Z (2017) Preparation and biological activity studies of resveratrol loaded ionically crosslinked chitosan-TPP nanoparticles. *Carbohydr Polym* 175:170–177
- Wu W, Chen L, Wang Y, Jin J, Xie X, Zhang J (2020) Hyaluronic acid predicts poor prognosis in breast cancer patients: a protocol for systematic review and meta analysis. *Medicine (Baltimore)* 99:e20438
- Xu Q, Hashimoto M, Dang TT, Hoare T, Kohane DS, Whitesides GM, Langer R, Anderson DG (2009) Preparation of monodisperse biodegradable polymer microparticles using a microfluidic flow-focusing device for controlled drug delivery. *Small* 5:1575–1581
- Yamada Y, Hashida M, Harashima H (2015) Hyaluronic acid controls the uptake pathway and intracellular trafficking of an octaarginine-modified gene vector in CD44 positive- and CD44 negative-cells. *Biomaterials* 52:189–198
- Yamawaki H, Hirohata S, Miyoshi T, Takahashi K, Ogawa H, Shinohata R, Demircan K, Kusachi S, Yamamoto K, Ninomiya Y (2009) Hyaluronan receptors involved in cytokine induction in monocytes. *Glycobiology* 19:83–92

- Yang C, Cao M, Liu H, He Y, Xu J, Du Y, Liu Y, Wang W, Cui L, Hu J, Gao F (2012) The high and low molecular weight forms of hyaluronan have distinct effects on CD44 clustering. *J Biol Chem* 287:43094–43107
- Yun YH, Goetz DJ, Yellen P, Chen W (2004) Hyaluronan microspheres for sustained gene delivery and site-specific targeting. *Biomaterials* 25:147–157
- Zhao C-X, He L, Qiao SZ, Middelberg APJ (2011) Nanoparticle synthesis in microreactors. *Chem Eng Sci* 66:1463–1479
- Zhong L, Liu Y, Xu L, Li Q, Zhao D, Li Z, Zhang H, Kan Q, Sun J, He Z (2019) Exploring the relationship of hyaluronic acid molecular weight and active targeting efficiency for designing hyaluronic acid-modified nanoparticles. *Asian J Pharm Sci* 14:521–530
- Zöller M (2011) CD44: can a cancer-initiating cell profit from an abundantly expressed molecule? *Nat Rev Cancer* 11:254–267



Theranostics Nanomaterials for Safe Cancer Treatment

5

Sindhu C. Pillai, Athira Anirudhan, and D. Sakthi Kumar

5.1 Introduction: Cancer and Nanomedicine

Cancer is one of the major causes of death worldwide, and it is estimated to increase by more than 70% in the coming years (Siegel et al. 2017). The 2020 report from National Cancer Registry Programme in India estimated that 94.1 per 100,000 males and 103.6 per 100,000 females were affected with cancer (Mathur et al. 2020). The six main hallmarks of cancer explained by Weinberg and Hanahan, which differentiate normal cells from cancerous, are sustained proliferative signaling, evading growth suppressors, activating invasion and metastasis, enabling replicative immortality, inducing angiogenesis, and resisting cell death (Hanahan and Weinberg 2011). Moreover, the functional activity of telomerase in cancer cells increases the DNA integrity, which helps them replicate infinitely. Another hallmark associated with a cancer cell is reprogramming of energy metabolism and evading the immune destruction process. In cancerous cells, the glucose transporter expression upregulates, which subsequently reprograms the metabolic pathway into aerobic glycolysis, increasing cell division and proliferation. In addition, the absence of surface marker in cancer cells mask its recognition from T lymphocytes and escape from the normal cellular elimination process (Hanahan and Weinberg 2011).

The conventional treatment method for cancer includes chemotherapy, radiation, and surgery. The major aim of chemotherapy is to destroy the growing cancerous cells; however, it also kills the normal surrounding tissues. The side effects of chemotherapy are drastic hair loss, bone marrow suppression, and gastrointestinal

S. C. Pillai · D. S. Kumar (✉)

Bio Nano Electronics Research Center, Graduate School of Interdisciplinary New Science, Toyo University, Kawagoe Campus, Saitama, Japan
e-mail: sakthi@toyo.jp

A. Anirudhan

Department of Nephrology, All India Institute of Medical Sciences, Bhopal, Madhya Pradesh, India

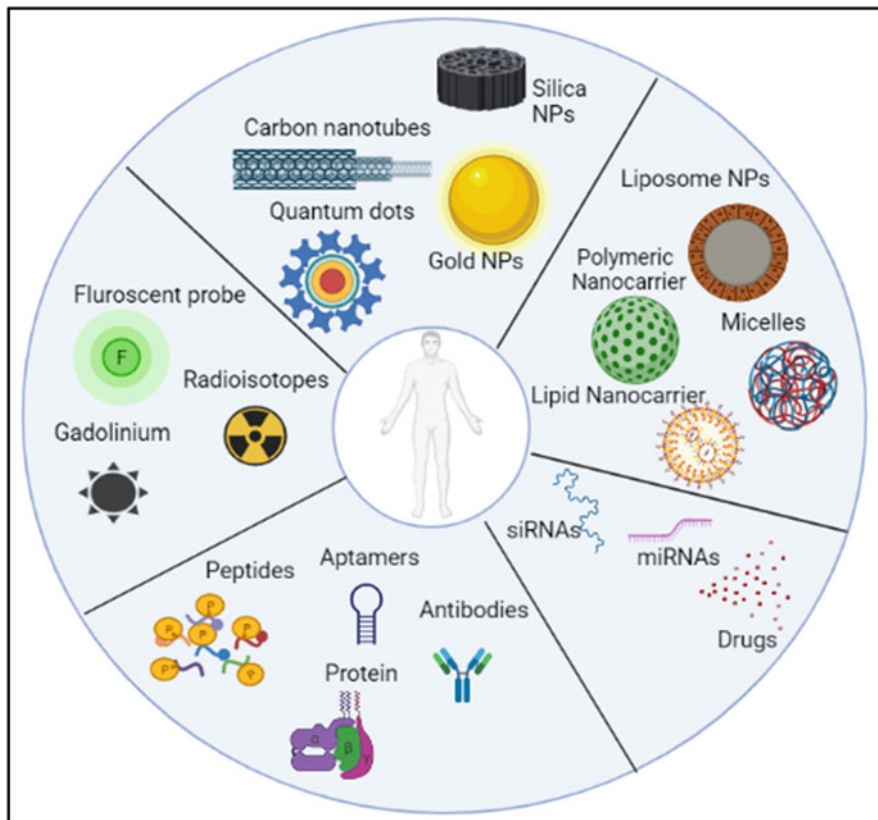


Fig. 5.1 The figure denotes different kinds of nanomedicine technologies

problems. The advancements in clinical diagnosis and treatment have improved the survival rate of cancer patients; though, these technologies still have limitations. Hence, there is an immense need to develop a therapy and diagnosis method that precisely targets cancerous cells by sparing normal cells to overcome the drawback of conventional methods. As a solution, nanomedicine technology was introduced (Fig. 5.1).

The current imaging contrast agents and tracers used in cancer diagnosis have limitations like lack of specificity, drug clearance, biodegradation, and side effects. Nanomedicine improves *in vivo* molecular diagnosis and targeted drug therapy using various contrast agents in cancer therapy. In nanomedicine, generally, the size of the nanoparticles ranges from 1 to 100 nm is synthesized and used (Wicki et al. 2015). The nanoparticles can target specific cancerous cells as the noninvasive method in *in vivo* and monitor the molecular changes. Another potential benefit of nanomedicine in cancer is that the drug-loaded nanocarriers delivered intravenously get absorbed directly by tumor vasculature via enhanced permeability and retention (EPR) effect. Similarly, these nanocarriers increase the half-life of chemotherapy

drugs thus being able to circulate long time resulting in an increase in its bioavailability and sustained drug release. In this chapter, we discuss the prospects of nanomedicines in the diagnosis and treatment of cancer. Table 5.1 represents the nanomedicines used against various cancers.

Recent nanomedicine research developed multifunctional nanoparticles that have both cancer diagnosis and treatment capability known as theragnosis (therapy + diagnosis) or theranostic nanoparticles. The term theranostic represents nanoparticles with two combined benefits of molecular imaging or diagnosis and therapeutic effect with loaded drug delivery (Fig. 5.2) (Andreou et al. 2017).

The multifunctional property of theranostic nanoparticle is subjected to its extremely small size with a large surface-area-to-volume ratio. The nanoparticles were synthesized in such a way as to improve their biocompatibility, stability in cancerous microenvironments, safety, drug loading and releasing capacity, target-specific delivery, molecular imaging, and sensitivity towards thermal or photodynamic stimuli. In addition, the reports suggest that the polymer used for theranostic nanoparticles are highly biocompatible and are readily biodegradable while used in vivo (Yildiz et al. 2018; Dobiasch et al. 2016; Belyanina et al. 2017; Lee et al. 2009). Among a diverse range of nanoparticles synthesized using different methodologies for biomedical applications, the bio-inspired nano vectors are most widely used compared with chemically synthesized materials to avoid the toxicity of chemical compounds. The common bio-inspired multifunctional theranostic NPs used are viral, protein NPs, apoferritin, aptamers, and solid-lipid NPs. The particle's outer surface was tagged with fluorophores and other contrast probes, which promotes sensitivity in imaging. They provide molecular imaging through contrast agents, measure therapeutic strategy by imaging probes and targeted drug delivery. The bioinspired theranostic nanoparticles are synthesized by following a few criteria: selection of accurate source material, methodology standardization for controlling physicochemical characteristics of nanoparticle, selection of therapeutics, imaging agents, and characterization of synthesized nanoparticles using various analytical techniques. Different theranostic nanoparticles are under clinical and preclinical trials (Table 5.2).

5.2 Bio-Inspired Organic Nanoparticles Used in Cancer

The diverse ranges of the green-synthesis approach to synthesize nanoparticles from natural sources, its cost-effectiveness, materials quality, and sustainability make researchers focus on constructing bio-inspired nanoparticles with unique characteristics for biomedical applications. Similarly, functional nanomaterials such as carbon nanotubes (CNTs), graphene, fullerenes, polymeric nanoparticles, and metal nanoparticles have physicochemical properties such as catalytic, dielectric, optical, and mechanical. These properties enable them to use in sensors, drug delivery, proteomics, and biomolecular electronics that provide a wide range of biomedical applications. On the other hand, some of these nanoparticles foster toxicity a bit higher, which may be suitable for killing cancer cells. In addition, the

Table 5.1 List of current nanomedicine used for cancer

Nanomedicine	Nanoparticle	Conjugated drug	Diameter (references)	Type of cancer
Zinostatin stimalamer	Polymer protein conjugate	Styrene maleic anhydride neocarzinostatin (SMANCS)	–	Renal cancer
Doxil/caelyx	Liposome (PEGylated)	Doxorubicin	80–90 nm (Cainelli and Vallone 2009)	HIV-associated Kaposi's sarcoma, ovarian cancer, metastatic breast cancer, and multiple myeloma
DaunoXome	Liposome (non-PEGylated)	Daunorubicin	45 nm (Chen et al. 2010)	HIV-associated Kaposi's sarcoma
Lipo-Dox	Liposome	Doxorubicin	180 nm (Conner et al. 2014)	Kaposi's sarcoma, breast, and ovarian cancer
DepoCyt	Liposome	Cytosine arabinoside (cytarabine)	10–20 μ m (Conner et al. 2014)	Neoplastic meningitis
Myocetf	Liposome	Doxorubicin	190 nm (Conner et al. 2014)	Breast cancer
Abraxane	Nanoparticle albumin-bound	Paclitaxel	130 nm (Miele et al. 2009a)	Advanced non-small-cell lung cancer, metastatic pancreatic cancer, metastatic breast cancer
Oncaspar	PEG protein conjugate	l-Asparaginase	50–200 nm (Conner et al. 2014)	Leukemia
Genexol-PM	PEG-PLA polymeric micelle	Paclitaxel	20–50 nm (Kim et al. 2004)	Breast cancer, lung cancer, ovarian cancer
MEPACT	Liposome (non-PEGylated)	Mifamurtide	–	Osteosarcoma
NanoTherm	Iron oxide nanoparticle	–	20 nm (Ledet and Mandal 2012)	Thermal ablation glioblastoma
Marqibo	Liposome (non-PEGylated)	Vincristine	100 nm (Silverman and Deitcher 2013)	Philadelphia chromosome-negative acute lymphoblastic leukemia
MM-398 (Onivyde)	Liposome (PEGylated)	Irinotecan	80–140 nm (Tran et al. 2017)	Metastatic pancreatic cancer (second line)

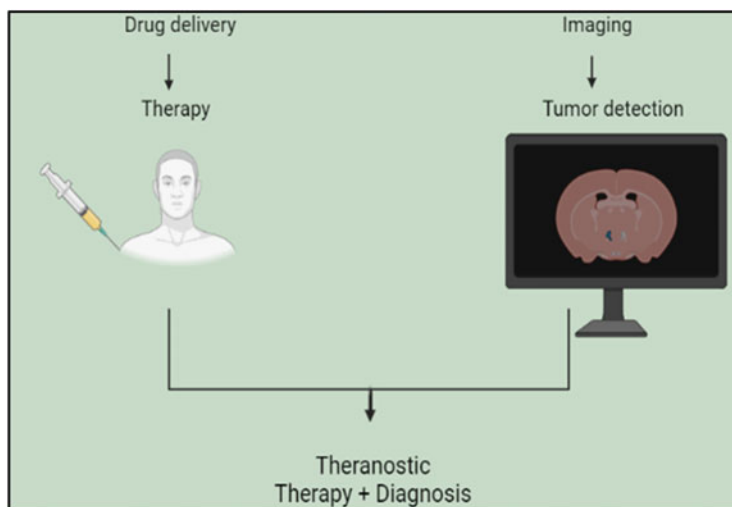


Fig. 5.2 Application of theranostic nanomedicine

nanomaterials synthesized from vesicles, viruses, cells, and other plant resources were also used in biomolecular diagnostic systems and defined as bio-inspired nanoparticles with less toxicity—this section reviews theranostic, bio-inspired nanoparticles, which have dual properties in cancer diagnosis and therapy.

5.2.1 Liposomes

Liposome nanoparticles are widely used for biomedical imaging applications and are readily self-assembled vesicles with spherical lipid bilayer shapes. The advantages of liposomes are that they engulf both lipophilic and hydrophobic compounds via lipid membrane and aqueous core. Moreover, liposomes are the most widely used as bio-nano theranostic particles because of their characteristics such as unilamellar lipid layer, high biocompatibility, biodegradability, ease to synthesize, high drug loading capacity, sustained drug release, less toxicity, and compatibility with both hydrophilic and hydrophobic chemotherapeutic drugs. Moreover, the liposome surfaces are easier to modify to target a specific region that needs cancer therapy (Silva et al. 2019). The imaging molecules were incorporated with loaded drugs either in an aqueous core medium or in a bilayer-lipid surface in the liposome. This versatile nature of liposome nanoparticles to integrate a wide range of diagnostic agents such as ^{64}Cu and ^{14}C isotopes, quantum dots (QDs), gadolinium (Gd)-based contrast agents, SPIONs, and fluorescent tags makes the therapeutic use of liposomes as theranostic nanoparticle material in cancer (Petersen et al. 2012; Al-Jamal et al. 2009; Wang and Chao 2018; Lamichhane et al. 2018; Martínez-González et al. 2016; Portnoy et al. 2015; Shen et al. 2017; Xing et al. 2018).

Table 5.2 Theranostic nanoparticles under clinical and preclinical trials

Stage	Nanoparticle type	Therapeutic agent	Diagnostic agent	Cancer type	Targets
Preclinical	Liposomes (100–200 nm)	Paclitaxel	pH-sensitive poly(ethylene oxide) (PEO)-modified poly(beta-amino ester) (PbAE) nanoparticles	Ovarian adenocarcinoma	EPR (Devalapally et al. 2007)
	Silica (100–200 nm)	Paclitaxel and camptothecin	Superparamagnetic iron oxide nanocrystals	Pancreatic cancer	Folic acid (Liong et al. 2008)
	Iron oxide (10–25 nm)	Anti-EGFR IgG	Iron oxide nanoparticles	Glioblastoma	EGFR (Hadjipanayis et al. 2010)
	Gold nanorod (10 x 40 nm)	Heat	Thermal/CT	Breast cancer	EPR (Von Maltzahn et al. 2009)
	Quantum dots (30–50 nm)	Paclitaxel, doxorubicin, 5-fluorouracil	Quantum dots	Many cancers	CD44, folic acid (Matea et al. 2017)
Clinical trials	Silica (6–7 nm)	cRGDY	Ultrasmall inorganic hybrid nanoparticles	Melanoma and malignant brain tumors	$\alpha_v\beta_3$ integrin (Phillips et al. 2014)
	Cyclodextrin (70 nm)	RNAi	Transferrin	Solid tumors	Transferrin receptor (Davis et al. 2010)
	Silica-gold nanoshell	Photothermal ablation	Nanoshell (MR and optical)	Head/neck cancer, primary and metastatic lung tumors	EPR (Singh et al. 2018)
	Gold (27 nm)	Tumor necrosis factor-alpha	Gold nanoparticles	Solid tumors	EPR (a passive mechanism) rhtTNF (active mechanism) (Libutti et al. 2010)
	Iron oxide	Endorem (superparamagnetic particles of iron oxide)	Iron oxide	Healthy volunteers	None (Richards et al. 2012)

5.2.2 Lipid-Based Theranostic Nanoparticles (LNPs)

The use of LNPs in cancer therapy is augmented due to their biocompatibility and feasibility to scale in various sizes (Tang et al. 2018). However, optimizing lipid theranostic nanoparticles with accurate size, shape, polydispersity index, surface charge, and stability is an excellent, challenging task. LNPs loaded with cyanine-based fluorescent dyes have a dual purpose, such as imaging and thermal ablation in cancer. They transform light energy into heat when exposed to NIR radiations (Yi et al. 2014; Feng et al. 2016; Weber et al. 2016; Feng et al. 2017). The DiR (1,1'-dioctadecyl-3,3,3',3'-tetramethyl indotricarbocyanine iodide) dyes have extended absorption of wavelengths, which helps in autofluorescence and increases penetration to promote antitumor activity (Pansare et al. 2012). The application of NIR dyes in conjugation with nanoparticles allows in vivo tracking of the nanoparticle. In general, the nanoparticles that were conjugated with DiR dye has lipophilic property and are used for treatment. These dyes show a high range of absorbance and fluorescence properties. Rajora et al. demonstrated that LNPs synthesized with apoE3 as targeted moiety while conjugating with porphyrin showed increased therapeutic effectiveness towards glioblastoma (Rajora et al. 2017). Similarly, Lin et al.'s LNPs conjugated with NIR dye and siRNA showed high sensitivity in NIR imaging and noninvasive method. These LNPs provide real-time monitoring of drug delivery and response mechanism in the orthotopic prostate tumor model (Lin et al. 2014).

5.2.3 Solid-Form Lipid Nanoparticles (SLNs)

The SLNs are modified lipid-based nanocarriers with high biocompatibility, high susceptibility to vascular uptake, and sustained drug release properties. They are small spherical (50–100 nm) colloidal form nanoparticles with low toxicity. Solid lipid nanoparticle core consists of fatty acids and triglycerides with an interfacial surfactant layer used as the theranostic particle in cancer treatment (Mehnert and Mäder 2001; Souto et al. 2007; Mussi and Torchilin 2013; Lopes et al. 2014). The imaging tags are encapsulated in a solidified lipid matrix. IR-780 iodide-loaded SLNs are targeted to tumor vasculature in glioblastoma tissue and monitored using PTT imaging (Kuang et al. 2017). The report suggests SLNs were incorporated with contrasting agents such as paramagnetic iron oxide, technetium-99, and quantum dots are used for cancer (Shuhendler et al. 2012; Bae et al. 2013). The study conducted by Bentolila et al. (2009) demonstrates that incorporating the chemotherapeutic drug (Paclitaxel) and siRNA in SLN shows synergistic anticancer activity via depositing in lung carcinoma cells. The fluorescence tag in siRNA promotes the target-specific uptake and migration of nanoparticles in in vivo cancer cells (Bentolila et al. 2009). Similarly, the combination of SLN with gadolinium (Gd) (III) complexes serves as a platform for oral contrast agents for MRI (Morel et al. 1998). In addition, only a limited number of studies reported the potential use of SLN theranostic nanoparticles in cancer diagnosis and treatment.

5.2.4 Lipid-Nano Structure (NLCs)

These nanoparticles are a combination of liquid and solid lipids. The major characteristic of NLCs is that their matrix ranges from crystalline to amorphous structures. The diversity in the matrix provided high drug loading and sustained release at the target compared to other nanocarriers (Videira et al. 2002; Wissing et al. 2004; Videira et al. 2006; Videira et al. 2012). Similarly, the loaded drug and imaging molecules were randomly dispersed in an aqueous and solid lipid hybrid matrix. Thus, the NLCs were used as multifunctional theranostic nano vectors for cancer therapy. Li et al. (2017) developed a dual-mode nano vector targeted towards breast cancer.

The nano vector consists of NIR dye IR780 in an aqueous core and an antagonist targeted to chemokine receptor CXCR4 in its outer shell. The result shows that the targeted antagonism and photothermal effect by dye combination provides a potential antitumor-antimetastatic property in the breast cancer model (Li et al. 2017). Furthermore, another promising approach was made in NLCs loaded with paclitaxel and Camptothecin drug in conjugation with QD as fluorescent imaging tag promotes the diagnosis and tracking of tumors in hepatocellular carcinoma in the murine model. Moreover, these nanocarriers help detect the lodging, internalization, cytotoxicity, and biodistribution of NLC nanomedicine (Olerile et al. 2017; Hsu et al. 2013).

5.2.5 Lipid-Based Nanocapsules (LNCs)

Lipid Nanocapsules (LNCs) are the next-level nanocarriers like lipoprotein structures with 1–100 nm size having intermediate properties of liposomes and polymeric nanoparticles with lipid core surrounded by tensioactive rigid membrane. These nanocapsules are synthesized using phase inversion of emulsion and organic solvent-free procedures (Huynh et al. 2009). Similarly, peptide-based targeted LNC made up of paclitaxel and DiD are used for glioblastoma treatment (Balzeau et al. 2013). Furthermore, LNCs were also used as gene delivery systems such as long-circulating DNA or plasmids DNA (Morille et al. 2010; David et al. 2013). In addition, to target tumorous cells, QD-tagged lipid nanocapsules conjugated with celecoxib and honokiol drugs were used, which showed high anticancer activity in breast cancer cells (Abdelhamid et al. 2018).

5.2.6 Lipid Micelles

Micelles are circular form lipid molecules in aqueous solutions. These micelles carry water-soluble chemotherapeutic drugs. The lipid micelle loaded with docetaxel has shown high therapeutic efficacy with lesser systemic toxicity in the xenograft breast cancer model (Ma et al. 2012). Ma et al. reported in their study the lipid-based micelles conjugated with docetaxel (M-DOC) as the therapeutic drug used as a

marker for anticancer and cancerous cell migration in xenograft breast cancer model (Ma et al. 2012).

5.2.7 Protein-Based Theranostic Nanoparticles

Protein-based nanocarriers are most widely used in cancer therapy and gained more attraction because of their biodegradability, biocompatibility, low toxicity, and ease of modifying the nanoparticles. The most commonly used proteins for the synthesis of nanoparticles are albumin, ferritin, gelatin, and transferrin.

Albumin nanoformulations—Albumins are common commercially available protein obtained from humans (HSA), bovine (BSA), rat (RSA) serum, and egg white (ovalbumin). The human serum albumin serves as a platform to isolate inorganic oxide to synthesize theranostic nanoparticles. HSA surfaces contain hydrophobic binding sites that help to bind non-covalently with different organic dyes and provide high fluorescence quantum yield. Recently, the conjugation of NIR dyes (IR780, indocyanine green (ICG), and IR825) are used for the synthesis of theranostic NPs for cancer. The main advantage of NIR dyes is deep penetration capacity with low inference.

Similarly, Chen et al. (2014) demonstrated that the HSA-IR825 complex formed by hydrophobic interactions shows high fluorescence yield at 600 nm during excitation and low at 808 nm excitation. This result infers that the complex has increased efficiency in imaging mechanisms (Chen et al. 2014). Abraxane, FDA approved nanocarrier, which contains albumin conjugated with paclitaxel drug, is used for imaging and drug delivery to tumors (Rosenberg et al. 1990; Takakura et al. 1990; Lohcharoenkal et al. 2014). Abraxane dosing is higher than normal paclitaxel, and it shows less toxicity with increased response in progression-free survival (Gradishar 2006; Miele et al. 2009b). Albumin protein is used as a platform for delivering low water-soluble drugs like rapamycin (Gonzalez-Angulo et al. 2013). Ferritin is another protein that efficiently encapsulates various non-native metallic NPs inside the protein core and acts as a nanocarrier for different functions. Zhen et al. reported that the conjugation of hydrophobic photosensitizer compound (Zn hexadecafluorophthalocyanine) in modified ferritin with NIR dye IR820 for fluorescence shows high potential in cancer diagnosis and imaging (Zhen et al. 2013a, b). Similarly, gelatin is characterized as polyampholyte protein with both anionic and cationic properties with hydrophobic groups.

Moreover, gelatin is biocompatible, biodegradable, water permeable, nontoxic, and easily soluble in water (Nezhadi et al. 2009). These natural characteristics of gelatin made this a good platform for synthesizing theranostic nanocarriers. Moreover, conjugation with iron oxide NPs and gold NPs increases the biocompatibility and stability of gelatin NPs. For instance, Tsai et al. show the importance of gelatin-coated gold NPs in fluorescence-based imaging during chemotherapy (Tsai et al. 2016). Transferrin is a glycoprotein that also has a promising role in theranostic NP-based cancer therapy and diagnosis. Transferrin is usually used for targeted tumor-specific delivery. Chen et al. (2013) show that the transferrin functionally

conjugated with graphene quantum dots is used to track and visualize tumor cells expressing the TfRs (Chen et al. 2013). Hence, these natural proteins offer a wide range of applications in cancer diagnosis and treatment.

5.2.8 Viral Nanoparticles (VNPs)

Viral nanoparticles (VNPs) are naturally occurring bio-nanomaterials obtained from plant viruses, bacteriophages, and mammalian viruses. The virus-encapsulated nanocarriers can accommodate a wide variety of molecules and can be easily modified to target specific tissue. The viral nanoparticles are synthesized by fermentation or molecular farming technology. Moreover, these VNPs are highly biocompatible, biodegradable, and used as vectors for delivering drugs because of availability and self-replication (Resch-Genger et al. 2008; Steinmetz 2010). These viral nanoparticles can be re-engineered with desirable target ligand, imaging moiety, and specific drug (Wen et al. 2012). The study shows that VNPs can be detected by noninvasive techniques such as PET and MRI scanning (Datta et al. 2008; Shukla and Steinmetz 2015). Flexman et al. demonstrate the PET scanning used for imaging fluoride and iron oxide particle conjugated with the Hemagglutinating virus of Japan (HVJ) (Flexman et al. 2008).

5.2.9 Oligonucleotide Theranostic Nanoparticles

Among different inorganic, organic, and polymeric nanoparticles, oligonucleotide-based theranostic nanoparticles are widely used for cancer therapy. The recent progress in theranostic nanoparticle development has shown oligonucleotide-based therapeutics have a potential role in cancer therapy. Targeting and delivering specific drugs using oligonucleotide is safe and effective. The studies suggest that after delivering, oligonucleotide nanoparticles conjugated with specific DNA or RNA performed the desired function at the targeted site during cell response imaging. The application of incorporating oligonucleotide in nanoparticles protects them from nuclease-induced degradation and promotes safety, stability, and effective drug delivery. In addition, the use of targeted oligonucleotide improves the early identification of tumorigenesis. The table below represents various kind of oligonucleotide theranostic particles (Table 5.3).

5.2.10 Peptide Theranostic Nanoparticles

Peptide-conjugated theranostic nanoparticles are currently used in cancer therapy. The main advantage of these peptides depended on the less immunogenicity process, cost-effectiveness, long-term stability, storage, and very easy to handle. Moreover, the smaller size provides feasibility for modifying the physicochemical properties of nanoparticles and less risk to the host immune. Similarly, the disadvantage of

Table 5.3 Oligonucleotide-based theranostic nanoparticles

Type of nanoparticle	Therapeutic oligonucleotide	Imaging compound	Spectroscopy
Gold nanoparticles	DNA and siRNA	GFP expression or knockdown	Fluorescence microscopy (Swierczewska et al. 2011)
SPIO nanoparticles	hTERT siRNA	SPIO nanoparticles	MRI (Bishop et al. 2015)
Quantum dots (QDs)	U6-enhanced-GFP (EGFP) siRNA, survivin siRNA	Quantum dots	Fluorescence microscopy (Boussif et al. 1995)
PEI-modified silica-coated magnetite nanoparticles	VEGF shRNA	Magnetite nanoparticles	MRI (Sunshine et al. 2012)
Manganese-doped iron oxide nanoparticles	Anti-GFP siRNA	Iron oxide nanoparticles	MRI (Li et al. 2014)
CdSe/CdS/ZnS QDs	EGFP siRNA	Quantum dots	Fluorescence microscopy (Lin et al. 2007)
1,4C-1,4 Bis-gold nanorod	Luc29 shRNA plasmid	Gold nanorod	Two-photon induced luminescence imaging (Ramos and Rege 2013)
PEGylated liposome Survivin siRNA Gadolinium-containing nanoparticles	Survivin siRNA	Gadolinium-containing lipids, Rhodamine-labeled cationic liposome, Alexa Fluor-labeled siRNA	MRI, fluorescence Microscopy (Lin et al. 2008)
Nanoparticles-human serum albumin	GL3 siRNA	Macrocyclic gadolinium complexes	MRI (Xia and Lin 2012)
QD-incorporated solid lipid nanoparticles	Bcl-2 siRNA	Quantum dots	Fluorescence imaging (Morin 1989)
Liposome-gold nanorod hybrids	PLK-1 siRNA	Gold nanorods	Multispectral optoacoustic tomography (Shay et al. 2001)
Poly (lactic-co-glycolic acid) nanoparticles	Hmger siRNA	Polymethine dyes	Intravital epifluorescence Microscopy (Philippi et al. 2010)
Chitosan-based hybrid nanocomplex	Survivin siRNA	Cy5.5	NIR fluorescence imaging (Zhu et al. 2013)

(continued)

Table 5.3 (continued)

Type of nanoparticle	Therapeutic oligonucleotide	Imaging compound	Spectroscopy
PEI-PEG-cografted polymeric nanoparticles	Choline kinase siRNA	[¹¹¹ In]1,4,7,10-tetraazacyclododecane-1,4,7,10-tetraacetic acid	Single-photon emission computed tomography (Chen et al. 2012a)

peptides is a low affinity towards the target and instability, which lead to enzymatic degradation. At the same time, peptide-based target selective theranostic particles with drug and contrast agents were synthesized for cancer therapy. The table listed below shows theranostic nanocarriers targeting based on peptides (Table 5.4).

5.3 Inorganic Theranostic Nanoparticles

The inorganic molecules such as iron, gold, silver, silica, and some oxides were used as theranostic nanoparticles for biomedical applications. The unique physicochemical properties of these nanoparticles help in sensing, imaging, and drug delivery (Patra et al. 2014). Moreover, implementing the green synthesis mechanism of inorganic nanoparticles has gained attention over the conventional procedure. This green synthesis has advantages such as easy, fast, and cost-effective method, completely toxic-free, extensive source of bioavailability in algae, plants, and bacteria, and easily soluble in water. Also, several studies have reported the advantage of biosynthesized theranostic gold and silver nanoparticles in cancer therapy (Lim et al. 2015).

5.3.1 Gold Theranostic Nanoparticles (AuNPs)

Among various inorganic molecules, gold nanoparticles have gained more attention in the optical bioimaging of cancer. This is because the gold nanoparticles have a very high surface-to-area ratio, making them more stable and biocompatible. Thus, the unique properties of gold nanoparticles made them ideal for photothermal therapy in cancer, and AuNPs are capable of converting light to heat in the presence of Infrared light that provides advantages for light-triggered treatments. Furthermore, they are used as nano vehicles to transport specific targeted probes or sensors. Currently, the synthesis of gold nanoparticles are active nanocarriers, metal catalysts, photosensitizers, and AuNPs generate reactive oxygen species in IR radiation, which defines the promising use of AuNPs in treatment and diagnostics (Wang et al. 2018; Vidal et al. 2018; Li et al. 2019; Mangadlao et al. 2018). In addition, easy surface modification of gold nanoparticles made them conjugate with specific antibodies, promoting direct electron microscopic visualization while

Table 5.4 List of peptide-mediated nanoparticles used for cancer treatment

Nanoparticle	Theranostic peptide	Target	Therapeutic agent	Diagnostic agent	Reference
Liposomes	cRGDFK	Integrin $\alpha v \beta 3$	Dox	BODIPY	Murphy et al. (2008)
	CSNIDARAC	Integrin $\alpha v \beta 6$	Dox	Cy7.5	He et al. (2011)
	CCK8	Cholecystokinin	Dox	^{111}In -DTPAGlu	Accardo et al. (2008)
Polymeric Micelles (PM)	[7-14]BN	GRP	Dox	^{111}In -DTPA	Accardo et al. (2012)
	GRGDS-NH2	Integrin $\alpha v \beta 3$	MTX	Gd MOF	Rowe et al. (2009)
	cRGD	Integrin $\alpha v \beta 3$	Dox	^{64}Cu -NOTA	Xiao et al. (2012)
	CRKRLDRNC	IL-4	Dox	Cy5.5	Wu et al. (2010)
	F3	Nucleolin	Photofrin	Iron oxide	Reddy et al. (2006)
Iron oxide nanoparticles	cRGD	Integrin $\alpha v \beta 3$	Dox	SPIO	Blanco et al. (2009)
	RGDLATLRQL	Integrin $\alpha v \beta 6$	Dox	SPIO	Guthi et al. (2010)
	RGD	Integrin $\alpha v \beta 3$	PAV	Iron oxide/Cy7	Gianella et al. (2011)
	CREKA/CRKDKC	–	–	SPIO/Cy7	Ageny et al. (2010)
	CGKRR	GBM	D[KLAKLAK] ₂	Iron oxide	Ageny et al. (2011)
	CTX	Brain	siRNA	Iron oxide	Mok et al. (2010)
	EPPT	uMUC-1	siRNA	SPION/Cy5.5	Kumar et al. (2010)
Gold Nanoparticles	tTF-RGD	Integrin $\alpha v \beta 3$	Dox/gold-NRs	SPIO	Von Maltzahn et al. (2011)
Quantum dots	cRGD	Integrin $\alpha v \beta 3$	Dox	QD	Hu et al. (2010)
Mesoporous silica	cRGDyK	Integrin $\alpha v \beta 3$	PdTPP	ATTO647N	Cheng et al. (2010)

minimizing toxicity and light scattering efficiency in various biomedical applications (Khlebtsov et al. 2013). Table 5.5 shows the various gold nanoparticles form (AuNPs) used in cancer.

5.3.2 Silver Nanoparticles as Theranostic Agents (AgNPs)

The unique physiochemical and light scattering characteristics of silver nanoparticles (AgNPs) enhance the potential role of silver nano vectors in cancer diagnosis and treatment (Austin et al. 2014). In the green synthesis procedure, the silver nanoparticles are synthesized from microorganisms such as fungi, yeast, bacteria, actinomycetes, plant extract, cell membranes, and viruses. The silver nanoparticles are attracted by researchers because of their high thermal conductivity, plasmonic properties, chemical stability, and antibacterial property. AgNPs are used as an anticancer diagnostic tool because they show a high penetration rate in cancerous cells and easy to track the path traveled by AgNP. Moreover, these AgNPs have a high surface-volume ratio, high rate of reproducibility, optical characteristics, and ease of functionalizing the surface of nanoparticles with high sensitivity and specificity make them more suitable for cancer therapy. The efficiency of AgNP to absorb or scatter light is estimated via the dipole approximation method (Zhang 2011). The optical characteristic of AgNPs to absorb specific wavelength help for imaging and photothermal therapy.

Similarly, the surface of nanoparticles can be functionalized using specific DNA/RNA molecules to target specific cancerous cells. The AgNPs act as biosensors for detecting serum-based specific tumor markers (Chen et al. 2012b). Lucas et al. (2015) demonstrated that the AgNPs size 45 nm synthesized using the SERS method had been used as a nanoprobe to detect epidermal growth factors associated with malignant tumors (Lucas et al. 2015). These AgNPs are conjugated with other nanomaterials like gold and silica, which improves the diagnostic properties. Raghav and Srivastava, 2015, reported that the combined gold-silver shell NPs enhance ovarian cancer diagnosis and prognosis (Raghav and Srivastava 2015). In addition, the silver nanoclusters are also used as fluorescence probes because of their extremely small size, less toxicity, high photostability, and fluorescence in NIR radiations (Oblisca et al. 2013). Similarly, the silver sulfide nanoparticle (AgS-NPs) conjugated with cyclic pentapeptide, which has high water-soluble properties and high affinity towards tumor-related integrins, are used for in vivo cancer imaging (Tang et al. 2015). Table 5.6 represents green synthesized silver nanoparticles (AgNPs) used in cancer treatment.

5.3.3 Iron Oxide Nanoparticles

Iron oxide nanoparticles come under the ferrimagnetic class of magnetic nanomaterials with a wide range of biomedical applications. These nanoparticles have applications in magnetic resonance imaging (MRI), magnetic particle imaging

Table 5.5 Various gold nanoparticle forms used for cancer therapy

Nanoforms	Particle synthesis procedure	Specification	References
Gold nanotube	Template synthesis	Easily adjustable plasmonic resonance in NIR region, wide functional area for molecules immobilization, large scattering and more sensitivity	Liu et al. (2020)
Gold nanorod	Template synthesis, seed-mediated methods, seedless methods, and green synthesis	Tunable plasmonic resonances in NIR region, more sensitivity, easy functionalize surface; antimicrobial activity, high magnitude of saturable absorption	Alkilany et al. (2012), Ma et al. (2017)
Gold nanocluster	Chemical etching and reduction, Sonochemical and Electrochemical synthesis and Microwave-assisted synthesis	Tunable plasmonic resonances in NIR region, ultra-small size, strong photoluminescence and photostability property, fast renal elimination; excellent biocompatibility; extremely large surface area	Zhang et al. (2018), Zhao et al. (2014)
Gold nanostar	Seed-mediated and seedless synthesis method; chemical reduction of gold salt method; Surfactant-free method	Multiple plasmon resonances with less toxicity, antibacterial activity, high surface plasmon resonance; surface functionalization easier.	Mousavi et al. (2020)
Gold nanocage	Galvanic replacement reaction	Increased absorption in NIR regions, the particle wall consist of hollow interiors and porous high scattering and absorption, easy surface functionalization	Xia et al. (2011)
Gold nanoshell	Gold nanoshells on SiO ₂ core, surfactant-assisted seeding method, single-step deposition-precipitation (DP) seeding; sandwiched gold-seeded shell Gold nanoshells on a polymer core: solvent-assisted approach; combined swelling-hetero aggregation; gold colloid seeding Hollow gold nanoshells: sacrificial template method	Tunable plasmonic resonances in NIR regions; highly effective for PTT and SERS	Ma et al. (2017)
Gold nanosphere	Wet chemistry method, seed-mediated growth	Single LSPR peak, small surface area, high cellular	Wozniak et al. (2017)

(continued)

Table 5.5 (continued)

Nanoforms	Particle synthesis procedure	Specification	References
		internalization, high colloidal stability; easy and available synthetic methods; easy surface functionalization	

(MPI), targeted delivery of drugs, proteins, antibodies, and nucleic acids, hyperthermia, biosensing, and tissue repair mechanism (Figuerola et al. 2010; Jin et al. 2014; Xu et al. 2011; Khandhar et al. 2013; Laurent et al. 2011; Haun et al. 2010; Siddiqi et al. 2016). Hence, various forms of iron oxide nanoparticles have broad applications in cancer diagnosis and therapy. Similarly, the development in nanomedicine introduced multifunctional magnetic nanoparticles and their different derivatives for bioimaging and therapies. The advantage of these multifunctional nanoparticles over others show high sensitivity in MRI, increased biocatalytic activity, advancement in magnetic hyperthermia treatment (MHT), applicable for photo-responsive therapy and drug delivery for chemotherapy, and gene therapy. Furthermore, these multifunctional nanoparticles act as a catalytic analog for peroxidase enzyme during cancer treatment via Fenton reaction. However, the hydroxyl compounds generated through catalysis induce high toxicity and lead the cancerous cell death (Torti and Torti 2019). Another category of iron oxide nanoparticles used for staging and monitoring cancer treatment are superparamagnetic iron oxide (SPIO) nanoparticles. SPIO nanoparticles were accumulated in cancer cells via the passive method through enhanced permeability and retention (EPR) effect or by active targeting with specific ligands (Matsumura and Maeda 1986). The SPIOs are used as route trackers for MRI during photodynamic therapy in cancer. The process utilizes several photosensitizing agents, which generate an excessive amount of reactive oxygen species underexposure to IR lights at a specific wavelength. Moreover, these iron oxide nanoparticles provide high tumor retention. Similarly, they are capable of generating hyperthermia because of Neel and Brownian relaxation effects. At this higher temperature (>42 °C), the cancerous cell membrane damages and leads to the apoptosis pathway. Overall, iron oxide nanoparticles have promising applications in improving cancer diagnosis and treatment.

5.4 Conclusion

In the last few decades, the possibility and application of theranostic nanoparticles are increased in cancer imaging and treatment. As a result, researchers accepted the most challenging question to construct multifunctional nanoparticles with multiple moieties corresponding to various functions. This crucial change paves the light in nanomedicine to choose multi-model cancer theranostic nanoparticles having targeting abilities for bioimaging and drug therapy in cancer.

Table 5.6 Silver nanoparticle used for cancer therapy

Silver nanoparticles (AgNPs)	Surface source	Targeted cancer	References
AgNP (12 nm)	PEG	MCF-7 cell line	Muhammad et al. (2016)
AgNP (20 nm)	Chitosan	A549 lung cancer cells	Arjunan et al. (2016)
AgNP (10–15 nm)	Potentilla fulgens Wall. Ex Hook extract	MCF-7 (human breast cancer) and U-87 (human glioblastoma) cancer cells	Mittal et al. (2015)
AgNP (20–80 nm)	Butea mono sperma leaf extract	B16F10 (mouse melanoma) and MCF-7 (breast cancer) cell lines	Patra et al. (2015)
AgNP (3.2–16 nm)	Pimpinella anisum seeds aqueous extract	Human neonatal skin stromal cells (hsscs) and colon cancer cells (HT115)	Alsahhi et al. (2016)
AgNP (20–80 nm)	Lonicera hypoglauca flower extract	MCF-7 (human breast cancer)	Jang et al. (2016)
AgNP (20 nm)	Cassia auriculata leaf extract	Lung carcinoma, adenocarcinoma mammary gland, and prostate carcinoma	Parveen and Rao (2015)
AgNP	Saccharina japonica extract	Hela cells (human cervical cancer)	Sreekanth et al. (2016a)
AgNP (23 nm)	Perilla frutescens leaf extract	Hela cells (human cervical Cancer)	Pandurangan et al. (2016a)
Silver-silica (10 nm)	3-(Aminopropyl)-trimethoxysilan	MG63 (human bone osteosarcoma)	Tudose et al. (2016)
Silver nanocomposites (60–80 nm)	Glutaraldehyde	Ovarian cancer cell line A2780 and lung cancer cell line A549	Baskar et al. (2016)
AgNP (33 nm)	Gymnemasylvestre leaf extract	Hep2 (human epithelioma)	Nakkala et al. (2015)
AgNP (7.8 nm)		Rat primary astrocytes and C6 rat glioma cells cultures	Salazar-García et al. (2015)
Chitosan-silver Hybrid nanoparticles (AgNP 5–10 nm)	Grape leaves aqueous extract	Hepg2 cells	El-Sherbiny et al. (2016)
Graphene oxide silver hybrid nanoparticles	Aqueous extract of dried jujube fruit	Human cervical cancer cell line (HeLa)	Sreekanth et al. (2016b)
AgNP	D. morbifera Léveille leaves Extract	A549 (lung cancer) and hepg2 (hepatocellular liver carcinoma) cell lines	Castro Aceituno et al. (2016)

(continued)

Table 5.6 (continued)

Silver nanoparticles (AgNPs)	Surface source	Targeted cancer	References
AgNP (10 nm)	–	Human cervical cancer cell line (HeLa)	Pandurangan et al. (2016b)
AgNP (24–150 nm)	<i>Commelina nudiflora</i> L. aqueous extract	HCT-116 colon cancer cells	Kuppusamy et al. (2016)
AgNP (33.5 nm)	<i>Aspergillus flavus</i>	Human acute promyelocytic leukaemia (HL-60) cell line	Sulaiman et al. (2015)

References

- Abdelhamid AS, Zayed DG, Helmy MW, Ebrahim SM, Bahey-El-Din M, Zein-El-Dein EA, El-Gizawy SA, Elzoghby AO (2018) Lactoferrin-tagged quantum dots-based theranostic nanocapsules for combined COX-2 inhibitor/herbal therapy of breast cancer. *Nanomedicine (Lond)* 13(20):2637–2656
- Accardo A, Tesaro D, Aloj L, Tarallo L, Arra C, Mangiapia G, Vaccaro M, Pedone C, Paduano L, Morelli G (2008) Peptide containing aggregates as selective nanocarriers for therapeutics. *ChemMedChem*:594–602
- Accardo A, Salsano G, Morisco A, Aurilio M, Parisi A, Maione F, Cicala C, Tesaro D, Aloj L, De Rosa G, Morelli G (2012) Peptide-modified liposomes for selective targeting of bombesin receptors overexpressed by cancer cells: a potential theranostic agent. *Int J Nanomedicine* 7: 2007–2017
- Agemy L, Sugahara KN, Kotamraju VR, Gujrati K, Girard OM, Kono Y, Mattrey RF, Park J-H, Sailor MJ, Jimenez AI, Cativiela C, Zanuy D, Sayago FJ, Aleman C, Nussinov R, Ruoslahti E (2010) Nanoparticle-induced vascular blockade in human prostate cancer. *Blood* 116:2847–2856
- Agemy L, Friedmann-Morvinski D, Kotamraju VR, Roth L, Sugahara KN, Girard OM, Mattrey RF, Verma IM, Ruoslahti E (2011) Targeted nanoparticle enhanced proapoptotic peptide as potential therapy for glioblastoma. *Proc Natl Acad Sci U S A* 108(42):17,450–17,455
- Al-Jamal WT, Al-Jamal KT, Tian B, Cakebread A, Halket JM, Kostarelos K (2009) Tumor targeting of functionalized quantum dot-liposome hybrids by intravenous administration. *Mol Pharm* 6(2):520–530
- Alkilany AM, Thompson LB, Boulos SP, Sisco PN, Murphy CJ (2012) Gold nanorods: their potential for photothermal therapeutics and drug delivery, tempered by the complexity of their biological interactions. *Adv Drug Deliv Rev* 64(2):190–199
- Alsali MS, Devanesan S, Alfuraydi AA, Vishnubalaji R, Munusamy MA, Murugan K, Nicoletti M, Benelli G (2016) Green synthesis of silver nanoparticles using *Pimpinellaanisum* seeds: antimicrobial activity and cytotoxicity on human neonatal skin stromal cells and colon cancer cells. *Int J Nanomed* 11:4439–4449
- Andreou C, Pal S, Rotter L, Yang J, Kircher MF (2017) “Molecular Imaging in Nanotechnology and Theranostics” (MINT) interest group. *Mol Imaging Biol* 19(3):363
- Arjuman N, Kumari HL, Singaravelu CM, Kandasamy R, Kandasamy J (2016) Physicochemical investigations of biogenic chitosan-silver nanocomposite as antimicrobial and anticancer agent. *Int J Biol Macromol* 92:77–87
- Austin LA, Mackey MA, Dreaden EC, El-Sayed MA (2014) The optical, photothermal, and facile surface chemical properties of gold and silver nanoparticles in biodiagnostics, therapy, and drug delivery. *Arch Toxicol* 88(7):1391–1417

- Bae KH, Lee JY, Lee SH, Park TG, Nam YS (2013) Optically traceable solid lipid nanoparticles loaded with siRNA and paclitaxel for synergistic chemotherapy with in situ imaging. *Adv Healthc Mater* 2(4):576–584
- Balzeau J, Pinier M, Berges R, Saulnier P, Benoit JP, Eyer J (2013) The effect of functionalizing lipid nanocapsules with NFL-TBS.40-63 peptide on their uptake by glioblastoma cells. *Biomaterials* 34(13):3381–3389
- Baskar G, Bikku George G, Chamundeeswari M (2016) Synthesis and characterization of asparaginase bound silver nanocomposite against ovarian cancer cell line A2780 and lung cancer cell line A549. *J Inorg Organomet Polym*. <https://doi.org/10.1007/s10904-016-0448-x>
- Belyanina I, Kolovskaya O, Zamay S, Gargaun A, Zamay T, Kichkailo A (2017) Targeted magnetic nanotheranostics of cancer. *Molecules* 22(6):975
- Laurent A, Bentolila, Yuval Ebenstein, Shimon Weiss. Quantum dots for in vivo small-animal imaging. *J Nucl Med* Apr 2009, 50 (4) 493–496;
- Bishop CJ, Tzeng SY, Green JJ (2015) Degradable polymer-coated gold nanoparticles for co-delivery of DNA and siRNA. *Acta Biomater* 11:393–403
- Blanco E, Kessinger CW, Sumer BD, Gao J (2009) Multifunctional micellar nanomedicine for cancer therapy. *Exp Biol Med (Maywood)* 234(2):123–131
- Boussif O, Lezoualc'h F, Zanta MA, Mergny MD, Scherman D, Demeneix B, Behr JP (1995) A versatile vector for gene and oligonucleotide transfer into cells in culture and in vivo: polyethylenimine. *Proc Natl Acad Sci U S A* 92(16):7297–7301
- Cainelli F, Vallone A (2009) Safety and efficacy of pegylated liposomal doxorubicin in HIV-associated Kaposi's sarcoma. *Biol Targets Ther* 3:385
- Castro Aceituno V, Ahn S, Simu SY, Wang C, Mathiyalagan R, Yang DC (2016) Silver nanoparticles from *Dendropanax moribifera* Léveillé inhibit cell migration, induce apoptosis, and increase generation of reactive oxygen species in A549 lung cancer cells. *In Vitro Cell Dev Biol Anim* 52(10):1012–1019
- Chen L, Shiah H, Chao T, Hsieh RK, Chen G, Chang J, Yeh G (2010) Phase I study of liposome irinotecan (PEP02) in combination with weekly infusion of 5-FU/LV in advanced solid tumors. *J Clin Oncol* 28(15_suppl):e13024
- Chen Z, Penet MF, Nimmagadda S, Li C, Banerjee SR, Winnard PT Jr, Artemov D, Glunde K, Pomper MG, Bhujwala ZM (2012a) PSMA-targeted theranostic nanoplex for prostate cancer therapy. *ACS Nano* 6(9):7752–7762
- Chen Z, Leim Y, Chen X (2012b) Immunoassay for serum alpha-fetoprotein using silver nanoparticles and detection via resonance light scattering. *Microchim Acta* 179:241–248
- Chen ML, He YJ, Chen XW, Wang JH (2013) Quantum-dot-conjugated graphene as a probe for simultaneous cancer-targeted fluorescent imaging, tracking, and monitoring drug delivery. *Bioconjug Chem*:387–397
- Chen Q, Wang C, Zhan Z, He W, Cheng Z, Li Y, Liu Z (2014) Near-infrared dye bound albumin with separated imaging and therapy wavelength channels for imaging-guided photothermal therapy. *Biomaterials* 35(28):8206–8214
- Cheng S-H, Lee C-H, Chen M-C, Souris JS, Tseng F-G, Yang C-S, Mou C-Y, Chen C-T, Lo L-W (2010) Tri-functionalization of mesoporous silica nanoparticles for comprehensive cancer theranostics-the trio of imaging, targeting and therapy. *J Mater Chem*:6149–6157
- Conner JB, Bawa R, Nicholas JM, Weinstein V (2014) Copaxone in the era of biosimilars and nanosimilars. In: *Handbook of clinical nanomedicine-from bench too bedside*. Pan Stanford Publishing Pte Ltd., Singapore, pp 1–31
- Datta A, Hooker JM, Botta M, Francis MB, Aime S, Raymond KN (2008) High relaxivity gadolinium hydroxypyridonate-viral capsid conjugates: nanosized MRI contrast agents. *J Am Chem Soc* 130(8):2546–2552
- David S, Passirani C, Carmoy N, Morille M, Mevel M, Chatin B et al (2013) DNA nanocarriers for systemic administration: characterization and *in vivo* bioimaging in healthy mice. *Mol Ther Nucleic Acids*:e64

- Davis ME, Zuckerman JE, Choi CH, Seligson D, Tolcher A, Alabi CA, Yen Y, Heidel JD, Ribas A (2010) Evidence of RNAi in humans from systemically administered siRNA via targeted nanoparticles. *Nature* 464(7291):1067–1070
- Devalapally H, Shenoy D, Little S, Langer R, Amiji M (2007) Poly (ethylene oxide)-modified poly (beta-amino ester) nanoparticles as a pH-sensitive system for tumor-targeted delivery of hydrophobic drugs: part 3. Therapeutic efficacy and safety studies in ovarian cancer xenograft model. *Cancer Chemother Pharmacol* 59(4):477–484
- Dobiasch S, Szanyi S, Kjaev A, Werner J, Strauss A, Weis C, Grenacher L, Kapilov-Buchman K, Israel LL, Lellouche JP, Locatelli E (2016) Synthesis and functionalization of protease-activated nanoparticles with tissue plasminogen activator peptides as targeting moiety and diagnostic tool for pancreatic cancer. *J Nanobiotechnol* 14(1):1–8
- El-Sherbiny IM, Salih E, Yassin AM, Elsayed EH (2016) Newly developed chitosan-silver hybrid nanoparticles: biosafety and apoptosis induction in HepG2 cells. *J Nanopart Res* 18:172
- Feng L, Gao M, Tao D, Chen Q, Wang H, Dong Z et al (2016) Cisplatin-prodrug-constructed liposomes as a versatile Theranostic nanoplatform for bimodal Imaging guided combination cancer therapy. *Adv Func Mater*:2207–2217
- Feng L, Cheng L, Dong Z, Tao D, Barnhart TE, Cai W, Chen M, Liu Z (2017) Theranostic liposomes with hypoxia-activated prodrug to effectively destruct hypoxic Tumors post-photodynamic therapy. *ACS Nano* 11(1):927–937
- Figueroa A, Di Corato R, Manna L, Pellegrino T (2010) From iron oxide nanoparticles towards advanced iron-based inorganic materials designed for biomedical applications. *Pharmacol Res* 62(2):126–143
- Flexman JA, Cross DJ, Lewellen BL, Miyoshi S, Kim Y, Minoshima S (2008) Magnetically targeted viral envelopes: a PET investigation of initial biodistribution. *IEEE Trans Nanobioscience* 7(3):223–232
- Gianella A, Jarzyna PA, Mani V, Ramachandran S, Calcagno C, Tang J, Kann B, Dijk WJ, Thijssen VL, Griffioen AW, Storm G, Fayad ZA, Mulder WJ (2011) Multi-functional nanoemulsion platform for imaging guided therapy evaluated in experimental cancer. *ACS Nano* 5(6):4422–4433
- Gonzalez-Angulo AM, Meric-Bernstam F, Chawla S, Falchook G, Hong D, Akcakanat A, Chen H, Naing A, Fu S, Wheler J, Moulder S, Helgason T, Li S, Elias I, Desai N, Kurzrock R (2013) Weekly nab-rapamycin in patients with advanced nonhematologic malignancies: final results of a phase I trial. *Clin Cancer Res* 19(19):5474–5484
- Gradishar WJ (2006) Albumin-bound paclitaxel: a next-generation taxane. *Expert Opin Pharmacother* 7(8):1041–1053
- Guthi JS, Yang SG, Huang G, Li S, Khemtong C, Kessinger CW, Peyton M, Minna JD, Brown KC, Gao J (2010) MRI-visible micellar nanomedicine for targeted drug delivery to lung cancer cells. *Mol Pharm* 7(1):32–40
- Hadjipanayis CG, Machaidze R, Kaluzova M, Wang L, Schuette AJ, Chen H, Wu X, Mao H (2010) EGFRvIII antibody-conjugated iron oxide nanoparticles for magnetic resonance imaging-guided convection-enhanced delivery and targeted therapy of glioblastoma. *Cancer Res* 70(15):6303–6312
- Hanahan D, Weinberg RA (2011) Hallmarks of cancer: the next generation. *Cell* 144(5):646–674
- Haun JB, Yoon TJ, Lee H, Weissleder R (2010) Magnetic nanoparticle biosensors. *Wiley Interdiscip Rev Nanomed Nanobiotechnol* 2(3):291–304
- He X, Na MH, Kim JS, Lee GY, Park JY, Hoffman AS, Nam JO, Han SE, Sim GY, Oh YK, Kim IS, Lee BH (2011) A novel peptide probe for imaging and targeted delivery of liposomal doxorubicin to lung tumor. *Mol Pharm* 8(2):430–438
- Hsu SH, Wen CJ, Al-Suwayeh SA, Huang YJ, Fang JY (2013) Formulation design and evaluation of quantum dot-loaded nanostructured lipid carriers for integrating bioimaging and anticancer therapy. *Nanomedicine (Lond)* 8(8):1253–1269

- Hu R, Yong KT, Roy I, Ding H, Law WC, Cai H, Zhang X, Vathy LA, Bergey EJ, Prasad PN (2010) Functionalized near-infrared quantum dots for in vivo tumor vasculature imaging. *Nanotechnology* 21(14):145105
- Huynh NT, Passirani C, Saulnier P, Benoit JP (2009) Lipid nanocapsules: a new platform for nanomedicine. *Int J Pharm* 379(2):201–209
- Jang SJ, Yang IJ, Tettey CO, Kim KM, Shin HM (2016) In-vitro anticancer activity of green synthesized silver nanoparticles on MCF-7 human breast cancer cells. *Mater Sci Eng C Mater Biol Appl* 68:430–435
- Jin R, Lin B, Li D, Ai H (2014) Superparamagnetic iron oxide nanoparticles for MR imaging and therapy: design considerations and clinical applications. *Curr Opin Pharmacol* 18:18–27
- Khandhar AP, Ferguson RM, Arami H, Krishnan KM (2013) Monodisperse magnetite nanoparticle tracers for in vivo magnetic particle imaging. *Biomaterials* 34(15):3837–3845. <https://doi.org/10.1016/j.biomaterials.2013.01.087>
- Khlebtsov BN, Tuchina ES, Khanadeev VA, Panfilova EV, Petrov PO, Tuchin VV, Khlebtsov NG (2013) Enhanced photoinactivation of staphylococcus aureus with nanocomposites containing plasmonic particles and hematoporphyrin. *J Biophotonics* 6:338–351
- Kim TY, Kim DW, Chung JY, Shin SG, Kim SC, Heo DS, Kim NK, Bang YJ (2004) Phase I and pharmacokinetic study of Genexol-PM, a cremophor-free, polymeric micelle-formulated paclitaxel, in patients with advanced malignancies. *Clin Cancer Res* 10(11):3708–3716
- Kuang Y, Zhang K, Cao Y, Chen X, Wang K, Liu M, Pei R (2017) Hydrophobic IR-780 dye encapsulated in cRGD-conjugated solid lipid Nanoparticles for NIR imaging-guided photothermal therapy. *ACS Appl Mater Interfaces* 9(14):12217–12226
- Kumar M, Yigit M, Dai G, Moore A, Medarova Z (2010) Image-guided breast tumor therapy using a small interfering RNA nanodrug. *Cancer Res* 70(19):7553–7561
- Kuppusamy P, Ichwan SJ, Al-Zikri PN, Suriyah WH, Soundharrajan I, Govindan N, Maniam GP, Yusoff MM (2016) In vitro anticancer activity of Au, Ag Nanoparticles synthesized using Commelinanudiflora L. aqueous extract against HCT-116 colon cancer cells. *Biol Trace Elem Res* 173(2):297–305
- Lamichhane N, Udayakumar TS, D'Souza WD, Simone CB 2nd, Raghavan SR, Polf J, Mahmood J (2018) Liposomes: clinical applications and potential for image-guided drug delivery. *Molecules* 23(2):288
- Laurent S, Dutz S, Häfeli UO, Mahmoudi M (2011) Magnetic fluid hyperthermia: focus on superparamagnetic iron oxide nanoparticles. *Adv Colloid Interf Sci* 166:8–23
- Ledet G, Mandal TK (2012) Nanomedicine: emerging therapeutics for the 21st century. *US pharm* 37(3):7–11
- Lee S, Ryu JH, Park K, Lee A, Lee SY, Youn IC, Ahn CH, Yoon SM, Myung SJ, Moon DH, Chen X (2009) Polymeric nanoparticle-based activatable near-infrared nanosensor for protease determination in vivo. *Nano Lett* 9(12):4412–4416
- Li D, Tang X, Pulli B, Lin C, Zhao P, Cheng J, Lv Z, Yuan X, Luo Q, Cai H, Ye M (2014) Theranostic nanoparticles based on bioreducible polyethylenimine-coated iron oxide for reduction-responsive gene delivery and magnetic resonance imaging. *Int J Nanomed* 9:3347–3361
- Li H, Wang K, Yang X, Zhou Y, Ping Q, Oupicky D, Sun M (2017) Dual-function nanostructured lipid carriers to deliver IR780 for breast cancer treatment: anti-metastatic and photothermal antitumor therapy. *Acta Biomater* 53:399–413
- Li S, Shen X, Xu QH, Cao Y (2019) Gold nanorod enhanced conjugated polymer/photosensitizer composite nanoparticles for simultaneous two-photon excitation fluorescence imaging and photodynamic therapy. *Nanoscale* 2019:19,551–19,560
- Libutti SK, Paciotti GF, Byrnes AA, Alexander HR Jr, Gannon WE, Walker M, Seidel GD, Yuldashva N, Tamarkin L (2010) Phase I and pharmacokinetic studies of CYT-6091, a novel PEGylated colloidal gold-rhTNF nanomedicine. *Clin Cancer Res* 16(24):6139–6149. <https://doi.org/10.1158/1078-0432.CCR-10-0978>

- Lim EK, Kim T, Paik S, Haam S, Huh YM, Lee K (2015) Nanomaterials for theranostics: recent advances and future challenges. *Chem Rev* 115:327–394
- Lin C, Zhong Z, Lok MC, Jiang X, Hennink WE, Feijen J, Engbersen JF (2007) Novel bioreducible poly(amido amine)s for highly efficient gene delivery. *Bioconjug Chem* 18(1):138–145
- Lin C, Blaauboer CJ, Timoneda MM et al (2008) Bioreducible poly(amido amine)s with oligoamine side chains: synthesis, characterization, and structural effects on gene delivery. *J Control Release* 126(2):166–174
- Lin Q, Jin CS, Huang H, Ding L, Zhang Z, Chen J, Zheng G (2014) Nanoparticle-enabled, image-guided treatment planning of target specific RNAi therapeutics in an orthotopic prostate cancer model. *Small* 10(15):3072–3082
- Liong M, Lu J, Kovoichich M, Xia T, Ruehm SG, Nel AE, Tamanoi F, Zink JI (2008) Multi-functional inorganic nanoparticles for imaging, targeting, and drug delivery. *ACS Nano* 2(5): 889–896
- Liu YL, Zhu J, Weng GJ, Li JJ, Zhao JW (2020) Gold nanotubes: synthesis, properties and biomedical applications. *Mikrochim Acta* 187:612
- Lohcharoenkal W, Wang L, Chen YC, Rojanasakul Y (2014) Protein Nanoparticles as drug delivery carriers for cancer therapy. *Biomed Res Int* 2014:180549
- Lopes RM, Gaspar MM, Pereira J, Eleutério CV, Carvalheiro M, Almeida AJ et al (2014) Liposomes versus lipid nanoparticles: comparative study of lipid-based systems as oryzalin carriers for the treatment of leishmaniasis. *J Biomed Nanotechnol*:3647–3657. <https://doi.org/10.1166/jbn.2014.1874>
- Lucas LJ, Tellez C, Castilho ML, Lee CLD, Hupman MA, Vieira LS et al (2015) Development of a sensitive, stable and EGFR-specific molecular imaging agent for surface enhanced Raman spectroscopy. *J Raman Spectrosc* 46:434–446
- Ma M, Hao Y, Liu N et al (2012) A novel lipid-based nanomicelle of docetaxel: evaluation of antitumor activity and biodistribution. *Int J Nanomed* 7:3389–3398
- Ma N, Wu FG, Zhang X, Jiang YW, Jia HR, Wang HY, Li YH, Liu P, Gu N, Chen Z (2017) Shape-dependent radiosensitization effect of gold nanostructures in cancer radiotherapy: comparison of gold nanoparticles, nanospikes, and nanorods. *ACS Appl Mater Interfaces* 9(15):13037–13048
- Mangadla JD, Wang X, McCreese C, Escamilla M, Ramamurthy G, Wang Z, Govande M, Basilion JP, Burda C (2018) Prostate-specific membrane antigen targeted gold nanoparticles for theranostics of prostate cancer. *ACS Nano* 12(4):3714–3725
- Martínez-González R, Estelrich J, Busquets MA (2016) Liposomes loaded with hydrophobic iron oxide Nanoparticles: suitable T2 contrast agents for MRI. *Int J Mol Sci* 17(8):1209
- Matea CT, Mocan T, Tabaran F, Pop T, Mosteanu O, Puia C, Iancu C, Mocan L (2017) Quantum dots in imaging, drug delivery and sensor applications. *Int J Nanomedicine* 12:5421
- Mathur P, Sathishkumar K, Chaturvedi M, Das P, Sudarshan KL, Santhappan S, Nallasamy V, John A, Narasimhan S, Roselind FS, ICMR-NCDIR-NCRP Investigator Group (2020) Cancer statistics, 2020: report from national cancer registry programme, India. *JCO Global Oncol* 6: 1063–1075
- Matsumura Y, Maeda H (1986) A new concept for macromolecular therapeutics in cancer chemotherapy: mechanism of tumorotropic accumulation of proteins and the antitumor agent smancs. *Cancer Res* 46(12 Pt 1):6387–6392
- Mehnert W, Mäder K (2001) Solid lipid nanoparticles: production, characterization and applications. *Adv Drug Deliv Rev* 47(2–3):165–196
- Miele E, Spinelli GP, Miele E, Tomao F, Tomao S (2009a) Albumin-bound formulation of paclitaxel (Abraxane® ABI-007) in the treatment of breast cancer. *Int J Nanomedicine* 4:99
- Miele E, Spinelli GP, Miele E, Tomao F, Tomao S (2009b) Albumin-bound formulation of paclitaxel (Abraxane ABI-007) in the treatment of breast cancer. *Int J Nanomed* 4:99–105
- Mittal AK, Tripathy D, Choudhary A, Aili PK, Chatterjee A, Singh IP, Banerjee UC (2015) Bio-synthesis of silver nanoparticles using *Potentilla fulgens* wall. Ex hook. and its therapeutic evaluation as anticancer and antimicrobial agent. *Mater Sci Eng C Mater Biol Appl* 53:120–127

- Mok H, Veiseh O, Fang C, Kievit FM, Wang FY, Park JO, Zhang M (2010) pH-sensitive siRNA nanovector for targeted gene silencing and cytotoxic effect in cancer cells. *Mol Pharm* 7(6): 1930–1939
- Morel S, Terreno E, Ugazio E, Aime S, Gasco MR (1998) NMR relaxometric investigations of solid lipid nanoparticles (SLN) containing gadolinium(III) complexes. *Eur J Pharm Biopharm* 45(2): 157–163
- Morille M, Montier T, Legras P, Carmoy N, Brodin P, Pitard B, Benoît JP, Passirani C (2010) Long-circulating DNA lipid nanocapsules as new vector for passive tumor targeting. *Biomaterials* 31(2):321–329
- Morin GB (1989) The human telomere terminal transferase enzyme is a ribonucleoprotein that synthesizes TTAGGG repeats. *Cell* 59(3):521–529
- Mousavi SM, Zarei M, Hashemi SA, Ramakrishna S, Chiang WH, Lai CW, Gholami A (2020) Gold nanostars—diagnosis, bioimaging and biomedical applications. *Drug Metab Rev* 52(2): 299–318
- Muhammad Z, Raza A, Ghafoor S, Naeem A, Naz SS, Riaz S, Ahmed W, Rana NF (2016) PEG capped methotrexate silver nanoparticles for efficient anticancer activity and biocompatibility. *Eur J Pharm Sci* 91:251–255
- Murphy EA, Majeti BK, Barnes LA, Makale M, Weis SM, Lutu-Fuga K, Wrasidlo W, Cheresch DA (2008) Nanoparticle-mediated drug delivery to tumor vasculature suppresses metastasis. *Proc Natl Acad Sci U S A* 105(27):9343
- Mussi SV, Torchilin VP (2013) Recent trends in the use of lipidic nanoparticles as pharmaceutical carriers for cancer therapy and diagnostics. *J Mater Chem B*:5201–5209
- Nakkala JR, Mata R, Bhagat E, Sadras SR (2015) Green synthesis of silver and gold nanoparticles from *Gymnemasylvestre* leaf extract: study of antioxidant and anticancer activities. *J Nanopart Res* 17:151
- Nezhadi SH, Choong PF, Lotfipour F, Dass CR (2009) Gelatin-based delivery systems for cancer gene therapy. *J Drug Target* 17(10):731–738
- Obliosca JM, Liu C, Yeh HC (2013) Fluorescent silver nanoclusters as DNA probes. *Nanoscale*:8443–8461
- Olerile LD, Liu Y, Zhang B et al (2017) Near-infrared mediated quantum dots and paclitaxel co-loaded nanostructured lipid carriers for cancer theragnostic. *Colloids Surf B Biointerfaces* 150:121–130
- Pandurangan M, Enkhtaivan G, Venkatasamy B, Mistry B, Noorzai R, Jin BY, Kim DH (2016a) Time and concentration-dependent therapeutic potential of silver Nanoparticles in cervical carcinoma cells. *Biol Trace Elem Res* 170(2):309–319
- Pandurangan M, Nagajyothi PC, Kim DH, Jung M-J, Shim J, Eom I-Y (2016b) Green synthesis and characterization of biologically active silver nanoparticles using *Perilla frutescens* leaf extract. *J Clust Sci* 28:81–90
- Pansare VJ, Hejazi S, Faenza WJ, Prud'homme RK (2012) Review of long-wavelength optical and NIR Imaging materials: contrast agents, fluorophores, and multi-functional Nano carriers. *Chem Mater*:812–827
- Parveen A, Rao S (2015) Cytotoxicity and genotoxicity of biosynthesized gold and silver nanoparticles on human cancer cell lines. *J Clust Sci* 26:775_788
- Patra CR, Mukherjee S, Kotcherlakota R (2014) Biosynthesized silver nanoparticles: a step forward for cancer theranostics? *Nanomedicine (Lond)*:1445–1448
- Patra S, Mukherjee S, Barui AK, Ganguly A, Sreedhar B, Patra CR (2015) Green synthesis, characterization of gold and silver nanoparticles and their potential application for cancer therapeutics. *Mater Sci Eng C Mater Biol Appl* 53:298–309
- Petersen AL, Hansen AE, Gabizon A, Andresen TL (2012) Liposome imaging agents in personalized medicine. *Adv Drug Deliv Rev* 64:1417–1435
- Philippi C, Loretz B, Schaefer UF, Lehr CM (2010) Telomerase as an emerging target to fight cancer—opportunities and challenges for nanomedicine. *J Control Release* 146(2):228–240

- Phillips E, Penate-Medina O, Zanzonico PB, Carvajal RD, Mohan P, Ye Y, Humm J, Gönen M, Kalaigian H, Schöder H, Strauss HW (2014) Clinical translation of an ultrasmall inorganic optical-PET imaging nanoparticle probe. *Sci Transl Med* 6(260):260ra149
- Portnoy E, Nizri E, Golenser J, Shmuel M, Magdassi S, Eyal S (2015) Imaging the urinary pathways in mice by liposomal indocyanine green. *Nanomedicine*:1057–1064
- Raghav R, Srivastava S (2015) Core_shellgold_silver nanoparticles based impedimetric immunosensor for cancer antigen CA125. *Sens Actuator B Chem* 220:557–564
- Rajora MA, Ding L, Valic M et al (2017) Tailored theranostic apolipoprotein E3 porphyrin-lipid nanoparticles target glioblastoma [published correction appears in *Chem Sci*. 2017 Aug 1;8(8):5803]. *Chem Sci* 8(8):5371–5384. <https://doi.org/10.1039/c7sc00732a>
- Ramos J, Rege K (2013) Poly(aminoether)-gold nanorod assemblies for shRNA plasmid-induced gene silencing. *Mol Pharm* 10(11):4107–4119
- Reddy GR, Bhojani MS, McConville P, Moody J, Moffat BA, Hall DE, Kim G, Koo YE, Woolliscroft MJ, Sugai JV, Johnson TD, Philbert MA, Kopelman R, Rehemtulla A, Ross BD (2006) Vascular targeted nanoparticles for imaging and treatment of brain tumors. *Clin Cancer Res*:6677–6686
- Resch-Genger U, Grabolle M, Cavaliere-Jaricot S, Nitschke R, Nann T (2008) Quantum dots versus organic dyes as fluorescent labels. *Nat Methods*:763
- Richards JMJ, Shaw CA, Lang NN, Williams MC, Semple SIK, MacGillivray TJ et al (2012) In vivo mononuclear cell tracking using superparamagnetic particles of iron oxide. *Circ Cardiovasc Imaging* 5:509–517
- Rosenberg SA, Aebersold P, Cornetta K, Kasid A, Morgan RA, Moen R, Karson EM, Lotze MT, Yang JC, Topalian SL, et al. Gene transfer into humans--immunotherapy of patients with advanced melanoma, using tumor-infiltrating lymphocytes modified by retroviral gene transduction. *N Engl J Med* 1990;323(9):570–578
- Rowe MD, Thamm DH, Kraft SL, Boyes SG (2009) Polymer-modified gadolinium metal-organic framework nanoparticles used as multi-functional nanomedicines for the targeted imaging and treatment of cancer. *Biomacromolecules*:983–993
- Salazar-García S, Silva-Ramírez AS, Ramirez-Lee MA, Hernandez HR, Rangel-Lopez E, Castillo CG et al (2015) Comparative effects on rat primary astrocytes and C6 rat glioma cells cultures after 24-h exposure to silver nanoparticles (AgNPs). *J Nanopart Res* 17:450
- Shay JW, Zou Y, Hiyama E, Wright WE (2001) Telomerase and cancer. *Hum Mol Genet* 10(7):677–685
- Shen J, Kim HC, Wolfram J, Mu C, Zhang W, Liu H, Xie Y, Mai J, Zhang H, Li Z, Guevara M, Mao ZW, Shen H (2017) A liposome encapsulated ruthenium polypyridine complex as a Theranostic platform for triple-negative breast cancer. *Nano Lett* 17(5):2913–2920
- Shuhendler AJ, Prasad P, Leung M, Rauth AM, Dacosta RS, Wu XY (2012) A novel solid lipid nanoparticle formulation for active targeting to tumor $\alpha(v)\beta(3)$ integrin receptors reveals cyclic RGD as a double-edged sword. *Adv Healthc Mater* 1(5):600–608
- Shukla S, Steinmetz NF (2015) Virus-based nanomaterials as positron emission tomography and magnetic resonance contrast agents: from technology development to translational medicine. *Wiley Interdiscip Rev Nanomed Nanobiotechnol* 7(5):708–721
- Siddiqi KS, Rahman A u, Husen A (2016) Biogenic fabrication of iron/iron oxide nanoparticles and their application. *Nanoscale Res Lett*:498
- Siegel RL, Miller KD, Fedewa SA, Ahnen DJ, Meester RG, Barzi A, Jemal A (2017) Colorectal cancer statistics, 2017. *CA Cancer J Clin* 67(3):177–193
- Silva CO, Pinho JO, Lopes JM, Almeida AJ, Gaspar MM, Reis C (2019) Current trends in cancer Nanotheranostics: metallic, polymeric, and lipid-based systems. *Pharmaceutics* 11(1):22
- Silverman JA, Deitcher SR (2013) Marqibo®(vincristine sulfate liposome injection) improves the pharmacokinetics and pharmacodynamics of vincristine. *Cancer Chemother Pharmacol* 71(3):555–564
- Singh P, Pandit S, Mokkapati VRSS, Garg A, Ravikumar V, Mijakovic I (2018) Gold Nanoparticles in diagnostics and therapeutics for human cancer. *Int J Mol Sci* 19(7):1979

- Souto EB, Almeida AJ, Müller RH (2007) Lipid Nanoparticles (SLN®, NLC®) for cutaneous drug delivery: structure, protection and skin effects. *J Biomed Nanotechnol*:317–331
- Sreekanth TVM, Pandurangan M, Jung MJ, Lee YR, Eom I-Y (2016a) Ecofriendlydecoration of graphene oxide with green synthesized silver nanoparticles: cytotoxic activity. *Res Chem Intermed* 42:5665–5676
- Sreekanth TVM, Pandurangan M, Kim DH, Lee YR (2016b) Greensynthesis:in-vitro anticancer activity of silver nanoparticles on human cervical cancer cells. *J Clust Sci* 27:671–681
- Steinmetz NF (2010 Oct) Viral nanoparticles as platforms for next-generation therapeutics and imaging devices. *Nanomedicine* 6(5):634–641
- Sulaiman GM, Hussien HT, Saleem MMNM (2015) Biosynthesis of silver nanoparticles synthesized by *aspergillus flavus* and their antioxidant, antimicrobial and cytotoxicity properties. *Bull Mater Sci* 38:639–644
- Sunshine JC, Peng DY, Green JJ (2012) Uptake and transfection with polymeric nanoparticles are dependent on polymer end-group structure, but largely independent of nanoparticle physical and chemical properties. *Mol Pharm* 9(11):3375–3383
- Swierczewska M, Lee S, Chen X (2011) Inorganic nanoparticles for multimodal molecular imaging. *Mol Imaging* 10(1):3–16
- Takakura Y, Fujita T, Hashida M, Sezaki H (1990) Disposition characteristics of macromolecules in tumor-bearing mice. *Pharm Res* 7(4):339–346
- Tang R, Xue J, Xu B, Shen D, Sudlow GP, Achilefu S (2015) Tunable ultrasmall visible-to-extended near-infrared emitting silver sulfide quantum dots for integrin-targeted cancer imaging. *ACS Nano* 9(1):220–230
- Tang WL, Tang WH, Li SD (2018) Cancer theranostic applications of lipid-based nanoparticles. *Drug Discov Today* 23(5):1159–1166
- Torti SV, Torti FM (2019) Winning the war with iron. *Nat Nanotechnol* 14:499–500
- Tran S, DeGiovanni PJ, Piel B, Rai P (2017) Cancer nanomedicine: a review of recent success in drug delivery. *Clin Transl Med* 6(1):1–21
- Tsai LC, Hsieh HY, Lu KY, Wang SY, Mi FL (2016) EGCG/gelatin-doxorubicin gold nanoparticles enhance therapeutic efficacy of doxorubicin for prostate cancer treatment. *Nanomedicine (Lond)* 11(1):9–30
- Tudose M, Culita DC, Musuc AM, Marinescu G, Somacescu S, Munteanu C et al (2016) Multi-functional silver nanoparticles-decorated silica functionalized with retinoic acid with antiproliferative and antimicrobial properties. *J Inorg Organomet Polym* 26:1043–1052
- Vidal C, Tomas-Gamasa M, Destito P, Lopez F, Mascarenas JL (2018) Concurrent and orthogonal gold(I) and ruthenium(II) catalysis inside living cells. *Nat Commun* 2018:1913
- Videira MA, Botelho MF, Santos AC, Gouveia LF, de Lima JJ, Almeida AJ (2002) Lymphatic uptake of pulmonary delivered radiolabelled solid lipid nanoparticles. *J Drug Target* 10(8):607–613
- Videira MA, Gano L, Santos C, Neves M, Almeida AJ (2006) Lymphatic uptake of lipid nanoparticles following endotracheal administration. *J Microencapsul* 23(8):855–862
- Videira M, Almeida AJ, Fabra A (2012) Preclinical evaluation of a pulmonary delivered paclitaxel-loaded lipid nanocarrier antitumor effect. *Nanomedicine* 8(7):1208–1215
- Von Maltzahn G, Park JH, Agrawal A, Bandaru NK, Das SK, Sailor MJ, Bhatia SN (2009) Computationally guided photothermal tumor therapy using long-circulating gold nanorod antennas. *Cancer Res* 69(9):3892–3900
- Von Maltzahn G, Park JH, Lin KY, Singh N, Schwöppe C, Mesters R, Berdel WE, Ruoslahti E, Sailor MJ, Bhatia SN (2011) Nanoparticles that communicate *in vivo* to amplify tumor targeting. *Nat Mater*:545–552
- Wang Q, Chao YM (2018) Multi-functional quantum dots and liposome complexes in drug delivery. *J Biomed Res* 32(2):91–106
- Wang C, Wang Y, Zhang L, Miron RJ, Liang J, Shi M et al (2018) Pretreated macrophage-membrane-coated gold nanocages for precise drug delivery for treatment of bacterial infections. *Adv Mater* 2018:e1804023

- Weber J, Beard PC, Bohndiek SE (2016) Contrast agents for molecular photoacoustic imaging. *Nat Methods* 13(8):639–650
- Wen AM, Lee KL, Yildiz I, Bruckman MA, Shukla S, Steinmetz NF (2012) Viral nanoparticles for in vivo tumor imaging. *J Vis Exp* (69):e4352
- Wicki A, Witzigmann D, Balasubramanian V, Huwyler J (2015) Nanomedicine in cancer therapy: challenges, opportunities, and clinical applications. *J Control Release* 200:138–157
- Wissing SA, Kayser O, Müller RH (2004) Solid lipid nanoparticles for parenteral drug delivery. *Adv Drug Deliv Rev* 56(9):1257–1272
- Wozniak A, Malankowska A, Nowaczyk G, Grzeskowiak BF, Tusnio K, Slomski R et al (2017) Size and shape-dependent cytotoxicity profile of gold nanoparticles for biomedical applications. *J Mater Sci Mater Med* 28:92
- Wu XL, Kim JH, Koo H, Bae SM, Shin H, Kim MS, Lee B-H, Park R-W, Kim I-S, Choi K, Kwon IC, Kim K, Lee DS (2010) Tumor-targeting peptide conjugated pH responsive micelles as a potential drug carrier for cancer therapy. *Bioconjug Chem*:208–213
- Xia W, Lin C (2012) Bioreducible polymer-delivered siRNA targeting human telomerase reverse transcriptase for human cancer gene therapy. *Ther Deliv* 3(4):439–442
- Xia Y, Li W, Cogley CM, Chen J, Xia X, Zhang Q et al (2011) Gold nanocages: from synthesis to theranostic applications. *Acc Chem Res* 44:914–924
- Xiao Y, Hong H, Javadi A, Engle JW, Xu W, Yang Y, Zhang Y, Barnhart TE, Cai W, Gong S (2012) Multifunctional unimolecular micelles for cancer-targeted drug delivery and positron emission tomography imaging. *Biomaterials* 33(11):3071–3082
- Xing J, Liu D, Zhou G et al (2018) Liposomally formulated phospholipid-conjugated novel near-infrared fluorescence probe for particle size effect on cellular uptake and biodistribution in vivo. *Colloids Surf B Biointerfaces* 161:588–596
- Xu H, Cheng L, Wang C, Ma X, Li Y, Liu Z (2011) Polymer encapsulated upconversion nanoparticle/iron oxide nanocomposites for multimodal imaging and magnetic targeted drug delivery. *Biomaterials* 32(35):9364–9373
- Yi X, Wang F, Qin W, Yang X, Yuan J (2014) Near-infrared fluorescent probes in cancer imaging and therapy: an emerging field. *Int J Nanomedicine* 9:1347–1365
- Yildiz T, Gu R, Zauscher S, Betancourt T (2018) Doxorubicin-loaded protease-activated near-infrared fluorescent polymeric nanoparticles for imaging and therapy of cancer. *Int J Nanomedicine* 13:6961
- Zhang YJ (2011) Investigation of gold and silver nanoparticles on absorption heating and scattering imaging. *Plasmonics*:393–397
- Zhang Q, Yang M, Zhu Y, Mao C (2018) Metallic nanoclusters for cancer imaging and therapy. *Curr Med Chem* 25(12):1379–1396
- Zhao JY, Cui R, Zhang ZL, Zhang M, Xie ZX, Pang DW (2014) Cytotoxicity of nucleus-targeting fluorescent gold nanoclusters. *Nanoscale*:13126–13134
- Zhen Z, Tang W, Guo C, Chen H, Lin X, Liu G, Fei B, Chen X, Xu B, Xie J (2013a) Ferritin nanocages to encapsulate and deliver photosensitizers for efficient photodynamic therapy against cancer. *ACS Nano* 7(8):6988–6996
- Zhen Z, Tang W, Chen H, Lin X, Todd T, Wang G, Cowger T, Chen X, Xie J (2013b) RGD-modified apoferritin nanoparticles for efficient drug delivery to tumors. *ACS Nano* 7(6):4830–4837
- Zhu D, Liu F, Ma L, Liu D, Wang Z (2013) Nanoparticle-based systems for T1-weighted magnetic resonance imaging contrast agents. *Int J Mol Sci* 14(5):10,591–10,607



Cardiovascular Safety Assessment of New Chemical Entities: Current Perspective and Emerging Technologies

6

Richa Tyagi and Shyam S. Sharma

6.1 Introduction and Importance of Cardiovascular Safety Studies

Before 1990, safety pharmacology was not a concept known to the pharmaceutical industry. Although, it has become evident over time that drugs appeared with rare lethal adverse effects at later stages in clinical trials, mostly during phase-3, not only causing wastage of resources, cost, and time but also posing a risk to trial participants. Even it became necessary for regulatory authorities to come up with a vigilant post-marketing surveillance (PMS) program for early detection of these events immediately after the acceptance for human use. The Food and Drug Administration of the United States (US FDA) and many other federal agencies utilized SRS (spontaneous reporting system) to observe the patterns of these rare adverse effects. This system collected reports from healthcare professionals and numerous hospitals worldwide to report rare adverse effects after huge reporting numbers. One such example which is also an epitome of such cases found in literature is terfenadine (Pugsley et al. 2008).

Terfenadine, an anti-histaminic drug, was discontinued for market use in mid-1990 due to increasing knowledge that the drug could be a major cause of a possibly fatal form of a cardiac syndrome known as torsades de pointes (TdP) syndrome (June and Nasr 1997). Before this event, the general viewpoint of the medical community was that only the compounds belonging to the class of cardiovascular (CVS) disorder treating drugs were considered to be the cause of such abnormalities. Surprisingly, terfenadine was used to treat hayfever, which is a very mild allergic reaction leading to a runny nose but was leading to such a

R. Tyagi · S. S. Sharma (✉)

Department of Pharmacology and Toxicology, National Institute of Pharmaceutical Education and Research (NIPER), Mohali, Punjab, India

e-mail: sssharma@niper.ac.in

life-threatening adverse effect suggesting the benefit being outweighed by the risk of using this drug since terfenadine is a non-CVS drug and possesses a little tendency to cause TdP rendering it so infrequent an incident that it counted on a million prescriptions before its accountability came into question (Rosen 1996).

This incident was of such a high significance to what we now know as Safety Pharmacology because predicting the risk of TdP caused due to terfenadine at its therapeutic dose was never attainable by preclinical toxicological studies or evaluation, which only suggested the adverse event profile of a drug at a very high/toxic/chronic doses. In addition, the measure of the outcome of terfenadine on QT interval is low, and the onset of its peak effects can also be delayed making it hard to detect (Ollerstam et al. 2007). Hence, it was suggestive of the situation, which could have been avoided if there would have been the presence of agenda that identified these risks in the drug discovery process by considering biomarkers or high-throughput screening methods for such adverse events (Pugsley et al. 2008). As a result, safety pharmacology developed into an industry-based discipline within a few years to link preclinical toxicology studies with drug discovery and development (Bass et al. 2004).

Regulatory guidance on physiological testing on organs was limited in the period before 1990. The US and European regulations presented extensive recommendations to assess the effects of the various drugs on the functioning of various organ systems (Gad 2004). Nonetheless, the Ministry of Health and Welfare in Japan introduced all-inclusive guidance for testing organ function in 1975. These guidelines elaborated on different organ systems to be evaluated as a first-tier evaluation (also known as category A studies) and made discrete suggestions related to study designs (selection of models, dose selection, and list of endpoints of investigations). The Second-tier of studies (aka category B studies) were also discussed in these guidelines. These studies were mainly necessity-based and were only conducted if any concerns arise from category A evaluation (Kinter and Valentin 2002). The concept was expanded upon by the International Council for Harmonisation of Technical Requirements for Pharmaceuticals for Human Use (ICH) safety pharmacology experts to explain three classes of pharmacological areas: primary pharmacodynamic, secondary pharmacodynamic, and safety pharmacology. At the same time, US, European, and Japanese regulatory authorities framed stances on general and safety pharmacology in the form of concept papers and guidance (Bass and Williams 2003). By 1998, draft documents were presented from Europe, Japan, and the USA. They were soon discussed at the pharmacology discussion group (later consolidated as the Safety Pharmacology Society (SPS) in 2000) meeting in September 1998. Consequently, the Ministry of Health and Welfare and the Japanese Pharmaceutical Manufacturer's Association approached the ICH steering committee and proposed the acceptance of an initiative on Safety Pharmacology. This proposal was later approved, accepted, and designated as topic S7 (Bass et al. 2004).

The term Safety Pharmacology first made its appearance in drafts of Topic M3 of the ICH guidelines "Non-Clinical Safety Studies for the Conduct of Human Clinical Trials for Pharmaceuticals," and Topic S6, "Preclinical Safety Evaluation of

Biotechnology derived Pharmaceuticals.” The work on the ICH Topic S7 (later redesignated as S7A) was initiated in 1999 by the Expert Working Group. A systematic safety pharmacology guideline was approved and embraced by the local regulatory agencies from 2000 to 2001 (Bass et al. 2004). However, the issue of evaluating the tendency of new chemical entities (NCEs) to cause potentially fatal ventricular tachyarrhythmia was not addressed initially. Even when the in vivo and in vitro methods were introduced for this purpose, the determination of the accuracy and translation to be used in human trials was still questionable. As a result, a new set of guidelines for evaluating the effect of NCEs on ventricular repolarization were called for by the ICH S7 expert working group. The ICH steering committee accepted the proposal in late 2000. It was adopted as ICH Topic S7B “Guideline on Safety Pharmacology Studies for Assessing the Potential for Delayed Ventricular Repolarization (QT Interval Prolongation) by Human Pharmaceuticals” (Bass et al. 2004).

Later ICH steering committee, upon a proposal from US FDA, accepted a similar guideline designated as ICH Topic E14, “The clinical evaluation of QT/QTc interval prolongation and proarrhythmic potential for non-anti-arrhythmic drugs” aimed at providing recommendations on clinical testing of NCEs for their potential of the prolonged QT interval (Bass et al. 2004). All these ICH guidelines concerning cardiovascular safety studies are further described in this chapter.

6.2 ICH S7A: Safety Pharmacology Studies for Human Pharmaceuticals

Safety Pharmacology studies deal with predicting even if a drug (in the widest sense of the word), upon administration into humans (or animal), is expected to be found harmful or unsafe, and its professional directive is to circumvent such an incidence (Pugsley et al. 2008). The prime objective of a safety pharmacology study is to protect clinical trial participants from any adverse effects and patients who are the recipient of marketed drugs from their potential adverse effects (ICH Harmonized Tripartite Guideline 2001). The guidelines narrate the principles and objectives of safety pharmacology, differing lines of investigations such as the core battery, follow-up studies and supplemental studies in a different organ system, and the timing of these studies concerning the clinical development of a new drug (ICH Harmonized Tripartite Guideline 2001). NCEs and biotechnology-derived products are subject to the safety studies mentioned in these guidelines. In addition, the marketed drugs can also fall in the scope of this guideline if major changes in their established pharmacological or biopharmaceutical properties are reported. For instance, a new formulation proposed for an established drug might change its bioavailability in the body and hence can have a significantly different effect which makes it necessary to conduct these safety studies before sending the formulation for a New Drug Application (NDA) approval.

Similarly, changes like a new route of administration, a new patient population, and new substantial adverse events render the product the subject of a safety

investigation (ICH Harmonized Tripartite Guideline 2001). These studies shall be performed prior to the first administration of agents in humans and before product approval (NDA). Some additional safety studies might also be carried out during the clinical development phase to explain and clarify the adverse effects observed during clinical development. These studies must be performed in compliance with good laboratory practices (GLP). The nature of these studies can be independent or combined with toxicology studies. However, after the introduction of frontloading, these studies were suggested to preferably be conducted during the lead optimization stage of drug discovery and development before the candidate selection (ICH Harmonized Tripartite Guideline 2001).

6.2.1 Safety Pharmacology Core Battery

Safety Pharmacological studies are categorized into essential core battery studies and supplemental studies, which are only carried out when necessary depending on the outcome of the core studies and pharmacological class of the drug. Safety pharmacology core battery studies aim to scrutinize the effects of the agent on crucial body functions. As the central nervous system, the cardiovascular and respiratory systems are usually considered vital organ systems. Hence, they are included in core battery studies (ICH Harmonized Tripartite Guideline 2001). Parameters to be assessed in safety pharmacology core battery studies are shown in Tables 6.1 and 6.2. Cardiac electrical activity and pump-muscle function are the two major pillars that sustain CVS functioning. Hence, CVS safety pharmacology is directed to investigate the effects of NCEs on the most pertinent components of this system and to detect harmful effects before the augmentation of clinical trials (ICH Harmonized Tripartite Guideline 2001). We have carried out safety pharmacology core battery studies of several new chemical entities (NCEs) and nanoformulations in the “National Centre for Safety Pharmacology, NIPER, Mohali, Punjab, India.”

Table 6.1 Parameters to be assessed in safety pharmacology core battery studies

Core battery studies	Parameters to be assessed
Central nervous system	Motor activity, neuro-muscular coordination, neuro-behavioral parameter estimation including sensory/motor reflex responses, and other CNS functions like regulation of body temperature and eating behavior.
Cardiovascular system	Systolic and diastolic blood pressure, heart rate, and the QT interval measurement by using an electrocardiogram. These studies can be performed in vivo, in vitro and/or ex vivo further to explore the means of repolarization and conductance abnormalities.
Respiratory system	Respiratory rate and other measures of respiratory function (e.g., hemoglobin oxygen saturation and tidal volume)

Table 6.2 Summary of key study design features of the CVS Safety Pharmacological evaluation according to ICH S7A guidelines

Attribute	Recommendation
Animal model	Conscious, unrestrained, telemetered, and trained
Test species	Rodent or non-rodent species, or most appropriate species based upon scientific considerations
Group size	Sufficient to rule out a significant effect of the drug
Controls	<ol style="list-style-type: none"> 1. Negative (vehicle or placebo). 2. Positive.
Route of administration	The best approximation of the clinical route
Test substance formulation	The best approximation of the clinical formulation, given constraints posted by the specific species
Dose range and schedule	Doses should include and exceed the primary pharmacodynamic or therapeutic range, single-dose administration studies

Table 6.3 Parameters to be assessed in various safety pharmacology follow-up studies

Follow-up Studies	Parameters to be assessed
Central nervous system	Learning and memory, analgesia, visual/auditory effects, EEG, proconvulsion, neurochemistry, ligand-specific binding, and PB-induced sleep
Cardiovascular system	Vascular resistance, ventricular contractility, coronary blood flow, Total peripheral resistance cardiac output, LVP (dp/dv), and effect of agents on CVS responses.
Respiratory system	Blood gases and pH, ventilator control (peripheral (NaCN response) and CNS (CO ₂ response), lung mechanics (dynamic compliance and Total pulmonary resistance), and pulmonary artery pressure

EEG Electroencephalogram, *PB* Phenobarbital, *LVP* Left ventricular pressure

6.2.2 Follow-up Safety Pharmacology Studies

Follow-up safety studies are performed to gain a deeper interpretation and reasoning for unexplainable results revealed in core battery studies. These studies can discover the mechanism of action for a pharmacological effect or an adverse effect, extent of the effect, and can even reveal the need for supplemental studies. Table 6.3 gives a list, not comprehensive, of additional studies that can be performed to evaluate further the effects of the agents in core systems of the body (ICH Harmonized Tripartite Guideline 2001).

6.2.3 Supplemental Safety Pharmacology Studies

As the name suggests, supplemental studies assess the possible harmful effects on organ system functions other than those included in the core battery studies, only if necessary. The necessity can be indicated by many factors like the pharmacological

class of the drugs (Non-Steroidal Anti-Inflammatory drugs aka NSAIDs infamous for gastric bleeding), concerning results arising from core battery studies, and extensive literature indicating adverse effects on these organ systems (ICH Harmonized Tripartite Guideline 2001). This includes the assessment of the effects of the test substance on (a) Autonomic Nervous System, (b) Renal/Urinary System, (c) Gastrointestinal System, and (d) Other Organ Systems.

6.3 ICH S7B Guidelines: The Nonclinical Evaluation of the Potential for Delayed Ventricular Repolarization (QT Interval Prolongation) by Human Pharmaceuticals

ICH S7B guideline elaborates a preclinical testing strategy for investigating the possibility of a new chemical entity to delay ventricular repolarization (QT Interval Prolongation) by human pharmaceuticals. This guideline is considered an extension of ICH guidance on S7A Safety Pharmacology Studies for Human Pharmaceuticals (Guideline, 2005). It delineates the nonclinical assay methods in addition to integrated risk assessment techniques (ICH Harmonized Tripartite Guideline 2005a).

The duration of both ventricular depolarization and repolarization sums up to QT interval. QT interval is described as the time from the start of the QRS complex to the T wave in an ECG recording. Most often, ventricular repolarization is the supreme cause of QT interval prolongation, which can take a severe form of ventricular tachyarrhythmia (ICH Harmonized Tripartite Guideline 2005a). It is important to understand the process of ventricular repolarization to explore the safety assessment methods to assess QT prolongation. The human cardiac action potential is comprised of five consecutive phases (Fig. 6.1) (Pinnell et al. 2007):

Phase 0: Opening of fast sodium channels and Na^+ influx (I_{Na}) leading to depolarization.

Phase 1: Rapid reduction in Na^+ passage upon closure of fast sodium channel and transient efflux of K^+ (I_{t0}) through K^+ channels leading to partial repolarization.

Phase 2: An influx of Ca^{2+} through L-type Ca^{2+} channels into the cell maintains the depolarization and presents a plateau phase.

Phase 3: Closure of sodium and calcium channels indicating repolarization. Membrane potential returns to baseline. Efflux of K^+ (I_{Kr} and I_{Ks}) through delayed rectifier K^+ channels occurs.

Phase 4: Activation of Na^+/K^+ ATPase pump creating negative intracellular potential and setting the final resting membrane potential (-90 mV).

Three major factors that can prolong the action potential are (a) increased activation of the Ca^{2+} current, (b) reduced inactivation of the inward Ca^{2+} or Na^+ currents, and (c) inhibition of the outward K^+ currents. However, the most important role in the determination of QT interval is played by the rapid and slow activating components of the delayed rectifier potassium current, I_{Kr} and I_{Ks} . The KCNH2 and KCNQ1 proteins, which constitute the α -subunits of the potassium channels responsible for I_{Kr} and I_{Ks} , are encoded by the human ether-a-go-go-related gene (hERG) and KvLQT1 gene, respectively. QT interval prolongation by

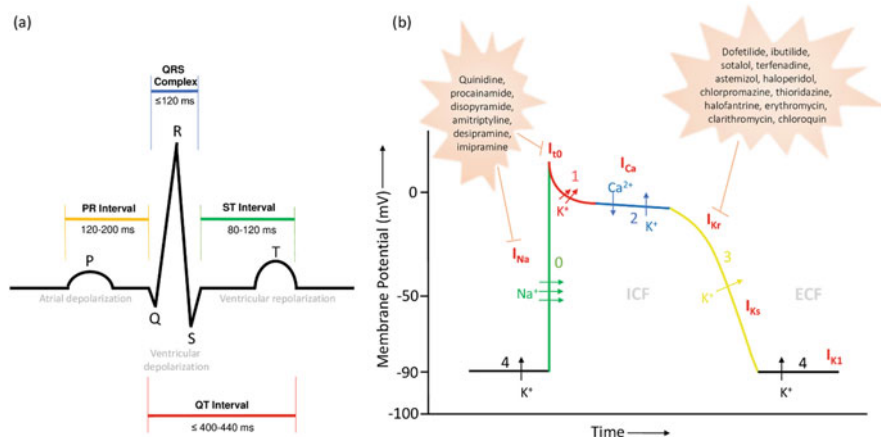


Fig. 6.1 (a) Figure showing a normal ECG wave along with the duration of intervals where PR interval represents the time between atrial depolarization and ventricular depolarization, QRS complex represents ventricular depolarization, ST interval represents the time between ventricular depolarization and repolarization, and QT interval represents the duration of ventricular systole. (b) graphical illustration of 0, 1, 2, 3 and 4 phase of cardiac action potential and movement of ions (respective currents) in between intracellular Fluid (ICF) and extracellular fluid (ECF) in the corresponding phase and various cardiac and non-cardiac drugs causing QT prolongation via I_{Kr} and I_{Na} blockage along with tabular representation of ion channels involved in various phases of cardiac action potential and resulting Transient Membrane Potential (TMP)

pharmaceuticals ubiquitously occurs due to inhibition of the delayed rectifier potassium channel (I_{Kr}) (ICH Harmonized Tripartite Guideline 2005a).

6.3.1 hERG Channels and QT Syndrome

The hERG gene was first termed and explained by Jeff Warmke and Barry Ganetzky. It is defined as the human homolog of the Ether-a-go-go gene prevalent in a fly called *Drosophila*. William D. Kaplan coined the term Ether-a-go-go in the 1960s after noticing flies starting to shake their legs after being anesthetized with ether. These flies specifically carried mutations in the Ether-a-go-go gene, and the shaking of legs resembled the dance moves, which were then popular at the Whisky A Go-Go nightclub in West Hollywood, California (Vandenberg et al. 2012). hERG potassium channels present six transmembrane domains (S1–S6) belonging to a Kv11.1 (KCNH2) family. The S4 domain carries a collective of positive charges, quintessentially of voltage-gated K^+ channels. As a characteristic of mammalian voltage-gated K^+ channels, hERGK⁺ channels also display strong inward rectification, primarily due to rapid inactivation, distinctively voltage-dependent. These channels exhibit slow deactivation, attributed to staying open for tens of milliseconds after repolarization and conducting a little current during this time as the electrochemical gradient for K^+ is minimum at the normal resting membrane potential \sim –85 mV.

Table 6.4 Recommendations for preclinical CVS safety assessment as per ICH S7B guideline

Parameters to be measured	Nonclinical methodologies
Ionic currents	In vitro: Cultured cardiac cell lines, heterologous expression systems for cloned human ion channels, and isolated animal or human cardiac myocytes
Action potential parameters	In vitro: Isolated cardiac preparations In vivo: Anesthetized animals—Specific electrophysiology parameters suggestive of action potential duration
ECG parameters	In vivo: Conscious or anesthetized animals
Proarrhythmic effects	In vivo and in vitro: Animals or isolated cardiac preparations

Although, if a premature stimulus ensues during this small time frame, hERG K^+ channels conduct a larger outward current that assists in suppressing the propagation of this premature beat (Vandenberg et al. 2012). Loss of hERG function is linked with long-QT syndrome type-2 (LQT2), distinguished by abnormally progressing ventricular repolarization, increased action potential duration, and high risk of TdP syndrome (Isbister and Page 2013). ICH S7B guideline shares its principles and recommendations with the S7A guideline. Its objective however is to detect the capability of a drug candidate/NCE to delay ventricular repolarization and, if found, to explore the relationship between the extent of this delay with the dose of the compound (ICH Harmonized Tripartite Guideline 2005a). The results from these studies not only divulge the risk of delayed ventricular repolarization but also help in illuminating its mechanism of action. Considerations regarding the study selection and design are shown in Table 6.4. The preclinical strategy for testing the pharmacological agents comprises of in vitro I_{K_r} assay, in vivo QT assay, consideration of pharmacological or chemical class of the agent, any relevant literature or information (clinical or nonclinical), and follow-up studies providing an integrated risk assessment which ultimately produces evidence of risk, if any (ICH Harmonized Tripartite Guideline 2005a). Both in vivo and in vitro electrophysiology studies are considered an integral part of CVS studies as per the ICH S7B guideline. In in vivo studies, the species selection is specific, including guinea pigs, rabbits, swine, ferret, dogs, and monkeys, because the phenomenon of ventricular repolarization and its ionic mechanism are quite similar to that of humans. These studies not only allow the measurement of QT interval but also elaborate on other safety parameters like QRS duration, blood pressure, PR interval, heart rate, and arrhythmia. Heart rate however since conversely related to QT interval, may influence the assessment of the drug effect on ventricular repolarization. Hence, any changes in heart rate due to species or any other external factor can alter the results, which necessitate the correction factor to be applied to the recorded QT interval during the experiment. Bazett or Fridericia are the two most commonly used correction formulae to rectify the QT interval for heart

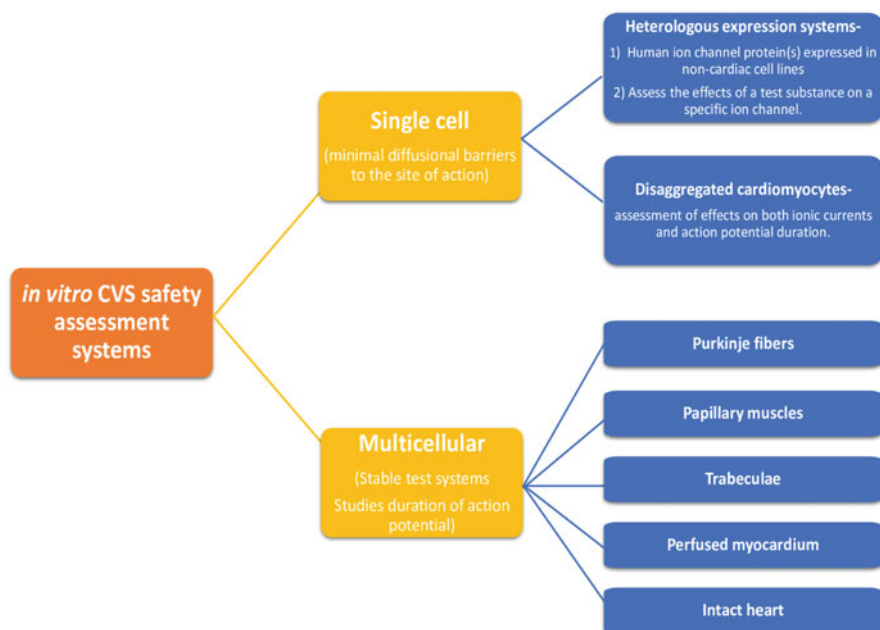


Fig. 6.2 In vitro systems used for primary Cardiovascular (CVS) safety studies as per ICH S7B Guideline

rate is known as QT_c, where c stands for corrected (ICH Harmonized Tripartite Guideline 2005a). On the other hand, in vitro studies can help in understanding the cellular mechanisms influencing the repolarization phenomenon in addition to the assessment of the potential for prolonged QT interval. These studies offer a much better and more accurate interpretation of results and save a lot of time and money, being an excellent alternative to in vivo studies (ICH Harmonized Tripartite Guideline 2005a). Figure 6.2 gives a detailed view of studies and systems incorporated in vitro safety assessment studies. As it is clear from the discussion above, ICH guideline S7B suggests several methods for assessing cardiac electrical activity. However, at the same time, innovation in these methods and techniques has always been encouraged by the committee. Figure 6.3 lists the conventional and emerging techniques in the field of CVS safety studies and are described further.

6.4 Conventional Techniques for CVS Safety Assessments

6.4.1 In Vivo Telemetry Technique

Telemetry has proven itself to be the best at measuring CVS parameters in freely moving conscious animals without any external hindrance and unnecessary stress hence producing reliable results for interpretation (Samson et al. 2011). Telemetric

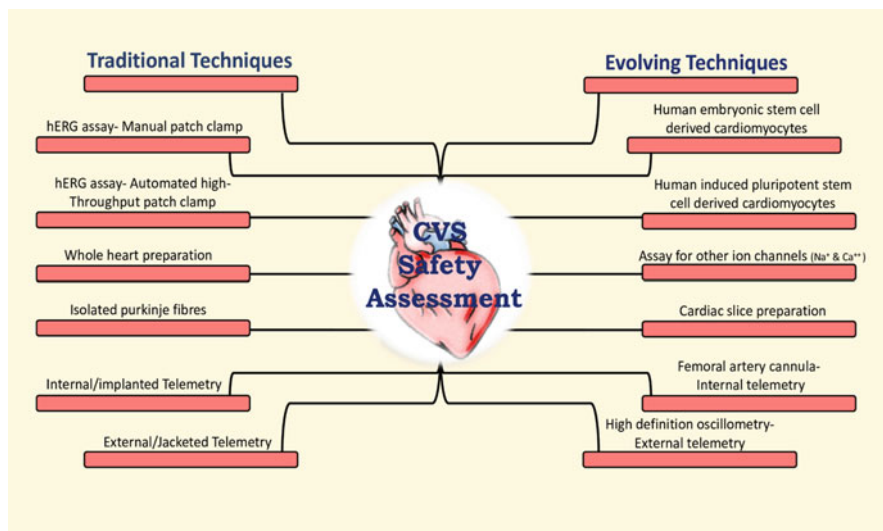


Fig. 6.3 Various techniques and systems employed in Cardiovascular (CVS) Safety assessment studies. (Left-hand side: Conventional techniques and Right-hand side: Evolved and newer techniques)

devices measure a broad range of CVS parameters which include heart rate, systolic and diastolic blood pressure (both arterial and ventricular), and almost all the Electroencephalogram (EEG) parameters: PR, QT, and ST intervals along with QRS complex. The corrected PR and QT intervals are considered for interpretation as inter-individual variation, and inter-species variation can influence these two parameters depending on the heart rate (Malik et al. 2002). Telemetry can be categorized as invasive and noninvasive. While the noninvasive technique, also known as external telemetry, makes use of an external jacket to be wrapped around an animal, the invasive technique requires a surgical procedure for the insertion of telemetric implants that allows the simultaneous measurement of hemodynamic and EEG parameters hence appropriately called as internal or implanted telemetry (Hamdam et al. 2013). One more advantage offered by internal telemetry is that it can be used for simultaneously measuring the parameters of other core organ systems in addition to CVS, making the concept of integrated core battery possible. This not only encourages the use of a fewer number of experimental animals but also saves a lot of research hours (Hamdam et al. 2013). Equal importance should be given to some other factors like concentration of plasma electrolytes, insulin and sugar levels, and alteration in body temperature while assessing the CVS parameters by using in vivo telemetry technique (Hamdam et al. 2013).

6.4.2 In Vitro hERG Assay and Isolated Systems

The role of hERG channels in QT prolongation and the occurrence of TdP syndrome is already discussed. Hence, it is essential to assess the effects of NCE on these channels, which can employ many screening techniques like automated voltage-clamp assays and radio-labeled ligand binding assays. A manual in vitro electrophysiology patch-clamp assay can also be employed to measure the extent of hERG inhibition induced by NCE (Hancox et al. 2008). These assays however can sometimes be challenging as these channels can be subject to inconclusiveness due to poorly known molecular mechanisms (Kaczorowski et al. 2011). Another method of quantifying the effects of NCE on cardiac action potential is using in vitro isolated myocardial systems, which include the entire isolated heart or an isolated myocardial tissue, for like papillary muscles and Purkinje fibers. These methods can not only screen the effects of NCE on action potential but, based on the choice of tissue, can also assess some additional influence of drug-like refractory period or force of contraction (Kågström et al. 2007). On the downside, these techniques require highly experienced and skilled electrophysiologists and are very expensive.

6.5 Emerging Technologies Techniques for CVS Safety Assessments

6.5.1 In Vivo Techniques

An advancement in external telemetry technique has emerged in the last decade, which combines jacketed telemetry with high-definition oscillometry (HDO). It offers two major advantages: (1) It can be used as an alternative to implanted telemetry and covers all the CVS safety parameters as the internal technique, and (2) It is cheaper and noninvasive (Meyer et al. 2010). Although, this technique still poses various limitations like shorter experimental periods, lack of knowledge regarding pharmacological validation techniques, and a lesser signal-to-noise ratio (Hamdam et al. 2013). However, all these limitations are reduced to a major extent after introducing femoral artery cannulation in an implanted telemetric technique that deploys a very small transducer in the artery and records for a longer duration with high output quality (McMahon et al. 2010).

6.5.2 In Vitro Techniques

It was discovered later that there are many channels, in addition to hERG, that can be either the note-worthy contributors or main culprits in causing ventricular arrhythmias in humans. These can be voltage-gated potassium channels, slow delayed rectifier potassium channels, potassium-permeable outward voltage-gated potassium channels, and inwardly rectifying potassium channels. Moreover, hyperpolarization-activated cyclic nucleotide-gated channel, L-Type calcium

channel, and voltage-gated sodium-permeable channel are also known to be involved in cardiac arrhythmia (Grant 2009; Nattel and Carlsson 2006). All these channels can be investigated using various electrophysiological techniques like the automated high-throughput patch-clamp program (Planer array technology) and can assess cardiac action potential (Laverty et al. 2011; Dunlop et al. 2008). These advanced techniques measure the magnitude of hERG blockade and can handle a vast number of NCEs in a significantly lesser time. Nevertheless, it is hard to achieve precise test concentrations in this approach and hence should use as an adjunct to other techniques (Guth and Rast 2010).

6.6 Newer Concepts in CVS Safety Assessment

6.6.1 Front-Loading

As mentioned earlier, for a better understanding of the potential of NCEs to cause various CVS adverse effects before in vivo studies, the concept of frontloading came into the picture that demands safety studies be conducted during the candidate selection phase of the drug discovery process (Lindgren et al. 2008). This offers various advantages like early detection of harmful substances, reduction in unnecessary in vivo studies, selection of safer and better candidates, and early discontinuation of potentially hazardous candidates, ultimately saving a lot of time and research cost (Hamdam et al. 2013).

6.6.2 Integrated Core Battery Safety Studies

We have discussed how telemetry is making its mark in providing a pertinent and reliable data set during in vivo safety studies. This technique has provided a chance to combine now two different core battery studies which were previously being performed distinctively. It does not only comply with the second R of the 4Rs principle (Replace, Reduce, Refine, and Rehabilitate) of animal use in research but strengthens the statistical power of the outcome (Moscardo et al. 2010; Tontodonati et al. 2007). CVS safety studies can either be paired with respiratory studies using automatic blood sampling and radio telemetry techniques or CNS safety studies with the help of radio telemetry (Kamendi et al. 2010). These studies also introduce the methodology for core system inter-dependency assessment as some times same pathological mechanisms may be involved in CNS as well as CVS disorders, or one can be the root cause of the other complication. Overall, it might be possible in the future to evaluate all core battery study endpoints in a sole study design with the help of integrated models (Pugsley et al. 2011).

6.6.3 Introduction of Alternate Models

It is now clear that abnormalities in cardiac functioning can not only be credited to hERG channels but various supplementary ion channels as well that significantly promote these complications. Hence, an alternate model is required, which inherently expresses both hERG channels as well as a variety of other ion channels. Human inducible pluripotent stem cell-derived 853 cardiomyocytes (hiPS-CM) and human embryonic stem cell-derived cardio-852 myocytes (hESC-CM) are two such models which fulfilled that requirement (Kraushaar et al. 2012). These systems are more sensitive as compared to conventional tissue preparations. They offer a screening of NCEs in both normal tissues and a disease-model style study as in hiPS-CM obtained from patients suffering long-QT syndrome (Moretti et al. 2010). However, these systems need to be properly standardized and validated as they appear with some limitations like genetic variation, stability of the phenotype, and reproducibility of differentiation (Hamdam et al. 2013).

6.6.4 Exploration of Targets

Cardiac sodium ion channel, worthy of focus—Even though the prime target for screening the NCEs for proarrhythmic potential has always been blockage of rapidly activating delayed rectifying potassium channels and respective inward rectifying potassium current (I_{Kr}), the focus has been gained by conduction and depolarization in the last decade. Both of them have been the target of drugs blocking sodium current (I_{Na}) (Harmer et al. 2011). This cardiac sodium channel as a target for drugs having the potential of prolonging ventricular repolarization was brought into the limelight by the catastrophic results of the Cardiac Arrhythmia Suppression Trial (Echt et al. 1991). These trials reported significantly high mortality among patients of acute myocardial infarction (MI) episodes with mild ventricular arrhythmia treated with class I anti-arrhythmic drugs (sodium channels blockers) in comparison to the placebo control group. This revealed a possibility that drugs that interfere with the activation of I_{Na} might present a tendency of causing ventricular arrhythmia (Farkas and Curtis 2002). Hence, the need for assessing the cardiac I_{Na} block was felt based on which safety margins for QRS prolongation and an in vitro method to gauge the cardiac I_{Na} blocking potential was proposed (Harmer et al. 2011).

6.7 Journey to an Evolved CVS Safety Assessment Approach

Constant efforts in improving the preexisting techniques and discovering new approaches were at their peak during the early 2000s. One example of such advancement is the report of a high number of false-positive outcomes, which was noticed in a study conducted by Cools et al. that used internal telemetry. The study demonstrated an increased prevalence of ventricular arrhythmia in healthy Beagle

dogs. This study implied the direct relation between the electrocardiogram (ECG) leads implantation and increased frequency of arrhythmic episodes (Cools et al. 2011). Another 6-month study conducted in telemetered normal Cynomolgus monkeys provided an exhaustive analysis of cardiac arrhythmia. The study assessed the changes in cardiac rate and rhythm with the help of pattern recognition software (ecgAUTO™). It was revealed that most of these non-human primates (NHPs) experienced several mild arrhythmias, which were variable every day. The incidence of severe arrhythmia was observed in a very small number of animals. This study reinforces the need to scrutinize the prescreening ECG as these inherently present arrhythmias (due to implantation procedure) might interfere with NCE assessment for its potential to cause ventricular arrhythmia (Chui et al. 2012).

As a solution to the abovementioned issue, a novel ECG algorithm was introduced, which could reduce the noise amplitudes by 85%, not only giving a clear and intelligible ECG signal content but also suggesting the improved sensitivity of the technique (Brockway and Hamlin 2011). Another proposition for the assessment of the effects of NCEs on ventricular refractoriness also came to light. This approach was focused at the cellular level, which investigates the effect of NCEs using quickly expanding stimulation trains (imitation of sequence related to the initiation of TdP). The drugs which lacked the potential of causing ventricular arrhythmia did not alter the rate of adaptation in rabbit myocytes. In contrast, the proarrhythmic drugs extended the rapid response at which myocytes stopped responding (Green et al. 2011). Detecting ventricular premature beats (VPB) can also be an alternative to forestall false outcomes. ARR30a is a new software application that can detect VPB in preclinical studies in a rapid, reliable, and automated manner. The software is appropriately validated with the help of an ECG database. It can detect five main types of arrhythmia, which include junctional beats, atrial beats, VPBs, sinus pause, and second-degree atrioventricular blockage, in various species like guinea pigs, minipigs, NHPs, dogs, and rats. The software has also shown remarkable predictivity and sensitivity in mentioned species (Koeppel et al. 2012).

Such technological advances were accompanied by various methodological ones, which are described below:

6.7.1 Application of Cardiac Stem Cells in CVS Safety Studies

Even though the *in vitro* hERG assay employing human myocyte cell lines is a sensitive approach for predicting the results of a clinical QT study, it still lacks specificity, which is only reasonably high at low exposure multiples (Wallis 2010). Also, as the concept of prognosis of TdP liability and QT prolongation is remarkably different, it may not be recommended to validate a channel screen based on a QT readout instead of TdP liability. The use of pluripotent stem cells serves as an excellent alternative to these conventional hERG screen models that use isolated human myocytes (Vidarsson et al. 2010). A variety of studies have explored these undifferentiated human stem cells of embryonic origin (hESC) and induced

pluripotent stem cells (iPSCs) of somatic origin for assessment of cardiac electrophysiological properties and their prospects of being a superior drug screening assay (Peng et al. 2010; Pugsley et al. 2010; Tanaka et al. 2009). Both Intracellular recordings from single cells and multi-electrode arrays have provided us with a method of measurement of calcium (Cav1.2), sodium (SCN5A), and potassium (I_{Kr} and I_{Ks}) currents (Peng et al. 2010). Although similarities between ion channel profiles of hESC and rabbit and canine Purkinje fibers have been discussed previously, a few differences like high potency for terfenadine and quinidine-induced I_{Kr} block and a decreased latency for the occurrence of channel block suggests the superiority of these systems (Peng et al. 2010). Several studies have utilized stem cells for preclinical CVS safety assessment and have received promising results (Moretti et al. 2010; Matsa et al. 2011; Itzhaki et al. 2011; Yazawa et al. 2011). For this technique, validation is necessitated to make the use of stem cells more prominent and reliable for CVS safety pharmacology during the drug screening process, and comprehensive information on specificity, sensitivity, and prognostic values of this model is also required to establish it as a primary nonclinical CVS safety model.

6.7.2 Cardiac Slice Preparation (In Vitro)

Preparation of thin cardiac slices has not yet attained the potential of carrying out a sole individual study but acts as one of the best complementary approaches to the traditional CVS models. These slicing methods better preserve and elaborate on the cellular architecture and tissue structure. Given the elasticity of the cardiac tissue, it is undoubtedly difficult to prepare such thin slices. Nevertheless, there exist a few techniques that prevent these slices from breakage and damage. Perfusion of the heart with high potassium solution can decrease the contractility, which can allow the slice preparation with vibratome after adhering the small portion of ventricular tissue to the agarose block. In proper storage conditions, a $\sim 350 \mu\text{m}$ thick vertical transmural slice can stay viable for 72 h. Even though the model allows the measurement of field potentials, determination of excitation, and recording of action potential and appropriate pharmacological responses, it still must be explored in terms of specificity and sensitivity towards various standard pharmacological agents for validation (Bussek et al. 2009).

6.7.3 Advanced and Superior Blood Pressure Recording with High Definition Oscillometry

A thorough and proper CVS safety assessment calls for a sensitive BP recording as it is the prime and an important parameter. Higher sensitivity is reported with HDO, which uses a cuff bladder to measure the blood pressure pulse waves as oscillations (Mitchell et al. 2010).

6.7.4 Cardiac Contractility a Core CVS Study Parameter

The CVS core battery studies are currently dominated by blood pressure (BP), heart rate and ECG parameter evaluation, and cardiac contractility are counted under supplementary or follow-up studies. However, the evaluation of contractility variables like left ventricular pressure (LVP) and rate of contraction and relaxation ($\pm dP/dt_{\max}$) can also be considered as a potential candidate for core safety assessment (Sarazan et al. 2011). The direct methods, both invasive and noninvasive, employed for the measurement of these contractility variables bear some limitations like induction of arrhythmia and high experimental cost (Pugsley and Curtis 2012). Hence, an alternative to these inefficient methods is the assessment of QA interval obtained from BP and ECG line. However, this QA interval requires a correction before the interpretation as the $\pm dP/dt_{\max}$, sometimes can be an unsuitable estimate of the inotropic state of the myocardium. Hence, this QA interval must be adjusted for LV end-diastolic volume, also known as preload (Hamlin and del Rio 2012). For this purpose, species-specific mathematical formulae for calculation of corrected myocardial contractility ($LV dP/dt_{\max}$) are determined, which corrects the parameter for changes in heart rate in primates, dogs, and minipigs (Markert et al. 2012; Sarazan et al. 2012). Table 6.5 collectively enlists a few research studies demonstrating the use of various techniques and technology in CVS safety assessment.

6.7.5 Organ on Chips

There are various models which were recently discussed for taking a step ahead in the innovation at CVS safety studies. Angiotensin II (ANG II)-induced in vitro cardiac model mimics myocardium laminar layers and is prepared by growing neonatal rat ventricular cardiomyocytes on corresponding muscular thin films (Horton et al. 2016). This model appropriately summarized the structural changes in the cardiac tissue and the development of proarrhythmic early after-depolarizations upon ANG II administration thus mimicking Ang II-induced cardiac damage. The use of murine (miCMs)-induced pluripotent stem-derived cells, human (hiCMs), and murine primary cardiomyocytes (mpCMs) are also in the running of a potentially novel in vitro screening assay for assessment of CVS safety. Pasqualini et al. presented a comparative in vitro physiology by using these systems, and the results suggested similar contractile cytoskeletal architecture with that observed in mpCM, reinforcing the idea of iPSCs to be used as a screening assay model (Pasqualini et al. 2015).

Table 6.5 List of research studies using different techniques and technologies in conducting various safety assessment studies

Purpose of study	Subject	Parameters assessment	Results	Dosing/ treatment	Inference	Ref.
To assess cardiorespiratory parameters for safety evaluation	Non-human primate	HR, BP, RR, MV, and QT interval	Increase in HR, BP, RR, MV at 2–7 h post administration Decrease in HR, TV, RR, MV at 5–23 h post administration Slight prolongation of QTcR at 1–11 h	Single-dose administration of test substance	Successful cardiorespiratory assessment in NHP for 24 h post administration.	Ingram-Ross et al. (2012)
To investigate the behavior of electro-mechanical (E-M) window—a surrogate marker for TdP	Anesthetized Guinea pigs.	BP and LVP signals, ECG parameters E-M window assessed for individual beats	Large (>50 ms) negative EMw followed by TdP	Single-dose administration of positive and negative control compounds	Negative EM windows are imperative for TdP induction	Guns et al. (2012)
To study the relation between EMw changes and occurrence of arrhythmia	Anesthetized beagle dogs.	EMw calculated as: QT interval-QLV Pend during atrial pacing	Administration of isoprenaline reduced the EMw (from 90 to 5 ms) and, in combination with an I _{Ks} blocker, lead to a large negative EMw (–109 ms) followed by TdP	Single-dose administration with atropine/ isoprenaline	EMw is a novel predictor of TdP risk in the given model	Van der Linde et al. (2010)
To compare internal and external telemetry techniques for ECG and BP measurement	Freely moving beagle dogs	MBP, SBP, DBP, heart rate, pulse pressure, PR, RR, QRS, QT, and QTcL interval were assessed for both methods.	For both methods, dec. in BP, HR, and pulse pressure with related ECG changes were observed with minoxidil administration. An increase in BP and pulse pressure and dec in HR and related ECG changes were observed on L-NAME administration	2 h pre-dose and 24 h post-dose with minoxidil, L-NAME, and vehicle	External jacketed telemetry techniques successfully measure both ECG and haemodynamic parameters in freely moving animals for approx. 26 h	Ward et al. (2012)

(continued)

Table 6.5 (continued)

Purpose of study	Subject	Parameters assessment	Results	Dosing/ treatment	Inference	Ref.
To demonstrate the use of mammalian cardiac tissue slices, long-term CVS safety studies	Freshly prepared cardiac slices from Guinea pig ventricle	Recording of intracellular action potentials and extracellular field potential parameters	24–28 h results upon administration with: E4031—Inc. FPD and APD Nifedipine—Dec in APD 4-aminopyridine—APD prolongation Carbenoxolone—Delayed propagation of FP	t/t with potassium channel blocker E4031 and 4-aminopyridine t/t with calcium channel blocker nifedipine t/t with gap junction blocker carbenoxolone	Cardiac slices could reproduce the responses for more than 24 h post preparation indicating its application for long-term CVS studies.	Bussek et al. (2012)

HR Heart rate, *RR* Respiratory rate, *EMw* Electro-mechanical window, *CVS* Cardiovascular, *MV* Minute volume, *TV* Tidal volume, *BP* Blood pressure, *ECG* Electrocardiogram, *QT interval* ECG parameter to assess ventricular repolarization, *QTc/QTcL/QTcR* Corrected QT interval, *APD* Action potential duration, *I/I* Treatment, *FP* Field potential, *FPD* Field potential duration, *LVP* Left ventricular pressure, *NHP* Non-human primate, *L-NAME* L-nitro arginine methyl ester, *PR/RR/QRS/ECG* parameters, *MBP* Mean blood pressure, *SBP* Systolic blood pressure, *DBP* Diastolic blood pressure, *TdP* Torsades de Pointes

6.8 ICH E14 Guideline: The Clinical Evaluation of QT/QTc Interval Prolongation and Proarrhythmic Potential for Non-Antiarrhythmic Drugs

As it is essential to conduct CVS safety studies in preclinical phases, the importance of testing drugs, with and without the potential of causing arrhythmia in humans, in the clinical phase is very substantial. ICH E14: The clinical evaluation of QT/QTc interval prolongation and proarrhythmic potential for non-antiarrhythmic drugs is a guideline that falls under the topic ICH-Efficacy and was advocated by the ICH steering committee at Step 1 Draft 2 (July 13, 2003). The final guideline was released in October 2005 by the US Department of Health and Human Services, Food and Drug Administration, Centre for Biologics Evaluation and Research (CBER) and Centre for Drug Evaluation and Research (CDER). The guideline focussed not only on testing the effects of new pharmacological agents of QT/QTc interval but also on reporting the myriad of other CVS adverse effects. It guides the sponsors regarding study design and its conduct, analysis and interpretation of the clinical studies to fathom the potential of new agents to cause QT/QTc prolongation in humans (Bass et al. 2004).

These guidelines apply to all the NCEs not classified as anti-arrhythmia drugs but also to market drugs for which a major change affecting their pharmacokinetic and pharmacodynamic characteristics is being introduced, e.g., a new route of administration or a new dose or a new formulation. The guideline briefly covers all the aspects of clinical trial planning, like the selection of subjects, exclusion criteria (repeated instances of a QTc interval >450 ms, on-going medication which prolongs QT/QTc interval, and presence of factors associated with TdP risk), safety monitoring and termination criteria (QT/QTc prolongation upto >500 ms or a total increase of >60 ms over baseline) (ICH Harmonized Tripartite Guideline 2005b).

A thorough QT/QTc study is a vital part of the clinical trial conducted under this guideline. The study is aimed at determining the potential of NCE to cause ventricular repolarization in a healthy human population. However, if these studies cannot be conducted in a healthy population due to tolerability/safety concerns, the guideline allows the study to be conducted in patients. The study is preferred to be conducted in the early stages of clinical development, which provides enough guidance to proceed in the later stages of clinical trials. However, the exact timing is always a matter of drug specifics. Where a positive QT/QTc study necessitates an extended ECG safety study later in the trials, a negative result will permit the on-therapy ECG study to be sufficient in drug safety assessment (ICH Harmonized Tripartite Guideline 2005b). Table 6.6 gives a brief overview of these “thorough QT/QTc studies.”

ECG changes recorded during QT/QTc studies which are considered atypical and adverse should be analyzed. This data must be consolidated with a successive assessment of equal rigor considering ECG data analysis. Standardization of the data collection process for indistinguishable research within a clinical trial program promotes a grouped analysis. Now, similar to the preclinical QT interval studies, QT interval recorded during the clinical trials must be corrected before submission (ICH

Table 6.6 Recommendations for clinical CVS safety assessment as per ICH E14 guideline

Aspects of 'thorough QT/QTc study'	Recommendation
Duration of dosing	Adequately planned to characterize the effect of NCE (and active metabolites) at various relevant concentrations
ECG collection	Timing to be directed by the pharmacokinetic profile of NCE
	Use of 12-lead surface ECGs and ambulatory ECG monitoring technique
	Submission of ECG data should be made as per regional guidance
Interpretation	Negative: Upper bound of the 95% one-sided CI for the highest time point-matched mean effect of the NCE on the QTc interval excludes 10 ms
	Positive: Largest time-matched difference exceeds the threshold (5 ms)

Harmonized Tripartite Guideline [2005b](#)). Researchers have the option to select from two types of correction formulae:

- (a) Formulae derived from within-subject data.
- (b) Formulae derived from population data which include Corrections based on linear regression techniques, Fridericia's correction: $QTc = QT/RR^{0.33}$, Bazett's correction: $QTc = QT/RR^{0.5}$ and Corrections using linear or nonlinear regression modeling on grouped data.

The QT/QTc data after analysis is required to be displayed as an analysis of central tendency and categorical analysis to obtain maximum pertinent information regarding clinical risk assessment (ICH Harmonized Tripartite Guideline [2005b](#)).

6.9 The Downside of the Current Approach on CVS Safety Assessment

Following the S7B and E14 guidelines, the pharmaceutical industry has always focussed on hERG blockage and the detection of the compounds responsible for this, using a myriad of preclinical assays. A comprehensive and accurate drug-induced I_{Kr} inhibition can only be measured by including an electrophysiological recording of native I_{Kr} in ventricular cardiomyocytes from a relevant species. Although this task does not seem to be this simple and poses a variety of challenges that includes need for mechanical and enzymatic myocyte dispersion from intact tissue, low amplitude of native I_{Kr} , low throughput measurements, and lack of pharmacological isolation from other overlapping currents (Hancox et al. [2008](#)). As a result, recombinant hERG channel assays and mammalian cell lines expressing these channels have been widely used by the industry.

Guideline S7B permits flexibility in user management of research protocols and measurement platforms. However, this can lead to an increased issue of variability among the data in the absence of a standardized approach. Currently, there is no ideal

protocol for studying the I_{Kr} sensitivity to NCEs. Hence, a standard procedure will reduce the variability in results (Fermini et al. 2016). The guideline also makes it confusing to distinguish safe hERG blockers from dangerous ones. It recommends obtaining full concentration-response relations for test compounds, except where physicochemical properties limit the maximal concentration that can be analyzed. Now that the infamous hERG pharmacology is known worldwide, it displays problems with NCE assessment and approx. 70% of them may interact with hERG at some concentration. In such a case, where redefining a safety margin may appear as a solution, it is not that easy as it does not address other problems like probable lack of C_{max} value required for accurate safety margin assessment, complete ignorance of other ionic currents, which may lead to QT prolongation and extreme complexity of relating QTc prolongation to safety margin values (Fermini et al. 2016).

6.10 Development of a New Prototype for the Assessment of NCE Cardiovascular Liability

Due to concerns like being the uneconomical and unmet assurance of clinical biomarkers to detect and foretellTdp, regulatory governing bodies have moved to foster a more powerful methodology for arrhythmia evaluation. These inventive endeavors are intended to decrease the requirement for a thorough QT (TQT) study. They are presently fixated on enhancing preclinical tests for assessing arrhythmogenesis and clinically distinguishing arrhythmia hazard using openness reaction examination and intensive ECG QT appraisal (IQT) in beginning-stage human studies (Lester and Olbertz 2016).

To evaluate this, the Consortium for Innovation and Quality in Pharmaceutical Development and the Cardiac Safety Research Consortium (IQ-CSRC) demonstrated a two-dose single ascending dose (SAD)-like trial in 20 individuals that involved six drugs (available in the market) known to cause QT-related effects. Out of the six compounds, five compounds infamously caused QT prolongation above the given threshold of regulatory concerns, and one compound had no considerable effect on QT whatsoever. ECG data were obtained and analyzed at different time intervals, based on analysis consortium conjectured, i.e., by employing concentration-effect modeling in which IQT data is evaluated in relation to sequential PK time points. By the above means, an exposure-response relationship could be determined, and hence the rapport of the compounds to lengthen the QTc interval (Darpo et al. 2014). The IQ-CSRC and US FDA see such kind of approach as “another option or choice” to the TQT trials. Although this study design is low-budget and detects QT liability in preliminary phases of drug development, it has a number of limitations, such as decreasing expenses and defining QT liability earlier in drug development. Also, researchers suggested that on the basis of a few compounds under study, a linear relationship cannot be established for a large spectrum of compounds. Further, this study could become complicated when the

metabolites of the compounds tend to cause QT/QTc prolongation or when the drug acts on multiple cardiac ion channels or the presence of a hysteresis effect due to bad tissue penetration (Postema and Wilde 2014).

The IQ-CSRC initiative also resulted in the updation of the ICH-E14 guidance to accommodate exposure-response (PK/PD) modeling as an essential assessment approach in FIH studies as an alternative to an exclusive TQT study (Xiao 2017). The fundamental components of this kind of investigation, as suggested by the FDA's Division of Cardio-renal Products, are being composed into a best practice report and incorporate (Lester and Olbertz 2016):

- A broad exposure margin of the NCE considering a disastrous clinical scenario focussing on the strength of 3–5 times higher than that which is established
- Improved and better quality clinical conduct and ECG data collection
- Planned specification of the modeling and statistical analysis plan and conducted diligent exposure-response study
- Relevant linearity and hysteresis examination in the whole collected data
- Inclusion of at least six placebo-treated subjects in the trial with classic group magnitude of 6–9 subjects

The promise of achieving adequately high medication exposure/concentrations is a key feature of this methodology. Such concentration is very likely to be a part of the clinical scenario considered as worst of all situations, which may include heightening the medication dosages to levels past a suprathereapeutic dose and calls for additional groups in SAD/MAD preliminaries. Likewise, the utilization of a standard drug (positive control) is not suggested if there is a placebo treatment gathering and drug concentrations accomplished are multifold of the clinically relevant exposure. Moreover, to alleviate a bogus obstructive examination in situations where drug exposure is deficient, another technique known as method bias sensitivity has been introduced by a few partners employing slope estimate of Bland-Altman as a marker of probable bias (Ferber et al. 2017).

6.11 Comprehensive In Vitro Proarrhythmia Assay (CiPA)

Another initiative, popularly known as the Comprehensive in vitro Proarrhythmia Assay (CiPA) initiative, utilizes a mechanical standpoint on establishing the pathogenesis of arrhythmias and is based on the advances of the last decade, both in terms of computer technology and pharmacology. Where S7B employs a binary approach (positive and negative) for the interpretation of assays, CiPA aims at determining the CVS liability in a graded manner (Sager et al. 2014). CiPA has now started to be officially announced by leaders in the academic community, industry, and regulatory agencies such as FDA and includes four foremost factors in a preclinical drug assessment.

First of all, an ion channel operating institution has improved and elaborative *in vitro* voltage-clamp studies of 7 different ion channels by taking advantage of high-throughput patch-clamp assays that modulate the cardiac AP and impact the risk of arrhythmia. Potassium channels (I_{Kr} , I_{Ks} , I_{to} , I_{K1}), peak and delayed Na^+ and Ca^{++} channels are currently targeted for these studies. The second initiative implements the O'Hara-Rudy computational model (O'Hara and Rudy 2012) of the human ventricular cardiomyocyte and is still under improvement via way of means of the *in silico* operating group. This model is created to propagate the cellular electrophysiology of different compounds and test the instability of the action potential along with its proclivity to early after depolarizations through *in silico* modeling. The third one involves the *in vivo* piece of this program and is backed up by a stem cell working group. It utilizes either human embryonic stem cell cardiomyocytes (hESC) or human-brought about pluripotent stem cell cardiomyocytes to corroborate the discoveries of the *in silico* modeling technique. In the last one, the clinical translational operating institution presents a set of 28 references or standard drugs marked as low, medium, and high risk of proarrhythmia. This list of 28 drugs is authorized by the FDA and will serve as a standard for rating the proarrhythmic risk of an NCE after a consolidation of the data obtained from the first three techniques of this paradigm. Overall, the CiPA initiative opposes the centralization of the QTc studies and aims to demarcate and certify the risk of proarrhythmia. This now no longer meant to rethink the necessity for *in vivo* telemetry research in species other than rodents. This approach will unavoidably expand the extent of arrhythmia recognition to become aware of compounds that can also increase the susceptibility to extreme arrhythmias through mechanisms aside from their action on I_{Kr} (O'Hara and Rudy 2012).

With the utilization of the preclinical CiPA paradigm in association with IQT tracking and exposure-response analysis in the early stages of medical research, it is expected that the current recommendation to conduct a TQT study on novel small-molecules will significantly subside. The FDA has also acknowledged that a gripping case for a TQT waiver would be dynamically taken into consideration if strong preclinical and medical evaluation did not occur any longer show any cardiac safety signs. Furthermore, the acquisition of this unified method can also result in decreased drug improvement costs, probably enhance the depiction of the risk of arrhythmia and marketing opportunities, and amplify the process of making early and knowledgeable decisions. However, despite high-throughput assays, the expense to be incurred in the CiPA scheme, interpretation of CiPA records by the regulators regarding ambiguous results, encouragement or discouragement of this method for the expansion of all non-biologic NCEs, and the concordance and prognostic potential of CiPA consequences remains to be in question until further discussion and judgment (Lester and Olbertz 2016). Figure 6.4 displays the key points of CiPA.



Fig. 6.4 Key features of Comprehensive *in vitro* Proarrhythmia Assay (CiPA) paradigm (*NCE* New chemical entity, *hiPSC* Human-induced pluripotent stem cells, *ECG* Electrocardiogram, *TQT* Thorough QT study)

6.12 In Silico Methods of CVS Safety Assessment: The Smart and Mathematical Future

CiPA has now familiarized us with *in silico* technique of assessing the risk of CVS toxicity as one of its initiative stepping towards the evolution of the CVS safety assessment. The concept introduced through CiPA includes *in silico* merging of electrophysiologic effects on the cellular level (Morissette et al. 2020). Even though *in vivo* and *in vitro* studies have been extremely helpful and are the primary line of study, they are carried out contemplating a small number of drugs. On the contrary, *in silico* assessment alone of a great number of drugs simultaneously predicts the TdP risk with an accuracy rate of 75% (Lawrence et al. 2008). Passini et al. demonstrated the accuracy of human *in silico* models upto 90% in predicting the

risk of arrhythmia and cardiac toxicity using approx. 60 standard drugs. In silico assessment not only helps in achieving high accuracy in results but also in the easy translation of preclinical data to humans. Hence, in silico human-based techniques are rapidly becoming an indispensable and critical tool for CVS safety studies by employing human stem cell-derived cardiomyocytes and computational multiscale human modeling (Bass et al. 2015; Rodriguez et al. 2015).

Multiscale in silico models have proven to be a strong and useful aid for assessing the anti-arrhythmic response of NCEs at the ECG level. The data produced can also assist in discovering novel biomarkers (ECG), which can determine the type of block, i.e., inward current block or outward (Vicente et al. 2016). One such investigation was carried out by Tixier et al. to spot new and improved biomarkers using machine learning and in silico model of multi-electrode array electrophysiology (Tixier et al. 2018). Similarly, Passini et al. also explored the prospects of a cellular surrogate for the EMw as a biomarker for detecting the risk of drug-induced arrhythmia in humans in silico trials. This research indicated better sensitivity of EMw in differentiating various compounds blocking calcium current (Passini et al. 2019).

In silico assays can also be a source of combined high-throughput assessment of TdP risk and mixed cardiac ion channel inhibition assessment during the early stages of drug development. The capability of in silico assays to predict the results of several time-consuming and error-prone in vivo models has also been evaluated and substantiated by a few studies (Beattie et al. 2013; Davies et al. 2012). Hence, in silico models and techniques are becoming promising by the day and rapidly taking over conventional animal models during the early stages of drug development.

In silico methodologies have also expanded to contribute to the understanding of arrhythmia and have made their mark to delineate the complex physiology, physiological variability, regulatory factors, both neural and hormonal, and many other complex processes involved in the pathology. Consequently, in silico modeling is extensively employed to investigate arrhythmia caused by a broad spectrum of etiology. In silico modeling has revealed the strong links between the following pathological events and proarrhythmic risk: (1) impaired local mitochondrial processes (Zhou et al. 2014), (2) role of Ca^{2+} releasing units and subcellular Ca^{2+} sparks in triggering arrhythmic events (Wang et al. 2015; Poláková et al. 2015) and (3) Neural stimulation especially β -adrenergic stimulation and its close involvement with Camp signaling (Yang et al. 2016; Surdo et al. 2017).

Population based-modeling approaches have also provided us with deeper insights regarding physiological variability (Passini et al. 2016). One speculation behind this cardiac variability modeling is the influence of external environmental factors over the regulation of the expression of ion channels which can cause the varying level of ionic conductance that can give rise to variable electrophysiological phenotypes (Zhou et al. 2018). Thus, an alliance of such in silico modeling and in vivo variability can not only add to the understanding of different types of cardiac abnormalities but also promote exploration of probable treatments for these illnesses (Zhou et al. 2018). All this newfound power and knowledge via in silico modeling

can take us one step forward towards the era of personalized medicines and treatment.

Recently Morissette et al. combined *in silico* qualitative endpoints with a mathematical translational pharmacokinetic/pharmacodynamic (tPKPD) model to improve the predictive outcome (QTc interval) of cardiovascular anesthetized guinea pig assay. The concept behind the merge was to determine the plasma concentration of the unbound drug at which it shows the proarrhythmic risk (prolongation of QTc interval) in advance. The results of the study advocated the union of the two approaches after finding comparative results, as in the case of *in vivo* assay. This has paved the way for much rapid identification of potential cardiotoxic or proarrhythmic agents at the expense of limited resources and time (Morissette et al. 2020).

There are still some unexplored areas that can be investigated with *in silico* approach in combination with persistent improvement in the representation of cardiac structure and function. The field is now prepared for its expansion in cardiotoxicity screening past ion channel blockage, equipment of cellular models with molecular dynamics enabling better comprehension of genetic defects, refined understanding of the regulation of signaling pathways by drug effects and external factors, and incorporation of clinical data into validation and structuration of these approaches (Zhou et al. 2018).

6.13 Conclusion

The field of cardiovascular safety assessment has come a long way from when it was started. We have now come face to face with the reality that the ICH safety guidelines crafted earlier certainly are capable of preventing NCEs with arrhythmogenic potential from commercialization but at the same time pose some major restrictions that halt the development of beneficial therapeutic agents. Hence, a considerable amount of research has been done on this matter, and new advances and strategies in the field have emerged. The core ideology, objectives, and vision have continued to be primarily the same throughout all these years, but the addition of new better methodologies and ideas have made their mark. Today, on the one hand, where we are equipped with the latest technology and both cost and time-efficient techniques, we still have to face the challenges of validation and substantiation. The future however is bright with *in silico* modeling and experimentation as this approach has not only been able to ensure the safety and effectiveness of new drugs but also can expose the vulnerability of various patient populations towards cardiac arrhythmia triggered by therapeutic agents. The expansion of translation of this approach into the industry and regulatory arrangement still demands the reliability of the technique, comparative analysis of the outcomes with already established approaches, and promotion of their execution with the help of user-friendly software. Altogether, the field has proven itself to be forever changing and advancing with no stagnation whatsoever.

Acknowledgments We acknowledge the financial support of PRDF, Department of Science and Technology (DST), Govt. of India and Department of Pharmaceuticals (DoP), Ministry of Chemicals and Fertilizers, Govt. of India to the “National Centre for Safety Pharmacology.”

References

- Bass A, Williams P (2003) Status of international regulatory guidelines on safety pharmacology, safety. *Pharmacology* 30:9–20
- Bass A, Kinter L, Williams P (2004) Origins, practices and future of safety pharmacology. *J Pharmacol Toxicol Methods* 49:145–151
- Bass AS, Hombo T, Kasai C, Kinter LB, Valentin J-P (2015) A historical view and vision into the future of the field of safety pharmacology. In *Principles of safety pharmacology*, pp 3–45
- Beattie KA, Luscombe C, Williams G, Munoz-Muriedas J, Gavaghan DJ, Cui Y, Mirams GR (2013) Evaluation of an in silico cardiac safety assay: using ion channel screening data to predict QT interval changes in the rabbit ventricular wedge. *J Pharmacol Toxicol Methods* 68:88–96
- Brockway M, Hamlin R (2011) Evaluation of an algorithm for highly automated measurements of QT interval. *J Pharmacol Toxicol Methods* 64:16–24
- Bussek A, Wettwer E, Christ T, Lohmann H, Camelliti P, Ravens U (2009) Tissue slices from adult mammalian hearts as a model for pharmacological drug testing. *Cell Physiol Biochem* 24:527–536
- Bussek A, Schmidt M, Bauriedl J, Ravens U, Wettwer E, Lohmann H (2012) Cardiac tissue slices with prolonged survival for in vitro drug safety screening. *J Pharmacol Toxicol Methods* 66:145–151
- Chui RW, Derakhchan K, Vargas HM (2012) Comprehensive analysis of cardiac arrhythmias in telemetered cynomolgus monkeys over a 6 month period. *J Pharmacol Toxicol Methods* 66:84–91
- Cools F, Janssens S, Vanlommel A, Teisman A, Towart R, Gallacher D (2011) ECG arrhythmias in non-implanted vs. telemetry-implanted dogs: need for screening before and sufficient recovery time after implantation. *J Pharmacol Toxicol Methods* 64:60–67
- Darpo B, Sarapa N, Garnett C, Benson C, Dota C, Ferber G, Jarugula V, Johannesen L, Keirns J, Krudys K (2014) The IQ-CSRC prospective clinical phase 1 study: “can early QT assessment using exposure response analysis replace the thorough QT study?”. *Ann Noninvasive Electrocardiol* 19:70–81
- Davies MR, Mistry HB, Hussein L, Pollard CE, Valentin J-P, Swinton J, Abi-Gerges N (2012) An in silico canine cardiac midmyocardial action potential duration model as a tool for early drug safety assessment. *Am J Physiol Heart Circ Physiol* 302:H1466–H1480
- Dunlop J, Bowlby M, Peri R, Vasilyev D, Arias R (2008) High-throughput electrophysiology: an emerging paradigm for ion-channel screening and physiology. *Nat Rev Drug Discov* 7:358–368
- Echt DS, Liebson PR, Mitchell LB, Peters RW, Obias-Manno D, Barker AH, Arensberg D, Baker A, Friedman L, Greene HL (1991) Mortality and morbidity in patients receiving encainide, flecainide, or placebo: the cardiac arrhythmia suppression trial. *N Engl J Med* 324:781–788
- Farkas A, Curtis MJ (2002) Limited antiarrhythmic effectiveness of clinically relevant concentrations of class I anti-arrhythmics in isolated perfused rat hearts. *J Cardiovasc Pharmacol* 39:412–424
- Ferber G, Zhou M, Dota C, Garnett C, Keirns J, Malik M, Stockbridge N, Darpo B (2017) Can bias evaluation provide protection against false-negative results in QT studies without a positive control using exposure-response analysis? *J Clin Pharmacol* 57:85–95
- Fermini B, Hancox JC, Abi-Gerges N, Bridgland-Taylor M, Chaudhary KW, Colatsky T, Correll K, Crumb W, Damiano B, Erdemli G (2016) A new perspective in the field of cardiac safety testing through the comprehensive in vitro proarrhythmia assay paradigm. *J Biomol Screen* 21:1–11

- Gad SC (2004) Safety pharmacology in pharmaceutical development and approval, 2nd edn. CRC Press
- Grant AO (2009) Cardiac ion channels. *Circ Arrhythm Electrophysiol* 2:185–194
- Green JR, Diaz GJ, Limberis JT, Houseman KA, Su Z, Martin RL, Cox BF, Kantor S, Gintant GA (2011) Ventricular rate adaptation: a novel, rapid, cellular-based in-vitro assay to identify proarrhythmic and torsadogenic compounds. *J Pharmacol Toxicol Methods* 64:68–73
- Guns P-J, Johnson DM, Weltens E, Lissens J (2012) Negative electro-mechanical windows are required for drug-induced Torsades de pointes in the anesthetized Guinea pig. *J Pharmacol Toxicol Methods* 66:125–134
- Guth B, Rast G (2010) Dealing with hERG liabilities early: diverse approaches to an important goal in drug development. *Br J Pharmacol* 159:22–24
- Hamdam J, Sethu S, Smith T, Alfirevic A, Alhaidari M, Atkinson J, Ayala M, Box H, Cross M, Delaunoy A (2013) Safety pharmacology—current and emerging concepts. *Toxicol Appl Pharmacol* 273:229–241
- Hamlin RL, del Rio C (2012) dP/dt_{max}—a measure of ‘baroinometry’. *J Pharmacol Toxicol Methods* 66:63–65
- Hancox JC, McPate MJ, El Harchi A, Zhang YH (2008) The hERG potassium channel and hERG screening for drug-induced torsades de pointes. *Pharmacol Ther* 119:118–132
- Harmer A, Valentin JP, Pollard C (2011) On the relationship between block of the cardiac Na⁺ channel and drug-induced prolongation of the QRS complex. *Br J Pharmacol* 164:260–273
- Horton RE, Yadid M, McCain ML, Sheehy SP, Pasqualini FS, Park S-J, Cho A, Campbell P, Parker KK (2016) Angiotensin II induced cardiac dysfunction on a chip. *PLoS One* 11:e0146415
- ICH Harmonized Tripartite Guideline (2001) Safety pharmacology studies for human pharmaceuticals S7A, pp 1–9
- ICH Harmonized Tripartite Guideline (2005a) The non-clinical evaluation of the potential for delayed ventricular repolarization (QT Interval Prolongation) by human pharmaceuticals, pp 1–10
- ICH Harmonized Tripartite Guideline (2005b) The clinical evaluation of QT/QTc interval prolongation and proarrhythmic potential for non-antiarrhythmic drugs E14, pp 1–14
- Ingram-Ross JL, Curran AK, Miyamoto M, Sheehan J, Thomas G, Verbeeck J, de Waal EJ, Verstynen B, Pugsley MK (2012) Cardiorespiratory safety evaluation in non-human primates. *J Pharmacol Toxicol Methods* 66:114–124
- Isbister GK, Page CB (2013) Drug induced QT prolongation: the measurement and assessment of the QT interval in clinical practice. *Br J Pharmacol* 76:48–57
- Itzhaki I, Maizels L, Huber I, Zwi-Dantsis L, Caspi O, Winterstern A, Feldman O, Gepstein A, Arbel G, Hammerman H (2011) Modelling the long QT syndrome with induced pluripotent stem cells. *Nature* 471:225–229
- June RA, Nasr I (1997) Torsades de pointes with terfenadine ingestion. *Am J Emerg Med* 15:542–543
- Kaczorowski GJ, Garcia ML, Bode J, Hess SD, Patel UA (2011) The importance of being profiled: improving drug candidate safety and efficacy using ion channel profiling. *Front Pharmacol* 2:78
- Kågström J, Sjögren E-L, Ericson A-C (2007) Evaluation of the Guinea pig monophasic action potential (MAP) assay in predicting drug-induced delay of ventricular repolarisation using 12 clinically documented drugs. *J Pharmacol Toxicol Methods* 56:186–193
- Kamendi HW, Brott DA, Chen Y, Litwin DC, Lengel DJ, Fonck C, Bui KH, Gorko MA, Bialecki RA (2010) Combining radio telemetry and automated blood sampling: a novel approach for integrative pharmacology and toxicology studies. *J Pharmacol Toxicol Methods* 62:30–39
- Kinter LB, Valentin JP (2002) Safety pharmacology and risk assessment. *Fundam Clin Pharmacol* 16:175–182
- Koepfel F, Labarre D, Zitoun P (2012) Quickly finding a needle in a haystack: a new automated cardiac arrhythmia detection software for preclinical studies. *J Pharmacol Toxicol Methods* 66:92–97

- Kraushaar U, Meyer T, Hess D, Gepstein L, Mummery CL, Braam SR, Guenther E (2012) Cardiac safety pharmacology: from human ether-a-gogo related gene channel block towards induced pluripotent stem cell based disease models. *Expert Opin Drug Saf* 11:285–298
- Lavery H, Benson C, Cartwright E, Cross M, Garland C, Hammond T, Holloway C, McMahon N, Milligan J, Park B (2011) How can we improve our understanding of cardiovascular safety liabilities to develop safer medicines? *Br J Pharmacol* 163:675–693
- Lawrence C, Pollard C, Hammond T, Valentin JP (2008) In vitro models of proarrhythmia. *Br J Pharmacol* 154:1516–1522
- Lester RM, Olbertz J (2016) Early drug development: assessment of proarrhythmic risk and cardiovascular safety: the age of repolarization cardiac toxicity. *Expert Rev Clin Pharmacol* 9: 1611–1618
- Lindgren S, Bass AS, Briscoe R, Bruse K, Friedrichs GS, Kallman MJ, Markgraf C, Patmore L, Pugsley MK (2008) Benchmarking safety pharmacology regulatory packages and best practice. *J Pharmacol Toxicol Methods* 58:99–109
- Malik M, Färbom P, Batchvarov V, Hnatkova K, Camm A (2002) Relation between QT and RR intervals is highly individual among healthy subjects: implications for heart rate correction of the QT interval. *Heart* 87:220–228
- Markert M, Trautmann T, Groß M, Ege A, Mayer K, Guth B (2012) Evaluation of a method to correct the contractility index LVdP/dtmax for changes in heart rate. *J Pharmacol Toxicol Methods* 66:98–105
- Matsa E, Rajamohan D, Dick E, Young L, Mellor I, Staniforth A, Denning C (2011) Drug evaluation in cardiomyocytes derived from human induced pluripotent stem cells carrying a long QT syndrome type 2 mutation. *Eur Heart J* 32:952–962
- McMahon C, Mitchell AZ, Klein JL, Jenkins AC, Sarazan RD (2010) Evaluation of blood pressure measurement using a miniature blood pressure transmitter with jacketed external telemetry in cynomolgus monkeys. *J Pharmacol Toxicol Methods* 62:127–135
- Meyer O, Jenni R, Greiter-Wilke A, Breidenbach A, Holzgreffe HH (2010) Comparison of telemetry and high-definition oscillometry for blood pressure measurements in conscious dogs: effects of torcetrapib. *J Am Assoc Lab Anim Sci* 49:464–471
- Mitchell AZ, McMahon C, Beck TW, Sarazan RD (2010) Sensitivity of two non-invasive blood pressure measurement techniques compared to telemetry in cynomolgus monkeys and beagle dogs. *J Pharmacol Toxicol Methods* 62:54–63
- Moretti A, Bellin M, Welling A, Jung CB, Lam JT, Bott-Flügel L, Dorn T, Goedel A, Höhnke C, Hofmann F (2010) Patient-specific induced pluripotent stem-cell models for long-QT syndrome. *N Engl J Med* 363:1397–1409
- Morissette P, Polak S, Chain A, Zhai J, Imredy JP, Wildey MJ, Travis J, Fitzgerald K, Fanelli P, Passini E (2020) Combining an in silico proarrhythmic risk assay with a tPKPD model to predict QTc interval prolongation in the anesthetized Guinea pig assay. *Toxicol Appl Pharmacol* 390: 114883
- Moscardo E, McPhie G, Faselli N, Dorigatti R, Meecham K (2010) An integrated cardiovascular and neurobehavioural functional assessment in the conscious telemetered cynomolgus monkey. *J Pharmacol Toxicol Methods* 62:95–106
- Nattel S, Carlsson L (2006) Innovative approaches to anti-arrhythmic drug therapy. *Nat Rev Drug Discov* 5:1034–1049
- O'Hara T, Rudy Y (2012) Quantitative comparison of cardiac ventricular myocyte electrophysiology and response to drugs in human and non-human species. *Am J Physiol Heart Circ Physiol* 302:H1023–H1030
- Ollerstam A, Visser S, Duker GR, Forsberg T, Persson AH, Nilsson LB, Björkman J-A, Gabrielsson J, Al-Saffar A (2007) Comparison of the QT interval response during sinus and paced rhythm in conscious and anesthetized beagle dogs. *J Pharmacol Toxicol Methods* 56: 131–144
- Pasqualini FS, Sheehy SP, Agarwal A, Aratyn-Schaus Y, Parker KK (2015) Structural phenotyping of stem cell-derived cardiomyocytes. *Stem Cell Reports* 4:340–347

- Passini E, Mincholé A, Coppini R, Cerbai E, Rodriguez B, Severi S, Bueno-Orovio A (2016) Mechanisms of proarrhythmic abnormalities in ventricular repolarisation and anti-arrhythmic therapies in human hypertrophic cardiomyopathy. *J Mol Cell Cardiol* 96:72–81
- Passini E, Trovato C, Morissette P, Sannajust F, Bueno-Orovio A, Rodriguez B (2019) Drug-induced shortening of the electro-mechanical window is an effective biomarker for in silico prediction of clinical risk of arrhythmias. *Br J Pharmacol* 176:3819–3833
- Peng S, Lacerda AE, Kirsch GE, Brown AM, Bruening-Wright A (2010) The action potential and comparative pharmacology of stem cell-derived human cardiomyocytes. *J Pharmacol Toxicol Methods* 61:277–286
- Pinnell J, Turner S, Howell S (2007) Cardiac muscle physiology. *BJA Educ* 7:85–88
- Poláková E, Illaste A, Niggli E, Sobie EA (2015) Maximal acceleration of Ca²⁺ release refractoriness by β -adrenergic stimulation requires dual activation of kinases PKA and CaMKII in mouse ventricular myocytes. *J Physiol* 593:1495–1507
- Postema PG, Wilde AAM (2014) The measurement of the QT interval. *Curr Cardiol Rev* 10:287–294
- Pugsley M, Curtis M (2012) Methodological innovations expand the safety pharmacology horizon. *J Pharmacol Toxicol Methods* 66:59–62
- Pugsley MK, Authier S, Curtis M (2008) Principles of safety pharmacology. *Br J Pharmacol* 154:1382–1399
- Pugsley M, Towart R, Authier S, Gallacher D, Curtis M (2010) Non-clinical models: validation, study design and statistical consideration in safety pharmacology. *J Pharmacol Toxicol Methods*
- Pugsley M, Towart R, Authier S, Gallacher D, Curtis M (2011) Innovation in safety pharmacology testing. *J Pharmacol Toxicol Methods* 64:1–6
- Rodriguez B, Carusi A, Abi-Gerges N, Ariga R, Britton O, Bub G, Bueno-Orovio A, Burton RA, Carapella V, Cardone-Noott L (2015) Human-based approaches to pharmacology and cardiology: an interdisciplinary and intersectorial workshop. *Europace* 18:1287–1298
- Rosen MR (1996) Of oocytes and runny noses. *Circulation* 94:607–609
- Sager PT, Gintant G, Turner JR, Pettit S, Stockbridge N (2014) Rechanneling the cardiac proarrhythmia safety paradigm: a meeting report from the cardiac safety research consortium. *Am Heart J* 167:292–300
- Samson N, Dumont S, Specq M-L, Praud J-P (2011) Radio telemetry devices to monitor breathing in non-sedated animals. *Respir Physiol Neurobiol* 179:111–118
- Sarazan RD, Mittelstadt S, Guth B, Koerner J, Zhang J, Pettit S (2011) Cardiovascular function in nonclinical drug safety assessment: current issues and opportunities. *Int J Toxicol* 30:272–286
- Sarazan RD, Kroehle JP, Main BW (2012) Left ventricular pressure, contractility and dP/dtmax in nonclinical drug safety assessment studies. *J Pharmacol Toxicol Methods* 66:71–78
- Surdo NC, Berrera M, Koschinski A, Brescia M, Machado MR, Carr C, Wright P, Gorelik J, Morotti S, Grandi E (2017) FRET biosensor uncovers cAMP nano-domains at β -adrenergic targets that dictate precise tuning of cardiac contractility. *Nat Commun* 8:1–14
- Tanaka T, Tohyama S, Murata M, Nomura F, Kaneko T, Chen H, Hattori F, Egashira T, Seki T, Ohno Y (2009) In vitro pharmacologic testing using human induced pluripotent stem cell-derived cardiomyocytes. *Biochem Biophys Res Commun* 385:497–502
- Tixier E, Raphael F, Lombardi D, Gerbeau J-F (2018) Composite biomarkers derived from micro-electrode array measurements and computer simulations improve the classification of drug-induced channel block. *Front Physiol* 8:1096
- Tontodonati M, Fasdelli N, Moscardo E, Giarola A, Dorigatti R (2007) A canine model used to simultaneously assess potential neurobehavioural and cardiovascular effects of candidate drugs. *J Pharmacol Toxicol Methods* 56:265–275
- Van der Linde H, Van Deuren B, Somers Y, Loenders B, Towart R, Gallacher D (2010) The electro-mechanical window: a risk marker for torsade de pointes in a canine model of drug induced arrhythmias. *Br J Pharmacol* 161:1444–1454
- Vandenberg JJ, Perry MD, Perrin MJ, Mann SA, Ke Y, Hill AP (2012) hERG K⁺ channels: structure, function, and clinical significance. *Physiol Rev* 92:1393–1478

- Vicente J, Johannesen L, Hosseini M, Mason JW, Sager PT, Pueyo E, Strauss DG (2016) Electrocardiographic biomarkers for detection of drug-induced late sodium current block. *PLoS One* 11:e0163619
- Vidarsson H, Hyllner J, Sartipy P (2010) Differentiation of human embryonic stem cells to cardiomyocytes for in vitro and in vivo applications. *Stem Cell Rev Rep* 6:108–120
- Wallis RM (2010) Integrated risk assessment and predictive value to humans of non-clinical repolarization assays. *Br J Pharmacol* 159:115–121
- Wang X, Weinberg SH, Hao Y, Sobie EA, Smith GD (2015) Calcium homeostasis in a local/global whole cell model of permeabilized ventricular myocytes with a Langevin description of stochastic calcium release. *Am J Physiol Heart Circ Physiol* 308:H510–H523
- Ward G, Milliken P, Patel B, McMahon N (2012) Comparison of non-invasive and implanted telemetric measurement of blood pressure and electrocardiogram in conscious beagle dogs. *J Pharmacol Toxicol Methods* 66:106–113
- Xiao LHJDER (2017) Introduction of ICH E14 clinical evaluation of QT prolongation caused by non-antiarrhythmic drug. *Q&As (R3)* 40:1378–1385
- Yang P-C, Boras BW, Jeng M-T, Docken SS, Lewis TJ, McCulloch AD, Harvey RD, Clancy CE (2016) A computational modeling and simulation approach to investigate mechanisms of subcellular cAMP compartmentation. *PLoS Comput Biol* 12:e1005005
- Yazawa M, Hsueh B, Jia X, Pasca AM, Bernstein JA, Hallmayer J, Dolmetsch RE (2011) Using induced pluripotent stem cells to investigate cardiac phenotypes in Timothy syndrome. *Nature* 471:230–234
- Zhou L, Solhjo S, Millare B, Plank G, Abraham MR, Cortassa S, Trayanova N, O'Rourke B (2014) Effects of regional mitochondrial depolarization on electrical propagation: implications for arrhythmogenesis. *Circ Arrhythm Electrophysiol* 7:143–151
- Zhou X, Bueno-Orovio A, Rodriguez B (2018) In silico evaluation of arrhythmia. *Curr Opin Physiol* 1:95–103



Toxicology of Pharmaceutical Products During Drug Development

7

Mishra Abhishek, Singla Rubal, Joshi Rupa, and Medhi Bikash

7.1 Introduction

Nonclinical safety attrition is a serious concern for the research and development of pharmaceutical products in their productivity, particularly in the early stages as well as compound optimization stage of clinical development. Numerous ways have been tried over the years to reduce the attrition related to nonclinical safety. Throughout human history, doctors have prescribed medications or various therapeutic agents for different diseases. Indeed, a distinguishing human trait is enthusiasm and readiness to take curative drugs, which otherwise be considered deadly. At sufficiently high doses however all chemical entities are hazardous. The therapeutic index (TI) is explained as the ratio between the toxic and therapeutic doses of a drug, and this term helps determine “safety margins” in clinical trials (Bucher et al. 1996). The margin of safety (MOS) is the most commonly used safety word in nonclinical toxicology examinations, which are aimed to give the safety data of the clinical trial. The MOS information must be viewed according to the disease type to be treated, the present therapies available, and the risk-benefit ratio of the available treatments. In fact, no treatment option is completely free of any type of risk. Thus, the drug development process necessitates the identification of potential risks as well as the comprehension of the benefits.

A drug can be defined as a substance that is utilized or intended to be employed to change or study the physiological systems or pathological conditions for the recipient’s benefit, according to the World Health Organization. The process of

Mishra Abhishek, Singla Rubal, and Joshi Rupa have contributed equally to this work.

M. Abhishek · S. Rubal · J. Rupa · M. Bikash (✉)
Department of Pharmacology, PGIMER, Chandigarh, India

discovery of a drug is a very complex, expensive, high-risk, complicated, and gratifying process. The main aim of the drug development process is discovering safe NCEs (New chemical entities) as well as NBEs (New biological entities) that are helpful in the treatment of the ailment being treated (Beary III 1997).

Toxicology refers to the branch of science that explains the effect of adverse effects of chemicals on humans, animals, plants, or microbes. It mainly deals with the nature as well as mechanisms by which these substances have toxic effects on living organisms or biological systems. The three major goals of these toxicological interpretations are determining the toxicological spectrum in laboratory animals over a wide dose range; response extrapolation to other species, with a focus on the potential negative impacts on humans; and determining the toxicological spectrum in humans (Calabrese and Baldwin 1994).

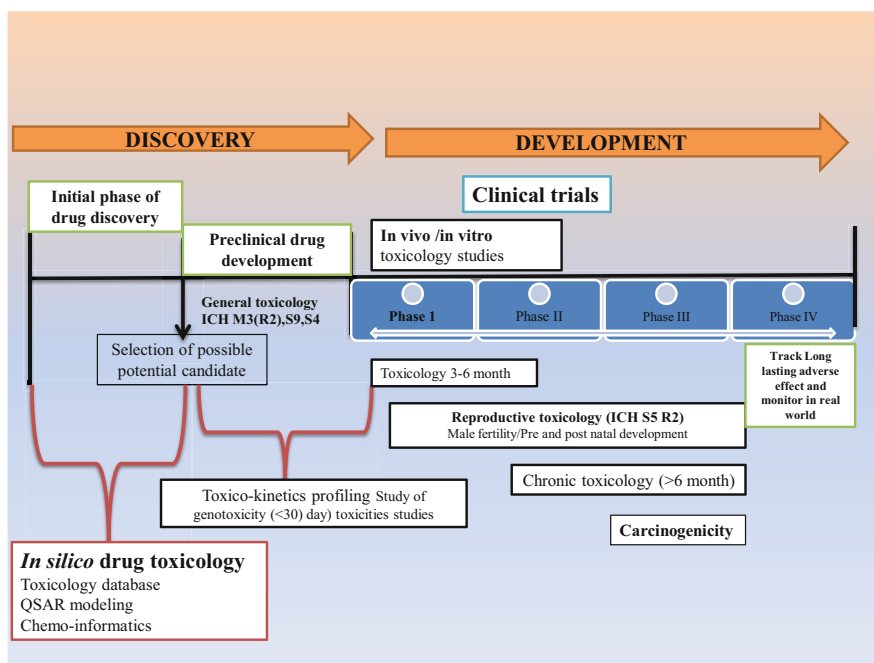
The European Union, the United States, and Japan tried to harmonize the regulatory guidelines for drug development (Bakke et al. 1995). The International Conference on Harmonization (ICH) developed a set of internationally agreed regulatory guidelines to aid global drug development. With studies undertaken in the United States, European Union, and Japan, this approach has been mainly effective. In each of the other regions, it is generally appropriate for submission. In each of the other regions, it is generally appropriate for submission. The Research and Development of Pharmaceutical products is a lengthy, difficult, and high-priced process and has yielded only around 10% of compounds that have entered phase 1 of the clinical trials.

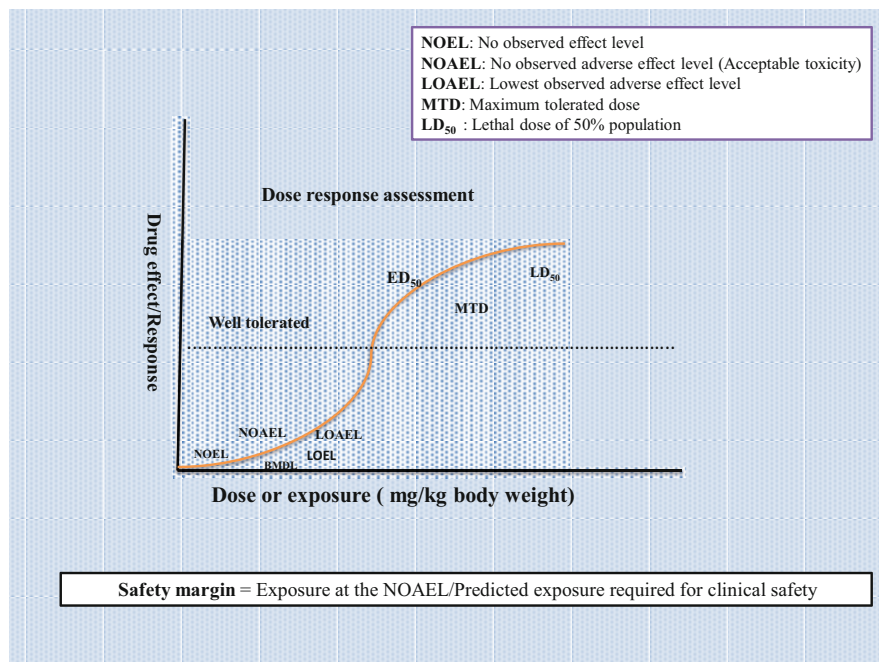
At the stage of discovery, failures are considerably more common, which leads to an increase in the cost of drug development in places where the medical needs are unmet, and also where the patients have limited access to medications with better safety and efficacy profiles (Baille et al. 2002). Increasing R & D spending has not translated into major gains in drug approvals during the last 30 years, resulting in the so-called pharmaceutical R & D productivity gap. A number of factors are responsible for increasing the productivity gap, and failure due to safety concerns is the most imperative among those factors (Centre for Medicines Research International 1998). The attrition related to nonclinical safety is less in oncology than in indications for which safety is a more important factor for success, for example, in the case of antiviral medicines or metabolic illnesses. Moreover, it is rare for a drug entity to fail because of a single cause. Thus, nonclinical toxicity is frequently employed as a fallback option.

Toxicological studies are being done according to the GLP-OECD principles. In an Investigational New Drug-enabling Good Laboratory Practice (GLP) toxicology study, given toxicity might be tolerated if seen with a secure anticipated margin of safety. The safety margin may be reduced to an undesirable amount in case of inaccurate prediction of human pharmacokinetics data; in that case, the termination will most likely be attributed to nonclinical toxicity, but in reality, it could be attributed to an inaccurate human PK prediction (Clewel and Andersen 1986).

In contrast, in phase I clinical investigation, a poor toxicological profile may limit the capacity to investigate the pharmacodynamic effects as well as in targeting engagement of an exploratory drug which could be classified as a failure of effectiveness or nonclinical toxicity. Liver and heart toxicity are two of the most common toxicities reported so far. The substances that target CNS will necessitate specific physicochemical properties, normally related to undesirable side effects like pharmacological promiscuity, whereas drugs acting on kidneys will necessitate relatively diverse physicochemical properties (Choudary et al. 1996).

This is mostly due to the fact that only some of the data points could be effectively understood in seclusion without considering additional contextual factors. Others have suggested that focusing on “what will not fail” is a superior strategy. Rather than using findings from these assays as a decision criterion for discontinuing drugs, these data are more likely to be utilized as “alerts” to affect a project’s overall nonclinical safety testing strategy, to put it another way. This chapter explained the role of toxicology studies in pharmaceutical product development, starting from the basics of toxicology to the regulatory requirements of toxicological studies in pharmaceutical product development.





7.2 Basic Principles of Toxicity Studies

Good Laboratory Practices (GLP) should be followed for toxicity studies. It means that toxicity testing should be done by qualified and trained personnel using standardized instruments and equipment. Moreover, all the experimental protocols should be performed per the preformulated SOPs (Standard Operating Procedures) duly verified by the authorized person. All the test substances/systems (in vitro as well as in vivo) should be accurately standardized. Furthermore, all the documentation, which includes the SOPs, raw files, histopathological slides, final reports as well as the tissue paraffin blocks, are to be archived and preserved for at least 5 years post-marketing of the drug.

7.3 Role of Preclinical Toxicity Animal Models in Drug Development

An experimental model should be selected such as to predict human toxicity for the assessment of an appropriate safety profile of a drug. To this purpose, one of the toxicology's core assumptions is the resemblance of the other rodents or non-human primates with the disease consequences in humans (Cavagnaro 1997). The toxicity

or side effect profile of a drug can be determined by considering the following factors:

1. The difference between the effect of control and the test should not be missed.
2. Differentiation between a treatment's non-unfavorable and adverse effects.

This method is consistent with the first ICH conference's view in which the unfavorable adverse effect produces risk to human health, and its consequences should be assessed appropriately.

To facilitate clinical trials, the ICH has employed significant decisions to remove vast disparities in the regulation of toxicity studies, e.g., duration, dose, species, etc. It is feasible to talk to regulators about the length of toxicological studies and, depending on the specifics of the test material, change these suggestions.

7.4 In-vivo Models

Since we have diminutive knowledge about the broad and complicated interactions across a variety of in-vitro systems, in vivo models are still have been considered the gold standard during toxicological studies. Selection of the proper species is crucial, as stated below, and depends upon the following factors:

- Studies comparing the metabolism of humans with animals will further help in studying the metabolic effects.
- The drug's sensitivity to a particular species, tissue, or organs
- Access to a sufficient historical control database
- Accessibility to the appropriate animal models from trustworthy sources.
- The facility's and staff's ability to offer proper animal care and maintenance

7.5 Different Animal Models in Toxicological Studies

1. Rodent (mouse, rat); non-rodent (monkey, dog)
Among rodents, rats and among non-rodents, dogs are generally preferred in toxicity studies as they have a very close resemblance to humans.
2. Ocular irritation: The ocular studies can easily be carried out in Rabbits
3. Dermal toxicity/irritation: Even dermal toxicity studies can also be carried out in rabbits. Moreover, the rats were also found to be a suitable model for dermal toxicities.
4. Dermal sensitization: Guinea pig
5. Phototoxicity: Among rodents, Guinea pigs and mice were commonly used to study the phototoxicity of the drugs.
6. Immunotoxicity: The mouse is considered to be an appropriate model for immunotoxicity studies. However, rats can also be used.
7. Developmental toxicity: Rodent (rat); non-rodent (rabbit)

8. Carcinogenicity: These studies are usually done in rodents like rat and mouse
9. Environmental toxicity: The studies employing environmental toxicity are typically carried out in lower organisms like rainbow trout, earthworm, *Daphnia*, etc.

Despite the rising usage of medications, significant human toxicity is still uncommon, demonstrating the validity of nonclinical safety testing. The concordance of medication toxicity in people and animals was assessed in a current assessment undertaken by the International Life Sciences Institute. For human toxicity, the true positive concordance rate was 71%. Erstwhile, at least one animal species with the same organ system predicted 71% of human target organ toxicities. The non-rodent (mainly dog) demonstrated almost 21% of the toxicity profile in humans, and rats predict around 7% of the human toxicities among rodents.

The majority of the significant discrepancies between the species are primarily due to their diverse biological systems, like changes in metabolic pathways and immunological responses. Moreover, a difference in animal and human exposure to nonclinical trials is also evident as per the following points:

1. The difference in the selection of doses (high) in animals results in a misrepresentation of the actual doses used in humans. It thus makes them inappropriate for use as a model in predicting safety in humans.
2. It is difficult to envisage the idiosyncratic reactions due to their poorly definable mechanism and rare occurrence. Moreover, it is not possible to study the relationship between dose and response in idiosyncratic reactions.
3. Presently, it is emphasized to conduct research on drugs specifically used in humans.

The choice of a suitable toxicity model is complicated by therapeutic goals. Human safety evaluation is by necessity conservative, assuming that animal toxicity is pertinent to humans unless demonstrated differently and that humans considered to be very can be more perceptive than other species examined for risk assessment purposes.

7.6 In-vitro Models

The increasing demand for quick screening assays with low cost and concern with the overuse of animals for research studies have led to the emergence of in vitro modeling techniques as an alternative to animal studies in the toxicological evaluation process (Bass and Scheibner 1987). These models also provide a method for the adverse properties to be determined at an initial stage in the process of drug discovery.

Alternative models provide the benefits of requiring tiny amounts of medicine, lower costs, and faster development times, all of which help speed up the drug research and development process. Furthermore, the number of *in vitro* systems has been established as unique instruments for probing and understanding distinct toxicity processes. In humans and animals, the final expression of toxicity is usually the result of a complex and broad set of cellular and biochemical interactions.

The *in vitro* models are well-defined and simple. These approaches allow for selective isolation as well as to evaluate a response which allows in selectively isolating and evaluating the drug response as well as helps in assistance in the mechanism of action of the drugs. From isolated organs to subatomic preparations, *in vitro* systems vary in structural and physiological complexity. For determining the applicability of the results to humans, a full understanding of the strengths and shortcomings of a specific model is essential.

Because of concerns about the brutal characteristics of the standard *in vivo* Draize test, more advanced ocular toxicity systems have been established. In most situations, rather than a single *in vitro* test, the combined data from a battery of assays are employed to afford the credence of evidence required to characterize toxicity. At last, all the information regarding the relative metabolism of the substance in humans and experimental animals usually used in toxicity assessment has been obtained using *in vitro* procedures.

Different *in-vitro* Models

1. Isolated, perfused organs
2. Tissue slices
3. Cells
4. Primary cell culture
5. Cultured cell lines
6. Subcellular preparation

7.7 Types of (Systemic) Toxicity Studies: Acute, Subchronic, and Chronic Toxicology

Acute toxicity testing usually consists of single-dose studies with a 14-days observation period, while subchronic toxicology testing consists of multiple-dose studies that span anywhere from 2 weeks to 6 months. Multiple-dose studies lasting 6 months are used in chronic toxicity.

Acute toxicity studies: It refers to studies in which single administration or several administrations within 24-h period. These are some of the key characteristics of these studies:

Animal species	2 rodent species (mice and rats)
No. of animals	5 animals of either sex/group
Route of administration	Identical to humans
Oral dose selection	Limit of 2 g/kg or 10× the normal dose

(continued)

Animal species	2 rodent species (mice and rats)
Treatment	Single bolus or several doses or continuous infusion within 24 h
Observation period	14 days after drug administration
Parameters to be observed	Effect on body weight, gross pathological changes, mortality (parenteral—Up to 7 days, oral—Up to 14 days)
Establish	MLD, MTD, LD50, LD10

Subchronic/subacute/Chronic toxicity studies: It refers to repeated administrations, daily or 5 times per week over a period of 10% of the life span, i. e., 3 months in rats, 1–2 years in dogs.

The procedures involved in these two types are very similar except for their duration. The following characteristics are involved:

Animal	At least two mammalian species, 1—rodent, 1—non-rodent.
Duration of treatment	14-, 28–90-, 180-days toxicity studies. Duration of the study depends on therapeutic indication.
Animal grouping	Group 1—Control group; group 2—Treatment group
Route of administration	The route intended for clinical use
Dose levels	Three graded dose levels

The dose selection criterion is as follows: The maximum dose must produce observable toxicity. Further, the intermediate dose was selected so that it may cause few symptoms but should not cause gross toxicity or death. The lowest dose should not cause observable toxicity.

Dose-ranging study: It is used for the detection of the target organ of toxicity and determination of maximum tolerated dose for successive studies.

Rodents	
No. of animals	5 animals/sex/group
Dose levels	At least 4 graded doses, including control
Duration of treatment	Exposure of animals to test subs daily for 10 consecutive days
Highest dose	MTD of single-dose study
Observation	Intoxication signs (body wt, laboratory parameter) Viscera and microscopic examination of the affected organ

The following criterion is also followed for the dose-ranging studies:

For the non-rodents: For the ascending MTD study phase, one male or female is taken. Following the preliminary parameters recording, the dosing is started. The initial dose chosen is three to five times that of the MTD or the effective dose. Further, the dose is increased every third day of the sample withdrawal from the animals. It is recommended to lower the dose in case of any observed toxicity signs. The test substance should be administered continually for about 10 days at tolerable dose limits, followed by sample collection for the laboratory parameters. The final step includes sacrificing the animals, autopsy of the tissues, and their microscopic examination.

7.8 Fourteen to Twenty-Eight Day Repeated-Dose Toxicity Studies

For these studies, 6–10 rodents or 2–3 non-rodents of either sex/group are taken. Three dose levels are included ranging from highest being the dose with observable toxicity to medium to least being the lowest dose are administered by the intended route. The parameters to be taken into account include bodyweight measurements, intake of water and food, biochemistry profile, hematological parameter recording as well as microscopic evaluation of the tissues and visceral organs.

7.9 Ninety-Day Repeated-Dose Toxicity Studies

In these studies, 15–30 rodents or 4–6 non-rodents of either sex per group are administered a grading of three dose levels. A “high-dose-reversal” group along with its subsequent control group is included in the study. The parameters to be noted include regular body weight measurement, account of the food and water intake, biochemistry and hematological screening, analysis of urine output, measuring weights of different organs, microscopic evaluation of tissues as well as checking the general signs of intoxication such as any changes in the appearance, behavior or activity of the animal.

7.10 180-Day Repeated-Dose Toxicity Studies

Fifteen to thirty rodents and 4–6 non-rodents per sex per group should be included with at least four groups with control. The dosing is done as per three graded levels by the intended route of administration. The parameters that are included are measurements of body weight and food intake, biochemistry and hematological parameters, microscopic examination of tissues, and signs of intoxication.

Male fertility study: It includes one rodent species (rat preferred) with six males per group. The dose should be selected from the 14–28 day toxicity studies. There should be three dose groups to be included with the highest dose that shows minimum toxicity during systemic studies. Additionally, one control group should also be included. Prior to mating/pairing, the treatment should be administered for a minimum of 28 days to a maximum of 70 days. The drug should be continued to the male animals even after pairing. The male and female animals should be separated either after 10 days of pairing or after the presence of a vaginal plug. Following 13 days of gestation, the pregnant females should be evaluated for the fertility index. Finally, the male animals are sacrificed, and the testis, as well as epididymis weights, should be noted. Also, the proper evaluation of the motility of the sperms should be done as well as the histological examination of these organs should be carried out.

7.11 Female Reproduction and Developmental Toxicity Studies

Female reproductive studies are required for the drugs indicated for women of childbearing age. It is categorized or divided into three segments

- Segment I—Female Fertility Study
- Segment II—Teratogenicity Study
- Segment III—Perinatal Study

7.11.1 Segment I—Female Fertility Study

These studies include one rodent species, preferably a rat. Here, the drug is administered (as per the intended route in humans) to both sexes with 15 animals per sex per group. The drug administration should be initiated approximately 28 days (males) or 14 days (females) before mating, and the treatment is continued during the time of mating as well as during the gestation phase (till the day of weaning). The drug treatment should be given in three graded doses, with the highest dose being the MTD. The parameters to be observed include regular body weight measurement, food/water intake, mating behaviors, any intoxication signs, the progress and length of gestation periods, the histological evaluation of the samples, and the health of the animals in the postnatal Phase.

7.11.2 Segment II—Teratogenicity Study

One rodent species, preferably rats or non-rodent species such as rabbit, is included with 20 pregnant rats/mice or 12 rabbits/group on each dose level. The drug treatment is given on three dose levels and is continued during the period of organogenesis. The route of drug administration is similar to that intended for therapeutic use, and dose levels are selected as per the segment 1 selection criterion. The highest dose selected should be the least toxic to the mother, while the lowest dose should be proportional to or a multiple of the dose intended for humans. The parameters to be observed for dams include measurement of body weights, food/water intake, any signs of intoxication, microscopic evaluation of the ovary, uterus, and its contents, calculating the number of implantation sites, corpora lutea numbers, number of resorptions. In addition to these, the observations to be made for the fetuses include checking the total number of fetuses, their gender, weight, body length, as well as evaluation of any skeletal, visceral abnormalities in the fetus.

7.11.3 Segment III: Perinatal Study

These studies should be included for the drugs that are indicated for pregnant or nursing women for a long duration or in case of any possibility of adverse effects on the fetus. It includes one rodent species (rat preferred) with four groups, each containing 15 dams/group. The dose levels of a drug should be selected in the multiples of the intended human dose. The administration of the drug should be continued through the last trimester (from gestation day 15). Finally, the dose which is selected should cause the lowest fetal loss, which is to be continued till the lactation as well as the weaning Phase. Ultimately, the dams are sacrificed, and the body weight, food/water intake, signs of intoxication, the progress of the gestation phase, and the histology of the affected organs is observed in the dams.

Further, a total of 15 males/females in each group, i.e., one male/female from each litter of F1 generation, is selected. These are then administered test drug or vehicle as per the above dose selection criteria all through the growth to sexual maturity, mating, gestation, and lactation phase. Following this, the performance in mating and fertility of the F1 generation is evaluated. Finally, the dams are sacrificed, and body weight, food/water intake, signs of intoxication, the progress of the gestation phase, and the histology of the affected organs are observed in the F2 generation.

7.12 Special Toxicities Studies

7.12.1 Local Toxicity

Evaluation of the local toxicity is considered necessary when new drug treatment is supposed to be used by special route of administration such as vaginal membrane and skin for determination of focal effect. These studies include two species with an increase in the group size with increased treatment duration. It includes three dosage levels and the untreated and/or vehicle-treated group. Local toxicity includes dermal, vaginal, rectal, and ocular toxicity studies.

7.12.2 Dermal Toxicity Study

Rat and rabbits were used for the assessment of dermal toxicity studies. More than three different concentrations should be used for the clinical dosage form studies. Material that is used for dermal toxicity should cover at least 10% of the total body surface area and should be applied on the hairless or shaved area of skin. The duration of application could vary from 7 to a maximum of 90 days based on the intended clinical use duration. In case some initial irritation to the skin is visible, there should be an inclusion of a repeated-dose group. The endpoints to be observed

include the appearance of any local edema or erythema along with the histological evaluation.

7.12.3 Photo-Allergy or Dermal Phototoxicity

These studies are required when a drug or its metabolite substance shows photosensitivity or the nature of its action indicates such potential. For example, drugs or agents that are used in leucoderma treatment. This study includes a pretest and the main test. In the pretest, a minimum of eight animals are screened for four concentrations and without UV exposure and application for up to 2 h, and the results can be recorded between 24 and 48 h.

In the main test, a minimum of 10 test animals and 5 controls are induced with the pretest dose for about 2 h, followed by UV exposure of 10 J/cm^2 . Further, between days 20 and 24, the animals are challenged with an equal concentration of test substance for approximately 2 h and observed for the formation of edema or erythema.

7.12.4 Vaginal Toxicity Test

These toxicity studies are performed in the rat or dog species with a minimum of 6–10 animals per group. Testing material should be applied topically over the vaginal mucosa as a cream, ointment, or pessary for 7–30 days. The observation parameters for vaginal toxicity include swelling, histopathological evaluation of the wall of the vagina, and introitus closure.

7.12.5 Rectal Tolerance Test

For the rectal toxicity test, the most preferred species include rabbits or dogs with 6–10 animals/group. The drug formulation should be applied many times daily to achieve a daily human dose. The extent of the application includes 7–30 days. The parameters that are observed in the rectal tolerance test include the presence of blood/mucus in the feces, checking the anal sphincter condition, and histological evaluation of the mucous membrane of the rectum.

7.12.6 Ocular Toxicity Studies

Ocular toxicities include the study of products that are meant for ocular implantation. The study should be performed on two species, with one being the albino rabbit (as it

has a large conjunctival sac). The formulation used in the ocular studies includes ointment, gels, and contact lenses. The duration of the study can be varied depending on the clinical duration of exposure with a maximum limit of 90 days. The parameters to be observed include changes in the intraocular pressure, slit lamp examination for detecting any changes in the iris, cornea, or aqueous humor, and histological evaluation.

7.12.7 Inhalation Toxicity Studies

For inhalation toxicity studies, one rodent, as well as another non-rodent species, are required with three dosage groups and one control group. For this study, gases and vapors must be applied on the entire body and aerosols have been given by nasal route only. The exposure time and concentration should be adjusted (5 mg/day), and duration may vary up to 6 h each day and 5 days per week. The temperature and humidity conditions, as well as the exposure flow rate, should be observed and recorded. The particle size of the formulation should be around 4 microns for aerosols. The parameters observed were respiratory rate evaluation, bronchial lavage, and histological examination, along with the normal observations of the systemic toxicity studies.

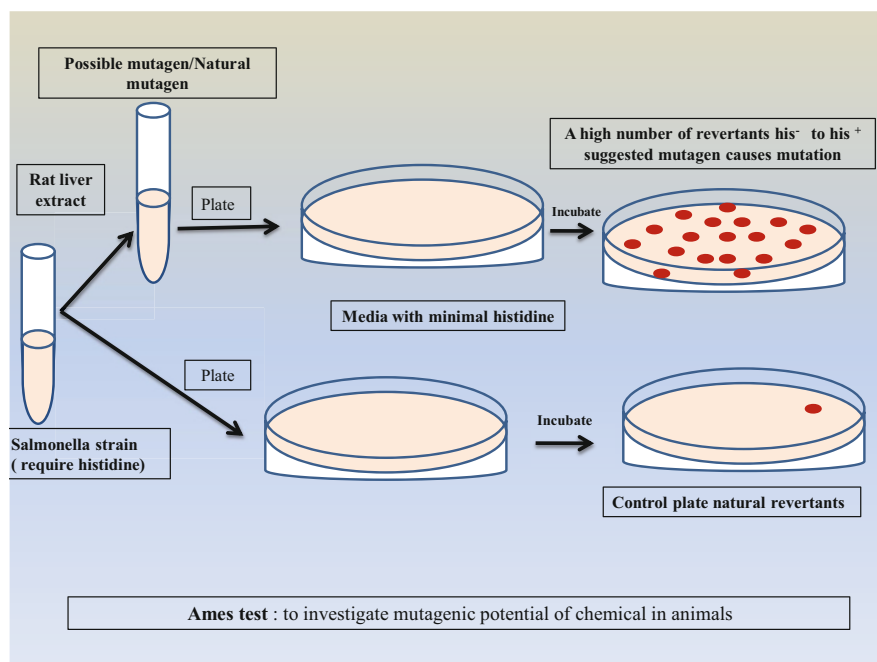
7.12.8 Allergenicity/Hypersensitivity

For the allergenicity and hypersensitivity studies, the standard tests are performed on two animal species, preferably guinea pig and mouse. The guinea pig maximization test involves two steps. The first step is the determination of maximum and minimum nonirritant doses performed for at least four doses which are tested by identical route of administration in a group of four males and females. The minimal dose that causes irritation is used for induction. The second step, which includes the main test, includes at least 6 male/female animals in each group. This test uses one control and one test group. The intradermal induction, which is performed on day 1, is accompanied by a topical challenge on day 21. In case of no response, a rechallenge is done from day 7 to 30 following the main challenge. The parameters observed include any presence of edema or erythema.

Further, in the case of local lymph node studies or assays, mice of either sex should be used with 6 mice per group. The test materials are to be applied on the skin of the ear in three graded doses on 3 consecutive days, and on the fifth day, the dissection of the draining auricular lymph nodes could be done 5 h following the intravenous administration of H-thymidine.

7.12.9 Genotoxicity Studies

Both types of studies, i.e., in vitro and in vivo, are performed for detecting the compounds that cause direct or indirect genetic deformity (Bolon 2004). Ames test has been widely used for genotoxicity studies. The most common strains of bacterium used for this test include *Salmonella typhimurium*—TA98, TA100, TA102, TA1535, TA97; *Escherichia coli*—WP2 *uvrA*, WP2 *uvrA* (pKM101). These strains show an auxotrophic effect because they require histidine for growth and cannot produce it. This test is used to check the ability of the tested substance to create mutations which results in a reversal of the prototrophic state that helps the cells to nurture on a histidine-free media. Further, the solvent/vehicle and positive control (Sodium azide or mitomycin C) should be used in these types of toxicity studies. The sign of positivity of this test is indicated by the raised number of revertants, increase in the number of aberrations in metaphase chromosomes or an increase in the number of micronuclei in polychromatic erythrocytes.



7.12.10 Carcinogenicity Studies

These types of studies are performed for all the medications that are predicted to be used clinically for more than 6 months, where the computation studies showed carcinogenicity risk, and where the repeated-dose toxicity studies show evidence of preneoplastic lesions (Ashton et al. 1999). The most commonly used species for

carcinogenicity studies are rodents, preferably rats, and should have a lower incidence or chance of spontaneous type tumors. At least three different doses should be used for the carcinogenicity studies. In this, the highest is the sublethal dose, i.e., the dose does not reduce the animal lifespan by more than 10% of the expected normal, intermediate dose includes the dose between the highest and the lowest dose and the lowest dose is selected as per the intended human therapeutic dose. The duration of dosing for these studies is nearly 24 months for rats and about 18 months for mice. The observation is based on autopsy, biopsy, and detailed macroscopic and microscopic histopathology of affected organ and tissue.

The nonclinical toxicity testing and safety evaluation data of an investigational new drug are required to perform various phases of clinical trials.

For Phase I Clinical Trials: It provides the data for the systemic type toxicities studies, male fertility studies, genotoxicity and local toxicities studies, hypersensitivity, and phototoxicity test.

For Phase II Clinical Trials: It includes providing all nonclinical safety data summaries submitted for the permission of Phase I clinical trials. For conduction of Phase II directly, nonclinical safety data obtained for the permission of Phase I trial needs to be submitted. It also includes repeated-dose and in vivo genotoxicity as well as reproductive and developmental toxicities studies.

For Phase III Clinical Trials: Nonclinical safety data is required for this Phase which was already submitted for obtaining permission for the initial phases of conducting clinical trials (Phase I and II). This Phase must be required reproductive and carcinogenicity studies.

For Phase IV Clinical Trials: In this Phase of a clinical trial, all Phase of data related to nonclinical safety is required in the case of starting Phase IV. Long-term adverse effect needs to be monitored in this Phase.

References

- Ashton GA, Griffiths SA, McAuslane JAN (1999) Industry experience with alternative models for the carcinogenicity testing of pharmaceuticals. Centre for Medicines Research International, Surrey, U.K.
- Baille TA, Cayen MN, Fouda H, Gerson RJ, Green JD, Grossman SJ, Klunk LJ, LeBlanc B, Perkins DG, Shipley LA (2002) Drug metabolites in safety testing. *Toxicol Appl Pharmacol* 182:188–196
- Bakke OM, Manocchia MA, deAbajo F, Kaitin KI, Lasagna L (1995) Drug safety discontinuations in the United Kingdom, the United States, and Spain from 1974 through 1993: a regulatory perspective. *Clin Pharmacol Ther* 58:108–117
- Bass R, Scheibner E (1987) Toxicological evaluation of biotechnology products: a regulatory viewpoint. *Arch Toxicol Suppl* 11:182–190
- Beary JF III (1997) The drug development and approval process. In *New drug approvals in 1997*. Pharmaceutical Research and Manufacturers of America, Washington, DC
- Bolon B (2004) Genetically engineered animals in drug discovery and development: a maturing resource for toxicologic research. *Basic Clin Pharmacol Toxicol* 95:154–161
- Bucher JR, Portier CJ, Goodman JI, Faustman EM, Lucier GW (1996) National Toxicology program studies: principles of dose selection and applications to mechanistic based risk assessment. *Fundam Appl Toxicol* 31:1–8

- Calabrese EJ, Baldwin LA (1994) Improved method for selection of the NOAEL. *Regul Toxicol Pharmacol* 19:48–50
- Cavagnaro JA (1997) Considerations in the preclinical safety evaluation of biotechnology derived products. In: Sipes IG, McQueen CA, Gandolphi J (eds) *Comprehensive toxicology*, vol 2: toxicological testing and evaluation. Elsevier Science Publishing, New York, pp 291–298
- Centre for Medicines Research International (1998) Safety evaluation of biotechnology-derived pharmaceutical: facilitating a scientific approach. In: Griffiths SA, Lumley CE (eds) *CHMP*. 2004. Position paper on nonclinical safety studies to support clinical trials with a single microdose. 23 June. CPMP/SWP/2599/02Rev1. Kluwer Academic Publishers, London
- Choudary J, Contrera JF, DeFelice A, DeGeorge JJ, Farrelly JG, Fitzgerald G, Goheer MA, Jacobs A, Jordan A, Meyers L, Osterberg R, Resnick C, Sun CJ, Temple RJ (1996) Response to Monro and Mehtaproposal for use of single-dose toxicology studies to support single-dose studies of new drugs in humans. *Clin Pharmacol Ther* 59:265–267
- Clewell HJ, Andersen ME (1986) Dose, species, and route extrapolation using physiologically based pharmacokinetic models. In *Pharmacokinetics in risk assessment, drinking*



Suradeep Basak, Joseph Lewis, Sudershan Rao Vemula,
and Prathapkumar Shetty Halady

8.1 Introduction

Food safety risk analysis is of paramount importance for assessing and managing the risks linked with hazards in food items (FAO/WHO 1995). This methodology has picked up its pace over a period of time as end-product testing of food items is time-consuming, and approaches are invasive to the sample tested; also, large sample sizes are needed to represent the batch of the food and also to ensure that the lot is not contaminated beyond the permissible limits or complying appropriate level of protection of consumers (FAO/WHO 1997). Food safety risk management involves consideration of process, control alternatives, scientific evidence of risks, and accordingly choosing and enforcing public food safety measurements by the government (National and International standard-setting bodies) in association with interested stakeholders (FAO/WHO 2006). Risk analysis is broadly identified as a key methodology to lay down the framework of food safety standards. According to FAO/WHO (1995) consultation report, risk analysis is composed of three integral components, namely risk assessment, risk management, and risk communication. Risk assessment is a science-based evaluation of the potential of hazards to cause foodborne illness through cumulative steps such as hazard identification, hazard

S. Basak

Department of Food Science and Technology, Pondicherry University, Pondicherry, India

Department of Biotechnology, Chandigarh University, Mohali, Punjab, India

J. Lewis

National Institute of Nutrition-ICMR, Hyderabad, India

S. R. Vemula

Regulatory Affairs, PFNDAI, Mumbai, India

P. S. Halady (✉)

Department of Food Science and Technology, Pondicherry University, Pondicherry, India

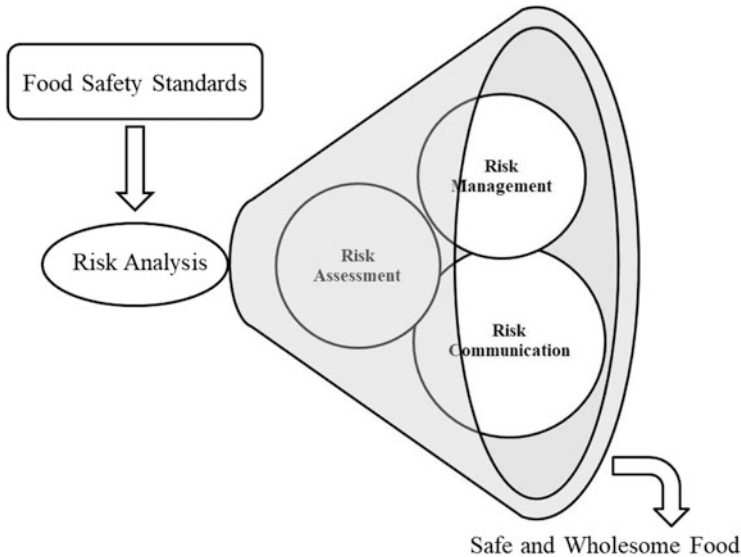


Fig. 8.1 Transformation of food safety standards into safe and wholesome food

characterization, exposure assessment, and risk characterization. The definition of risk management defined by Codex Alimentarius Commission (CAC) suggested the adoption of appropriate measures to minimize or reduce the evaluated or assessed risks in food items (FAO 1999) (Fig. 8.1).

Risk communication involves the creation of awareness about the risks in the food items through interactive sessions among risk assessor, risk manager, and other interested stakeholders. Key international scientific advisory bodies that maintain standards advisory bodies are Food and Agriculture Organization (FAO)/World Health Organization (WHO) joint expert committees on Food additives and joint meeting on pesticide residues, United States Environmental Protection Agency, United States Food and Drug Administration, European Food Safety Authority, European Medicines Agency, European Chemicals Agency within the Registration, Evaluation, Authorisation and Restriction of Chemicals directives, Food Safety Commission of Japan to name a few (EFSA 2014). Codex Alimentarius Commission (CAC) is the international body that defines risk assessment principles and practices for all foodborne hazards and also directs the application of codex standards through risk analysis principles (FAO 1999). Likewise, the Food Safety and Standards Authority of India has formed a risk assessment cell in their framework under sections 10, 16 (1) (i) (c) and 18 (1) (2) (b) (c) and its prime objectives are as follows (FSSAI 2021). As shown in Fig. 8.2, Risk assessment is broadly divided into four categories, namely hazard identification, exposure assessment, dose-response assessment, and risk characterization (NRC 1983).

Under the risk-based framework, a food safety management system is the basis for placing safe and wholesome foods on the market. At the basic level, prerequisite

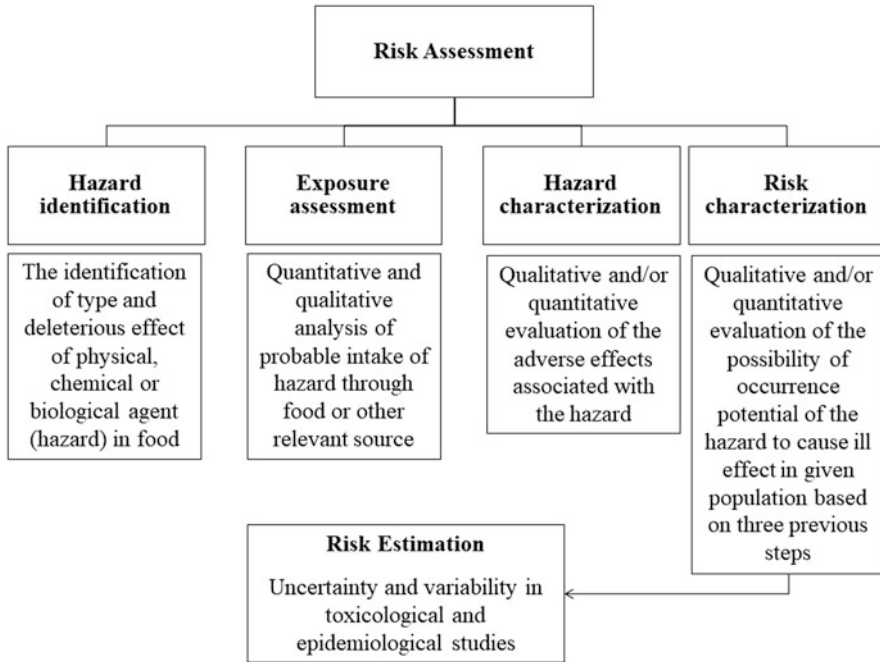


Fig. 8.2 Risk assessment framework (Lammerding and Fazil 2000)

programs, namely good agricultural practices (GAP), good manufacturing practices (GMP), and good hygienic practices (GHP), should be in place prior to moving upwards with hazard analysis critical control points (HACCP). Several trivial or unlikely hazards present in the food can lead to product failures through unverified processes; therefore, correct essential identification of control points (CCP) is necessary so that their limits can be specified and appropriate corrective measures are taken in order to optimize the HACCP system (Gaze et al. 2002).

8.1.1 Chemical Risk Assessment

The objective of chemical risk assessment is to quantify and qualify exposure of chemicals from pertinent sources, namely water, food, skin, inhalation in a said population (exposure assessment), followed by determination of the permissible limit of the hazard (hazard identification and hazard characterization) and finally quantification of risk linked with such exposure (risk characterization) (Ingenbleek et al. 2021). Toxic chemicals causing adverse effects on human health are intended and unintended contaminants, such as pesticides, biocides, food additives, organic pollutants, heavy metals, dioxins, perfluoroalkyl substances, and brominated flame retardants mycotoxin, ciguatoxin (Dorne and Fink-Gremmels 2013).

The procedure of risk assessment requires a fair amount of toxicological and epidemiological data obtained using internationally accepted standard protocols. Hazard identification and characterization of chemical toxicity involve toxicokinetics which is the response of the human body towards the toxic chemical, toxicodynamics which is better understood by the toxic effect of the chemical in the human body, and, finally, the determination of safety levels of the exposure of untoward chemicals (Dorne and Fink-Gremmels 2013). Risk assessment commences with a clear and precise term of reference, problem statement. Thereafter, it moves to the accumulation of scientific evidence, technical clarity, associated uncertainties, followed by evaluation and interpretation of the applicable data using suitable mathematical models. The outcome of problem formulation includes a questionnaire regarding the problems identified and the time required to address the problems (Hardy et al. 2017).

Risk assessors follow tiered approaches to produce fit-for-purpose risk assessments depending on the time and resources. The low-tier approach is followed under limited time and resources, whereas high-tier approaches are involved under the situation when available data is vast for better estimation of uncertainties using probabilistic approaches including Bayesian methods (Meek et al. 2011; Hardy et al. 2015; More et al. 2019). The occurrence of uncertainty and variability in the raw data should also be considered so as to have a quantitative and qualitative variance of the risk estimates (FAO/WHO 1995). The assessment is based on real-time exposure scenario that includes various extreme situations, like people belonging to susceptible and high-risk population group, minority opinions, etc., and the conclusion is presented to risk managers and other risk assessors so as to review their assessment.

8.1.1.1 Exposure to Toxic Substances Ingested Through Food

Exposure assessment deals with the amount of the toxic chemical a person is exposed to by ingestion of all foods consumed in a diet containing the toxic chemical. The dietary exposure to such toxic chemicals depends on the dose of the chemical in food, daily intake of the same through diet and body weight, which is calculated using the following equation:

$$E_i = \sum_{k=1}^n \frac{C_{i,k} \times L_k}{W_i} \quad (8.1)$$

where E_i is the daily dietary exposure normalized by consumption units; $C_{i,k}$ is the daily dietary intake; L_k is the concentration of the toxic chemical in food; W_i is body weight

Two distinct strategies for chemical risk assessment in foods are followed to collect occurrence data. According to Official Controls Regulation 2017/625/EC, the first strategy relies on data from food control systems, i.e., nationwide food surveillance and monitoring programs collected, collated, and analyzed at regular intervals to keep a check on specific compliance requirements of the contaminant and its level in foods consumed by the population (Dorne et al. 2009; European Commission

2017). The second strategy involves total diet study (TDS), which is an alternate approach where foods belonging to the staple diet of the region are selected based on food consumption data and subsequently pooled for analysis (EFSA, FAO, and WHO 2011; EFSA 2011). To analyze the contaminants in food samples up to trace level of parts per billion (ng/g) or parts per trillion (pg/g) using selective, sensitive, and robust analytical techniques are employed. These analytical techniques include sample preparation followed by quantification using various chromatographic techniques coupled with or without spectrometry, namely gas-chromatography, liquid chromatography, and mass-spectrometry (Ridgway et al. 2007; Farré et al. 2014; Pico et al. 2020). According to the international recommendation by EFSA, FAO, and WHO (2011), robust occurrence data is generated only when the analytical method used to quantify contaminants are fit-for-purpose, validated properly, and have been submitted to proficiency testing. Additionally, they have used certified reference material while testing (Van Leeuwen et al. 2006). Validation of testing method is adjudged by the parameters, namely the limit of detection, the limit of quantification, precision, accuracy, and recovery.

Exposure assessment through food consumption is estimated based on any of the following strategies: food balance sheet, food consumption data from household budget surveys, and individual quantitative food consumption data. The food balance sheet of any country is about statistical estimates of food available for consumption based on total food production added with total imports, less exported food commodities, which are readily available on a global database (FAOSTAT 2021). However, a food balance sheet gives a broad perspective of food consumption of any nation irrespective of variation in food habits within a nation based on geographical locations and demography. It also does not provide insight into food consumption among population subgroups, such as infants, young children, and lactating or pregnant women (Ingenbleek et al. 2021).

Food consumption data collected from the food balance sheet should involve the use of male equivalent if gender and age of subjects are part of the surveys (Weissell and Dop 2012). Food consumption data can also be obtained indirectly by collecting data for food consumption of a different household in various clusters by conducting household budget surveys followed by converting food expenditure data collected for 15 days into food consumption data considering food price. This will certainly provide a perceptivity of food consumption, especially in countries having more number of people with low and medium-income groups (Ingenbleek et al. 2017). However, the disadvantage of a household budget survey to estimate food consumption is the unavailability of food consumption of each individual in a household, or in other words, we can say this strategy does not allow us to generate data on individual food consumption in a given household. Therefore, a direct approach to obtain individual food consumption data through repeated 24 h dietary recalls is applied. This method renders quantitative information on the diet of each and every individual in a household, including their gender and age (Osadchiy et al. 2020). As this method involve two nonconsecutive 24 h diet recalls, the sample size should be fairly large for robust data. Global and individual food consumption summary

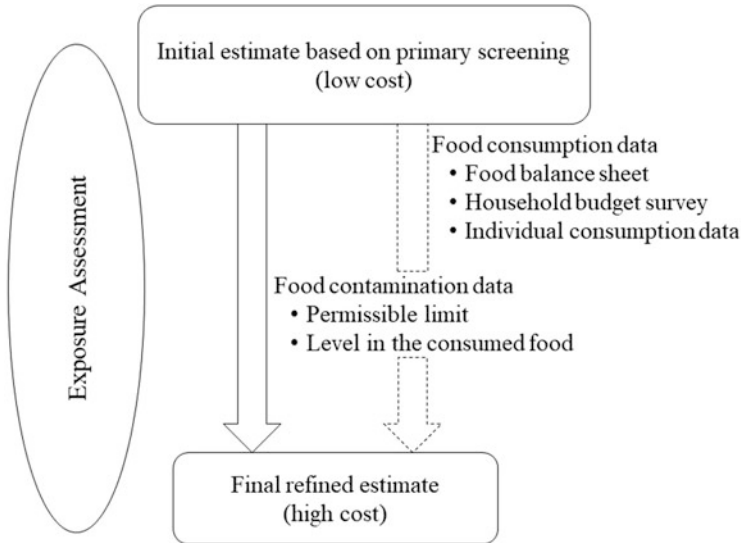


Fig. 8.3 Step-wise approach of dietary exposure assessment (FAO/WHO 2009)

statistics are open-access databases, available for use and reference (FAO/WHO 2021a; FAO/WHO 2021b).

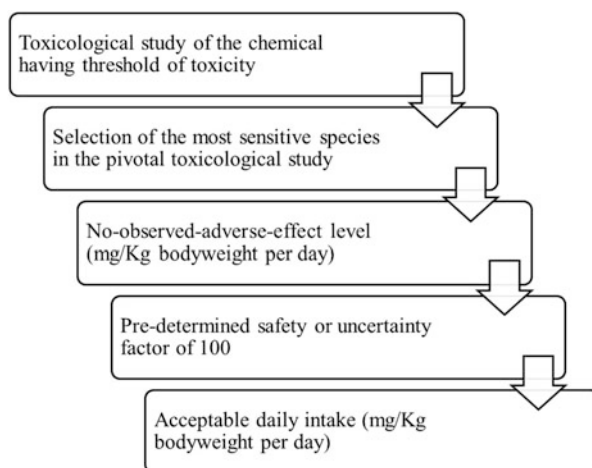
Dietary exposure assessments are therefore dependent on the availability of food consumption and contamination. Appropriate to the situation, exposure assessments can be probabilistic, where food consumption data and contaminant in that food are crossed, or it can be deterministic, where point estimation of the contaminant is performed from a given pooled sample (More et al. 2019). Finally, to implement TDS within a cluster or specific population, one should identify the core foods, collect food consumption data, pool the food samples as consumed to quantify contaminants, and calculate exposure assessment according to Eq. (8.1) (Ingenbleek et al. 2021). Figure 8.3 summarizes the stepwise approach of dietary exposure assessment as suggested by the institutional bodies, such as WHO and FAO (FAO/WHO 2009).

8.1.1.2 Identifying and Characterizing Hazards

Hazard identification should be as precise as possible in relation to the type and nature of the adverse effects arising from the presence of any chemical, physical, or biological agent with the potential to cause harm to the food for any given population or subpopulation. Precision in hazard identification will present the required outcomes to counter the effects arising from an outbreak or due to prolonged exposure to a particular hazard.

Hazard characterization is a qualitative and quantitative evaluation of adverse effects associated with the identified hazard. It involves an assessment of dose-response data (including uncertainties or variation) to provide risk managers with

Fig. 8.4 Steps to determine the acceptable daily intake of toxic chemicals in food items



information from toxicological and epidemiological considerations for setting permissible limits of chemical contaminants in foods (FAO/WHO 2009). The chronology of deleterious or adverse effect of contaminant commences with its exposure through foods followed by assimilation inside the body (toxicokinetic) then finally the appearance or manifestation of signs and symptoms specific to the dose (toxicodynamic).

According to the Joint FAO/WHO Expert Committee on Food Additives (JECFA), the constitution of acceptable daily intake (ADI) in hazard characterization ensures the daily dietary exposure estimate to the chemical (food additive, pesticides, or veterinary drugs) is below the acceptable limit. Also, to regulate the dietary intake of chemicals having a longer half-life (heavy metals, dioxins, etc.), the term tolerable dietary intake (TDI) is used as these chemicals do not have an immediate adverse effect on the human body upon consumption, but prolonged exposure and accumulation of the same will lead to deleterious effect (FAO/WHO 1987).

Tolerable intake expressed on a weekly basis is termed as provisional tolerable weekly intakes (PTWI) as an accumulation of the chemical can be limited over a period of time, and the assessment, which includes daily variation in the data, emphasize the significance of limiting the intake of such contaminants (Herrman and Younes 1999). While using this approach (Fig. 8.4), a safety (or uncertainty) factor of 100 is applied to consider an inter- and intra-species variation to no-observed-effect levels (NOELs) and no-observed-adverse-effect levels (NOAELs) to calculate ADI (Larsen 2006).

The event of chemical exposure to its biological response and progression can be studied either at a basic level, i.e., exposure to apical toxicity or up to an advanced level of knowledge, i.e., exposure to internal dose metabolism to its toxicity in the target organ resulting in cascade reactions leading to biological responses (Ingenbleek et al. 2021). These events have been validated in two frameworks by

WHO (2010) and other collaborative groups as a mode of action and adverse outcome pathway (AOP).

The mode of action (MoA) framework describes biologically possible key events (cytological and biochemical) that lead to the tangible effect of the contaminant supported by robust experimental and mechanistic data, i.e., both toxicokinetic and toxicodynamic data are considered; however, the toxic effect at molecular level is not included in the framework (Boobis et al. 2008; Culleres et al. 2008). This framework assists in decision-making regarding the relationship between dose and response, the relevance of apparent effect in the animal model to humans and uncertainty or variability of response within a population, including subpopulation with enhanced vulnerabilities (Guyton et al. 2008). Over the period of time, the MoA framework has accommodated the MoA analysis of genotoxic and non-genotoxic chemicals (Bertail et al. 2010). So far, various collaborative groups, namely International Programme on Chemical Safety, International Life Sciences Institute, and US Environmental Protection Agency, have developed the MoA framework for examining and applying MoA data in human health risk assessment of chemical contaminants.

Adverse outcome pathway is defined as a sequence of events starting from exposure of chemical contaminant to an individual or population through to a final toxic effect from both human health and environmental point of view. If an individual is concerned, then the pattern and cascade of events leading to the adverse effect of the contaminant will be considered as a human health concern, whereas the same will be an environmental concern if a population or subpopulation is affected by exposure to the chemical substances through food items (Ankley et al. 2010; Ankley and Edwards 2018). The feature of AOP is described by a molecular initiating event and a series of intermediate key events, which results in deleterious effects of the contaminants. Also, AOP mostly deals with the toxicodynamics study than the kinetic study of toxic chemicals upon exposure, but with the aggregate exposure pathway framework, toxicokinetic study can also be integrated into the AOP framework (Teeguarden et al. 2016; Price et al. 2020).

Risk characterization is the penultimate stage of risk assessment where comparison is made between exposure and nature of the hazard so as to estimate (qualitative as well quantitative) the possibility of occurrence and seriousness of any known or potential outbreak of any health issue in a given population based on initial steps of risk assessment, i.e., hazard identification, characterization, and exposure assessment (Ingenbleek et al. 2021). Acceptable daily intake or tolerable daily intake of chemicals presumed to have thresholds of toxicity are compared with the human exposure to the hazard and estimated using previously mentioned tiered approaches to infer the health risks associated with the chemical. Exposure assessment of such chemicals provides a toxicological profile of the chemical for setting up acceptable limits of the same in the different foods so that any deviation in the predefined level can be characterized using a probabilistic approach. Therefore, based on ADI/TDI level, safety metrics of any population or subpopulation can be determined; however, it is acceptable to have level of exposure that exceeds ADI/TDI occasionally because the ADI/TDI calculation includes safety or uncertainty factors (Dorne and

Fink-Gremmels 2013). The margin of exposure (MOE) or ADI for genotoxic and carcinogenic compounds is derived from benchmark dose lower confidence limit (BMDL) and human exposure (EFSA Scientific Committee et al. 2017). On deriving the BMDL using animal data, MOE values greater than or equal to 10,000 are considered as situations of low concern, whereas MOE values less than 10,000 are interpreted as situations of critical care and where risk management strategies are applied to minimize the severity of the exposure (EFSA 2012).

According to several international agencies involved in monitoring standards and framing guidelines for food safety, risk assessment of human exposure to multiple chemicals or chemical mixtures is achieved using two approaches, namely the whole mixture approach and the component-based approach (EFSA et al. 2020). The whole mixture approach is applicable to chemical mixtures whose composition is partly known or poorly characterized (e.g., a mixture of petroleum hydrocarbons into aromatic and aliphatic fractions). Hence, it is difficult to acquire information about individual components of such mixtures. In that case, the mixture is considered a single unit and the dose-response data is interpreted, or in case of inadequate dose-response data, a similar mixture is referred to further the risk assessment (Boobis et al. 2011). However, this approach is restricted to chemical mixtures whose composition does not change significantly (SCHER, SCENIHR, and SCCS 2012). On the contrary, the component-based approach is commonly used for a chemical mixture whose composition is well-known and documented. The individual components of the mixture are grouped into assessment groups based on its toxicity, physiological properties, and exposure and risk assessment steps are carried out (More et al. 2019). This is based on the fact that toxicity of chemical mixture as a unit is a cumulative effect of toxicity of individual chemicals, i.e., dose addition model as default model unless otherwise applicable, which is the presence of interactions among components in synergism or antagonism (Ingenbleek et al. 2021). For such approaches, risk characterization of the chemical mixture is targeted by comparison of the ratio of combined exposure of the chemical mixture to the quantitative metrics for its toxicity for a distinct species, population, subpopulation, and community. So, basically, the hazard metrics and parameters for exposure assessment are evaluated either for the individual chemical or the mixture as a single unit in the assessment group and equated for risk characterization. For example, if a chemical A and B are to be assessed for their associated risk, then hazard metrics (e.g., NOAEL or BMDL) for chemical A and chemical B will be evaluated individually and will be compared with the sum of exposure metrics using the hazard index or reference point index (More et al. 2019). Uncertainty is factored in risk characterization when combined toxicity of chemicals.

Finally, the risk assessment is concluded if the risk characterization for multiple chemicals does not show any health concern, and if otherwise, it suggests the requirement of additional data or any further risks, then the risk management step is activated to neutralize the adversity of the situation. It is of utmost importance to identify uncertainty in each and every mixture that departs from dose addition (Quignot et al. 2019).

8.1.2 Microbiological Risk Assessment

The framework for risk assessment of microorganisms in a food item is similar in steps and sequence as used for chemical contaminants comprising hazard identification, exposure assessment, hazard characterization, and risk characterization (Fig. 8.5).

Formally, the first step in microbial risk assessment (MRA) is to identify the microorganism present (agent with the potential to cause harm) in the food and its adverse effect on human health (CAC 1999). The major source of food pathogen and the pathogen of concern are determined in this initial step of MRA (Lammerding and Fazil 2000). The evaluation of risk issuing from this step is qualitative, and the preliminary information obtained are analyzed in detail in further steps of the risk framework. Epidemiological evidences in association with clinical and microbiological are included to identify the hazard carrying the potential to cause foodborne illness or outbreaks.

The probability of the consumer being exposed to the pathogen and its microbial load in the food and in a single-serve upon ingestion is estimated in exposure assessment (CAC 1999). This step involves investigation of the source of microbial contamination right from the farm to fork, i.e., production, processing, distribution, handling, and consumption of the food (FAO/WHO 2008). Various predictive microbiological tools are applied to characterize the nature of pathogens present in foods under varying extrinsic and intrinsic conditions (McKellar and Lu 2004; McMeekin et al. 2010). The amount of food consumed and frequency of consumption of the same is of paramount importance to assess the severity of the exposure to the microbial contaminant.

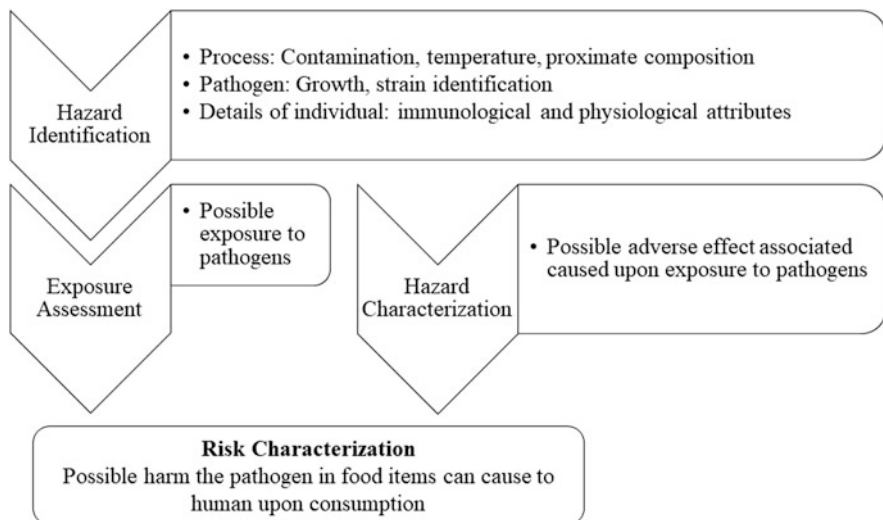


Fig. 8.5 Basic framework of microbial risk assessment

Hazard identification defines the nature and adversity of the pathogenic microorganism on humans on ingestion based on exposure assessment (Buchanan et al. 2000). The dose-response relationship suggests the direct relationship between the adverse effect and ingestion of microbial load through foods. The immunological and physiological state of the human is also an important factor affecting the magnitude of severity caused by the same load of pathogens among different individuals in the population or subpopulation (Gerba et al. 1996; Lund and O'Brien 2011). Traditionally, it has always been presumed that a minimum infectious dose is necessary to establish infection criteria, and exposure below this dose will not cause any infection; however, with the advance of scientific investigation, the concept of non-threshold infection is well established. The concept of single-hit suggests that low microbial load or exposure below the acceptable limit can eventually cause infection due to the ability of a pathogen to acclimatize in adverse growing conditions and multiply to establish pathogenesis (Lammerding 2013). The timeline of any foodborne illness upon ingestion of contaminated food is mentioned in Fig. 8.5. Factors that influence the process of pathogenesis, namely microbial resistance to the host's defense mechanism, the ability of the pathogen to colonize and virulence factor of the microorganism, immunological and physiological state of the host, type of food responsible for the infection, are considered to characterize the hazard (FAO/WHO 2003).

8.1.2.1 Risk Characterization

Risk characterization is the qualitative and/or quantitative estimation considering attendant uncertainty or variability using the information and data interpreted in preceding steps (hazard identification, exposure assessment, and hazard characterization) forms the basic premise of risk characterization (Buchanan et al. 2000; Ross and McMeekin 2009). The risk estimates should be based on available and updated scientific data; however expert opinion and uncertainty is an indispensable part of risk characterization and eventually MRA as a whole. Expert handling of a wide range of qualitative and/or quantitative data is achieved using some prerequisite, such as knowledge of mathematical models, microbiology, and the process involved. This step can be divided into six stages which is an integration of previous steps of MRA, summarizing the identified risks, considering the variability in risks, validation of analysis method, and tracking the uncertainty of all inputs to MRA (Voysey et al. 2002). The decision tree involved in risk characterization is conveyed to risk assessors and risk managers (FAO/WHO 2009). Risk characterization is performed in such a way that it could offer an insight (such as the prominent cause for the occurrence of risk) about the nature beyond a simple qualitative and quantitative statement of the risk.

Microbial risk assessment may focus on a single point or condition in the food chain, or it can accommodate its entire continuum of food ecosystem, i.e., farm to fork (FAO/WHO 2008). Further, the assessment may be scheduled on a single pathogen in a single food or all pathogens associated with foodborne illness; for example, the risk associated with *Salmonella* contamination in eggs—or all products associated with the pathogen, e.g., meats—in a particular region or the entire

country. In food industries, the MRA of a newly developed food product and/or its process is performed when significant variability and uncertainty exist to resolve food safety concerns. MRA can be achieved using several strategies to gather and analyze relevant information in the steps mentioned in the basic framework of the assessment (FAO/WHO 2010). Based on assumption and presentation of data, MRA can be qualitative and quantitative, with qualitative MRA involving categorization or depiction of hazard, its nature or exposure, whereas quantitative MRA is about quantitation of severity of the hazard or associated using numerical data and mathematical models (Lammerding 2013). Quantitative risk assessments use the information on microbial load for a given time and temperature, the initial microbial load, decimal reduction time (D -value), and nature of the pathogen as mentioned in Eqs. (8.2a) and (8.2b) to formulate a numerical expression of risk:

$$\log \frac{N_T}{N_0} = - \frac{t}{D} \quad (8.2a)$$

$$\log \frac{D}{D_R} = - \frac{(T_R - T)}{z} \quad (8.2b)$$

where N_T is microbial load or contamination after thermal treatment for time t and temperature T ; N_0 is initial microbial load or contamination; D_R is D -value at the reference temperature T_R ; z is the prominent attributes of the pathogen. MRA involves several such relationships being determined and estimated using mathematical models. Variability and uncertainty are incorporated in the mathematical model through the variation in the input factors and uncertainty in the model parameters defining the variable input factors, respectively (Voysey et al. 2002; Ross and McMeekin 2009). With the recent advancement of scientific knowledge, the semi-quantitative MRA approach is found to be the most useful in obtaining a structured way to enlist the risk based on the magnitude of its severity which further assists the risk assessor set its priorities. This approach uses both descriptive analyses of qualitative assessment and numerical modeling of quantitative assessment.

8.1.3 Application of Risk Assessment in the Context of Target Exposures

Risk-based systems are holistic (end to end), they begin with predicting emerging risks from the current monitoring database, thereafter precisely identify the hazard, characterizing severity of harm to general or especially vulnerable groups, assessing exposure routes (ingestion, inhalations) and enormity of spread (local, national, geopolitical) and based on these factors, characterize the risk (high or low). Such a framework is designed to deal with public health and is about balancing risk and economic activity.

Just as there is always some risk associated with any drug, so also in the case of food and substances added, where uncertainty exists or adverse events emerge over

time, provisional risk management measures are necessary to ensure an appropriate level of health protection is adopted, pending further scientific information for a more comprehensive risk assessment; however, “the measures adopted shall be proportionate and no more restrictive of trade than is required to achieve an appropriate level of health protection, regard being had to technical and economic feasibility and other factors regarded as reasonable and proper in the matter under consideration” (FSSAI 2006). Where risks are anticipated or limited to certain vulnerable groups of people, proper caution is communicated.

Risk communication is a simple matter of informing all relevant entities, including the public, of the true nature of risk. Risk communication is defined as the exchange of information and opinions concerning risk and risk-related factors among risk assessors, risk managers, consumers, and other interested parties (FAO/WHO 2016). The FSSA (FSSAI 2006) more elaborately defines it as the interactive exchange of information and opinions throughout the risk analysis process concerning risks, risk-related factors, and risk perceptions among risk assessors, risk managers, consumers, industry, the academic community, and other interested parties, including the explanation of risk assessment findings and the basis of risk management decisions. Adverse public health events require government authorities to communicate with civil society in an objective and transparent manner.

Exposure assessments rely upon results obtained from diet surveys. Total diet studies (TDS) are well recognized as being more accurate in revealing the actual amounts of nutrients or adverse substances, they are expensive and take years to complete. Since surveys involve substantial variations in cost, logistics, and time, their purpose, scale, and scope should be explicitly defined. In assessing individual dietary intakes, a popular method is a retrospective reporting from the recent past (24-h recall) or at remote time periods however considering that memory recalls diminish with time. Every method has its strengths and weakness, none is perfect, and the investigator’s choice is to be examined not merely for errors or fragility of inferences but whether its summary of findings, an indication of trends, or exposure of risks are sufficiently plausible to take notice, alert risk managers and prioritize risk. Wherever necessary, confirmatory surveys may be carried out.

Where the likelihood of a national character emerging on dietary intakes appears remote, targeted surveys of a small associative group should be the order of the day prior to embarking on a TDS, if necessary. Targeted surveys have three important features, namely, they are cost-effective, provide multicultural segmental exposure differences, and are completed in a shorter time duration. Where risks are suspected or evidence scant or absent, for countries with divergent dietary practices, small group surveys selected on well-reasoned criteria may be an expedient source of information. India is a diverse country, more significantly in the dietary practices of its population. The likelihood of a national character emerging on dietary intakes appears remote, whereas small associative group surveys should be the order of the day prior to embarking on a TDS.

Secondly, a judicious selection of food(s) majorly consumed (e.g., staples, such as rice, wheat, milk) combined with foods frequently consumed but in lower amounts (e.g., spices, herbs, etc.) exposures to chemical risks provide leading

indicators of population risk. Studies on consumption and exposures are more refined and realistic when intake levels are determined on foods for table use are analyzed, i.e., at the point of ingestion. It is likely that processing may affect levels from washing, comminution, or heat degradation and reflects realistic intakes in population diets.

The first task in risk-based ecosystems is using risk assessment in predicting emerging hazards and proactive preparedness by risk managers in containing the exposure or transmission of the hazard, whether by ingestion (food and waterborne) or inhalation (pandemic). Early warning of an adverse public health event is of critical importance than post-event responses (reactive), deeply entrenched in current policy and planning. Containment strategies are crucial at the initial stage before propagation spirals out of control; the latter stage increases costs, allocation of resources, and public confidence is governance. There is no “one size fits all” regulatory approach, and India must develop its own response to public health risks.

Exposure assessments are perhaps the most critical step in food safety control. With globalization and the availability of food products from all over the world, changes in lifestyle behaviors and consequent changing dietary preferences require robust systems to measure their implications. Exposures arising from these changes with ingesting chemicals, such as food additives, pesticide residues, toxins, and contaminants, need continuous monitoring and surveillance. Food consumption data also provide nutrition-based information on nutrient intakes of vitamins, minerals, fat, sugar, salt, and others for framing policy and advocacy petitions.

Diet surveys are expensive, and in a multicultural country with varying dietary habits, exposure analysis on small and relevant group(s) segments can provide fairly realistic estimations. More such studies provide more data which in the absence of a national total diet study is a dependable alternative.

8.1.4 Case Studies on Targeted Exposure Assessments

With the introduction of carbonated caffeine beverages, popularly known as energy drinks, over recent years, exposure to caffeine may raise issues regarding the safe intake of caffeine.

The EFSA Panel on Dietetic Products, Nutrition and Allergies (EFSA Panel on Dietetic Products and Nutrition and Allergies 2015) provided a scientific opinion that caffeine intakes from all dietary sources do not give rise to concerns about adverse health effects for the general healthy population and subgroups thereof. “Single doses of caffeine up to 200 mg (about 3 mg/kg body weight for a 70 kg adult). Habitual caffeine consumption of up to 400 mg per day does not give rise to safety concerns for nonpregnant adults. Habitual caffeine consumption of up to 200 mg per day by pregnant women does not give rise to safety concerns for the fetus. Single doses of caffeine and habitual caffeine intakes up to 200 mg consumed by lactating women do not give rise to safety concerns for breastfed infants. For children and adolescents, the information available is insufficient to derive a safe caffeine intake. The Panel considers that caffeine intakes of no concern derived for

Table 8.1 Consumption of caffeine per day from energy drinks

	% Students	Caffeine per day (mg)
Rarely	32.6	–
Per month	8.3 (80 mg/30 days)	2.7
Per fortnightly	25.8 (80 mg/14 days)	5.7
Twice weekly	7.6 (160 mg/7 days)	22.9

250 mL is a single-serve pack

acute caffeine consumption by adults (3 mg/kg body weight per day) may serve as a basis to derive single doses of caffeine and daily caffeine intakes of no concern for these population subgroups.”

In a measure to control the overall intake of caffeine, India put out a standard for “caffeinated beverage” that set the maximum level of 75 mg of caffeine per can (250 mL) (Bedi et al. 2014). In a questionnaire administered in a study by Ravichandran et al. 2018, 180 respondents aged 13–40 years (132 students and 48 employed), showed the frequency of energy drink consumption by students was rarely (32.6%), followed by fortnightly (25.8%), once a week (11.4%), once a month (8.3%), twice a week (7.6%), and everyday (2.3%). Whereas among working employees, 33.3% of them consumed rarely, followed by fortnightly (16.7%), once a month (12.5%), twice a week (10.4%), and once a week or every day (2.1%). Table 8.1 provides the intake of caffeine from the consumption of energy drinks. Suitable and appropriate conclusions on the risk presented to the total intake of caffeine from all sources.

In modern food law, public health safety begins with government obligations of assessing whether its population(s) is at risk. Only what is consumed is what puts populations at risk. Exposure assessment is perhaps the most critical step in food safety control. While risk exists from consumption of all foods, the level of human exposure (from consumption) to physical, chemical, and biological hazards over a lifetime without adverse consequences is of concern. Executive functions/duties require installation of surveillance, monitoring, and evaluation processes (databased) for taking proportionate measures at appropriate times. Stakeholders are informed on the progression of measures taken in mitigating risks. The absence of such capabilities in a food control system leads to false conclusions. Exposure analysis can be used to project the level of consumption of certain food(s) the specific hazard will exceed the safety limit; it is a predictive system.

Governments worldwide are concerned with ensuring public health through systematic reductions of risks associated with the ingestion of unwanted substances, and these are prioritized on seriousness and immediacy of action. Monitoring public health is an ongoing activity to assess the impact of existing regulatory measures and whether the trend will meet targets. Public health goals are achieved only if exposure assessment reveals a risk mitigation trajectory is progressing towards the established goal. Small associative group studies are expedient for such predictions.

Lead and cadmium are among the most abundant heavy metals and are particularly toxic (Bhaskarachary et al. 2014). Plant or seafood from sources exposed to

Table 8.2 Intake of various foods (g) in different age and physiological groups

Age group	2–4 years		16–17 years		Sedentary worker		Pregnant women	
	Mean	95th	Mean	95th	Mean	95th	Mean	95th
Cereals	172	345	510	836; 644 ^a	426	689; 600 ^a	401	659
Pulses	12	37	37	123; 95	32	92; 86	14	97
Milk/buttermilk	81	298	106	284; 308	139	388; 392	141	652
Potato	12	50	44	182; 91	39	146; 111	33	161
Fruits	33	166	451	186; 175	44	173; 205	58	260
Cooking oil	7	19	23	57; 36	20	52; 43	14	34

^aFirst value is for male, second is for female

Table 8.3 Concentration of heavy metal contaminants in table-ready foods at the point of ingestion

Foods	N ^a	Lead (µg/kg) ^a , Mean (SD)	Cadmium (µg/kg) ^a , Mean (SD)
Rice	24	55.4(45.8) -	0.2(0.49)—FSSAI value
Sorghum	21	73.7(81.13)	0.06(0.20)
Red gram dal	24	1.4(5.29)	0.05(0.17)
Eggplant	24	0.5(1.32)	0.5(1.0)
Milk	24	11.2(15.23)	0.01 (0.04)
Buttermilk	22	17.4 (25.89)	0.03 (0.11)
Tamarind	24	30.1(44.54)	BDL ^b
Red chili powder	23	10.4(23.21)	4.7(12.16)
Groundnut oil	24	8.4(22.76)	BDL ^b
Water	24	0.2(0.55)	0.1(0.36)

^aMicrogram per kilogram of fresh weight

^bBDL: below detection limit

^cNumber of people tested

polluted waters or sewage reflects higher levels of toxic metals. Planning of exposure studies should take into account agricultural practices ranging from large well-irrigated fields to local small plots often unhygienically watered. In a study by NIN, Hyderabad (Bhaskarachary et al. 2014), 22 most commonly consumed foods were selected from various food groups, including drinking water. The amounts of a few selected foods among different age and physiological groups are shown in Table 8.2.

Indian diets predominantly derive over 55–65% of daily energy from cereals, and pulses, as seen from data in Table 8.2. Table 8.3 provides the concentration of heavy metals, lead, and cadmium, which are the major contaminants in the food supply chain in table-ready foods, taking into consideration the various methods for processing the selected foods. They have the potential to accumulate in the body, raising concerns about adverse health effects.

Dietary exposures are obtained by calculating the total intake of the contaminant from all food sources. Typically, commodity foods in staple or subsistence diets are consumed in larger amounts (cereals, milk, potato), frequently, even daily. Other

Table 8.4 Dietary exposure (Mean intake level)

Age group	Lead			Cadmium		
	Exposure ($\mu\text{g}/\text{kg bw}$)		% PTWI	Exposure ($\mu\text{g}/\text{kg bw}$)		% PTWI
	Per day	Per week		Per day	Per week	
1–3 years	1.10	7.70	30.81	0.01	0.07	0.97
16–17 years	0.63	4.42	17.69	0.01	0.05	0.77
Sedentary worker	0.53	3.72	14.86	0.01	0.05	0.65
Pregnant women	0.59	4.15	16.60	0.01	0.06	0.91

Table 8.5 Dietary exposure (95th percentile intake level)

Age group	Lead			Cadmium		
	Exposure ($\mu\text{g}/\text{kgbw}$)		% PTWI	Exposure ($\mu\text{g}/\text{kgbw}$)		% PTWI
	Per day	Per week		Per day	Per week	
1–3 years	2.73	19.11	76.44	0.029	0.20	0.42
16–17 years (M)	1.26	8.82	35.28	0.024	0.17	0.35
Sedentary worker (M)	1.04	7.28	29.12	0.022	0.15	0.31
Pregnant women	1.02	7.14	28.56	0.019	0.13	0.47

foods or ingredients are typically added for their sensorial attributes and are consumed in smaller quantities; however, some of them, tamarind and red chilies, may have higher concentrations of chemical substances. Exposure levels of representative foods selected from staple categories (cereals, milk, etc.) and those used for sensory purposes (chilies, tamarind) can serve as leading indicators for monitoring risk and progress on public health goals. In the case of contaminants, a safety indicator of habitual intake (weekly or monthly) is the provisional tolerable weekly intake (PTWI). The exposure levels as a percentage of the PTWI of several foods are presented in Tables 8.4 and 8.5.

Food risks arise not only from the processing industry but also from climatic zones that favor the growth and propagation of toxins. In a country, like India, with varied climatic zones, dietary consumptions, and agricultural postharvest conditions, coordinated nationwide studies are required, monitored by States or Regional nodes. However, where dietary intakes are majorly driven by staples and other food grains, the gap narrows, where hazards are likely to thrive. Geographical climates and conditions of warm, humid, unseasonal rains, and floods also favor fungal infection of standing crops and contamination in stored grains (Tables 8.6 and 8.7).

Foods generally consumed in staple diets are agricultural produce minimally processed (cleaning, drying, grinding, or pasteurization) are the direct entry points for chemical substances, such as contaminants, toxins, and pesticide residues into the food supply chain. Reduction or removal of chemical substances is not viable in downstream processes and must be reduced by good agricultural practices, hitherto unmonitored or informally regulated. As a point of discussion, the intake of the lead 95th percentile of 29.12 indicates 95% of the population has an exposure of approximately one-third of the provisional tolerable weekly intake level. A single

Table 8.6 Concentration of pesticide residues in foods ($\mu\text{g}/\text{kg}$ fresh weight)

Pesticides	Rice	Milk	Potato	Water
α -HCH	1.42(6.4)	0.83 (0.67)	0.03(0.16)	BDL
β -HCH	0.13(0.64)	BDL	0.01(0.040)	BDL
γ -HCH	0.029(0.11)	0.65(0.71)	0.13(0.41)	0.89(1.81)
δ -HCH	0.25(0.77)	0.5 (0.28)	BDL	0.1(0.27)
α -Endosulfan	0.19 (0.59)	0.3(0.14)	0.055(0.16)	0.016(0.06)
β -Endosulfan	0.239 (0.46)	0.157(0.11)	0.004(0.02)	0.143(0.32)
2'4 DDT	0.015(0.06)	0.9(0.71)	BDL	0.071(0.24)
4'4 DDT	0.204(0.36)	0.778(0.32)	0.028(0.09)	0.322(0.41)
Cypermethrin	2.737 (6.12)	2.967(2.01)	1.028(1.02)	2.973(2.73)

Table 8.7 Estimated daily intake of pesticide residues, % ADI, by target groups at 95th percentile ($\mu\text{g}/\text{Kg}$ bw)

Pesticide	1–3 years		16–17 years (male)		Sedentary worker male		Pregnant women	
	Per day	% ADI	Per day	% ADI	Per day	% ADI	Per day	% ADI
α -HCH	0.154	0.307	0.072	0.143	0.059	0.118	0.059	0.117
β -HCH	0.048	0.095	0.016	0.032	0.014	0.027	0.016	0.033
γ -HCH	0.029	0.059	0.009	0.018	0.009	0.018	0.013	0.026
δ -HCH	0.045	0.90	0.017	0.034	0.015	0.030	0.018	0.035
α -Endosulfan	0.036	0.061	0.015	0.026	0.013	0.022	0.015	0.025
β -Endosulfan	0.033	0.055	0.014	0.024	0.012	0.020	0.012	0.021
2'4 DDT	0.025	0.245	0.006	0.06	0.007	0.069	0.011	0.106
4'4 DDT	0.064	0.639	0.020	0.198	0.019	0.192	0.025	0.251
Cypermethrin	0.378	0.756	0.166	0.333	0.142	0.284	0.157	0.314

data point reveals much less than the true risk prevailing. The leading indicator for metallic contaminants (chemicals not intentionally added to food produce) is trend analysis of exposures conducted at predetermined time intervals (e.g., 5 years) and whether these are under control under public health goals.

While heavy metals discussed earlier are not intentionally added to foods but present nevertheless as a consequence of soil pollution, waste disposal, and untreated discharge, there are other chemicals intentionally added that remain as residues. Exposure studies are not intended to inform governments of the mitigatory measures taken and their effect. Surveillance, monitoring, and evaluation of these measures are the core of any predictive food safety management system installed by governments and progress towards public health goal targets. Of particular concern are persistent organic pollutants (POP) which linger in soils for several years, and the continuing presence of banned pesticides or those restricted to vector control only; these should be undetectable at the lowest level of detection (LLOD) (Jonnalagadda et al. 2015). Preventative safety assessments are only possible if robust surveillance, monitoring, and evaluation system are in place to detect the presence of banned pesticides.

Following through, exposures to pesticide residues of the same foods (Table 8.3) were calculated. The total exposure from foods prepared for table use is presented in Tables 8.4 and 8.5. Finally, the exposures were expressed as $\mu\text{g}/\text{kg}$ body mass per day, which was compared with the ADIs (FAO 1997), Dietary intake of 15 pesticides.

While heavy metals discussed earlier are not intentionally added to foods but enter the food chain as a consequence of soil pollution by waste disposal and untreated discharge, and ineffective preventive measures. Exposure studies are not intended as much to inform consumers than require regulators to implement and monitor mitigation measures and long-term surveillance. Of particular concern are persistent organic pollutants (POP) which linger in soils for several years, and the continuing presence of banned pesticides or those restricted for vector control in the food chain; these should be undetectable at the LLOD (Jonnalagadda et al. 2015).

Reactive food control systems inherently built on product failures are incapable of dealing with the ingress of hazards along the food chain. For example, a study on monitoring of pesticide residues at the national level (FSSAI 2019) reported that of 23,666 samples analyzed, 19.1% (4510 samples) were detected with residues, of which 2.2% (523 exceeded the maximum residue limit (MRL). Consequently, maintaining a strict vigil by drawing samples from manufacturers, wholesalers, and retailers was the enforcement advice. Three major weaknesses emerge here compared with a risk-based system. Reactive systems are post failures, contrary to predictive risk-based systems; the latter is continuously monitored and surveillance. In the case of agricultural contaminants and chemical treatments (pesticide residues), downstream activities (manufacturing, distribution, and retailing) are incapable of addressing the risk. The action taken should be at the source of ingress into the food chain. Monitoring may be designed to “identify crops and regions” having a preponderance of “particular pesticide residues,” which requires a different plan and execution framework. As argued earlier, diversity in food dietary habits presents the case for a policy decision that every State or Region conducts periodically dietary surveys for intakes of adverse substances. Risk-based ecosystems (food supply chain) being predictive are used for monitoring public health goals and preventing failures instead of predominantly taking recourse to penal impositions.

8.1.5 Risk Communication and Risk Perception

The risk analysis framework widely adopted globally describes the essential features of food safety communications. The Food Safety and Standards Act (2006) of Indian legislation comprehensively defines risk communication as “the interactive exchange of information and opinions throughout the risk analysis process concerning risks, risk-related factors, and risk perceptions, among risk assessors, risk managers, consumers, industry, the academic community and other interested parties, including the explanation of risk assessment findings and the basis of risk management decisions.”

Risk communication is about the preparedness of food safety authorities to deal with public health issues, transparently sharing information on the failure objectively and the risk involved. Countries face challenges in providing effective risk communication when institutional capabilities are inadequate. For example, insufficient resources of relevant expertise and infrastructure for collecting, collating, and analysis of food hazards “at points” in the supply chain reduce communication authenticity. Lack of reliable data on food hazards and risks impedes communication in a timely and accurate manner (FAO/WHO 2016).

Oxytocin, a hormone produced by the hypothalamus and secreted by the nearby pituitary gland: plays an important role in releasing milk in humans and animals. Fears of adverse health consequences have been expressed on the common practice of injecting milch cattle with oxytocin, which is carried over in milk and consumed as food. In the absence of scientifically verified public information, perceptions are formed and among stakeholders of all manner of professions and transmitted until the overwhelming view is that harm is likely. Following the logical steps in risk assessment, in such a case, is not merely about exposure to the hormone but whether, in the first instance, a hazard exists, defined as an “agent with the potential to cause an adverse health effect” (FSSAI 2006). Studies carried out (Pullakhandam et al. 2014) have shown that exogenous administrations of oxytocin injections to milch cattle do not influence its content in milk. For example, milch cattle administered oxytocin injections showed content in milk of 0.06 ± 0.031 ng/mL, while cattle not injected had similar mean oxytocin levels (0.06 ± 0.028 ng/mL) thereby concluding that oxytocin is a natural constituent of milk and injections administered had no effect on its milk content. Further oxytocin present in milk rapidly degrades during intestinal digestion, ruling out its absorption and associated adverse health consequences, if any.

If purpose-led scientific studies such as these are designed to raise public awareness as part of creating a vibrant risk-based ecosystem, health authorities should routinely put out such findings in a compelling but simple manner. Academia edged into confining these to scientific journals and libraries should be made part of an organized risk communications structure, contributing their scientific expertise to a wider audience. Equitable infrastructural arrangements are required for risk communication, similar to risk assessment and risk management.

It is unknown whether public information of these findings had diminished unfounded perceptions, post-wide publication, as a final step of the intended study. A cognitive application of “commercial supply chains” of organized resources, access and procurement of relevant studies, wide publication in media including social media, and following through on its impact in diminishing perception for factual understanding should be a dominant feature of risk communication.

Risk perceptions are subjective judgments about a current concern of adverse effects. A common assumption in risk perception research is that people’s knowledge and certainty about a risk determines how they will perceive it (Paek and Hove 2017). People who are unaware of the natural toxins present in frequently consumed foods, albeit at safe levels, are startled when the fact appears in media, often the first communicators.

Communicators must be quick as consumers react instantly, desisting from buying a perfectly safe food whose naturally present toxin was revealed for the first time. Reports of the presence of formalin in fish, commonly consumed communities off the Indian west coast would have been less alarming if the data on its natural prevalence in the food chain was put out quickly based on available surveillance, monitoring, and evaluation capabilities of a risk-based national food control structure. Not communicating openly from data on whether amounts of formalin found was within or exceeded its natural levels led to people panicking and stress in trade. Risk communication and risk perception are two sides of the coin. When the former is not conveyed in time or not understood by stakeholders, perceptions are formed. Even though food scientists and nutritionists are aware that safe food does not mean zero risk; however, a deemed belief of people is, it should be zero. Scientist relies on analytical thinking, experimental verification, and conclusive evidence, whereas people rely on experiential observations and emotions.

8.2 Conclusion

Modern food safety legislations worldwide provide a risk-based framework for protecting human health, taking into consideration that measures implemented are appropriate with the risk presented. The science-based approach through validated risk assessments precedes the framing of national policy and public health goals. Increasingly many countries are using risk-based predictive approaches in food control over outdated and reactive inspection systems, which are hazard-based and often unduly restrictive of trade or insensitive to health objectives. The science-based approach of risk assessment opens a new dimension for applying investigative sciences in populations, subgroups studies, and planning of appropriate measures. It can aid in policy planning, nutrition strategies, infrastructural capacities, and the adoption of health goals.

References

- Ankley GT, Edwards SW (2018) The adverse outcome pathway: a multifaceted framework supporting 21st century toxicology. *Curr Opin Toxicol* 9(2018):1–7. <https://doi.org/10.1016/j.cotox.2018.03.004>
- Ankley GT, Bennett RS, Erickson RJ, Hoff DJ, Hornung MW, Johnson RD, Mount DR et al (2010) Adverse outcome pathways: a conceptual framework to support ecotoxicology research and risk assessment. *Environ Toxicol Chem* 29(3):730–741. <https://doi.org/10.1002/etc.34>
- Bedi N, Dewan P, Gupta P (2014) Energy drinks: potions of illusion. *Indian Pediatr* 51:529–533
- Bertail P, Cléménçon S, Tressou J (2010) Statistical analysis of a dynamic model for dietary contaminant exposure. *J Biol Dyn* 4(2):212–234. <https://doi.org/10.1080/17513750903222960>
- Bhaskarachary K, Betsy A, Vemula SR, Rao VV, Polasa K (2014) Dietary exposure assessment of Lead and cadmium in rural population of Andhra Pradesh—India—a total diet study approach. *Int J Food Nutr Sci* 3(4):45–52. <https://doi.org/10.18527/2500-2236-2017-4-1-ii-iv>
- Boobis AR, Doe JE, Barbara Heinrich-Hirsch ME, Meek SM, Ruchirawat M, Schlatter J, Seed J, Vickers C (2008) IPCS framework for analysing the relevance of a noncancer mode of action for humans. *Crit Rev Toxicol* 38(2):87–96. <https://doi.org/10.1080/10408440701749421>

- Boobis A, Budinsky R, Collie S, Crofton K, Embry M, Felter S, Hertzberg R et al (2011) Critical analysis of literature on low-dose synergy for use in screening chemical mixtures for risk assessment. *Crit Rev Toxicol* 41(5):369–383. <https://doi.org/10.3109/10408444.2010.543655>
- Buchanan RL, Smith JL, Long W (2000) Microbial risk assessment: dose-response relations and risk characterization. *Int J Food Microbiol* 58(3):159–172. [https://doi.org/10.1016/S0168-1605\(00\)00270-1](https://doi.org/10.1016/S0168-1605(00)00270-1)
- Codex Alimentarius Commission (CAC) 1999 Principles and guidelines for the conduct of a microbiological risk assessment (CAC/GL–30). Rome, Italy
- Commission E (2017) Regulation (EU) 2017/625 on official controls and other official activities performed to ensure the application of food and feed law, rules on animal health and welfare, plant health and plant protection products. *Off J Eur Union* 95(1):1–142. <http://eur-lex.europa.eu/legal-content/EN/TXT/PDF/?uri=CELEX:32017R0625&rid=1>
- Culleres DB, Boesten J, Bolognesi C, Boobis A, Büchert A, Coggon D, Hardy A et al (2008) Opinion of the scientific panel on plant protection products and their residues to evaluate the suitability of existing methodologies and, if appropriate, the identification of new approaches to assess cumulative and synergistic risks from pesticides to human health with a view to set MRLs for those pesticides in the frame of regulation (EC) 396/2005. *EFSA J* 6(5):1–84. <https://doi.org/10.2903/j.efsa.2008.705>
- Dorne JLCM, Fink-Gremmels J (2013) Human and animal health risk assessments of Chemicals in the Food Chain: comparative aspects and future perspectives. *Toxicol Appl Pharmacol* 270(3): 187–195. <https://doi.org/10.1016/j.taap.2012.03.013>
- Dorne JLCM, Dorne JLCM, Bordajandi LR, Amzal B, Ferrari P, Verger P (2009) Combining analytical techniques, exposure assessment and biological effects for risk assessment of Chemicals in Food. *TrAC Trends Anal Chem* 28(6):695–707. <https://doi.org/10.1016/j.trac.2009.03.008>
- EFSA (2011) Overview of the procedures currently used at EFSA for the assessment of dietary exposure to different chemical substances. *EFSA J* 9(12):1–33. <https://doi.org/10.2903/j.efsa.2011.2490>
- EFSA (2012) Statement on the applicability of the margin of exposure approach for the safety assessment of impurities which are both genotoxic and carcinogenic in substances added to food/feed. *EFSA J* 10(3):6–10. <https://doi.org/10.2903/j.efsa.2012.2578>
- EFSA (2014) Modern methodologies and tools for human Hazard assessment of chemicals. *EFSA J* 12(4):1–87. <https://doi.org/10.2903/j.efsa.2014.3638>
- EFSA Panel on Dietetic Products, and Nutrition and Allergies (2015) Scientific opinion on the safety of caffeine. *EFSA J* 13(5). <https://doi.org/10.2903/j.efsa.2015.4102>
- EFSA Scientific Committee, Hardy A, Benford D, Halldorsson T, Jeger MJ, Knutsen KH, More S et al (2017) Update: use of the benchmark dose approach in risk assessment. *EFSA J* 15(1): 1–41. <https://doi.org/10.2903/j.efsa.2017.4658>
- EFSA, FAO, WHO (2011) Towards a harmonised Total diet study approach: a guidance document. *EFSA J* 9(11):1–66. <https://doi.org/10.2903/j.efsa.2011.2450>
- EFSA, Dorne JLCM, Crépet A, Biesebeek JD, Machera K, Hogstrand C (2020) Human risk assessment of multiple chemicals using component-based approaches: a horizontal perspective, vol 17. EFSA Supporting Publications. <https://doi.org/10.2903/sp.efsa.2020.EN-1759>
- FAO (1997) Codex general standard for contaminants and toxins in foods and feed, Codex Stan193-1995 (Rev.1- 1997), vol 47. Codex Alimentarius International Food Standards, FAO, p 53
- FAO (1999) Principles and guidelines for the conduct of microbiological risk assessment. FAO: Agric Consumer Protect 63:68. <http://www.fao.org/docrep/004/y1579e/y1579e05.htm>
- FAO/WHO (1987) Principles for the safety assessment of food additives and contaminants in food. Environmental Health Criteria, Geneva, Switzerland. <https://apps.who.int/iris/handle/10665/37578>
- FAO/WHO (1995) Application of risk analysis to food standards issues: report of the joint FAO/WHO expert consultation. Switzerland, Geneva

- FAO/WHO (1997) "Risk management and food safety: report of a joint FAO/WHO expert consultation." FAO Food and Nutrition Paper. Vol. 65. Rome. doi: <https://doi.org/10.4081/jna.2011.6.s2.e5>
- FAO/WHO (2003) Hazard characterisation for pathogens in food and water [microbiological risk assessment series 3]. Geneva, Switzerland. <http://apps.who.int/iris/bitstream/handle/10665/42693/9241562374.pdf?sequence=1%0Ahttp://www.fao.org/docrep/006/y4666e/y4666e00.htm>
- FAO/WHO (2006) The use of microbiological risk assessment outputs to develop practical risk management strategies: metrics to improve food safety. A Joint FAO/WHO Expert Meeting, Kiel, Germany
- FAO/WHO (2008) Exposure assessment of microbiological hazards in food [microbiological risk assessment series 7]. Geneva, Switzerland
- FAO/WHO (2009) Principles and methods for the risk assessment of Chemicals in Food-Environmental Health Criteria 240. Geneva, Switzerland
- FAO/WHO (2010) Risk characterisation of microbiological hazards in food [microbial risk assessment series 17]. Geneva, Switzerland. <http://www.fao.org/docrep/012/i1134e/i1134e.pdf>
- FAO/WHO (2016) Risk communication applied to food safety. Food and Agriculture Organization of the United Nations and World Health Organization, Rome. www.fao.org/food/food-safety-quality%0Awww.who.int/foodsafety
- FAO/WHO (2021a) FAO/WHO chronic individual food consumption—summary statistics (FAO/WHO CIFOcOss). 2021. <https://www.who.int/teams/nutrition-and-food-safety/databases>
- FAO/WHO (2021b) Global individual food consumption data tool. 2021. <http://www.fao.org/gift-individual-food-consumption/en/>
- FAOSTAT. 2021. "Food and Agriculture Data." 2021. <http://www.fao.org/faostat/en/#home>
- Farré M, Picó Y, Barceló D (2014) Application of ultra-high pressure liquid chromatography linear ion-trap orbitrap to qualitative and quantitative assessment of pesticide residues. *J Chromatogr A* 1328:66–79. <https://doi.org/10.1016/j.chroma.2013.12.082>
- FSSAI (2006) Food safety and standard act, 2006. Ministry of Law and Justice (Legislative Department), India
- FSSAI (2019) Monitoring of pesticide residues at national level. File No 7(5) 2019/Pesticide Residues/RCD/FSSAI
- FSSAI (2021) Risk assessment. 2021. <https://fssai.gov.in/cms/Risk-Assessment.php>
- Gaze R, Betts R, Stringer MF (2002) HACCP systems and microbiological risk assessment. In: Brown M, Stringer M (eds) *Microbiological risk assessment in food processing*. Woodhead Publishing Limited, Cambridge, pp 248–265
- Gerba CP, Rose JB, Haas CN (1996) Sensitive populations: who is at the greatest risk? *Int J Food Microbiol* 30(1–2):113–123. [https://doi.org/10.1016/0168-1605\(96\)00996-8](https://doi.org/10.1016/0168-1605(96)00996-8)
- Guyton KZ, Barone S, Brown RC, Euling SY, Jinot J, Makris S (2008) Mode of action frameworks: a critical analysis. *J Toxicol Environ Health B Crit Rev* 11(1):16–31. <https://doi.org/10.1080/10937400701600321>
- Hardy A, Dorne JLCM, Aiassa E, Alexander J, Bottex B, Chaudhry Q, Germini A et al (2015) Editorial: increasing robustness, transparency and openness of Scientific assessments. *EFSA J* 13:3. <https://doi.org/10.2903/j.efsa.2015.e13031>
- Hardy A, Benford D, Halldorsson T, Jeger MJ, Knutsen HK, More S, Naegeli H et al (2017) Guidance on the use of the weight of evidence approach in Scientific assessments. *EFSA J* 15(8). <https://doi.org/10.2903/j.efsa.2017.4971>
- Herrman JL, Younes M (1999) Background to the ADI/TDI/PTWI. *Regul Toxicol Pharmacol* 30(2 II):109–113. <https://doi.org/10.1006/rtp.1999.1335>
- Ingenbleek L, Zajet E, Dzossa AD, Adebayo SB, Ogungbange J, Dansou S, Diallo ZJ et al (2017) Methodology design of the regional sub-Saharan Africa total diet study in Benin, Cameroon, Mali and Nigeria. *Food Chem Toxicol* 109:155–169. <https://doi.org/10.1016/j.fct.2017.08.017>
- Ingenbleek L, Lautz LS, Dervilly G, Darney K, Astuto MC, Tarazona J, Liem AKD et al (2021) Risk assessment of chemicals in Food and Feed: principles, applications and future

- perspectives. In: Harrison RM (ed) Environmental pollutant exposures and public health. Royal Society of Chemistry, pp 1–38. <https://doi.org/10.1039/9781839160431-00001>
- Jonnalagadda PR, Vemula SR, Rao VV, Polasa K (2015) Dietary exposure to pesticide residues by various physiological groups of population in Andhra Pradesh, South India. *Int J Food Nutr Sci* 4(1):139–148
- Lammerding A (2013) Microbial food safety risk assessment. In: Glenn Morris J Jr, Potter ME (eds) Foodborne infections and intoxications, 4th edn. Academic Press, pp 37–51. <https://doi.org/10.1016/B978-0-12-416041-5.00003-2>
- Lammerding A, Fazil A (2000) Hazard identification and exposure assessment for microbial food safety risk assessment. *Int J Food Microbiol* 58:147–157. www.elsevier.nl/locate/ijfoodmicro
- Larsen JC (2006) Risk assessment of chemicals in european traditional foods. *Trends Food Sci Technol* 17(9):471–481. <https://doi.org/10.1016/j.tifs.2006.04.007>
- Lund BM, O'Brien SJ (2011) The occurrence and prevention of foodborne disease in vulnerable people. *Foodborne Pathog Dis* 8(9):961–973. <https://doi.org/10.1089/fpd.2011.0860>
- McKellar R, Lu X (2004) Modelling microbial responses in foods. CRC Press, Boca Raton, FL
- McMeekin TA, Hill C, Wagner M, Dahl A, Ross T (2010) Ecophysiology of foodborne pathogens: essential knowledge to improve food safety. *Int J Food Microbiol* 139(SUPPL. 1):S64–S78. <https://doi.org/10.1016/j.ijfoodmicro.2010.01.041>
- Meek ME, Bette AR, Boobis KM, Crofton GH, Van Raaij M, Vickers C (2011) Risk assessment of combined exposure to multiple chemicals: a WHO/IPCS framework. *Regul Toxicol Pharmacol* 60(2):S1–S14. <https://doi.org/10.1016/j.yrtph.2011.03.010>
- More SJ, Hardy A, Bampidis V, Benford D, Bennekou SH, Bragard C, Boesten J et al (2019) Guidance on harmonised methodologies for human health, animal health and ecological risk assessment of combined exposure to multiple chemicals. *EFSA J* 17:3. <https://doi.org/10.2903/j.efsa.2019.5634>
- National Research Council (NRC) (1983) Risk assessment in the Federal Government: managing the process. National Academy Press, Washington, DC
- Osadchiy T, Poliakov I, Olivier P, Rowland M, Foster E (2020) Progressive 24-hour recall: usability study of short retention intervals in web-based dietary assessment surveys. *J Med Internet Res* 22(2):1–12. <https://doi.org/10.2196/13266>
- Paek H-J, Hove T (2017) Risk perceptions and risk characteristics risk and risk perception: definitions and dimensions. *Oxford Research Encyclopedia of Communication*, no. March: 1–15
- Pico Y, Alfarhan AH, Barcelo D (2020) How recent innovations in gas chromatography-mass spectrometry have improved pesticide residue determination: an alternative technique to be in your radar. *TrAC Trends Anal Chem* 122:115720. <https://doi.org/10.1016/j.trac.2019.115720>
- Price PS, Jarabek AM, Burgoon LD (2020) Organising mechanism-related information on chemical interactions using a framework based on the aggregate exposure and adverse outcome pathways. *Environ Int* 138(March):105673. <https://doi.org/10.1016/j.envint.2020.105673>
- Pullakhandam R, Palika R, Vemula SR, Polasa K, Boindala S (2014) Effect of oxytocin injection to Milching buffaloes on its content & stability in milk. *Indian J Med Res* 139(6):933–939. <https://pubmed.ncbi.nlm.nih.gov/25109729>
- Quignot N, Wiecek W, Amzal B, Dorne JL (2019) The Yin–Yang of CYP3A4: a bayesian meta-analysis to quantify inhibition and induction of CYP3A4 metabolism in humans and refine uncertainty factors for mixture risk assessment. *Arch Toxicol* 93(1):107–119. <https://doi.org/10.1007/s00204-018-2325-6>
- Ravichandran AS, Vemula R, Mendu VVR, Konapur A, Subba RM, Gavaravarapu. (2018) Perceptions and practices related to consumption of ‘energy drinks’. *Indian J Nutr Dietetics* 55(4):412–422
- Ridgway K, Lalljie SPD, Smith RM (2007) Sample preparation techniques for the determination of trace residues and contaminants in foods. *J Chromatogr A* 1153(1–2):36–53. <https://doi.org/10.1016/j.chroma.2007.01.134>

- Ross T, McMeekin TA (2009) Risk assessment and pathogen management. In: Blackburn C d W, McClure PJ (eds) *Foodborne pathogens: hazards, risk analysis and control*, 2nd edn. Woodhead Publishing Limited, pp 113–153. <https://doi.org/10.1533/9781845696337.1.113>
- SCHER, SCENIHR, and SCCS (2012) Toxicity and assessment of chemical mixtures. doi: <https://doi.org/10.2772/21444>
- Teeguarden JG, Tan YM, Edwards SW, Leonard JA, Anderson KA, Corley RA, Kile ML et al (2016) Completing the link between exposure science and toxicology for improved environmental health decision making: the aggregate exposure pathway framework. *Environ Sci Technol* 50(9):4579–4586. <https://doi.org/10.1021/acs.est.5b05311>
- The Food Safety and Standards Act, 2006 (2006) <https://doi.org/https://legislative.gov.in/actsofparliamentfromtheyear/food-safety-andstandards-act-2006>
- Van Leeuwen SPJ, Van Cleuvenbergen R, Abalos M, Pasini AL, Eriksson U, Cleemann M, Hajslova J, De Boer J (2006) New certified and candidate certified reference materials for the analysis of PCBs, PCDD/fs, OCPs and BFRs in the environment and food. *Trends Anal Chem* 25(4):397–409. <https://doi.org/10.1016/j.trac.2006.01.011>
- Voysey P, Jewell K, Stringer M (2002) Risk characterisation. In: Brown M, Stringer M (eds) *Microbial risk assessment in food processing*. Woodhead Publishing Limited, pp 127–154
- Weisell R, Dop MC (2012) The adult male equivalent concept and its application to household consumption and expenditures surveys (HCES). *Food Nutr Bull* 33(3 Suppl):157–162. <https://doi.org/10.1177/15648265120333s203>
- WHO (2010) WHO human health risk assessment toolkit : chemical hazards. IPCS Harmonization Project Document



Nontoxic Natural Products as Regulators of Tumor Suppressor Gene Function

9

Dibya Ranjan Jalli and Debasmita Pankaj Alone 

9.1 Introduction

Cancer is a complex, multifactorial genetic disorder that includes misguided cell proliferation, invasion, metastasis, neo-angiogenesis (Baluk et al. 2005) and alteration of many physiological processes such as developing resistance to apoptosis. Any unregulated proliferation of cells is termed a tumor or neoplasm. When they evade surrounding normal tissue through the blood or lymph, it is called metastasis. Cancer specifically refers to malignant tumor or metastasis, and the overall process is known as carcinogenesis (Baba and Catoi 2007). Loss of function or gain of function mutation that contributes to abnormal cell proliferation is the key event in the process of carcinogenesis (Knudson 1986).

9.2 Cancer Critical Genes

Any genetic and epigenetic changes in a gene responsible for cancer are called cancer critical genes or drivers of cancer. These cancer critical genes are broadly classified into two different categories, i.e., proto-oncogenes and tumor suppressor genes. The protein products of proto-oncogenes are normally growth factors or transcription factors involved in cell growth and division (Albert et al. 2002), but any changes or mutations turn these genes into cancer-causing oncogenes. Mutation of a single copy of proto-oncogene drives the healthy cell to behave abnormally. So,

D. R. Jalli · D. P. Alone (✉)

School of Biological Sciences, National Institute of Science Education and Research (NISER)
Bhubaneswar, Khurda, Odisha, India

Homi Bhabha National Institute (HBNI), Mumbai, India

e-mail: debasmita@niser.ac.in

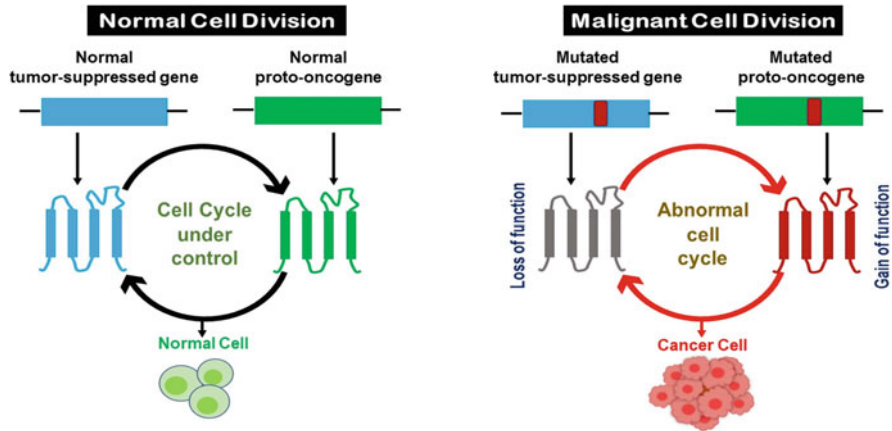


Fig. 9.1 In normal cell division, both the proto-oncogenes and tumor suppressor genes contribute towards regular cell growth and cell differentiation. But, a gain of function mutation of proto-oncogenes allows the cells to grow uncontrollably, whereas loss of function of tumor suppressor genes sets free brakes for cell proliferation thus leading the cell fate towards a cancerous state. Due to alteration in proto-oncogenes and tumor suppressor genes, the healthy cells transform into cancer cells. This figure is modified and retrieved from <https://app.biorender.com/biorender-templates/t-5ed6b0f2cc82d300ae329495-tumor-suppressor-genes-and-proto-oncogenes>

it acts dominantly like gain of function by a single mutation causing the cell to be cancerous (Fig. 9.1). On the other hand, tumor suppressor genes are normal genes which regulate controlled cell division and cell cycle arrest when the DNA is mutated (Cooper Geoffrey 2000).

9.2.1 Tumor Suppressor Genes

As the name suggests, tumor suppressor genes are good genes and are involved in normal cell growth and division. The products of these genes act on cell cycle checkpoints that will not allow unwanted cell proliferation. Mutations in these genes are usually recessive, which means it requires both copies of the genes either to be deleted or to be inactivated in a normal cell for it to transform into a cancerous cell. The protein products of tumor suppressor genes are cell division regulatory proteins, proteins regulating programmed cell death, and proteins involved in cell growth and survival (Wang et al. 2018). And the protein products perform the following functions.

- To regulate the expression of cell cycle checkpoint proteins
- To act on different cell cycle checkpoints to stop the abnormal growth
- To relay information regarding normal cell proliferation
- Receptors for growth and survival pathway
- Proteins that regulate response to damaged DNA

Tumor suppressor genes broadly fall under two categories: (1) Gatekeeper Genes and (2) Caretaker Genes.

A. Gatekeeper Genes

Gatekeeper genes are those genes or products of tumor suppressor genes that directly regulate or inhibit cell growth. Whenever there is a loss of function mutation or inactivation of both copies of these genes, the inhibitory product for cell growth fails to be formed, which allows the cells to grow uncontrollably thus initiating tumorigenesis. The cell loses control over its growth because of the absence or altered gatekeeper tumor suppressor genes. Gatekeeper genes generally have three different functions (Mina and Kumar 2016), which are as follows:

- Cell cycle regulator genes (e.g., *RBI*, *APC*, and *P53*)
- Cell cycle checkpoint genes (e.g., *CIP* or *KIP* family genes, namely *p21*, *p27*, *p57*, and *INK4* family genes, namely *p15*, *p16*, *p18*, and *p19*)
- Apoptosis-related genes (e.g., *BCL-XL*, *BCL-2*, and *BAX*)

B. Caretaker Genes

Caretaker genes are those tumor suppressor genes that maintain overall genetic stability. These involve DNA repair genes and the genes that are required in maintaining genome stability. Mutation or any alteration in caretaker genes may lead to the loss of function of other vital genes. Caretaker genes are not directly involved in the regulation of cell proliferation, but they slow down cell division so that the cells get enough time to repair their damaged DNA thereby preserving the overall genomic stability. Mutations in these genes may end up in an altered expression of the products of gatekeeper genes which directly leads to the process of carcinogenesis. *BRCA1*, *BRCA2*, *MSH2*, and *MLH1* are some examples of caretaker tumor suppressor genes (Table 9.1). Some other tumor suppressor genes are *WT-1*, *NF-1*, *VHL*, and *PTEN* (Deiningner 1999).

Table 9.1 List of a few tumor suppressor genes, their chromosomal and cellular location, and function

Gene	Chromosome	Location	Function
<i>Rb</i>	13	Nucleus	Cell cycle
<i>APC</i>	5	Cytoskeleton	Cell-cell recognition
<i>p53</i>	17	Nucleus	DNA repair, apoptosis
<i>INK4A</i>	9	Nucleus	Cell cycle/p53function
<i>Bcl2</i>	18	Mitochondria	Apoptosis
<i>Brca2</i>	17	Nucleus	DNA repair

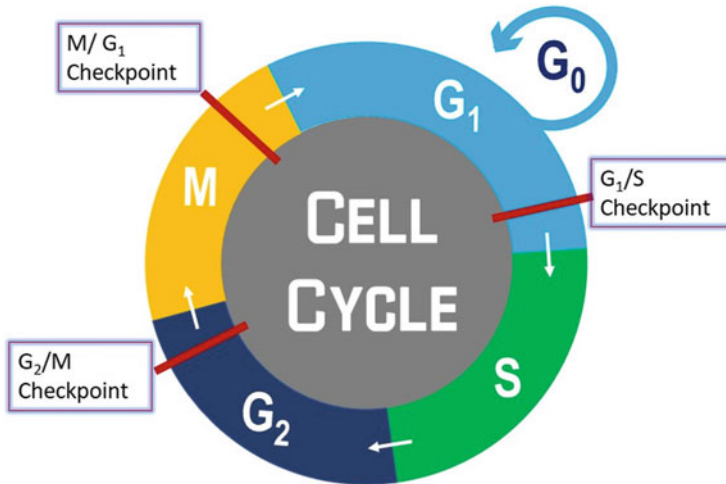


Fig. 9.2 A schematic representation of different steps of the cell cycle and its checkpoints. The blue arrow mark shows the G₀ resting phase, and the red lines are the checkpoints of different steps in the cell cycle. G₁/S checkpoint checks for nutrients, growth factors, and damaged DNA. G₂/M checkpoint analyzes the cell content, DNA replication, and genome integrity. If minor errors are found, the cell cycle halts and the cell performs several repairs in response to the damaged DNA. But in case of irreparable damage, cell signals for apoptosis pathway to ensure the damaged DNA is not passed on to the daughter cells. M/G₂ or spindle checkpoints check for proper chromosome spindle attachment. If the external conditions are not favorable, like temperature, improper nutrients, and energy, then the cell enters into the G₀ phase until the condition becomes favorable. This figure is modified and retrieved from <https://app.biorender.com/biorender-templates/t-5ecc32496890b000b56a3678-cyclins-cell-cycle-regulators>

9.2.2 Cell Cycle Check Points

Cell cycle or division of cells occurs in a sequence with high accuracy and fidelity to assure each daughter cell receives an equal and exact amount of genetic material. Chromosome duplication and cell division must occur in a regulated manner. Normal cells proceed through the cell cycle in a regulated manner, which ensures cell division in favorable conditions. Also, by examining the signals from internal and external sources, cells will decide when to proceed, wait, or stop division. Numerous stops have been set throughout the cell cycle to ensure the cells are prevented from dividing in adverse conditions. These points are known as cell cycle checkpoints (Fig. 9.2). They help the cell to halt cell division if the DNA is damaged, so the cell will get enough time to repair the damage and proceed to the next step. If the damage is irreparable, the cell will undergo apoptosis (Surova and Zhivotovsky 2013). Deviation in the regulation of these checkpoints drives the cells to become cancerous. These checkpoints are as follows:

- (a) G1 checkpoints or G1/S transition
- (b) G2 checkpoints or G2/M transition
- (c) Spindle checkpoint, i.e., during the transition from metaphase to anaphase

9.2.3 Cell Cycle Control System

A significant factor or the protein complex that induces mitosis or has a remarkable role in cell maturation is identified as the maturation-promoting factor (MPF). MPF acts like an engine that drives the progression of the cell cycle from one step to the next. MPF mainly comprises two subunits, i.e., cyclins (regulatory component) and cyclin-dependent kinases or CDKs (catalytic component and acts as a protein kinase). These two subunits are activated when they combine to form a complex, and this complex helps the cell to cross various checkpoints of the cell cycle (Malumbrace 2014). Cyclins are so named as these proteins are continuously made and degraded during the cell cycle.

Cyclins regulate the cell cycle when they are bound to CDKs. To be fully active, the cyclin-CDK complex needs to be phosphorylated at specific positions. There are four types of cyclins that are present in eukaryotic cells, namely cyclin A, cyclin B, cyclin D, and cyclin E. The concentration of these cyclins fluctuates throughout the cell cycle. On the other hand, CDKs are a group of proteins that constitute the family of protein kinases. Kinases fall under the class-III enzyme category, which adds a phosphate group to the target (Malumbrace 2014).

CDKs are so named because their activities are regulated by cyclins. They catalyze their target by phosphorylating the specific serine-threonine residues. As CDKs are cyclin-dependent and different cyclins are present in various steps of the cell cycle (Fig. 9.3), the target proteins that are to be activated for smooth progression of the cell cycle are also different. The target protein phosphorylated by the cyclin-CDK complex helps the cell cycle advance to the next phase. The concentration of CDKs is stable throughout the cell cycle. The phosphorylation event of the target protein by the Cyclin-CDKs complex is transient and reversible. Once the cell complex disappears, the target protein gets dephosphorylated. CDK4/6, CDK2, and CDK1 are involved with different cyclins to form their respective complex and are found in eukaryotic cells. Different cyclins bind with CDKs to form a complex and catalyze the target proteins at specific points of the cell cycle and thus regulate the cell cycle.

9.2.4 Role of CKIs in the Regulation of Cell Cycle Control

Cyclin-dependent Kinase Inhibitors, abbreviated as CKIs, are the protein involved in cell cycle regulation. These CKIs include two major families, i.e., the CIP/KIP (CDKs Inhibitory Protein/Kinase Inhibitory Protein) family and INK4 (Inhibitors of CDK4) family. Both these CIP/KIP and INK4 family proteins are categorized under tumor suppressor gene as primarily they inhibit the activities of all CDKs responsible for the regulation of cell cycle in unfavorable conditions. The CIP or KIP family includes three proteins, namely p21, p27, and p57, that attach and suppress

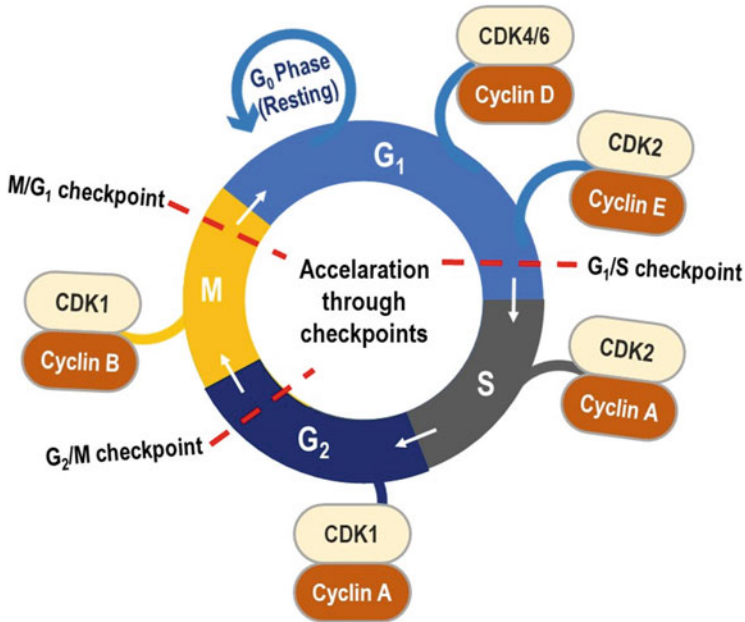


Fig. 9.3 This diagram depicts the cell cycle control system. Various CDKs bind with cyclins to make regulatory complexes. These complexes act on various checkpoints and phases of the cell cycle to trigger the cell cycle to transition from one point to the next. Cyclin D and CDK4/6 complex works in the early G1 phase. Cyclin E and CDK2 complex regulate the event at the G1/S checkpoint. Cyclin A-CDK2 complex regulates the completion of the S phase. CyclinA-CDK1 complex acts as a molecular switch that regulates the events in the G2/M checkpoint. Cyclin B-CDK1 complex is responsible for the M phase. All these cyclin-CDKs complexes act at different phases of the cell cycle by phosphorylating different target protein downstream. This figure is modified and retrieved from <https://app.biorender.com/biorender-templates/t-60087bed1a8a0000a4a460f0-cell-cycle-deregulation-in-cancer>

the activities of all CDKs (Starostina and Kipreos 2012), whereas the INK4 family has four proteins; p15, p16, p18, and p19 that specifically bind either to CDK4 or CDK6 and impede the action of cyclin D (Fig. 9.4) (Roussel 1999).

9.2.5 Role of RB in Cell Cycle Control

The first phenotypic tumor suppressor gene to be discovered is the *RB1* (Retinoblastoma1) gene that codes for a protein known as pRB. The protein product of the *RB* gene negatively regulates the cell cycle. When the cell is ready to divide, pRB gets phosphorylated and becomes inactive to allow cell cycle progression. The function of pRB in the cell cycle is mainly regulated by the E2F family of transcription factors (Giacinti and Giordano 2006). Loss of function mutation of *RB1* gene is associated with retinoblastoma, a malignant tumor of the retina, and many other tumors. This *RB1* gene is located on chromosome 13q14.2, and the molecular weight of this

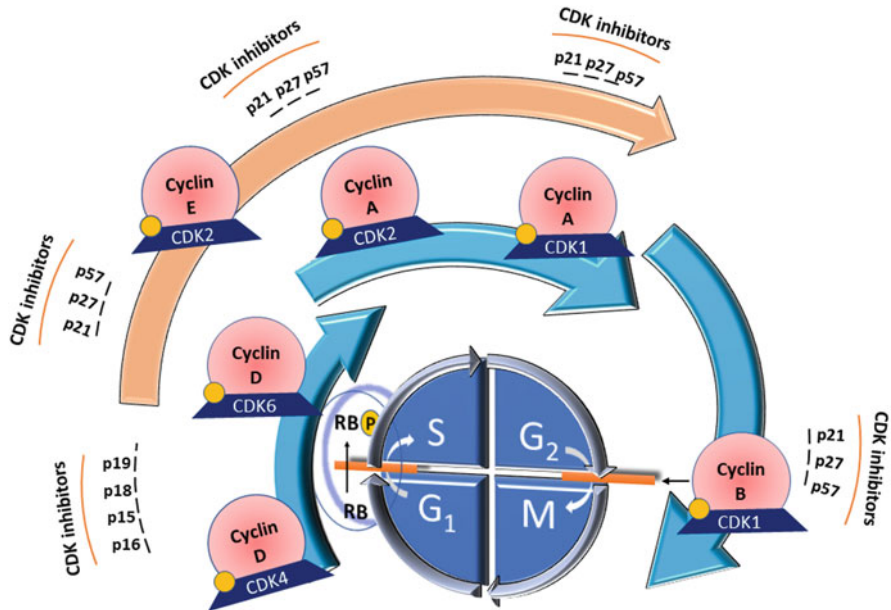


Fig. 9.4 Schematic representation of CKIs family proteins regulate the cell cycle at different checkpoints by catalyzing with cyclin-CDKs complexes. These tumor suppressor proteins act on cell cycle checkpoints and stop uncontrolled growth. The RB proteins sense the mutagenic stress from the environment and counter it by applying brakes in cell proliferation. Growth inhibition is triggered by inhibiting phosphorylation of RB protein; thus, the E2F transcription factor cannot get released to take part in the replication of DNA. Thus, cell cycle arrest is done at the G1 phase. These biochemical processes suggest that CKIs family proteins act as a tumor suppressor or anti-oncogenic. This figure is modified and reprinted from Lucia, C., leal-Esteban., et al., “Cell cycle regulation in cancer cell metabolism,” *Biochimica et Biophysica Acta (BBA)- Molecular Basis of Disease*, 1866 (2020): 165715.doi: <https://doi.org/10.1016/j.bbadis.2020.165715>

protein is 110 kDa. It helps in excessive cell cycle progression as well as its differentiation by binding with the E2F transcription factor. E2F transcription factor helps in the synthesis of Cyclin A protein which is needed in the S phase of the cell cycle (Fig. 9.5). So unphosphorylated or hypo-phosphorylated pRb protein blocks the cell cycle progression.

9.2.6 Role of P53 Protein in Cell Cycle Regulation

The TP53 protein with an apparent molecular weight of 53 kDa is encoded by the tumor suppressor gene *p53*. It protects the cell from becoming cancerous by checking unregulated cell growth, activates the expression of other genes to fix damaged DNA, and promotes programmed cell death or apoptosis if the damage cannot be reverted. It is also known as the “guardian of the genome” because it is

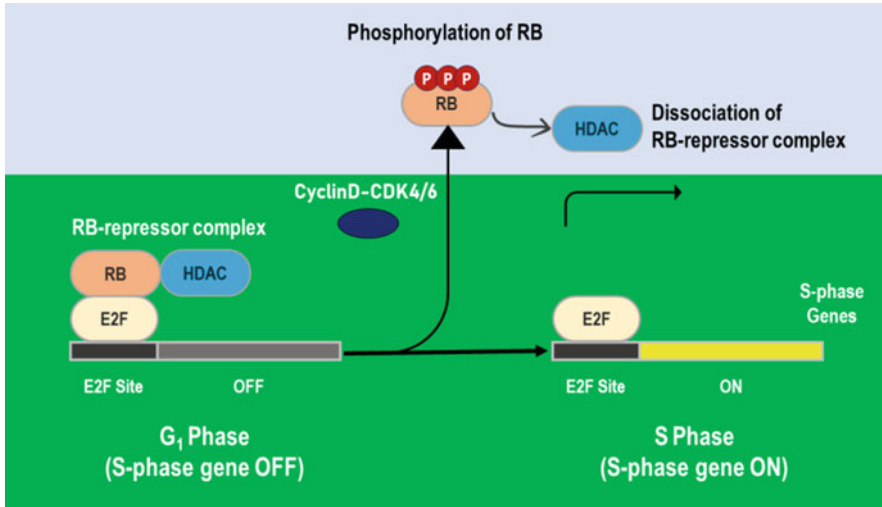


Fig. 9.5 Rb and Rb-PPP illustrate the unphosphorylated and the phosphorylated morphs of the retinoblastoma protein. The association of RB protein with the E2F transcription factor blocks its transactivation domain at G0 and early G1. Around the late G1 phase, due to the cyclinD-CDK4/6 complex, RB protein gets phosphorylated and detached from E2F to permit the synthesis of protein products needed for the S phase. Generally, RB protein attaches with HDAC (Histone Deacetylase) to repress the expression of genes for the S phase. Cyclin-CDK4/6 complexes regulate the RB/E2F activity. The phosphorylation of RB protein accompanied by cyclin D-CDK 4/6 and cyclin E-CDK2 complexes in G0 and G1, respectively, that triggers the release of the E2F transcription factor to produce cyclin A protein needed for the cell cycle to enter into the S phase. This figure is modified and retrieved from <https://app.biorender.com/biorender-templates/t-5f2c644eb9908c00b11d9ed7-g1s-checkpoint>



Fig. 9.6 A simplified diagram depicts the growth arrest response by p53 protein when the cell is under stress. Whenever the cell senses stress like DNA damage or oxidative stress, p53 protein acts as a transcription factor for the *p21* gene and binds DNA, that triggers the synthesis of p21 protein, which in turn interacts with CDC2, cell division stimulating protein. After p21 forms a complex with CDK2, the cell cycle is halted. Due to the inhibition of the CDK2 enzyme by p21, the progression of the cell cycle to the S phase is declined. CDC2 is cumulatively obstructed by p21, GADD45, and 14-3-3, so a succession of the cell cycle to M phase is ceased. The expression of these inhibitory proteins is regulated by p53 thus causing growth arrest. This image is modified and retrieved from <http://www.bioinformatics.org/p53/introduction.html>. Assessed on 22 Dec 2021

essential for regulating DNA repair and cell division. It is located on human chromosome 17p13.1. It performs major functions like cell cycle regulation and apoptosis (Fig. 9.6). Mutation in the *p53* gene leads the normal cell to proliferate



Fig. 9.7 It depicts the p53-mediated apoptosis pathway. Bax is a proapoptotic protein, also known as Bcl-2-associated protein in the Bcl-2 gene family. Under cellular stress, p53 binds to the *Bax* gene and allows its transcription to produce Bax protein. Bax protein creates small holes in the mitochondrial membrane. That results in the release of cytochrome-c into the cytosol, where it reacts with Apaf1 protein to activate caspase9 and the subsequent dimerization of caspase9 leads to apoptosis. The p53 protein also acts as a transcription factor for other proapoptotic proteins like NOXA and PUMA. This figure is modified and retrieved from <http://www.bioinformatics.org/p53/introduction.html>. Assessed on 22 Dec 2021

abnormally and become cancerous. Almost 50% of all human tumors are generated due to mutation in the *p53* gene. Usually, normal cells have low levels of p53 because of its proteasomal degradation by MDM2 (Mutant Double Minute2), functioning as E3 ubiquitin ligase (Haupt et al. 1997). Any genotoxic stress leads to an increase in p53 protein levels. It normally responds to cellular stress like DNA damage, oxidative stress, and DNA replication stress by accomplishing the following events (Pflaum et al. 2014):

- Growth arrest
- DNA repair
- Apoptosis
- Antioxidant defense
- Senescence

So any alteration or deletion mutation in the *TP53* gene does not allow the cell to grow and divide uncontrollably and triggers the cell to become cancerous.

P53 triggers growth arrest by regulating the p21 expression when the cell is under stress or mostly with damaged DNA (Macleod et al. 1995), P21 arrests the cell at G1 phase by directly acting on the cell cycle stimulating proteins. In response to this halt, the cell repairs all of its damaged DNA and signals to the regulators to proceed further. But if the cell contains damaged DNA or the damaged DNA is irreparable, then the cell undergoes a suicidal apoptotic mechanism to prevent unwanted proliferation (Fig. 9.7). If the cell has mutated the *p53* gene, then arrest at G1 phase will not occur, which will drive the cell to become cancerous.

Because of its ability to trigger apoptosis, the effectiveness to target p53 in treatment options like chemotherapy and radiation is more promising. Due to the mutation in p53, cancer cells will not be able to divert towards apoptosis and get extremely unresponsive to further treatments. So p53 is also known as a cellular gatekeeper or molecular policeman that can sense cellular stress and responds by performing growth arrest, DNA repair, and apoptosis.

9.2.7 Role of APC as a Tumor Suppressor Gene

Besides the mutations in RB and P53, a number of mutations in tumor suppressor genes are observed to play a role in some cancers. Thousands of precancerous polyps or adenomas from the epithelial cells that line the colon wall develop in inherited Familial Adenomatous Polyposis, abbreviated as FAP. If not removed, the cells within the polyps are very likely to transform into fully cancerous cells. This is due to a deletion of a small region in the long arm of chromosome 5, which is identified as the gene encoding Adenomatous Polyposis Coli or APC. In case of loss of function mutation of APC, the epithelial cells of the colon wall lose their controlled growth ability and over-proliferate to form polyps instead of normal epithelial cells lining the wall (Nagase and Nakamura 1993). It is not only found in inherited cases but also 80% of sporadic cases are developing this devastated FAP. For instance, somatic mutation of the *APC* gene is associated with carcinomas of the stomach, pancreas, colon (Nakatsuru et al. 1993), and melanoma (Worm et al. 2004).

The APC protein or Adenomatous Polyposis Coli is a protein found in humans encoded by the *APC* gene that negatively regulates β -catenin levels and interacts with E-cadherin, which is involved in cell adhesion (Kwong and Dove 2009). β -catenin generally elevates the expression of such proteins, which have a key role in cell growth and multiplication and differentiation. The protein product of the *APC* gene is a key tumor suppressor protein having multiple domains through which it binds to various proteins and generates a destruction complex that checks the level of β -catenin inside the cell. Loss of function mutation of *APC* will result in a loss of control over the production of β -catenin, which allows the cells to grow and divide in a misguided manner resulting in a malignant state. It plays a significant role in other cellular processes like the protein product of *APC* gene ensures correct arrangements of chromosomes following the cell division in alliance with proteins that take part in the cell growth signaling pathway. Protein APC interacts with mitotic spindles and guides them towards accurate attachment with the kinetochore complex of sister chromatids to ensure faithful chromosome arrangements (Tarafa et al. 2003).

9.2.8 BRCA1 and BRCA2

BRCA1 (Breast Cancer susceptibility gene 1) and *BRCA2* (Breast Cancer susceptibility gene 2) are the caretaker tumor suppressor genes that have been associated with most inherited cases of breast cancer and also incriminated in some ovarian cancers (having a very high mortality rate) (Antoniou et al. 2003). The *BRCA1* gene is located on 17q21, and the cytogenetic position of *BRCA2* is 13q12.3. We are all born with two copies of the *BRCA1* and *BRCA2* genes. Some individuals have a genetic mutation on one of their copies. This causes the gene to deviate from its usual course of downstream regulatory action, and, in doing so, it heightens the risk of falling prey to certain cancer types. Men and women who carry a *BRCA1* and *BRCA2* gene mutation may also be at an elevated risk of developing other cancers like pancreatic cancer, melanoma, colon cancer, and stomach cancer. A harmful

BRCA1 and *BRCA2* gene can be inherited from either of the parents. The effect of a mutation can also be seen even if the alternate copy of the gene is normal. Both men and women can be equally affected by this cancer if they have a mutation in both copies of the gene. Both these genes have two distinct roles, i.e., as a transcription factor and a part of the cell's DNA repair machinery (Tai et al. 2007). Whenever a cell senses double-stranded DNA break, both BRCA genes will allow the production of ATM (Ataxia Telangiectasia Mutated) and Chk2 (Checkpoint kinase2) by acting as a transcription factor to *ATM* and *Chk2* genes (Junran et al. 2004). These are the damage recognition proteins that phosphorylate the BRCA1 + BRCA2 + RAD51 complex in association with other proteins to repair the double-stranded break (Orhan et al. 2021). If the damage is irreparable, it leads to the activation of p53, which in turn acts as a transcription factor for p21 that binds to and inhibits CDKs activity and blocks the entry of cells into the S phase.

9.2.9 PTEN

Phosphatases and TENs in homolog is a phosphatase abbreviated as PTEN and is encoded by the *PTEN* gene located on chromosome 10q23.31. *PTEN* is a tumor suppressor gene encoding the protein PTEN of 403 amino acids, which has both lipid and protein phosphatase activities. PTEN is found in all tissues of the body. It is the most common tumor suppressor in human cancers, and its deregulation is also implicated in several other diseases as the phosphate intricately involved in cell cycle regulation will not allow the cell to grow and divide uncontrollably. Protein encoded by the PTEN tumor suppressor gene is an interesting example of antagonism between oncogenes and tumor suppressor gene products. PTEN prevents irregular cell growth, proliferation and survival by downregulating the PI3 kinase-dependent pathway (Carracedo and Pandolfi 2008). PTEN dimer hydrolyzes PI3 (Phosphatidylinositol 3, 4, 5-triphosphate), resulting in the generation of PIP2, a dephosphorylation product of PIP3. By dephosphorylation of PIP3, PTEN antagonizes the activities of PI3 kinase and AKT. *PI3 kinase* and *AKT* act as oncogenes by promoting cell survival. Conversely, the loss of function mutation of PTEN can contribute to tumor development as a result of increased levels of PI3 kinase and AKT and inhibition of programmed cell death. Loss of function of PTEN gene makes defective PTEN protein that is unable to apply the brakes on cell growth or cannot trigger the deregulated cells to die hence leading to the occurrence of tumor. Any change in PTEN protein like phosphorylation at its active site, covalent modification by ubiquitinylation, oxidation reaction, and addition of acetyl group can cause an alteration in its activity. Phosphorylation and dephosphorylation at the C-terminal end of PTEN protein lead its way towards its inactive and active state, respectively. Active PTEN guards the cell cycle at G1/S transition, and in case of any deviation, it will not allow the cell to enter in S phase by upregulating p27, which inhibits the formation of cyclin C/CDK2 complex (Mamillapalli et al. 2001). PTEN also regulates the movement and relocation of cells, and any change in the PTEN gene leads to flag the event of metastasis.

9.2.10 WT1

WT1 (Wilm's Tumor 1) is Wilm's tumor-associated gene located on chromosome 11p13. Normal function of the *WT1* gene is the synthesis of protein WT1 required for the development of kidney (Kreidberg et al. 1993) and gonads (ovaries of female and testes in male) at the embryonic stage (Wilhelm and Englert 2002). After birth, the activity of WT1 is restricted to form glomerulus, present in the Bowman's capsule of the nephron and helps in filtering blood through the kidney. The WT1 protein regulates the transcription of numerous genes and functions both as an activator and a transcriptional coactivator or as a repressor of gene expression. Due to the ability of WT1 to bind to RNA, it can also be detected in the cytoplasm of many cells. WT1 plays a vital role in cell growth, proliferation, and differentiation, after which the cell will mature to carry out specific functions at concerned locations. This protein has the ability to bind to different regions on DNA thus influencing the expression of different genes necessary for cell survival and growth. Due to the presence of four zinc finger motifs and proline/glutamine-rich domain at C- and N-terminus, respectively, it can potentially bind to DNA (Hirose 1999). WT1 represses the transcription of growth factors like Platelet-Derived Growth Factor and Insulin-like Growth Factor 1 thus arresting cell proliferation (Wang et al. 1992; Gangyi et al. 1997).

9.2.11 VHL

VHL is a tumor suppressor gene; loss of function mutation causes Von Hippel-Lindau syndrome. It is an autosomal dominant syndrome in which the patient has a high incidence of cysts in multiple organs and may also be associated with tumor risk. The *VHL* gene is located on chromosome 3p25. The protein product of the *VHL* gene acts as a component of substrate recognition in a protein complex that includes a series of other proteins. The main function of VHL protein is its E3 ubiquitin ligase activity that downgrades the concerned protein target (Fig. 9.8). The main target of this protein product is HIF 1 α (Hypoxia Inducible factor 1 α) which allows enhanced angiogenesis by promoting the expression of angiogenesis factors like Platelet Derived Growth Factor and Vascular Endothelial Growth Factor (Na et al. 2003).

9.2.12 NF1

Neurofibromatosis abbreviated as NF is a group of genetic disorders that causes tumors in nervous tissue. These are two types, namely, NF1 and NF2. The *NF1* is a tumor suppressor gene found in the human chromosome 17, involved in normal cell growth and division. Any change in NF1 makes it lose its ability to synthesize neurofibromin, allowing over-proliferation in the cells. Neurofibromin is a tumor suppressor protein and a GTPase activating enzyme, which is a negative regulator of the *ras* gene. Neurofibromin increases the rate of GTP hydrolysis of RAS. When the NF1-RAS complex assembles, active RAS binds to the catalytic domain of NF1 and

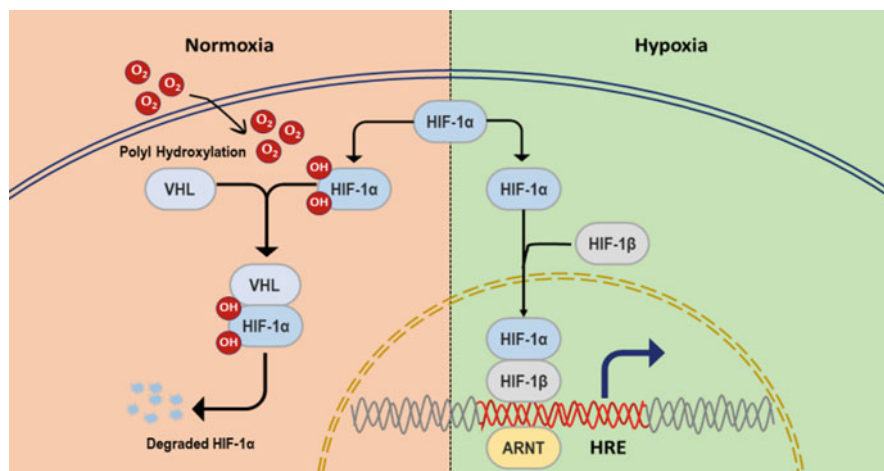


Fig. 9.8 This image represents the regulation of HIF 1 α (Hypoxia Inducible Factor 1 α) by VHL. Under normal conditions, there is a proteasomal degradation of HIF 1 α by the E3 ubiquitinase activity of VHL. VHL can attach to HIF 1 α via the hydroxylated proline residues. Under hypoxia condition, proline residues of VHL are not hydroxylated, so it cannot bind to HIF 1 α . Now the free HIF 1 α acts as a transcription factor for downstream angiogenesis growth factors by allowing the expression of HRE (Hypoxia Response Element). Due to a mutation in the *VHL* gene, it loses its property to degrade HIF 1 α . Free HIF 1 α will maintain a hypoxia environment which is more suitable for the malignant cells to proliferate abnormally. This figure is revised and retrieved from <https://app.biorender.com/biorender-templates/t-5ffe0f2123ca6b00a7467b51-hif-signaling>

thus decreases the activity of RAS (Bollag and Clapp 1996). The deficiency of neurofibromin increases GTP and upregulates the RAS pathway because RAS binds to GTP only and not GDP. This results in dysregulated cell division.

9.3 Natural Products and its Role in Regulating Tumor Suppressor Genes Function

Cancer is a devastating disease and is often chronic in nature with an increased death rate. Currently, available treatment options like radiotherapy, chemotherapy, and surgery are not sufficient to combat this disease. As cancer is a multistep disorder in terms of its numerous oncogenic factors and the several physiological processes they affect, targeting a single step provides disappointing cure rates. Combinatorial medications or pharmaceuticals are the newly emerged treatment option nowadays. Most pharmaceuticals are natural compounds or secondary metabolites of natural products used since ancient times to cure diseases. Moreover, herbs are natural compounds that are ingested with diet to prevent the occurrence of various diseases. A long history exists of natural products derived from plants, fungi, and microorganisms that have been used in the treatment and prevention of chronic diseases. Many natural products have been showing chemo-preventive and

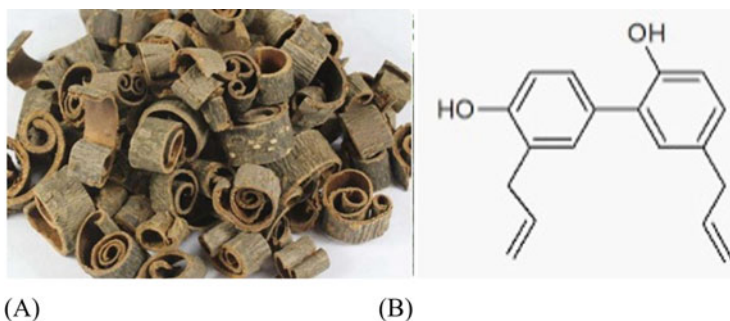


Fig. 9.9 (a) and (b) represent the bark of *Magnolia officinalis* from which the herb is extracted and the structure of honokiol, respectively. Honokiol is a biphenolic natural product. (Source credit: [Google.com](https://www.google.com))

anticancer activities. There is an emerging focus on natural products that include dietary phytoconstituents in preventing cancer onset and treatment options. Owing to the chemo-preventive action of natural products and other medicinal properties, these are being considered for in-depth research as pharmaceutical agents for preventing, blocking, or altering the progression of invasive cancers. The systematic consumption of natural products in diets like fruits, vegetables, and herbs provides promising chemoprevention or delay in the development or onset of cancer due to a multitude of effects of these products on diverse molecular signaling pathways with no or minimal toxicity to normal cells. Here, we will discuss a few natural products and their activities, such as growth arrest and induction of apoptosis by regulating tumor suppressor genes.

9.3.1 Honokiol

Honokiol is a bioactive compound extracted from the bark of *Magnolia officinalis* from the family Magnoliaceae (Fig. 9.9). The seed flowers and bark of *Magnolia sp.* have long been used as sources of traditional medicines. Honokiol has already been tested in human prostate cancer cell lines, namely PC-3 and LNCaP, in which a sharp decline in cancer cell number was observed in a concentration- and time-dependent manner. The molecular pathways suggest honokiol arrests the cell cycle at G0 and G1 phase triggering the upregulated expression of p21 and p27, which in turn binds with CDKs to accomplish growth arrest. Also, honokiol-treated prostate cancer cell lines show a distinct decline in the pRB protein level that reduces the transcriptional activities of E2F. As E2F activity is suppressed, it is unable to transcribe the genes needed for the S phase thus the cell cycle is halted. It also increases the PTEN expression, which in turn inhibits the PI3k/AKT pathway that allows the cells to proliferate (Fried and Arbiser 2009).

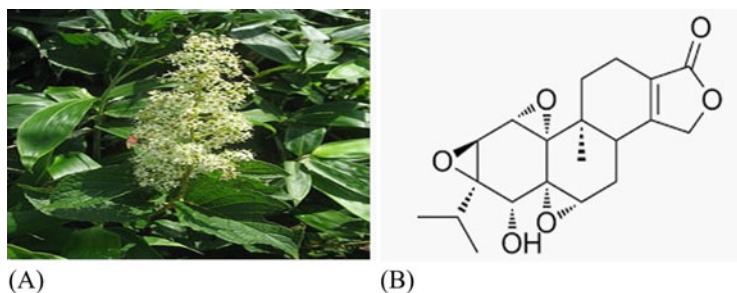


Fig. 9.10 (a) and (b) show the herb *Tripterygium wilfordii* is a vine from which the drug is extracted and the structure of Triptolide. (Source credit: [Google.com](https://www.google.com))

9.3.2 Triptolide

Triptolide is extracted from a herb called *Tripterygium wilfordii*, sometimes called thunder god vine but most popularly known as thunder duke vine (Fig. 9.10a). It exhibits anti-proliferative and proapoptotic functions. Triptolide shows increased p21 expression (Huang 2013). The p21 protein (gene located on chromosome 6) regulates the cell cycle by binding with cyclin-CDK 1, 2, 4/6 complexes thus inhibiting their activity to impair cell growth. It also reduces pRB phosphorylation that does not allow the transcription activity of E2F needed for downstream expression of cell cycle proteins (Tao et al. 2011). It has high anti-tumor activities, but its physical and severe toxicity limits its therapeutic potential. Pharmaceutical formulation of this herb has a wide variety of secondary metabolites, which are potentially showing high antiproliferative activity with less toxicity.

9.3.3 Lichochalcone A

Lichochalcone, a well-known novel estrogen, is obtained from the herb *Glycyrrhiza glabra* (commonly known as licorice root), which is a flowering plant of the bean family Fabaceae (Fig. 9.11). This is an aromatic chemical that can be extracted from the root and which shows anti-tumor activities in various human cells. Lichochalcone does not allow the phosphorylation of pRB by downregulating the expression of cyclin D and CDK 4/6. Thus, pRB does not detach from E2F to allow it to make necessary protein for the S phase (Kitagishi et al. 2012). This triggers the cell cycle arrest at G1 phase. Lichochalcone A activates JNK1 (c-Jun N-terminal kinase) which increases the expression of p21. Then p21 interacts with CDK1 to block the cell at G2 checkpoint. JNK1 also activates p53 through a cascade of intermediates if the cell is under severe stress, p53 transcribes the *Bax* gene, which induces cell apoptosis via intrinsic pathway (Lin and Tian 2017).

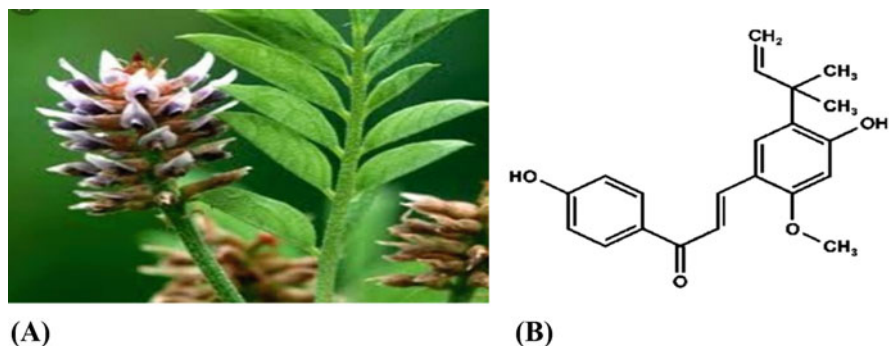


Fig. 9.11 (a) and (b) depicts *Glycyrrhiza glabra*, the plant from which this product is extracted and the molecular structure of Lichochalcone, a chalconoid. (Source credit: [Google.com](https://www.google.com))



Fig. 9.12 (a) shows the *Acanthopanax gracilistilus* with blackberries and (b) shows the bark of herb and AGE extract in powder form. (Source credit: [Google.com](https://www.google.com))

9.3.4 *Acanthopanax gracilistilus*

Acanthopanax is a herb of thorny shrubs and trees that has long been used as a popular Chinese medicinal herb from the family Araliaceae. *Acanthopanax gracilistilus* extract or AGE is prepared from dried barks and has been used in the treatment of various autoimmune diseases and cancer in China (Fig. 9.12). In vitro testing in MT-1, HL-60, and HSC-2 cell lines has revealed an inhibitory effect of this herb on the proliferative potential of cancer cells. The pathophysiology of AGE suggests that it decreases the expression of CDK2/4 that will not be able to phosphorylate the pRB protein needed for cell cycle progression to the next phase. Thus, it triggers growth arrest at G0 and G1 stages (Shan et al. 2000).

9.3.5 Ginsenosides

Ginsenosides, extracted from the plant *Panax ginseng*, have been used in traditional medicine for a long time (Fig. 9.13). Ginsenosides are derived from several parts of the plant, especially from the root. Till date, around 40 ginsenoside compounds have been discovered. Rb1, Rg1, Rg3, Re, Rd., and Rh1 are the most commonly used ginsenosides. Each ginsenoside has the ability to bind to monomeric, dimeric, or trimeric sugar as they have at least two (at carbon position 3 and 20) or three (at carbon position 3, 6, and, 20) free hydroxyl groups. On the basis of their chemical structure, they are broadly classified into two different categories: Protopanaxatriols (Re, Rf, Rg1, Rg2, and Rh1) and Protopanaxadiols (Rb1, Rb2, Rc, Rd., Rg3, Rh2, and Rh3). Ginsenosides inhibit tumor growth by regulating the cell cycle and apoptosis. Ginsenosides Rg3 has already been tested in osteosarcoma cell lines in which it triggered programmed cell death and cell cycle arrest at G0/G1 phase by upregulating the expression of p53 and p21, which in turn suppresses the activity of cyclin B-CDK2, 4, and 6 complexes. The apoptotic molecular pathology suggests ginsenoside Rg3 did not allow the proteasomal degradation of p53 by inhibiting the action of MDM2, which directed the cell to sense cellular stress and prompt it towards the intrinsic apoptosis pathway (Zhang and Li 2015).

Ginsenosides promote apoptosis via both endogenous and exogenous pathways. Some ginsenosides such as Rg3, Rg5, Rh2, Rk1, Ck, and PPD can promote endogenous programmed cell death. They upregulate the proapoptotic proteins like Bax and downregulate the antiapoptotic proteins like Bcl-2 and Bcl-x that results in the loss of membrane potential of mitochondria and activates caspase9. Rg3, Rh2, Ck, and PPD can also trigger extrinsic programmed cell killing by upregulating P53 expression. These natural products also trigger DR4, DR5, and Fas to activate caspase8 (Chen et al. 2018). Both the intrinsic and extrinsic death induces pathways that stimulate the downstream effector receptors to finally activate

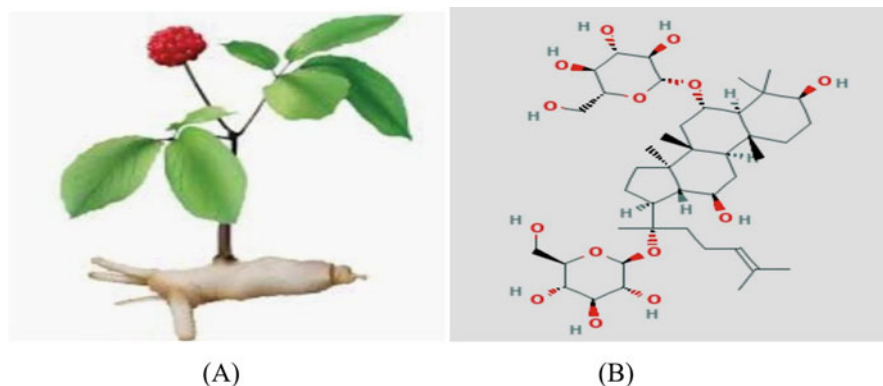


Fig. 9.13 (a) and (b) represent the plant *Panax ginseng* from which it is extracted and the molecular structure of Ginsenosides. (Source credit: [Google.com](#))

caspase3 and caspase7, which break down PARP (polyadenosine diphosphate ribose polymerase) to allow the cancerous cell to enter apoptosis.

9.3.6 Curcumin

Curcumin is derived from the roots of *Curcuma longa*, a flowering plant of the ginger family Zingiberaceae (Fig. 9.14). The yellow color of turmeric is due to the presence of curcumin which is a natural phenol derivative. It shows keto-enol tautomer, i.e., which exists in enolic form in organic solvents and keto form in water. Curcumin has a wide variety of pharmacological activities like antifungal, antibacterial, anti-inflammatory, antioxidant, and anticancer. Curcumin can be used as a therapeutic agent in almost all human cancer types as it targets diverse signaling pathways involved in tumorigenesis. In conjugated form, curcumin downregulates tumor-inducing proteins like p13k, AKT, MAPK, and ROS (Rafiq et al. 2018). Besides, curcumin also suppresses the activity of cyclin-CDKs complexes by upregulating p21 and p27 protein levels. It also downregulates the expression of numerous proteins that are directly involved in cell growth and proliferation thus triggering cell cycle arrest at different phases of the cell cycle (Zhou et al. 2011). Curcumin inhibits tumor growth in *l(2)glDrosophila* in-vivo brain tumor model through ROS-mediated action (Das et al. 2014).

It has been observed that curcumin inhibits the expression of the *Akt* gene and activates the *p53* gene for downstream signals like DNA repair, apoptosis, and cell cycle arrest. Molecular targets of curcumin involve almost all tumor suppressor genes. Curcumin also inhibits WT1 gene expression in leukemia cell lines and PANC1 (Glienke and Maute 2009). WT1 protein is involved in cell differentiation. In the leukemic k562 cell line, the WT1 expression decreases as curcumin affects the promoter binding region of *WT1* gene (Anuchapreeda 2006). The effect of curcumin

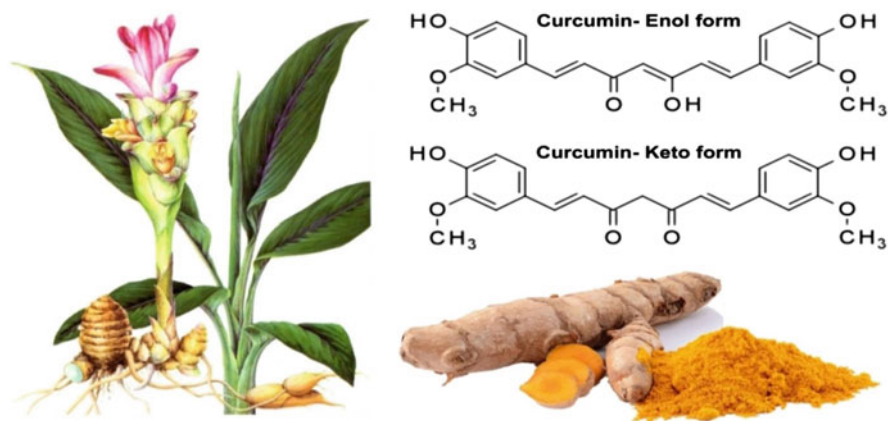


Fig. 9.14 The figure depicts the rhizomes of the plant *Curcuma longa*, the molecular structure of curcumin, along with the turmeric powder. (Source credit: [Google.com](https://www.google.com))

on WT1 expression may be useful in the future development of therapeutics for leukemic patients. Activated cancer-associated fibroblast (CAFs) is a disease which is repressed by curcumin. It upregulates p16 and other proteins while inactivating the JAK2/STAT3 pathway. Curcumin can trigger DNA damage-independent and safe senescence in stromal fibroblasts.

9.3.7 Genistein

Genistein is extracted from soybeans or soy products from the plant *Genista tinctoria*, which is a species of flowering plant in the family of Fabaceae (Fig. 9.15). It is popularly known as the dyer's greenwood or dyer's broom. It structurally resembles the class of compounds called isoflavones. It regulates tumor growth by inducing apoptosis, cell cycle arrest and acts as an inhibitor of many angiogenic factors (Yu and Zhu 2012). Primarily, genistein induces apoptosis by increasing the expression of Bax proapoptotic protein (Kim et al. 2009). It represses and downgrades the cell proliferation marker known as Cdc25C, which plays a vital role in stimulating the cyclin B-CDK1 complex (Randall and Keith 2003).

9.3.8 Sesquiterpenoids

Sesquiterpenoids are extracted from ginger oil. Both sesquiterpenoids and sesquiterpene sometimes play a vital role in human health because of their potential for treatment against cancer and cardiovascular diseases. These natural compounds can be taken in a balanced diet or as pharmaceutical agents. Sesquiterpenoids enhance the chemosensitivity of tumor cells through redox regulations of STAT3 signaling

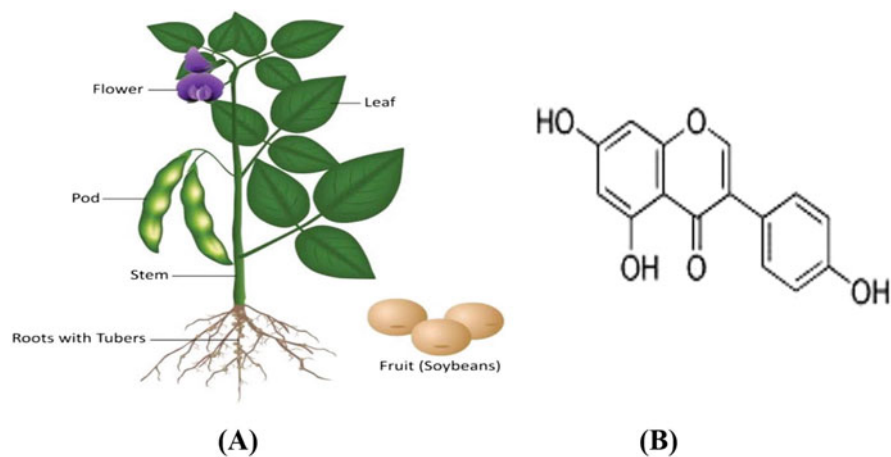


Fig. 9.15 (a) represents the plant *Genista tinctoria* from the fruits from which genistein is extracted. (b) Molecular structure of Genistein. (Source credit: [Google.com](https://www.google.com))

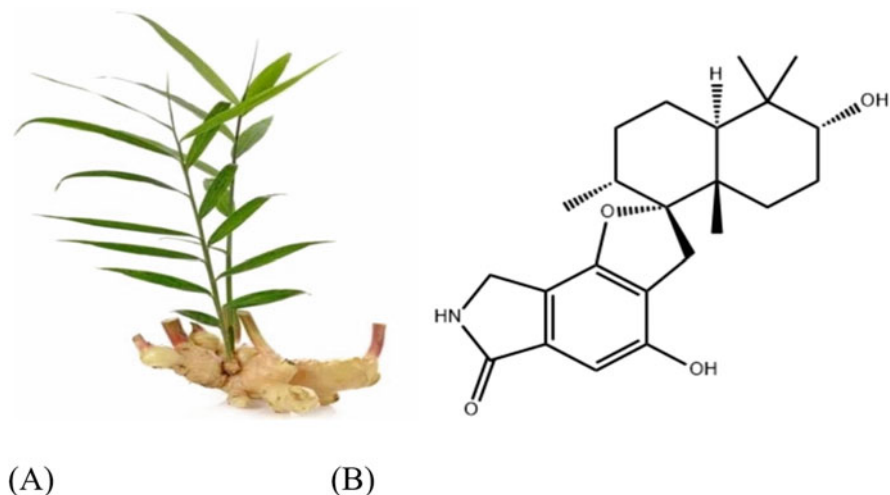


Fig. 9.16 (a) represents a Ginger root, while (b) represents the molecular structure of Sesquiterpenoid. (Source credit: [Google.com](https://www.google.com))

(Jang et al. 2019). STAT3 is a nuclear transcriptional factor that regulates the genes involved in the cell cycle. Sesquiterpene lactones are Sesquiterpenoids containing three isoprene rings and a lactone ring (Fig. 9.16). Sesquiterpene lactones significantly inhibit cell proliferation by arresting the cell at G2/M interphase by decreasing the expression of CDK1 together with cyclin B (Lohberger et al. 2013).

9.3.9 Piperine

Piperine is an alkaloid present in *Piper nigrum*, popularly known as black pepper, which is one of the most used spices worldwide (Fig. 9.17). Piperine has very low solubility in water, so it is extracted by using organic solvents like dichloromethane. Piperine induces cell death depending on the different cell varieties and nature of tumor cells. Piperine directly attacks and stops cell multiplication by binding to various target proteins at cell cycle checkpoints G1, G1/S, and G2/M. Piperine-treated tumor cells impair the cyclin D-CDKs 4/6 activity by increasing the level of P21 expression, which causes the cell cycle arrest at the G1 checkpoint (Fofaria et al. 2014). Similarly, it does not allow the phosphorylation of pRB protein; consequently, the action of cyclin E-CDKs 2 complex gets hampered in allowing the cell to enter into the S phase thus halting the cell at G1/S transition. Further upregulation of P21 by piperine reduces the activity of cyclin A-CDKs 1 complex, which in turn arrests the cell at G2/M transition (Rather and Bhagat 2018). Overall, piperine does not allow for irregular multiplication of cells as it influences cell cycle inhibitors.

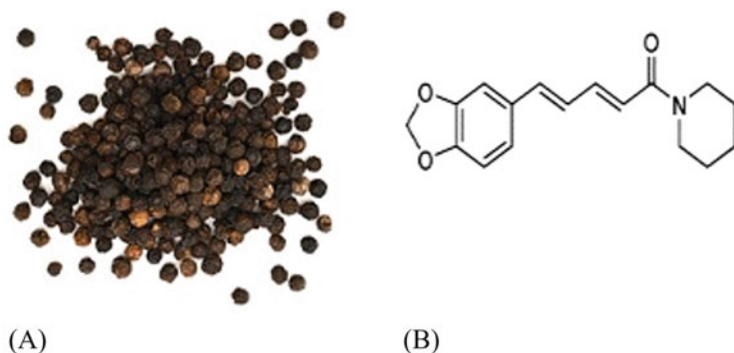


Fig. 9.17 (a) and (b) represent the Black pepper and the molecular structure of piperine. (Source credit: [Google.com](https://www.google.com))

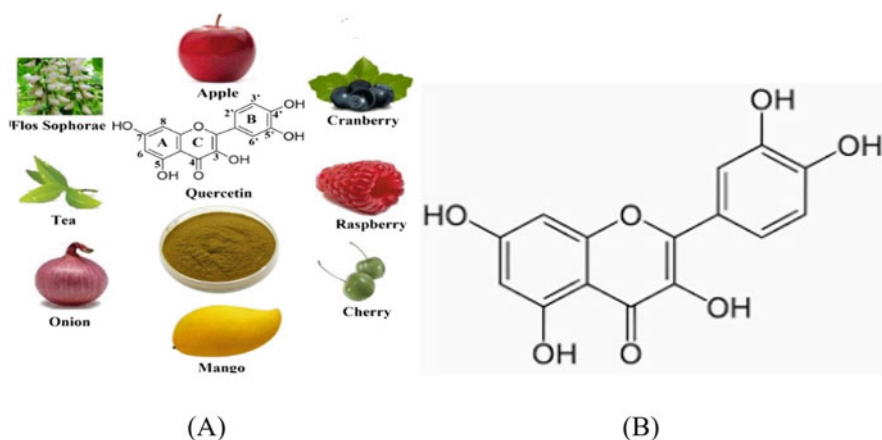


Fig. 9.18 (a) represents various sources of quercetin, while (b) shows the structure of quercetin. (Source credit: [Google.com](https://www.google.com))

9.3.10 Quercetin

Quercetin is a natural pigment in fruits, vegetables, and grains. It is a derivative of a plant compound known as flavonoid that is abundant in healthy foods, including fruits and vegetables, particularly in onions, apples, and broccoli as well as red wine (Fig. 9.18). Quercetin plays an important role as an antiproliferative and anticancer agent and also stimulates apoptosis. Quercetin allows transcription of Bax and BAD proteins that create a pore in the mitochondrial membrane (Lee et al. 2008). As a result, cytochrome C is released from the mitochondria, and it triggers the intrinsic apoptosis pathway. Quercetin also regulates the expression of p21 protein that regulates the cell cycle arrest at G1 phase (Ranelletti et al. 2000).

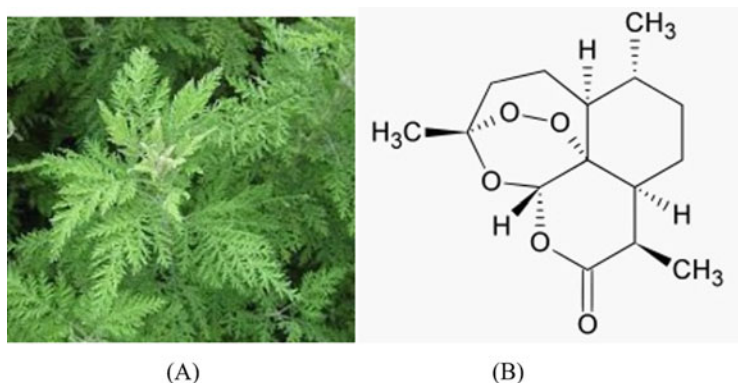


Fig. 9.19 (a) and (b) represent the *Artemisia annua* and the molecular structure of Artemisinin. (Source credit: [Google.com](https://www.google.com))

9.3.11 Artemisinin

Artemisinin is an antimalarial lactone derived from the plant *Artemisia annua*, also known as sweet wormwood (Fig. 9.19). Its semi-synthetic derivatives are also used to treat malaria. Artemisinin and its semi-synthetic derivatives like dihydroartemisinin, artesunate, and artemether are well-known antimalarial drugs. Recent studies suggest that artemisinin and its semi-synthetic metabolites possess anticancer potential. The antiproliferative actions of artemisinin downregulate CDK transcription and increase the expression of CDK inhibitors like p21 and p27 (Zhang et al. 2014). Artemisinin individually and in combination with curcumin promotes cell apoptosis by producing an excess amount of ROS (Das et al. 2014). Artemisinin, when administered, binds with Fe, and forms a Fe(III)–artemisinin complex, which might harm the lysosome of tumor cells by permeabilizing its membrane thus releasing free radicals into the cytosol, generating a high amount of ROS (Crespo and Wei 2012).

9.3.12 Plumbagin

Plumbagin (5-hydroxy-2-methyl-1, 4- naphthoquinones- C11-H8-O3) is a naphthoquinone isolated from the root plant *Plumbago zeylanica* (Fig. 9.20). It is a stirring yellow pigment that patently appears in the Plumbaginaceae family. *Plumbago zeylanica* has been extensively studied for its cytotoxic activities on different cancer cell lines and animal models. Plumbagin stops abnormal cell proliferation by inducing the cells to undergo growth arrest at different checkpoints and also promotes the intrinsic mode of apoptosis depending on the cancer cell type. It was observed that plumbagin causes cell cycle arrest at G1 phase by inhibiting the expression of cyclin D and cyclin E and increasing the expression of P53 in human breast cancer cell lines. Further, it showed downregulation of antiapoptotic proteins

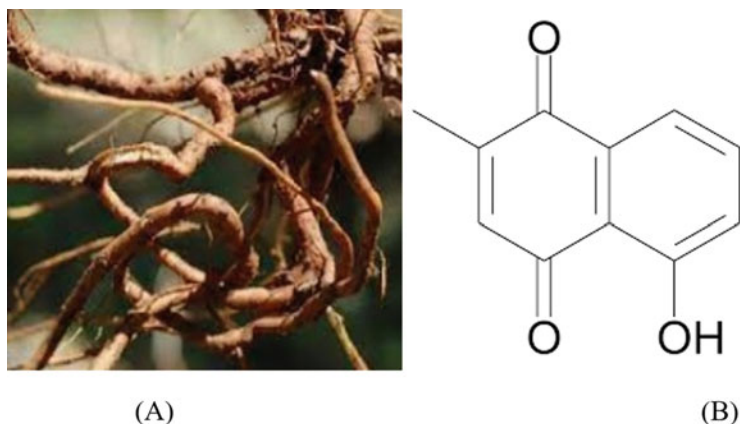


Fig. 9.20 (a) represents the root of *Plumbago zeylanica* and (b) represents the structure of plumbagin. (Source credit: [Google.com](https://www.google.com))

like Bax and Bcl and activated expression of Bcl-xL and Bcl-2 antiapoptotic proteins (Zhang et al. 2016). It was also seen that plumbagin-treated breast cancer cells exhibited increased P21 expression with reduced amounts of cyclin A, cyclin B, and CDKs-1 thus blocking the cell growth at the G2-M checkpoint (Kuo and Hsu 2006). Plumbagin triggers the intrinsic death pathway by modulating the ratio of proapoptotic and antiapoptotic proteins that paves the way towards proapoptosis signaling and production of intracellular ROS to induce apoptosis (Tian et al. 2012).

9.3.13 Thymoquinone

Thymoquinone is the most abundant bioactive phytochemical extracted from the seeds of the plant *Nigella sativa* (Fig. 9.21). This plant is popularly known as black cummin in Middle East countries, and dietary oils have been extracted from the seeds. Thymoquinone has been intensively studied by healers from ancient times to researchers till date for its therapeutic effects on various diseases including cancer. It is a promising anticancer agent from natural sources due to its inhibitory effect on carcinogenesis and neo-angiogenesis (Banerjee et al. 2010). Thymoquinone checks inhibition of cell proliferation associated with G1 phase growth arrest when treated with P53 mutant breast cancer lines. It also induced intrinsic programmed cell death by activating caspase-dependent and independent apoptosis pathways in a dose- and time-dependent manner (Sutton et al. 2014). Thymoquinone has a significant cytotoxic effect on bladder cancer cell lines. It induces apoptosis through the endoplasmic reticulum stress-mediated mitochondrial pathway in which an increased ratio of Bax/Bcl-2 as well as cytochrome is found (Zhang et al. 2018).

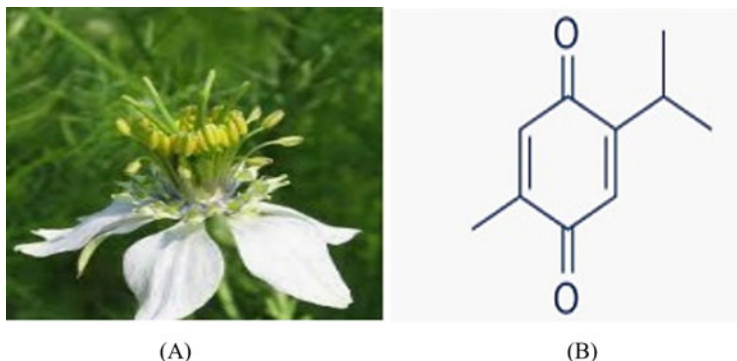


Fig. 9.21 Image (a) shows the *Nigella sativum* and (b) represents the molecular structure of Thymoquinone. (Source credit: [Google.com](https://www.google.com))

9.4 Conclusion

Natural phytochemicals potentiate and play a strong role in preventing cancer. In this work, a number of these compounds have been discussed. The natural compounds have excellent anti-tumor activity and have the capability to target various molecular processes.

Since precedent days, natural products, herbs, and spices have been used for preventing several diseases, including cancer. Cancer is a dreaded disease and a major cause of morbidity with a poor prognosis worldwide. Natural products like honokiol, curcumin, and ginsenosides inhibit tumor growth by targeting the dysregulated cell cycle and inducing apoptosis. They have several varieties of pharmacological activities like antifungal and antibacterial properties, which can be put to implementation for the development of effective therapeutic agents in almost all human cancers as it targets a wide array of signaling networks involved in tumorigenesis. Many known pharmaceuticals today use the natural compounds or the secondary metabolite of natural products. Natural dietary phytochemicals have been widely used in cancer prevention and treatment studies. Most of the natural products and some of their secondary metabolites had been tested *in vitro* to establish their efficacy against cancer cell lines and its minimum effective concentration. Some of these have shown successful results in animal models and clinical trials. Regular consumption of fruits and vegetables and herbs that are rich in phytochemicals along with physical exercise provides several health benefits and keep diseases, including cancer, at bay.

Furthermore, cancer being a multifactorial disease, these natural products harboring medicinal properties have been put to optimal usage in cases of combinatorial treatment for cancer. This not only augments the other anticancer component's activity but also reduces the previously associated toxicity to a minimal or negligible level. As cancer chemoprevention and treatment using natural phytochemicals have

been such an attractive and effective approach, further efforts are fully justifiable to thoroughly understand their potencies. Today there are multiple opportunities for the development of normal analogs and pro-drugs. Natural product research is a powerful approach for the discovery of these compounds which are biologically active and carry numerous benefits, and it will continue to be a promising and active research area in cancer biology in the near future.

Acknowledgements This work is supported by an intramural grant (RIN-4002-SBS) from National Institute of Science Education and Research (NISER), an autonomous organization under Department of Atomic Energy, Government of India.

References

- Albert B et al (2002) *Molecular biology of the cell*. Garland Science, New York. ISBN-10: 0-8153-3218-1
- Antoniou A et al (2003) Average risks of breast and ovarian cancer associated with BRCA1 or BRCA2 mutations detected in case series unselected for family history: a combined analysis of 22 studies. *Am J Hum Genet* 72:1117–1130. <https://doi.org/10.1086/375033>
- Anuchapreeda S (2006) Curcumin inhibits WT1 gene expression in human leukemic K562 cells. *Acta Pharmacol Sin* 27:360–366. <https://doi.org/10.1111/j.1745-7254.2006.00291.x>
- Baba AL, Catoi C (2007) *Comparative oncology*. The Publishing House of Romanian Academy, Bucharest. ISBN-10:973-27-1457-3
- Baluk P et al (2005) Cellular abnormalities of blood vessel as targets in cancer. *Curr Opin Genet Dev* 15:102–111. <https://doi.org/10.1016/j.gde.2004.12.005>
- Banerjee S, Padhye S, Azmi A, Wang Z, Philip PA, Kucuk O, Sarkar FH, Mohammad RM (2010) Review on molecular and therapeutic potential of thymoquinone in cancer. *Nutr Cancer* 62(7): 938–946. <https://doi.org/10.1080/01635581>
- Bollag G, Clapp DW (1996) Loss of NF1 results in activation of the Ras signaling pathway and leads to aberrant growth in haematopoietic cells. *Nat Genet* 12:144–148. <https://doi.org/10.1038/ng0296-144>
- Carracedo A, Pandolfi P (2008) The PTEN–PI3K pathway: of feedbacks and cross-talks. *Oncogene* 27:5527–5541. <https://doi.org/10.1038/onc.2008.247>
- Chen T, Li B et al (2018) Functional mechanism of ginsenosides on tumor growth and metastasis. *Saudi J Biol Sci* 25:917–922. <https://doi.org/10.1016/j.sjbs.2018.01.012>
- Cooper Geoffrey M (2000) *The cell, a molecular approach*. Sunderland, Sinauer Associates. ISBN-10:0-87893-106-6
- Crespo OMP, Wei MQ (2012) Antitumor activity of artemisinin and its derivatives: from a well-known antimalarial agent to a potential anticancer drug. *J Biomed Biotechnol*:247597. <https://doi.org/10.1155/2012/247597>
- Das SS, Nanda GG, Alone DP (2014) Artemisinin and curcumin inhibit *Drosophila* brain tumor, prolong life span, and restore locomotor activity. *IUBMB Life* 66:496–506. <https://doi.org/10.1002/iub.1284>
- Deininger P (1999) Genetic instability in cancer: caretaker and gate keeper genes. *Ochsner J* 4:206–209
- Fofaria NM et al (2014) Piperine causes G1 phase cell cycle arrest and apoptosis in melanoma cells through checkpoint kinase-1 activation. *PLoS One* 9:e94298. <https://doi.org/10.1371/journal.pone.0094298>
- Fried LE, Arbiser JL (2009) Honokiol, a multifunctional antiangiogenic and antitumor agent. *Antioxid Redox Signal* 11:1139–1148. <https://doi.org/10.1089/ars.2009.2440>

- Gangyi D et al (1997) Decreased expression of Wilms' tumor gene WT-1 and elevated expression of insulin growth factor-II (IGF-II) and type I IGF receptor genes in prostatic stromal cells from patients with benign prostatic hyperplasia. *J Clin Endocrinol Metabol* 82:2198–2203. <https://doi.org/10.1210/jcem.82.7.4067>
- Giacinti C, Giordano A (2006) RB and cell cycle progression. *Oncogene* 25:5220–5227. <https://doi.org/10.1038/sj.onc.1209615>
- Glienke W, Maute L (2009) Wilms' tumour gene 1 (WT1) as a target in curcumin treatment of pancreatic cancer cells. *Eur J Cancer* 45:874–880. <https://doi.org/10.1016/j.ejca.2008.12.030>
- Haupt Y et al (1997) MDM2 promotes rapid degradation of P53. *Nature* 387:296–299. <https://doi.org/10.1038/387296a0>
- Hirose M (1999) The role of Wilms' tumorigenes. *J Med Investig* 46:130–140
- Huang M (2013) Triptolide inhibits MDM2 and induces apoptosis in acute lymphoblastic leukemia cells through a p53-independent pathway. *Mol Cancer Ther* 12:184–194. <https://doi.org/10.1158/1535-7163.MCT-12-0425>
- Jang HJ, Lim HJ et al (2019) STAT3-inhibitory activity of sesquiterpenoids and diterpenoids from *Curcuma phaeocalis*. *Bioorg Chem* 93:103267. <https://doi.org/10.1016/j.bioorg.2019.103267>
- Junran Z et al (2004) chk2 phosphorylation of BRCA1 regulates DNA double strand break repair. *Mol Cell Biol* 24:708–718. <https://doi.org/10.1128/MCB.24.2.708-718.2004>
- Kim SH et al (2009) Involvement of both extrinsic and intrinsic apoptotic pathways in apoptosis induced by genistein in human cervical cancer cells. *Ann N Y Acad Sci* 1171:196–201. <https://doi.org/10.1111/j.1749-6632.2009.04902.x>
- Kitagishi Y et al (2012) Protection against cancer with medicinal herb via activation of tumor suppressor. *J Oncol* 2012:7. <https://doi.org/10.1155/2012/236530>
- Knudson AG (1986) Genetics of human cancer. *Ann Rev Genet* 20:231–251
- Kreidberg JA et al (1993) WT-1 is required for early kidney development. *Cell* 74:679–691. [https://doi.org/10.1016/0092-8674\(93\)90515-r](https://doi.org/10.1016/0092-8674(93)90515-r)
- Kuo P-L, Hsu Y-L (2006) Plumbagin induces G2-M arrest and autophagy by inhibiting the AKT/mammalian target of rapamycin pathway in breast cancer cells. *Mol Cancer Ther* 5:3209–3221. <https://doi.org/10.1158/1535-7163.MCT-06-0478>
- Kwong LN, Dove WF (2009) APC and its modifiers in colon cancer. *Adv Exm Med Biol* 656:85–106. https://doi.org/10.1007/978-1-4419-1145-2_8
- Lee DH, Szczepanski M, Lee YJ (2008) Role of Bax in quercetin-induced apoptosis in human prostate cancer cells. *Biochem Pharmacol* 75:2345–2355. <https://doi.org/10.1016/j.bcp.2008.03.013>
- Lin X, Tian L (2017) Antitumor effects and the underlying mechanism of licochalcone A combined with 5-fluorouracil in gastric cancer cells. *Oncol Lett* 13:1695–1701. <https://doi.org/10.3892/ol.2017.5614>
- Lohberger B et al (2013) Sesquiterpene lactones downregulate G2/M cell cycle regulator proteins and affect the invasive potential of human soft tissue sarcoma cells. *PLoS One* 8:e66300. <https://doi.org/10.1371/journal.pone.0066300>
- Macleod KF et al (1995) P53 dependent and independent expression of P21 during cell growth and differentiation and DNA damage. *Genes Dev* 9:935–944. <https://doi.org/10.1101/gad.9.8.935>
- Malumbrace M (2014) Cyclin dependent kinases. *Genome Biol* 15(122):1–10. <https://doi.org/10.1186/gb4184>
- Mamillapalli R et al (2001) PTEN regulates the ubiquitin-dependent degradation of the CDK inhibitor p27(KIP1) through the ubiquitin E3 ligase SCF(SKP2). *Curr Biol* 11:263–267. [https://doi.org/10.1016/s0960-9822\(01\)00065-3](https://doi.org/10.1016/s0960-9822(01)00065-3)
- Minna U, Kumar P (2016) Lifescience, fundamental & practice. Path Finder, New Delhi. ISBN-978-81-906427-7-4
- Na X, Wu G et al (2003) Overproduction of vascular endothelial growth factor related to von Hippel-Lindau tumor suppressor gene mutations and hypoxia-inducible factor-1 alpha expression in renal cell carcinomas. *J Urol* 170:588–592. <https://doi.org/10.1097/01.ju.0000074870.54671.98>

- Nagase H, Nakamura Y (1993) Mutation of APC (adenomatous polyposis coli) gene. *Hum Mutat* 2: 425–434. <https://doi.org/10.1002/humu.1380020602>
- Nakatsuru S, Yanagisawa A et al (1993) A somatic mutations of the APC gene in precancerous lesion of the stomach. *Hum Mol Genet* 9:1463–1465. <https://doi.org/10.1093/hmg/2.9.1463>
- Orhan E et al (2021) Regulation of RAD51 at the transcriptional and functional levels: what prospects for cancer therapy? *Cancers (Basel)* 13:2930. <https://doi.org/10.3390/cancers13122930>
- Pflaum J et al (2014) P53 family and cellular stress responses in cancer. *Front Oncol* 4:285. <https://doi.org/10.3389/fonc.2014.00285>
- Rafiq S, Raza M et al (2018) Molecular targets of curcumin and future therapeutic role in leukemia. *J Biosci Med* 6:33–50. <https://doi.org/10.4236/jbm.2018.64003>
- Randall SF, Keith W (2003) Genistein activates p38 mitogen-activated protein kinase, inactivates ERK1/ERK2 and decreases Cdc25C expression in immortalized human mammary epithelial cells. *J Nutr* 133:226–231. <https://doi.org/10.1093/jn/133.1.226>
- Ranelletti FO et al (2000) Quercetin inhibits p21-RAS expression in human colon cancer cell lines and in primary colorectal tumors. *Int J Cancer* 85:438–445
- Rather RA, Bhagat M (2018) Cancer chemoprevention and piperine: molecular mechanisms and therapeutic opportunity. *Front Cell Dev Biol* 6:00010. <https://doi.org/10.3389/fcell.2018.00010>
- Roussel M (1999) The INK4 family of cell cycle inhibitors in cancer. *Oncogene* 18:5311–5317. <https://doi.org/10.1038/sj.onc.1202998>
- Shan BE et al (2000) Chinese medicinal herb, *Acanthopanax gracilistylus*, extract induces cell cycle arrest of human tumor cells in vitro. *Jap J Cancer Res* 91:383–389. <https://doi.org/10.1111/j.1349-7006.2000.tb00956.x>
- Starostina NG, Kipreos ET (2012) Multiple degradation pathways regulate versatile CIP/KIP CDK inhibitors. *Trends Cell Biol* 22:33–41. <https://doi.org/10.1016/j.tcb.2011.10.004>
- Surova O, Zhivotovsky B (2013) Various modes of cell death induced by DNA damage. *Oncogene* 32:3789–3797. <https://doi.org/10.1038/onc.2012.556>
- Sutton KM et al (2014) Thymoquinone, a bioactive component of black caraway seeds, causes G1 phase cell cycle arrest and apoptosis in triple-negative breast cancer cells with mutant p53. *Nutr Cancer* 66:408–418. <https://doi.org/10.1080/01635581.2013.878739>
- Tai YC, Domchek S et al (2007) Breast cancer risk among male BRCA1 and BRCA2 mutation carriers. *J Natl Cancer Inst* 99:1811–1814. <https://doi.org/10.1093/jnci/djm203>
- Tao R, Lu L et al (2011) Triptolide inhibits rat vascular smooth muscle cell proliferation and cell cycle progression via attenuation of ERK1/2 and Rb phosphorylation. *Exp Mol Pathol* 90:137–142. <https://doi.org/10.1016/j.yexmp.2010.12.001>
- Tarafa G, Prat E et al (2003) Common genetic evolutionary pathway in familial Adenomatous polyposis Tumors. *Cancer Res* 63:5731–5737
- Tian L, Yin D et al (2012) Plumbagin induces apoptosis via the p53 pathway and generation of reactive oxygen species in human osteosarcoma cells. *Mol Med Rep* 5:126–132. <https://doi.org/10.3892/mmr.2011.624>
- Wang ZY, Madden SL, Deuel TF, Rauscher FJ 3rd. (1992) The Wilms' tumor gene product, WT1, represses transcription of the platelet-derived growth factor A-chain gene. *J Biol Chem* 267: 21,999–22,002
- Wang LH et al (2018) Loss of tumor suppressor gene function in human cancer, an overview. *Cell Physiol Biochem* 51:2647–2693. <https://doi.org/10.1159/000495956>
- Wilhelm D, Englert C (2002) The Wilms tumor suppressor WT1 regulates early gonad development by activation of Sf1. *Genes Dev* 16:1839–1851. <https://doi.org/10.1101/gad.220102>
- Worm J, Christensen C, Grønbaek K et al (2004) Genetic and epigenetic alterations of the APC gene in malignant melanoma. *Oncogene* 23:5215–5226. <https://doi.org/10.1038/sj.onc.1207647>
- Yu X, Zhu J (2012) Anti-angiogenic genistein inhibits VEGF-induced endothelial cell activation by decreasing PTK activity and MAPK activation. *Med Oncol* 29:349–357. <https://doi.org/10.1007/s12032-010-9770-2>

- Zhang F, Li M (2015) 20(S)-ginsenoside Rg3 promotes senescence and apoptosis in gallbladder cancer cells via the p53 pathway. *Drug Des Dev Ther* 9:3969–3987. <https://doi.org/10.2147/DDDT.S84527>
- Zhang HT et al (2014) Artemisinin inhibits gastric cancer cell proliferation through up regulation of p53. *Tumour Biol* 35:1403–1409. <https://doi.org/10.1007/s13277-013-1193-1>
- Zhang XQ, Yang CY et al (2016) Plumbagin shows anti-cancer activity in human breast cancer cells by the upregulation of p53 and p21 and suppression of G1 cell cycle regulators. *Eur J Gynaecol Oncol* 37:30–35
- Zhang M et al (2018) Thymoquinone induces apoptosis in bladder cell via endoplasmic reticulum stress dependent mitochondrial pathway. *Chemico-Biol Interaction* 292:65–75. <https://doi.org/10.1016/j.cbi.2018.06.013>
- Zhou Q, Wang XF et al (2011) Curcumin enhanced antiproliferative effect of mitomycin C in human breast cancer MCF-7 cells *in vitro* and *in vivo*. *Acta Pharmacol Sin* 2:1402–1410. <https://doi.org/10.1038/aps.2011.97>



Advancements in the Safety of Plant Medicine: Back to Nature

10

Ankita Misra, Bhanu Kumar, Deepali Tripathi, and Sharad Srivastava

10.1 Introduction

India has a glorious history of its traditional systems of medicine (TSM), and in modern times, these stand collectively as “AYUSH”—Ayurveda, Unani, Yoga and naturopathy, Siddha and Homeopathy. The ancient Vedic and other scriptures also have evidences about these TSM, and it is well-known that the concept of Ayurveda in treating and managing medical conditions was developed between 2500 and 500 BC (Subhose et al. 2005). *Ayurveda* teaches us about balancing the various elements of the body like *Panchamahabhuta* (five basic elements) and *Tridosha* (Vatta, Pitta, Kapha). The use of traditional system of medicine is not limited to Indian boundaries only, across the globe, several alternative systems like *Amchi*, traditional Chinese system of medicine (TCM), Tibetan system of medicine (Sowa Rigpa), traditional Korean system of medicines, Japanese system of medicines, etc., are in practices since ages. Over the years, in the race of modernization, these traditional systems have matured into well-oriented and scientifically validated alternatives of allopathic medicines. A large number of populations living in low- and middle-income countries are still dependent on natural resources for their daily healthcare needs. Thus, it is advocated to explore the benefit of plant resources around us in a holistic way (Pandey et al. 2013).

World Health Organization (WHO) in the year 1998 has framed a new policy for health at a global scale entitled “Health for all in twenty-first century,” which was aimed to achieve security and equity in health, increased expectancy of healthy life and access to basic, quality health care for everyone. Later in 2013, WHO launched “WHO Traditional Medicine Strategy 2014–2023,” with the purpose of

A. Misra · B. Kumar · D. Tripathi · S. Srivastava (✉)
Pharmacognosy Division, CSIR-National Botanical Research Institute, Lucknow, Uttar Pradesh, India
e-mail: sharad@nbri.res.in

incorporating traditional and complementary medicines to achieve and promote global healthcare. The strategy also ensures that the safety, quality, and efficacy of such herbal medicines/plant-derived products must be regulated (World Health Organization (WHO) 2013). The scientifically validated herbal medicines, owing to their efficacy, safety, and cost-effectiveness, have emerged as a suitable alternative for many of the modern medicines which have been repeatedly found to impart harmful side effects to the human body. Herbal medicines, on the other hand, are more compatible with the human system as they are a complex mixture of many active ingredients and often work in synergy by complementing and supplementing each other's functions. India is one of the largest producers of medicinal plants, and the rich biodiversity of India has around 20,000 medicinal plants, among them, only 7000–7500 have been used by traditional practitioners. According to WHO, the international trade of medicinal plants will reach five trillion US \$ by the year 2050, and this reflects the global acceptance of medicinal plants and/or plant-based products. The huge resurgence in the use of herbal products is due to various factors, i.e., side effects of modern medicine, long-term medication affecting human health, high cost, and drug resistance, etc. Therefore, in this present context, the challenges in medicinal plants and the approaches for the advancement in herbal products for the benefit of mankind, along with strategies to conserve, restore, and flourish biodiversity, were summarized. This will give insight into the modernization of herbal products and regulations in quality and efficacy in parallel with biodiversity conservation (Pandey et al. 2013).

10.2 Relevance of Medicinal Plants/Plant-Derived Products and Challenges

During the nineteenth century, medical science had achieved significant advances around the globe and due to which the rate of mortality decreases and life expectancy increases. The development of several lifesaving drugs has an ancestral linkage with plant sources, and the world is shifting its attention towards mother nature, and as per WHO, around 25% of discovered drugs/drug molecules have a natural origin. However, despite such benefits, the utilization of medicinal plants in the mainstream healthcare system in India is still on midway, and there are several challenges that need to be addressed. Industrialization and profit earning from the pharmaceutical sector has created a burden on natural resources, and the rising demand of herbal raw material is the first challenge. The global herbal market size was US\$ 83 billion (2019) and is increasing at a steady pace which leads to the over-harvesting/ indiscriminate collection from wild sources and ends up in biodiversity loss of potential species.

A golden example is *Taxus baccata*, which is continuously harvested from nature for taxol metabolite. Similarly, other medicinal plants having a promising pharmacological activity like *Aconitum* spp., *Nardostachys grandiflora*, *Gloriosa superba*, *Polygonatum verticillatum*, *Swertia* spp., *Gentiana* spp., etc., were enlisted, off and on (at times) in red data book due to various factors including excessive exploitation.

Further, unlike a single conventional drug which may have one direct action, the medicinal plants have multifarious benefits, and therefore a single plant is used in various conditions, e.g., 34 types of diseases can be cured using *Hemidesmus indicus*, *Aegle marmelos* in 31, *Phyllanthus emblica* in 29, and *Gloriosa superba* in 28 (Jain n.d.). This has led to collection of some selected plants in higher quantities for commercial aspects and further worsens the situation. The harvesting of medicinal plants along with destructive harvesting of underground parts should be checked so that the regeneration of species may not get affected. In addition, for sustainable availability of raw material, the maturity, season, and time of harvest should be monitored along with the promotion of commercial cultivation at specific locations where agro-climatic conditions support the higher biomass and maximum yield of active metabolites. The second challenge associated with rising demand is *biodiversity loss* or rarity in the availability of species, particularly in the case of medicinal plants growing in specific climatic conditions. The collection of commonly growing plants with a wide distribution from natural sources is admissible; however, in the case of plants growing in specific micro-climates like *Coptis teeta*, *Aconitum hetrophylla*, *Saussurea lappa*, the concern is serious, and, therefore, collection and formulation development with such species is a costly affair and not advisable also, unless we have either alternate sources or cultivated raw material. There are various other causes which affect the diversity pattern of species, such as restricted distribution, slow germination rate, invasion of exotic species, habitat alteration, climate shift, grazing, human interventions, fragmentation and degradation of population, and genetic changes (Kala 2000; Weekley and Race 2001; Oostermeijer et al. 2003; Kale 2005). One classic example is “Daruharidra” in *Ayurveda*. The authentic drug is *Berberis aristata*, but due to over-exploitation for its various usages, now the species is rarely available in the wild. The consumption is however met with alternate *Berberis* species with comparable chemical profiles like *B. asiatica*, *B. lyceum*, etc., under the same common name of “Daruharidra.”

The third challenge is *Bio-prospection and biopiracy*, with the increase in commercialization and demand of natural products, the former concept of the remote forest has now converted into profit-generating natural resources. Flora and fauna of any country is its national wealth, and thus its protection is relevant in current times. It is now challenging for policymakers to draw a line between exploring natural wealth and exploiting it. The bio-prospection of plants and their usage within a country abides by its legal framework in established law. In India, National Biodiversity Authority plays a significant role in dealing with plant products, plant breeding, plant varieties, commercial utilization, patents, etc. However, the exchange of plant resources across the national boundary of India is a punishable offense under “*biopiracy*.” Besides, some other challenges are *slow rate of growth*, *unavailability of suitable agro-techniques*, *lack of commercial cultivation practices*, *less production*, *improper harvesting*, *pest and cattle infestation*, *fluctuation in demand-supply chain*, *improper marketing infrastructure*, etc. The herbal drug market in India has several loops and needs to be strengthened, as it involves several stakeholders ranging from plant collectors, local buyers, middlemen, traders, wholesalers, manufacturers, exporters, and herbal healers, and thus a lot of monitoring

involvement is there which creates brawl. The deep pin issue is that growers located in the wild are uneducated, and they are unaware of the gold they are producing or farming. The local buyers are taking advantage of this to gain profit, for example, in some villages of Chamoli, Uttarakhand (India), farmers are cultivating *Saussurea costus* (Kut) and *Rheum emodi* (Dolu) but are unable to sell them at fixed price due to lack of knowledge or disturbed market linkage. However, the regulatory bodies in India like the Ministry of AYUSH, Department of Science and Technology, Botanical Survey of India, ICAR-National Bureau of Plant Genetic Resources, and MoEF are constantly working on it to bring such economically lagged people into the mainstream for a better economy generation from local resources and socioeconomic upliftment. Lastly, the most challenging issue in herbal drugs is its *quality control, pharmacovigilance (safety, toxicity, and adverse drug reaction), and clinical trial* (Sen and Chakraborty 2017).

10.3 Quality Control and Modernization of Herbal Product Development

In spite of several hurdles, traditional medicines are flourishing decently, and the world is recognizing their potential. The untiring efforts of the public, scientific bodies, and government agencies are bringing herbal medicines into the mainstream with the backing of scientifically validated data. However, before approaching the advancement in herbal medicines, it is necessary to look into the problems regarding the quality of raw materials. The medicinal plants used as raw material for the manufacturing of herbal formulations are prone to various factors like change in climate, soil-microflora, genetic changes, and other biotic-abiotic factors and this ultimately affects their potency, safety, and efficacy. With the change in inter-natural boundaries, the biodiversity changes and is the sole reason for the wider acceptability of chemically produced drugs. To regulate this issue in 2014, USFDA released “Guidelines for Industry: Botanical Drugs Product,” which focuses on ensuring the quality and therapeutic efficacy of botanical drug batches as sold in the market.

The three predominant issues which require necessary action for the development of scientifically validated herbal medicine are (1) uniformity in regulation and standardization protocol, (2) availability of enormous scientific/clinical data to establish therapeutic efficacy, and (3) toxicity data. Further to establish global acceptance of the developed herbal product, the following points must be kept in mind:

- The drug and its every batch after production must comply with the standard of consistency.
- The identity of the drug can be estimated through botanical and chemical (analytical techniques) methods like HPTLC, HPLC, GC-MS, etc.
- The product must comply with the permissible limit of heavy metals, aflatoxins, microbial load as per the regulatory bodies of the country.

- The product should not have toxic metabolites like cardiac glycosides, cyanogenic glycosides, etc.
- It must be safe as supported by *in vivo* animal studies (Srivastava and Misra 2018).

The quality standardization of herbal products is tedious due to enormous variation in raw materials used for preparation and the lack of regulatory guidelines in the particular sector. The quality is susceptible to being compromised, starting from the stage of collection of raw materials due to lack of knowledge, less availability, deliberate adulteration or substitution, lack of postharvesting/storage practices, lack of standardized manufacturing protocols, etc. More specifically, the possible factors affecting the quality of herbal products are:

- Intricate phytochemical composition responsible for claimed pharmacological activity.
- Bioactive phytochemical component is generally unknown and/or uncertainty of active component and whole extract exert synergistic response.
- Non-availability of chemical profiling to identify the variations within batches.
- Variability in wild and cultivated plant species with change in environmental conditions, and
- Variation in pharmacological activities.

The consistency in quality of herbal medicine is correlated with homogeneity or bioequivalence of raw material/finished product. Initially, the consistency in terms of chemical components depends on analyzing/evaluating the single component only. However, with advancement in R & D techniques, it has been established that the efficacy is due to the synergistic action of several known and unknown phytomolecules, and, thus, the concept of multi-component analysis was evolved, which targets analyzing various components simultaneously or even similarity in characteristic fingerprinting profile. Further, in the twentieth century, regulatory bodies in India, i.e., Indian Pharmacopoeia Commission, Ministry of AYUSH, CDSCO, etc., have coined a new term “Phytopharmaceuticals.” Phytopharmaceutical drug is defined as “purified and standardized fraction with defined minimum four bioactive or phytochemical compounds (qualitatively and quantitatively assessed) of an extract of a medicinal plant or its part, for internal or external use of human beings or animals for diagnosis, treatment, mitigation, or prevention of any disease or disorder but does not include administration by parenteral route” (Ministry of Health and Family Welfare Gazette Notification G.S.R. 918(E) *n.d.*). The quantification of the single component has the disadvantage that it can be deliberately added to the raw material and finished product. Therefore, looking at the drawbacks of both approaches, analysis of complete fingerprints is recommended nowadays. The chemical quantification, either single or multi-component or complete fingerprint, can be achieved through sophisticated analytical techniques like HPTLC, HPLC, HPLC-MS/MS, HPLC-TOF-ESI-MS Fingerprint, UPLC-MS/MS, GC-MS, NMR, etc. (Anonymous *n.d.*).

To standardize the chemical equivalence in raw material, it is essential to identify the metabolites which need to be targeted (quantified) and the major metabolites based on their bioactivity should be selected. Further, as explained above, the plant metabolite varies considerably due to changes in their habitat and environmental conditions. Thus, for product development, superior-quality raw material should be selected. If we deepen our thought on searching for superior quality material, then tracing such material is possible only when we have studied and quantified the metabolites from samples (plant materials) collected from a wide range of geographical areas. Thus, an approach of “chemotaxonomy” was coined to identify the superior quality raw material, i.e., elite chemotypes, based on high metabolite content (Misra and Srivastava 2016). The detailed concept and cases studied by our groups are discussed further.

10.4 Chemotaxonomic Approach for Sustainable Use of Natural Resources

Modern science, taking leads from traditional indigenous knowledge, has advanced the field of herbal drugs by generating scientifically validated data and developing herbal drugs as per the requirement of global standards. In the past, several highly valuable plant-derived therapeutic molecules have been identified, e.g., aspirin, taxol, vincristine, vinblastine, colchicine, withanolides, etc., and developed medicines that are very effective against many diseases. The chemotaxonomy approach is a major step towards identifying superior quality germplasms growing in different eco-geographical conditions of a country. It deals with the exploration of targeted medicinal plants from different locations of phytogeographical zones and the collection of medicinal plants for chemical profiling. It also includes documentation of crucial information related to specific medicinal plants such as prevailing environmental conditions, soil type, associated species growing nearby, GPS details, and development of a passport data sheet. This is very important in a holistic view as supportive parameters for developing suitable agro-technology for commercial cultivation. These details also help in a future collection of germplasm from the same location for researchers/industries with respect to variations in chemical profile with time, climate change, the effect of pollution, etc.

The chemical profiling of samples of a single plant species collected from different locations gives a very interesting as well as challenging set of data that is to be correlated with the concentration of bioactive metabolites versus all other variables. The statistical analysis of generated data coupled with bioclimatic niche characterization based on the Environmental Rasters for Ecological Modelling (ENVIREM) dataset gives a holistic idea about the distribution pattern in different eco-geographical regions and its relation with the chemical profile. This approach enables us to identify locations for direct collection of superior quality raw material subjected to its abundance, while on the other hand, it gives insights regarding the suitable set of agronomic parameters for optimum yield of bioactive compounds.

This practice is also very important for the reasonable harvesting of plant material from the field and helps in the conservation of natural resources.

10.5 Case Studies on Chemotaxonomic Approach

The interest in the identification of elite sources of raw material and chemotypes has grown worldwide in the recent past. With the advent of modern, sophisticated tools, it is now possible to determine the bioactive metabolite profile in medicinal plants with precision and their use for industrial application. There are success stories that exhibit the importance of chemotaxonomic analysis of medicinal plants in order to identify superior chemotypes of high-value medicinal plants. A few of them are discussed below (Fig. 10.1):

10.6 *Acorus calamus* L.

Acorus calamus L. (fam. Acoraceae) is a perennial, aromatic herb commonly known as sweet flag, with creeping rhizomes and a strong, characteristic odor. In *Ayurveda*, its rhizomes are described to be useful as tonic, stimulant, expectorant, aphrodisiac, and diuretic (Mukherjee et al. 2007). It is known for its insecticidal, antimicrobial, antispasmodic, and antidepressant properties. The species is also used to treat

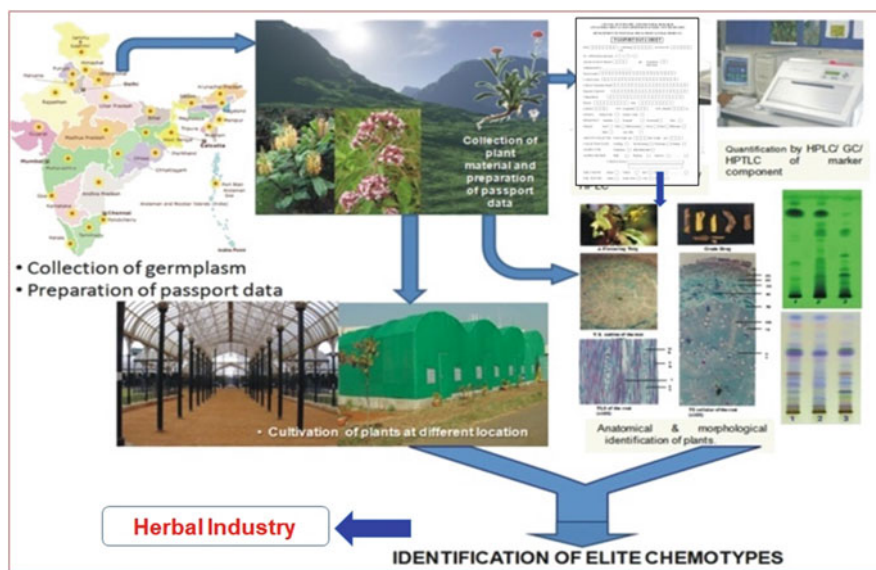


Fig. 10.1 The industrial chemotaxonomy study design

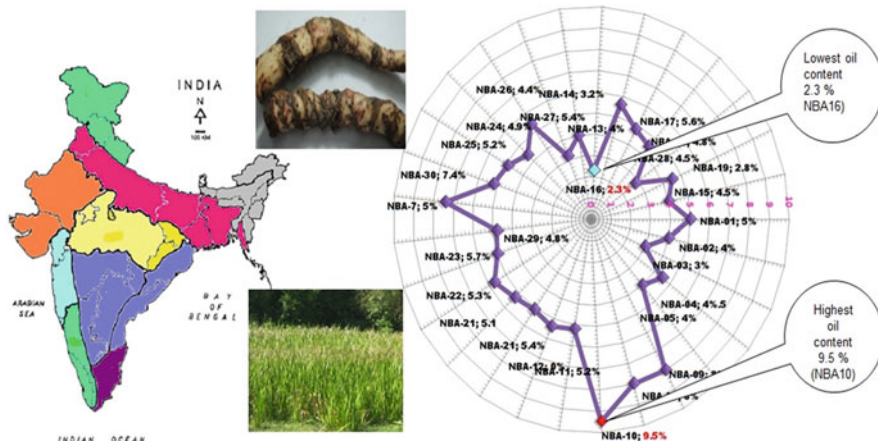


Fig. 10.2 Chemotaxonomic study on *Acorus calamus*

insomnia and epilepsy (Rana et al. 2013). The rhizome is used widely in folklore medicine for various ailments related to diarrhea, throat, and nervous system (Viswanathan 1995). A large number of volatile organic compounds have been reported in the essential oil obtained from the rhizome, and α and β -asarone and acorenone were the major compounds present (Gyawali and Kim 2009). In our study, 29 germplasms of *A. calamus* were collected, and chemical profiling was done through GC-MS. It was found that the oil content varied largely (2.3–9.5%) in samples collected from different locations (Fig. 10.2).

10.7 *Gloriosa superba* L.

Gloriosa superba is traditionally used in the treatment of snakebite, gout, and respiratory disorders. It exhibits analgesic, anti-inflammatory, antimicrobial, larvicidal, anti-poxviral, anti-thrombotic, and anti-tumor properties (Misra et al. 2021). Its therapeutic importance is due to the presence of phytochemicals such as colchicine and gloriosine which are very useful in treating cancer and other diseases (Jain et al. 2004). In our study, a total of 128 accessions of *G. superba* L. were collected from different phytogeographical zones of India to study the variation in content of colchicine. A wide variation, ranging from 0.0052% to 0.860% was observed among the collected samples. However, the maximum content was observed in samples collected from Western Ghats (Gutuput, Kerala) and minimum content was recorded in NBG-75 from Upper Gangetic plains (Navgarh, U.P) (Srivastava et al. 2014a; Misra et al. 2017, 2020) (Fig. 10.3).

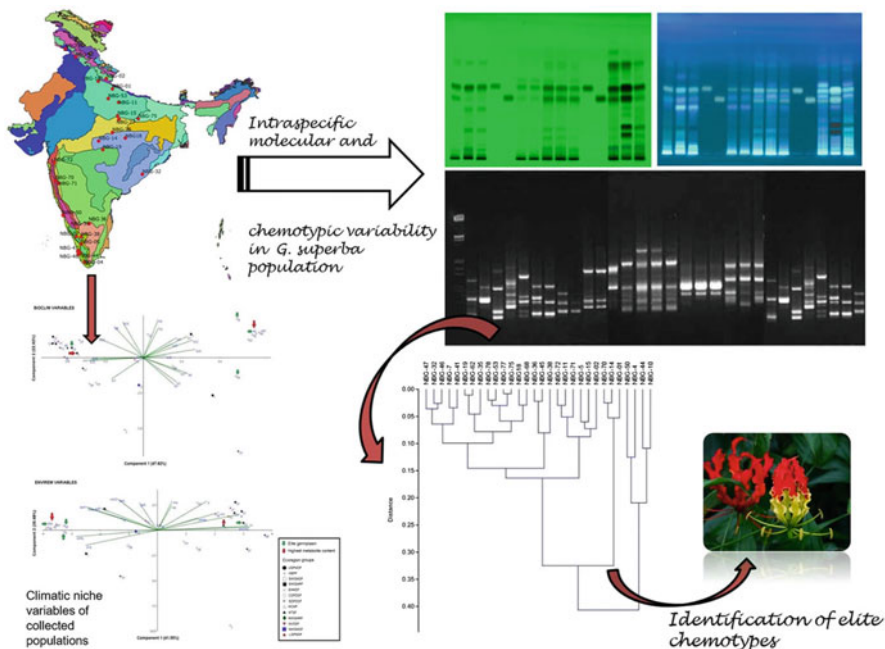


Fig. 10.3 Chemotaxonomic study on *Gloriosa superba*

10.8 *Tribulus terrestris* L.

Tribulus terrestris (fam. Zygophyllaceae), commonly known as Gokharu, has great importance in Indian systems of medicine. *Tribulus terrestris* (fruits) is known for its multifarious medicinal properties and is also used as dietary application. It is used for its various health benefits as digestive, cooling, expectorant, aphrodisiac, etc. (Chhatre et al. 2014). The species is a rich source of protodioscin and prototribestin steroidal saponins. The studies on identification and quantification of protodioscin and prototribestin in *T. terrestris* fruits collected from different phytogeographical zones of India have been done, and significant variation was found in metabolite content. Maximum content of protodioscin (0.317%) was found in samples collected from the Western Ghats, while prototribestin was found maximum (0.636%) in the arid zone of India (Rawat et al. 2013) (Fig. 10.4).

10.9 *Coleus forskohlii* Briq

Coleus forskohlii (fam. Lamiaceae) has been used for treating heart diseases traditionally. In recent times, *C. forskohlii* is preferred as a functional food due to its potency as obesity reducing agent and weight management (Kamohara 2016). This

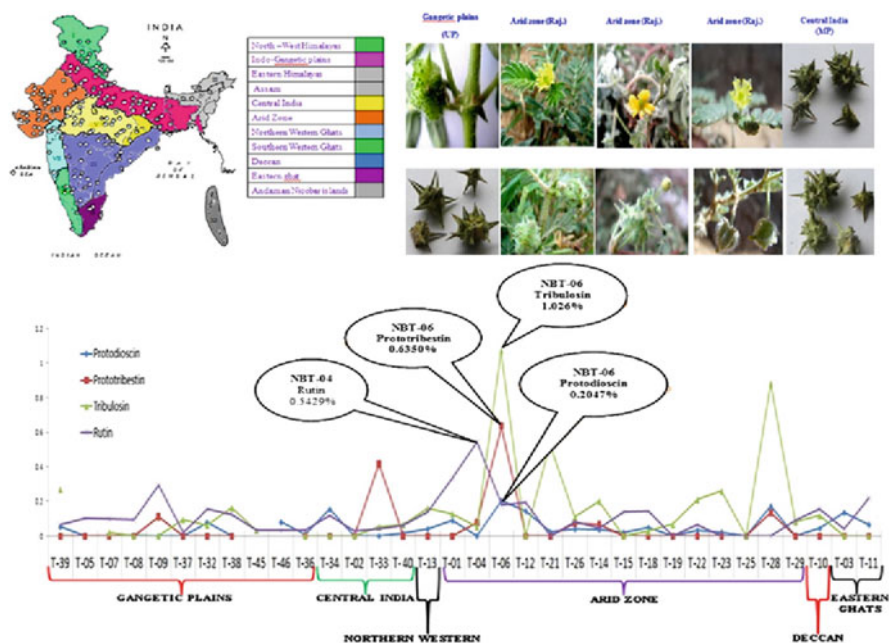


Fig. 10.4 Chemotaxonomic study on *Tribulus terrestris*

is the only natural source of the diterpenoid forskolin used for eczema, asthma, psoriasis, cardiovascular disorders, and hypertension. India exported *Coleus forskohlii* worth USD 38,776,700 with a total quantity of 271,163 metric tonnes. Japan is the largest buyer worth USD 21,707,204, followed by the United States and the United Arab Emirates worth USD 10,867,931 and USD 2,823,936, respectively (Srivastava et al. 2017). In our study, a total of 74 accessions of *C. forskohlii* were collected from various phyto-geographical zones of India. The minimum concentration of forskolin was reported in NBC-36 (0.004%) from the Western Ghats, while the maximum concentration was found in NBC-46 (1.153%) from the western coast of Malabar (Shukla et al. 2016, 2017) (Fig. 10.5).

10.10 *Costus speciosus* (Koen. Ex Retz) Sm

Costus speciosus, commonly known as the insulin plant, is a well-known plant in the traditional medicine system. As per ethnobotanical claims, *Costus* rhizomes are used in various ailments like jaundice, bronchial asthma, dropsy, diabetes, leprosy, and severe headache (El-Far et al. 2018). In our study, the rhizomes of 34 samples of *Costus speciosus* were collected from Gangetic plains of India. In plants, diosgenin is found in glycosidic form (inactive and associated with sugar moiety), and

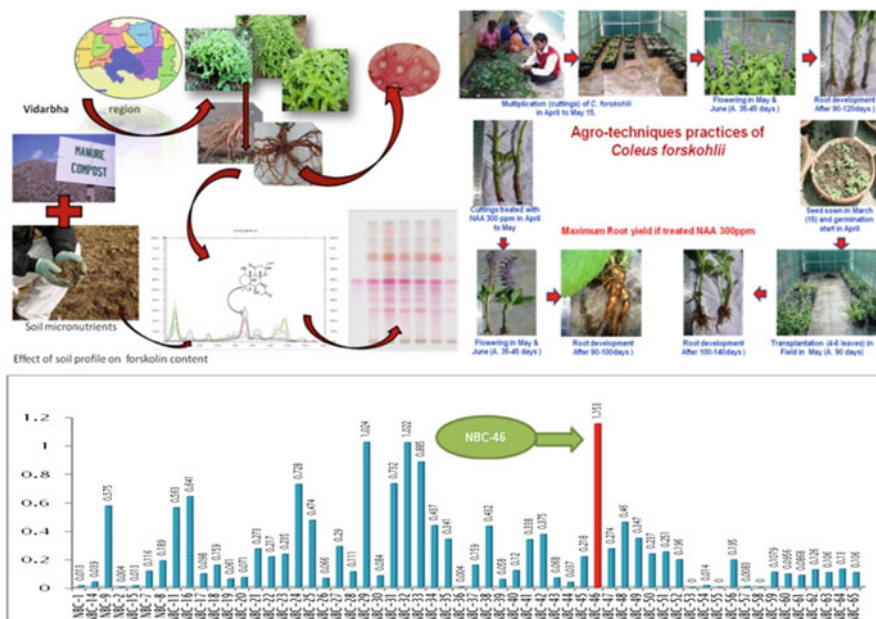


Fig. 10.5 Chemotaxonomic study on *Coleus forskohlii*

therefore it needs to be hydrolyzed to set it free, activated form. The results revealed that after acid hydrolysis diosgenin content was higher (0.15–1.88%) than non-hydrolysis (0.009–0.368%) plant extract. Germplasms collected from Central India were identified as elite chemotypes based on hierarchical clustering analysis (Kumar et al. 2020; Rawat et al. 2021) (Fig. 10.6).

10.11 *Ageratum conyzoides* L.

Ageratum conyzoides is widely used as an ethnomedicine by traditional healers and rural communities across the globe. It is used for treating cattle from an infestation of ectoparasites, wound healing, to treat skin diseases, and as an antimicrobial agent. Total of 110 germplasms were collected from different phyto-geographical zones of India. Chemical profiling of two bioactive compounds, precocene I and precocene II, was done through HPTLC, and in vitro anti-tick potential was studied. Maximum precocene I content was 0.095%, while maximum precocene II content was 0.338%. A significant anti-tick potential was reported in 95% alcoholic extract of *A. conyzoides* (Kumar et al. 2019, 2018, 2015) (Fig. 10.7).

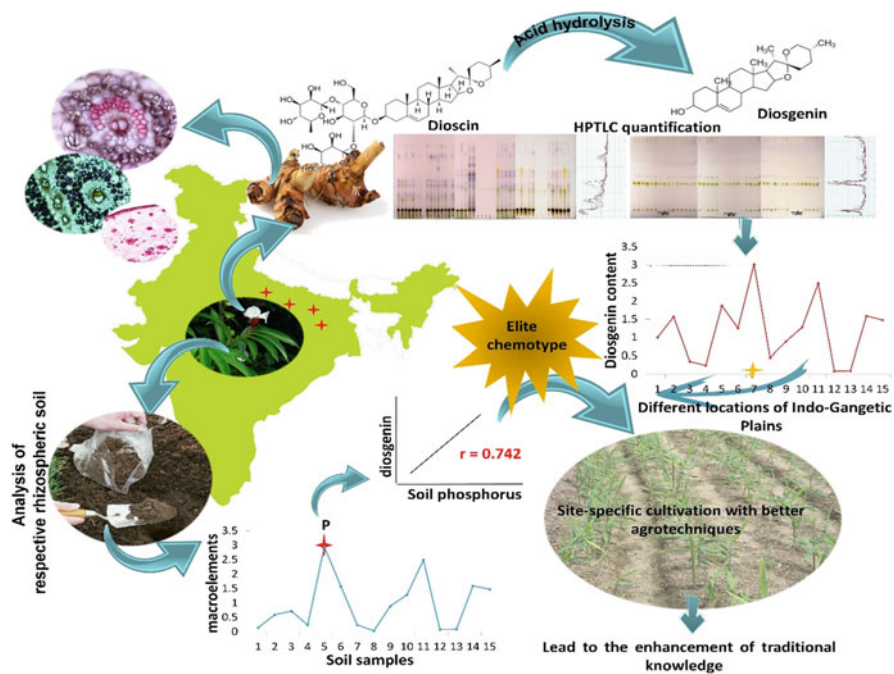


Fig. 10.6 Chemotaxonomic study on *Costus speciosus*

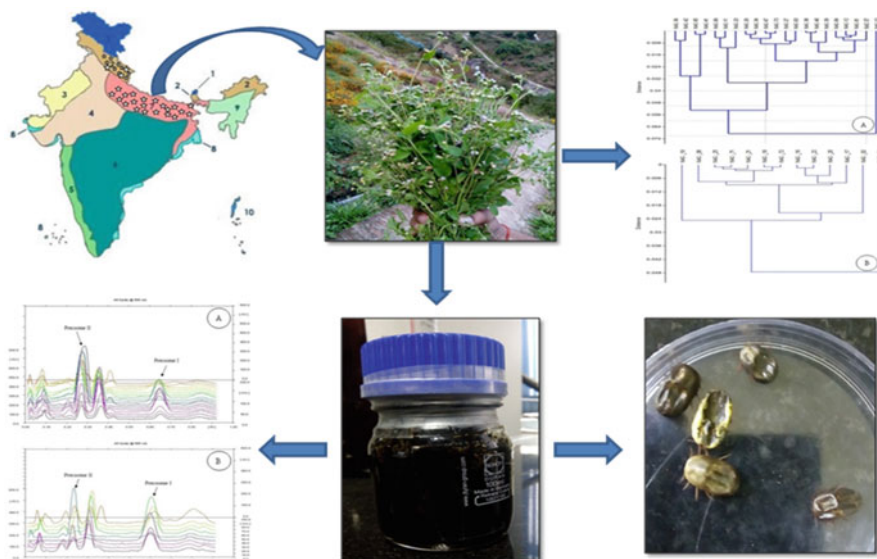


Fig. 10.7 Chemotaxonomic study on *Ageratum conyzoides*

10.12 *Centella asiatica* L. (Urban)

Centella asiatica (fam. Apiaceae) is an important medicinal plant in *Ayurveda* and has been used in neuropsychiatric disorders and wound healing for ages. For ages, the species has been used for the treatment of depression, neurological conditions, and anxiety burns and wound healing, ulcer, and as a brain tonic. In our study, a total of 109 germplasm were collected. The content of asiatic acid, madecassic acid, asiaticoside, and madecassoside varies from 3.2 to 0.02%, 3.06 to 0.02%, 4.3 to 0.02%, and 4.8 to 0.01%, respectively (Srivastava et al. 2014b). Results of PCA and associated dendrogram signify that the samples from the ecoregions of South Western Ghats Montane Rain Forests and East Deccan Dry-Evergreen Forests were rich in centellosides metabolite. Among them, CA-109, CA-134, and CA-122 were identified as elite chemotypes (Gupta et al. 2014) (Fig. 10.8).

Once the elite chemotypes are identified, commercial cultivation of medicinal species can be easily promoted. The knowledge about propagation techniques of medicinal plants is <10%, and the scores of agro-techniques developed for enhanced cultivation were less than 1% globally. This trend signifies that the development of agro-techniques for commercially/industrially valuable medicinal plants is a burning segment for future R & D. The data from chemotaxonomic studies will result in the identification of specific locations which is favored by nature for the growth of superior quality planting material. Thus, the reproduction of such ecological-niche factors under optimum conditions will help in developing agronomic practices/agro-techniques. In the same context, industry-sponsored cultivation of medicinal crop at

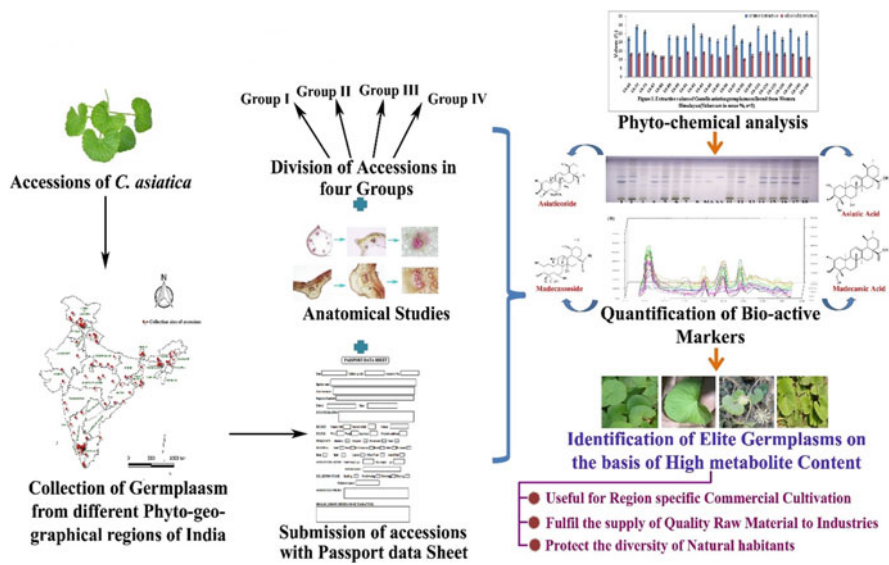


Fig. 10.8 Chemotaxonomic study on *Centella asiatica*

specific sites will create a channel for sustainable availability of quality raw material to the herbal drug industry and also reduce the load on wild sources.

Further, there will be a scope for socioeconomic upliftment of manpower involved in cultivation practices. The next step, after standardization of chemical constancy of raw material and/or finished herbal product, is to ensure biological safety. The efficacy of the developed product must be tested along with the safety and toxicity profile and should be maintained in every batch during the production for market acceptability and consumer safety. The efficacy can be evaluated using various protocols based on the targeted disease. The traditional and classical method to evaluate the safety, efficacy, and toxicity is through using the experimental animals, either using whole animal or animal part. The addition of biological quality assessment is a new addition to the identification of the quality of plant material along with a classical method of chemical assessment of plant drugs. Biological assessment of plant material/products involves regular pharmacological activity procedures, i.e., test design, experimental grouping, data recording, etc., along with data generation in terms of pharmaceutical analysis such as precision, repeatability, and accuracy. The various methods for biological assessment of any herbal products can be achieved through *Bioassays*, *Bio-response profile*, *Biological gene expression profile*, *Biomarker based activity assessments*, *Metabolomics*, *Proteomics*, etc., with the intervention of sophisticated hyphenated techniques. Currently, herbal product development is translating towards a new horizon, which is an amalgamation of both the chemical and biological identity of raw plant materials, i.e., ingredients used as well as the finished products/formulations.

10.13 Integration of Herbal Products in the Mainstream: Policy Regulations

The first national policy in India was framed under the Drug and Cosmetics Act, 1940, and Rule, which was revised several times. Over time, several changes and development were done to include the Indian traditional systems of medicine in regulations and gazette documents. Finally, in the year 2013 the department of Ayurveda, Yoga and Naturopathy, Unani, Siddha and Homeopathy (AYUSH) was constituted, and later a separate Ministry of AYUSH was formed in the year 2014. Similarly, a Pharmacopeial laboratory was established to ensure the standardization of drugs/products under Ayurveda, Siddha, Homeopathy and Unani systems of medicine and their testings also. Recently the AYUSH division was also formed in DGCI for the approval and clinical trial registration of herbal products under AYUSH mode. The advancement of such infrastructure results in the timely release of Official gazetted documents, and the developed products/raw materials have to abide with these regulations before commercialization in the Indian market. Ayurvedic Pharmacopeia of India and Indian Pharmacopeia along with the AYUSH ministry are major players in deciding the policy issues related to herbal drugs. Besides this, a collaborative database under the name “Traditional Knowledge Digital Library (TKDL)” was formed by CSIR and AYUSH to document the

traditional, folklore, and ethnobotanical information regarding these Indian traditional systems of medicine. This TKDL contains informations about 500 Ayurvedic, 500 Unani, and 200 Siddha formulations and is shared with different patent offices to regulate intellectual property (IP) protection. In nutshell, the development of new herbal products/formulations based on traditional knowledge is the key path and to achieve this, “reverse pharmacology” is the suitable approach. This approach is classical yet keeping pace with modernization in product development; the inverse route “disease to experiment” will be adopted in cohesion with the chemical and botanical assessment of raw material as well as a finished product to increase consumer acceptability. The use of various sophisticated analytical techniques, pharmacological data to establish the safety, toxicity, and efficacy profile along with clinical studies (as per DCGI/AYUSH guidelines) will serve as a powerful hammer to nail the coffin.

10.14 Emerging Concept of Plant-Based Nano-Formulations: A New Face of Traditional Ayurvedic *Bhasmas*

A section of Ayurveda, “*Rasa Shastra*,” i.e., Vedic chemistry, deals with herbo-mineral preparations called Bhasma (Prakash n.d.; Pal et al. 2014). Bhasma, literally meaning ash, is unique “Ayurvedic herbo-mineral-metallic compounds of nano-dimensions (usually 5–50 nm) as established by modern microscopic and spectroscopic techniques” (Kumar et al. 2006). It is prepared through a chain of processes involving purification (shodhana) and incineration (marana), aimed at reducing the particle size, for example, *Swarna Bhasma* (gold ash) has been characterized as globular particles of gold of 1–2 μm . The end product is expected to be a tasteless, biocompatible, bioassimilable, absorbable, and suitable powder intended for the human body. There are several types of *Ayurvedic* bhasmas, namely metallic, mineral, or herbal bhasma, each having its characteristic properties (Mohaptra and Jha 2010). The manufacturing process is very systematic and elaborate, called “Bhasmikarana,” which converts the metal from its original state to a higher oxidation state (Wadekar et al. 2005). This leads to the elimination of toxicity associated with metal and metal-oxides with high medicinal value. The metals, when treated with medicinal plants or their oil, lead to the adhesion of medicinally important phytochemicals on the metal surface. In this way, various phytochemicals, such as phenolics and flavonoids, are easily transported inside the cell due to the small size and high absorbability of the *Bhasma* and maintain sustained and prolonged bio-availability. During the preparation of *Swarna Bhasma*, the gold leaves are heated and then dipped in *Sesamum indicum* oil, followed by processing with buttermilk, decoction of kulattha (*Dolichous biflorus*), radish (*Raphanus sativus*), and kanji (*Oryza sativa*). Mandura (Iron) Bhasma is prepared and processed with fresh triphala decoction, lemon juice, and *Aloe vera*. Naga Bhasma is processed with several herbs, including Chichiri (*Plectranthus cuesta*) and Vaasa (juice of *Adhatoda vasica* Leaf) (Farooq et al. 2019).

The concept of *Bhasmas* is very old, but its preparation methodology is scientifically acceptable in today's time and corresponds to nanoparticles, and is similar (physicochemical) to nano-crystalline materials. The prime difference between *Bhasma* and synthetic nano-material is due to the usage of organic, mineral materials, and herbs during the preparation. The therapeutic potential of *Bhasmas* is dependent on the potency/efficacy of plant and animal products used for the preparation. Drugs having low solubility leads to various bioavailability issues, after product development like bio-assimilation after oral intake, due to less diffusion high quantity are required for intravenous delivery, and various other side effects. However, such complications could be resolved by the use of nanotechnological approaches in the drug delivery system. An extensive study has been done regarding drug designing at the nano-scale, and is one of the most advanced and acceptable technology in nanoparticle applications. This technique has tremendous potential to modify properties of drugs like solubility, diffusion, drug release profiles, immunogenicity, and bioavailability (Beutler 2009). Due to their nano size, the product particles will easily penetrate into the tissue system, facilitating the cellular drug uptake, permitting an efficient drug delivery, and thus targeted action is achieved. Hence, nano-formulation(s) ensure direct interaction with the targeted site, exhibiting improved efficiency and reduced side effects (Patra et al. 2018). However, the properties of a nanoparticle which make them unique for their importance in industrial and biomedical applications had also raised several safety concerns. For example, carbon-based nanoparticles have been found to be toxic in several in vitro and in vivo assay (Johnston et al. 2010). Iron, Silver, and Gold nanoparticles sometimes demonstrate cytotoxicity under certain conditions (Wang et al. 2013; Kim et al. 2012; Pan et al. 2007), and therefore formulation development should be done with caution.

Considering the harmful aspects of artificial nanotechnology, researchers nowadays are moving back towards ancient nanoparticles, i.e., *Bhasmas* giving them a new outlook under the banner of "Green nanoparticles" involving phytochemical processing of nanoparticles. These phytochemicals act as the reducing agent for nanoparticles and simultaneously act as an effective capping agent to prevent the aggregation of nanoparticle. The methodology may be novel but is just a modified version of the traditional "Ayurvedic *Bhasmasikaran*" procedure where the metals are treated with plants (Pal et al. 2014). Copper oxide nanoparticles were prepared using an aqueous extract of herbal tea (*Stachys lavandulifolia*) flowers leading to green and cost-effective biogenesis of nano-catalyst (Veisi et al. 2021). Silver nanoparticles synthesized with aqueous extract of *Acanthospermum austral* exhibit potential antimicrobial activity along with the potential modulator of cytotoxic and immune responses, owing to capping with plant extract (Mussin et al. 2021). Similarly, copper nanoparticles prepared in an aqueous solution using *Crocus sativus* leaf extract were found to be a neuroprotective promotor and were under clinical trial (Zhang et al. 2020). In the same context, treatment of neurodegenerative disorders, plant-based nanoparticles having the ability to cross the blood-brain-barrier involving curcumin, piperine, quercetin, etc., were developed with increased bioavailability and improved pharmacokinetics (Moradi et al. 2020). Poly Lactic

Glycolic Acid or Poly Lactic Acid was approved by FSSAI and is used as a nano-carrier for several phytochemical nanoparticles like resveratrol, silybin, silymarin, etc., for the treatment of diabetes (Dewanjee et al. 2020). Berberine-loaded nanoparticles and artemisinin nano-capsules were tested in the treatment of cancer (Youfang et al. 2009; Habtemariam 2020). Looking at the advantages offered by medicinal plants in the form of nano-formulations, nano-medicines are neither undeniable nor unavoidable. However, there is a strict need for rigorous safety-related studies in order to reduce toxicity. In this regard, *Ayurvedic Bhasma* may hold strong relevance to serve as an excellent template for the development of nano-medicine as efficient therapeutics.

10.15 Conclusion

It is not exaggerated to say that the utilization of medicinal plants for health benefits is an integral part of human lives since immortal. However, the modernization of our knowledge of scientific tools and techniques has risen our consciousness to explore the scientific evidence behind every pharmacological benefit of medicinal plants. This is well understood that with advancements in the human race, the health care system should be made affordable and reachable to each one of us across the globe, and, therefore, global acceptance of traditional systems of medicine (TSM) will be the possible alternative. There is still hesitation in society about accepting the TSM as the first line of treatment, although it cannot be ignored that still, more than 70% of the world's population rely on traditional herbal medicines for their primary health care needs.

This brings in responsibility on official bodies that necessary guidelines, rules, and regulations must be framed out and implemented on various strata involved in/dealing with medicinal plants. Various challenges which focus on standardizing the authenticity of raw material, its chemical characterization, and biological efficacy should be addressed, specifically by the concerned authorities in implementation, manufacturer/dealer/retailer for the product development, and by the R & D professionals in generating scientific evidences/methodologies. The Indian government, regulatory bodies, and premier R & D institutions are endlessly working to bring the goodness of our rich tradition of the traditional system of medicines like the Ministry of AYUSH into the mainstream healthcare system of India. A long path has been covered but still a long way to go to achieve milestones.

References

- Anonymous (n.d.). <https://cmjournal.biomedcentral.com/track/pdf/10.1186/s13020-020-00335-9.pdf>
- Beutler JA (2009) Natural products as a foundation for drug discovery. *Curr Protocols Pharmacol* 46(1):9–11
- Chhatre S, Nesari T, Somani G, Kanchan D, Sathaye S (2014) Phytopharmacological overview of *Tribulus terrestris*. *Pharmacogn Rev* 8(15):45

- Dewanjee S, Chakraborty P, Mukherjee B, De Feo V (2020) Plant-based antidiabetic nanoformulations: the emerging paradigm for effective therapy. *Int J Mol Sci* 21(6):2217
- El-Far AH, Shaheen HM, Alsenosy AW, El-Sayed YS, Al Jaouni SK, Mousa SA (2018) *Costus speciosus*: traditional uses, phytochemistry, and therapeutic potentials. *Pharmacogn Rev* 12(23)
- Farooq S, Mehmood Z, Qais FA, Khan MS, Ahmad I (2019). Nanoparticles in ayurvedic medicine: potential and prospects. In *New look to phytomedicine*. pp 581–596. Academic Press
- Gupta A, Verma S, Kushwaha P, Srivastava S, Aks R (2014) Quantitative estimation of asiatic acid, asiaticoside & madecassoside in two accessions of *Centella asiatica* (L) urban for morpho-chemotypic variation. *Indian J Pharm Educ Res* 48(3):75–79
- Gyawali R, Kim KS (2009) Volatile organic compounds of medicinal values from Nepalese *Acorus calamus* L. *Kathmandu Univ J Sci Eng Technol* 5:51
- Habtemariam S (2020) Recent advances in berberine inspired anticancer approaches: from drug combination to novel formulation technology and derivatisation. *Molecules* 25(6):1426
- Jain SK (n.d.) *Dictionary of folk medicine and ethnobotany*. Deep Publications, New Delhi
- Jain A, Katewa SS, Chaudhary BL, Galav P (2004) Folk herbal medicines used in birth control and sexual diseases by tribals of southern Rajasthan, India. *J Ethnopharmacol* 90(1):171–177
- Johnston HJ, Hutchison GR, Christensen FM, Peters S, Hankin S, Aschberger K, Stone V (2010) A critical review of the biological mechanisms underlying the in vivo and in vitro toxicity of carbon nanotubes: the contribution of physico-chemical characteristics. *Nanotoxicology* 4(2): 207–246
- Kala CP (2000) Status and conservation of rare and endangered medicinal plant in the Indian trans-Himalaya. *Biol Conserv* 93:371–379
- Kale CP (2005) Indigenous uses, population density, and conservation of threatened medicinal plants in protected areas of the Indian Himalayas. *Conserv Biol* 19:268–378
- Kamohara S (2016) An evidence-based review: anti-obesity effects of *coleus forskohlii*. *Personalised Med Universe* 5:16–20
- Kim TH, Kim M, Park HS, Shin US, Gong MS, Kim HW (2012) Size-dependent cellular toxicity of silver nanoparticles. *J Biomed Mater Res A* 100(4):1033–1043
- Kumar A, Nair AG, Reddy AV, Garg AN (2006) Unique ayurvedic metallic-herbal preparations, chemical characterisation. *Biol Trace Elem Res* 109(3):231–254
- Kumar B, Srivastava S, Rawat AK (2015) Intra-specific variation of precocene I in the wild population of *Ageratum conyzoides* L. from the Western Himalayas. *JPC-J Planar Chromatogr Modern TLC* 28(5):391–394
- Kumar B, Misra A, Rawat AK, Rawat YS, Srivastava S (2018) Simultaneous quantification of Precocene I and Precocene II through high-performance thin-layer chromatography validated method in *Ageratum conyzoides* L. germplasms from the western Himalayas. *Pharmacogn Mag* 14(55):141
- Kumar B, Misra A, Kumar S, Rawat AK, Rawat YS, Ghosh S, Srivastava S (2019) Antitick potential and chemical variability among *Ageratum conyzoides* L. germplasms collected from Eastern and Western Ghats of India. *Int J Acarol* 45(8):488–496
- Kumar M, Misra A, Srivastava A, Shukla PK, Tewari LM, Srivastava S (2020) Comparative pharmacognostical and pharmacological evaluation of *Costus speciosus* (Koen) JE Sm. Germplasm Collected from Eastern Ghats of India. *Pharmacogn J* 12(1)
- Ministry of Health and Family Welfare Gazette Notification G.S.R. 918(E) (n.d.) [Last accessed on 2016 Feb 18]. Available from: <http://www.cdsc0.nic.in/writeraddata/GSR%20918-E-dated-30-11-2015.pdf>
- Misra A, Srivastava S (2016) Chemotaxonomy: an approach for conservation & exploration of industrially potential medicinal plants. *J Pharmacogn Nat Prod* 2:4
- Misra A, Shukla PK, Kumar B, Chand J, Kushwaha P, Khalid M, Rawat AK, Srivastava S (2017) High-performance thin-layer chromatographic-densitometric quantification and recovery of bioactive compounds for identification of elite chemotypes of *Gloriosa superba* L. collected from Sikkim Himalayas (India). *Pharmacogn Mag* 13(Suppl 3):S700

- Misra A, Kumar B, Shukla P, Srivastava S (2020) Simultaneous HPTLC-UV quantification of colchicine and gloriosine alkaloids in the natural population of *Gloriosa superba* L., collected from eastern Ghats of India for the identification of elite chemotypes. *J Liq Chromatogr Relat Technol* 43(9–10):351–360
- Misra A, Mishra P, Kumar B, Shukla PK, Kumar M, Singh SP, Sundaresan V, Adhikari D, Agrawal PK, Barik SK, Srivastava S (2021) Chemodiversity and molecular variability in the natural populations (India) of *Gloriosa superba* (L.) and correlation with eco-geographical factors for the identification of elite chemotype (s). *Fitoterapia* 150:104,831
- Mohaptra S, Jha CB (2010) Physicochemical characterisation of ayurvedic bhasma (Swarna makshikabhasma): an approach to standardisation. *Int J Ayurveda Res* 1(2):82
- Moradi SZ, Momtaz S, Bayrami Z, Farzaei MH, Abdollahi M (2020) Nanoformulations of herbal extracts in the treatment of neurodegenerative disorders. *Front Bioeng Biotechnol* 7:238
- Mukherjee PK, Kumar V, Mal M, Houghton PJ (2007) *Acorus calamus*.: scientific validation of ayurvedic tradition from natural resources. *Pharm Biol* 45(8):651–666
- Mussin J, Robles-Botero V, Casañas-Pimentel R, Rojas F, Angiolella L, San Martín-Martínez E, Giusiano G (2021) Antimicrobial and cytotoxic activity of green synthesis silver nano-particles targeting skin and soft tissue infectious agents. *Sci Rep* 11(1):1–2
- Oostermeijer JGB, Luijten SH, Den Nijs JCM (2003) Integrating demographic and genetic approaches in plant conservation. *Biol Conserv* 113:389–398
- Pal D, Sahu CK, Haldar A (2014) Bhasma: the ancient Indian nanomedicine. *J Adv Pharm Technol Res* 5(1):4
- Pan Y, Neuss S, Leifert A, Fischler M, Wen F, Simon U, Schmid G, Brandau W, Jahnen-Dechent W (2007) Size-dependent cytotoxicity of gold nanoparticles. *Small* 3(11):1941–1949
- Pandey MM, Rastogi S, Rawat AKS (2013) Indian traditional ayurvedic system of medicine and nutritional supplementation. *Evid Based Complement Alternat Med*. <https://doi.org/10.1155/2013/376327>
- Patra JK, Das G, Fraceto LF, Campos EV, del Pilar R-TM, Acosta-Torres LS, Diaz-Torres LA, Grillo R, Swamy MK, Sharma S, Habtemariam S (2018) Nano based drug delivery systems: recent developments and future prospects. *J Nanobiotechnol* 16(1):1–33
- Prakash B (n.d.) (01) Use of metals in ayurvedic medicine
- Rana TS, Mahar KS, Pandey MM, Srivastava SK, Rawat AK (2013) Molecular and chemical profiling of ‘sweet flag’ (*Acorus calamus* L.) germplasm from India. *Physiol Mol Biol Plants* 19(2):231–237
- Rawat AK, Srivastava A, Tiwari SS, Srivastava S (2013) Quantification of protodioscin and prototribestin in fruits of *Tribulus terrestris* L. collected from different phytoecographical zones of India. *J Liq Chromatogr Relat Technol* 36(13):1810–1821
- Rawat P, Kumar M, Srivastava A, Kumar B, Misra A, Pratap Singh S, Srivastava S (2021) Influence of soil variation on diosgenin content profile in *Costus speciosus* from Indo-Gangetic Plains. *Chem Biodivers* 18:e2000977
- Sen S, Chakraborty R (2017) Revival, modernisation and integration of Indian traditional herbal medicine in clinical practice: importance, challenges and future. *J Tradit Complement Med* 7: 234–244
- Shukla PK, Misra A, Kumar M, Rajan S, Agrawal PK, Rawat AK, Srivastava S (2016) Intra-specific chemotypic variability of forskolin content in *Coleus forskohlii* (wild.) Briq. Growing in Nilgiri Hills of India. *JPC-J Planar Chromatogr Modern TLC* 29(5):347–355
- Shukla PK, Misra A, Kumar M (2017) Simultaneous quantification of forskolin and iso-forskolin in *Coleus forskohlii* (Wild.) Briq. And identification of elite chemotype, collected from eastern ghats (India). *Pharmacogn Mag* 13(Suppl 4):S881
- Srivastava S, Misra A (2018) Quality control of herbal drugs: advancements and challenges. In: Singh B, Peter KV (eds) *New age herbals*. Springer Nature Singapore Pte Ltd. https://doi.org/10.1007/978-981-10-8291-7_10
- Srivastava S, Misra A, Shukla PK, Kumar B, Lata S, Rawat AK (2014a) A validated over pressured layered chromatography (OPLC) method for separation and quantification of colchicine in

- Gloriosa superba* (L.) tubers from different geographical regions. RSC. Advances 4(105): 60,902–60,906
- Srivastava S, Verma S, Gupta A, Rajan S, Rawat A (2014b) Studies on chemotypic variation in *Centella asiatica* (L.) urban from Nilgiri range of India. JPC-J Planar Chromatogr Modern TLC 27(6):454–459
- Srivastava S, Misra A, Mishra P, Shukla P, Kumar M, Sundaresan V, Negi KS, Agrawal PK, Rawat AK (2017) Molecular and chemotypic variability of forskolin in *Coleus forskohlii* Briq., a high-value industrial crop collected from western Himalayas (India). RSC Adv 7(15):8843–8851
- Subhose V, Srinivas P, Narayana A (2005) Basic principles of pharmaceutical science in ayurveda. Bull Indian Inst Hist Med 35(2):83–92
- Veisi H, Karmakar B, Tamoradi T, Hemmati S, Hekmati M, Hamelian M. Biosynthesis of CuO nanoparticles using aqueous extract of herbal tea (*Stachys Lavandulifolia*) flowers and evaluation of its catalytic activity. Sci Rep 2021;11(1):1–3
- Viswanathan K (1995) Survey on medicinal spices of the Nilgiris. Anc Sci Life 14(4):258
- Wadekar MP, Rode CV, Bendale YN, Patil KR, Prabhune AA (2005) Preparation and characterisation of a copper-based Indian traditional drug: Tamrabhasma. J Pharm Biomed Anal 39(5):951–955
- Wang B, Yin JJ, Zhou X, Kurash I, Chai Z, Zhao Y, Feng W (2013) Physicochemical origin for free radical generation of iron oxide nano-particles in biomicroenvironment: catalytic activities mediated by surface chemical states. J Phys Chem C 117(1):383–392
- Weekley CW, Race T (2001) The breeding system of *Ziziphus celata* judd and D.W. Hall (Rhamnaceae), a rare endemic plant of the Lake, vol 100. Implications for Recovery, Biological Conservation, Wales Ridge, FL, pp 207–2013
- World Health Organization (WHO) (2013) Traditional medicine strategy 2014–2023. World Health Organization, Geneva
- Youfang C, Xianfu L, Hyunjin P, Richard G (2009) Evaluation of artemisinin nano-particles. Nanomed Nanotechnol Biol Med 5:316–322
- Zhang P, Cui J, Mansooridara S, Kalantari AS, Zangeneh A, Zangeneh MM, Sadeghian N, Taslimi P, Bayat R, Şen F (2020) RETRACTED ARTICLE: suppressor capacity of copper nano-particles biosynthesised using *Crocus sativus* L. leaf aqueous extract on methadone-induced cell death in adrenal pheochromocytoma (PC12) cell line. Sci Rep 10(1):1–5



Chemicals and Their Interaction in the Aquaculture System

11

T. A. Jose Priya and Sudha Kappalli

11.1 Introduction

Aquaculture is a growing agribusiness across the world. Commercially important aquatic animals are often prone to diseases caused by biotic and abiotic factors. Amplification and transmission of diseases are the significant risks of aquaculture farming systems, leading to substantial effects on the economy. Specifically, more rapid and severe outbreaks of viral, bacterial, fungal, protists, and metazoan diseases commonly result in higher cumulative mortalities of cultured animals such as fishes, crustaceans, and mollusks.

Disease vulnerability frequently affects the culturing status of the most valued aquatic species populations. Various control measures have been introduced over the years. These include disinfectants, antibiotics, pesticides, chemotherapeutics, antibiotics, and drugs (Pathak et al. 2000; Rodgers and Furones 2009; Romero et al. 2012; Idowu and Sogbesan 2017). The chemicals often cause adverse effects such as environmental damage and the development of resistant strains of pathogens. Antimicrobial use in aquaculture leads to the development and spread of antimicrobial-resistant bacteria, resistance genes, and antimicrobial residues in aquaculture products and the environment (Aly and Albutti 2014; Cabello et al. 2016; Nakayama et al. 2017).

In India, the Guidelines issued under Coastal Aquaculture Authority (CAA) rules state that chemicals must be avoided in aquaculture ponds (<http://caa.gov.in/>). Antibiotics of concern include chloramphenicol, nitrofurantoin parent compounds, metabolites, furazolidone, furaltadone, nitrofurantoin, nitrofurazone, and so forth. (Romero et al. 2012; Carvalho et al. 2012; Rasul and Majumdar 2017). For risk

T. A. Jose Priya · S. Kappalli (✉)

Department of Zoology, School of Biological Sciences, Central University of Kerala, Kasaragod, India

e-mail: sudhakappalli@cukerala.ac.in

assessment, the chemicals present in the culture ponds have to be detected. It is rather hard to find the presence of chemicals in the culture system. Specific chemicals cannot be detected easily if the culture farms use a mixture of chemicals indiscriminately. National Residue Control Plan (NRCP) of Marine Products Export Development Authority (MPEDA), India, is a statutory requirement for the export of marine and aquaculture products to European Union countries (MPEDA 1987). NRCP will monitor substances like antibacterial/veterinary medicinal products and environmental contaminants in hatcheries, feed mills, aquaculture farms, processing plants, and so forth.

11.2 Chemical Practices in Aquaculture Systems

Several chemicals have been used for aquaculture mainly to treat diseased animals and, to a lesser degree, improve water quality in culture facilities. On the business side, the main advantage of chemical application is the quick achievement of results (Table 11.1). Chemicals used in grow-out farming and hatchery operations are classified into the following categories:

1. Water/soil quality enhancers
2. Fertilizers
3. Disinfectants
4. Anesthetics
5. Antimicrobials
6. Feed additives
7. Pesticides
8. Immunostimulants
9. Breeding inducing agents

11.3 Aquaculture Species of Commercial Importance: Worldwide Review

Global aquaculture is a flourishing sector and is one of the most vital primary industries. The primary culture species being cultured in different parts of the world and the chemical usage is discussed below. The Asia–Pacific region (China, India, Indonesia, Vietnam), Africa, Europe, Latin America, Canada, Brazil, the United States, Saudi Arabia, Australia, and Russia are significant aquaculture producers reported.

China accounts for nearly 70% of world aquaculture production. A wide variety of freshwater and marine fishes, shellfish, crustaceans, and aquatic plants, have been cultured in China (Cao et al. 2015; Gui et al. 2018). The major aquatic species of commercial importance include Chinese carp species, yellow croaker, grouper and sea bream, mollusks, and seaweed. Land-based farming, such as tank culture for flounder and turbot, is also popular in northeast China. Familiar but rare species such

Table 11.1 Chemicals used in aquaculture systems

S. No	Category	Subcategory	Chemical ingredients
1	Water and soil conditioners	Liming	Oxides, hydroxides and silicates of calcium or magnesium
		EDTA treatment	Disodium Ethylene Diamine Tetraacetate
		KMnO ₄ treatment	Potassium permanganate
		Other	Calcium sulfate (Gypsum), Chloramine T (N-Chloro-p-toluene sulfonamide), Acriflavin, Aluminum sulfate (alum), Iodophores, Organophosphates, Sodium chloride
2	Fertilizers	Organic fertilizers	Livestock manures, plant crop residues, food processing wastes, fresh-cut or dry grass
		Inorganic fertilizers	Urea, triple superphosphate (TSP), Ammonium nitrate, Calcium nitrate, Sodium nitrate, Potassium nitrate, Ammonium sulfate, Diammonium phosphate, Monoammonium phosphate, Superphosphate, Ammonium polyphosphate, Potassium chloride
3	Disinfectants	Chlorination	Chlorine gas (Sodium/Calcium hypochlorite)
		Formalin treatment	Formaldehyde Methanol
		BKC treatment	Benzaklonium chloride
		Iodine treatment	Povidone-iodine (PVP-I)
		Hydrogen peroxide treatment	Aqueous H ₂ O ₂ , Sodium percarbonate
		Malachite green treatment	Malachite green
4	Anesthetics	Benzocaine	Ethyl 4-aminobenzoate
		Other	Quinaldine, Halothane, Isoflurane, Lignocaine, MS222, Phenoxyethanol, CO ₂ , and clove oil
5	Antimicrobials	Antibiotics	Quinolones, tetracyclines, amphenicols, sulfonamides
6	Feed additives	Supplementary fish feeds	Vitamins, minerals, pigments, antioxidants, chemoattractants, and preservatives
7	Pesticides	Herbicides	Copper sulfate (bluestone), fluridone, Glyphosate, 2,4-D, Diquat
		Insecticides	Pyrethroids (deltamethrin, cypermethrin), organophosphates (dichlorvos, dipeterex)
8	Immunostimulants	Vaccines	Live, attenuated, peptide, and genetic vaccines
		Cytokines	TNF, interleukins (IL)

(continued)

Table 11.1 (continued)

S. No	Category	Subcategory	Chemical ingredients
9	Breeding inducing agents	Hypophysation	Pituitary gland extract
		Sex control agents	17 α methyltestosterone, 17 β methyl progestins
		Synthetic hormones	Estrogens and androgens

as abalone, holothurians, and scallops are also cultured using specialized aquaculture techniques.

In India, there are many candidate species of commercial importance in aquaculture. The species are Tiger shrimp (*Penaeus monodon*), Giant Freshwater prawn (*Macrobrachium rosenbergii*), Pacific white-legged shrimp (*Penaeus vannamei*), Indian white shrimp (*Penaeus indicus*), Milkfish (*Chanoschanos*), Mullet (*Mugil cephalus*), Asian Sea bass (*Lates calcarifer*), Nile Tilapia (*Oreochromis niloticus*), Cobia (*Rachycentron canadum*), Tiger Grouper (*Epinephelus fuscoguttatus*), Mangrove crabs (*Scylla serrata*), Edible oyster (*Crassostrea madrasensis*), Pearl oyster (*Pinctada fucata*, *P. margaritifera*), Mussels (*Perna viridis*, *P. indica*), Yellow Clam (*Paphiamalabarica*), and Clams (*Anadara granosa*, *Villoritacyprinoides*) (Jana and Jana 2003; De Jong 2017; Jayasankar 2018).

In Indonesia, the species raised by aquaculture farms include salmon, catfish, tilapia, cod, and others (Yusuf 1995; Tran et al. 2017). Vietnam, an ideal country boasting for its seafood industry, is dominated by freshwater fish ponds, rice-cum-fish and marine cage culture in the northern region, and the intensive culture of giant tiger prawn in the central region. The southern region has the most diversified farming activities, including shrimp culture, rice-cum-fish, rice-cum-prawn and mangrove-cum-aquaculture, marine cage culture of finfish and lobster, pond and fence cultures of catfish, and other indigenous species such as snakehead fish, climbing perch, and giant river prawn. Key aquaculture species include pangasius, shrimp, tilapia, and bivalves and marine fishes such as cobia, seabass, and grouper (Aquaculture Vietnam 2021).

On the other hand, Africa contributes insignificantly to the world aquaculture, albeit the larger-scale investments in Egypt, Nigeria, Uganda, Ghana, Tunisia, Kenya, Zambia, Madagascar, Malawi, and South Africa for the production of fish. Almost 99% of the production is from the inland freshwater systems dominated mainly by the culture of indigenous and abundant species of tilapia and African catfish (Halwart 2020; Satia 2011; Satia 2017; Cai et al. 2017; FAO 2016, 2018).

Aquaculture production in Europe is very diverse in terms of farming species and methods of production. Sea cages, ponds, raceways, and on-land recirculating aquaculture systems have been widely used. The major aquaculture-producing EU countries are Spain, France, Italy, and Greece. Despite the diversity of aquaculture, the EU aquaculture production is concentrated on only a few species: mussels, salmon, seabream, rainbow trout, seabass, oysters, and carp (Oceans and Fisheries, European Commission n.d.).

Aquaculture production in Latin America and the Caribbean account for 3% of the global output. The primary regional cultures are exotic species, mainly salmonids, marine shrimp, and tilapia (Hernández-Rodríguez et al. 2001; Lovatelli 2021). Latin America mainly exports shrimp and salmonids, and Ecuador being the top shrimp-producing country, especially the white leg shrimp.

Atlantic salmon (*Salmo salar*) and the white sturgeon (*Acipenser transmontanus*) are the commercially important species of North America, Canada, and the United States. Along with these, channel catfish (*Ictalurus punctatus*) and chinook salmon remain the dominant species produced in North America and the North-eastern Pacific of Canada, respectively. Golden shiner, rainbow trout, tilapia, and coho salmon are also commercially important species of North America. In addition to this finfish farming, invertebrate species were also added to their culture system. The main invertebrate products include red swamp crawfish, American oyster, blue mussel, northern quahog, abalone, european flat oyster, and pacific oyster (Olin 2001; Masser and Bridger 2007; Olin et al. 2012; Clements and Chopin 2017).

All aquaculture operations directly or indirectly demand drugs and other chemicals such as antibiotics and other therapeutic compounds, disinfectants, sedatives and anesthetics, herbicides and pesticides, sex manipulators, spawning aids, immunostimulants, and vaccines.

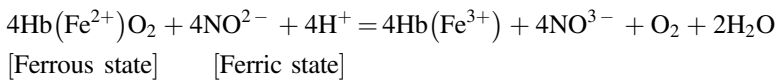
11.4 Chemical Ingredients Purposed for Water Quality Management in Aquaculture

Intensive culture systems are often coupled with formulated feed, water quality management, and disease control. Aquaculture productivity largely depends upon soil and water quality variables such as pH, salinity, and temperature. All these parameters have to be maintained at optimum levels; otherwise, the growth and survival of the cultured species will be highly affected. Various chemical treatment methodologies include liming, potassium permanganate usage, and EDTA treatment.

The most important factor affecting the growth of aquaculture species is the water quality. Natural water is composed of negatively charged chlorides (Cl^-), sulfates (SO_4^-), carbonates (CO_3^-) and bicarbonates (HCO_3^-) and positively charged sodium (Na^+), potassium (K^+), magnesium (Mg^{++}) and Calcium (Ca^{++}). Traces of other ions, including copper, iron, zinc, fluoride, cobalt, and molybdenum, are also necessary for the growth of aquaculture species. Apart from the ions, the principal gases dissolved in water are oxygen (O_2), carbon dioxide (CO_2), and nitrogen (N_2). Minimum levels of ammonia and nitrites, optimum water hardness, pH, and temperature are also necessary for the optimum growth of aquatic animals (Pattillo 2014). Outside the optimum ranges, cultured animals can become stressed and vulnerable. For instance, if the pH of the water is far beyond or far below the optimum range, cultured animals are prone to mortality. Inappropriate pH (low or high) also favors the solubility of chemicals and heavy metals in the water, increasing the chance of water toxicity to the cultured species. pH also affects the growth and reproduction of

the cultured species. Extremely high pH is associated with alkalosis. The water's high alkalinity (pH of or above 9.6) affects the fish by denaturing the cellular membranes of gills, skin, and eyes, causing death. Extremely high pH also leads to the conversion of ionized ammonium (NH₄) into toxic-free (unionized) ammonia (NH₃), which in turn causes gill and kidney damage, impaired growth, and disease susceptibility (Randall and Tsui 2002; Zeitoun and Mehana 2014). Free or unionized ammonia is highly toxic compared to ionized ammonium, and the lethal concentration of ammonia being 0.2–0.5 mg/L. The clinical signs of ammonia poisoning include anorexia (stop feeding), behavioral and swimming abnormalities, neurological and respiratory symptoms. Nitrite poisoning also causes breathing difficulties, depigmentation/hyperpigmentation, and behavioral abnormalities in cultured animals.

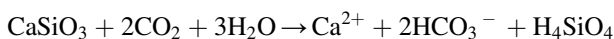
Aquatic animals in freshwater are often hyperosmotic and require an active uptake of ions through their gills to compensate for the loss of ions via urine and passive efflux across the gills. Nitrite poisoning however affects the branchial Cl⁻ uptake mechanism. The high nitrite concentration in the water enters the blood plasma. It diffuses into the red blood cells, oxidizing iron in hemoglobin (Hb) into a ferric (Fe³⁺) state. It is called ferrihemoglobin or methemoglobin, which cannot bind oxygen, and leads to tissue hypoxia. It causes methemoglobinemia or brown blood disease in fish.



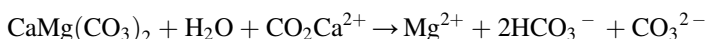
11.4.1 Liming

Lime is a significant chemical used to improve the bottom condition during the preparation of a grow-out pond. Lime changes the chemistry of water and pond soils thereby making nutrients available to cultured organisms. Liming is considered an integral part of water and soil management in aquaculture. Liming helps to neutralize sulfides and acids, decrease soil acidity, and increase the total alkalinity (Boyd and Pillai 1985; Boyd and Tucker 1998; Wurts and Masser 2004). Liming is used to correct the bottom of culture ponds and to stabilize water pH.

The chemicals used for the liming are oxides, hydroxides, and silicates of calcium or magnesium. Liming substances include Calcium (CaCO₃) and dolomite (calcium-magnesium carbonate/CaMg(CO₃)₂). The common liming substances are calcitic limestone and dolomite limestone. Various types of lime at varying doses are being used in aquaculture for different purposes. Commercial calcium carbonate, also known as agriculture lime or limestone/crushed shell, is prepared by crushing the limestone to fine particle size. It has the same chemical composition as limestone crushed to make it. More refined limestone dissolves much faster than coarser limestone.

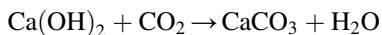


Calcium hydroxide ($\text{Ca}(\text{OH})_2$), also known as flaked lime, slaked lime, hydrated lime, or builders' lime, is prepared by hydrating calcium oxide. Quicklime/insulated lime/burnt lime or burnt shell lime (CaO) is caustic and hygroscopic and often recommended to apply to acidic soils only. Dolomite or dolomite lime ($\text{CaMg}(\text{CO}_3)_2$) is the lime used during the culture period because the carbonates in the dolomite lime are the least reactive. Therefore, aquaculturists recommend using dolomite [$\text{CaMg}(\text{CO}_3)_2$] during the culture period. Carbon dioxide in water reacts with dolomite as follows:

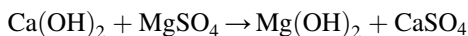


Dolomite traps CO_2 without being lost to the atmosphere by reacting with the free CO_2 in the water. CO_2 is released from the decomposition of organic matter. After liming treatment, the equilibrium concentrations of CO_2 are higher. Also, the problems of low alkalinity and low Mg content in aquaculture ponds can be solved by applying dolomite.

Lime is also used to remove chemicals that cause carbonate hardness. When lime is added, hardness-causing minerals such as calcium and magnesium will form insoluble precipitates. Calcium hardness is precipitated as calcium carbonate (CaCO_3), and magnesium hardness is precipitated as magnesium hydroxide ($\text{Mg}(\text{OH})_2$) by liming treatment.



[Lime]



After each cultivation, the bottom soil may become heavily polluted and acidic due to the accumulation of humus organic substances. Liming materials can neutralize the organic acids released from humus substances, raise the pH value of bottom soil, and increase the degradation of organic substances. Humus organic substances can be reutilized as fertilizer during the subsequent cultivation. An overview of the lime treatment process in an aquarium is shown in Fig. 11.1.

Caution needs to be exercised while selecting the type of lime as well as for its optimum dosage. Most agricultural lime available in the market is granular, which has excessive moisture, affecting the filtration capacity. Overdosage of lime often cause disadvantages such as the reduction of micronutrients like Zn, Fe, etc., in the culture bottom. The high lime dosage often results in the rapid rise of pH in the farming ground, which may cause the mortality of fish and other farmed organisms. Lime treatment also has other disadvantages like carbonation and sulfate attack.

Co-application of lime with fertilizers is also practiced; when the pH of the bottom mud is increased by lime, the availability of phosphorus added in fertilizer also increases. However, excessive liming can be damaging because it decreases

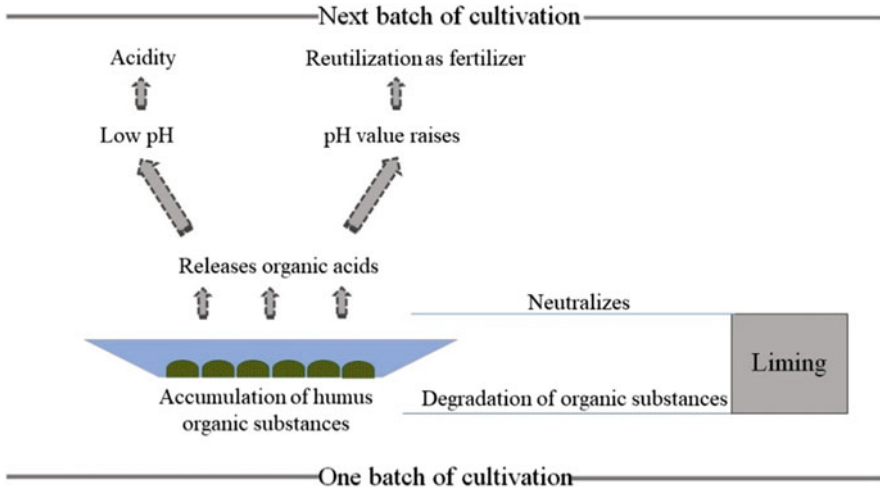


Fig. 11.1 An overview of the lime treatment process in an aquarium

phosphorus availability through the precipitation of insoluble calcium or magnesium phosphate.

The advantages of liming include minimizing the microorganisms, especially the micro-parasites, improving the fine-textured bottom soil, and enhancing the decomposition of organic substances by bacteria creating increased oxygen and carbon reserves. Liming precipitates the suspended or soluble organic materials, decreases biological oxygen demand (BOD), and increases light penetration into the water (waters may be cleared of humid stains of vegetative origin, which restrict light penetration). It enhances nitrification and neutralizes the harmful action of certain substances like sulfides and acids. Liming also increases phytoplankton growth which in turn leads to increased fish/shrimp/prawn production. However, improper lime treatment favors excessive phytoplankton, which causes chronic high pH through excessive photosynthesis by consuming more CO₂ during the daytime.

Disadvantages of liming are: certain types of lime-like pelletized lime and fluid lime are of high cost, and other types such as burnt lime and lime wastes may potentially raise the pH to toxic levels. Most types of lime provide short-term effects.

11.4.2 EDTA treatment

Disodium Ethylene Diamine Tetraacetate or EDTA is a chemical or chelating agent used to reduce heavy metal concentrations and improve water quality. EDTA is used in many hatcheries as a treatment measure against ectocommusal fouling and to stimulate juvenile molting. EDTA is also applied to remove organic substances from the water.

Heavy metals + EDTA → Chelates

11.4.3 Potassium Permanganate treatment

Potassium Permanganate (KMnO₄) is one of the first chemicals used as a chemotherapeutic in aquaculture. It has been applied since the early part of the century. It is used to treat external parasites, such as monogeneans, particularly in the aquarium fish industry. When applied at about 5 ppm, it is also a good treatment for external bacterial infections such as *Columnaris* and *Aeromonas hydrophila*. For aquarium fish, it can be used up to 500 ppm as a dip treatment for 5 min.

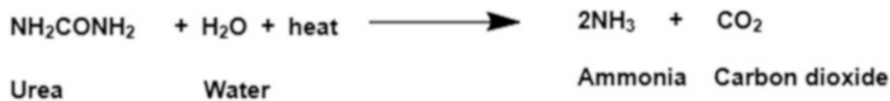
11.5 Fertilizers

Organic and chemical fertilizers are being applied to aquaculture farms for optimum production (Biao 2008; Green 2015; Boyd 2018). Fertilization is a fundamental part of pond preparation that increases nitrogen, phosphorus, and other plant nutrients and stimulates phytoplankton growth. Phytoplankton can remove the potentially toxic ammonia nitrogen from water and food for herbivorous fish such as tilapia, milkfish, and carps. Fertilization is also done after chlorination and before stocking of culture species such as shrimps.

Organic fertilizers include livestock manure, plant crop residues, food processing wastes, and fresh-cut or dry grass. Livestock manure comes mainly from farm animals, and the commonly used manures are cow dung, pig dung, poultry droppings, etc. Organic fertilizers contain nitrates and phosphates.

There are a wide variety of commercial inorganic fertilizers available for aquaculture. Nitrogen, phosphorus, and potassium are called the primary fertilizer nutrients. Nitrogen and phosphorus fertilizers are the common forms used before the production cycle to stimulate beneficial phytoplankton to post-larval stages of fish and shrimp. Most nitrogen fertilizers are made from ammonia industrially. Potassium fertilizers are applied to increase potassium concentrations for low salinity in the inland culture of shrimp and marine fish.

The two most commonly used commercial chemical fertilizers are urea and triple superphosphate (TSP). Urea is an organic compound that hydrolyses in water to ammonia, nitrogen and carbon dioxide.



The chemical molecular formula of TSP is $\text{Ca}(\text{H}_2\text{PO}_4)_2 \cdot \text{H}_2\text{O}$. This water-soluble superphosphate fertilizer contains 44–51% of available P_2O_5 .

Other common fertilizers used in aquaculture are ammonium nitrate, calcium nitrate, sodium nitrate, potassium nitrate, ammonium sulfate, diammonium phosphate, monoammonium phosphate, superphosphate, ammonium polyphosphate, and potassium chloride.

The significant difference between organic and chemical fertilizers is that organic fertilizers release nutrients by microbial decomposition, while chemical fertilizers dissolve themselves to release nutrients (Boyd, 1995; Boyd and Tucker 1998). Organic fertilizers have lower concentrations of N_2 , P_2O_5 and K_2O than chemical fertilizers. Organic fertilizers are less expensive and can be applied in larger quantities. Organic fertilizers often result in a 3–5-fold increase in yield than that of commercial chemical fertilizers. Fertilization is often most effective when organic fertilizers are applied in combination with commercial fertilizers.

11.6 Disinfectants

Optimal water quality is required for aquaculture at high densities to suppress pathogens. There are several chemicals recommended for pond and hatchery disinfection. Chlorine, iodine, formalin, and benzalkonium chloride (BKC) are commonly used as disinfectants in aquaculture. Numerous commercial disinfectants are available on the Indian market, but almost all contain any one of the above as primary ingredients.

11.6.1 Chlorination

Chlorination is a common practice of disinfection in aquaculture. Chlorination is usually applied as gaseous chlorine or hypochlorite (OCl^- or ClO^-). Hypochlorites are potential germicidal agents. Traditionally, sodium and calcium hypochlorites have been used in the aquaculture industry. Sodium hypochlorite or household bleach is a chemical compound with NaOCl or NaClO chemical formula. It comprises a sodium cation (Na^+) and a hypochlorite anion (OCl^- or ClO^-). Hypochlorites act more effectively in acidic conditions, even though they kill most microorganisms at neutral pH (7.0). Hypochlorites act by releasing hypochlorous acid, which is the primary active disinfectant.

Water + Chlorine gas = hypochlorous acid + hydrogen ion + chloride ion

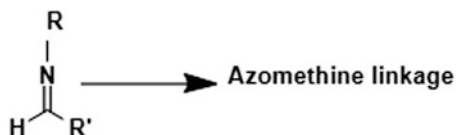
Water + sodium hypochlorite = hypochlorous acid + Sodium hydroxide

The chlorine gas reaction is swift, and therefore sodium hypochlorite is often recommended for a rapid rise in the pH of the aquaculture ponds. However, hypochlorites are not recommended during the culture period or for prophylaxis

due to their toxic effect on tissues. In order to avoid toxicity, chlorinated waters should be dechlorinated before introducing the culture species into them. Chlorination is also applied when the aquaculture water is intended to be discharged into natural waters. Dechlorination should also be done during such situations. Passive dechlorination could be done by exposure to sunlight and air.

11.6.2 Formalin Treatment

Formalin is one of the most popular disinfectants in aquaculture. It is prepared as an aqueous solution of formaldehyde stabilized with methanol. Formalin condenses the amino acids of microorganisms into azomethines thereby killing a wide range of microorganisms (bacteria, fungi, and other ectoparasites, especially protozoan parasites). At standard dosage rates, it shows high treatment efficiency against parasites.



R = amino part

R' = aldehyde or ketonic part

However, formalin is a very slow active chemical, and it is not effective against internal infections. Excess use of formalin causes oxygen depletion.

11.6.3 BKC Treatment

Benzalkonium Chloride (BKC) is one of the broad-spectrum disinfectants specially used for the aquaculture of shrimp. In many shrimp farms, it is used to reduce the density of plankton and dinoflagellates.

The disadvantage of BKC treatment is that it should be applied in large amounts to kill even a minimum plankton concentration. Moreover, if used in large quantities, the resulting decomposition of organic matter will have a deleterious effect on animal health.

11.6.4 Iodine Treatment

Iodine is used as a disinfectant in hatcheries and ponds to eliminate aquatic bacteria and other pathogens. Iodine is usually sprayed in liquid form over the pond bottom.

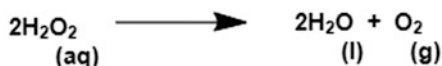
11.6.5 Hydrogen Peroxide

Hydrogen peroxide is mainly used against ectoparasites and fungi in freshwater species. It is one of the most potent oxidizers being used. However, it is easily decomposed in water, particularly in organic matter, light, and turbulence thereby not leaving any toxic products.



Like other disinfectants, there are many risk factors related to the use of hydrogen peroxide, primarily their concentration and dosage. Overdosing can lead to potential disruption of biofilter processes, whereas under-dosing causes less treatment efficiency.

Hydrogen peroxide is available in aqueous solutions, peracetic acid solutions or can be liberated from a granular formulation as sodium percarbonate ($2\text{Na}_2\text{CO}_3 \cdot 3\text{H}_2\text{O}_2$)



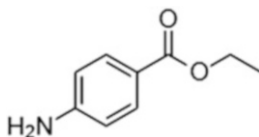
11.6.6 Malachite Green

Malachite green is a disinfectant widely used to treat aquatic protozoa and oomycetes. More specifically, it is used in pond bottoms to eradicate *Icthyophthirius* cysts in aquariums and finfish farms and control *Lagenidium* in shrimp hatcheries.

11.7 Anesthetics

Sedation and anesthesia work as allies in aquafarming for stress-relieving procedures. Transportation, human handling, size sorting, weighing process, etc., exhibit physiological stress in aquaculture practices. Increased stress alters fish plasma cortisol, glucose, lactase, chloride, sodium, and lymphocyte concentrations. The use of anesthetics could mitigate the stress and thereby increase production and profitability. Anesthetics are sparingly used in aquaculture, particularly during the long-distance transport of broodstock and fish seed. Anesthetics use in aquaculture is limited due to the high cost, least availability, risk, and side effects on culture species

and consumers. The two commercial anesthetics options are tricaine and benzocaine. Since tricaine is very expensive, benzocaine ($C_9H_{11}NO_2$) is the most demanded one. Benzocaine is also called Anesthesin, Ethyl 4-aminobenzoate, 94-09-7, Ethyl aminobenzoate, Ethyl p-aminobenzoate, etc.



11.8 Chemical Structure of Benzocaine

Other Anesthetics include Quinaldine, Halothane, Isoflurane, Lignocaine, MS222, Phenoxyethanol, CO_2 , and clove oil. Due to the cost efficiency, clove oil is most preferred by aquaculturists. However, clove oil could only immobilize the fish, so it is not suitable for painful procedures.

11.9 Antimicrobials

Infections due to bacteria are major disease problems in both freshwater and brackish water aquaculture. Diseases caused by *Aeromonas hydrophila* and various species of *Vibrio* are significant problems in the freshwater and brackish water farming of fish and shrimp. In order to treat the diseased species, antibiotics are generally applied via different delivery routes such as oral (in feed flakes and encapsulated diets) or by injection. Worldwide, quinolones, tetracyclines, amphenicols, and sulfonamides are the most commonly used classes of antimicrobials. The main active ingredients include oxytetracycline, chlortetracycline, amoxicillin, co-cotrimoxazole, sulfadiazine, and sulfamethoxazole (Table 11.2).

Antibiotic usage also has several disadvantages. Antibiotics are most effective only when they are administered at the initial stages of a disease. It is because the cultured species lacks the feeding habit once infected. It may initiate environmental pollution problems and affect human health due to the drug residues in cultured products. Antimicrobial use in aquaculture also creates public health hazards. Antimicrobial-resistant strains could be developed, and traces of antimicrobial residues could be detected in aquaculture products and the environment. Antibiotics content in the aquaculture produce could be tested in Government of India Laboratories, ICAR Laboratories, CSIR Laboratories, MPEDA Laboratories, EIA Laboratories, and State Government or Private NABL (National Accreditation Board for Testing and Calibration Laboratories). Uncontrolled use of antibiotics results in severe environmental contamination and a deleterious impact on public health.

Table 11.2 Widely used antibiotics and their treatment option in aquaculture

S. No.	Antibiotic	Treatment option	Target species	Safety concerns
1	Erythromycin	bacterial infection (E.g., Vibriosis)	Carps, catfish, shrimp	Nephrotoxicity, allergies, human and environmental issues
2	Nitrofurans	Vibrio spp. Infection	Shrimp larvae, carps, catfish	Potential carcinogenic effects
3	Oxytetracycline	Vibriosis, columnaris disease	Freshwater and brackish water fish	severe environmental contamination and impact on public health
4	Chloramphenicol	Aerobacteriumliquefaciens, Haemophiluspiscium and A. salmonicida	Carp, trout	Antibiotic resistance
5	Acriflavine	Bacteria (<i>Flexibactercolumnaris</i>) and external protozoans	Seabass, catfish	Environmental issues
6	Copper compound	external protozoan infestation	Fish culture and shrimp farms	Copper accumulation in the pond bottom
7	Dipterex	systemic ectodermal and mesodermal baculovirus (SEMBV) and yellowhead disease (YHD)	pond-cultured fish and shrimp	Environmental issues
8	Oxolinic Acid	treatment of vibriosis, Aeromonas hydrophila	Shrimp and freshwater fishes	Environmental issues
9	Macrolides	streptococcus, Chlamydia, piscirickettsia infections and Bacterial kidney disease	Fish juveniles during transport	Environmental issues

11.9.1 Chloramphenicol

Chloramphenicol is a bacteriostatic prophylactic agent which acts on bacteria by inhibiting protein synthesis. It prevents protein chain elongation by inhibiting the peptidyl transferase activity of the bacterial ribosome. Chloramphenicol diffuses through the bacterial cell wall and reversibly binds to the bacterial 50S ribosomal subunit. It binds to the A2451 and A2452 residues in the 23S rRNA of the 50S ribosomal subunit. The binding interferes with peptidyl transferase activity thereby preventing the transfer of amino acids to the growing peptide chains and blocking peptide bond formation (MacDougall and Chambers 2011) (Fig. 11.2).

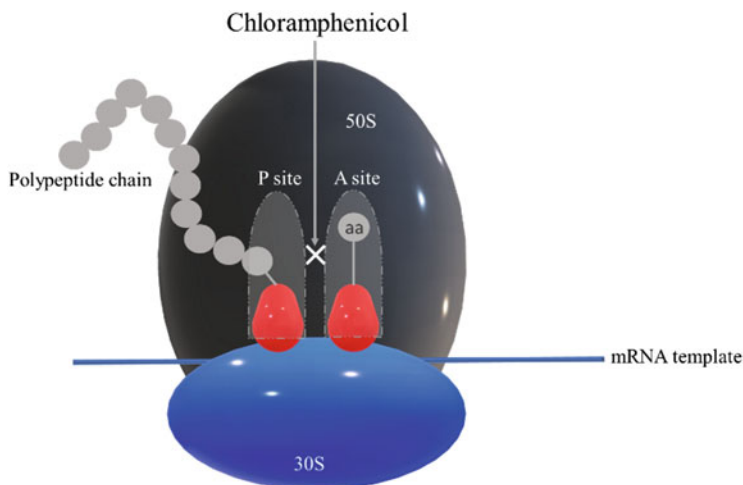


Fig. 11.2 Mechanism of action of chloramphenicol on bacterial cell

Chloramphenicol is used as a prophylactic agent against carp dropsy disease (caused by *Aerobacterium liquefaciens*), trout ulcer disease (caused by *Haemophilus piscium*), and furunculosis disease (caused by *A. salmonicida*).

11.9.2 Acriflavine

Acriflavine is applied in fish farms and aquariums to treat bacteria and external protozoans. It is usually recommended as a treatment option for *Flexibacter columnaris* infections in seabass and catfish.

11.9.3 Copper Compound

Copper compound (Cutrine Plus) is an approved chemical for shrimp culture. It is also used in fish culture farms. It is a parasiticide that acts against external protozoan infestation. It is also recommended for treatment against filamentous bacteria in shrimp farms. However, continuous use of copper is not recommended because copper may accumulate in the pond bottom, which is dangerous to shrimp.

11.9.4 Dipterex

Metrifonate, also called Trichlorfon or chlorophos, is an organophosphorus compound marketed under the brand name Dipterex. It is widely used to treat crustacean, monogenean, and protozoan parasites in pond-cultured fish. Dipterex is applied in

water storage canals and reservoirs to eliminate wild crustacean vectors of shrimp viruses (systemic ectodermal and mesodermal baculovirus (SEMBV) and yellowhead disease virus (YHD)).

11.10 Feed Additives

For better aquaculture practices, instead of the supplementary fish feeds comprising agricultural wastes and by-products, complete feeds should be developed to meet the complete nutritional requirements of the species being cultured. These complete feeds are supplied with additives in pigments, vitamins, phospholipids, chemoattractants, and preservatives, like mold inhibitors and antioxidants.

In most cases, aquatic organisms require only minute amounts of essential nutrients for average growth, metabolism, and reproduction. Therefore, the natural feed may be abundant enough to provide essential vitamins and minerals. Due to the limitation of natural feed, vitamins and minerals are added to the diet as a complete feed. Among the vitamins, vitamin C is widely used in shrimp diets. The added minerals include Calcium, Phosphorus, Magnesium, Sodium, Potassium, Zinc, Copper, Manganese, Iron, Cobalt, and Selenium. Similarly, antioxidants like Ethoxyquin, Butylated hydroxy are also added.

11.11 Pesticides

Pesticides are often used in aquaculture to control aquatic weeds, insect infestation, and fungal diseases. Pesticides with synthetic chemicals are most extensively used for pest management. The commonly used pesticides are Dichlorvos (Nuvan), Malathion (Cythion), Quinophos (Ecalux), Benzene hexachloride (Gammexene), Copper sulfate, Sodium chloride, Calcium oxide, Oxytetracycline, Chlortetracycline, and Doxycycline. Based on their target action, pesticides can be divided into herbicides, insecticides, and fungicides.

11.11.1 Herbicides

Aquatic plant problems ranging from microscopic plankton algae to larger plants rooted in the pond bottom frequently interfere with commercial fish production, and dealing with these weeds is challenging. This weed management always requires a combination of management practices. For intensive fish farming, large amounts of nutrients are to be introduced into the water as commercial feed and inorganic fertilizers. The availability of nutrients often creates an ideal habitat for aquatic weeds “growth.” Culture farms with dense weed infestations are difficult to be removed. Freeing the culture species from the weeds is also a cumbersome process. Aquatic plants that cause weed problems are of different groups, including algae, floating weeds, emersed weeds, and submerged weeds (Shelton and Murphy 2011).

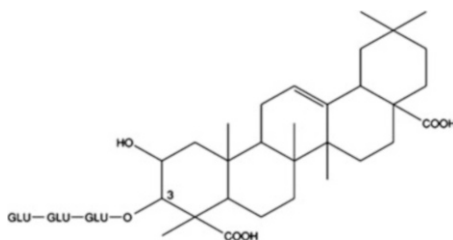
Copper has been widely used as a herbicide in aquaculture operations. It is not only an effective algicide but it is also used against parasite infections. Copper sulfate is water-soluble, and it could be applied as a spray solution over the surface of culture farms or ponds. For a larger area, such as lake farming, copper sulfate can be easily spread on the water surface through an adequately equipped boat.

Copper sulfate pentahydrate ($\text{CuSO}_4 \cdot 5\text{H}_2\text{O}$) is widely used for the management of algae. Since the algae can overgrow following herbicide applications, copper sulfate treatment is a short-time management method. However, it could be made effective in the long term when combined with other management methods. Other than algae, copper is occasionally used against other weeds. Recently, there have been a large number of herbicides available in the market against selected aquatic weeds.

The most significant risk of using copper sulfate is the accumulation and decaying of algal or plant materials, limiting the amount of dissolved oxygen.

11.11.2 Insecticides

Insecticides are often applied to ponds to kill predators or unwanted species before stocking. For example, saponin, used as a molluscicide, is often applied as powdered or cake forms.



The chemical structure of saponin consists of an aglycone unit linked to one or more carbohydrate chains.

The primary chemical groups of other insecticides are Organophosphate, Carbamates, Organochlorine, Pyrethroids, and Necotenoides.

11.12 Immunostimulants

Using immune stimulators against infectious diseases is more advantageous than using antibiotics in aquaculture. Because some strains of pathogens become resistant to certain antibiotics due to their overuse or misuse, also, antibiotic residues may accumulate in aquaculture products, which affects safety. Glucan and peptidoglycan are the most common immunostimulants used in aquaculture.

Glucans are polysaccharides derived from glucose monomers. Glycosidic bonds link the monomers. Four types of glucans are available: 1,6- (starch), 1,4- (cellulose), 1,3- (laminarin), and 1,2-bonded glucans. Glucans stimulate the nonspecific defense mechanism of aquatic animals against bacterial infection.

Peptidoglycan, the primary structural polymer in most bacterial cell walls, consists of glycan chains. Glycan chains comprise repeats of N -acetylglucosamine and N -acetylmuramic acid residues, cross-linked by peptide side chains. Peptidoglycan is used as an immunostimulant for increasing the growth rate, survival and feed conversion of aquaculture animals. It also enhances the phagocytic activity of hemocytes in shrimp and other crustaceans.

Besides peptidoglycan and glucan, the commonly used immunostimulants in aquaculture are Muramyl dipeptide, Chitin, Chitosan, Lentinan, Schizophyllan and Oligosaccharide, Levamisole, Yeast derivatives, and so forth.

Recently, efficient preventive pathogen-specific strategy is being practiced in many commercial aquaculture farms. Among them, vaccination is an essential strategy in large-scale commercial fish farming. There are several vaccines, including live, attenuated, peptide, and genetic vaccines that have been licensed against bacterial, viral, and protozoan infections. However, aquaculture vaccines are not used as widely as human vaccines.

In addition, cytokines which are the crucial regulators of the immune system, also have potential applications not only used for the development of vaccines but can also be applied directly as immunostimulants. Pro-inflammatory cytokines like tumor necrosis factors (TNF), IL-6 and IL-17 family, T(H)1 type interleukins (IL-2, IL-15, IL-12 alpha and beta, IL-18), IL-10 family (IL-10, IL-19/20, IL-22, and IL-26), and Interferons have great potential for immune stimulation in aquaculture. However, there is a significant hurdle in discovering these cytokine molecules from aquaculture organisms due to their low identities to their mammalian counterparts.

11.13 Breeding Inducing Agents

Induced breeding practices are being done for the artificial propagation of culture species in aquaculture. In many culture farms, induced breeding practices are established as a dependable source of culture seeds. In natural fisheries, there is a possibility of reducing stocks, which in turn significantly reduces production. Since the overall aquaculture production depends on the continuous supply of seeds, induced breeding is essential. There is a high demand for artificial reproduction technology in commercially valuable species. Breeding inducing agents are applied to improve the reproductive potential of culture species.

Hypophysation is a methodology used for the breeding of fish. The technology employs the injection of pituitary gland extract. Brazil was the first country which develops hypophysation technology on a commercial scale.

In addition, sex control agents such as 17α methyltestosterone for the male population and 17β methyl progestins for the female population are also in practice.

Synthetic hormones are also used for artificial reproduction and sex reversal. The most critical synthetic sex hormones used in fish farming are estrogens and androgens. Hormones such as corticosteroids, anabolic steroids, and other steroids have been incorporated into the feed of shrimp hatcheries to make the larvae look healthy and uniform in size.

11.14 Conclusion

In recent years, as aquaculture has become more intensive, the use of chemicals has also intensified. Major chemicals used in aquaculture and their interaction with the aquaculture system were discussed in this chapter. Though there has been an increasing concern about the usage of chemicals, aqua farmers must use the chemicals with great caution. Chemicals can cause damage not only to cultured animals but also to human consumers and the environment if misused. For instance, drugs and chemicals are often applied in aquaculture to improve water quality and reduce the risk of diseases. However, frequent exposure to chemicals causes environmental degradation, affecting the water quality unsuitable for long-term aquaculture. Good management practices are to be followed, which can considerably reduce the usage of chemicals. Overuse of chemicals, especially antibiotics, not only increases production costs but also intensifies adverse consequences. Therefore, the strategy of chemical usage should be adopted as a last resort. For the success of aquaculture, chemicals must be judiciously and responsibly used. For better management, the adverse impacts of chemical use in aquaculture should not outweigh the advantages. Chemical residues in aqua food products and the ponds' chemical residuals after harvest periods should be monitored. The aggressive promotion of chemical products by sales associates should not influence the farmers to increase their use of drugs and chemicals.

Despite all of this, chemicals and drugs will continue to play an essential role in aquaculture development. Nevertheless, if they are used with the utmost caution, adverse effects such as environmental damage and the development of resistant strains of pathogens could be avoided. Furthermore, implementing specific legislation on the restricted use of therapeutic drugs and chemicals in aquaculture could improve the situation.

References

- Aly SM, Albutti A (2014) Antimicrobials use in aquaculture and their public health impact. *J Aquaculture Res Dev* 5(4):1
- Aquaculture Vietnam (2021). <https://www.aquafishesexpo.com/vietnam/en-us/news-updates/vietnam-aquaculture-overview>
- Biao X (2008) The development of and prospects for organic aquaculture worldwide. *Outlook Agric* 37(4):255–260
- Boyd CE (2018) Aquaculture pond fertilisation. *CAB Rev* 13(002):1–12

- Boyd CE, Pillai VK (1985) Water quality management in aquaculture. CMFRI Special Publication 22:1–44
- Boyd CE, Tucker CS (1998) Liming. In Pond aquaculture water quality management, pp. 178–225. Springer, Boston, MA
- Cabello FC, Godfrey HP, Buschmann AH, Dölz HJ (2016) Aquaculture as yet another environmental gateway to the development and globalisation of antimicrobial resistance. *Lancet Infect Dis* 16(7):e127–e133
- Cai J, Quagrainie K, Hishamunda N (2017) Social and economic performance of tilapia farming in Africa. *FAO Fisheries Aquac Circular* C1130
- Cao L, Naylor R, Henriksson P, Leadbitter D, Metian M, Troell M, Zhang W (2015) China's aquaculture and the world's wild fisheries. *Science* 347(6218):133–135
- Carvalho E, David GS, Silva RJ (eds) (2012) Health and environment in aquaculture. *BoD–Books on Demand*
- Clements JC, Chopin T (2017) Ocean acidification and marine aquaculture in North America: potential impacts and mitigation strategies. *Rev Aquac* 9(4):326–341
- De Jong J (2017) Aquaculture in India. Rijksdienst voor Ondernemend Nederland
- FAO (2016) The state of world fisheries and aquaculture 2016. Contributing to food security and nutrition for all. FAO, Rome, p 200
- FAO (2018) The state of world fisheries and aquaculture 2018–Meeting the sustainable development goals. License: CC BY-NC-SA 3.0 IGO.
- Green BW (2015) Fertilisers in aquaculture. In *Feed and feeding practices in aquaculture*, pp. 27–52. Woodhead Publishing
- Gui JF, Tang Q, Li Z, Liu J, De Silva SS (eds) (2018) *Aquaculture in China: success stories and modern trends*. John Wiley & Sons
- Halwart M (2020) Fish farming was high on the global food system agenda in 2020. *FAO Aquac Newslett* 61:II–III
- Hernández-Rodríguez A, Alceste-Oliviero C, Sanchez R, Jory D, Vidal L, Constain-Franco LF (2001) Aquaculture development trends in Latin America and the Caribbean. In: Subasinghe R, Bueno PB, Phillips MJ, Hough C, McGladdery SE, Arthur JR (eds) *Aquaculture in the third millennium*, pp 317–340
- Idowu TA, Sogbesan OA (2017) Synthetic chemical application in aquaculture production. *Int J Environ Agric Sci* 1(2):1–10
- Jana BB, Jana S (2003) The potential and sustainability of aquaculture in India. *J Appl Aquaculture* 13(3-4):283–316
- Jayasankar P (2018) Present status of freshwater aquaculture in India—a review. *Indian J Fisheries* 65(4):157–165
- Lovatelli A (2021) Webinar: regional review on status and trends in aquaculture development in Latin America and the Caribbean–2020. *FAO Aquaculture Newslett* 63:27–28
- MacDougall C, Chambers H (2011) Protein synthesis inhibitors and miscellaneous antibacterial agents. In: Goodman and Gilman's the pharmacological basis of therapeutics. McGraw-Hill, New York, pp 1521–1547
- Masser MP, Bridger CJ (2007) A review of cage aquaculture: North America. *FAO Fisheries Technical Paper*, 498, 105
- MPEDA C (1987) The marine products export development authority
- Nakayama T, Hoa TTT, Harada K, Warisaya M, Asayama M, Hinenoya A et al (2017) Water metagenomic analysis reveals low bacterial diversity and the presence of antimicrobial residues and resistance genes in a river containing wastewater from backyard aquacultures in the Mekong Delta, Vietnam. *Environ Pollut* 222:294–306
- Oceans and Fisheries, European Commission (n.d.) Overview of E.U. aquaculture (fish farming). https://ec.europa.eu/oceans-and-fisheries/ocean/blue-economy/aquaculture/overview-eu-aquaculture-fish-farming_en
- Olin PG (2001) Current status of aquaculture in North America. In: Subasinghe RP, Bueno P, Phillips MJ, Hough C, McGladdery SE, Arthur JR (eds) *Aquaculture in the third millennium*.

- Technical proceedings of the conference on aquaculture in the third millennium, Bangkok, Thailand, 20-25 February 2000. NACA, Bangkok, pp 377–396. and FAO, Rome
- Olin PG, Smith J, Nabi R (2012) Regional review on status and trends in aquaculture development in North America: Canada and the United States of America—2010
- Pathak SC, Ghosh SK, Palanisamy K (2000) The use of chemicals in aquaculture in India
- Pattillo DA (2014) Water quality management for recirculating aquaculture. Extension aquaculture specialist. Iowa State University Extension and Outreach
- Randall DJ, Tsui TKN (2002) Ammonia toxicity in fish. *Marine Pollut Bull* 45(1–12):17–23
- Rasul MG, Majumdar BC (2017) Abuse of antibiotics in aquaculture and its effects on humans, aquatic animal and the environment. *Saudi J Life Sci* 2(3):81–88
- Rodgers CJ, Furones MD (2009) Antimicrobial agents in aquaculture: practice, needs and issues. *Options Méditerranéennes* 86:41–59
- Romero J, Feijóo CG, Navarrete P (2012) Antibiotics in aquaculture—use, abuse and alternatives. *Health Environ Aquaculture* 159
- Satia BP (2011) Regional review on status and trends in aquaculture development in sub-saharanafrica—2010/Revue régionale sur la situation et les tendances dans l'aquacultureenafriquesubsaharienne—2010. FAO Fisheries and Aquaculture Circular, I, III, IV, V, 1-7, 9-23, 25-33, 35-41, 43-45, 47-51, 53-59, 61-67, 69-117, 119-137, 139-161, 163-191
- Satia PB (2017) Regional review on status and trends in aquaculture development in sub-saharanafrica—2010/Revue régionale sur la situation et les tendances dans l'aquacultureenafriquesubsaharienne - 2010. FAO Fisheries and Aquaculture Circular, I, III, IV, V, 1-7, 9-23, 25-33, 35-41, 43-45, 47-51, 53-59, 61-67, 69-117, 119-137, 139-161, 163-191
- Shelton J, Murphy T (2011) Aquatic weed management: control methods
- Tran N, Rodriguez UP, Chan CY, Phillips MJ, Mohan CV, Henriksson PJG et al (2017) Indonesian aquaculture futures: An analysis of fish supply and demand in Indonesia to 2030 and role of aquaculture using the AsiaFish model. *Marine Policy* 79:25–32
- Wurts WA, Masser MP (2004) Liming ponds for aquaculture. Southern Regional Aquaculture Center
- Yusuf D (1995) Aquaculture in Indonesia. In *Towards sustainable aquaculture in Southeast Asia and Japan: Proceedings of the Seminar-Workshop on Aquaculture Development in Southeast Asia*, Iloilo City, Philippines, 26-28 July 1994 (pp. 109-115). Aquaculture Department, South-east Asian Fisheries Development Center
- Zeitoun MM, Mehana EE (2014) Impact of water pollution with heavy metals on fish health: overview and updates. *Global Veterinaria* 12(2):219–231



Zebrafish as a Biomedical Model to Define Developmental Origins of Chemical Toxicity **12**

Jennifer L. Freeman

12.1 Introduction

Most commonly, chemical toxicity tests are completed and assessed within a life stage. For example, developmental toxicity tests will expose organisms during developmental stages and then immediately assess toxicity. At the other end of the spectrum, chemical exposures may occur in aged organisms to address questions on neurodegeneration or similar outcomes. Some toxicity assays do address multiple life stages, such as the prenatal developmental toxicity study (OECD TG 414), which provides general information on the effects of prenatal exposure on the pregnant animal and the developing organism. Most recently, a newer chemical exposure paradigm is gaining traction, which focuses on how early-life chemical exposures may influence that individual throughout their life and potentially make them more susceptible to a variety of adverse health outcomes later in their life. This research idea is most commonly referred to as the “Developmental Origins of Health and Disease” or “DOHaD.”

The current DOHaD research field originates from the “Barker hypothesis,” which emerged in the 1990s as proposed by the British epidemiologist David Barker that intrauterine growth retardation, low birth rate, and premature birth could be associated with hypertension, coronary heart disease, and non-insulin-dependent diabetes in middle age (Barker et al. 1993; Barker 2007), but is based on research that goes back to the 1930s (Gluckman et al. 2016). Overall, these initial findings reported that undernutrition during gestation could shape the risk of adult cardiac and metabolic disorders. This relationship has been referred to by a number of different names, including “Barker’s hypothesis,” “fetal origins of adult disease,”

J. L. Freeman (✉)

School of Health Sciences, Purdue University, West Lafayette, IN, USA

e-mail: jfreema@purdue.edu

and most recently “DOHaD.” Since this time, DOHaD has generated global interest in the research area of developmental plasticity in many different additional fields and themes beyond the initial cardiovascular impacts, including obesity, cancer, neurological disorders, and neurodegenerative diseases, among other noncommunicable diseases, with the appreciation that there can be different windows during development that are the most sensitive. Additionally, the mechanisms driving these adverse health outcomes are being investigated with the main focus on a wide range of epigenetic alterations. Furthermore, the DOHaD paradigm has gained traction in environmental health, understanding how developmental chemical exposure may influence the risk of developing various noncommunicable diseases. Early studies in environmental health included a number of chemicals spanning environmental chemicals (e.g., heavy metal lead) and drugs (e.g., diethylstilbestrol), among many others (Needleman et al. 1982; Robboy et al. 1977). Since that time, studies in the DOHaD paradigm in environmental health have greatly expanded, encompassing environmental epidemiology and laboratory-based toxicology studies in a variety of animal model organisms. These studies include using the zebrafish, which is becoming a stronghold as a complementary vertebrate model system to mammals given several strengths for toxicity testing, especially within the DOHaD paradigm (Hill et al. 2005; Horzmann and Freeman 2018). In this chapter, the paradigm and mechanisms behind DOHaD are discussed. Second, studies employing the zebrafish to define mechanisms of toxicity using the DOHaD paradigm are detailed, linking the strengths of this vertebrate animal model in providing connections between early-life chemical exposures and later-in-life adverse health outcomes.

12.2 Mechanisms of the DOHaD Paradigm

The DOHaD paradigm recognizes that development is a critical period of susceptibility to environmental insults (Barker 2004; Grandjean et al. 2015; Haugen et al. 2015; Heindel et al. 2015). The most sensitive developmental window may be the in utero period, but in other cases can be following the birth or into childhood, as well as even early adulthood dependent on the development of different biological systems. For example, in humans, we know that the brain continues to develop through early adulthood, and, thus, it is critical to assess the impacts of chemical exposure throughout this longer developmental period. Heindel et al. (2015) proposed DOHaD impacts in the research area of environmental health have common aspects to those in nutrition and stress, including acting during specific windows of developmental plasticity, resulting in subtle functional changes not necessarily detectable without molecular approaches, latency in between chemical exposure and disease or dysfunction, increased susceptibility to disease, the potential for sex-specific effects, and acting partially through epigenetic mechanisms. In fact, epigenetic modifications are the most commonly explored mechanism of the DOHaD paradigm.

Upon discovering the connection of early life influences on adverse health outcomes later in life, researchers began seeking answers to identify the mechanisms responsible for driving these outcomes. Several mechanisms are being explored among multiple research fields investigating DOHaD questions spanning excessive exposure to stress hormones, permanent dysfunction due to alterations in organ structure, genetic mutations, and deregulation of gene expression mediated through epigenetic modifications. To date, most of this research within the toxicity field has emphasized epigenetic mechanisms given the lack of observed structural malformations, extensive knowledge already available on genetic mechanisms of chemical toxicity, and that the adverse health outcomes in the DOHaD paradigm are being observed with chemical exposures at low doses without mutagenic activity. Moreover, it is recognized that epigenetic marks undergo dynamic changes during development and that epigenetic modifications frequently co-occur or precede the emergence of a disease phenotype arising from chemical exposure. Epigenetic modifications span multiple mechanisms, including DNA methylation, histone post-translational modifications [e.g., lysine methylation and acetylation of core histone proteins (H2A, H2B, H3, and H4)], and non-coding RNAs. DNA methylation is the most common investigated in toxicity studies and consists of a covalent attachment of a methyl group to the fifth carbon on the cytosine (mainly the cytosine-phosphate-guanine (CpG) dinucleotides) (Bird 2002; Miranda and Jones 2007). Generally, DNA hypermethylation at gene promoter regions is associated with transcriptional suppression, while DNA hypomethylation is associated with active transcription (Ng and Bird 1999). DNA methylation is modulated by DNA methyltransferase (i.e., DNMTs) and methyl-cytosine dioxygenase (i.e., TETs), and, thus, is dynamic in nature with a single epigenetic modification typically co-regulated by “reader” and “eraser” proteins. As such, these epigenetic modifications are conceptually reversible.

Other than DNA methylation, histone posttranslational modifications regulate gene transcriptional state by modulating chromatin accessibility (Klemm et al. 2019; Gibney and Nolan 2010). The roles of these histone posttranslational modifications on gene expression are diverse. For example, H3K4me3 and H3K27ac mark euchromatin for gene activation (Wysocka et al. 2006), while H3K27me3 marks facultative heterochromatin for gene repression (Wiles and Selker 2017). In addition, H3K9me3 marks heterochromatin for permanent gene silencing (Mozzetta et al. 2015). Similar to DNA methylation, the level of histone lysine methylation is modulated by their corresponding “writers” and “erasers,” including the H3K9me3 eraser histone lysine demethylase 4A (KDM4A) and the H3K27me3 erasers histone lysine demethylase 6A and 6B (KDM6A and KDM6B). Several studies confirm chemical exposure can alter heterochromatin markers [e.g., (Xie et al. 2021, Lin et al. 2021)], but unlike DNA methylation modifications, these changes tend to persist in the genome and as such, may serve as a better biomarker for past chemical exposure (Eid et al. 2016). In summation, studies completed to date support that epigenetic modifications occur following chemical exposure and may persist in the genome, increasing the susceptibility of cells and thus organisms in the DOHaD paradigm to adverse health outcomes.

12.3 Overview of DOHaD Studies in Environmental Health

To date, a variety of environmental chemicals have been investigated for their influence on the DOHaD. An extensive review was published in 2017 that included publications through 2014 that met the criteria for evaluating the DOHaD hypothesis in environmental epidemiology (Heindel et al. 2017). The authors identified a robust literature of 425 studies with over 60 different chemicals studied at that time. Unfortunately, though ~38% of the 425 studies focused primarily on PCBs (100 of the 425 studies) and organochlorine pesticides (60 of the 425 studies), while 114 of the 425 studies targeted the metals mercury and lead. In addition, it was reported that almost 50% of these studies focused on in utero exposures and health outcome in childhood, with a strong emphasis on neurodevelopmental and neurobehavioral outcomes (211 of the 425 studies). Additional adverse health outcomes included cancer (59 studies), respiratory illnesses (50 studies), metabolic outcomes (35 studies), reproductive health (31 studies), immune disorders (29 studies), endocrine dysfunction (22 studies), and cardiovascular alterations (12 studies). These findings documented the limits of knowledge for the role of environmental chemicals in the DOHaD hypothesis at that time and also reflected difficulty in long-term tracking of individuals from in utero to adulthood in addressing DOHaD questions in human populations with only 43 studies examining endpoints with populations aged 18 years or older. Epidemiologists are taking advantage of publicly available databases (e.g., the National Health and Nutrition Examination Survey, NHANES, US Centers for Disease Control and Prevention) and are pooling or comparing large epidemiology cohorts to address DOHaD research questions. In addition, many of the initial studies are continuing to track these individuals as they age, expanding the data attained into older age.

Further, several animal models are being utilized in toxicity testing that addresses the DOHaD hypothesis to assist in expanding the number of environmental chemicals being investigated and to identify mechanisms of toxicity in the DOHaD paradigm. The controlled laboratory-based studies permit questions on dose-response, sensitive developmental windows, and multiple biological systems and molecular assessments to be defined while taking advantage of the shorter life periods of most animal systems to attain life course assessments. While rodents are still the most commonly used animals in these studies, there has been a rapid adaptation to using the zebrafish as a complementary whole animal vertebrate model to mammals. Similar to other toxicology research areas, researchers are recognizing the strengths that the zebrafish can offer in addressing the DOHaD hypothesis.

12.4 Strengths of the Zebrafish to Address the DOHaD of Environmental Chemicals

One of the leading issues in environmental health revolves around the limitation on understanding adverse health outcomes and overall health risks of most chemicals. Today there are over 90,000 chemicals in commerce. Of these chemicals, only a couple of hundred are thoroughly assessed for their toxicity and human health risks. To address these limitations in chemical toxicity knowledge, complementary and alternative methods are being developed globally. This includes the adoption of complementary whole organisms to include in this toxicity beyond the common mammalian assays.

The zebrafish (*Danio rerio*) is now a well-recognized biological model system for toxicology research. The zebrafish is being used to study toxicity from molecular initiating events to alterations in organismal health and behavior and is being applied as a complementary vertebrate whole organism model to mammals. Zebrafish can be used for high-throughput chemical toxicity testing, allowing for quick, large-scale screening similar to *in vitro* assays. On the other hand, zebrafish are complex organisms with highly conserved organ systems and metabolic pathways that enable the evaluation of toxicokinetics and toxicodynamics of environmental chemicals similar to mammalian models. Zebrafish are small, have easy husbandry, and are more economic to maintain than mammals (Bailey et al. 2013). Developmental phases of the zebrafish are well-described (Kimmel et al. 1995) and, with embryonic development *ex vivo*, allow for easy chemical exposure. Zebrafish developmental periods are rapid, with all major body systems formed by 72 h post-fertilization (hpf), which is known as the end of embryogenesis (Fig. 12.1). During these early stages of development, zebrafish are also optically near-transparent, allowing for visualizing all internal structures from fertilization until around 120 hpf or later. The zebrafish genome is sequenced (Howe et al. 2013) with amenability to genetic manipulation (Varshney et al. 2015) and omics-based evaluations (Horzmann and Freeman 2017). The zebrafish is reported to perform comparably to mammalian models in developmental toxicity assays (Sipes et al. 2011; Gustafson et al. 2012; Ball et al. 2014). Traditionally given strengths and characterization, the zebrafish was widely used in developmental biology and toxicology, but recent years have witnessed an expansion of zebrafish in studies at all life stages and continual characterization of zebrafish aging and disease progression (Kiper and Freeman 2021). The application of zebrafish in DOHaD studies has grown, including those within the toxicology research area (Sasaki and Kishi 2013). Moreover, there are now many studies that demonstrate epigenetic modifications in zebrafish following chemical exposure; thus, permitting identification of epigenetic mechanisms driving DOHaD in these toxicity studies (Bouwmeester et al. 2016; Sanchez et al. 2017; Wirbisky-Hershberger et al. 2017; Horzmann et al. 2021).

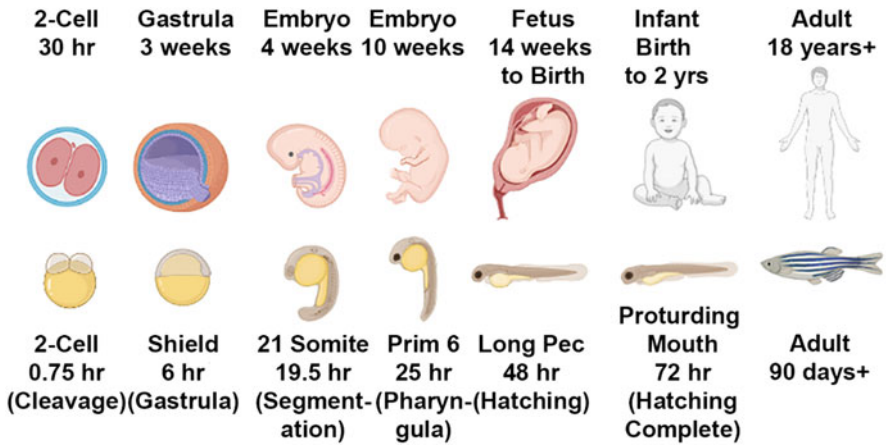


Fig. 12.1 Comparable life stages of humans and zebrafish. Zebrafish embryogenesis is rapid and complete by 72 h post-fertilization (hpf). Comparable embryonic developmental parameters in the zebrafish in hours and days can be aligned to similar developmental progression in humans in hours, days, weeks, and months. Zebrafish hatch from their chorion, usually between 48 and 72 hpf and enter the eleutheroembryo stage, where all organs are developed, but the fish are not yet free feeding, which can be roughly compared to human birth and early infant stages. Zebrafish are considered larval fish until sexual differentiation occurs around 30 days post fertilization (dpf). During the juvenile stage of zebrafish (~30–89 dpf), the reproductive system matures until the zebrafish is able to actively reproduce around 90 dpf, when the adult phase begins. Detailed knowledge of these zebrafish developmental phases enables a general comparison to human life stages. Image created in BioRender

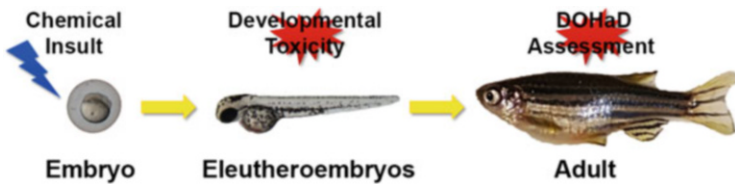


Fig. 12.2 Demonstration of DOHaD exposure paradigm in the zebrafish. Zebrafish are exposed to a chemical during development, the chemical exposure is ceased, and insults are assessed at a later life stage. In this example, zebrafish are exposed to a chemical during embryogenesis, and outcome endpoints are assessed immediately following chemical exposure in eleutheroembryos to address developmental toxicity. In addition, the remaining zebrafish are rinsed of chemicals to cease exposure and allowed to mature into an adult. Outcome endpoints are then investigated in the adult fish to inform on chemical influence on later life health impacts in the DOHaD paradigm

12.5 DOHaD Toxicity Studies Using Zebrafish

Studies within the DOHaD paradigm use the zebrafish to characterize how developmental exposures may influence the risk of adverse health outcomes throughout the lifespan (Lee and Freeman 2014) (Fig. 12.2). Examples of these studies are

discussed in this section, and similar to the environmental epidemiology studies, include polychlorinated dibenzodioxins, metals, pesticides, and other chemicals (Table 12.1). One of the earlier studies in this area investigated persistent life course alterations, including reproductive outcomes following exposure to 2,3,7,8-tetrachlorodibenzo-p-dioxin (TCDD) for 1 h per week from 0 to 7 weeks of age (King Heiden et al. 2009). Initial developmental toxicity analysis included exposure concentrations up to 400 pg/mL, but only zebrafish in the 25 and 50 pg/mL treatment survived to adulthood. Further sample sizes were only large enough in the lower treatment concentration (25 pg/mL) for analysis later in life. Sex-specific analyses were completed in the adults beginning at 3 mpf. Overall, more severe effects were observed in males, which were found to be the primary contributor to reproductive dysfunction. Craniofacial defects (at 3 mpf) and liver lesions (at 11 mpf) in adult males were also identified. In a follow-up study, the exposure paradigm was altered to 50 pg/mL TCDD for 1 h either early in embryogenesis (4 hpf) or during sexual determination at 3 weeks and repeated at 7 weeks (Baker et al. 2013). Significant effects were observed in adults with repeated exposure during sexual differentiation. Specifically, there were more females in the population compared to males (60–40%) and the presence of intersex fish. A decrease in egg release and fertilization success, along with craniofacial and spinal skeletal abnormalities, were also observed (Baker et al. 2013).

Metal toxicity has also been assessed in the DOHaD paradigm with zebrafish. Ruiters et al. (2016) exposed zebrafish to cadmium during embryogenesis (0–72 hpf) and reported altered antioxidative physiology and prolonged response to physical stress at 10–12 weeks of age in treatment groups exposed to concentrations 50–3200-fold below direct embryotoxic concentration. Alternatively, in their DNA methylation analysis select molecular targets were only identified at embryotoxic concentrations for *cyp19a2* and *vtg1*. No alterations were observed for the *vasa* promoter region. The authors further explored the literature on potential mechanisms and hypothesized thiols as the major contributor to the later-in-life effects. In addition, several studies have explored the influence of a developmental lead (Pb) exposure on neurotoxic outcomes, aligning with comparable studies in non-human primates and rodents (Wu et al. 2008; Bihagi et al. 2014, 2018; Dash et al. 2016; Eid et al. 2016, 2018). Two studies evaluated adult brain transcriptome alterations in each sex at age 12 months following an embryonic (1–72 hpf) exposure to 10 or 100 ppb ($\mu\text{g/L}$) Pb (Lee and Freeman 2016; Lee et al. 2018). These studies reported more significant alterations in genes associated with the central nervous system and Alzheimer's disease in the female brain, while gene alterations were involved in cancer pathways in the male brain. Further, several studies have assessed behavioral outcomes in adult zebrafish with a developmental Pb exposure. An exposure from 1 to 120 hpf at 100 ppb altered color preference in adult males aged 12 months in behavioral assays, showing a decreased preference towards shorter wavelengths (Bault et al. 2015). A similar exposure from 6 to 120 hpf but at slightly lower treatment concentrations of 25 and 50 ppb Pb detected learning and memory impairments at 150 dpf (Chen et al. 2012). Two studies also showed that a shorter exposure from 2 to 24 hpf was suffice to see altered visual responses at 4 mpf

Table 12.1 Example toxicity studies using the zebrafish in the DOHaD paradigm

Chemical	Chemical Exposure Age and Duration	Age of Endpoint Assessment	Chemical Concentrations	Summary of Study Outcomes	Reference
2,3,7,8-tetrachlorodibenzo-p-dioxin (TCDD)	0–7 weeks, 1 h per week (first exposure at 4–6 hpf)	3 and 11 mpf	0 and 25 pg/mL	Impaired egg production, fertility, and gamete quality; craniofacial defects in males at 3 mpf; ovarian lesions in females at 3 mpf; lesion in the liver of males at 11 mpf	King Heiden et al. (2009)
2,3,7,8-tetrachlorodibenzo-p-dioxin (TCDD)	4 hpf or 3 wpf and 7 wpf for 1 h each	16 wpf for abnormalities and sex ratios; 20 wpf for reproduction; 12 mpf for histopathology	0 and 50 pg/mL	In 3 and 7 wpf exposure groups: Shift to 60% female populations and craniofacial and spinal skeletal abnormalities at 16 wpf; decreased egg release and fertilization at 20 wpf; altered ovarian development and maturation and intersex fish	Baker et al. (2013)
Cadmium (CdCl ₂)	0–72 hpf	10–12 wpf	0, 1.0, 3.2, 10, 32, 67, and 100 µM	Altered antioxidant physiology prolonged and behavioral response to physical stress at non-embryotoxic concentrations (<32 µM); methylation alterations in <i>cyp19a2</i> and <i>vfg1</i> but only at embryotoxic concentrations (+32 µM)	Ruiter et al. (2016)
Lead (Pb acetate)	6–120 hpf	150 dpf	0, 25, and 50 ppb (µg/L)	Learning and memory impairments in all Pb treatments	Chen et al. (2012)
Lead (Pb chloride)	2–24 hpf	4 mpf	0, 3, 10, 30, and 100 nM	Altered visual response at all Pb concentrations	Rice et al. (2011)

Lead (Pb chloride)	2–24 hpf	12 mpf	0–10 μ M	Altered social behavior in both sexes	Weber and Ghorai (2013)
Lead (Pb acetate)	1–72 hpf	12 mpf	0 and 10 ppb (μ g/L)	Brain transcriptome showed more pronounced neurological gene alterations in the female brain	Lee and Freeman (2016)
Lead (Pb acetate)	1–72 hpf	12 mpf	0 and 100 ppb (μ g/L)	Sex-specific brain transcriptome alterations with increased changes in the nervous system in females and cancer in males; p38 MAPK was confirmed as an upstream regulator in the male brain	Lee et al. (2018)
Lead (Pb acetate)	1–120 hpf	12 mpf	0 and 100 ppb (μ g/L)	Color preference was altered in adult male fish with Pb exposure	Bault et al. (2015)
Atrazine	1–72 hpf	6 mpf	0, 0.3, 3, and 30 ppb (μ g/L)	Male adult zebrafish had genes altered in the brain and testes associated with the hypothalamus-pituitary-adrenal axis and the hypothalamus-pituitary-gonadal axis in all treatment groups; no changes in gonadosomatic index, testes histology, or testosterone were detected	Wirbisky et al. (2016a)
Atrazine	1–72 hpf	6 mpf	0, 0.3, 3, and 30 ppb (μ g/L)	A significant decrease in spawning and an increase in follicular atresia and progesterone in the 30 ppb treatment group; ovarian transcriptome analysis identified alterations in genes associated with endocrine system development and function, tissue development, and behavior in all treatment groups	Wirbisky et al. (2016b)

(continued)

Table 12.1 (continued)

Chemical	Chemical Exposure Age and Duration	Age of Endpoint Assessment	Chemical Concentrations	Summary of Study Outcomes	Reference
Atrazine	1–72 hpf	6 or 9 mpf	0, 0.3, 3, and 30 ppb (µg/L)	At 9 mpf, a significant decrease in 5-HIAA (3 ppb) and serotonin turnover (0.3 and 3 ppb) in the female brain with no changes in male brain; brain transcriptome analysis of female brain aged 6 months identified molecular targets in the serotonergic pathway in all treatment groups	Wirbisky et al. (2015)
Atrazine	1–72 hpf	9 mpf	0, 0.3, 3, and 30 ppb (µg/L)	Males had decreased locomotor parameters in all treatment groups; brain transcriptome changes in genes associated with organismal development, cancer, and nervous and reproductive system development and function in all treatment groups; decreased cells in brain raphe populations in 30 ppb treatment group; no significant changes in global DNA methylation of brain	Horzmann et al. (2021)
Bisphenol A (BPA)	8–120 hpf	8 mpf	0, 0.01, 0.1, and 1 µM	Deficits in the first reversal learning task and T-maze in all treatment groups	Saili et al. (2012)

Bisphenol A (BPA)	6 hpf to 5 mpf; 6 dpf to 5 mpf; or 3 mpf to 5 mpf	5 mpf	0, 0.001, 0.01, and 0.1 μM	BPA did not effect growth; testes weight decreased in earliest exposure group at 0.001 μM; A reduction in sperm volume, density, motility, and volume at 0.001 μM in all exposure duration groups; overall more severe effects at a low dose of 0.001 μM compared to 0.01 and 0.1 μM	Chen et al. (2017)
Mono-2-ethylhexyl phthalate (MEHP)	6–120 hpf	15 dpf	0 and 200 ppb (μg/L)	MEHP exposure increased hepatic steatosis and increased expression of PPARα target, <i>fabp1a1</i>	Sant et al. (2021a)
Perfluorooctanesulfonic acid (PFOS)	1–5 dpf or 1–15 dpf	15 and 30 dpf	0, 16, and 32 μM	Increased incidence of aberrant islet morphologies (32 μM) at 15 dpf, principal islet areas (16 and 32 μM) at 15 and 30 dpf, and adiposity (16 and 32 μM) at 15 and 30 dpf in longer exposure group; no significant changes in larval spontaneous behavior at 15 dpf	Sant et al. (2021b)

Abbreviations: *dpf* Days post fertilization, *hpf* Hours post fertilization, *mpf* Months post fertilization, *wpf* weeks post fertilization

at Pb concentrations as low as 3 nM (Rice et al. 2011) and impairments in social behaviors at 12 mpf at Pb concentrations up to 10 μ M (Weber and Ghorai 2013).

The agricultural herbicide atrazine (2-chloro-4-ethylamino-6-isopropylamino-1,3,5-triazine) has also been investigated for later-in-life impacts of an embryonic (1–72 hpf) exposure at 0, 0.3, 3, and 30 ppb (μ g/L), which spans the current regulatory limit in drinking water in the United States (3 ppb). Alterations along the hypothalamus-pituitary-gonadal axis have primarily been assessed in both sexes at 6 and 9 mpf. At 6 mpf, a decrease in spawning in the 30 ppb treatment group was observed with increased follicular atresia and ovarian progesterone in the same treatment groups (Wirbisky et al. 2016b). At 6 mpf, ovarian transcriptome analysis revealed alterations in genes associated with endocrine system development and function, tissue development, and behavior in all treatment groups, while female brain transcriptome analysis identified a number of molecular targets associated with the serotonergic system (Wirbisky et al. 2015). As such, neurotransmitter levels were measured in the female and male brain at 9 mpf. Females had a decrease in 5-HIAA (5-hydroxyindoleacetic acid) and serotonin turnover. No changes were observed for dopamine or GABA, along with no impacts on any of the neurotransmitters in the male brain (Wirbisky et al. 2015). To further assess potential influences of the embryonic atrazine exposures in males, brain and testes transcriptome analysis was completed and coupled with testes histology and hormone levels. No alterations in body or testes weight, gonadosomatic index, testes histology, or levels of 11-ketotestosterone or testosterone were observed. Transcriptome analysis did reveal alterations in pathways associated with abnormal cell and neuronal growth and morphology; molecular transport, quantity, and production of steroid hormones; and neurotransmission in all treatment groups. To further investigate potential neurotoxic outcomes in the males, behavior, brain transcriptome, brain methylation status, and neuropathology were assessed at 9 mpf (Horzmann et al. 2021). Decreased locomotor parameters were identified in a battery of behavior tests in all treatment groups. Brain transcriptome analysis identified alterations in genes associated with organismal development, cancer, and nervous and reproductive system development and function similar to as observed at 6 mpf (Wirbisky et al. 2016a). Decreased cell numbers of raphe populations were also detected in the 30 ppb treatment group, but global methylation levels of the brain were not changed (Horzmann et al. 2021). Overall, these studies indicate that embryonic atrazine exposure at concentrations around drinking water regulatory levels impacts reproductive and neurological outcomes in the DOHaD paradigm.

The DOHaD hypothesis has also been incorporated to assess the toxicity of the plasticizers, bisphenol A (BPA) and mono-2-ethylhexyl phthalate (MEHP), and of the perfluoroalkyl substance, perfluorooctanesulfonic acid (PFOS). In one study, exposure of 0.01, 0.1, and 1 μ M BPA from 8 to 120 hpf resulted in learning deficits as assessed in a reversal-learning task and in a T-maze in adult zebrafish aged 8 months (Saili et al. 2012). An additional study investigated impacts to the male reproductive system following three different BPA exposure periods encompassing embryogenesis (6 hpf to 5 mpf), larval development (6 dpf to 5 mpf), and sexual differentiation (3–5 mpf) (Chen et al. 2017). BPA exposures included 0.001, 0.01,

and 0.1 μM . While BPA did not affect growth, a decrease in testes weight in the 0.001 μM treatment group from only the embryonic exposure period and a reduction in sperm volume, density, motility, and volume in the 0.001 μM treatment group from all exposure periods was observed. Overall, this study concluded a non-monotonic dose response with the most severe impacts at the lowest test concentration. Exposure to 200 ppb of another plasticizer, MEHP, from 6 to 120 hpf increased hepatic steatosis and expression of the PPAR α target, *fabp1a1*, at 15 dpf (Sant et al. 2021a). This study concluded that developmental exposure to MEHP was suffice to increase hepatic steatosis, but the findings indicated that Nrf2a did not play a major role in the outcome (Sant et al. 2021a). In addition, the toxicity of PFOS is beginning to be investigated in the DOHaD paradigm. Specifically, two exposure periods were initiated at 1–5 dpf or 1–15 dpf at 16 and 32 μM (Sant et al. 2021b). The most significant insults were observed with the longer exposure period of 1–15 dpf. An increased incidence of aberrant islet morphologies in the higher treatment group (32 μM) was observed at 15 dpf. In addition, alterations in principal islet areas and adiposity were seen in both treatment groups at 15 and 30 dpf. No significant changes in larval spontaneous behavior at 15 dpf were observed, and the authors concluded a developmental PFOS exposure could alter metabolic programming that could persist following cessation of the chemical exposure.

Overall, this series of studies using the zebrafish to address various adverse health outcomes in the DOHaD exposure paradigm assists in further defining risks of exposure to various environmental chemicals. Studies are incorporating different exposure periods and several adverse outcome assessments. The zebrafish DOHaD studies included in this section are not an inclusive list but serve to represent examples of these types of studies that have been conducted to date and to support future studies applying zebrafish to address questions in this research area to inform human health risk.

Beyond the DOHaD paradigm, many of the aforementioned studies and others expand the assessments to include multi- or transgenerational endpoints. These studies incorporate a variety of exposure periods (similar to the studies described in Table 12.1), including developmental and adult life stages. The developmental exposures align with the DOHaD paradigm initiating exposure sometimes the following fertilization (e.g., King Heiden et al. 2009; Baker et al. 2013, 2014; Wirbisky et al. 2016b; Chen et al. 2017; Meyer et al. 2020), while the adult exposures are considering exposure of gametes and subsequent generational effects (e.g., Liu et al. 2016).

12.6 Study Design Considerations

Currently, there are no standard operating protocols or exposure parameters that zebrafish researchers follow. As such, there can be limitations when comparing studies among multiple studies. For example, developmental stages are dynamic, resulting in potential differences to be observed in DOHaD studies if exposure periods are not aligned. In the current research literature, there are a number of

variations in embryonic and larval exposure periods that may be initiated immediately after fertilization (often at 1 or 2 hpf) or with a slight delay at 6 hpf. Researchers take these different approaches to either try to capture the earliest of developmental periods (e.g., those that start at 1–2 hpf) or may choose to start exposures at 6 hpf when fertilized versus non-fertilized eggs are better confirmed. In addition, there is great variability in the age at which the chemical exposure may cease. Studies often choose to stop chemical exposure at 72 hpf to align with the end of embryogenesis, 96 hpf to align with historic toxicity exposure protocols used for lethality that fit within the 5-day work week (e.g., 96 hr-LC₅₀), 120 hpf to target the end of major organ formation at which several reference malformation charts are available and common behavioral assays are performed, among other ages (Brannen et al. 2010; Panzica-Kelly et al., 2010; Sipes et al. 2011). As such, special consideration should be given when comparing studies to the exact exposure period enacted in the study and the differences that may be observed in DOHaD studies dependent on what developmental stages the chemical exposure occurred. Other husbandry parameters should also be noted, including the temperature at which zebrafish were reared as developmental progression is influenced by temperature. Zebrafish at higher temperatures develop more rapidly compared to lower temperatures (e.g., 28 °C compared to 26 °C, which are both common in zebrafish studies).

12.7 Future Directions and Challenges

While these findings are laying the groundwork for zebrafish DOHaD-based studies, significant challenges exist in delineating the mechanisms of these later-in-life adverse health outcomes. The role that epigenetics plays in driving the progression and ultimately establishing a disease phenotype in the DOHaD paradigm is complicated. Epigenetic alterations are intrinsically complex, with multiple modifications possible on a single target. As such, not only do multiple epigenetic targets need to be addressed, but studies need to work to identify the specific alterations occurring for each target. We also know now that epigenetic alterations are dynamic and change with time at varying timescales. For example, histone acetylation changes within a cell cycle (~days), while DNA methylation changes can last life-long (~years). As this field progresses, it will be important to track epigenetic changes caused by chemical exposures in real-time to understand these dynamics to further our understanding of toxicity mechanisms linking the developmental exposure and later-in-life adverse health outcomes. Overall, the zebrafish is well-suited to address these challenges moving forward, taking advantage of the many strengths mentioned previously, spanning *ex vivo* embryonic development of a near-transparent organism to shorter life periods.

Furthermore, advances in genetic models and technologies for labeling molecular features of epigenetic modifications will enable the zebrafish to identify and track the impacts of these chemical insults beginning at the earliest stages of development and throughout the lifespan (Kiper and Freeman 2021). Detailed toxicokinetic understanding of most chemicals is also limited currently for the zebrafish, but similar to

other research areas with the zebrafish; this knowledge base is rapidly expanding (Kirla et al. 2016; Ahkin Chin Tai et al. 2021). In addition, while this chapter has primarily focused on adverse health outcomes in the exposed generation, multiple studies are now incorporating multi- or transgenerational analyses that include progeny or individuals from multiple generations of the initially exposed generation.

References

- Ahkin Chin Tai JK, Horzmann KA, Franco J, Jannasch AS, Cooper BR, Freeman JL (2021) Developmental atrazine exposure in zebrafish produces the same major metabolites as mammals, along with altered behavioural outcomes. *Neurotoxicol Teratol* 85:106971. <https://doi.org/10.1016/j.ntt.2021.106971>
- Bailey J, Oliveri A, Levin ED (2013) Zebrafish model systems for developmental neurobehavioral toxicology. *Birth Defects Res C Embryo Today* 99:14–23. <https://doi.org/10.1002/bdrc.21027>
- Baker TR, Peterson RE, Heideman W (2013) Early dioxin exposure causes toxic effects in adult zebrafish. *Toxicol Sci* 135:241–250. <https://doi.org/10.1093/toxsci/kft144>
- Baker TR, Peterson RE, Heideman W (2014) Using zebrafish as a model system for studying the transgenerational effects of dioxin. *Toxicol Sci* 138:403–411. <https://doi.org/10.1093/toxsci/kfu006>
- Ball JS, Stedman DB, Hillegass JM, Zhang CX, Panzica-Kelly J, Coburn A, Enright BP, Tornesi B, Amouzadeh HR, Hetheridge M, Gustafson A-L, Augustine-Rauch KA (2014) Fishing for teratogens: a consortium effort for a harmonized zebrafish developmental toxicology assay. *Toxicol Sci* 139:210–219. <https://doi.org/10.1093/toxsci/kfu017>
- Barker DJP (2004) The developmental origins of adult disease. *J Am Coll Nutr* 23:588S–595S. <https://doi.org/10.1080/07315724.2004.10719428>
- Barker DJP (2007) The origins of the developmental origins theory. *J Intern Med* 261:412–417. <https://doi.org/10.1111/j.1365-2796.2007.01809.x>
- Barker DJP, Godfrey KM, Gluckman PD, Harding JE, Owens JA, Robinson JS (1993) Fetal nutrition and cardiovascular disease in adult life. *Lancet* 341:938–941. [https://doi.org/10.1016/0140-6736\(93\)91224-A](https://doi.org/10.1016/0140-6736(93)91224-A)
- Bault ZA, Peterson SM, Freeman JL (2015) Directional and colour preference in adult zebrafish: implications in behavioural and learning assays in neurotoxicology studies. *J Appl Toxicol* 35:1502–1510. <https://doi.org/10.1002/jat.3169>
- Bihaqi SW, Bahmani A, Subaiea GM, Zawia NH (2014) Infantile exposure to lead and late-age cognitive decline: relevance to AD. *Alzheimers Dement* 10:187–195. <https://doi.org/10.1016/j.jalz.2013.02.012>
- Bihaqi SW, Alansi B, Masoud AM, Mushtaq F, Subaiea GM, Zawia NH (2018) Influence of early life Lead (pb) exposure on α -synuclein, GSK-3 β and Caspase-3 mediated tauopathy: implications on Alzheimer's disease. *Curr Alzheimer Res* 15:1114–1122. <https://doi.org/10.2174/1567205015666180801095925>
- Bird A (2002) DNA methylation patterns and epigenetic memory. *Genes Dev* 16:6–21. <https://doi.org/10.1101/gad.947102>
- Bouwmeester MC, Ruiter S, Lommelaars T, Sippel J, Hodemaekers HM, van den Brandhof E-J, Pennings JLA, Kamstra JH, Jelinek J, Issa J-PJ, Legler J, van der Ven LTM (2016) Zebrafish embryos as a screen for DNA methylation modifications after compound exposure. *Toxicol Appl Pharmacol* 291:84–96. <https://doi.org/10.1016/j.taap.2015.12.012>
- Brannen KC, Panzica-Kelly JM, Danberry TL, Augustine-Rauch KA (2010) Development of a zebrafish embryo teratogenicity assay and quantitative prediction model. *Birth Defect Res B* 89:66–77. <https://doi.org/10.1002/bdrb.20223>

- Chen J, Chen Y, Liu W, Bai C, Liu X, Liu K, Li R, Zhu J-H, Huang C (2012) Developmental lead acetate exposure induces embryonic toxicity and memory deficit in adult zebrafish. *NeurotoxicolTeratol* 34:581–586. <https://doi.org/10.1016/j.ntt.2012.09.001>
- Chen J, Saili KS, Liu Y, Li L, Zhao Y, Jia Y, Bai C, Tanguay RL, Dong Q, Huang C (2017) Developmental bisphenol A exposure impairs sperm function and reproduction in zebrafish. *Chemosphere* 169:262–270. <https://doi.org/10.1016/j.chemosphere.2016.11.089>
- Dash M, Eid A, Subaiea G, Chang J, Deeb R, Masoud A, Renehan WE, Adem A, Zawia NH (2016) Developmental exposure to lead (pb) alters the expression of the human tau gene and its products in a transgenic animal model. *Neurotoxicology* 55:154–159. <https://doi.org/10.1016/j.neuro.2016.06.001>
- Eid A, Bihaqi SW, Renehan WE, Zawia NH (2016) Developmental lead exposure and lifespan alterations in epigenetic regulators and their correspondence to biomarkers of Alzheimer's disease. *Alzheimers Dement (Amst)* 2:123–131. <https://doi.org/10.1016/j.dadm.2016.02.002>
- Eid A, Bihaqi SW, Hemme C, Gaspar JM, Hart RP, Zawia NH (2018) Histone acetylation maps in aged mice developmentally exposed to lead: epigenetic drift and Alzheimer-related genes. *Epigenomics* 10:573–583. <https://doi.org/10.2217/epi-2017-0143>
- Gibney ER, Nolan CM (2010) Epigenetics and gene expression. *Heredity* 105:4–13. <https://doi.org/10.1038/hdy.2010.54>
- Gluckman PD, Buklijas T, Hanson MA (2016) The developmental origins of health and disease (DOHaD) concept, in the epigenome and developmental origins of health and disease. Elsevier:1–15. <https://doi.org/10.1016/B978-0-12-801383-0.00001-3>
- Grandjean P, Barouki R, Bellinger DC, Casteleyn L, Chadwick LH, Cordier S, Etzel RA, Gray KA, Ha E-H, Junien C, Karagas M, Kawamoto T, Lawrence BP, Perera FP, Prins GS, Puga A, Rosenfeld CS, Sherr DH, Sly PD, Suk W, Sun Q, Toppari J, van den Hazel P, Walker CL, Heindel JJ (2015) Life-long implications of developmental exposure to environmental stressors: new perspectives. *Endocrinology* 156:3408–3415. <https://doi.org/10.1210/en.2015-1350>
- Gustafson A-L, Stedman DB, Ball J, Hillegass JM, Flood A, Zhang CX, Panzica-Kelly J, Cao J, Coburn A, Enright BP, Tornesi MB, Hetheridge M, Augustine-Rauch KA (2012) Inter-laboratory assessment of a harmonised zebrafish developmental toxicology assay—Progress report on phase I. *Reprod Toxicol* 33:155–164. <https://doi.org/10.1016/j.reprotox.2011.12.004>
- Haugen AC, Schug TT, Collman G, Heindel JJ (2015) Evolution of DOHaD: the impact of environmental health sciences. *J Dev Orig Health Dis* 6:55–64. <https://doi.org/10.1017/S2040174414000580>
- Heindel JJ, Balbus J, Bimbaum L, Brune-Drise MN, Grandjean P, Gray K, Landrigan PJ, Sly PD, Suk W, Slechta DC, Thompson C, Hanson M (2015) Developmental origins of health and disease: integrating environmental influences. *Endocrinology* 156:3416–3421. <https://doi.org/10.1210/en.2015-1394>
- Heindel JJ, Skalla LA, Joubert BR, Dilworth CH, Gray KA (2017) Review of developmental origins of health and disease publications in environmental epidemiology. *Reprod Toxicol* 68:34–48. <https://doi.org/10.1016/j.reprotox.2016.11.011>
- Hill AJ, Teraoka H, Heideman W, Peterson RE (2005) Zebrafish as a model vertebrate for investigating chemical toxicity. *Toxicol Sci* 86:6–19. <https://doi.org/10.1093/toxsci/kfi110>
- Horzmann KA, Freeman JL (2017) Toxicogenomic evaluation using the zebrafish model system. In: Meyers RA (ed) *Encyclopedia of analytical chemistry*. John Wiley & Sons, Ltd, Chichester, pp 1–19. <https://doi.org/10.1002/9780470027318.a9628>
- Horzmann KA, Freeman JL (2018) Making waves: new developments in toxicology with the zebrafish. *Toxicol Sci* 163:5–12. <https://doi.org/10.1093/toxsci/kfy044>
- Horzmann KA, Lin LF, Taslakjian B, Yuan C, Freeman JL (2021) Embryonic atrazine exposure and later in life behavioural and brain transcriptomic, epigenetic, and pathological alterations in adult male zebrafish. *Cell Biol Toxicol* 37:421–439. <https://doi.org/10.1007/s10565-020-09548-y>
- Howe K, Clark MD, Torroja CF, Torrance J, Berthelot C, Muffato M, Collins JE, Humphray S, McLaren K, Matthews L, McLaren S, Sealy I, Caccamo M, Churcher C, Scott C, Barrett JC,

- Koch R, Rauch G-J, White S, Chow W, Kilian B, Quintais LT, Guerra-Assunção JA, Zhou Y, Gu Y, Yen J, Vogel J-H, Eyre T, Redmond S, Banerjee R, Chi J, Fu B, Langley E, Maguire SF, Laird GK, Lloyd D, Kenyon E, Donaldson S, Sehra H, Almeida-King J, Loveland J, Trevanion S, Jones M, Quail M, Willey D, Hunt A, Burton J, Sims S, McLay K, Plumb B, Davis J, Clee C, Oliver K, Clark R, Riddle C, Elliot D, Elliott D, Threadgold G, Harden G, Ware D, Begum S, Mortimore B, Mortimer B, Kerry G, Heath P, Phillimore B, Tracey A, Corby N, Dunn M, Johnson C, Wood J, Clark S, Pelan S, Griffiths G, Smith M, Glithero R, Howden P, Barker N, Lloyd C, Stevens C, Harley J, Holt K, Panagiotidis G, Lovell J, Beasley H, Henderson C, Gordon D, Auger K, Wright D, Collins J, Raisen C, Dyer L, Leung K, Robertson L, Ambridge K, Leongamornlert D, McGuire S, Gilderthorp R, Griffiths C, Manthavadi D, Nichol S, Barker G, Whitehead S, Kay M, Brown J, Murnane C, Gray E, Humphries M, Sycamore N, Barker D, Saunders D, Wallis J, Babbage A, Hammond S, Mashreghi-Mohammadi M, Barr L, Martin S, Wray P, Ellington A, Matthews N, Ellwood M, Woodmansey R, Clark G, Cooper JD, Cooper J, Tromans A, Grafham D, Skuce C, Pandian R, Andrews R, Harrison E, Kimberley A, Garnett J, Fosker N, Hall R, Garner P, Kelly D, Bird C, Palmer S, Gehring I, Berger A, Dooley CM, Ersan-Ürün Z, Eser C, Geiger H, Geisler M, Karotki L, Kirn A, Konantz J, Konantz M, Oberländer M, Rudolph-Geiger S, Teucke M, Lanz C, Raddatz G, Osoegawa K, Zhu B, Rapp A, Widaa S, Langford C, Yang F, Schuster SC, Carter NP, Harrow J, Ning Z, Herrero J, Searle SMJ, Enright A, Geisler R, Plasterk RHA, Lee C, Westerfield M, de Jong PJ, Zon LI, Postlethwait JH, Nüsslein-Volhard C, Hubbard TJP, RoestCrollius H, Rogers J, Stemple DL (2013) The zebrafish reference genome sequence and its relationship to the human genome. *Nature* 496:498–503. <https://doi.org/10.1038/nature12111>
- Kimmel CB, Ballard WW, Kimmel SR, Ullmann B, Schilling TF (1995) Stages of embryonic development of the zebrafish. *Dev Dyn* 203:253–310. <https://doi.org/10.1002/aja.1002030302>
- King Heiden TC, Spitsbergen J, Heideman W, Peterson RE (2009) Persistent adverse effects on health and reproduction caused by exposure of zebrafish to 2,3,7,8-tetrachlorodibenzo-p-dioxin during early development and gonad differentiation. *Toxicol Sci* 109:75–87. <https://doi.org/10.1093/toxsci/kfp048>
- Kiper K, Freeman JL (2021) Use of zebrafish genetic models to study Etiology of the amyloid-beta and neurofibrillary tangle pathways in Alzheimer's disease. *CN* 19. <https://doi.org/10.2174/1570159X19666210524155944>
- Kirla KT, Groh KJ, Steuer AE, Poetzsch M, Banote RK, Stadnicka-Michalak J, Eggen RIL, Schirmer K, Kraemer T (2016) From the cover: zebrafish larvae are insensitive to stimulation by cocaine: importance of exposure route and toxicokinetics. *Toxicol Sci* 154:183–193. <https://doi.org/10.1093/toxsci/kfw156>
- Klemm SL, Shipony Z, Greenleaf WJ (2019) Chromatin accessibility and the regulatory epigenome. *Nat Rev Genet* 20:207–220. <https://doi.org/10.1038/s41576-018-0089-8>
- Lee J, Freeman JL (2014) Zebrafish as a model for investigating developmental lead (pb) neurotoxicity as a risk factor in adult neurodegenerative disease: a mini-review. *Neurotoxicology* 43:57–64. <https://doi.org/10.1016/j.neuro.2014.03.008>
- Lee J, Freeman JL (2016) Embryonic exposure to 10 µg/L(–1) lead results in female-specific expression changes in genes associated with nervous system development and function and Alzheimer's disease in the aged adult zebrafish brain. *Metallomics* 8:589–596. <https://doi.org/10.1039/c5mt00267b>
- Lee J, Horzmann KA, Freeman JL (2018) An embryonic 100µg/L lead exposure results in sex-specific expression changes in genes associated with the neurological system in females or cancer in male adult zebrafish brains. *Neurotoxicol Teratol* 65:60–69. <https://doi.org/10.1016/j.ntt.2017.10.006>
- Lin LF, Xie J, Sánchez OF, Bryan C, Freeman JL, Yuan C (2021) Low dose lead exposure induces alterations on heterochromatin hallmarks persisting through SH-SY5Y cell differentiation. *Chemosphere* 264:128486. <https://doi.org/10.1016/j.chemosphere.2020.128486>
- Liu Q, Klingler RH, Wimpee B, Dellinger M, King-Heiden T, Grzybowski J, Gerstenberger SL, Weber DN, Carvan MJ (2016) Maternal methylmercury from a wild-caught walleye diet

- induces developmental abnormalities in zebrafish. *Reprod Toxicol* 65:272–282. <https://doi.org/10.1016/j.reprotox.2016.08.010>
- Meyer DN, Crofts EJ, Akemann C, Gurdziel K, Farr R, Baker BB, Weber D, Baker TR (2020) Developmental exposure to Pb²⁺ induces transgenerational changes to zebrafish brain transcriptome. *Chemosphere* 244:125527. <https://doi.org/10.1016/j.chemosphere.2019.125527>
- Miranda TB, Jones PA (2007) DNA methylation: the nuts and bolts of repression. *J Cell Physiol* 213:384–390. <https://doi.org/10.1002/jcp.21224>
- Mozzetta C, Boyarchuk E, Pontis J, Ait-Si-Ali S (2015) Sound of silence: the properties and functions of repressive Lys methyltransferases. *Nat Rev Mol Cell Biol* 16:499–513. <https://doi.org/10.1038/nrm4029>
- Needleman HL, Leviton A, Bellinger D (1982) Lead-associated intellectual deficit. *N Engl J Med* 306:367. <https://doi.org/10.1056/NEJM198202113060619>
- Ng H-H, Bird A (1999) DNA methylation and chromatin modification. *Curr Opin Genet Dev* 9: 158–163. [https://doi.org/10.1016/S0959-437X\(99\)80024-0](https://doi.org/10.1016/S0959-437X(99)80024-0)
- Panzica-Kelly JM, Zhang CX, Danberry TL, Flood A, DeLan JW, Brannen KC, Augustine-Rauch KA (2010) Morphological score assignment guidelines for the dechorionated zebrafish teratogenicity assay. *Birth Defects Res Part B* 89:382–395
- Rice C, Ghorai JK, Zalewski K, Weber DN (2011) Developmental lead exposure causes startle response deficits in zebrafish. *Aquat Toxicol* 105:600–608. <https://doi.org/10.1016/j.aquatox.2011.08.014>
- Robboy SJ, Scully RE, Welch WR, Herbst AL (1977) Intrauterine diethylstilbestrol exposure and its consequences: pathologic characteristics of vaginal adenosis, clear cell adenocarcinoma, and related lesions. *Arch Pathol Lab Med* 101:1–5
- Ruiter S, Sippel J, Bouwmeester M, Lommelaars T, Beekhof P, Hodemaekers H, Bakker F, van den Brandhof E-J, Pennings J, van der Ven L (2016) Programmed effects in neurobehavior and antioxidative physiology in zebrafish embryonically exposed to cadmium: observations and hypothesised adverse outcome pathway framework. *IJMS* 17:1830. <https://doi.org/10.3390/ijms17111830>
- Sailli KS, Corvi MM, Weber DN, Patel AU, Das SR, Przybyla J, Anderson KA, Tanguay RL (2012) Neurodevelopmental low-dose bisphenol A exposure leads to early life-stage hyperactivity and learning deficits in adult zebrafish. *Toxicology* 291:83–92. <https://doi.org/10.1016/j.tox.2011.11.001>
- Sanchez OF, Lee J, Yu King Hing N, Kim S-E, Freeman JL, Yuan C (2017) Lead (Pb) exposure reduces global DNA methylation level by non-competitive inhibition and alteration of dnmt expression. *Metallomics* 9:149–160. <https://doi.org/10.1039/c6mt00198j>
- Sant KE, Annunziato K, Conlin S, Teicher G, Chen P, Venezia O, Downes GB, Park Y, Timme-Laragy AR (2021a) Developmental exposures to perfluorooctanesulfonic acid (PFOS) impact embryonic nutrition, pancreatic morphology, and adiposity in the zebrafish, *Danio rerio*. *Environ Pollut* 275:116644. <https://doi.org/10.1016/j.envpol.2021.116644>
- Sant KE, Moreau HM, Williams LM, Jacobs HM, Bowsher AM, Boisvert JD, Smolowitz RM, Pantazis J, Annunziato K, Nguyen M, Timme-Laragy A (2021b) Embryonic exposures to mono-2-Ethylhexyl phthalate induce larval steatosis in zebrafish independent of Nrf2a signaling. *J Dev Orig Health Dis* 12:132–140. <https://doi.org/10.1017/S2040174420000057>
- Sasaki T, Kishi S (2013) Molecular and chemical genetic approaches to developmental origins of ageing and disease in zebrafish. *Biochem Biophys Acta* 1832:1362–1370. <https://doi.org/10.1016/j.bbadis.2013.04.030>
- Sipes NS, Padilla S, Knudsen TB (2011) Zebrafish: as an integrative model for twenty-first-century toxicity testing. *Birth Defects Res C Embryo Today* 93:256–267. <https://doi.org/10.1002/bdrc.20214>
- Varshney GK, Sood R, Burgess SM (2015) Understanding and editing the zebrafish genome. *Adv Genet* 92:1–52. <https://doi.org/10.1016/bs.adgen.2015.09.002>

- Weber DN, Ghorai JK (2013) Experimental design affects social behaviour outcomes in adult zebrafish developmentally exposed to lead. *Zebrafish* 10:294–302. <https://doi.org/10.1089/zeb.2012.0780>
- Wiles ET, Selker EU (2017) H3K27 methylation: a promiscuous repressive chromatin mark. *Curr Opin Genet Dev* 43:31–37. <https://doi.org/10.1016/j.gde.2016.11.001>
- Wirbisky SE, Weber GJ, Sepúlveda MS, Xiao C, Cannon JR, Freeman JL (2015) Developmental origins of neurotransmitter and transcriptome alterations in adult female zebrafish exposed to atrazine during embryogenesis. *Toxicology* 333:156–167. <https://doi.org/10.1016/j.tox.2015.04.016>
- Wirbisky SE, Sepúlveda MS, Weber GJ, Jannasch AS, Horzmann KA, Freeman JL (2016a) Embryonic atrazine exposure elicits alterations in genes associated with neuroendocrine function in adult male zebrafish. *Toxicol Sci* 153:149–164. <https://doi.org/10.1093/toxsci/kfw115>
- Wirbisky SE, Weber GJ, Sepúlveda MS, Lin T-L, Jannasch AS, Freeman JL (2016b) An embryonic atrazine exposure results in reproductive dysfunction in adult zebrafish and morphological alterations in their offspring. *Sci Rep* 6:21337. <https://doi.org/10.1038/srep21337>
- Wirbisky-Hershberger SE, Sanchez OF, Horzmann KA, Thanki D, Yuan C, Freeman JL (2017) Atrazine exposure decreases the activity of DNMTs, global DNA methylation levels, and dnmt expression. *Food Chem Toxicol* 109:727–734. <https://doi.org/10.1016/j.fct.2017.08.041>
- Wu J, Basha MR, Zawia NH (2008) The environment, epigenetics and amyloidogenesis. *J Mol Neurosci* 34:1–7. <https://doi.org/10.1007/s12031-007-0009-4>
- Wysocka J, Swigut T, Xiao H, Milne TA, Kwon SY, Landry J, Kauer M, Tackett AJ, Chait BT, Badenhorst P, Wu C, Allis CD (2006) A PHD finger of NURF couples histone H3 lysine 4 trimethylation with chromatin remodelling. *Nature* 442:86–90. <https://doi.org/10.1038/nature04815>
- Xie J, Lin L, Sánchez OF, Bryan C, Freeman JL, Yuan C (2021) Pre-differentiation exposure to low-dose of atrazine results in persistent phenotypic changes in human neuronal cell lines. *Environ Pollut* 271:116379. <https://doi.org/10.1016/j.envpol.2020.116379>



Green Synthesis of Nontoxic Nanoparticles 13

K. B. Megha, X. Joseph, and P. V. Mohanan

13.1 Introduction

Nanotechnology has gained much remarkable research achievement in the last decades due to its most significant and astonishing properties. Nanoparticles (NPs) are synthesized with controlled and unique morphology that directly affects their distinctive property. Nanoparticle synthesis is mainly restricted over their particle size, shape, and crystalline structure, making them applied for various applications in biomedical, bio-remediation, bio-sensors, and low-cost electrodes (Antonyraj et al. 2013; Neville et al. 2009; Staniland 2007; Mandeep 2020). Generally, nanotechnology is defined as the science in which materials are manipulated at their atomic level by the combined approach of engineering, chemistry, and biology (Cauerhff and Castro 2013). The concept of nanotechnology has a long history and has been utilized in the ninth century by Mesopotamians where they used gold and silver nanoparticles to glitter their pots and utensils (Faraday 1857). Michael Faraday gave the first scientific explanation on nanoparticle properties in his famous work entitled “Experimental relations to gold and other metals to light” (Faraday 1857; Singh et al. 2011). But the term “nanotechnology” was introduced by Richard Feynman in 1959, which is considered as the remarkable beginning for nanotechnology (Singh et al. 2011).

Much considerable attention has been gained for the synthesis of NPs by implementing newer techniques for developing NPs with different kinds of composition and biological sources. However, currently prevailing methods used to synthesize nanoparticles are really expensive, hazardous to the environment, and unproductive. Several factors such as the time, method chosen for the synthesis,

K. B. Megha · X. Joseph · P. V. Mohanan (✉)

Toxicology Division, Biomedical Technology Wing, Sree Chitra Tirunal Institute for Medical Sciences and Technology (Govt. of India), Poojapura, Trivandrum, Kerala, India

© The Author(s), under exclusive license to Springer Nature Singapore Pte Ltd. 2023

P. V. Mohanan, S. Kappalli (eds.), *Biomedical Applications and Toxicity of Nanomaterials*, https://doi.org/10.1007/978-981-19-7834-0_13

319



Fig. 13.1 The 12 principles of green chemistry (Anastas and Warner 1998)

pH, temperature, pressure, and pore size significantly affect the quality and quantity of the nanoparticles and their characterization and application. Bioactive molecules that are present in plants, algae, fungi, and yeast were identified to promote an active part in the formation of NPs with peculiar shapes and sizes. It thereby acts as a suitable enhancer to develop a safe, green, and environmentally compatible protocol for NP synthesis. Several synthetic methods are employed until now to prepare and synthesize NP with varying sizes and morphology. Even though these methods made the development of more extensive NP, an improved mass production protocol is a requisite for different applications like industry, medicines, agriculture, home appliances, and communication technology in targeting environment-friendly approach.

The green synthesis of NPs utilizes different biological moieties that can overcome many of the negative impacts caused by chemical and physical methods. Currently, biological/green synthesis is preferred due to its safe, clean, economic capability and can be scaled up for the synthesis of nanomaterials. The applications of NP are increasing day by day due to their exceptional characteristics such as anti-inflammatory and anti-microbial activity, highly biocompatible, bioavailability, effective drug delivery, tumor targeting, and bioactivity (Elfeky et al. 2020; Dulinska-Molak et al. 2018; Sharaf et al. 2019; Hassan et al. 2019; Mohamed et al. 2019; Fouda et al. 2019, 2018; Shaheen and Fouda 2018; Tomar et al. 2014; Vidhu and Philip 2014; Kotil et al. 2017). Green synthesis of nanoparticles mainly prefers mild pressure, temperature, and pH at significantly low cost (Fouda et al. 2017). Paul Anastas and John Warner established the 12 principles of green chemistry to impart NP synthesis, design, and reduce the hazardous effect on humans and the environment (Anastas and Warner 1998) (Fig. 13.1).

13.2 Synthesis of Nanoparticles Using a Green Approach

Nanoparticles are synthesized by various physical, chemical, biological, or hybrid methods (Mohanpuria et al. 2008; Tiwari et al. 2008; Luechinger et al. 2010). The production of NPs using the conventional chemical or physical method results in the release of toxic by-products, which are extremely hazardous to the environment. And also, these particles cannot be used for the application of medical or clinical purposes due to their extreme toxicity (Parashar et al. 2009a, b). The conventional approach is mainly employed for nanoparticle production in large quantities with well-defined size and shape within a short period of time. However, complicated procedure with high cost, ineffective and obsolete makes them inappropriate for many biomedical applications. This made the growing interest in an environmentally friendly approach. It is reported that the NPs synthesized from green technology are superior to the particle synthesized from chemical or physical methods since no expensive chemicals are involved in any of the steps, consumption of less energy, and finally generate eco-friendly particles and by-products. The green synthesis approach does not generate toxic wastes during the whole manufacturing process (Daniel and Astruc 2004; Li et al. 2011; Chauhan et al. 2012) (Fig. 13.2).

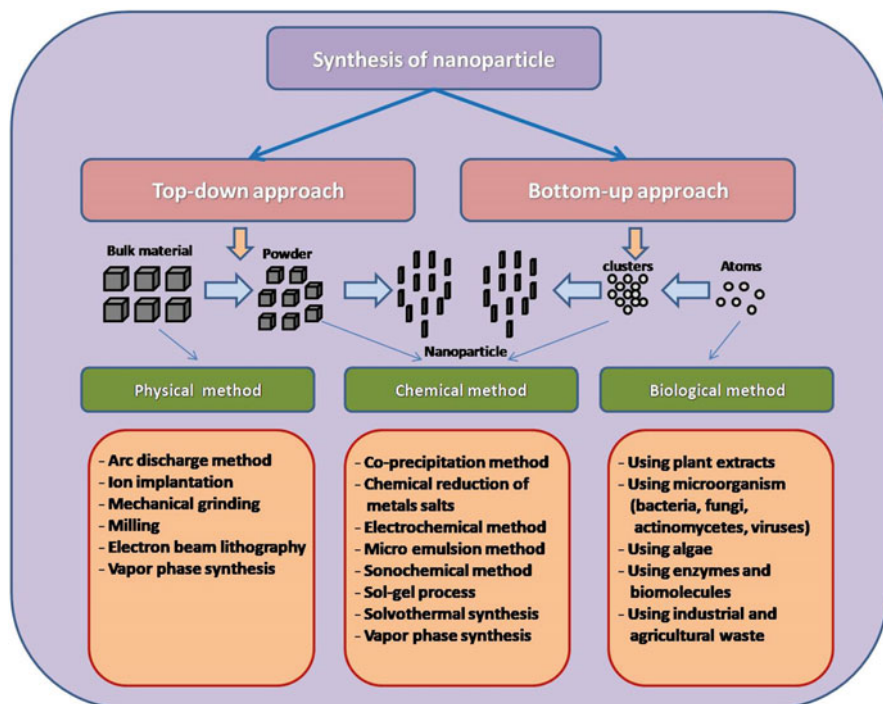


Fig. 13.2 Different strategies and techniques for synthesizing nanoparticles

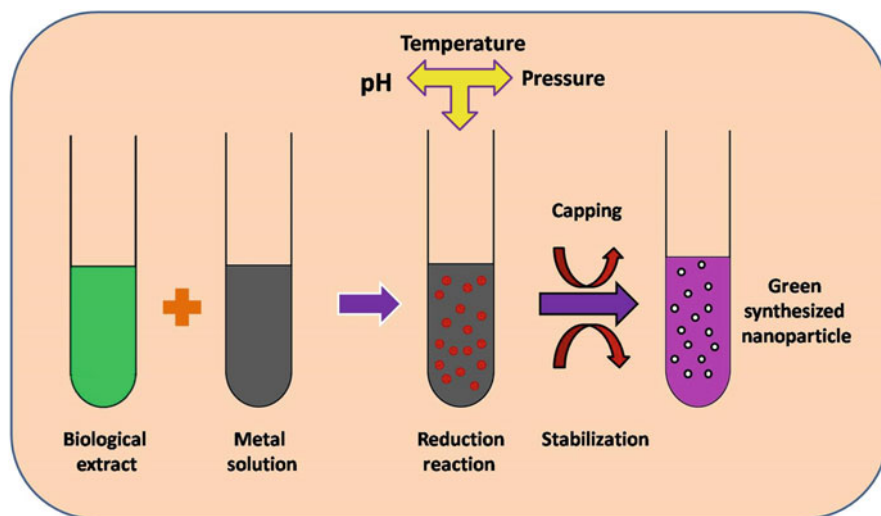


Fig. 13.3 Biological synthesis of nanoparticles using green approach

The green synthesis of NPs utilizes the bottom-up approach in which synthesis happens in the presence of stabilizing and reducing agents. Their synthesis involves three main steps (a) solvent media selection, (b) selection of environmentally suitable reducing agent, and (c) selection of nontoxic material for synthesis (Fierascu et al. 2010). NP synthesis is mainly based on the green approach acquired with the main objective to reduce waste and energy, utilize recyclable matter, and implement the technique to reduce environmental hazards thereby generating NPs that can be used for multipurpose applications. It is reported in the literature that a living system can act as the biological working station for the development of metal oxides and metal nanoparticles (Ashraf et al. 2018; Bibi et al. 2017a, b; Nazar et al. 2018). The different types of microorganisms, including bacteria (Shivaji et al. 2011), fungi (Syed et al. 2013), and plant extract (Akhtar et al. 2013), act as the biologically derived precursor molecule for the synthesis of nanoparticles with a wide range of applications. The plant extracts of root, leaf, seed, stem, and latexes are excellent source of reducing and stabilizing agents (Fig. 13.3).

In addition, different algae are also utilized to synthesize nanoparticles due to their exceptional tendency to bio-remediation of unsafe heavy metals by converting them to less hazardous eco-friendly forms. Another better and convenient selection is the utilization of plant extracts for nanoparticle synthesis. It provides a rapid, nontoxic, and inexpensive intermediate for the large-scale production of NPs (Njagi et al. 2011). In the current situation of environmental pollution due to the release of hazardous chemicals from NP synthesis, emphasis is needed for better adoption of a new eco-friendly strategy for the production and application of nanomaterials is highly essential (Nwamezie 2018; Remya et al. 2017). It has been reported from the studies that a variety of microorganisms, especially bacteria and fungus, synthesize

NPs of silver (Ag), gold (Au), alginate, titanium (Ti), and magnesium (Mg) (Duran et al. 2014).

Green synthesis mainly works on the bottom-up approach where nanoparticles are formed by the oxidation-reduction of metallic ions secreted by the biomolecules, especially enzymes, proteins, sugars, etc. (Prabhu and Poulouse 2012). However, a complete understanding of the NP synthesis from the microbial origin is yet to be understood as different microbes exhibit another mechanism of interaction with the metal ions. The biochemical interaction of the precise microorganism as well as the environmental conditions like temperature, pH together contribute towards the size and shape of the newly synthesized NPs (Makarov et al. 2014).

Even though NP synthesis based on green synthesis highlights so many beneficial effects yet some challenges are to be overcome during the process. Initial criteria stand for the requirement of optimizing the process that determines the size and shape of the particle. The identification of each role contributed by the compounds in the biological synthesis of the particles needs to be investigated. The procedure for scaling up the nanoparticle synthesis needs more exploration to apply for commercial purposes. And also, the green approach needs more multidisciplinary involvement from basic science, chemical engineering, and industry to synthesize novel material for commercial practice.

13.3 Nanoparticle Synthesis Mediated by Bacteria

Bacteria have become the most preferred and widely studied microorganism for nanoparticle synthesis as it requires slight growth conditions, easiness in extraction and purification, and have the highest yield. *Bacillus thuringiensis*, *Bacillus licheniformis*, *Klebsiella pneumoniae*, and *Morganellapsychrotolerans* were utilized to synthesize silver nanoparticles (John et al. 2020). Titanium dioxide (TiO₂) is synthesized with the aid of *Bacillus subtilis* and *Lactobacillus* sp. (Khan and Fulekar 2016). *Pseudomonas aeruginosa*, *Escherichia coli* DH5 α , *Rhodopseudomonas capsulata*, *Bacillus subtilis*, and *Bacillus licheniformis* are used for gold nanoparticle synthesis (Srinath et al. 2018), whereas *Clostridium thermoaceticum*, *Rhodopseudomonas palustris*, and *Escherichia coli* were exploited for cadmium nanoparticle synthesis (Sweeney et al. 2004). The bacteria act as a biocatalyst or as a bio-scaffold for mineralisation and synthesis of nanoparticles. *Streptomyces* HBUM171191 is reported for the biosynthesis of manganese and zinc nanoparticles (Waghmare et al. 2011). After the preferred incubation period, bacteria can synthesize nanoparticles in the broth provided either extracellularly or intracellularly. This phenomenon makes the biosynthesis of nanoparticles more reasonable, malleable, and the most proper technique for large-scale production. The endurance of bacteria to withstand the physical and chemical growth conditions such as pH, temperature, culturing time, and media composition influence the synthesis of nanoparticles.

13.4 Nanoparticle Synthesis Mediated by Fungus and Yeast

Fungus holds higher priority for the synthesis of NPs than bacteria as it exhibits greater bearing capacity, the tendency to agglomerate metals, and better linking ability. It is very easy to handle and maintain in laboratory conditions. Fungus release enzymes, which can reduce the metal ions for the production of nanoparticles (Mandal and Bolander 2006). The application of fungus in the synthesis of metallic nanoparticles is found to be preferable due to the highest release of enzymes and proteins. The fungus of different species such as *Phanerochaete chrysosporium*, *Schizophyllum commune*, *Pleurotussajor-caju*, and *Coriolus versicolor* exhibits the ability to produce Au and Ag nanoparticles (El Domany et al. 2018; Elamawi et al. 2018). It has been reported that the oxides of zinc (Zn) and iron (Fe)NPs are synthesized with the aid of *Fusarium keratoplasticum*, *Fusarium oxysporum*, *Aspergillus niger*, *Aspergillus terreus*, and *Alternaria alternata* (Mohamed et al. 2019; Sarkar et al. 2017). *Helminthosporium tetramera*, *Schizophyllum radiatum*, *Fusarium keratoplasticum*, and *Fusarium* spp. were utilized to synthesize silver NPs (Mohamed et al. 2017; Gaikwad et al. 2013; Shelar and Chavan 2014; Metuku et al. 2014). Interestingly, *Fusarium oxysporum* is detailed for the ability to synthesize cadmium sulfide (CdS), zinc sulfide (ZnS), lead sulfide (PbS), and molybdenum sulfide (MoS₂) NPs under a controlled condition with appropriate salt in their growth media (Ahmad et al. 2002). The biological synthesis of platinum (Pt)NPs is synthesized with the help of the fungus *Neurospora crassa* and is produced intracellularly (Castro et al. 2013). However, the secretion of higher levels of proteins and enzymes makes it possible for the fungus to synthesize NPs with increased productivity. The pathogenicity of specific fungus creates potential safety concerns (Minuto et al. 2006). Nevalainen and coworkers described in their study that the non-pathogenic fungus *Trichoderma asperellum* and *Trichoderma reesei* are ideal for the synthesis of NPs (Nevalainen et al. 1994; Mukherjee et al. 2008; Khabat et al. 2011) (Fig. 13.4).

Yeasts own the highest ability to take up and accumulate a good quantity of metal ions due to their large surface vicinity (Bhattacharya and Gupta 2005; Mandal et al. 2006). It is reported that yeasts especially strain MKY3, *Candida albicans*, *Candida utilis*, and *Saccharomyces boulardii* supported in the biosynthesis of Ag-NPs (Soliman et al. 2018). Yeasts isolated from the extreme acid source have shown efficacy in synthesizing Au and AgNPs (Rónavári et al. 2018). The production of stable selenium (Se)NPs has been explored in *Magnusiomycesingens* LHF1 intracellularly (Lian et al. 2019). The mechanism of NP synthesis modified by yeast varies accordingly, resulting in increased permanence and alteration in particle size and characteristic properties. When exposed to cadmium (Cd) salts, *Candida glabrata* synthesizes CdS quantum dots intracellularly (Dameron and Winge 1990). In the presence of Pb ions, *Torulopsis* sp. produces PbS quantum dots, and similarly, *Pichia jadinii* synthesizes AuNPs after exposure to Au ions in the medium.

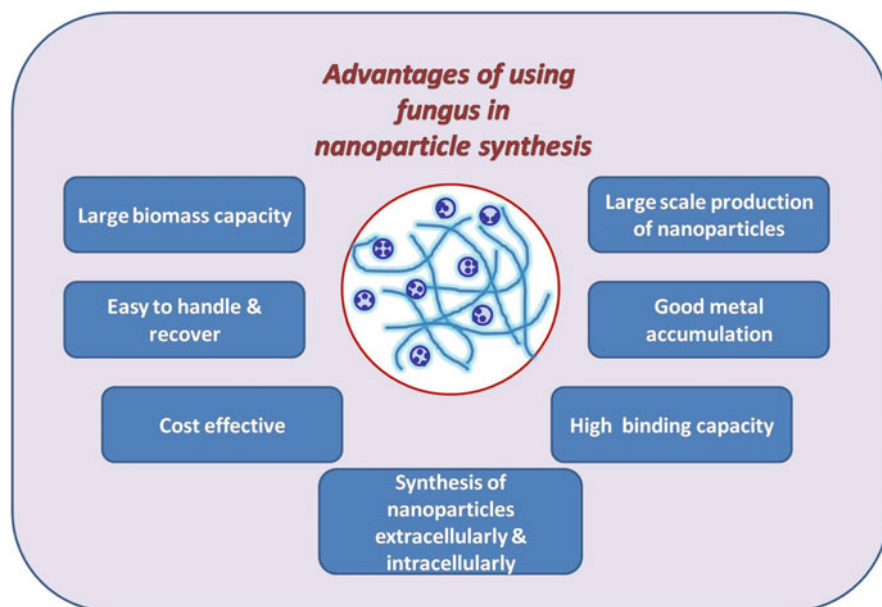


Fig. 13.4 Advantages of using fungus-mediated nanoparticle synthesis

13.5 Nanoparticle Synthesis Mediated by Algae

Algae are considered to have the capability to accumulate heavy metals from the environment and to synthesize nanoparticles. The bio-reduction ability of algae has shown the potential of a wide range of metallic and metal oxide nanoparticles from gold, silver, palladium (Pd), platinum, cadmium sulfate (CdSO_4), zinc oxide (ZnO), and copper oxide (CuO) (Azizi et al. 2014; Jena et al. 2013; Lengke et al. 2006; Momeni and Nabipour 2015; MubarakAli et al. 2012). The dried unicellular alga, namely *Chlorella vulgaris* could synthesize gold nanoparticles by reducing tetrachloroaurate ions to form Au-NPs of different shapes like tetrahedral, decahedral, and icosahedral (Luangpipat et al. 2011). *Sargassum wightii* marine algae can synthesize Au, Ag, and Au/Ag bimetallic nanoparticles extracellularly (Tang et al. 2009). *Phaeodactylum tricoratum*, a phytoplanktonic alga, possesses the ability to fabricate the Cd nanocrystals using phytochelation (Scarano and Morelli 2003). *Shewanella* algae have the potential to reduce aqueous platinum chloride (PtCl_2) to elemental Pt and finally to NPs in their periplasm (Konishi et al. 2007). The study reported by Brayner and coworkers features the importance of cyanobacteria in the synthesis of Au, Pt, Ag, and PdNPs (Brayner et al. 2007). Another species of algae, namely *Turbinariaconoides*, are used for Au NP synthesis (Rajeshkumar et al. 2014). Contrarily, four marine macroalgae like *Colpomeniasinusa*, *Pterocladia capillatae*, *Ulva faciata*, and *Janiarubens* were

applied for Au NP biosynthesis (Rajeshkumar et al. 2014; El-Rafie et al. 2013; Azizi et al. 2013). The edible blue-green algae *Spirulina platensis* was also used to synthesize Ag, Au, and Au/Ag bimetallic nanoparticles (Tang et al. 2009). The exact mechanism of intracellular and extracellular formation of nanoparticles by algal biomass is yet to be recognized.

13.6 Nanoparticle Synthesis Mediated by Viruses

The application of virus for NP synthesis is of a novel approach that has the potential to generate inorganic NPs like silicon dioxide (SiO_2), CdS, ZnS, and iron oxide (Fe_2O_3). The utilization of the whole virus has been of great research thought for the last few decades intended for the synthesis of quantum dots (Zeng et al. 2013). Novel synthesis routes of semiconductor nano-heterostructures were developed by Chuanbin Mao's group in 2003 using M13 bacteriophage (Mao et al. 2003). One of the attractive characteristic features of utilizing viral mediators is their complex capsid proteins that are highly responsive to metal ion precursors (Makarov et al. 2014). Biologically synthesized nano-generators of high performance were developed using barium titanate (BaTiO_3) by Yoon Sung Nam and coworkers using the M13 viral template with possible genetic modification (Jeong et al. 2013). The difficulty in synthesizing inorganic nanocrystals using bacteria and fungus could be overcome by utilizing viral mediators. By applying genetic engineering and molecular cloning, phage-based tobacco mosaic virus (TMV) was genetically structured, having the potential to generate NP of requisite dimension (Shenton et al. 1999).

13.7 Nanoparticle Synthesis Mediated by Plants

The utilization of plants for the synthesis of NPs is considered to be the most suitable strategy than using microbes since it is an easily available, non-pathogenic form, and many of the possible pathways that may be involved for synthesis are researched thoroughly. The synthesis of NPs using plant extracts was first reported by the Gardea-Torresdey group by successfully synthesizing silver NPs using *Alfalfa* sprouts (Gardea-Torresdey et al. 2003). One of the major outstanding features shown by the NP in this approach is their higher surface area to volume ratio (Kato 2011). The production of homogenous Ag NP from silver nitrate (AgNO_3) salt within 4 h is attained by using *Jatrocurcas* extract (Bar and Kr 2009). In another study, the seed exudates of *Medicago sativa* could synthesize Ag NP (Borges et al. 2017). The fruit extract of *Terminalia chebula* also exhibited the potential to synthesize Ag NP (Edison and Sethuraman 2012). The spherical Au NPs (20 nm) were synthesized with the aid of flower extract from *Nyctanthes arbor tristis* (night jasmine) (Das et al. 2011). It is reported by Kasturi et al. in their study that the phyllanthin extracted from *Phyllanthus amarus* can be used for the synthesis of Ag and Au nanoparticles. It is observed that the concentration of phyllanthin directly

influenced the size and shape of the particle. In the presence of low phyllanthin concentration, triangular- and hexagonal-shaped NPs are formed whereas, in the presence of higher concentration, spherical-shaped NP is produced (Kasthuri et al. 2009).

The extracts of soya, *Tridax procumbens* and *Aloe barbadensis* are used for the synthesis of Cu and CuONPs (Gunalan et al. 2012; Rafique et al. 2020). The synthesis of ZnO NPs is accomplished with the help of plants, namely *Zingiber officinale*, *Ficus benghalensis*, *Parthenium hysterophorus*, *Sapindus rarak*, *Passiflora foetida* and *Ficus benghalensis* (Shekhawat et al. 2015). Interestingly, the latex from the stem of *Euphorbia nivulia* is used to synthesize a class of Cu NPs which is stabilized and coated with the peptides and terpenoids present in the latex (Valodkar et al. 2011). Initially, the synthesis of Pt NPs was made with the help of *Diospyros kaki* (Persimmon) leaf extract (Jae et al. 2010) and the presence of the ketones in the extract acts as a reducing agent for Pt ions. Moreover, *Gardenia jasminoides* (Cape jasmine) extract is used to synthesize Pd NPs and the antioxidants present in the extract act as stabilizing and reducing agents (Chen et al. 2009). Plant extract-based nanoparticle synthesis is more advantageous than microbes. It follows a single-step process, nonpathogenic condition, easily available and economical, a significant amount of metabolite production, low hazardous chemical waste, and is an environmentally beneficial approach (Ahn et al. 2019).

13.8 Factors Affecting the Biosynthesis of Nanoparticles

The synthesis, characterization, and application of NPs depend on several factors. Even a slight modification in the type of the adsorbate and the change in the activity of catalysts influence the synthesis process (Ajayan 2004; Somorjai and Park 2008). The dynamic nature of the particle gets altered with a change in time and temperature (Pennycook et al. 2012). Various important other factors directly affect the synthesis, including the pH and temperature of the solution, the concentration of the extract and raw material used, and the procedure chosen for the process (Baker et al. 2013). The method varies from physical techniques using mechanical procedure to chemical and biological processes. The process selected holds the highest priority as it should be eco-friendly and more acceptable than the other conventional methods (Kharissova et al. 2013; Varahalarao et al. 2014). The pH of the solution mixture directly influences the texture and size of the synthesized nanoparticle. So, by controlling the pH, the size of the NP can be adjusted. Another important parameter that affects the synthesis is the temperature. Most physical method prefers a temperature above 350 °C, whereas the chemical method require a temperature below 350 °C and in the biological method temperature, less than 100 °C is desirable. The temperature of the reaction medium influence the nature of the particle formed (Rai et al. 2006).

The pressure applied to the medium influence the shape and size of the synthesized NPs, and also, the reduction rate of metal ions is much faster at appropriate pressure (Pandey 2012; Tran and Le 2013). Time is an important feature that affects the quality and size of the NP. The incubation time of the reaction

mixture greatly influences the synthesis process (Darroudi et al. 2011). For the efficient application of NPs for different purposes, the cost associated with the production should be able to regulate and control. The biological synthesis is found to be cost-effective and can be implemented for large-scale purposes. The particle size is influenced by determining the properties of the NPs. The quality and application of the nanoparticle are greatly influenced by the porosity, especially for biomedical and drug delivery applications. An efficient extraction method for synthesized NPs from the reaction medium also dramatically affects their application in the biomedical and pharmaceutical sectors (Kowalczyk et al. 2011).

13.9 Characterization of the Synthesized Nanoparticle

The characterization of NPs faces immense challenges that affect the detailed features and finally affect their properties. The ultimate task is choosing the appropriate technique for the characterization studies. The characterization is mainly performed to address the particle size distribution, porosity, surface area, pore size, solubility, zeta potential, aggregation, crystallinity, intercalation, dispersion, etc. (Ingale and Chaudhari 2013). To determine the NP parameters, several techniques are employed such as UV-visible spectrometry, Fourier transformation infrared spectroscopy (FT-IR), Electron microscopy, Energy-dispersive spectroscopy (EDS), Dynamic light scattering (DLS), Zeta potential, X-ray diffraction (XRD), Atomic Force Microscopy (AFM), and other techniques designed to measure the parameters are detailed in Table 13.1.

13.10 Safety Aspects of Green Synthesized Nanoparticles

The advancement in nanotechnology research has created a potential solution to so many areas of day-to-day life. So, laws and approvals are obligatory to regulate the applications of nanomaterials due to their toxicity and impact on health, which stands really of great concern. Effective regulation is of higher priority as the benefits obtained from these techniques can be transferred to society. The necessary rules are required in the following stages production, handling, distribution, storage, and disposal (Seaton et al. 2010). In early 2000, the first product of nanotechnology came into the market. The United States took the first step to form regulations for nanomaterials by forming “The Interagency Working Group on Nanotechnology” (IWGN) under the National Science and Technology Council. In India, RIS—“Research and Information System” for Developing countries launched “Nanomaterials Program: Sciences and Devices”, which is in the 12th five-year plan from 2012 to 2017 which is proposed for performing research and development programs to introduce 14 products, processes, and technologies in the field of nanotechnology (Kumar 2014). One important factor to be carefully considered while comparing with other synthesis methods is that NPs synthesized by the green method are less toxic than others thereby providing an eco-friendly approach.

Table 13.1 Commonly used instruments for the characterization of nanoparticles

Characterization tools	Functions
UV visible spectroscopy	To detect the surface plasmon resonance (SPR), which is contributed to the reverberation of electron band on the surface of metal nanoparticles using lightwave
Transmission, scanning, and high-resolution electron microscopy (TEM, SEM, and HR-TEM)	To clarify the morphological shapes, size, and aggregation of nanoparticles
Fourier transformation infrared spectroscopy (FT-IR)	To detect the functional groups required for the stabilization of nanoparticles
Dynamic light scattering (DLS)	To detect the agglomeration and size distribution of nanoparticles
Energy-dispersive spectroscopy (EDX)	To identify the purity and elemental composition of green synthesized nanoparticles
Zeta potential	To detect the surface charge of the nanoparticles, which determines their stability
X-ray diffraction (XRD)	To determine the crystallographic shape and crystalline size of the nanoparticle
Atomic force microscope (AFM)	To analyze the 2D and 3D morphology of nanoparticles
Thermogravimetric analysis	To evaluate the thermal behavior of the particle
Mass spectrometry (MS)	To study the chemical state, elemental, and molecular compositions of NPs and also to determine conjugation with biomolecules
Inductively coupled plasma-MS (ICP-MS)	To assess the size distribution, chemical composition, and concentration of NPs
Ferromagnetic resonance (FMR)	To identify NP size, shape, distribution, and surface composition.
Differential centrifugal sedimentation (DCS)	To detect the NP size based on the sedimentation rate

However, research is still needed to understand the best technique for evaluating the efficiency and risk of nanoparticles synthesized by green approach. It is also necessary to standardize the experiment and establish special regulations for the application of green synthesized NPs.

13.11 Application of Nanoparticles Developed by Green Synthesis

A wide range of NPs has been produced using green synthesis approach. They have been successfully used in the field of pharmaceuticals, agriculture, anti-microbial agents, cosmetics, water treatment, textile industry, drug delivery, imaging purpose, etc. (Fig. 13.5). The NP used in the medical application significantly impacted the early detection system, diagnostic ideal, especially for imaging and treatment of many drug-resistant microbial pathogens (Luo et al. 2014; Fahimmunisha et al.

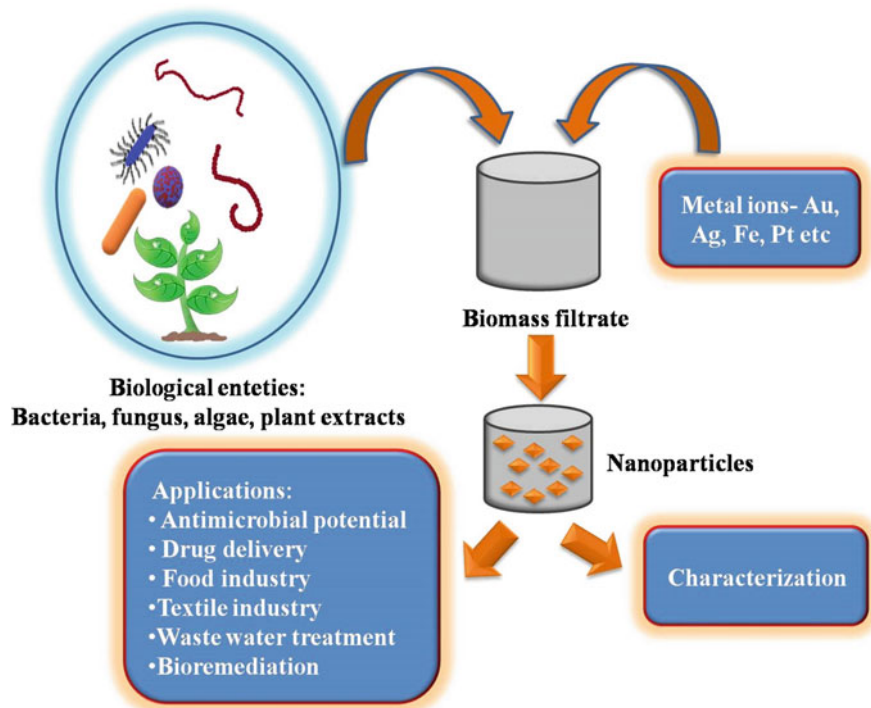


Fig. 13.5 Green synthesis of NPs and their prospective applications

2020). The biologically synthesized NPs, especially from microbial and plant origin, ensure high anti-microbial properties. The Ag-NP synthesized by *Pestalotia* sp. has antibacterial potential against human pathogens (Raheman et al. 2011). It is similarly reported to have antifungal activity against *Candida albicans* and efficient larvicidal action against *Aedes aegypti* (Suresh et al. 2014). ZnONPs synthesized from green approach exhibited anti-microbial activity towards both Gram-positive and Gram-negative, especially *E.coli*, *Salmonella typhimurium*, *Pseudomonas aeruginosa*, *Listeria monocytogens*, and *Staphylococcus aureus* (Fouda et al. 2020; Ogunyemi et al. 2019). The large diversity in the nanomaterials has been investigated for improved and efficient cancer therapy and also to reduce the side effects compared to conventional treatment strategies (Unal et al. 2020).

The inorganic metal and metal oxide NPs such as Ag, Au, Nickel (Ni), ZnO, Fe₂O₃, and (TiO₂) is the most gifted materials applicable in medicine, especially for imaging, drug and gene delivery, targeted therapy, and biosensing. One of the most predicted functions for therapeutic application of nanoparticles is to deliver the drug effectively to the target site in which green NP exhibit sufficient potential for targeted drug delivery. The green synthesis of AuNPs is effective for targeted drug delivery for an anthracycline anti-cancer compound doxorubicin. Another important application of NP is in the textile industry, as it improves the performance of finished

fabrics. For example, Ag-NPs has been used up for their improved antibacterial property, UV obstructing, and self-cleaning ability of smooth and finished fabric materials (Fouda et al. 2017; Mohamed et al. 2017).

Similarly, ZnNPs is also being used in the textile industry as it exhibits good anti-microbial property (Mohamed et al. 2019). As NPs have a large surface area to volume ratio, it results in substantial effectiveness in blocking UV radiation compared to initial bulk material (Mohamed et al. 2019). The application of nanotechnology can solve the foremost issue concerned with the scarcity and quality of water (Uddandarao et al. 2019). Nanotechnology can offer a high-performance water treatment facility for wastewater treatment to remove heavy materials and impurities (Zonaro et al. 2017). A variety of nanoparticles has shown the ability to disinfect the wastewater, especially by Ag, ZnO, CuO, TiO₂, etc. (Salvadori 2019; Rafique et al. 2020). Now nanotechnology has become the accepted strategy for water management.

NPs have exposed their application in the food industry mainly in packaging and delivery systems, particularly nanometal oxides such as the ZnO nanoparticles incorporated with polymeric materials are used for packaging purposes, which aids in improved anti-microbial properties (Espitia et al. 2012). Nanomaterials support packaging facility as a part of food safety precautions. The application of NPs in the food industry would benefit from controlling microbial growth, especially biofilm formation (Beeler and Singh 2016). Nanotechnology influenced different sectors of agriculture. One of the main advantages of using NP is to control plant pathogens and is applied as pesticides, fertilizers, and insecticides. CuNPs were synthesized biologically using *Streptomyces* spp. and exhibited antifungal activity against *Pythium ultimum*, *Aspergillus niger*, *Fusarium oxysporum*, and *Alternaria alternata* (Hassan et al. 2019, 2018). One of the problems encountered in the agricultural sector is the usage of excessive chemical fertilizers, shortage in water resources, and low soil fertility, which negatively affects the agricultural sector. It is reported that the minerals and crystals of zeolites can be used as nanofertilizers (Guo et al. 2018). Another application of NP is as nanopesticides in which metal oxides and polymer ingredients in different form and formulation has been accomplished and used as pesticides for various pests, pathogens, insects that threaten the agricultural fields.

The highly persistent and xenobiotic natured pollutants such as dyes, azo dyes, cationic dyes, and acid dyes can be treated biologically and have gained much attention. These hazardous pollutants can create much terrific negative impact on aquatic life when it gets disposed into water bodies, especially in lakes, streams, ponds, sea, etc. (Sharma et al. 2015). Various studies have described that the catalytic activity of certain nanomaterials can reduce these xenobiotics and can lessen the hazards to the environment in a biological way (Zhao et al. 1998). Excitingly, AgNPs have shown a good catalytic ability to reduce organic dyes and to decolorise them. It exhibited the degradation of dyes with good reaction time and efficiency (Zhao et al. 1998). Similarly, both Ag and Au NPs catalyze the degradation of dyes thereby reducing the time required for the dye removal process.

13.12 Conclusion and Future Perspectives

Nanotechnology has provided directions for the application of materials at the nanoscale level. It exhibited a wide range of characteristic properties due to its small size and high surface area to volume ratio compared to its bulk material. A variety of methodologies are used for the synthesis of nanoparticles. The conventional synthesis method in both physical and chemical approaches creates toxic chemical waste and is hazardous to the environment. The alternate approach is the “green synthesis” method, in which biological agents such as bacteria, fungus, yeasts, algae, and plants are utilized as a part of their synthesis. The green approach provides many advantages like availability and synthesis, cost-effectiveness, less toxic, and eco-friendly than conventional strategies. The green synthesis of NPs opened the way for many applications in biotechnology. The production of metal and metal oxide NPs using green synthesis has been used for anti-microbial and anti-tumor activities, controlling pathogens, food industry, agriculture sector, bioremediation, and water treatment.

The mechanism of green synthesis still needs to be more explored. The green synthesis method requires more optimization studies for the specific size and shape of the NPs and to understand the physicochemical characteristic properties to be applied in the field of biomedical science. The majority of the research in this approach is restricted to metallic NPs rather, research needs to be expanded for synthesizing lipid, polymeric, silica, and other types using green approach. The metabolites that are involved in the biosynthesis of NPs need to be thoroughly investigated, and also the role played by each candidate metabolite need to be studied. For the commercialization of the green synthesized NPs, the scale-up of the production is the next challenging issue. Further research is required to develop new biosynthesis methods, and their application in various disciplines is of higher priority.

References

- Ahmad A, Mukherjee P, Mandal D, Senapati S, Khan MI, Kumar R, Sastry M (2002) Enzyme mediated extracellular synthesis of CdS nanoparticles by the fungus, *Fusarium oxysporum*. *J Am Chem Soc* 124(41):12,108–12,109
- Ahn EY, Jin H, Park Y (2019) Assessing the antioxidant, cytotoxic, apoptotic and wound healing properties of silver nanoparticles green-synthesised by plant extracts. *Mater Sci Eng C* 101:204–216
- Ajayan PM (2004) How does a nanofibre grow? *Nature* 427(6973):402–403
- Akhtar MS, Panwar J, Yun YS (2013) Biogenic synthesis of metallic nanoparticles by plant extracts. *ACS Sustain Chem Eng* 1(6):591–602
- Anastas PT, Warner JC (1998) Principles of green chemistry. *Green Chem Theory Pract* 29
- Antonyraj CA, Jeong J, Kim B, Shin S, Kim S, Lee KY, Cho JK (2013) Selective oxidation of HMF to DFF using Ru/ γ -alumina catalyst in moderate boiling solvents toward industrial production. *J Ind Eng Chem* 19(3):1056–1059

- Ashraf R, Sultana B, Riaz S, Mushtaq M, Iqbal M, Nazir A et al (2018) Fortification of phenolics, antioxidant activities and biochemical attributes of radish root by plant leaf extract seed priming. *Biocatal Agric Biotechnol* 16:115–120
- Azizi S, Namvar F, Mahdavi M, Ahmad MB, Mohamad R (2013) Biosynthesis of silver nanoparticles using brown marine macroalga, *Sargassum muticum* aqueous extract. *Materials* 6(12):5942–5950
- Azizi S, Ahmad MB, Namvar F, Mohamad R (2014) Green biosynthesis and characterisation of zinc oxide nanoparticles using brown marine macroalga *Sargassum muticum* aqueous extract. *Mater Lett* 116:275–277
- Baker S, Rakshith D, Kavitha KS, Santosh P, Kavitha HU, Rao Y, Satish S (2013) Plants: emerging as nanofactories towards facile route in the synthesis of nanoparticles. *Bioimpacts* 3(3):111
- Bar H, Kr D (2009) Bhui, GP Sahoo, P. Sarkar, SP De, and A. Misra. *Colloids Surf., A*, 339, 134–139
- Beeler E, Singh OV (2016) Extremophiles as sources of inorganic bio-nanoparticles. *World J Microbiol Biotechnol* 32(9):1–11
- Bhattacharya D, Gupta RK (2005) Nanotechnology and potential of microorganisms. *Crit Rev Biotechnol* 25(4):199–204
- Bibi I, Kamal S, Ahmed A, Iqbal M, Nouren S, Jilani K et al (2017a) Nickel nanoparticle synthesis using *camellia sinensis* as reducing and capping agent: growth mechanism and photocatalytic activity evaluation. *Int J Biol Macromol* 103:783–790
- Bibi I, Nazar N, Iqbal M, Kamal S, Nawaz H, Nouren S et al (2017b) Green and eco-friendly synthesis of cobalt-oxide nanoparticles: characterisation and photocatalytic activity. *Adv Powder Technol* 28(9):2035–2043
- Borges LGA, Savi A, Teixeira C, de Oliveira RP, De Camillis MLF, Wickert R et al (2017) Mechanical ventilation weaning protocol improves medical adherence and results. *J Crit Care* 41:296–302
- Brayner R, Barberousse H, Hemadi M, Djedjat C, Yéprémian C, Coradin T et al (2007) Cyanobacteria as bioreactors for the synthesis of Au, Ag, Pd, and Pt nanoparticles via an enzyme-mediated route. *J Nanosci Nanotechnol* 7(8):2696–2708
- Castro L, Blázquez ML, Muñoz JA, González F, Ballester A (2013) Biological synthesis of metallic nanoparticles using algae. *IET Nanobiotechnol* 7(3):109–116
- Cauerhff A, Castro GR (2013) Bionanoparticles, a green nanochemistry approach electronic journal of biotechnology, vol. 16, núm. 3, 2013, pp. 1–10 Pontificia Universidad Católica de Valparaíso Valparaíso, Chile. *Electron J Biotechnol* 16(3):1–10
- Chauhan RP, Gupta C, Prakash D (2012) Methodological advancements in green nanotechnology and their applications in the biological synthesis of herbal nanoparticles. *Int J Bioassays* 1:6–10
- Chen G, Liu H, Somesfalean G, Liang H, Zhang Z (2009) Upconversion emission turning from green to red in Yb³⁺/Ho³⁺-codoped NaYF₄ nanocrystals by tridoping with Ce³⁺ ions. *Nanotechnology* 20(38):385704
- Dameron CT, Winge DR (1990) Characterisation of peptide-coated cadmium-sulfide crystallites. *Inorg Chem* 29(7):1343–1348
- Daniel MC, Astruc D (2004) Gold nanoparticles: assembly, supramolecular chemistry, quantum-size-related properties, and applications toward biology, catalysis, and nanotechnology. *Chem Rev* 104(1):293–346
- Darroudi M, Ahmad MB, Zamiri R, Zak AK, Abdullah AH, Ibrahim NA (2011) Time-dependent effect in green synthesis of silver nanoparticles. *Int J Nanomedicine* 6:677
- Das RK, Gogoi N, Bora U (2011) Green synthesis of gold nanoparticles using *Nyctanthes arbortristis* flower extract. *Bioprocess Biosyst Eng* 34(5):615–619
- Dulinska-Molak I, Chlanda A, Li J, Wang X, Bystrzejewski M, Kawazoe N et al (2018) The influence of carbon-encapsulated iron nanoparticles on the elastic modulus of living human mesenchymal stem cells examined by atomic force microscopy. *Micron* 108:41–48
- Duran N, Gaikwad S, Rai M, Gade A (2014) Green synthesis of silver nanoparticles by *Phoma glomerata*. *Micron* 59:52–59

- Edison TJI, Sethuraman MG (2012) Instant green synthesis of silver nanoparticles using *Terminalia chebula* fruit extract and evaluation of their catalytic activity on reduction of methylene blue. *Process Biochem* 47(9):1351–1357
- El Domany EB, Essam TM, Ahmed AE, Farghali AA (2018) Biosynthesis physico-chemical optimisation of gold nanoparticles as anti-cancer and synergetic anti-microbial activity using *Pleurotus ostreatus* fungus. *J Appl Pharm Sci* 8:119–128
- Elamawi RM, Al-Harbi RE, Hendi AA (2018) Biosynthesis and characterisation of silver nanoparticles using *Trichoderma longibrachiatum* and their effect on phytopathogenic fungi. *Egypt J Biol Pest Contr* 28(1):1–11
- Elfeky AS, Salem SS, Elzaref AS, Owda ME, Eladawy HA, Saeed AM et al (2020) Multifunctional cellulose nanocrystal/metal oxide hybrid, photo-degradation, antibacterial and larvicidal activities. *Carbohydr Polym* 230:115711
- El-Rafie HM, El-Rafie M, Zahran MK (2013) Green synthesis of silver nanoparticles using polysaccharides extracted from marine macroalgae. *Carbohydr Polym* 96(2):403–410
- Espitia PJP, Soares NDF, dos Reis Coimbra JS, de Andrade NJ, Cruz RS, Medeiros EAA (2012) Zinc oxide nanoparticles: synthesis, anti-microbial activity and food packaging applications. *Food Bioprocess Technol* 5(5):1447–1464
- Fahimmunisha BA, Ishwarya R, AlSalhi MS, Devanesan S, Govindarajan M, Vaseeharan B (2020) Green fabrication, characterisation and antibacterial potential of zinc oxide nanoparticles using aloe socotrina leaf extract: a novel drug delivery approach. *J Drug Deliv Sci Technol* 55:101,465
- Faraday M (1857) LIX. Experimental relations of gold (and other metals) to light. —The Bakerian lecture. London, Edinburgh, and Dublin *Philos Magaz J Sci* 14(96):512–539
- Fierascu R, Iona R, Dumitriu I (2010) Noble metals nanoparticles synthesis in plant extracts. *Synthesis* 1:22
- Fouda A, Mohamed A, Elgamal MS, El-Din Hassan S, Salem Salem S, Shaheen TI (2017) Facile approach towards medical textiles via myco-synthesis of silver nanoparticles. *Der Pharma Chemica* 9:11–18
- Fouda A, Saad EL, Salem SS, Shaheen TI (2018) In-vitro cytotoxicity, antibacterial, and UV protection properties of the biosynthesised zinc oxide nanoparticles for medical textile applications. *Microb Pathog* 125:252–261
- Fouda A, Abdel-Maksoud G, Abdel-Rahman MA, Salem SS, Hassan SED, El-Sadany MAH (2019) Eco-friendly approach utilising green synthesised nanoparticles for paper conservation against microbes involved in biodeterioration of archaeological manuscript. *Int Biodeterior Biodegradation* 142:160–169
- Fouda A, Hassan SED, Abdo AM, El-Gamal MS (2020) Anti-microbial, antioxidant and larvicidal activities of spherical silver nanoparticles synthesised by endophytic streptomyces spp. *Biol Trace Elem Res* 195(2):707–724
- Gaikwad SC, Birla SS, Ingle AP, Gade AK, Marcato PD, Rai M, Duran N (2013) Screening of different fusarium species to select potential species for the synthesis of silver nanoparticles. *J Braz Chem Soc* 24:1974–1982
- Gardea-Torresdey JL, Gomez E, Peralta-Videa JR, Parsons JG, Troiani H, Jose-Yacamán M (2003) Alfalfa sprouts: a natural source for the synthesis of silver nanoparticles. *Langmuir* 19(4):1357–1361
- Gunalan S, Sivaraj R, Venkatesh R (2012) Aloe barbadensis Miller mediated green synthesis of mono-disperse copper oxide nanoparticles: optical properties. *Spectrochim Acta A Mol Biomol Spectrosc* 97:1140–1144
- Guo H, White JC, Wang Z, Xing B (2018) Nano-enabled fertilisers to control the release and use efficiency of nutrients. *Curr Opin Environ Sci Health* 6:77–83
- Hassan SED, Salem SS, Fouda A, Awad MA, El-Gamal MS, Abdo AM (2018) New approach for anti-microbial activity and bio-control of various pathogens by biosynthesised copper nanoparticles using endophytic actinomycetes. *J Radiat Res Appl Sci* 11(3):262–270

- Hassan SED, Fouda A, Radwan AA, Salem SS, Barghoth MG, Awad MA et al (2019) Endophytic actinomycetes streptomyces spp mediated biosynthesis of copper oxide nanoparticles as a promising tool for biotechnological applications. *JBIC J Biol Inorg Chem* 24(3):377–393
- Ingale AG, Chaudhari AN (2013) Biogenic synthesis of nanoparticles and potential applications: an eco-friendly approach. *J Nanomed Nanotechnol* 4(165):1–7
- Jae YS, Kwon EY, Kim BS (2010) Biological synthesis of platinum nanoparticles using *Diospyros kaki* leaf extract. *Bioprocess Biosyst Eng* 33:159–164
- Jena J, Pradhan N, Dash BP, Sukla LB, Panda PK (2013) Biosynthesis and characterisation of silver nanoparticles using microalga *Chlorococcum humicola* and its antibacterial activity. *Int J Nanomater Biostruct* 3(1):1–8
- Jeong CK, Kim I, Park KI, Oh MH, Paik H, Hwang GT et al (2013) Virus-directed design of a flexible BaTiO₃ nano-generator. *ACS Nano* 7(12):11,016–11,025
- John MS, Nagoth JA, Ramasamy KP, Mancini A, Giuli G, Natalello A et al (2020) Synthesis of bioactive silver nanoparticles by a pseudomonas strain associated with the antarctic psychrophilic protozoan *Euplates focardii*. *Mar Drugs* 18(1):38
- Kasthuri J, Kathiravan K, Rajendiran N (2009) Phyllanthin-assisted biosynthesis of silver and gold nanoparticles: a novel biological approach. *J Nanopart Res* 11(5):1075–1085
- Kato H (2011) Tracking nanoparticles inside cells. *Nat Nanotechnol* 6(3):139–140
- Khabat V, Mansoori GA, Karimi S (2011) Biosynthesis of silver nanoparticles by fungus *Trichoderma Reesei*. *Insciences J* 1(1):65–79
- Khan R, Fulekar MH (2016) Biosynthesis of titanium dioxide nanoparticles using *Bacillus amyloliquefaciens* culture and enhancement of its photocatalytic activity for the degradation of a sulfonated textile dye reactive red 31. *J Colloid Interface Sci* 475:184–191
- Kharisova OV, Dias HR, Kharisov BI, Pérez BO, Pérez VMJ (2013) The greener synthesis of nanoparticles. *Trends Biotechnol* 31(4):240–248
- Konishi Y, Ohno K, Saitoh N, Nomura T, Nagamine S, Hishida H et al (2007) Bioreductive deposition of platinum nanoparticles on the bacterium *Shewanella algae*. *J Biotechnol* 128(3): 648–653
- Kotil T, Akbulut C, Yön ND (2017) The effects of titanium dioxide nanoparticles on ultrastructure of zebrafish testis (*Danio rerio*). *Micron* 100:38–44
- Kowalczyk B, Lagzi I, Grzybowski BA (2011) Nanoseparations: strategies for size and/or shape-selective purification of nanoparticles. *Curr Opin Colloid Interface Sci* 16(2):135–148
- Kumar A (2014) Nanotechnology development in India: an overview. *Research and Information System for Developing Countries*
- Lengke MF, Fleet ME, Southam G (2006) Synthesis of platinum nanoparticles by reaction of filamentous cyanobacteria with platinum (IV)–chloride complex. *Langmuir* 22(17):7318–7323
- Li X, Xu H, Chen ZS, Chen G (2011) Biosynthesis of nanoparticles by microorganisms and their applications. *J Nanomater* 2011
- Lian S, Diko CS, Yan Y, Li Z, Zhang H, Ma Q, Qu Y (2019) Characterisation of biogenic selenium nanoparticles derived from cell-free extracts of a novel yeast *Magnusiomyces ingens*. *3Biotech* 9(6):1–8
- Luangpipat T, Beattie IR, Chisti Y, Haverkamp RG (2011) Gold nanoparticles produced in a microalga. *J Nanopart Res* 13(12):6439–6445
- Luechinger NA, Grass RN, Athanassiou EK, Stark WJ (2010) Bottom-up fabrication of metal/metal nanocomposites from nanoparticles of immiscible metals. *Chem Mater* 22(1):155–160
- Luo QY, Lin Y, Li Y, Xiong LH, Cui R, Xie ZX, Pang DW (2014) Nanomechanical analysis of yeast cells in CdSe quantum dot biosynthesis. *Small* 10(4):699–704
- Makarov VV, Love AJ, Sinitsyna OV, Makarova SS, Yaminsky IV, Talianky ME, Kalinina NO (2014) “Green” nanotechnologies: synthesis of metal nanoparticles using plants. *Acta Naturae (англоязычная версия)* 6(1):20
- Mandal D, Bolander ME (2006) ME; Mukhopadhyay, D.; Sarkar, G.; Mukherjee, P. *Appl Microbiol Biotechnol* 69, 485

- Mandal D, Bolander ME, Mukhopadhyay D, Sarkar G, Mukherjee P (2006) The use of microorganisms for the formation of metal nanoparticles and their application. *Appl Microbiol Biotechnol* 69(5):485–492
- Mandeep PS (2020) Microbial nanotechnology for bioremediation of industrial wastewater. *Front Microbiol* 11
- Mao C, Flynn CE, Hayhurst A, Sweeney R, Qi J, Georgiou G et al (2003) Viral assembly of oriented quantum dot nanowires. *Proc Natl Acad Sci* 100(12):6946–6951
- Metuku RP, Pabba S, Burra S, Gudikandula K, Charya MS (2014) Biosynthesis of silver nanoparticles from *Schizophyllum radiatum* HE 863742.1: their characterisation and antimicrobial activity. *3 Biotech* 4(3):227–234
- Minuto A, Spadaro D, Garibaldi A, Gullino ML (2006) Control of soilborne pathogens of tomato using a commercial formulation of *Streptomyces griseoviridis* and solarisation. *Crop Prot* 25(5): 468–475
- Mohamed A, Fouda A, Elgamel M, El-Din Hassan S, Shaheen T, Salem S (2017) Enhancing of cotton fabric antibacterial properties by silver nanoparticles synthesised by new Egyptian strain *Fusarium keratoplasticum* A1-3. *Egyptian Journal of Chemistry*, 60(Conference Issue (The 8th International Conference of The Textile Research Division (ICTRD 2017), National Research Centre, Cairo 12622, Egypt.)), pp 63–71
- Mohamed AA, Fouda A, Abdel-Rahman MA, Hassan SED, El-Gamal MS, Salem SS, Shaheen TI (2019) Fungal strain impacts the shape, bioactivity and multifunctional properties of green synthesised zinc oxide nanoparticles. *Biocatal Agric Biotechnol* 19:101103
- Mohanpuria P, Rana NK, Yadav SK (2008) Biosynthesis of nanoparticles: technological concepts and future applications. *J Nanopart Res* 10(3):507–517
- Momeni S, Nabipour I (2015) A simple green synthesis of palladium nanoparticles with sargassum alga and their electrocatalytic activities towards hydrogen peroxide. *Appl Biochem Biotechnol* 176(7):1937–1949
- MubarakAli D, Gopinath V, Rameshbabu N, Thajuddin N (2012) Synthesis and characterisation of CdS nanoparticles using C-phycoerythrin from the marine cyanobacteria. *Mater Lett* 74:8–11
- Mukherjee, Roy M, Mandal BP, Dey GK, Mukherjee PK, Ghatak J et al (2008) Green synthesis of highly stabilised nanocrystalline silver particles by a non-pathogenic and agriculturally important fungus *T. asperellum*. *Nanotechnology* 19(7):075103
- Nazar N, Bibi I, Kamal S, Iqbal M, Nouren S, Jilani K, Umair M, Ata S (2018) Cu nanoparticles synthesis using biological molecule of *P. granatum* seeds extract as reducing and capping agent: growth mechanism and photocatalytic activity. *Int J Biol Macromol* 106:1203–1210
- Nevalainen H, Suominen P, Taimisto K (1994) On the safety of *Trichoderma reesei*. *J Biotechnol* 37(3):193–200
- Neville F, Pchelintsev NA, Broderick MJ, Gibson T, Millner PA (2009) Novel one-pot synthesis and characterisation of bioactive thiol-silicate nanoparticles for biocatalytic and biosensor applications. *Nanotechnology* 20(5):055612
- Njagi EC, Huang H, Stafford L, Genuino H, Galindo HM, Collins JB et al (2011) Biosynthesis of iron and silver nanoparticles at room temperature using aqueous sorghum bran extracts. *Langmuir* 27(1):264–271
- Nwamezie OUIF (2018) Green synthesis of iron nanoparticles using flower extract of *Piliostigmathamningii* and their antibacterial activity evaluation. *Chem Int* 4(1):60–66
- Ogunyemi SO, Abdallah Y, Zhang M, Fouad H, Hong X, Ibrahim E et al (2019) Green synthesis of zinc oxide nanoparticles using different plant extracts and their antibacterial activity against *Xanthomonas oryzae* pv. *oryzae*. *Artif Cells Nanomed Biotechnol* 47(1):341–352
- Pandey BD (2012) Synthesis of zinc-based nanomaterials: a biological perspective. *IET Nanobiotechnol* 6(4):144–148
- Parashar U, Saxena S, Srivastava A (2009a) Bioinspired synthesis of silver nanoparticles. *Digest J Nanomater Biostruct* 4(1)

- Parashar V, Parashar R, Sharma B, Pandey AC (2009b) Parthenium leaf extract mediated synthesis of silver nanoparticles: a novel approach towards weed utilisation. *Digest J Nanomater Biostruct* 4(1)
- Pennycook TJ, McBride JR, Rosenthal SJ, Pennycook SJ, Pantelides ST (2012) Dynamic fluctuations in ultrasmall nanocrystals induce white light emission. *Nano Lett* 12(6):3038–3042
- Prabhu S, Poulouse EK (2012) Silver nanoparticles: mechanism of anti-microbial action, synthesis, medical applications, and toxicity effects. *Int Nano Lett* 2(1):1–10
- Rafique M, Shafiq F, Gillani SSA, Shakil M, Tahir MB, Sadaf I (2020) Eco-friendly green and biosynthesis of copper oxide nanoparticles using *Citrofortunellamicrocarpa* leaves extract for efficient photocatalytic degradation of Rhodamin B dye from textile wastewater. *Optik* 208: 164,053
- Raheman F, Deshmukh S, Ingle A, Gade A, Rai M (2011) Silver nanoparticles: novel anti-microbial agent synthesised from an endophytic fungus *Pestalotia* sp. isolated from leaves of *Syzygiumcumini* (L). *Nano Biomed Eng* 3(3):174–178
- Rai A, Singh A, Ahmad A, Sastry M (2006) Role of halide ions and temperature on the morphology of biologically synthesised gold nanotriangles. *Langmuir* 22(2):736–741
- Rajeshkumar S, Malarkodi C, Paulkumar K, Vanaja M, Gnanajobitha G, Annadurai G (2014) Algae mediated green fabrication of silver nanoparticles and examination of its antifungal activity against clinical pathogens. *Int J Metals* 2014
- Remya VR, Abitha VK, Rajput PS, Rane AV, Dutta A (2017) Silver nanoparticles green synthesis: a mini-review. *Chem Int* 3(2):165–171
- Rónavári A, Igaz N, Gopisetty MK, Szerencsés B, Kovács D, Papp C et al (2018) Biosynthesized silver and gold nanoparticles are potent antimicrobials against opportunistic pathogenic yeasts and dermatophytes. *Int J Nanomedicine* 13:695
- Salvadori MR (2019) Processing of nanoparticles by biomatrices in a green approach. In *Microbial nanobionics* (pp. 1–28). Springer, Cham
- Sarkar J, Mollick MMR, Chattopadhyay D, Acharya K (2017) An eco-friendly route of γ -Fe₂O₃ nanoparticles formation and investigation of the mechanical properties of the HPMC- γ -Fe₂O₃ nanocomposites. *Bioprocess Biosyst Eng* 40(3):351–359
- Scarano G, Morelli E (2003) Properties of phytochelatin-coated CdSnanocrystallites formed in a marine phytoplanktonic alga (*Phaeodactylumtricornutum*, Bohlin) in response to cd. *Plant Sci* 165(4):803–810
- Seaton A, Tran L, Aitken R, Donaldson K (2010) Nanoparticles, human health hazard and regulation. *J Roy Soc Interf* 7(suppl_1):S119–S129
- Shaheen TI, Fouda A (2018) Green approach for one-pot synthesis of silver nanorod using cellulose nanocrystal and their cytotoxicity and antibacterial assessment. *Int J Biol Macromol* 106:784–792
- Sharaf OM, Al-Gamal MS, Ibrahim GA, Dabiza NM, Salem SS, El-Ssayad MF, Youssef AM (2019) Evaluation and characterisation of some protective culture metabolites in free and nano-chitosan-loaded forms against common contaminants of Egyptian cheese. *Carbohydr Polym* 223:115094
- Sharma K, Singh G, Kumar M, Bhalla V (2015) Silver nanoparticles: facile synthesis and their catalytic application for the degradation of dyes. *RSC Adv* 5(33):25,781–25,788
- Shekhawat MS, Ravindran CP, Manokari M (2015) An eco-friendly method for the synthesis of zinc oxide nanoparticles using *Lawsoniainermis* L. aqueous extracts. *Int J Innov* 5(1):1
- Shelar GB, Chavan AM (2014) Fungus-mediated biosynthesis of silver nanoparticles and its antibacterial activity. *Arch Appl Sci Res* 6:111–114
- Shenton W, Douglas T, Young M, Stubbs G, Mann S (1999) Inorganic–organic nanotube composites from template mineralisation of tobacco mosaic virus. *Adv Mater* 11(3):253–256
- Shivaji S, Madhu S, Singh S (2011) Extracellular synthesis of antibacterial silver nanoparticles using psychrophilic bacteria. *Process Biochem* 46(9):1800–1807
- Singh M, Manikandan S, Kumaraguru AK (2011) Nanoparticles: a new technology with wide applications. *Res J Nanosci Nanotechnol* 1(1):1–11

- Soliman H, Elsayed A, Dyaa A (2018) Anti-microbial activity of silver nanoparticles biosynthesised by *Rhodotorula* sp. strain ATL72. *Egypt J Basic Appl Sci* 5(3):228–233
- Somorjai GA, Park JY (2008) Colloid science of metal nanoparticle catalysts in 2D and 3D structures. Challenges of nucleation, growth, composition, particle shape, size control and their influence on activity and selectivity. *Top Catal* 49(3–4):126–135
- Srinath BS, Namratha K, Byrappa K (2018) Eco-friendly synthesis of gold nanoparticles by *Bacillus subtilis* and their environmental applications. *Adv Sci Lett* 24(8):5942–5946
- Staniland SS (2007) Magnetosomes: bacterial biosynthesis of magnetic nanoparticles and potential biomedical applications. *Nanotechnol Life Sci Online*
- Suresh G, Gunasekar PH, Kokila D, Prabhu D, Dinesh D, Ravichandran N et al (2014) Green synthesis of silver nanoparticles using *Delphinium denudatum* root extract exhibits antibacterial and mosquito larvicidal activities. *Spectrochim Acta A Mol Biomol Spectrosc* 127:61–66
- Sweeney RY, Mao C, Gao X, Burt JL, Belcher AM, Georgiou G, Iverson BL (2004) Bacterial biosynthesis of cadmium sulfide nanocrystals. *Chem Biol* 11(11):1553–1559
- Syed A, Saraswati S, Kundu GC, Ahmad A (2013) Biological synthesis of silver nanoparticles using the fungus *Humicola* sp. and evaluation of their cytotoxicity using normal and cancer cell lines. *Spectrochim Acta A Mol Biomol Spectrosc* 114:144–147
- Tang J, Xiong L, Wang S, Wang J, Liu L, Li J et al (2009) Distribution, translocation and accumulation of silver nanoparticles in rats. *J Nanosci Nanotechnol* 9(8):4924–4932
- Tiwari DK, Behari J, Sen P (2008) Time and dose-dependent anti-microbial potential of silver nanoparticles synthesized by a top-down approach. *Curr Sci*:647–655
- Tomar RS, Chauhan PS, Shrivastava V (2014) A critical review on nanoparticle synthesis: physicochemical v/s biological approach. *World J Pharm Res* 4(1):595–620
- Tran QH, Le AT (2013) Silver nanoparticles: synthesis, properties, toxicology, applications and perspectives. *Adv Nat Sci Nanosci Nanotechnol* 4(3):033001
- Uddandarao P, Balakrishnan RM, Ashok A, Swarup S, Sinha P (2019) Bioinspired ZnS: Gd nanoparticles synthesised from an endophytic fungi *Aspergillus flavus* for fluorescence-based metal detection. *Biomimetics* 4(1):11
- Unal IS, Demirbas A, Onal I, Ildiz N, Ocsoy I (2020) One-step preparation of stable gold nanoparticles using red cabbage extracts under UV light and its catalytic activity. *J Photochem Photobiol B Biol* 204:111,800
- Valodkar M, Jadeja RN, Thounaojam MC, Devkar RV, Thakore S (2011) Biocompatible synthesis of peptide capped copper nanoparticles and their biological effect on tumour cells. *Mater Chem Phys* 128(1–2):83–89
- Varahalarao V, Kaladhar DS, Mohan B, Kishore Naidu G, Sujatha B (2014) Review: green synthesis of silver and gold nanoparticles. *Middle East J Sci Res* 19(6):834–842
- Vidhu VK, Philip D (2014) Catalytic degradation of organic dyes using biosynthesised silver nanoparticles. *Micron* 56:54–62
- Waghmare SS, Deshmukh AM, Kulkarni SW, Oswaldo LA (2011) Biosynthesis and characterisation of manganese and zinc nanoparticles. *Universal J Environ Res Technol* 1(1)
- Zeng Q, Wen H, Wen Q, Chen X, Wang Y, Xuan W et al (2013) Cucumber mosaic virus as drug delivery vehicle for doxorubicin. *Biomaterials* 34(19):4632–4642
- Zhao J, Wu T, Wu K, Oikawa K, Hidaka H, Serpone N (1998) Photoassisted degradation of dye pollutants. 3. Degradation of the cationic dye rhodamine B in aqueous anionic surfactant/TiO₂ dispersions under visible light irradiation: evidence for the need of substrate adsorption on TiO₂ particles. *Environ Sci Technol* 32(16):2394–2400
- Zonaro E, Piacenza E, Presentato A, Monti F, Dell'Anna R, Lampis S, Vallini G (2017) *Ochrobactrum* sp. MPV1 from a dump of roasted pyrites can be exploited as bacterial catalyst for the biogenesis of selenium and tellurium nanoparticles. *Microb Cell Factories* 16(1):1–17



Synthesis, Characterization and Applications of Titanium Dioxide Nanoparticles

14

Remya Rajan Renuka, Narenkumar Jayaraman, Angeline Julius, Velmurugan Palanivel, Vasudevan Ramachandran, Rajesh Pandian, Umesh Luthra, and Suresh Kumar Subbiah

14.1 Introduction

Titania or Titanium dioxide (TiO_2) is an inorganic substance of commercial importance and has a wide range of applications. It has improved functioning in the area of photocatalytic uses to remove various organic contaminants from air and water and is widely used as a dielectric and pigment in paints (Ziental et al. 2020). It is also thought to be a viable option for photoelectrochemical energy generation. Titania, due to its biocompatible and nontoxic nature, is used in biomedical sciences, particularly in bone tissue engineering and pharmaceuticals (Jafari et al. 2020).

TiO_2 is found in both crystalline and amorphous forms, with the three crystalline polymorphous anatase, rutile, and brookite being the most common. Brookite has an orthorhombic structure, whereas anatase and rutile have a tetragonal structure (Mamaghani et al. 2019). The immobilization of TiO_2 nanoparticles on a suitable substrate has gained widespread acceptance because it has the potential to reduce the cost of phase separation procedures and increase the practical aspect of these catalysts as a process for industrial development (Al-Madanat et al. 2021). Nanotechnology is concerned with the synthesis and characterization of nanoscale materials, as well as the comprehension and application of their prospective uses (El Shafey 2020). Materials at the nanoscale scale are emerging as interdisciplinary fields encompassing physics, chemistry, and biology. Many fundamental properties of materials, such as optical, electrical, catalytic, and mechanical, were previously understood to be a result of their size, composition, and structural order (Nasrollahzadeh et al. 2019b).

R. R. Renuka · N. Jayaraman · A. Julius · V. Palanivel · V. Ramachandran · R. Pandian · U. Luthra · S. K. Subbiah (✉)

Centre for Materials Engineering and Regenerative Medicine, Bharath Institute of Higher Education and Research, Chennai, Tamil Nadu, India

e-mail: pvc_gp@bharathuniv.ac.in

© The Author(s), under exclusive license to Springer Nature Singapore Pte Ltd. 2023

P. V. Mohanan, S. Kappalli (eds.), *Biomedical Applications and Toxicity of Nanomaterials*, https://doi.org/10.1007/978-981-19-7834-0_14

339

Pigments, optic filters, antireflective coatings, chemical detectors or sensors, catalytic converters, and sterilizing materials are just a few of the uses for TiO₂ (Mandeh et al. 2012). Because of its electrical and structural qualities, it has a wide range of uses. The high visible spectral transmission, high refractive index, chemically stable, photocatalytic, and antibacterial properties are all key qualities of this material. Anatase, rutile, and brookite are the three crystal forms of TiO₂ (Parrino et al. 2020). The functional characteristics, surface area, quantity of defects, transition temperature phases, and distinct phases stability are all influenced by the size and shape of TiO₂ particles (Zhang and Banfield 2014). Furthermore, the crystalline phase, crystallite size, and porosity of TiO₂ affect its optical, textural, and catalytic properties. Because of the new features expected, TiO₂ synthesis of nanoparticles with a suitable specific surface and high porosity for specific applications is attractive (Patil et al. 2011). Rutile is the phase that works best in sonocatalysis, and anatase is the most efficient phase in photocatalysis, according to research on TiO₂ as a catalyst. In addition, sunscreen lotion with TiO₂ nanoparticles can be used for blocking UV-A and UV-B rays (Viana et al. 2010). The size, shape, and phases of synthesized TiO₂ nanoparticles influence the efficacy of solar radiation backscattering (Cerro-Prada et al. 2019).

The biogenesis of nanoparticles has piqued the interest of a number of researchers due to the high cost of chemical and physical procedures as well as the radical reaction conditions (Qiao and Qi 2021). As a result, in their search for new low-cost nanoparticle manufacturing pathways, researchers turned to microbes and plant extracts (El-Naggar and Shoueir 2020). In aqueous media, titanium dioxide (TiO₂) is stable and accepts both alkaline and acidic solutions. Photocatalysts, cosmetics, and pharmaceuticals have all used TiO₂ nanoparticles. Because of their small size, the particles can easily enter bacterial surfaces and cause injury. Several researchers are interested in titanium nanoparticles because of their inexpensive cost compared to noble metals like Au, Pt, and Ag (Abdussalam-Mohammed 2020).

Sol-gel, hydrothermal, solvothermal, spray pyrolysis, coprecipitation, and other processes have all been used to synthesize ultrafine titania powders both physically and chemically. Microorganisms have been shown to manufacture inorganic compounds both intracellularly and extracellularly. TiO₂ nanoparticles were recently synthesized using lactobacillus and yeast (Rani and Shanker 2020). Biological sources like *Bacillus subtilis*, *Eclipta prostrata* leaf aqueous extract, *Fusarium oxysporium*, and *Aspergillus flavus* were used to make TiO₂ nanoparticles (Zhu et al. 2019). The fabrication of latex, proteins, and phytochemicals from plant sources for metal nanoparticle manufacturing is particularly advantageous because it eradicates the requirement for handling, culturing, and maintenance, unlike that of microbes (Nasrollahzadeh et al. 2019a). The use of the biomaterials indicated above for the synthesis of metal nanoparticles has the added benefit of acting as a reducing and capping agent (Velmurugan and Incharoensakdi 2018).

Previous research on the application of TiO₂ claimed that the bactericidal and catalytic capabilities of TiO₂ may be enhanced by the addition of noble metallic particles like gold (Au), copper (Cu), or silver (Ag) on its surface (Nguyen et al. 2019). TiO₂ is a valuable semiconducting transition metal oxide material with

unique properties, such as ease of control, low cost, and nontoxicity, as well as strong chemical erosion resistance, making it suitable for solar cells, chemical sensors, and environmental distillation (Theerthagiri et al. 2019). These nanoparticles differ from their bulk counterparts in terms of electrical, magnetic, and optical properties. Titanium dioxide is found in amorphous and crystalline forms, with the most common crystalline polymorphs being anatase, rutile, and brookite (Parrino et al. 2020).

Removal of toxic substances is done using a variety of physiochemical techniques that were previously used, including sedimentation-flocculation, coagulation, molecular sieving, ion exchange, reverse osmosis, membrane filtration, ozonation, chlorination, chemical precipitation, adsorption, photocatalysis, chemical methods, and electrochemical techniques, among others. However, these procedures are inefficient and inadequate in terms of cost, energy, environmental friendliness, and purifying capabilities, necessitating expensive and intricate technologies, poor adsorption rates, and a lack of total pollutant destruction. Furthermore, most organic dyes, detergents, and pesticide chemicals contain benzene and naphthalene rings, which are difficult to breakdown using traditional physical, biological, and chemical processes (Thomas et al. 2018). An enhanced heterogeneous photocatalysis of TiO_2 was proposed as a simple model that works at ambient conditions, with high stability, and is cost-effective, energy-saving, and safe for the environment. Furthermore, the procedures do not cause secondary pollution in the environment (Ibhadon and Fitzpatrick 2013).

As TiO_2 is becoming one of the most exciting aspects in recent years, this review focuses on the physical, chemical, and biological methods of synthesizing TiO_2 nanoparticles. Other attempts were made to concentrate the developments, including industrial, environmental, and biomedical applications.

14.2 Methods for Synthesis of TiO_2 Nanoparticles

14.2.1 Physical Methods

14.2.1.1 Spray Pyrolysis Synthesis and Electrophoretic Concentration of TiO_2 NPs

The technique of spray pyrolysis is a chemical synthesis protocol of TiO_2 that requires spraying precursor solution by a furnace. The synthesis of dense, uniform nanofilms makes this technique widely accepted. Among its disadvantages is low-cost effectiveness due to the employment of low temperature that requires energy hence limiting large-scale production of TiO_2 . Other concerns include the emission of airborne particles during the synthesis that requires expensive equipment for particulate control (Rehan et al. 2011).

Titanium precursors, including titanium isopropoxide (TTIP), water-soluble TC-300[®], and TC-400[®] can be used. A solution of TTIP can be prepared using diluted nitric acid and ethanol. During the process, TTIP is slowly added to the nitric acid solution and mixed vigorously using a magnetic stirrer for an hour to result in a

clear, hydrolyzed titanium precursor. Ethanol and water can be used as solvents for the preparations of clear yellow solutions of TC-300[®] and TC400[®] (Wang et al. 2005).

Electrophoretic synthesis is the use of nonaqueous solvents that cause water pollution and adversely affect the destruction of aquatic habitat and air pollution due to nonaqueous solvent evaporation.

14.2.1.2 Microwave-Assisted Method for Synthesis

The microwave-aided method for synthesizing TiO₂ is a widely accepted approach involving rapid and homogenous heating of the reaction mixture that saves time. Limitations for large-scale mass production include the high cost of production since it requires intensive microwave heating, and the time-dependent growth monitoring of the TiO₂ nanoparticle production is not possible.

In acidic/alkaline synthesis, TTIP is added by a drop in a 0.01 M HNO₃ solution/NaOH solution. After heating the precursor solutions for 6 h at 80 °C, the solution is stored in a modified domestic microwave oven. The synthesis temperature is between 110 and 150 °C, and the time for synthesis is maintained between 2 and 60 min. Following synthesis, the solution is rinsed in water and preceded with characterization (May-Masnou et al. 2018).

14.2.1.3 Laser Ablation

Pulsed laser ablation has become a promising technique, with several advantages, including simplicity and low cost. The titanium oxide NPs are developed using an experimental device. A pulsed laser is focused using a glass lens and steered perpendicular to the surface of a titanium disc target. The titanium disc was dipped in distilled water and rotated. A beaker is filled with 20 mL, and the water thickness layer above the titanium disc is 2–3 mm. A plasma plume occurs above the laser dot due to the interaction between the laser light and the titanium target. The chemical composition of the ablated particles will be titanium oxide. Nanoparticles are produced at the energy level of 40 mJ/pulse and are spherical in shape, and the large particles are a result of the aggregation of the smaller particles to attain a more stable condition (Nikolov et al. 2009).

14.2.1.4 Electrochemical Method

The electrochemical method of TiO₂ nanoparticles synthesis includes the use of a stabilizing agent, the tetra propyl ammonium bromide salt in tetrahydrofuran and acetonitrile in the ratio of 4:1. The sizes of the nanoparticles are controlled by the use of several factors, such as the density and polarity of the solvent. Metal oxidation occurs in the anode, and cations migrate to the cathode, followed by metal oxide reduction and formation. In an experimental setup for the synthesis of titanium dioxide nanoparticles, a Titanium metal sheet is used as the anode, and a platinum sheet is used as the cathode, placed a cm apart. Tetra Propyl Ammonium Bromide in acetonitrile/tetrahydrofuran is used as an electrolyte. Clusters of titanium dioxide stabilized with tetra propyl ammonium bromide (TPAB) is obtained, and the solvent is decanted and washed with tetrahydrofuran several times to remove the stabilizing

reagent and dried in a vacuum. Calcination is performed at 550 °C and stored under ambient conditions (Anandgaonker et al. 2019).

14.2.2 Chemical Methods

14.2.2.1 Sol–Gel Route of Synthesis

A sol represents colloidal particles in a liquid are classified as lyophobic and lyophilic, depending on the interactive strength. Stabilization of the sols is when the forces between the two particles prevent the agglomeration and hence coagulate. As sol can be transformed into a gel when the particle charges are removed by an additive (Danks et al. 2016). A gel, on the other hand, is a porous three-dimensional inter-connected solid network that accounts for elasticity. Polymeric and colloidal gel formation depend on the transition, caused by either physicochemical effect or chemical bonding (Dannert et al. 2019).

Though Sol–gel synthesis is widely researched to produce high crystalline nanoparticles, the cost employed in the production makes it less feasible among other methods of production, involving raw materials, organic material removal by the drying process, and reduction volume of synthesized TiO₂ (Macwan et al. 2011). Several other criteria including control of the size and shape of NPs, ease in synthesis, profitability, high temperature and pressure, high energy and eco-toxicity, and environmental durability are still prevalent.

The TiO₂ nanopowder can be synthesized through a simple sol–gel method. An ethanolic solution of the precursor Titanium tetraisopropoxide (TTIP) of pH 1.6 is equipped by adjusting the pH with HCl. The TTIP precursor (5 mL) is added drop by drop to ethanol under continuous stirring for 2 h with a magnetic stirrer at normal room temperature. The solution was heated to 125 °C and temperature is maintained for an hour. The sol–gel was subsequently heated at 300 °C for 2 h. TiO₂ nanocrystals will be obtained after annealing (Sharma et al. 2020).

14.2.2.2 Coprecipitation Method

A simple and cost-effective procedure for synthesizing TiO₂ nanoparticles has been reported by Horti et al. adapting titanium oxysulfate and sodium hydroxide as primary sources using the chemical coprecipitation method (Horti et al. 2019). Calcination of the nanopowder was performed at a temperature ranging 300 °C–600 °C. The influence of the calcining temperature on the optical properties is investigated and confirmed (Ellouzi et al. 2020).

In this method of synthesis, 1.596 g (0.01 M) of TiOSO₄ powder is dissolved in 100 mL of demineralized water and stirred uniformly at a temperature of 700 °C for half an hour. A 0.02 M solution of sodium hydroxide is prepared and added dropwise under uniform stirring for an hour. In synthesis, the colorless solution becomes a white precipitate that can be filtered using Whatman No.1 filter paper. The precipitate is washed with deionized water and ethanol and heated at 80 °C for an hour in a hot air oven to eliminate impurities. Recrystallization of the nanopowder is performed by heating at 200 °C for 5–6 h. The nanopowder is calcinated at

temperatures ranging from 300 °C to 600 °C for 2 h in a muffle furnace following separation by filtration. Higher calcination temperatures ensure a pure anatase phase. The formation of TiO₂ is confirmed by the FTIR and EDX spectra (Chen et al. 2015b).

14.2.2.3 Solvothermal Method

TiO₂ nanoparticles can be prepared by low-temperature solvothermal technique, involving a mixture of nonaqueous solvents using an autoclave. Usage of mixed solvents in the solvothermal method ensures the synthesis of size-controlled TiO₂ nanoparticles with size uniformity. The use of organic solvents in the solvothermal process is considered the safest and environmentally safe (Mamaghani et al. 2019).

An optimized protocol uses 0.1 M Titanium Tetraisopropoxide (TTIP) added to 50 mL of anhydrous ethanol with continued stirring to attain homogeneity, for an hour. A prepared mixture of ethanol and deionized water in the ratio of 1:1 was added to the solution and vigorously agitated for an hour. Hydrolysis was initiated by adding a few drops of Sulfuric Acid. The solution was transferred to a tightly sealed reagent bottle, and solvothermal growth was carried out at 90 °C for different growth times. The solution is then centrifuged and washed with deionized to eradicate impurities from the nanopowder. The nanopowder is dried and annealed at temperatures 400, 450, and 500 °C for 1 h for annealing temperature optimization (X. Chen and Mao 2007).

14.2.2.4 Hydrothermal Method

The hydrothermal method, involving a single step, is capable to generate uniform sized nanoparticles, identical to the particle size of the solvothermal method, employing high temperature and pressure inside a closed system, namely, an autoclave. The hydrothermal method of nanoparticle synthesis involves aqueous solvents in contrast to the solvothermal method (Asim et al. 2014). The use of hydrothermal method of synthesis of nanoparticles is limited because of the use of surfactants which are toxic to the ecosystem, specifically aquatic life.

Hydrothermal treatment of sol-gels produces TiO₂ nanoparticles. A 0.5 M solution of titanium butoxide in 2-propanol was added to distilled water in the proportion of 1:4, subjected to constant agitation for 45 min, and filtered to retrieve the hydrolyzed precipitate of Titanium. The precipitated Titanium was then added to dilute solutions of Nitric acid and Tertiary Butyl Alcohol and then heated at 70 °C for an hour and continuously stirred to emit the acidic/alkaline peptized gels (Ismagilov et al. 2012). Nanoparticles are produced from hydrothermal treatment of the gels subjected to characterization techniques such as scanning electron microscopy, transmission electron microscopy, X-ray photoelectron spectroscopy, and Fourier transform infrared spectroscopy.

14.2.2.5 Laser Vaporization and Condensation

Laser vaporization and condensation work on a principle combining metal laser vaporization under controlled condensation to synthesize nanoscale metal oxide, with particle sizes 10–20 nm of well-defined composition. The ejected atoms of the

laser pulse react with the gas and condense to form nanoparticles. The small particles are removed by convection so that they are interrupted before forming large particles. The nanocrystals produced aggregate to form a webbed microstructure with a large surface area (Samy and Li 1997).

Colloidal solution of TiO₂ Nanoparticles can be synthesized using pulsed laser ablation. Neodymium-doped yttrium aluminum garnet laser operating at 35 mJ/pulse energy is used for the ablation of titanium target placed in water. Violet-colored, colloidal solution with high stability is produced that can be characterized by UV-Visible absorption, X-ray diffraction, SEM, and FTIR spectroscopic technique.

14.2.3 Biological Methods

The biological or green method of nanoparticle synthesis can be compared to the chemical reduction process, where the most expensive chemicals have been replaced with plants and microbial extracts. This has the potential to reduce toxicity, economic, environmental, and sustainability impacts and enhance its biomedical applications (Pantidos and Horsfall 2014; Zuverza-Mena et al. 2017). The method of nanoparticle synthesis requires a precursor salt and is combined with the biological extracts, which may act as reducing, capping, or stabilizing agents due to the presence of active molecules. The product obtained was washed, lyophilized, and stored for further analysis. Morphology and size distribution may be restrained by alterations in metrics like temperature, pH, incubating period, salt concentrates, etc. TiO₂ synthesized has crystal and amorphous forms and can occur in any of the three polymorphic crystal natures such as anatase, rutile and brookite (Mahshid et al. 2007). Sources of biological extracts include microbes such as fungi and bacteria; plants and other biological entities have been used in TiO₂ nanoparticle synthesis (Nadeem et al. 2018).

Plants are generally preferred for the biosynthesis of nanoparticles as they are naturally available and safe. Different parts of plants such as leaves (Thakur et al. 2019; Ahmad et al. 2020), seeds (Mathew et al. 2021), roots (Suman et al. 2015; Al-Shabib et al. 2020; Bekele et al. 2021), fruits (Hossain et al. 2019), and flowers (Aravind et al. 2021) have been primarily used for producing metallic nanoparticles (Sun et al. 2019). When developing TiO₂ nanoparticles, many researchers explained the use of natural products based on medicinal plants such as *Calotropis gigantean*, *Psidium guajava*, *Aloe barbadensis* Miller, *Ageratina altissima* L, *Vitex negundo*, *Psidium guajava*, *Curcuma longa*, *Vigna unguiculata*, *Eclipta prostrata*, and *Moringa oleifera* (Zhu et al. 2019). Microbes are also very promising, energetic, and adaptive due to the presence of high metabolic flows, and the compassion abilities of microbes have been taken into account for efficient nanoparticle synthesis (Kirthi et al. 2011; Rajakumar et al. 2012; Taran et al. 2018). The competencies of the microbes have not been exploited for metal nanoparticle or oxide synthesis (Jha et al. 2009). The biological sources utilized in the TiO₂ synthesis are presented in Table 14.1.

Table 14.1 TiO₂ nanoparticles synthesis using biological sources

S. No	Biological Sources	References
<i>Microbial sources</i>		
1	<i>Lactobacillus sp.</i>	Jha et al. (2009)
2	<i>Sachharomyces cerevisiae</i>	Jha et al. (2009)
3	<i>Bacillus subtilis</i>	Kirthi et al. (2011)
4	<i>Aspergillus flavus TFR7</i>	Raliya and Tarafdar (2012)
5	<i>Bacillus mycoides</i>	Órdenes-Aenishanslins et al. (2014)
6	<i>Bacillus amyloliquefaciens</i>	Khan and Fulekar (2016)
<i>Plant sources</i>		
7	<i>Syzygium cumini</i>	Sethy et al. (2020)
8	<i>Echinacea purpurea</i>	Dobrucka (2017)
9	<i>Cassia fistula</i>	Swathi et al. (2019)
10	<i>Psidium guajava</i>	Santhoshkumar et al. (2014)
11	<i>Aloe barbadensis</i>	Rajkumari et al. (2019)
12	<i>Euphorbia prostrata</i>	Zahir et al. (2015)

14.3 Characterization

The TiO₂ nanoparticles synthesized using physical, chemical, or biological approaches are evaluated using UV-visible (UV-vis) spectroscopy, X-Ray Diffraction (XRD) spectroscopy, Fourier Transmission Infrared (FTIR) spectroscopy, Scanning Electron Microscopy (SEM) with Energy Dispersive X-ray (EDX) spectroscopy, High Resolution-Transmission Electron Microscopy (HR-TEM) with Selected area electron diffraction (SAED), zeta potential, Atomic Force Microscopy (AFM), Brunauer–Emmett–Teller(BET) analysis, Single Particle-Inductively Coupled Plasma Mass Spectroscopy (SP-ICPMS), Thermal Gravimetric Analysis (TGA). The different methods used to synthesize and characterize TiO₂ are illustrated in Fig. 14.1.

The optical attributes of bio-reduced TiO₂ nanoparticles used to be recorded employing a UV-vis spectrophotometer at different wavelengths of 200–800 nm (Saranya et al. 2018).

Sample XRD peaks have been achieved with the degree range of diffraction (2 θ) calibrated from 20° to 90° by means of a diffractometer. It was equipped with a graphite monochromator and operated at 40 kV with a Cu K α source of radiation of 30 mA (Wei et al. 2013). The resulting model was compared with the Joint Committee on Powder Diffraction Standards (JCPDS) dataset file.

The functional groups of the samples are identified using FTIR. The sample is mixed with KBr to get a fine homogeneous powder of small particle size and made into pellets to record Infrared (IR) spectra. Transparent oxide semiconductor samples were prepared to form a disc of a few tenths of a millimeter thickness with a density between 10 and 100 mg/cm³. The sample discs were formed by applying pressure at ambient temperature under dry conditions. FTIR was utilized to detect the stretching

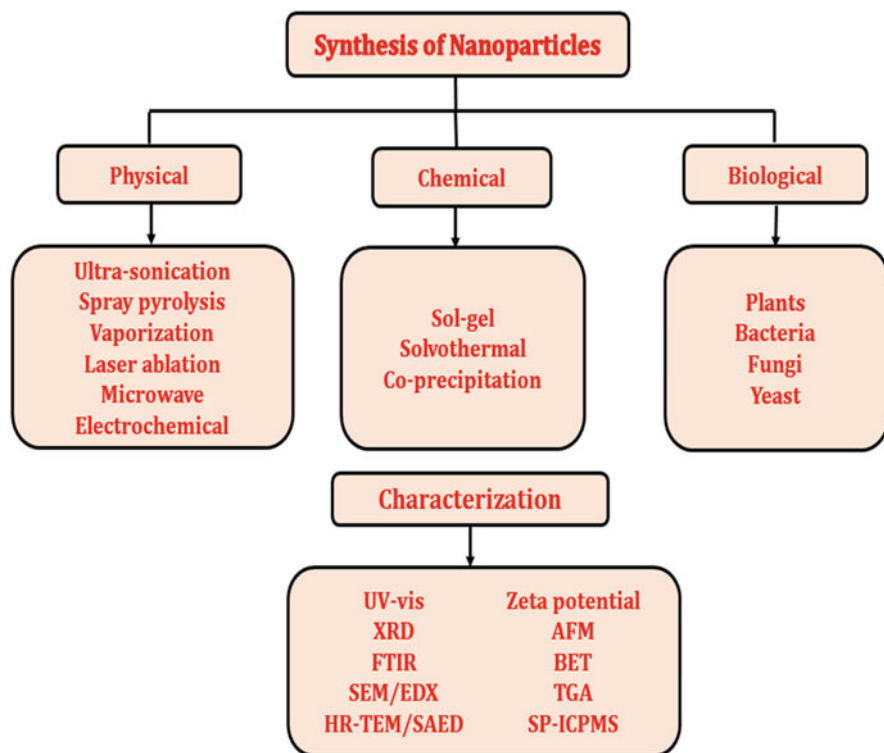


Fig. 14.1 TiO₂ nanoparticle synthesis and characterization

of metal-oxygen bonding attenuated total reflectance mode and the spectral range of 4000–400 cm⁻¹ (León et al. 2017).

The synthesized TiO₂ nanoparticles are placed on a carbon-coated copper grid and later permitted to dehydrate below a mercury lamp for 5 min. SEM characterizes the detailed morphology of a sample, and the elemental compositions are analyzed using EDX (Jalali et al. 2020).

The HR-TEM micrographs of TiO₂ nanoparticles could clearly elucidate single, separable, and aggregated nanoparticles. The size measurement can be carried out along the largest diameter of the particles showing a wide size distribution varying from 1 to 100 nm. The SAED pattern is used to determine the diffraction ring and scattered dots to the diffraction planes (Ramalingam et al. 2020).

The Zeta Potential Assessment was performed to examine the stability that is important for many applications. Surface zeta potentials were evaluated using the zeta analyzer to investigate the surface potential of TiO₂ nanoparticles. A Zeta potential of 30 mV or greater, i.e., positive or negative charge, is generally essential for achieving moderate stability of the dispersion (Sentein et al. 2009).

Surface morphology analysis, roughness, and texture of nanoparticles are observed by AFM. This is done to get a better overview of the topological map of

the surface, which are uneven due to the presence of clusters or agglomeration of TiO₂ nanoparticles (Ramalingam et al. 2020). Surface, pore size distribution, and pore volume for TiO₂ nanoparticles were investigated using the BET technique (Sethy et al. 2020).

The thermal properties, together with identifying the amount of surface coating of the synthesized TiO₂ nanoparticles, were studied using a thermogravimetric analysis (TGA) instrument (Saranya et al. 2018).

SP-ICPMS emerges as one of the most effective detection techniques for nanoparticles and also for measuring very small nanoparticles at extremely low concentrations, i.e., levels of parts by a trillion (Hadioui et al. 2019). Following the measurement, it provides the mean size, size distribution, and particle number concentration of the nanoparticles (Mozhayeva and Engelhard 2020).

14.4 Applications

Nanotechnology has been extensively established and implemented in the fields of medicine, materials, energy, information technology and protection of the environment, the food industry, and agriculture. Titanium dioxide (TiO₂) nanostructures have numerous advantages, making them essential resources with capable usage in different areas (Table 14.2). TiO₂ nanomaterial is used as a significant material in advanced applications. Its physical and biological properties are responsible for protective applications against ultraviolet light (Hwang et al. 2003). TiO₂ nanostructures are magnificently used for dental, osteosynthesis, and orthopedic applications (Mahltig et al. 2005). In recent times, primary practical research on TiO₂ has been used to degrade photoassisted organic molecules (Hwang et al. 2003).

Table 14.2 Titanium oxide Nanoparticles application in industry/Environmental

S. No	Synthesis	Source	Application	Reference
<i>Industry</i>				
1	Chemical	Nanocrystalline	Gas sensors	Zahra et al. (2020)
2	Chemical	Zinc oxide	White pigment	Abdullah and Kamarudin (2017)
3	Chemical	Titanium tetrachloride	Photocatalytic degradation	Haider et al. (2017)
4	Chemical	Phosphate	Water pollution	Illarionov et al. (2020)
5	Biological	<i>Matricaria chamomilla</i>	Lithium batteries	Pakseresht et al. (2021)
<i>Environmental</i>				
1	Chemical	Polymer nanocomposites	Environmental remediation	Ziental et al. (2020)
2	Biological	<i>Catharanthus roseus</i>	Antimicrobial	Nadeem et al. (2018)
3	Biological	<i>Scenedesmus obliquus</i>	Wastewater treatment	Naseem and Durrani (2021)

Applications using this method include disinfection, wastewater purification, and self-cleaning coatings in urban buildings. The sections below provide an explanation of the different applications of TiO₂ nanostructures.

14.5 Industrial Application

14.5.1 Lithium Batteries

In modern society, the most favorable energy storage technology, lithium-ion batteries, are regarded as the best for electric vehicles, renewables, and mobile electronics (Arico et al. 2011). The commercial success in lithium batteries was particularly in their nanostructures, where scientists have been carrying out TiO₂ polymorphs and their composites. Lithium insertion anatase and bronze polymorphs are moderately well understood, whereas Li-insertion TiO₂ (B) appears different from the anatase. Compared to the Li-insertion, TiO₂ (B) has higher energy storage than the rutile and anatase (Yang et al. 2009). The essential factors in lithium-ion batteries (LIB) are the size of the particle and crystallographic nanostructure alignments (Arico et al. 2011). The TiO₂ (B) crystallographic orientations confirmed that lithium-ion mobility $b > c \ll a$ -axis channel (Yang et al. 2009).

14.5.2 Gas Sensors

Gas sensors are based on semiconductor oxides; the advantages of the sensor are low cost, devices in front of the usual monitoring systems, easy implementation, and reduced size, being even similar to microelectronic systems (Ruiz et al. 2004). TiO₂ has been widely used for gas sensor applications because the adsorption of the gases causes a modification of the electrical conductivity (Miyazaki et al. 2005). Consequently, TiO₂ is generally used as a gaseous oxygen instrument to determine the fuel combustion process to control fuel pollution of the environment and consumption in car engines (Ali et al. 2018).

14.5.3 Paper Industry

In the paper industry, they used pigment. It has the most abundant component in the coating materials due to the strongest stability refractive index, colorless, and comparatively small and consistent uptake of visible light. Generally, clays are widely used in the paper industry as coating pigments, especially hydrous aluminum silicates combined with numerous mineral species (Ali et al. 2018). Kaolinite is the primary mineral in kaolin clay and was used as the main white pigment in various applications such as paper fillers, paper coating, paint, ceramics, cracking catalyst, cement, wastewater treatment, and pharmaceutical industries, respectively. Kaolin is a low cost and commercially available paper coating pigment that has been

commonly used where the light scattering index is inferior to that of the micro TiO₂ powder (Murray and Kogel 2005). TiO₂ has recently developed into a central white pigment source of light scattering have been synthesized using processes such as hydrothermal and hydrolysis (El-Sherbiny et al. 2014). In the paper industry, the usage of the nano pigments formed is revealed in a slight quantity of titanium dioxide owing to scattering light, brightness, and opacity.

14.5.4 Food Industry

Nanotechnology could change the conventional food industry and the production, processing, packaging, transport, and consumption of food (Rashidi and Khosravi-Darani 2011). Novel nanosensors for the development of packaging/food quality techniques have changed the manner in which food is preserved and delivered (Chen et al. 2014). TiO₂ nanoparticles are regarded to be one of the nanomaterials produced in significant quantities around the world (Keller et al. 2013). Meanwhile, from 2002, the US Food and Drug Administration, the European Union, and China have formally approved TiO₂ to be used in food additives and simply declared that the added quantity must not exceed 1% of the total weight of the foodstuff. Besides, the photocatalytic activity of TiO₂ nanoparticles is applied in food packing with good antibacterial capacity. As a result of these outstanding benefits, the production of TiO₂ nanoparticles and their percentage in the food category has risen exponentially (Hendren et al. 2011).

14.6 Environmental

14.6.1 Photocatalyst

Photocatalysis demonstrates the chemical reaction that happens as light passes by a chemical compound susceptible to light. It destroys the particle and leads to the degradation of biological contaminants, odors, etc., and this photocatalysis reaction has numerous significant results. In a photocatalytic mechanism, free radical formation takes place that has been linked to the negative health consequences of TiO₂ in sunscreen. In order to protect the biological compositions of organisms, sunscreens containing TiO₂ require photostability (Dar et al. 2020). Since anatase is more photoactive than rutile, free radical production is probably higher during the anatase stage. As a result, the rutile is preferred in compositions of sunscreen. In addition, in photocatalysis, a combination of anatase and rutile is more effective than every single phase, which is dependent on the rate of electron–hole recombination, crystallinity, adsorptive affinity, and particle interconnectivity (Laux et al. 2018). The combination of these qualities almost always ensures photocatalysis success, as demonstrated with commercial powder Degussa P-25. Photocatalytic activity of immobilized TiO₂ particles on macroporous ceramic alumina foams has been reported earlier. Crosslinked macroporous ceramic foam with an open 3D structure

and low flow resistance was found to be a very promising medium for photocatalytic applications and water purification systems (Lu 2018). Ambient factors such as light, oxygen, water vapor, temperature, and microorganisms all have an impact on the quality of perishable goods such as foods and medications. Packaging can act as a protective barrier, allowing them to avoid degenerative diseases (Mustafa and Andreescu 2020).

14.6.2 Photocatalytic Elimination of Water Pollutants

Water bodies are among the most valuable and essential Earth's natural resources. There is a lack of clean and safe water that can be utilized in great quantities (Mekonnen and Hoekstra 2016). Water resources are habitually contaminated with harmful pollutants like dyes (textile and cosmetic industries), heavy metals (paint industries, automobile manufacturing, and electrical industries), as well as microorganisms that are reasons for a variety of biological and human-related diseases (Gopinath et al. 2020).

TiO₂ has a number of limitations when used as a photocatalytic in the treatment of water. It absorbs visible and actual ultraviolet radiation that falls to the surface by less than 5% (Yin et al. 2003). While using the nano-form, they have a tendency to agglomerate and convert to larger particles that reduce the surface and active sites. They also have very high dispersion thereby reducing efficiency (Gao et al. 2011; Mallakpour and Nikkhoo 2014).

14.6.3 Removal of Pollution/Deodorization Applications

TiO₂ eliminates elements of environmental pollution, such as nitrogen oxides (NO_x) emitted by atmospheric exhaust. Sulfur oxides (SO_x), an inorganic material harmful to the environment, are also decomposed. TiO₂ excludes odors, such as conventional air fresheners and air sprayers. It breaks up the odor by causing the odor source to degrade (ammonia, aldehyde gas, etc.).

14.7 Biomedical Application

Recently, there has been an increase of using nanoparticles in biomedical applications such as drug delivery and discovery, surgeries, bio-imaging, and biosensors. In addition, they have widely used both in vitro and in vivo modes of diagnostic approaches, regenerative medicine, and tissue engineering. (McNamara and Tofail 2017; Bharathala and Sharma 2019). Among many nanoparticles, metal oxide has dominated many applications, particularly Iron oxide, Zinc oxide, and titanium dioxide used in many biomedical, therapeutic, and diagnostic purposes such as bio-imaging, ultrasonic techniques, magnetic particle hyperthermia, and much more applications and mainly used because of their excellent features like the

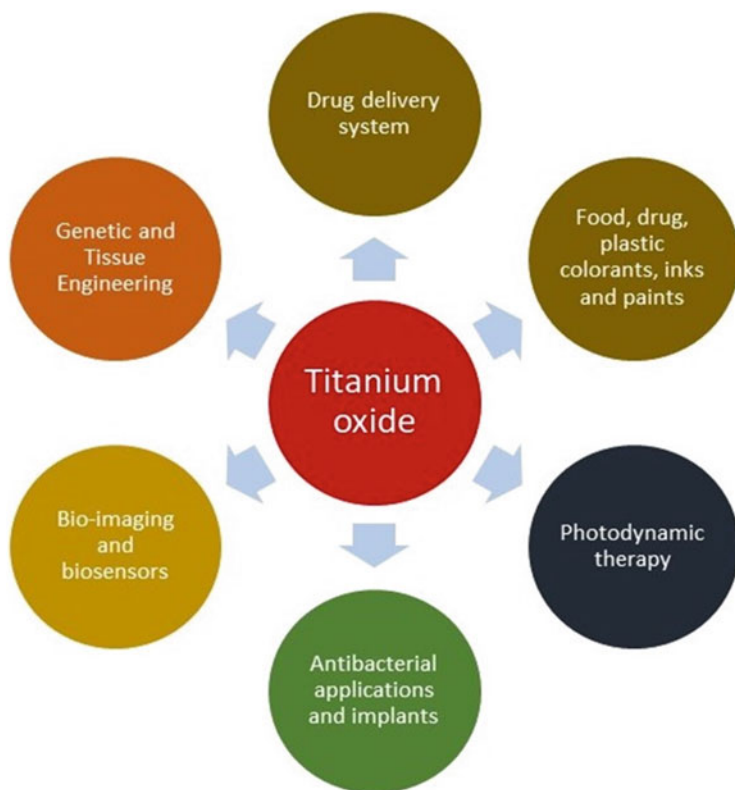


Fig. 14.2 Multifunctional applications of TiO₂ nanoparticles in biomedical and medicine

chemical stability, biocompatibility, nontoxicity, high-magnetic susceptibility, and high-saturation magnetization (Oh et al. 2006; Hong et al. 2011; Liu et al. 2016). Titanium dioxide (TiO₂) is widely used in bone-regeneration materials, as the TiO₂ contact with biofluid and emerges immediately on the exterior part of metallic Titanium (Brammer et al. 2012). Figure 14.2 illustrates the applications of TiO₂ in various industries.

14.7.1 Photodynamic Therapy (PDT)

Recently, in PDT, combined dyes and nanoparticles increased the photosensitizer's selectivity and the therapy's efficacy (Ziental et al. 2020). Among those nanoparticles, the annual production and the usage of TiO₂ as a photosensitizing agent increased rapidly for treating cancer and in photodynamic inactivation of antibiotic-resistant bacteria (Xu et al. 2007). Geraets et al. (2014) noticed that TiO₂ excretion by the kidneys in rats slowly indicates its potential accumulation of

tissue. It is not severe as the photosensitizer is administered once/several times during the PD.

14.7.2 Targeted Drug Delivery

Targeted drug administration and the controlled diffusion of drugs into cancer treatments improve the therapeutic effect and reduce side effects (Fig. 14.3). TiO₂ nanostructures are considered a candidate for the therapeutic effect of chemotherapeutic agents for their ability in controlled release, high biocompatibility, and low toxicity (Çeşmeli and Biray Avcı 2019). A study suggested the one-dimensional synergistic effect of TiO₂ on the internalization and accumulation of daunorubicin in human hepatocellular carcinoma (SMMC-7721) cell lines as a drug dispensing agent in cancer therapy (Li et al. 2009). Similarly, another study found that the combination of doxorubicin and TiO₂ nanoparticles produced a synergistic response against breast cancer (MCF-7) cell lines (Akram et al. 2019).

14.7.3 Antibacterial Activity

TiO₂ nanoparticles could be used as an effective microbicide agent for their safety and stability in comparison with organic antimicrobial agents. TiO₂ is an antimicrobial agent used in several antimicrobial industries such as dentistry and orthopedic

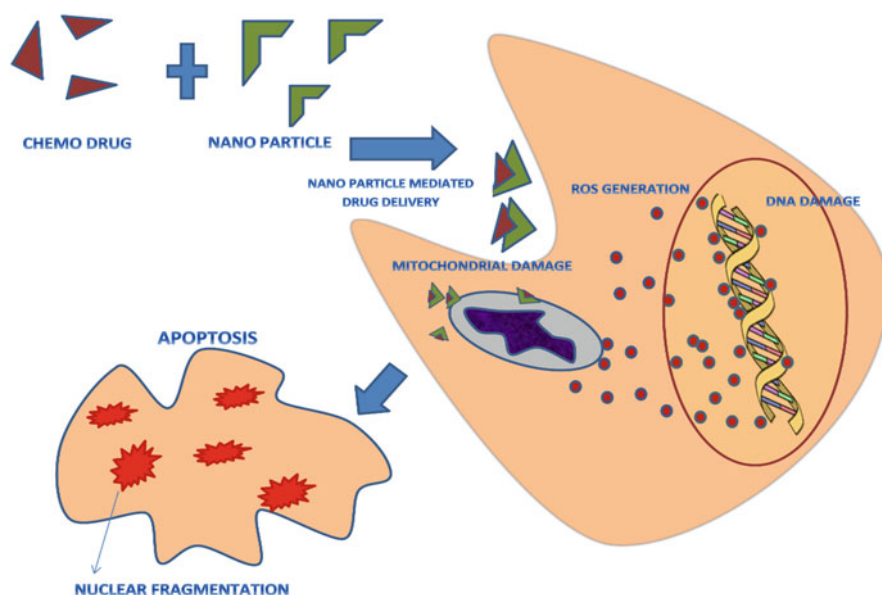


Fig. 14.3 Nanoparticle-mediated targeted drug delivery

implants. The implant failure could be due to contamination of titanium-based dental implants. In order to control infection and the long-term success of dental implants, another way of placing implants in bones is important. The modification of the implant surface is one of the best options to strengthen it. Hence, TiO₂ nanotubes could be the choice for their unique features of antibacterial functions at a proper concentration, and enhance the osteogenic activity of implants efficacy due to cytocompatibility and improve cell adherence, proliferation, and mobility of cells (W. Liu et al. 2015; Choi et al. 2019). TiO₂ has been commonly used for antimicrobial applications due to microbial growth and biofilm inhibition activity (Ağçeli et al. 2020). This technique was identified as advantageous as it was observed to be the simple approach of TiO₂ nanoparticles with the most promising approach for overcoming multiresistant pathogens (Jayaseelan et al. 2013). Titanium nanoparticles are capable of reacting with OH and O₂ formed on their surfaces to generate oxygen and hydroxyl free radicals. The area that interacts with bacterial pathogens rises as the surface area of nanoparticles grows, making them appropriate as an antibacterial agent (Gopinath et al. 2020).

14.7.4 Bone and Dental Implants

As a result of the flexible, high resistance to corrosion and tensile strength, TiO₂ is considered an enhancement for implantation (Chen et al. 2015a). An experiment shows the impact of TiO₂ on enhancing mechanical strength, setting time, and hydraulic response of calcium phosphate bone cement in the short term. The outcome of the study indicated that the thickness of the nanometres, the high porous structure, and the surface area of the TiO₂ nanotubes greatly improved cell adhesion and improved bone growth (Brammer et al. 2012).

The surface topography and the porous surface are vital to attaining appropriate osseointegration in dental implants as they will be helpful for drug loading and biocompatibility. TiO₂ nanotubes are considered the best candidate to cover the surface of dental implants because of their peculiar features. Using an anodic oxidation method, TiO₂ nanotubes were grown on dental implant surfaces with a length of 10 μm and diameter of 60 nm loaded with bone morphogenetic protein-2 and showed enhanced osseointegration (Shim et al. 2014). The unique properties and characteristics such as nontoxicity and nano topographical of TiO₂ had given more attention to the production of implants.

14.8 Conclusion

TiO₂ nanoparticles are cost-effective, require a large amount of energy, and produce toxic by-products that are harmful to the environment. Hence, synthesis using physical, chemical, and biological methods is extensive lately. Consequently, biofabrication using plants and microbial sources have favored the synthesis of TiO₂ nanoparticles that are less expensive and environmentally friendly. TiO₂

nanostructures and its composites, because of its unique characteristics, have gained attraction in diverse applications such as gas sensors, paper industry, lithium batteries, photocatalytic, and environmental applications. Additionally, it has a vital role to play in biomedical applications. In view of all the general features, it can be stated that TiO₂ nanomaterials offer better development for advanced technological applications. However, to further develop and utilize TiO₂ nanomaterials in other advanced areas, detailed studies such as toxicity assessment and detailed clinical trials are required.

References

- Abdullah M, Kamarudin SK (2017) Titanium dioxide nanotubes (TNT) in energy and environmental applications: An overview. *Renew Sust Energ Rev* 76:212–225
- Abdussalam-Mohammed W (2020) Comparison of chemical and biological properties of metal nanoparticles (Au, Ag), with metal oxide nanoparticles (ZnO-NPs) and their applications. *Adv J Chem Sect A* 3(2):192–210
- Ağçeli GK, Hamideh Hammachi S, Kodal P, Cihangir N, Aksu Z (2020) A novel approach to synthesise TiO₂ nanoparticles: biosynthesis by using streptomyces Sp. HC1. *J Inorg Organomet Polym Mater* 30(8):3221–3229
- Ahmad W, Jaiswal KK, Soni S (2020) Green synthesis of titanium dioxide (TiO₂) nanoparticles by using Mentha Arvensis leaves extract and its antimicrobial properties. *Inorg Nano-Metal Chem* 50(10):1032–1038
- Akram MW, Raziq F, Fakhar-e-Alam M, Aziz MH, Alimgeer KS, Atif M, Amir M, Hanif A, Aslam W, Farooq. (2019) Tailoring of au-TiO₂ nanoparticles conjugated with doxorubicin for their synergistic response and photodynamic therapy applications. *J Photochem Photobiol A Chem* 384:112040
- Ali I, Suhail M, Alothman ZA, Alwarthan A (2018) Recent advances in syntheses, properties and applications of TiO₂ nanostructures. *RSC Adv* 8(53):30125–30147
- Al-Madanat O, AlSalka Y, Ramadan W, Bahnemann DW (2021) TiO₂ photocatalysis for the transformation of aromatic water pollutants into fuels. *Catalysts* 11(3):317
- Al-Shabib NA, Husain FM, Qais FA, Ahmad N, Khan A, Alyousef AA, Arshad M, Noor S, Khan JM, Alam P (2020) Phyto-mediated synthesis of porous titanium dioxide nanoparticles from Withania Somnifera root extract: broad-spectrum attenuation of biofilm and cytotoxic properties against HepG2 cell lines. *Front Microbiol* 11:1680
- Anandgaonker P, Kulkarni G, Gaikwad S, Rajbhoy A (2019) Synthesis of TiO₂ nanoparticles by electrochemical method and their antibacterial application. *Arab J Chem* 12(8):1815–1822
- Aravind M, Amalanathan M, Mary MSM (2021) Synthesis of TiO₂ nanoparticles by chemical and green synthesis methods and their multifaceted properties. *SN Appl Sci* 3(4):1–10
- Arico AS, Bruce P, Scrosati B, Tarascon J-M, Van Schalkwijk W (2011) Nanostructured materials for advanced energy conversion and storage devices. In *Materials for sustainable energy: a collection of peer-reviewed research and review articles from Nature Publishing Group*, pp 148–59
- Asim N, Ahmadi S, Alghoul MA, Hammadi FY, Saeedfar K, Sopian K (2014) Research and development aspects on chemical preparation techniques of photoanodes for dye sensitized solar cells. *Int J Photoenergy* 2014:518156
- Bekele ET, Zereffa EA, Gultom NS, Kuo D-H, Gonfa BA, Sabir FK (2021) Biotemplated synthesis of titanium oxide nanoparticles in the presence of root extract of kniphofia schemperi and its application for dye sensitized solar cells. *Int J Photoenergy* 2021
- Bharathala S, Sharma P (2019) Biomedical applications of nanoparticles. In *Nanotechnology in modern animal biotechnology*, pp 113–32. Elsevier

- Brammer KS, Frandsen CJ, Jin S (2012) TiO₂ nanotubes for bone regeneration. *Trends Biotechnol* 30(6):315–322
- Cerro-Prada E, García-Salgado S, Quijano M, Varela F (2019) Controlled synthesis and microstructural properties of sol-gel TiO₂ nanoparticles for photocatalytic cement composites. *Nanomaterials* 9(1):26
- Çeşmeli S, Biray Avci C (2019) Application of titanium dioxide (TiO₂) nanoparticles in cancer therapies. *J Drug Target* 27(7):762–766
- Chen X, Mao SS (2007) Titanium dioxide nanomaterials: synthesis, properties, modifications, and applications. *Chem Rev* 107(7):2891–2959
- Chen H, Seiber JN, Hotze M (2014) ACS select on nanotechnology in food and agriculture: a perspective on implications and applications. ACS Publications
- Chen X, Liu L, Huang F (2015a) Black titanium dioxide (TiO₂) nanomaterials. *Chem Soc Rev* 44(7):1861–1885
- Chen H-T, Shu H-Y, Chung C-J, He J-L (2015b) Assessment of bone morphogenic protein and hydroxyapatite–titanium dioxide composites for bone implant materials. *Surf Coat Technol* 276: 168–174
- Choi S-H, Jang Y-S, Jang J-H, Bae T-S, Lee S-J, Lee M-H (2019) Enhanced antibacterial activity of titanium by surface modification with polydopamine and silver for dental implant application. *J Appl Biomater Funct Mater* 17(3):2280800019847067
- Danks AE, Hall SR, Schnepf ZJM (2016) The evolution of ‘sol–Gel’ Chemistry as a technique for materials synthesis. *Mater Horizons* 3(2):91–112
- Dannert C, Stokke BT, Dias RS (2019) Nanoparticle-hydrogel composites: from molecular interactions to macroscopic behavior. *Polymers* 11(2):275
- Dar GI, Saeed M, Wu A (2020) Toxicity of TiO₂ Nanoparticles. In *TiO₂ nanoparticles: applications in nanobiotechnology and nanomedicine*, pp 67–103
- Dobrucka R (2017) Synthesis of titanium dioxide nanoparticles using *echinacea purpurea* Herba. *Iran J Pharm Res IJPR* 16(2):756
- El Shafey AM (2020) Green synthesis of metal and metal oxide nanoparticles from plant leaf extracts and their applications: a review. *Green Process Synthesis* 9(1):304–339
- Ellouzi I, Harir M, Schmitt-Kopplin P, Laänab L (2020) Coprecipitation synthesis of Fe-doped TiO₂ from various commercial TiO₂ for photocatalytic reaction. *Int J Environ Res* 14(6):605–613
- El-Naggar ME, Shouair K (2020) Recent advances in polymer/metal/metal oxide hybrid nanostructures for catalytic applications: a review. *J Environ Chem Eng* 8(5):104175
- El-Sherbiny S, Morsy F, Samir M, Fouad OA (2014) Synthesis, characterisation and application of TiO₂ nanopowders as special paper coating pigment. *Appl Nanosci* 4(3):305–313
- Gao B, Yap PS, Lim TM, Lim T-T (2011) Adsorption-photocatalytic degradation of acid red 88 by supported TiO₂: effect of activated carbon support and aqueous anions. *Chem Eng J* 171(3): 1098–1107
- Geraets L, Oomen AG, Krystek P, Jacobsen NR, Wallin H, Laurentie M, Verharen HW, Brandon EFA, de Jong WH (2014) Tissue distribution and elimination after oral and intravenous administration of different titanium dioxide nanoparticles in rats. *Part Fibre Toxicol* 11(1):1–21
- Gopinath KP, Madhav NV, Krishnan A, Malolan R, Rangarajan G (2020) Present applications of titanium dioxide for the photocatalytic removal of pollutants from water: a review. *J Environ Manag* 270:110906
- Hadioui M, Knapp G, Azimzada A, Jreije I, Frechette-Viens L, Wilkinson KJ (2019) Lowering the size detection limits of ag and TiO₂ nanoparticles by single particle ICP-MS. *Anal Chem* 91(20):13275–13284
- Haider AJ, Hassan R, Anbari AL, Kadhim GR, Salame CT (2017) Exploring potential environmental applications of TiO₂ nanoparticles. *Energy Procedia* 119:332–345
- Hendren CO, Mesnard X, Dröge J, Wiesner MR (2011) Estimating production data for five engineered nanomaterials as a basis for exposure assessment. ACS Publications
- Hong H, Shi J, Yang Y, Zhang Y, Engle JW, Nickles RJ, Wang X, Cai W (2011) Cancer-targeted optical imaging with fluorescent zinc oxide nanowires. *Nano Lett* 11(9):3744–3750

- Horti NC, Kamatagi MD, Patil NR, Nataraj SK, Sannaikar MS, Inamdar SR (2019) Synthesis and photoluminescence properties of titanium oxide (TiO₂) nanoparticles: effect of calcination temperature. *Optik* 194:163070
- Hossain A, Yasmine Abdallah M, Masum AM, Islam M, Li B, Sun G, Meng Y, Wang Y, An Q (2019) Lemon-fruit-based green synthesis of zinc oxide nanoparticles and titanium dioxide nanoparticles against soft rot bacterial pathogen *Dickeya Dadantii*. *Biomol Ther* 9(12):863
- Hwang DK, Moon JH, Shul YG, Jung KT, Kim DH, Lee DW (2003) Scratch resistant and transparent UV-protective coating on polycarbonate. *J Sol-Gel Sci Technol* 26(1):783–787
- Ibhadon AO, Fitzpatrick P (2013) Heterogeneous photocatalysis: recent advances and applications. *Catalysts* 3(1):189–218
- Illarionov GA, Morozova SM, Chrishtop VV, Einarsrud M-A, Morozov MI (2020) Memristive TiO₂: synthesis, technologies, and applications. *Front Chem* 8
- Ismagilov ZR, Shikina NV, Mazurkova NA, Tsikoza LT, Tuzikov FV, Ushakov VA, Ishchenko AV, Rudina NA, Korneev DV, Ryabchikova EI (2012) Synthesis of nanoscale TiO₂ and study of the effect of their crystal structure on single cell response. *Sci World J* 2012
- Jafari S, Mahyad B, Hashemzadeh H, Janfaza S, Gholikhani T, Tayebi L (2020) Biomedical applications of TiO₂ nanostructures: recent advances. *Int J Nanomedicine* 15:3447
- Jalali E, Maghsoudi S, Noroozian E (2020) A novel method for biosynthesis of different polymorphs of TiO₂ nanoparticles as a protector for *Bacillus thuringiensis* from ultra violet. *Sci Rep* 10(1):1–9
- Jayaseelan C, Rahuman AA, Roopan SM, Kirthi AV, Venkatesan J, Kim S-K, Iyappan M, Siva C (2013) Biological approach to synthesise TiO₂ nanoparticles using *Aeromonas hydrophila* and its antibacterial activity. *Spectrochim Acta A Mol Biomol Spectrosc* 107:82–89
- Jha AK, Prasad K, Kulkarni AR (2009) Synthesis of TiO₂ nanoparticles using microorganisms. *Colloids Surf B: Biointerfaces* 71(2):226–229
- Keller AA, McFerran S, Lazareva A, Suh S (2013) Global life cycle releases of engineered nanomaterials. *J Nanopart Res* 15(6):1–17
- Khan R, Fulekar MH (2016) Biosynthesis of titanium dioxide nanoparticles using *Bacillus amyloliquefaciens* culture and enhancement of its photocatalytic activity for the degradation of a sulfonated textile dye reactive red 31. *J Colloid Interface Sci* 475:184–191
- Kirthi AV, Abdul Rahuman A, Rajakumar G, Marimuthu S, Santhoshkumar T, Jayaseelan C, Elango G, Abdul Zahir A, Kamaraj C, Bagavan A (2011) Biosynthesis of titanium dioxide nanoparticles using bacterium *Bacillus subtilis*. *Mater Lett* 65(17–18):2745–2747
- Laux P, Tentschert J, Riebeling C, Braeuning A, Creutzenberg O, Epp A, Fessard V, Haas K-H, Haase A, Hund-Rinke K (2018) Nanomaterials: certain aspects of application, risk assessment and risk communication. *Arch Toxicol* 92(1):121–141
- León A, Reuquen P, Garín C, Segura R, Vargas P, Zapata P, Orihuela PA (2017) FTIR and Raman characterization of TiO₂ nanoparticles coated with polyethylene glycol as carrier for 2-methoxyestradiol. *Appl Sci* 7(1):49
- Li Q, Wang X, Xiaohua L, Tian H, Jiang H, Lv G, Guo D, Chunhui W, Chen B (2009) The incorporation of daunorubicin in cancer cells through the use of titanium dioxide whiskers. *Biomaterials* 30(27):4708–4715
- Liu W, Penglei S, Chen S, Wang N, Wang J, Liu Y, Ma Y, Li H, Zhang Z, Webster TJ (2015) Antibacterial and osteogenic stem cell differentiation properties of photoinduced TiO₂ nanoparticle-decorated TiO₂ nanotubes. *Nanomedicine* 10(5):713–723
- Liu H, Zhang J, Chen X, Xue-Song D, Zhang J-L, Liu G, Zhang W-G (2016) Application of iron oxide nanoparticles in glioma imaging and therapy: from bench to bedside. *Nanoscale* 8(15):7808–7826
- Lu X (2018) Immobilisation of photocatalyst on supporting materials for pollutant control. Deakin University
- Macwan DP, Dave PN, Chaturvedi S (2011) A review on Nano-TiO₂ sol-gel type syntheses and its applications. *J Mater Sci* 46(11):3669–3686

- Mahlting B, Böttcher H, Rauch K, Dieckmann U, Nitsche R, Fritz T (2005) Optimized UV protecting coatings by combination of organic and inorganic UV absorbers. *Thin Solid Films* 485(1–2): 108–114
- Mahshid S, Askari M, Ghamsari MS (2007) Synthesis of TiO₂ nanoparticles by hydrolysis and peptization of titanium isopropoxide solution. *J Mater Process Technol* 189(1–3):296–300
- Mallakpour S, Nikkhoo E (2014) Surface modification of nano-TiO₂ with trimellitylimido-amino acid-based diacids for preventing aggregation of nanoparticles. *Adv Powder Technol* 25(1): 348–353
- Mamaghani AH, Haghighat F, Lee C-S (2019) Hydrothermal/solvothermal synthesis and treatment of TiO₂ for photocatalytic degradation of air pollutants: preparation, characterization, properties, and performance. *Chemosphere* 219:804–825
- Mandeh M, Omidi M, Rahaie M (2012) In vitro influences of TiO₂ nanoparticles on barley (*Hordeum vulgare* L.) tissue culture. *Biol Trace Elem Res* 150(1):376–380
- Mathew SS, Sunny NE, Shanmugam V (2021) Green synthesis of anatase titanium dioxide nanoparticles using cuminum cyminum seed extract; effect on mung bean (*Vigna Radiata*) seed germination. *Inorg Chem Commun* 126:108485
- May-Masnou A, Soler L, Torras M, Salles P, Llorca J, Roig A (2018) Fast and simple microwave synthesis of TiO₂/au nanoparticles for gas-phase photocatalytic hydrogen generation. *Front Chem* 6:110
- McNamara K, Tofail SAM (2017) Nanoparticles in biomedical applications. *Adv Phys X* 2(1): 54–88. <https://doi.org/10.1080/23746149.2016.1254570>
- Mekonnen MM, Hoekstra AY (2016) Four billion people facing severe water scarcity. *Sci Adv* 2(2):e1500323
- Miyazaki H, Hyodo T, Shimizu Y, Egashira M (2005) Hydrogen-sensing properties of anodically oxidized TiO₂ film sensors: effects of preparation and pretreatment conditions. *Sensors Actuators B Chem* 108(1–2):467–472
- Mozhayeva D, Engelhard C (2020) A critical review of single particle inductively coupled plasma mass spectrometry—a step towards an ideal method for nanomaterial characterization. *J Anal At Spectrom* 35(9):1740–1783
- Murray HH, Kogel JE (2005) Engineered clay products for the paper industry. *Appl Clay Sci* 29(3–4):199–206
- Mustafa F, Andreescu S (2020) Nanotechnology-based approaches for food sensing and packaging applications. *RSC Adv* 10(33):19309–19336
- Nadeem M, Tungmunnithum D, Hano C, Abbasi BH, Hashmi SS, Ahmad W, Zahir A (2018) The current trends in the green syntheses of titanium oxide nanoparticles and their applications. *Green Chem Lett Rev* 11(4):492–502
- Naseem T, Durrani T (2021) The role of some important metal oxide nanoparticles for wastewater and antibacterial applications: a review. *Environ Chem Ecotoxicol*
- Nasrollahzadeh M, Sajjadi M, Sajadi SM, Issaabadi Z (2019a) Green nanotechnology. *Interf Sci Technol* 28:145–198. Elsevier
- Nasrollahzadeh M, Sajadi SM, Issaabadi Z, Sajjadi M (2019b) Biological sources used in green nanotechnology. *Interf Sci Technol* 28:81–111
- Nguyen VT, Viet Tien V, Nguyen TA, Tran VK, Nguyen-Tri P (2019) Antibacterial activity of TiO₂-and ZnO-decorated with silver nanoparticles. *J Composites Sci* 3(2):61
- Nikolov AS, Atanasov PA, Milev DR, Stoyanchov TR, Deleva AD, Peshev ZY (2009) Synthesis and characterisation of TiO_x nanoparticles prepared by pulsed-laser ablation of Ti target in water. *Appl Surf Sci* 255(10):5351–5354
- Oh J, Feldman MD, Kim J, Condit C, Emelianov S, Milner TE (2006) Detection of magnetic nanoparticles in tissue using magneto-motive ultrasound. *Nanotechnology* 17(16):4183
- Órdenes-Aenishanslins NA, Saona LA, Durán-Toro VM, Monrás JP, Bravo DM, Pérez-Donoso JM (2014) Use of titanium dioxide nanoparticles biosynthesized by bacillus mycooides in quantum dot sensitized solar cells. *Microb Cell Factories* 13(1):1–10

- Pakseresht S, Cetinkaya T, Al-Ogaili AWM, Halebi M, Akbulut H (2021) Biologically synthesised TiO₂ nanoparticles and their application as lithium-air battery cathodes. *Ceram Int* 47(3): 3994–4005
- Pantidos N, Horsfall LE (2014) Biological synthesis of metallic nanoparticles by bacteria, fungi and plants. *J Nanomed Nanotechnol* 5(5):1
- Parrino F, Pomilla FR, Camera-Roda G, Loddo V, Palmisano L (2020) Properties of titanium dioxide 2. In *Titanium dioxide (TiO₂) and its applications*, pp 13
- Patil SR, Hameed BH, Škapin AS, Štangar UL (2011) Alternate coating and porosity as dependent factors for the photocatalytic activity of sol-gel derived TiO₂ films. *Chem Eng J* 174(1): 190–198
- Qiao J, Qi L (2021) Recent progress in plant-gold nanoparticles fabrication methods and bio-applications. *Talanta* 223:121396
- Rajakumar G, Abdul Rahuman A, Mohana Roopan S, Gopiesh Khanna V, Elango G, Kamaraj C, Abdur Zahir A, Velayutham K (2012) Fungus-mediated biosynthesis and characterisation of TiO₂ nanoparticles and their activity against pathogenic bacteria. *Spectrochim Acta A Mol Biomol Spectrosc* 91:23–29
- Rajkumari J, Maria Magdalane C, Siddhardha B, Madhavan J, Ramalingam G, Al-Dhabi NA, Arasu MV, Ghilan AKM, Duraipandiayan V, Kaviyarasu K (2019) Synthesis of titanium oxide nanoparticles using aloe *Barbadensis* mill and evaluation of its antibiofilm potential against *Pseudomonas aeruginosa* PAO1. *J Photochem Photobiol B Biol* 201:111667
- Raliya R, Tarafdar JC (2012) Novel approach for silver nanoparticle synthesis using *Aspergillus terreus* CZR-1: mechanism perspective. *J Bionanosci* 6(1):12–16
- Ramalingam V, Harshavardhan M, Hwang I (2020) Titanium decorated iron oxide (Ti@ Fe₂O₃) regulates the proliferation of bovine muscle satellite cells through oxidative stress. *Bioorg Chem* 105:104459
- Rani M, Shanker U (2020) Green photocatalytic synthesis activity of TiO₂ and its. *Handb Smart Photocatal Mater Fundamentals Fabrications Water Resour Appl* 22:11
- Rashidi L, Khosravi-Darani K (2011) The applications of nanotechnology in food industry. *Crit Rev Food Sci Nutr* 51(8):723–730
- Rehan M, Lai X, Kale GM (2011) Hydrothermal synthesis of titanium dioxide nanoparticles studied employing in situ energy dispersive X-ray diffraction. *Cryst EngComm* 13(11):3725–3732
- Ruiz AM, Cornet A, Morante JR (2004) Study of La and Cu influence on the growth inhibition and phase transformation of Nano-TiO₂ used for gas sensors. *Sensors Actuators B Chem* 100(1–2): 256–260
- Samy, S, and Shoutian Li. 1997. "Synthesis of nanoparticles by a laser-vaporisation-controlled condensation technique." In Ramachandran N (edds) *Materials research in low gravity*, 3123: 98–109. International Society for Optics and Photonics
- Santhoshkumar T, Rahuman AA, Jayaseelan C, Rajakumar G, Marimuthu S, Kirthi AV, Velayutham K, Thomas J, Venkatesan J, Kim S-K (2014) Green synthesis of titanium dioxide nanoparticles using *Psidium guajava* extract and its antibacterial and antioxidant properties. *Asian Pac J Trop Med* 7(12):968–976
- Saranya KS, Padil VVT, Senan C, Pilankatta R, Saranya K, George B, Waclawek S, Černík M (2018) Green synthesis of high-temperature stable anatase titanium dioxide nanoparticles using gum kondagogu: characterisation and solar driven photocatalytic degradation of organic dye. *Nano* 8(12):1002
- Sentein C, Guizard B, Giraud S, Yé C, Ténégal F (2009) Dispersion and stability of TiO₂ nanoparticles synthesized by laser pyrolysis in aqueous suspensions. *J Phys Conf Ser* 170: 12,013. IOP Publishing
- Sethy NK, Arif Z, Mishra PK, Kumar P (2020) Green synthesis of TiO₂ nanoparticles from *Syzygium Cumini* extract for photo-catalytic removal of Lead (Pb) in explosive industrial wastewater. *Green Process Synthesis* 9(1):171–181

- Sharma R, Sarkar A, Jha R, Sharma AK, Sharma D (2020) Sol-gel-mediated synthesis of TiO₂ nanocrystals: structural, optical, and electrochemical properties. *Int J Appl Ceram Technol* 17(3):1400–1409
- Shim SC, Choe BH, Jang IS, Choi DS, Lee JK, Cha BK, Choi WY (2014) Effect of TiO₂ nanotube arrays on osseointegration for dental implant. In: Mishra B, Ionescu M, Chandra T (eds) *Advanced materials research*, vol 922, pp 71–74. *Trans Tech Publ*
- Suman TY, Ravindranath RRS, Elumalai D, Kaleena PK, Ramkumar R, Perumal P, Aranganathan L, Chitrarasu PS (2015) Larvicidal activity of titanium dioxide nanoparticles synthesised using *Morinda Citrifolia* root extract against *Anopheles Stephensi*, *Aedes aegypti* and *Culex quinquefasciatus* and its other effect on non-target fish. *Asian Pacific J Trop Dis* 5(3): 224–230
- Sun Y, Wang S, Zheng J (2019) Biosynthesis of TiO₂ nanoparticles and their application for treatment of brain injury—An in-vitro toxicity study towards central nervous system. *J Photochem Photobiol B Biol* 194:1–5
- Swathi N, Sandhiya D, Rajeshkumar S, Lakshmi T (2019) Green synthesis of titanium dioxide nanoparticles using *Cassia fistula* and its antibacterial activity. *Int J Res Pharm Sci* 10:856–860
- Taran M, Rad M, Alavi M (2018) Biosynthesis of TiO₂ and ZnO nanoparticles by *Halomonas Elongata* IBRC-M 10214 in different conditions of medium. *BioImpacts: BI* 8(2):81
- Thakur BK, Kumar A, Kumar D (2019) Green synthesis of titanium dioxide nanoparticles using *Azadirachta Indica* leaf extract and evaluation of their antibacterial activity. *S Afr J Bot* 124: 223–227
- Theerthagiri J, Sunitha Salla RA, Senthil PN, Madankumar A, Arunachalam P, Maiyalagan T, Kim H-S (2019) A review on ZnO nanostructured materials: energy, environmental and biological applications. *Nanotechnology* 30(39):392001
- Thomas S, Pasquini D, Leu S-Y, Gopakumar DA (2018) *Nanoscale materials in water purification*. Elsevier
- Velmurugan R, Incharoensakdi A (2018) Nanoparticles and organic matter: process and impact. In: Tripathi DK et al (eds) *Nanomaterials in plants, algae, and microorganisms*. Elsevier, pp 407–428
- Viana MM, Soares VF, Mohallem NDS (2010) Synthesis and characterisation of TiO₂ nanoparticles. *Ceram Int* 36(7):2047–2053
- Wang W-N, Wuled Lenggoro I, Terashi Y, Kim TO, Okuyama K (2005) One-step synthesis of titanium oxide nanoparticles by spray pyrolysis of organic precursors. *Mater Sci Eng B* 123(3): 194–202
- Wei X, Zhu G, Fang J, Chen J (2013) Synthesis, characterisation, and photocatalysis of well-dispersible phase-pure anatase TiO₂ nanoparticles. *Int J Photoenergy* 2013:726872
- Xu J, Sun Y, Huang J, Chen C, Liu G, Jiang Y, Zhao Y, Jiang Z (2007) Photokilling cancer cells using highly cell-specific antibody–TiO₂ bioconjugates and electroporation. *Bioelectrochemistry* 71(2):217–222
- Yang Z, Choi D, Kerisit S, Rosso KM, Wang D, Zhang J, Graff G, Liu J (2009) Nanostructures and lithium electrochemical reactivity of lithium titanites and titanium oxides: a review. *J Power Sources* 192(2):588–598
- Yin S, Zhang Q, Saito F, Sato T (2003) Preparation of visible light-activated titania photocatalyst by mechanochemical method. *Chem Lett* 32(4):358–359
- Zahir AA, Chauhan IS, Bagavan A, Kamaraj C, Elango G, Shankar J, Arjaria N, Roopan SM, Rahuman AA, Singh N (2015) Green synthesis of silver and titanium dioxide nanoparticles using *Euphorbia Prostrata* extract shows shift from apoptosis to G0/G1 arrest followed by necrotic cell death in *Leishmania Donovanii*. *Antimicrob Agents Chemother* 59(8):4782–4799
- Zahra Z, Habib Z, Chung S, Badshah MA (2020) Exposure route of TiO₂ NPs from industrial applications to wastewater treatment and their impacts on the agro-environment. *Nano* 10(8): 1469

- Zhang H, Banfield JF (2014) Structural characteristics and mechanical and thermodynamic properties of nanocrystalline TiO₂. *Chem Rev* 114(19):9613–9644
- Zhu X, Pathakoti K, Hwang H-M (2019) Green synthesis of titanium dioxide and zinc oxide nanoparticles and their usage for antimicrobial applications and environmental remediation. In: Shukla A, Irvani S (eds) *Green synthesis, characterisation and applications of nanoparticles*. Elsevier, pp 223–263
- Ziental D, Czarczynska-Goslinska B, Mlynarczyk DT, Glowacka-Sobotta A, Stanis B, Goslinski T, Sobotta L (2020) Titanium dioxide nanoparticles: prospects and applications in medicine. *Nano* 10(2):387
- Zuverza-Mena N, Martínez-Fernández D, Wenchao D, Hernandez-Viezcás JA, Bonilla-Bird N, López-Moreno ML, Komárek M, Peralta-Videa JR, Gardea-Torresdey JL (2017) Exposure of engineered nanomaterials to plants: insights into the physiological and biochemical responses-a review. *Plant Physiol Biochem* 110:236–264



Characterization of Nontoxic Nanomaterials for Biological Applications

15

Ashna Poulouse, T. Shibina, T. Sreejith, Anitta Sha Mercy, Drisya Das, K. Haritha, A. K. Sijo, George Mathew, and Pramod K. S.

Abbreviations

^1H NMR	Proton nuclear magnetic resonance spectroscopy
AAS	Atomic absorption spectroscopy
AFM	Atomic Force Microscopy
BET	Brunauer–Emmett–Teller analysis
BIF	Back field imaging mode
BSE	Back scattered electrons
CARS	Coherent anti-Stokes Raman spectroscopy
DLS	Dynamic light scattering
DMA	Dynamic mechanical analysis
DSC	Differential scanning calorimetry
DTA	Differential thermal analysis
ED	Electron diffraction mode
EGA	Evolved gas analysis
EPR	Electron paramagnetic resonance
ESR	Electron spin resonance spectroscopy
EXAFS	Extended X-ray absorption fine structures
FCC	Face centered cubic
FTIR	Fourier transform infrared spectroscopy
HAADF	High angle annular dark field
HRTEM	High-resolution TEM
ICDD	International Centre for Diffraction Data
ICP-MS	Inductively coupled plasma mass spectrometry

A. Poulouse · T. Shibina · T. Sreejith · A. S. Mercy · D. Das · K. Haritha · A. K. Sijo · G. Mathew · P. K. S. (✉)
Department of Physics, St. Mary's College, Sulthan Bathery, Kerala, India

© The Author(s), under exclusive license to Springer Nature Singapore Pte Ltd. 2023

P. V. Mohanan, S. Kappalli (eds.), *Biomedical Applications and Toxicity of Nanomaterials*, https://doi.org/10.1007/978-981-19-7834-0_15

363

ICP-OES	Inductively coupled plasma optical emission spectroscopy
IR	Infrared
Mossbauer	Mossbauer spectroscopy
MRI	Magnetic resonance imaging
NGR	Nuclear gamma resonance spectroscopy
NMR	Nuclear magnetic resonance spectroscopy
NPs	Nanoparticles
PL	Photoluminescence
PLE	PL excitation spectroscopy
ppm	Parts-per-million
ppq	Parts-per-quadrillion
ppt	Parts-per-trillion
QUELS	Quasi-elastic light scattering
RAMAN	Raman spectroscopy
SEM	Scanning electron microscope
SERS	Surface-enhanced Raman scattering spectroscopy
SPM	Scanning probe microscopy
STEM	Scanning TEM
TEM	Transmission electron microscope
TERS	Tip-enhanced Raman scattering spectroscopy
TGA	Thermogravimetric analysis
TMA	Thermomechanical analysis
UV-Visible	UV-visible spectroscopy
VSM	Vibrating-sample magnetometer
XANES	X-ray absorption near edge structure
XAS	X-ray absorption spectroscopy
XPS	X-ray photoelectron spectroscopy
XRD	X-ray diffraction

15.1 Introduction

Richard P. Feynman, in his famous talk “There is plenty of room at the bottom,” predicted that one day we will be making things at the atomic level. And since these small things will build upwards, we will be able to make them more precisely and control what we want them to do.

There are two unique aspects of nanomaterials.

1. Compared to bulk materials, nanoscale materials have a high surface area to volume ratio. This will provide a large area for reactions and thereby an exponential increase in reaction rate per molecule.
2. As the particle size reduces beyond 100 nm, the visible light (400–700 nm) starts to interact with these particles, which manifests as different colors, for example,

the color of nanogold is not golden but red, orange or blue and the color depends on the particle size of nanoparticles. Thus, the optical, chemical, electrical, thermal, and mechanical properties of nanoparticles may differ from that of bulk counterparts. These surprising and interesting features enable the extensive use of nanoparticles in various fields. In this context, it is very important to evaluate the size and structural features of novel nanoparticles. The precise and detailed characterization enables the proper use of nanomaterials, ultimately deciding their acceptance in society.

While thinking about the preparation, characterization, and end use of nanomaterials, two facts deserve much importance.

1. It may be easy to prepare nanoparticles of size less than 100 nm, but it is not very easy to keep these nanoparticles at the required size range. They tend to agglomerate and form micro-particles unless capping agents are used during their preparation stage.
2. Even though many nanomaterials serve mankind in multiple ways, all nanomaterials are not bio-friendly. They can be environmentally hazardous and may be toxic to life forms. Therefore, their use in optimized concentrations must be ensured, and for this, the characterization of their properties is essential.

This chapter throws light on the various techniques used for the characterization of nanoparticles and nanomaterials. These include microscopic, chemical and biological techniques, spectral analysis, optical property characterizations and techniques for assessing magnetic, rheological, and electrical properties.

For a quick grasp of content, the reader is directed to Fig. 15.1, which presents all the characterization techniques discussed in this chapter.

15.2 Physical and Morphological Characterization

Some of the main physical and morphological characterization techniques are Scanning Electron Microscopy (SEM), Transmission Electron Microscopy (TEM), BET Surface Area analysis, and Atomic Force Microscopy (AFM). These techniques can provide information regarding the size, size distribution, aspect ratio, surface area, degree of aggregation, porous nature, etc. The importance of morphological characterization lies in fact and saying that “*Seeing is believing.*”

15.2.1 Scanning Electron Microscopy (SEM)

Conventional optical microscopy uses optical light. Its resolution is limited to its optical wavelength of the order of 500 nm with a maximum magnification of about a thousand times. The characterization of structures on a nanoscale is often best performed by electron microscopy. It yields information about topography,

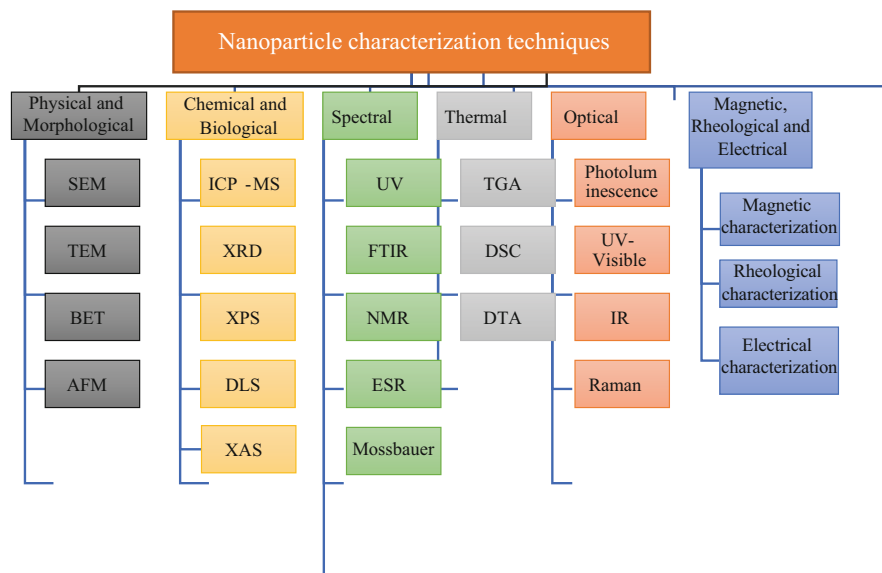


Fig. 15.1 Techniques for the characterization of nanoparticles

morphology, composition, and crystallographic information. Electron microscopy uses the principle of high energy-focused electron beam as a radiation source to image the sample with nanometer precision. The electron microscopy techniques use the high energy focused electrons beam as scanning signal, which has de Broglie wavelength of the order of 0.4 nm. Therefore, it can provide better resolution and magnification compared to an optical microscope. When a sample is exposed to a beam of high-energy electrons, there are many possible events that can happen. These are represented in Fig. 15.2.

In SEM, information collected about the sample is obtained from the scattered electrons and X-ray photons from the sample (Egerton 2005; McMullan 1995). SEM can provide information about surface roughness (Banerjee et al. 2009), chemical composition (SEM-EDAX) (Srinivasan et al. 2007), electrical behavior, and crystal structure of the surface of the sample (Sujata and Jennings 1991). Figure 15.3 shows the Schematic representation of SEM.

In SEM, the primary electrons emitted by the electron gun are accelerated to high kinetic energy. This is done by passing them through an anode connected to a large positive potential of the order of 2–40 keV with respect to the electron gun. Electromagnetic condenser lenses focus the electron beam into a fine probe. This focused beam passes through a scanning coil, which deflects the beam into the desired direction and scans the desired spot on the sample. The objective lens is used to focus the electron beam into a small region on the sample surface. When a highly focused electron beam strikes the sample, some of these electrons are scattered elastically with an angle greater than 90° to the incident direction and with kinetic energy almost the same as that of incident primary electrons. These are called Back

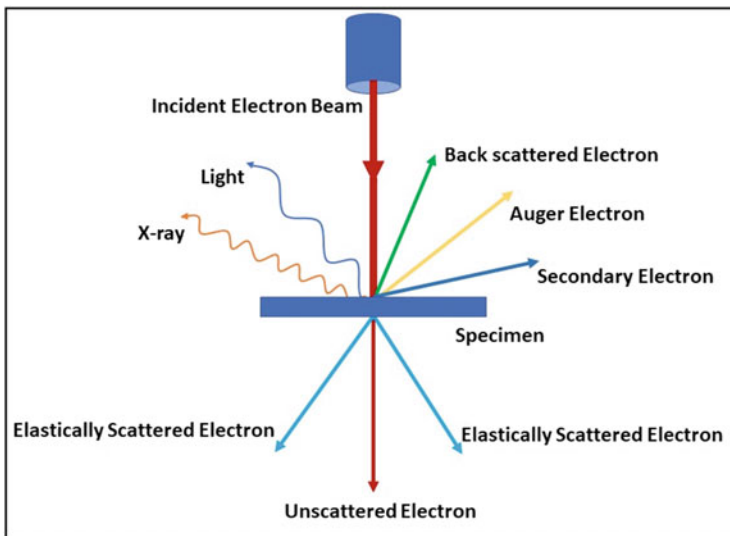


Fig. 15.2 Interaction of electron beam with the sample

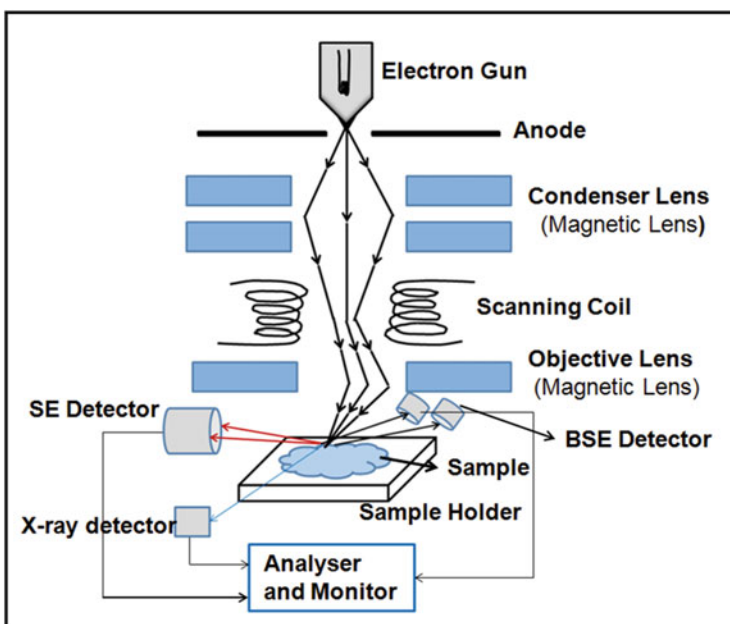
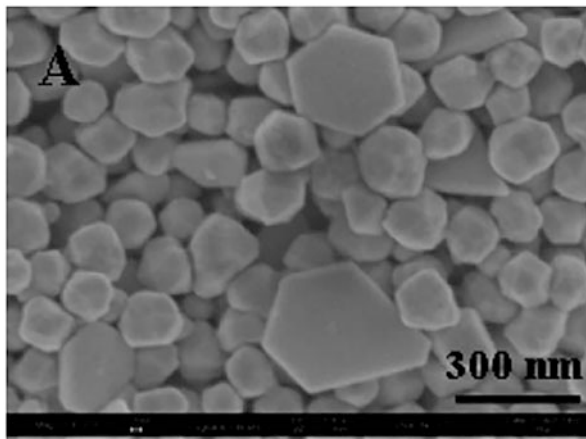


Fig. 15.3 Schematic representation of SEM instrument

Fig. 15.4 SEM images of the gold nanoparticles formed by the reaction of 1 mM HAuCl_4 and 5% Diopyros kaki leaf broth at 25 °C (Song et al. 2009)



Scattered Electrons (BSE). Some valance electrons of atoms at the sample surface get emitted due to their interaction (inelastic) with primary electrons. They are called Secondary Electrons (SE). Characteristic X-rays are generated from the sample atom when the incident beam knocks out an inner shell electron, and at the same time, an outer shell electron moves into the empty orbit. These SE, BSE, and X-rays are collected by various detectors arranged in a specimen chamber. The signals from each detector and synchronized incident beam signal (raster-scanned signal) are fed to the analyzer, which produces the magnified image of the sample, and the image is displayed on the display system.

One of the advantages of SEM over other electron microscopes is that it does not need any special sample preparation, as in the case of TEM. SEM permits the nondestructive evaluation of the sample. The main limitations of the SEM are that it can image only the surface of a few nanometers deep, it cannot examine live cell specimens, and it can give only black and white images (Fig. 15.4).

15.2.2 Transmission Electron Microscope (TEM)

It is an already established fact that the uniqueness of nanomaterials is their very high surface area to volume ratio. This becomes more important for porous materials where internal surface area also comes in to picture, especially in use as catalysts and adsorbents, etc. Internal cavities and canals present in nanoparticles can effectively reduce the required concentration of nanomaterials for a certain activity. Their characterizations therefore deserve importance. In Transmission electron microscopy (TEM), a beam of electrons is transmitted through a very thin specimen to form an image that reveals the sample's internal structure. An image is formed from the interaction of the electrons with the sample as the beam is transmitted through the specimen. The image is then magnified and focused onto an imaging device, such as a fluorescent screen, a layer of photographic film, or a sensor such as a scintillator

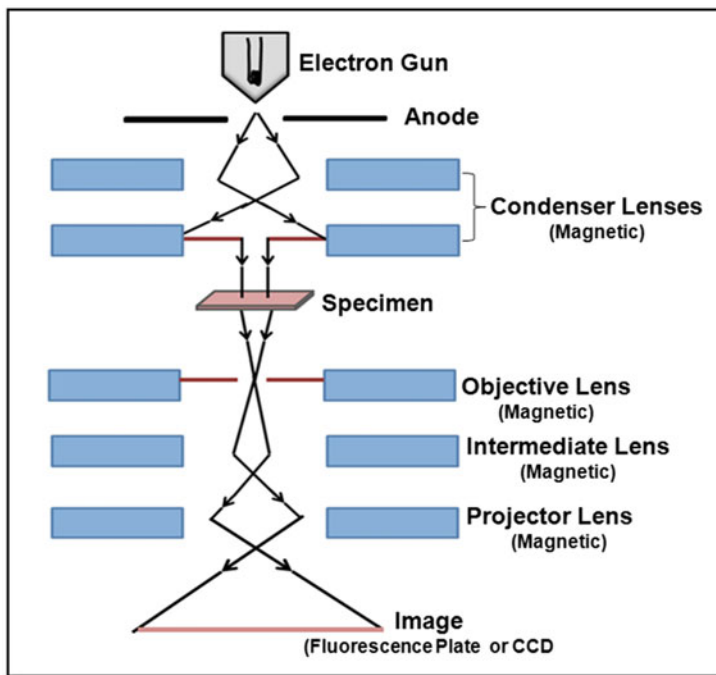
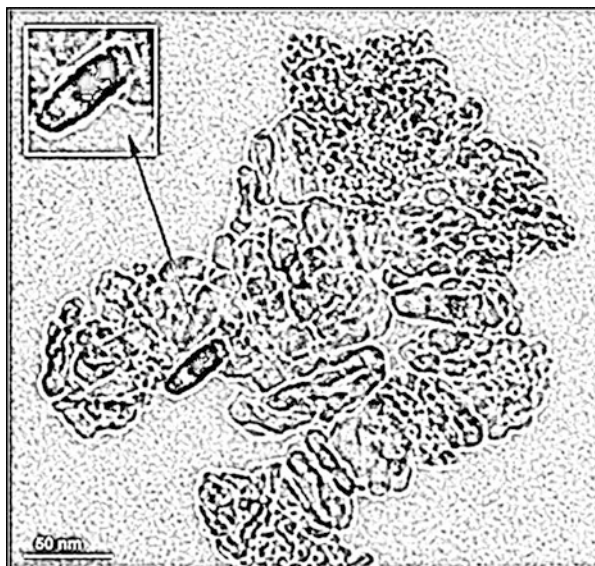


Fig. 15.5 Schematic representation of TEM

attached to a charge-coupled device. TEM specifically gives information about the inner structure of the sample, such as topographical, morphological composition, and crystalline structure, and produces magnification power up to 2 million times the specimen. One of the crucial aspects while using TEM is that the sample must be ultrathin to transmit the electron, and hence it requires special sample preparation techniques. TEM gives a depth resolution of 1–10 nm and lateral resolution of 0.1–1 nm (Fultz and Howe 2012; Wang 2000; Reimer and Kohl 2013). TEM has multiple imaging modes that enable the examination of specimens from various aspects. Back Field imaging mode (BIF), Electron Diffraction mode (ED), High-Resolution TEM (HRTEM), Scanning TEM (STEM), and High Angle Annular Dark Field (HAADF) are some imaging modes. TEM provides information about the internal microstructure rather than just the internal structure as SEM. Figure 15.5 is the schematic representation of TEM.

In TEM, electrons emitted by the electron gun are accelerated to high energy intense beam by applying a large positive potential (80–200 kV) to an anode electrode with respect to the electron gun. Therefore, these electrons can penetrate the thickness up to 1 μm . Electromagnetic condenser lenses will focus this beam into a specially prepared ultrathin sample, which is to be observed. The transmitted electron beam is focused by the electromagnetic objective lens towards the projector lens, magnifying the transmitted beam and focusing on the fluorescence screen or

Fig. 15.6 A representative image of TiO_2 nanoparticles characterized by TEM (Palaniappan and Pramod 2011)



CCD. It produces an image of the sample. The image formed will be two-dimensional and black and white. TEM works under a high vacuum which is essential to ensure electrons do not collide with gas atoms (Fig. 15.6).

15.2.3 Brunauer–Emmett–Teller (BET) Surface Area Analysis

One of the main criteria to entitle a material as a nanomaterial is its specific surface area. Owing to very small particle size, the surface area to volume ratio of nanomaterials is very high compared to bulk materials. Many interesting features of nanoparticles rise from their small size and very large surface area, for example, the use as a catalyst and the ability to exhibit adsorption. For bulk, the surface area to volume in relation to the number of atoms is insignificant. Brunauer–Emmett–Teller (BET) analysis is used to determine the specific surface area of nanomaterials. The physical adsorption of gas molecules on the exposed surface of a material is utilized to measure the specific surface area and understand the porous material's texture. This adsorption also depends on the experimental conditions like temperature, gas pressure, and the interaction between gas and the sample material (Ansari et al. 2018). The usual gas used in BET analysis is nitrogen because of its availability in high purity and the ability to form strong interaction with most of the solids. Prior to the experiment, the samples must be dried and degassed at the required temperatures. This can ensure the removal of water and already adsorbed gases. The samples are usually maintained in low temperatures for strong interaction with the sample surface and the gas. Known amounts of nitrogen gas are released successively to the sample under controlled pressure. Pressure transducers are used to monitor

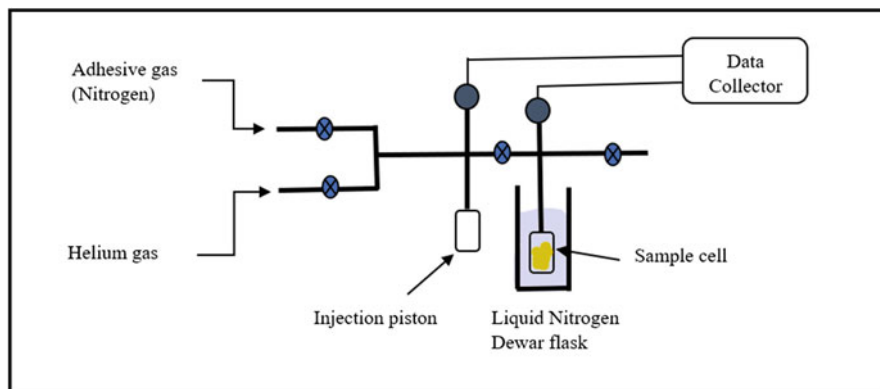


Fig. 15.7 Schematic representation of BET

pressure changes accurately and precisely. After the formation of the adsorption layer, the sample is removed from the nitrogen atmosphere and heated to release the adsorbed gas (Raja and Barron 2021). A BET isotherm is plotted with the amount of gas adsorbed as a function of the relative pressure. The information from the isotherm is used to determine the specific surface area of the sample. The specific surface area is expressed in the units of area per mass of sample (m^2/g) (Sing 2001). Figure 15.7 shows the schematic representation of BET analysis.

The BET analysis confirms the results from XRD and TEM methods. If the nanoparticles are assumed to be spherical, the average diameter can be calculated by the below equation,

$$D = \frac{6000}{\rho S_w} \quad (15.1)$$

where S_w is specific surface area in m^2/g and ρ is the theoretical density in g/cm^3 (Wei et al. 2009a, b). Correlation between the results of size determination through different methods needed for size-depending applications. The difference in the sample size obtained through BET indicates the agglomeration of nanosized particles to micro size range. This, in turn, reduces the specific surface area of the particle size to become large.

15.2.4 Atomic Force Microscopy (AFM)

Atomic force microscopy (AFM) is a very high-resolution type of scanning probe microscopy (SPM), with demonstrated resolution on the order of fractions of a nanometer. It is more than 1000 times better than the optical diffraction limit. AFM is usable in various disciplines such as fundamental surface science, routine surface roughness analysis, and spectacular 3D imaging. This imaging tool has a vast dynamic range, spanning the realms of optical and electron microscope. It is also a

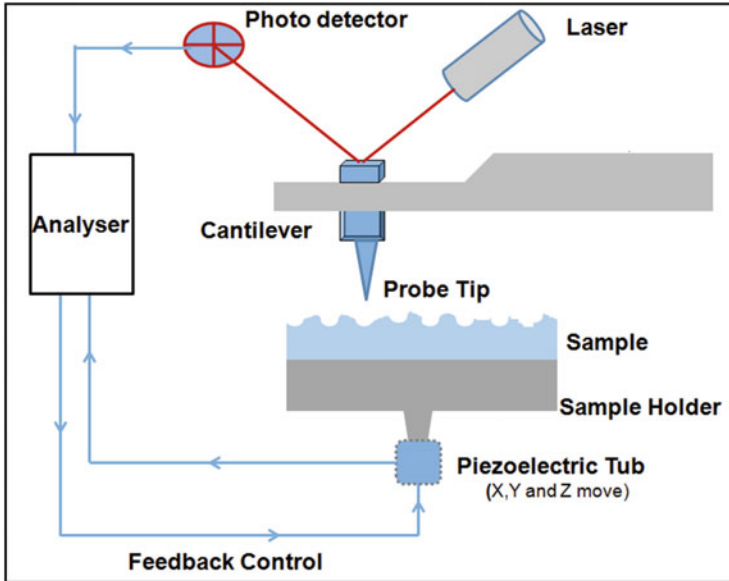


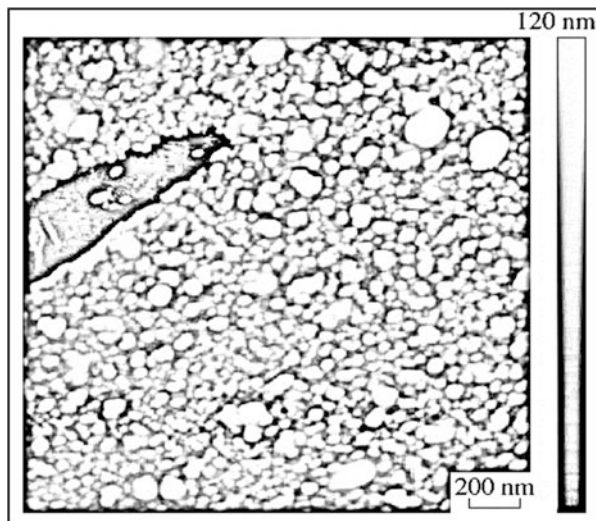
Fig. 15.8 Schematic representation of AFM

profiler with unprecedented 3D resolution. In some cases, AFM can measure physical properties such as surface conductivity, static charge distribution, and elastic moduli. AFM can image both conducting and nonconducting samples at atomic resolution (Eaton and West 2010; Rugar and Hansma 1990; Giessibl 2003). It uses the principle of a thin cantilever with a spring constant weaker than the equivalent spring between atoms. This allows scanning over a sample surface mechanically with a sharp tip attached to the cantilever to get the image of atomic-scale topography. A schematic of AFM is given in Fig. 15.8.

The main components of AFM are a sharp tip mounted on a soft cantilever spring, a way of sensing the cantilever deflection (LASER and Photodetector), a feedback system to monitor and control the deflection and interactive forces. A mechanical scanning system (usually piezoelectric) that moves the sample with respect to the tip in a raster pattern and display system that convert measured data into an image. When the probe tip of AFM is brought into proximity of the sample surface, the forces such as Vander Waal's force, electrostatic force, magnetic force, and other forces which arises due to the physical interaction between the surface atoms of the sample and probe tip causing deflection of the cantilever tip. The deflections are synchronized with the Laser and photodetector system and which produces the 3D images of the sample.

The atomic force microscope (AFM) is used for the examination of forensic evidence examination and has found many applications in biological sciences. The AFM can be used to image the structure of soft biological materials in their inherent environments, in product development, quality control in the optical, semiconductor,

Fig. 15.9 AFM image of a glass portion entirely covered by nanoparticles formed by femtosecond laser modification of C–Si surface at a residual pressure of 0.1 mbar (Golovan et al. 2009)



and magnetic recording industries and biological applications such as the sequencing of DNA, and to watch biological processes such as polymerization of the blood coating protein fibrin. (Lopour 2001; Liu and Wang 2010) (Fig. 15.9).

15.3 Chemical and Biological Characterization

Irrespective of the bulk material and its chemical composition, the chemistry of the surface has considerable importance. It is this surface chemistry that makes a surface polar or nonpolar, inert or reactive, frictionless or rough. One of the main areas that emerged in this field is chameleon coatings, where the surface roughness is tunable with preferential migration of one of the components to the surface as temperature changes. In this context, the surface chemistry of nanomaterials deserves much importance. The chemical composition, surface chemistry, stability, crystalline nature and structure, concentration in biological fluids, etc., of nanoparticles can be obtained through various chemical and biological characterization techniques. The following section provides a brief overview of some of the chemical and biological characterization techniques.

15.3.1 X-Ray Diffraction (XRD)

X-ray diffraction (XRD) is a rapid analytical nondestructive technique that provides information about the crystallographic texture of nanomaterials. It enables crystal structure identification, crystallite grain size, and calculation of lattice parameter calculation precisely and accurately. This establishes the relationships between the crystal structure and the physical and chemical properties of the nanomaterial under

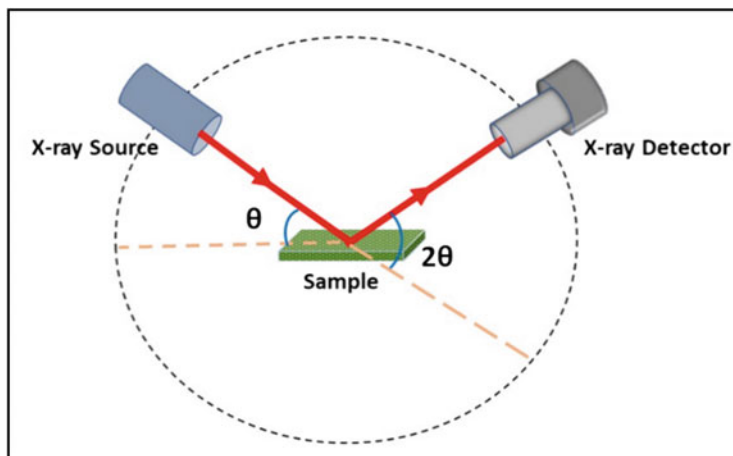


Fig. 15.10 Schematic representation of XRD

investigation. XRD is an ideal method for material studies because of its non-contact and nondestructive nature. When X-rays with a certain frequency encounter a material, they are scattered by the electrons of the material elastically. If the scattered beams are in phase, they interfere constructively and get the intensity maximum at that particular angle (Sharma et al. 2012). The interaction of the incident rays with the sample produces constructive interference when conditions satisfy Bragg's Law.

$$n\lambda = 2d \sin \theta \quad (15.2)$$

where λ is the wavelength of electromagnetic radiation (here, X-ray), θ is the diffraction angle, d is the lattice spacing in a crystalline sample, and n is an integer. Usually, the wavelength of X-rays, ranging from 0.1 to 100 Å, which is in the range of interatomic distances (Lavina et al. 2014). Figure 15.10 shows the schematic representation of the XRD instrument, where the X-ray source and the X-ray detector are situated on the circumference of the focusing circle and specimen stage at the center of the circle.

From the diffraction pattern, the particle sizes can also be quantitatively evaluated using the Debye–Scherrer equation,

$$d = \frac{k\lambda}{\beta \cos \theta} \quad (15.3)$$

which gives a relationship between peak broadening in XRD and particle size. Where d is the particles size, k is the Debye–Scherrer constant (0.89), λ is the wavelength of X-ray (0.15406 nm), and β is the full width at half maximum and θ is the Bragg angle (Dung et al. 2009). X-ray diffraction patterns with broad peaks indicate the ultrafine nature and small crystallite size of the samples (Zipare et al. 2018).

The diffraction pattern is like a fingerprint of the crystal structure. By comparing the reference pattern from International Centre for Diffraction Data (ICDD) database, the structure of the particles can be evaluated (Mourdikoudis et al. 2018). In the case of iron oxide nanoparticles, Fe_3O_4 (magnetite phase) and $\gamma\text{-Fe}_2\text{O}_3$ (maghemite phase), their formation is confirmed using the XRD pattern. Magnetite has face-centered cubic (FCC) crystal structure with sharp and intense peaks, confirming its highly crystalline nature. Maghemite has a slight shift of peaks compared to magnetite. Thus, we can identify the formation of both phases (Krishna et al. 2012). XRD is also used to check the coating in the nanomaterial surface, which increases the size of the particle. Cation distributions in nanocomposites are evaluated by relatively integrated intensity calculations from the XRD data (Zipare et al. 2018). Even though XRD is a versatile tool for determining the crystalline nature of a sample, it is very difficult to identify two or more chemicals that occupy the same crystallographic site.

15.3.2 Inductively Coupled Plasma Mass Spectrometry (ICP-MS)

The detection of metals, especially metal nanoparticles in drug formulations, polluted water, and foodstuff, is very important. The presence of metals in ppm levels can be analyzed by AAS (atomic absorption spectroscopy), in ppt levels by ICP-OES (inductively coupled plasma optical emission spectroscopy), and in ppq levels by inductively coupled plasma mass spectrometry (ICP-MS). ICP-MS is an analytical technique used to measure the concentration and size distribution of NPs at trace levels in biological fluids. It also provides molecular information about the composition, structure, and chemical state of nanoparticles (Mourdikoudis et al. 2018). For obtaining the best quality, sample preparation and sample introduction methods are very crucial in the ICP-MS method. In this technique, as the name indicates, the sample materials are lead through a plasma source and become ionized. Based on their mass, ions are sorted. This method has an extremely low detection limit, so highly diluted samples are analyzed (Olesik 1991). Figure 15.11 shows the main parts of the ICP-MS instrument.

The induction system consists of a device that carries the sample to the nebulizer. That may include a peristaltic pump and an autosampler. The nebulization system transforms the liquid sample into a spray of light drops. Then the nebulized sample is entered into the ICP compartment containing argon plasma, where the sample is ionized instantaneously. These ions are then transferred to an interface region consisting of a skimmer and the sampler cone. This subsequent cone helps to focalize the ions into small volumes. The next part is the Mass spectrometer, where the ions are separated according to their mass. The last part is a detection system that converts the ionic signals into electric pulses (Aceto 2016; Wilschefski and Baxter 2019).

ICP-MS, which is one of the best examples of the hyphenated technique, is usually applied during the synthesis of nanoparticles so that the total concentration of nanoparticles in the colloidal solution can be precisely determined. This method is

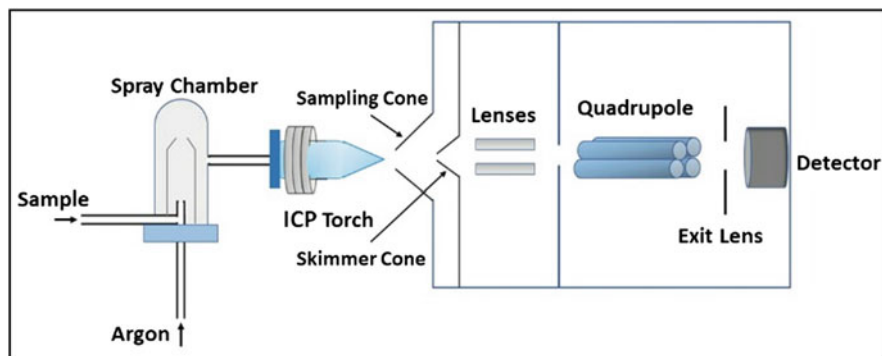


Fig. 15.11 Schematic diagram of ICP-MS

used to determine the size distribution of gold nanoparticles. But ICP-MS signal does not provide direct information on the size of the particle. If the particle shape and density are known, then the size can be estimated from the total mass of the measuring element (Olesik and Gray 2012). The intensity of the signal at the detector indicates the mass of the nanoparticle (Scheffer et al. 2008). The incorporation of different functional groups and biomolecules in nanomaterials can also be detected by using this technique. Quantification of the amount and size distribution of metallic nanoparticles suspended in aqueous matrices is done precisely by the ICP-MS method (Lee et al. 2014).

15.3.3 X-Ray Photoelectron Spectroscopy (XPS)

Surface chemistry of materials is important, not only for catalytic properties resulting from surface porosity and roughness but also on the perspective of the surface polarity of printable materials. Very smooth surfaces must be converted to rough by treatment with a corona discharge and very nonpolar surfaces to polar surfaces by proper surface chemical modifications. The extent of surface chemical modification can be analyzed by XPS. Elemental composition, contaminants at the surface of nanomaterial, chemical state, binding energies within nanomaterial, and peculiarities of electronics states are determined through this technique. The basic principle behind XPS is the photoelectric effect. The monochromatic X-rays penetrate the nanomaterial and eject an electron from the core-level orbitals of an atom within the nanomaterial. These ejected electrons with unique energy values are characterized by an electron energy analyzer. Every element has a particular set of peaks in the photoelectron spectrum corresponding to photon energy and binding energies. The intensity of peaks indicates the concentration of the selected element. XPS method provides information without any significant damage to the sample (Holbrook et al. 2015).

For surface-modified nanomaterials, XPS identifies the depth of the surface layer. XPS is applied to study the surface composition and interactions of the deposited nano complexes. For this relatively small amount of nano, a complex suspension is needed (Korin et al. 2017). In the case of nanocatalyst preparation, the interaction between the precursor and the substrate is confirmed by using XPS (Arroyo-Ramírez et al. 2009). XPS is used to determine the thickness of protein coating in coated gold nanoparticles. The absorbed peptides in the interfaces of the gold nanoparticle are also detected by this method (Belsey et al. 2015). XPS can provide information about elemental distributions, surface coating thickness and surface functionalities of nanomaterials, and various natural materials with nano-size (Baer and Engelhard 2010).

15.3.4 Dynamic Light Scattering (DLS)

DLS is also known as photon correlation spectroscopy or quasi-elastic light scattering (QUELS), employed to find the size of nanoparticles in colloidal dispersions. Due to the continuous Brownian motion of nanoparticles in colloidal solution, the light scattering intensity fluctuates. This fluctuation is directly related to the diffusion coefficient of the particle. This is, in turn, related to the hydrodynamic radius of the particle. Thus, the size of the particle can be determined by measuring the light scattering intensity (Holbrook et al. 2015). For effective measurements, low nanoparticle concentration is desired. In hyperthermia studies using magnetic nanoparticles, the effect of aggregation on the heating abilities of nanomaterial is evaluated by using DLS (Guibert et al. 2015; Kusigerski et al. 2019). During aqueous ferrofluid preparation, the colloidal properties like hydrodynamic size, polydispersity index, and zeta potential are obtained by DLS (Behdadfar et al. 2012).

15.3.5 X-Ray Absorption Spectroscopy (XAS)

XAS is a broadly used method to investigate the chemical composition and electronic states of nanomaterials. It measures the X-ray absorption coefficient of a material as a function of energy. Each element has a specific set of X-ray absorption patterns corresponding to its electron binding energies. XAS is a highly sensitive technique convenient to identify the chemical state of species even at very low concentrations (Mourdikoudis et al. 2018). XAS consists of high intensity, coherent X-ray beam with a wide energy range. XAS spectra consist of three major classes of features. The first energy range is due to the absorption of an incident photon by core-level electron ejection. The next feature above this energy range is known as X-ray absorption near-edge structure (XANES). The near-edge regime of XAFS provides information on the unoccupied electronic states of a system (Mårtensson et al. 2013). At higher energies, extended X-ray absorption fine structures (EXAFS) are seen. The elemental composition, oxidation state, and electronic structure of the

selected sample can be evaluated by analyzing the above features and referring to the known structure (Holbrook et al. 2015).

XAS has been employed in the characterization of many nanomaterial-containing systems. Nanoparticle ferrites with iron atoms and additional metals in ferrites are investigated by X-ray absorption near-edge spectroscopy (XANES) and extended X-ray absorption fine structure (EXAFS) to determine the type of their spinel ferrite structure (Nilsen et al. 2007). XANES is used to understand the nature of the growing Ge nanoparticles. Also, XAS/EXAFS is utilized as a method to monitor the mechanism and kinetics of the Ge nanoparticle formation reaction from Mg_2Ge and $GeCl_4$ (Pugsley et al. 2011).

15.4 Spectral Characterization

Matter and radiation are the children of the universe. The interaction of matter with radiation gives rise to spectra, and the branch is called spectroscopy. While spectroscopy deals with the interaction of matter and radiated energy, spectrometry is the study of measuring a specific spectrum and the measurement of radiation intensity and wavelength.

The spectral behavior of nanoparticles is different from that of their bulk counterparts. The response of nanoparticles with various ranges of electromagnetic magnetic radiation is determined through different spectroscopic techniques. The following sections illustrate various spectroscopic techniques used for the characterization of nanoparticles.

15.4.1 UV-VIS Spectroscopy

UV-Vis spectroscopy (UV-Vis) is a technique used to measure the intensity of light absorbed and scattered by a sample. A sample is placed between a light source and a photodetector, and the intensity of UV-Vis light is measured before and after passing through the sample. The intensity of light transmitted is plotted as a function of wavelength. UV-Vis spectroscopy allows the identification and spectral characterization of nanomaterials. It even gives the idea about the stability of nanoparticles in colloidal solutions. Block diagram and details of UV-Vis spectroscopy are included in Sect. 15.6.2.

15.4.2 Fourier Transform Infrared Spectroscopy (FTIR)

FTIR spectroscopy is a powerful tool for identifying the chemical constituents and chemical bonds in nanomaterials by producing an infrared absorption spectrum. In the IR region, the electromagnetic waves mainly couple with the vibrational motion of the molecule. Depending on the elements and type of bonds, particular IR frequency radiation is being absorbed. The wavelength of radiation absorbed is

specific for each constituent. So, by comparing with the known results, one can easily identify the composition of a nanomaterial. Block diagram and some characterization results using FTIR are included in Sect. 15.6.3.

15.4.3 Nuclear Magnetic Resonance Spectroscopy (NMR)

The energy of radiofrequency radiation is very small to vibrate, rotate, or excite an atom or molecule, but it is sufficient to affect the nuclear spin of the atoms. NMR spectroscopy is an analytical technique that exploits the magnetic properties of nuclei. In NMR spectroscopy, radiofrequency waves induce transitions between magnetic energy levels of nuclei of a molecule. The theory behind NMR comes from the spin of a nucleus, and it generates a magnetic field, the nuclear spins are in random directions. In an external magnetic field, the nuclei align themselves either with or against the external field, an energy transfer is also possible from ground to excited state. When the spin returns to the ground state level, the absorbed radiofrequency energy is emitted that gives the NMR spectrum of the specific nucleus. Both liquid and solid types of samples can be used in NMR spectroscopy. The NMR spectrum is a plot of the intensity of NMR signals vs magnetic field (frequency) (Fig. 15.12).

Proton nuclear magnetic resonance spectroscopy (^1H NMR) is one of the most powerful tools to give information about the type and number of hydrogen atoms in a molecule. ^1H NMR spectra of most organic compounds are characterized by chemical shifts and by spin-spin coupling between protons. It can also be used for purity determination providing the structure and molecular weight of the compound. The best-known application of NMR is Magnetic resonance imaging (MRI) for medical

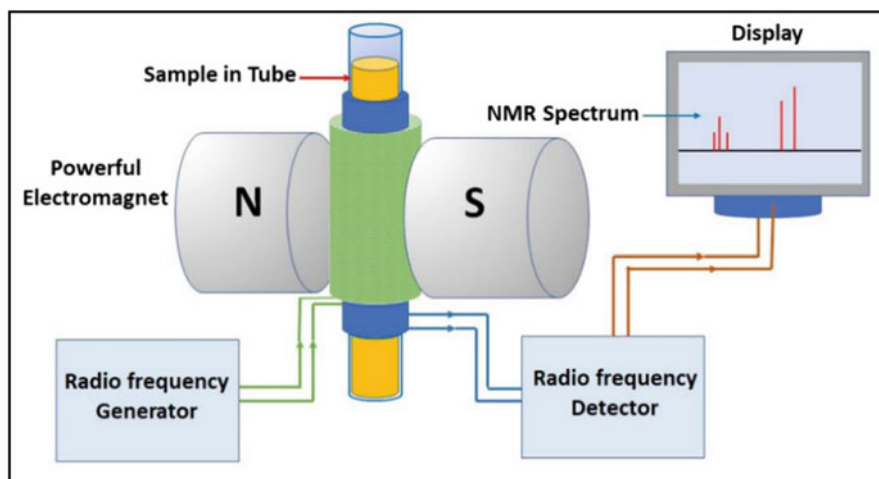


Fig. 15.12 Schematic diagram of key components of NMR spectroscopy

diagnosis. It is useful for identifying drug leads and determining the conformations of the compounds bound to enzymes, receptors, and other proteins.

15.4.4 Electron Spin Resonance Spectroscopy (ESR)

It is a nondestructive analytical technique also known as Electron paramagnetic resonance (EPR) or Electron magnetic resonance (ESR) that is based on the absorption of microwave radiation by a paramagnetic substance when it is exposed to a strong magnetic field. When a paramagnetic material (containing unpaired electrons) is subjected to a magnetic field, spin energy level splitting of an electron occurs. Applied suitable microwave radiation causes the transition between these spin levels. The resulting absorption of microwave radiation is modulated to record. Klystron tube act as microwave source stabilized against temperature fluctuations. The modulation of the signal is accomplished by a small alternating variation of the magnetic field, which is produced by supplying an AC signal to the modulation coil oriented to the sample (Fig. 15.13).

It is a direct method to detect the presence of free radicals and to identify the paramagnetic species. It can be used to study the reaction mechanism of free radicals, photochemical, and polymerization reactions. Its applicability is seen in the determination of oxidation state and conducting properties of the superconducting materials and determination of the presence of oil under the earth. Many studies have been reported based on EPR spectra, including the detection of free radicals in human skin biopsies during UV irradiation (Herrling et al. 2003), organic radicals identified in natural marine appetites (Gilinskaya 2010), and the

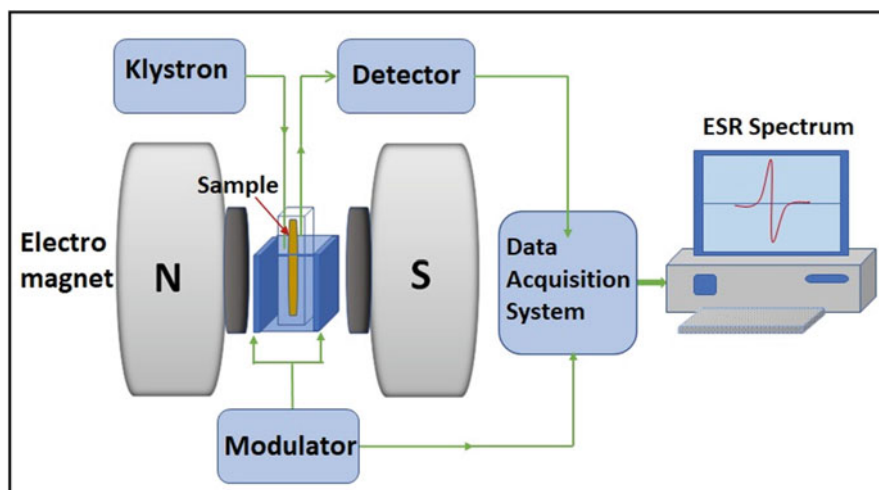


Fig. 15.13 Schematic diagram of ESR spectroscopy

radical intermediates formed upon photoinduced reactions on TiO_2 (Dvoranová et al. 2014).

15.4.5 Mossbauer Spectroscopy

Mossbauer Spectroscopy is a useful analytical tool also known as Nuclear Gamma Resonance Spectroscopy (NGR) that is based on the resonance fluorescence of gamma radiation (Mossbauer effect). The production of Mossbauer spectrum involves recoil-free emission and absorption of gamma rays by atomic nuclei bound in the solid with Mossbauer active elements such as Fe, Sn, Sb, and I. Mossbauer effect cannot be observed in liquids and gases because the recoil energy cannot be dissipated in these states of matter. The spectrum observed by the Mossbauer effect helps to obtain information on the chemical environment within the molecule by hyperfine interactions such as chemical isomer shift, quadrupole splitting, and magnetic splitting. These interactions alone or in combination are the primary characteristics of Mossbauer spectra.

The isomer shift arises from the nuclear energy shift caused by the Coulomb interaction between the nucleus and the electron density at the site of the nucleus. It is mainly affected by the outermost occupied s-orbital electrons, and the screening effect of p-, d-, and f-electrons decreases this s-density at the nucleus. A positive chemical isomer shift is due to an increase in s-electron density at the nucleus. Quadrupole splitting reflects the interaction between nuclear energy levels and surrounding electric field gradients. Nuclei in states with non-spherical charge distributions produce an asymmetrical spherical field that splits the nuclear energy levels. Magnetic splitting is the result of interaction between the nucleus and the surrounding magnetic field. Mossbauer spectrum can be used to find out the oxidation state, spin state, and magnetic ordering of the Fe atoms in a nanoparticle sample. The superparamagnetic behavior of nanoparticles can also be confirmed by this method (Sijo et al. 2019) (Fig. 15.14).

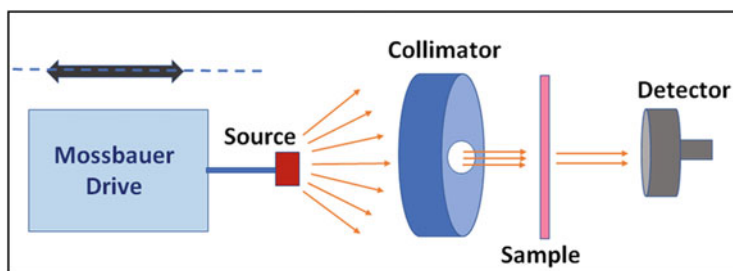


Fig. 15.14 Schematic diagram of key components of Mossbauer spectrometer

15.5 Thermal Characterization

The uniqueness of high-performance materials mainly lies not only in their performance but also in their durability. A material having a superior performance for a long duration of time will have high market demands. But sometimes, easy degradability of the material (e.g., one-time use plastics) through thermal, optical, and other modes may also be a requirement. In this context, the thermal characterization of the material in different atmospheres (air, nitrogen) deserves much importance.

Various properties of nanosized materials or their modified form with respect to the change in temperature or time over a wide range of temperatures can be measured by different methods, including thermogravimetric analysis (TGA), differential scanning calorimetry (DSC), evolved gas analysis (EGA), differential thermal analysis (DTA), dynamic mechanical analysis (DMA), and thermomechanical analysis (TMA). These techniques provide information like sample composition, surface coating, crystallinity, reaction enthalpies, and kinetics (Mansfield 2013). Details of some main techniques and possible outcomes from each method are described in the following sections.

15.5.1 Thermogravimetric Analysis (TGA)

TGA is a quick and common method for analyzing the constituent of a sample and its thermal stability. When a material is heated, the mass of the sample will either increase or decrease due to physical and chemical changes (Mansfield 2013). The change in the mass of material is recorded under a range of temperatures. Various thermal effects, such as decomposition temperature of the nanomaterial, thermal stability, adsorption and desorption, combustion and dehydration, are recognized by monitoring the weight change (Seifi et al. 2020).

The samples are usually kept in a controlled atmosphere using a vacuum or inert gases like Argon or Nitrogen. In some cases, reactive gases like oxygen or air are introduced (Guo et al. 2013). Then the sample is heated at a specific rate by using a specific temperature program. The equipment measures the temperature and weight of the sample many times in a second. Outputs are presented as thermograms of weight percentage versus temperature or time. Thermogram at specified conditions (at a given temperature and time) is characteristic of each nanoparticle and nanocomposite. Therefore, this method can be also used to identify the sample. The transitions in the curve indicate various changes in the material under the temperature changes.

The main advantage of analyzing nanocomposites using TGA is the ability to identify the extent of binding with each constituent (Parikh and Parekh 2015). The thermogram of the composite must be different from that of individual constituents. Decomposition temperature, water, and solvent content in the sample, purity of the sample, and percentage of each component (Wang et al. 2018) are easily determined using TGA. The exact temperature for each change is also obtained through this method. We must be careful about the conditions during the analysis because the

reaction rate may be varied with heating rate, purge gas, sample shape, and the pan used to hold the sample. It is also difficult to distinguish between constituents with similar decomposition temperatures through this method.

15.5.2 Differential Scanning Calorimetry (DSC)

Differential scanning calorimetry is a powerful and versatile thermal analyzer used to measure material transitions as a function of time or temperature. Identification of phase transitions, such as glass transition, melting, and crystallization, are obtained through this technique (Seifi et al. 2020). This method requires a very small amount of sample (about 2–10 mg). Especially DSC is used when the nanoparticles are modified by surfactant and during composite preparation with suitable polymers (Karimzadeh et al. 2016). This will enable to find effective bonding or coordination within the nanoparticle and other constituents. DSC is also used to check the purity of a sample (Araújo et al. 2010).

In DSC analysis, a sample of known mass in a pan and an empty reference pan are placed over a small platform within the DSC chamber. This chamber is maintained in continuous N₂ flow. Both the sample and reference are maintained at nearly the same temperature throughout the experiment. Reference and sample are identical, except those references are empty. When the sample undergoes a physical transformation, such as phase transitions, more or less heat will need to flow to it than the reference to maintain both at the same temperature. Whether less or more heat must flow to the sample depends on whether the process is exothermic or endothermic. These transitions involve energy changes or heat capacity changes detected by thermocouple sensors lying below the pans. The sensor of DSC is designed to give superior performance, high sensitivity, and excellent resolution. The sample is heated or cooled, and the changes in its heat capacity are tracked as changes in the heat flow. Heat flow to the sample from the furnace is measured relative to the heat flow to the reference material. The output is the difference in the heat flow between the reference and sample.

DSC measurements can be made in two ways: by measuring the electrical energy provided to heaters below the pans necessary to maintain the two pans at the same temperature (power compensation) or by measuring the heat flow (differential temperature) as a function of sample temperature (heat flux). The DSC ultimately outputs the differential heat flow (heat/time) between the material and the empty reference pan. Heat capacity may be determined by taking the ratio of heat flow to the heating rate. Thus,

$$C_p = \frac{Q}{\Delta T} \quad (15.4)$$

Here C_p is the heat capacity of the material, Q is the heat flow through the material over a given time, and ΔT is the change in temperature over that same time.

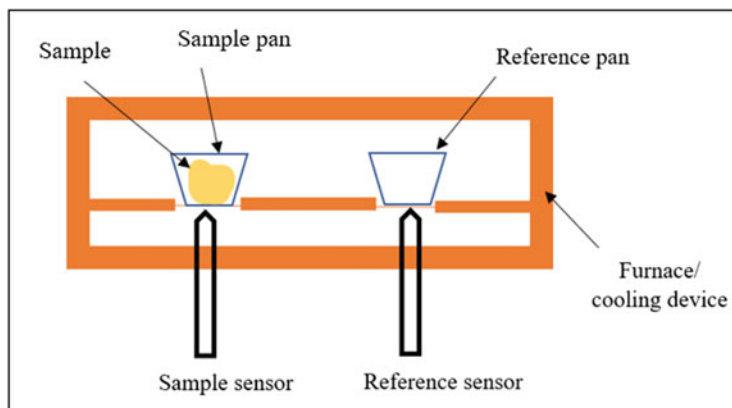


Fig. 15.15 Schematic representation of DSC

The result of a DSC experiment is a curve of heat flux versus temperature or versus time. This curve can be used to calculate the enthalpies of transitions. This is done by integrating the peak corresponding to a given transition. It can be shown that the enthalpy of transition can be expressed using the following equation,

$$\Delta H = KA \quad (15.5)$$

where ΔH is the enthalpy of transition, K is the calorimetric constant, and A is the area under the curve. The calorimetric constant will vary from instrument to instrument and can be determined by analyzing a well-characterized sample with known enthalpies of transition. DSC has the advantages of the rapidity with which the measurements are made and the small amount of sample is required. But it is not suitable for double-phase mixtures and cannot detect gas generation. Figure 15.15 shows the schematic diagram of DSC.

15.5.3 Differential Thermal Analysis (DTA)

Similar to the abovementioned methods, differential thermal analysis is also used to quantitatively analyze the chemical composition of nanomaterials. It uses the same principle as DSC. If a material is heated, it undergoes phase transitions with emission or absorption of heat. Like DSC, the temperature difference between the sample and reference materials is recorded as a function of time or temperature. The specific temperature span is provided by programming. In the case of DTA, the reference may not be an empty vessel like in DSC. It may be $\alpha\text{-Al}_2\text{O}_3$. DTA is used to analyze the nature of bonding between the nanoparticle and the coating material in surface-functionalized nanoparticles. It is considered as a supporting method for the above-described two techniques. It confirms the results from DSC and TGA (Can et al. 2017; Zoccal et al. 2010). Because we get information about crystallization, phase

Fig. 15.16 Average TG curves for the decomposition of the control, TiO₂ bulk, and nTiO₂ exposed Zebrafish bones

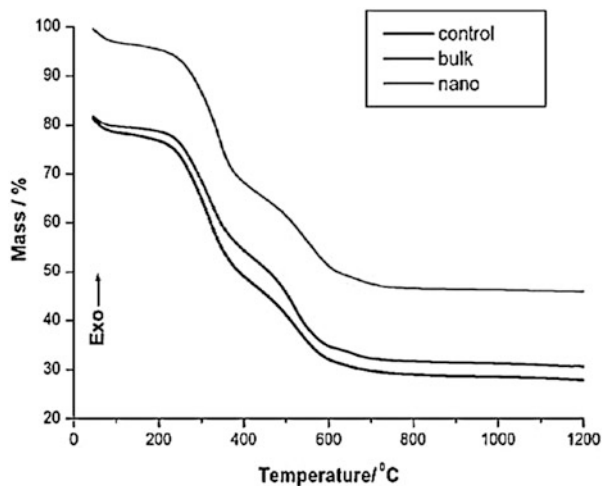
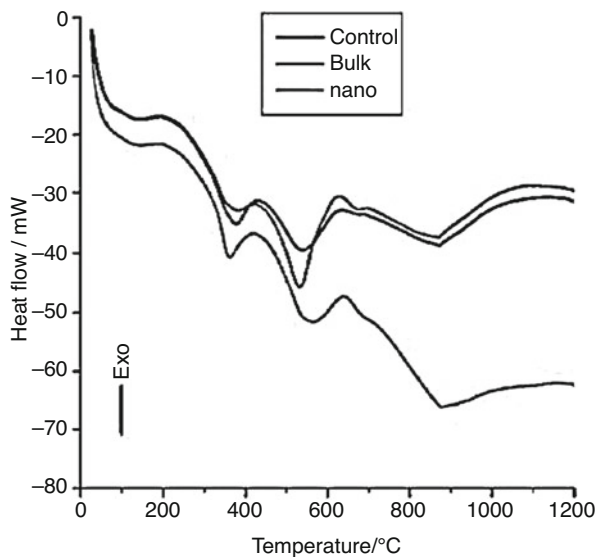


Fig. 15.17 The average DSC curves for the control, TiO₂ bulk, and nTiO₂ exposed Zebrafish bones



transitions, endothermic and exothermic, and complete thermal decomposition (Abdul et al. 2011).

Figures 15.16 and 15.17 shows the results from the experiments using a simultaneous TG-DSC-DTA unit on the effect of TiO₂ exposure on the thermal properties of Zebrafish (*Danio rerio*) bones, respectively (Pramod et al. 2012). The first mass loss step in the TG curve is due to the water desorption, the second step indicates the combustion of the organic components, and the third step represents the decomposition of the inorganic phases. Thermal behavior of control bones and TiO₂ (both bulk and nano) exposed bones are compared and found that the nano TiO₂ exposed has

higher residue mass. Similar to the TG curve, the DSC thermogram also has three well-defined exothermic peaks due to three effects of mass loss, i.e., the evolution of water, decomposition process of the organic material and inorganic materials. The result shows the drastic change in calorimetric enthalpy values due to the nano TiO₂ exposure. When a biological structure undergoes any changes, its thermodynamic characteristics will change. Thus, TG-DSC-DTA analysis is a capable tool to analyze the effect of exposure of nanoparticles on the thermal properties of a biological sample.

15.6 Optical Characterization Techniques

The optical properties are closely related to electric and electronic properties. As we move from bulk to nanoscale, surface area to volume ratio increases and quantum effects get dominated. Optical characterization methods take advantage of electrical and mechanical characterization by giving characteristics of nanomaterial without damaging them due to their non-contact and noninvasive nature. Common optical characterization methods include absorbance/transmittance, photoluminescence, and Raman scattering measurements by analyzing UV-Visible absorption (UV-vis), Photoluminescence (PL), Infrared absorption (IR), and Raman scattering spectrum. The above spectrums are formed by light-matter interaction, which causes electronic excitation and molecular vibrations in liquids and gases, electronic excitation, and optical phonons in solids.

15.6.1 Photoluminescence Spectroscopy

Photoluminescence (PL) spectroscopy is a useful technique for the study and characterization of materials, especially semiconductors. PL is useful in quantifying optical emission efficiencies (Roushan et al. 2012), the composition of the material (Lu et al. 2009), impurity content (Nakarmi et al. 2009) of semiconductors. Luminescence is the result of electronic excitation by different mechanisms. Cathode luminescence is the result of electron beam excitation, Triboluminescence results from mechanical excitation, and Incandescence results from thermal excitation (Fig. 15.18).

Photoluminescence (PL) is a result of optical excitation. Electrons in the sample material move to the excited states by optical excitation and their deexcitation to lower energy states with the release of energy by radiative (i.e., emission of light or luminescence) or non-radiative process. The emitted light has a longer wavelength, $\lambda = hc/(E_2 - E_1)$ or lower energy than the absorbed light (causes excitation) because a part of the energy may release in the non-radiative process like vibrational relaxation, quenching with surrounding molecules or internal conversion. Radiative emission may occur in the form of Fluorescence or Phosphorescence. Fluorescence occurs only during the excitation, but Phosphorescence may continue for a considerable time after the removal of the excitation source. PL spectrum provides

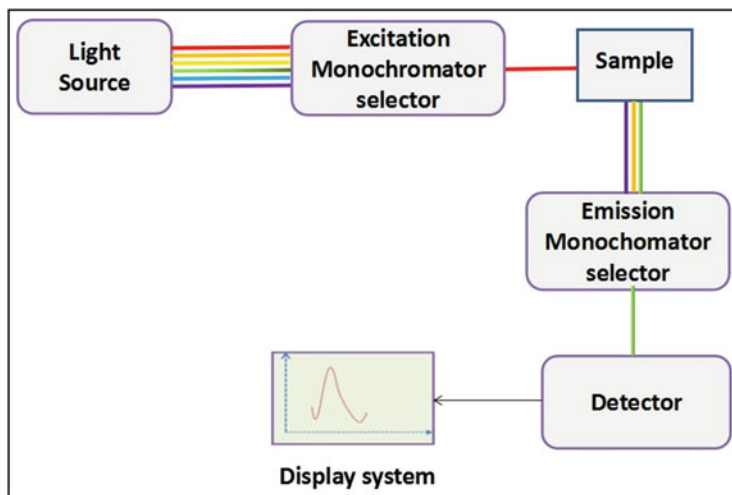


Fig. 15.18 Schematic diagram of key components in a luminescence experiment: emission spectrum is produced for a fixed excitation wavelength

information about the defect structure of solid or the purity and crystalline quality of semiconductors since non-radiative processes are associated with localized defects. Photoluminescence Spectroscopy includes PL Spectroscopy, PL Excitation Spectroscopy (PLE), and Time-resolved PL Spectroscopy.

Luminescence spectrum is a graph showing the variation of emission intensity with excitation wavelength similar to absorbance Vs wavelength in absorption spectra. The shift in the peak of absorption and emission spectra is called Stokes's shift, it is due to the longer wavelength shift of emission peak compared to absorption peak. PL spectrum is sensitive to factors such as temperature (Biju et al. 2005; Walker et al. 2003), pressure (Hannah et al. 2013), excitation intensity, and wavelength (Amans et al. 2002).

15.6.2 UV-Visible Spectroscopy

This technique is based on the measurement of light absorption by a sample. If the sample absorbs light at some wavelength, the transmitted light will be reduced. The intensity of the transmitted light plotted as a function of light wavelength will give a spectrum of the sample absorption. Most spectrometers cover the wavelength range of about 200–800 nm. Here absorption occurs due to the electronic transition of molecules. Since the absorption in the UV-visible region involves mostly electronic transitions, it is also named electronic absorption spectroscopy. Here the absorption of light occurs by excitation of electronic transition, which changes the dipole moment in molecules or solids, which yield information on the presence of certain



Fig. 15.19 Schematic diagram of key components in a UV-vis spectrometer

species, the number of species with high sensitivity, conformation, orientation, and the effect of solvation on electronic states (Fig. 15.19).

Absorbance (A) is defined as $-\log T$, with T being transmittance I/I_0 (where I is transmitted light intensity and I_0 is incident light intensity). An absorbance of 1 implies that the sample absorbed 90% of incoming light, or we can say that 10% of the incident light was transmitted through the sample. Based on Beer-Lambert law, the relation between absorbance (A) and extinction coefficient (α) is

$$A = \log(I_0/I) = \alpha cd \quad (15.6)$$

where c is the concentration of absorbing species and d is the length of the beam in the absorbing (Swinehart 1962). Absorbance (A) can be determined experimentally. The extinction coefficient is wavelength dependent, so the plot of α as a function of λ is characteristic of the given sample and reflects the fundamental electronic properties of the sample. UV-vis spectroscopy is used in quantifying protein and DNA (Sirajuddin et al. 2013; Tajmir-Riahi et al. 2009). The sample concentration should be optimized to get an undistorted or real spectrum. Proper blank or background should be taken before the sample spectrum is measured. Agglomeration of particles (floaters) in the sample will cause significant scattering and distorted spectrum, so floaters can be precipitated out by centrifugation (Mehta et al. 2009). The excitonic absorption peak of CdS nanoparticles blue shifts with decreasing particle size while the molar absorption coefficient increases with decreasing size (Vossmeier et al. 1994).

15.6.3 Infrared (IR) Spectroscopy

Absorption of electromagnetic radiation in the IR region can cause changes in the rotational and vibrational energy states. Since the energy associated with vibrations of interatomic chemical bonds in a molecule is close to IR light, it can absorb the light if the bond can exhibit a dipole moment. Different bonds within functional groups which possess a dipole moment will absorb at different areas of the IR spectrum. The presence of functional groups in a colloidal system of nanoparticles can be analyzed by IR spectroscopy, mainly Fourier Transform Infrared Spectroscopy FTIR (Yudianti et al. 2011). Absorption peaks associated with functional groups such as $-\text{OH}$ and $-\text{COOH}$ appear at specific wavenumbers in the spectrum. The peaks can be analyzed to get the structure of the compound. IR spectra reveal the

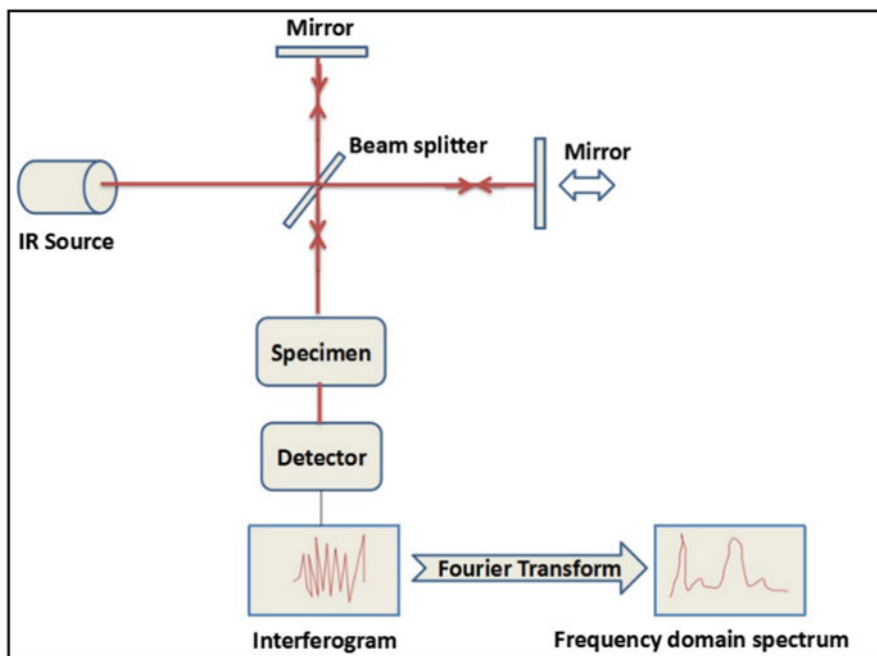


Fig. 15.20 Schematic diagram of key components in IR spectrometer

vibrational signatures of the constituents present in the surrounding media of the nanoparticles and surface structure of metal oxide nanoparticles (López-Lorente and Mizaikoff 2016) (Fig. 15.20).

The sample needs to be thin or dilute enough, so Beer's law is valid similar to UV-vis spectroscopy. The sample used can be solid, liquid, or gaseous state. Light source and optical components used are appropriate for IR light. Many of the nanomaterials are capable of entering into living cells, and thereby structural changes may occur that can be studied using IR spectroscopy.

Figure 15.21 shows the average FTIR spectra of the control of $n\text{TiO}_2$ on the biochemical constituents of gill tissues of Zebrafish in the region of $3050\text{--}2800\text{ cm}^{-1}$, the bands assigned to C–H stretching vibrations of proteins and lipids are located (Palaniappan and Pramod 2010).

15.6.4 Raman Spectroscopy

Raman Scattering is a powerful technique in characterizing nanoparticles by measuring the frequency shift of inelastically scattered light from the sample when incident light strikes the sample. In the inelastic scattering process, some of the energy of the incident photon is lost or increased (energy is not conserved). In Raman spectroscopy, we measure the difference in energy between the incident and

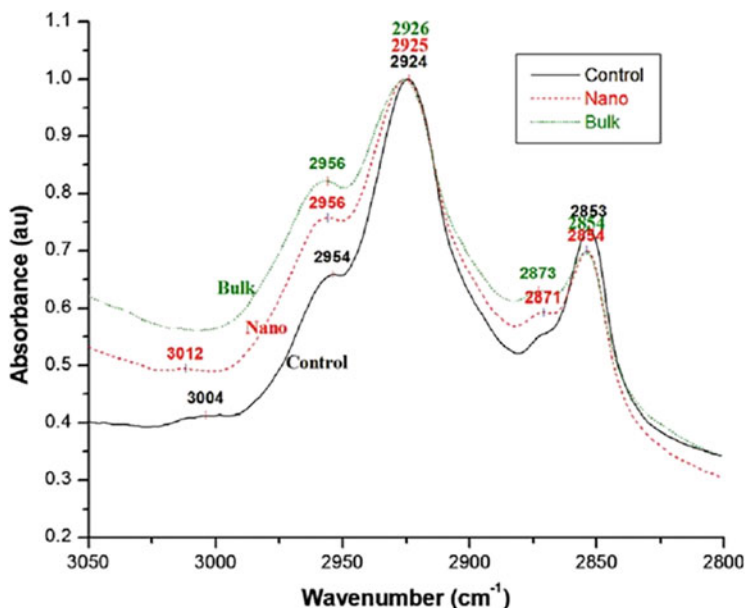


Fig. 15.21 The average FTIR spectra ($n = 9$) of the control, $n\text{TiO}_2$ and TiO_2 bulk exposed gill tissues of *D. rerio* in the $3050\text{--}2800\text{ cm}^{-1}$ region. (The spectra were normalized with respect to the amide A band at 2924 cm^{-1})

scattered photon called Raman shift (expressed in wave number cm^{-1}), which corresponds to the energy required to excite a molecule to a higher vibrational mode. Raman scattering depends on the polarization change, which will be the result of molecular vibrations. Raman spectroscopy has been used in a real-time monitoring system to detect illegal drugs (Dies et al. 2018), toxic material in the environment (Song et al. 2019), and chemical and biological warfare agents (Yan and Vo-Dinh 2007) (Fig. 15.22).

Figure 15.23 shows a shift to a higher wave number and an increase in the intensity of the band observed at $\sim 1087\text{ cm}^{-1}$ in the TiO_2 exposed tissues, suggesting that some of the conformational changes resulted from the partial alterations in the helical conformations (Palaniappan and Pramod 2011).

Two mechanisms responsible for the enhancement of Raman signal are Surface plasmon resonance and resonance enhancement. A variety of Raman-enhanced techniques have emerged Surface-Enhanced Raman Scattering Spectroscopy (SERS), Tip-enhanced Raman Scattering Spectroscopy (TERS), Coherent anti-Stokes Raman Spectroscopy (CARS), etc. (Fig. 15.24).

Owing to plasmonic effects, strong electromagnetic field enhancement at the surface of nanostructured metallic particles occurs in surface-enhanced Raman spectroscopy (SERS) (Ru 2008). Advanced Raman spectroscopic techniques are utilized in plant disease diagnostics (Payne and Kurouski 2021) detection of

Fig. 15.22 Schematic of key components in Raman spectroscopy

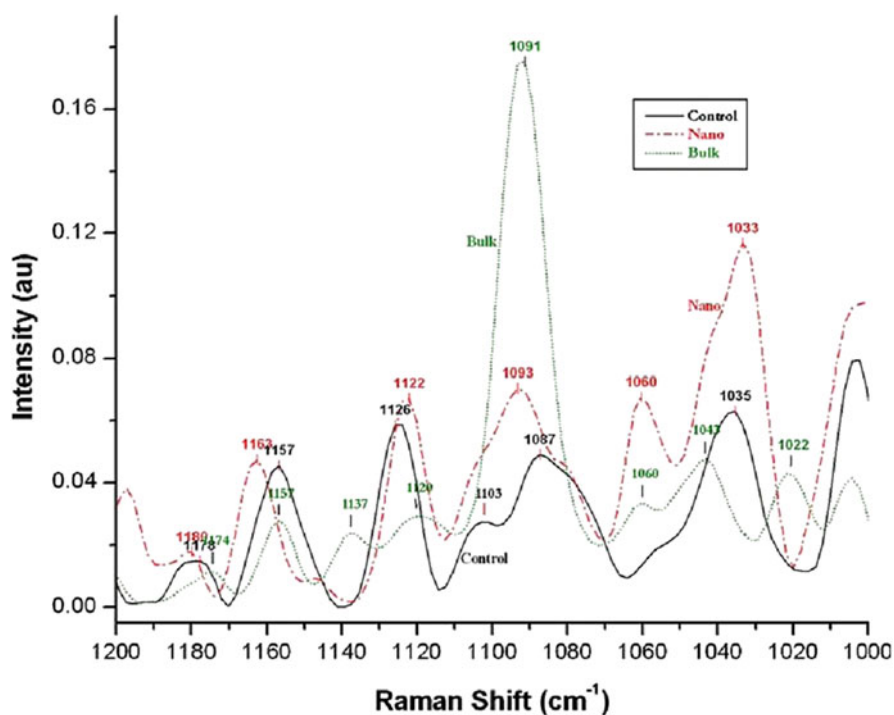
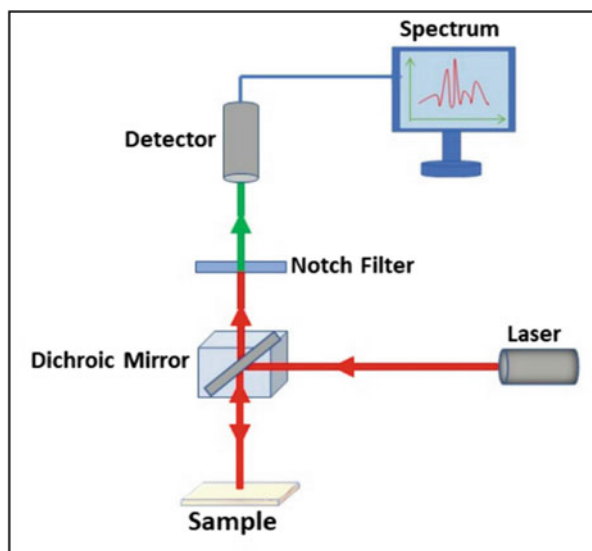


Fig. 15.23 Averaged FT-Raman spectra of liver tissues of Zebrafish (*D. rerio*) in the region of 1200–1000 cm^{-1} for the control, $n\text{TiO}_2$ and TiO_2 bulk (Palaniappan and Pramod 2011)

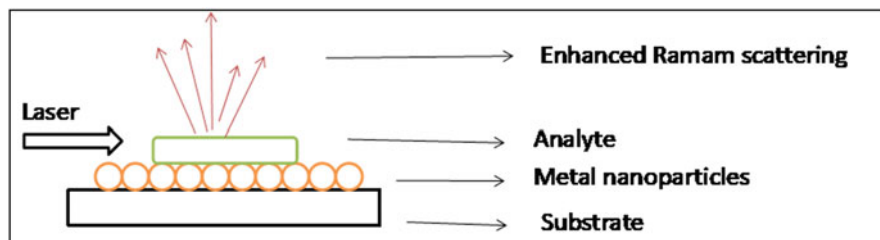


Fig. 15.24 Schematic of surface-enhanced Raman scattering system

biological molecules (Guzelian et al. 2002). SERS techniques have been used for the detection, identification, and quantification of bacteria (Akanny et al. 2021).

15.7 Magnetic, Rheological, and Electrical Characterization

For some specific applications like hyperthermia, proper knowledge about the magnetic properties of synthesized nanoparticles is necessary. Sufficiently small nanoparticles under a finite temperature, its magnetic moment flips from one direction to the other frequently. If external magnetic field is applied to such systems, the particle temperature rises due to the hysteresis loss. This introduces magnetic hyperthermia (Raland et al. 2017). Rheological techniques evaluate the flow behavior of nanomaterials. With the decrease in size, nanoparticles show interesting electrical properties. The below section explains some important magnetic, rheological, and electrical characterization techniques for nanoparticles.

15.7.1 Magnetic Characterization

Magnetic nanoparticles are an essential class in inorganic nanomaterials. They are zero-dimensional materials with metal-based configurations. When the particle size of the nanomaterial is reduced to a critical size, they show some interesting magnetic properties like superparamagnetism (Kaykan et al. 2020). The hysteresis loop of superparamagnetic materials shows zero remanences and coercivity at room temperature. Also, these particles can be easily manipulated using an external magnetic field. Due to the enhanced features, magnetic nanoparticles have a wide range of applications like drug and gene delivery, MRI, magnetic hyperthermia, biosensor, labeling (Gul et al. 2019), etc. Before introducing them into a biological system, proper characterization of the magnetic nanoparticles are necessary. That will ensure the minimal and productive use of synthesized nanoparticles. We need to understand the fundamental magnetic properties like magnetic moment, saturation magnetization, remanent magnetization, and coercive field before utilization. Vibrating-sample magnetometer (VSM), superconducting quantum interference devices (SQUID), and pulse-field hysteresis loop tracer are some magnetic characterization instruments.

VSM is the most common, simple, fast, and relatively inexpensive method for analyzing the magnetic properties of a nanomaterial. It is a direct current magnetometry technique where the physically moving sample is placed in a uniform and constant field to induce the magnetic field change, and magnetic moment is recorded by measuring the change in the voltage (Sandler et al. 2019). M–H loop (Hysteresis loop) analysis provides information about magnetic behavior of the material like saturation magnetization (Kaykan et al. 2020), remnant magnetization, coercive field, and superparamagnetism (Sijo and Dutta 2018). The magnetic behavior of zinc ferrite nanoparticles is quickly recorded using a pulse-field hysteresis loop tracer at room temperature (Somvanshi et al. 2019). Hysteresis loop tracer consists of a solenoid, pickup coil system, micro-controller integrated circuit, and data acquisition system. Software is used to calculate hysteresis parameters followed by plotting the hysteresis loop (Likhite et al. 2011). The most recent and advanced characterization method is SQUID. The output voltage of a SQUID is recorded in the form of a flux profile (Clarke 2014). Compared with other techniques, SQUID has high sensitivity and low noise levels (Saari et al. 2015). In some cases, SQUID analysis is performed to confirm the unaffected magnetic properties of nanomaterials after some modifications.

15.7.2 Rheological Characterization

Rheology, the science of flow behavior of materials, is important in the conversion of a nanomaterial from a less useful shape to a more useful shape for the service of the society. Nanocomposites find wide use in engineering applications (like oilfield industries), and their rheological properties (flow behavior) must be well investigated. The rheometer is the main equipment used to find the rheological properties like viscosity, viscoelastic moduli, yield stress, storage modulus, etc., stress-controlled rotational rheometer with parallel-plate geometry (Baek and Kim 2011), compact rheometer (Kumar and Sharma 2018), and stress-controlled rheometer with a cone-and-plate geometry (Li et al. 2015) are the major types of rheometers.

The rheological characterization is necessary for nanocomposites rather than pure nanomaterials. Because whenever some nanomaterial is added to gel (Baek and Kim 2011) or engine oil (Rabiee et al. 2018), their flow behavior changes. Rheological studies on native gel and nanomaterial-added gel are performed to address the changes (Nanda et al. 2013). In most cases, the yield stress of the gel is increased with an increase in the concentration of nanoparticles (Rabiee et al. 2018). The viscosity of the gel increases with the concentration of nanoparticles up to a limit. After that, there is an abrupt decrease (Baek and Kim 2011). The proper knowledge about the flowing behavior of nanocomposites makes its effective use in oilfield operations.

15.7.3 Electrical Characterization

Electrical measurements are mandatory for comparing the effect of coating in nanoparticles with the uncoated ones. Also, native nanoparticles and nanocomposites have different electrical properties like resistivity and conductivity. These properties depend on particle size, structure, concentration, dispersion, and orientation of nanoparticles (Bokobza 2017). In the field of polymers, there are polymers like high-frequency insulators such as polyethylene as well as electrically conducting polymers such as polyaniline. For many applications, the electrical properties must be finely tuned between the extremes such as conductor and insulator. The variation of electrical conductivity with temperature also is very important in this aspect. The inherent electrical property of a polymer can be changed by the addition of nanoparticles, whose electrical properties are very important. Therefore, these properties of nanomaterials must be carefully characterized. The electrical measurements are done by using the two-probe configuration of the electrodes. Current-voltage (I–V) curves are plotted by providing a DC source. Electrometer voltmeter is another instrument ensuring the direct current measurements (Yurkov et al. 2007). Due to the large surface area to volume ratio, the electrical properties of the nanomaterials are unique compared to their bulk counterparts.

15.8 Conclusion

Proper nanomaterial characterization plays a significant role in their various applications. There are different characterization techniques for evaluating each property. Each method follows specific criteria for effective analysis. Some single techniques provide different features associated with nanoparticles. But for the acquisition of full features of nanomaterial, numerous techniques are required. Even for confirming a single property, we need more than one method. Based on the advantages and disadvantages, the techniques can be combined to get valuable information with minimal time consumption. Indicating that characterization methods are complementary to each other. The appropriate knowledge about each technique will help to choose the most suitable technique for characterization.

References

- Abdul M, Khan M, Kumar S, Ahamed M, Alrokayan SA (2011) Structural and thermal studies of silver nanoparticles and electrical transport study of their thin films. *Nanoscale Res Lett*. <http://www.nanoscalereslett.com/content/6/1/434>
- Aceto M (2016) The use of ICP-MS in food traceability. In: *Advances in food traceability techniques and technologies: improving quality throughout the food chain*, Elsevier Ltd., Duxford. <https://doi.org/10.1016/B978-0-08-100310-7.00008-9>
- Akanny E, Bonhommé A, Bessueille F, Bourgeois S, Bordes C (2021) Surface enhanced Raman spectroscopy for bacteria analysis: a review. *Appl Spectrosc Rev* 56(5):380–422. <https://doi.org/10.1080/05704928.2020.1796698>

- Amans D, Guillois O, Ledoux G, Porterat D, Reynaud C (2002) Influence of light intensity on the photoluminescence of silicon nanostructures. *J Appl Phys* 91(8):5334–5340. <https://doi.org/10.1063/1.1461064>
- Ansari MA, Baykal A, Asiri S, Rehman S (2018) Synthesis and characterisation of antibacterial activity of spinel chromium-substituted copper ferrite nanoparticles for biomedical application. *J Inorg Organomet Polym Mater* 28(6):2316–2327. <https://doi.org/10.1007/s10904-018-0889-5>
- Araújo AA, Souza MD, Bezerra S, Storpirtis S, Matos JDR (2010) Determination of the melting temperature, heat of fusion, and purity analysis of different samples of zidovudine (AZT) using DSC. *Braz J Pharm Sci* 46(1):37–43. <https://doi.org/10.1590/S1984-82502010000100005>
- Arroyo-Ramírez L, Montano-Serrano R, Raptis RG, Cabrera CR (2009) Nanostructural formation of Pd-Co bimetallic complex on HOPG surfaces: XPS and AFM studies. *Res Lett Nanotechnol* 2009:1–5. <https://doi.org/10.1155/2009/971423>
- Baek G, Kim C (2011) Rheological properties of carboxypol containing nanoparticles. *J Rheol* 55(2): 313–330. <https://doi.org/10.1122/1.3538092>
- Baer DR, Engelhard MH (2010) XPS analysis of nanostructured materials and biological surfaces. *J Electron Spectrosc Relat Phenom* 178–179(C):415–432. <https://doi.org/10.1016/j.elspec.2009.09.003>
- Banerjee S, Yang R, Courchene CE, Conners TE (2009) Scanning electron microscopy measurements of the surface roughness of paper. *Ind Eng Chem Res* 48(9):4322–4325
- Behdadfar B, Kermanpur A, Sadeghi-Aliabadi H, Del Puerto M, Morales, and Morteza Mozaffari. (2012) Synthesis of aqueous ferrofluids of ZnXFe₃-XO₄ nanoparticles by citric acid assisted hydrothermal-reduction route for magnetic hyperthermia applications. *J Magn Magn Mater* 324(14):2211–2217. <https://doi.org/10.1016/j.jmmm.2012.02.034>
- Belsey NA, Shard AG, Minelli C (2015) Analysis of protein coatings on gold nanoparticles by XPS and liquid-based particle sizing techniques. *Biointerphases* 10(1):019012. <https://doi.org/10.1116/1.4913566>
- Biju V, Makita Y, Sonoda A, Yokoyama H, Baba Y, Ishikawa M (2005) Temperature-sensitive photoluminescence of CdSe quantum dot clusters. *J Phys Chem B* 109(29):13899–13905. <https://doi.org/10.1021/jp0504241>
- Bokobza L (2017) Mechanical and electrical properties of elastomer nanocomposites based on different carbon nanomaterials. *C (J Carbon Res)* 3(10):1–22. <https://doi.org/10.3390/c3020010>
- Can HK, Kavlak S, Parvizikhosroshahi S, Güner A (2017) Preparation, characterisation and dynamical mechanical properties of dextran-coated iron oxide nanoparticles (DIONPs). *Artif Cells Nanomed Biotechnol*:1–12. <https://doi.org/10.1080/21691401.2017.1315428>
- Clarke J (2014) SQUID (superconducting quantum interference device). In: AccessScience. McGraw-Hill Education, New York. <https://doi.org/10.1036/1097-8542.649800>
- Dies H, Raveendran J, Escobedo C, Docoslis A (2018) Rapid identification and quantification of illicit drugs on nanodendritic surface-enhanced Raman scattering substrates. *Sensors Actuators B Chem* 257:382–388. <https://doi.org/10.1016/j.snb.2017.10.181>
- Dung DTK, Hai TH, Phuc LH, Long BD, Vinh LK, Truc PN (2009) Preparation and characterisation of magnetic nanoparticles with chitosan coating. *J Phys Conf Ser* 187:6–11. <https://doi.org/10.1088/1742-6596/187/1/012036>
- Dvoranová D, Barbieriková Z, Brezová V (2014) Radical intermediates in photoinduced reactions on TiO₂ (an EPR spin trapping study). *Molecules* 19(11):17279–17304. <https://doi.org/10.3390/molecules191117279>
- Eaton P, West P (2010) Atomic force microscopy. Oxford University Press, Oxford. <https://doi.org/10.1093/acprof:oso/9780199570454.001.0001>
- Egerton RF (2005) Physical principles of electron microscopy. Springer
- Fultz B, Howe JM (2012) Transmission electron microscopy and diffractometry of materials. Springer Science & Business Media, Heidelberg
- Giessibl FJ (2003) Advances in atomic force microscopy. *Rev Mod Phys* 75:949

- Gilinskaya LG (2010) Organic radicals in natural apatites according to EPR data: potential genetic and paleoclimatic indicators. *J Struct Chem* 51(3):471–481. <https://doi.org/10.1007/s10947-010-0069-0>
- Golovan LA, Djun IO, Dokukina AE, Zabotnov SV, Ezhov AA, Kashkarov PK, Maslova NE, Ostapenko IO, Panov VI, Timoshenko VU (2009) AFM investigation of nanoparticles formed on silicon surface by femtosecond laser pulses. *Bull Russ Acad Sci Phys* 73(1):39–41. <https://doi.org/10.3103/S1062873809010122>
- Guibert C, Dupuis V, Peyre V, Fresnais J (2015) Hyperthermia of magnetic nanoparticles: experimental study of the role of aggregation. *J Phys Chem C* 119(50):28148–28154. <https://doi.org/10.1021/acs.jpcc.5b07796>
- Gul S, Khan SB, Rehman IU, Khan MA, Khan MI (2019) A comprehensive review of magnetic nanomaterials modern day theranostics. *Front Mater* 6(July):1–15. <https://doi.org/10.3389/fmats.2019.00179>
- Guo J, Hongbo G, Wei H, Zhang Q, Haldolaarachchige N, Li Y, Young DP, Wei S, Guo Z (2013) Magnetite–polypyrrole metacomposites: dielectric properties and magnetoresistance behavior. *J Phys Chem C* 117:10191
- Guzelian AA, Sylvia JM, Janni JA, Clauson SL, Spencer KM (2002) SERS of whole-cell bacteria and trace levels of biological molecules. Vibrational spectroscopy-based sensor systems. *Int Soc Opt Photon* 4577:183–192
- Hannah DC, Yang J, Podsiadlo P, Chan MKY, Demortiere A, Gosztola DJ, Prakapenka VB, Schatz GC, Kortshagen U, Schaller RD (2013) On the origin of efficient photoluminescence in silicon nanocrystals. In: 2013 Conference on lasers and electro-optics, CLEO 2013. https://doi.org/10.1364/cleo_qels.2013.qtu2o.2
- Herrling T, Fuchs J, Rehberg J, Groth N (2003) UV-induced free radicals in the skin detected by ESR spectroscopy and imaging using nitroxides. *Free Radic Biol Med* 35(1):59–67. [https://doi.org/10.1016/S0891-5849\(03\)00241-7](https://doi.org/10.1016/S0891-5849(03)00241-7)
- Holbrook RD, Galyean AA, Gorham JM, Herzing A, Pettibone J (2015) Overview of nanomaterial characterization and metrology. *Front Nanosci* 8. <https://doi.org/10.1016/B978-0-08-099948-7.00002-6>
- Karimzadeh I, Dizaji HR, Aghazadeh M (2016) Preparation, characterisation and PEGylation of superparamagnetic Fe₃O₄ nanoparticles from ethanol medium via cathodic electrochemical deposition (CED) method. *Mater Res Express* 3(9):1–11. <https://doi.org/10.1088/2053-1591/3/9/095022>
- Kaykan L, Sijo Antoni AK, Julia Ž, Khrystyna M (2020) Tailoring of structural and magnetic properties of nanosized lithium ferrites synthesised by sol–gel self-combustion method. *Appl Nanosci* 0123456789:4–10. <https://doi.org/10.1007/s13204-020-01413-y>
- Korin E, Froumin N, Cohen S (2017) Surface analysis of nanocomplexes by X-ray photoelectron spectroscopy (XPS). *ACS Biomater Sci Eng* 3(6):882–889. <https://doi.org/10.1021/acsbomaterials.7b00040>
- Krishna R, Titus E, Krishna R, Bardhan N, Bahadur D, Gracio J (2012) Wet-chemical green synthesis of l-lysine amino acid stabilized biocompatible iron-oxide magnetic nanoparticles. *J Nanosci Nanotechnol* 12(8):6645–6651. <https://doi.org/10.1166/jnn.2012.4571>
- Kumar RS, Sharma T (2018) Stability and rheological properties of nanofluids stabilized by SiO₂ nanoparticles and SiO₂-TiO₂ nanocomposites for oilfield applications. *Colloids Surf A Physicochem Eng Asp* 539(2010):171–183. <https://doi.org/10.1016/j.colsurfa.2017.12.028>
- Kusigerski V, Illes E, Blanus J, Gyergyek S, Boskovic M, Perovic M, Spasojevic V (2019) Magnetic properties and heating efficacy of magnesium doped magnetite nanoparticles obtained by co-precipitation method. *J Magn Magn Mater* 475:470–478. <https://doi.org/10.1016/j.jmmm.2018.11.127>
- Lavina B, Dera P, Downs RT (2014) Modern X-ray diffraction methods in mineralogy and geosciences. *Rev Mineral Geochem* 78(1):1–31. <https://doi.org/10.2138/rmg.2014.78.1>

- Lee S, Bi X, Reed RB, Ranville JF, Herckes P, Westerhoff P (2014) Nanoparticle size detection limits by single particle ICP-MS for 40 elements. *Environ Sci Technol* 48(17):10291–10300. <https://doi.org/10.1021/es502422v>
- Li MC, Qinglin W, Song K, Lee S-y, Yan Q, Yiqiang W (2015) Cellulose nanoparticles: structure-morphology-rheology relationships. *ACS Sust Chem Eng*, pp 1–45
- Likhite SD, Likhite P, Radha S (2011) PC based pulsed field hysteresis loop tracer. *AIP Conf Proc* 1349(Part A):495–496. <https://doi.org/10.1063/1.3605950>
- Liu S, Wang Y (2010) Application of AFM in microbiology: a review. *Scanning* 32(2):61–73. <https://doi.org/10.1002/sca.20173>
- López-Lorente AI, Mizaiikoff B (2016) Recent advances on the characterisation of nanoparticles using infrared spectroscopy. *TrAC Trends Anal Chem* 84:97–106. <https://doi.org/10.1016/j.trac.2016.01.012>
- Lopour F (2001) AFM—a tool for a study of surfaces and micro/nanostructures. In: *Conference Proceedings Brno, Czech Republic*, vol 29, pp 567–574
- Lu X, Beaton DA, Lewis RB, Tiedje T, Zhang Y (2009) Composition dependence of photoluminescence of GaAs_{1-x}Bix alloys. *Appl Phys Lett* 95(4):3–5. <https://doi.org/10.1063/1.3191675>
- Mansfield E (2013) Recent advances in thermal analysis of nanoparticles: methods, models and kinetics. In: *Modeling, characterisation and production of nanomaterials*. Elsevier Ltd., pp 167–178. <https://doi.org/10.1016/B978-1-78242-228-0.00006-5>
- Mårtensson N, Söderstrom J, Svensson S, Travnikova O, Patanen M, Miron C, Sæthre LJ et al (2013) On the relation between X-Ray photoelectron spectroscopy and XAFS. *J Phys Conf Ser* 430(1). <https://doi.org/10.1088/1742-6596/430/1/012131>
- McMullan D (1995) Scanning electron microscopy 1928–1965. *Scanning* 17(3):175–185
- Mehta SK, Kumar S, Chaudhary S, Bhasin KK (2009) Effect of cationic surfactant head groups on synthesis, growth and agglomeration behavior of ZnS nanoparticles. *Nanoscale Res Lett* 4(10): 1197–1208. <https://doi.org/10.1007/s11671-009-9377-8>
- Mourdikoudis S, Pallares RM, Thanh NTK (2018) Characterisation techniques for nanoparticles: comparison and complementarity upon studying nanoparticle properties. *Nanoscale*. <https://doi.org/10.1039/c8nr02278j>
- Nakarmi ML, Nepal N, Lin JY, Jiang HX (2009) Photoluminescence studies of impurity transitions in Mg-doped AlGaIn alloys. *Appl Phys Lett* 94(9):2009–2011. <https://doi.org/10.1063/1.3094754>
- Nanda J, Biswas A, Adhikari B, Banerjee A (2013) A gel-based trihybrid system containing nanofibers, nanosheets, and nanoparticles: modulation of the rheological property and catalysis. *Angew Chem Int Ed* 52(19):5041–5045. <https://doi.org/10.1002/anie.201301128>
- Nilsen MH, Nordhei C, Ramstad AL, Nicholson DG, Poliakov M, Cabanas A (2007) XAS (XANES and EXAFS) investigations of nanoparticulate ferrites synthesised continuously in near critical and supercritical water. *J Phys Chem C* 111(17):6252–6262. <https://doi.org/10.1021/jp062672z>
- Olesik JW (1991) Elemental analysis using ICP-OES and ICP/MS. *Anal Chem* 63(1):12–21. <https://doi.org/10.1021/ac00001a001>
- Olesik JW, Gray PJ (2012) Considerations for measurement of individual nanoparticles or microparticles by ICP-MS: determination of the number of particles and the analyte mass in each particle. *J Anal At Spectrom* 27(7):1143–1155. <https://doi.org/10.1039/c2ja30073g>
- Palaniappan PLRM, Pramod KS (2010) FTIR study of the effect of NTiO₂ on the biochemical constituents of gill tissues of zebrafish (*Danio Rerio*). *Food Chem Toxicol* 48(8–9):2337–2343. <https://doi.org/10.1016/j.fct.2010.05.068>
- Palaniappan PR, Pramod KS (2011) Raman spectroscopic investigation on the microenvironment of the liver tissues of zebrafish (*Danio Rerio*) due to titanium dioxide exposure. *Vib Spectrosc* 56(2):146–153. <https://doi.org/10.1016/j.vibspec.2011.01.005>
- Parikh N, Parekh K (2015) Technique to optimise magnetic response of gelatin coated magnetic nanoparticles. *J Mater Sci Mater Med* 26(7):1–9. <https://doi.org/10.1007/s10856-015.5534-z>

- Payne WZ, Kurouski D (2021) Raman spectroscopy enables phenotyping and assessment of nutrition values of plants: a review. *Plant Methods*. <https://doi.org/10.1186/s13007-021-00781-y>
- Pramod KS, Krishnakumar N, Vijayasundaram V, Palaniappan PLRM (2012) The effect of titanium dioxide exposure on the thermal properties of zebrafish (*Danio Rerio*) bones. *J Therm Anal Calorim* 108(1):133–139
- Pugsley AJ, Bull CL, Sella A, Sankar G, McMillan PF (2011) XAS/EXAFS studies of Ge nanoparticles produced by reaction between Mg 2Ge and GeCl₄. *J Solid State Chem* 184(9): 2345–2352. <https://doi.org/10.1016/j.jssc.2011.06.020>
- Rabiee F, Akbari V, Taheri A (2018) A novel experimental investigation on the effect of nanoparticles composition on the rheological behavior of nano-hybrids. *J Mol Liq* 17:1–20. <https://doi.org/10.1016/j.molliq.2017.11.147>
- Raja PMV, Barron AR (2021) Physical methods in chemistry and nano science. OER LibreTexts. <https://doi.org/10.1002/jctb.5000533702>
- Raland RD, Saikia D, Borgohain C, Borah JP (2017) Heating efficiency and correlation between the structural and magnetic properties of oleic acid coated MnFe₂O₄ nanoparticles for magnetic hyperthermia application. *J Phys D Appl Phys* 50:32. <https://doi.org/10.1088/1361-6463/aa77e9>
- Reimer L, Kohl H (2013) Transmission electron microscopy: physics of image formation and microanalysis. Springer, Berlin
- Roushan M, Zhang X, Li J (2012) Solution-processable white-light-emitting hybrid semiconductor bulk materials with high photoluminescence quantum efficiency. *Angew Chem Int Ed* 51(2): 436–439. <https://doi.org/10.1002/anie.201105110>
- Ru ECL, Etchegoin PG (2008) Principles of surface-enhanced raman spectroscopy: and related plasmonic effects. Elsevier, Amsterdam
- Rugar D, Hansma P (1990) Atomic force microscopy. *Phys Today* 43(10):23–30
- Saari MM, Sakai K, Kiwa T, Sasayama T, Yoshida T, Tsukada K (2015) Characterisation of the magnetic moment distribution in low-concentration solutions of iron oxide nanoparticles by a high-Tc superconducting quantum interference device magnetometer. *J Appl Phys* 117(17). <https://doi.org/10.1063/1.4919043>
- Sandler SE, Fellows B, Thompson Mefford O (2019) Best practices for characterisation of magnetic nanoparticles for biomedical applications. *Anal Chem* 91(22):14159–14169. <https://doi.org/10.1021/acs.analchem.9b03518>
- Scheffer A, Engelhard C, Sperling M, Buscher W (2008) ICP-MS as a new tool for the determination of gold nanoparticles in bioanalytical applications. *Anal Bioanal Chem* 390(1):249–252. <https://doi.org/10.1007/s00216-007-1576-5>
- Seifi H, Gholami T, Seifi S, Mehdi S (2020) A review on current trends in thermal analysis and hyphenated techniques in the investigation of physical, mechanical and chemical properties of nanomaterials. *J Anal Appl Pyrolysis* 149(May):1–14. <https://doi.org/10.1016/j.jaap.2020.104840>
- Sharma R et al (2012) X-ray diffraction: a powerful method of characterising nanomaterials. *Recent Res Sci Technol* 4(8):77–79
- Sijo AK, Dutta DP (2018) Size-dependent magnetic and structural properties of CoCrFeO₄ nanopowder prepared by solution self-combustion. *J Magn Magn Mater* 451:450–453
- Sijo AK, Jha VK, Kaykan LS, Dutta DP (2019) Structure and cation distribution in superparamagnetic NiCrFeO₄ nanoparticles using Mössbauer study. *J Magn Magn Mater* 497:166047. <https://doi.org/10.1016/j.jmmm.2019.166047>
- Sing K (2001) The use of nitrogen adsorption for the characterisation of porous materials. *Colloids Surf A Physicochem Eng Asp* 188:3–9
- Sirajuddin M, Ali S, Badshah A (2013) Drug-DNA interactions and their study by UV-visible, fluorescence spectroscopies and cyclic voltametry. *J Photochem Photobiol B Biol* 124:1–19. <https://doi.org/10.1016/j.jphotobiol.2013.03.013>

- Somvanshi SB, Vipin Kumar R, Kounsalye JS, Saraf TS, Jadhav KM (2019) Investigations of structural, magnetic and induction heating properties of surface functionalized zinc ferrite nanoparticles for hyperthermia applications. *AIP Conf Proc* 2115. <https://doi.org/10.1063/1.5113361>
- Song JY, Jang HK, Kim BS (2009) Biological synthesis of gold nanoparticles using *Magnolia kobus* and *Diopyros kaki* leaf extracts. *Process Biochem* 44(10):1133–1138. <https://doi.org/10.1016/j.procbio.2009.06.005>
- Song D, Yang R, Long F, Zhu A (2019) Applications of magnetic nanoparticles in surface-enhanced Raman scattering (SERS) detection of environmental pollutants. *J Environ Sci (China)* 80:14–34. <https://doi.org/10.1016/j.jes.2018.07.004>
- Srinivasan C, Mullen T, Hohman JN, Anderson ME (2007) Scanning electron microscopy of nanoscale chemical patterns. *ACS Nano* 1(3):191–201
- Sujata K, Jennings HM (1991) Advances in scanning electron microscopy. *MRS Bull* 16(3):41–45
- Swinehart DF (1962) The Beer-Lambert law. *J Chem Educ* 39(7):333–335. <https://doi.org/10.1021/ed039p333>
- Tajmir-Riahi HA, N'Soukpoé-Kossi CN, Joly D (2009) Structural analysis of protein-DNA and protein-RNA interactions by FTIR, UV-visible and CD spectroscopic methods. *Spectroscopy* 23(2):81–101. <https://doi.org/10.3233/SPE-2009-0371>
- Vossmeier T, Katsikas L, Giersig M, Popovic IG, Diesner K, Chemseddine A, Eychmüller A, Weller H (1994) CdS nanoclusters: synthesis, characterisation, size dependent oscillator strength, temperature shift of the excitonic transition energy, and reversible absorbance shift. *J Phys Chem* 98(31):7665–7673. <https://doi.org/10.1021/j100082a044>
- Walker GW, Sundar VC, Rudzinski CM, Wun AW, Bawendi MG, Nocera DG (2003) Quantum-dot optical temperature probes. *Appl Phys Lett* 83(17):3555–3557. <https://doi.org/10.1063/1.1620686>
- Wang ZL (2000) Transmission electron microscopy of shape-controlled nanocrystals and their assemblies. *J Phys Chem B* 104(6):153–1175
- Wang G, Qian K, Mei X (2018) A theranostic nanoplatfrom: magneto-gold@fluorescence polymer nanoparticles for tumor targeting: T1 & T2-MRI/CT/NIR fluorescence imaging and induction of genuine autophagy mediated chemotherapy. *R Soc Chem* 10(22):10467–10478. <https://doi.org/10.1039/c8nr02429d>
- Wei Z, Qiao H, Yang H, Zhang C, Yan X (2009a) Characterisation of NiO nanoparticles by anodic arc plasma method. *J Alloys Compd* 479(1–2):855–858. <https://doi.org/10.1016/j.jallcom.2009.01.064>
- Wei Z, Zhou M, Qiao H, Zhu L, Yang H, Xia T (2009b) Particle size and pore structure characterisation of silver nanoparticles prepared by confined arc plasma. *J Nanomater* 2009: 5–10. <https://doi.org/10.1155/2009/968058>
- Wilschefski SC, Baxter MR (2019) Inductively coupled plasma mass spectrometry: introduction to analytical aspects. *Clin Biochem Rev* 40(3):115–133. <https://doi.org/10.33176/AACB-19-00024>
- Yan F, Vo-Dinh T (2007) Surface-enhanced Raman scattering detection of chemical and biological agents using a portable Raman integrated tunable sensor. *Sensors Actuators B Chem* 121(1): 61–66. <https://doi.org/10.1016/j.snb.2006.09.032>
- Yudianti R, Onggo H, Saito Y, Iwata T, Azuma J-I (2011) Analysis of functional group sited on multi-wall carbon nanotube surface. *Open Mater Sci J* 5:242–247
- Yurkov G, Yu AS, Fionov YA, Koksharov VV, Koleso, and S. P. Gubin. (2007) Electrical and magnetic properties of nanomaterials containing iron or cobalt nanoparticles. *Inorg Mater* 43(8): 834–844. <https://doi.org/10.1134/S0020168507080055>
- Zipare KV, Bandgar SS, Shahane GS (2018) Effect of Dy-substitution on structural and magnetic properties of Mn–Zn ferrite nanoparticles. *J Rare Earths* 36(1):86–94. <https://doi.org/10.1016/j.jre.2017.06.011>

Zoccal JVM, de Oliveira Arouca, F, Gonçalves JAS (2010) Synthesis and characterisation of TiO₂ nanoparticle by the method pechini. In: Seventh international Latin American conference on powder technology, pp 449–455



X. Joseph, Akhil, Arathi, K. B. Megha, U. Vandana, and P. V. Mohanan

16.1 Introduction

Nanoparticles are considered as materials of size less than 100 nm. The physical and chemical properties of nanoparticles can vary significantly from the bulk counterpart, such as the electronic and chemical properties can improve, solubility in the biological fluid can increase, circulation time in the circulatory system can increase, toxicity profile may change, and so on, due to this nanoparticle is considered superior in many scenarios. For example, silicon nanoparticles in solar cells improve energy efficiency, aluminum nanoparticles in rocket fuel improve energy release, nanoparticles act as a carrier for drug delivery, improve the water filtration process, and absorb UV light. The broad spectrum of features of nanoparticles makes them span across various industries such as healthcare, cosmetics, food production, electronics, agriculture, and so on.

The application of nanoparticles in numerous fields may result in the contact of such particles with humans or other organisms during their life cycle. Many reports have pointed out that nanoparticles have critical applications in human health care, but some of them are toxic. Exposure to nanoparticles can cause cell death through a variety of mechanisms. The oxidative stress development is the primary reason for nanoparticle-induced toxicity. The toxicity of nanoparticles depends on the size, chemical composition, shape, and solubility of the particles (Fig. 16.1). The toxicity of the nanoparticles is generally found to increase with an increase in

X. Joseph, K. B. Megha and U. Vandana contributed equally to this work.

X. Joseph · Akhil · Arathi · K. B. Megha · U. Vandana · P. V. Mohanan (✉)

Toxicology Division, Biomedical Technology Wing, Sree Chitra Tirunal Institute for Medical Sciences and Technology (Govt. of India), Trivandrum, Kerala, India

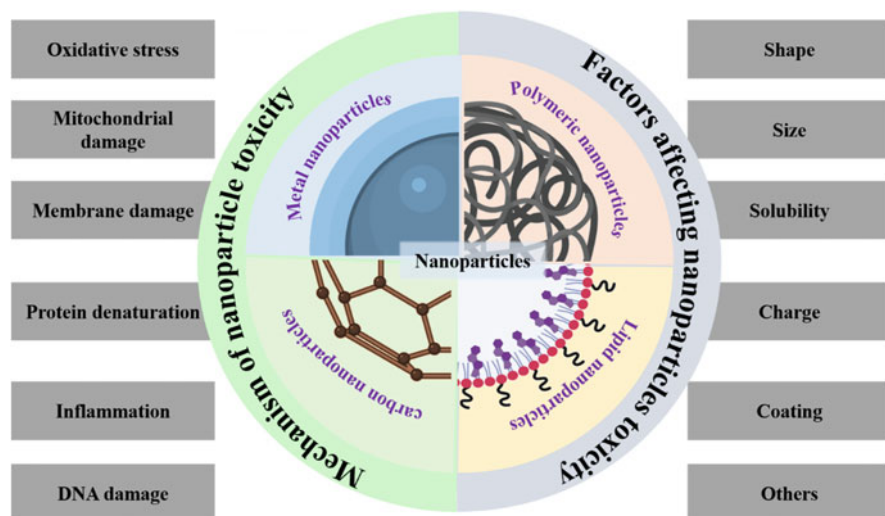


Fig. 16.1 Factors and mechanism of toxicity associated with nanoparticles

electro-positivity. The nanoparticle with a positive charge tends to interact with the negatively charged cell membrane rather than the neutral or negatively charged particles. Alternatively, the toxicity decreases with an increase in size or spherical shape. Nanoparticles with low solubility tend to accumulate in organs and eliminate very slowly with time. The low solubility of the nanoparticles can therefore increase the toxicity.

Similarly, the non-coated nanoparticles can exert more toxic effects than nanoparticles coated with biomolecules. The coating of nanoparticles is also beneficial in improving solubility by preventing aggregation in the biological environment. Therefore, it is necessary to evaluate and characterize the nanoparticle according to its toxicity carefully. This chapter describes the potential mechanisms of nanoparticle-induced toxicity and various methods to evaluate the toxicity associated with nanoparticle exposure.

16.2 Potential Mechanism of Nanoparticle-Induced Toxicity

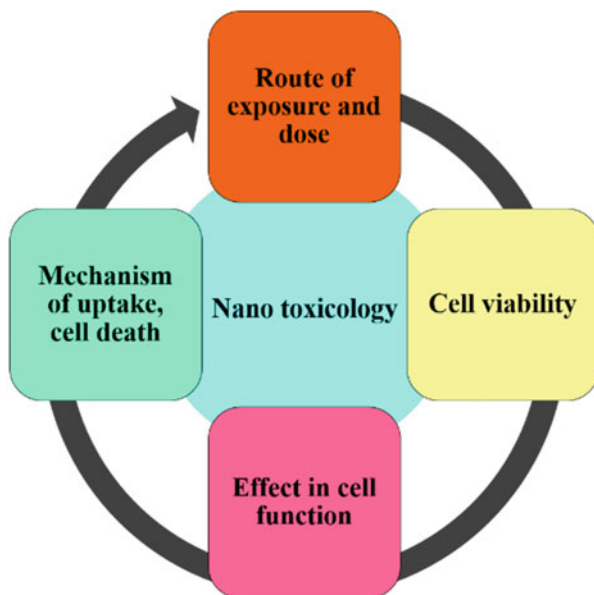
Inhalation and dermal contact are the primary way of nanoparticle entry to the body and secondarily through ingestion or injection. During nanoparticle exposure through inhalation, the nanoparticles are deposited throughout the respiratory tract, and the biological effect depends on the residence time of nanoparticles in the respiratory tract. The nanoparticle's entry in dermal exposure can facilitate through the hair follicles and broken or flexed skin. However, the nanoparticle exposed through the ingestion was primarily eliminated through the feces. The entry of nanoparticles through the gastrointestinal tract depends on the charge and size of

the particles (Fig. 16.1). Negatively charged mucus can result in the trapping of positively charged nanoparticles. Nanoparticle charge is also a critical factor in platelet uptake and clot formation. Intravenously injected nanoparticles can quickly translocate through the circulatory system and reach the target. Many nanoparticles have demonstrated their ability to pass the blood-brain barrier. Cells can take up the nanoparticle via phagocytosis or clathrin-dependent/independent pinocytosis. The smaller sized particles quickly gain entry to the cell than the larger sized particles. Upon uptake of nanoparticles into the cell, they can translocate to various organelles or nuclei. The nanoparticles further increase the permeability of the cell membrane and can damage the ionic exchange across the membrane. Nanoparticles can also lead to DNA damage, histone modification, chromosomal abbreviation, or mutation. Alternatively, the nanoparticle presence in the cytoplasm may lead to the generation of oxidative stress and various intrinsic enzyme failures. The generation of reactive oxygen species (ROS) in cells due to nanoparticle exposure induces inflammation. ROS generation also impairs the mitochondrial membrane potential, interferes with mitochondrial respiration, increases misfolded and unfolded protein content in the endoplasmic reticulum, and further leads to stress. The cumulative effect of cellular activity changes can activate various specific pathways and synergistically lead to cell death. Cell death can be programmed (apoptosis) or necrotic. Based on different pathways present in cell death, various cytotoxicity experiments have been developed till now. Due to the interaction of nanoparticles with various specific cells, the selection of cell lines to assess the cytotoxicity of a nanoparticle is essential.

16.3 Toxicity Assessments

Identifying and accessing toxicity associated with nanoparticles is essential to implement them for human use. Proper hazard identification and risk assessment are also necessary for predicting the impact of nanoparticles on public health. The toxicity assessment studies the death of the cell and the effect of nanoparticles on cell viability, various cellular function, and the cellular mechanism of uptake, translocation, and degradation. Based on the *in vitro* assays, one can predict the dose and route of nanoparticle exposure in model organisms (Fig. 16.2). The primary parameter of nanoparticle-associated toxicity is the dose. Therefore, to evaluate the cytotoxicity of the nanoparticles and associated pathways, various assays have been developed. Different *in vitro* assays can determine the cellular level of cytotoxicity associated with nanoparticles (Fig. 16.3), and organ-level toxicity can be monitored through *in vivo* assays. As mentioned earlier, selecting suitable cell lines and model organisms is necessary to evaluate nanoparticle's toxicity.

Fig. 16.2 Schematic representation of steps in nanoparticle toxicity assessment



In-vitro Toxicity assays	MTT assay	Mitochondrial enzymes in the viable cells converts MTT to formazan
	Neutral red uptake assay	The ability of a viable cell to incorporate the dye in the lysosome
	LDH assay	Measures loss of the intracellular LDH to the extracellular medium due to the cell death
	Sulforhodamine B assay	Quantification of cellular protein contents
	Resazurin reduction assay	Oxidoreductase enzymes present in the active cells reduce the weak-fluorescent resazurin to highly fluorescent resorufin

Fig. 16.3 Overview of various in vitro assays used in toxicity assessment of nanoparticle

16.3.1 In Vitro Toxicity Assessment

16.3.1.1 MTT Assay

MTT is a tetrazolium salt with a chemical name of 3-(4,5-dimethylthiazol-2-yl)-2,5-diphenyl tetrazolium bromide, which can be used for the estimation of cell viability. Viable cells that can convert the insoluble MTT into a soluble formazan crystal. The catalytic reduction of MTT to formazan is carried out by the succinate dehydrogenase enzymes present in the mitochondria. Therefore, MTT-based cytotoxicity assay measures the mitochondrial activity of the cell, which can indirectly correlate with

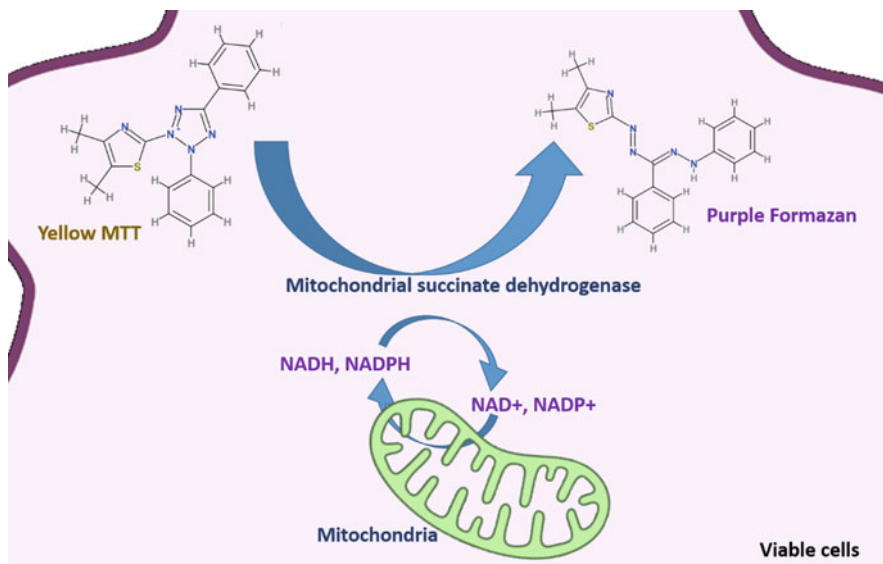


Fig. 16.4 Pictorial representation of MTT reduction

the cellular energy or viability. MTT assay is a colorimetry-based simple method of accessing the cell viability of a population of cells in which the live cell density is directly proportional to the color developed. Nevertheless, the MTT assay requires a solubilizing agent to dissolve the formazan crystal produced and develop color. The production of colored formazan products can quantify by measuring the absorbance using a multi-plate reader. From the development of the MTT assay by Mosmann (1983), it is considered a gold standard in estimating cell viability and proliferation. Significant improvisation has been carried out to improve the sensitivity, accuracy, and to simplify the assay steps. The protocol described by Mosmann utilized an acid-isopropanol solution for solubilization of the formazan crystal (Mosmann 1983). However, Hansen et al., in 1989, modified the protocol by replacing acid-isopropanol solution with DMF for the solubilization of formazan crystal (Hansen et al. 1989) and later Van Rensburg et al. with DMSO in 1997 (Van Rensburg et al. 1997) (Fig. 16.4).

Subsequently, modified tetrazolium-based assays such as MTS, XTT, and WST assays have been described to avoid the washing and solubilization steps present in the traditional MTT assay. Even though significant modifications have been made to simplify the steps involved in the conventional assay, the MTT assay is still considered the standard and well-established assay. Although the well-established MTT assay can provide high-throughput screening and offer miniaturization, it is associated with some challenges and limitations. A reduction in the production of formazan crystal can be observed with a depletion in essential nutrients such as D-glucose, NADPH or due to the change in pH level in the cell culture media. Mitochondria can be intact during the initial phases of cell death through apoptosis,

resulting in MTT reduction to an extent. The molecules or drugs that interfere with mitochondrial activity can influence and alter the cell viability values obtained through MTT assay.

Similarly, some molecules with reductive potential, including ascorbic acid, DTT, paclitaxel, polyphenols, antioxidants, and metal alloy corrosion products, can interact with the tetrazolium salt with the results obtained from the MTT assay. The MTT assay depends on the metabolic rate of cells. The confluent situation in adherent culture reduces the cell's metabolic activity due to contact inhibition, decreasing the MTT reduction. Moreover, some nanoparticles or the media compounds like phenol red can interfere with the absorbance of the formazan crystals and lead to false results due to the enhancement of colorimetry data. Therefore, it is necessary to include the controls (culture medium with MTT and nanoparticles without cells) to avoid false positives and improve the data.

MTT assay can be carried out by adding the MTT reagent with a final concentration of 0.2–0.5 mg/mL to the cells after the nanoparticle treatment. After incubating for 3 h, an organic solvent such as DMSO or isopropanol must be added to solubilize the formazan product formed. After incubating for 15 min under gentle shaking in the dark, the absorbance can be read at 540 nm using a multi-plate reader. Proper controls, including (1) cell alone with MTT and without nanoparticle treatment (negative control), (2) media with MTT and nanoparticle without cell, and (3) positive control (hydrogen peroxide or phenol), should be included in the test. The percentage cell viability can be estimated by taking the relative absorbance of cells treated with varying concentration nanoparticles with respect to the negative control.

16.3.1.2 Modified Tetrazolium Salts

3-(4,5-Dimethylthiazol-2-yl)-5-(3-carboxymethoxyphenyl)-2-(4-sulfophenyl)-2H-tetrazolium (MTS) is a modified tetrazolium salt that can be used for accessing the cell viability, proliferation rate, and cytotoxicity. MTS assay measures the mitochondrial activity of cells, and it can be correlated with cell viability. Unlike MTT assay, MTS assay does not require any formazan solubilizing agent to dissolve the formazan product; however, it requires an electron coupling agent (e.g., phenazine methosulfate, phenazine ethosulfate) to facilitate the reduction (Braydich-Stolle et al. 2005). The reduction of MTS salt results in a formazan product, and it can be directly quantified by taking absorbance at 490 nm using a multi-plate reader. Quantification of cell viability without disturbing the cell is one of the main advantages of MTS assay. Similar to the MTT assay, the presence of ascorbic in the culture media can cause the reduction of MTS salt (Huang et al. 2004).

WST-1 or 4-[3-(4-iodophenyl)-2-(4-nitrophenyl)-2H-5-tetrazolio]-1,3-benzene disulfonate is a modified tetrazolium salt that can be used for one-step cytotoxicity and cell viability assay (Ishiyama et al. 1996). The WST-1 works similar to the MTT by measuring mitochondrial activity by the reaction of succinate dehydrogenase enzymes present in the mitochondria with the tetrazolium salt and forming formazan products. However, WST-1 reduction forms a soluble and stable formazan product in contrast to the insoluble formazan product of MTT assay (Ngamwongsatit et al. 2008), and it is not cytotoxic therefore allowing the rapid and easy measure of

viability. Similar to MTS, the bioreduction of WST-1 to the formazan product requires electron coupling agents such as phenazine methosulfate.

2,3-Bis(2-methoxy-4-nitro-5-sulfohenyl)-5-[(phenylamino)carbonyl]-2H-tetrazolium hydroxide (XTT) is another modified tetrazolium salt used for the estimation of cytotoxicity and cell viability. Similar to WST and MTS assay, the bioreduction of XTT in the presence of an electron coupling agent will result in the formation of a water-soluble formazan product (Roehm et al. 1991). XTT assay can be performed for the cell viability estimation of cells grown in three-dimensional scaffolds (Huyck et al. 2012).

16.3.1.3 Neutral Red Uptake Assay

3-Amino-7-dimethyl-2-methyl phenazine hydrochloride or neutral red (NR) is a supravital dye that can be used to estimate cell viability quantitatively (Repetto et al. 2008). The NR uptake assay is based on the principle of the ability of a viable cell to incorporate the dye. The weak cationic NR dye at physiological pH can penetrate through the plasma membrane of viable cells by nonionic diffusion. Upon uptake of the dye, it accumulates in the lysosome of a viable cell. The acidic environment of the lysosome protonated the NR dye through the electrostatic, hydrophobic interaction of the phosphate/anionic groups of the lysosomal matrix with NR dye (Ates et al. 2017). Subsequently, the charged NR dye retains in the lysosome. However, the cell with a damaged or compromised membrane due to nanoparticle exposure cannot take the NR. The dye can be extracted from the cells using the acidified ethanol solution and measured spectrophotometrically by taking the absorbance at 540 ± 10 nm. Therefore, the cell viability is measured and expressed as the reduction of the cellular uptake of NR dye based on the treatment with nanoparticles.

The neutral red uptake predominantly relies on the cell's ability to maintain the pH gradients by ATP production. The charge of the dye at physiological pH is around zero, which facilitates the uptake. The low pH condition in the lysosome enables the protonation of the dye. The neutral red uptake assay for the assessment of cell viability has certain challenges that need to describe, for example, the toxic materials that require metabolic activation, material that interact with serum protein, chemicals that induces the irreversible crystallization of NR dye and nanoparticles with localized effect on the lysosome (Fig. 16.5).

The NR uptake assay to evaluate the cell viability can be performed by adding the dye solution of a concentration of 0.1% and incubating for 3 h at 37 °C, 5% CO₂, followed by the treatment of nanoparticles on cells. The excess dye should be removed by washing with PBS after incubation. The NR dye retained in the lysosome can be extracted by adding a desorbing agent (glacial acetic acid, 95% ethanol, deionized water in the ratio of 1:50:49) and incubating in the dark for around 15 min with gentle shaking. The absorbance of the NR dye retained can be measured by a multi-plate reader at 540 nm.

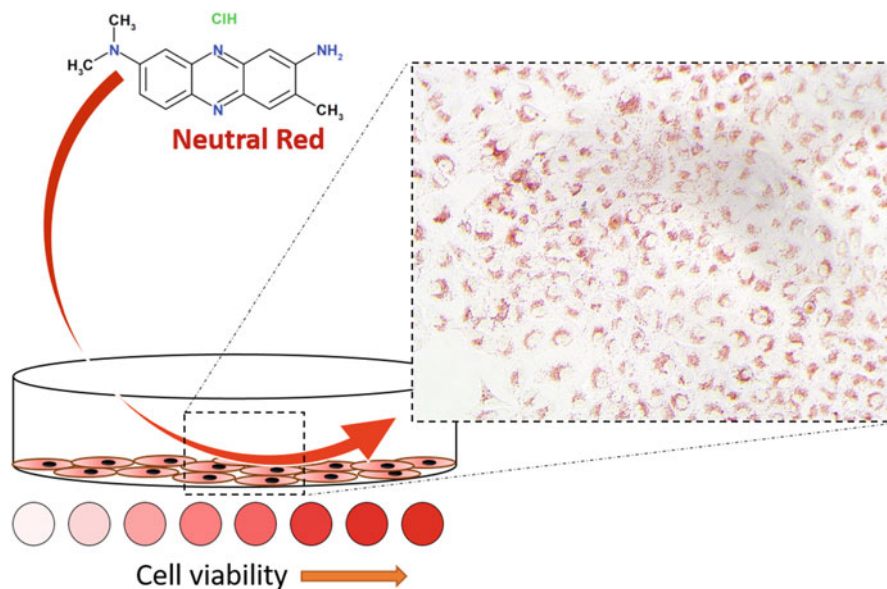


Fig. 16.5 Neutral red uptake assay for the determination of cell viability

16.3.1.4 Lactate Dehydrogenase Assay

Lactate dehydrogenase (LDH) is a soluble and stable enzyme present in the cytoplasm of a cell that catalyzes the interconversion of L-lactate to pyruvate and NAD^+ to NADH during glycolysis. The damage of the cell membrane or the cell death due to nanoparticle exposure will lead to the leakage of the LDH enzyme into the culture medium. Therefore, the LDH leakage assay measures the loss of the intracellular LDH to the extracellular medium due to the compromise of cell membrane integrity (Fig. 16.6).

A colorimetric or fluorometric coupled reaction can estimate the released LDH. In colorimetric LDH assay, the LDH released to the extracellular medium was measured using a coupled reaction that includes the conversion of yellow 2-*p*-iodophenyl-3-*p*-nitrophenyl tetrazolium chloride (INT) to the red colored formazan product. The formazan crystal produced can be measured by taking absorbance at 492 nm using a multi-plate reader. If LDH is present in the culture media, it converts the lactate to pyruvate by reducing NAD^+ to NADH and H^+ . The diaphorase enzyme transfers the H/H^+ generated from the conversion of NAD^+/NADH to the INT salt and forms the formazan product. Hence, the formation of the formazan product is directly proportional to cell death. Alternatively, in fluorometry assay, the NAD^+ to NADH conversion through the oxidation of lactate to pyruvate converts the non-fluorescent resazurin to the fluorescent resorufin. The phenol red and serum present in the cell culture media and detergents such as SDS and cetrimide can influence the LDH assay. Phenol red can generate background absorbance. The normalized value using culture media control or phenol red-free medium can

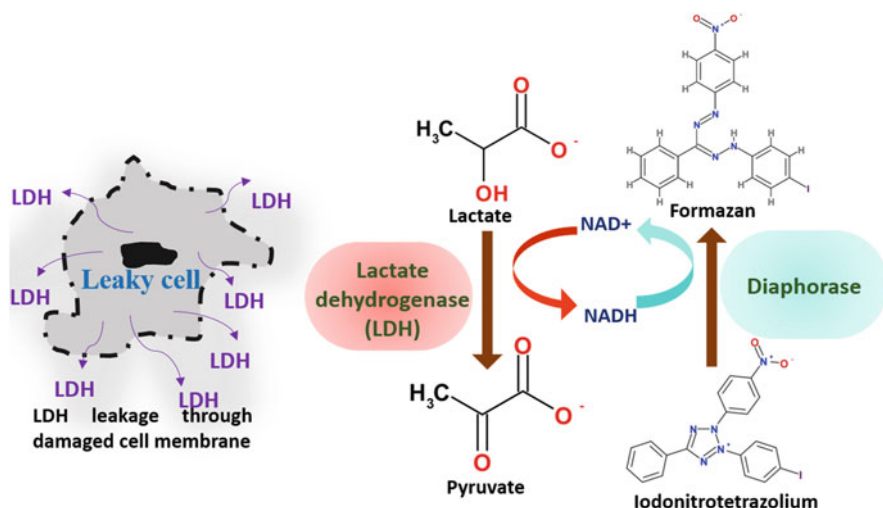


Fig. 16.6 Lactate dehydrogenase assay for cytotoxicity assessment

therefore reduce the background absorbance. Similarly, serum exhibits significant LDH activity. Heat inactivated serum, or reduced serum media (~5%) can minimize the error (Kumar et al. 2018). Certain media components such as sodium pyruvate can inhibit LDH activity and lead to low or comparably no signal. Similarly, test compounds may interact with the LDH activity (Kendig and Tarloff 2007). Hence, careful experimental design and optimization of the steps are required to obtain meaningful data (Kaja et al. 2017).

16.3.1.5 Sulforhodamine B Assay

Sulforhodamine B (SRB), an amino xanthene fluorescent protein stain with two sulfonic groups, can be used to estimate cell numbers through the quantification of cellular protein contents (Skehan et al. 1990). SRB binds to the basic amino acid groups of the cellular proteins and can colorimetrically measure the dye's binding. Due to the direct interaction of dye with the cellular protein, test material interference can be avoided in SRB assay. However, SRB assay requires a fixing step using trichloroacetic acid. The fixing ensures the electrostatic, pH-dependent binding of the dye to the basic amino acid residues of the fixed cells (Skehan et al. 1990). The fixing step offers indefinite stability to the cells. The dye can be extracted in mild basic conditions. Even though the SRB assay did not clearly distinguish the live or dead cells, it can be used for cytotoxicity experiments on the assumption that the detached dead cells can be washed away during repeated washing steps. SRB assay provides a large-scale screening with higher sensitivity (Keepers et al. 1991) and better linearity with the cell number (Rubinstein et al. 1990). Light exposure can result in the degradation of SRB dye; hence, light contamination should be avoided while performing the assay.

16.3.1.6 Resazurin Reduction Assay

Resazurin is a redox dye that can quantify cell viability because the oxidoreductase enzymes present in the mitochondria, cytosol, and microsome of the metabolically active cells reduce the weak-fluorescent resazurin to highly fluorescent resorufin. Stable and nontoxic resorufin produced by the bioreduction of resazurin can be measured fluorometrically or colorimetrically (Czekanska 2011). The reduction of resazurin is therefore directly proportional to the number of viable cells present in the culture. Resazurin reduction assay allows the continuous monitoring of the cell proliferation both in end-point or kinetic assay, and it can be used in conjunction with other assays (Anoopkumar-Dukie et al. 2005). The enzymes such as nicotinamide adenine dehydrogenase, flavin mononucleotide dehydrogenase, flavin adenine dinucleotide dehydrogenase, and the cytochrome present in the mitochondria primarily take part in the reduction of resazurin. Similarly, enzymes such as flavin reductase, NADPH: quinone oxidoreductase, and cytochromes present in the cytosol and microsome also perform the catalysis of the resazurin. The maximum peak of excitation and emission spectra for resorufin is 579 and 584 nm, respectively. Alternatively, the maximum absorbance wavelength of resazurin and resorufin is 605 and 573 nm. Optimization of cell-seeding density, incubation time, and dye concentration are required to produce reproducible and meaningful data. Cells with high metabolic activity and long incubation time can further convert the highly fluorescent resorufin to hydroresorufin. The hydroresorufin produced through the secondary reduction resazurin is colorless and non-fluorescent. The media components with intrinsic antioxidant capacity, such as ascorbic acid and cysteine, can result in inaccurate results.

16.3.1.7 Assay of Intracellular ATP

The intracellular level of adenosine triphosphate (ATP), the primary cellular energy source, is a good index for measuring cytotoxicity. The intracellular content of ATP can be measured by the luciferin-luciferase method (Andreotti et al. 1995). Even though ATP luminescence assay was initially developed to assess chemotherapeutic sensitivity of various drug molecules (Kurbacher and Cree 2005), it can be used to evaluate cell viability in nanoparticle treatment experiments (Braun et al. 2018). Briefly, viable and metabolically active cells maintain intracellular levels. However, cell death or damage due to nanoparticle exposure may lead to the desist of cellular respiration and rapid reduction of ATP levels. The decrease in the ATP levels will cause the loss of luminescence of luciferin-luciferase. Hence, the decline in the ATP level can be correlated to cell death (AshaRani et al. 2009). ATP-based assays provide more sensitivity than other fluorescent-based assays due to the very minimal probability of unintentional interaction of the dye with test cytotoxic nanoparticles (Maehara et al. 1987).

16.3.1.8 Calcein-AM/PI Dual Staining

Cell viability assay or cytotoxicity analysis can be performed microscopically or flow cytometrically by calcein-AM/PI dual staining. Calcein-AM is a lipophilic and membrane-permeable acetomethyl ester of calcein. Upon the cell entry, the esterase

in the viable cells converts the non-fluorescent calcein-am to highly green fluorescent calcein (λ_{ex} 490 nm, λ_{em} 515 nm) (Bratosin et al. 2005). Therefore, it measures intracellular enzyme activity and cell membrane integrity. However, propidium iodide (PI) is a nuclear dye that can penetrate the damaged, compromised cell membrane and not the viable cell's membrane. PI can intercalate with the DNA present in the nucleus and emits bright red fluorescence (λ_{ex} 535 nm, λ_{em} 617 nm). Calcein-AM/PI dual staining requires multiple washing steps (Ramirez et al. 2010), and its toxicity to several cell lines (Jonsson et al. 1996; Liminga et al. 1995) are the major drawback of this assay.

16.3.2 In Vivo Toxicity Assessments

In vivo toxicity assessments generally evaluate the organ-level toxicity associated with nanoparticle treatment. Different model organisms can be used for the determination of toxicity (Table 16.1). The selection of model organisms depends on the toxicity of interest. For example, the embryonic zebrafish assay can be performed for evaluating developmental toxicity (Truong et al. 2011). Histopathology analysis and specific biomarker monitoring should be performed to find out the specific toxicity of the materials. The preparation of histopathology slides and the staining process are critical to assess the toxicity. Similarly, the assessment of nanoparticle-related genotoxicity, reproductive toxicity, and carcinogenicity are essential for hazard identification and risk assessment. Depending on the properties and functionalities, certain nanoparticles can cross the cell membrane, translocate to the nucleus, and interfere with nuclear components such as DNA and certain proteins. The interaction of nanoparticles with DNA may lead to lesion formation and alter cell division. ROS generation due to nanoparticle exposure also has a negative effect on the cell cycle.

16.3.2.1 Embryonic Zebrafish Assay

The embryonic zebrafish assay is primarily used for accessing the developmental toxicity associated with nanoparticle exposure. Toxicity assessment using embryonic zebrafish offers both time and cost-effective methods for determining toxicity (Aspatwar et al. 2019). The zebrafish embryo model system can be considered the intact organism that provides functional homeostatic feedback mechanisms and demonstrates intracellular signaling pathways. Zebrafish models only require less infrastructure and fewer nanoparticles to perform the experiments compared to other animal models. Additionally, more than 90% of open reading frames of humans are homologous to the fish's genes (Kimmel et al. 1995). The analogy existing in the early development of zebrafish with higher order vertebrates makes them an exclusive model organism to predict toxicity and conduct high-throughput screening.

The nanoparticle treatment can be performed either by waterborne exposure or by direct delivery by microinjection. Waterborne exposure can be achieved by dissolving the nanoparticle in fish water. Microinjection ensures accurate delivery of a particular dose to the embryo. The toxicity assessment can be performed after the nanoparticle treatment by evaluating the cell viability, perturbation in the

Table 16.1 Examples of in vivo model systems used in toxicity assessment

Type of nanoparticles (NPs) used	In vivo model	Findings	Reference
ZnCl ₂ and ZnO-NPs	Zebrafish larvae (<i>Danio rerio</i>)	Cytotoxic and DNA damage	Boran and Ulutas (2016)
ZnO-NPs	<i>Drosophila melanogaster</i>	Cytotoxic at a higher dose of nanoparticle	Carmona et al. (2016)
Ag-NPs	Zebrafish (<i>Danio rerio</i>)	Cytotoxic, oxidative stress generation, and genotoxic	Krishnaraj et al. (2016)
CuO-nano rods	<i>Hydra magnipapillata</i>	Dose-dependent cell death, oxidative stress induction genotoxic	Murugadas et al. (2016)
ZnO-NPs	<i>Allium cepa</i> roots	Chromosomal aberrations, ROS generation in a dose-dependent manner	Ahmed et al. (2017)
CuO NPs	<i>Drosophila melanogaster</i>	Antigenotoxic activity	Alaraby et al. (2017)
Maghemite (γ -Fe ₂ O ₃) – NPs	Zebrafish (<i>Danio rerio</i>)	Genotoxic	Villacis et al. (2017)
TiSiO ₄ -NPs	<i>Eisenia andrei</i>	Genotoxic	Correia et al. (2017)
CeO ₂ NPs	<i>Corbicula fluminea</i> (freshwater bivalve)	DNA damage	Koehlé-Divo et al. (2018)
MnO-NPs	<i>Physcomitrella patens</i> gametophores	Epigenetic alterations	Ghosh et al. (2019)
AuNPs-indolicidin	<i>Saccharomyces cerevisiae</i>	ROS induction, DNA damage	de Alteriis et al. (2018)
CuO NPs	<i>Allium cepa</i>	Cytotoxic and genotoxic	Singh and Singh (2019)
ZnO-NPs	Seaurchin (<i>Paracentrotus lividus</i>)	Spermiotoxic	Oliviero et al. (2019)
ZnO-NPs	Zebrafish (<i>Danio rerio</i>)	Teratogenicity and genotoxic and cytotoxic	Suriyaprabha et al. (2019)
CeO ₂ -NPs	<i>Oncorhynchus mykiss</i>	Dose-dependent toxicity	Correia et al. (2020)
Nano-CeO ₂	<i>Chironomus riparius</i> larvae	Genotoxic	Savić-Zdravković et al. (2020)
Au-NPs	Gilthead seabream (<i>Sparus aurata</i>)	Accumulation of Au NP liver and spleen	Barreto et al. (2020)
Ag ₂ O and Ag ₂ CO ₃ doped TiO ₂ NPs and pure TiO ₂ particles	Zebrafish (<i>Danio rerio</i>)	Histological lesions, apoptosis, and oxidative stress	Mahjoubian et al. (2021)
Co-exposure of iron oxide NPs and		Genotoxic and mutagenic	

(continued)

Table 16.1 (continued)

Type of nanoparticles (NPs) used	In vivo model	Findings	Reference
glyphosate-based herbicide	Guppy (<i>Poecilia reticulata</i>)		de Souza Trigueiro et al. (2021)
Nanorod, nanosphere, and nanowire forms of TiO ₂	<i>Drosophila melanogaster</i>	Dose-dependent toxicity	Demir (2020)

developmental progression, and the changes in the contraction and movements present in the embryos (Truong et al. 2011). The changes in the larval morphology and behavioral end-points such as the motility and tactile response can be monitored for the prediction of toxicity especially, the developmental toxicity.

16.3.2.2 Reproductive Toxicity Assessment Using *Drosophila melanogaster*

Drosophila melanogaster, commonly known as the fruit fly, can be used for assessing the reproductive and developmental toxicity associated with nanoparticle exposure (Pompa et al. 2011). The nanoparticle treatment of flies can be carried out by dispersing the nanoparticles in the fly's food. Lifespan experiments can be conducted by maintaining the flies in the vials with treated food and normal food. The fertility and reproductive capacity changes elicited by nanoparticle exposure can be monitored by isolating and mating the virgin flies that emerged from nanoparticle-treated food vial and controlling the food vial. The reproductive performance can be analyzed by counting the total number of eggs laid by the female and its mean egg production, and the number of flies that emerged from the eggs. Similarly, the toxic effect of nanoparticles in flies can be assessed by monitoring the expression levels of various proteins (Heat shock proteins, signaling proteins involved in DNA damage repair and apoptosis, etc.) and biomarkers (ROS generation, antioxidant enzymes, etc.). For example, the silver nanoparticle exposure studies in *Drosophila melanogaster* have demonstrated DNA damage, apoptosis through the upregulation of heat shock protein, oxidative stress development, increased activities of antioxidant enzyme, and upregulation of apoptosis markers (caspase-3 and caspase-9) (Ahamed et al. 2010).

16.3.2.3 Toxicity Assessment Using *Daphnia magna*

Recent years have witnessed a surge in the production of nano-based materials. The large-scale production of the nanoscale product can lead to their entry into the aquatic system. Therefore, identifying potential risks and hazards associated with nanoparticle exposure in the aquatic environment is necessary (Magro et al. 2018). The toxicity assessment of nanoparticle exposure in an aqueous environment can be emulated by using various model organisms. *Daphnia magna* is a flea and can be used as a model organism to assess environmental toxicity and bioaccumulation studies of various nanoparticles in the aquatic system (Hu et al. 2018). The

nanoparticle exposure in toxicity studies using daphnids can be dietborne or waterborne (Zhao and Wang 2011). The acute toxicity of nanoparticles using *Daphnia magna* as a model organism can be performed according to Organization for Economic Co-operation and Development (OECD) (1994) with some slight modifications. Briefly, the neonates collected from the pregnant female and placed in the media/surface water containing the nanoparticle and the mobility of the neonates were assessed after 24 and 48 h of the exposure, and the neonates who were not able to swim within 15 s considered as immobilized. Alternatively, the chronic exposure studies can be carried out according to OECD 211 protocol for 21 days. The experiment conditions are similar to acute toxicity studies, except the nanoparticle-containing media/surface water refreshed every 24 h to maintain a steady level of nanoparticle concentration. The death of the neonates can be assessed microscopically by observing the heartbeat. Toxicity assessment using daphnids can also be monitored by recording changes in the appendage curling rate (Xu et al. 2020), growth rate, heartbeat rate, and swimming performance (Magro et al. 2018).

16.3.2.4 Chick Chorioallantoic Membrane (CAM) Assay

The chorioallantoic membrane (CAM) is a highly vascularized extra-embryonic membrane found in hen's eggs (Ribatti 2016). The mammalian placental analogy of CAM allows them to employ as an alternative to animal models (Eckrich et al. 2020). The presence of the circulatory system and various organic functions facilitates using CAM assay in the teratogenicity, embryotoxicity, mucous membrane irritation testing, etc. (Luepke 1985). Nanotoxicology assessments by CAM assay can use in vivo microscopic analysis and immunohistochemistry to determine the lethal dose (LD₅₀), distribution, and accumulation of nanoparticles in various organs. The nanoparticle exposure can be performed by intravascular injection on the 10th day of egg development (Eckrich et al. 2020). CAM assay is a promising technique to evaluate the accumulation and toxicity of nanoparticles. The CAM assay does not require much ethical clearance as compared to other in vivo animal models. Tumor formation with vasculature and stromal cells can be initiated in the CAM of a fertilized egg by transplanting the cancer cell onto the membrane (Vu et al. 2018). Therefore, different nanoparticles can screen for their potential anticancer activity using fertilized eggs. Various research groups have demonstrated the use of fertilized hen eggs as an in vivo model for toxicity evaluation of nanoparticles. The in vivo toxicity assessment of single-walled carbon nanotubes (SWCNT) using chicken embryos has exhibited angiogenesis inhibition in CAM and interfered with embryo development, which eventually led to the death of SWCNTs-treated embryos (Roman et al. 2013). However, the exposure of platinum nanoparticles in chicken embryos did not cause any changes in the embryo's development but induced apoptosis and decreased the proliferation of cells of the brain (Prasek et al. 2013). Similarly, the silver nanoparticle injection in embryo did not demonstrate any changes in the developmental process however have resulted in the reduction of the number and size of lymph follicular and changed the nuclei profile of cells in the bursa of fabricius (Grodzik and Sawosz 2006).

16.3.2.5 Acute and Chronic Toxicity Studies

In recent years, the world has witnessed increased use and production of nanoscale material for various applications. Even though the intrinsic properties of nanoparticles are advantageous in many areas, toxicity is still a concern to address. This is due to the difference in the properties of nanoscale products from their bulk counterpart. Hence, thorough toxicity studies are required to rule out potential toxic responses before the intended application on a large scale. Various *in vitro* and *in vivo* studies are often necessary for the same. Animal *in vivo* models such as mice and rats can be used for evaluating the toxicity response elicited by nanoparticles. Parameters such as serum chemistry, clearance rate, distribution kinetics, histopathology analysis, and hematological analysis can be used for toxicity evaluation (Kumar et al. 2017). The organ-level toxicity can be obtained from the histopathological examination of various organs after the exposure of nanoparticles (Lei et al. 2008). Also, the loss of appetite, changes in fur color, behavioral change, and weight loss after nanoparticle exposure in mice can account for the toxicity evaluation (Chen et al. 2009).

The nanoparticle exposure in mice and rats can be performed by different routes such as intravenous, subcutaneous, inhalation, dermal, oral, and intraperitoneal. After exposure, the nanoparticle is absorbed into the body, interacts with various bio moieties, is distributed across various organs, and finally eliminated from the body. Therefore, the route of exposure, properties of nanoparticles, and their biological interaction can impact the toxicity response (Jia et al. 2017). The acute toxicity of nanoparticles can be evaluated by exposing nanoparticles to Sprague-Dawley rats. The nanoparticle in the prescribed dose (mg of nanoparticle/kg of animal) should inject intravenously. Proper vehicle control (e.g., sucrose solution) and positive control (e.g., cyclophosphamide) should also be administered in different animal groups for the appropriate comparison of toxicity measurements. The changes in the body weight and clinical signs should be monitored and recorded to analyze the nanoparticle's effect on animals. Finally, the biochemical parameters analysis, nanoparticle distribution studies, and histopathological analysis of various tissues collected from rats provide ideas about the distribution of nanoparticles in different organs and their effect on the targets. Oral toxicity of nanoparticles can be performed by orally administering the nanoparticle in a prescribed dose in rats. The changes in various parameters such as the liver function enzyme's activity, ROS generation, and lipid hydroperoxide concentration can identify the potential effect of nanoparticles in animals.

16.3.2.6 Micronucleus Assay

Micronucleus (MN) assay is a simple and highly sensitive method commonly used for *in vitro* and *in vivo* genotoxic evaluation of environmental pollutants, medical devices, pharmaceutical products, and various chemicals, including nanomaterials (Hayashi 2016). Micronucleus are small, round chromatin-containing bodies formed from chromosome or chromosome fragments that lag behind cell division and are considered a potential sign of chromosome instability induced by clastogens and aneugens. *In vitro* MN assay is one of the most widely accepted techniques for

assessing nanomaterial genotoxicity (OECD 2016a). *In vitro* MN assays using human peripheral blood lymphocytes (Thomas and Fenech 2011) or cell lines (e.g., CHO, V79, CHO/IU, L5178Y, etc.), the inclusion of cytochalasin B, which blocks cytokinesis by inhibiting actin polymerization, allows the scoring of MN in binucleated cells which avoids false results that might have occurred due to altered cell division kinetics, and is termed as cytokinesis block micronucleus (CBMN) assay (Fenech 2008). CBMN assay may be modified as a multi-end point method for simultaneous detection of cytotoxicity, cytostasis, and genotoxicity and hence referred to as CBMN cyto assay. In CBMN cyto assay, quantitative measure of micronuclei, nucleoplasmic bridges (NPBs), and nuclear buds (NBUDs) provide evidence of genotoxic events, and cytostasis can be measured from the ratio of mononucleated cells, binucleated cells, and multinucleated cells, and cytotoxicity by detecting apoptosis and necrosis. Many published studies involving *in vivo* genotoxicity assays had adopted the method specified by OECD 474 for the *in vivo* mammalian cell MN test (OECD 2016b). Automated scoring of micronuclei by flow cytometry or image analysis software enables to analyze the data more precisely (Avlasevich et al. 2011).

16.3.2.7 Chromosomal Aberrations Assay

Chromosomal aberration assay, *in vitro* or *in vivo*, is used to detect structural chromosomal aberrations like chromosome or chromatid breaks and exchanges caused by genotoxic agents (George et al. 2017). Many studies have been done by *in vitro* and *in vivo* chromosomal aberration tests for the genotoxic assessment of nanomaterials (Patel et al. 2017). Primary human peripheral blood lymphocytes or established cell lines like CHO cells are preferred for *in vitro* studies (OECD 2016c). Culture can be done either in the presence or absence of S9, a metabolic activator, depending on the cell type used. *In vivo* studies, as suggested by OECD 475, can be done in rodents (mice or rat) or in any other mammalian species with proper justification (OECD 2016d). Addition of metaphase-arresting agent colchicine arrest cells at the metaphase stage of mitosis by hindering the action of spindle fiber, and structural aberrations can be scored very well from metaphase preparations made following chromosome harvest from treated or exposed cells.

16.3.2.8 DNA Damage Assay

Comet assay is a sensitive, simple, reliable, versatile, and widely accepted gel-electrophoresis-based method used to detect DNA strand breaks induced by chemicals or mutagens. This technique has immense application in epidemiological research and toxicological screening for potential genotoxic agents (Vandghanooni and Eskandani 2011). In the comet assay, cells pretreated with test chemicals embedded in a thin layer of agarose gel spread on a microscopic slide are lysed in the presence of high salt/detergent concentration, electrophoresed under alkaline conditions (pH > 13), stained with chromatin-specific fluorescent dyes and examined under a fluorescent microscope (Bowman et al. 2012). Cells exhibiting DNA damage migrate more towards anode from the nucleus, resembling the “tail” of a comet and undamaged nucleoid body remains like the “head” of a comet hence

termed as comet assay. The degree of DNA damage due to strand breaks can be assessed from the percentage of tail DNA fraction after fluorescent staining (Lorenzo et al. 2013). This method can be done *in vitro* using primary cultures (e.g., peripheral blood lymphocytes) or by using established cell lines; or *in vivo* with cells isolated from target organs of animals (e.g., rodents) exposed to the test material. Comet assay had been commonly used in the genotoxicity studies of nanomaterials like C60 fullerenes, single-walled carbon nanotubes (SWCNTs), multi-walled carbon nanotubes (MWCNTs), metal and metal oxide nanoparticles, carbon black, silica nanoparticles, etc.

16.3.2.9 Immunotoxicity Assays

The immune toxicity can be performed by repeated dose exposure (28 or 90 days) of the nanoparticle. The nanoparticle enters the body and interacts with various immune cells such as macrophages, dendritic cells, etc. Hence, the assessment of immune toxicity requires special consideration. The immunotoxicity assays monitor the signs of immunostimulation and immunosuppression.

16.3.2.10 Buehler Test (BT)

Buehler Test (BT) is used for finding the allergenicity of the test material. The BT consists of two phases, the induction phase and the challenge phase. The induction phase comprised topical induction of nanoparticles on days 0, 7, and 21 for 6 h and challenge phase on week 5 and rechallenge on week 7, respectively (Buehler 1965). The challenging sites can be graded from one to four based on the erythematous response and presence of edema (Frankild et al. 2000).

16.3.2.11 The Guinea Pig Maximization Test (GPMT)

The Guinea pig maximization test (GPMT) is used to evaluate the possible formation of allergic reactions elicited by nanoparticle exposure. The GPMT consists of two phases, namely, the induction phase and the challenge phase. During the induction phase, test nanoparticles were exposed to animals twice. Initially, the test material, along with an adjuvant (Freund's complete adjuvant), need to inject intradermally into the animal for enhancing the immune reaction (day 0) and later the occluded topical induction (day 7) of the test material. In the second phase of GPMT, nanoparticles with a lower concentration need to be exposed to the treated animal group (day 21) and rechallenged on day 35. Subsequently, the scoring of individual animals for possible allergic reactions, including swelling and erythema, needs to be performed to determine the sensitization reaction (Magnusson 1980).

16.3.2.12 Local Lymph Node Assay (LLNA)

Local lymph node assay (LLNA) is a highly sensitive immunotoxicity assessment test that measures lymphocyte proliferation and correlates with the material's allergic potential. Murine models are used for performing LLNA. The LLNA test is an alternative to GPMT and BT since it avoids the challenging and rechallenging phase and incorporates earlier end points. The test material is applied to the mice topically on day 0, day 1, and day 3 (three consecutive days). ^3H -thymidine is injected on the

6th day, and hours later, the animal is sacrificed, and the lymphocytes in the draining lymph node are tested for radioactivity (Rovida et al. 2012). The radioactivity level is proportional to lymphocyte proliferation (Gerberick et al. 2007).

16.4 Challenges and Future Perspective in Toxicity Assessment of Nanoparticles

The toxicity of nanoparticles can be carried out using various *in vitro* and *in vivo* analyses. The nanoparticle size and properties can affect the toxicity of the particle. Therefore, to predict the toxicity profile of nanoparticles, proper physiochemical characterization is required. Commonly used *in vitro* cytotoxicity assays based on tetrazolium salts depend on the ability of mitochondrial enzymes present in the viable cells to reduce the tetrazolium salt to formazan product. However, certain media components and the test particle itself can interfere with the tetrazolium salt or the activity of the enzyme, causing underestimation or overestimation of cell viability. Similarly, the interferences are also observed in other assays such as neutral red, resazurin reduction assay, or LDH assay. Hence, careful optimization and proper controls are required for meaningful cell viability data.

Animal models are used for predicting toxicity in humans. The animal models can provide valuable information regarding nanoparticle treatment and associated toxicity. Animal models are necessary for understanding the toxicity kinetics and systemic response. However, the differences in the genetic makeup, pathophysiology, and various signaling pathways will cause ambiguity in the results obtained from animal models. Hence, a proper system that is mimicking human physiology is required. Organ-on-a-chip is a recently developed technology that can emulate actual organ functions. Organ-on-a-chip models manipulate the physiological forces affecting the cellular microenvironment to mimic physiology-relevant conditions (Joseph et al. 2021). Multiple such organ-on-a-chip platforms can combine and ultimately develop a human-on-a-chip that can replace animal models for performing toxicity experiments.

Acknowledgments The authors wish to express their sincere thanks to the Director and Head, Biomedical Technology Wing, Sree Chitra Tirunal Institute for Medical Sciences and Technology (Govt. of India), Trivandrum, for their support and for providing the infrastructure to carry out this work.

References

- Ahamed M, Posgai R, Gorey TJ, Nielsen M, Hussain SM, Rowe JJ (2010) Silver nanoparticles induced heat shock protein 70, oxidative stress and apoptosis in *Drosophila melanogaster*. *Toxicol Appl Pharmacol* 242:263–269. <https://doi.org/10.1016/j.taap.2009.10.016>
- Ahmed B, Dwivedi S, Abdin MZ, Azam A, Al-Shaeri M, Khan MS, Saquib Q, Al-Khedhairi AA, Musarrat J (2017) Mitochondrial and chromosomal damage induced by oxidative stress in Zn

- (2+) ions, ZnO-bulk and ZnO-NPs treated allium cepa roots. *Sci Rep* 7:40685. <https://doi.org/10.1038/srep40685>
- Alaraby M, Hernández A, Marcos R (2017) Copper oxide nanoparticles and copper sulphate act as antigenotoxic agents in *drosophila melanogaster*. *Environ Mol Mutagen* 58:46–55. <https://doi.org/10.1002/em.22068>
- Andreotti PE, Cree IA, Kurbacher CM, Hartmann DM, Linder D, Harel G, Gleiberman I, Caruso PA, Ricks SH, Untch M (1995) Chemosensitivity testing of human tumors using a microplate adenosine triphosphate luminescence assay: clinical correlation for cisplatin resistance of ovarian carcinoma. *Cancer Res* 55:5276–5282
- Anoopkumar-Dukie S, Carey JB, Conere T, O'Sullivan E, van Pelt FN, Allshire A (2005) Resazurin assay of radiation response in cultured cells. *Br J Radiol* 78:945–947. <https://doi.org/10.1259/bjr/54004230>
- AshaRani PV, Mun GLK, Hande MP, Valiyaveetil S (2009) Cytotoxicity and genotoxicity of silver nanoparticles in human cells. *ACS Nano* 3:279–290. <https://doi.org/10.1021/nl800596w>
- Aspatwar A, Hammaren MM, Parikka M, Parkkila S (2019) Rapid evaluation of toxicity of chemical compounds using zebrafish embryos. *J Vis Exp*. <https://doi.org/10.3791/59315>
- Ates G, Vanhaecke T, Rogiers V, Rodrigues RM (2017) Assaying cellular viability using the neutral red uptake assay. *Methods Mol Biol* 1601:19–26. https://doi.org/10.1007/978-1-4939-6960-9_2
- Avlasevich S, Bryce S, De Boeck M, Elhajouji A, Van Goethem F, Lynch A, Nicolette J, Shi J, Dertinger S (2011) Flow cytometric analysis of micronuclei in mammalian cell cultures: past, present and future. *Mutagenesis* 26:147–152. <https://doi.org/10.1093/mutage/geq058>
- Barreto A, Carvalho A, Campos A, Osório H, Pinto E, Almeida A, Trindade T, Soares A, Hylland K, Loureiro S (2020) Effects of gold nanoparticles in gilthead seabream—a proteomic approach. *Aquat Toxicol* 221:105445
- Boran H, Ulutas G (2016) Genotoxic effects and gene expression changes in larval zebrafish after exposure to ZnCl₂ and ZnO nanoparticles. *Dis Aquat Org* 117:205–214. <https://doi.org/10.3354/dao02943>
- Bowman L, Castranova V, Ding M (2012) Single cell gel electrophoresis assay (comet assay) for evaluating nanoparticles-induced DNA damage in cells. *Methods Mol Biol* 906:415–422. https://doi.org/10.1007/978-1-61779-953-2_34
- Bratosin D, Mitrofan L, Palič K, Estaquier J, Montreuil J (2005) Novel fluorescence assay using calcein-AM for the determination of human erythrocyte viability and aging. *Cytometry A* 66A:78–84. <https://doi.org/10.1002/cyto.a.20152>
- Braun K, Stürzel CM, Biskupek J, Kaiser U, Kirchhoff F, Lindén M (2018) Comparison of different cytotoxicity assays for in vitro evaluation of mesoporous silica nanoparticles. *Toxicol In Vitro* 52:214–221. <https://doi.org/10.1016/j.tiv.2018.06.019>
- Braydich-Stolle L, Hussain S, Schlager JJ, Hofmann M-C (2005) In vitro cytotoxicity of nanoparticles in mammalian germline stem cells. *Toxicol Sci* 88:412–419. <https://doi.org/10.1093/toxsci/kfi256>
- Buehler EV (1965) Delayed contact hypersensitivity in the guinea pig. *Arch Dermatol* 91:171–177. <https://doi.org/10.1001/archderm.1965.01600080079017>
- Carmona ER, Inostroza-Blancheteau C, Rubio L, Marcos R (2016) Genotoxic and oxidative stress potential of nanosized and bulk zinc oxide particles in *Drosophila melanogaster*. *Toxicol Ind Health* 32:1987–2001. <https://doi.org/10.1177/0748233715599472>
- Chen Y-S, Hung Y-C, Liao I, Huang GS (2009) Assessment of the in vivo toxicity of gold nanoparticles. *Nanoscale Res Lett* 4:858. <https://doi.org/10.1007/s11671-009-9334-6>
- Correia B, Lourenco J, Marques S, Nogueira V, Gavina A, da Graça Rasteiro M, Antunes F, Mendo S, Pereira R (2017) Oxidative stress and genotoxicity of an organic and an inorganic nanomaterial to *Eisenia andrei*: SDS/DDAB nano-vesicles and titanium silicon oxide. *Ecotoxicol Environ Saf* 140:198–205

- Correia AT, Rodrigues S, Ferreira-Martins D, Nunes AC, Ribeiro MI, Antunes SC (2020) Multi-biomarker approach to assess the acute effects of cerium dioxide nanoparticles in gills, liver and kidney of *Oncorhynchus mykiss*. *Comp Biochem Physiol C Toxicol Pharmacol* 238:108842
- Czekanska EM (2011) Assessment of cell proliferation with resazurin-based fluorescent dye. *Methods Mol Biol* 740:27–32. https://doi.org/10.1007/978-1-61779-108-6_5
- de Alteriis E, Falanga A, Galdiero S, Guida M, Maselli V, Galdiero E (2018) Genotoxicity of gold nanoparticles functionalised with indolicidin towards *Saccharomyces cerevisiae*. *J Environ Sci* 66:138–145. <https://doi.org/10.1016/j.jes.2017.04.034>
- de Souza Trigueiro NS, Gonçalves BB, Dias FC, de Oliveira Lima EC, Rocha TL, Sabóia-Morais SMT (2021) Co-exposure of iron oxide nanoparticles and glyphosate-based herbicide induces DNA damage and mutagenic effects in the guppy (*Poecilia reticulata*). *Environ Toxicol Pharmacol* 81:103521. <https://doi.org/10.1016/j.etap.2020.103521>
- Demir E (2020) An in vivo study of nanorod, nanosphere, and nanowire forms of titanium dioxide using *Drosophila melanogaster*: toxicity, cellular uptake, oxidative stress, and DNA damage. *J Toxicol Environ Health A* 83:456–469. <https://doi.org/10.1080/15287394.2020.1777236>
- Eckrich J, Kugler P, Buhr CR, Ernst BP, Mendler S, Baumgart J, Brieger J, Wiesmann N (2020) Monitoring of tumor growth and vascularisation with repetitive ultrasonography in the chicken chorioallantoic-membrane-assay. *Sci Rep* 10:1–14
- Fenech M (2008) The micronucleus assay determination of chromosomal level DNA damage. *Methods Mol Biol* 410:185–216. https://doi.org/10.1007/978-1-59745-548-0_12
- Frankild S, Vølund A, Wahlberg JE, Andersen KE (2000) Comparison of the sensitivities of the Buehler test and the guinea pig maximisation test for predictive testing of contact allergy. *Acta Derm Venereol* 80:256–262. <https://doi.org/10.1080/000155500750012126>
- George JM, Magogotya M, Vetten MA, Buys AV, Gulumian M (2017) From the cover: an investigation of the genotoxicity and interference of gold nanoparticles in commonly used in vitro mutagenicity and genotoxicity assays. *Toxicol Sci* 156:149–166. <https://doi.org/10.1093/toxsci/kfw247>
- Gerberick GF, Ryan CA, Dearman RJ, Kimber I (2007) Local lymph node assay (LLNA) for detection of sensitisation capacity of chemicals. *Methods* 41:54–60. <https://doi.org/10.1016/j.ymeth.2006.07.006>
- Ghosh I, Sadhu A, Moriyasu Y, Bandyopadhyay M, Mukherjee A (2019) Manganese oxide nanoparticles induce genotoxicity and DNA hypomethylation in the moss *Physcomitrella patens*. *Mutat Res* 842:146–157. <https://doi.org/10.1016/j.mrgentox.2018.12.006>
- Grodzik M, Sawosz E (2006) The influence of silver nanoparticles on chicken embryo development and bursa of Fabricius morphology. *J Anim Feed Sci* 15:111–114. <https://doi.org/10.22358/jafs/70155/2006>
- Hansen MB, Nielsen SE, Berg K (1989) Re-examination and further development of a precise and rapid dye method for measuring cell growth/cell kill. *J Immunol Methods* 119:203–210
- Hayashi M (2016) The micronucleus test—most widely used in vivo genotoxicity test. *Genes Environ* 38:18. <https://doi.org/10.1186/s41021-016-0044-x>
- Hu Y, Chen X, Yang K, Lin D (2018) Distinct toxicity of silver nanoparticles and silver nitrate to *Daphnia magna* in M4 medium and surface water. *Sci Total Environ* 618:838–846. <https://doi.org/10.1016/j.scitotenv.2017.08.222>
- Huang KT, Chen YH, Walker AM (2004) Inaccuracies in MTS assays: major distorting effects of medium, serum albumin, and fatty acids. *BioTechniques* 37:406–412. <https://doi.org/10.2144/04373ST05>
- Huyck L, Ampe C, Van Troys M (2012) The XTT cell proliferation assay applied to cell layers embedded in three-dimensional matrix. *Assay Drug Dev Technol* 10:382–392. <https://doi.org/10.1089/adt.2011.391>
- Ishiyama M, Tominaga H, Shiga M, Sasamoto K, Ohkura Y, Ueno K (1996) A combined assay of cell viability and in vitro cytotoxicity with a highly water-soluble tetrazolium salt, neutral red and crystal violet. *Biol Pharm Bull* 19:1518–1520

- Jia Y-P, Ma B-Y, Wei X-W, Qian Z-Y (2017) The in vitro and in vivo toxicity of gold nanoparticles. *Chin Chem Lett* 28:691–702. <https://doi.org/10.1016/j.ccllet.2017.01.021>
- Jonsson B, Liminga G, Csoka K, Fridborg H, Dhar S, Nygren P, Larsson R (1996) Cytotoxic activity of calcein acetoxymethyl ester (Calcein/AM) on primary cultures of human haematological and solid tumours. *Eur J Cancer* 32:883–887
- Joseph X, Akhil V, Arathi A, Mohanan PV (2021) Comprehensive development in organ-on-a-chip technology. *J Pharm Sci*. <https://doi.org/10.1016/j.xphs.2021.07.014>
- Kaja S, Payne AJ, Naumchuk Y, Koulen P (2017) Quantification of lactate dehydrogenase for cell viability testing using cell lines and primary cultured astrocytes. *Curr Protoc Toxicol* 72:2.26.1–2.26.10. <https://doi.org/10.1002/cptx.21>
- Keepers YP, Pizao PE, Peters GJ, van Ark-Otte J, Winograd B, Pinedo HM (1991) Comparison of the sulforhodamine B protein and tetrazolium (MTT) assays for in vitro chemosensitivity testing. *Eur J Cancer Clin Oncol* 27:897–900. [https://doi.org/10.1016/0277-5379\(91\)90142-Z](https://doi.org/10.1016/0277-5379(91)90142-Z)
- Kendig DM, Tarloff JB (2007) Inactivation of lactate dehydrogenase by several chemicals: implications for in vitro toxicology studies. *Toxicol In Vitro* 21:125–132. <https://doi.org/10.1016/j.tiv.2006.08.004>
- Kimmel CB, Ballard WW, Kimmel SR, Ullmann B, Schilling TF (1995) Stages of embryonic development of the zebrafish. *Dev Dyn* 203:253–310. <https://doi.org/10.1002/aja.1002030302>
- Koehl -Divo V, Cossu-Leguille C, Pain-Devin S, Simonin C, Bertrand C, Sohm B, Mouneyrac C, Devin S, Giamb rini L (2018) Genotoxicity and physiological effects of CeO2 NPs on a freshwater bivalve (*Corbicula fluminea*). *Aquat Toxicol* 198:141–148
- Krishnaraj C, Harper SL, Yun S-I (2016) In vivo toxicological assessment of biologically synthesised silver nanoparticles in adult Zebrafish (*Danio rerio*). *J Hazard Mater* 301:480–491. <https://doi.org/10.1016/j.jhazmat.2015.09.022>
- Kumar V, Sharma N, Maitra SS (2017) In vitro and in vivo toxicity assessment of nanoparticles. *Int Nano Lett* 7:243–256
- Kumar P, Nagarajan A, Uchil PD (2018) Analysis of cell viability by the lactate dehydrogenase assay. *Cold Spring Harb Protoc* 2018. <https://doi.org/10.1101/pdb.prot095497>
- Kurbacher CM, Cree IA (2005) Chemosensitivity testing using microplate adenosine triphosphate-based luminescence measurements. *Methods Mol Med* 110:101–120. <https://doi.org/10.1385/1-59259-869-2:101>
- Lei R, Wu C, Yang B, Ma H, Shi C, Wang Q, Wang Q, Yuan Y, Liao M (2008) Integrated metabolomic analysis of the nano-sized copper particle-induced hepatotoxicity and nephrotoxicity in rats: a rapid in vivo screening method for nanotoxicity. *Toxicol Appl Pharmacol* 232:292–301
- Liminga G, Nygren P, Dhar S, Nilsson K, Larsson R (1995) Cytotoxic effect of calcein acetoxymethyl ester on human tumor cell lines: drug delivery by intracellular trapping. *Anti-cancer Drugs* 6:578–585
- Lorenzo Y, Costa S, Collins AR, Azqueta A (2013) The comet assay, DNA damage, DNA repair and cytotoxicity: hedgehogs are not always dead. *Mutagenesis* 28:427–432. <https://doi.org/10.1093/mutage/get018>
- Luepke NP (1985) Hen’s egg chorioallantoic membrane test for irritation potential. *Food Chem Toxicol* 23:287–291. [https://doi.org/10.1016/0278-6915\(85\)90030-4](https://doi.org/10.1016/0278-6915(85)90030-4)
- Maehara Y, Anai H, Tamada R, Sugimachi K (1987) The ATP assay is more sensitive than the succinate dehydrogenase inhibition test for predicting cell viability. *Eur J Cancer Clin Oncol* 23:273–276. [https://doi.org/10.1016/0277-5379\(87\)90070-8](https://doi.org/10.1016/0277-5379(87)90070-8)
- Magnusson B (1980) Identification of contact sensitizers by animal assay. *Contact Dermatitis* 6:46–50. <https://doi.org/10.1111/j.1600-0536.1980.tb03894.x>
- Magro M, De Liguoro M, Franzago E, Baratella D, Vianello F (2018) The surface reactivity of iron oxide nanoparticles as a potential hazard for aquatic environments: a study on *Daphnia magna* adults and embryos. *Sci Rep* 8:13017. <https://doi.org/10.1038/s41598-018-31483-6>

- Mahjoubian M, Naeemi AS, Sheykhani M (2021) Toxicological effects of Ag(2)O and Ag(2)CO (3) doped TiO(2) nanoparticles and pure TiO(2) particles on zebrafish (*Danio rerio*). *Chemosphere* 263:128182. <https://doi.org/10.1016/j.chemosphere.2020.128182>
- Mosmann T (1983) Rapid colorimetric assay for cellular growth and survival: application to proliferation and cytotoxicity assays. *J Immunol Methods* 65:55–63
- Murugadas A, Zeeshan M, Thamaraiselvi K, Ghaskadbi S, Akbarsha MA (2016) Hydra as a model organism to decipher the toxic effects of copper oxide nanorod: eco-toxicogenomics approach. *Sci Rep* 6:29663. <https://doi.org/10.1038/srep29663>
- Ngamwongsatit P, Banada PP, Panbangred W, Bhunia AK (2008) WST-1-based cell cytotoxicity assay as a substitute for MTT-based assay for rapid detection of toxigenic *Bacillus* species using CHO cell line. *J Microbiol Methods* 73:211–215. <https://doi.org/10.1016/j.mimet.2008.03.002>
- OECD (1994) OECD guidelines for the testing of chemicals. Organization for Economic, Paris
- OECD (2016a) Test No. 487: In vitro mammalian cell micronucleus test. <https://doi.org/10.1787/9789264264861-en>
- OECD (2016b) Test No. 474: Mammalian erythrocyte micronucleus test. <https://doi.org/10.1787/9789264264762-en>
- OECD (2016c) Test No. 473: In vitro mammalian chromosomal aberration test. <https://doi.org/10.1787/9789264264649-en>
- OECD (2016d) Test No. 475: Mammalian bone marrow chromosomal aberration test. <https://doi.org/10.1787/9789264264786-en>
- Oliviero M, Schiavo S, Dumontet S, Manzo S (2019) DNA damages and offspring quality in sea urchin *Paracentrotus lividus* sperms exposed to ZnO nanoparticles. *Sci Total Environ* 651:756–765. <https://doi.org/10.1016/j.scitotenv.2018.09.243>
- Patel S, Patel P, Bakshi SR (2017) Titanium dioxide nanoparticles: an in vitro study of DNA binding, chromosome aberration assay, and comet assay. *Cytotechnology* 69:245–263. <https://doi.org/10.1007/s10616-016-0054-3>
- Pompa PP, Vecchio G, Galeone A, Brunetti V, Sabella S, Maiorano G, Falqui A, Bertoni G, Cingolani R (2011) In vivo toxicity assessment of gold nanoparticles in *Drosophila melanogaster*. *Nano Res* 4:405–413
- Prasek M, Sawosz E, Jaworski S, Grodzik M, Ostaszewska T, Kamaszewski M, Wierzbicki M, Chwalibog A (2013) Influence of nanoparticles of platinum on chicken embryo development and brain morphology. *Nanoscale Res Lett* 8:251. <https://doi.org/10.1186/1556-276X-8-251>
- Ramirez CN, Antczak C, Djaballah H (2010) Cell viability assessment: toward content-rich platforms. *Expert Opin Drug Discov* 5:223–233. <https://doi.org/10.1517/17460441003596685>
- Repetto G, del Paso A, Zurita JL (2008) Neutral red uptake assay for the estimation of cell viability/cytotoxicity. *Nat Protoc* 3:1125–1131
- Ribatti D (2016) The chick embryo chorioallantoic membrane (CAM). A multifaceted experimental model. *Mech Dev* 141:70–77
- Roehm NW, Rodgers GH, Hatfield SM, Glasebrook AL (1991) An improved colorimetric assay for cell proliferation and viability utilising the tetrazolium salt XTT. *J Immunol Methods* 142:257–265
- Roman D, Yasmeen A, Mireuta M, Stiharu I, Al Moustafa A-E (2013) Significant toxic role for single-walled carbon nanotubes during normal embryogenesis. *Nanomedicine* 9:945–950. <https://doi.org/10.1016/j.nano.2013.03.010>
- Rovida C, Ryan C, Cinelli S, Basketter D, Dearman R, Kimber I (2012) The local lymph node assay (LLNA). *Curr Protoc Toxicol* Chapter 20:Unit 20.7. <https://doi.org/10.1002/0471140856.tx2007s51>
- Rubinstein LV, Shoemaker RH, Paull KD, Simon RM, Tosini S, Skehan P, Scudiero DA, Monks A, Boyd MR (1990) Comparison of in vitro anticancer-drug-screening data generated with a tetrazolium assay versus a protein assay against a diverse panel of human tumor cell lines. *JNCI J Natl Cancer Inst* 82:1113–1117. <https://doi.org/10.1093/jnci/82.13.1113>
- Savić-Zdravković D, Milošević D, Uluer E, Duran H, Matic S, Stanić S, Vidmar J, Ščančar J, Dikić D, Jovanović B (2020) A multiparametric approach to cerium oxide nanoparticle toxicity

- assessment in non-biting midges. *Environ Toxicol Chem* 39:131–140. <https://doi.org/10.1002/etc.4605>
- Singh Z, Singh I (2019) CTAB surfactant assisted and high pH nano-formulations of CuO nanoparticles pose greater cytotoxic and genotoxic effects. *Sci Rep* 9:5880. <https://doi.org/10.1038/s41598-019-42419-z>
- Skehan P, Storeng R, Scudiero D, Monks A, McMahon J, Vistica D, Warren JT, Bokesch H, Kenney S, Boyd MR (1990) New colorimetric cytotoxicity assay for anticancer-drug screening. *JNCI J Natl Cancer Inst* 82:1107–1112. <https://doi.org/10.1093/jnci/82.13.1107>
- Suriyaprabha R, Balu KS, Karthik S, Prabhu M, Rajendran V, Aicher WK, Maaza M (2019) A sensitive refining of in vitro and in vivo toxicological behavior of green synthesised ZnO nanoparticles from the shells of *Jatropha curcas* for multifunctional biomaterials development. *Ecotoxicol Environ Saf* 184:109621. <https://doi.org/10.1016/j.ecoenv.2019.109621>
- Thomas P, Fenech M (2011) Cytokinesis-block micronucleus cytome assay in lymphocytes. *Methods Mol Biol* 682:217–234. https://doi.org/10.1007/978-1-60327-409-8_16
- Truong L, Harper SL, Tanguay RL (2011) Evaluation of embryotoxicity using the zebrafish model. *Methods Mol Biol* 691:271–279. https://doi.org/10.1007/978-1-60761-849-2_16
- Van Rensburg CE, Anderson R, Jooné G, Myer MS, O'Sullivan JF (1997) Novel tetramethylpiperidine-substituted phenazines are potent inhibitors of P-glycoprotein activity in a multidrug resistant cancer cell line. *Anticancer Drugs* 8:708–713
- Vandghanooni S, Eskandani M (2011) Comet assay: a method to evaluate genotoxicity of nano-drug delivery system. *Bioimpacts* 1:87–97. <https://doi.org/10.5681/bi.2011.012>
- Villacis RAR, José Filho S, Pina B, Azevedo RB, Pic-Taylor A, Mazzeu JF, Grisolia CK (2017) Integrated assessment of toxic effects of maghemite (γ -Fe₂O₃) nanoparticles in zebrafish. *Aquat Toxicol* 191:219–225
- Vu BT, Shahin SA, Croissant J, Fatieiev Y, Matsumoto K, Le-Hoang Doan T, Yik T, Simargi S, Conteras A, Ratliff L, Jimenez CM, Raehm L, Khashab N, Durand J-O, Glackin C, Tamanoi F (2018) Chick chorioallantoic membrane assay as an in vivo model to study the effect of nanoparticle-based anticancer drugs in ovarian cancer. *Sci Rep* 8:8524. <https://doi.org/10.1038/s41598-018-25573-8>
- Xu EG, Cheong RS, Liu L, Hernandez LM, Azimzada A, Bayen S, Tufenkji N (2020) Primary and secondary plastic particles exhibit limited acute toxicity but chronic effects on *Daphnia magna*. *Environ Sci Technol* 54:6859–6868. <https://doi.org/10.1021/acs.est.0c00245>
- Zhao C-M, Wang W-X (2011) Comparison of acute and chronic toxicity of silver nanoparticles and silver nitrate to *Daphnia magna*. *Environ Toxicol Chem* 30:885–892. <https://doi.org/10.1002/etc.451>



Safety of Nanoparticles: Emphasis on Antimicrobial Properties

17

Kuljit Singh, Shimona Ahlawat, Diksha Kumari, Uma Matlani, Meenakshi, Tejinder Kaur, and Alka Rao

17.1 Introduction

Nanotechnology is the branch of science (nanoscience) that deals with manipulating and tailoring nanosized particles for the desired applicability. The building block of nanotechnology is the nanoparticles (NPs), and this new innovative technology offers an edge over conventional diagnostics and therapeutic approaches (Yetisgin et al. 2020). The properties such as optimal shape, size, larger surface area, biodegradability, biocompatibility, and immune-compatibility make nanomaterials attractive to researchers (Gurunathan et al. 2020). This technology has enabled better bioimaging and improved diagnostic devices, which have further increased therapy success rates in the medical field (Ibrahim 2020). Nanotechnology in agricultural industries has potential applications in crop production, crop improvement, assurance of healthy food, pathogen identification, and removal (Ghorbanpour et al.

K. Singh (✉) · D. Kumari
Infectious Diseases Division, CSIR-Indian Institute of Integrative Medicine, Jammu, India
Academy of Scientific and Innovation Research (AcSIR), Ghaziabad, India
e-mail: singh.kuljit@iiim.res.in

S. Ahlawat · A. Rao (✉)
Academy of Scientific and Innovation Research (AcSIR), Ghaziabad, India
CSIR-Institute of Microbial Technology, Chandigarh, India
e-mail: raoalka@imtech.res.in

U. Matlani · T. Kaur
CSIR-Institute of Microbial Technology, Chandigarh, India

Meenakshi
Academy of Scientific and Innovation Research (AcSIR), Ghaziabad, India

© The Author(s), under exclusive license to Springer Nature Singapore Pte Ltd. 2023

P. V. Mohanan, S. Kappalli (eds.), *Biomedical Applications and Toxicity of Nanomaterials*, https://doi.org/10.1007/978-981-19-7834-0_17

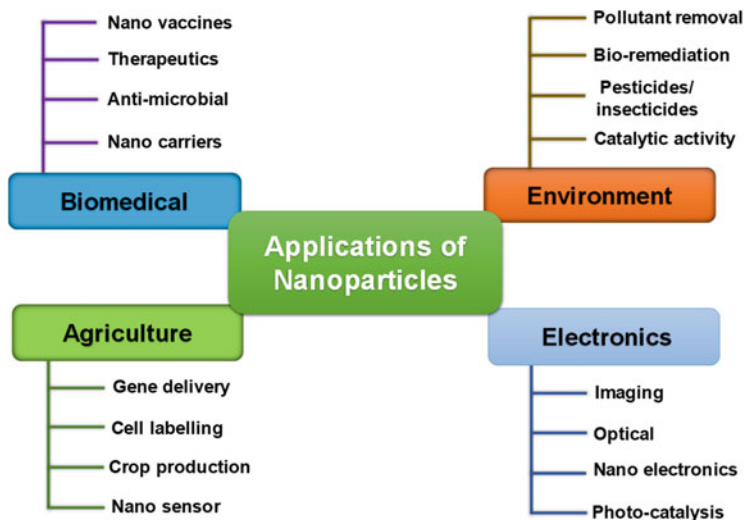


Fig. 17.1 Various applications of nanotechnology

2020). Invention like “Nanosensors” can detect and measure the material derived from bacterial growth and metabolism. Thus, nanosensors can check bacterial and viral toxicity at extremely low concentrations (Rahmati et al. 2020; Kumar et al. 2020). Nanotechnology can also provide solutions for a clean and green environment. A nano fabric towel can absorb 20 times its weight in oil utilized for clean-up purposes (Jin et al. 2018). The use of water-repellent magnetic NPs in oil spills can remove the oil from the water mechanically. Nanotechnology promises an efficient and cost-effective waste-water treatment and thus can help cope with the ever-increasing water demands in the human population. Graphene oxide NPs are increasingly used to filter out air pollutants and purify the air. New NPs-based catalyst has the efficiency to minimize the effect of air pollutants from industrial plants and automobiles (Skinder and Hamid 2020).

NPs are useful in cosmetics, paints, automobiles, space science, and sports utilities. The use of NPs in textiles and fabrics makes them stain resistant, increases sustainability, enhances the quality of food packaging material, and increases the food preservation period, accordingly (Thangadurai et al. 2020). An overview of various applications of nanotechnology is shown in Fig. 17.1. The antimicrobial properties of NPs are of particular interest to researchers. The characteristic of NPs to restrict the growth and metabolism of microbes better than their macroscale counterparts has proved advantageous to overcome the multidrug-resistant mechanism (Wang et al. 2020). For example, cerium oxide NPs cause oxidative stress to eliminate microorganisms (Farias et al. 2018). NPs can serve as antibacterial, antifungal, and antiviral agents (Gudkov et al. 2021; Chen and Liang 2020; Mba and Nweze 2020) both in metallic and biogenic forms (Saleem et al. 2019; Bagchi

and Chauhan 2018). This chapter, in particular, elaborates on the current understanding of NP-based technology for its use as antimicrobial agent.

17.2 Nanoparticles: An Overview

According to the international organization for standardization (ISO), NPs are defined as nano entities that have all three dimensions (3D) in the nanoscale (Sudha et al. 2016). NPs can be formed of several elements, primarily metals, polymers, metal oxides, ceramics, and organic molecules, having salient features that make them desirable for various industrial and pharmaceutical applications (Gharpure et al. 2020). These can be synthesized by chemical processes or environment-friendly methods such as microbes, enzymes, and plants (Hasan 2014). The best-explored applications of NPs include early diagnosis, treatment, and cure of diseases such as cancer, diabetes, and cardiovascular diseases.

17.2.1 Nanoparticles as Drug Carriers

The traditional drug delivery system possesses various constraints such as insolubility of drug, low permeability to the plasma membrane, high dosage of injections, and adverse side effects. The nanotechnology-based drug delivery approach is a novel and emerging concept to overcome the pitfalls of conventional drug delivery approaches (Patra et al. 2018). One can encapsulate the drugs in the internal cavity of the NPs through non-covalent interactions and accomplish the administration of such nanomaterials-based drugs passively. After reaching its target position, the encapsulated structure unfolds, releasing the desired drug to the absolute target. Alternatively, in the self-delivery method, the drug is directly conjugated to the nanocarrier. For target drug delivery, special consideration is necessary during the early drug designing process itself. The coupling between the drug and the carrier NPs is crucial. It has to ensure that the drug does not dissociate too early from the nanocarrier, or else it will be cleared from the body without reaching its required destination. Also, if the drug is not cleaved from its nanocarrier at the optimum time, it will reduce its biological efficacy significantly (Lu et al. 2016). The following section describes the different forms of nanocarriers used for drug delivery with pictorial representation shown in Fig. 17.2.

17.2.1.1 Chitosan

It is a biopolymer extracted from the chitinous shells of sea crustaceans. It is a nontoxic, stable, non-immunogenic, biodegradable polymer employed for the drug delivery process (Ahmad et al. 2021).

17.2.1.2 Alginate

It is a natural polysaccharide derived from the cell walls or intracellular compartments of brown algae, namely *Ascophyllum nodosum* and *Laminaria*

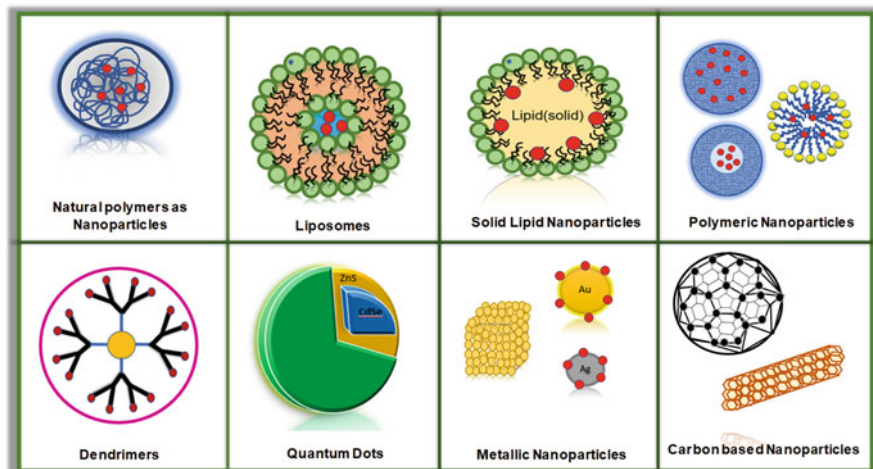


Fig. 17.2 Various forms of nanoparticles used for drug delivery purposes

digitata. With excellent stability, biocompatibility, biodegradability, and reduced toxicity, alginate is a proven agent for various pharmaceutical applications (Hariyadi and Islam 2020).

17.2.1.3 Liposomes

These are the spherical vesicles consisting of an inner aqueous core encapsulated around a phospholipid bilayer. Both water-loving (hydrophilic) and water-repelling (hydrophobic) drugs can form liposomes. Due to their structural similarity with the cell membrane phospholipids and superior pharmacokinetics, liposomes are attractive drug delivery tools in therapeutics (Xing et al. 2016). Apart from making the compound more stable, liposomes fulfill the 3Bs—biodegradable, biocompatible, and biodistribution. However, they are costly to produce (Yadav et al. 2017).

17.2.1.4 Solid Lipid Nanoparticles

As a substitute to conventional carrier systems, namely liposomes, emulsification, and polymeric NPs, solid lipid NPs are another form of nanocarriers for precise drug administration, non-degenerative, and a budget-friendly approach. It consists of a solid lipid matrix, a surfactant such as an emulsifier, a co-surfactant such as water or solvent, and active ingredients, particularly drugs (Basha et al. 2020). Formulations of solid lipid NPs are possible for oral, dermal, and parenteral administration.

17.2.1.5 Polymeric Nanoparticles

The 10–100 nm diametric amphiphilic solid colloidal particles formed of block copolymers hydrophobic core containing hydrophobic drug and water-soluble hydrophilic shell balancing the core are called polymeric nanoparticles. The use of polymeric nanocarriers reduces cytotoxicity and improves the stability and solubility of the drug in the bloodstream. While chitosan and dextran are natural polymers,

polyamide, polyesters, and polyphosphazene are synthetic polymers (Lu et al. 2016). Polymeric micelles have a core and a shell that are hydrophilic. The hydrophilic drug is loaded in the core region of micelles.

Similarly, polymeric nanovesicles have an aqueous core and amphiphilic shell. Thus, nanovesicles can integrate both hydrophobic and hydrophilic materials like proteins, genes, and drugs. However, these structures dissociate into the linear form below its critical micelle concentration; therefore, the nanogel—a more stable polymeric nanoparticle form—is in better demand (Lu et al. 2016).

17.2.1.6 Dendrimers

The term is derived from two Greek words, “dendron” and “meros,” which means trees and the parts, respectively (Heera and Shanmugam 2015). Dendrimers indeed are highly branched nanostructures widely used for cancer treatment and bioimaging. With the properties like symmetrical molecular structure and numerous functional groups that can be modified desirably, this becomes a useful candidate for various therapeutics and drug delivery (Abbasi et al. 2014). However, the positively charged dendrimers can alter the cellular membranes and become poisonous to the cell.

17.2.1.7 Quantum Dots

Quantum dots are mini beads of free electrons possessing unique electronic and optical properties. It is a luminescent semiconductor nanocrystal with a 2–10 nm nano-diametric range (Cartaxo 2016). They are generally of two types: simple or core quantum dots (composed of a single material) and core-shell quantum dots (in which the material with a wider energy gap is enclosed by a material having a smaller energy gap). The commonly used material for quantum dots are indium phosphide, cadmium selenide, cadmium telluride, zinc sulfide, and indium arsenide (Ilaiyaraja et al. 2018). These tiny devices are reportable therefore suitable for therapeutic, biosensing, bioimaging, and protein-specific applications or targeting (Riyaz et al. 2019).

17.2.1.8 Metallic Nanoparticles

Metallic NPs consist of metals such as silver, titanium, and gold, metal oxides such as ZnO, magnetic oxides, and semiconductors such as CdS. These are easily transported to the cells due to their appropriate size (10–100 nm) and are not affected by the *in vivo* environment (Ojea-Jimenez et al. 2013). They are efficient in drug delivery and possess antioxidant properties (Khiev et al. 2021).

17.2.1.9 Carbon-Based Nanoparticles

The different allotropic forms of Carbon are helpful for pharmaceutical applications. Carbon-based NPs include carbon nanotubes, fullerene, and nanodiamonds. Fullerene is a highly symmetrical icosahedron having 60 carbons. Carbon nanotubes are single-walled or multi-walled nanotubes. These have a wide range of applications as they exhibit unique properties, namely elasticity, rigidity, electric conductivity, and thermal conductivity (Wilczewska et al. 2012).

17.2.2 Advantages of Drug Administration Employing Nanoscience

Nanostructure-mediated drug delivery comes with increased solubility, more surface area, high dissociation rates, decreased dosage amount reducing toxicity, improved stability, and many more benefits. Nanoparticle-based therapeutics exhibit better efficiency and site-specific drug release due to their nano size and bioavailability to specific tissue/organs. Also, it reduces the side effects of various drugs (Pardhiya and Paulraj 2016). It prolongs the circulation time of the drug, and increases drug penetration. Nanocarriers are generally biodegradable in nature, and, thus, are risk-free. It also protects the drug from premature degradation, increasing its life span. Particle size and surface characteristics of NPs can be easily manipulated to achieve both passive and active drug targeting after parenteral administration (Mitchell et al. 2020).

17.2.3 Disadvantages of Drug Administration Employing Nanoscience

The advantages provided by the NPs are immense, yet some of the limitations need mention and may not be ignored. The large surface area of nanosized particles makes these particles highly sensitive to the biological environment. Similarly, some NPs, such as polymeric NPs, have limited drug-loading capacity, which is a serious disadvantage. Some forms of NPs may cause systemic toxicity, which is an important consideration for clinical use. The small size and increased surface area may also lead to the accumulation of particles, making the physical management of NPs difficult both in dry and liquid states (Mohanraj and Chen 2006). Nanoparticle synthesis may not be economical and may require sophisticated technology and skilled human resource for large-scale manufacturing.

17.3 Applications of Nanoparticles

17.3.1 Nanoparticles as Antibacterial Agents

At least 1% of the bacteria present in the ecosystem are responsible for causing illness in humans. What might appear small percentage includes a plethora of highly infectious organisms, including but not limited to *Escherichia coli*, *Pseudomonas aeruginosa*, *Klebsiella pneumoniae*, *Mycobacterium tuberculosis*, *Staphylococcus aureus*, and *Clostridioides difficile*. The frequent and prolonged use of commonly available antibiotics has led to antibiotic resistance in bacteria, making them less effective and creating a major public health problem. The pipeline for new drugs has been static for quite a while; therefore, there is a desperate need to find creative solutions to bacterial infections and combat antimicrobial resistance. According to the WHO's 2020 annual review of the clinical and preclinical antibacterial pipelines (World Health Organization 2021), five key criteria were highlighted: (a) Target

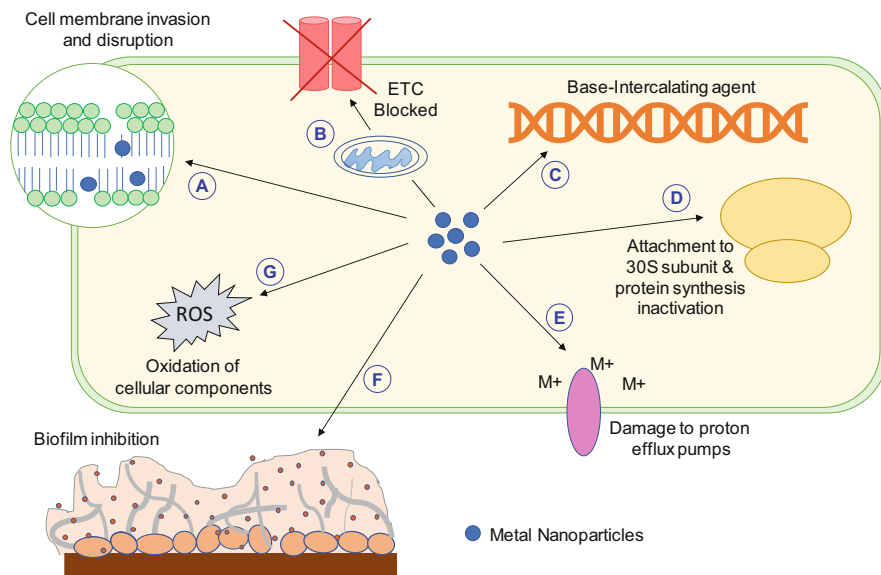


Fig. 17.3 Mechanisms of action and targets of metallic NPs in a bacterial cell. (A) Bacterial cell walls have an overall negative charge on them, attracting metal ions released from NPs to the membrane. The ions penetrate the membrane, creating pores and destabilizing its structure. (B) Mitochondrial toxicity by causing a loss in membrane potential and inhibiting ATPases thereby blocking the electron transport chain (ETC) and ATP generation. (C) The metal ions released from NPs enter the bacterial genome and intercalate between bases by attaching to their S or P groups leading to cytotoxic mutations. (D) Ions released from amassed NPs in the cytoplasm denature the ribosomal subunits and hinder protein synthesis. (E) NPs block the proton efflux pumps on bacterial membranes and thereby prevent them from extruding toxins. (F) NPs affect biofilm integrity by inhibiting EPS production and interrupting bacterial communication required for quorum sensing. (G) NPs can induce oxidative stress in the bacterial cell by generating reactive oxygen species, which oxidize glutathione, leading to suppression of the bacterial antioxidant defense system and allowing the metal ions to freely interact with cellular organs and disrupt their functions, leading to cell death

priority pathogens, (b) Overcome existing resistance, (c) Address a public health need, (d) Preserve effectiveness, and (e) Make accessible to all. Metal NPs with antibacterial activity meet all these criteria and have emerged as non-traditional but promising antibacterial agents. Different synthesis methods can produce NPs of varied shapes and dimensions, which shows strong and extended antimicrobial activity against a broad-spectrum of infectious bacteria (Correa et al. 2020). It has also been theorized that the ability of NPs to target multiple biomolecules in an organism can potentially bring the evolution of resistant bacteria to a standstill (Slavin et al. 2017). A diagrammatic representation of various mechanisms of action and targets of metal NPs in a bacterial cell is shown in Fig. 17.3. This chapter summarizes the latest understanding of the antimicrobial potential of NPs, wherein we have outlined the most recent and most cited papers that progressively endorse metallic NPs as the new antibiotic alternatives.

Silver (Ag) is the most sought-after metal for synthesizing NPs. In a study by Mohanta's group (2020), spherical silver NPs were synthesized in conjugation with fresh leaf extracts from three plants *Semecarpus anacardium* (SA), *Glochidion lanceolarium* (GL), and *Bridelia retusa* (BR). Successful synthesis was confirmed by observing a color change in the solution from the pale-yellow mixture of leaf extract to a deep brown color. Results from SEM micrographs determined their size range as 52–96 nm. The particles exhibited antibacterial and antibiofilm activity against three pathogenic bacteria: *E. coli*, *P. aeruginosa*, and *S. aureus*. SA-AgNPs showed the best antibacterial and antibiofilm with minimum inhibitory concentration (MIC) values. Antibacterial MICs are as follows, *E. coli*: 23.49 $\mu\text{g/mL}$, *P. aeruginosa*: 12.9 $\mu\text{g/mL}$, *S. aureus*: 33.72 $\mu\text{g/mL}$, and antibiofilm MICs are *E. coli*: 23.42 $\mu\text{g/mL}$, *P. aeruginosa*: 12.9 $\mu\text{g/mL}$, *S. aureus*: 33.77 $\mu\text{g/mL}$, respectively. Comparative analysis also indicated that GL-AgNPs were more active against gram-positive organisms (*S. aureus*), whereas SA-AgNP and BR-AgNPs had the most potent activity against gram-negative organisms (*P. aeruginosa* and *E. coli*) (Table 17.1). In a similar study, Ahmed's group (2020) involved green synthesis of silver NPs using the culture of silver-resistant *Bacillus safensis* TEN12 strain. UV-Vis spectroscopy was used to confirm the formation of AgNPs at an absorption peak at 426.18 nm, and FTIR analysis revealed that the AgNPs were stabilized by capping proteins and alcohols. The NPs were spherical, with sizes ranging between 20 and 45 nm, as confirmed by SEM and TEM. Disk diffusion and dilution assays revealed antibacterial activity against *S. aureus* with a zone of inhibition (ZOI) of 20.35 mm along with $\sim 78\%$ growth reduction and in *E. coli* ZOI was 19.69 mm and $\sim 75\%$ reduced growth. MTT assay with the NPs on the HepG2 cell line reported $\sim 36\%$ viability of cells. Both studies clearly showcase the strong potential of AgNPs as antibacterial therapeutic agents.

Rozilah's group (2020) reported the production of antibacterial polymer films made of sugar palm starch biopolymer composite films and AgNPs (0%, 2%, 3%, 4%). At higher AgNPs percentages, there was a noted increase in film elasticity and reduced molecular mobility of matrix, making the nanocomposite films more resistant to breaks, wear, and tear. FE-SEM was used to characterize the nanostructures of films, and the average size of AgNPs was 67.73 ± 6.39 nm. The nanocomposites with thickness ranging from 0.180 to 0.250 ± 0.05 mm were cut into circular disks and immersed in bacterial cultures to determine their activity against *S. aureus*, *E. coli*, and *S. choleraesuis*. Maximum inhibitory activity (ZOI ranging from 7 to 8 mm) was observed against gram-negative bacteria using bio-composite films with 3–4% AgNPs, which can further be explored to prepare films with food packaging applications. In retrospect, silver is a metal with attractive antibacterial potential, and therefore AgNPs must be pushed forward as commercial broad-spectrum antibacterial therapeutic agents. The anti-infective activity of AgNPs inspired the exploration of other metals for similar properties against infectious bacteria. Al-Musawi's group (2020) developed gold nanofibers by conjugating Honey/tripolyphosphate/chitosan (HTCs) fibers with *Capsicum annum* (CA) and gold NPs. FE-SEM analysis revealed a size range of 351 ± 78 nm and a fibrous, dense, smooth, clear, and bead-free morphology. Disk diffusion assay confirmed

Table 17.1 Nanoparticles as antibacterial agents

Publication year	NPs and conjugates	Metal	Characterization	Size (nm)	Shape	Activities	Ref.
2020	Leaf extracts from <i>Semecarpus anacardium</i> , <i>Glochidion lanceolarium</i> , and <i>Bridelia retusa</i>	Silver	UV-vis, ATR-FTIR, DLS, SEM	52–96	Spherical	While GL-AgNPs were more active against gram-positive organisms, SA-AgNP and BR-AgNPs had the strongest activity against gram-negative organisms	Mohanta et al. (2020)
2020	Green synthesis using <i>Bacillus safensis</i> TEN12 strain culture	Silver	UV-vis, FTIR, XRD, SEM, TEM, EDXS	22–46	Spherical	Green NPs showed antibacterial (disk diffusion and MIC) activity against <i>E. coli</i> and <i>S. aureus</i> , and anticancer activity at 20 µg/mL AgNP concentration	Ahmed et al. (2020)
2020	The organic-inorganic hybrid of antibacterial sugar palm starch biopolymer composite films and silver NPs	Silver	FTIR, TGA, FE-SEM	67 ± 6.39	Spherical	ZOI for gram-negative bacteria in the range of 7–8 mm was observed with 3% and 4% of AgNPs	Rozilah et al. (2020)
2020	Honey/tripolyphosphate/chitosan (HTCs) nanofibers loaded with capsaicin derived from <i>Capsicum annum</i> and loaded with gold NPs	Gold	FE-SEM	351 ± 78	Fibrous, dense, smooth, clear, and bead-free	The HTC-CA/AuNP were significantly effective against three gram-negative and one gram-positive organisms. Nanofibers also showed good wound-healing ability	Al-Musawi et al. (2020)

(continued)

Table 17.1 (continued)

Publication year	Publication	Metal	Characterization	Size (nm)	Shape	Activities	Ref.
2020	NPs and conjugates Edible biopolymer (pullulan/carrageenan), D-limonene (DL), and copper sulfide NPs	Copper	FE-SEM, FTIR, XRD, WVP, WCA, MC	47.5 µm film thickness	Greenish intact films	Antibacterial activity against <i>E. coli</i> and a popular foodborne pathogen, <i>L. monocytogenes</i> was also observed	Roy and Rhim (2020)
2020	Citric acid-coated silver and iron oxide NPs	Silver and Iron	TEM, AFM, XRD	~10	Spherical, cubic, and spiral	Inhibited the growth of <i>E. coli</i> and <i>S. typhimurium</i> at a concentration of 100 µg/mL	Gabrielyan et al. (2020)
2020	Zinc NPs conjugated with pineapple peel waste and synthesized at different temperatures	Zinc	FTIR, XRD, FE-SEM, EDXS, TEM	Non-heated: 8–45 nm and heated 73–123 nm	Non-heated: spherical and rod-shaped. Heated: Flower rod shapes	ZOI ranging from 8–15 mm were noted on a <i>B. subtilis</i> lawn using the disk diffusion method. 3% non-heated zinc NPs showed the best antibacterial activity with ZOI of 15 mm	Basri et al. (2020)
2020	Extract of mushroom, <i>Fomes fomentarius</i> , with aqueous solutions of titanium isopropoxide and silver nitrate	Titanium and silver	XRD, DR-UV-S, FTIR, SEM, TEM	80–120	Irregular, rough surface, and aggregated	Disk diffusion using titanium NPs showed ZOI of 15 and 11 mm for <i>E. coli</i> and <i>S. aureus</i> lawns, respectively	Rehman et al. (2020)
2020	Rifampicin encapsulated in mesoporous silica NPs	Silica	QCM-D, TIRF, TGA, FTIR-ATR	~47	Spherical and mesoporous	A 2.5-fold reduction in colony-forming units (CFU) was observed. Calcined NPs tended to	Joyce et al. (2020)

2020	Selenium NPs coated with recombinant spider silk protein eADF4 (κ 16)	Selenium	Zeta potential, SEM, TEM, EDXS, ATR-FTIR, FSD	46	Spherical and monodispersed	Inhibited <i>E. coli</i> growth to 0.3×10^8 CFU/mL. The minimum bactericidal concentration observed was 8 ± 1 μ g/mL	Huang et al. (2020)
2020	Leaf extracts of two medicinal plants, <i>Cassia fistula</i> and <i>Melia azedarach</i> , conjugated with zinc NPs	Zinc	XRD, FTIR, SEM, UV-vis, DLS	10–68	Spherical, clustered, rough surface	<i>Cassia fistula</i> zinc NPs showed better activity against <i>E. coli</i> (ZOI: 44 mm), and <i>Melia azedarach</i> zinc NPs were more effective against <i>S. aureus</i> (ZOI: 38 mm)	Naseer et al. (2020)

AFM atomic force microscopy, *ATR-FTIR* attenuated total reflection-Fourier transform infrared spectra, *DLS* dynamic light scattering, *DR-UV-S* diffuse reflectance UV-visible spectroscopy, *EDS* electron diffraction spectroscopy, *EDXS* energy-dispersive X-ray spectroscopy, *FE-SEM* field-emission scanning electron microscopy, *FTIR* Fourier transform infrared spectroscopy, *FSD* Fourier self-deconvolution, *MC* moisture content, *QCM-D* quartz crystal microbalance with dissipation, *SEM* scanning electron microscopy, *TEM* transmission electron microscopy, *TIFR* total internal reflection fluorescence, *UV-vis* ultraviolet-visible spectroscopy, *WVP* water vapor permeability, *WCA* water contact angle, *XRD* X-ray diffraction

antibacterial activity against *P. multocida*: 34 mm (HTC-CA/AuNPs), *K. rhinoscleromatis*: 31.5 mm (HTC-CA/AuNPs), *S. pyogenes*: 30.5 mm (HTC-CA/AuNPs), *V. vulnificus*: 34 mm (HTC-CA/AuNPs). Although, HTC-CA and HTC-AuNPs showed better results for *P. multocida*, *K. rhinoscleromatis*. MTT assay for HTC-CA/AuNP showed 61% cell viability, over 20% greater than the other nanofibers. HTC-CA/AuNP also demonstrated superior wound healing abilities compared to HTC-CA and HTC-AuNPs dressings thereby indicating the multi-pronged potential of these nanofibers.

Roy's group (2020) developed an antibacterial biofilm from Edible biopolymer (pullulan/carrageenan), D-limonene (DL) and copper sulfide NPs (CuSNPs). The CuSNPs and DL fillers enhanced the UV-light shielding and mechanical properties of the film without altering the thermal stability and transparency. The greenish films showed a reduction of 7 log cycles for *E. coli* and about 2 log cycles for *L. monocytogenes*, a common pathogenic food microbe. In another study, Gabrielyan's group (2020) demonstrated citric acid-coated Ag and iron oxide NPs with antagonistic activity towards two strains of *E. coli* K12 (Wild type) and pARG25 (kanamycin-resistant) and *Salmonella typhimurium*. AgNPs effect was more pronounced on all the strains but iron oxide NPs also suppressed the bacterial growth rate of *E. coli* wild type, *E. coli* (kanamycin-resistant), and *S. typhimurium* by 1.3-, 2.5-, and 4-folds, respectively. A study on zinc NPs by Basri's group (2020) explored an exciting approach of conjugating zinc NPs with pineapple peel waste under temperature control and embedding zinc NPs in starch films to test for their antibacterial activity. Morphological experiments by SEM and TEM showed the non-heated (28 °C) zinc NPs as a mixture of spherical and rod-shaped (8–45 nm), whereas the heated (60 °C) zinc NPs were flower rod shapes (73–123 nm), and the zinc-starch nanocomposite films were 6 mm in diameter. The nanocomposite films prepared with non-heated zinc NPs showed higher efficacy than heated zinc NPs against *B. subtilis* at three NP concentrations 1%, 3%, and 5%. *B. subtilis* lawn indicated that films formed with 3% zinc non-heated and heated NPs showed the best antibacterial activity with ZOI of 15 and 12.33 mm, respectively. Therefore, this strategy could be further explored as a narrow-spectrum antibacterial agent. An intriguing study by Rehman's group (2020) illustrated the synthesis of titanium NPs in combination with intracellular extract of a wild mushroom, *Fomes fomentarius*. FE-SEM showed titanium NPs as aggregated, irregularly shaped with a rough surface in the size range of 80–120 nm. Antibacterial disk diffusion assay showed promising titanium NPs against *E. coli* (ZOI: 15 mm) and *S. aureus* (ZOI: 11 mm). Other recent studies using Silica, Selenium, and Zinc NPs with conjugates significantly indicate their antibacterial potential against *E. coli* and *S. aureus* (Joyce et al. 2020; Huang et al. 2020; Naseer et al. 2020). The NPs in these studies could be strong prospects of broad-spectrum antibacterial agents against the most commonly observed, virulent gram-positive and gram-negative microorganisms.

17.3.2 Nanoparticles as Antifungal Agents

Fungal pathogens are the most common cause of bloodstream infections in hospitalized patients (Pfaller et al. 2020). The fungal toxins cause severe and life-threatening infections in humans and animals, leading to hepato- and nephrotoxicity, pulmonary infections, immunosuppression, and cancer (Khatoun et al. 2015; Claeys et al. 2020). Severe fungal infections begin with fungal colonization followed by microbial colonies leading to complex multicellular biofilms, which are very hard to fight off with conventional antifungal agents (Paul et al. 2018; Guerra et al. 2020). The use of several antifungal agents for the treatment of fungal infections has been proposed, but most of them are not approved due to limited clinical data (Arastehfar et al. 2020; Wall and Lopez-Ribot 2020). The production and characterization of NPs synthesized using a variety of metallic/nonmetallic components, and variable sizes and shapes have diversified their applications in healthcare and the food sector (Shakibaie et al. 2015). NPs facilitate efficient, targeted delivery of active ingredients with slow-release and long-lasting effectiveness (Silva Viana et al. 2020). Several research groups have evaluated the use of metal NPs alone and as conjugates with antifungal drugs, algal extracts having antifungal properties (Guerra et al. 2020; Cleare et al. 2020; Sattary et al. 2020). Silver is the most commonly applied metal for antifungal assessment, owing to its broad antimicrobial spectrum and less toxicity in mammals (Guerra et al. 2020; Silva Viana et al. 2020). However, the use of other metals like gold, zinc, titanium, and selenium (Pariona et al. 2019; Osonga et al. 2020), and nonmetallic substances like silica and chitosan has also been described (Kalagatur et al. 2018). Discussed below are relevant studies from the past year as available on PubMed, which reported a high antifungal potential of NPs and conjugates (Table 17.2).

Guerra's group (2020) tested the effectiveness of AgNPs against pathogenic *Candida tropicalis* and nonpathogenic probiotic *Saccharomyces boulardii*. The rationale behind the study was to search nanomaterials with significant inhibition of the growth of pathogen microorganisms without eradicating other nonpathogenic species like *S. boulardii*. Synthesized AgNPs have a polygonal-like shape with an average size of 35 ± 15 nm having 1.2% weight of metallic silver stabilized with 18.8% weight of polyvinylpyrrolidone (PVP) in 80% weight of distilled water. The results revealed that 25 $\mu\text{g/mL}$ AgNPs are sufficient to inhibit 90% of the *C. tropicalis* cell growth in comparison to 60% by Fluconazole at 35 $\mu\text{g/mL}$ and 95% inhibition by Amp B at 5 $\mu\text{g/mL}$. The results indicate selective inhibition of pathogenic fungi by AgNPs as approximately 50% of the *S. boulardii* cell population remains viable in the presence of AgNPs, which can initiate further cell multiplication. Hosseini's group (2020) investigated the antifungal effect of zinc oxide (ZnO) NPs and Nystatin on inhibiting the growth of *C. albicans* isolates, causing vulvovaginal candidiasis (VVC). All isolates were susceptible to treatment at the lowest MIC value of ZnO-NPs (0.02 $\mu\text{g/mL}$) and Nystatin (0.6 $\mu\text{g/mL}$), respectively. The results indicate that both ZnO-NPs and Nystatin might be suitable inhibitors of *Candida* sp., with the highest sensitivity to ZnO at MIC 90, ≥ 0.5 $\mu\text{g/mL}$ compared to the non-treated control samples. Therefore, ZnO can act as a potential

Table 17.2 Nanoparticles as antifungal agents

Publication year	NPs and conjugates	Metal	Target pathogen	Characterization	Size (nm)	Shape	Activities	Ref.
2020	Silver NPs with <i>Ligustrum lucidum</i> leaf extract	Silver	<i>Setosphaeria turcica</i> (Phytopathogen)	TEM, UV-Vis	4–42	Spherical	Antifungal activity against <i>S. turcica</i> with IC ₅₀ at a concentration of 170.20 µg/mL.	Huang et al. (2020)
2020	Silver NPs	Silver	<i>Candida tropicalis</i> , <i>Saccharomyces boulardii</i>	TEM, UV-Vis	35 ± 15	Polygonal	Capable of inhibiting 90% cell growth in <i>C. tropicalis</i> , whereas ~50% population of probiotic yeast is still viable, demonstrating selective inhibition of pathogens	Guerra et al. (2020)
2020	Niitic oxide NPs	Niitic oxide	<i>Candida auris</i>	DLS	200–2000	Spherical	Significant ($p < 0.05$) growth inhibition of <i>C. auris</i> strains with a >70% reduction in biofilm formation at 10 mg/mL of NPs	Cleare et al. (2020)
2020	Mesoporous silica NPs encapsulated with lemongrass and clove oil	Silica	<i>Gaeumannomyces graminis</i>	FTIR, BET, TGA, UV-Vis	50–70	Spherical	Antifungal effects of the encapsulated oils increased threefold after encapsulation into NPs with a 70% disease control in vivo	Sattary et al. (2020)
2020	Zinc oxide NPs and Nystatin	Zinc	<i>Candida albicans</i>	UV-Vis	NA	Spherical	VVC <i>Candida</i> sp. showed the highest sensitivity to ZnO at MIC 90 ≥0.5 µg/mL compared to the non-treated control samples	Hosseini et al. (2020)
2020	Gold NPs	Gold	<i>Candida albicans</i> , <i>C. glabrata</i> , <i>C. tropicalis</i> , <i>C. krusei</i>	TEM, XRD	10–50	Rod-shaped	Gold nanorods led to a significant reduction in filament formation, growth inhibition, and prevention of biofilm formation following the incubation of conidia with NPs	Piktel et al. (2020)
2021	Gold NPs synthesized by green algae <i>Chlorella sorokiniana</i>	Gold	<i>Candida tropicalis</i> , <i>C. glabrata</i> , <i>C. albicans</i>	UV-Vis, DLS, XRD, FTIR, SEM, ICP-MS, TEM	5–40	Spherical	Significant antifungal activity against the <i>Candida</i> sp. was observed	Gürsoy and Öztürk (2021)

2020	Tungsten trioxide-doped Zinc oxide NPs	Tungsten	<i>Aspergillus niger</i> , <i>A. flavus</i> , <i>Penicillium notatum</i>	EDS, SEM, TEM, XRD	18–30	Spherical and rod	Superior antifungal activity as compared to the standard drug Fluconazole	Anshad et al. (2020)
2020	Chitosan-stabilized gold NPs and Carbon NPs	Gold, Carbon	<i>Fusarium oxysporum</i> DSM 62338, <i>F. oxysporum</i> DSM 62060	AFM, DLS, UV-Vis	Gold: 80 Carbon: 23	Spherical	A reduction in colony diameter of phytopathogenic fungal strains of <i>F. oxysporum</i> and <i>F. oxysporum</i> affecting tomato production was recorded	Lipisa et al. (2020)
2021	Zinc-based NPs	Zinc	<i>Fusarium oxysporum</i> , <i>Curvularia lanata</i> , <i>Macrophomina phaseolina</i>	FTIR, TEM, UV-Vis, XRD	8–210	Quasi-spherical to hexagonal	Maximum mycelial inhibitory activity was recorded in order: <i>F. oxysporum</i> > <i>C. lanata</i> > <i>M. phaseolina</i>	Kalia et al. (2021)
2020	Titanium dioxide NPs green synthesized and by sol-gel method	Titanium	<i>Ustilago tritici</i> (Wheat rust)	EDS, FTIR, SEM, XRD	15	Spherical	Green prepared titanium NPs were found to have the best antifungal activity against <i>U. tritici</i> wheat rust, especially NPs synthesized with the extract of <i>C. quinoa</i>	Irshad et al. (2020)
2020	Copper NPs	Copper	<i>Colletotrichum gloeosporioides</i> (tropical fruit pathogen)	DLS, TEM	100–300	Spherical	A 100% growth inhibition of <i>C. gloeosporioides</i> at a concentration of 200 ppm copper was observed	Nguyen et al. (2020)
2021	Selenium NPs synthesized by <i>Bacillus megaterium</i> ATCC 55000	Selenium	<i>Rhizoctonia solani</i> RCMB 031001	DLS, TEM, UV-Vis, XRD	41	Spherical	Influent antifungal activity against <i>R. solani</i> in vitro as well as in vivo	Hashem et al. (2021)

(continued)

Table 17.2 (continued)

Publication year	NPs and conjugates	Metal	Target pathogen	Characterization	Size (nm)	Shape	Activities	Ref.
2021	Zinc oxide NPs	Zinc	<i>Alternaria alternata</i> CGJM 3078, <i>Alternaria alternata</i> CGJM 3006, and <i>Fusarium verticillioides</i> CGJM 3823	BET, EDS, FTIR, UV-Vis, XRD, SEM, TEM, TGA	47–65	Spherical	Maximum inhibition was recorded at a concentration of 0.002–5 mg/mL with the largest zone of inhibition against <i>A. alternata</i> CGJM 3006 followed by <i>F. verticillioides</i> CGJM 3823 and <i>A. alternata</i> CGJM 3078	Akpomie et al. (2021)
2021	Copper NPs	Copper	<i>Aspergillus niger</i> , <i>Fusarium oxysporum</i> , and <i>Alternaria alternata</i>	UV-Vis, FTIR, NTA, TEM, XRD, Zeta potential	5–12	Spherical	Significant antifungal effect against the target pathogen is reported	Shende et al. (2021)

AFM atomic force microscopy, BET Brunauer-Emmett-Teller, DLS dynamic light scattering, EDS energy-dispersive X-ray spectrometry, FTIR Fourier transform infrared spectrometry, ICP-MS inductively coupled plasma mass spectrometer, NA not applicable, NTA NPs tracking and analysis system, SEM scanning electron microscopy, TEM transmission electron microscopy, TGA thermo gravimetric analysis, UV-Vis ultraviolet-visible spectroscopy, XRD X-ray diffraction

agent for the control, prevention, and treatment of VVC. Similar observations against Amp B-resistant *C. albicans* are recorded using gold, silver, and selenium NPs (Lotfali et al. 2021). Piktel's group (2020) demonstrated a significant reduction in filament formation following the incubation of conidia with average survival rates of $16.50 \pm 11.12\%$, $10.8 \pm 13.25\%$, $1.67 \pm 0.19\%$, and $0.9 \pm 0.51\%$ for the tested *C. albicans*, *C. glabrata*, *C. tropicalis*, and *C. krusei* isolates at a dose of 1 ng/mL. No hemolytic activity was recorded at fungicidal doses, along with a reduction in biofilm formation at relatively low doses of 0.5–5 ng/mL. Cleare's group (2020) also demonstrated significant growth inhibition of *Candida auris* strains and a >70% decrease in biofilm viability after treatment with 10 mg/mL of nitric oxide NPs. Green synthesized gold NPs synthesized using algae *Chlorella sorokiniana* displayed prominent activity against *Candida tropicalis*, *C. glabrata*, and *C. albicans* (Gürsoy and Öztürk 2021). The effectiveness of metallic NPs against *Aspergillus* sp. is also widely explored. Although lower than the conventional fluconazole antifungal drug, tungsten trioxide-doped zinc oxide NPs are found effective against *Aspergillus* sp. (*A. niger* and *A. flavus*) and *Penicillium notatum* (Arshad et al. 2020). Further, improvements with such rarely used metal NPs can be made by optimizing the metal concentration and reaction conditions.

Apart from the human pathogenic fungi, the use of antifungal NPs has overcome the persistent limitations of using conventional chemical fungicides in the management of plant diseases. Studies have reported the antifungal activity of metal NPs against a soil-borne plant pathogen, *Fusarium oxysporum*. A reduction in colony diameter of phytopathogenic fungal strains of *Fusarium* (*F. oxysporum* DSM 62338 and *F. oxysporum* DSM 62060) that affect tomato production was recorded when treated with chitosan-stabilized gold (AuNPs) and Carbon (CNPs) (Lipşa et al. 2020). A mycelial growth inhibition rate of 100% was achieved in the case of *F. oxysporum* DSM 62060 using 5 mL of three different concentrations of NPs (AuNP25, AuNP50, AuNP75). However, maximum growth inhibition of 54.1% was observed in the case of *F. oxysporum* DSM 62338. CNPs resulted in maximum inhibition of 42.4% and 36.5% for *F. oxysporum* DSM 62338 and *F. oxysporum* DSM 62060. Another study by Kalia's group (2021) reported extensive leakage of the cytoplasmic material from the hyphal tissue along with the swelling of the hyphae cells in the tested fungal species (*Fusarium oxysporum* > *Curvularia lunata* > *Macrophomina phaseolina*) at a 40 mg/L concentration of zinc oxide NPs. Wheat rust caused by *Ustilago tritici* is responsible for global losses in wheat production and harvesting. Irshad's group (2020) has reported a high antifungal potential of green synthesized titanium dioxide-based NPs, especially those produced using *C. quinoa* extract. Similarly, phytopathogenic *Setosphaeria turcica* is responsible for severe foliar disease in maize crops. Spherical AgNPs with an average size of 13 nm, synthesized with *Ligustrum lucidum* leaf extract, effectively against *S. turcica* with IC₅₀ of 170.20 µg/mL (Huang et al. 2020). Sattery's group (2020) reported antifungal effects of the mesoporous silica NPs encapsulated with lemongrass and clove oil increased threefold after encapsulation into NPs with a 70% disease control confirmed by in vivo studies. One of the most delicious tropical fruit, mango, suffers severe damage due to anthracnose produced by

phytopathogenic *Colletotrichum gloeosporioides* (Kamle and Kumar 2016). Anthracnose is responsible for huge (sometimes up to 100%) postharvest loss for mangoes produced under wet or humid conditions. A promising dose-dependent antifungal activity of copper NPs in the size range of 100–300 nm has been reported against *C. gloeosporioides* with 100% growth inhibition at 200 ppm copper (Nguyen et al. 2020). Hashem's group (2021) reported antifungal activity of selenium NPs against *Rhizoctonia solani* RCMB 031001 both in vitro and in vivo with minimum inhibition and minimum fungicidal concentrations of 0.0625 and 1 mM, respectively. A decrease in the severity of root rot disease was noted after treatment. Another report (Akpomie et al. 2021) on plant pathogenic fungi describes a maximum inhibition of *Alternaria* sp. and *F. oxysporum* after treatment with zinc NPs. The largest zone (25.09–36.28 mm) against *A. alternata* CGJM 3006 was observed at a concentration of 0.002–5 mg/mL, followed by *F. verticillioides* CGJM 3823 (23.77–34.77 mm) and *A. alternata* CGJM 3078 (22.73–30.63 mm) in comparison to a positive control (5% bleach). Lastly, copper NPs have shown promising activity against *A. niger*, *F. oxysporum*, and *A. alternata* (Shende et al. 2021).

17.3.3 Nanoparticles as Antiviral Agents

Viruses are the disease-causing agent and have been the causative agent of various diseases in humans. They have a global presence and are responsible for pandemics and epidemics in the past. Viral infections have high morbidity and mortality rate as more than half a million (0.69 million) people died from AIDS-related illnesses in 2019 (Mahy et al. 2019). Respiratory viral infections are easily transmissible and result in a high death rate. Since the exposure of Corona virus disease 2019 (COVID-19), 50 million people were affected, and 3.15 million deaths were observed until April 2021, making it the highest pandemic of the century (Riffe and Acosta 2021). They also cause severe infections, as seen in the case of the Zika virus that results in encephalopathy and meningitis (Nunes et al. 2016). This also affects socioeconomic ratios and impacts the quality of life, as we have seen in the recent pandemic of COVID-19. Considering how prevalent these viral infections are, there is a smaller number of antiviral drugs available. The available vaccines need to be upgraded as the virus mutates rapidly, leading to a new strain, making the available vaccine less effective. Although the search and development of new antiviral are difficult but new and promising therapies have been suggested. NPs have very compelling properties that include optimal size, shape, immuno-compatibility, biodegradability, slow release in bloodstream, and importantly can cross blood-air as well as the blood–brain barrier thus can be precise for a target. NPs alone or in conjugation with antiviral drugs seem to be potential antiviral therapy candidates (Jiao et al. 2018; Szunerits et al. 2015; Gurunathan et al. 2018). The snapshot of antiviral mechanisms of NPs is presented in Fig. 17.4. Thus, to explore the role of the potential impact of NPs in antiviral therapy, we have discussed past 1-year studies retrieved from PubMed using keywords as antiviral and nanoparticles in the advance search option (Table 17.3).

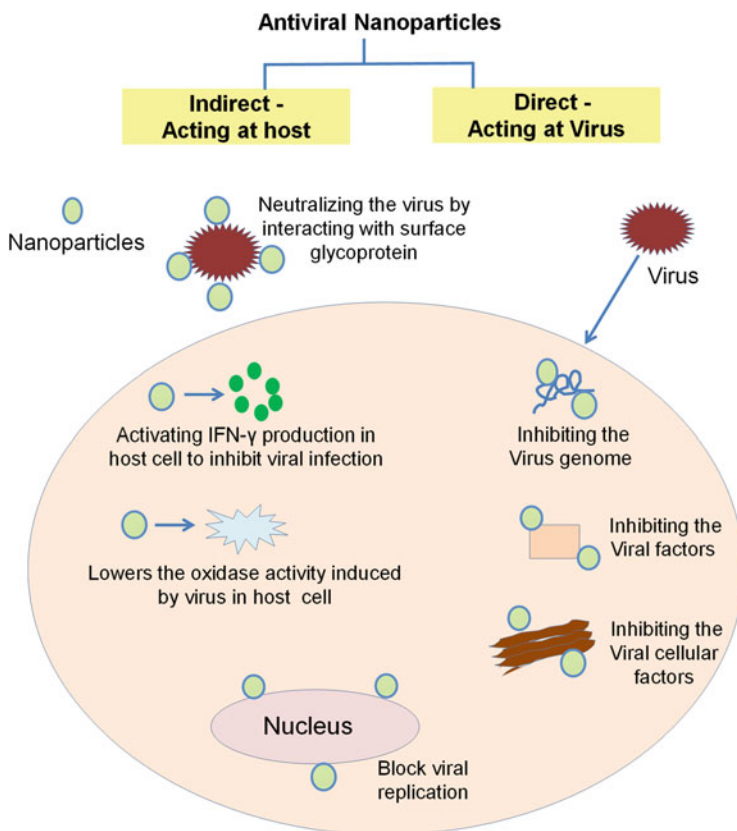


Fig. 17.4 Pictorial representation of NPs as antiviral agents

The study done by Bharti's group (2021) explored the potential of colloidal and immobilized glass silver NPs against water-borne bacteriophages. The particles were synthesized using a chemical reduction approach and immobilized by post-immobilized method on a glass substrate having amines as a functional group. SEM and TEM platforms characterized NPs. Colloidal silver NPs inactivated the T4 bacteriophage and MS2 at the concentration of 60 $\mu\text{g}/\text{mL}$, making the drinking water free from these viruses. As the COVID pandemic is going on, there is an urgent need for a vaccine. So, many NPs emerged as potential candidates against SARS-CoV2. In a study done by Wang's group (2021), cell membrane-based NPs were formed by the classical extrusion method, in which HEK-293 T-hACE2 cells were used for experimentation. These NPs exhibit affinity towards ACE2 receptors to attach to S1 of spike protein, making the virus less available to HK-2 cells and reducing the infection. The TEM analysis revealed a diameter of size 100 nm. The conjugated NPs efficiently reduced the adherence of severe acute respiratory syndrome corona virus 2 (SARS-CoV2) and its mutant D614G-S1 (which is prevalent globally) to HK-2 cells. IC_{50} to neutralize the SARS-CoV2 pseudovirions is 431.2

Table 17.3 Nanoparticles as antiviral agents

Publication year	NPs and conjugates	Metal	Target pathogen	Characterization	Size (nm)	Shape	Activities	Ref.
2021	Colloidal Silver NPs	Silver	MS2, and T4 bacteriophage	SEM, TEM	1–10	Spherical	At the dose of 60 µg/mL completely inactivate MS2 and T4 bacteriophage within 30 and 50 min with an initial concentration of 10 ³ PFU/mL	Bharti et al. (2021)
2021	Cell membrane-based NPs	NA	SARS-CoV2, D614G-S1, pseudovirions	TEM, DLS	100	Spherical	Effectively neutralized the virus with an IC ₅₀ 431.2 µg/mL. Also inhibited the apoptosis induced by translocation of S1 into the cytoplasm of the virus	Wang et al. (2021)
2020	Nanodecoy (cellular membrane nanovesicles)	NA	SARS-CoV2	TEM	100	Round	Neutralize inflammatory cytokines, including IL-6 and GM-CSF. In vivo suppress acute pneumonia in mice model	Rao et al. (2020)
2020	Silver NPs	Silver	SARS-CoV2	TEM	2–15	Spherical	AgNPs inhibits the SARS-CoV2 in veroE6 cell/TMPRSS2, at a concentration of 2 ppm	Jeremiah et al. (2020)
2020	Ivermectin-loaded PLGA- <i>b</i> -PEG-MAL-NPs	NA	SARS-CoV2	TEM	70–80	Spherical	Inhibit the expression of spike protein and ACE2 at the transcription level	Sumar et al. (2020)
2021	<i>Linga chenduram</i> NPs	Mercury and sulfur	Hepatitis C virus	SEM, TEM, FTIR, XRD, EDAX	9–18	Spherical	Inhibit the viral activity in a dose-dependent manner	Al-Ansari et al. (2021)
2021	Poly (lactico-glycolic acid) curcumin NPs	NA	Zika Virus	FTIR, SEM, DLS, DSC	210 ± 40	Polygonal	PLGA-curcumin inhibits ZIKA virus growth and reduces the viral RNA synthesis and protein expression	Pachon et al. (2021)

2020	Monoolein based NPs	NA	HIV	TEM	155 ± 7	Spherical	Monoolein-iodinavir suppresses the growth of HIV virions	Bianchin et al. (2021)
2020	Silver NPs	Silver	H1N1	TEM	20–25	Spherical	AgNPs lower the oxidase activity and increase the life expectancy of mice	Kiseleva et al. (2020)
2021	Nano-Mn	Manganese	MHV-A59 (Murine coronavirus)	TEM, DLS	20–30	Spherical	Nano-Mn activates the IFN- γ production and also suppresses the virus infection in C57/BL-6 mice.	Sun et al. (2021)

DLS dynamic light scattering, *DSC* differential scanning calorimetry, *EDAX* energy-dispersive X-ray analysis, *FTIR* Fourier transform infrared spectroscopy, *SEM* scanning electron microscope, *TEM* transmission electron microscope, *XRD* X-ray diffraction

ng/mg. It is nontoxic, both in vitro and in vivo, making it a potential candidate against the virus. A similar study against SARS-CoV2 by Rao's group (2020) has taken membrane vesicle nanodecoy with 100 nm in size analyzed by TEM. They have shown that it binds and neutralizes inflammatory cytokines, including interleukin 6 (IL-6) and granulocyte-macrophage colony-stimulating factor (GM-CSF). In vivo study also showed that it suppresses pneumonia in mice models. In an interesting study done by Jeremiah's group (2020), to determine the size and concentration at which silver NPs inhibit the SARS-CoV2. They have taken different sizes and concentrations and found that at around 10 nm, a concentration ranging from 1 to 10 ppm showed an inhibitory effect. The concentration above 20 ppm causes cytotoxicity in veroE6 cells/TMPRS22, and they also showed that AgNPs inhibit the viral entry by destroying the integrity of the virus, confirmed by luciferase-based assay. Surnar's group (2020) using ivermectin drug loaded with poly(lactide-co-glycolide)-*b*-poly(ethylene glycol)-maleimide (PLGA-*b*-PEG-Mal) polymer and tagged with Fc immunoglobulin fragment. Ivermectin is a clinically antiviral-approved drug, but its single dose is toxic to the body, and fast clearance results in the noneffectiveness of the drug. So, the NPs are loaded with medicine cause it is slowly released into the bloodstream. Further attachment to Fc helps in crossing the gut epithelial barrier to reach the bloodstream. It has been shown in the study that free ivermectin is less effective in inhibiting or reducing the expression of pseudo-SARS-CoV2 as well as HEK293T expressing spike protein than ivermectin NPs. There are other studies also which proposed that Silver NPs are a potential candidate for inhibiting SARS-CoV2 shown by homology modeling and other bioinformatics studies (Pilaquinga et al. 2021; Varahachalam et al. 2021). Plants extract with known antiviral properties has been taken in nano form against Hepatitis C virus, as seen in a study by Al-Ansari's group (2021). Traditional medicine formed from the herbal mineral Linga chenduram was used. It consists of mercury and sulfur elements in large amounts, but other metals like silver, iron, and molybdenum were also present in trace amounts shown by EDAX analysis. The particles are in the range of 9.71–18.40 nm, having spherical, but other shapes like triangular, cubic, and hexagonal also exist. The inhibitory effect was seen on Huh-7 hepatoma cell line, showing a strong impact in a dose-dependent manner. It is nontoxic to the cell line and in vivo in the male albino rat. In a study against the ZIKA virus, curcumin is used, which has antiviral antibacterial activity. The NPs are made using Poly-lactic-co-glycolic acid (PLGA) as a polymer matrix. The size of the NP is 210 ± 40 nm, as observed from SEM, whereas DLS shows 780 nm size. This difference arises due to the aggregation of NPs in DLS as performed at 25 °C. In an in vitro study, in Vero cells, the E_{50} value was 3.7 ± 0.05 mm. The antiviral activity of PLGA-curcumin is more than free curcumin. Also, the synthesis of virus protein in Vero cells reduces as there has been a reduction of 68% in E-protein synthesis when incubating with PLGA-curcumin compared to only 20% reduction seen with free curcumin (Pacho et al. 2021). In a fascinating study done by Bianchin's group (2021), they made children-friendly drugs for HIV using monoolein-based NPs containing indinavir drug, a particle size of 155 ± 7 nm. The monoolein successfully masked the bitter taste of the known anti-HIV drug indinavir, making it suitable for children to eat. Another study against

the influenza virus done by Kiseleva's group (2020) using silver NPs reported that it lowers the oxidase activity, prevents the lesion, and increases the life expectancy of female CBA mice. The characterization is done by TEM with a mean average size of 20–25 nm.

17.3.4 Nanoparticles as Anti-leishmanial Agents

Leishmaniasis is a widespread neglected tropical disease caused by protozoan parasites belonging to the genus *Leishmania*. Clinically, the disease is classified into three primary forms, cutaneous, mucocutaneous, and visceral leishmaniasis. Among them, visceral leishmaniasis is the fatal one and annually, 20,000–30,000 deaths occur due to this disease. Treatment regimens rely upon a few numbers of drugs such as pentavalent antimonials, Amp B, Miltefosine, and Paromomycin (Singh et al. 2016; Altamura et al. 2020). With increasing drug resistance and toxicities against these drugs, it is the need of the hour to improve the drug delivery approach to fight against leishmaniasis. In the following section, we have tried to discuss the last 1-year research publications retrieved from PubMed, which elucidate the role of NPs in anti-leishmanial therapy (Table 17.4).

Saqib's group (2020) assessed the anti-leishmanial activity of polycaprolactone (NPs) containing Amp B against two strains of the parasite (*L. donovani* and *L. tropica* KWH23). NPs formed were spherical with an average size of 183 nm and encapsulation efficiency of ~86% analyzed by UV-visible spectrophotometer. Macrophages cell line (J774) was infected with *L. donovani* and *L. tropica* KWH23 parasites, and anti-leishmanial activities of NPs, Amp B, and Ambisome were evaluated in a dose-dependent manner. As reported, inhibitory concentration (IC₅₀) of NPs, Amp B, and Ambisome against *L. donovani* are 0.23, 0.21, and 0.28, respectively, and against *L. tropica* KWH23 these values are 0.03, 0.19, and 0.25 µg/mL, respectively. IC₅₀ of NPs against *L. tropica* KWH23 was significantly lower as compared to the standard drugs. Thus, this formulation can provide a novel option for treating cutaneous infections caused by the *L. tropica* parasite. In another study, Almayouf's group (2020) determined the effect of silver NPs against cutaneous infection of leishmaniasis in female Balb/c mice. Silver NPs containing Fig and Olive extracts were biosynthesized, and TEM studies confirmed the spherical shape of NPs, along with size ranging from 50 to 100 nm. Infection in Balb/c mice was developed by giving a subcutaneous injection of *L. tropica* parasites above the tail area. After the completion of 3 weeks, the mice group which were pretreated with NPs reported significantly reduced skin lesions as compared to the untreated group. Pretreatment with NPs also reduced oxidative stress and increased antioxidant enzyme activities in *L. major* infected Balb/c mice. NPs pretreated mice group also showed a marked decrease in the mRNAs expression levels of interleukin (IL)-1β and tumor necrosis factor (TNF)-α. In another study, Awad's group (2021) synthesized silver NPs using *Commiphora molmol* (myrrh) and performed in vitro and in vivo assays against *L. major*. Dose-dependent reduction in the growth of *L. tropica* promastigotes was observed during in vitro studies and in vivo studies in

Table 17.4 Nanoparticles as anti-leishmanial agents

Publication year	Publication	Metal	Characterization	Size (nm)	Shape	Activities	Ref.
2020	NPs and conjugates Polycaprolactone NPs containing Amp B	NA	SEM	183	Spherical	Inhibited the growth of both <i>Leishmania tropica</i> and <i>Leishmania donovani</i> amastigotes with an IC ₅₀ value of 0.03 and 0.023 µg/mL, respectively	Saqib et al. (2020)
2020	Silver NPs containing Fig and Olive extracts	Silver	TEM	50–100	Spherical or polygonal	Effective in reducing lesions in mice infected with <i>Leishmania major</i> and also enhanced the activity of antioxidant enzymes	Almayouf et al. (2020)
2021	Silver NPs containing <i>Commiphora molmol</i> (myrrh)	Silver	TEM, EDS	49	Spherical	During in vitro studies, dose-dependent (10–150 µL/100 µL) inhibition of <i>Leishmania major</i> promastigote was observed and in vivo studies report the healing of skin lesions in mice model	Awad et al. (2021)
2021	Cadmium oxide and chitosan NPs	Cadmium	SEM, TEM, EDS	18–40	Spherical	Reduced the growth of <i>Leishmania major</i> promastigote with an IC ₅₀ value of 0.6 µg/mL and also induced apoptosis-mediated cell death	Bahraminegad et al. (2021)
2020	Chitosan NPs containing Amp B	NA	SEM, TEM	69 ± 8	Spherical	Amp B-loaded chitosan NPs were more effective in reducing lesions and parasite	Riezk et al. (2020)

2020	Titanium dioxide NPs doped with Zinc and hypericin	TiO ₂	SEM, TEM, EDS	~20	Spherical	Inhibited the growth of <i>Leishmania amazonensis</i> with an IC ₅₀ value of 17.5 µg/mL and reduced the parasite load by 43–58% in the BALB/c mice model of CL	Sepulveda et al. (2020)
2020	Silver NPs containing xylan	Silver	SEM, AFM, EDS	~102	Spherical	Inhibited the growth of <i>Leishmania amazonensis</i> promastigote with an IC ₅₀ value of 25 µg/mL	Silva Viana et al. (2020)
2020	Silver NPs containing extract of <i>Mentha arvensis</i> and <i>Mentha longifolia</i>	Silver	SEM, AFM, EDS	20–100	Spherical	Significantly reduced the growth of <i>Leishmania tropica</i> promastigote with an in vitro IC ₅₀ activity of 10–13 µg/mL	Javed et al. (2020a, b)
2020	Biogenic gold-silver bimetallic NPs	Gold and Silver	TEM, EDS	10–12	Spherical	Inhibited the growth of <i>Leishmania donovani</i> promastigote as well as amastigote with an IC ₅₀ value of 0.03–0.035 µg/mL	Alti et al. (2020)
2020	Gold NPs containing Amp B	Gold	DLS, FTIR, TEM	~48	Spherical	Significantly reduced the growth of <i>Leishmania donovani</i> promastigote with an IC ₅₀ value ~20 nM and also activated immunostimulatory Th1 (IL-12 and interferon-γ) response	Kumar et al. (2019)

(continued)

Table 17.4 (continued)

Publication year	NPs and conjugates	Metal	Characterization	Size (nm)	Shape	Activities	Ref.
2020	Guar gum NPs containing Amp B and piperine	NA	DLS	<200	Spherical	During <i>In vitro</i> assay, the growth of <i>Leishmania donovani</i> promastigote was inhibited with an IC ₅₀ value of 24 ng/mL and <i>in vivo</i> studies in a golden hamster model of VL displayed ~90% parasite inhibition	Ray et al. (2020)
2020	2-Hydroxypropyl- β -cyclodextrin (HPCD) modified solid lipid NPs with Amp B and paromomycin	NA	SEM, TEM	141 \pm 3.2	Spherical	Inhibited the growth of intracellular <i>L. donovani</i> amastigotes with an IC ₅₀ value of 0.013 μ g/mL and also significantly reduced the parasite load by 70–90% in BALB/c mice model of VL	Parvez et al. (2020a)
2020	Chitosan solid lipid NPs containing Amp B and paromomycin	NA	SEM, TEM	373 \pm 1.4	Spherical	Ex vivo anti-leishmanial activity on intracellular amastigotes of <i>L. donovani</i> was reported to be 0.018 μ g/mL, which is significantly lower as compared to Amp B alone	Parvez et al. (2020b)

AFM atomic force microscopy, *DLS* dynamic light scattering, *EDS* electron diffraction spectroscopy, *EDS* energy-dispersive X-ray spectroscopy, *FTIR* Fourier transform infrared spectroscopy, *NA* not applicable, *SEM* scanning electron microscopy, *TEM* Transmission Electron Microscopy

BALB/c mice also reported complete healing of the skin lesions within 3 weeks of infection. In both studies mentioned above, lesion healing was significantly better as compared to the standard drug pentostam. Other recent studies also signify the protective efficacy of NPs against cutaneous infection caused by the *Leishmania* parasite (Bahraminegad et al. 2021; Riezk et al. 2020; Sepulveda et al. 2020; Silva Viana et al. 2020). In an interesting study, Javed's group (2020a) explored the role of non-oxidative biocompatible silver NPs synthesized from an aqueous extract of *Mentha arvensis* against *L. tropica*. The average size of NPs was 20–100 nm, and they were structurally anisotropic, confirmed by SEM and AFM studies. Biocompatible NPs were highly effective against *L. tropica* promastigotes as 10 µg/mL dose of NPs killed ~50% of the parasite. In a similar study by the same group (Javed et al. 2020b), silver NPs were phyto-synthesized from an aqueous extract of *Mentha longifolia*. They reported dose-dependent killing of *L. tropica* parasites, with 10 µg/mL dose of NPs killing ~67% of the parasite. Both silver, as mentioned earlier NPs were also effective in killing various plant bacterial pathogens (Javed et al. 2020a, b).

As the drug resistance cases against the current treatment regimen for visceral leishmaniasis are on the rise, Altı's group (2020) synthesized biogenic bimetallic NPs using herbal leaf extracts to evaluate the anti-leishmanial effect against promastigote and amastigote forms of *L. donovani*. TEM and EDX studies confirmed that NPs formed were well separated, spherical, and had an average size of 10–12 nm. As reported, IC₅₀ of bimetallic NPs against promastigote was significantly lower (0.035 µg/mL) than the standard drug miltefosine (10 µg/mL). Bimetallic NPs were also successful in reducing the amastigote form of the parasite by 30–45% in *L. donovani* infected THP-1 cell line. Mechanistic studies revealed that parasite cell death occurred due to reactive oxygen species-induced apoptosis.

Similarly, Kumar's group (2019) also reported improved anti-leishmanial efficacy (~5 folds) of gold NPs conjugated with Amp B compared to Amp B alone during ex vivo studies. The above studies suggest that the metallic NPs-based drug delivery approach can be explored as an alternative option to the available standard drugs. In an attempt to increase the bioavailability of Amp B, Ray's group (2020) developed enteric-coated guar gum NPs containing natural bioenhancer (piperine) and Amp B suitable for oral administration. These NPs displayed controlled drug release and also protected the drug from the acidic pH of the stomach. In vitro studies of these NPs against promastigotes and amastigotes of *L. donovani* parasites exhibited two to threefolds higher IC₅₀ than Amp B drug alone. Golden hamster animal model infected with *L. donovani* also showed significant anti-leishmanial activity with ~90% parasite clearance along with enhanced drug bioavailability confirmed by pharmacokinetics and biodistribution studies. In another study, Parvez's group (2020a) reported the use of 2-hydroxypropyl-β-cyclodextrin (HPCD)-based solid lipid NPs composed of Amp B and paromomycin as an oral drug delivery approach. NPs were spherical with an average size of 141 ± 3.2 nm, confirmed by SEM and TEM studies. The safety and biocompatibility of formulated NPs were confirmed by cytotoxicity studies performed in the J774A.1 macrophage cell line and Swiss albino mice model. Ex vivo studies reported the inhibition of

growth of *L. donovani* amastigotes with an IC_{50} value of 0.013 $\mu\text{g/mL}$, and in vivo experiments performed in BALB/c mice infected with *L. donovani* also showed a 70–90% decrease in parasite burden. In a similar study by the same group (Parvez et al. 2020b), the use of chitosan-based NPs containing Amp B and paromomycin drugs proved effective in inhibiting the growth of the *L. donovani* parasite. Thus, the above studies suggest that NPs-based oral drug delivery approach is the way forward to fight against leishmaniasis.

17.4 Conclusion and Future Perspectives

It is evident from the above context that the synergistic effect of nanotechnology with nanoscience has revolutionized the path of therapeutics approaches. With the excellent efficacy of NPs as antibacterial, antifungal, antiviral, and anti-leishmanial candidates, it is the future ray of hope in overcoming drug resistance and enhancing the killing efficacy of the drug. The use of metallic, liposomal, solid lipid NPs and polymeric micelles aided in on-point drug delivery, treatment shortening controlled drug release, and reduced considerable toxicity. The major action mechanisms employing NPs are enhancing oxidative/nitrosative production in parasites and bacteria, inhibiting biofilm formation in fungi and bacteria, and remodeling viral capsid proteins to disrupt its function and halt replication machinery of the virus. However, NPs are mostly restricted to the study and do not enter clinical trials owing to extensive cost, complicated synthesis mechanism, and low drug loading capacity. Despite these limitations, NPs carry significant potential pertaining to drug delivery approaches. Developing improved preclinical animal models along with a well-versed biological concept can improve the NPs-mediated drug delivery system. Eventually, alliance with theoretical and experimental researches across academia, pharmaceutical industry, and medicine will assist in taking forward these discoveries from research laboratories to the standard population. Therefore, there is an imperative urge to overdue these downfalls and explored realistic applications of NPs for next-generation drug delivery platforms.

References

- Abbasi E, Aval SF, Akbarzadeh A, Milani M, Nasrabadi HT, Joo SW, Hanifehpour Y, Nejati-Koshki K, Pashaei-Asl R (2014) Dendrimers: synthesis, applications, and properties. *Nanoscale Res Lett* 9:1–10
- Ahmad MZ, Rizwanullah M, Ahmad J, Alasmary MY, Akhter MH, Abdel-Wahab BA, Warsi MH, Haque A (2021) Progress in nanomedicine-based drug delivery in designing of chitosan nanoparticles for cancer therapy. *Int J Polym Mater Polym Biomater* 71:1–22
- Ahmed T, Shahid M, Noman M, Niazi MBK, Zubair M, Almatroudi A, Khurshid M, Tariq F, Mumtaz R, Li B (2020) Bioprospecting a native silver-resistant *Bacillus safensis* strain for green synthesis and subsequent antibacterial and anticancer activities of silver nanoparticles. *J Adv Res* 24:475–483

- Akpomie KG, Ghosh S, Gryzenhout M, Conradie J (2021) One-pot synthesis of zinc oxide nanoparticles via chemical precipitation for bromophenol blue adsorption and the antifungal activity against filamentous fungi. *Sci Rep* 11:1–17
- Al-Ansari MM, Singh AR, Al-Khattaf FS, Michael JJ (2021) Nano-formulation of herbo-mineral alternative medicine from *linga chenduram* and evaluation of antiviral efficacy. *Saudi J Biol Sci* 28:1596–1606
- Almayouf MA, El-Khadragy M, Awad MA, Alolayan EM (2020) The effects of silver nanoparticles biosynthesized using fig and olive extracts on cutaneous leishmaniasis-induced inflammation in female balb/c mice. *Biosci Rep* 40. <https://doi.org/10.1042/BSR20202672>
- Al-Musawi S, Albukhaty S, Al-Karagoly H, Sulaiman GM, Alwahibi MS, Dewir YH, Soliman DA, Rizwana H (2020) Antibacterial activity of honey/chitosan nanofibers loaded with capsaicin and gold nanoparticles for wound dressing. *Molecules* 25:4770
- Altamura F, Rajesh R, Catta-Preta CMC, Moretti NS, Cestari I (2020) The current drug discovery landscape for trypanosomiasis and leishmaniasis: challenges and strategies to identify drug targets. *Drug Dev Res* 83:1–28
- Alti D, Veeramohan Rao M, Rao DN, Maurya R, Kalangi SK (2020) Gold–silver bimetallic nanoparticles reduced with herbal leaf extracts induce ROS-mediated death in both promastigote and amastigote stages of *Leishmania donovani*. *ACS Omega* 5:16238–16245
- Arastehfar A, Gabaldón T, Garcia-Rubio R, Jenks JD, Hoenigl M, Salzer HJ, Ilkit M, Lass-Flörl C, Perlin DS (2020) Drug-resistant fungi: an emerging challenge threatening our limited antifungal armamentarium. *Antibiotics* 9:877
- Arshad M, Ehtisham-ul-Haque S, Bilal M, Ahmad N, Ahmad A, Abbas M, Nisar J, Khan M, Nazir A, Ghaffar A (2020) Synthesis and characterization of Zn doped WO₃ nanoparticles: photocatalytic, antifungal and antibacterial activities evaluation. *Mater Res Express* 7:015407
- Awad MA, Al Olayan EM, Siddiqui MI, Merghani NM, Alsaif SSA-L, Aloufi AS (2021) Antileishmanial effect of silver nanoparticles: green synthesis, characterization, in vivo and in vitro assessment. *Biomed Pharmacother* 137:111294
- Bagchi T, Chauhan S (2018) Nanotechnology-based approaches for combating tuberculosis: a review. *Curr Nanomater* 3:130–139
- Bahraminegad S, Pardakhty A, Sharifi I, Ranjbar M (2021) The assessment of apoptosis, toxicity effects and anti-leishmanial study of Chitosan/CdO core-shell nanoparticles, eco-friendly synthesis and evaluation. *Arab J Chem* 14:103085
- Basha SK, Dhandayuthabani R, Muzammil MS, Kumari VS (2020) Solid lipid nanoparticles for oral drug delivery. *Mater Today Proc* 36:313–324
- Bharti S, Mukherji S, Mukherji S (2021) Antiviral application of colloidal and immobilized silver nanoparticles. *Nanotechnology* 32:205102
- Bianchin MD, Prebianca G, Immich MF, Teixeira ML, Colombo M, Koester LS, Araújo BVD, Poletto F, Kulkamp-Guerreiro ICJDD, Pharmacy I (2021) Monoolein-based nanoparticles containing indinavir: a taste-masked drug delivery system. *Drug Dev Ind Pharm* 47:83–91
- Cartaxo ALP (2016) Nanoparticles types and properties—understanding these promising devices in the biomedical area
- Chen L, Liang J (2020) An overview of functional nanoparticles as novel emerging antiviral therapeutic agents. *Mater Sci Eng C* 112:110924
- Claeys L, Romano C, De Ruyck K, Wilson H, Fervers B, Korenjak M, Zavadil J, Gunter MJ, De Saeger S, De Boevre M (2020) Mycotoxin exposure and human cancer risk: a systematic review of epidemiological studies. *Comp Rev Food Sci Food Saf* 19:1449–1464
- Cleare LG, Li KL, Abuzeid WM, Nacharaju P, Friedman JM, Nosanchuk JD (2020) NO *Candida auris*: nitric oxide in nanotherapeutics to combat emerging fungal pathogen *Candida auris*. *J Fungi* 6:85
- Correa MG, Martiñez FB, Vidal CPO, Streitt C, Escrig J, de Dicastillo CL (2020) Antimicrobial metal-based nanoparticles: a review on their synthesis, types and antimicrobial action. *Beilstein J Nanotechnol* 11:1450–1469

- Farias IAP, Santos CCLD, Sampaio FBC (2018) Antimicrobial activity of cerium oxide nanoparticles on opportunistic microorganisms: a systematic review. *Biomed Res Int* 2018: 1923606
- Gabrielyan L, Badalyan H, Gevorgyan V, Trchounian A (2020) Comparable antibacterial effects and action mechanisms of silver and iron oxide nanoparticles on *Escherichia coli* and *Salmonella typhimurium*. *Sci Rep* 10:1–12
- Gharpure S, Akash A, Ankamwar B (2020) A review on antimicrobial properties of metal nanoparticles. *J Nanosci Nanotechnol* 20:3303–3339
- Ghorbanpour M, Bhargava P, Varma A, Choudhary DK (2020) Biogenic nanoparticles and their use in agro-ecosystems. Springer, Singapore
- Gudkov SV, Burmistrov DE, Serov DA, Rebezov MB, Semenova AA, Lisitsyn AB (2021) A mini review of antibacterial properties of ZnO nanoparticles. *Front Phys* 9:641481. <https://doi.org/10.3389/fphy>
- Guerra JD, Sandoval G, Patron A, Avalos-Borja M, Pestryakov A, Garibo D, Susarrey-Arce A, Bogdanchikova N (2020) Selective antifungal activity of silver nanoparticles: a comparative study between *Candida tropicalis* and *Saccharomyces boulardii*. *Colloid Interface Sci Commun* 37:100280
- Gürsoy N, Öztürk BY (2021) Synthesis of intracellular and extracellular gold nanoparticles with a green machine and its antifungal activity. *Turk J Biol* 45:196
- Gurunathan S, Kang M-H, Qasim M, Kim J-H (2018) Nanoparticle-mediated combination therapy: two-in-one approach for cancer. *Int J Mol Sci* 19:3264
- Gurunathan S, Qasim M, Choi Y, Do JT, Park C, Hong K, Kim JH, Song H (2020) Antiviral potential of nanoparticles-can nanoparticles fight against coronaviruses? *Nanomaterials (Basel)* 10:1645
- Hariyadi DM, Islam N (2020) Current status of alginate in drug delivery. *Adv Pharmacol Pharm Sci* 2020:8886095
- Hasan S (2014) A review on nanoparticles: their synthesis and types. *Res J Recent Sci* 2277:2502
- Hashem AH, Abdelaziz AM, Askar AA, Fouda HM, Khalil A, Abd-Elsalam KA, Khaleil MM (2021) *Bacillus megaterium*-mediated synthesis of selenium nanoparticles and their antifungal activity against *Rhizoctonia solani* in faba bean plants. *J Fungi* 7:195
- Basri HH, Talib RA, Sukor R, Othman SH, Ariffin H (2020) Effect of synthesis temperature on the size of ZnO nanoparticles derived from pineapple peel extract and antibacterial activity of ZnO-starch nanocomposite films. *Nanomaterials* 10:1061
- Heera P, Shanmugam S (2015) Nanoparticle characterization and application: an overview. *Int J Curr Microbiol App Sci* 4:379–386
- Hosseini SS, Joshaghani H, Shokohi T, Ahmadi A, Mehrbakhsh Z (2020) Antifungal activity of ZnO nanoparticles and Nystatin and downregulation of SAP1-3 genes expression in fluconazole-resistant *Candida albicans* isolates from vulvovaginal candidiasis. *Infect Drug Resist* 13:385
- Huang T, Kumari S, Herold H, Bargel H, Aigner TB, Heath DE, O'Brien-Simpson NM, O'Connor AJ, Scheibel T (2020) Enhanced antibacterial activity of Se nanoparticles upon coating with recombinant spider silk protein eADF4 (κ 16). *Int J Nanomedicine* 15:4275
- Ibrahim H (2020) Nanotechnology and its applications to medicine: an over view. *QJM Int J Med* 113. <https://doi.org/10.1093/qjmed/hcaa060.008>
- Ilaiyaraja N, Fathima SJ, Khanum F (2018) Quantum dots: a novel fluorescent probe for bioimaging and drug delivery applications. In: *Inorganic frameworks as smart nanomedicines*. Elsevier, pp 529–563
- Irshad MA, Nawaz R, ur Rehman MZ, Imran M, Ahmad J, Ahmad S, Inam A, Razzaq A, Rizwan M, Ali S (2020) Synthesis and characterization of titanium dioxide nanoparticles by chemical and green methods and their antifungal activities against wheat rust. *Chemosphere* 258:127352

- Javed B, Raja NI, Nadhman A (2020a) Understanding the potential of bio-fabricated non-oxidative silver nanoparticles to eradicate Leishmania and plant bacterial pathogens. *Appl Nanosci* 10: 2057–2067
- Javed B, Nadhman A, Mashwani Z-U-R (2020b) Phytosynthesis of Ag nanoparticles from *Mentha longifolia*: their structural evaluation and therapeutic potential against HCT116 colon cancer, Leishmanial and bacterial cells. *Appl Nanosci* 10:3503–3515
- Jeremiah SS, Miyakawa K, Morita T, Yamaoka Y, Ryo A (2020) Potent antiviral effect of silver nanoparticles on SARS-CoV-2. *Biochem Biophys Res Commun* 533:195–200
- Jiao Y, Tibbitts A, Gillman A, Hsiao M-S, Buskohl P, Drummy LF, Vaia RA (2018) Deformation behavior of polystyrene-grafted nanoparticle assemblies with low grafting density. *Macromolecules* 51:7257–7265
- Jin L, Hu B, Kuddannaya S, Zhang Y, Li C, Wang ZJPC (2018) A three-dimensional carbon nanotube–nanofiber composite foam for selective adsorption of oils and organic liquids. *Polym Compos* 39:E271–E277
- Joyce P, Ulmefors H, Maghrebi S, Subramaniam S, Wignall A, Jøemetsa S, Höök F, Prestidge CA (2020) Enhancing the cellular uptake and antibacterial activity of rifampicin through encapsulation in mesoporous silica nanoparticles. *Nanomaterials* 10:815
- Kalagatur NK, Nirmal Ghosh OS, Sundararaj N, Mudili V (2018) Antifungal activity of chitosan nanoparticles encapsulated with *Cymbopogon martinii* essential oil on plant pathogenic fungi *Fusarium graminearum*. *Front Pharmacol* 9:610
- Kalia A, Kaur J, Tondey M, Manchanda P, Bindra P, Alghuthaymi MA, Shami A, Abd-Elsalam KA (2021) Differential antimycotic and antioxidant potentials of chemically synthesized zinc-based nanoparticles derived from different reducing/complexing agents against pathogenic fungi of maize crop. *J Fungi* 7:223
- Kamle M, Kumar P (2016) *Colletotrichum gloeosporioides*: pathogen of anthracnose disease in mango (*Mangifera indica* L.). In: *Current trends in plant disease diagnostics and management practices*. Springer, Cham, pp 207–219
- Khatoun N, Mishra A, Alam H, Manzoor N, Sardar M (2015) Biosynthesis, characterization, and antifungal activity of the silver nanoparticles against pathogenic *Candida* species. *Bionanoscience* 5:65–74
- Khiev D, Mohamed ZA, Vichare R, Paulson R, Bhatia S, Mohapatra S, Lobo GP, Valapala M, Kerur N, Passaglia CL (2021) Emerging nano-formulations and nanomedicines applications for ocular drug delivery. *Nanomaterials* 11:173
- Kiseleva IV, Farroukh MA, Skomorokhova EA, Rekstin AR, Bazhenova EA, Magazenkova DN, Orlov IA, Rudenko LG, Brogginini M, Puchkova LV (2020) Anti-influenza effect of nanosilver in a mouse model. *Vaccine* 8:679
- Kumar P, Shivam P, Mandal S, Prasanna P, Prasad SR, Kumar A, Das P, Ali V, Singh SK (2019) Synthesis, characterization, and mechanistic studies of a gold nanoparticle–amphotericin B covalent conjugate with enhanced antileishmanial efficacy and reduced cytotoxicity. *Int J Nanomedicine* 14:6073
- Kumar P, Mahajan P, Kaur R, Gautam S (2020) Nanotechnology and its challenges in the food sector: a review. *Mater Today Chem* 17:100332
- Lipşa F-D, Ursu E-L, Ursu C, Ulea E, Cazacu A (2020) Evaluation of the antifungal activity of gold–chitosan and carbon nanoparticles on *Fusarium oxysporum*. *Agronomy* 10:1143
- Lotfali E, Toreyhi H, Sharabiani KM, Fattahi A, Soheili A, Ghasemi R, Keymaram M, Rezaee Y, Iranpanah S (2021) Comparison of antifungal properties of gold, silver, and selenium nanoparticles against amphotericin B-resistant *Candida glabrata* clinical isolates. *Avicenna J Med Biotechnol* 13:47
- Lu H, Wang J, Wang T, Zhong J, Bao Y, Hao H (2016) Recent progress on nanostructures for drug delivery applications. *J Nanomater* 2016. <https://doi.org/10.1155/2016/5762431>
- Mahy M, Marsh K, Sabin K, Wanyeki I, Daher J, Ghys PD (2019) HIV estimates through 2018: data for decision-making. *AIDS (London, England)* 33:S203

- Mba IE, Nweze EI (2020) The use of nanoparticles as alternative therapeutic agents against *Candida* infections: an up-to-date overview and future perspectives. *World J Microbiol Biotechnol* 36:1–20
- Mitchell MJ, Billingsley MM, Haley RM, Wechsler ME, Peppas NA, Langer R (2020) Engineering precision nanoparticles for drug delivery. *Nat Rev Drug Discov* 20:1–24
- Mohanraj VJ, Chen Y (2006) Nanoparticles—a review. *Trop J Pharm Res* 5:561–573
- Mohanta YK, Biswas K, Jena SK, Hashem A, Abd-Allah EF, Mohanta TK (2020) Anti-biofilm and antibacterial activities of silver nanoparticles synthesized by the reducing activity of phytoconstituents present in the Indian medicinal plants. *Front Microbiol* 11. <https://doi.org/10.3389/fmicb.2020.01143>
- Naseer M, Aslam U, Khalid B, Chen B (2020) Green route to synthesize Zinc Oxide Nanoparticles using leaf extracts of *Cassia fistula* and *Melia azadarach* and their antibacterial potential. *Sci Rep* 10:1–10
- Nguyen VT, Dang-Thi M-S, Trinh KS (2020) Antifungal activity of Gelatin-Tapioca starch film and coating containing copper nanoparticles against *Colletotrichum gloeosporioides* causing anthracnose. *J Chem* 2020:6667450
- Nunes ML, Carlini CR, Marinowic D, Neto FK, Fiori HH, Scotta MC, Zanella PLÁ, Soder RB, da Costa JC (2016) Microcephaly and Zika virus: a clinical and epidemiological analysis of the current outbreak in Brazil. *J Pediatr* 92:230–240
- Ojea-Jimenez I, Comenge J, Garcia-Fernandez L, Megson ZA, Casals E, Puentes VF (2013) Engineered inorganic nanoparticles for drug delivery applications. *Curr Drug Metab* 14:518–530
- Osonga FJ, Akgul A, Yazgan I, Akgul A, Eshun GB, Sakhaee L, Sadik OA (2020) Size and shape-dependent antimicrobial activities of silver and gold nanoparticles: a model study as potential fungicides. *Molecules* 25:2682
- Pacho MN, Pugni EN, Díaz Sierra JB, Morell ML, Sepúlveda CS, Damonte EB, García CC, D'Accorso NB (2021) Antiviral activity against Zika virus of a new formulation of curcumin in poly lactic-co-glycolic acid nanoparticles. *J Pharm Pharmacol* 73:357–365
- Pardhiya S, Paulraj R (2016) Role of nanoparticles in targeted drug delivery system. *Nanotechnol Drug Deliv* 2:21–51
- Pariona N, Mtz-Enriquez AI, Sánchez-Rangel D, Carrión G, Paraguay-Delgado F, Rosas-Saito G (2019) Green-synthesized copper nanoparticles as a potential antifungal against plant pathogens. *RSC Adv* 9:18835–18843
- Parvez S, Yadagiri G, Gedda MR, Singh A, Singh OP, Verma A, Sundar S, Mudavath SL (2020a) Modified solid lipid nanoparticles encapsulated with Amphotericin B and Paromomycin: an effective oral combination against experimental murine visceral leishmaniasis. *Sci Rep* 10:1–14
- Parvez S, Yadagiri G, Karole A, Singh OP, Verma A, Sundar S, Mudavath SL (2020b) Recuperating the biopharmaceutical aspects of amphotericin B and paromomycin using a chitosan functionalized nanocarrier via oral route for enhanced anti-leishmanial activity. *Front Cell Infect Microbiol* 10:576
- Patra JK, Das G, Fraceto LF, Campos EVR, del Pilar Rodriguez-Torres M, Acosta-Torres LS, Diaz-Torres LA, Grillo R, Swamy MK, Sharma S (2018) Nano based drug delivery systems: recent developments and future prospects. *J Nanobiotechnol* 16:1–33
- Paul S, Mohanram K, Kannan I (2018) Antifungal activity of curcumin-silver nanoparticles against fluconazole-resistant clinical isolates of *Candida* species. *Int Q J Res Ayurveda* 39:182
- Pfaller MA, Carvalhaes CG, Smith CJ, Diekema DJ, Castanheira M (2020) Bacterial and fungal pathogens isolated from patients with bloodstream infection: frequency of occurrence and antimicrobial susceptibility patterns from the SENTRY Antimicrobial Surveillance Program (2012–2017). *Diagn Microbiol Infect Dis* 97:115016
- Piktel E, Suprewicz Ł, Depciuch J, Cieśluk M, Chmielewska S, Durnaś B, Król G, Wollny T, Deptuła P, Kochanowicz J (2020) Rod-shaped gold nanoparticles exert potent candidacidal activity and decrease the adhesion of fungal cells. *Fut Med* 15:2733–2752

- Pilaquinga F, Morey J, Torres M, Seqqat R, de Las Nieves Piña M (2021) Silver nanoparticles as a potential treatment against SARSCoV-2: a review. *Wiley Interdiscip Rev Nanomed Nanobiotechnol* 77:e1707
- Rahmati F, Hosseini SS, Safai SM, Lajayer BA, Hatami M (2020) New insights into the role of nanotechnology in microbial food safety. *3 Biotech* 10:1–15
- Rao L, Xia S, Xu W, Tian R, Yu G, Gu C, Pan P, Meng Q-F, Cai X, Qu D et al (2020) Decoy nanoparticles protect against COVID-19 by concurrently adsorbing viruses and inflammatory cytokines. *J Proc Natl Acad Sci* 117:27141–27147
- Ray L, Karthik R, Srivastava V, Singh SP, Pant AB, Goyal N, Gupta KC (2020) Efficient antileishmanial activity of amphotericin B and piperine entrapped in enteric coated guar gum nanoparticles. *Drug Deliv Transl Res* 11:118–130
- Rehman S, Farooq R, Jermy R, Asiri SM, Ravinayagam V, Jindan RA, Alsalem Z, Shah MA, Reshi Z, Sabit H (2020) A Wild Fomes fomentarius for biomediation of one pot synthesis of titanium oxide and silver nanoparticles for antibacterial and anticancer application. *Biomol Ther* 10:622
- Riezak A, Van Bocxlaer K, Yardley V, Murdan S, Croft SL (2020) Activity of amphotericin B-loaded chitosan nanoparticles against experimental cutaneous leishmaniasis. *Molecules* 25:4002
- Riffe T, Acosta E (2021) Data resource profile: COVerAGE-DB: a global demographic database of COVID-19 cases and deaths. *Int J Epidemiol* 50:390–390f
- Riyaz B, Sudhakar K, Mishra V (2019) Quantum dot-based drug delivery for lung cancer. In: *Nanotechnology-based targeted drug delivery systems for lung cancer*. Elsevier, pp 311–326
- Roy S, Rhim J-W (2020) Fabrication of copper sulfide nanoparticles and limonene incorporated pullulan/carrageenan-based film with improved mechanical and antibacterial properties. *Polymers* 12:2665
- Rozilah A, Jaafar CN, Sapuan SM, Zainol I, Ilyas RA (2020) The effects of silver nanoparticles compositions on the mechanical, physiochemical, antibacterial, and morphology properties of sugar palm starch biocomposites for antibacterial coating. *Polymers* 12:2605
- Saleem K, Khursheed Z, Hano C, Anjum I, Anjum S (2019) Applications of nanomaterials in leishmaniasis: a focus on recent advances and challenges. *Nanomaterials* 9:1749
- Saqib M, Ali Bhatti AS, Ahmad NM, Ahmed N, Shahnaz G, Lebaz N, Elaissari A (2020) Amphotericin B loaded polymeric nanoparticles for treatment of leishmania infections. *Nanomaterials* 10:1152
- Sattary M, Amini J, Hallaj R (2020) Antifungal activity of the lemongrass and clove oil encapsulated in mesoporous silica nanoparticles against wheat's take-all disease. *Pestic Biochem Physiol* 170:104696
- Sepulveda AAL, Velasquez AMA, Linares IAPO, de Almeida L, Fontana CR, Garcia C, Graminha MAS (2020) Efficacy of photodynamic therapy using TiO₂ nanoparticles doped with Zn and hypericin in the treatment of cutaneous leishmaniasis caused by *Leishmania amazonensis*. *Photodiagn Photodyn Ther* 30:101676
- Shakibaie M, Mohazab NS, Mousavi SAA (2015) Antifungal activity of selenium nanoparticles synthesized by *Bacillus* species Msh-1 against *Aspergillus fumigatus* and *Candida albicans*. *Jundishpur J Microbiol* 8:e26381
- Shende S, Bhagat R, Raut R, Rai M, Gade A (2021) Myco-fabrication of copper nanoparticles and its effect on crop pathogenic fungi. *IEEE Trans Nanobioscience* 20:146–153
- Silva Viana RL, Pereira Fidelis G, Medeiros MJC, Morgano MA, Alves MGCF, Passero LFD, Pontes DL, Theodoro RC, Arantes TD, Sabry DA (2020) Green synthesis of antileishmanial and antifungal silver nanoparticles using corn cob xylan as a reducing and stabilizing agent. *Biomol Ther* 10:1235
- Singh K, Garg G, Ali V (2016) Current therapeutics, their problems and thiol metabolism as potential drug targets in leishmaniasis. *Curr Drug Metab* 17:897–919
- Skinder BM, Hamid S (2020) Nanotechnology: a modern technique for pollution abatement. In: *Bioremediation and biotechnology*, vol 4. Springer, Cham, pp 295–311

- Slavin YN, Asnis J, Häfeli UO, Bach H (2017) Metal nanoparticles: understanding the mechanisms behind antibacterial activity. *J Nanobiotechnol* 15:1–20
- Sudha PN, Sangeetha K, Vijayalakshmi K, Barhoum A (2016) Nanomaterials history, classification, unique properties, production and market. In: *Emerging applications of nanoparticles and architecture nanostructures*. Elsevier, pp 341–384
- Sun Y, Yin Y, Gong L, Liang Z, Zhu C, Ren C, Zheng N, Zhang Q, Liu H, Liu W (2021) Manganese nanodepot augments host immune response against coronavirus. *Nano Res* 14:1260–1272
- Surnar B, Kamran MZ, Shah AS, Dhar S (2020) Clinically approved antiviral drug in an orally administrable nanoparticle for COVID-19. *ACS Pharmacol Transl Sci* 3:1371–1380
- Szunerits S, Barras A, Khanal M, Pagneux Q, Boukherroub R (2015) Nanostructures for the inhibition of viral infections. *Molecules* 20:14051–14081
- Thangadurai D, Sangeetha J, Prasad R (2020) *Nanotechnology for food, agriculture, and environment*. Springer, Cham
- Varahachalam SP, Lahooti B, Chamaneh M, Bagchi S, Chhibber T, Morris K, Bolanos JF, Kim N-Y, Kaushik A (2021) Nanomedicine for the SARS-CoV-2: state-of-the-art and future prospects. *Int J Nanomedicine* 16:539
- Wall G, Lopez-Ribot JL (2020) Current antimycotics, new prospects, and future approaches to antifungal therapy. *Antibiotics* 9:445
- Wang CY, Makvandi P, Zare EN, Tay FR, Niu LN (2020) Advances in antimicrobial organic and inorganic nanocompounds in biomedicine. *Adv Therap* 3:2000024
- Wang C, Wang S, Chen Y, Zhao J, Han S, Zhao G, Kang J, Liu Y, Wang L, Wang X (2021) Membrane nanoparticles derived from ACE2-rich cells block SARS-CoV-2 infection. *ACS Nano* 15:6340–6351
- Wilczewska AZ, Niemirowicz K, Markiewicz KH, Car H (2012) Nanoparticles as drug delivery systems. *Pharmacol Rep* 64:1020–1037
- World Health Organization (2021) 2020 Antibacterial agents in clinical and preclinical development: an overview and analysis. Available at: <https://www.who.int/publications/i/item/9789240021303>. Accessed 5 May 2021
- Xing H, Hwang K, Lu Y (2016) Recent developments of liposomes as nanocarriers for theranostic applications. *Theranostics* 6:1336
- Yadav D, Sandeep K, Pandey D, Dutta RK (2017) Liposomes for drug delivery. *J Biotechnol Biomater* 7:276
- Yetisgin AA, Cetinel S, Zuvin M, Kosar A, Kutlu O (2020) Therapeutic nanoparticles and their targeted delivery applications. *Molecules* 25:2193



Akhil, Arathi, K. B. Megha, X. Joseph, V. P. Sangeetha,
and P. V. Mohanan

18.1 Introduction

Nanotechnology has immensely contributed to the scientific and technological advancement witnessed over the past few years (Wilkinson 2003). Nanomaterials have become an integral part of almost all fields of science and engineering with their intriguing applications (Kolahalam et al. 2019). Out of the nanomaterials, zero-dimensional nanomaterials like Quantum Dots are getting broad interest due to their attractive properties. Quantum dots are semiconductor crystalline nanoparticles with inherent fluorescence properties. Due to their exceptional photophysical characteristics, they have been used widely for imaging in the biomedical arena (Jamieson et al. 2007).

The beginning of the eighteenth century witnessed a massive surge in the development of Quantum dots in terms of their synthesis and conceptualization. QDs are mainly comprised of an inorganic core. This inorganic core contributes to their peculiar optical characteristics. The exciton confinement occurring inside the nanocrystals is the primary reason behind the photophysical properties. More technically, the exciton has a definite size inside the crystal called the exciton Bohr radius. The energy levels will become discrete leading to quantum confinement when the size of the semiconductor nanocrystal is smaller than the size of the exciton Bohr radius. Hence, the exciton Bohr radius plays a crucial role in the properties of

V. Akhil, K. B. Megha, X. Joseph, V. P. Sangeetha and P. V. Mohanan contributed equally to this work.

Akhil · Arathi · K. B. Megha · X. Joseph · V. P. Sangeetha · P. V. Mohanan (✉)

Toxicology Division, Biomedical Technology Wing, Sree Chitra Tirunal Institute for Medical Sciences and Technology (Govt. of India), Trivandrum, Kerala, India

the QDs (Kouwenhoven and Marcus 1998). These desirable properties can be achieved by stringent control over synthesis parameters.

Some of the salient photophysical features of QDs include tunable light emission, broad absorption spectra, narrow emission spectra, high quantum yield, and high photostability. These desirable properties can be achieved by stringent control over synthesis parameters. The irreplaceable properties of QDs led to their use as a probe for imaging purposes. Visual analysis of cells and biomolecules serves as an integral part of biomedical research (Haustein and Schwille 2007). Fluorescent organic dyes or proteins were considered the gold standard for fluorescence imaging and sensing so far (Juette et al. 2014).

Nevertheless, there existed many problems in standard dye-based imaging. Low stability and narrow excitation spectra are the significant issues related to these organic dyes (Juette et al. 2014). In addition, multiple fluorophores with distinct excitation and emission were the only method to achieve multicolor imaging.

In contrast, the broad absorption spectral property allows the QDs to emit different colors upon excitation with a single wavelength (Kouwenhoven and Marcus 1998). Furthermore, the narrow emission properties nullify overlapping issues when compared to the organic dyes. The emission spectra of the QDS can be tuned by varying various parameters such as core size, elemental composition, and surface modifications. NIR QDs with light emission at the NIR region (700–1000 nm) are widely used for deep tissue imaging (Zhao et al. 2018). High photostability is another factor that distinguishes QDs from conventional organic fluorophores. Several studies exhibited the higher stability of QDs against the highest stable organic dye Alexa488 (Montón et al. 2009).

Even though the unique features enable the QDs as promising substitutes for conventional fluorescent dyes or proteins, the safety issues are still debatable. Only a few reports are describing the toxicity concerns of various QDs. This chapter describes the application of QDs *in vitro* and *in vivo* bioimaging. It also focuses on the vital safety concern raised by these QDs intended for imaging applications (Fig. 18.1).

18.2 Features of QDs

18.2.1 Tunable Light Emission

The light emission from the QDs is dependent on various factors such as size and composition. Generally, the size of QDs ranges from 2 to 10 nm. Varying the size to even 1 nm can change the properties of the QDs in terms of their emission. The high bandgap energy arising from the smaller QDs creates QDs having shorter wavelength emission, i.e., towards the blue region. When size increases, the QDs will emit colors with higher wavelengths, i.e., towards the red area (Gan et al. 2008).

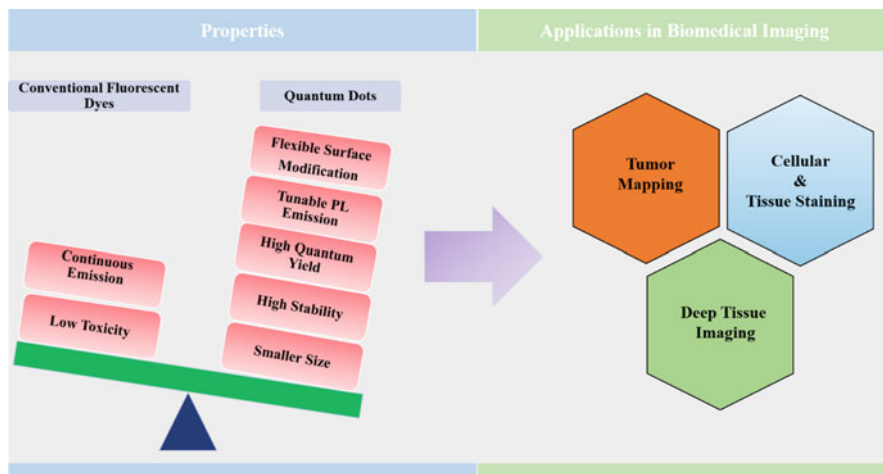


Fig. 18.1 Schematic showing the various properties and applications of QDs in biomedical imaging

18.2.2 Broad Absorption Spectra and Narrow Emission Spectra

The broad absorption spectra arising from the quantum confinement effects allow the QDs for multicolor imaging. The narrow emission spectra overcome the issues of overlapping of spectra while multiplexing (Resch-Genger et al. 2008).

18.2.3 High Quantum Yield and High Absorption Extinction Coefficient

Due to the quantum confinement effects, the QDs show high absorption extinction coefficient. This suggests that the molar absorption is directly proportional to the quantum confinements. The high brightness of the QDs is due to the high quantum yield and high molar absorption coefficient. These features will make the QDs superior in imaging deep tissues with reduced autofluorescence and scattering (Rezaei and Tanhaei 2016; Leatherdale et al. 2002).

18.2.4 Excellent Photostability

Due to its inorganic core and shell, most of the inorganic QDs are highly stable. This property makes them excellent and effective imaging probes over a long period. The excellent stability also contributes to the extended circulation time of QDs inside the body when used for in vivo imaging applications (Jain et al. 2008).

18.3 Synthesis of Quantum Dots

Even after the first synthesis of QDs, the synthetic approaches underwent a series of optimizations and improvements due to the profound interest in its applications. The first synthesis of QDs was reported by Bawendi et al. (1993). The synthesis of QDs is mainly followed by either a Top-down or Bottom-up approach, as shown in Fig. 18.2 (Valizadeh et al. 2012). Both the approaches were modified by various research groups depending on the nature of QDs required in terms of size, morphology, and emission properties. The top-down approach generally utilizes the breakdown of bulk precursors into nano-sized particles. The major top-down processes utilized for the synthesis of QDs are electron beam lithography (Grützmacher et al. 2007), focused ion beam (Holleitner et al. 2001), reactive-ion etching (Farahani et al. 2005), electrochemical exfoliation (Zhou et al. 2007), and laser ablation (Sun et al. 2006). The bottom-up strategy utilizes the assembly of small molecules or atoms to form QDs. The main processes utilized for the strategy are chemical vapor deposition (Burda et al. 2005) and wet chemical methods such as hydrothermal method (Xu et al. 2015a), microwave method (Zhu et al. 2009), ultrasonication (Zhang et al. 2015), microemulsion process (Li et al. 2010), and sol-gel process (Lin et al. 2005). Each method has its advantages and features. Even though the top-down approach is the more accessible and greener method for retaining the chemical and physical properties of the precursors, the unpredictability of size and the morphological parameter is still a major concern. The most widely used approach for the synthesis of QD is based on a bottom-up strategy due to the high performance rendered by the QDs. The QDs synthesized using this method showed a higher quantum yield. Moreover, surface functionalization can be done effectively using this protocol.

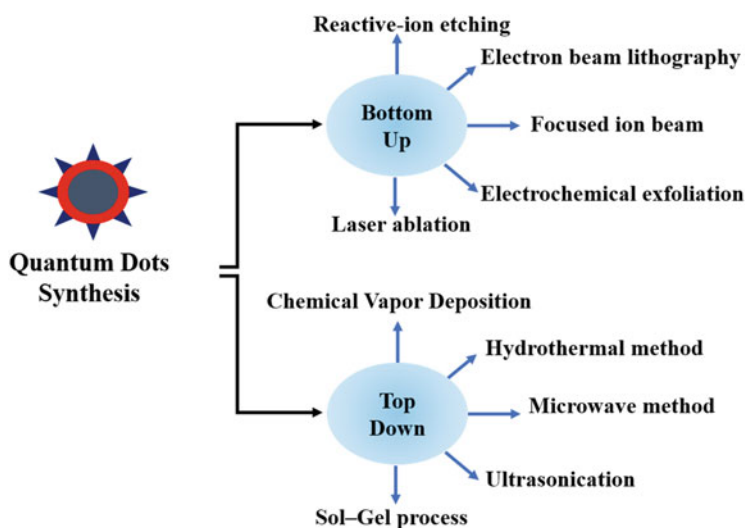


Fig. 18.2 Schematic depicting the different strategies in the top-down and bottom-up approaches

18.4 Classification/Types of Quantum Dots

Based on the elemental composition of the QDs, they can be classified into many types. The traditional QDs are composed of a heavy metal core and a shell. The shell around the QD core reduces the surface deficiency and enhances the quantum yield. A few examples of conventional core-shell QDs comprise CdTe, CdSe, PbSe, and GaAs QDs with a core consisting of Group II–IV, IV–VI, or III–V semiconductors of the periodic table with ZnS or SiO₂ shells (Dabbousi et al. 1997). Cadmium-based QDs (Cd QDs) are the widely studied quantum dots so far (Zhang et al. 2014). The Cd-based QDs include CdSe, CdTe, CdS, and CdTe/CdSe core/shell QDs with a protective layer of ZnS or ZnSe. The toxic responses of Cd-based QDs paved the way for the synthesis of other QDs.

Indium-based QDs represent the other class of QDs with promising features (Ramasamy et al. 2017). They show improved photostability than cadmium-based QDs due to the presence of covalent bonds. In contrast, these QDs must be coated with wider bandgap materials to compact their low quantum yield. Among Silver-based QDs (Di et al. 2016), Ag₂S (Du et al. 2010) and Ag₂Se (Zhu et al. 2013) are of enormous interest due to their NIR emission range. Carbon-based QDs (Xu et al. 2019) and Silicon-based QDs (Warner et al. 2005) are other types of Cd-free QDs. The significant advantage of QDs relies on its single wavelength tunable emission. Various QDs and their emission are depicted in Fig. 18.3.

Transition metal dichalcogenide (TMDC) QDs are the newest members with multifaceted applications (Fouladi-Oskouei et al. 2018). The major QDs belonging to this group are Molybdenum disulfide QDs (Guo and Li 2020) (MoS₂ QDs) and Tungsten Disulfide QDs (Xu et al. 2015b) (WS₂ QDs). The 2D chemical structure and the NIR absorption ability make them promising nanomaterials in bioimaging applications. QDs of this type can be both prepared using a top-down and bottom-up approach. Owing to the 2D sheet structure, these types of QDs can be efficiently designed through ultrasonic exfoliation. Transition dichalcogenides-based QDs are superior materials with exciting photothermal and photodynamic properties (Fouladi-Oskouei et al. 2018). Recent efforts have developed NIR QDs (Ma 2010) synthesized from the same class of molecules discussed above but can be efficiently utilized in the near-infrared region.

18.5 Imaging Applications of Quantum Dots

As discussed in the previous sections, the intriguing properties such as excellent photostability and high quantum yield of the quantum dots place them in the top position among the other fluorescent molecules used for bioimaging purposes. The use of quantum dots with a high molar extinction coefficient is widely used for bioimaging applications. The bioimaging applications can be broadly classified into two-QDs for in vitro imaging and QDs for in vivo imaging (Guo and Li 2020).

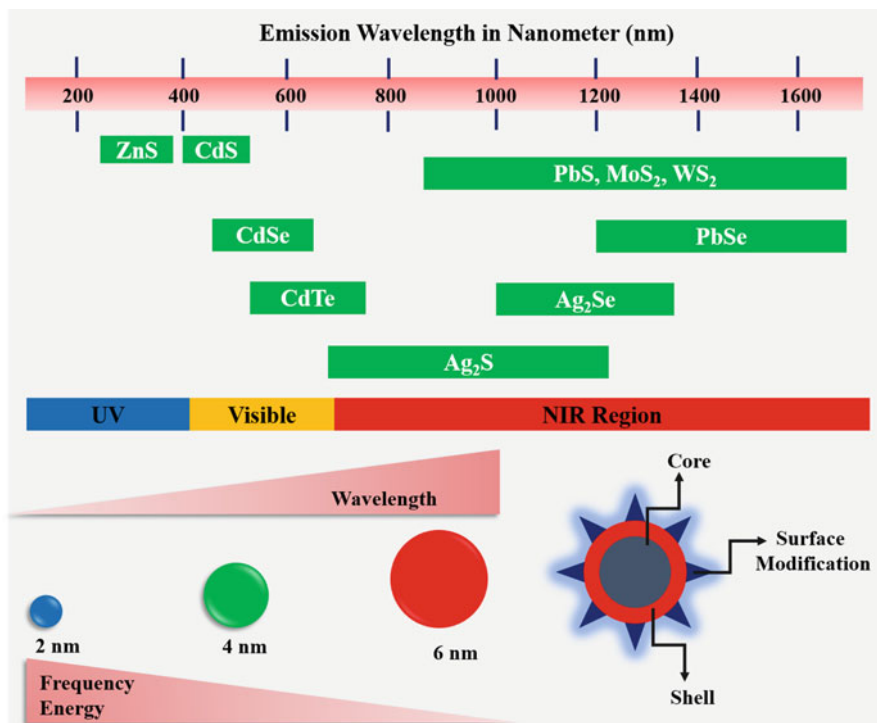


Fig. 18.3 Schematic showing the various emission wavelengths of QDs

18.5.1 In Vitro Imaging

Long-term stability and multi-signal detection properties forge QDs as efficient cellular nanoprobes. The *in vitro* applications such as QDs for cellular imaging, live-cell imaging, biomolecular detection, tracking, and binding assays are discussed below (Xu et al. 2015b).

18.5.1.1 Cellular and Biomolecular Imaging

Cell imaging is essential to understand the unknown cellular properties as well as biological interactions of biomolecules. In this context, developing and investigating bioimaging probes using QDs are highly rewarding. The ideal cellular imaging nanoprobe should be smaller, bright, detectable, water-soluble, less toxic, and have specific binding properties. Almost all types of QDs have been widely used for this purpose, irrespective of the elemental composition. The initial cellular targeting was based on the conjugation of QDs with actin-binding molecules like transferrin or phalloidin (Ma 2010).

A recent report from our group also showed the cellular imaging applications of zwitterionic carbon quantum dots. Highly fluorescent zwitterionic CQDs were synthesized through microwave pyrolysis and utilized for imaging HEK 293 cells.

The cellular responses exhibited the biocompatible nature of the synthesized QDs. The zwitterionic nature and the smaller size of the QDs highlighted their importance as potential cellular imaging probes (Sangeetha et al. 2021).

QDs can also be employed for the labeling of plasma membranes. The plasma membrane of cells is a highly crucial part of mediating cell signaling and transport mechanisms. Among the functions, membrane electrical activity is critical since the membrane electrical activity can directly give information regarding the functioning of neuronal circuits. At neutral pH, CdSe@ZnS-GSH QDs with size 2 and 520 nm emission effectively labeled the plasma membrane of HEK 293 cells, PC-12 cells, and primary rat neurons. In addition, CdSe@ZnS-GSH QDs exhibit excellent optical stability during continuous fluorescence imaging for up to 60 min. Moreover, CdSe@ZnS-GSH QDs also effectively label cells without affecting the proliferation, disturbing the membrane integrity, or causing apoptosis and necrosis of cells. Moreover, the synthesized QDs showed excellent long-term photostability for up to 60 min and were nontoxic to cells (Chen et al. 2019).

Black phosphorous QDs are also studied for their cellular imaging property. BP nanodots were synthesized through the ultrasonication method and evaluated their cellular imaging efficiency on C2C12 skeletal myoblasts. The green fluorescence upon excitation with visible light showed the effective entry of cells inside the cells. Not only Black phosphorous QDs but the other QDs in the MXene family can also be used as cellular imaging probes (Shin et al. 2018).

Tracking biomolecules inside cells is of enormous interest in clinical biotechnology due to the underlying information regarding cellular processes. The real-time monitoring of biomolecules inside cells can answer many unsolved problems like cellular responses towards various cues, cellular interactions, and particle movements. Moreover, tracking biomolecules such as biomarkers of different diseases can give us essential information regarding the condition. This can hasten the early diagnosis, treatment, and progression of diseases like cancer.

18.5.1.2 Tissue Staining

The improved brightness of the QDs allows them to be used as effective tissue staining probes. The emission from the QDs is brighter than the autofluorescence from the formalin-fixed and paraffin-embedded (FFPE) tissue samples. Moreover, the QDs fluorescence intensity will remain intact even after exposing continuously to excitation light in contrast to the photobleaching of conventional dyes. Traditional detection of biological molecules in tissue specimens was based on the visualization of fluorophores attached to the secondary antibodies. Recent strategies use QD-conjugated antibodies for immunohistochemical detection of tissue specimens.

Wang and coworkers successfully demonstrated the application of QDs in detecting signals from different channels (multiplex detection) and quantifying biomarkers. The authors optimized the efficiency of QD-based IHF staining of the tissue specimens and compared the results with the conventional western blot and IHC staining methods. QD-Ab conjugates were prepared using the 1-ethyl-3-[3-dimethylaminopropyl] carbodiimide hydrochloride EDC coupling of

commercially available carboxylic acid-functionalized QDs with emission ranging from 529 to 623 nm to secondary antibody (Xu et al. 2013).

QD-based IHF studies also revealed the possible mechanisms in the pathogenesis of Diabetic Nephropathy (DN). DN is a major renal complication associated with diabetes. Investigations showed that Aldose reductase (AR) and Toll-like receptor 4 (TLR4) are involved in the progression of DN. CdSe/CdS/ZnS quantum dots having 620 nm emission were synthesized and conjugated with mouse monoclonal AR antibodies to investigate the role of possible mechanisms related to the renal tissue. The QD-based IHF study revealed the presence and upregulation of AR, and the TLR4 proteins were upregulated in the renal tissues of diabetic rats. The dual color immunofluorescent labeling efficiently exhibited the simultaneous visualization of AR and TLR4 proteins and their interactions in renal tissues. Both the proteins can be visualized through excitation using UV light with no spectral overlapping (Liu et al. 2015).

To identify the multiple targets (overexpressed antigens) in human lymphoid tissue specimen's streptavidin-conjugated quantum dots with distinct emission spectra were synthesized. The simultaneous detection of differentially expressed antigens successfully showed the ability of the synthesized streptavidin-conjugated quantum dots in multispectral staining. The combination of quantum dots with antibodies is superior to the traditional fluorophore staining for the simultaneous detection of multiple targets in fixed tissue (Fontaine et al. 2006).

18.5.1.3 Binding Assays

Binding assays based on QDs were mainly dependent on the QD-mediated Forster Resonance Energy Transfer (FRET) mechanism. The general definition of FRET describes the non-radiative fluorescence energy transfer from a donor molecule to an acceptor molecule within proximity distance called Forster distance. QDs can be used as donors or acceptors, depending on the point of evaluation. When QD is used as a donor, the most crucial point to be noted is selecting an acceptor with enough spectral overlap and efficient quantum yield for FRET detection. Long lifetime donors are required when QD acts as an acceptor.

Numerous QD-based FRET sensing probes were developed so far for the detection and imaging of cellular responses. Since pH plays a crucial role in the growth and proliferation of cells, pH-sensitive QD-based FRET nanoprobe are used to detect intracellular pH. Bao and coworkers fabricated a pH sensor by coupling a commercial semiconductor QD *Qdot ITK* carboxyl quantum dots with fluorescent monomeric proteins mOrange and mOrange M163K. The 525 nm emitting QD acted as a donor, whereas the fluorescent proteins served as the acceptor in the FRET pair with pH-dependent emission intensity. As a result, the energy transfer efficiency was directly proportional to the pH of the environment with maximum sensitivity in the acceptor proteins' pK_a range. Both mOrange and mOrange M163K showed efficient detection in the physiological pH with pK_a values 6.9 and 7.89, respectively. To track the intracellular pH changes, the authors incubated the QD-FP FRET pair with HeLa cells. The FRET pair was conjugated with a C-terminal polyarginine sequence for effective endosomal uptake. The cellular studies showed the changes in the

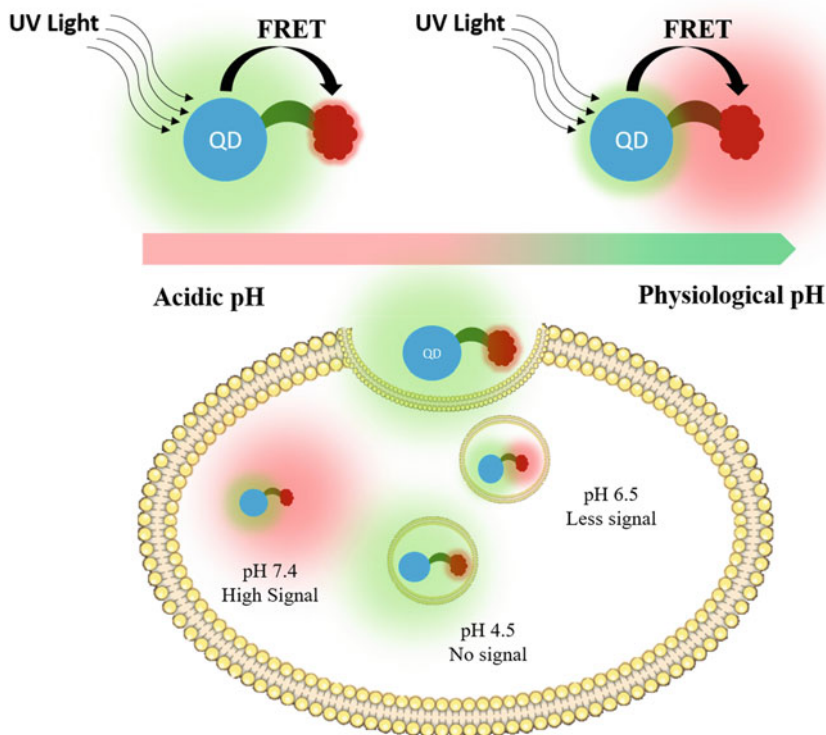


Fig. 18.4 Schematic showing the concept of pH-based intracellular imaging

emission intensity of the FRET pair to the pH changes in the endocytic pathway. In neutral pH of the extracellular environment and early endosome, the QD-FP FRET pair exhibited high intensity, whereas low emission in the late endosome due to the acidic pH (Fig. 18.4) (Dennis et al. 2012).

The functions of QD FRET pairs are not limited to pH-sensitive systems. They are well-studied for investigating protein interactions, enzyme activity studies, immunoassays, and so on. Recent reports also showed the effective functionalization of QDs with DNA for sensing studies (Banerjee et al. 2016).

18.5.2 In Vivo Imaging

Due to their high photostability inside the body, various attempts have been made for the synthesis of QDs for different in vivo applications. In vivo tracking is an important parameter as it enables the proper understanding of the action of the biomolecule or bioprocess of interest inside the human body. Nevertheless, the development of an efficient in vivo fluorescent nanoprobe is not an easy task. There are many factors to be considered while designing them. Interference from

other physiological factors inside the body and the circulation lifetime are the significant factors to be solved. Additionally, selecting an appropriate ligand for specific targeting and the determination of an effective dose for imaging are crucial steps in development. The major *in vivo* applications include *in vivo* tracking of nanomaterials inside the body, tumor mapping, and deep tissue imaging.

18.5.2.1 Tumor Imaging

Early detection and diagnosis of cancer are essential in reducing the fatality caused by the deadly disease. The imaging will give information regarding the extent of metastasis and the area to be targeted for delivering drugs. The active targeting of tumor cells can be achieved by functionalizing QDs with suitable ligands that can recognize biomolecules or proteins specific to tumor cells. Angiogenesis, the formation of new blood vessels, is highly essential for the progression of the tumor. Hence, tumors can be easily imaged with QDs conjugated with ligands that can selectively bind to critical factors in tumor angiogenesis and progression.

Based on the fact that the VEGF factor is overexpressed in cancer metastasis, Vascular endothelial growth factor (VEGF) targeting imaging probes can be used to detect the tumor. In one of the examples, QDs-bevacizumab conjugates were synthesized and utilized for the noninvasive imaging of tumors in mice through specific targeting of VEGF factor in tumor cells by Bevacizumab. The as-synthesized QD-Bevacizumab conjugate effectively imaged the tumor sites in mice, binding the VEGF factor within 12 h. In another example, arginine-glycine-aspartic acid (RGD) peptide conjugated CdTe/ZnS QDs were used for imaging tumors *in vivo*. The conjugation of RGD to a PEG-modified CdTe/ZnS QD yields QDs that can specifically bind to Integrin $\alpha\beta_3$, which is overexpressed in tumor sites. The high fluorescent intensity and the multivalency of RGD ligands effectively made a high-standard *in vivo* imaging probe with efficient tumor targeting (Cai et al. 2006). Folate receptors overexpressed in cancer cells are also an attractive target for imaging using QDs-based nanoprobe. PbS/CdS core/shell quantum dots (QDs) conjugated with folic acid with NIR emission were used to image mice tumors. The NIR emission of the conjugated QDs can be modulated for multi-imaging of various physiological events and tumor mapping (Jeong et al. 2018) (Fig. 18.5).

18.5.2.2 Deep Tissue Imaging

Normal light under 700 nm cannot penetrate deep into the body due to the high level of scattering occurring inside the body. The near-infrared region of the spectrum can overcome the issues of normal range with reduced scattering and autofluorescence from nearby tissues. Hence, synthesizing QDs with NIR emission can improve the quality of imaging and deep tissue penetration. The NIR biological windows can be further divided into two—NIR I with spectral range (650–950 nm) and NIR-II with spectral range (1000–1400 nm).

Using NIR-II fluorescent QDs, Sentinel Lymph Node (SLN) mapping can be done fastly with high accuracy and precision. CdTe/CdSe core/shell QDs were synthesized and coated with oligomeric phosphine for improving solubility. The size of the QDs enabled them to retain in the SLN without leaking into the nearby

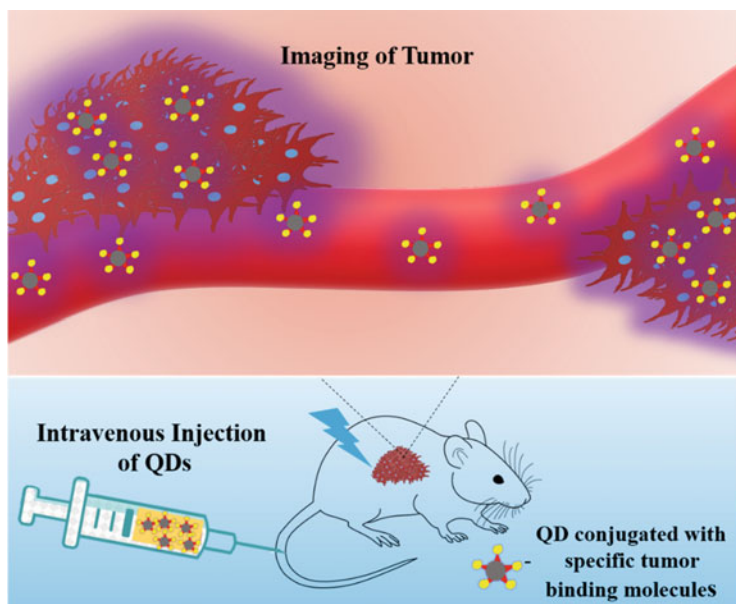


Fig. 18.5 Schematic showing the imaging of tumor using QDs

cells. The QDs mapped the Lymph system of the pig within 5 mins after intradermal injection. This study successfully showed the advancement of NIR QDs in targeting lymph nodes in a big animal model (Frangioni et al. 2007).

The interesting photophysical features of the NIR QDs facilities them a suitable candidate for image guide therapy applications. CdTe QDs of size 4.5 nm conjugated with an RGD peptide were utilized for targeting the tumor and image-guided surgical removal of cancer. The high affinity of RGD peptides towards glioblastoma (U87 MG) played a vital role in identifying tumor sites in athymic nude mice. The CdTe-RGD NIR QDs showed a significant NIR signal after intravenous tail injection and accumulated in the target site. The image-guided removal of the tumor was performed successfully with excellent real-time NIR imaging of the quantum dots (Li et al. 2012).

18.6 Safety Concerns of QDs

Although there are many achievements in the synthesis of QDs for imaging applications, there exist many challenges also. Biosafety is a significant concern that needs to be addressed in the case of biomedical applications. The safety aspects of the QDs can be determined through in vitro and in vivo toxicity studies. In vivo toxicity evaluation of QDs is of more interest since it is a more physiologically relevant model system. The in vivo studies can give a better picture of the ADME of the QDs. However, the in vitro studies can provide the cellular fate and mechanism

of toxicity induced by the QDs when interacting with the cells. Both examinations are equally important from a regulatory point of view. The generation of QD toxicity mainly occurs in two ways (1) toxicity generated from the leaching of heavy metalcore, (2) reactive oxygen species (ROS) generation-mediated toxicity. ROS are caused by the transfer of energy to oxygen molecules in the surrounding environment.

Most of the QDs are made up of heavy metal-based semiconductor cores like Cadmium, Lead, Selenium, etc. Out of that, most heavy metal-based QDs used for bioimaging applications are based on Cadmium-based QDs (Cd QDs). Cadmium is a potent carcinogen with an LD₅₀ value of 100–300 mg/kg. Bhatia and coworkers studied the *in vitro* toxicity of CdSe QDs synthesized using a bottom-up approach using primary rat hepatocytes as a liver model. The results demonstrated that the QDs were showing acute toxicity to hepatocytes. The toxicity was due to the leaching of Cd²⁺ ions from the core. Reduced Cd surface formed by the surface oxidation of the core resulted in the leaching of free ions. These Cd ions can bind to the mitochondrial proteins through sulfhydryl groups, leading to the thiol group inactivation. This oxidative stress, in turn, leads to mitochondrial dysfunction. The *in vivo* studies also were consistent with the toxic response of cadmium-containing QDs through the accumulation of the QDs in the liver and kidney (Derfus et al. 2004).

Another report highlighted the importance of core and shell composition in determining the toxicity of QDs. The chemical composition of the nanoparticle core and the design of the outer capping layer are essential factors affecting QD toxicity. The authors compared the toxic responses of standard CdTe quantum dots with ZnS-coated CdSe CDs against Human breast cancer cells (MCF-7 cell line). The uncapped CdTe showed toxicity towards the cell, whereas the ZnS-capped CdSeQDs were nontoxic. By quantifying the amount of ROS generated, the authors succeeded in claiming that the toxicity is not solely dependent on the Cd²⁺ concentration (Cho et al. 2007). Another comparative study of ZnS capped, lipid-coated cadmium selenide (CdSe) and indium gallium phosphide (InGaP) with similar sizes also showed the toxic nature of Cadmium-based QDs against porcine renal proximal tubule cells (LLC-PK1). Further experimental data suggested that the toxicity was not dependent on the core material but also on the final material. Cadmium-based QDs also damage plasma membrane (Lovrić et al. 2005).

Since the endothelial cells are lining the body's blood vessels, investigating the toxicity of QDs on endothelial cells is vital. The endothelial cells are the primary contact of QDs indirect injection into the body for *in vivo* imaging studies. Hence, *in vitro* toxicity studies with human umbilical vein endothelial cells (HUVEC) provides the details regarding the interaction of QDs. Moreover, most cardiovascular diseases show early symptoms of endothelial dysfunction (Choy et al. 2001). So, the irregularities in the functioning of endothelial cells can give the early diagnosis of cardiovascular diseases in humans. Toxicity evaluation of mercaptosuccinic acid (MSA)-capped CdTe QDs on endothelial cells even revealed its toxic nature towards endothelial cells. Even a concentration of 0.1–100 µg/mL induced apoptosis in HUVEC cells. A twofold increase in the generation of ROS

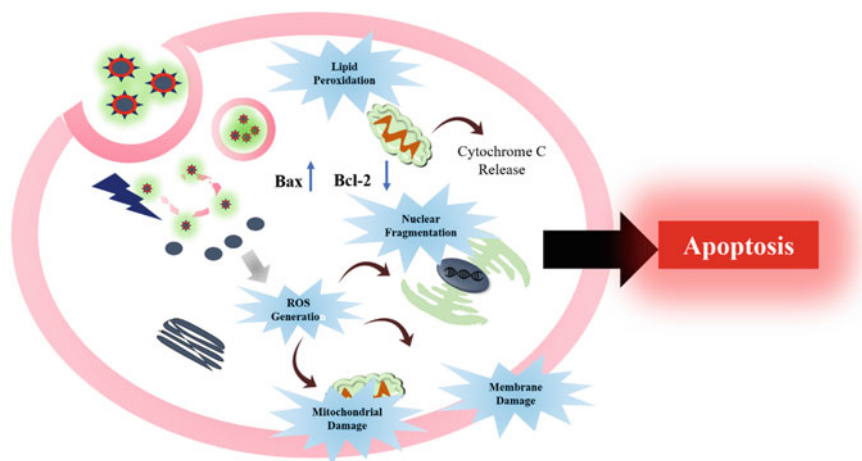


Fig. 18.6 Schematic showing the mechanism of toxicity induced by the QDs

was observed after 12 h treatment with the QDs. ROS generation is considered to be the main reason for the toxicity of CdTe QDs (Yan et al. 2011). ROS generation can lead to a series of mechanisms inside the cellular environment that leads to cell death. Apart from ROS generation, the uptake of QDs can induce mitochondrial damage such as disruption of membrane integrity, swelling of mitochondria, cytochrome c release, and mitochondrial hyperplasia (Choi et al. 2007). The ROS generation, which in turn activates the mitochondrial apoptosis pathway. All these can lead to apoptosis. The primary toxicity mechanisms induced by QDs are shown in Fig. 18.6.

The majority of the studies depicted the issues related to QD in terms of their safety, mainly Cadmium-based QDs. The requirement of QDs with low toxicity compared to toxic Cadmium-based QDs resulted in the synthesis and studies of a new class of QDs named Cadmium-free QDs (Xu et al. 2016). QDs synthesized from semiconductor materials other than Cadmium belong to this group. Major cadmium-free QDs utilized for imaging applications due to their reduced toxicity effects are Carbon QDs (Xu et al. 2019), MXene-based QDs (Xue et al. 2017), Silicon-based QDs (Warner et al. 2005), Indium-based QDs (Long et al. 2021), and Black phosphorous-based QDs (Lee et al. 2016). Surface capping of QDs is also utilized for reducing the toxicity concerns raised by the QDs. The surface modification reduces toxicity issues and improves the photophysical properties of QDs, such as brightness and stability. Modifying the surface with biomolecules that can scavenge the ROS is one of the most utilized strategies for reducing toxicity.

18.7 Conclusion

Quantum Dots are up-and-coming candidates with broad applicability in many areas due to their excellent photophysical properties. Owing to their high stability and quantum yield, they have been explicitly used for bioimaging purposes. Various QDs have been synthesized and studied for various *in vitro* and *in vivo* imaging applications. Depending on the nature of the semiconductor material, the properties of QDs considerably varied. The quest for highly efficient QDs with improved imaging properties resulted in the synthesis of cadmium-free QDs. The NIR QDs represent the newest class of QDs that can even be used for image-guided therapies.

Even though there are many reports on QDs intended for biomedical applications, there is a lack of proper safety studies. The toxicity of QDs are crucial since they are used inside the body for imaging purposes. The size and even elemental composition of QDs can contribute to toxicity. Furthermore, the interaction of QDs with other biomolecules inside the physiological environment can induce potential toxicity. Hence, an accurate understanding of the cytotoxic mechanism is highly needed for the proper prediction of their safety. The standard toxicity studies involve *in vivo* and *in vitro* toxicity assessment. The existing toxicity studies are not sufficient to predict the safety of QDs. The need for a proper standard protocol is high for the proper prediction of toxicity. Without doubt, a detailed understanding of the toxicity and its mechanism can explore further applications of QDs as future smart imaging probes.

Acknowledgments The authors wish to express their sincere thanks to the Director and Head, Biomedical Technology Wing, Sree Chitra Tirunal Institute for Medical Sciences and Technology (Govt. of India), Trivandrum, for their support and for providing the infrastructure to carry out this work.

References

- Banerjee A, Pons T, Lequeux N, Dubertret B (2016) Quantum dots–DNA bioconjugates: synthesis to applications. *Interface Focus* 6(6):20160064
- Burda C, Chen X, Narayanan R, El-Sayed MA (2005) Chemistry and properties of nanocrystals of different shapes. *Chem Rev* 105(4):1025–1102
- Cai W, Shin D-W, Chen K, Gheysens O, Cao Q, Wang SX, Gambhir SS, Chen X (2006) Peptide-labeled near-infrared quantum dots for imaging tumor vasculature in living subjects. *Nano Lett* 6(4):669–676
- Chen G, Zhang Y, Peng Z, Huang D, Li C, Wang Q (2019) Glutathione-capped quantum dots for plasma membrane labeling and membrane potential imaging. *Nano Res* 12(6):1321–1326
- Cho SJ, Maysinger D, Jain M, Röder B, Hackbarth S, Winnik FM (2007) Long-term exposure to CdTe quantum dots causes functional impairments in live cells. *Langmuir* 23(4):1974–1980
- Choi AO, Cho SJ, Desbarats J, Lovrić J, Maysinger D (2007) Quantum dot-induced cell death involves Fas upregulation and lipid peroxidation in human neuroblastoma cells. *J Nanobiotechnol* 5(1):1–13
- Choy JC, Granville DJ, Hunt DWC, McManus BM (2001) Endothelial cell apoptosis: biochemical characteristics and potential implications for atherosclerosis. *J Mol Cell Cardiol* 33(9):1673–1690

- Dabbousi BO, Rodriguez-Viejo J, Mikulec FV, Heine JR, Mattoussi H, Ober R, Jensen KF, Bawendi MG (1997) (CdSe) ZnS core-shell quantum dots: synthesis and characterization of a size series of highly luminescent nanocrystallites. *J Phys Chem B* 101(46):9463–9475
- Dennis AM, Rhee WJ, Sotto D, Dublin SN, Bao G (2012) Quantum dot-fluorescent protein FRET probes for sensing intracellular pH. *ACS Nano* 6(4):2917–2924
- Derfus AM, Chan WCW, Bhatia SN (2004) Probing the cytotoxicity of semiconductor quantum dots. *Nano Lett* 4(1):11–18
- Di J, Xia J, Ji M, Wang B, Yin S, Huang Y, Chen Z, Li H (2016) New insight of Ag quantum dots with the improved molecular oxygen activation ability for photocatalytic applications. *Appl Catal B Environ* 188:376–387
- Du Y, Bing X, Tao F, Cai M, Li F, Zhang Y, Wang Q (2010) Near-infrared photoluminescent Ag₂S quantum dots from a single source precursor. *J Am Chem Soc* 132(5):1470–1471
- Farahani JN, Pohl DW, Eisler H-J, Hecht B (2005) Single quantum dot coupled to a scanning optical antenna: a tunable superemitter. *Phys Rev Lett* 95(1):017402
- Fouladi-Oskouei J, Shojaei S, Liu Z (2018) Robust tunable excitonic features in monolayer transition metal dichalcogenide quantum dots. *J Phys Condens Matter* 30(14):145301
- Fountaine TJ, Wincovitch SM, Geho DH, Garfield SH, Pittaluga S (2006) Multispectral imaging of clinically relevant cellular targets in tonsil and lymphoid tissue using semiconductor quantum dots. *Mod Pathol* 19(9):1181–1191
- Frangioni JV, Kim S-W, Ohnishi S, Kim S, Bawendi MG (2007) Sentinel lymph node mapping with type-II quantum dots. In: *Quantum dots*. Humana Press, Totowa, NJ, pp 147–159
- Gan C, Zhang Y, Battaglia D, Peng X, Xiao M (2008) Fluorescence lifetime of Mn-doped ZnSe quantum dots with size dependence. *Appl Phys Lett* 92(24):241111
- Grützmacher D, Fromherz T, Dais C, Stangl J, Müller E, Ekinci Y, Solak HH et al (2007) Three-dimensional Si/Ge quantum dot crystals. *Nano Lett* 7(10):3150–3156
- Guo Y, Li J (2020) MoS₂ quantum dots: synthesis, properties and biological applications. *Mater Sci Eng C* 109:110511
- Haustein E, Schwille P (2007) Trends in fluorescence imaging and related techniques to unravel biological information. *HFSP J* 1(3):169–180
- Holleitner AW, Decker CR, Qin H, Eberl K, Blick RH (2001) Coherent coupling of two quantum dots embedded in an Aharonov-Bohm interferometer. *Phys Rev Lett* 87(25):256802
- Jain PK, Huang X, El-Sayed IH, El-Sayed MA (2008) Noble metals on the nanoscale: optical and photothermal properties and some applications in imaging, sensing, biology, and medicine. *Acc Chem Res* 41(12):1578–1586
- Jamieson T, Bakhshi R, Petrova D, Pocock R, Imani M, Seifalian AM (2007) Biological applications of quantum dots. *Biomaterials* 28(31):4717–4732
- Jeong S, Jung Y, Bok S, Ryu Y-M, Lee S, Kim Y-E, Song J et al (2018) Multiplexed in vivo imaging using size-controlled quantum dots in the second near-infrared window. *Adv Healthc Mater* 7(24):1800695
- Juette MF, Terry DS, Wasserman MR, Zhou Z, Altman RB, Zheng Q, Blanchard SC (2014) The bright future of single-molecule fluorescence imaging. *Curr Opin Chem Biol* 20:103–111
- Kolahalalam LA, Viswanath IVK, Diwakar BS, Govindh B, Reddy V, Murthy YLN (2019) Review on nanomaterials: synthesis and applications. *Mater Today Proc* 18:2182–2190
- Kouwenhoven L, Marcus C (1998) Quantum dots. *Phys World* 11(6):35
- Leatherdale CA, Woo W-K, Mikulec FV, Bawendi MG (2002) On the absorption cross section of CdSe nanocrystal quantum dots. *J Phys Chem B* 106(31):7619–7622
- Lee HU, Park SY, Lee SC, Choi S, Seo S, Kim H, Won J et al (2016) Black phosphorus (BP) nanodots for potential biomedical applications. *Small* 12(2):214–219
- Li H, Li Y, Cheng J (2010) Molecularly imprinted silica nanospheres embedded CdSe quantum dots for highly selective and sensitive optosensing of pyrethroids. *Chem Mater* 22(8):2451–2457
- Li Y, Li Z, Wang X, Liu F, Cheng Y, Zhang B, Shi D (2012) In vivo cancer targeting and imaging-guided surgery with near infrared-emitting quantum dot bioconjugates. *Theranostics* 2(8):769

- Lin K-F, Cheng H-M, Hsu H-C, Lin L-J, Hsieh W-F (2005) Band gap variation of size-controlled ZnO quantum dots synthesized by sol-gel method. *Chem Phys Lett* 409(4-6):208-211
- Liu X, Rui H, Lian H, Liu Y, Liu J, Liu J, Lin G et al (2015) Dual-color immunofluorescent labeling with quantum dots of the diabetes-associated proteins aldose reductase and Toll-like receptor 4 in the kidneys of diabetic rats. *Int J Nanomedicine* 10:3651
- Long Z, Zhang W, Tian J, Chen G, Liu Y, Liu R (2021) Recent research on the luminous mechanism, synthetic strategies, and applications of CuInS₂ quantum dots. *Inorg Chem Front* 8(4):880-897
- Lovrić J, Cho SJ, Winnik FM, Maysinger D (2005) Unmodified cadmium telluride quantum dots induce reactive oxygen species formation leading to multiple organelle damage and cell death. *Chem Biol* 12(11):1227-1234
- Ma Q, Su X (2010) Near-infrared quantum dots: synthesis, functionalization and analytical applications. *Analyst* 135(8):1867-1877
- Montón H, Nogués C, Rossinyol E, Castell O, Roldán M (2009) QDs versus Alexa: reality of promising tools for immunocytochemistry. *J Nanobiotechnol* 7(1):1-10
- Murray CB, Norris DJ, Bawendi MG (1993) Synthesis and characterization of nearly monodisperse CdE (E = sulfur, selenium, tellurium) semiconductor nanocrystallites. *J Am Chem Soc* 115(19):8706-8715
- Ramasamy P, Kim N, Kang Y-S, Ramirez O, Lee J-S (2017) Tunable, bright, and narrow-band luminescence from colloidal indium phosphide quantum dots. *Chem Mater* 29(16):6893-6899
- Resch-Genger U, Grabolle M, Cavaliere-Jaricot S, Nitschke R, Nann T (2008) Quantum dots versus organic dyes as fluorescent labels. *Nat Methods* 5(9):763-775
- Rezaei G, Tanhaei MH (2016) Optical absorption coefficients and refractive index changes of an on-centerhydrogenic impurity in a multi-layered spherical quantum dot: Effects of external fields and geometrical size. *Opt Quant Electron* 48(1):73
- Sangeetha VP, Smriti S, Solanki PR, Mohanan PV (2021) Mechanism of action and cellular responses of HEK293 cells on challenge with zwitterionic carbon dots. *Colloids Surf B Biointerfaces* 202:111698
- Shin YC, Song S-J, Lee YB, Kang MS, Lee HU, Jin-Woo O, Han D-W (2018) Application of black phosphorus nanodots to live cell imaging. *Biomater Res* 22(1):1-8
- Sun Y-P, Zhou B, Lin Y, Wang W, Fernando KAS, Pathak P, Meziani MJ et al (2006) Quantum-sized carbon dots for bright and colorful photoluminescence. *J Am Chem Soc* 128(24):7756-7757
- Valizadeh A, Mikaeili H, Samiei M, Farkhani SM, Zarghami N, Akbarzadeh A, Davaran S (2012) Quantum dots: synthesis, bioapplications, and toxicity. *Nanoscale Res Lett* 7(1):1-14
- Warner JH, Hoshino A, Yamamoto K, Tilley RD (2005) Water-soluble photoluminescent silicon quantum dots. *Angew Chem Int Ed* 44(29):4550-4554
- Wilkinson JM (2003) Nanotechnology applications in medicine. *Med Device Technol* 14(5):29-31
- Xu H, Jing X, Wang X, Daqing W, Chen ZG, Wang AY (2013) Quantum dot-based, quantitative, and multiplexed assay for tissue staining. *ACS Appl Mater Interfaces* 5(8):2901-2907
- Xu Q, Pu P, Zhao J, Dong C, Gao C, Chen Y, Chen J, Liu Y, Zhou H (2015a) Preparation of highly photoluminescent sulfur-doped carbon dots for Fe (III) detection. *J Mater Chem A* 3(2):542-546
- Xu S, Li D, Peiyi W (2015b) One-pot, facile, and versatile synthesis of monolayer MoS₂/WS₂ quantum dots as bioimaging probes and efficient electrocatalysts for hydrogen evolution reaction. *Adv Funct Mater* 25(7):1127-1136
- Xu G, Zeng S, Zhang B, Swihart MT, Yong K-T, Prasad PN (2016) New generation cadmium-free quantum dots for biophotonics and nanomedicine. *Chem Rev* 116(19):12234-12327
- Xu Q, Li W, Ding L, Yang W, Xiao H, Ong W-J (2019) Function-driven engineering of 1D carbon nanotubes and 0D carbon dots: mechanism, properties and applications. *Nanoscale* 11(4):1475-1504
- Xue Q, Zhang H, Zhu M, Pei Z, Li H, Wang Z, Huang Y et al (2017) Photoluminescent Ti₃C₂ MXene quantum dots for multicolor cellular imaging. *Adv Mater* 29(15):1604847

- Yan M, Zhang Y, Xu K, Fu T, Qin H, Zheng X (2011) An in vitro study of vascular endothelial toxicity of CdTe quantum dots. *Toxicology* 282(3):94–103
- Zhang F, Yi D, Sun H, Zhang H (2014) Cadmium-based quantum dots: preparation, surface modification, and applications. *J Nanosci Nanotechnol* 14(2):1409–1424
- Zhang X, Lai Z, Liu Z, Tan C, Huang Y, Li B, Zhao M, Xie L, Huang W, Zhang H (2015) A facile and universal top-down method for preparation of monodisperse transition-metal dichalcogenide nanodots. *Angew Chem Int Ed* 54(18):5425–5428
- Zhao J, Zhong D, Zhou S (2018) NIR-I-to-NIR-II fluorescent nanomaterials for biomedical imaging and cancer therapy. *J Mater Chem B* 6(3):349–365
- Zhou J, Booker C, Li R, Zhou X, Sham T-K, Sun X, Ding Z (2007) An electrochemical avenue to blue luminescent nanocrystals from multiwalled carbon nanotubes (MWCNTs). *J Am Chem Soc* 129(4):744–745
- Zhu H, Wang X, Li Y, Wang Z, Yang F, Yang X (2009) Microwave synthesis of fluorescent carbon nanoparticles with electrochemiluminescence properties. *Chem Commun* 34:5118–5120
- Zhu C-N, Jiang P, Zhang Z-L, Zhu D-L, Tian Z-Q, Pang D-W (2013) Ag₂Se quantum dots with tunable emission in the second near-infrared window. *ACS Appl Mater Interfaces* 5(4): 1186–1189



Genotoxicity Evaluation of Nanosized Materials

19

V. P. Sangeetha, Vandana Arun, and P. V. Mohanan

19.1 Introduction

Nanoparticles are (NPs) nanoscaled materials with sizes less than 100 nm. The physicochemical features ensure its unique magical properties. Nanomaterial exhibits unique features, including size, large surface area, shape, and high mechanical, thermal, and electrical properties (Fubini et al. 2010). In recent years, nanomaterials with new intended applications increased drastically. Hence, the risk associated with the use of nanoparticles must be well-defined and properly addressed. Both in vitro and in vivo studies have addressed the toxicological potential of different nanomaterials. However, studies also reported the limitation of assessing the toxicity of nanomaterials using conventional toxicity methods due to their unique properties (Abdalaziz et al. 2014). Geno-nano toxicology is yet another emerging field, mainly addressing the genotoxicity potential of nanomaterials, interaction of nanomaterial with DNA, or induction of oxidative stress may lead to genotoxicity. The literature provides detailed information on genotoxic effects on various nanoparticles. Different traditional and new methods are available to assess the genotoxicity of nanomaterials both in vitro and in vivo.

V. P. Sangeetha and Vandana Arun contributed equally with all other contributors.

V. P. Sangeetha · V. Arun · P. V. Mohanan (✉)

Toxicology Division, BMT Wing, Sree Chitra Tirunal Institute for Medical Sciences and Technology (Govt. of India), Trivandrum, Kerala, India

© The Author(s), under exclusive license to Springer Nature Singapore Pte Ltd. 2023

P. V. Mohanan, S. Kappalli (eds.), *Biomedical Applications and Toxicity of Nanomaterials*, https://doi.org/10.1007/978-981-19-7834-0_19

477

19.2 Genotoxicity Evaluation of Nanomaterials

Genotoxicity is the ability of a substance to induce genetic damage, and it may further lead to mutation. Genotoxicity tests are well designed to assess the toxicity of the chemical, and it is well established. Different regulatory agencies have recommended various tests to assess the genotoxicity of different substances. As per FDA, it is mandatory to undergo genotoxicity tests before marketing a product. Generally, OECD guidelines are followed for conducting genotoxicity studies for any chemicals. DNA breaks, gene mutations, and chromosomal alternations are key measures to assess genotoxicity. The genetic toxicology studies use the following assays: Comet assay, Micronuclei assay, g-H2Ac immunostaining assay, measuring 8-hydroxy-2'-deoxyguanosine levels, and DNA deletions as a genetic instability endpoint. General genotoxicity endpoint assay as per OECD is followed to assess nanomaterials' genotoxicity in the literature. Genotoxicity assays widely known include *in vitro* and *in vivo* comet assay, micronucleus assay, chromosomal aberration studies, and mouse lymphoma gene mutation assay, which check the chromosomal, gene alternations, and mutations. The need for standard guidelines for genotoxicity has been raised by different researchers regarding the genotoxicity of nanomaterials. The battery of tests for genotoxicity assessment of chemicals is considered inappropriate for nanoparticles, but still, the same is used to assess the genotoxicity of nanomaterials with some modifications.

In general, nanoparticles are classified into three broad categories: organic, carbon-based material, and inorganic. Metal and metal oxide nanomaterials are considered organic nanomaterials, which include silver (Ag), gold (Au), aluminum (Al), cadmium (Cd), copper (Cu), iron (Fe), zinc (Zn), and lead (Pb) (ZnO), copper oxide (CuO), magnesium aluminum oxide ($MgAl_2O_4$), titanium dioxide (TiO_2), cerium oxide (CeO_2), iron oxide (Fe_2O_3), silica (SiO_2), and iron oxide (Fe_3O_4); carbon-based nanomaterials include Graphene, fullerene, single-walled carbon nanotubes, multiwalled carbon nanotube, carbon fiber, an activated carbon, and carbon black. Dendrimers, cyclodextrin, liposome, and micelle are categorized as organic-based nanomaterials (Golbamaki et al. 2015). Composite-based nanomaterials are nanomaterials that include any combinations of the classification mentioned above. The most represented group is inorganic nanomaterials, including carbon nanotubes, fullerene particles, metal and metal oxide nanoparticles. Metal and metal oxide nanoparticles are a particular focus because they are easily synthesized and modified chemically and have widespread potential in medicine, consumer, industrial products, and military applications. Different genotoxicity test conducted for different nanoparticles recently is tabulated in Table 19.1. Different test strategies for genotoxicity assessment of nanomaterials include; Mutagenicity, Chromosomal damage, and DNA damage (Armand et al. 2016). Figure 19.1 depicts nanomaterial-induced genotoxicity and its testing strategies.

Table 19.1 In vitro and in vivo genotoxicity test performed for different nanomaterials

Assays	Nanomaterials studied (in vitro)	Cell lines	Nanomaterials studied (in vivo)	Animal model	Reference
Comet	TiO ₂ , silver, iron, Au, carbon-based nanomaterial, Ni and NiO, cadmium oxide (CdO), CeO ₂ , MgO, ZnO ₂ , indium tin oxide (ITO), CuO, CoFe ₂ O ₄ , SiO ₂ , ZnO ₂ , Bi(III) oxide (Bi ₂ O ₃), ZnO, coated and uncoated ferric cobalt boron (FeCoB), cerium oxide, Concanavalin A immobilized—ZnO, Co (Co, CoO, and Co ₃ O ₄), oleic acid-coated iron oxide	A549, human peripheral blood lymphocytes, BEAS-2B, mice oocytes, mouse embryonic fibroblast MEF Ogg1 +/+ and Ogg1 -/- cells, HepG2 (liver), NRK-52E (kidney), Caco-2 (intestine), A549 (lung) cell lines. Balb/3T3 (mammalian cell line of murine origin), A549 (human type II alveolar epithelial cell line), (BMECs), Astrocytes, NHDF HepG2, NRK-52E, human fibroblasts from the foreskin, SH-SY5Y (neuron cells), 3D human bronchial models, human nasal mucosa Mussel hemocytes, gill cells, human cell line (pulmonary TT1 cells), HT29-MTX-E12 human peripheral blood	ZnO, titanium dioxide, poly-L-lysine-coated superparamagnetic iron oxide, silica-coated cobalt-zinc-iron, MgO, TiO ₂ P25, CeO ₂ and BaSO ₄ , WO ₃ , Cr ₂ O ₃ , yttrium oxide nano- and microparticles, citrated-coated Ag, silica, halloysite nanotubes (HNTs)	Swiss albino mice, C57BL/6J BomTac mice (intratracheal), Lewis rats (intracranial implantation) Wistar rats-(oral, inhalation), Sprague-Dawley rats (intratracheal), Wistar rats (inhalation), wistar rats (oral), Rabbits-IV	Branica et al. (2016), Ghosh et al. (2016), Rubio et al. (2016), Preaubert et al. (2016), Annangi et al. (2016), Mahmood et al. (2016), Stoccoro et al. (2016), Latvala et al. (2016), Akyil et al. (2016), Ljan et al. (2017), Netzer et al. (2018), Abudayyak et al. (2017a, b), Harvanova et al. (2017), Haase et al. (2017), Di Buccianico et al. (2017, 2018), Hackenberg et al. (2017), Katsumiti et al. (2018), Vila et al. (2018), Zal et al. (2018), Naeem et al. (2017), Fernández-Bertólez et al. (2018a, b), Moratin et al. (2018), De Carli et al. (2018), Montazeri et al. (2018), May et al. (2018), Klingelfus et al. (2019), Ávalos et al. (2018), Cappellini et al. (2018), Kazimirova et al.

(continued)

Table 19.1 (continued)

Assays	Nanomaterials studied (in vitro)	Cell lines	Nanomaterials studied (in vivo)	Animal model	Reference
		<p>cultures, TK6 cells, human mesenchymal bone marrow stem cells, V79 cell line, human A172 glioblastoma cells, HL-60-(human promyelocytic leukemia cells)</p> <p>RTG-2 cells line (rainbow trout gonadal HL-60—(tumoral human leukemia cells) and HepG2-human hepatoma cells A549 type II epithelial cell lines</p>			<p>(2019), Zangeneh et al. (2019), Gea et al. (2019), Mittag et al. (2019), Dumaia et al. (2019), Efthimiou et al. (2020), Laban et al. (2020), Siivola et al. (2020), Vuković et al. (2020), Franz et al. (2020), Arslan and Akbaba (2020), Demir et al. (2020), Wallin et al. (2017) (In vitro)</p> <p>Rubio et al. (2016), Novotna et al. (2017), Mangalampalli et al. (2017), Relier et al. (2017), Cordelli et al. (2017), Chinde and Grover (2017), Hadrup et al. (2019, 2021), Panyala et al. (2019), Kim et al. (2019), Barfod et al. (2020), Fatima and Ahmad (2019) (In vivo)</p>

MN	Coated and uncoated ferric cobalt boron (FeCoB), cerium (IV) oxide (CONPs), ZnO-NPs Gold nanoparticles TiO ₂ , SiO ₂ , CeO ₂ , Ag	HepG2 (liver), NRK-52E (kidney), Caco-2 (intestine), and A549 human colon adenocarcinoma cell line (Caco-2) Human peripheral blood lymphocytes FaDu cells astrocytes NHDF (normal human dermal fibroblasts) V79 cell line human A172 glioblastoma cells TK6 lymphoblastoid cells	ZnO, MgO, CeO ₂ , BaSO ₄ , WO ₃ Cr ₂ O ₃ , yttrium oxide nano- and microparticles	Swiss albino mice, Wistar rats (oral), Sprague-Dawley rats Intratracheal Wistar rats (inhalation)	Branica et al. (2016), Akyl et al. (2016), Abudayyak et al. (2017b), Fernández-Bertólez et al. (2018b), May et al. (2018), Di Bucchianico et al. (2018), Cappellini et al. (2018), Laban et al. (2020) (In vitro) Rubio et al. (2016), Relier et al. (2017), Cordelli et al. (2017), Chinde and Grover (2017), Hadrup et al. (2019), Kim et al. (2019), Fatima and Ahmad (2019), Ali et al. (2019) (In vivo)
Chromosomal aberration	Carbon-based nanomaterials, Co-based NPs (Co, CoO, and Co ₃ O ₄), cerium (IV) oxide nanoparticles (CONPs)	A549 type II epithelial cell lines TK6 and HepG2 cells	ZnO, MgO, tungsten oxide (WO ₃) NPs, chromium oxide NPs (Cr ₂ O ₃ NPs), (TiO ₂ NPs)	Swiss albino mice, Wistar rats (Oral)	Rubio et al. (2016), Relier et al. (2017), Hadrup et al. (2019), Ali et al. (2019), Levy et al. (2019) (In vivo)

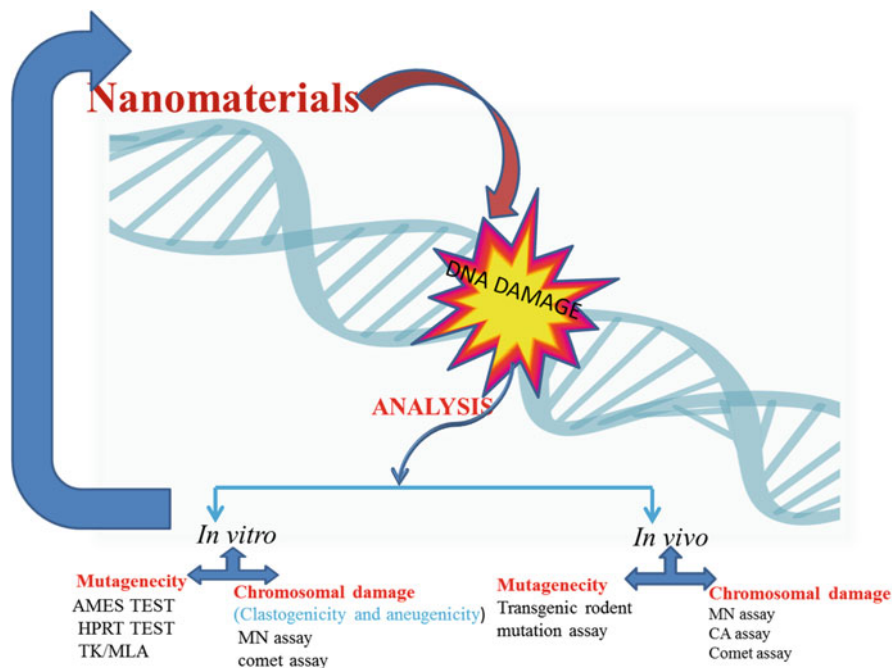


Fig. 19.1 Different genotoxicity testing methods for nanomaterials. *MN* micronucleus, *CA* chromosomal abrasion

19.3 Mutagenicity Assay

19.3.1 In Vitro Mutagenicity

Mutagenicity is the key endpoint of genotoxicity, which refers to the induction or permanent alternation in DNA of a cell or organism, and it is transferred to the subsequent generation (OECD). Heritable DNA changes or mutations include:

- Alternation in a single base pair, multiple genes, chromosomes
- Breaks in chromosomes
- Alternation in chromosome number (aneuploidy)
- Mitotic recombination

In vitro mutagenicity tests performed for different nanomaterials according to OECD guidelines in bacteria and mammalian cells are discussed below.

19.3.1.1 The Ames Test

The Ames test, the bacterial reverse mutation test developed by Bruce Ames, assesses compounds' mutagenicity in bacterial strains. The principle behind this

test is that the mutagenic compound restores the ability to synthesize essential amino acid histidine in bacteria (*Salmonella typhimurium* or *Escherichia coli*). Different modes of mutation induction, such as frameshift and base substitution mutation, can be determined by this method. Mutagens can revert point mutation in histidine or tryptophan biosynthesis genes in *Salmonella typhimurium* or *Escherichia coli* thereby restoring the ability of bacteria to synthesize essential amino acids. The revertant bacteria can grow without amino acids (Doak et al. 2012) even though this has been considered the accepted genotoxicity test for assessing mutagenicity, which is inappropriate for nanomaterials. However, this is routinely included in the assessment of the genotoxicity of nanomaterial; documented evidence on the negative and positive test for Ames test on different nanomaterials has been reported in the literature. Researchers claim that the Ames test was inadequate to assess nanomaterials' genotoxicity. The gram-negative strains of bacteria lack uptake mechanisms that normally happen in the mammalian cell, such as end pin phagocytosis (Landsiedel et al. 2009; Warheit and Donner 2010; Dewangan et al. 2018).

19.3.2 In Vitro Mammalian Cell Gene Mutation Test

19.3.2.1 Hypoxanthine-Guanine Phosphoribosyl Transferase Test

In vitro mammalian cell gene mutation test assess the gene mutations at the *hprt* or *xprt* reporter locus. This clonal selection assay has been performed for different nanomaterials as per OECD guidelines to assess the mutation of the Hypoxanthine-guanine phosphoribosyltransferase gene on the mammalian cells X chromosome and a transgene of xanthine-guanine phosphoribosyltransferase (*Xprt*) on a somatic chromosome. Base pair substitutions, frameshifts, small deletions, and insertions can be detected by *hprt assay*. The *XPRT* test determines large deletions and possibly mitotic recombination. The principle behind this test is that normal cells with *hprt* positive gene are sensitive to purine analog 6-thioguanine and resulting in inhibition of cellular metabolism. In contrast, mutant cells restrict the cooperation of lethal 6-thioguanine (6-TG) into the DNA and result in the growth of cells in a medium containing 6-thioguanine and form colonies (OECD 2016a). The cell lines recommended for this are used for *XPRT* assay include CHO-derived AS52 cells and as per literature, the most frequently used cells include: Chinese hamster ovary [CHO], Chinese hamster lung [V79], mouse lymphoma L5178Y, and human TK6 (OECD TG 476) (Lloyd and Kidd 2012). The *HPRT* mutant frequency was calculated as Cloning efficiency (CE) = colonies seeded cells per dish/Seeded cells per dish.

The factors to be considered for the selection of cells include:

- Sensitivity to mutagens
- Cloning efficiency
- A stable karyotype
- Spontaneous mutant frequency

19.3.2.2 Xanthine-Guanine Phosphoribosyl Transferase Test

Xanthine-guanine phosphor ribosyl transferase, XPRT test, and mutation at Glutamic-pyruvic transaminase (*gpt*) transgene are analyzed. Similar to the hprt assay, point mutations were detected together with large deletions and possibly mitotic recombination is determined by the XPRT test. The autosomal location of *gpt* transgene may detect larger deletions, OECD (476) (Lloyd and Kidd 2012). Both mutagenic assays detect different levels of mutation. Mutant frequency is measured by counting mutant colonies observed when grown in selective media.

19.3.2.3 The In Vitro Mouse Lymphoma Assay (Mutation at Tk Gene)

The mammalian cell Tk gene mutation assay (OECD TG 490) determines mutation at the thymidine kinase (Tk) reporter locus of L5178Y mouse lymphoma Tk+/- cells (OECD 2015). As per OECD, this test is conducted in both L5178Y Tk+/- - 3.7.2C mouse lymphoma cell line and TK6 human lymphoblastoid cell lines. The principle behind this test is that Tk+/- cells are unable to grow in lethal nucleoside analog trifluorothymidine, as it cooperates with DNA and inhibits the replication process, whereas this mutation at tk locus (Tk-/-) results in the growth of cells with lethal nucleoside analog trifluorothymidine. Larger colonies are formed due to point mutation. Its colonies often result from chromosomal mutation. Similar to these, TK6 cells were also used to assess mutations at the tk locus for evaluating mutations induced at the TK locus (Prabhakar et al. 2012).

The key endpoints of mutagenicity such as gene mutation, clastogenicity, and aneuploidy of different nanomaterials are assessed. The literature provides evidence on the commonly performed mutagenicity assay of nanoparticles; It mainly includes Tk (thymidine kinase) or Hprt (hypoxanthine phosphoribosyltransferase) genes mutation assays (Lloyd and Kidd 2012; ECHA 2020). Both in vitro and in vivo studies have been performed. In vitro studies were conducted on bacterial and mammalian cells. Recently, regarding the size of nanomaterials and bacterial cells, the Ames test is not recommended for mutagenicity of nanomaterials as bacterial cell wall limits the uptake of nanomaterials (Manshian et al. 2011; Wang et al. 2007). Recommended mutagenicity studies on metal and metal oxide in the last 10 years have been discussed. Nanomaterials namely titanium dioxide (TiO₂) nanoparticles (NPs) key components with a wide range of applications, including in the food industry genotoxicity assessment is of great importance (Asakura et al. 2010). It has been documented that mutagenicity is induced by TiO₂ and carbon nanotubes (Armand et al. 2016; Huang et al. 2009). In contradictory, studies also reported negative mutagenicity in response to TiO₂ and carbon nanotubes (Gulledge 2007; Chen et al. 2001). This may be due to the difference in nanomaterial characterization or sensitivity towards different cell lines. UF-TiO-induced increased mutation frequency was observed on HPRT assay in WIL2-cells (Chen et al. 2014). It was also documented that the dose-dependent mutagenic effect of TiO₂ in V79 cells (Kazimirova et al. 2020; Manshian et al. 2013). A recent study has documented that the lack of mutagenic effects was independent of the dispersion of nanomaterial, TiO₂ (Guichard et al. 2016). Similarly, few studies are performed with metal nanoparticles to assess the mutagenicity. SiO₂, MWCNT mutagenic potential was

assessed in L5178Y TK+/- cell and CHO cells, negative results were obtained, and no evident mutagenicity was observed (Mrakovcic et al. 2015; Thybaud et al. 2003).

19.3.3 In Vivo Mammalian Mutagenicity Assay

In vivo Transgenic Rodent (TGR) mutation assays are determined gene mutations under standard conditions. This provides a quick and reliable assay in assessing mutation in DNA of any tissue of interest (Wahnschaffe et al. 2005). A transgenic mutation test system is a foreign gene construct containing a target *gene* as a target for mutations and a *shuttle vector* for recovering the target gene DNA from the tissue of the transgenic animal (Nohmi et al. 2017). Transgenic rodent mutation assay, transgenic rats and mice that contain multiple copies of chromosomally integrated plasmid or phage shuttle vectors. Transgenic models widely used are: lacZ bacteriophage mouse (Muta Mouse), lacZ plasmid mouse; gpt delta (gpt and Spi-); lacI mice or rat (Big Blue rat or mice) are used under standard conditions (Nohmi et al. 2000; Kohler et al. 1991). A wide range of transgenic models are available, and they can be selected according to the test requirement; mainly, mouse models are used. TGR mutation models enable the assessment, quantify, and sequencing of mutations in both somatic and germ cells. The key factors considered for Transgenic Rodent (TGR) mutation assays as per OECD guidelines include:

- Selection of animals
- The duration of treatment
- Dose selection
- Route of administration

19.3.3.1 *LacI* and *LacZ* Transgenic Mouse Model (Somatic Cells)

Transgenic mouse models are constructed by integrating *E. coli LacI* and *LacZ* genes into the mouse. *LacI* transgenic mouse or rat contains 30–40 copies of a lambda LIZ α shuttle phage vector integrated into its genome at a single locus on chromosome 4, and *lacZ* mouse models contain about 80 copies of the shuttle vector at chromosome (Gossen et al. 1989). The principle behind this assay is that a transgene-containing reporter gene is used to assess mutation. This test can be performed as a single or repeated-dose study. Upon treatment with the test compound, tissue of interest DNA is extracted (contains transgene), followed by in vitro phage packaging and introduced into *E. coli* cell. The *E. coli* cells are grown in media containing chromogenic substances (X-gal). Mutation at the *LacI* gene may result in blue plaques, and non-mutated *lacI* forms colorless plaques. A similar test was performed in *LacZ* transgenic mouse model to assess mutagenesis at the *lacZ* gene (Louro et al. 2014). The blue and white plaque ratio was observed, and it is considered the indicator of mutation or measure of the mutagenicity. Figure 19.2 represents transgenic rodent mutagenicity assessment in the transgenic mouse model. In vivo mutagenicity of TiO₂ nanomaterial was assessed using LacZ plasmid-based transgenic mice. The mice were exposed to intravenous injection of

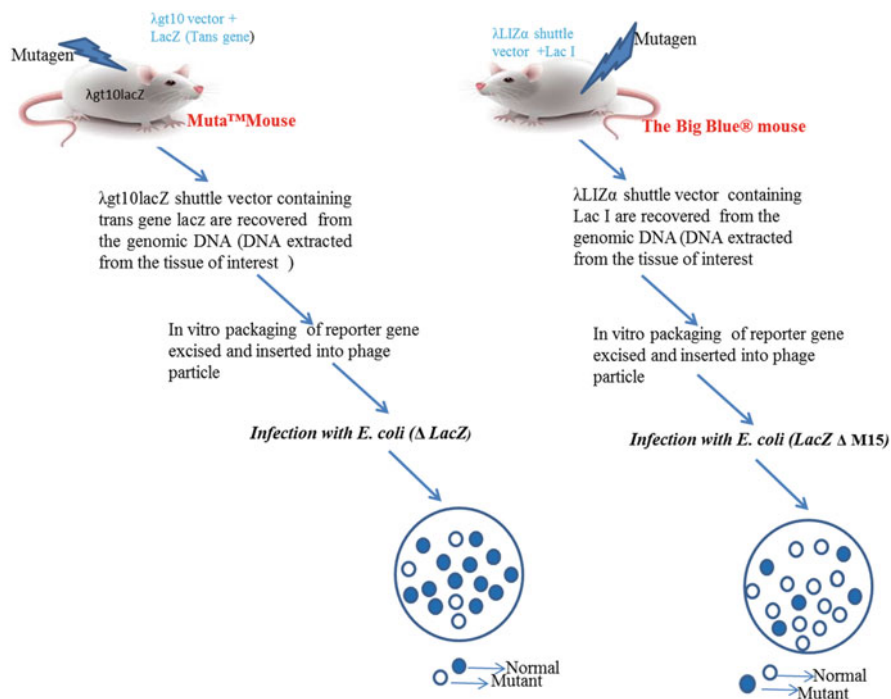


Fig. 19.2 In vivo transgenic rodent assay in different transgenic models

two daily doses of 10 and 15 mg/kg of body weight/day of TiO₂ NM; no genotoxicity was observed (Suzuki et al. 2016). In another study, frequencies of point mutation and deletions in the liver induced by TiO₂-P25 in gpt Delta mice were assessed by gpt and Spi– mutation assays; no mutation was observed in liver DNA even though more deposition of TiO₂ in the liver was analyzed (Douglas et al. 1995). *LacI* and *LacZ* transgenic mouse model (somatic cells) assay procedures are represented in Fig. 19.2.

19.3.3.2 Transgenic Rodent Assays (Germ Cell)

As per OECD guidelines mentioned earlier, transgenic rodent assays with few alternations are followed for germ cell mutagenesis (Marchetti et al. 2018). The process of the rescue of a transgene from male germ cells is as follows: the germ cells of mature sperm cells are collected from cauda epididymis and the vas deferens, in comparison to somatic cell mutation, the tissue collection or sampling time for mice and rat varies in case of germ cells: 49 days after exposure to test compound for mice and 70 days in case of the rat. The mentioned duration is necessary for the maturation of spermatogonial stem cells to sperm and to reach the vas deferens and cauda epididymis (Miura et al. 2008a). Recently it has been documented that mutagenicity can be assessed 28 days after treatment followed by 28 days expression period (Miura et al. 2008a).

19.3.3.3 Pig-a Assay in Rodents and Humans

Phosphatidylinositol glycan complementation group A (Pig-a) gene is a reporter gene that assesses mutation (Miura et al. 2008b; Dertinger et al. 2011). Approximately two copies of 30 genes are involved in the biosynthesis of GPI anchors, while Pig-a gene presents as one functional copy on the X chromosome of the cell. Mutations at the Pig-a gene result in the loss of glycosyl phosphatidyl inositol-anchored proteins in the cell surface, and thus the mutant cells fail to express surface markers CD59 or CD24. The presence of these cell surface antigens can be assessed by flow cytometry. This assay can be combined with rodent 28-day repeated-dose toxicity (Khanal et al. 2018; Kimoto et al. 2016), which may reduce the use of animals. The assay is considered very quick and cost-effective as it requires only a small volume of blood. Pig-a conserved gene; hence, it can be performed in rats, mice, and humans. This is considered to be the follow-up assay of *in vivo* mutagenicity assay. The evaluation score of Pig-a assay is recorded as positive (P), negative (N), equivocal (E), or inconclusive (I). Peripheral blood reticulocytes and total RBCs are analyzed to assess Pig-a mutant frequency.

Pig-a mutant phenotype assessment is established for erythrocytes (mature and immature) in peripheral blood (Olsen et al. 2017). Technical guidelines for this assay is under the development of OECE. Pig-a assay in rodents has been explored to assess the mutagenicity of nanomaterials. The mutation potency of TiO₂ has been determined by assessing the frequency of Pig-mutants in erythrocytes TiO₂ was well dispersed (so that it could reach the bone marrow) and intravenously administered to mice. After 9 days of treatment, blood was collected, and no significant mutant frequency was observed (Li et al. 2014). Contradictory results to the above were also observed in another study. This may be due to differences in the characterization of nanomaterials. It has been documented that PVP-coated AgNP administered at different concentrations intravenously to B6C3F1 mice did not induce any mutant frequencies in the Pig-a gene assay (Zhu et al. 2020), both Ag NPs and TiO₂ NPs did not induce Pig-a gene mutation frequency in TK6 cells (Horibata et al. 2017). On Pig-a gene assay, a single intratracheal instillation of MWCNTs was non-mutagenic to the bone marrow (Magdolenova et al. 2014). CeO₂ and BaSO₄ inhalation exposure to rats for a period of 6/4 months did not show any mutagenicity on Pig-a gene assay (Collins 2004).

19.4 Chromosomal Damage Assays

19.4.1 Single Cell Gel Electrophoresis (SCGE) Assay/Comet Assay

Single cell gel electrophoresis is one of the most common, simple, reliable, and widely applied DNA damage assays in nanogenotoxicology. It is a very sensitive and versatile technique that can detect single and double-strand DNA breaks, excision repair sites, alkali-labile sites (ALS), basic sites, and cross-links (Azqueta and Dusinska 2015; Vandghanooni and Eskandani 2011). In this *in situ* gel electrophoresis technique, the test material treated cells embedded in low melting agarose

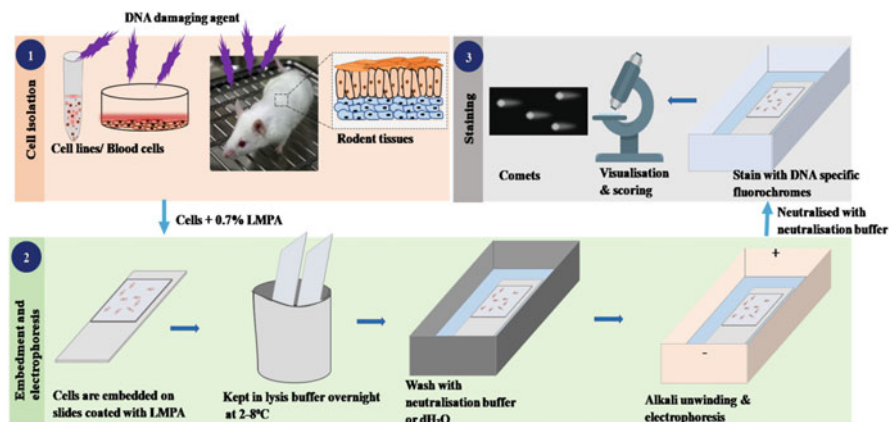


Fig. 19.3 The diagrammatic representation of Comet assay

gel spread on a microscopic slide are lysed in the presence of detergent and high salt concentration to remove cell membrane and proteins. Then electrophoresis has to be carried out to allow the migration of damaged DNA from the undamaged nucleoid body, which acquires a “comet” structure when stained with DNA-specific fluorochromes hence termed as “comet assay.” As the DNA is negatively charged, the smaller damaged DNA fragments will move faster towards the anode under electric current resembling the “tail” of “comet” than the unbroken part, which looks like the “head” of “comet.” The amount of DNA in the tail region signifies the extent of DNA damage in the cell due to genotoxic events induced by test material (Huk et al. 2014, 2015; Magdolenova et al. 2012). Figure 19.3 represents the process involved in the comet assay.

19.4.2 General Requirements

Genotoxicity assessment of the same nanomaterials may show variations in the test findings due to differences in size distribution, dispersion stability, and changes in physicochemical characteristics like size, shape, charge, and surface coatings; hence, the physicochemical properties and exposure conditions should be validated accordingly. The exposure concentration of the nanomaterials can be expressed in terms of mass per volume ($\mu\text{g}/\text{mL}$), mass per area ($\mu\text{g}/\text{cm}^2$), or mass per cell ($\mu\text{g}/\text{cell}$). The concentration of nanomaterials can also be indicated in terms of several nanomaterials, i.e., no. of NM/mL (NM/mL), number of NM per surface area (NM/cm^2), number of NM (NM/cell) or in terms of the surface area of nanomaterials, i.e., the surface area of NM per mL ($\text{NM cm}^2/\text{mL}$), the surface area of NM per area ($\text{NM cm}^2/\text{cm}^2$) or surface area of NM/cell ($\text{NM cm}^2/\text{cell}$) (Dusinska and NanoTEST Consortium 2009; Guadagnini et al. 2014; Magdolenova et al. 2015; Stone et al. 2009).

To ensure the reliability of genotoxicity assays, exposure concentrations are expressed in terms of two different units; in addition to mass, concentrations in many nanomaterials or the surface area are also recommended. Cytotoxicity assessment should be done prior to genotoxicity testing to confirm the dose range, as genotoxic events can occur secondary to cytotoxicity, which may lead to a false interpretation of the results. The selected exposure concentrations should cover nontoxic to around 80% viability in cytotoxic assays and should signify levels of possible human exposure. Moreover, the concentration, which causes excessive agglomeration of nanomaterials, has to be avoided. Genotoxicity assays of nanomaterials commonly use a prolonged exposure time of about 24 h, but positive responses of comet assay were obtained with a short exposure time of 2–3 h (Ostling 1984; Singh et al. 1988; Pu et al. 2015).

The comet assay can be done *in vitro* using single cells from primary cell lines like peripheral blood mononuclear cells and immortalized cell lines or *in vivo* using cells from homogenized tissue biopsies (Magdolenova et al. 2012, 2015; Huk et al. 2014; Dusinska and NanoTEST Consortium 2009; Guadagnini et al. 2014; Stone et al. 2009; Ostling 1984). Depending on the characteristics of the nanomaterial, the test method (*in vitro* or *in vivo*), cell type (human or mammalian), and the target organ to be studied in case of *in vivo* assay are chosen. Most *in vitro* assays were done using human peripheral blood lymphocytes and established immortalized cell lines of human or mammalian origin. Mice and rats are preferred for *in vivo* studies as per OECD guidelines, and in most cases, target tissues chosen are lungs, liver, blood, and BAL (Huk et al. 2014; Dusinska and NanoTEST Consortium 2009; Guadagnini et al. 2014; Magdolenova et al. 2015; Stone et al. 2009; Ostling 1984).

19.4.3 In Vitro Comet Assay

19.4.3.1 Alkaline Single Cell Gel Electrophoresis/Alkaline Comet Assay

The technique was first developed as a microgel electrophoresis technique by Ostling and Johanson (1984) (Singh et al. 1988). This procedure was modified by Singh et al. (1988) by providing high pH (Pu et al. 2015). In this technique, the cells with test materials are embedded in 0.5% low melting point agarose and layered onto a microscopic slide precoated with 1.5% normal-melting agarose. After the solidification of agarose, an extra layer of agarose can be added. The slides are then kept in the detergent solution overnight (cell lysis), followed by electrophoresis for 20 min in the alkaline buffer to unwind DNA. Then slides are gently washed with neutralization buffer or phosphate-buffered saline and stained with a fluorescent dye (George et al. 2017).

For detecting DNA strand breaks by alkaline comet assay, the maximum dose selected should ideally have at least 60% viability, as more cytotoxic concentration may provide false-positive results. A reliable method to detect cytotoxicity like relative growth activity or colony-forming assay, rather than conventional colorimetric assays (e.g., MTT) must be done along with the same assay using the same cell type (George et al. 2017; Gehlhaus et al. 2008). The concentration, which

intensifies agglomeration, must be eliminated as agglomeration may affect the bioavailability of nanomaterials (NMs) in the cells, leading to a false interpretation of results. NMs concentration should be expressed in at least two units (commonly used are $\mu\text{g/mL}$ or $\mu\text{g/cm}^2$), depending on the type of NM and culture plate used (Huk et al. 2015; George et al. 2017; Gehlhaus et al. 2008).

Both positive and negative controls should be incorporated into the assay to ensure the test's accuracy and reliability. Negative control, preferably solvent alone, which shows the background DNA damage and positive control, which produces a significant level of strand breaks, ascertain quality control of the assay. Hydrogen peroxide (2–100 μM for 5–10 min) and photosensitiser Ro 19-8022 with visible light are commonly used in the comet assay as positive controls to induce strand breaks. An appropriate nano-specific positive control, which can induce adequate levels of DNA damage, has yet to be validated (Ostling 1984). NM coatings, stabilizers, or solvents may evoke toxicity and hence should be included separately in the assay. The leachable particular metal ions from the metal NMs and carbon nanotubes can induce a form of reactive oxygen species, which may lead to toxicity and have to be ruled out to avoid false elucidation of the results (Stone et al. 2009; Ostling 1984).

Experimental controls (positive and negative controls) have to be included in each assay to maintain quality. Negative control can be dispersion media alone, processed in the same manner for NM dispersion without the addition of NM. Positive controls used, commonly 5 mM EMS, photosensitiser Ro 19-8022 or 20–100 μM H_2O_2 , must induce significantly increased levels of DNA strand breaks (Gehlhaus et al. 2008).

19.4.3.2 Preparation of Sample

The assay can be conducted using human or mammalian primary cells or cell lines; the method of selection and cell type solely depend on the characteristics of test NMs and the possible route of human exposure. The assay steps should be ensured to not introduce any additional DNA strand breaks or repair during cell isolation and processing (Könen-Adıgüzel and Ergene 2018). It is advisable to select the dose of NM for genotoxicity assessment based on cytotoxicity by a reliable method like relative growth activity or colony-forming assay as NMs may interfere with colorimetric assays like MTT. The suggested dose for alkaline comet assay should exhibit at least 60% cell viability as DNA strand breaks secondary to cytotoxicity may cause false-positive results (Souza et al. 2016). The dose range selection based on possible occupational and environmental exposure is also recommended (Nadin et al. 2001; OECD 2014, 2016b). Human peripheral blood samples from healthy nonsmoking donors are preferred. Triplicate cultures from each sample should be included in the assay. It is recommended to conduct each assay three times to maintain specificity. Genotoxicity assessment using comet assay was conducted for CeO_2 NPs by Konen-Adıgüzel et al. (2018) (Souza et al. 2016). Blood samples were mixed with equal volumes of histoplaque-1077 and centrifuged for 30 min at 2000 rpm. The obtained suspension (0.5 mL) was added to RPMI (4.5 mL) containing 20% fetal calf serum, 2 mM L-glutathione, 10 mg/mL PHA (phytohaemagglutinin), and antibiotic-antimycotic agents. The culture tubes were incubated for 24 h at 37 °C and 5%

CO₂. Subsequently, NP treatment was given for 3 h; 2% LMPA agarose was mixed with 100 μL of treated lymphocyte suspension and applied onto slides precoated with 5% standard melting agarose and electrophoresed (Souza et al. 2016). The genotoxic effects of silver nanoparticles were assessed by Souza et al. (2016) using CHO-K1 and CHO-XR55 cell lines (Martínez-Luna et al. 2015). The cells were seeded at a density of 2.5×10^5 cells/flask and incubated to subconfluency; subsequently, adequate doses of Ag NPs treatment were given for 24 h. After treatment, cells were washed in PBS, trypsinized, and centrifuged. To avoid further DNA damage, a low concentration of trypsin (0.005%) is suggested for harvesting. The cell button was mixed in 100 μL of 0.5% low-melting point agarose and embedded in slides spread with 1.5% normal-melting point agarose. The slides are allowed to solidify and then kept for 24 h in ice-cold (4 °C) lysis buffer having Triton X-100 (1%), DMSO (10%), 2.5 mM NaCl, 100 mM disodium EDTA, and 100 mM Tris. After 24 h, the slides were maintained for 20 min in freshly prepared electrophoresis buffer with 1 mM disodium EDTA and 300 mM NaOH for DNA unwinding. After that, electrophoresis was performed using 25 V and 300 mA for 20 min. Electrophoresed slides were immersed in a neutralization buffer for 15 min and then fixed in ethanol. The 50 cells were scored after staining with SYBR green. DNA intensity in comet tails was quantified by comet assay IV software (Martínez-Luna et al. 2015).

19.4.3.3 Preparation of Slides for Electrophoresis and Visualization of Comets

Slide preparation is critical as a uniform layer of gel is required for better visualization of comets with less background noise, especially in cases of high DNA migration to avoid overlapping comets. A thin flat layer of agarose is made on frosted and chilled microscopic slides by dipping in normal-melting point agarose and letting it solidify. A single cell suspension made in low-melting point agarose at 37 °C is added to the solidified layer of agarose, a coverslip is placed over it to level the surface, and the slide is chilled to enhance gelling process. Agarose concentration and cell count in the suspension should be optimized to ensure adequate analysis of cells. During slide preparation, direct contact with light should be avoided to circumvent additional DNA damage, which may mislead the scoring interpretation (Collins 2004; Gehlhaus et al. 2008; Könen-Adıgüzel and Ergene 2018; Souza et al. 2016; Martínez-Luna et al. 2015). After the slide preparation, the slides were placed in lysis buffer with high salt/detergent concentration for 1–24 h to promote cell lysis after solidification. Lysis buffer having 1% Triton X-100, 10% DMSO, 2.5 mM NaCl, 100 mM disodium EDTA, and 100 mM Tris is generally used. Chilled lysis buffer is preferred to maintain the firmness of agarose gel, and the isolated DNA after cell lysis may be subjected to proteinase K treatment to remove residual protein. The tagging of DNA with site-specific repair enzymes or antibodies is advisable following cell lysis to identify the type of genotoxic event (Collins 2004; Ostling 1984; Martínez-Luna et al. 2015; Nadin et al. 2001). After lysis, the slides must be washed thrice with neutralization buffer (0.4 M Tris-HCl, pH 4.5) at 4 °C and kept in alkaline electrophoresis buffer (pH > 13) having 1 mM EDTA and 300 mM NaOH for

20 min for alkali unwinding and isolation of ssDNA (Dusinska and NanoTEST Consortium 2009; Guadagnini et al. 2014). Electrophoresis has to be carried out after alkali unwinding using the same buffer (pH > 13) for 10–20 min with 25 V and 300 mA. The required voltage/ampere is optimized depending on the DNA migration seen in control and treated cells (Gehlhaus et al. 2008). Following electrophoresis, the slides should be stained with fluorescent dye specific for chromatin, like 0.6 μM ethidium bromide or DAPI (1 $\mu\text{g}/\text{mL}$) or SYBR gold, put coverslip, and the comets have to be examined under a fluorescent microscope. As ethidium bromide is carcinogenic, care should be taken while handling it. The silver staining technique for visualizing comets developed by Nadin et al. (2001) is shown to be highly sensitive, reproducible, and avoids the risk of using ethidium bromide (OECD 2016b). Comet scoring must be done from 100 randomly selected cells, and the ratio of the percentage of DNA content in the tail to total (head and tail) is analyzed manually or using the software. The manual scoring includes grading of comets from 0 to 4 based on the proportion of DNA damage.

19.4.4 In Vivo Comet Assay

In vivo mammalian alkaline comet assay is a commonly used method in nanogenotoxicology for detecting DNA strand breaks in cells isolated from animal tissues, particularly from rodents, as suggested by OECD 489. This assay reveals DNA damages regarding in vivo ADME, i.e., absorption, distribution, metabolism, and excretion of the test material. As part of reducing animal usage in agreement with the 3Rs principle (Reduction, refinement, replacement), comet assay can be performed along with other genotoxic assays in rodents. Non-rodent species may be used for the assay and other toxicity studies with proper scientific and ethical justification (OECD 2014, 2016b, c; Organisation for Economic Co-operation and Development 2002; Oliviero et al. 2019). Many studies have been reported for nanomaterial genotoxicity testing using in vivo comet assay by adopting OECD 489. Wallin et al. (2017) had done in vivo comet assay for assessing the genotoxicity of TiO_2 -NPs via Intratracheal exposure in C57BL/6J BomTac mice. Novotna et al. (2017) reported that no significant increase in oxidative damage had been produced in Lewis rats by poly-lysine-coated superparamagnetic iron oxide NPs and silica-coated cobalt, zinc, iron-NPs following intracranial implantation. Kim et al. (2019) reported citrated-coated Ag NPs-induced DNA damage in rabbit liver tissues following intravenous administration as evidenced by in vivo comet assay. As part of genotoxicity studies, comet assay had been done in *Paracentrotus lividus* sperms (Oliviero et al. 2019) and adult zebrafish (*Danio rerio*) embryo peripheral blood (Suriyaprabha et al. 2019) to detect DNA strand breaks caused by ZnO-NPs (Novotna et al. 2017; Mangalampalli et al. 2017; Barfod et al. 2020; Blakey and Douglas 1990). The vehicles selected should be compatible with the test system, and the use of aqueous solvents/vehicles is preferable. The selected dose of positive control (e.g., EMS) must produce moderate demonstrable effects that can ensure the sensitivity and reliability of the assay. Ethyl methanesulfonate, ethyl nitrosourea,

methyl methanesulfonate, *N*-methyl-*N'*-nitro-*N*-nitrosoguanidine, 1,2-dimethylhydrazine 2HCl, and *N*-methyl-*N*-nitrosourea can be selected as positive controls as specified by OECD 489. In the case of *in vivo* studies, administration of tungsten carbide–cobalt mixture (1 mg/mouse) by pharyngeal aspiration 24 h prior to euthanasia gives remarkable DNA damage in lung cells and bronchioalveolar lavage (BAL). Negative controls group administered with vehicle alone, which does not induce any genotoxic events, should be included in the study (OECD 2014, 2016b, c; Organisation for Economic Co-operation and Development 2002; Oliviero et al. 2019).

19.4.4.1 Selection of Animals and Experimental Design

Healthy adult rodents, mainly rats and mice of 6–10 weeks, are usually preferred for the assay. The assay can be done in other species according to the likely route of NM exposure and should be justified. Rodents should be kept in small groups of same sex with proper identification markings. A room temperature of 22 ± 3 °C and relative humidity of 50–60% is to be provided. Alternate dark/light cycles with fresh air changes, conventional laboratory diets and appropriate drinking water are essential. Animals must be randomly selected and acclimatized for not less than 5 days prior to the study. According to OECD 489, each test group shall have five analyzable animals of one sex or each sex if both sexes are employed. For the positive control, at least three animals of one sex or each sex (if study groups consist of animals from both sexes) should be included (OECD 2014, 2016c; Organisation for Economic Co-operation and Development 2002).

The route of administration of test nanomaterial will be following all available data regarding the test material like a possible route of human exposure, other toxicity study results, and available ADME profiling and structural alerts for genotoxicity. The liver is the main organ involved in metabolism, and it has been extensively studied for genotoxic events. The test materials, which are expected to have an oral route of exposure stomach, are chosen as relevant site-of-contact tissue. However, the duodenum and jejunum can also be considered. Genotoxic events following inhalation toxicity can be studied in lungs and bronchioalveolar lavage cells. The test can also be conducted in other tissue like the kidney, urinary bladder, skin, or multiple organs (OECD 2014, 2016b, c). It has been reported that germ cell genotoxicity assessment using alkaline comet assay produces significant background DNA damage. Hence, the assay should be validated and standardized accordingly before using gonadal tissues (OECD 2014, 2016c; Organisation for Economic Co-operation and Development 2002).

Animals are administered with test material through a proper route for a selected period of exposure. After the exposure time, target tissues must take out, make single cell/nuclei suspension, embed in agarose gel, and lysis of the cell membranes and proteins using high salt/detergent concentration. The lysis breaks down cellular and nuclear membrane proteins permitting chromatin contents, including the DNA loop (nucleoids) and fragmented DNA fractions get released. Electrophoreses after lysis under high pH (>13) cause the migration of DNA fragments further from the nucleoid, resembling a “comet,” in which the fragments represent “tail” and the

nucleoid the “head.” The comets can be visualized using a fluorescent microscope after staining with DNA-specific dyes. The intensity of DNA content in “tail” in comparison to the total intensity, i.e., DNA content of the head and tail together signifies the DNA destruction induced by genotoxic events (Azqueta and Dusinska 2015; Vandghanoooni and Eskandani 2011; OECD 2014, 2016c; Organisation for Economic Co-operation and Development 2002),

19.4.4.2 Dose Selection, Administration, and Sampling

Appropriate nanomaterial concentrations should be exposed to animals for two time periods, 3–6 and 24 h, to assure the entry of NMs into cells. In the case of studies involving poorly soluble NMs, an exposure time of 24 h is required for mice and rats to allow DNA damage (Latvala et al. 2016). Acute oral toxicity-fixed-dose procedure specified by OECD 420 had been reported in many studies involving acute oral exposure to test NMs (Netzer et al. 2018). As per OECD 489, the preferable treatment schedule suggests the administration of 2 or more doses at 24 h intervals and samples to be collected 2–6 h after final exposure (Mangalampalli et al. 2017; Barfod et al. 2020; OECD 2014, 2016c; Organisation for Economic Co-operation and Development 2002).

If the dose range cannot be determined from the available data of the same material, a preliminary dose-finding study should be performed in the same laboratory using the same species and animal strain. This preliminary study should determine the maximum tolerated dose (MTD), the maximum feasible dose, maximum exposure, or limit dose of the test material. For carrying out acute or sub-acute comet assay, besides maximum tolerated dose, two additional doses, ideally those having a difference of $<\sqrt{10}$, have to be included such that the dose range could cover maximum to those producing moderate or no cytotoxicity. In case of nontoxic test material, for studies requiring more than 14 days exposure to test a maximum dose of 1000 mg/kg body weight/day and for studies requiring less than 14 days exposure, a maximum dose of 2000 mg/kg body weight/day are recommended by OECD 489 (OECD 2014, 2016c; Organisation for Economic Co-operation and Development 2002; Oliviero et al. 2019).

The route of administration has to be selected according to the possible route of environmental exposure and can be oral, topical, subcutaneous, intravenous, inhalation, intratracheal, or via implantation. The maximum volume given should depend upon the animal's size and must not exceed 1 mL/100 g body weight, but for an aqueous solution, a maximum volume of 2 mL/100 g body weight can be given (OECD 2014, 2016c).

Clinical signs, food and water intake, and changes in body weight of the animals should be monitored. The optimum time for collecting samples will depend on the chemical composition of the test and selected route of administration and should be able to detect DNA strand breaks induced by test material before rectifying those breaks by repair mechanisms or priming to cell death. The sampling time can be decided from the time (T_{\max}) at which the concentration (C_{\max}) of the test will attain its maximum in plasma or steady state in cases of studies demanding multiple exposures. If such kinetic data is not available, the sample can be collected at

2–6 h after the last exposure for studies with multiple treatments and studies involving single administration samplings at 2–6 and 16–26 h is recommended.

19.4.4.3 Preparation of Sample and Work Procedure

At the appropriate sampling time, euthanize the animals humanely, collect the target organs, and prepare the cell/nuclei suspension for the comet assay as early as possible because the DNA lesions detected by the comet assay may last only for a short period. The tissue slices should be preserved in an ice-cold mincing buffer until processing, and the main steps are as follows homogenization, mincing, enzymatic treatment, and filtration (Novotna et al. 2017; OECD 2014, 2016c; Organisation for Economic Co-operation and Development 2002; Oliviero et al. 2019). Slides should be prepared immediately after obtaining single cell/nuclei suspension, and all the procedures should be done avoiding direct contact with light. An adequate volume of single cell/nuclei suspension is to be added to 0.5–1% LMPA such that the final concentration of LMPA may not be less than 0.45%. After preparing the slides, keep them in chilled lysis buffer having high salt and detergent for at least 1 h or overnight in the refrigerator. Following the cell and nuclear membrane lysis, the slide should be rinsed using neutralization buffer, phosphate buffer, or distilled water to remove the remaining salt/detergent of lysis buffer (Novotna et al. 2017; Mangalampalli et al. 2017; Barfod et al. 2020; OECD 2014, 2016c; Organisation for Economic Co-operation and Development 2002; Oliviero et al. 2019; Blakey and Douglas 1990; Hartmann et al. 2003; Olive et al. 2012; Kumaravel et al. 2009). Place the slides in the electrophoretic unit (with active cooling and high-capacity power supply) with an alkaline buffer for 20 min to unwind the DNA. The duration of electrophoresis and applied potential difference are critical factors in considering DNA migration; preferably, these can be 0.7 v/cm for 20 min. The temperature of the electrophoretic buffer has to be maintained within 2–10 °C throughout unwinding and electrophoresis. Once the electrophoresis gels are completed, the slides should be rinsed in neutralization buffer for 5 min, stain the gels and score as early as possible, preferably within 1–2 days. After drying, the slides can be stored for 1–2 weeks at room temperature or in the refrigerator after dehydration by dipping in absolute ethanol for 5 min (Novotna et al. 2017; Mangalampalli et al. 2017; Barfod et al. 2020; OECD 2014, 2016c; Organisation for Economic Co-operation and Development 2002; Oliviero et al. 2019; Blakey and Douglas 1990; Hartmann et al. 2003; Olive et al. 2012; Kumaravel et al. 2009; Burlinson et al. 2007; Wiklund and Agurell 2003).

Mangalampalli et al. (2017) conducted an alkaline comet assay as part of genotoxicity assessment of MgO NPs in female albino Wistar rats following oral exposure. They have selected 6–8-weeks-old animals having a weight range of 120–140 g. The dose ranges for oral exposure have been selected based on acute oral toxicity-fixed dose method as per OECD 420 (Oliviero et al. 2019). The study had five groups, negative control administered with Milli Q water alone, low dose (100 mg of MgO NPs/kg body weight), medium dose (500 mg of MgO NPs/kg body weight), high dose (1000 mg of MgO NPs/kg body weight), and positive control or CP (Cyclophosphamide) group. All animals were sacrificed by cervical dislocation

at 24 and 72 h sampling following exposure. Whole blood collected from retro-orbital plexus in EDTA tubes and liver tissue were used for alkaline comet assay, in which increased tail intensity was noted in the highest concentration (Relier et al. 2017).

19.4.4.4 Analysis and Interpretation

Scoring comets can be done using automated or semi-automated image analysis software after staining with fluorochromes (e.g., SYBR Gold, Green I, Propidium iodide, ethidium bromide) at a suitable magnification of about 200 \times using a fluorescent microscope. The comets can be graded as “scorable” having different heads and tails separated from adjacent cells, “non-scorable,” and “hedgehogs.” A total of 150 scorable cells (from 2 or 3 slides) per animal (5 animals per group) should be scored. Non-scorable cells can be avoided, and “hedgehogs” have to be analyzed visually and separately noted. The negative control, positive controls, and test-treated groups should be scored separately. The percentage tail DNA or % tail intensity is determined for the interpretation of results and is defined as the percentage of tail DNA to total DNA content (head + tail) in the cell. “Hedgehogs,” clouds, or ghosts are damaged cells with small or indistinct heads and large spread-out tails, indicating severely damaged cells. The hedgehogs are difficult and unreliable to be assessed by the image analyzing software, and hence they are not involved in the final analysis (Mangalampalli et al. 2017; Bright et al. 2011; Lovell and Omori 2008; Ghosh et al. 2019; Perotti et al. 2015; Lewies et al. 2014; Georgieva et al. 2017; Gleit et al. 2009). In addition to DNA damage, excessive degree cytotoxicity of target tissues may also produce positive findings in the comet assay. Assessment of parameters related to cytotoxicity should be considered in genotoxicity studies, especially in cases with increased DNA migration. The median of percentage tail DNA is assessed from each slide, and from the median values, the mean for each animal is calculated. The mean of the individual animal determines the group mean. For a test to be acceptable negative and positive controls will produce results compatible with the historical data. The positive control must show a statistically significant difference compared to the negative control. Moreover, an appropriate number of cells and doses should be analyzed and scored (Mangalampalli et al. 2017; Azqueta and Dusinska 2015; OECD 2014; Georgieva et al. 2017; Gleit et al. 2009; Tice and Vasquez 1998; Fenech 2000). For proper interpretation, test results should be statistically compared with negative control results or historical negative control data (Azqueta and Dusinska 2015; OECD 2014, 2016c; Organisation for Economic Co-operation and Development 2002; Tice and Vasquez 1998).

19.5 Micronucleus Assay

The micronucleus assay is the most commonly used and highly sensitive genotoxicity test method for screening genotoxic agents or mutagens. It can be done *in vitro*/*in vivo* for reliable assessment of chromosome loss and chromosome or chromatid breakage induced by test chemicals.

19.5.1 In Vitro Mammalian Cell Micronucleus (MN) Assay

In vitro micronucleus assay is one of the commonly used genotoxicity tests to detect micronuclei (MN) in the cytoplasm of interphase cells. MN assay can detect gross chromosomal changes and is widely recognized as one of the widely accepted in vitro techniques for the genotoxic assessment of chemicals. MN may arise from the acentric chromosome (lacks a centromere) or chromatid fragments or whole chromosome, which lags in cell division, i.e., unable to move to poles during the anaphase. MN can be identified after DNA staining as single or multiple membrane-bound chromatins containing structures in the cytoplasm with no observable linkage to the cell's nucleus. They have similar morphology as interphase nuclei except for their small size and are therefore named "micronuclei." The micronucleus assay is a widely accepted test in nanogenotoxicology as it easily detects aneugenic (numerical chromosomal aberration) and clastogenic (structural chromosomal aberration) effects induced by the test material (Landsiedel et al. 2009; OECD 2016d).

Most of the published studies conducted to detect genotoxic effects of nanomaterials have adopted the testing principles specified by OECD 487 with modifications based on the physicochemical characteristics of the test nanomaterial. It had been demonstrated that high concentrations of silicon dioxide (SiO₂), titanium dioxide (TiO₂), Cerium oxide (CeO₂), Multiwalled carbon nanotubes (MWCNTs), silver, and gold nanoparticles might induce MN formation, indicating a positive genotoxic response. In the studies conducted so far, a wide variation in the selection of cell lines, time of NM exposure, use of cytochalasin along with NM to obtain binucleate cells, and the number of cells to be scored are observed (OECD 2016e; ISO/TR 10993-22:2017 2017; Elespuru et al. 2018; Li et al. 2012; Benameur et al. 2015; Muller et al. 2008; Kumar and Dhawan 2013).

In cytokinesis-block micronucleus assay (CBMN), using cultured mammalian cells, the addition of actin polymerization inhibitor cytochalasin B or cyt-B (3–6 µg/mL) restricted the scoring of MN frequency in once divided cells only, i.e., cells having binucleated appearance. As thousands of cells are scored per treatment, an MN assay is more reliable and reproducible than a chromosomal aberration assay. Hence, the MN may have whole chromosomes, and aneugenic effects induced by test materials can also be detected in MN assay, which is a challenging one in conventional chromosomal aberration assay (Dewangan et al. 2018; OECD 2016e; ISO/TR 10993-22:2017 2017; Elespuru et al. 2018; Li et al. 2012). Figure 19.4 represents polychromatic erythrocytes (PCE) with micronucleus from bone marrow cells of Swiss albino mice and binucleated cells on acridine orange staining.

19.5.1.1 General Principle

The test material treatment can be given with and without an exogenous source of metabolic activation (e.g., S9) depending on the cell type, for a sufficient time of exposure to actuate chromosome damage, resulting in the formation of micronuclei in the interphase cell. The scoring of MN should be done in the stained interphase cells that have completed nuclear division after the exposure of the test material. This can be ensured by selectively analyzing binucleated cells in CBMN by adding cyt-B,

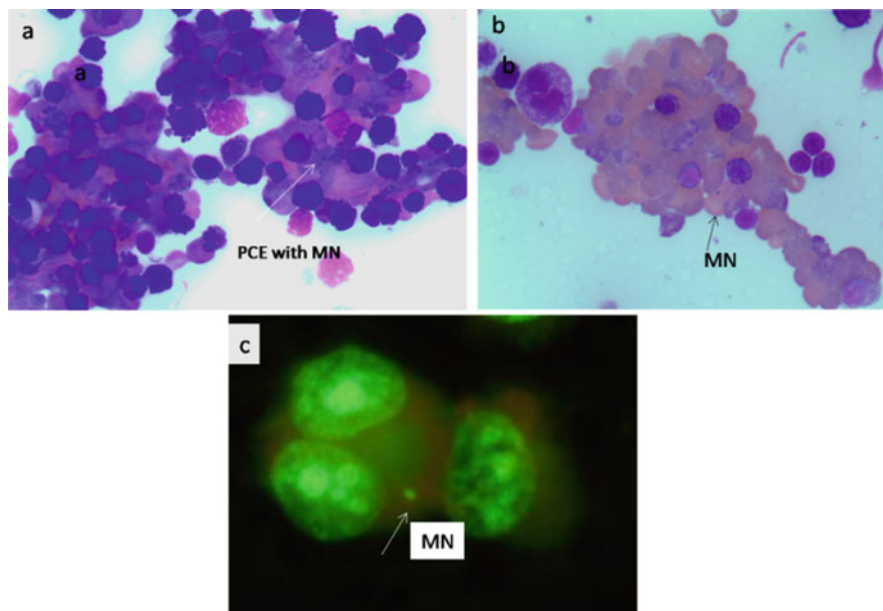


Fig. 19.4 Bone marrow cells of mice stained with May Grunwald-Giemsa showing PCE with micronucleus (a, b) and binucleated cells on acridine orange staining (c)

which inhibits cytokinesis by hindering microfilament ring assembly. In MN assays without cyt-B administration, the mononucleated cells selected for MN should go through at least one cell division after the test material administration. Cell proliferation in control and treated cells should be evaluated along with the cytotoxicity of treated cells (Dewangan et al. 2018; Maffei et al. 2014).

19.5.1.2 Experimental Design

The cells selected for studying MN frequency should have less background incidence of micronucleated cells. The incidence of MN in the negative control should be correlated with that of the historical negative control data. Human peripheral blood lymphocytes from healthy nonsmoking donors or Syrian hamster embryo cultures can be used. Cell line like CHO, V79, CHL/IU, and L5178/Y are also suggested by OECD. The peripheral blood collected from more than one donor should be documented, and blood from male and female donors is not advisable to be pooled. The cultures must be maintained using suitable cell culture media, and appropriate culturing conditions like the temperature of 37 °C and 5%CO₂ should be ensured. Cell lines should be devoid of mycoplasma contamination and with a stable modal chromosome number. The cell cycle length of cultures used for the test must be confirmed in the laboratory and correlated with the published data for the cell type (Zangeneh et al. 2019; Dewangan et al. 2018; OECD 2016e; ISO/TR 10993-22:2017 2017; Elespuru et al. 2018; Murgia et al. 2008; Moratin et al. 2018). The cell type can be selected based on the expected route of human exposure and the

physicochemical characteristics of the test NM. Several NM genotoxicity studies using other cell lines like TK6 lymphoblastoid cells, human bronchial epithelial cells (BEAS-2B), normal human dermal fibroblasts (NHDF), and human promyelocytic leukemia cells (HL-60) have been published so far (Abudayyak et al. 2017a; Montazeri et al. 2018; Cappellini et al. 2018).

The seeding density of the cell lines used should be appropriate. The cells are ensured to be maintained in the exponential growth phase from the start of treatment until harvest to expose the test nanoparticle to different stages of the cell cycle. Heparinized whole blood or isolated lymphocytes was added with mitogen, e.g., phytohemagglutinin (PHA), to stimulate cell division before administering test material. If the cells in the test system have inadequate metabolizing capacity, an exogenous source of metabolic activation system should be used. Post mitochondrial fraction (S9, 1–2% v/v) supplemented with co-factor prepared from the liver of rodents especially rats by treating with enzyme-activating (e.g., Aroclor 1254 or a blend of phenobarbital and β -naphthoflavone) (Montazeri et al. 2018; Cappellini et al. 2018; OECD 2016e; ISO/TR 10993-22:2017 2017; Elespuru et al. 2018; Raja et al. 2020).

NP doses should be freshly prepared before administration for ensuring the stability of the test material. Solid particles are to be diluted in suitable solvents, and liquids may be dosed directly before the treatment of cells. Solvents selected should be compatible with the test system, and aqueous solvents (<10% v/v in the final treatment media) are preferable. In order to confirm that cells scored must go through mitosis after test NP exposure or postexposure incubation, the use of CytoB may be considered. CytoB blocks cytokinesis by inhibiting actin assembly, which results in the formation of binucleated cells (Landsiedel et al. 2009; OECD 2016e; ISO/TR 10993-22:2017 2017; Elespuru et al. 2018; Li et al. 2012; Ng et al. 2010). The commonly selected concentration of CytoB is 3–6 $\mu\text{g}/\text{mL}$ and must be optimized as per cells used. CytoB can interfere with actin filaments and may affect the uptake of certain types of NM. In these cases, co-exposure of cytoB with test NM may be avoided; instead, posttreatment or delayed co-treatment can be followed. After NM exposure, the media is removed, and, subsequently, cytoB is added to obtained binucleate cells, i.e., cytoB is added during the posttreatment period. In delayed co-treatment, NM exposure may be given for 6–24 h, and after that, cytoB is added for the rest of the exposure period. OECD recommends an exposure time of 1.5–2 normal cell cycle length for long-term treatment, most of the studies that have been conducted to assess the genotoxic potential of NM provide 24 h treatment for long-term exposure, and this seems to be sufficient as 24 h exposure can allow the cells to pass through one cell cycle in the presence of test NM (Wallin et al. 2017; Landsiedel et al. 2009; OECD 2016e; ISO/TR 10993-22:2017 2017; Elespuru et al. 2018; Fenech 2020).

CBMN assay can be elaborated as a multipoint cytogenetic technique capable of evaluating chromosomal instability, cytostatic, and cytotoxicity; hence, can be regarded as CBMN cytome assay. Nucleoplasmic bridges (NPBs) that might have resulted from telomeric end-fusions, failure to repair DNA breaks, or incomplete chromatid separation can be very well assessed by inhibiting cytokinesis from

obtaining binucleated cells by adding cytoB. Nuclear buds (NBUDs) formed during the extrusion of amplified genes, and excess DNA repair complexes can also be detected. Quantitative analysis of MNi, NPBs, and NBUDs, considered potent biomarkers of genotoxic events, provides chromosomal instability induced by test material. Relative frequencies of mononucleated cells, binucleated cells, and multinucleated cells indicate cell proliferation and cytostasis. Detection of cytotoxicity by assessing apoptosis and necrosis helps quantify dead cells and type of cell death (Li et al. 2017).

In in vitro MN, the highest dose of NM should not cause severe cytotoxicity, precipitation in the media, or change in pH. All these changes may result in a false interpretation of results. If test material exposure causes any change in pH, it is advised to adjust the pH in the final media and should be documented. In studies in which CytoB is not used, cell proliferation has to be assessed by cell counts, population doubling time, and measuring cytotoxicity. Here RPD (Relative Population Doubling) or RICC (Relative Increase in Cell Count) must be evaluated to ensure that cells scored have gone through cell division with or after treatment. In studies involving the use of CytoB, cytostasis is determined by measuring CBPI (Cytokinesis-Block Proliferation Index) or RI (Replication Index) (Arslan and Akbaba 2020; Wallin et al. 2017; OECD 2016e; ISO/TR 10993-22:2017 2017; Elespuru et al. 2018; Li et al. 2012; Fenech 2020; Heshmati et al. 2019). The serum concentration of the media may enhance or reduce NM uptake depending on the physicochemical properties and peculiarities of the cell type used. So, it is recommended to conduct genotoxicity studies with and without serum content in the media, and the difference in the outcome has to be noted (Landsiedel et al. 2009; OECD 2016e).

The dose range should cover a minimum of three analyzable concentrations if the test is shown to produce cytotoxicity including, the highest with 50–70% cytotoxicity, a moderate degree of cytotoxicity, and without cytotoxicity/cytostasis. For the test material, which are non-cytotoxic the maximum dose recommended is 0.01 M, 5 mg/mL, or 5 μ L/mL (Arslan and Akbaba 2020; OECD 2016e; ISO/TR 10993-22:2017 2017; Elespuru et al. 2018; Li et al. 2012; Fenech 2020; Heshmati et al. 2019).

It is essential to keep both positive and negative controls to interpret the study results accurately. Negative controls, including solvents/vehicles alone in treatment media, should be included along with every test. CdSO₄ and the use of other non-genotoxic compounds at non-cytotoxic concentrations had been used in several studies. Positive control selected should produce the reproducible and analyzable level of micronucleus at the selected dose level. No aneugens requiring metabolic activation have been reported yet. Clastogens not requiring metabolic activation as recommended by OECD are Methyl methane sulfonate, Mitomycin C, 4-Nitroquinolone-*N*-Oxide, and Cytosine arabinoside. Benzo(a)pyrene and cyclophosphamide do not require metabolic activation. Colchicine and vinblastine are commonly used aneugens (Li et al. 2017). Adequate exposure to ionizing radiations like X-rays induces MN formation and hence can be taken as a positive control (Wallin et al. 2017).

19.5.1.3 Experimental Procedure

The exposure regime can be short term or long term as recommended by OECD 487 is summarized below:

1. In the presence of cytoB, the treatment may be given as mentioned below:
 - (a) Short-term treatment with the addition of an external source of metabolic activation (e.g., S9)
Cell cultures are exposed to test material for 3–6 h with S9.
S9 and treatment media are removed, and fresh media having cytoB are added.
A sampling at 1.5–2.0 normal cell cycle length after the initiation of treatment.
 - (b) Short-term treatment without the addition of an external source of metabolic activation
Cell cultures are exposed to test material for 3–6 h with S9.
Treatment media are removed, and fresh media with cytoB is added.
Sampling was done at 1.5–2 normal cell cycle length at the initiation of the treatment.
 - (c) Long term without metabolic activation
Cell cultures are exposed to test material for 1.5–2 normal cell lengths with cytoB.
Sampling was done after the treatment period.
2. In the absence of cytoB
Cell cultures are exposed continuously with test material y without adding cytoB and S9 for 1.5–2 normal cell cycle length, and sampling is done at the end of the treatment period.
For tests and controls, duplicate cultures should be kept. The treatment schedule and inclusion of cytoB can be selected based on the physicochemical characteristics of test nanoparticles (Fig. 19.5).

19.5.1.4 Analysis and Interpretation of In Vitro Micronucleus Assay

Cells are harvested from each culture separately, and slides are prepared adequately. Cells should remain intact with cell membrane and cytoplasm, which enables easy recognition of micronuclei and binucleate cells in cytokinesis-block assays. The slides can be stained with Giemsa or fluorescent DNA-specific dyes (e.g., acridine orange). The FISH technique using pancentrometric DNA probes and DNA counterstaining can be included to determine the origin of micronuclei (Efthimiou et al. 2020; Arslan and Akbaba 2020; Heshmati et al. 2019; Wilde et al. 2017). In cytoB-treated cultures, micronuclei have to be scored from at least 2000 binucleate cells per concentration of test, and control should be counted. Binucleated cells with irregular shapes, multinucleated cells which are not well separated, cells with more than two main nuclei, or cells with main nuclei having major size differences should not be included while scoring. In cases of test material that is known to interfere with the action of cytoB, the scoring of mononucleated cells is recommended. In assays not using cytoB, micronuclei have to be scored in 2000 cells per concentration of test

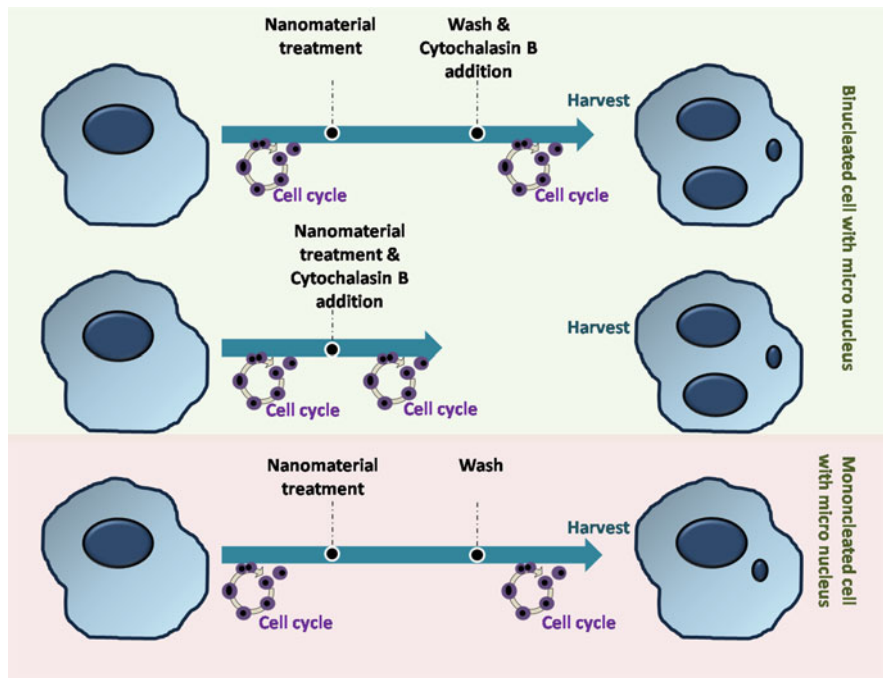


Fig. 19.5 Procedure for Micronucleus assay on treatment with nanomaterial treatment

and controls. The scoring can be done manually or using automated techniques (e.g., flow cytometry, laser scanning cytometry, and image analysis software).

Along with the quantification of micronuclei relative increase in cell counts (RICC) or relative population doubling (RPD), cytokinesis-block proliferation index (CBPI) should be detected for assessing cell proliferation. The test should be repeated if less than 1000 cells (1000 binucleated cells in case of cytoB-treated cultures) per concentration are only obtained with more cells or less cytotoxic concentration. The outcome of negative and positive control of the assay should be correlated with the historical control database for negative and positive control, respectively (Efthimiou et al. 2020; Vuković et al. 2020; Arslan and Akbaba 2020; Heshmati et al. 2019; Wilde et al. 2017; Di Bucchianico et al. 2014).

Positive control results should exhibit a statistically significant increase compared to the negative control. Test results have to be compared with negative control data for accurate interpretation of the results (OECD 2016e; Fenech 2020; Heshmati et al. 2019; Wilde et al. 2017; Di Bucchianico et al. 2014). The addition of kinetochore or centromeric staining in the *in vitro* MN assay allows differentiating between aneugenic and clastogenic events resulting in micronuclei formation, which gives an idea about the mechanism of nanomaterial-induced DNA damage (Landsiedel et al. 2009; OECD 2016e).

Genotoxicity of nickel (II) oxide NPs by *in vitro* MN assay using human peripheral lymphocytes had reported by Dumala et al. (2019). Peripheral blood was collected in EDTA tubes from healthy, nonsmoking male volunteers aged 25–30 years. Lymphocytes were isolated by centrifugation with Histopaque 1087, followed by the addition of RBC lysis buffer. RPMI 1640, having 10% FBS and 1% AB/AM, was used for blood culture. NiO NPs exposure had been given for 6, 12, and 18 h. Subsequently, cytoB (3 $\mu\text{g}/\text{mL}$) was added to prevent cytoplasmic division. The cells were harvested, slide prepared, and stained with 10% giemsa, and micronucleated binuclear cells were scored. A dose- and time-dependent increase in MN incidence suggestive of clastogenic events were noted in the study (Efthimiou et al. 2020).

Masoumeh Heshmati et al. (2019) conducted a genotoxicity evaluation of Ag NPs in the Chinese hamster ovary (CHO-K1) cell line. The medium used was RPMI 1640, containing 10% serum. The maximum dose used for CBMN produces approximately 80% cytotoxicity. Long-term treatment of NPs (24 h) with cytoB (3 $\mu\text{g}/\text{mL}$) was given. Ag NPs induced significantly increased MN frequency in some of the test concentrations (Wilde et al. 2017).

Siivola et al. (2020) had done a cytokinesis-block micronucleus assay (CBMN) as part of the genotoxic assessment of CuO NPs and reported a dose-dependent increase in MN frequency. Transformed human bronchial epithelial cells (BEAS-2B) cultured in BEGM bronchial epithelial cell growth media at 37 °C and 5% CO₂ had been used for the assay. The maximum dose selected for genotoxicity studies produced $55 \pm 5\%$ cytotoxicity. The CuO NPs were dispersed in BEGM bronchial epithelial cell growth media with 0.6 mg/mL BSA (Bovine Serum Albumin). After 6 h of NP treatment, cytochalasin B was added to block cytokinesis. The cells were harvested, processed, and stained using acridine orange (32 $\mu\text{g}/\text{mL}$) and DAPI (5 $\mu\text{g}/\text{mL}$). Mitomycin C (150 ng/mL) was used as a positive control. Cytokinesis-Block Proliferation Index (CBPI) and % cytostasis were also assessed (Vuković et al. 2020).

Au NPs (5 and 15 nm) show a statistically significant increase in MN frequency compared to control in CBMN assay conducted in Raw2647 and human peripheral blood lymphocytes after an exposure of 48 h. However, a negative response was obtained in CBMN using CHO cells treated with 14 nm Au NPs. Au NPs (5 or 50 nm) also did not induce MN formation in any test concentration in the study using human bronchial epithelial cells (Lebedová et al. 2018; Wang et al. 2020; Di Virgilio et al. 2010; Hovhannisyan 2010). A genotoxicity study of TiO₂ NPs (21 nm) was done by Kazimirova et al. (2019) using TK6 cells. TiO₂ NPs at a concentration of 3, 15, and 75 $\mu\text{g}/\text{cm}^2$ are exposed to two sets of TK6 cells cultured in RPMI 1640 supplemented with L glutamine and 10% FBS for two-time points 4 and 24 h. Subsequently, cytochalasin B (6 $\mu\text{g}/\text{mL}$) was added and incubated for 24 h to obtain a total exposure period of 28 and 48 h, respectively. Mitomycin C (0.05 $\mu\text{g}/\text{mL}$) and cells without any treatment served as positive and negative control, respectively. Slides were prepared, and the incidence of MN in binucleated cells was analyzed. TiO₂ did not exhibit a statistically significant difference in MN compared to the control at any of the tested concentrations (Zangeneh et al. 2019). Di Virgilio et al.

(2010) reported CBMN assay as part of the genotoxic assessment of TiO₂ NPs. The study was done in CHO-K1 cells cultured in a Ham F10 culture medium. TiO₂, 0.5, 1.5, 10 µg/mL were exposed to 24 h along with cytoB (4.5 µg/mL). A statistically significant increase in MN frequency compared to negative control was reported in the study (Wiklund and Agurell 2003). These controversial results obtained for the same material in different studies might have been due to different cell lines used. Hence, it is recommended to do the genotoxic assays with at least two cell lines in parallel (OECD 2016f).

19.5.2 In Vivo MN Assay

Mammalian erythrocyte micronucleus assay has been used to evaluate micronucleus formation resulting from chromosome or chromatid damage induced by a test material in mitotic apparatus of mammalian erythroblast, especially of rodents. Micronucleus may contain lagging chromosome fragments or entire chromosome, which lags in cell division, and the increased frequency of immature erythrocyte or polychromatic erythrocyte or reticulocyte in the test material-treated animals signifies structural or numerical chromosome aberrations induced by test chemical. Micronucleated immature erythrocytes can be scored accurately from bone marrow samples of young adult rodents. However, mammalian peripheral blood samples may also be considered for analysis (Hadrup et al. 2021; Mahjoubian et al. 2021).

Test material, negative and positive control treatments were given to animals for an adequate exposure time, and animals were humanely euthanized. Bone marrow is harvested, processed, stained, and examined for the presence of immature erythrocyte or polychromatic erythrocyte, either visually by microscopic examination or by automated techniques like flow cytometry, image analysis, or laser scanning cytometry. Peripheral blood samples can also be analyzed for the presence of micronucleated immature erythrocytes or reticulocytes (Hadrup et al. 2021).

19.5.2.1 Experimental Design and General Requirements

The historical control database generated by the laboratories should be agreeing with the published control range and distribution for selected controls. As per OECD 474, healthy rodents of 6–10 weeks of age can be considered for the study. The use of other species is allowed with proper scientific and ethical justification. The selected animals can be caged as small groups of the same sex inappropriate temperature of 22 ± 3 °C, relative humidity of 50–60%, and 12-h alternate light/dark cycles. Animals should be provided with an adequate supply of drinking water and conventional laboratory feeds. Randomly selected animals should be acclimatized to the laboratory for a minimum of 5 days. Kim et al. (2019) reported DNA damage induced by citrate-coated Ag NPs in rabbit liver tissue following intravenous administration. Several studies regarding genotoxicity of metal and metal oxide NMs have been reported in zebrafish (*Danio rerio*), Guppy (*Poecilia reticulata*), and *Drosophila melanogaster* in relation to consequences following environmental exposure of NMs (Wallin et al. 2017; Barfod et al. 2020; Hadrup

et al. 2021; Fatima and Ahmad 2019; Mahjoubian et al. 2021; de Souza Trigueiro et al. 2021; Turner et al. 2011).

Three test dose groups, positive, and negative control groups, each with at least five analyzable animals of single sex or of either sex (for studies involving both sexes), should be included in the assay. The maximum tolerated dose (MTD), i.e., the dose, which can withstand the animals without producing death or severe signs of toxicity requiring euthanasia, has to be determined by a preliminary range-finding study carried out in the same laboratory using the same species of animal. In case of studies requiring administration of 14 days or more, the maximum recommended dose is 1000 mg/kg body weight/day, and for studies requiring less than 14 days of administration, a maximum dose of 2000 mg/kg body weight/day can be considered. The dose range selected should produce maximum to mild or no toxicity. The dose-finding study should be conducted using the same animal strain in the same laboratory conducting the final experiment (Mahjoubian et al. 2021; Giubilato et al. 2020; Hayashi et al. 2000; Hayashi 2016).

The route of administration can be oral, topical, subcutaneous, intravenous, intraperitoneal, inhalation, or via implantation, and should be selected based on the expected exposure route of the test nanomaterial. The treatment can be given as two or more regimens at 24 h intervals. However, split doses of two or more treatments at 2–3 h intervals can also be used for administering large volumes. As suggested by OECD, the bone marrow samples can be collected at two time periods, the first one not before 24 h after administration and the second one after a specific time interval but not beyond 48 h after administration. In the case of peripheral blood collection, samples can be taken from the same group at two time periods, the first sample not before 36 h after treatment and the second after a specific time interval but not beyond 72 h after administration (Mahjoubian et al. 2021; Hayashi et al. 2000; Hayashi 2016).

For studies using two daily treatments at 24 h intervals, bone marrow samples can be collected at 18–24 h after the final treatment, and peripheral blood can be collected at 36–48 h after treatment. These harvest times have been optimized based on the appearance and disappearance of micronuclei in the target sites. In the case of studies utilizing three or more daily treatments at 24 h intervals, sampling of bone marrow should be done not beyond 24 h after the final treatment, and peripheral blood sampling should be done before 40 h after final treatment (Mahjoubian et al. 2021; Hayashi 2016).

Solvents/vehicles chosen should be compatible with the test system without inducing any adverse chemical reactions affecting the test. In the case of inhalation toxicity studies, the test material exposure can be given as gas, vapor, or solid-liquid aerosol. The use of aqueous solvents like water, physiological saline, methylcellulose solution, carboxymethyl cellulose sodium salt solution, corn oil, or olive oil should be preferred. Positive control groups administered with a substance capable of producing a detectable increase in micronuclei like ethyl methanesulfonate, methyl methanesulfonate, ethyl nitrosourea, mitomycin C, cyclophosphamide, triethylenemelamine, or colchicine have to be incorporated in each assay. Negative

control groups treated with solvents/vehicles alone without test materials should be kept with each assay (OECD 2016f; Mahjoubian et al. 2021).

19.5.2.2 Analysis and Interpretation of In Vivo Micronucleus Assay

Clinical signs and changes in the body weight of all animals should be recorded. Plasma levels of administered test chemicals can be done at appropriate intervals for ensuring bone marrow exposure to test chemicals. Peripheral blood can be collected from animals from the tail vein or other appropriate blood vessels as per animal ethical requirements. Bone marrow samples can be collected from the tibia or femur of animals following humane sacrifice. The blood or bone marrow preparations are made, either supravitaly stained or prepared smears are stained with specific dyes (e.g., Giemsa) for manual scoring by microscope or processed for flow cytometric analysis (Zangeneh et al. 2019; Mahjoubian et al. 2021; Giubilato et al. 2020; Hayashi et al. 2000; Hayashi 2016).

Differentiation of clastogenic and aneugenic events, i.e., whether the origin of micronuclei is from chromosome/chromosomal fragments, can be determined by specific methods using antikinetochore antibodies or FISH or in situ hybridization using pancentromeric probes (Wallin et al. 2017; Fenech 2020; Hovhannisyan 2010; OECD 2016f; Mahjoubian et al. 2021). As per OECD 474 revised in 2016, 4000 immature erythrocytes have been scored for the presence of micronuclei. The ratio of immature to total (immature + mature) erythrocytes per animal must be done from 500 erythrocytes for bone marrow and 2000 erythrocytes for peripheral blood (Mahjoubian et al. 2021).

The negative and positive control data obtained should be compatible with the historical control database. The test material can be considered distinctly positive if either test dose shows a significant increase in micronucleated immature erythrocytes on statistical comparison with negative control or a dose-dependent increase is obtained by a suitable trend test or any tested dose tested is found outside the historical negative control database (Mahjoubian et al. 2021; Giubilato et al. 2020; Hayashi et al. 2000; Hayashi 2016).

ZnO-NPs-induced genotoxic changes were assessed by Ghosh et al. (2016) using in vivo comet assay (OECD 489), chromosomal aberration (OECD 475), and micronucleus assay (OECD 474) in male Swiss albino mice. The study group included: Animals treated with ZnO-NPs at three different concentrations 25, 50, and 100 mg of ZnO-NPs/kg body weight, vehicle (sterile filtered PBS), and positive control (MMC). The test and control treatments were given at 0, 24, and 45 h. The animals were sacrificed by cervical dislocation 3 h after the final treatment, followed by a collection of bone cells from femur bone, processed, and stained using May-Gruenwald/Giemsa. Percentage of polychromatic cells (% PCE), frequency of micronucleated-PCE (MN-PCE), and % MN-PCE were calculated for each animal and statistically compared with the vehicle control. A statistically significant increase was noted compared to the control in all concentrations of ZnO tested (Rubio et al. 2016).

Female Wistar rats were used for studying the genotoxic effects of magnesium oxide nanoparticles (MgO NPs) by Mangalampalli et al. (2017). The genotoxic

assessment was done using the *in vivo* comet assay, chromosomal aberration, and micronucleus assay after acute exposure of MgO NPs (low dose—100 mg/kg body weight, medium dose—500 mg/kg body weight, and high dose—1000 mg/kg body weight), control (MilliQ water) and positive control (cyclophosphamide) dose was fixed by an initial range-finding study as per OECD 420. Bone marrow cells were collected after the humane sacrifice of the animals after 24 and 72 h oral exposure. A significant increase in micronucleated bone marrow cells was noted compared to the negative control (Relier et al. 2017).

Repeated oral toxicity (28 days) study was conducted for the toxicological assessment of tungsten oxide nanoparticles (WO₃ NPs) in Wistar rats by Chinde and Grover (2017). The animals were divided into five groups—three test groups (low dose, medium dose, and high dose), one control, and CP group; each group had ten animals (five males and five females). All the animals were sacrificed humanely 24 h after the last exposure. CP group was injected with 40 mg/kg body weight intraperitoneally 24 h before sacrifice. The dose, which showed signs of toxic effects without severe distress, was fixed as the highest dose of WO₃ NPs. The highest dose administered showed a significant increase in MN frequency compared to the control (Hadrup et al. 2019).

Harmonizing with 3R (Replacement, Reduction, and Refinement) principle as part of animal welfare requirements combination of *in vivo* micronucleus assay with comet assay or conducting micronucleus assay as a part of other toxicological assessments like acute toxicity studies or repeated-dose toxicity studies can be considered (Ema et al. 2013).

19.6 Chromosomal Aberration Assay

Chromosomal aberration assay detects structural aberrations of chromosomes induced by test material in mammalian cells and is one of the commonly used assays for assessing genotoxicity induced by engineered nanomaterials. Several studies have been conducted for analyzing the genotoxicity of C60 fullerene, multiwalled carbon nanotubes (MWCNTs), Ag, Au, and TiO₂ nanomaterials by chromosomal aberration assay. It has been reported that Ag NPs induce significant chromosomal aberrations in human mesenchymal stem cells at a concentration of 0.1 µg/mL. Genotoxic effects have also been reported for Au NPs, SWCNTs, and Ni NPs. Most of the published studies adopted the testing strategies signified by OECD guidelines for testing chemicals to conduct genotoxicity testing of nanomaterials. OECD 473 specifies criteria to detect genotoxicity of test materials by *in vitro* chromosomal aberration assay. ISO/TR 10993-22:2017 includes guidance on genotoxicity testing of biomedical devices, which may have nanomaterial components and are expected to liberate nanosized wear particles in the biological system (Kim et al. 2019; OECD 2016e; ISO/TR 10993-22:2017 2017; Tian et al. 2020). The procedure followed for the chromosomal aberration assay is represented in Fig. 19.6.

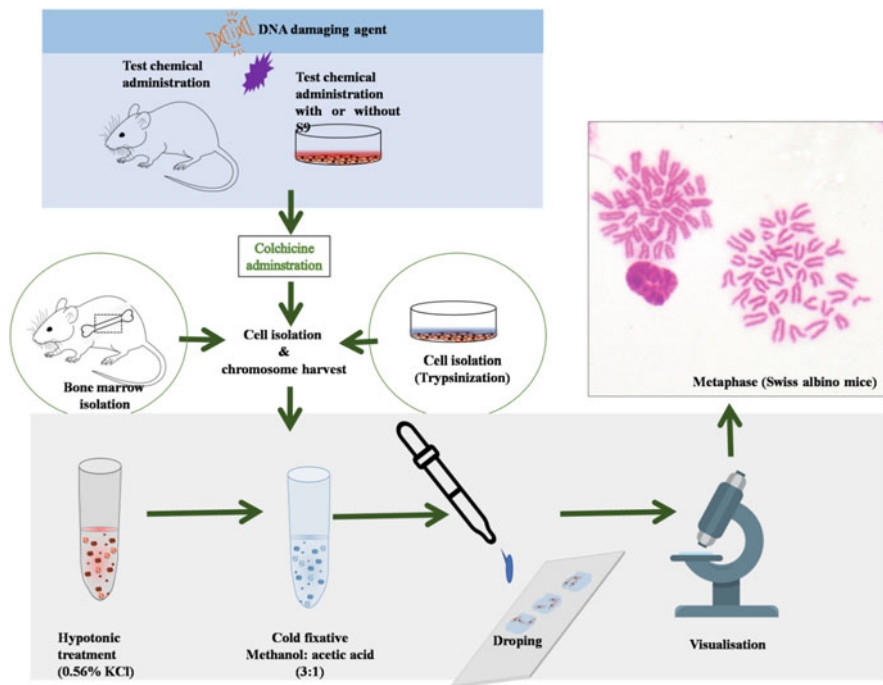


Fig. 19.6 Work procedure for performing chromosomal aberration assay

19.6.1 In Vitro Chromosomal Aberration Test

In vitro chromosomal aberration test detects structural chromatid or chromosomal aberration in cells treated with test chemical. Established cell lines or primary cultures of human or rodent origin can be selected for the assay (OECD 2016; ISO/TR 10993-22:2017 2017). Clastogenic events are best demonstrated in the metaphase stage of mitosis. The use of a metabolic activation system (e.g., S9) can be considered in the case of assays using cells that are not metabolically competent with the test material. Test materials are exposed to cells in the presence and absence of a metabolic activator (e.g., S9) for a sufficient period, followed by arresting the cells at cell metaphase by adding colcemid or colchicine (metaphase-arresting agent). Chromosomes are harvested, processed, stained using chromatin-specific dyes, and microscopically analyzed for the presence of structural aberrations in chromosomes or chromatids (ISO/TR 10993-22:2017 2017; Miller et al. 1997).

19.6.1.1 Selection and Preparation of Sample

Preferably, cell lines like Chinese Hamster Ovary (CHO) cells, Chinese Hamster Lung (CHL/IU), V79, TK6, or primary cells of human or other mammalian origin and peripheral blood lymphocytes, are used for in vitro chromosomal aberration test. Peripheral blood lymphocytes should be collected from young, healthy, nonsmoking

individuals who were not recently exposed to genotoxic chemicals or ionizing radiations. The cells must be maintained in the exponential phase of growth until the time of harvest for exposing the test material to various cell cycle stages, which ensures the reliability of the assay. Cell lines or primary culture must be sustained in suitable cell culture media at adequate conditions (e.g., 37 °C and 5% CO₂). The normal cell cycle length of the selected cells evaluated in the laboratory should be agreed with published data. Cell lines should have a consistent modal chromosome number and be devoid of mycoplasma contamination (ISO/TR 10993-22:2017 2017; Kanda et al. 1994).

Whole blood (anticoagulated by heparin) or separated lymphocytes stimulated by mitogen like phytohemagglutinin can be used for primary culture. For assays using cell lines with inadequate endogenous metabolizing capacity, an external source of metabolic activation system like post mitochondrial fraction isolated from the liver of rodents supplemented with cofactors (S9) is commonly used at a final concentration of 1–2% (v/v) or a maximum of 10% (v/v) (Mangalampalli et al. 2017; Kimoto et al. 2016; Olsen et al. 2017; Zhu et al. 2020). All doses should be freshly prepared. Solvents used should be compatible with the test system and do not induce any adverse reaction. Preferably, aqueous solvent (e.g., saline or water) or culture media must be used. Aqueous solvents at a concentration of less than 10% and organic solvents at a concentration of less than 1% in the final treatment media are recommended (Kim et al. 2019; ISO/TR 10993-22:2017 2017; Tian et al. 2020; Miller et al. 1997).

The highest concentration to be tested for genotoxicity should be decided based on cell proliferation and cytotoxicity. The test concentration, which causes marked cytotoxicity, should be eliminated. Relative Population Doubling (RPD) or Relative Increase in Cell Count (RICC) for cell lines and Mitotic Index (MI) for primary cultures for lymphocytes are recommended for assessing cytotoxicity. A minimum of three analyzable concentrations ranging from highest showing $55 \pm 5\%$ cytotoxicity to moderate and no cytotoxicity should be included. Concurrent positive and negative controls must be incorporated into the assay. If the test material is found to be non-cytotoxic, the highest concentration recommended by OECD is 10 mM, 2 mg/mL, or 2 μ L/mL, and the three analyzable concentrations of two- to threefold difference are preferable (Kim et al. 2019; ISO/TR 10993-22:2017 2017; Tian et al. 2020; Miller et al. 1997).

Negative control, ideally solvent alone without treatment processed in the same manner as the test, should be included in the assay. Cells alone without any treatment are preferred as a negative control in most published studies. Positive controls which needed S9 like benzo(a)pyrene, cyclophosphamide, and those not needed S9 like methyl methane sulfonate, mitomycin C, 4-nitroquinolone-*N*-oxide, and cytosine arabinoside are commonly preferred for the assay (ISO/TR 10993-22:2017 2017; Tian et al. 2020; Kanda et al. 1994). To ensure reliability, short-term treatment with and without S9 and long-term treatment without S9 must be done. Short-term treatment involves exposing test material to cultures at the exponential growth phase with and without S9 for a period of 3–6 h, removing the treatment media, replacing it with fresh media, and harvest after 1.5 normal cell cycle length.

Long-term treatment involves exposing test material continuously for a period of 1.5 normal cell cycle lengths to cells at the exponential phase, followed by chromosome harvesting (ISO/TR 10993-22:2017 2017; Miller et al. 1997).

19.6.1.2 Chromosome Harvest and Analysis

Metaphase-arresting agents, colchicine or colcemid at a concentration of about 0.1–0.2 µg/mL, must be added 1–3 h before chromosome harvesting. The tests and control cultures should be processed separately, and the steps are hypotonic treatment (with 0.56% or 0.075 M KCl), fixation (ideally freshly prepared ice-cold methanol:acetic acid 3:1), and staining with 4–5% Giemsa in Sorensen's buffer for 5 min or DNA-specific fluorescent dyes (Demir et al. 2020; ISO/TR 10993-22:2017 2017; Kanda et al. 1994; Patlolla et al. 2012).

Tests and control slides should be labeled properly and independently analyzed for the presence of chromosome/chromatid aberrations. For an appropriate evaluation, a minimum of 300 well-spread metaphases with modal chromosome number \pm two should be scored for each concentration of test and control. Chromatid and chromosome aberrations, including gaps, breaks, and exchanges, should be noted separately. Each laboratory should set an unhistorical control database for the positive and negative control, which should be compatible with the published data for the same material. The results of each test concentration are statistically compared with that of the negative control value and if a statistically significant increase is observed in any test concentration compared to negative control or the observed increase is dose-dependent, or the results of the test are beyond historical negative control range and distribution, the test can be considered as positive or potentially genotoxic, as per OECD 475 (Lian et al. 2017; Cappellini et al. 2018; Demir et al. 2020; ISO/TR 10993-22:2017 2017; Tian et al. 2020; Miller et al. 1997; Kanda et al. 1994; Patlolla et al. 2012; Al-Ahmadi 2019; Mrđanović et al. 2009; OECD 2016g).

Arslan and Akbaba (2020) conducted *in vitro* chromosomal aberration test as part of the genotoxic assessment of cerium (IV) oxide NPs (CONPs) using human peripheral blood lymphocytes. They have used blood samples collected from healthy nonsmoking male volunteers who have no systemic or genetic disease. Distilled water and mitomycin C were selected as negative and positive controls, respectively. After 70 h and 15 min of incubation, colcemid was added and incubated for a further 1 h and 45 min to arrest cells at metaphase. Following centrifugation (78 g for 10 min), hypotonic treatment was given by adding 0.075 M KCl drop by drop. After 15–20 min of incubation at 37 °C, tubes were centrifuged, the supernatant removed, and cold fixative solution (methanol:acetic acid 3:1 v/v) was added drop by drop, centrifuged, and the supernatant removed. This step was repeated twice. The cell suspension was dropped onto cold slides, and slides were air-dried and stained with Giemsa for 15 min. CONPs induce a statistically significant level of chromosomal aberrations in all the concentrations of CONPs tested (Demir et al. 2020).

Genotoxicity studies of nickel nanoparticles (Ni NPS) and nickel oxide nanoparticles (NiO NPs) were done by Di Bucchianico et al. (2018). They have conducted CBMN assay (OECD 487), chromosomal aberration assay (OECD 473), and comet assay for genotoxic evaluation of Ni NPs and NiO NPs. Bronchial

epithelial cell line (BEAS-2B) cultured in the epithelial cell growth medium was used in the study. The dose range was selected based on cytotoxicity data, and non-cytotoxic or concentration showing a maximum of 30% cytotoxicity was used for the assay. The appropriate density of BEAS-2B cells was seeded in a 6-well plate, and incubated for 24 h. Dispersions of NPs were added directly to obtain a final concentration of 5 μg of Ni per mL and incubated further for 48 h. Cells without any treatment and MMC at a concentration of 0.05 $\mu\text{g}/\text{mL}$ served as positive and negative control, respectively. Metaphase-arresting agent demecolcine (0.05 $\mu\text{g}/\text{mL}$) was added 3 h prior to harvesting. After hypotonic treatment, they were using 0.075 M KCl and three times washing with cold fixative (methanol:acetic acid, 3:1). The cell suspension was kept at $-20\text{ }^{\circ}\text{C}$ overnight. The cell suspension was dropped onto cold slides, air-dried, and stained using 4% (v/v) Giemsa solution in Sorensen's buffer pH 7 for 6 min. Microscopic analysis of stained slides revealed that Ni NPs induce chromatid-type aberrations, inter- and intra-arm exchanges, dicentric chromosomes, and endo-reduplications. However, the aberrations produced by NiO NPs were shown to be chromosome breaks and acentric fragments (Cappellini et al. 2018).

19.6.2 In Vivo Chromosomal Aberration Test

The mammalian chromosomal aberration test evaluates structural chromosome or chromatid aberration induced by test material in the bone marrow cells of animals, especially rodents. Generally, auegenic events cannot be detected by chromosomal aberration assays and require *in vivo* or *in vitro* micronucleus assays. Animal groups are treated with test material, negative and positive controls via a suitable route for a specific time of exposure, subsequently injected with metaphase-arresting substance (e.g., colchicine or colcemid) 1–3 h prior to sacrifice, animals are humanely euthanized, bone marrow cells are harvested, processed, stained, and cells at metaphase stage of mitosis are analyzed for the evidence of chromosome or chromatid type of structural aberrations. As part of proficiency testing, each laboratory should establish its historical control database compatible with the published data for negative and positive controls (Rubio et al. 2016; Relier et al. 2017; Hadrup et al. 2019; Hayashi 2016; Shinohara et al. 2009; Liu et al. 2014).

19.6.2.1 Experimental Design and Sample Preparation

Healthy, young adult animals of 6–10 weeks of age and adequate weight, commonly rodents (rats and mice), are preferred for the study. The use of other species may be allowed with proper scientific and ethical justification. Animals should be kept in small groups of the same sex with optimum housing conditions like a temperature of $22 \pm 3\text{ }^{\circ}\text{C}$, 50–60% humidity, alternate 12 h dark/light cycles, and adequate fresh air changes. Animals must be supplied with common laboratory feed for the species and adequate drinking water. The selection of test and control animals shall be random, and each animal should be identified by proper labeling (Rubio et al. 2016; Relier et al. 2017; Hadrup et al. 2019; Hayashi 2016; Zhang et al. 2015). Solid test materials

are diluted to appropriate concentrations using suitable solvent/vehicles before administration. Liquid test materials can be directly administered or diluted accordingly prior to administration. For the oral route of exposure, the materials can be dosed along with diet or drinking water. Inhalation toxicity studies are conducted by exposing the test materials like gas, vapor, or solid/liquid aerosol. Solvents used should be compatible with the test system without inducing any adverse chemical reaction. Preferably, aqueous solvent/vehicles must be used (Shinohara et al. 2009; Parasuraman 2011; Garcia-Canton et al. 2012).

Positive control animal groups treated with a known clastogen (e.g., ethyl methanesulfonate, methyl methanesulfonate, ethyl nitrosourea, mitomycin C, cyclophosphamide) must be included in the study. The negative control animal group can be treated with solvent/vehicle alone without test material. Test and control groups should include at least five analyzable animals of one sex or both sexes (in case of studies involving both sexes (Shinohara et al. 2009; Parasuraman 2011; Garcia-Canton et al. 2012), maximum tolerated dose (MTD). This maximum dose can be withstood by animals without death or any symptoms of severe pain or distress requiring euthanasia. Instead, animals must show mild to moderate symptoms like body weight depression, and effects on the hematopoietic system. The dose range selected should cover a maximum to one with moderate or no little toxicity. The assay should include the negative control, positive control, and three analyzable test dose with ideally a twofold difference in concentration. In the case of substances that are found to be nontoxic from published data or from the preliminary study for identifying dose, a maximum dose of 2000 mg/kg body weight can be administered. For studies with an exposure period of greater than 14 days, the limit dose should be 1000 mg/kg body weight, and for studies with an exposure period of fewer than 14 days or less, the limit dose of 2000 mg/kg/body weight/day is recommended (Suzuki et al. 2016; Shinohara et al. 2009; Parasuraman 2011; Garcia-Canton et al. 2012). The administration route can be oral, topical, subcutaneous, intravenous, intraperitoneal, intratracheal, or implantation and should be based on the anticipated route of human exposure. A maximum volume of 1 mL/100 g body weight is recommended for administration and should depend on the animal's size. However, for an aqueous solution, the maximum volume of 2 mL/100 g body weight can be used (Levy et al. 2019; Shinohara et al. 2009; Parasuraman 2011; Fatima and Ahmad 2019; Garcia-Canton et al. 2012).

19.6.2.2 Chromosome Harvest Analysis and Interpretation

General clinical signs, morbidity, mortality, and body weight changes of all animals should be monitored following the administration of test, negative, and positive controls. In the case of studies involving single sample exposure, two sampling times, first after 1.5 normal cell cycle length and later at 24 h following the first sampling, are recommended. If the studies involve more than one exposure, samples can be collected at a 1.5 normal cell cycle after the last administration. Metaphase-arresting agents (e.g., colchicine or colcemid) should be injected intraperitoneally prior (3–5 h for mice and 2–5 h for rats) to sacrifice. Immediately after sacrifice, bone marrow cells (femur or tibia) are harvested, treated with a hypotonic agent (e.g.,

0.56% or 0.075 M KCl), fixed with freshly prepared methanol: acetic acid in the ratio 3:1, stained with Giemsa or DNA-specific fluorochromes and analyzed microscopically for chromosome or chromatid aberrations. Plasma levels of the test chemicals can be monitored from blood samples taken at a specific time interval to ensure the target tissue exposure to the chemical. All the slides of the test, positive, and negative controls, should be scored blind, and scoring of at least 200 well-spread metaphases with modal chromosome number \pm two is required. The mitotic index must be measured from 1000 cells per animal to determine cytotoxicity (Rubio et al. 2016; Relier et al. 2017; Hadrup et al. 2019; Shinohara et al. 2009).

Suppose a statistically significant difference is observed in any of the test concentrations compared to the negative control, or a dose-dependent increase is observed in test values, or any test value is found outside the negative control range and distribution. In that case, the test can be considered positive or genotoxic (Shinohara et al. 2009). As part of toxicity assessment of TiO₂ NPs (21 and 80 nm), Ali et al. (2019) reported a chromosomal aberration assay done in Swiss albino mice following 5 days of oral exposure. Colchicine was injected intraperitoneally 2 h prior to sacrifice, and 100 well-spread metaphases (per animal) prepared from bone marrow cells were analyzed for chromosome aberrations like gaps, breaks, fragments, and deletions. In this study, a dose-dependent increase in the percentage of aberrant cells was shown compared to control (Levy et al. 2019). Genotoxicity of chromium oxide (Cr₂O₃ NPs) was assessed by chromosomal aberration, MN assays, and detection of sperm abnormalities by repeated oral exposure in Wistar rats.

Similarly, Cr₂O₃ NPs mediated genotoxicity was noticed (Ali et al. 2019). Chinde and Grover (2017) did *in vivo* chromosomal aberration assay as part of genotoxicity evaluation of tungsten oxide (WO₃ NPs) nanoparticles in female Wistar rats by acute oral exposure based on the protocol depicted by OECD 475 (Hadrup et al. 2019). After acute oral exposure of WO₃, NP study groups were euthanized at 18 and 24 h.

19.7 DNA Damage

19.7.1 Double-Strand Breaks (DSB) Assay

Histone H2AX phosphorylation, γ -H2AX, biomarker is commonly used in genotoxicity studies to assess for DNA damage. DNA double-strand breaks (DSBs) formation induced by genotoxicity can be assessed by phosphorylation of the histone H2AX to γ -H2AX. This is considered an early DNA damage response (Rogakou et al. 1998). Multiple copies of γ -H2AX production at DSBs can be detected *in vitro* using well-established immuno-histochemical methods. In response to DNA damage near the DNA double-stranded break, phosphorylation of histone H2AX molecules at serine 139 are ameliorated and form γ -H2AX foci (Ji et al. 2017). The detection of γ -H2AX relies on immunological techniques using specific monoclonal and polyclonal antibodies against the H2AX C-terminal phosphorylated peptide. γ -H2AX levels generated can be measured both in cell or tissue lysates (Zhu

et al. 2007). Cells are exposed for a defined period followed by fixing, permeabilization, and finally stained with anti- γ -H2AX, followed by the secondary fluorescent antibody. γ -H2AX foci are detected microscopically, and Literature provides evidence that recent years' studies on different nanomaterials utilized H2AX phosphorylation technique to assess double-stranded DNA breaks, which includes carbon nanotubes (Cveticanin et al. 2010; Valdiglesias et al. 2013), zinc oxide (Chattopadhyay et al. 2013), gold (Msiska et al. 2010), silica (Paget et al. 2015), polystyrene (Ling et al. 2021), and titanium dioxide (Elje et al. 2020).

19.8 High-ThroughPut Methods and Recent In Vitro Models

With the rapid development in the field of nanotechnology, safety assessment of it is the greatest concern. For genotoxicity, the conventional methods were found to be time-consuming and highly laborious. Hence, the development of a new high-throughput method for screening genotoxicity is in high demand. Some of the high-throughput methods for genotoxicity assessment are discussed here: To meet the genotoxicity assessment of different nanomaterials in a time, cost-effective, and accurate way, newer versions of existing genotoxicity assays have been developed. As the number of nanomaterials and nano-based products is increasing day by day, it paved the way for developing new models and high-throughput methods of assessing genotoxicity, and a few are listed below. Minimizing animal experiments by considering the 3Rs policy to reduce, refine, and replace, new in vitro models are being developed successfully to assess the toxicity of nanomaterials and advanced in vitro models are the representations of the tissue or organ to be studied as the liver is the primary site of the accumulation of nanomaterials (Pfuhrer et al. 2020). 3D models for skin, airways, and liver have been developed for genotoxicity assessment (Tahara et al. 2019; Dubiak-Szepietowska et al. 2016).

Recently a three-dimensional (3D) mini organ cultures (MOCs) of human nasal mucosa have been maintained to assess the genotoxicity of ZnO nanoparticles, and results showed that repetitive exposure to low concentrations of ZnO-NPs leads to DNA damage (Katsumiti et al. 2018). EpiAirwayTM 3D human bronchial models as a higher throughput model to assess the genotoxicity SiO₂, ZrO₂, and silver nanomaterials (Di Bucchianico et al. 2017). The efficiency of 2D monolayer and 3D spheroid cultures of HepG2 human liver cells in response to TiO₂, Ag, and ZnO-NPs for assessing genotoxicity has been studied; 3D cultures mimic the in vivo tissue behavior more in comparison with 2D culture (Elje et al. 2019). The difference in toxicity response in 2D and 3D cultures has been reported in various studies (Shah et al. 2018; Mandon et al. 2019; Kermanizadeh et al. 2014). Commercial InspheroTM liver microtissues for evaluating genotoxicity effects of NPs including zinc oxide (ZnO), MWCNTs, and TiO₂ NPs have been reported (Corvi and Madia 2017), in vitro liver model has been developed to complement the micronucleus assay, as this is one of the two in vitro assays recommended in the battery for genotoxicity testing (Dong and Sun 2016).

To overcome the existing limitations of cell culture, compiling a micro-fluid network with 3D models, i.e., organ on a chip (OCC), has been developed recently. OCC has been developed for each organ of the human body. Recently, microfabricated chip technologies for the screening of cytotoxicity and genotoxicity of NMs have been developed (Vecchio et al. 2014; Shaposhnikov et al. 2010; Gutzkow et al. 2013). It can platform for the single cell gel electrophoresis (comet) assay, CometChip, to assess DNA damage and genotoxic potential. Different versions of the conventional comet assay, such as 12 mini gels per slide, 96 mini gels on Gel Bond film, and 96 well multi-chamber plates, are newly developed (Stang and Witte 2009; Wood et al. 2010). It could analyze different types of nanoparticles at a time. Regarding micronucleus assay, an automated evaluation system flow cytometry analysis of both nuclei and micronuclei has been developed (Witt et al. 2008). Gamma H2AX conventional assay is also modified by different computerized approaches. The modified versions of the existing genotoxicity assays are discussed below.

19.8.1 Modified Versions of the Comet Assay

19.8.1.1 Medium Throughput Methylation-Sensitive Comet Assay

The comet assay is a relevant method used for detecting genotoxic events induced by different types of NMs. By incorporating an additional step of DNA digestion using lesion-specific restriction endonucleases in the conventional comet assay, the reliability and specificity of the assay can be enhanced. These modified versions can detect the type of DNA damage. One among them is the methylation-sensitive modified version of the comet assay, which allows the detection of global methylation and CpG island DNA methylation. DNA methyltransferase enzyme can add methyl ($-\text{CH}_3$) group at 5' position of cytosine residues, and this covalent modification occurs in all organisms. The methylation-sensitive comet assay utilizes isoschizomer properties of restriction enzymes Hpa11 and Msp1 for identifying global methylation. Hpa11 and Msp1 recognize the identical tetranucleotide sequence, 5'-CCGG-3' but possess different sensitivity to DNA methylation. Msp1 and Hpa11 cannot cleave 5'-CCGG-3', but Msp1 can cleave 5'-CmCCGG-3'. Ghosh et al. (2018) used a methylation-sensitive comet assay using Hpa11 and Msp1 for determining Mno-NPs induced DNA damage and DNA hypomethylation in *Physcomitrella patens* gametophores (Burlinson et al. 2007; Wiklund and Agurell 2003). In this assay, the slides taken from lysis buffer must be treated in an enzyme-reaction buffer having an adequate concentration of Hpa11 and Msp1 before proceeding with the rest of the steps, i.e., unwinding, electrophoresis, and neutralization. The DNA strand breaks can be evaluated by % tail DNA content. The maximum extent of DNA fragmentation is produced by Msp1 cleavage, and DNA fragments obtained from Hpa11 digestion are inversely related to DNA methylation (Azqueta and Dusinska 2015; Perotti et al. 2015; Lewies et al. 2014; Georgieva et al. 2017; Glej et al. 2009).

19.8.1.2 Endo III and FPG-Modified Comet Assay

This modified version of the comet assay uses DNA repair enzymes, endonuclease III (Endo III), and formamide pyrimidine-DNA glycosylase (FPG) to identify DNA strand breaks and oxidative DNA damage. Comet assay with Fpg and ENDO III had been employed by Novotna et al. (2017) to assess strand breaks and oxidative damage produced in brain cells of Lewis rats following intracranial exposure of poly-L-lysine-coated superparamagnetic iron oxide NPs and silica-coated cobalt-zinc-iron NPs (Mangalampalli et al. 2017; Azqueta and Dusinska 2015).

19.8.1.3 Comet-FISH

Comet-FISH method, a combination of single gel cell electrophoresis (comet assay) and fluorescence in situ hybridization (FISH), helps to detect overall and genome region-specific DNA damage (Tice and Vasquez 1998).

19.8.1.4 High-Throughput Screening Using Comet Chip

High-throughput techniques like comechip allow rapid screening of frequently exposing NMs from suspension cultures and cell lines. These methods are found to be sensitive, rapid, and less time-consuming than conventional comet assays. The most commonly used one employs microfabrication technology to develop 96 well microwells in the agarose layer. This microarray can be processed automated for detecting DNA breaks, a basic and alkali-sensitive sites from the cell suspension pretreated with test NMs (Fenech 2000; Weingeist et al. 2013; Watson et al. 2014; Karlsson et al. 2014).

19.8.1.5 ToxTracker Assay

A novel reporter assay determines the genotoxicity of a compound and its associated mechanism. This Green fluorescent protein (GFP) reporter gene was integrated into the mouse-based embryonic cell line to assess genotoxicity. The mouse stem cell lines with biomarkers identify the mechanism of toxicity (216). GFP-tagged reporter targets a particular cellular signaling pathway. Recently, we developed an in vitro assay called ToxTracker that can rapidly provide mechanistic insights into the biological damage induced by chemicals (Hendriks et al. 2016). ToxTracker mES reporter cell assay efficiently evaluates the mode of action of different nanomaterials. A study recently reported using ToxTracker mES reporter cell assay to distinguish genotoxicity and its associated mechanism of efficiently characterized metal oxide nanoparticles (CuO, ZnO, NiO, CeO₂, Fe₃O₄, and TiO₂) (Ates et al. 2016). The ToxTracker assay, a mechanism-based assessment of genotoxicity, consists of a panel of mouse embryonic stem (mES) cell lines that each contain a different GFP-tagged reporter for a distinct cellular signaling pathway. Response or Induction of different reporters in the cell lines indicates the mode of action of the toxicant and the damage induced. Reporters activate different responses, Srxn1-GFP reporter involved in oxidative response and regulation of antioxidant gene (Hendriks et al. 2016; Ates et al. 2016), the Rtkn-GFP and Bsc12-GFP activate in response to DNA damage, Ddit3-GFP reporter is associated with protein damage. The ToxTracker assay determines the mode of action of genotoxicants, whether the toxicity is via

direct DNA interaction, oxidative stress, or general cellular stress. In this assay, a reporter gene identifies different responses against the test compound. Chromosomal and DNA damage, inhibition of proteins involved in cell division, microtubule disruption, and oxidative stress are evaluated. The biomarkers associated with DNA damage and repair are also estimated. This assay is based on, as mentioned early on, genetically engineered cell lines with a promoter activated by genotoxic insult (e.g., p53 response element) fused to one or more reporter genes (e.g., β -lactamase). Activation of reporter genes is visualized using automated micro-confocal imaging, fluorescent microscope, and flow cytometry. As reported by the United States Tox21 program listed, some reporter assays include ToxTracker (Ates et al. 2016; Hastwell et al. 2006), Green Screen (McCarrick et al. 2020) antibody assays (e.g., p53RE, γ H2AX, ATAD5). A recent study investigated the mechanism of toxicity of different nanoparticles using ToxTracker assay showed that nanomaterials such as CdTe QDs, Mn, Mn_3O_4 , Sb, Sb_2O_3 , and Sn induced Ddit3-GFP reporter indicating protein damage, also Mn, Mn_3O_4 nanoparticle showed a prominent ToxTracker response with activation of reporters: Srxn1-GFP, Rtkn-GFP, Ddit3-GFP involved in oxidative stress, DNA damage, protein damage, respectively (Xie et al. 2011).

19.8.2 Modified Techniques for MN Detection

19.8.2.1 Flow Cytometry Method

Flow cytometry-based MN scoring has been developed as a high-throughput, reliable, robust, faster, and highly scalable technique for assessing the genotoxic potential of engineered nanomaterials (EMNs). This technique provides faster data acquisition and analysis and can be applied to any NMs or cell line. SiO_2 and TiO_2 -induced MN formation was analyzed by Pauline Franz et al. (2020), by flow cytometry-based scoring of micronucleus and compared the results obtained using the comet assay to establish the suitability of flow cytometry-based assays (Arslan and Akbaba 2020). By applying this automated technique, reliable data can be obtained faster than time and more operator-dependent conventional microscopic scoring (Arslan and Akbaba 2020; Wallin et al. 2017; Wang et al. 2020; Di Virgilio et al. 2010; Hovhannisyanyan 2010). In vitro MN assay by flow cytometry had been conducted by Demir et al. (2020) for assessing the genotoxicity of CdO NPs using TK6 cells and obtained a dose-dependent increase in micronucleus induction (Wallin et al. 2017).

19.8.2.2 In Vitro Micronucleus Assay and FISH Analysis

Cytokinesis-block micronucleus cytome (CBMN-cyt) assay has been developed as a versatile technique for detecting cytogenetic damage, cytostatic and cytotoxicity of chemicals, including ENMs. In combination with fluorescence in situ hybridization (FISH), the CBMN-cyt assay can be used as an efficient tool for assessing structural chromosomal aberrations (clastogenic) and numerical chromosomal aberrations (aneugenic) induced by test NMs. FISH analysis using pancentromeric DNA probes

distinguishes MN from whole chromosome loss (centromere positive) or acentric chromosome (centromere negative) fragment in binucleate cells resulting after cytoB treatment. Centromere, telomere, and chromosome painting probes are commonly selected for FISH analysis (Li et al. 2017; Heshmati et al. 2019; Wilde et al. 2017; Di Bucchianico et al. 2014; Lebedová et al. 2018; Wang et al. 2020; Di Virgilio et al. 2010; Hovhannisyan 2010; OECD 2016f).

19.9 Advantages and Limitations of Genotoxicity Assays

In vitro and in vivo mutagenicity assays, comet assay, and MN assays are common methods used in the literature to evaluate the genotoxicity of nanomaterials. These assays showed both limitations and advantages in identifying genotoxicity. With regard to nanomaterials, the Ames test is no longer considered for genotoxicity as nanomaterials showed negative results in the Ames test found to be positive in vitro mammalian cell genotoxicity test. It has been suggested, and simply the test cannot be ruled out without a proper investigation by a regulatory agency. Alternations in the method must be performed to proper uptake of nanoparticles into the Ames test bacteria to reduce the potential for false-negative results. However, different types of mutations can be determined by HPRT and MLA assay by sequencing the mutated Tk or Hprt loci. This assay has the capacity to characterize a diverse range of possible mutations. As MLA assay is limited to rodent cell lines, HPRT can also be applied to human monolayer suspension cell types (male TK6 or MCL-5) (Dewangan et al. 2018). In vivo transgenic rodent assay have many advantages, as mutation can be identified from any rodent tissue at any stage of development. Any route of administration can be selected, and the reproducibility of results is high. The limitation of this assay is increased cost, high mutation frequency, and limited sensitivity to clastogens.

In the case of the comet assay, it is considered a fast, inexpensive, rapid, and highly sensitive technique commonly used to detect DNA damage. Comet assays require a relatively small number of cells and can be done using proliferating and non-proliferating cells. Several peculiarities of nanoparticles may interfere with the comet assay like adsorption capacity, optical characteristics, hydrophobic nature, physicochemical properties, charge, and the tendency to agglomerate (Vandghanooni and Eskandani 2011; Huk et al. 2015; George et al. 2017). Studies have reported that the dispersion protocol employed may affect the genotoxicity of nanoparticles (Gehlhaus et al. 2008; Könen-Adıgüzel and Ergene 2018). The same nanomaterials exhibit high variations in the test result of the comet assay, and this may be due to size distributions, methods employed in the preparation of dispersions, dispersion stability, conditions of exposure, constituents of culture media, serum protein concentration used, size, charge, and surface coatings used. Coating materials or stabilizers must be tested separately along with the main assay to eliminate false positive or negative results. Complete data regarding nanomaterials uptake must be needed for accurate interpretation of the results (Vandghanooni and Eskandani 2011; Huk et al. 2015; Magdolenova et al. 2012).

Micronucleus assay cannot be considered an alternative to chromosomal aberration assay as it did not directly analyze the cells in the metaphase stage of the cell cycle. Instead, it is an independent and widely accepted genotoxic assay with many advantages and limitations. Unlike chromosomal aberration test, micronucleus assay can be modified for any dividing cells irrespective of its karyotype and is easy to conduct and interpret. Analysis of micronucleus assay, especially *in vivo* MN assays are more easy and precise as the only chromatin content in cells to analyze is the micronucleus. The main nucleus is removed from the erythrocytes of mammals during the last stages of erythropoiesis, and this feature enables easy quantification of the micronucleated cells by automated image analysis or flow cytometry. In the MN assay response of the test, materials can be detected for a longer duration. The outcome of toxins affecting spindle fibers can also be analyzed compared to CA assays. The use of metaphase-arresting agents like colcemid is not needed in MN assays, and the background frequency of micronucleated cells was shown to be quite stable. Different types of chromosomal aberrations are difficult to analyze by conventional MN assays, and the pseudo-micronucleated cells, if present, may interfere with the accurate interpretation of the data (OECD 2016e; ISO/TR 10993-22:2017 2017; Mahjoubian et al. 2021; Ema et al. 2013).

19.10 General Mechanisms of Genotoxicity

Nanoparticles are known to be classified into different categories. These include organic, inorganic, and hybrid particles. The versatile properties of nanomaterials increased its demand in different applications. With its merits, its increased demand can lead to an adverse effect on the biological system (Dusinska et al. 2011a, b; Chan 2006; Vega-Villa et al. 2008). The physicochemical properties of each nanomaterial vary, which in turn contributes to the toxicity of nanomaterials. As discussed earlier, different genotoxicity toxicity tests are performed to assess the toxicity, with that diverse mechanisms of toxicity can be addressed (Dusinska et al. 2017).

Numerous studies have been conducted to assess the genotoxic effects of different nanomaterials and their associated mechanisms involved in the induction of genetic changes. As per the literature, the existing knowledge on the mechanism of toxicity of nanomaterials includes oxidative stress, inflammation, immunotoxicity, and genotoxicity (Goldberg et al. 2007). Drug delivery is one of the key applications of developed nanoparticles for targeted delivery, and new controlled synthetic strategies have been developed to include bioresponsive moieties (Collins et al. 2013). Nanomaterials of small size enter the nucleus and may interact with DNA and associated proteins, which may induce genotoxicity. The genotoxicity of nanomaterials is categorized as primary (direct or indirect) or secondary genotoxicity with respect to its mechanism of action. Engineered nanomaterials for various intended applications may induce genotoxicity either by directly interacting with the genetic material or indirectly induced by ROS production, and result in damage to DNA. The key factors that influence the genotoxicity of nanomaterial and different mechanisms of genotoxicity are expressed in Fig. 19.7.

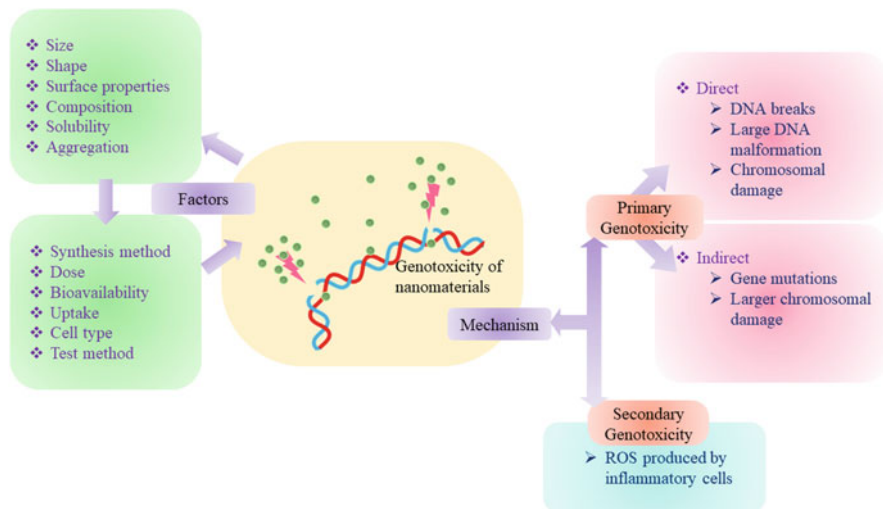


Fig. 19.7 Mechanism of genotoxicity of nanomaterials

19.10.1 Primary Genotoxicity

Primary direct genotoxicity involves the direct interaction of nanomaterials with the genome, and nanomaterials should enter the nucleus to elicit genotoxicity. Small nanoparticles can easily enter the nucleus through nuclear pores and result in the induction of DNA alternations or chromosomal damage. The effect or consequence of the interaction depends on the stages of the cell cycle nanomaterials interact and influence the replication and transcription process (Kohl et al. 2020). On the other hand, primary indirect genotoxicity is known to be due to nanomaterial-induced ROS generation.. The process of uptake and entry of nanoparticles into the nucleus is key to distinguishing direct and indirect genotoxicity (De Marzi et al. 2013). The generated ROS may induce oxidation of purine and pyrimidine and breakage of DNA strands. Finally, these may lead to mutations. Numerous studies on metal oxide nanomaterials documented that it can interfere with nuclear proteins involved in various processes of the cell cycle and induce ROS production in cellular compartments, inhibiting antioxidant defense proteins (Park et al. 2011; Petersen and Nelson 2010). It was also reported that indirect DNA damage might be the result of ROS-mediated oxidative stress induced by metal oxide nanomaterials (Kruszewski et al. 2013; Yang et al. 2009). A study has documented that SiO₂ nanoparticles enter the cell and result in aberrant clusters of topoisomerase I formation (Baweja et al. 2011). An in silico study reported an abiding site for fullerene-engineered nonmaterial on human DNA topoisomerase II alpha, and it led to DNA damage (Evans et al. 2017).

19.10.2 Secondary Genotoxicity

Secondary genotoxicity is the key mechanism of the genotoxicity of nanomaterials, mediated by inflammatory cells such as macrophages and neutrophils. These immune cells initiate the generation of reactive oxygen species, which activates the release of proinflammatory cytokines through different signaling pathways (Forman and Torres 2002; Borm et al. 2018). Cytokines activate the generation of intracellular nitric oxide synthesis. Both ROS and nitric oxide contribute to secondary genotoxicity leading to DNA damage. Secondary genotoxicity is considered the key genotoxicity mechanism for in vivo studies in crystalline silica (Catalán et al. 2016) and certain carbon nanotubes (Åkerlund et al. 2019). A recent study has documented that induce the Ni and NiO NPs release inflammatory cytokines, and secondary genotoxicity was observed in lung epithelial cells.

19.11 Conclusion

Nanomaterials-induced genotoxicity is a matter of great concern nowadays due to the exponential rise in nanotechnology. A battery of genotoxicity tests is available guided by different regulatory agencies. To date, no specific genotoxicity tests for nanomaterials are available. Hence, recommended in vitro and in vivo OECD guidelines for genotoxicity assessment are followed for nanomaterials. Even though few limitations are documented with conventional genotoxicity testing strategies for nanomaterials. Variations in genotoxicity results for similar nanomaterials are observed, and it affects the interpretation of genotoxicity of different nanomaterials. The literature also provides evidence that the variation and contradictory results may be due to improper characterization of nanomaterials. Gaining the importance of nanomaterials emphasizes the need for the development of new tools for the assessment of genotoxicity. High-throughput techniques and new models need to be explored for efficient analysis of the genotoxicity of nanomaterials.

Acknowledgments The authors wish to express their sincere thanks to the Director and Head, Biomedical Technology Wing, Sree Chitra Tirunal Institute for Medical Sciences and Technology (Govt. of India), Trivandrum, for their support and for providing the infrastructure to carry out this work.

References

- Abdalaziz MA, Annangi B, Marcos R (2014) Testing the genotoxic potential of nanomaterials using *Drosophila*. In: Genotoxicity and DNA repair. Humana Press, New York, pp 297–304
- Abudayyak M, Öztaş E, Arici M, Özhan G (2017a) Investigation of the toxicity of bismuth oxide nanoparticles in various cell lines. *Chemosphere* 169:117–123
- Abudayyak M, Gurkaynak TA, Özhan G (2017b) In vitro toxicological assessment of cobalt ferrite nanoparticles in several mammalian cell types. *Biol Trace Elem Res* 175(2):458–465

- Åkerlund E, Islam MS, McCarrick S, Alfaro-Moreno E, Karlsson HL (2019) Inflammation and (secondary) genotoxicity of Ni and NiO nanoparticles. *Nanotoxicology* 13(8):1060–1072
- Akyıl D, Eren Y, Konuk M, Tepekozcan A, Sağlam E (2016) Determination of mutagenicity and genotoxicity of indium tin oxide nanoparticles using the Ames test and micronucleus assay. *Toxicol Ind Health* 32(9):1720–1728
- Al-Ahmadi MS (2019) Cytogenetic and molecular assessment of some nanoparticles using *Allium sativum* assay. *Afr J Biotechnol* 18(29):783–796
- Ali SA, Rizk MZ, Hamed MA, Aboul-Ela EI, El-Rigal NS, Aly HF, Abdel-Hamid AH (2019) Assessment of titanium dioxide nanoparticles toxicity via oral exposure in mice: effect of dose and particle size. *Biomarkers* 24(5):492–498
- Annanji B, Rubio L, Alaraby M, Bach J, Marcos R, Hernández A (2016) Acute and long-term in vitro effects of zinc oxide nanoparticles. *Arch Toxicol* 90(9):2201–2213
- Armand L, Tarantini A, Beal D, Biola-Clier M, Bobyk L, Sorieul S, Pernet-Gallay K, Marie-Desvergne C, Lynch I, Herlin-Boime N, Carriere M (2016) Long-term exposure of A549 cells to titanium dioxide nanoparticles induces DNA damage and sensitizes cells towards genotoxic agents. *Nanotoxicology* 10(7):913–923
- Arslan K, Akbaba GB (2020) In vitro genotoxicity assessment and comparison of cerium (IV) oxide micro- and nanoparticles. *Toxicol Ind Health* 36(2):76–83. <https://doi.org/10.1177/0748233720913349>. PMID: 32279649
- Asakura M, Sasaki T, Sugiyama T, Takaya M, Koda S, Nagano K, Arito H, Fukushima S (2010) Genotoxicity and cytotoxicity of multi-wall carbon nanotubes in cultured chinese hamster lung cells in comparison with chrysotile A fibres. *J Occup Health* 52:155–166
- Ates G, Favvys D, Hendriks G, Derr R, Mertens B, Verschaevae L et al (2016) The Vitotox and ToxTracker assays: a two-test combination for quick and reliable assessment of genotoxic hazards. *Mutat Res* 810:13–21. <https://doi.org/10.1016/j.mrgentox.2016.09.005>
- Ávalos A, Haza AI, Mateo D, Morales P (2018) In vitro and in vivo genotoxicity assessment of gold nanoparticles of different sizes by comet and SMART assays. *Food Chem Toxicol* 120:81–88
- Azqueta A, Dusinska M (2015) The use of the comet assay for the evaluation of the genotoxicity of nanomaterials. *Front Genet* 6:239
- Barfod KK, Bendtsen KM, Berthing T, Koivisto AJ, Poulsen SS, Segal E, Verleysen E, Mast J, Holländer A, Jensen KA, Hougaard KS (2020) Increased surface area of halloysite nanotubes due to surface modification predicts lung inflammation and acute phase response after pulmonary exposure in mice. *Environ Toxicol Pharmacol* 73:103266
- Baweja L, Gurbani D, Shanker R, Pandey AK, Subramanian V, Dhawan A (2011) C60-fullerene binds with the ATP binding domain of human DNA topoisomerase II alpha. *J Biomed Nanotechnol* 7(1):177–178
- Benameur L, Auffan M, Cassien M, Liu W, Culcasi M, Rahmouni H, Stocker P, Tassistro V, Bottero JY, Rose J, Botta A (2015) DNA damage and oxidative stress induced by CeO2 nanoparticles in human dermal fibroblasts: evidence of a clastogenic effect as a mechanism of genotoxicity. *Nanotoxicology* 9(6):696–705
- Blakey DH, Douglas GR (1990) The role of excision repair in the removal of transient benzo [a] pyrene-induced DNA lesions in Chinese hamster ovary cells. *Mutat Res DNA Repair* 236(1): 35–41
- Borm PJA, Fowler P, Kirkland D (2018) An updated review of the genotoxicity of respirable crystalline silica. *Part Fibre Toxicol* 15(1):23. <https://doi.org/10.1186/s12989-018-0259-z>
- Branica G, Mladinić M, Omanović D, Želježić D (2016) An alternative approach to studying the effects of ZnO nanoparticles in cultured human lymphocytes: combining electrochemistry and genotoxicity tests. *Arh Hig Rada Toksikol* 67:277–288
- Bright J, Aylott M, Bate S, Geys H, Jarvis P, Saul J, Vonk R (2011) Recommendations on the statistical analysis of the Comet assay. *Pharm Stat* 10(6):485–493
- Burlinson B, Tice RR, Speit G, Agurell E, Brendler-Schwaab SY, Collins AR, Escobar P, Honma M, Kumaravel TS, Nakajima M, Sasaki YF (2007) Fourth international workgroup on

- genotoxicity testing: results of the in vivo Comet assay workgroup. *Mutat Res Genet Toxicol Environ Mutagen* 627(1):31–35
- Cappellini F, Hedberg Y, McCarrick S, Hedberg J, Derr R, Hendriks G, Odnevall Wallinder I, Karlsson HL (2018) Mechanistic insight into reactivity and (geno) toxicity of well-characterized nanoparticles of cobalt metal and oxides. *Nanotoxicology* 12(6):602–620
- Catalán J, Siivola KM, Nymark P, Lindberg H, Suhonen S, Järventaus H, Koivisto AJ et al (2016) In vitro and in vivo genotoxic effects of straight versus tangled multi-walled carbon nanotubes. *Nanotoxicology* 10(6):794–806. <https://doi.org/10.3109/17435390.2015.1132345>
- Chan VS (2006) Nanomedicine: an unresolved regulatory issue. *Regul Toxicol Pharmacol* 46:218–224
- Chattopadhyay N, Cai Z, Kwon YL, Lechtman E, Pignol JP, Reilly RM (2013) Molecularly targeted gold nanoparticles enhance the radiation response of breast cancer cells and tumor xenografts to X-radiation. *Breast Cancer Res Treat* 137:81–91
- Chen Z, Wang Y, Ba T, Li Y, Pu J, Chen T, Song Y, Gu Y, Qian Q, Yang J, Albertini RJ et al (2001) HPRT mutations in humans: biomarkers for mechanistic studies. *Mutat Res* 489:1–16
- Chen Z, Wang Y, Ba T, Li Y, Pu J, Chen T, Song Y, Gu Y, Qian Q, Yang J, Jia G (2014) Genotoxic evaluation of titanium dioxide nanoparticles in vivo and in vitro. *Toxicol Lett* 226(3):314–319. <https://doi.org/10.1016/j.toxlet.2014.0>
- Chinde S, Grover P (2017) Toxicological assessment of nano and micron-sized tungsten oxide after 28 days repeated oral administration to Wistar rats. *Mutat Res Genet Toxicol Environ Mutagen* 819:1–3
- Collins AR (2004) The comet assay for DNA damage and repair. *Mol Biotechnol* 26(3):249–261
- Collins AR, Kumar A, Dhawam A, Stone V, Dusinska M (2013) Mechanisms of genotoxicity. Review of recent in vitro and in vivo studies with engineered nanoparticles. *Nanotoxicology* 52(2):1–70
- Cordelli E, Keller J, Eleuteri P, Villani P, Ma-Hock L, Schulz M, Landsiedel R, Pacchierotti F (2017) No genotoxicity in rat blood cells upon 3-or 6-month inhalation exposure to CeO₂ or BaSO₄ nanomaterials. *Mutagenesis* 32(1):13–22
- Corvi R, Madia F (2017) In vitro genotoxicity testing-can the performance be enhanced. *Food Chem Toxicol* 106:600–608
- Cveticanin J, Joksic G, Leskovic A, Petrovic S, Sobot AV, Neskovic O (2010) Using carbon nanotubes to induce micronuclei and double strand breaks of the DNA in human cells. *Nanotechnology* 21:015102
- De Carli RF, Chaves DD, Cardozo TR, de Souza AP, Seeber A, Flores WH, Honatel KF, Lehmann M, Dihl RR (2018) Evaluation of the genotoxic properties of nickel oxide nanoparticles in vitro and in vivo. *Mutat Res Genet Toxicol Environ Mutagen* 836:47–53
- De Marzi L et al (2013) Cytotoxicity and genotoxicity of ceria nanoparticles on different cell lines in vitro. *Int J Mol Sci* 14(2):3065–3077
- de Souza Trigueiro NS, Gonçalves BB, Dias FC, de Oliveira Lima EC, Rocha TL, Sabóia-Morais SM (2021) Co-exposure of iron oxide nanoparticles and glyphosate-based herbicide induces DNA damage and mutagenic effects in the guppy (*Poecilia reticulata*). *Environ Toxicol Pharmacol* 81:103521
- Demir E, Qin T, Li Y, Zhang Y, Guo X, Ingle T, Yan J, Orza AI, Biris AS, Ghorai S, Zhou T (2020) Cytotoxicity and genotoxicity of cadmium oxide nanoparticles evaluated using in vitro assays. *Mutat Res Genet Toxicol Environ Mutagen* 850:503149
- Dertinger SD, Phonethpawth S, Weller P, Nicolette J, Murray J, Sonders P et al (2011) International *Pig-a* gene mutation assay trial: evaluation of transferability across 14 laboratories. *Environ Mol Mutagen* 52(9):690–698. <https://doi.org/10.1002/em.20672>
- Dewangan J, Pandey PK, Divakar A, Mishra S, Srivastava S, Rath SK (2018) Detection of gene mutation in cultured mammalian cells. In: Kumar A, Dobrovolsky VN, Dhawan A, Shanker R (eds) *Mutagenicity: assays and applications*. Elsevier, London, pp 49–67

- Di Bucchianico S, Fabbrizi MR, Cirillo S, Uboldi C, Gilliland D, Valsami-Jones E, Migliore L (2014) Aneuploidogenic effects and DNA oxidation induced in vitro by differently sized gold nanoparticles. *Int J Nanomedicine* 9:2191
- Di Bucchianico S, Cappellini F, Le Bihanic F, Zhang Y, Dreij K, Karlsson HL (2017) Genotoxicity of TiO₂ nanoparticles assessed by mini-gel comet assay and micronucleus scoring with flow cytometry. *Mutagenesis* 32(1):127–137
- Di Bucchianico S, Gliga AR, Åkerlund E, Skoglund S, Wallinder IO, Fadeel B, Karlsson HL (2018) Calcium-dependent cyto- and genotoxicity of nickel metal and nickel oxide nanoparticles in human lung cells. *Part Fibre Toxicol* 15(1):1–4
- Di Virgilio AL, Reigosa M, Arnal PM, De Mele MF (2010) Comparative study of the cytotoxic and genotoxic effects of titanium oxide and aluminium oxide nanoparticles in Chinese hamster ovary (CHO-K1) cells. *J Hazard Mater* 177(1–3):711–718
- Doak SH, Manshian B, Jenkins GJ, Singh N (2012) In vitro genotoxicity testing strategy for nanomaterials and the adaptation of current OECD guidelines. *Mutat Res* 745(1–2):104–111. <https://doi.org/10.1016/j.mrgentox.2011.09.013>
- Dong H, Sun H (2016) A microchip for integrated single-cell gene expression profiling and genotoxicity detection. *Sensors* 16:1489
- Douglas GR, Jiao J, Gingerich JD, Gossen JA, Soper LM (1995) Temporal and molecular characteristics of mutations induced by ethylnitrosourea in germ cells isolated from seminiferous tubules and in spermatozoa of lacZ transgenic mice. *Proc Natl Acad Sci U S A* 92(16):7485–7489. <https://doi.org/10.1073/pnas.92.16.7485>
- Dubiak-Szepietowska M, Karczmarczyk A, Jönsson-Niedziolka M, Winckler T, Feller KH (2016) Development of complex-shaped liver multicellular spheroids as a human-based model for nanoparticle toxicity assessment in vitro. *Toxicol Appl Pharmacol* 294:78–85
- Dumala N, Mangalampalli B, Grover P (2019) In vitro genotoxicity assessment of nickel (II) oxide nanoparticles on lymphocytes of human peripheral blood. *J Appl Toxicol* 39(7):955–965
- Dusinska M, NanoTEST Consortium (2009) Testing strategies for the safety of nanoparticles used in medical application. *Nanomedicine* 4:605–607
- Dusinska M, Fjellsbø LM, Magdolenova Z, Ravnum S, Rinna A, Rundén-Pran E (2011a) Chap. 11: Safety of nanoparticles in medicine. In: *Nanomedicine in health and disease*. Science Publishers, Boca Raton, FL, pp 203–226
- Dusinska M, Rundén-Pran E, Carreira SC, Saunders M (2011b) Chap. 4: *In vitro* and *in vivo* toxicity test methods. In: Fadeel B, Pietroiusti A, Shvedova A (eds) *Adverse effects of engineered nanomaterials: exposure, toxicology and impact on human health*. Academic Press, London
- Dusinska M, Tulinska J, El Yamani N, Kuricova M, Liskova A, Rollerova E, Rundén-Pran E, Smolkova B (2017) Immunotoxicity, genotoxicity and epigenetic toxicity of nanomaterials: new strategies for toxicity testing? *Food Chem Toxicol* 109:797–811
- ECHA (2020) Registration dossier aluminum oxide. Available online: <https://echa.europa.eu/fr/registrationdossier/-/registered-dossier/16039/7/7/1>. Accessed on 5 Jan 2020
- Efthimiou I, Georgiou Y, Vlastos D, Dailianis S, Deligiannakis Y (2020) Assessing the cytogenotoxic potential of model zinc oxide nanoparticles in the presence of humic-acid-like-polycondensate (HALP) and the leonardite HA (LHA). *Sci Total Environ* 721:137625
- Elespuru R, Pfuhler S, Aardema MJ, Chen T, Doak SH, Doherty A, Farabaugh CS, Kenny J, Manjanatha M, Mahadevan B, Moore MM (2018) Genotoxicity assessment of nanomaterials: recommendations on best practices, assays, and methods. *Toxicol Sci* 164(2):391–416
- Elje E, Hesler M, Rundén-Pran E, Mann P, Mariussen E, Wagner S, Dusinska M, Kohl Y (2019) The comet assay applied to HepG2 liver spheroids. *Mutat Res Genet Toxicol Environ* 845:403033
- Elje E, Mariussen E, Moriones OH, Bastús NG, Puentes V, Kohl Y, Dusinska M, Rundén-Pran E (2020) Hepato (Geno) toxicity assessment of nanoparticles in a HepG2 liver spheroid model. *Nanomaterials* 10(3):54

- Ema M, Imamura T, Suzuki H, Kobayashi N, Naya M, Nakanishi J (2013) Genotoxicity evaluation for single-walled carbon nanotubes in a battery of in vitro and in vivo assays. *J Appl Toxicol* 33(8):933–939
- Evans SJ, Clift MJ, Singh N, de Oliveira Mallia J, Burgum M, Wills JW, Wilkinson TS, Jenkins GJ, Doak SH (2017) Critical review of the current and future challenges associated with advanced in vitro systems towards the study of nanoparticle (secondary) genotoxicity. *Mutagenesis* 32(1): 233–241. <https://doi.org/10.1093/mutage/gew054>
- Fatima R, Ahmad R (2019) Hepatotoxicity and chromosomal abnormalities evaluation due to single and repeated oral exposures of chromium oxide nanoparticles in Wistar rats. *Toxicol Ind Health* 35(8):548–557
- Fenech M (2000) The in vitro micronucleus technique. *Mutat Res Fundam Mol Mech Mutagen* 455(1–2):81–95
- Fenech M (2020) Cytokinesis-Block micronucleus cytome assay evolution into a more comprehensive method to measure chromosomal instability. *Genes* 11(10):1203
- Fernández-Bertólez N, Costa C, Brandão F, Kiliç G, Teixeira JP, Pásaro E, Laffon B, Valdiglesias V (2018a) Neurotoxicity assessment of oleic acid-coated iron oxide nanoparticles in SH-SY5Y cells. *Toxicology* 406:81–91
- Fernández-Bertólez N, Costa C, Brandão F, Kiliç G, Duarte JA, Teixeira JP, Pásaro E, Valdiglesias V, Laffon B (2018b) Toxicological assessment of silica-coated iron oxide nanoparticles in human astrocytes. *Food Chem Toxicol* 118:13–23
- Forman HJ, Torres M (2002) Reactive oxygen species and cell signaling: respiratory burst in macrophage signaling. *Am J Respir Crit Care Med* 166(Suppl_1):S4–S8. <https://doi.org/10.1164/rccm.2206007>
- Franz P, Bürkle A, Wick P, Hirsch C (2020) Exploring flow cytometry-based micronucleus scoring for reliable nanomaterial genotoxicity assessment. *Chem Res Toxicol* 33(10):2538–2549
- Fubini B, Ghiazza M, Fenoglio I (2010) Physicochemical features of engineered nanoparticles relevant to their toxicity. *Nanotoxicology* 4:347–363
- García-Canton C, Anadón A, Meredith C (2012) γ H2AX as a novel endpoint to detect DNA damage: applications for the assessment of the in vitro genotoxicity of cigarette smoke. *Toxicol In Vitro* 26(7):1075–1086
- Gea M, Bonetta S, Iannarelli L, Giovannozzi AM, Maurino V, Bonetta S, Hodoroaba VD, Armato C, Rossi AM, Schilirò T (2019) Shape-engineered titanium dioxide nanoparticles (TiO₂-NPs): cytotoxicity and genotoxicity in bronchial epithelial cells. *Food Chem Toxicol* 127:89–100
- Gehlhaus M, Osier M, Lladós F, Plewak D, Lumpkin M, Odin M, Rooney A (2008) Toxicological review of cerium oxide and cerium compounds (CAS No. 1306-38-3). In: Support of summary information on the integrated risk information system (IRIS)
- George JM, Magogoty M, Vetten MA, Buys AV, Gulumian M (2017) From the cover: an investigation of the genotoxicity and interference of gold nanoparticles in commonly used in vitro mutagenicity and genotoxicity assays. *Toxicol Sci* 156(1):149–166
- Georgieva M, Rasydov NM, Hajduch M (2017) DNA damage, repair monitoring and epigenetic DNA methylation changes in seedlings of Chernobyl soybeans. *DNA Repair* 50:14–21
- Ghosh M et al (2018) Differences in MWCNT- and SWCNT-induced DNA methylation alterations in association with the nuclear deposition. *Part Fibre Technol* 15(1)
- Ghosh M, Sinha S, Jothiramajayam M, Jana A, Nag A, Mukherjee A (2016) Cyto-genotoxicity and oxidative stress induced by zinc oxide nanoparticle in human lymphocyte cells in vitro and Swiss albino male mice in vivo. *Food Chem Toxicol* 97:286–296
- Ghosh I, Sadhu A, Moriyasu Y, Bandyopadhyay M, Mukherjee A (2019) Manganese oxide nanoparticles induce genotoxicity and DNA hypomethylation in the moss *Physcomitrella patens*. *Mutat Res Genet Toxicol Environ Mutagen* 842:146–157
- Giubilato E, Cazzagon V, Amorim MJ, Blosi M, Bouillard J, Bouwmeester H, Costa AL, Fadeel B, Fernandes TF, Fito C, Hauser M (2020) Risk management framework for nano-biomaterials used in medical devices and advanced therapy medicinal products. *Materials* 13(20):4532

- Glei M, Hovhannisyan G, Pool-Zobel BL (2009) Use of Comet-FISH in the study of DNA damage and repair. *Mutat Res Rev Mutat Res* 681(1):33–43
- Golbamaki N, Rasulev B, Cassano A, Robinson RL, Benfenati E, Leszczynski J, Cronin MT (2015) Genotoxicity of metal oxide nanomaterials: review of recent data and discussion of possible mechanisms. *Nanoscale* 7:2154
- Goldberg M, Langer R, Jia X (2007) Nanostructured materials for applications in drug delivery and tissue engineering. *J Biomater Sci Polym Ed* 18(3):241–268. <https://doi.org/10.1163/156856207779996931>
- Gossen JA, De Leeuw WJF, Tan CHT, Zwarthoff EC, Berends F, Lohman PHM, Knook DL, Vijg J (1989) Efficient rescue of integrated shuttle vectors from transgenic mice: a model for studying mutations in vivo. *Proc Natl Acad Sci U S A* 86:7971–7975
- Guadagnini R, Kenzaoui HB, Cartwright L et al (2014) Toxicity screenings of nanomaterials: challenges due to interference with assay processes and components of classic in vitro tests. *Nanotoxicology* [Epub ahead of print], in press
- Guichard Y, Fontana C, Chaviniere E, Terzetti F, Gaté L, Binet S, Darne C (2016) Cytotoxic and genotoxic evaluation of different synthetic amorphous silica nanomaterials in the V79 cell line. *Toxicol Ind Health* 32(9):1639–1650
- Gulledge WP (2007) Re: cyto- and genotoxicity of ultrafine TiO₂ (2) particles in cultured human lymphoblastoid cells. *Mutat Res* 634(1–2):241
- Gutzkow KB, Langley TM, Meier S, Graupner A, Collins AR, Brunborg G (2013) High-throughput comet assay using 96 minigels. *Mutagenesis* 28:333–340
- Haase A, Dommershausen N, Schulz M, Landsiedel R, Reichardt P, Krause BC, Tentschert J, Luch A (2017) Genotoxicity testing of different surface-functionalized SiO₂, ZrO₂ and silver nanomaterials in 3D human bronchial models. *Arch Toxicol* 91(12):3991–4007
- Hackenberg S, Scherzed A, Zapp A, Radloff K, Ginzkey C, Gehrke T, Ickrath P, Kleinsasser N (2017) Genotoxic effects of zinc oxide nanoparticles in nasal mucosa cells are antagonized by titanium dioxide nanoparticles. *Mutat Res Genet Toxicol Environ Mutagen* 816:32–37
- Hadrup N, Rahmani F, Jacobsen NR, Saber AT, Jackson P, Bengtson S, Williams A, Wallin H, Halappanavar S, Vogel U (2019) Acute phase response and inflammation following pulmonary exposure to low doses of zinc oxide nanoparticles in mice. *Nanotoxicology* 13(9):1275–1292
- Hadrup N, Aimonen K, Ilves M, Lindberg H, Atluri R, Sahlgren NM, Jacobsen NR, Barfod KK, Berthing T, Lawlor A, Norppa H (2021) Pulmonary toxicity of synthetic amorphous silica—effects of porosity and copper oxide doping. *Nanotoxicology* 15(1):96–113
- Hartmann A, Agurell E, Beevers C, Brendler-Schwaab S, Burlinson B, Clay P, Collins A, Smith A, Speit G, Thybaud V, Tice RR (2003) Recommendations for conducting the in vivo alkaline Comet assay. *Mutagenesis* 18(1):45–51
- Harvanova MP, Jiravova J, Malohlava J, Tomankova KB, Jirova D, Kolarova H (2017) Raman imaging of cellular uptake and studies of silver nanoparticles effect in BJ human fibroblasts cell lines. *Int J Pharm* 528(1–2):280–286
- Hastwell PW, Chai LL, Roberts KJ, Webster TW, Harvey JS, Rees RW et al (2006) High-specificity and high-sensitivity genotoxicity assessment in a human cell line: validation of the GreenScreen HC *GADD45a-GFP* genotoxicity assay. *Mutat Res* 607(2):160–175. <https://doi.org/10.1016/j.mrgentox.2006.04.011>
- Hayashi M (2016) The micronucleus test—most widely used in vivo genotoxicity test. *Genes Environ* 38(1):1–6
- Hayashi M, MacGregor JT, Gatehouse DG, Adler ID, Blakey DH, Dertinger SD, Krishna G, Morita T, Russo A, Sutou S (2000) In vivo rodent erythrocyte micronucleus assay. II. Some aspects of protocol design including repeated treatments, integration with toxicity testing, and automated scoring. *Environ Mol Mutagen* 35(3):234–252
- Hendriks G, Derr RS, Misovic B, Morolli B, Calléja FMGR, Vrieling H (2016) The extended ToxTracker assay discriminates between induction of DNA damage, oxidative stress, and protein misfolding. *Toxicol Sci* 150(1):190–203. <https://doi.org/10.1093/toxsci/kfv323>

- Heshmati M, Bidgoli SA, Khoei S, Mahmoudzadeh A, Sorkhabadi SM (2019) Cytotoxicity and genotoxicity of silver nanoparticles in Chinese Hamster ovary cell line (CHO-K1) cells. *Nucleus* 62(3):221–225
- Horibata K, Ukai A, Ogata A, Nakae D, Ando H, Kubo Y, Nagasawa A, Yuzawa K, Honma M (2017) Absence of *in vivo* mutagenicity of multi-walled carbon nanotubes in single intratracheal instillation study using F344 *gpt* delta rats. *Genes Environ* 39:4. <https://doi.org/10.1186/s41021-016-0065-5>
- Hovhannisyann GG (2010) Fluorescence in situ hybridization in combination with the comet assay and micronucleus test in genetic toxicology. *Mol Cytogenet* 3(1):1–1
- Huang S, Chueh PJ, Lin YW, Shih TS, Chuang SM (2009) Disturbed mitotic progression and genome segregation are involved in cell transformation mediated by nano-TiO₂ long-term exposure. *Toxicol Appl Pharmacol* 241:182–194
- Huk A, Izak-Nau E, Reidy B, Boyles M, Duschl A, Lynch I, Dušinska M (2014) Is the toxic potential of nanosilver dependent on its size? *Part Fibre Toxicol* 11(1):1–6
- Huk A, Collins AR, El Yamani N, Porredon C, Azqueta A, de Lapuente J, Dusinska M (2015) Critical factors to be considered when testing nanomaterials for genotoxicity with the comet assay. *Mutagenesis* 30(1):85–88
- ISO/TR 10993-22:2017 (2017) Biological evaluation of medical devices—part 22: guidance on nanomaterials
- Ji J, Zhang Y, Redon CE, Reinhold WC, Chen AP, Fogli LK, Holbeck SL, Parchment RE, Hollingshead M, Tomaszewski JE, Dudon Q, Pommier Y, Doroshow JH, Bonner WM (2017) Phosphorylated fraction of H2AX as a measurement for DNA damage in cancer cells and potential applications of a novel assay. *PLoS One* 12(2):e0171582. <https://doi.org/10.1371/journal.pone.0171582>
- Kanda R, Jiang T, Hayata I, Kobayashi S (1994) Effects of colcemid concentration on chromosome aberration analysis in human lymphocytes. *J Radiat Res* 35(1):41–47
- Karlsson HL, Gliga AR, Calléja FM et al (2014) Mechanism-based genotoxicity screening of metal oxide nanoparticles using the ToxTracker panel of reporter cell lines. *Part Fibre Toxicol* 11:41. <https://doi.org/10.1186/s12989-014-0041-9>
- Katsumiti A, Thorley AJ, Arostegui I, Reip P, Valsami-Jones E, Tetley TD, Cajaraville MP (2018) Cytotoxicity and cellular mechanisms of toxicity of CuO NPs in mussel cells in vitro and comparative sensitivity with human cells. *Toxicol In Vitro* 48:146–158
- Kazimirova A, Baranokova M, Staruchova M, Drlickova M, Volkovova K, Dusinska M (2019) Titanium dioxide nanoparticles tested for genotoxicity with the comet and micronucleus assays in vitro, ex vivo and in vivo. *Mutat Res Genet Toxicol Environ Mutagen* 843:57–65
- Kazimirova A, El Yamani N, Rubio L, García-Rodríguez A, Baranokova M, Marcos R, Dusinska M (2020) Effects of titanium dioxide nanoparticles on the Hprt gene mutations in V79 hamster cells. *Nanomaterials* 10(3):465
- Kermanizadeh A, Gaiser BK, Johnston H, Brown DM, Stone V (2014) Toxicological effect of engineered nanomaterials on the liver. *Br J Pharmacol* 171:3980–3987
- Khanal S, Singh P, Avlasevich SL, Torous DK, Bemis JC, Dertinger SD (2018) Integration of liver and blood micronucleus and *Pig-a* gene mutation endpoints into rat 28-day repeat-treatment studies: proof-of-principle with diethylnitrosamine. *Mutat Res* 828:30–35. <https://doi.org/10.1016/j.mrgentox.2018.02.005>
- Kim YJ, Rahman MM, Lee SM, Kim JM, Park K, Kang JH, Seo YR (2019) Assessment of in vivo genotoxicity of citrated-coated silver nanoparticles via transcriptomic analysis of rabbit liver tissue. *Int J Nanomedicine* 14:393
- Kimoto T, Horibata K, Miura D, Chikura S, Okada Y, Ukai A et al (2016) The PIGRET assay, a method for measuring *Pig-a* gene mutation in reticulocytes, is reliable as a short-term in vivo genotoxicity test: summary of the MMS/JEMS-collaborative study across 16 laboratories using 24 chemicals. *Mutat Res* 811:3–15. <https://doi.org/10.1016/j.mrgentox.2016.10.003>

- Klingelfus T, Disner GR, Voigt CL, Alle LF, Cestari MM, Leme DM (2019) Nanomaterials induce DNA-protein crosslink and DNA oxidation: A mechanistic study with RTG-2 fish cell line and Comet assay modifications. *Chemosphere* 215:703–709
- Kohl Y, Rundén-Pran E, Mariussen E, Hesler M, El Yamani N, Longhin EM, Dusinska M (2020) Genotoxicity of nanomaterials: advanced in vitro models and high throughput methods for human hazard assessment—a review. *Nanomaterials* 10(10):1911
- Kohler SW, Provost GS, Fieck A, Kretz PL, Bullock WO, Putman DL, Sorge JA, Short JM (1991) Analysis of spontaneous and induced mutations in transgenic mice using a lambda ZAP/lacI shuttle vector. *Environ Mol Mutagen* 18:316–321
- Könen-Adıgüzel S, Ergene S (2018) In vitro evaluation of the genotoxicity of CeO₂ nanoparticles in human peripheral blood lymphocytes using cytokinesis-block micronucleus test, comet assay, and gamma H2AX. *Toxicol Ind Health* 34(5):293–300. <https://doi.org/10.1177/0748233717753780>. PMID: 29554819
- Kruszewski M, Grądzka I, Bartłomiejczyk T, Chwastowska J, Sommer S, Grzelak A, Zuberek M, Lankoff A, Dusinska M, Wojewódzka M (2013) Oxidative DNA damage corresponds to the long term survival of human cells treated with silver nanoparticles. *Toxicol Lett* 219(2):151–159
- Kumar A, Dhawan A (2013) Genotoxic and carcinogenic potential of engineered nanoparticles: an update. *Arch Toxicol* 87(11):1883–1900
- Kumaravel TS, Vilhar B, Faux SP, Jha AN (2009) Comet assay measurements: a perspective. *Cell Biol Toxicol* 25(1):53–64
- Laban B, Ralević U, Petrović S, Leskovic A, Vasić-Anićijević D, Marković M, Vasić V (2020) Green synthesis and characterization of nontoxic L-methionine capped silver and gold nanoparticles. *J Inorg Biochem* 204:110958
- Landsiedel R, Kapp MD, Schulz M, Wiench K, Oesch F (2009) Genotoxicity investigations on nanomaterials: methods, preparation and characterization of test material, potential artifacts and limitations—many questions, some answers. *Mutat Res Rev Mutat Res* 681(2–3):241–258
- Latvala S, Hedberg J, Di Bucchianico S, Möller L, OdnevallWallinder I, Elihn K, Karlsson HL (2016) Nickel release, ROS generation and toxicity of Ni and NiO micro-and nanoparticles. *PLoS One* 11(7):e0159684
- Lebedová J, Hedberg YS, OdnevallWallinder I, Karlsson HL (2018) Size-dependent genotoxicity of silver, gold and platinum nanoparticles studied using the mini-gel comet assay and micronucleus scoring with flow cytometry. *Mutagenesis* 33(1):77–85
- Levy DD, Zeiger E, Escobar PA, Hakura A, Van der Lee de BJM, Kato M et al (2019) Recommended criteria for the evaluation of bacterial mutagenicity data (Ames test). *Mutat Res* 848:403074. <https://doi.org/10.1016/j.mrgentox.2019.07.004>
- Lewies A, Van Dyk E, Wentzel JF, Pretorius PJ (2014) Using a medium-throughput comet assay to evaluate the global DNA methylation status of single cells. *Front Genet* 5:215
- Li Y, Chen DH, Yan J, Chen Y, Mittelstaedt RA, Zhang Y, Biris AS, Heflich RH, Chen T (2012) Genotoxicity of silver nanoparticles evaluated using the Ames test and in vitro micronucleus assay. *Mutat Res Genet Toxicol Environ Mutagen* 745(1–2):4–10
- Li Y, Bhalli JA, Ding W, Yan J, Pearce MG, Sadiq R, Cunningham CK, Jones MY, Monroe WA, Howard PC, Zhou T, Chen T (2014) Cytotoxicity and genotoxicity assessment of silver nanoparticles in mouse. *Nanotoxicology* 8(Suppl 1):36–45. <https://doi.org/10.3109/17435390.2013.855827>
- Li Y, Doak SH, Yan J, Chen DH, Zhou M, Mittelstaedt RA, Chen Y, Li C, Chen T (2017) Factors affecting the in vitro micronucleus assay for evaluation of nanomaterials. *Mutagenesis* 32(1):151–159
- Lian D, Chonghua Z, Wen G, Hongwei Z, Xuetao B (2017) Label-free and dynamic monitoring of cytotoxicity to the blood-brain barrier cells treated with nanometre copper oxide. *IET Nanobiotechnol* 11(8):948–956
- Ling C, An H, Li L, Wang J, Lu T, Wang H, Hu Y, Song G, Liu S (2021) Genotoxicity evaluation of titanium dioxide nanoparticles in vitro: a systematic review of the literature and meta-analysis. *Biol Trace Elem Res* 199:2057–2076

- Liu Y, Xia Q, Liu Y, Zhang S, Cheng F, Zhong Z, Wang L, Li H, Xiao K (2014) Genotoxicity assessment of magnetic iron oxide nanoparticles with different particle sizes and surface coatings. *Nanotechnology* 25(42):425101
- Lloyd M, Kidd D (2012) The mouse lymphoma assay. *Methods Mol Biol* 817:35–54. https://doi.org/10.1007/978-1-61779-421-6_3
- Louro H, Tavares A, Vital N, Costa PM, Alverca E, Zwart E, de Jong WH, Fessard V, Lavinha J, Silva MJ (2014) Integrated approach to the in vivo genotoxic effects of a titanium dioxide nanomaterial using LacZ plasmid-based transgenic mice. *Environ Mol Mutagen* 55(6):500–509
- Lovell DP, Omori T (2008) Statistical issues in the use of the comet assay. *Mutagenesis* 23(3):171–182
- Maffei F, Zolezzi Moraga JM, Angelini S, Zenesini C, Musti M, Festi D, Cantelli-Forti G, Hrelia P (2014) Micronucleus frequency in human peripheral blood lymphocytes as a biomarker for the early detection of colorectal cancer risk. *Mutagenesis* 29(3):221–225
- Magdolenova Z, Bilaničová D, Pojana G, Fjellsbø LM, Hudecova A, Hasplova K, Marcomini A, Dusinska M (2012) Impact of agglomeration and different dispersions of titanium dioxide nanoparticles on the human related in vitro cytotoxicity and genotoxicity. *J Environ Monit* 14(2):455–464
- Magdolenova Z, Collins A, Kumar A, Dhawan A, Stone V, Dusinska M (2014) Mechanisms of genotoxicity. A review of in vitro and in vivo studies with engineered nanoparticles. *Nanotoxicology* 8(3):233–278
- Magdolenova Z, Drlickova M, Henjum K, Rundén-Pran E, Tulinska J, Bilanicova D, Pojana G, Kazimirova A, Barancokova M, Kuricova M, Liskova A (2015) Coating-dependent induction of cytotoxicity and genotoxicity of iron oxide nanoparticles. *Nanotoxicology* 9(Suppl 1):44–56
- Mahjoubian M, Naeemi AS, Sheykhan M (2021) Toxicological effects of Ag₂O and Ag₂CO₃ doped TiO₂ nanoparticles and pure TiO₂ particles on Zebrafish (*Danio rerio*). *Chemosphere* 263:128182
- Mahmoud A, Ezgi Ö, Merve A, Özhan G (2016) In vitro toxicological assessment of magnesium oxide nanoparticle exposure in several mammalian cell types. *Int J Toxicol* 35(4):429–437
- Mandon M, Huet S, Dubreil E, Fessard V, Le Hegarat L (2019) Three-dimensional HepaRG spheroids as a liver model to study human genotoxicity in vitro with the single cell gel electrophoresis assay. *Sci Rep* 9:10548
- Mangalampalli B, Dumala N, Grover P (2017) Acute oral toxicity study of magnesium oxide nanoparticles and microparticles in female albino Wistar rats. *Regul Toxicol Pharmacol* 90:170–184
- Manshian BB, Mikhail J, Jenkins GJS, Barron A, Wright CJ, Doak SH (2011) DNA damaging potential of single walled carbon nanotubes. *Mutagenesis* 26:701
- Manshian BB, Jenkins GJ, Williams PM, Wright C, Barron AR, Brown AP, Hondow N, Dunstan PR, Rickman R, Brady K, Doak SH (2013) Single-walled carbon nanotubes: differential genotoxic potential associated with physico-chemical properties. *Nanotoxicology* 7(2):144–156
- Marchetti F, Aardema MJ, Beevers C, Van Benthem J, Godschalk R, Williams A et al (2018) Identifying germ cell mutagens using OECD test guideline 488 (Transgenic Rodent Somatic and Germ Cell Gene Mutation Assays) and integration with somatic cell testing. *Mutat Res* 832–833:7–18. <https://doi.org/10.1016/j.mrgentox.2018.05.021>
- Martínez-Luna G, Castillo-Cadena J, Serment-Guerrero JH (2015) Modified procedure to assess DNA breakage in spermatozoa by means of the comet assay. *Rev Int Contam Ambient* 31(1):39–45
- May S, Hirsch C, Rippl A, Bohmer N, Kaiser JP, Diener L, Wichser A, Bürkle A, Wick P (2018) Transient DNA damage following exposure to gold nanoparticles. *Nanoscale* 10(33):15723–15735
- McCarrick S, Cappellini F, Kessler A, Moelijker N, Derr R, Hedberg J, Wold S, Blomberg E, Odnevall Wallinder I, Hendriks G, Karlsson HL (2020) ToxTracker reporter cell lines as a tool for mechanism-based (geno) toxicity screening of nanoparticles—metals, oxides and quantum dots. *Nanomaterials* 10(1):110

- Miller B, Albertini S, Locher F, Thybaud V, Lorge E (1997) Comparative evaluation of the *in vitro* micronucleus test and the *in vitro* chromosome aberration test: industrial experience. *Mutat Res Genet Toxicol Environ Mutagen* 392(1–2):45–59
- Mittag A, Schneider T, Westermann M, Gleis M (2019) Toxicological assessment of magnesium oxide nanoparticles in HT29 intestinal cells. *Arch Toxicol* 93(6):1491–1500
- Miura D, Dobrovolsky VN, Kasahara Y, Katsuura Y, Heflich RH (2008a) Development of an *in vivo* gene mutation assay using the endogenous *Pig-A* gene: I. Flow cytometric detection of CD59-negative peripheral red blood cells and CD48-negative spleen T-cells from the rat. *Environ Mol Mutagen* 49:614–621. <https://doi.org/10.1002/em.20414>
- Miura D, Dobrovolsky VN, Mittelstaedt RA, Kasahara Y, Katsuura Y, Heflich RH (2008b) Development of an *in vivo* gene mutation assay using the endogenous *Pig-A* gene: II. Selection of *Pig-A* mutant rat spleen T-cells with proaerolysin and sequencing *Pig-A* cDNA from the mutants. *Environ Mol Mutagen* 49:622–630. <https://doi.org/10.1002/em.20413>
- Montazeri A, Zal Z, Ghasemi A, Yazdannejat H, Asgarian-Omran H, Hosseini-mehr SJ (2018) Radiosensitizing effect of cerium oxide nanoparticles on human leukemia cells. *Pharm Nanotechnol* 6(2):111–115
- Moratin H, Scherzad A, Gehrke T, Ickrath P, Radeloff K, Kleinsasser N, Hackenberg S (2018) Toxicological characterization of ZnO nanoparticles in malignant and non-malignant cells. *Environ Mol Mutagen* 59(3):247–259
- Mrakovic M, Meindl C, Leitinger G, Roblegg E, Fröhlich E (2015) Carboxylated short single-walled carbon nanotubes but not plain and multi-walled short carbon nanotubes show *in vitro* genotoxicity. *Toxicol Sci* 144(1):114–127
- Mrđanović J, Šolajić S, Bogdanović V, Stankov K, Bogdanović G, Djordjević A (2009) Effects of fullerene C60 (OH) 24 on the frequency of micronuclei and chromosome aberrations in CHO-K1 cells. *Mutat Res Genet Toxicol Environ Mutagen* 680(1–2):25–30
- Msiska Z, Pacurari M, Mishra A, Leonard SS, Castranova V, Vallyathan V (2010) DNA double-strand breaks by asbestos, silica, and titanium dioxide. *Am J Respir Cell Mol Biol* 43:210–219
- Muller J, Decordier I, Hoet PH, Lombaert N, Thomassen L, Huaux F, Lison D, Kirsch-Volders M (2008) Clastogenic and aneugenic effects of multi-wall carbon nanotubes in epithelial cells. *Carcinogenesis* 29(2):427–433
- Murgia E, Ballardin M, Bonassi S, Rossi AM, Barale R (2008) Validation of micronuclei frequency in peripheral blood lymphocytes as early cancer risk biomarker in a nested case-control study. *Mutat Res Fundam Mol Mech Mutagen* 639(1–2):27–34
- Nadin SB, Vargas-Roig LM, Ciocca DR (2001) A silver staining method for single-cell gel assay. *J Histochem Cytochem* 49(9):1183–1186
- Naem A, Alam M, Khan TA, Husain Q (2017) A biophysical and computational study of concanavalin A immobilized zinc oxide nanoparticles. *Protein Pept Lett* 24(12):1096–1104
- Netzer K, Jordakieva G, Girard AM, Budinsky AC, Pilger A, Richter L, Kataeva N, Schotter J, Godnic-Cvar J, Ertl P (2018) Next-generation magnetic nanocomposites: cytotoxic and genotoxic effects of coated and uncoated ferric cobalt boron (FeCoB) nanoparticles *in vitro*. *Basic Clin Pharmacol Toxicol* 122(3):355–363
- Ng CT, Li JJ, Bay BH, Yung LY (2010) Current studies into the genotoxic effects of nanomaterials. *J Nucleic Acids* 2010:947859
- Nohmi T, Suzuki T, Masumura K (2000) Recent advances in the protocols of transgenic mouse mutation assays. *Mutat Res* 455(1–2):191–215. [https://doi.org/10.1016/S0027-5107\(00\)00077-4](https://doi.org/10.1016/S0027-5107(00)00077-4)
- Nohmi T, Masumura K, Toyoda-Hokaiwado N (2017) Transgenic rat models for mutagenesis and carcinogenesis. *Genes Environ* 39:11. <https://doi.org/10.1186/s41021-016-0072-6>
- Novotna B, Herynek V, Rossner P Jr, Turmovcova K, Jendelova P (2017) The effects of grafted mesenchymal stem cells labeled with iron oxide or cobalt-zinc-iron nanoparticles on the biological macromolecules of rat brain tissue extracts. *Int J Nanomedicine* 12:4519

- OECD (2014) Reports of the JaCVAM initiative international pre-validation and validation studies of the in vivo rodent alkaline comet assay for the detection of genotoxic carcinogens, Series on testing and assessment, Nos. 195 and 196. OECD Publishing, Paris
- OECD (2015) Test No. 490: In vitro mammalian cell gene mutation tests using the thymidine kinase gene. OECD, Paris
- OECD (2016a) Test No. 476: *In vitro* mammalian cell gene mutation tests using the *Hprt* and *xprt* genes, OECD guidelines for the testing of chemicals, Section 4. OECD Publishing, Paris. <https://doi.org/10.1787/9789264264809-en>
- OECD (2016b) OECD guideline for testing of chemicals, 489: *In vivo* mammalian alkaline comet assay
- OECD (2016c) Overview of the set of OECD genetic toxicology test guidelines and updates performed in 2014-2015. ENV Publications. Series on testing and assessment, No. 234. OECD, Paris
- OECD (2016d) Test No. 487: *In vitro* mammalian cell micronucleus test
- OECD (2016e) Test No. 473: *In vitro* mammalian chromosomal aberration test
- OECD (2016f) Test No. 474: Mammalian erythrocyte micronucleus test
- OECD (2016g) Test no. 475: Mammalian bone marrow chromosomal aberration test
- Olive PL, Banáth JP, Durand RE (2012) Heterogeneity in radiation-induced DNA damage and repair in tumor and normal cells measured using the “comet” assay. *Radiat Res* 178(2):AV35–AV42
- Oliviero M, Schiavo S, Dumontet S, Manzo S (2019) DNA damages and offspring quality in sea urchin *Paracentrotus lividus* sperms exposed to ZnO nanoparticles. *Sci Total Environ* 651:756–765
- Olsen AK, Dertinger SD, Krüger CT, Eide DM, Instanes C, Brunborg G, Hartwig A, Graupner A (2017) The Pig-a gene mutation assay in mice and human cells: a review. *Basic Clin Pharmacol Toxicol* 121:78–92
- Organisation for Economic Co-operation and Development (2002) Test No. 420: Acute oral toxicity-fixed dose procedure. OECD Publishing, Paris
- Ostling KJ (1984) Microelectrophoretic study of radiation-induced DNA damages in individual mammalian cells. *Biochem Biophys Res Commun* 123(1):291–298
- Ostling O, Johanson KJ (1984) Microelectrophoretic study of radiation-induced DNA damages in individual mammalian cells. *Biochem Biophys Res Commun* 123(1):291–298. [https://doi.org/10.1016/0006-291x\(84\)90411-x](https://doi.org/10.1016/0006-291x(84)90411-x)
- Paget V, Dekali S, Kortulewski T, Grall R, Gamez C, Blazy K, Aguerre-Chariol O, Chevillard S, Braun A, Rat P et al (2015) Specific uptake and genotoxicity induced by polystyrene nanobeads with distinct surface chemistry on human lung epithelial cells and macrophages. *PLoS One* 10: e0123297
- Panyala A, Chinde S, Kumari SI, Rahman MF, Mahboob M, Kumar JM, Grover P (2019) Comparative study of toxicological assessment of yttrium oxide nano- and microparticles in Wistar rats after 28 days of repeated oral administration. *Mutagenesis* 34(2):181–201
- Parasuraman S (2011) Toxicological screening. *J Pharmacol Pharmacother* 2(2):74
- Park MVDZ et al (2011) Genotoxicity evaluation of amorphous silica nanoparticles of different sizes using the micronucleus and the plasmid lacZ gene mutation assay. *Nanotoxicology* 5(2): 168–181
- Patlolla AK, Berry A, May L, Tchounwou PB (2012) Genotoxicity of silver nanoparticles in *Vicia faba*: a pilot study on the environmental monitoring of nanoparticles. *Int J Environ Res Public Health* 9(5):1649–1662
- Perotti A, Rossi V, Mutti A, Buschini A (2015) Methy-sens Comet assay and DNMTs transcriptional analysis as a combined approach in epigenotoxicology. *Biomarkers* 20(1):64–70
- Petersen EJ, Nelson BC (2010) Mechanisms and measurements of nanomaterial-induced oxidative damage to DNA. *Anal Bioanal Chem* 398(2):613–650
- Pfuhler S, van Benthem J, Curren R, Doak SH, Dusinska M, Hayashi M, Heflich RH, Kidd D, Kirkland D, Luan Y et al (2020) Use of in vitro 3D tissue models in genotoxicity testing:

- strategic fit, validation status and way forward. Report of the working group from the 7th International Workshop on Genotoxicity Testing (IWGT). *Mutat Res Toxicol Environ Mutagen* 850–851:503135
- Prabhakar PV, Reddy UA, Singh SP, Balasubramanyam A, Rahman MF, InduKumari S, Agawane SB, Murty US, Grover P, Mahboob M (2012) Oxidative stress induced by aluminum oxide nanomaterials after acute oral treatment in Wistar rats. *J Appl Toxicol* 32:436–445
- Preaubert L, Courbiere B, Achard V, Tassistro V, Greco F, Orsiere T, Bottero JY, Rose J, Auffan M, Perrin J (2016) Cerium dioxide nanoparticles affect *in vitro* fertilization in mice. *Nanotoxicology* 10(1):111–117
- Pu X, Wang Z, Klaunig JE (2015) Alkaline comet assay for assessing DNA damage in individual cells. *Curr Protoc Toxicol* 65(1):3–12
- Raja IS, Lee JH, Hong SW, Shin DM, Lee JH, Han DW (2020) A critical review on genotoxicity potential of low dimensional nanomaterials. *J Hazard Mater* 409:124915
- Relier C, Dubreuil M, Lozano García O, Cordelli E, Mejia J, Eleuteri P, Robidel F, Loret T, Pacchierotti F, Lucas S, Lacroix G (2017) Study of TiO₂ P25 nanoparticles genotoxicity on lung, blood, and liver cells in lung overload and non-overload conditions after repeated respiratory exposure in rats. *Toxicol Sci* 156(2):527–537
- Rogakou EP, Pilch DR, Orr AH, Ivanova VS, Bonner WM (1998) DNA double-stranded breaks induce histone H2AX phosphorylation on serine 139. *J Biol Chem* 273(10):5858–5868
- Rubio L, Annangi B, Vila L, Hernández A, Marcos R (2016) Antioxidant and anti-genotoxic properties of cerium oxide nanoparticles in a pulmonary-like cell system. *Arch Toxicol* 90(2):269–278
- Shah UK, Mallia JO, Singh N, Chapman KE, Doak SH, Jenkins GJS (2018) A three-dimensional *in vitro* HepG2 cells liver spheroid model for genotoxicity studies. *Mutat Res* 825:51–58
- Shaposhnikov S, Azqueta A, Henriksson S, Meier S, Gaivão I, Huskisson NH, Smart A, Brunborg G, Nilsson M, Collins AR (2010) Twelve-gel slide format optimised for comet assay and fluorescent *in situ* hybridisation. *Toxicol Lett* 195:31–34
- Shinohara N, Matsumoto K, Endoh S, Maru J, Nakanishi J (2009) *In vitro* and *in vivo* genotoxicity tests on fullerene C60 nanoparticles. *Toxicol Lett* 191(2–3):289–296
- Sivvola KM, Suhonen S, Hartikainen M, Catalán J, Norppa H (2020) Genotoxicity and cellular uptake of nanosized and fine copper oxide particles in human bronchial epithelial cells *In Vitro*. *Mutat Res Genet Toxicol Environ Mutagen* 856:503217
- Singh NP, McCoy MT, Tice RR, Schneider EL (1988) A simple technique for quantitation of low levels of DNA damage in individual cells. *Exp Cell Res* 175(1):184–191
- Souza TA, Franchi LP, Rosa LR, da Veiga MA, Takahashi CS (2016) Cytotoxicity and genotoxicity of silver nanoparticles of different sizes in CHO-K1 and CHO-XRS5 cell lines. *Mutat Res Genet Toxicol Environ Mutagen* 795:70–83
- Stang A, Witte I (2009) Performance of the comet assay in a high-throughput version. *Mutat Res Genet Toxicol Environ Mutagen* 675:5–10
- Stoccoro A, Di Bucchianico S, Uboldi C, Coppedè F, Ponti J, Placidi C, Blosi M, Ortelli S, Costa AL, Migliore L (2016) A panel of *in vitro* tests to evaluate genotoxic and morphological neoplastic transformation potential on Balb/3T3 cells by pristine and remediated titania and zirconia nanoparticles. *Mutagenesis* 31(5):511–529
- Stone V, Johnston H, Schins RP (2009) Development of *in vitro* systems for nanotoxicology: methodological considerations. *Crit Rev Toxicol* 39:613–626
- Suriyaprabha R, Balu KS, Karthik S, Prabhu M, Rajendran V, Aicher WK, Maaza M (2019) A sensitive refining of *in vitro* and *in vivo* toxicological behavior of green synthesized ZnO nanoparticles from the shells of *Jatropha curcas* for multifunctional biomaterials development. *Ecotoxicol Environ Saf* 184:109621
- Suzuki T, Miura N, Hojo R, Yanagiba Y, Suda M, Hasegawa T, Miyagawa M, Wang RS (2016) Genotoxicity assessment of intravenously injected titanium dioxide nanoparticles in gpt delta transgenic mice. *Mutat Res Genet Toxicol Environ Mutagen* 802:30–37

- Tahara H, Sadamoto K, Yamagiwa Y, Nemoto S, Kurata M (2019) Investigation of comet assays under conditions mimicking ocular instillation administration in a three-dimensional reconstructed human corneal epithelial model. *Cutan Ocul Toxicol* 38:375–383
- Thybaud V, Dean S, Nohmi T, de Boer J, Douglas GR, Glickman BW, Gorelick NJ, Heddle JA, Heflich RH, Lambert I, Martus HJ (2003) In vivo transgenic mutation assays. *Mutat Res Genet Toxicol Environ Mutagen* 540(2):141–151
- Tian S, Cyr A, Zeise K, Bryce SM, Hall N, Bemis JC, Dertinger SD (2020) 3Rs-friendly approach to exogenous metabolic activation that supports high-throughput genetic toxicology testing. *Environ Mol Mutagen* 61(4):408–432
- Tice R, Vasquez M (1998) Protocol for the application of the pH > 13 alkaline single cell gel (SCG) assay to the detection of DNA damage in mammalian cells. *Sigma (x-100)* 503:465–8353
- Turner PV, Pekow C, Vasbinder MA, Brabb T (2011) Administration of substances to laboratory animals: equipment considerations, vehicle selection, and solute preparation. *J Am Assoc Lab Anim Sci* 50(5):614–627
- Valdiglesias V, Costa C, Kiliç G, Costa S, Pásaro E, Laffon B, Teixeira JP (2013) Neuronal cytotoxicity and genotoxicity induced by zinc oxide nanoparticles. *Environ Int* 55:92–100
- Vandghanooni S, Eskandani M (2011) Comet assay: a method to evaluate genotoxicity of nano-drug delivery system. *BioImpacts* 1(2):87
- Vecchio G, Fenech M, Pompa PP, Voelcker NH (2014) Lab-on-a-chip-based high-throughput screening of the genotoxicity of engineered nanomaterials. *Small* 10:2721–2734
- Vega-Villa KR, Takemoto JK, Yáñez JA, Remsberg CM, Forrest ML, Davies NM (2008) Clinical toxicities of nanocarrier systems. *Adv Drug Deliv Rev* 60:929–938
- Vila L, García-Rodríguez A, Cortés C, Marcos R, Hernández A (2018) Assessing the effects of silver nanoparticles on monolayers of differentiated Caco-2 cells, as a model of intestinal barrier. *Food Chem Toxicol* 116:1
- Vuković B, Milić M, Dobrošević B, Milić M, Ilić K, Pavičić I, Šerić V, Vrček IV (2020) Surface stabilization affects toxicity of silver nanoparticles in human peripheral blood mononuclear cells. *Nanomaterials* 10(7):1390
- Wahnschaffe U, Bitsch A, Kielhorn J, Mangelsdorf I (2005) Mutagenicity testing with transgenic mice. Part I: comparison with the mouse bone marrow micronucleus test. *J Carcinog* 4:3
- Wallin H, Kyjovska ZO, Poulsen SS, Jacobsen NR, Saber AT, Bengtson S, Jackson P, Vogel U (2017) Surface modification does not influence the genotoxic and inflammatory effects of TiO₂ nanoparticles after pulmonary exposure by instillation in mice. *Mutagenesis* 32(1):47–57
- Wang JJ, Sanderson BJ, Wang H (2007) Cyto- and genotoxicity of ultrafine TiO₂ particles in cultured human lymphoblastoid cells. *Mutat Res* 628:99–106
- Wang Y, Zhang H, Shi L, Xu J, Duan G, Yang H (2020) A focus on the genotoxicity of gold nanoparticles. *Nanomedicine*. <https://doi.org/10.2217/nmm-2019-0364>
- Warheit DB, Donner EM (2010) Rationale of genotoxicity testing of nanomaterials: regulatory requirements and appropriateness of available OECD test guidelines. *Nanotoxicology* 4(4):409–413
- Watson C, Ge J, Cohen J, Pyrgiotakis G, Engelward BP, Demokritou P (2014) High-throughput screening platform for engineered nanoparticle-mediated genotoxicity using CometChip technology. *ACS Nano* 8(3):2118–2133
- Weingeist DM, Ge J, Wood DK, Mutamba JT, Huang Q, Rowland EA, Yaffe MB, Floyd S, Engelward BP (2013) Single-cell microarray enables high-throughput evaluation of DNA double-strand breaks and DNA repair inhibitors. *Cell Cycle* 12(6):907–915
- Wiklund SJ, Agurell E (2003) Aspects of design and statistical analysis in the Comet assay. *Mutagenesis* 18(2):167–175
- Wilde S, Dambowsky M, Hempt C, Sutter A, Queisser N (2017) Classification of in vitro genotoxicants using a novel multiplexed biomarker assay compared to the flow cytometric micronucleus test. *Environ Mol Mutagen* 58(9):662–677
- Witt KL, Livanos E, Kissling GE, Torous DK, Caspary W, Tice RR, Recio L (2008) Comparison of flow cytometry- and microscopy-based methods for measuring micronucleated reticulocyte

- frequencies in rodents treated with nongenotoxic and genotoxic chemicals. *Mutat Res* 649:101–113
- Wood DK, Weingeist DM, Bhatia SN, Engelward BP (2010) Single cell trapping and DNA damage analysis using microwell arrays. *Proc Natl Acad Sci* 107(22):10008–10013
- Xie H, Mason MM, Wise JP Sr (2011) Genotoxicity of metal nanoparticles. *Res Environ Health* 26: 251–268
- Yang H, Wu Q, Tang M, Kong L, Lu Z (2009) Cell membrane injury induced by silica nanoparticles in mouse macrophage. *J Biomed Nanotechnol* 5:528–535, Chapter 5
- Zal Z, Ghasemi A, Azizi S, Asgarian-Omran H, Montazeri A, Hosseinimehr SJ (2018) Radioprotective effect of cerium oxide nanoparticles against genotoxicity induced by ionizing radiation on human lymphocytes. *Curr Radiopharm* 11(2):109–115
- Zangeneh M, Nedaei HA, Mozdarani H, Mahmoudzadeh A, Salimi M (2019) Enhanced cytotoxic and genotoxic effects of gadolinium-doped ZnO nanoparticles on irradiated lung cancer cells at megavoltage radiation energies. *Mater Sci Eng C* 103:109739
- Zhang Q, Zeng SX, Lu H (2015) Determination of maximum tolerated dose and toxicity of Inauhzin in mice. *Toxicol Rep* 2:546–554
- Zhu L, Chang DW, Dai L, Hong Y (2007) DNA damage induced by multiwalled carbon nanotubes in mouse embryonic stem cells. *Nano Lett* 7:3592–3597
- Zhu HM, Huang PC, Zhao TT, Zhou CH, Li RW, Yu CR, Chen ZY, Gu LF, Chang Y (2020) In vitro genotoxicity study of silver nanoparticles and titanium dioxide nanoparticles. *Yi Chuan* 42(12):1192–1200. <https://doi.org/10.16288/j.ycz.20-161>



S. Ajikumaran Nair and V. Gayathri

20.1 Introduction

The term scaffold refers to a tailor-made plinth to support, repair, and augment the performance of an edifice. Scaffolds have a peerless role in accelerating tissue regeneration and repair. The scaffold acts as an interim synthetic extracellular matrix (ECM) for cell-cell interaction prior to forming new tissue. Scaffolds should provide ample space for cell adhesion, proliferation, and differentiation. It must be strong enough to impart mechanical strength, highly porous to act as an artificial ECM required to accommodate pluripotent cells for growth and regeneration in three dimensions. The scaffolds are an inevitable part of tissue engineering (TE) and regenerative medicine, the toxicity of scaffolds, along with the other two components, such as growth factors and cells (stem cells), influences the success. The inherent toxicity of the scaffold materials or its by-products formed due to biodegradation elicits various cascades of immunological reactions, including inflammation, necrosis, and graft rejection. So every scaffold should be validated thoroughly for its possible toxicity in tissue microenvironment *in vitro* or *in vivo* by assessing their actions, such as cytotoxicity, proliferation, cell morphology, tissue architecture, cytopathy, cell interconnectivity, and protein and gene expressions.

S. Ajikumaran Nair and V. Gayathri contributed equally to this work.

S. A. Nair · V. Gayathri (✉)

Phytochemistry and Phytopharmacology Division, KSCSTE-Jawaharlal Nehru Tropical Botanic Garden and Research Institute (KSCSTE-JNTBGRI), Palode, Thiruvananthapuram, Kerala, India
e-mail: gayathriyaswer@jntbgri.res.in

This chapter discussed the scaffold materials and their applications linked to toxicity in detail.

20.2 Various Scaffold Materials and Their Possible Toxicity

The scaffolds are classified into two main groups, synthetic (polymeric and inorganic) and natural. The synthetic scaffolds possess greater mechanical strength and regulated degradation pattern, but they have inherent toxicity when implanted inside live tissue. To circumvent the problem, scaffolds are engineered so as to minimize the toxicity by adding various substances like polycarbonates, which produce less acidic degradation products. For higher mechanical support of scaffolds, poly (fumarate)s are incorporated, which can be crosslinked due to the double carbon bond in their backbone suitable for hard and soft TE applications. Recently more advanced scaffolds are synthesized by natural product materials. Natural product materials are proven to be less toxic from time immemorial and are eco-friendly too. Scaffolds of 2D/3D architecture were synthesized either from synthetic or natural products, but more compatible and less toxic scaffolds were synthesized as composite materials from these two classes.

20.2.1 Synthetic Scaffolds Materials

The main demands on biomaterials for TE scaffolds are that they serve the bulk mechanical and structural requirements of the target tissue and enable molecular interactions with cells that promote tissue healing. In this context, synthetic polymers are attractive materials for constructing scaffolds, which are typically more flexible than natural materials. Moreover, it is reasonably easy to control its mechanical and chemical properties, and they are readily available and relatively inexpensive too. Synthetic scaffold materials are generated by chemical/physical processes as polymeric or inorganic biomaterials suitable for TE. Some of the best known polymeric synthetic scaffold materials are poly(ethylene glycol) (PEG), poly(vinyl alcohol) (PVA), poly(acrylic acid) (PAA), poly(2-hydroxyethyl methacrylate) (PHEMA), poly(lactic acid) (PLA), poly(glycolic acid) (PGA), poly(lactic-co-glycolic acid) (PLGA), poly(ϵ -caprolactone) (PCL), poly(phosphazene)s, and polypropylene fumarate (PPF). Inorganic ceramic, synthetic scaffold materials include bioactive glass, alumina, zirconia, hydroxyapatite (HA), sintered hydroxyapatite, α and β tricalcium phosphate (TCP), tetra calcium phosphate and calcium phosphate. The biocompatibility and toxicity of these synthetic scaffolds are varying. Poly(ethylene glycol) (PEG) or poly(ethylene oxide) (PEO, at high molecular weights) is an extremely hydrophilic polymer with excellent solubility in a range of solvents and high solution mobility. It is used extensively in TE, particularly as a component of hydrogels due to its ability to imbibe water. It is inert to housekeeping enzymes and constitutive protein thus not interfering with biological cues. Although these features are ideal, they cannot fully provide an ideal environment for cell adhesion

and tissue formation due to their bio-inert nature. In TE applications, PVA is a widely used polymer due to its exceptional weight-bearing properties, high porosity, and compatibility. The literature showed PVA has good biomechanical properties and forms highly porous scaffolds in combination with agents like sucrose. Still, the lack of *in vivo* biocompatibility of this composite material and inflammatory responses, when implanted in preclinical animal models, are the major limitations (Place et al. 2009). In addition, the toxicity of the material is a major challenge as they cause the accumulation of material in the form of xenobiotics, which are either conjugated to get eliminated from the system or accumulate over time in the circulation, causing foreign body interaction with the immune cells.

Even though PVA hydrogels are widely used in constructing mono or bilayered scaffolds, they demonstrated acute tissue responses in animal models (Onuki et al. 2008). To reduce the acute inflammatory response of PVA, its composites of sucrose, PLGA, PGA or N, O-carboxymethyl chitosan (NOCC) were used, which bear high strength and porosity compatible to produce cardiovascular devices, dialysis membranes, wound dressings and are suitable for drug delivery. In an *in vivo* biocompatibility and toxicity study of PVA/NOCC scaffold in rats, the subcutaneous implantation of the composite elicited low tissue toxicity and limited inflammatory responses. The serum biochemical parameters of the test (PVA/NOCC) are significantly close to the control animals, but the tissue sensitivity and inflammatory responses deviate from the standard values (Place et al. 2009; Kamarul et al. 2014). PVA/PAA and its derivatives, such as poly(2-hydroxyethyl methacrylate) (PHEMA), are nonbiodegradable. While implanting these scaffolds as permanent ones, they must be chemically modified (e.g., by introducing ester linkages) or used with low polydispersity index materials to ensure elimination from the body. The biodegradability of PHEMA hydrogels was increased by adding PCL segments, and the degradation rate can be controlled by PCL chain length and crosslinking density in the PHEMA backbone (Atzet et al. 2008).

The most widely used synthetic biodegradable polymers are poly(α -hydroxy acids), e.g., PLA, PGA, PCL, and their copolymers, approved by the FDA as bioscaffolds. They can persist in a robust state for sufficient time to allow for the formation of new tissue, ultimately degrading and becoming replaced by tissue/s. These polyesters degrade by hydrolysis, eventually releasing oligomers or monomers that are the products of normal metabolic pathways. This scaffold is versatile in the medical field as wound dressings, degradable sutures, stents, etc. Still, the challenging problem is their inherent hydrophobicity associated with poor wetting nature and lack of cellular attachment/interaction (Vroman and Tighzert 2009). Though these materials possess less toxicity, their remnant in the body may act as a foreign substance for the immune cells thus increasing the immune response over time, resulting in a toxic burden to tissues. PPF is linear polyester, based upon fumaric acid backbone, which on biodegradation resulted in propylene glycol, poly-(acrylic acid-co-fumaric acid), and fumaric acid, an intermediary substance of Krebs cycle. The tissue response to PPF depends on both the polymer and its degradation by-products. PPF has already been shown to be non-cytotoxic to many cells. However, the toxicity of degradation products of PPF is not evaluated in an

in vivo approach (Kasper et al. 2009). Propylene glycol, one of the by-products of PPF, is toxic in large intravenous doses; it induces renal insufficiency, hepatic dysfunction, hyperosmolality, lactic acidosis, acute kidney injury, and sepsis-like syndrome in patients (Zar et al. 2007).

A relatively new (and promising) class of polymer is the poly(phosphazene)s, which are attractive due to their structural adaptability to afford a high level of control over degradation, crystallinity, and other characteristics (Song et al. 2018). However, the toxicity of this material is still in question as the degraded products are not completely eliminated, and the immune response is high.

Bioactive glass is another vital scaffold material in bone TE. The uniqueness of these scaffolds is the easiness of specifying the desired rate of degradation by controlling its chemical composition. This advantage is optimized by setting their chemical composition, thermal and environmental processing mechanisms. Even though the glass scaffolds are easy to use in bone TE, the primary defect is their limited load-bearing capacity, mechanical strength, and fracture toughness (Fu et al. 2011). Due to the less load-bearing capacity, this material rarely supports cell adhesion, which accelerates morphological changes in the cells due to the long duration of cell-material interaction, leading to cellular toxicity and undesirable immunogenicity. A specific composite scaffold constructed with a ceramic mimic bone structural hierarchy with a thin polymer layer improves mechanical properties, cell attachment, and proliferation. HA-modified by MnO_2 for bone TE applications by sol-gel and precipitation methods demonstrated that they possessed higher compressive strength, toughness, hardness, and density when compared to the pure HA scaffolds. The in vitro biological analysis using human osteoblast cells reveals that HA-modified scaffolds are biocompatible with adequate ALP activity (Azizi et al. 2020). Many biocompatible ceramic scaffolds are designed with HAP, calcium hydroxyapatite (CHA), and PLGA, named as ALBO-OS with very high porosity. HAP and CHA were chosen as one of the most widely used ceramic materials in bone TE as it represents the component of natural bone. Besides improving mechanical properties, PLGA coating enhances the scaffold surface for various cell activities, like adhesion, density, and proliferation (Polo-Corrales et al. 2014). Likewise, the HAP-Burr hole button (HAP-BHB) scaffolds were seeded with mesenchymal stem cells for quick regeneration processes showing that the scaffold material is nontoxic up to 0.5 g/mL in MTT assay. The apoptotic activity of HAP-BHB is similar to control cells, but a deviation in the generation of reactive oxygen species was designated. In scanning electron and confocal microscopic evaluation, the scaffold is biocompatible, and it lacks toxicological cellular response to immune cells (Gayathri et al. 2016). In cultured fibroblast treated with finely ground HAP powders exhibits cytotoxicity than larger particles and concluded that it is because of their physical presence independent of any toxic chemical effect (Evans 1991). Hydrolytic degradation of ester linkages and crystallinity are the major factors deciding the controlled degradation of synthetic scaffolds; maintaining an ideal condition for these factors is complex, and hence it is considered a major drawback in synthetic scaffolds. Another vital character need for an excellent scaffold is the accessibility of water into the scaffold; this is decided by the

polymer's glass transition temperature (T_g) and crystallinity. Maintaining a suitable T_g and crystallinity in synthetic scaffold for accessing water to the polymer chains is another major task (Nikolova and Chavali 2019; Chen and Liu 2016).

A wide array of synthetic scaffolds are used in TE applications, but most of them lack biological cues inherent in natural materials so that synthetic scaffolds can promote desirable cell responses minimally and lack ample toxicity evaluation protocol (Nikolova and Chavali 2019). In view of this, alternate natural processes can be recreated in biomaterials by incorporating matrix proteins such as chitosan, collagen, or fibrin to facilitate tissue regeneration and vascularization (Chen and Liu 2016). They need to be cell inductive and conductive, possessing mechanical properties, geometrically and functionally designed to mimic the native ECM environment. 3D printed scaffolds play an essential role in TE as they allow tissue ingrowth with the degradation of scaffolds (Nikolova and Chavali 2019; Wang et al. 2015). Nevertheless, as already discussed, toxicological screening and the *in vitro*/*in vivo* toxicity is again a challenge as the by-products of these materials get converted to xenobiotics triggering the cellular immune response.

20.2.2 Natural Products Scaffold Materials

Natural products in scaffold development is a fascinating arena that is still in its infancy. Owing to green technology and environmentally safe, natural product biomaterials draw considerable attention in the area of scaffold construction and the development of new devices for biomedical applications. Advancements in pharmaceutical chemistry, especially in continuous flow chemistry, augment the generation of more unique scaffolds of natural product origin. These flow protocols facilitate effective comparison between chemical approaches and natural products hand in hand (Antonella et al. 2021). Major natural products utilised in scaffold synthesis are pectin, bacterial cellulose, chitosan sulfate, alginate, hyaluronan, gellan gum (GG), β -chitin, silk fibroin, gelatin, collagen, and glycosaminoglycans (GAGs). Soy protein and β -chitin are the natural by-products turned out from food industries which are excellent biomaterials for the synthesis of sponge-like 3D scaffolds (Las Heras et al. 2020). The sponge-like scaffolds (SLS) possess exceptional physico-chemical properties, which provide cues for cell adhesion, proliferation, and high cell loading capacity. Furthermore, cytotoxicity is negligible *in vitro*; prominent collagen fibers deposition together with enhanced neovascularization makes it an excellent biocompatible material (Las Heras et al. 2020). Simultaneously, these materials cause immunotoxicity which is greater due to the undesired eliciting of a major histocompatibility complex. Pectin is another plant-derived material smooth, hairy, or branched in nature obtained from the citrus industry. It has suitable gelling properties, solubility, and is nontoxic; hence, it is used in TE, drug delivery, wound dressings, and other medical applications. Highly porous 3D pectin scaffold synthesized by freeze-drying technique *in vivo* experiment shows the anti-adhesion effect with enhanced mesenchymal stem cell growth in the peritoneal cavity (Kulikouskaya et al. 2019). Pectin/polysaccharide and peptides unit-based

biopolymers are used as an alternative for ECM. Pectin from plant cells mimics the artificial ECM. Derivatives of pectin scaffolds are used as a substitute for bone scaffold preparations, wherein the scaffold microsphere enhances the adhesion, proliferation, and differentiation of mesenchymal stem cells to osteocytes. These properties listed pectin as a suitable vehicle for green bone scaffold preparation (Munarin et al. 2011). The major challenge in the pectin-based scaffold is its purity; otherwise, it contains mutagenic agents prompting mutagenicity in cells. Another natural, green, and safe material is silk fibroin which exhibits biocompatibility, biodegradability, and enhanced biological and mechanical strength. Modification of the 3D porous structure of silk fibroin with graphene oxide (GO) results in a scaffold with good biodegradability, drug release, and biocompatible properties. Silk fibroin and titanium dioxide (TiO₂) gave nanocomposite scaffolds for bone tissues with enhanced bioactivity, biocompatibility, and structural strength (Johari et al. 2020; Nguyen et al. 2019). Polysaccharides in the form of biomaterials from *Beta vulgaris* were electrospun in a nylon matrix as nanofibers provided good mechanical strength. Immunocytochemistry testing of these composites was comparable to the native skin tissues, and these green composite scaffolds retained keratinocytes function (Ranjbarvan et al. 2018; Jahangirian et al. 2018). In the skin regeneration test, a scaffold made out of hydroxyethyl cellulose (HEC)/silver nanoparticles showed enhanced skin regeneration with sustained cell morphology, high water absorption capacity, and desirable biodegradation. It is devoid of toxicity because the silver ions produced are reduced by HEC without any chemical template (Zulkifli et al. 2017; El-Sheikh et al. 2013). Bacterial cellulose (BC) is another crucial candidate in biomedical applications as it has good biodegradability, network structure, high mechanical strength, good water absorption capacity, and easiness of preparation. Scaffold prepared from BC of *Gluconacetobacter xylinus* displayed 50% increment in human chondrocytes proliferation without inducing significant activation of pro-inflammatory cytokine (Svensson et al. 2005). However, its insufficient porosity structure and low biocompatibility in humans limit its application in TE. Though the above scaffolds showed no cytotoxicity, they may elicit an immune response as their degraded by-products are not entirely metabolized in the body leading to metabolic toxicity.

Electrospun hydrophilic nanofibrous mat fabricated from the polycaprolactone, chitosan sulfate, and gelatin mixture showed significant cell proliferation due to surface porosity, water contact angle, mechanical strength, chemical structure, and degradability in water (Gomes et al. 2017). Composite glycosaminoglycans (GAGs) scaffolds with gelatin and hyaluronan demonstrated controlled diffusion, improved cell adhesion, and proliferation when seeded with human keratinocyte, fibroblast, and mesenchymal stem cells (Bhowmick et al. 2016). Gelatin nanofibers crosslinked in situ with 1,4-butanediol diglycidyl ether showed mimicked ECM, which displayed no toxicity against fibroblasts and was suitable for skin TE. Collagen and GAG help in re-epithelialization, neovascularization, reduce skin scarring, and accelerate healing mechanisms (Jahangirian et al. 2018; Law et al. 2017). An in vivo experiment in rats with bioscaffolds of gelatin methacryloyl and methacryloyl substituted tropoelastin showed desired characteristics like superior

biocompatibility, mechanical strength, ample porosity, biodegradability, swellability, and significant adhesive activity in hydrogels (Soucy et al. 2018). Besides having many advantages, these scaffolds are selective to specific type of cells and may sometimes show overgrowth of cells affecting cell morphology. Tissue regeneration through clinically effective means of treatment of injured body organs with scaffold has problems of resilience and mechanical power, donor-site morbidity, regular losing of volume, and fibrous capsular structure. Even in 3D constructs, issues of cytotoxicity and cytocompatibility exist. Over and above, the biological scaffolds of composite nature display immune response pose a major challenge.

A composite scaffold is synthesized using chitosan-gelatin hydrogel in bilayered tubular architecture with a non-porous outer layer. In MTT assay and confocal microscopy, this tubular construct seeded with human dermal fibroblasts displayed cell proliferation and cellular adhesion. It also showed 50% *in vitro* biodegradation at 16 days and maintained excellent tubular architecture (Badhe et al. 2017). An electroactive muscle scaffold material made with gellan gum (GG), sponge-like hydrogels (SLH), and polypyrrole (PPy) to PPy-GG-SLH complex seeded with L929 and C2C12 myoblast cells showed less toxicity and significant adhesion and proliferation (Berti et al. 2017). Even though it provides an alternative electroactive platform for testing electrical stimulation on skeletal muscle, the toxicity of leached remnants from the PPy-GG-SLH material is a challenge. Recently, a core-shell nanofiber mesh-GelMA is synthesized by coaxial electrospinning and photo-crosslinking of gelatin and polycaprolactone units for vascular TE. Here, the polycaprolactone act as the core and functionalized gelatin is the shell, wherein water contact angle and amount of gelatin are inversely proportional. Normal human dermal fibroblast cells seeded in the GelMA mesh showed cell proliferation *in vitro* with excellent biocompatibility; attenuated hemolytic and thrombogenic characters (Coimbra et al. 2017).

A modified scaffold of alginate hydrogel conjugated with gelatin and heparin (Alg-G-H) in the presence of skeletal muscle ECM augments proliferation and differentiation of human skeletal muscle progenitor cells (hSMPCs) *in vitro* (Yi et al. 2017). In addition, even though these materials are cytocompatible, they enhance immunotoxicity by eliciting major histocompatibility complex and other immune cells.

Green and safe systems for generating myelinated Schwann cells (SC) are important aspects for treating peripheral nerve damage (Jessen et al. 2015). Polyurethane scaffold prepared by the polycondensation of poly(glycerol sebacate) and aniline pentamer helps to regenerate SC myelin gene expression and neurotrophin secretion. These biodegradable polyurethanes are useful in nerve TE (Vogt et al. 2021; Wu et al. 2016).

Collagen is a triple-helix structural protein found in skin, bones, cartilage, tendons, and ligaments extensively used in the synthesis/fabrication of various scaffold materials. In a study, a cellular scaffold synthesized from PLGA microcarriers with collagen as the adhesive agent provided an excellent platform for cell support and proliferation to engineered NT-3 overexpressing cells. This 3D

scaffold is sufficient to overexpress the neurotrophin-3 and the expression of tyrosine hydroxylase, which promotes the intracellular signaling pathway of dopaminergic neuron differentiation. This is a promising result in the treatment of neuronal damage by TE (Dhandayuthapani et al. 2011). Nerve conduits peripheral nerve fasciculi were constructed with multiwalled silk fibroin/silk sericin conduits instigated nerve regeneration aiding in the treatment of nerve damage (Wang et al. 2018). The electrospun core of PLLA nanofibrous incorporated with vascular endothelial growth factor (VEGF) and recombinant human nerve growth factor (NGF) proved effective management for nerve malfunction in nerve injury. These core-shell nanofibrous scaffolds helped in sciatic nerve restoration (Chen et al. 2015a; Nazarnezhad et al. 2020). Hurdles in neural TE include toxicity associated with inflammation and fibrosis upon implantation of external material into the nervous system as the self-renewal of cells and neural tissues is limited. Among the other well-known nerve conduits of silk fibroin composite origin, nerve regeneration in a silk fibroin-blended poly(L-lactide-co- ϵ -caprolactone) SF/P(LLA-CL) is better than that poly(L-lactide-co- ϵ -caprolactone) P(LLA-CL) conduit. The study shows that SF/P(LLA-CL) enhances fibroblast growth in vitro; neovascularization, and regeneration of axon and Schwann cells in vivo (Wang et al. 2018). Wound dressing material fabricated by electrospun recombinant spider silk protein/PCL blend (pNSR16/PCL) submicrofibrous mat seeded with NIH-3T3 cells in MTT assay displayed less toxicity. NIH-3T3 cells on pNSR16/PCL composite scaffolds showed better cell adhesion than PCL scaffolds; moreover, immunohistochemistry proved no cytotoxicity on normal cell growth. However, the pNSR16/PCL composite meets the criteria for a good biomaterial, and the actual efficacy as a human scaffold material is not yet validated (Zhao et al. 2013).

Decellularized natural scaffold materials have gained interest, as the growth of cells is much faster in these constructs compared to the other bio-engineered ones. The severity of immunogenicity of the host toward the decellularized scaffold and grafted cells depends on the biocompatibility of the construct. Although these scaffolds showed less cytotoxicity, a series of in vitro and in vivo biocompatibility tests are needed to assess the toxicity. Decellularized matrices obtained from animals or humans underwent rigorous toxicity evaluation to look upon their possible biocompatibility by determining their in vitro/in vivo cytotoxicity, pathogenicity, immunogenicity, and biodegradability (Hussein et al. 2016). In a study, scaffolds constructed from bladder submucosa, small intestinal submucosa, acellular corpus spongiosum matrix, and polyglycolic acid seeded with rabbit corporal smooth muscle cells in MTT assay and mechanical evaluation displayed all are nontoxic and biocompatible.

Furthermore, although each scaffold demonstrated suitable mechanical properties for TE, the acellular corpus spongiosum matrix showed superior qualities for urethral reconstruction applications (Rashidbenam et al. 2019). In addition to the synthetic/natural product macro/micro composite materials, scaffolds of nano-scales were also developed. These materials draw significant advances in the area of TE due to their superior qualities, and hence their toxicological evaluation is an important factor.

20.3 Advances in Scaffold Engineering: Nanoscaffolds and Related Toxicity

Casting biodegradable polymer into a porous fibrous nanoscaffold through thermally induced phase separation (TIPS) to resemble ECM is a beneficial approach in TE. Apatite ceramic component incorporated into polymer forms nanofibrous scaffolds, which provides a structure that aids in cell adhesion, proliferation, and differentiation in bone TE. It is noted that the incidence of apoptosis in polymer alone scaffold is greater than ceramic–polymer scaffolds. The development of a synthetic analog of the extracellular matrix (ECM) is a painstaking task as it involves characteristics to regulate cell behavior and tissue progression for various biomedical applications. It also involves micro- and nanofabrication techniques to produce scaffolds with tight control over its characteristics, including the physical, chemical, geometrical, and mechanical characteristics. Advanced constructs consist of dual layers of cells and nano-scale biocompatible polyelectrolyte (PE) in an alternate fashion to mimic the *in vivo* co-layered cells. Herein, the PE scaffold aided in hepatocytes morphology, cytoskeletal structure, and the nanoscaffold provided a cell-adhesive surface for proliferation thus maintaining the layered architecture of the liver (Rajagopalan et al. 2006). The approach signifies nanoparticle integration into the nano-structured scaffolds to deliver biologically active molecules like growth and differentiation factors so as to regulate cell behavior for optimal tissue regeneration (Nikolova and Chavali 2019). Amine-capped aniline trimer with dimethylol propionic acid, polylactide, and hexamethylene diisocyanate on elastomeric polyurethane–urea copolymers nanomaterial provided a surface for elastic tissues like skeletal muscle, cardiac muscle, and nerve to regenerate (Jahangirian et al. 2018; Chen et al. 2015b). The major hurdle in organ transplantation is tissue rejection. To avoid this, the use of TE regenerates required tissues or organs. This can be done by biocompatible dendrimers, which mimic the 3D microenvironment of human-ECM. In neural TE, dendritic nanoparticles are introduced into the scaffold to increase its effectiveness, and here also the toxicology evaluation platform is not available for the same (Accardo et al. 2020). Neural regenerative medicine is a complex system involving ECM and tight junctions where neurons are synapsed and are supported by the ECM (Ferrer-Ferrer and Dityatev 2018). Treatment of peripheral nerve injuries is limited. Furthermore, the nanobiomaterials are supplemented with growth factors that produce unique biological niches that promote nerve regeneration and functional recovery (Aijie et al. 2018). Nanofibrous structures made of PLLA and polyaniline for cardiac TE- and CM-based 3D bio actuators have been reported of nontoxicity. These PLLA/polyaniline conductive nano compounds displayed great electroactivity, cell viability, cell-cell interactions, maturation, and increased differentiation of H9c2 cardiomyoblasts (CM). It was also noted that these sheets augmented the automatic beating frequency of primary CMs, which was similar to ECM in cardiac tissue (Wang et al. 2017).

As discussed in this section, nano scaffolds give great opportunity in TE, but the major challenge faced by nanomaterials is their toxicity. The toxicity of nanomaterial is due to its dissolution as individual components inside the body

which are taken up by the immune cells and trigger an immune response involving cytokines and chemokines, which make the body immune and susceptible to various infections over a period of time. They also demonstrated cellular apoptosis and necrosis, which have to be tackled.

20.4 Toxicity Evaluation Tests of Scaffolds

The main limitation of toxicological assessment in current scaffold engineering is the lack of complete and acceptable guidelines to evaluate scaffold material toxicity. Hence, we depend on tests approved by various international standard organizations. International Standards Organization (ISO) 10993 sets a series of 20 standard tests to evaluate the biocompatibility of scaffold materials for utilizing in medical devices and clinical studies. In this way, before going for the tests, one has to decide the type of tests the medical device has to undergo, considering various factors involved in the toxicity of scaffold materials. The factors influencing the toxicity of scaffold materials are summarized in Fig. 20.1.

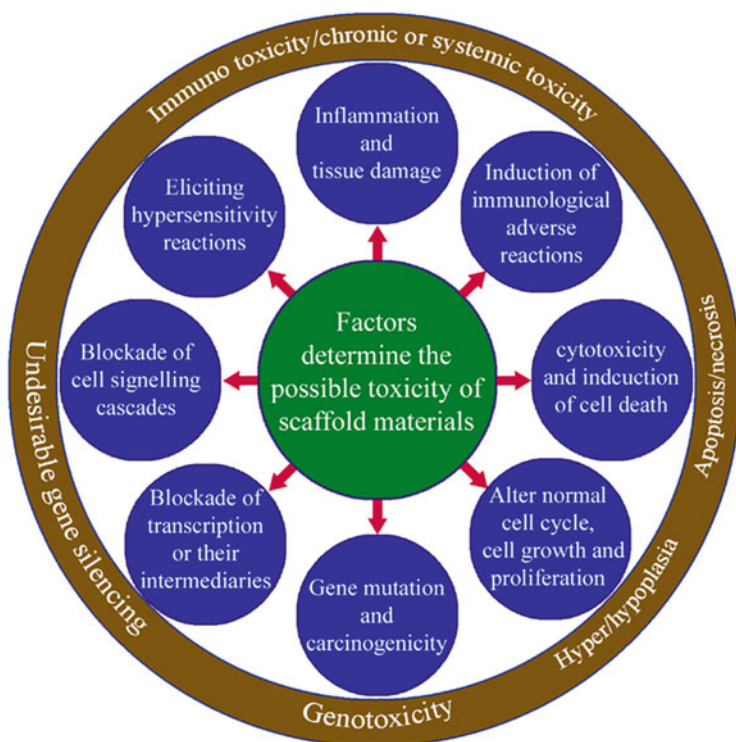


Fig. 20.1 Major factors to be considered to evaluate the toxicity of scaffold materials to determine their utility in TE purposes and medical device applications (Seyedmajidi et al. 2018; Cao et al. 2009; Yan et al. 2019; Leng et al. 2020; Reddy et al. 2021; Copes et al. 2019; Clowes 1993)

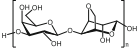
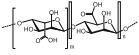
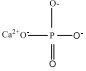
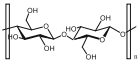
In addition to these factors, the nature of body contact, contact duration, and clinical trials would need to comply with the guidelines of ISO 10993, Good Manufacturing Practices (GMP), Organisation for Economic Co-operation and Development (OECD), and International Council for Harmonisation (ICH). Together with regulatory authorities and pharmaceutical industries, these guidelines determine the technical requirements for medical devices and pharmaceuticals for human use. Some basic criteria for the suitability and toxicity of a scaffold for their use in TE regardless of the tissue type are addressed below:

1. **Cytocompatibility and biocompatibility:** Scaffold must be cell compatible, wherein they must allow cell adhesion, function, and migration onto the surface and penetrate through the scaffold to proliferate in the new matrix. Even though it has cytocompatibility, certain scaffold materials eliciting severe inflammatory responses culminate in graft rejection (Chen and Liu 2016).
2. **Degradability and storage properties:** Scaffolds are a support system that eventually allows the body's own cells to replace the implanted scaffold thus producing ECM. Scaffold degradation is an important point; the degradation by-products may also be nontoxic and must be eliminated from the body without interference with other organs. A scaffold needs to be economical, and it also needs to follow good manufacturing practice (GMP) standards during its construction. This determines the shelf life of the construct before its end-use (Chan and Leong 2008).
3. **Mechanical and porosity properties:** The scaffold should preferably possess mechanical properties similar to the anatomical site of implantation. A challenge faced is the healing rate which is age-dependent in an individual. Many materials have greater mechanical strength and high porosity but fail in *in vivo* implantation due to insufficient capacity for vascularization and poor cell infiltration in the scaffold (Chen and Liu 2016).
4. **Scaffold architecture and cellular interactions:** Cellular penetration and diffusion of nutrients between the cells and ECM are very much evident in scaffolds with high porosity. Additionally, these features support the diffusion of waste like degradation products of scaffold material out of the body without affecting surrounding organs and tissues. The interaction between scaffolds and cells is usually through chemical groups called ligands on the surface of the scaffold material (Chan and Leong 2008).
5. **Choice of biomaterial:** Material used to fabricate a scaffold is also a deciding factor for toxicity. Raw materials used in the TE scaffold need to be assessed for toxicity before the fabrication (Chen and Liu 2016).

Scaffold materials used in various medical applications exhibit different levels of toxicity influenced by the above-described criteria and the factors specified in Fig. 20.1. A precise list of scaffold materials, their application/s, advantages, and possible toxicity are provided in Table 20.1.

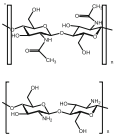
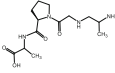
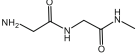
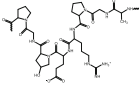
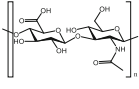
A scaffold biomaterial is advised for a chain of tests in preclinical animal models before approaching clinical trials. Hence, full-proof predictive *in vitro* systems is

Table 20.1 A brief list of scaffold materials and their bio-properties

Scaffold material	Biomedical applications	Advantages	Toxicity (if any)
Agarose (Salati et al. 2020; Varoni et al. 2012) 	Drug delivery, TE, cancer therapy, disease diagnosis, and regenerative medicine.	Biocompatible, cell proliferative, controlled self-gelling properties, high water absorbance capacity, adjustable mechanical properties, increase cell adhesion.	Nontoxic generally, but a phlogistic reaction was reported with neutrophils and mild inflammation around agarose scaffolds.
Alginate (Sahoo and Biswal 2021; Rychen et al. 2017; BIBRA (Bibra Toxicology Advice & Consulting) 1988) 	Bone, skin and cartilage TE, wound dressing, drug delivery.	Biocompatible, biodegradable, quick gelation, abundant availability, and easy to process.	Nontoxic generally, but mild irritation to the eyes and skin sensitization observed. Repeated oral dose of alginic acid and its sodium salt displayed laxative effects in humans and experimental animals.
Bioactive glass (Rahaman et al. 2011)	Bone regeneration	Biocompatible, 3D architecture for excellent cell adhesion and proliferation, controlled biodegradation.	Concentration of boron above threshold level displayed in vitro and in vivo toxicity.
Calcium phosphate cements (Xu et al. 2017; Krambeck et al. 2010) 	Bone TE, drug, and biological molecule delivery.	Biocompatible, predominant compressive strength, osteoconductive, molding capacity, injectable.	In Donryu rats, CPC exhibit slight inflammatory reactions. It also showed in vivo blood clotting and embolism.
Cellulose (Hickey and Pelling 2019; Cullen et al. 2002) 	Cardiac, bone and neural TE, artificial skin development, skin and wound dressing.	Biocompatible, biodegradable, enhance cell adhesion, covalently attach to many bioactive molecules.	Nontoxic generally, but short-term inhalation of cellulose showed toxicity and inflammation. Nanofibrillated cellulose did not exhibit any toxicity to skin and eyes but demonstrated significant cytotoxicity to skin cells.

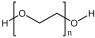
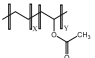
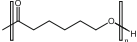
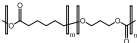
(continued)

Table 20.1 (continued)

Scaffold material	Biomedical applications	Advantages	Toxicity (if any)
Chitin/chitosan (Cullen et al. 2002; Croisier and Jérôme 2013) 	Skin, bone, cartilage, and neural TE, drug delivery system, wound dressing.	Biocompatible, biodegradable, mucoadhesive, antimicrobial, cell proliferative, gel-forming properties.	CS is less toxic; the micro- and nanoparticles of CS induce inflammasome by macrophages.
Collagen (Ibrahim and El-Zairy 2015; Khan and Khan 2013) 	Blood vessel, bone, cartilage, ligament, nerve, skin tendon TE, wound dressings, drug delivery system.	Biocompatible, biodegradable, porous, high tensile strength, fibril-forming ability, abundant.	Nontoxic generally. Crosslinked collagen displayed mild toxicity. In rabbits, soluble collagen infusion induces respiratory distress, agitation, convulsions, increases in total cardiac and hepatic lactate dehydrogenase, and liver damage.
Fibrinogen and fibrin (Gomes et al. 1991) 	Skin TE, drug delivery system, as bioadhesive.	Biocompatible, biodegradable; increase cell adhesion and proliferation.	Nontoxic generally and exhibits minimal inflammation.
Gelatin (García 2018; Bello et al. 2020) 	Artificial skin, stents, implants, drug delivery systems, engineered grafts, cell sheets.	Biocompatible, biodegradable, resistant to heat and enzymatic denaturation.	Nontoxic generally, but scaffold synthesized of with other agents like glutaraldehyde showed mild to moderate cytotoxicity.
Glycosaminoglycans (Moeller et al. 2016; Ayerst et al. 2017) 	Cardiac implants, wound dressings, bone, vascular, neural, skin and cartilage TE.	Biocompatible, biodegradable, antithrombotic, and anticoagulant properties.	Nontoxic generally, but microbial contamination-associated toxicity and pathogenesis are frequently observed. In addition, it acts as a pathological chaperone, inducing amyloidosis.

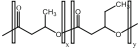
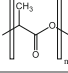
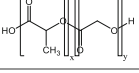
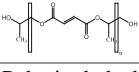
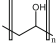
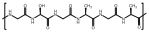
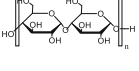
(continued)

Table 20.1 (continued)

Scaffold material	Biomedical applications	Advantages	Toxicity (if any)
Hydroxyapatite (Iannuzzi et al. 2015; Kattimani et al. 2016)	Bone TE.	Biocompatible, bioaffinitive, bioactive, osteoconductive, osteointegrative, osteoinductive.	Nontoxic generally, but HAP nanoparticles at high concentrations caused genotoxicity and cytotoxicity due to its oxidative stress in hepatocytes.
Poly(ethylene glycol) (Sonmez et al. 2016) 	Bone, skin TE, wound dressings, and controlled-release devices	Biocompatible, muco- and bioadhesive, hydrophilic, having elasticity, non-ionic, less immunogenic in normal conditions.	Nontoxic. Prolonged use of PEG initiates a signaling cascade mediated by reactive oxygen species and associated immunological adverse reactions.
Poly(ethylene-co- vinylacetate) (Xu et al. 2017; Osman et al. 2020) 	Implants, contraceptive applications, drug delivery	Biocompatible hydrophilicity.	Observed toxicity associated with higher oxygen consumption <i>Lumbriculus variegatus</i> .
Poly(ϵ -caprolactone) (Meng 2014) 	Bone TE, implants, and drug delivery.	Biocompatible, cytocompatible, regulated cell proliferation, angiogenesis, controled hydrolytic degradation.	Nontoxic in local tissue. The acidic degradation product of PCL (caproic acid, succinic acid, valeric acid, and butyric acid) accumulated in cultured cells reported a negative effect. Caproic acid is an irritant to the lungs, causing cough, shortness of breath, and pulmonary edema.
Poly(caprolactone- co-trimethylene carbonate) (Hajiali et al. 2017) 	Orthopedic implants, cardiac patches, vascular grafts, adhesion barriers, stents, ear implants, drug delivery systems.	Biocompatible, excellent biodegradability, high porosity, superior mechanical strength.	Nontoxic generally. In the exceptional cellular microenvironment, caprolactone hydrolyses to yield hydroxycarboxylic acid, which displayed toxicity.
Poly (3-hydroxybutyrate-	Surgical sutures, drug delivery, tissue	Biocompatible, biodegradable, high	D-3-hydroxybutyrate produced from

(continued)

Table 20.1 (continued)

Scaffold material	Biomedical applications	Advantages	Toxicity (if any)
co-3-hydroxyvalerate) (Rocha et al. 2014; Wang et al. 2013) 	regeneration devices, cardiovascular stents.	absorption capacity, wettability, thermoplasticity.	PHBV is a normal blood constituent, but low toxicity was observed in an in vivo experiment.
Poly(lactic acid (Rivera-Briso and Serrano-Aroca 2018; Tyler et al. 2016) 	Bio-absorbable screws, stents, sutures and are used in peripheral nerve and spinal cord injury regeneration.	Biocompatible, higher mechanical strength, cytocompatibility, good degradation rate, suitable carrier of hydrophilic drugs.	Nontoxic in solid form, but toxic if inhaled and/or absorbed into the skin or eyes as a vapor or liquid.
Poly(lactic-co-glycolic acid (Da Silva et al. 2018; Pandey and Jain 2015; Makadia and Siegel 2011) 	Bone regeneration, gene therapy, implants, tumor targeting.	Excellent cell adhesion, proliferation, accelerated biodegradation.	Accumulation of lactic acid and glycolic acids at high concentrations will cause renal toxicity and alter normal biological responses.
Polypropylene fumarate (Elmowafy et al. 2019) 	Bone tissue engineering.	High tensile strength, biocompatible, lower degradation rate, biostable.	No toxicity was reported.
Poly(vinyl alcohol (Cai et al. 2019) 	Contact lenses, drug delivery systems, wound dressing materials.	Biocompatible, water-soluble; excellent elasticity to support scaffold, non-carcinogenic.	No toxicity was reported.
Silk fibroin (Gaaz et al. 2015; Kundu et al. 2013) 	Bone, vascular, neural, skin, cartilage, ligaments, tendons, cardiac, ocular, and bladder TE.	Biocompatible, biodegradable, bioresorbable, excellent mechanical strength.	Silk fibroin nanoparticles displayed induction of oxidative stress and ROS generation.
Starch (Naserzadeh et al. 2018; Kaur et al. 2007) 	Bone, skin TE drug delivery system	Biocompatible, biodegradable, good swelling power, solubility, gelatinization, rheological characteristics, mechanical behavior, and enzymatic digestibility.	Nontoxic generally but in chemically modified starch- based scaffolds release toxic by-products and also reduce its degradation rate.

recommended. These tests are applicable to the raw components, final material, or finished scaffolds. It is also noted that routine biochemical screening assays are recommended prior to preclinical testing. Chronic, local, and systemic toxicity are also the major criteria in the toxicity evaluation of implantable scaffolds (Myers et al. 2017; International Organization for Standardization (ISO) 10993 2018). Three stages of testing of scaffold materials are necessary to utilize the scaffold materials in TE/in medical device applications. Stage I includes the primary level of testing, which comprises the acute/subacute toxicity phase and more detailed studies, such as establishing the mutagenic and carcinogenic activity of the material (OECD 2018–2020; ICH Topic M3 (R2) 2008). This gives an idea of the bio-function ability of the material/scaffold. In stage II, the test material/scaffold is implanted in an animal model before being used in patients/clinical studies. Information from stage I will help to conduct the procedure. In stage III, the scaffold material which satisfactorily meet all the desired qualities without any conspicuous toxicity will be tested in humans. Some of the systemic biocompatibility tests used to determine the utility of scaffold materials in the clinical application are as follows:

- (a) Cytotoxicity test: The cellular toxicity can be tested by an in vitro platform using MTT and LDH assays, wherein the material interacts with the cells of interest or the end-use of the scaffold. It may be a direct or indirect contact assay (ISO 10993-5:2009(en) 2009).
- (b) Sensitization test: This test involves scaffold or their constituent materials to produce skin sensitization. Sensitization will be ranged from irreversible damage to the skin with visible necrosis in the epidermis, dermis ulceration, or may be manifested as pruritus, erythema, edema, papules, vesicles, or bullae. In immunologically mediated allergic contact dermatitis, the hypersensitive reaction involves a cutaneous reaction to scaffold materials or degradation products. Adjuvant mediated guinea pig maximization test (GPMT) is a commonly used test (ISO 10993-10:2021 2021).
- (c) Irritation test: This test involves localized nonspecific inflammatory response to the material in the form of erythema (redness) of the skin and maybe necrosis. Patch assay in rabbits is the standard test (ISO 10993-10:2021 2021).
- (d) Intracutaneous reactivity test: This test is mainly used to detect irritant chemicals in scaffolds or leach out from scaffolds made up of polymers, ceramics, plastics, etc. Test material will be injected into the Rabbit skin on one side and control material on the other side (ISO 10993-10:2021 2021).
- (e) Systemic toxicity test: This test helps to find the system distribution and absorption of a toxicant from the entry route to the circulation where deleterious effects are manifested. Rat, Mice, or suitable animals can be used (ISO 10993-11, OECD and WHO guidelines) (ISO 10993-11:2017 2017).
- (f) Acute, subacute, and chronic toxicity tests: These toxicity tests can provide preliminary information (serum biochemical and hematological) on the toxic nature of a material for which no other toxicology information is available (OECD 423, 407, 452, OECD and WHO guidelines) (OECD 2020).

- (g) Genotoxicity test: The test using mammalian or non-mammalian cells, bacteria, yeasts, fungi, or whole animals to determine whether gene mutations, changes in chromosome structure, or other DNA or gene changes are caused by the test scaffold materials (ISO 10993-3:2014 [2014](#)).
- (h) Carcinogenicity test: This test determines the carcinogenic potential of scaffold materials or their by-products in multiple exposures on test animals and is observed for a significant portion of its life span (ISO 10993-3:2014 [2014](#)).
- (i) Reproductive or developmental toxicity test: The test describes the male and female reproductive performance when exposed to the scaffold materials. Toxicity is evaluated from necropsy and histopathological findings (OECD 421) (ISO 10993-3:2014 [2014](#)).
- (j) Hemocompatibility test: The test determines the blood compatibility of scaffold materials or their by-products for possible thrombosis, coagulation, platelet function, and immunogenicity (ISO 10993-4:2017 [2017](#)).
- (k) Immunotoxicology test: In this test, hypersensitivity, photosensitivity, induced autoimmunity, developmental immunotoxicity, immune suppression, and stimulation of scaffold materials in cultured cells will be determined (ISO/TS 10993-20:2006 [2006](#)).

Recently some modified testing recommendations in ISO Standard 10993-5 have been introduced. These modifications denote a novel method for absorbable scaffold cytotoxicity. However, the approach is not foolproof (ISO 10993-5:2009(en) [2009](#)). The gene/protein expressions influenced by the scaffold materials are also a major area to determine the toxicity of scaffolds. For this purpose, we can rely on transcriptome analysis, proteomics, and metabolomics along with the abovementioned tests in feature.

20.5 Conclusion

Biological scaffolds of natural, synthetic, or mixed origin are important in ameliorating various ailments associated with tissue/organ damage. Booming research in this area draws significant attention to improve the qualities of scaffolds to increase biocompatibility, cell growth, attachment, differentiation, remodulation without cytotoxicity, and immunological reactions. Many 2D or 3D composite macro, micro, and nano scaffolds showed higher mechanical strength, porosity, integrity, cytocompatibility, cell adhesion, biodegradability, differentiation, and migration. Among the wide variety of synthetic scaffold materials used in tissue-micro environments, some trigger an immunological cascade of reactions that lead to graft rejection due to the toxic by-products of enzymatic biodegradation. Natural scaffold materials show the lowest toxicity and higher biocompatibility in TE than synthetic ones.

Moreover, the scaffold natural products are cheaper, and abundant and only a minor resource is still being utilized in this aspect. Many synthetic composite materials are inherited with microbial contamination, oxidative stress, eliciting

hypersensitivity reactions, anti-angiogenesis, etc. These problems can be circumvented by using newer natural products scaffold materials with antioxidant, cell proliferative, anti-hypersensitive, angiogenic, cell-binding, differentiation, and migration properties. Biocompatibility, efficacy, and toxicity evaluation of scaffolds have prime importance in the development of scaffolds of the desired choice, and hence an array of tests are utilized. Generally, ISO, WHO, OECD, and ICH tests/guidelines are suitable to test scaffold materials' toxicity. In vitro cytotoxicity or cell proliferation activities of all scaffolds can be determined by MTT/XTT assays and fluorescent/confocal microscopy. Irritation tests and biofunctionality assays are used to assess cell immune response, neoangiogenesis, percentage mineralization, and fibroplasia. Acute, subacute, and systemic toxicity evaluation (serum biochemical and hematological parameters) with detailed look-up on the gene and protein expression are integral parts of toxicity evaluation of scaffolds. The Utilization of next-generation sequencing, transcriptome analysis, and modern bioinformatics tools pave a new vista for the development of new biocompatible scaffold materials with no or minimum toxicity.

References

- Accardo A, Ventre M, Chiappini C, Onesto V, Coluccio ML, Netti P, Gentile F (2020) Chapter 3: Nanoscaffolds for neural regenerative medicine. In: Razavi M (ed) Neural regenerative nanomedicine. Academic Press, London, pp 47–88. <https://doi.org/10.1016/B978-0-12-820223-4.00003-6>
- Aijie C, Xuan L, Huimin L, Yanli Z, Yiyuan K, Yuqing L, Longquan S (2018) Nanoscaffolds in promoting regeneration of the peripheral nervous system. *Nanomedicine* 13(9):1067–1085. <https://doi.org/10.2217/nmm-2017-0389>
- Antonella IA, Margherita B, Heiko L (2021) Flow synthesis approaches to privileged scaffolds—recent routes reviewed for green and sustainable aspects. *Green Chem* 23:2233–2292. <https://doi.org/10.1039/D0GC03883K>
- Atzet S, Curtin S, Trinh P, Bryant S, Ratner B (2008) Degradable poly(2-hydroxyethyl methacrylate)-co-polycaprolactone hydrogels for tissue engineering scaffolds. *Biomacromolecules* 9(12): 3370–3377. <https://doi.org/10.1021/bm800686h>
- Ayerst BI, Merry C, Day AJ (2017) The good the bad and the ugly of glycosaminoglycans in tissue engineering applications. *Pharmaceuticals (Basel, Switzerland)* 10(2):54. <https://doi.org/10.3390/ph10020054>
- Azizi F, Heidari F, Fahimipour F, Sajjadnejad M, Vashae D, Tayebi L (2020) Evaluation of mechanical and biocompatibility properties of hydroxyapatite/manganese dioxide nanocomposite scaffolds for bone tissue engineering application. *Int J Appl Ceram Technol*. <https://doi.org/10.1111/ijac.13549>
- Badhe RV, Bijukumar D, Chejara DR, Mabrouk M, Choonara YE, Kumar P, Pillay V (2017) A composite chitosan-gelatin bi-layered, biomimetic macroporous scaffold for blood vessel tissue engineering. *Carbohydr Polym* 157:1215–1225. <https://doi.org/10.1016/j.carbpol.2016.09.095>
- Bello AB, Kim D, Kim D, Park H, Lee SH (2020) Engineering and functionalisation of gelatin biomaterials: from cell culture to medical applications. *Tissue Eng Part B Rev*. <https://doi.org/10.1089/ten.teb.2019.0256>
- Berti FV, Srisuk P, da Silva LP, Marques AP, Reis RL, Correlo VM (2017) Synthesis and characterisation of electroactive gellan gum spongy-like hydrogels for skeletal muscle tissue engineering applications. *Tissue Eng Part A*. <https://doi.org/10.1089/ten.tea.2016.0430>

- Bhowmick S, Scharnweber D, Koul V (2016) Co-cultivation of keratinocyte-human mesenchymal stem cell (hMSC) on sericin loaded electrospun nanofibrous composite scaffold (cationic gelatin/hyaluronan/chondroitin sulfate) stimulates epithelial differentiation in hMSCs: *in vitro* study. *Biomaterials* 88:83–96. <https://doi.org/10.1016/j.biomaterials.2016.02.034>
- BIBRA (Bibra Toxicology Advice & Consulting) (1988) Toxicity profile for alginate and its common salts. BIBRA, Wallington, pp 1–8. Available online: <https://www.bibra-information.co.uk/downloads/toxicity-profile-for-alginate-and-its-commonsalts-1988>
- Cai Z, Wan Y, Becker ML, Long Y-Z, Dean D (2019) Poly(propylene fumarate)-based materials: synthesis, functionalisation, properties, device fabrication and biomedical applications. *Biomaterials*. <https://doi.org/10.1016/j.biomaterials.2019.03.038>
- Cao H, Chai C, Chew SY (2009) Scaffold-based gene silencing approach to regenerative medicine. *Mol Ther* 17:S389–S390. [https://doi.org/10.1016/s1525-0016\(16\)39382-0](https://doi.org/10.1016/s1525-0016(16)39382-0)
- Chan BP, Leong KW (2008) Scaffolding in tissue engineering: general approaches and tissue-specific considerations. *Eur Spine J* 17(Suppl 4):467–479. <https://doi.org/10.1007/s00586-008-0745-3>
- Chen FM, Liu X (2016) Advancing biomaterials of human origin for tissue engineering. *Prog Polym Sci* 53:86–168. <https://doi.org/10.1016/j.progpolymsci.2015.02.004>
- Chen X, Wang J, An Q, Li D, Liu P, Zhu W, Mo X (2015a) Electrospun poly(L-lactide-co-ε-caprolactone) fibers loaded with heparin and vascular endothelial growth factor to improve blood compatibility and endothelial progenitor cell proliferation. *Colloids Surf B Biointerfaces* 128:106–114. <https://doi.org/10.1016/j.colsurfb.2015.02.023>
- Chen J, Dong R, Ge J, Guo B, Ma PX (2015b) Biocompatible, biodegradable, and electroactive polyurethane-urea elastomers with tunable hydrophilicity for skeletal muscle TE. *ACS Appl Mater Interfaces* 7(51):28273–28285. <https://doi.org/10.1021/acsami.5b10829>
- Clowes AW (1993) Chapter 17: Intimal hyperplasia and graft failure. *Cardiovasc Pathol* 2(3): 179–186. [https://doi.org/10.1016/1054-8807\(93\)90058-a](https://doi.org/10.1016/1054-8807(93)90058-a)
- Coimbra P, Santos P, Alves P, Miguel SP, Carvalho MP, de Sá KD, Ferreira P (2017) Coaxial electrospun PCL/Gelatin-MA fibers as scaffolds for vascular tissue engineering. *Colloids Surf B Biointerfaces* 159:7–15. <https://doi.org/10.1016/j.colsurfb.2017.07.065>
- Copes F, Pien N, Van Vlierberghe S, Boccafroschi F, Mantovani D (2019) Collagen-based tissue engineering strategies for vascular medicine. *Front Bioeng Biotechnol* 7. <https://doi.org/10.3389/fbioe.2019.00166>
- Croisier F, Jérôme C (2013) Chitosan-based biomaterials for tissue engineering. *Eur Polym J* 49(4): 780–792. <https://doi.org/10.1016/j.eurpolymj.2012.12.009>
- Cullen R, Brian M, Alan J, Davis J (2002) Toxicity of cellulose fibres. *Ann Occup Hyg* 46. https://doi.org/10.1093/annhyg/46.suppl_1.81
- Da Silva D, Kaduri M, Poley M, Adir O, Krinsky N, Shainsky-Roitman J, Schroeder A (2018) Biocompatibility, biodegradation and excretion of polylactic acid (PLA) in medical implants and theranostic systems. *Chem Eng J* 340:9–14. <https://doi.org/10.1016/j.cej.2018.01.010>
- Dhandayuthapani B, Yoshida Y, Maekawa T, Kumar DS (2011) Polymeric scaffolds in tissue engineering application: a review. *Int J Polym Sci* 2011:1–19. <https://doi.org/10.1155/2011/290602>
- Elmowafy EM, Tiboni M, Soliman ME (2019) Biocompatibility, biodegradation and biomedical applications of poly(lactic acid)/poly(lactic-co-glycolic acid) micro and nanoparticles. *J Pharm Investig*. <https://doi.org/10.1007/s40005-019-00439-x>
- El-Sheikh MA, El-Rafie SM, Abdel-Halim ES, El-Rafie MH (2013) Green synthesis of hydroxyethyl cellulose-stabilized silver nanoparticles. *J Polymer* 2013:650837. <https://doi.org/10.1155/2013/650837>
- Evans E (1991) Toxicity of hydroxyapatite in vitro: the effect of particle size. *Biomaterials* 12(6): 574–576. [https://doi.org/10.1016/0142-9612\(91\)90054-e](https://doi.org/10.1016/0142-9612(91)90054-e)
- Ferrer-Ferrer M, Dityatev A (2018) Shaping synapses by the neural extracellular matrix. *Front Neuroanat* 12. <https://doi.org/10.3389/fnana.2018.00040>

- Fu Q, Saiz E, Rahaman MN, Tomsia AP (2011) Bioactive glass scaffolds for bone tissue engineering: state of the art and future perspectives. *Mater Sci Eng C* 31(7):1245–1256. <https://doi.org/10.1016/j.msec.2011.04.022>
- Gaaz T, Sulong A, Akhtar M, Kadhum A, Mohamad A, Al-Amiery A (2015) Properties and applications of polyvinyl alcohol, halloysite nanotubes and their nanocomposites. *Molecules* 20(12):22833–22847. <https://doi.org/10.3390/molecules201219884>
- García MC (2018) Drug delivery systems based on nonimmunogenic biopolymers. In: *Engineering of biomaterials for drug delivery systems*. Woodhead Publishing, Duxford, pp 317–344. <https://doi.org/10.1016/b978-0-08-101750-0.00012-x>
- Gayathri V, Harikrishnan V, Mohanan PV (2016) Integration of rabbit adipose derived mesenchymal stem cells to hydroxyapatite burr hole button device for bone interface regeneration. *Int J Biomater* 2016:1–9. <https://doi.org/10.1155/2016/1067857>
- Gomes SA, Thomson M, Ali M, Alnaqeeb M, Khater SH (1991) Collagen toxicity in rabbits. *Toxicol Lett* 56(1–2):229–235. [https://doi.org/10.1016/0378-4274\(91\)90110-r](https://doi.org/10.1016/0378-4274(91)90110-r)
- Gomes S, Rodrigues G, Martins G, Henriques C, Silva JC (2017) Evaluation of nanofibrous scaffolds obtained from blends of chitosan, gelatin and polycaprolactone for skin tissue engineering. *Int J Biol Macromol* 102:1174–1185. <https://doi.org/10.1016/j.ijbiomac.2017.05.004>
- Hajjali F, Tajbakhsh S, Shojaei A (2017) Fabrication and properties of polycaprolactone composites containing calcium phosphate-based ceramics and bioactive glasses in bone tissue engineering: a review. *Polym Rev* 58(1):164–207. <https://doi.org/10.1080/15583724.2017.1332640>
- Hickey RJ, Pelling AE (2019) Cellulose biomaterials for tissue engineering. *Front Bioeng Biotechnol* 7:45. <https://doi.org/10.3389/fbioe.2019.00045>
- Hussein KH, Park KM, Kang KS, Woo HM (2016) Biocompatibility evaluation of tissue-engineered decellularised scaffolds for biomedical application. *Mater Sci Eng C* 67:766–778. <https://doi.org/10.1016/j.msec.2016.05.06>
- Iannuzzi C, Irace G, Sirangelo I (2015) The effect of glycosaminoglycans (GAGs) on amyloid aggregation and toxicity. *Molecules* 20(2):2510–2528. <https://doi.org/10.3390/molecules20022510>
- Ibrahim HM, El-Zairy EMR (2015) Chitosan as a biomaterial—structure, properties, and electrospun nanofibers, concepts, compounds and the alternatives of antibacterials. In: Bobbarala V (ed) *Concepts, compounds and the alternatives of antibacterials*. IntechOpen, London. <https://doi.org/10.5772/61300>. <https://www.intechopen.com/books/concepts-compounds-and-the-alternatives-of-antibacterials/chitosan-as-a-biomaterial-structure-properties-and-electrospun-nanofibers>
- ICH Topic M3 (R2) (2008) Non-clinical safety studies for the conduct of human clinical trials and marketing authorization for pharmaceuticals
- International Organization for Standardization (ISO) 10993 (2018) ISO/TC 194, Biological and clinical evaluation of medical devices—part 1: evaluation and testing within a risk management process. ISO 10993-1
- ISO 10993-10:2021(2021) Biological evaluation of medical devices—part 10: tests for irritation and skin sensitisation
- ISO 10993-11:2017 (2017), Biological evaluation of medical devices—part 11: tests for systemic toxicity
- ISO 10993-3:2014 (2014) Biological evaluation of medical devices—part 3: tests for genotoxicity, carcinogenicity and reproductive toxicity
- ISO 10993-4:2017 (2017) Biological evaluation of medical devices—part 4: selection of tests for interactions with blood
- ISO 10993-5:2009(en) (2009) Biological evaluation of medical devices—part 5: tests for in vitro cytotoxicity
- ISO/TS 10993-20:2006 (2006) Biological evaluation of medical devices—part 20: principles and methods for immunotoxicology testing of medical devices

- Jahangirian H, Ghasemian Lemraski E, Rafiee-Moghaddam R, Webster T (2018) A review of using green chemistry methods for biomaterials in tissue engineering. *Int J Nanomedicine* 13:5953–5969. <https://doi.org/10.2147/ijn.s163399>
- Jessen KR, Mirsky R, Lloyd AC (2015) Schwann cells: development and role in nerve repair. *Cold Spring Harb Perspect Biol* 7(7):a020487. <https://doi.org/10.1101/cshperspect.a020487>
- Johari N, Madaah Hosseini HR, Samadikuchaksaraei A (2020) Mechanical modeling of silk fibroin/TiO₂ and silk fibroin/fluoridated TiO₂ nanocomposite scaffolds for bone TE. *Iran Polym J*. <https://doi.org/10.1007/s13726-020-00789-6>
- Kamarul T, Krishnamurthy G, Salih ND, Ibrahim NS, Raghavendran HR, Suhaeb AR, Choon DS (2014) Biocompatibility and toxicity of poly(vinyl alcohol)/N, O-carboxymethyl chitosan scaffold. *ScientificWorldJournal*. <https://doi.org/10.1155/2014/905103>
- Kasper FK, Tanahashi K, Fisher JP, Mikos AG (2009) Synthesis of poly(propylene fumarate). *Nat Protoc* 4(4):518–525. <https://doi.org/10.1038/nprot.2009.24>
- Kattimani VS, Kondaka S, Lingamaneni KP (2016) Hydroxyapatite—past, present, and future in bone regeneration. *Bone Tissue Regen Insights* 7:BTRI.S36138. <https://doi.org/10.4137/btri.s36138>
- Kaur L, Singh J, Liu Q (2007) Starch—a potential biomaterial for biomedical applications. In: Mozafari MR (ed) *Nanomaterials and nanosystems for biomedical applications*. Springer, Dordrecht. https://doi.org/10.1007/978-1-4020-6289-6_5
- Khan R, Khan MH (2013) Use of collagen as a biomaterial: an update. *J Ind Soc Periodontol* 17(4):539–542. <https://doi.org/10.4103/0972-124X.118333>
- Krambeck AE, Handa SE, Evan AP, Lingeman JE (2010) Brushite stone disease as a consequence of lithotripsy? *Urol Res* 38(4):293–299. <https://doi.org/10.1007/s00240-010-0289-y>
- Kulikouskaya V, Kraskouski A, Hileuskaya K, Zhura A, Tratsyak S, Agabekov V (2019) Fabrication and characterisation of pectin-based 3D porous scaffolds suitable for treatment of peritoneal adhesions. *J Biomed Mater Res A*. <https://doi.org/10.1002/jbm.a.36700>
- Kundu B, Rajkhowa R, Kundu SC, Wang X (2013) Silk fibroin biomaterials for tissue regenerations. *Adv Drug Deliv Rev* 65(4):457–470. <https://doi.org/10.1016/j.addr.2012.09.043>
- Las Heras K, Santos E, Garrido T, Guitierrez FB, Aguirre JJ, de la Caba K, Guerrero P, Igartua M, Hernandez RM (2020) Soy protein and chitin sponge-like scaffolds: from natural by-products to cell delivery systems for biomedical applications. *Green Chem*. <https://doi.org/10.1039/d0gc00089b>
- Law JX, Liao LL, Saim A, Yang Y, Idrus R (2017) Electrospun collagen nanofibers and their applications in skin tissue engineering. *Tissue Eng Regen Med* 14(6):699–718. <https://doi.org/10.1007/s13770-017-0075-9>
- Leng Q, Chen L, Lv Y (2020) RNA-based scaffolds for bone regeneration: application and mechanisms of mRNA, miRNA and siRNA. *Theranostics* 10(7):3190–3205. <https://doi.org/10.7150/thno.42640>
- Makadia HK, Siegel SJ (2011) Poly lactic-co-glycolic acid (PLGA) as biodegradable controlled drug delivery carrier. *Polymers* 3(3):1377–1397. <https://doi.org/10.3390/polym3031377>
- Meng TT (2014) Volatile organic compounds of polyethylene vinyl acetate plastic are toxic to living organisms. *J Toxicol Sci* 39(5):795–802. <https://doi.org/10.2131/jts.39.795>
- Moeller C, Fleischmann C, Thomas-Rueddel D, Vlasakov V, Rochweg B, Theurer P, Gattinoni L, Reinhart K, Hartog CS (2016) How safe is gelatin? A systematic review and meta-analysis of gelatin-containing plasma expanders vs crystalloids and albumin. *J Crit Care* 35:75–83. <https://doi.org/10.1016/j.jcrc.2016.04.011>
- Munarin F, Guerreiro SG, Grellier MA, Tanzi MC, Barbosa MA, Petrini P, Granja PL (2011) Pectin-based injectable biomaterials for bone tissue engineering. *Biomacromolecules* 12(3):568–577. <https://doi.org/10.1021/bm101110x>
- Myers DK, Goldberg AM, Poth A, Wolf MF, Carraway J, McKim J, Coleman KP, Hutchinson R, Brown R, Krug HF, Bahinski A, Hartung T (2017) From *in vivo* to *in vitro*: the medical device testing paradigm shift. *ALTEX Altern Anim Exp* 34(4):479–500. <https://doi.org/10.14573/altex.1608081>

- Naserzadeh P, Mortazavi SA, Ashtari K, Salimi A, Farokhi M, Pourahmad J (2018) Evaluation of the toxicity effects of silk fibroin on human lymphocytes and monocytes. *J Biochem Mol Toxicol* 32(6):e22056. <https://doi.org/10.1002/jbt.22056>
- Nazarnazhad S, Bairo F, Kim HW, Webster TJ, Kargozar S (2020) Electrospun nanofibers for improved angiogenesis: promises for tissue engineering applications. *Nanomaterials (Basel, Switzerland)* 10(8):1609. <https://doi.org/10.3390/nano10081609>
- Nguyen TP, Nguyen QV, Nguyen VH, Le TH, Huynh V, Vo DN, Trinh QT, Kim SY, Le QV (2019) Silk fibroin-based biomaterials for biomedical applications: a review. *Polymers* 11(12):1933. <https://doi.org/10.3390/polym11121933>
- Nikolova MP, Chavali MS (2019) Recent advances in biomaterials for 3D scaffolds: a review. *Bioactive Mater* 4:271–292. <https://doi.org/10.1016/j.bioactmat.2019.10.005>
- OECD (2018–2020) OECD guidelines for testing of chemicals
- OECD (2020) OECD guidelines for testing of chemicals, test guidelines
- Onuki Y, Bhardwaj U, Papadimitrakopoulos F, Burgess DJ (2008) A review of the biocompatibility of implantable devices: current challenges to overcome foreign body response. *J Diabetes Sci Technol* 2(6):1003–1015. <https://doi.org/10.1177/193229680800200610>
- Osman AF, Hamid ARA, Fitri TFM, Fauzi AAA, Halim KAA (2020) Poly (ethylene-co-vinylacetate) copolymer-based nanocomposites: a review. *IOP Conf Ser Mater Sci Eng* 864:012121
- Pandey A, Jain DS (2015) Poly lactic-co-glycolic acid (PLGA) copolymer and its pharmaceutical application. In: *Handbook of polymers for pharmaceutical technologies*. Wiley, Hoboken, NJ, pp 151–172. <https://doi.org/10.1002/9781119041412.ch6>
- Place ES, George JH, Williams CK, Stevens MM (2009) Synthetic polymer scaffolds for tissue engineering. *Chem Soc Rev* 38(4):1139. <https://doi.org/10.1039/b811392k>
- Polo-Corrales L, Latorre-Esteves M, Ramirez-Vick JE (2014) Scaffold design for bone regeneration. *J Nanosci Nanotechnol* 14(1):15–56. <https://doi.org/10.1166/jnn.2014.9127>
- Rahaman MN, Day DE, Bal BS, Fu Q, Jung SB, Bonewald LF, Tomsia AP (2011) Bioactive glass in tissue engineering. *Acta Biomater* 7(6):2355–2373
- Rajagopalan P, Shen CJ, Berthiaume F, Tilles AW, Toner M, Yarmush ML (2006) Polyelectrolyte nano-scaffolds for the design of layered cellular architectures. *Tissue Eng* 12(6):1553–1563. <https://doi.org/10.1089/ten.2006.12.1553>
- Ranjbarvan P, Mahmoudifard M, Kehtari M, Babaie A, Hamed S, Mirzaei S, Hosseinzadeh S (2018) Natural compounds for skin TE by electrospinning of nylon-Beta vulgaris. *ASAIO J* 64(2):261–269. <https://doi.org/10.1097/mat.0000000000000611>
- Rashidbenam Z, Jasman MH, Hafez P, Tan GH, Goh EH, Fam XI, Ho C, Zainuddin ZM, Rajan R, Nor FM, Shuhaili MA, Kosai NR, Imran FH, Ng MH (2019) Overview of urethral reconstruction by tissue engineering: current strategies, clinical status and future direction. *Tissue Eng Regen Med* 16(4):365–384. <https://doi.org/10.1007/s13770-019-00193-z>
- Reddy MSB, Ponnamma D, Choudhary R, Sadasivuni KK (2021) A comparative review of natural and synthetic biopolymer composite scaffolds. *Polymers* 13:1105. <https://doi.org/10.3390/polym13071105>
- Rivera-Briso A, Serrano-Aroca Á (2018) Poly(3-hydroxybutyrate-co-3-hydroxyvalerate): enhancement strategies for advanced applications. *Polymers* 10(7):732. <https://doi.org/10.3390/polym10070732>
- Rocha DN, Brites P, Fonseca C, Pêgo AP (2014) Poly(trimethylene carbonate-co-ε-caprolactone) promotes axonal growth. *PLoS One* 9(2):e88593. <https://doi.org/10.1371/journal.pone.0088593>
- Rychen G, Aquilina G, Azimonti G, Bampidis V, Bastos ML, Bories G, Chesson A, Cocconcelli PS, Flachowsky G, Kolar B, Kouba M, Lopez-Alonso M, Lopez Puente S, Mantovani A, Mayo B, Ramos F, Saarela M, Villa RE, Wallace RJ, Wester P, Lundebye AK, Nebbia C, Renshaw D, Innocenti M, Gropp J, EFSA FEEDAP Panel (EFSA Panel on Additives and Products or Substances used in Animal Feed) (2017) Scientific opinion on the safety and efficacy of sodium and potassium alginate forpets, other non-food-producing animals and

- fish. *EFSA (European Food Safety Authority) J* 15(7):4945, 13 pp. <https://doi.org/10.2903/j.efs.a.2017.4945>
- Sahoo DR, Biswal T (2021) Alginate and its application to tissue engineering. *SN Appl Sci* 3:30. <https://doi.org/10.1007/s42452-020-04096-w>
- Salati MA, Khazai J, Tahmuri AM, Samadi A, Taghizadeh A, Taghizadeh M, Zarrintaj P, Ramsey JD, Habibzadeh S, Seidi F, Saeb MR, Mozafari M (2020) Agarose-based biomaterials: opportunities and challenges in cartilage tissue engineering. *Polymers* 12(5):1150. <https://doi.org/10.3390/polym12051150>
- Seyedmajidi S, Seyedmajidi M, Zabihi E, Hajian-Tilaki K (2018) A comparative study on cytotoxicity and genotoxicity of the hydroxyapatite-bioactive glass (HA/BG) and fluorapatite-bioactive glass (FA/BG) nanocomposite foams as tissue scaffold for bone repair. *J Biomed Mater Res A*. <https://doi.org/10.1002/jbm.a.36452>
- Song R, Murphy M, Li C, Ting K, Soo C, Zheng Z (2018) Current development of biodegradable polymeric materials for biomedical applications. *Drug Des Devel Ther* 12:3117–3145. <https://doi.org/10.2147/dddt.s165440>
- Sonmez E, Cacciatore I, Bakan F, Turkez H, Mohtar Y, Togar B, Stefano A (2016) Toxicity assessment of hydroxyapatite nanoparticles in rat liver cell model in vitro. *Hum Exp Toxicol* 35(10):1073–1083. <https://doi.org/10.1177/0960327115619770>
- Soucy JR, Shirzaei Sani E, Portillo Lara R, Diaz D, Dias F, Weiss AS, Koppes AN, Koppes RA, Annabi N (2018) Photocrosslinkable gelatin/tropoelastin hydrogel adhesives for peripheral nerve repair. *Tissue Eng Part A* 24(17–18):1393–1405. <https://doi.org/10.1089/ten.TEA.2017.0502>
- Svensson A, Nicklasson E, Harrah T, Panilaitis B, Kaplan DL, Brittberg M, Gatenholm P (2005) Bacterial cellulose as a potential scaffold for tissue engineering of cartilage. *Biomaterials* 26(4):419–431. <https://doi.org/10.1016/j.biomaterials.2004.02.049>
- Tyler B, Gullotti D, Mangraviti A, Utsuki T, Brem H (2016) Polylactic acid (PLA) controlled delivery carriers for biomedical applications. *Adv Drug Deliv Rev* 107:163–175. <https://doi.org/10.1016/j.addr.2016.06.018>
- Varoni E, Tschon M, Palazzo B, Nitti P, Martini L, Rimondini L (2012) Agarose gel as biomaterial or scaffold for implantation surgery: characterisation, histological and histomorphometric study on soft tissue response. *Connect Tissue Res* 53(6):548–554. <https://doi.org/10.3109/03008207.2012.712583>
- Vogt L, Ruther F, Salehi S, Boccaccini AR (2021) Poly(glycerol sebacate) in biomedical applications—a review of the recent literature. *Adv Health Care Mater*. <https://doi.org/10.1002/adhm.202002026>
- Vroman I, Tighzert L (2009) Biodegradable polymers. *Materials* 2(2):307–344. <https://doi.org/10.3390/ma2020307>
- Wang L, Du J, Cao D, Wan Y (2013) Recent advances and the application of poly (3-hydroxybutyrate-co-3-hydroxyvalerate) as tissue engineering materials. *J Macromol Sci A Pure Appl Chem* 50:885–893
- Wang MO, Piard CM, Melchiorri A, Dreher ML, Fisher JP (2015) Evaluating changes in structure and cytotoxicity during in vitro degradation of three-dimensional printed scaffolds. *Tissue Eng Part A* 21(9–10):1642–1653. <https://doi.org/10.1089/ten.tea.2014.0495>
- Wang L, Wu Y, Hu T, Guo B, Ma PX (2017) Electrospun conductive nanofibrous scaffolds for engineering cardiac tissue and 3D bioactuators. *Acta Biomater* 59:68–81. <https://doi.org/10.1016/j.actbio.2017.06.036>
- Wang C, Jia Y, Yang W, Zhang C, Zhang K, Chai Y (2018) Silk fibroin enhances peripheral nerve regeneration by improving vascularisation within nerve conduits. *J Biomed Mater Res A* 106(7):2070–2077. <https://doi.org/10.1002/jbm.a.36390>
- Wu Y, Wang L, Guo B, Shao Y, Ma PX (2016) Electroactive biodegradable polyurethane significantly enhanced Schwann cells myelin gene expression and neurotrophin secretion for peripheral nerve tissue engineering. *Biomaterials* 87:18–31. <https://doi.org/10.1016/j.biomaterials.2016.02.010>

- Xu HH, Wang P, Wang L, Bao C, Chen Q, Weir MD, Reynolds MA (2017) Calcium phosphate cements for bone engineering and their biological properties. *Bone Res* 5:17056. <https://doi.org/10.1038/boneres.2017.56>
- Yan X, Chen Y, Song Y, Yang M, Ye J, Zhou G, Yu J (2019) Scaffold-based gene therapeutics for osteochondral tissue engineering. *Front Pharmacol* 10. <https://doi.org/10.3389/fphar.2019.01534>
- Yi H, Forsythe S, He Y, Liu Q, Xiong G, Wei S, Li G, Atala A, Skardal A, Zhang Y (2017) Tissue-specific extracellular matrix promotes myogenic differentiation of human muscle progenitor cells on gelatin and heparin conjugated alginate hydrogels. *Acta Biomater* 15(62):222–233. <https://doi.org/10.1016/j.actbio.2017.08.022>
- Zar T, Graeber C, Perazella MA (2007) Reviews: recognition, treatment, and prevention of propylene glycol toxicity. *Semin Dial* 20(3):217–219. <https://doi.org/10.1111/j.1525-139x.2007.00280.x>
- Zhao L, Chen D, Wei M, Yao Q, Li M (2013) Preparation of a recombinant spider silk protein/Pcl blend submicrofibrous mat and its cytocompatibility. *Polym Polym Compos* 21(2):85–92. <https://doi.org/10.1177/096739111302100205>
- Zulkifli FH, Hussain FSJ, Zeyohannes SS, Rasad MSBA, Yusuff MM (2017) A facile synthesis method of hydroxyethyl cellulose-silver nanoparticle scaffolds for skin tissue engineering applications. *Mater Sci Eng C* 79:151–160. <https://doi.org/10.1016/j.msec.2017.05.028>



Biological Safety and Cellular Interactions of Nanoparticles

21

Arathi, K. B. Megha, X. Joseph, and P. V. Mohanan

21.1 Introduction

The application of nanoparticles (NPs) spans multi-disciplines of science, including industrial, electronics, environmental, energy, food and agriculture, textile, biomedical, and pharmaceuticals. The development of nanoparticle-mediated medical applications has surged in recent decades and provides a dependable and potent alternative for various medical issues. The interaction of nanoparticles with cells and the cellular environment is evident as nanoparticles-based biomedical and pharmaceutical applications are attaining major milestones day by day.

The biological fate of molecules entering the cell depends on its uptake and the consequent interactions between the cell and the molecules. Any molecule that needs to enter the cells should primarily encounter the plasma membrane, comprising mainly lipids and proteins. The negatively charged lipids act as the boundary of cells, and proteins regulate the trafficking of molecules in and out of the cell (Alberts et al. 1994). Likewise, the fate of nanoparticle-based biomedical applications also majorly depends upon its cellular uptake. The cells take up the nanoparticle through various internalization mechanisms; they reach the target organs via the bloodstream, accumulate there, and are later eliminated.

The nanoparticles designed for functioning in the cellular environment must be thoroughly studied for their interactions in the biological environment. The consequences of cell-nanoparticle interaction must be deciphered well-advanced to

A. Arathi, K. B. Megha, X. Joseph and P. V. Mohanan contributed equally to this work.

Arathi · K. B. Megha · X. Joseph · P. V. Mohanan (✉)

Toxicology Division, Biomedical Technology Wing, Sree Chitra Tirunal Institute for Medical Sciences and Technology (Govt. of India), Trivandrum, Kerala, India

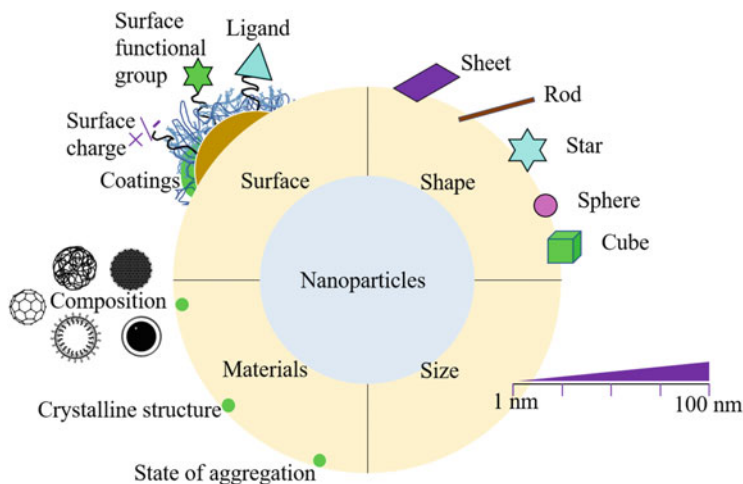


Fig. 21.1 Factors affecting NPs-cells interaction

eliminate any pernicious consequences. The biological medium containing various biomolecules like polysaccharides, lipids, proteins, and nucleotides may interact with the nanoparticles, and these interactions could result in advantageous and disadvantageous outcomes. The cellular target of nanoparticles also determines the type of interactions occurring between the nanoparticles and the cellular environment. For example, the nanoparticle intended for drug delivery should reach the blood vessels. The interaction of nanoparticles with blood and its components will also contribute to the outcomes of nanoparticle-mediated drug delivery.

The manipulation of nanoparticles to cope with the adverse effects of cellular interactions can be a better approach for escalating the efficiency of nanoparticle-mediated biomedical applications. The interaction of nanoparticles with cells depends on various aspects related to both cells and the nanoparticles. The interactions vary with varying cell types and the properties of nanoparticles. The physicochemical properties of nanoparticles, including size, shape, surface functionalization, can determine the cellular uptake, their interactions, and the preceding toxicity (Fig. 21.1). Also, the nanoparticles, when exposed to the biological environment, form a protein corona by the adsorption of proteins on the nanoparticle surface, which can alter the cellular interactions. The protein corona also affects the interaction of nanoparticles with blood and its components (Bertrand et al. 2017).

The biological responses accompanying the introduction of nanoparticles into the cellular environment are not fully elucidated. The effectiveness of the existing methods and protocols to evaluate the possible hazards allied with the engineered nanoparticles is of great concern. The potential application of nanoparticles is mainly involved in nanomedicine and drug delivery. The nanoparticle-cellular interactions are defined by the double-layered plasma membrane, the cellular uptake pathway, the intracellular trafficking of nanoparticles, the protein corona formation, and the

associated cytotoxicity. This chapter focuses on all these aspects of cellular nanoparticle interactions.

21.2 The Dynamics of Nanoparticle-Cell Interaction

As mentioned in the introduction, the nanoparticles, like any other foreign substance entering the cell, undergo internalization, accumulation in the target tissue, and finally get eliminated. The nanoparticles enter the human body via gastrointestinal and dermal routes. For successful biomedical applications, the nanoparticles must evade the plasma membrane, escape the endosomes, and cross the nuclear envelope in many instants. The biomolecules present in the media conjugate the nanoparticles in the extracellular media and help in the internalization. The efficacies of the nanoparticles are determined by the ability of the nanoparticles to reach the target location finally.

21.2.1 Cellular Internalization of Nanoparticles

Since the cell membrane is not readily permeable to foreign substances, different internalization mechanisms of nanoparticles (detailed in the next section) produce the desired physiological response inside the body. Toxicity can be an implication if the nanoparticles enter the cells through nonspecific internalization. The nanoparticles sized in the range of 10–100 nm are highly allowed inside the cells. As the size decrease, the entry of nanoparticles is mediated by the cost of energy. The phagocytic cells help in the internalization and targeted movement of nanoparticles above the size of 100 nm. The size and surface chemistry of the nanoparticles are highly linked as the forces acting on the surface play a fundamental role in the interaction of the nanoparticles with the biological system. The relationship between the uptake mechanism and zeta potential also is essential for the interaction of nanoparticles. The nanoparticles are internalized based on their specific interaction with different moieties and target them to the desired location. For instance, an antibody-coated nanoparticle shows a highly increased efficiency of internalization than that of the internalization based on charged molecules (Wilhelm et al. 2003).

The cellular internalization also depends on the adsorption of surface proteins onto the nanoparticles. This protein conjugation might change size, shape, and surface morphology that would be advantageous or disadvantageous for the uptake process and the desired biological application. Nonspecific internalization of nanoparticles can be prevented by studying the adsorption mechanisms thereby increasing the efficient uptake of nanoparticles by the cells (Zhao and Stenzel 2018).

21.2.2 Interaction of Nanoparticles with Tumor Tissue

Nanoparticles are actively involved in tumor therapy, and nanoparticles such as dendrimers, polymeric micelles, and liposomes are majorly employed for targeted therapies for tumors. The nano-drug delivery of nanoparticles is based on the cellular interactions that allow passive and active targeting strategies. The ligand present in the nanoparticles binds to the receptors in the tumor cells via active targeting (Wang et al. 2010). Once the binding occurs, the drug-loaded nanoparticles release the drugs to the tumor microenvironment (TME) upon cellular cues like pH and temperature. The tumor microenvironment is in many ways different from the typical cell environment. The abnormalities surrounding the TME, such as blood supply, oxygen supply, pH, and immune responses, are targeted by engineered nanoparticles to reduce the effects (Fig. 21.2). Understanding the physiological effects of functionalized nanoparticles on the tumor microenvironment could improve the tumor-targeting mechanisms and enhance the efficiency of tumor therapy.

Various research groups around the world have extensively studied the anticancer effects of nanoparticles. The nanoparticles affect the tumor environment by (1) inducing autophagy of the cells, (2) inhibiting angiogenesis and tumor growth, (3) cutting off the cross talk between the cancer cells with the associated fibroblasts and endothelial cells, (4) Inducing ROS mediated stress—eventually leading to the inactivation of the tumor cells (Huai et al. 2019).

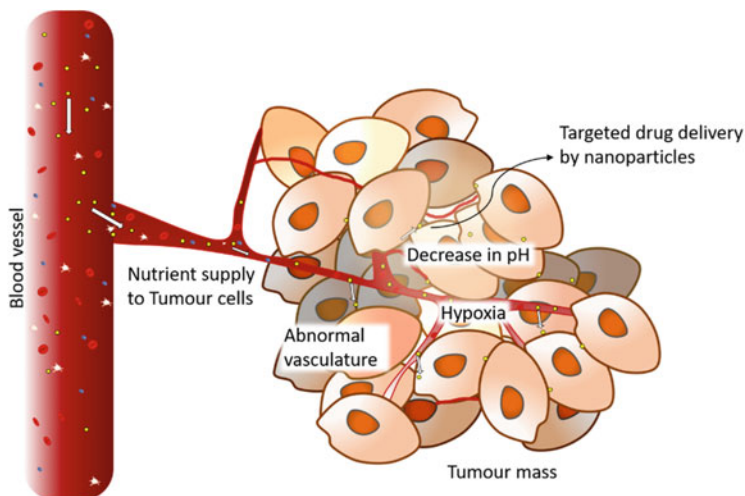


Fig. 21.2 Nanoparticle targeting tumor mass

21.3 Cellular Pathways for Nanoparticle Uptake

The primary task of any nanoparticle entering the cells is to breach the cell membrane barrier comprising the lipid bilayer and integral membrane proteins. The initial interaction of nanoparticles with the cell membrane mediates the uptake of these particles. The biological activity of any molecule entering the cells is determined by the interaction of the molecule with the plasma membrane and the subsequent cell uptake process. The cellular internalization of each type of nanoparticle follows a specific pathway. The two main ways through which the nanoparticle enters the cells are direct translocation and endocytosis. Translocation or diffusion is the energy-independent process where the movement into the cell is mediated by the concentration gradient or the solubility of nanoparticles. Molecules like proteins and nanoparticles cannot permeate through the cell membrane by a simple diffusion process and hence require an active cellular process that helps in the entry.

The cellular uptake pathway of the nanoparticles determines the fate of the nanoparticles inside the cells. Alternatively, in other words, the target site of the nanoparticles inside the cells decides the uptake mechanisms. The surface functionality of nanoparticles also plays a significant role in selecting the endocytosis pathway. The functionalities such as size, charge, shape, and nature of the core material will facilitate the regulation of specific endocytotic pathways suitable for the nanoparticle's intended function (Means et al. 2021). Most of the natural polymers, synthetic polymers, dendrimers, carbon-based, metallic nanoparticles, and lipids are taken up by the cells mainly through clathrin-mediated endocytosis (CME), caveolae-dependent endocytosis (CVME) and macropinocytosis. CME was the primary mechanism of entry of Chitosan Nanoparticles into RAW 264.7 (Jiang et al. 2017).

Endocytosis is an energy-dependent process that helps move particles from the exterior of the cell to the internal environment through vesicles formed from the cell membrane (Doherty and McMahon 2009). The endocytotic pathways act as a gateway into the cells and subcellular organelles for the therapeutic nanoparticles. Endocytosis refers to the different pathways that help the nanoparticle enter the cells. The endocytosis can be generally divided into phagocytosis and pinocytosis (Fig. 21.3). Phagocytosis, carried out by the phagocytotic cells like macrophages and dendritic cells, aids in engulfing particulate matter, while the pinocytosis pathways help in the acquiring of fluids and other small molecules by the cells. It is again grouped into macropinocytosis and receptor-mediated endocytosis (caveolae-dependent and clathrin-mediated endocytosis) (Mosquera et al. 2018). The endocytosis of the nanoparticles results in the formation of vesicles enclosing the nanoparticles such as macropinosomes, phagosomes, and endosomes. These vesicles hinder the immediate and direct contact of nanoparticles with the cytoplasm and the cellular organelles.

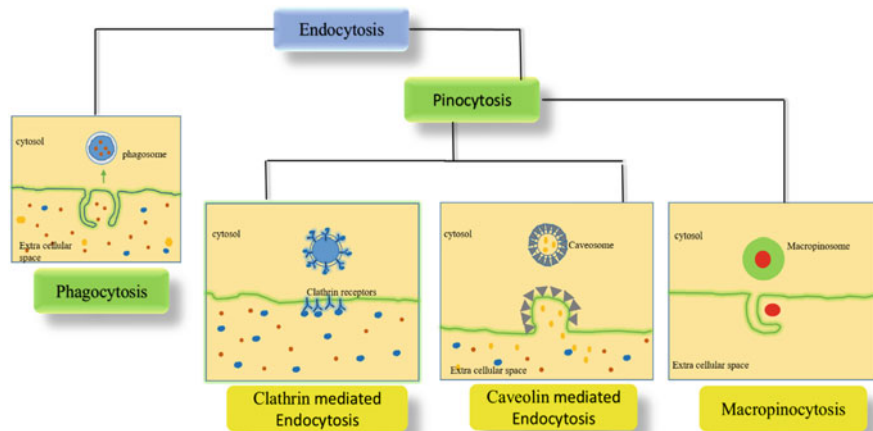


Fig. 21.3 Schematic diagram of the different types of cellular uptake mechanisms

21.3.1 Phagocytosis

Immune cells such as macrophages, dendritic cells, B lymphocytes, and neutrophils exercise phagocytosis to eliminate the substances identified as foreign to the cellular environment. The nanoparticles of size larger than 500 nm bind to the receptors of the phagocytotic cells (Fc receptors, complement receptors, mannose receptors, and scavenger receptors) and are cleared from circulation (Chen et al. 2017). The nanoparticles are opsonized by adding complement proteins, serum proteins, and immunoglobulins to the surface, and this adsorption results in the recognition of the nanoparticles by the phagocytes. Once entering the phagocytes, nanoparticles are entrapped in vesicles called phagosomes that ultimately fuse with the lysosomes forming phagolysosomes. The nanoparticles get digested within the phagolysosomes (Sahay et al. 2010). This clearance of nanoparticles can be a challenge to the effective functioning of the nanoparticles inside the body. Hence, the nanoparticles intended to produce specific cellular functions need to be carefully engineered to overcome the rapid sequestration by the macrophages and other mononuclear phagocyte systems (MPS) cells. The nanoparticles administered intravenously are rapidly opsonized while interacting with the blood tissue (Lazarovits et al. 2015). The surface modification of nanoparticles is an effective method to reduce the opsonization of cells and thereby prevent the sequestration of nanoparticles by the MPS system. The polyethylene glycol (PEG)-coated nanoparticles reduce opsonization thereby enhancing cellular targeting and uptake of these nanoparticles (Li et al. 2014). The uptake of nanoparticles can also be increased by exhibiting surface ligands that mark the molecules as “self” and allow increased uptake by reducing the phagocytosis (Rodriguez et al. 2013).

21.3.2 Macropinocytosis

In macropinocytosis, the actin stabilized plasma membrane extensions engulf the incoming fluids and solutes nonspecific. The process is different from other cellular uptake mechanisms so that it is established through actin filaments. The characteristic vacuoles of the mechanism, the macropinosomes with a size ranging from 200 nm to 5 μm engulf the nanoparticles that mediate a change in pH and exhibition of endosome markers. The decrease in the pH causes the fusion of the macropinosomes with late endosomes or lysosomes. Ligand functionalized nanoparticles mainly use the pathway to achieve entry into the cell (Li and Pang 2021). PEGylated chitosan/siRNA nanoparticles (Yang et al. 2017) and Bis-quaternary Gemini surfactants (Cardoso et al. 2014) utilized macropinocytosis for their cellular uptake.

21.3.3 Clathrin-Mediated Endocytosis

The important endocytotic pathway for the uptake of nanoparticles is mediated by the protein clathrin and is referred to as the clathrin-coated uptake. The plasma membrane recruits clathrin and initiates the interaction of the receptor on the surface of the nanoparticle leading to the alignment of clathrin to coat the vesicle (Popova et al. 2013). The clathrin-coated vesicles with a size of approximately 100–500 nm entrap the nanoparticles and transport the nanoparticles into the endosomes. Nanoparticles enter into the endo-lysosomal system and eventually induce their desired function in the physiological system. The clathrin-mediated pathways of different nanoparticles were studied in different cellular models. The uptake mechanisms investigated the toxicity of silver nanoparticles in *C. elegans*. The study revealed that the nematodes took up silver nanoparticles in the clathrin-dependent cellular uptake and played a significant role in the cytotoxic outcomes (Eom and Choi 2019). The uptake of gold nanoparticles that have promising biomedical applications was evaluated by various microscopic techniques and found that gold nanoparticles with an approximate size of 20 nm were taken up by clathrin-mediated endocytosis (Ng et al. 2015). The vascular smooth muscle cells showed significantly reduced uptake of PLGA when the clathrin-mediated endocytosis pathway was inhibited. The study also provided a hint that the positively charged nanoparticles are endocytosed in a clathrin-dependent manner (Panyam et al. 2002).

21.3.4 Caveolae-Mediated Endocytosis

Another major pathway that aids in the uptake of nanoparticles is the caveolin-mediated endocytosis pathway. Caveolae are the small pits present in the cell membrane that embeds caveolin, the cholesterol-binding protein. The nanoparticles, when reaching the cell surface, the plasma membrane produces invaginations of approximately 70 nm size and take up the particles. Compared with the

clathrin-mediated endocytosis with a reversible association with the receptors, caveolin-1 does not dissociate from the vesicles (Pelkmans et al. 2004). Fullerenes, a promising nanoparticle with various biomedical applications, were surface-functionalized with phenylalanine (Bucky amino acid, Baa) poly-lysine derivative with a FITC label (Baa-Lys (FITC)-(Lys) 8-OH). The functionalized nanoparticle was uptaken by HEK cells via a caveolae-mediated pathway. The ATP-dependent endocytosis was mediated by a scavenger receptor-specific pathway (Zhang et al. 2009). There exists a variety of cellular mechanisms for the transport of a substance across cells. However, after the specific targeting, nanoparticles utilizes the endocytosis mechanism for internalization to ensure the entire drug release. It was studied that the lipid-coated perfluorocarbon emulsions, a class of nanoparticles, endure specific cellular interaction and distribute the lipophilic molecules avoiding the complete internalization of the nanoparticle. This was possible as the lipophilic molecules were delivered following the caveolae-dependent pathway (Partlow et al. 2008).

21.3.5 Clathrin- and Caveolin-Independent Endocytosis

Additionally, several other uptake mechanisms mediate the interaction of nanoparticles and their cellular internalization that does not depend on clathrin- and caveolin-mediated endocytosis. Some nanoparticles can enter the cell membrane without mediation by receptors. Since this is not a significant pathway for nanoparticle uptake, it is not discussed elaborately in this chapter.

21.4 Physicochemical Properties of Nanoparticles Influencing the Interaction Mechanisms

There are countless studies conducted to identify the cellular interactions of nanoparticles. These studies implicated that the physicochemical properties of the nanoparticles greatly determine the cell-nanoparticle interaction. All the cellular events starting from the cellular adhesion, uptake, intracellular trafficking, and the nanoparticle's exocytosis depend on the properties of nanomaterials such as size, shape, charge, composition, and rigidity. The significant factors, size shape, and surface charge are discussed below and summarized in Table 21.1.

21.4.1 Size

The size of the nanoparticles plays a crucial role in mediating the interactions with the cellular environment. The cellular processes such as cellular uptake greatly depend on the size of the nanoparticles. The nano-sized particles have a comparatively higher uptake than the micro-sized particles (Zauner et al. 2001). The intracellular uptake of gold nanoparticles with different sizes was determined in HeLa

Table 21.1 Effect of physicochemical properties of NPs on cellular interactions

Physicochemical factors affecting the cellular interactions	Specifications	Nanoparticle type	Cell lines/animal model	Cellular effects	Reference
Size		AgNPs	RBCs	Adsorption, uptake, hemolytic activity	Chen et al. (2015)
	37 nm	PVP-coated iron oxide	RAW 264.7	Cellular uptake	Huang et al. (2010b)
	30 nm	TiO ₂	MC3T3-E1	Cellular uptake	Brammer et al. (2009)
	100 nm	Poly(ethylene glycol)- bi-poly(propylene sulfide)	THP-1	Cellular uptake	Shann et al. (2012)
Shape	Rod	SiNPs	HepG2, HL-7702	Increased uptake, oral bioavailability	Shao et al. (2017)
		AuNPs	Glioblastoma	Cytotoxic	Bandyopadhyay et al. (2018)
	Sheet	Polymeric NPs	4T1 cells	Prolonged circulation in blood	Zhang et al. (2016)
		Dendrimers	4T1 cells	Antitumor efficiency, high tumor accumulation	Guo et al. (2018)
	Sphere and rod	AuNPs	STO cells, HeLa cells, SNB19 cells	Cellular uptake internalization	Chithrani and Chan (2007)
			HeLa cells	Cellular uptake	Graillon et al. (2008)
Star-shaped	AuNPs	Human skin fibroblasts, RFPECs	Cytotoxicity	Favi et al. (2015)	

(continued)

Table 21.1 (continued)

Physicochemical factors affecting the cellular interactions		Specifications	Nanoparticle type	Cell lines/animal model	Cellular effects	Reference
Charge		Antionic	AuNPs	U14 tumors	Prolonged circulation, enhanced accumulation	Wang et al. (2016)
			QDs	MDA-MB231 and RAW 264.7 macrophages	Increased uptake, prolonged circulation	Liu et al. (2015)
		Cationic	Polymeric	THP-1 macrophages and non-phagocytic A549 cells	Uptake	Jeon et al. (2018)
Surface modification			Liposome	U87MG and NIH/3T3	Uptake	Kang et al. (2017)
			Graphene oxide	In vitro and in vivo assesment	Improved biocompatibility	Xu et al. (2016)
			Polystyrene nanoparticles	(M2) Macrophages	Selective evasion of phagocytic clearance	Qie et al. (2016)
Rigidity/elasticity			Magnetic iron oxide nanoparticles	A549, HeLa	Biocompatibility	Malvindi et al. (2014)
			PEG-based hydrogel nanoparticles	J774 macrophages, bEnd.3, 4T1 cells	Circulation, phagocytosis, endocytosis	Anselmo et al. (2015)

cells. The 50 nm-sized gold particles showed higher uptake than the nanoparticles with sizes of 14 and 74 nm (Chithrani et al. 2006). The cellular uptake and the localization of silver nanoparticles were also dependent on the size. The effect of different particle size (5, 20, 50, 100 nm) of silver nanoparticles in B16 mouse melanoma cell lines suggested that the particle size not only enhance the efficiency of cellular uptake but also affect the endocytosis and the internal trafficking of the nanoparticles (Wu et al. 2019). In general, the effects of particle size on cellular interactions are widely studied, and the synthesis of nanoparticles with smaller sizes can be promising for various nanomedicine and drug delivery applications.

21.4.2 Shape

The shape of the nanoparticles also has an influence on cellular interactions. The shape of the nanoparticle is identified as a new factor that exerts tremendous impact on cellular interactions, including uptake, bio-distribution, and the in vivo effectiveness of the nanoparticle. The shape-dependent interactions of the nanoparticle with the cells have been studied in various nanoparticles. Mesoporous silica nanoparticles synthesized with three different shapes have been studied. It was noted that the particle with higher aspect ratios was taken up more effectively by the A375 human melanoma (A375) cells. It was also found that cellular functions such as cell proliferation, adhesion, migration, and apoptosis were impacted by particles with higher aspect ratios (Huang et al. 2010a). Recently nonspherical nanoparticles have been used to improve the therapeutic efficiency of anticancer agents and have been a remarkable finding relating to the particle shape. Apart from the spherical nanoparticles, nonspherical nanoparticles provide unique surface areas that can accommodate better methods of surface modifications using various ligands and thereby enhance targeted drug delivery (Jindal 2017).

21.4.3 Charge and Surface Hydrophobicity

The surface charge of the nanoparticles influences the interaction of nanoparticles with the cell. The alterations in the electrostatic property relate directly to the cellular uptake, internalization, intracellular transport, and the elimination of nanoparticles. Many studies are pointing out the relationship between the surface charge and the cellular interaction of nanoparticles. Most of them conclude that the cells internalize positively charged nanoparticles more efficiently than negatively charged nanoparticles. The magnetic iron oxide nanoparticles with different coatings on the surface that generated three different nanoparticles with negative and positive charges were studied on Oral Squamous Carcinoma Cell KB. The cellular uptake of the positively charged CS-DMSA@MNPs was the highest and little uptake was shown by the negatively charged DMSA@MNPs (Ge et al. 2009). The magnetic nanoparticles were functionalized with a positive polyethyleneimine (PEI-MNPs) and a negative polyacrylic acid (PAA-MNPs). The results demonstrated the

incorporation of larger amounts of PEI-MNPs than PAA-MNPs (Calatayud et al. 2014).

21.5 The Cell Mechanics Influencing Nanoparticle-Cell Interaction

Most of the studies focusing on nanoparticle-cell interactions deal with the physico-chemical properties of nanoparticles and their effect on various cellular processes such as cellular uptake, biokinetics, and toxicity. Even though cell mechanics have been widely studied, the effects of nanoparticles on the mechanics of cells are not studied elaborately. Cell mechanics can determine the cell functions and health of the cell. The interaction of nanoparticles with the cytoskeletal structures and the cellular organelles is essential for fundamental cellular processes like cell growth, differentiation, cell migration, and tissue integrity. Hence, it is beneficial to understand the cell mechanics and their influence on the cellular processes when nanoparticles are introduced to the system (Septiadi et al. 2018). The cellular adhesion and cytoskeleton systems are the two main constituent fields of cell and tissue mechanics. The cellular junctions, cell-extracellular matrix (ECM) junctions, and proteins that mediate adhesion like cadherins, integrins, and selectins constitute the cell adhesion system. These systems help analyze and withstand the force exerted by the cell's exterior, including a neighboring cell or the ECM (Discher et al. 2005). The cytoskeleton deploys force onto the cell's surroundings to keep the cellular shape intact through the dynamic assembly and disassembly of actin and tubulin with the help of other motor proteins. The cytoskeleton regulates processes like cell migration, which aids in wound healing, cancer metastasis, and maintains the elastic properties of cells.

The nanoparticles used for various applications can induce or inhibit cellular processes and interact with the cytoskeleton structures and the cellular organelles. Due to their unique physicochemical properties, nanoparticles that are internalized by the cells react with the cellular membrane, cellular organelles, and cytoskeleton structures. These interactions can change the physiological functions of the cell. Compared to the number of cell viability studies reported for the nanoparticles, few studies report the effects of nanoparticle exposure on cell mechanics. Thus, it is worthwhile to identify the potential changes that occur in the cell mechanics upon exposure to nanoparticles.

21.5.1 Cellular Adhesion

Adhesion is the primary cellular activity encountered by nanoparticles when entering a biological system. The nanoparticles bind with the cell or the ECM through protein-protein interactions. The cell adhesion molecules like integrins, cadherins, and immunoglobulin superfamily CAMs perform specific functions and enhance the adhesion of the nanoparticles.

The nanoparticles entering the cells get adhered to the cell membrane or are endocytosed by various mechanisms. This interaction is known to cause changes in cellular processes. The nanoparticles could either enhance or inhibit the adhesion properties depending upon the various factors related to the cells and the nanoparticles. The exposure of silver nanoparticles in a triple coculture model of blood–brain barrier including pericytes, astrocytes, and endothelial cells in rat were studied for the effect of nanoparticles on tight junctions. The study pointed out that the protein ZO-1 that mediates tight junction activity is decreased in this case and leads to neurotoxic effects in rats. This was followed by shrinkage of mitochondria, formation of vacuoles, and enlarging of the endoplasmic reticulum (Xu et al. 2015). The interaction of cadherin, the cell junction protein in an endothelial cell with TiO₂ nanoparticles, induced the leakage of the endothelial cell. This leads to the remodeling of actin filaments and the degradation of the cadherin protein. The pulmonary metastasis of the melanoma-lung metastasis model in mice was increased as the TiO₂ nanoparticles caused the leakage of subcutaneous blood vessels (Setyawati et al. 2013).

There are a number of molecules that mediates the adhesion of nanoparticles and cells. The molecules can vary in varying cell types as there are specific proteins related to specific cellular responses in each kind of cell. The immunoglobulin superfamily (IgSF) is the protein superfamily present in the cell surface and soluble proteins that are engaged in relaying the recognition, binding, and adhesion of the cells. For instance, in endothelial cells, intracellular adhesion molecules (ICAM) and vascular adhesion molecules (VCAM) belong to the immunoglobulin superfamily that aids in the adhesion of endothelial cells (Jin et al. 2018). Alumina nanoparticles were shown to induce the expression of mRNA and protein of ICAM-1 and VCAM-1 in human umbilical vein endothelial cells and porcine pulmonary artery endothelial cells (Oesterling et al. 2008). The nanoparticle interaction with the cells can clearly affect the cell adhesion properties. Even though the exact mechanisms are not elaborated in many instances, the knowledge about these interactions can add upon to the effective synthesis of suitable nanoparticles for biomedical applications.

21.5.2 Cytoskeleton Interactions

The cytoskeleton of the cell performs various functions, including the organization of cell components, establishing the proper cellular shape, providing mechanical support to the cells connecting the cells with their environment, cell division, and cell migration. The cytoskeleton comprises a dynamic network of proteins extended all over the cytoplasm and with the extracellular components. The intracellular trafficking of the molecules presents inside the cells is mediated by the cytoskeleton structures. The interaction of nanoparticles with the cytoskeleton has been studied in various *in vitro* and *in vivo* (Ispanixtlahuatl-Meráz et al. 2018). Most of these studies describe the effects of nanoparticles on the cytoskeleton as a function of the cellular structure, and the cytoskeletal disruptions that lead to the disintegration of other cellular processes are less known.

The physicochemical properties, the dosage, and the time of exposure of nanoparticles can affect the cytoskeleton interactions. The microtubule, microfilaments, and intermediate filaments that constitute the cytoskeleton can impact exposure to nanoparticles. The effect of gelatin nanoparticles on the cytoskeleton organization was studied in human fibroblasts. The actin and tubulin structure of the cells were found to be disorganized with the treatment of the nanoparticles at a concentration of 0.2 mg/mL (Gupta et al. 2004). A decrease in the expression of α -actin was observed in the RT-qPCR studies in MRC-5 cells (mouse lung fibroblasts) and human primary lung fibroblasts when treated with TiO₂ nanospheres (Boland et al. 2014). All the reported literature depicts that those cytoskeletal modifications upon nanoparticles' interactions are interconnected with the cellular stress responses. Hence, the changes in cytoskeleton structures should be studied in cellular responses rather than confining them to the cell shape modifications.

21.6 Cell–Nanoparticle Interactions and Hemostasis

The nanoparticles entering the living system, via various administration routes, reach their target organs by transport through blood. Although the various types of nanoparticles have various cellular destinations, they have to encounter systemic circulation at some point in their journey in the system. The interactions of nanoparticles with the blood systems can be desirable and non-desirable. Most of the *in vitro* and *in vivo* studies conducted to characterize nanoparticles in the living system neglect the interactions of nanoparticles with blood and its components. In order to fully account for the physiological responses related to the uptake of nanoparticles, it is more beneficial to study the interaction of nanoparticles with the blood cells also. The critical evaluation of the damaging effects of the cellular interactions between any foreign particle and the various constituents of blood is essential in applications of nanoparticles demanding therapeutic efficiencies (Szebeni and Haima 2013).

21.6.1 The Formation of Protein Corona

With the entry of nanoparticles into the bloodstream, the immune cells instantly identify the nanoparticles and initiate the processes that eliminate nanoparticles from the bloodstream. This prevents the interaction of nanoparticles with the destined tissues. The process of recognition by the immune cells is marked by the adsorption of proteins onto the surface of nanoparticles. This adsorption of proteins onto the nanoparticle surface upon entry into the blood is termed the protein corona formation or the biological corona formation (de la Harpe et al. 2019). As described in Sect. 21.3.1, the phagocytotic cells mediate along with the proteins, immunoglobulins, and the complement proteins opsonize the nanoparticle and tag them for clearance from the blood (Fig. 21.4). The consequential interaction of nanoparticles results

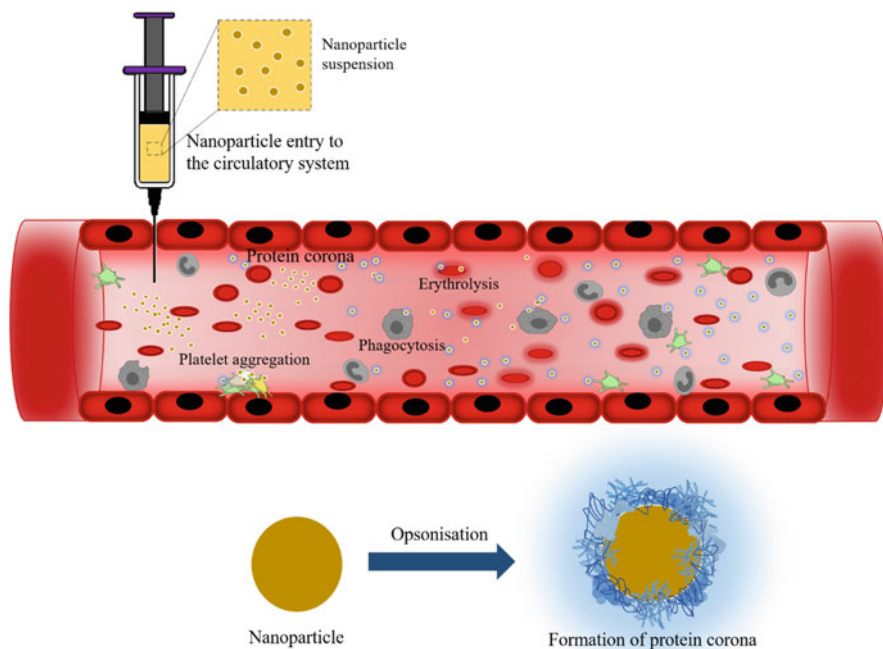


Fig. 21.4 Schematic representation of NPs interaction with blood cells

from the adsorption of the proteins on these nanoparticles and also the nature of the corona formed. The protein corona formation of a nanoparticle can be understood by studying the various immune responses happening with the entry of nanoparticles into the cells. The formation of protein corona can alter the physicochemical properties of the nanoparticles and make them a different entity compared with its actual synthetic identity. Also, the physiological factors including bioavailability, cellular uptake, intracellular trafficking, bio-distribution, and toxicity can endure detrimental effects on the formation of the protein corona (Simon et al. 2018).

The protein corona formation has been detected in various nanoparticles, such as silica nanoparticles, iron oxide nanoparticles, polymeric nanoparticles, quantum dots, and gold nanoparticles, to name a few. Since the most abundant protein in the serum is albumin, the protein corona was also composed of albumin on most of the nanoparticles, along with fibrinogens, immunoglobulins, and apolipoproteins. The dynamic nature of protein corona formation results in the production of soft and hard corona around the nanoparticles. The soft corona is formed as the result of the initial interactions with the serum proteins. The weakly interacting proteins with lower affinity are replaced timely by the high-affinity protein that binds tightly to the nanomaterials forming the hard corona (Fleischer and Payne 2014).

In *in vivo* systems, the drug release ability and targeting of nanoparticles are severely affected by protein corona formation. To conquer the opsonization process,

there are numerous approaches to hide the nanoparticles from the phagocytotic cells. Surface coating of nanoparticles with suitable substances like hydrophilic ligands, pre-coating with specific proteins, stealth polymers, and protein corona shields would help to increase the retention time in blood. Hence, the synthesis and development of nanoparticles for biological applications should demand a comprehensive understanding of the physiological effects stirred up by the protein corona formation (Caracciolo et al. 2017).

21.6.2 Nanoparticles and the Interaction with Blood Cells

Instantly after the entry of NPs into the blood system, they confront various components of blood systems, including blood cells (erythrocytes, leukocytes, and thrombocytes) and the associated proteins. These components have structure-based functions that regulate cellular processes. The nanoparticles could sometimes alter the structure and function of the proteins thereby leading to undesired toxic responses. The NP-cellular interactions can affect the significant properties of blood like hemorheology and processes like axial margination that can have a significant impact on the underlying cellular functions (Brass et al. 2019). The nanoparticle interaction with erythrocytes could alter the parameters influencing blood viscosity that could, in turn, change the resistance of blood flow and impairment of major organs. The nanoparticle interaction with the erythrocyte can also cause hemolysis. The hemolysis-inducing nanoparticles can be a major threat to the clinical implications of nanoparticles (Mocan 2013). The serious hemolytic activity in nanoparticles, including the most widely studied hydroxyapatite and silver nanoparticles, poses major concerns. Even though the critical mechanisms leading to hemolysis are not fully understood, the processes like cellular uptake, internalization, and the direct nanoparticle-membrane interaction of erythrocytes can be plausible explanations. Silver nanoparticles induce the lysis of RBCs by direct interaction with the cellular membrane causing oxidative stress and membrane injury (Chen et al. 2015). The oxygen transport mechanism of erythrocytes can also be altered by the interaction of nanoparticles with the erythrocyte membrane. The flexibility and deformability of erythrocytes were affected by the graphene quantum dots (Kim et al. 2016) and PEGylated gold NPs (He et al. 2014). The deformability of erythrocytes hinders blood flow and contributes to the aggregation of erythrocytes in the spleen, disrupting the functions of the organs (Zhao et al. 2011). The nanoparticle interaction could increase the aggregation properties of erythrocytes abnormally and result in the occlusion of narrow blood vessels thereby decreasing the availability of blood to the target organs (Barshtein et al. 2018).

The inorganic and polymeric nanoparticles were studied to assess their influence on the composition of RBCs. The mutual interactions of RBCs when exposed to nanodiamonds showed adverse effects compared to other nanoparticles. They caused the formation of larger RBC aggregates (Avsieievich et al. 2019). Platelets also play a major role in hemostasis, and accessing their interactions with nanoparticles is necessary to avoid any adverse effects on their intended function.

Platelets ensure hemostasis by undergoing three distinct phases, namely adhesion, activation, and aggregation. The burden induced by nanoparticles at any of these stages may change the functions thereby causing antagonistic functions. Silica nanoparticles were shown to accelerate vascular endothelial dysfunction by negatively regulating the L6R/STAT/TF signaling pathway (Feng et al. 2019). The influence of silica nanoparticles on endothelial cells and their effect on platelet adhesion was studied by Saikia et al. (2018). The number of platelets adhered on the surface of the endothelial cells in the presence of the nanoparticles showed an increasing pattern. The expression levels of PECAM also increased thereby increasing the adhesion of platelets to the surface of endothelial cells (Fig. 21.4). The platelet activation was also increased when treated with silver nanoparticles. The physicochemical characteristics of the nanoparticle could determine the interaction of nanoparticles with platelets. The surface chemistry of the nanoparticles could enhance the interaction of platelets. Positively charged nanoparticles would enhance the platelet–platelet interaction by neutralizing the negative charge on the platelets and thereby forming aggregates. Platelet aggregation is also elevated by the dendrimeric nanoparticles like PPI, PAMAM, and carbosilane dendrimers. In CD1 mice, PAMAM dendrimers are found to cause lethal DIC-like coagulation. The platelets were activated by cationic G7 PAMAM dendrimers and altered the morphology. This, in turn, changed the function of platelets thereby increasing the aggregation tendency and adherence to surfaces (Jones et al. 2012). Another essential component of the blood system is the leukocytes comprising monocytes, granulocytes, and lymphocytes. The lymphocytes are the key components of the immunity system. The immune system and the coagulation system depend on the activation of leukocytes; the hemocompatibility of nanoparticles is dependent on leukocytes. The engineered nanoparticles are recognized as non-self-bodies by the leukocytes and phagocytosed thereby eliminating them from circulation. Hence, the interaction of nanoparticles with the different blood cells must be thoroughly monitored during the synthesis of nanoparticles, especially for targeted drug delivery.

The effect of different nanoparticles on blood cells can vary according to the physicochemical factors of the nanoparticles. Hence, hemocompatibility studies are mandated to elucidate the complete cellular behavior of newly produced nanoparticles. The toxic responses can also significantly differ based on this factor. There are many studies reporting on the exciting application of nanoparticles for various pharmaceutical purposes. However, the clinical translation of these drugs compared to studies conducted is lesser due to the fact that there are many overlooked factors that facilitate the cell-nanoparticle interaction. One of them can be the unforeseen mechanisms of toxicity happening with the encounter of NPs with the blood circulation system (Zia et al. 2018). The nano-based drug delivery can have major advantages over the existing drug delivery systems characterized by reduced shelf life, easily degradable, high dosage, and nonspecific delivery. The nanoparticle-mediated drugs that are engineered to target the systemic circulation and the coagulation processes specifically can prove desirable and overcome many challenges related to the clinical applications of drugs targeting the coagulation

processes. On the contrary, the interaction of nanoparticles with the blood cells, including the endothelial cells, various proteins, and the components of the coagulation pathway, including platelets and coagulation factors, could harness unintended toxic effects in the living system. Overlooking the interactions of nanoparticles with the blood components could also invite life-threatening severities and lead to nanoparticle-induced coagulopathies (Ruckerl et al. 2006). The studies also report that the hemostasis balance can be disturbed by the nanoparticles causing severe toxicity like disseminated intravascular coagulation and deep vein thrombosis (Ilinskaya and Dobrovolskaia 2016).

21.7 Intracellular Trafficking of NPs

The transport of nanoparticles to specific intracellular destinations is the important stage after the uptake of nanoparticles into the cells. The nanoparticles after the endocytosis reside in the membrane-lined endosomes and need to be shipped to the target by traveling across the cytoplasm and the cellular trafficking. Based on the uptake mechanism and internalization, the nanoparticle trapped inside the endosomes can be eliminated, recycled, or transported to various subcellular organelles, including mitochondria, Golgi, endoplasmic reticulum, or lysosomes. The complex nature of the intracellular transport mechanisms makes it difficult to elucidate the big picture of all the processes inside the cells.

21.7.1 Endosomal Escape

The trafficking of endosomes across the cells is a sophisticated process that involves the movement of motor proteins carrying the vesicles along the microtubules. The sorting of the vesicles to their various destinations is carried out at this stage. Moreover, the vesicles are fused to early endosomes or matured into late lysosomes depending on the cellular process required. The change in pH of the vesicles is a notable event occurring during the maturation of the endosomal vesicles (Such et al. 2015). The entrapment of nanoparticles can be desirable and non-desirable according to the function assigned to them. The nanoparticles designed for functioning inside the lysosomes or the endosomal network do not require to come out of the vesicle, so the entrapment is desirable (Bareford and Swaan 2007). However, for the majority of nanomedicine applications, the nanoparticles need to be targeted outside the endosomal vesicles. The acidification of the endosomal vesicles upon maturation from early to late endosomes can degrade and digest the nanoparticles trapped inside the vesicles thereby destroying their functional aspects. Hence, the nanoparticles need to be engineered with mechanisms that would help them escape from the endosomal network.

To synthesize an efficient nano-delivery system, the endosomal escape mechanism must be carefully understood. The nanoparticles have been engineered with several mechanisms to overcome endosomal entrapment. The incorporation of

envelopes like membrane-based or viral capsids that have the capability to fuse with the membrane of endosomes has been utilized (Li et al. 2009). This method has been used to transport a variety of molecules, including drugs and nanoparticles, from the endosomal vesicles to the cytoplasm. With the complexity in synthesizing such membrane-bound nanoparticles and the immunogenicity of the viral capsids, the enveloping approach is not accepted widely. The application of pH-sensitive approaches is an acceptable approach for preparing the nanoparticles for endosomal escape. The nanoparticles are coated with moieties that are pH-sensitive and would encounter structural distortions when the endosomal pH changes to acidic and thereby resulting in the rupturing of the endosomal vesicle (Kobayashi et al. 2009). Also, the “proton sponge effect” can be utilized where the nanoparticles are coated with polymers with a buffering range of 5–7 pH that initiates an osmotic swelling of the endosomes and subsequent burst leading to the escape of the nanoparticle (Chou et al. 2011).

The interaction of nanoparticles with the cellular membranes can be accessed via various assays and can be studied as a manifestation of the endosomal escape involved. The relation between the physicochemical properties and the endosomal escape ability can also be determined by the assays. For instance, the endosomal escape mechanism of polymeric nanoparticles can be investigated by the RBC lysis and dye leakage from dye-loaded liposomes. There are several mechanisms that enable the escape of nanoparticles from the endosomes. For the synthesis of nanoparticles with ideal properties, the factors that control the escape must be thoroughly understood. The endocytosis mechanisms do play a major role in determining the effectiveness of endosomal escape as well. The main mechanisms that help in the endosomal escape through osmotic pressure change, through membrane fusion, escape via nanoparticle swelling, and membrane destabilization (Smith et al. 2018). More research on the detailed understanding of these mechanisms is required to design nanoparticles that can efficiently work for their desired function.

21.7.2 Organelle and Subcellular Targeting

The cellular functions are precisely carried out by the presence of various cellular organelles. The mitochondria, nucleus, endoplasmic reticulum, Golgi apparatus, and lysosomes, among the major organelles, play their role in organizing and regulating cellular functions. All the major cellular processes, including cell division, replication, energy metabolism, and synthesis of proteins and lipids, are well regulated by the cellular organelles, and any abnormality in the regulation invites the dysfunction of the cellular environment, eventually leading to the diseased state of the body. Nanoparticles mediated drug targeting is a promising tool to treat the abnormalities occurring in cellular processes, and hence the targeting of organelles is an essential step for the treatment using nanoparticles. The physicochemical properties of the nanomaterials can be manipulated in such a way that it makes the specific targeting of organelles possible. Along with the proper surface functionalities, the

manipulations based on size and charge can also aid in specific delivery to the subcellular organelles.

The nucleus is a sought-after destination for targeting nanoparticles as the genetic material is inhabited inside them. The novel treatment methods for many gen-related diseases can be a great success if the targeting of nanoparticles to the nucleus is well explored. The nuclear membrane complex actively transports nanoparticles into the cells along with the nuclear localization signals (NLS). The size plays a vital role in the nuclear targeting of nanoparticles. The smaller nanoparticles tend to localize in the nucleus while larger ones remain in the cytoplasm. The nanoparticles with a diameter of up to 50 nm enter the nucleus through the nuclear pore channel by active uptake (Pan et al. 2012). The nuclear pore channel has a diameter of approximately 6–9 nm, and hence the nanoparticles having a diameter less than the pore size can enter the nucleus via passive diffusion (Eibauer et al. 2015). The nuclear targeting in HepG2 cells was studied using peptide complexed nanoparticles, and the study revealed various means of assessing the efficiency of nuclear targeting (Tkachenko et al. 2003). Another important organelle for intracellular targeting of the nanoparticles is the mitochondria. The surface functionalization of nanopolymers with suitable moieties targeted the nanoparticle to the mitochondria. The targeting of mesoporous silica nanoparticles conjugated with ligand to deliver doxorubicin to mitochondria was performed. The targeting efficiency in mitochondria was analyzed in HeLa cells by the localization study. The results highlighted the promising application of nanoparticle targeting to mitochondria for anticancer treatments (Qu et al. 2015).

The folding and transport of proteins occur in the endoplasmic reticulum and hence is an essential organ for cellular targeting. Any abnormalities in the genetic or environmental aspects induce ER stress and are tagged for the development of diseases. The ER targeting strategies include small molecule-mediated targeting (ligand-receptor, lipophilic membrane, enzyme), peptide-mediated targeting, and carrier-based ER targeting (Shi et al. 2021). The Golgi apparatus is also targeted for nanomedicine therapy as the organelle is critical for the posttranslational modifications of synthesized proteins. A Golgi apparatus targeting nanoparticle prodrug was synthesized by retinoic acid conjugated chondroitin sulfate. The nanoparticle targeted the multistep approach that enhanced the antimetastasis effect combined with chemotherapy (Li et al. 2019).

21.7.3 Exocytosis

The process of expelling the membrane-bound vesicles and their constituents to the extracellular matrix is termed exocytosis. Basically, it is the process of eliminating unwanted substances from the intracellular spaces. The excretion of nanoparticles from the cellular environment is a necessary process that affects the interaction of cells and nanoparticles. The timely removal of the nanoparticle thereby preventing its accumulation in the cellular spaces is essential to avoid any harmful effects. However, the fast rate of exocytosis can also affect the efficiency of the

nanoparticles. The prolonged residency time of the nanoparticle can be helpful in the drug delivery process. The ICP-MS study of the gold nanoparticles modified with quarternary amines revealed that the compounds stayed in cells avoiding exocytosis and did not cause cytotoxicity for 24 h (Kim et al. 2015). Compared to the entry of cells into the cells, the exit also is dependent upon the cell types. The excretion process of the same nanoparticle can be different for different cell lines, even though the endocytosis mechanism seems to be similar. The interaction of human cells with silica nanoparticles was performed to gain insight into the entry and exit of nanoparticles into the cell. The exocytosis of silica nanoparticles in three different cell lines showed that the exocytosis mechanisms were different in these cell lines (Chu et al. 2011). A better understanding of the exocytosis of the nanomaterials can enhance the potential applications of drug delivery applications.

21.8 Cell-Nanoparticle Interactions and Cytotoxicity

The nanoparticle exposure in the cell can promote reactive oxygen species (ROS) generation, DNA damage, inflammation, lysosomal damage, mitochondrial damage, cell division inhibition, and finally, cell death. The oxidative stress due to nanoparticle-induced ROS generation is the primary reason for cellular toxicity. ROS is an indispensable signaling molecule, that mediates homeostasis and assists in diverse cell signaling pathways, and its generation can be intrinsic or extrinsic. Mitochondria, microsomes, peroxisomes, and inflammatory reactions occurring in the cell are the primary sources of ROS generation. However, the nanoparticle (NP) can act as the exogenous source of ROS generation. Even though it is a ROS key molecule in various cellular reactions, it is produced in trace amounts. NPs activate the mitogen-activated protein kinase (MAPK) pathway, various transcription factors, regulate cytokine production, and interfere with calcium pump through the free radicle generation. Cells have the intrinsic ability to detoxify the free radicle generated via the antioxidant system (enzymatic or nonenzymatic). Cells regulate the mild and intermediate oxidative stress conditions by activating the phase II antioxidant system and a pro-inflammatory response via MAPK and nuclear factor kappa light chain enhancer of activated B cells (NF- κ B). The high level of oxidative stress results in the electron chain's dysfunction by damaging the mitochondrial membrane. The highly reactive free radical perturbs the normal redox state and results in lipid peroxidation, impaired protein folding, DNA damage, and meddling with various signaling pathways (Lewinski et al. 2008).

Many of the nanoparticles developed have been shown to induce ROS generation due to their reactive surface. The surface-bound pro-oxidant functional groups present on the surface of nanoparticles facilitate ROS generation. The reduced size and altered electronic properties of nanoparticles can result in the formation of reactive sites. The electron acceptor/donor present in such reactive sites reacts with molecular oxygen to produce reactive oxygen species. Nanoparticle with transition metals on the surface reacts with H_2O_2 and produce oxidized metal ion and $OH\bullet$. Similarly, the oxidized metal ion can react with H_2O_2 and further induce $OH\bullet$. Upon

entry of NPs into the cell, they can translocate to mitochondria. Once reaching the mitochondria, the NPs can interfere and impair the electron transport chain and further damage structural integrity, leading to the membrane depolarization of mitochondria, ultimately, the endogenous ROS generation. NPs exposure to the cell can trigger the pro-inflammation cascade via activation of various signaling pathways, recruits immune cells, and they release ROS to eliminate the NPs. The ROS generated due to the nanoparticle exposure can induce DNA damage via strand breaks, fibrosis through ECM deposition, mitochondrial dysfunction, and lipid peroxidation (Wydra et al. 2015).

NPs translocation to the nucleus can result in their intercalation within grooves of DNA. NPs such as carbon nanotubes (CNT) can mimic the microtubule system. Some reports have suggested that CNTs can impair cell division by interfering with mitotic spindle formation and perturbing centromeres. The stress developed in cells due to NPs through the protein misfolding and damage, endoplasmic reticulum (ER) and mitochondrial stress, impaired gene regulation and expression, and various signaling cascades may induce autophagic cell death. However, surface modification can change the autophagy potential of nanoparticles. The nanoparticles in the lysosome can induce oxidative stress, promote osmotic swelling, result in alkalization, and finally the structural damage to the lysosome. A schematic diagram of the various cytotoxicity mechanisms is depicted in Fig. 21.5.

21.9 Exploring the Cellular Interaction of Nanoparticles

The expeditious development of nanotechnology-based medical applications needs effective tracking methods to understand the interactions of nanoparticles with biological molecules. The contemporary methods used to track the interactions of nanoparticles are schematically represented in Fig. 21.6. The most widely accepted tool to probe cellular interactions is through imaging. Bioimaging techniques have witnessed a drastic evolution since the beginning of their application for understanding cellular interaction. Recent advances in bioimaging have aided in the successful monitoring of cellular interactions with nanoparticles. Fluorescence microscopy has been widely accepted for its ability to track multiple wavelengths in the natural cellular environment. Other than imaging, insights into the molecular interactions and the sequential effects of these interactions on the phenotypic and genotypic characteristics of the cells can be analyzed by various analytic tools, including cytometry, high-content analysis, and super-resolution techniques, new technologies need to be implemented as the experimental cell-based models are paving the way to advanced technologies such as organ on a chip (Joseph et al. 2022). Single-molecule data analysis and super-resolution technology have been employed to analyze the nanoparticle interaction during the uptake process (van der Zwaag et al. 2016). To detangle the cellular effects of silver nanoparticles in human umbilical vein endothelial cells, high-content (HC) imaging combined with high-content gene expression studies were employed (Manshian et al. 2015). Establishing newer platforms that could directly capture the nano-metric resolutions and provide mechanistic

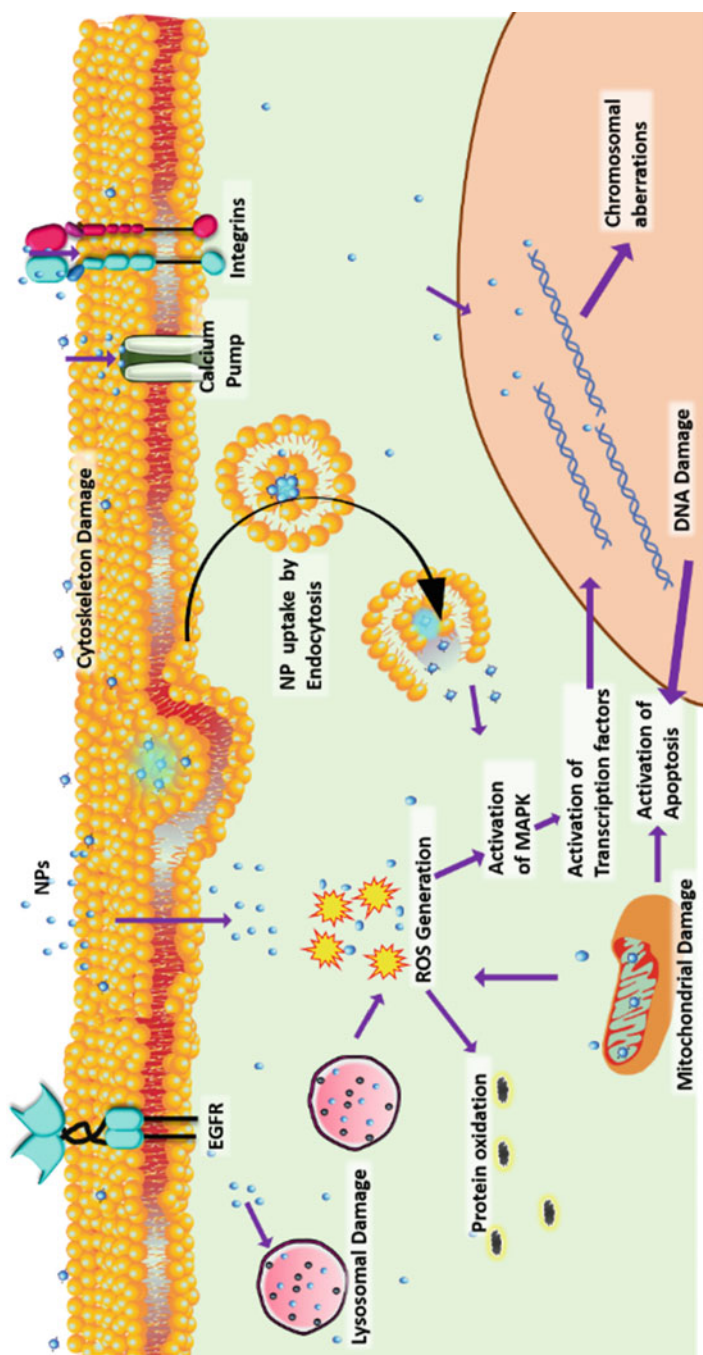


Fig. 21.5 Schematic representation of toxicity elicited by nanoparticles on cells



Fig. 21.6 Methods used to analyze the cellular interactions of nanoparticles

insights on cellular interactions must be the futuristic application of nanotechnology in medical applications.

21.10 Conclusion

Numerous types of nanoparticles are synthesized for various biomedical applications. The cellular interactions of nanoparticles are an essential aspect as nanoparticle-based applications are finding momentum in numerous biological fields, including medicine, drug delivery, and pharmaceuticals. Nanoparticles can regulate different cellular processes like cellular uptake, intracellular trafficking, cell signaling, and exocytosis and can mediate both beneficial and harmful effects in the living system. The influence of nanoparticles on cell adhesion, cytoskeleton arrangements, and migration need to be thoroughly studied. The current advances in the experimental processes have paved the way for the synthesis of novel nanoscale particles with defined biological implications. Even though plenty of studies report the interactions of nanoparticles with cells, many challenges need to be solved to ameliorate the disadvantages of nanoparticle-based biological applications, including toxicity concerns. The existing experimental analysis is not sufficient to

thoroughly understand the behavior of cells and the association of biomolecules with nanoparticles. The current experimental analysis should be improvised in such a way that it can capture the true dynamic nature of the cellular environment and the influence of nanoparticles on the cellular mechanisms. The cellular interactions of nanoparticles must be studied in all ways possible to avoid the detrimental effects arising when they are translated into a therapeutic approach and to avoid toxicological concerns.

Acknowledgments The authors wish to express their sincere thanks to the Director and Head, Biomedical Technology Wing, Sree Chitra Tirunal Institute for Medical Sciences and Technology (Govt. of India), Trivandrum, for their support and for providing the infrastructure to carry out this work.

References

- Alberts B, Johnson A, Lewis J, Raff M, Roberts K, Walter P (1994) Chapter 4: Molecular biology of the cell. Garland Science, New York, p 4
- Anselmo AC, Zhang M, Kumar S, Vogus DR, Menegatti S, Helgeson ME, Mitragotri S (2015) Elasticity of nanoparticles influences their blood circulation, phagocytosis, endocytosis, and targeting. *ACS Nano* 9(3):3169–3177
- Avsievich T, Popov A, Bykov A, Meglinski I (2019) Mutual interaction of red blood cells influenced by nanoparticles. *Sci Rep* 9(1):1–6
- Bandyopadhyay S, McDonagh BH, Singh G, Raghunathan K, Sandvig A, Sandvig I, Andreassen JP, Glomm WR (2018) Growing gold nanostructures for shape-selective cellular uptake. *Nanoscale Res Lett* 13(1):1–12
- Bareford LM, Swaan PW (2007) Endocytic mechanisms for targeted drug delivery. *Adv Drug Deliv Rev* 59(8):748–758
- Barshtein G, Arbell D, Yedgar S (2018) Hemodynamic functionality of transfused red blood cells in the microcirculation of blood recipients. *Front Physiol* 9:41
- Bertrand N, Grenier P, Mahmoudi M, Lima EM, Appel EA, Dormont F, Lim JM, Karnik R, Langer R, Farokhzad OC (2017) Mechanistic understanding of *in vivo* protein corona formation on polymeric nanoparticles and impact on pharmacokinetics. *Nat Commun* 8(1):1–8
- Boland S, Hussain S, Baeza-Squiban A (2014) Carbon black and titanium dioxide nanoparticles induce distinct molecular mechanisms of toxicity. *Wiley Interdiscip Rev Nanomed Nanobiotechnol* 6(6):641–652
- Brammer KS, Oh S, Cobb CJ, Bjursten LM, van der Heyde H, Jin S (2009) Improved bone-forming functionality on diameter-controlled TiO₂ nanotube surface. *Actabiomaterialia* 5(8):3215–3223
- Brass LF, Tomaiuolo M, Welsh J, Poventud-Fuentes I, Zhu L, Diamond SL, Stalker TJ (2019) Hemostatic thrombus formation in flowing blood. In: *Platelets*. Academic Press, London, pp 371–391
- Calatayud MP, Sanz B, Raffa V, Riggio C, Ibarra MR, Goya GF (2014) The effect of surface charge of functionalised Fe₃O₄ nanoparticles on protein adsorption and cell uptake. *Biomaterials* 35(24):6389–6399
- Caracciolo G, Farokhzad OC, Mahmoudi M (2017) Biological identity of nanoparticles *in vivo*: clinical implications of the protein corona. *Trends Biotechnol* 35(3):257–264
- Cardoso AM, Morais CM, Silva SG, Marques EF, de Lima MCP, Jurado MAS (2014) Bis-quaternary gemini surfactants as components of nonviral gene delivery systems: a comprehensive study from physicochemical properties to membrane interactions. *Int J Pharm* 474(1–2): 57–69

- Chen LQ, Fang L, Ling J, Ding CZ, Kang B, Huang CZ (2015) Nanotoxicity of silver nanoparticles to red blood cells: size dependent adsorption, uptake, and hemolytic activity. *Chem Res Toxicol* 28(3):501–509
- Chen F, Wang G, Griffin JI, Brennehan B, Banda NK, Holers VM, Backos DS, Wu L, Moghimi SM, Simberg D (2017) Complement proteins bind to nanoparticle protein corona and undergo dynamic exchange *in vivo*. *Nat Nanotechnol* 12(4):387–393
- Chithrani BD, Chan WC (2007) Elucidating the mechanism of cellular uptake and removal of protein-coated gold nanoparticles of different sizes and shapes. *Nano Lett* 7(6):1542–1550
- Chithrani BD, Ghazani AA, Chan WC (2006) Determining the size and shape dependence of gold nanoparticle uptake into mammalian cells. *Nano Lett* 6(4):662–668
- Chou LY, Ming K, Chan WC (2011) Strategies for the intracellular delivery of nanoparticles. *Chem Soc Rev* 40(1):233–245
- Chu Z, Huang Y, Tao Q, Li Q (2011) Cellular uptake, evolution, and excretion of silica nanoparticles in human cells. *Nanoscale* 3(8):3291–3299
- de la Harpe KM, Kondiah PP, Choonara YE, Marimuthu T, du Toit LC, Pillay V (2019) The hemocompatibility of nanoparticles: a review of cell–nanoparticle interactions and hemostasis. *Cell* 8(10):1209
- Discher DE, Janmey P, Wang YL (2005) Tissue cells feel and respond to the stiffness of their substrate. *Science* 310(5751):1139–1143
- Doherty GJ, McMahon HT (2009) Mechanisms of endocytosis. *Annu Rev Biochem* 78:857–902
- Eibauer M, Pellanda M, Turgay Y, Dubrovsky A, Wild A, Medalia O (2015) Structure and gating of the nuclear pore complex. *Nat Commun* 6(1):1–9
- Eom HJ, Choi J (2019) Clathrin-mediated endocytosis is involved in uptake and toxicity of silica nanoparticles in *Caenorhabditis elegans*. *Chem Biol Interact* 311:108774
- Favi PM, Gao M, Johana SepúlvedaArango L, Ospina SP, Morales M, Pavon JJ, Webster TJ (2015) Shape and surface effects on the cytotoxicity of nanoparticles: gold nanospheres versus gold nanostars. *J Biomed Mater Res A* 103(11):3449–3462
- Feng L, Yang X, Liang S, Xu Q, Miller MR, Duan J, Sun Z (2019) Silica nanoparticles trigger the vascular endothelial dysfunction and prethrombotic state via miR-451 directly regulating the IL6R signaling pathway. *Part Fibre Toxicol* 16(1):1–13
- Fleischer CC, Payne CK (2014) Nanoparticle–cell interactions: molecular structure of the protein corona and cellular outcomes. *Acc Chem Res* 47(8):2651–2659
- Ge Y, Zhang Y, Xia J, Ma M, He S, Nie F, Gu N (2009) Effect of surface charge and agglomerate degree of magnetic iron oxide nanoparticles on KB cellular uptake *in vitro*. *Colloids Surf B Biointerfaces* 73(2):294–301
- Gratton SE, Ropp PA, Pohlhaus PD, Luft JC, Madden VJ, Napier ME, DeSimone JM (2008) The effect of particle design on cellular internalisation pathways. *Proc Natl Acad Sci* 105(33):11613–11618
- Guo Y, Zhao S, Qiu H, Wang T, Zhao Y, Han M, Dong Z, Wang X (2018) Shape of nanoparticles as a design parameter to improve docetaxel antitumor efficacy. *Bioconjug Chem* 29(4):1302–1311
- Gupta AK, Gupta M, Yarwood SJ, Curtis AS (2004) Effect of cellular uptake of gelatin nanoparticles on adhesion, morphology and cytoskeleton organisation of human fibroblasts. *J Control Release* 95(2):197–207
- He Z, Liu J, Du L (2014) The unexpected effect of PEGylated gold nanoparticles on the primary function of erythrocytes. *Nanoscale* 6(15):9017–9024
- Huai Y, Hossen MN, Wilhelm S, Bhattacharya R, Mukherjee P (2019) Nanoparticle interactions with the tumor microenvironment. *Bioconjug Chem* 30(9):2247–2263
- Huang X, Teng X, Chen D, Tang F, He J (2010a) The effect of the shape of mesoporous silica nanoparticles on cellular uptake and cell function. *Biomaterials* 31(3):438–448
- Huang J, Bu L, Xie J, Chen K, Cheng Z, Li X, Chen X (2010b) Effects of nanoparticle size on cellular uptake and liver MRI with polyvinylpyrrolidone-coated iron oxide nanoparticles. *ACS Nano* 4(12):7151–7160

- Ilnskaya AN, Dobrovolskaia MA (2016) Nanoparticles and the blood coagulation system. In: Handbook of immunological properties of engineered nanomaterials, Haematocompatibility of engineered nanomaterials, vol 2. World Scientific Publishing, Hackensack, NJ, pp 261–302
- Ispanixtlahuatl-Meráz O, Schins RP, Chirino YI (2018) Cell type specific cytoskeleton disruption induced by engineered nanoparticles. *Environ Sci Nano* 5(2):228–245
- Jeon S, Clavdetscher J, Lee DK, Chankeshwara SV, Bradley M, Cho WS (2018) Surface charge-dependent cellular uptake of polystyrene nanoparticles. *Nanomaterials* 8(12):1028
- Jiang LQ, Wang TY, Webster TJ, Duan HJ, Qiu JY, Zhao ZM, Yin XX, Zheng CL (2017) Intracellular disposition of chitosan nanoparticles in macrophages: intracellular uptake, exocytosis, and intercellular transport. *Int J Nanomedicine* 12:6383
- Jin K, Luo Z, Zhang B, Pang Z (2018) Biomimetic nanoparticles for inflammation targeting. *Acta Pharm Sin B* 8(1):23–33
- Jindal AB (2017) The effect of particle shape on cellular interaction and drug delivery applications of micro-and nanoparticles. *Int J Pharm* 532(1):450–465
- Jones CF, Campbell RA, Franks Z, Gibson CC, Thiagarajan G, Vieira-de-Abreu A, Sukavaneshvar S, Mohammad SF, Li DY, Ghandehari H, Weyrich AS (2012) Cationic PAMAM dendrimers disrupt key platelet functions. *Mol Pharm* 9(6):1599–1611
- Joseph X, Akhil V, Arathi A, Mohanan PV (2022) Comprehensive development in organ-on-a-chip technology. *J Pharm Sci* 111:18–31
- Kang JH, Jang WY, Ko YT (2017) The effect of surface charges on the cellular uptake of liposomes investigated by live cell imaging. *Pharm Res* 34(4):704–717
- Kim C, Tonga GY, Yan B, Kim CS, Kim ST, Park MH, Zhu Z, Duncan B, Creran B, Rotello VM (2015) Regulating exocytosis of nanoparticles via host–guest chemistry. *Org Biomol Chem* 13(8):2474–2479
- Kim J, Nafiujjaman M, Nurunnabi M, Lee YK, Park HK (2016) Hemorheological characteristics of red blood cells exposed to surface functionalised graphene quantum dots. *Food Chem Toxicol* 97:346–353
- Kobayashi S, Nakase I, Kawabata N, Yu HH, Pujals S, Imanishi M, Giralt E, Futaki S (2009) Cytosolic targeting of macromolecules using a pH-dependent fusogenic peptide in combination with cationic liposomes. *Bioconjug Chem* 20(5):953–959
- Lazarovits J, Chen YY, Sykes EA, Chan WC (2015) Nanoparticle–blood interactions: the implications on solid tumour targeting. *Chem Commun* 51(14):2756–2767
- Lewinski N, Colvin V, Drezek R (2008) Cytotoxicity of nanoparticles. *Small* 4(1):26–49
- Li YX, Pang HB (2021) Macropinocytosis as a cell entry route for peptide-functionalised and bystander nanoparticles. *J Control Release* 329:1222–1230
- Li F, Zhang ZP, Peng J, Cui ZQ, Pang DW, Li K, Wei HP, Zhou YF, Wen JK, Zhang XE (2009) Imaging viral behavior in mammalian cells with self-assembled capsid–quantum-dot hybrid particles. *Small* 5(6):718–726
- Li Y, Kröger M, Liu WK (2014) Endocytosis of PEGylated nanoparticles accompanied by structural and free energy changes of the grafted polyethylene glycol. *Biomaterials* 35(30):8467–8478
- Li H, Zhang P, Luo J, Hu D, Huang Y, Zhang ZR, Fu Y, Gong T (2019) Chondroitin sulfate-linked prodrug nanoparticles target the golgi apparatus for cancer metastasis treatment. *ACS Nano* 13(8):9386–9396
- Liu Q, Li H, Xia Q, Liu Y, Xiao K (2015) Role of surface charge in determining the biological effects of CdSe/ZnS quantum dots. *Int J Nanomedicine* 10:7073
- Malvindi MA, De Matteis V, Galeone A, Brunetti V, Anyfantis GC, Athanassiou A, Cingolani R, Pompa PP (2014) Toxicity assessment of silica coated iron oxide nanoparticles and biocompatibility improvement by surface engineering. *PLoS One* 9(1):e85835
- Manshian BB, Pfeiffer C, Pelaz B, Heimerl T, Gallego M, Moller M, Del Pino P, Himmelreich U, Parak WJ, Soenen SJ (2015) High-content imaging and gene expression approaches to unravel the effect of surface functionality on cellular interactions of silver nanoparticles. *ACS Nano* 9(10):10431–10444

- Means N, Elechalawar CK, Chen WR, Bhattacharya R, Mukherjee P (2021) Revealing macropinocytosis using nanoparticles. *Mol Asp Med* 83:100993
- Mocan T (2013) Hemolysis as expression of nanoparticles-induced cytotoxicity in red blood cells. *BMBN* 1(1):7–12
- Mosquera J, García I, Liz-Marzán LM (2018) Cellular uptake of nanoparticles versus small molecules: a matter of size. *Acc Chem Res* 51(9):2305–2313
- Ng CT, Tang FMA, Li JJE, Ong C, Yung LLY, Bay BH (2015) Clathrin-mediated endocytosis of gold nanoparticles in vitro. *Anat Rec* 298(2):418–427
- Oesterling E, Chopra N, Gavalas V, Arzuaga X, Lim EJ, Sultana R, Butterfield DA, Bachas L, Hennig B (2008) Alumina nanoparticles induce expression of endothelial cell adhesion molecules. *Toxicol Lett* 178(3):160–166
- Pan L, He Q, Liu J, Chen Y, Ma M, Zhang L, Shi J (2012) Nuclear-targeted drug delivery of TAT peptide-conjugated monodisperse mesoporous silica nanoparticles. *J Am Chem Soc* 134(13):5722–5725
- Panyam J, Zhou WZ, Prabha S, Sahoo SK, Labhasetwar V (2002) Rapid endo-lysosomal escape of poly (DL-lactide-co-glycolide) nanoparticles: implications for drug and gene delivery. *FASEB J* 16(10):1217–1226
- Partlow KC, Lanza GM, Wickline SA (2008) Exploiting lipid raft transport with membrane targeted nanoparticles: a strategy for cytosolic drug delivery. *Biomaterials* 29(23):3367–3375
- Pelkmans L, Bürlü T, Zerial M, Helenius A (2004) Caveolin-stabilised membrane domains as multifunctional transport and sorting devices in endocytic membrane traffic. *Cell* 118(6):767–780
- Popova NV, Deyev IE, Petrenko AG (2013) Clathrin-mediated endocytosis and adaptor proteins. *Acta Nat* 5(3):62–73
- Qie Y, Yuan H, Von Roemeling CA, Chen Y, Liu X, Shih KD, Knight JA, Tun HW, Wharen RE, Jiang W, Kim BY (2016) Surface modification of nanoparticles enables selective evasion of phagocytic clearance by distinct macrophage phenotypes. *Sci Rep* 6(1):1–11
- Qu Q, Ma X, Zhao Y (2015) Targeted delivery of doxorubicin to mitochondria using mesoporous silica nanoparticle nanocarriers. *Nanoscale* 7(40):16677–16686
- Rodriguez PL, Harada T, Christian DA, Pantano DA, Tsai RK, Discher DE (2013) Minimal “self” peptides that inhibit phagocytic clearance and enhance delivery of nanoparticles. *Science* 339(6122):971–975
- Ruckerl R, Ibalid-Mullı A, Koenig W, Schneider A, Woelke G, Cyrys J, Heinrich J, Marder V, Frampton M, Wichmann HE, Peters A (2006) Air pollution and markers of inflammation and coagulation in patients with coronary heart disease. *Am J Respir Crit Care Med* 173(4):432–441
- Sahay G, Alakhova DY, Kabanov AV (2010) Endocytosis of nanomedicines. *J Control Release* 145(3):182–195
- Saikia J, Mohammadpour R, Yazdimamaghani M, Northrup H, Hlady V, Ghandehari H (2018) Silica nanoparticle–endothelial interaction: uptake and effect on platelet adhesion under flow conditions. *ACS Appl Biomater* 1(5):1620–1627
- Septiadi D, Crippa F, Moore TL, Rothen-Rutishauser B, Petri-Fink A (2018) Nanoparticle–cell interaction: a cell mechanics perspective. *Adv Mater* 30(19):1704463
- Setyawati MI, Tay CY, Chia SL, Goh SL, Fang W, Neo MJ, Chong HC, Tan SM, Loo SCJ, Ng KW, Xie JP (2013) Titanium dioxide nanomaterials cause endothelial cell leakiness by disrupting the homophilic interaction of VE–cadherin. *Nat Commun* 4(1):1–12
- Shann SY, Lau CM, Thomas SN, Jerome WG, Maron DJ, Dickerson JH, Hubbell JA, Giorgio TD (2012) Size-and charge-dependent non-specific uptake of PEGylated nanoparticles by macrophages. *Int J Nanomedicine* 7:799
- Shao D, Lu MM, Zhao YW, Zhang F, Tan YF, Zheng X, Pan Y, Xiao XA, Wang Z, Dong WF, Li J (2017) The shape effect of magnetic mesoporous silica nanoparticles on endocytosis, biocompatibility and biodistribution. *Actabiomaterialia* 49:531–540
- Shi Y, Wang S, Wu J, Jin X, You J (2021) Pharmaceutical strategies for endoplasmic reticulum-targeting and their prospects of application. *J Control Release* 329:337–352

- Simon J, Müller LK, Kokkinopoulou M, Lieberwirth I, Morsbach S, Landfester K, Mailänder V (2018) Exploiting the biomolecular corona: Pre-coating of nanoparticles enables controlled cellular interactions. *Nanoscale* 10(22):10731–10739
- Smith SA, Selby LI, Johnston AP, Such GK (2018) The endosomal escape of nanoparticles: toward more efficient cellular delivery. *Bioconjug Chem* 30(2):263–272
- Such GK, Yan Y, Johnston AP, Gunawan ST, Caruso F (2015) Interfacing materials science and biology for drug carrier design. *Adv Mater* 27(14):2278–2297
- Szebeni J, Haima P (2013) Hemocompatibility of medical devices, blood products, nanomedicines and biologicals. In: TECOmedical clinical & technical review. TECOmedical, Sissach
- Tkachenko AG, Xie H, Coleman D, Glomm W, Ryan J, Anderson MF, Franzen S, Feldheim DL (2003) Multifunctional gold nanoparticle–peptide complexes for nuclear targeting. *J Am Chem Soc* 125(16):4700–4701
- van der Zwaag D, Vanparijs N, Wijnands S, De Rycke R, De Geest BG, Albertazzi L (2016) Super resolution imaging of nanoparticles cellular uptake and trafficking. *ACS Appl Mater Interfaces* 8(10):6391–6399
- Wang J, Sui M, Fan W (2010) Nanoparticles for tumor targeted therapies and their pharmacokinetics. *Curr Drug Metab* 11(2):129–141
- Wang JY, Chen J, Yang J, Wang H, Shen X, Sun YM, Guo M, Zhang XD (2016) Effects of surface charges of gold nanoclusters on long-term *in vivo* biodistribution, toxicity, and cancer radiation therapy. *Int J Nanomedicine* 11:3475
- Wilhelm C, Billotey C, Roger J, Pons JN, Bacri JC, Gazeau F (2003) Intracellular uptake of anionic superparamagnetic nanoparticles as a function of their surface coating. *Biomaterials* 24(6):1001–1011
- Wu M, Guo H, Liu L, Liu Y, Xie L (2019) Size-dependent cellular uptake and localisation profiles of silver nanoparticles. *Int J Nanomedicine* 14:4247
- Wydra RJ, Rychahou PG, Evers BM, Anderson KW, Dziubla TD, Hilt JZ (2015) The role of ROS generation from magnetic nanoparticles in an alternating magnetic field on cytotoxicity. *Acta Biomaterialia* 25:284–290
- Xu L, Dan M, Shao A, Cheng X, Zhang C, Yokel RA, Takemura T, Hanagata N, Niwa M, Watanabe D (2015) Silver nanoparticles induce tight junction disruption and astrocyte neurotoxicity in a rat blood–brain barrier primary triple co-culture model. *Int J Nanomedicine* 10:6105
- Xu M, Zhu J, Wang F, Xiong Y, Wu Y, Wang Q, Weng J, Zhang Z, Chen W, Liu S (2016) Improved *in vitro* and *in vivo* biocompatibility of graphene oxide through surface modification: poly (acrylic acid)-functionalisation is superior to PEGylation. *ACS Nano* 10(3):3267–3281
- Yang C, Gao S, Dagnæs-Hansen F, Jakobsen M, Kjems J (2017) Impact of PEG chain length on the physical properties and bioactivity of PEGylated chitosan/siRNA nanoparticles *in vitro* and *in vivo*. *ACS Appl Mater Interfaces* 9(14):12203–12216
- Zauner W, Farrow NA, Haines AM (2001) *In vitro* uptake of polystyrene microspheres: effect of particle size, cell line and cell density. *J Control Release* 71(1):39–51
- Zhang LW, Yang J, Barron AR, Monteiro-Riviere NA (2009) Endocytic mechanisms and toxicity of a functionalised fullerene in human cells. *Toxicol Lett* 191(2–3):149–157
- Zhang H, Liu Y, Chen M, Luo X, Li X (2016) Shape effects of electrospun fiber rods on the tissue distribution and antitumor efficacy. *J Control Release* 244:52–62
- Zhao J, Stenzel MH (2018) Entry of nanoparticles into cells: the importance of nanoparticle properties. *Polym Chem* 9(3):259–272
- Zhao Y, Sun X, Zhang G, Trewyn BG, Slowing II, Lin VSY (2011) Interaction of mesoporous silica nanoparticles with human red blood cell membranes: size and surface effects. *ACS Nano* 5(2):1366–1375
- Zia F, Kendall M, Watson SP, Mendes PM (2018) Platelet aggregation induced by polystyrene and platinum nanoparticles is dependent on surface area. *RSC Adv* 8(66):37789–37794



Role of Artificial Intelligence in the Toxicity Prediction of Drugs 22

Manisha Malani, Anirudh Kasturi, Md. Moinul, Shovanlal Gayen, Chittaranjan Hota, and Jayabalan Nirmal

22.1 Introduction

22.1.1 Toxicity Due to Chemicals and Drugs

Toxicity is defined as the adverse effect on an individual from any substance due to its exposure. Based on the longevity of adverse effect, toxicity can be broadly categorized as acute toxicity and chronic toxicity. Acute toxicity is for a shorter duration of time, whereas chronic toxicity is for a longer duration of time, usually for months and years. Toxicity can be measured both qualitatively and quantitatively as low, moderate or high and Lethal dose-50, respectively. Exposure to the substance can also be acute (single dose) or chronic (multiple exposures) (Raies and Bajic 2016). Factors that determine the toxicity of substances comprise of nature of the substance, including its structural and physicochemical properties or the route of exposure, dose of exposure, its interaction with endogenous molecules, and other biological properties of individuals such as body mass, age, and gender (Pérez Santín et al. 2021).

M. Malani · J. Nirmal (✉)

Translational Pharmaceutics Research Laboratory (TPRL), Department of Pharmacy, Birla Institute of Technology and Science-Pilani, Hyderabad Campus, Hyderabad, Telangana, India

A. Kasturi · C. Hota

Department of Computer Science and Information Systems (CSIS), Birla Institute of Technology and Science-Pilani, Hyderabad Campus, Hyderabad, Telangana, India

M. Moinul

Department of Pharmaceutical Sciences, Dr. Harisingh Gour University, Sagar, Madhya Pradesh, India

S. Gayen

Laboratory of Drug Design and Discovery, Department of Pharmaceutical Technology, Jadavpur University, Kolkata, West Bengal, India

Traditionally *in vivo* experiments were set as the gold standard for measuring the efficacy and toxicity of drug substances, but in a developing era, usage of animals has to be minimized due to ethical reasons, and therefore alternatives are developed to implement the 3Rs system (Replacement, Reduction, Refinement). Replacement defines “the alternatives to be used in place of animals,” Reduction denotes “to minimize the use of animals” if no alternatives are present, and Refinement refers “to proper handling and providing plausible comfort to animals” (Vinardell Martínez-Hidalgo 2007). *In vitro* methods are developed to mimic the physiology of the body; though they have been successful in replacing the use of animals to a certain extent, they cannot imitate the truly complex nature of the body.

One of the greatest challenges in toxicology is recognizing the toxicity of drug molecules by use of high-throughput screening, i.e., to avoid the usage of animals in the early phase of drug discovery and development (Mayr and Bojanic 2009). Early detection leads to the reduction of attrition of pharmaceutical products in the later phase of development and also improves the safety of existing drug molecules. Therefore, *in silico* predictions have been evolving ever since the knowledge of machine learning models has been widespread in all the fields of science. Computational modeling has been successfully established in toxicity prediction of chemicals and drugs and are acceptable by regulatory authorities upon following certain guidelines.

22.1.2 Artificial Intelligence

As computer science progressed in the 1950s, scientists first developed computers that needed human interaction and they spent nearly a decade constructing computers that could learn on their own. This breakthrough was significant not only in computer science but also in various industries, including pharmaceutical companies and society. In certain ways, computers have progressed to the point where they can perform new tasks on their own. Artificial intelligence (AI) in the future will adapt to people’s natural language, actions, and emotions in order to engage with them. Humans will not only live in real physical space but also in a digital virtualized network as the adoption and interconnection of various intelligent terminals grow. The distinctions between humans and robots will be blurred in this cyberspace (Goertzel and Pennachin 2007; Russell and Norvig 2016; Došilovic et al. 2018). AI is any theory, method, or technique that aids machines (particularly computers) in analyzing, simulating, exploiting, and exploring human thought processes and behavior. It is the intelligent computation and calculation of data. AI is the study of characteristics of human behaviors with the goal of building an intelligent system that allows computers to perform jobs that previously only humans could do and to use computer hardware and software to imitate the underlying processes. AI is a multidisciplinary and interdisciplinary organic science and social science that developed over 60 years (Mata et al. 2018; Murphy 2012; Tan and Lim 2018). In specific industrialization and marketing projects, AI is more widely used and shows new trends in development such as

- (a) The mainstream for AI development is Deep Learning plus Big Data. Artificial Neural Networks (ANN) make it possible for robots to learn, think, and handle more complex tasks.
- (b) AI has gradually entered the phase of technological Research and Development (R & D) and experimental research industrialization. Commercial products have matured in image and speech recognition, Natural Language Processing, predictive analyses, etc.
- (c) AI has been applied in various fields ranging from the manufacturing and agricultural fields to commercial and service sectors, increasing its focus on and expansion of AI's general technologies and fundamental techniques.

The field of artificial intelligence has been around for decades. AI is defined by some as the combination of machine learning (ML) and deep learning (DL). On the other hand, DL is a subdivision of ML and ML is a subdivision of AI. In addition to DL, artificial neural networks are also part of AI. The term deep learning refers to ANNs with several layers (Albawi et al. 2017). There is a fundamental difference between deep learning and other neural networks, such as feedforward neural networks and feedback neural networks, which all use feedforward networks but implement them in different ways. It employs more complicated ways of linking layers, as well as more neurons and greater computer capacity, to use complex models and extract features automatically. So, DL can be characterized as a neural network (NN) that includes networks with a variety of pretrained variables as well as unsupervised, convolutional, and recursive NNs. The use of deep learning (DL) in speech recognition, computer vision, pattern identification, pharmacophore, toxicological predictions, etc., has been demonstrated to be very beneficial, with some situations yielding spectacular results. Advances in image identification, object detection, image classification, and face detection are more recent examples of DL. According to the research conducted, DL is currently being used in computer vision for object recognition, and it can be implemented quickly in that field (Zhou et al. 2017). Additionally, a newly published literature talks about the popularity of DL architectures and how they apply in industrial and practical settings. A complete evaluation of four DL architectures includes DBNs (deep belief networks), constrained Boltzmann machine, AEs (auto encoders), VAEs (variational auto encoders), and convolutional neural network (CNN) (da Silva Júnior et al. 2020).

Convolutional neural networks (CNNs) are among the most popular deep neural networks. CNNs are extensions of NNs that span many locations in space, using shared weights. CNN is built to recognize images because it has convolutions that are placed throughout the system and enable it to identify the item in an image. CNN consists of a number of different layers, all of which are fully connected; includes a pooling layer, convolutional, and nonlinear layers. Fully connected and convolutional layers, for example, have a list of parameters, whereas nonlinear layers and pooling layers do not. According to recent research, CNN does a great job with machine learning (ML) problems (Albawi et al. 2017). It is especially in picture data that these processes are quite beneficial.

A core principle of deep learning (DL) is to augment how well you handle ideas (abstraction) rather than volumes of information (events). About half of the ideas at the advanced levels are described in detail using the fewest possible quality ideas, while the other half are explained simply using the concept(s) already known. These hierarchical levels of learning allow systems to accurately and completely understand complicated or multi-complex presentations from raw input. An effective quality is bringing deep learning to different fields, including Information and Technology, Food and Pharma companies, etc.

22.1.3 Machine Learning Models

Machine learning techniques or models can be broadly classified into three categories:

- (a) *Supervised*: In supervised learning, the input dataset is labeled, i.e., correct values are provided for the data, and based on these input values, the algorithm shows a labeled output. It classifies the objects in a pool using a set of characteristics while excluding annotations.
- (b) *Unsupervised*: In unsupervised learning, the input dataset is not labeled, i.e., the algorithm has to find a pattern in the given input data in the form of groups or clusters. It groups all the objects within an area so that likeness is established, and once the groupings are made, they are categorized into plausible groups.
- (c) *Reinforcement learning*: In reinforcement learning, the algorithm works on reward and action phenomena in an environment. The algorithm has an environment where it sequentially solves the task and modifies its actions based on the experience to get a reward and maximize the performance. In simple terms, a reinforcement-enabled system can learn from the consequences of prior interactions with the environment and monitor how these results impact future interactions. The overall purpose of reinforcement learning is to pick actions that maximize future benefits.

22.1.4 Algorithms

Several machine learning algorithms have been developed to do a quick classification, finding patterns in biological data. They are the actual base of model development which analyses the input data and predicts the outputs. Every algorithm works on a different principle and identifies the patterns in different orders. Based on our application, i.e., input dataset and expected output, one of the algorithms can be used. To improve the efficiency of developed models, they can also be used in combinations known as consensus model where the final output can be predicted in two ways—one takes the average of predictions from each model and do not consider their contribution difference, known as averaged consensus, and another performs logistic regression where the prediction from each model is considered as

an input variable, and the consensus prediction is the output, known as weighted consensus (Plewczynski 2009). Some of the algorithms are mentioned here briefly,

- (a) *Regression analysis*: It may refer to the linear regression modeling for continuous data, and for categorical data, logistic regression is used. The main aim of linear regression is to predict the linear relationship between the set of predicted variables, and one linear line is drawn that minimizes the distance between data point along the dimension of a set of the outcome variable. This logistic regression and multiple linear regressions are most commonly used in supervised ML algorithms. Here dependent variable is predicted using the given set of independent variables, and the final result gives only two outcomes (either True or False).
- (b) *k-Nearest Neighbors (k-NN)*: Here, the data containing labeled and unlabelled nodes situated from the nearest nodes are subject to a query that follows the majority voting rule. Here k represented the number of nearest neighbors participating in the voting system. This method is used for supervised learning in both classification and regression problems.
- (c) *Support Vector Machine (SVM)*: SVM can be applied for linear and nonlinear data. Each data point is plotted into n -dimensional space, and the value of a particular domain keeps the value of each domain. The SVM classifier fits the best line that can separate the n -dimensional space into the class label known as hyperplane. This hyperplane finds the exact category for upcoming new data points.
- (d) *Artificial neural network (ANN)*: ANN is the same as natural neurons, where artificial neurons are arranged in layers in order to process information. Each neuron in an ANN receives numerous input signal from different sources and then do the sum of the input and finally develop an activation response through a nonlinear activation function and passes the output signal to the next connected neuron. ANN has been widely used in the modeling of QSAR and as well as in pharmacokinetics and pharmacodynamics analysis.
- (e) *Decision tree*: It is a supervised machine learning approach in which the data is continuously split according to certain parameters. This classifier is like a tree structure where internal nodes represent a feature, leaves for the class label, and edges show the feature conjunction for leading the class labels. The path goes from root to leave, and that follows the decision rule. The leaves are the decision or outcome, and the decision node contains the split data.
- (f) *Random forest (RF)*: The random forest is an ensemble supervised classifier built up of a collection of the decision tree. Each decision tree is constructed on a training sample, and the final prediction is based on the majority prediction from each tree. This classifier is trained using the bagging method. The responsibility of the bagging method boots up the overall classification result by combining the learning models. The random forest can be applied to both regression problems and classification problems.

22.1.5 Performance Evaluation Measures

Numerous criteria are used to assess the performance of developed models. Different measures evaluate the different features of a classifier produced by an algorithm. A developed classifier can have two classes (binary classifier) or multiple classes (multi classifier). As the number of classes increases, the complexity of evaluating a model increases and the classes are now related hierarchically (Sokolova et al. 2006). Usually, binary classification is used for developing and predicting the class of unknown components. Binary classification is evaluated based on flat performance measures, which are well-defined from a matrix known as the confusion matrix (Costa et al. 2007). The confusion matrix is a table that defines the performance of a developed classifier based on the number of true and false outcomes on a test or validation dataset (Narkhede 2018a). As mentioned above, it is used for a binary classifier, it has only two classes, either positive or negative. The predicted class of test data is compared with the actual class of data (already known), and then based on the true or false outcome, the dataset can be categorized as true positive, false positive, true negative, and false negative as depicted in Fig. 22.1. In a confusion matrix, predicted classes are described as positive or negative, whereas the actual classes are described as true or false. The four categories of confusion matrix are given as

True positive (TP): The predicted class is positive, and the actual class is also positive (true)

True negative (TN): The predicted class is negative, and the actual class is also negative (true)

False positive (FP): The predicted class is positive, but the actual class is negative (false)

False negative (FN): The predicted class is negative, but the actual class is positive (false)

These four categories of confusion matrix are the basis of the performance evaluation of a classifier. Different measures used to evaluate the performance of binary classifiers are accuracy, error, sensitivity, specificity, precision, *F*-measure, and Receiver Operating Characteristic (ROC) (Costa et al. 2007).

Fig. 22.1 Confusion matrix

Actual Class \ Predicted Class	Positive	Negative
	Positive	True Positive (TP)
Negative	False Positive (FP)	True Negative (TN)

- (a) *Accuracy (A)*: Accuracy defines the true predicted outcomes of all the classes as given in Eq. (22.1)

$$\text{Accuracy} = \frac{\text{TP} + \text{TN}}{\text{TP} + \text{TN} + \text{FP} + \text{FN}} \quad (22.1)$$

- (b) *Error (E)*: Error defines the false predicted outcomes of all the classes, as given in Eq. (22.2)

$$\text{Error} = (1 - \text{Accuracy}) = \frac{\text{FN} + \text{FP}}{\text{TP} + \text{TN} + \text{FP} + \text{FN}} \quad (22.2)$$

- (c) *Sensitivity or recall (R)*: It is defined as a true positive rate, i.e., the number of positive predicted outcomes from the total number of actual positive data as shown in Eq. (22.3)

$$\text{Recall or sensitivity} = \frac{\text{TP}}{\text{TP} + \text{FN}} \quad (22.3)$$

- (d) *Specificity (S)*: It is defined as a true negative rate, i.e., number of negative predicted outcomes from the total number of actual negative data as shown in Eq. (22.4)

$$\text{Specificity} = \frac{\text{TN}}{\text{TN} + \text{FP}} \quad (22.4)$$

- (e) *Precision (P)*: It is defined as a measure to estimate the probability of true positive outcomes from all the positive predicted outcomes as shown in Eq. (22.5)

$$\text{Precision} = \frac{\text{TP}}{\text{TP} + \text{FP}} \quad (22.5)$$

- (f) *F-measure*: It is obtained by a combination of recall and precision. It is useful, especially when it is not easy to relate the models with low recall and high precision or vice versa. It helps to analyze recall and precision simultaneously by utilizing harmonic means instead of the arithmetic mean. A constant (β) is an applied trade-off between recall and precision, as given in Eq. (22.6a), but as the value is generally set to 1, it is not used generally as shown in Eq. (22.6b).

$$F\text{-measure} = \frac{(\beta^2 + 1) * P * R}{\beta^2 * (P + R)} \quad (22.6a)$$

(or)

$$F\text{-measure} = \frac{2 * P * R}{(P + R)} \quad (22.6b)$$

(g) *Receiver operating characteristic (ROC)*: It is obtained by a combination of recall (sensitivity) and specificity. It is used when the threshold values are the determining factors for the outcomes of the developed model.

ROC values range between 0 to 1, where 0 represents that all the predictions are reciprocating, i.e., positive is predicted as negative and vice versa, 1 represents that the model is able to differentiate between the classes, and 0.5 represents that model cannot differentiate between classes (Costa et al. 2007; Narkhede 2018b).

22.1.6 Machine Learning Model Development

The important components of any machine learning model are the input dataset, descriptors used for the dataset, algorithms, and the output data. A model is built by various descriptors for the input dataset, and only the significant descriptors are chosen for model development. Dataset is split into training (again split into training and validation dataset) and testing dataset, usually in the ratio of 70:30 or 80:20. The model is trained using a training dataset using different algorithms, and then the best model is chosen based on the evaluation parameters of each model on the testing dataset. Using the output on the testing dataset, data is divided into TP, TN, FP, or FN, followed by evaluating the performance of the developed model in terms of accuracy, sensitivity, specificity, precision, *F*-measure, and ROC. Best is selected to screen or predict the activity of unknown compounds. The process of machine learning model development is shown in Fig. 22.2. The details of developing a

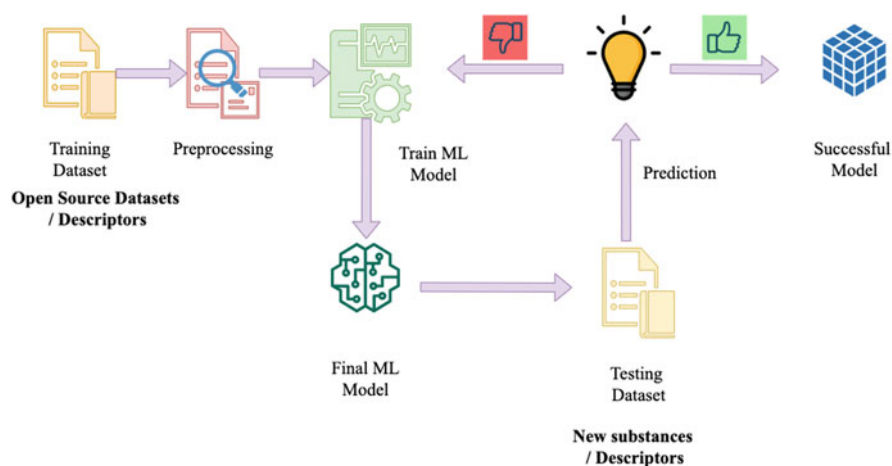


Fig. 22.2 Representation of machine learning model development

machine learning model are described elsewhere (Alpaydin 2020; Müller and Guido 2016).

On the other hand, it is important to focus on the different errors while developing a model such as generalization error in a classifier is the likelihood that a randomly selected instance would be incorrectly classified. Generalization error is one of the major concerns in building a classifier. A test data set should not be used during training to calculate the generalization error. If sample data is employed as a means of measuring accuracy or error, then the measures utilized to assess that property are referred to as sample accuracy or sample error, respectively. Training error is the sample error measured on the training data, which should be observed and analyzed during evaluation. Contrary, if the test error (which is almost always worse) differs significantly from the training error, the classifier's generalization may be poor because it has become overly specific to the training data. The value discovered from the analysis of the test set and the training set should be used to compare the test set error with the training set error. To aid in finding the best values of the prediction function parameters, an ML process's main goal is to search for the hypotheses that have the highest value. When it comes to optimizing a classifier, the focus should be on the hypothesis parameters. Finding the best hypothesis parameters can be a difficult computational challenge. In some cases, the computational cost of the search is reduced by approximating the optimum with a more advanced approach.

22.2 Tools Used in Artificial Intelligence

22.2.1 Neural Networks

The popularity of artificial neural networks (ANNs), especially in image classification, category, object detection, recommendation engines, and next-word predictions, has grown recently (Dave and Dutta 2014). Some of the other hotspots in AI are information security, Internet of things, cloud computing, robotics, and cloud. ANNs can be assessed using factors like accuracy, processing speed, latency, performance, fault tolerance, size, and convergence for data analysis (He and Garcia 2009; Mozaffari et al. 2019). One of the major advantages of ANNs is the ability to do parallel executions, making research in this direction more interesting and important (Izeboudjen et al. 2014). ANNs can be used to recognize photos, analyze natural language, etc. ANNs are widely used for the universal approximation of functions in numerical paradigms because of their high self-study characteristics, adaptiveness, tolerance for errors, nonlinearity, and enhanced input for output mapping (Wang et al. 2017a). These variables for data analysis provide more grounds for the high level of ANNs to be efficient, effective, and successful in dealing with complicated challenges in many sectors of life. ANNs can deal with agricultural, scientific, medical, and commodity trading. Even though ANNs have a broad range of purposes, it becomes increasingly important to design an effective method for their performance development. When we consider some of the other concerns, it is, for example, an approach that considers the challenges surrounding

the use of data sets (size, volume, size, and other), data correctness, data tools, data standards, data entry method, data division, and data preprocessing. Furthermore, some of the prominent issues with the modeling of ANN that are of interest and which require further study in the future include development techniques which can improve the development of solid models, improve the transparency of patterns and allow useful knowledge from experienced ANNs. Moreover, there are challenges to improving the capacity for extrapolation and better convergence. Additionally, these variables, such as gradient enigma and variable issues, and noise must be continually quantified. Additionally, variable convergence and time-consuming difficulties are typical of most artificial neural systems, and supervised learning is required to overcome this issue. The following are some of these problems,

- (a) Improving robust model design: model robustness means that ANN types can predict a wider variety of data, such as training data. For instance, textual data and knowledge are used to improve the financial market modeling forecast. Some experts believe it is suitable for calibrating and validating data that ANNs are globally accepted and achieve maximum potential. But predictions of the correlation and robustness of models under all sorts of conditions are plausible (Xing et al. 2018; Kingston et al. 2005). Error-validated ANNs can predict conditions like those in the trained data accurately.
- (b) Improved model transparency and the ability to extract the knowledge from educated ANN: means the possibility of interpreting ANN models so that the impact of model inputs on outputs can be fully understood.
- (c) Enhanced extrapolation capability, the capacity of the model to accurately predict external data ranges used in the calibration of the ANN model is an extrapolation of ANN models. ANNs are most effective if the data for design or model calibration are not exceeding the range (Flood and Kartam 1994; Minns and Hall 1996; Tokar and Johnson 1999).
- (d) Further restrictions of ANNs, including uncertainty, in unconsidered predictions. If uncertainty is not reported, measuring the quality of predictions of ANN becomes difficult, which can limit or reduce the effectiveness of predictions critically. Although ANNs have had problems, new approaches such as cognitive computing and deep learning have significantly enhanced support in those areas. There may still be a synthetic machine unavailable, but systems such as ANN, which help improve human life, are here.

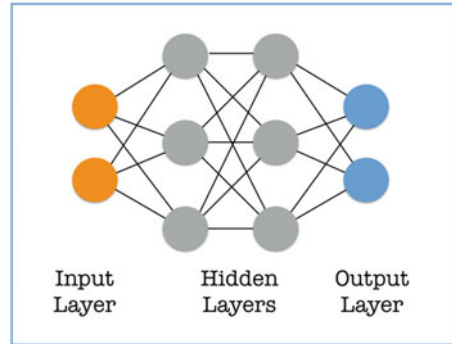
ANNs are frequently used for human requirements in a range of industries. Many companies are investing in neural networks to overcome the issues that operational research has faced in a wide variety of sectors and the economic sector (Boyacioglu et al. 2009). Because of its broad applicability, in addition to its usefulness in science and engineering, artificial information is often promoted for data analysis by academics in the areas of the social sciences and the arts (Haykin and Network 2004). For example, in several areas such as industrial production, oil exploration, and business, artificial intelligence (AI) was widely applied in solving optimization problems (Rahmanifard and Plaksina 2019; Araque et al. 2017).

One of the advantages of employing ANNs is that it can make it easier to utilize and more accurate models from complex natural systems with large inputs (Abiodun et al. 2018). The ANN was found to be a very new and valued paradigm for addressing problems and learning machines. The ANN model is an information manager that works in the human brain similarly to the biological nervous system. The global research interest in brain functions has recently increased (Wang et al. 2017b). According to Haykin, an ANN is a machine designed to do a task in the same way that the human brain does (Donahue et al. 2014). In diverse sectors of human need, many people are now utilizing ANNs. Many organizations, historically an area where operational research (OR) is applied, devote resources to neural networks for usage in different industries and the economy. The most distinctive feature of artificial intelligence, albeit important in science and engineering, is mainly employed to analyze data by academics in the social sciences and arts. While ANNs may aid modeling from complex natural systems with massive inputs to be more user-friendly and accurate, there are benefits of using this application, such as making more complex models easier to build. The ANN has been shown to be a novel model for solving problems and machine learning that is very relevant.

There has recently been a tremendous increase in interest in the workings of the brain around the world (Wang et al. 2017b). Haykin states that an ANN can perform a given task in the same way the human brain does, and hence the ANN can be considered a kind of machine produced by the brain. To take a more specific example, “the human brain is quite large and exceptionally efficient.” The man’s brain functions like an information-processing machine, like a machine based on a variety of complex signal-computing operations. The most critical feature of this brain is its unique processing capabilities. It is made up of multiple interconnected “neurons” known as elements that function together to resolve daily issues. Neural networks have applications across a wide range of disciplines, such as the human brain, which connects to send and receive signals for human action (Haykin and Network 2004).

A feedforward neural network (FFNN) resembles human neural network processing units, but it has layers arranged sequentially instead of concurrently. Layers in FFNN have connections to each other; As each connection has a different weight or strength, the overall layer connection weight or strength does not equal each connection weight or strength. In determining the overall capacity of the network, the weights of the network connections weigh in. Nodes are another name for NN units. In the network, the information is first captured by the input units and then flows from one layer until it is available at the output units. In the absence of any feedback between layers, NN usually operates. Only in one direction: input nodes, hidden nodes, and output nodes. These neural networks are commonly referred to as feedforward neural networks (Hertz et al. 2018). A simple perceptron model is shown in Fig. 22.3 with 1 input layer, 2 hidden layers, and 1 output layer. The input layer has 2 input units or neurons, all depicted as circles colored in orange, connected to the hidden nodes (colored in grey) in the next layer. The hidden layer is then connected to the output layer (colored in blue).

Fig. 22.3 Simple perceptron model



Control of dynamical systems and classic machine learning techniques are the main classifications of FFNN applications (Kuschewski et al. 1993; Xiang et al. 2016; De Martino and De Martino 2018). Deep networks are referred to as NNs with two or more hidden layers. Unlike FFNN, FBNN can use “memory” (a store of information) for the data input sequence. This means that FFNN can process tasks on a first-come, first-served basis depending on the number of inputs. When a job like unsegmentation or pattern recognition requires feedback in the opposite direction, it is done as part of the process (connected handwriting recognition). Using a feedback neural network, this application area has roles that include mathematical proofs, fitting data from seismic surveys, medical procedures, etc. When backpropagation or feedback NNs are used to connect nodes, a coordinated graph is produced. In order to exhibit dynamic terrestrial behavior, real-time feedback NNs can dynamically generate consecutive graphs in tandem. For many examples, see: There are numerous instances of self-organizing maps (including Kohonen’s) and recurrent neural networks (RNN). In order to keep the previous time step’s network state, the input edges instead of the next layer were utilized. For instance, RNN can recognize text or speech if we have a text or speech signal. The presence of short-term memory results in a cycle in the network.

22.2.2 Deep Learning Frameworks and Libraries

22.2.2.1 Cafe

Convolutional Architecture for Fast Feature Embedding (CAFE) is a prominent open-source deep learning framework that is used in popular coffee shops, such as Starbucks, for example. The Neuromation framework is also the first open-source deep learning framework to share all of its code, algorithms, and information in the field. At the moment, the responsibility for upkeep at the Berkeley Vision and Learning Center is being held by Berkeley Vision and Learning Center. In recent GitHub rankings, Cafe was put second in the machine learning projects section, while TensorFlow was top. The computational photography software is particularly well-suited for image processing using convolutional neural networks in C and C++.

Despite the fact that some developers see it as a general-purpose framework, Cafe is a computer vision framework. “Decaf,” the previous incarnation of the cafe, personifies this. After decaf, we learned that CNN’s amazing portability has been shown; in other words, the findings obtained by utilizing CNN for image feature extraction may be applied to other visual tasks and will provide positive results. Additionally, the study about the Decaf project determined that the convolution and full connection layers are the most computationally taxing operations since they operate on a huge number of matrices (Donahue et al. 2014).

For example, because Cafe delivers outstanding performance with CUDA and GPUs, it demonstrates the particular figures shown above. A single K40 or Titan GPU can process up to 40 million images per day at a rate of around 2.5 ms per image (Jia et al. 2014). In industries where core algorithms are used as a primary function, Cafe’s high performance is ideal. Cafe is a leader in image categorization with convolutional neural networks, and it is the developer’s first choice when it comes to this task. Cafe also offers the following benefits.

- (a) Many classic neural networks, such as AlexNet and LeNet, have a lot of support, and only a small amount of code can be used in real-world engineering.
- (b) Cafe allows beginners to get up and run quickly. Rather than writing code, models and optimizations are written in text. To ease fast access, Cafe provides the model definition, optimization parameters, and pretraining weights.
- (c) Fast and transplant. The framework transplant is achievable because the majority of the underlying layer is written in C++. Cafe enables GPU-accelerated operations, resulting in a high-performance framework.
- (d) Hardware vendor support is excellent, particularly from NVIDIA, which has optimized GPU computing and assisted in the promotion of Cafe. Similarly, Cafe has several drawbacks, such as the need to install a full Cafe, which necessitates the installation of numerous programs. It is simple to make mistakes throughout the installation process. In other circumstances, C++ and CUDA must be directly modified to support the new GPU when using Cafe to build sophisticated neural networks such as Google Net (needs roughly 2000 lines of code to describe the whole Google Net network).

22.2.2.2 Theano

Theano was founded in 2007, and it was the first deep learning library. Theano is a Python library that efficiently defines, optimizes, and evaluates mathematical statements involving multidimensional arrays, according to its official introduction. It has been one of the most widely used CPU and GPU mathematical compilers, particularly in the machine learning community, since its inception and has demonstrated constant performance increases (Team et al. 2016). Theano is a mathematical expression compiler. We use sign language to describe our results, then Theano compiles the code, and the application runs efficiently on a GPU or CPU. Theano, as a Python library with an integrated NumPy library, is better-suited for numerical optimization than other libraries, such as Numpy or SciPy. Theano and TensorFlow’s functions are comparable. Theano, as a research platform, has a

greater chance of going to the bottom than other deep learning libraries; however, it needs effort to create the model.

As a result, multiple deep learning libraries built on Theano have arisen, many of which include packages such as Keras, Lasagne, and others. The powerful language Keras encapsulates neural networks, making it possible to do back-end calculations with little effort. One thing about Keras is that components are pluggable modules. Connecting new components, such as a roll layer and activation function, is only a matter of connecting them while loading the model at discovery time. Besides the obvious, there are additional favorites in the intellectual world, such as lasagna from the library. In addition to being the top layer of the Theano package, lasagne is also the topmost layer of the Theano package, which has very rigid definitions for each layer of the neural network. That means there are two further packages related to lasagna-based neural networks: Scikit neural networks. These Theano higher package library blocks, such as Deep or Pylearn2, may be regarded as a huge family. Python's deep learning libraries could be limited if Theano is not accessible. NumPy would not exist without SciPy, Scikit-Learn, and Scikitimage. Without them, SciPy, Scikit-Learn, and Scikitimage would not exist either. Deep learning is currently being used by a majority of researchers, which is why Theano is considered the industry standard. However, due to its academic background, Theano was built with academics in mind, and as a result, it is frequently used by deep learning professionals. However, the rapid growth of TensorFlow with Google's assistance has reduced the number of Theano users, but Theano, being a 10-year-old deep learning library, still has a number of advantages:

- (a) Because of the Python and NumPy combo, Theano offers a minimal learning curve.
- (b) RNN can be used with a computation graph.
- (c) Keras, as Theano's high-level API, is relatively simple to use.
- (d) Theano's calculation stability allows it to calculate the output value accurately with a minimal function.

Theano's flaws are also readily apparent:

- (a) Multi-GPU and horizontal expansion are not supported.
- (b) There is a lack of support for the traditional model.

There are a lot of high-quality documents on Theano, and a lot of researchers have done a lot of study on it. The performance of Theano is discussed in-depth in other publications (Bahrampour et al. 2015). On the MNIST dataset, all of the following data is available at the LeNet neural network.

22.2.2.3 TensorFlow

By incorporating their operating principles, Google created their second-generation open-source artificial intelligence learning system, TensorFlow, on the concept of disbelief. An N -dimensional array is called a tensor, but a calculation based on

flowcharts is called a flow. TensorFlow is a machine learning framework that uses artificial neural networks to handle and analyze complicated data formats. In contrast to that, one of the most widely used uses of TensorFlow is doing computations on a variety of heterogeneous platforms, from mobile phones and tablets to large-scale distributed systems with hundreds of computers and thousands of processing devices like GPU cards (Abadi et al. 2016). Most people are familiar with TensorFlow for deep neural network training and inference. However, TensorFlow is also widely utilized for a range of other activities. An ML platform where machine learning systems, including speech recognition, computer vision, robotics, information retrieval, and natural language processing, are tested, developed, and deployed (Abadi 2016).

TensorFlow can be viewed as a combination of Theano and Cafe characteristics that have been synthesized and extended. On the one hand, it, like Theano, allows for automatic derivation, and the user is relieved of the necessity to calculate the gradient via reverse propagation. TensorFlow, on the other hand, has a stronger deployment capacity than Cafe and can execute complicated models on devices with limited memory and CPU capabilities, which appeals to many embedded developers. With SWIG (Simplified Wrapper and Interface Generator), you can do research and development in Python on a superior machine while deploying models in a resource- and latency-hungry embedded environment or you may utilize C++ to perform more advanced tasks. SWIG provides a range of supported languages for supplying C/C++ code, making it possible to implement interfaces for more scripting languages in the future quickly. In the majority of frameworks, the use of cuDNN in single GPU conditions is currently required, which limits the impact of hardware power or memory allocation. The only problem with this is that the vast amount of data required for large-scale deep learning slows down training. In order to do these two tasks at present moment, distributed computing is necessary to train a model while also creating parallel computing on the CPU and GPU clusters. TensorFlow was made available as open source under the Apache 2.0 license in April 2016. It can accomplish 40 times the speed and 15 times the performance using only a single GPU, and it uses 16 GPUs to deliver a whopping 15-fold increase in performance. The few deep learning frameworks that now have distributed features natively only are TensorFlow, CNTK, DeepLearning4J, and MXNet.

Two additional essential supplementary components of TensorFlow are now available: TensorFlow Serving and TensorBoard. When you run TensorFlow Serving, you have the option to export models that have been trained in TensorFlow and then deploy them to a RESTful interface for predictive services. This component, consisting of the training model, debugging parameters, and packaging model, may take TensorFlow from research to production. TensorFlow Serving will significantly contribute to industry standards using TensorFlow.

TensorBoard is a suite of TensorFlow Web applications for monitoring the TensorFlow run process, also known as the visual Computation Graph. Scalars, pictures, audio, histograms, and Computation Graphs are the four modes of visualization that TensorBoard now offers. The Events Dashboard in TensorBoard may be used to track critical metrics such as loss, learning rate, and accuracy on the

verification set in real time. The user settings stored photographs during training, such as training intermediate results with Matplotlib made out of the picture, can be seen in Image Dashboard. A TensorFlow calculation graph can be seen entirely in Graph Explorer, which also supports scaling drag and viewing node characteristics.

TensorFlow has good development possibilities as a result of Google's frequent upgrades. TensorFlow's overall architecture design is also extremely solid, and when compared to its Python-based older competitors Theano, TensorFlow is more mature and powerful. Because Google, as a large corporation, has invested significantly more resources in TensorFlow's development than colleges or individual developers, it is likely that in the future, TensorFlow's progress will be swift and may have extended well beyond institutions or individuals who own or maintain the deep learning framework.

TensorFlow is a popular and powerful deep learning framework; however, it is still under development, and several issues have to be fixed. As the saying goes, the benefits of TensorFlow are obvious:

- (a) Future support for several programming languages.
- (b) The two characteristics of a high-performance system are performance and multi-processor, GPU, or hybrid platform support.
- (c) The portability of TensorFlow is more than other frameworks; innovation is connected to research and products, and it is simple to add new ideas by using TensorFlow Serving.

When in use, TensorFlow supports a small number of shortboards: Even if it uses socket-based RPC instead of RDMA, the distributed performance of distributed communication is limited. Performance concerns arise when Python is used as a TensorFlow interface. A small or short process or amount of time could generate a substantial delay. A number of articles have covered TensorFlow in-depth, and a lot of people use TensorFlow. The NVIDIA Titan X GPU is also used to perform a TensorFlow benchmark (with four convolutional models) on a six-core Intel Core i7-5930K CPU, which runs at 3.5 GHz (Abadi et al. 2016).

TensorFlow is also highly approachable to non-techies. Similarly, there have been many high-level APIs created on Theano, such as TFlern and TensorLayer. Some of these higher level APIs are designed to make developing huge frameworks faster, and, possibly in the future, they will be used by runtimes. Those who have never encountered deep learning developers will have an easier time using a deep learning network to construct one. TFlern and TensorLayer are not very popular; however, there is an extensive TFlern-related study with a code sample that describes how to use TFlern, as well as comparisons to a variety of conventional high-level APIs (Keras, Lasagne). The summary combing method was implemented using TensorLayeras given below:

- (a) Keras: Theano was brought to the public, and now there are many users. Sickie-learn style programming is used to obscure the data stream's complexity. The overall performance of TensorFlow is subpar, and scalability is lacking (to be

compatible with TensorFlow at the sacrifice of efficiency). Debugging is a demanding undertaking, to say the least.

- (b) **TensorLayer**: Academic communities have many advantages, including flexibility, and it is simple to build a dynamic network structure (Neural Modular Network). Because the industry moves swiftly, it has an advantage. It is quite helpful, plus it comes with a Google TensorFlow implementation that is modular. Newbies can use the Sickie-learn API and professional-grade API at the same time during the transition.
- (c) **TFlearn**: Unlike TensorLayer, which is highly compatible with both backends, Keras is far less efficient when it comes to compatibility with both backends. Disadvantages: The upkeep is a tad tedious. As a secondary benefit, Lasagne is nicely sealed, making it great for people who are accustomed to Theano.

Instead of hiding all of Theano's methods and objects, Lasagne included a number of them as well as supporting functions at the bottom of the stack. The biggest drawback of lasagne is that it lacks varied communities of communication. The latest version of TensorLayer has been made available. TensorLayer is an industrial library, which provides academics with a powerful and flexible method-building methodology. With TensorFlow's rapidly developing technology, it is expected that good features from TensorLayer will support it.

22.2.2.4 Torch

Torch, a data-science-focused computing platform, emphasizes GPUs, offers substantial support for machine learning algorithms, and incorporates experimental and theoretical computational approaches. Thanks to LuaJIT, a simple and speedy scripting language, and a C/CUDA implementation, the tool is simple to use and efficient (Wang et al. 2019). Python was frequently used in machine learning when it was created, although Lua was created in Brazil in the 1990s. The complexity of learning Lua and Python, in particular, is on the lower end of the spectrum. Although machine learning (specifically in academia) has almost always relied on the latter, the latter has undeniably dominated the field of machine learning. As with other programmers, commercial programmers have little or no familiarity with Lua. The promotion of torches has become more difficult because of this. Even if it is strong, people have a generally negative impression of Torch. In the following ways, you can see the power of the torch:

- (a) LuaJIT's general-purpose computation capability is significantly superior to Python's ability. When a large number of data structures are employed, LuaJIT's performance suffers. Meanwhile, LuaJIT allows us to modify C pointers directly.
- (b) Torch's framework includes self-contained Lua and entirely Python-based programs for many platforms; nevertheless, the system's portability is limited, and it relies heavily on other libraries.
- (c) The FFI expansion interface in LuaJIT is simple to learn and may be used to connect other libraries to Torch.

Torch also created the Tensor N -Dimension array type object. Torch Tensor is a memory view, and while a piece of memory may have many view (Tensor) points, its design also considers performance (directly for memory) and convenience. Torch also includes a number of related libraries, including linear algebra, convolution, Fourier transform, graphics, and statistics. Because of these advantages, a modified version of Torch has been developed to aid AI research by a number of Internet behemoths. Facebook, Twitter, and DeepMind are among the companies involved (already acquired by Google). When compared to the HTK (Speech Recognition Toolkit), the performance (training/decoding time) is nearly the same. Number95 is a data collection.

In a similar vein, when contrasted to SVMlight (a well-known software for training support vector machines), yielded nearly identical results. Torch, on the other hand, is a far more extensive tool than HTK as well as SVMlight (Collobert et al. 2002). Torch is a library for machine learning. Torch is beneficial since it eliminates the need to write C++ code. Torch is more flexible than TensorFlow and Theano. Torch's most common uses are in the field of increased security. The learning library is highly modular, versatile, and simple to use, to be able to develop levels tailored to our specifications, and to employ a big pool of highly trained models. What developers will have to do is figure out how to use the torch. Lua has been around since the beginning because it was created for computers. Torch and Theano were put on display, where Collobert et al. served as conductor of a comparison between them (Collobert et al. 2011). Torch vs Theano neural network topologies trained on SGD. Each of the following cores (one CPU core, four OpenMP cores, and GPU options), as well as GPU options, were considered. In order to measure performance, the number of processed instances is counted. OpenMP will be indirectly supported via the Intel MKL library. Right now, Theano has built-in support for OpenMP, so accessing it directly will be faster. It outperforms Theano on most benchmarks. The performance for tiny architectures is on the slower side, which could provide an issue. Python's high runtime explains this.

22.2.2.5 PyTorch

One additional feature PyTorch has is GPU-based tensor calculation, which may be used in most situations where NumPy is employed. The second phase is to design a neural network that is distinct from others. The problem with using a Lua-based torch is that Lua's thread restrictions have always been a limiting factor. Even while multithreading is helpful in this area, Python has an edge because of this. In order to be able to make use of the simplicity of Python, you may integrate Torch into it. In the context of Torch development, the incorporation of Python is also favorable.

There are several other static frameworks to choose from, including TensorFlow, Theano, and Cafe. A neural network must be first created and reused as many times as necessary. Only by starting from the beginning will you be able to customize the network. PyTorch offers a reverse-mode auto-differentiation approach for network optimization without latency or overhead. This PyTorch-exclusive technique is an efficient implementation thus far due to its major edge over competing frameworks.

22.2.2.6 Scikit-Learn

In general, frameworks that include machine learning or deep learning implementation tend to employ Python as part of the API interface. One of the most widely used machine learning frameworks, Scikit-learn, is built within the native Python package. Scikit-learn was created in 2007 by machine learning researcher David Cournapeau, who also developed the Scikit-learn project, which includes additional Python programs such as NumPy and SciPy. Unlike other projects, the codebase is being maintained primarily by volunteers. It is possible that the increased cost of development upkeep for Scikit-learn is to blame for its recent conservatism. People express themselves in two ways: Another advantage of Scikit-learn is that it does not add to the size of the field of machine learning. The second advantage of Scikit-learn is that it does not use algorithms that have not been reviewed and assessed. These are the six fundamental functions of Scikit-learn: Classification, regression, clustering, dimensionality reduction, model selection, and data preprocessing. The MLP implementation in Scikit-learn is not suitable for large-scale challenges, as it does not support deep learning or GPU acceleration. While other similar frameworks, like Keras and Theano, should be considered if you are using Python for deep learning; other frameworks, like these, should be used if they are needed. One of the best aspects of using Scikit-learn is its regression algorithm, which is adequate for most developers and serves as a short tutorial on the use of each strategy. Most of the prominent machine learning algorithms are already included in Scikit-learn, and it is essential in the Python open-source community. All of the machine learning algorithm's modular implementations are included in Scikit-learn, and the model can accept raw data directly to achieve the desired output. Scikit-Learn is useful because of its numerous advantages.

Machine learning models that have been tested and work well have been completed. It is easy to set up as only a few Python packages are necessary (compared with Cafe). It is readily apparent that the issues with Scikit-learn are glaring. Since it is inflexible, useful for working with tiny- and medium-sized data volumes, it is well-suited for this purpose. GPU acceleration is not supported by Scikit-learn. Multilayer neural networks do not have to be employed for great performance. Scikit-learn works effectively because it is compiled with Cython, a third-party tool that allows C-based code to execute on top of the Scikit-learn framework. Despite not being suitable for broad, deep learning, Scikit-learn is an excellent option for a few specific uses. Scikit-learn is useful for classifying and training models using unlabeled data sets. The researchers in this study found that Scikit-Learn (a machine learning Python library) was more accurate than several other Python-based machine learning libraries, including machine learning Python (Pedregosa et al. 2011; Albanese et al. 2012). Scikit-learn is considerably more stable under different algorithms than other machine learning libraries.

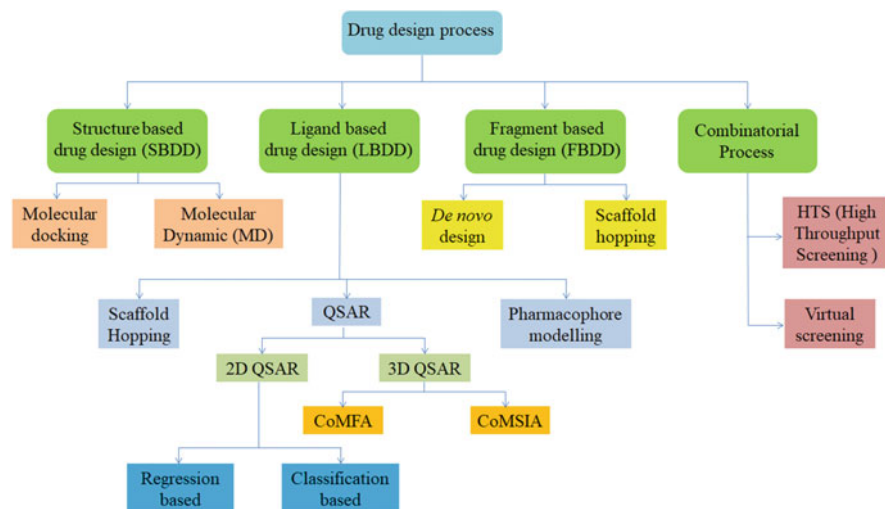


Fig. 22.4 Computer-aided drug design process

22.2.3 Quantitative Structure-Activity Relationship (QSAR)

The drug discovery and drug development process are complex and time-consuming. The main aim is to design safe and effective drug molecules with no or minimum toxicity drug molecules. Computer-aided drug design (CADD) is nowadays used most preferably than conventional drug discovery process because of minimization of the time and cost. Figure 22.4 represents various drug design processes.

Quantitative Structure-Activity Relationship (QSARs) is a computerized statistical method used to find a mathematical relationship between measurable physico-chemical parameters and their biological activity. This is expressed by equation $\Phi = f(C)$ where Φ is expressed as biological activity, and C is expressed as physiochemical or structural properties of chemical structure (Wexler et al. 2005). This follows the principle of similarity. This technique assumes that the molecules having similar structure will have identical chemical properties. However, the information provided by a set of compounds with a target is used for the identification of new compounds from other databases by the virtual screening method (Wexler et al. 2005; Roy et al. 2015). The Discovery of a new drug molecule is a complex process and takes a lot of time and money for fulfillment. QSAR-based rational drug design minimizes time and money needed in comparison to traditional drug design. In 1960, Corwin Hansch (Hansch et al. 1962), Father of QSAR, observed further momentum to QSAR research by using Hammett constants and hydrophobicity parameters that were later described by an equation known as Hansch and Fujita (Eq. 22.7).

$$\text{Log} \frac{1}{C} = k_1\pi + k_2\alpha + k_3E_s + k_4 \quad (22.7)$$

where k_1 , k_2 , and k_3 are the coefficient term and k_4 is constant. On the other hand, π , α , and E_s are substituents constant, Hammett sigma, and steric descriptors, respectively. At the same time, another QSAR approach was designed by Free and Wilson, where the total influence of the parent moiety and each structural feature present in a molecule are represented as a biological activity (Free and Wilson 1964). Equation (22.8) defines the Free-Wilson approach. So biological activity (BA) is represented as

$$\text{BA} = \sum a_i x_i + \mu \quad (22.8)$$

where μ is the overall average activity of parent moiety and x_i is the variable of the i th substituent with a value of 0 and 1 if absent and present, respectively, and a_i is the contribution of the i th structural feature of a substituent to BA.

22.2.3.1 Descriptors Based on a Different Dimension

Molecular descriptors are numerical values that describe the specific information about the studied molecules that may describe the correlation of chemical structure with the different physical and chemical properties. Different types of descriptors are used for QSAR studies according to a dimension which is listed in Table 22.1 (Roy et al. 2015; Ojha Lokendra et al. 2013; Abdel-Ilah et al. 2017).

22.2.3.2 Model-Based QSAR Approach

A model is an exact copy of the original object. QSAR model defined the relationship between chemical structures with biological activity. QSAR models are

Table 22.1 Various types of descriptors in QSAR

Descriptors	Description
1D	One dimension represents the correlation between fundamental molecular property and molecular fragments, i.e., molecular weight (MW), Molecular refractory, log P , pK_a with the biological property.
2D	Correlation of various 2D properties that contain topological information, i.e., physicochemical property including some thermodynamic parameter with biological activity.
3D	It describes the correlation of 3D property with surrounding molecules, i.e., Electronic parameter, particular parameter, MSA parameters (Molecular shape analysis), MFA parameters (Molecular field analysis), Receptor surface analysis.
4D	Describe the ligand-receptor interaction with 3D protein structure, i.e., GRID, raptor, etc.
5D	It describes the induced fit model in 4D QSAR with explicit representation, i.e., flexible protein docking.
6D	It added different solvation circumstances along with the information obtained from 5D descriptors.
7D	It comprises real receptor or target-based model data.

developed by using probability distribution or by different statistical methods like linear regression, partial least square (PLS) (Stanton 2012), principal component analysis (PCA) (Dunteman 1989), and genetic function algorithm (GFA) (Sukumar et al. 2014). Both regression and classification methods are used for the development of the model (Amin et al. 2018). A good QSAR model can define the endpoint, having an unambiguous algorithm for an appropriate measure of goodness of fit. A QSAR model can be described by equation $Y = f(X) + \text{error}$, where X is the set of descriptors and Y is the endpoint (Roy 2017). For the development of the QSAR model, firstly, raw data are collected from different literature and public database (Roy 2017). Then different descriptors are calculated and further develop a model. Further models are evaluated or validated by different statistical measures like accuracy, sensitivity, specificity, ROC (receiver operating characteristics), and MCC (Matthews's correlation coefficient). Various methods like Bayesian classification study, Recursive Partitioning, and smile-based Monte Carlo optimization are mostly used to develop the QSAR model (Amin et al. 2018; Roy 2017; Neves et al. 2018; Patel et al. 2014).

22.2.3.3 3D QSAR

The three-dimensional QSAR approach is the most prominent computational means for the development of QSAR-based drug discovery. The main goal of 3D QSAR is to develop a relationship between biological activity and special properties of chemical structures like steric, electrostatic, and lipophilic properties (Roy et al. 2015). However, a 3D QSAR analysis helps to identify the pharmacophore arrangement of molecules in a space and also provides guidelines for the design of the succeeding generation compounds with improved selectivity and biological activity. The advantage of the 3D QSAR over the 2D QSAR method is that it shows a 3D structure of the ligand and is also applicable for structurally diverse molecules. However, some drawbacks are that this technique is not applicable for huge datasets containing thousands of compounds and is based on only assumptions. The most commonly used methods for 3D QSAR are comparative molecular field analysis (CoMFA) and comparative molecular similarity analysis (CoMSIA) (Roy et al. 2015; Patel et al. 2014; Verma et al. 2010).

22.2.3.3.1 Comparative Molecular Field Analysis (CoMFA)

Cramer et al. developed this model that is molecular alignment-dependent, field-based, and ligand-based method, which helps in the development of the quantitative relationship of molecular structures and its response property, especially the steric (as a Lennard-Jones function) and electrostatic (as coulomb function) one. Due to its descriptor-based alignment-dependent property, all aligned ligand is placed in an energy grid, especially in the center with a spacing of 2 Å. Then in each lattice point, appropriate probes are situated for energy calculation. Interestingly this computed value serves as a descriptor for the development of model. Moreover, for visual understanding of the correlation between descriptors and biological response, linear regression methods like partial least squares (PLS) are used that can differentiate favorable and unfavorable electrostatic and steric potential. There are different

factors which are responsible for the performance of the CoMFA. The binding mode, binding affinity, and an extensive range of biological response of the ligand molecules may affect the performance of the CoMFA (the more significant the range of the biological activity, the better the performance).

Moreover, the alignment of the molecules and molecular interaction energy fields may induce the performance of CoMFA. CoMFA shows many advantages over classical QSAR that are like, it can be applied in any series of molecules and represent the interaction energy of an entire ligand, not only the small fragment of the ligand. On the other hand, there are some limitations that are low signal-to-noise ratio and too many variables considered here.

22.2.3.3.2 Comparative Molecular Similarity Indices Analysis (CoMSIA)

CoMSIA is a modified version of the CoMFA that is a linear, ligand-based, and alignment-dependent methodology, developed to overcome the certain limitation of CoMFA. Klebe et al. developed this method that is based on similarity indices which are adapted from the SEAL algorithm. CoMFA mainly enlightens on the alignment of the molecules that create problems in the interpretation of steric potential and electrostatic potential and also alignment sensitivity which is solved by employing Gaussian potential in CoMSIA. Here steric, electrostatic, hydrophobic potential, and hydrogen bond properties are used. Further, for analyzing the property of the molecules in a dataset, a common probe is placed into the grid box, and then similarity at each grid point is measured.

There are some other methodologies like CoMSA (comparative molecular surface analysis), CoRIA, CoMPIA (comparative molecule/pseudo receptor interaction analysis), CoMASA (comparative molecular active site analysis), and SOMFA (self-organizing molecular field analysis) used in 3D QSAR based drug discovery (Roy et al. 2015; Patel et al. 2014; Malik et al. 2013).

22.2.3.4 Machine Learning in QSAR

Development of correlation of chemical molecules with their biological activities based on their chemical structure by QSAR model through machine learning approach has proved to be the best model. This approach is known as “ML-QSAR” (Lo et al. 2018). Here machines can learn from data rather than following only programmed instructions in the simple QSAR model. Nowadays, the design and discovery of new drug molecules through the machine learning approach create a lot of interest. It mainly helps develop a QSAR model later used in virtual screening for filtration of several libraries for a specific type of drug design and finding the different physiochemical properties of the drug molecules like metabolism, toxicity, and drug-drug interaction carcinogenicity.

In the QSAR model, supervised and unsupervised learning are mostly used. Interestingly machine learning can be used in both regression and classification problems (Lo et al. 2018; Shahlai 2013). For better understanding the QSAR, various types of algorithms are used, most of them are Decision Tree, Random Forest, Support Vector Machine, Ada Boost, and Artificial neural network (ANN) (Lo et al. 2018; Shahlai 2013; Gertrudes et al. 2012).

22.2.3.5 Application of QSAR

QSAR has been applied for several decades to find the best model for the activity of any bioactive substances. It applies in vast areas like rationalization of the active lead compound with enhanced biological activity, activity prediction, determination of physicochemical properties that will be best for any biological activation, and, finally, in finding toxicology. Donepezil, Norfloxacin, and Ipconazole are some successful drugs that were designed by QSAR-based approach. However, the QSAR model is not only used in the pharmaceutical industry for drug discovery but also applied in the food industry and chemicals for industrial processes and rational design of numerous other products such as surface-active agents, perfume, dyes, and fine chemicals.

Initially, the ideology to develop QSAR for the prediction of pharmacological or toxicological effects of chemicals and drugs was based on the physicochemical properties of drugs related to their biological response. However, recently due to improvements in the technology and development of computational models, the sophistication levels of a model have increased, which made it feasible to use numerous features of drug molecules, including physical and chemical properties, to compute a model with higher efficiency (Vedani et al. 2006). Moreover, it has been proved that the additional data from *in vitro* cell line studies can greatly impact the performance of QSAR models by increasing their accuracy (Vayer et al. 2009). Apart from the physicochemical properties of drugs and their biological responses, the common fingerprints of drug molecules causing toxicity can also act as biomarkers in predicting toxicity. Most of these computational approaches depend on the QSAR technique or molecular profiling, or *in vitro* cell studies to predict or identify the similarity between molecules (Antczak et al. 2010). Though computational techniques along with QSAR have been continuously developing improved models to predict the toxicity of drugs, better approaches are required to predict the toxicity of drugs by improving the accuracy and precision of the developed model.

22.2.4 Docking

Molecular docking is a computational process working on structures of molecules for drug designing where a theoretical simulation is taken place for predicting the binding position, orientation, and affinity of the ligand with receptor protein in the active binding site. Here optimization of the complex conformation takes place for the minimization of free energy. Therefore, docking plays a vital role in identifying the activity of any drug molecules in the drug discovery process and studying them at the molecular level (Chaudhary and Mishra 2016; Tao et al. 2020).

X-ray crystallography and NMR technique are used for structural biology for the identification of the protein active site. However, these techniques may not be possible for the identification of molecular features which are responsible for specific biological activity and prediction of the compounds modification that can improve potency and further characterization of the thermodynamic and dynamic change of intermolecular interaction. The concept of docking came from the “lock and key”

model (based on recognition of the enzyme active site for substrate), proposed by Fischer (1894) (Koshland 1995). Here ligand and protein are used as a rigid body. But due to some problem related to rigid-body docking later, it was converted to the “induced fit” model, proposed by Koshland (1958) (Koshland 1995, 1963), where ligand and protein both are used as flexible, and now this is described as a binding event more accurately. Interestingly, the first molecular docking software, DOCK, came in early 1982 (Tao et al. 2020).

The main aim of docking is to develop accurate structural modeling and accurate prediction of activity. The docking process comprises special matching and energy matching between receptor protein and ligand for optimal conformation (Chaudhary and Mishra 2016). Here at the time of binding of the ligand with protein, the conformation of the active site change simultaneously until a successful stable bond has been formed with the lowest binding energy. There are various types of docking like protein-protein docking, protein-ligand, protein-amino acid, and protein-DNA. Here we mainly focus on protein-ligand docking.

There are different types of interaction between the docked protein and ligand. Most of them are electrostatic forces (e.g., dipole-dipole, charged-dipole, charge-charge), hydrogen bond, hydrophobic interaction, electrostatic forces (e.g., Vander Waals interaction), and steric forces. However, hydrogen bond and hydrophobic interaction are crucial for evaluating the affinity between ligands and receptors because they stabilize the biochemical environments (Chaudhary and Mishra 2016; Yan and Zou 2017; Kuntz et al. 1982).

22.2.4.1 Steps in Molecular Docking

Docking can be done in two interrelated steps: the first step is done by sampling conformation of the ligand into active site of the protein and then followed by the second step in which scoring function is used to rank the conformations (Meng et al. 2011). During the first step, different sample algorithms are used in docking software that helps in the reproducibility of the experimental binding mode. There are different algorithms; most of them are matching algorithms (based on geometry, i.e., ligand fits with the active site of protein or molecular shape mapping) (Norel et al. 1994), incremental construction (a list of fragments put into active site by incremental fashion) (Rarey et al. 1996), LUDI (mainly focus on hydrogen bond and hydrophobic contacts) (Böhm 1992), MCSS (Multiple Copy of Simultaneous Search) (Miranker and Karplus 1991), Monte Carlo (poses of the ligand are generated by bond rotation) (Hart and Read 1992), and genetic algorithm (Stochastic method, that utilizes randomly modifying ligand conformations to explore the conformational space) (Morris et al. 1998). In addition, the scoring function is used for the depiction of the correct poses from incorrect poses and further estimation of the binding affinity by calculating binding free energy. However, several types of scoring functions are used, like force field-based (binding energy is evaluated by calculating the non-bonded interaction) (Kollman 1993), empirical (binding energy divided into energy components and then multiplied by a coefficient and final total gives the ultimate result) (Jain 1996) and knowledge-based scoring (based on an assumption where maybe interaction will be more significant).

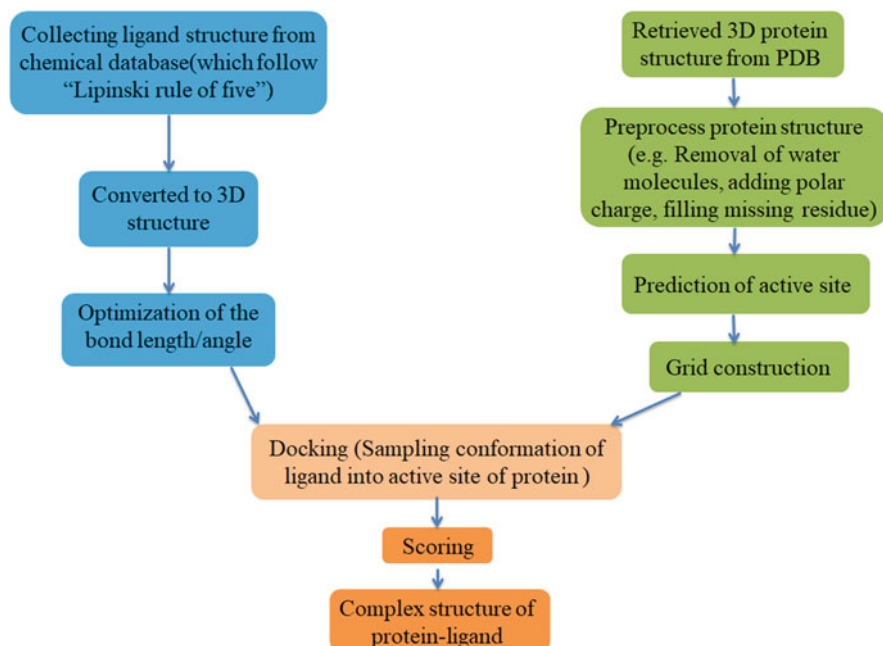


Fig. 22.5 Schematic representation of different steps in molecular docking

Table 22.2 Representation of different types of docking

Type of docking	Classification	References
Based on binding site	(a) Blind docking (b) Site-specific docking	Hassan et al. (2017) Kong et al. (2019)
Based on interacting molecules	(a) Protein-ligand docking (b) Protein-protein docking (c) Protein-peptide docking (d) Protein-DNA docking (e) DNA-ligand docking	Forli et al. (2016) Yan et al. (2017) Ciemny et al. (2018) Yan et al. (2017) Jayaram et al. (2012)
Based on flexibility	(a) Rigid-body docking (b) Semi-rigid docking (c) Flexible docking	Meng et al. (2011) Meng et al. (2011) Meng et al. (2011)
Other special dockings	(a) Induced fit docking (b) Hydrated docking	Barreca et al. (2009) Forli and Olson (2012)

Figure 22.5 represents the schematic representation of the different steps in molecular docking.

22.2.4.2 Different Types of Molecular Docking

There are different types of dockings, as listed in Table 22.2. Blind docking is mainly used when the active site of the receptor is not found properly. Here grid box is used for full receptors. But in the case of site-specific docking, the active site of the

protein is already known from before or already reported in the paper. However, docking can be classified according to the flexibility of the macromolecules and ligands (Chaudhary and Mishra 2016; Meng et al. 2011).

- (a) *Rigid-body docking*: This type of docking happened when both ligand and receptor are treated as a rigid body, and here search space is minimal and has three transitional and rotational degree of freedom. It follows the old “lock and key” theory. This docking is mainly used for the first time in DOCK, FLOG, and in some protein-protein docking. This process is very easy and does not need multiple mathematical calculations.
- (b) *Semi-flexible docking*: This type of docking contains fixed protein and a small ligand molecule, especially fragments. Here ligand can bind any position of the receptors and change its pose for minimum energy required for the perfect fit in the complex. It follows the induced fit program.
- (c) *Flexible docking*: Here, both ligand and protein are flexible. During this process, both ligand and receptor modify their conformation repeatedly. It is a complicated process. Currently, various methods are available for the flexibility of receptors, one among them is soft docking that decreases the van der Waals repulsion energy, which is termed in scoring function to allow for a degree of atom-atom overlap between the ligand and receptor. Nowadays, AutoDock, GLIDE, and GOLD software is more favorably used for flexible docking.

22.2.4.3 Machine Learning in Docking

The most essential part of molecular docking is the scoring function. In conventional docking, the scoring function is mainly developed by a force field, knowledge-based, or empirical process that limits docking power and is cost-effective in drug discovery. In some studies (Ashtawy and Mahapatra 2013), it was found that the machine learning-based scoring function has an 80% success rate, whereas in conventional showed a 70% success rate. Various nonparametric machine learning methods are employed here. In the machine learning approach, MLs are used in two cases, firstly for prediction of the binding affinities and use this score to differentiate the promising pose from the less promising one. Further second set build a scoring function for the prediction of RMSD (Root Mean Square Deviation) value. A different algorithm like multiple linear regression, k-nearest neighbors, support vector machine, and random forest are used most commonly for the development of docking model (Ashtawy and Mahapatra 2013; Khamis et al. 2015; Jiménez-Luna et al. 2020).

22.2.4.4 Application of Molecular Docking

Molecular docking is nowadays used in a vast area of drug design and discovery. It is not only used in ligand-target binding for finding structural determinants necessary for receptor-ligand docking but also used in virtual screening (hit identification) for disease-related target finding. In addition, it is also helpful in reverse docking that allows the prediction of biological targets for the particular molecule, which represent an effective approach for target fishing and profiling. Moreover, it can be used in

drug repositioning, prediction of active site, prediction of adverse drug reaction, and polypharmacology.

Reverse docking helps to predict the toxicity of drug molecules based on their structure and interaction with various target receptors, transporters, enzymes, and other biomolecules. Molecular docking is also used for regulatory purposes to predict the toxicity of drug molecules based on the developed classification models. As docking helps us understand the binding between two molecules, it is an important tool to predict the toxicity of drug molecules by understanding their mechanism of binding with various targets, including receptors, enzymes, and transporters (Trisciuzzi et al. 2018).

Molecular docking is mainly used for predicting the desired orientation of drug molecules that can fit into the binding pocket of their target. This can be achieved by determining their lowest energy conformation and is often used to perform receptor-based, enzyme-based, and transporter-based virtual screening to recognize the drug molecule that best fits the binding site of the target (Pu et al. 2019).

22.3 OECD Guidelines for Testing Chemicals

The organisation for Economic Co-operation and Development (OECD) is an organization where the government can work together to share knowledge, experience, and solutions to common obstacles. It joins hands with governments to get an idea about what drives economic, social, and environmental change. It calculates productivity and international flows of investment and trade. It regulates global standards of various things, including agriculture, tax, and the safety of chemicals. OECD also focuses on issues which directly affect the lives of humans, such as the process of payment of tax and other social securities. It relates different socio-economic policies of various countries to improve the quality of life (OECD 1994, 2022a).

Guidelines given by OECD for the testing of chemicals are an exclusive tool for evaluating the plausible effects of chemicals on the environment and human health. It is recognized globally as a standard protocol for the safety testing of chemicals. These guidelines are used by experts in academia, industry, and also by governmental agencies involved in the testing and evaluation of chemicals. OECD guidelines are expanding continuously and updated regularly to ensure they imitate the state-of-the-art science and techniques to meet the regulatory needs of its members. The guidelines are expanded with the assistance of professionals in academia, industry, regulatory agencies, animal, and environmental welfare organizations (OECD 1994, 2022a). OECD has proposed five basic principles in the regulatory context for using computational techniques, which include a defined endpoint, defined domain of applicability, definite algorithm, suitable measures for robustness, prediction, and reliability of the developed model, and also the interpretation of mechanism if possible (Pérez Santín et al. 2021).

Guidelines given by OECD for the testing of chemicals is a set of about 150 most significant agreed testing methods globally, used by independent laboratories,

Table 22.3 OECD Guidelines for the Testing of Chemicals, Section 4: guidelines for various toxicity related to health issues and tests performed

Toxicity	Guideline/test numbers
Chronic toxicity/carcinogenicity	417, 451–453
Dermal toxicity	402, 404, 410, 411
Developmental toxicity	414, 421, 422, 426
Genotoxicity	471, 473–490
Inhalation toxicity	403, 412, 413, 433, 436
Neurotoxicity	418, 419, 424
Ocular toxicity	405, 437, 438, 460, 491, 492, 494, 496
Oral toxicity	401, 407, 408, 409, 420, 423, 425
Phototoxicity/photoreactivity	432, 495
Reproduction toxicity	415, 416, 421, 422, 443
Skin sensitization	406, 427–431, 435, 439, 442 A/B/C/D/E, 498
Steroid hormones (estrogen receptor/androgen receptor)	440, 441, 455–458, 493

industry, and government to recognize and characterize the potential dangers of chemicals. They are a collection of tools for experts used mostly in safety testing and consequent chemical product notification, registration, and evaluation. In addition, they can be used for the selection and ranking of chemicals for the development of novel chemicals in toxicology research (OECD 1994, 2022b). OECD Guidelines for the Testing of Chemicals are broadly categorized into five sections:

Section 1: Physical–Chemical properties—This section involves physical and chemical properties (OECD 2022c).

Section 2: Effects on Biotic systems—This section involves effects on biotic systems (OECD 2022d).

Section 3: Environmental Fate and Behavior—This section involves environmental fate and behavior (OECD 2022e).

Section 4: Health effects—This section involves health effects (OECD 2022f).

Section 5: Other Test Guidelines—This section involves other test guidelines (OECD 2022g).

Each section consists of an ample number of tests which defines a detailed protocol for a variety of tests to be followed (OECD 2022b). The guidelines for studying the effect of chemicals and drugs on the health of individuals by *in vitro* and *in vivo* models are given in detail in Section 4, comprising a total of 80 tests, each with different criteria as mentioned in Table 22.3 (OECD 2022f). It describes various tests for different types of toxicity, including dermal toxicity, skin sensitization, ocular toxicity, genotoxicity, reproductive, and developmental toxicity. These guidelines give the detailed protocol regarding the use of animals, their handling, dosing of drugs in case of acute and chronic studies, and also evaluating parameters. For a particular test, new guidelines are published or updated whenever required.

They help us to screen molecules in the initial phase of drug discovery and also suggest the replacement, reuse, and refinement of animals. Preclinical toxicity evaluation in non-primates, usually rodents and primates, is a prerequisite for the drugs to enter clinical trials, and hence these guidelines are essential in the drug discovery process as they establish protocols starting from formulation of a drug to its efficacy and toxicity performed *in vitro* and *in vivo*, along with its impact on the environment.

22.4 Importance of Artificial Intelligence in Toxicity Predictions

AI-based modeling to predict toxicity has been promoted over the past decade and continues to emerge as a developing area. The knowledge about AI modeling has improved vastly in all fields. In addition, it is the best alternative for animal studies because of ethical aspects, the suffering of animals, and, more importantly, for the reliability of results when compared with many *in vivo* tests (Pérez Santín et al. 2021). To develop *in silico* models, a variety of databases is required along with pharmacophores, QSAR, similarity finder, i.e., common fingerprints, machine learning models, molecular modeling, and other network analysis tools that involve the usage of computers (Ekins et al. 2007). Computational models are built for predicting the toxicity of molecules in the environment and health issues. Various properties of molecules, both chemical and biological, are considered while developing a model, such as the structure of molecules, dose and time response, pharmacokinetics data, and pharmacodynamics data (Wu and Wang 2018).

Earlier, the models were constructed based on single parameters, such as chemical structure or any biological property, but as the field is diverging new models are developed using a combination of structural and biochemical parameters to predict a better outcome with high accuracy. The developed model measures toxicity only against one target system (Wu and Wang 2018). Apart from using multifeatured input data, more advanced models are computed by a combination of perturbations and machine learning which integrates different biological and chemical data to predict the toxicity against diverse living organisms (Kleandrova et al. 2015). As the chemical structure of molecules can be related to their biological activity, including efficacy and toxicity, it is important for academia and pharma companies to predict the safety of novel chemical entities even before synthesizing the molecule, which can save both time and cost for researchers. These models are required in the process of drug discovery and predicting toxicity by understanding their affinity to a particular target by molecular docking studies or by characterization of their structural, physical, and chemical properties.

Strangely, estimations of toxicity as true predictions using *in silico* methods range between 85% and 90% as it out-turns that the available literature and biological data showing the experimental proofs are limited. Also, the selection of descriptors used for input data is limited. Hence, it is crucial to understand the working of these models to identify the significant characteristics or the descriptors to be used for developing a model which gives a reliable output with reproducibility (Hutter 2018).

22.4.1 Toxicity Due to Drugs

Drugs are a boon to human health, but if not used precisely, they can also be a curse to us. Most of the drugs used today are associated with some minor or major adverse effects. Though these drugs have US-FDA approval after clinical trials, their chronic usage is not usually considered before approval. Therefore, most of these drugs showing toxicity due to long-term usage can only be found by physicians treating their patients. Apart from efficacy, the toxicity of drug molecules also plays a crucial role in determining their fate. On one side, the Food and Drug Administration (FDA) approves novel drugs for treating various diseases, on the contrary, the FDA Adverse Event Reporting System (FAERS) records more than 10 million Adverse Event reports, out of which more than 5 million reports were associated with chronic conditions and around 1.1 million reports were associated with death (Basile et al. 2019). It is reported that many new drug entities fail due to various reasons, including toxicity though they are found to be very efficacious. Drug development process usually takes 10–15 years to get launched in the market, and therefore it is very crucial to understand the possible adverse effects of drugs as soon as possible to reduce the effort, cost, and time in developing new drugs (Kennedy 1997). Most of the approved and marketed drugs are withdrawn due to toxicity in various organs. Hepatotoxicity is the leading cause of the withdrawal of drugs and is highly variable, ranging from asymptomatic alterations in liver functioning to chronic liver failure (Mehta et al. 2010).

Most pharmaceutical industries are now interested in determining the toxicity of new drugs even before their manufacturing to reduce the cost and time consumed for drug development. Hence, many innovative techniques are on their way to predict the toxicity of drug molecules along with their mechanisms, including Artificial Intelligence (AI)-based machine learning models. AI-based machine models are developing recklessly to understand the toxicity caused by various chemicals, drugs, and other molecules. Computational methods are important as thousands of drug features can be computed, analyzed, filtered, and selected based on algorithms; moreover, it is beyond the scope of humans to study these features individually for all the existing and emerging drug molecules (Khuri and Deshmukh 2018). AI-based models can predict toxicities of molecules based on their physicochemical properties such as topological surface area, $\text{Log}P$ or $\text{Log}D$ values, the number of acceptor and donor groups, presence of various functional groups such as hydroxyl and amine groups, molecular weight, molecular volume, aromatic rings and also based on the structure of molecules which helps in determining its interaction and binding efficacy with various biomolecules in body.

22.4.2 Toxicity Due to Drug-Drug Interactions

Patients suffering from multiple chronic diseases frequently follow polypharmacy, i.e., co-prescription of various drugs. It is prescribed as a consequence of aiming for disease-specific targets to treat patients with multiple chronic diseases. One of the

major limitations of polypharmacy is adverse drug reactions due to drug-drug interactions. This risk of adverse drug reactions due to drug-drug interactions increases in any patient with the increase in coexistence of diseases and the multiple drugs prescribed (Marengoni and Onder 2015).

Interactions between multiple drugs at both the target site and the non-target site can further influence the therapeutic efficacy and safety of drug molecules. It is well-known that a combination of drugs can improve the efficiency of treatment by showing synergistic effects; however, it could also lead to antagonist effects or adverse reactions if the interactions are not favorable. Around 30% of adverse drug events are associated with drug-drug interactions (Pirmohamed and L'E Orme 1998). Moreover, many licensed drugs are withdrawn from the market due to drug-drug interactions as these adverse drug events are usually not observed during clinical trials (Herrero-Zazo et al. 2016). Therefore, an early understanding of the interactions between commonly used drug molecules or for combination therapy is a prerequisite to reduce adverse drug events and also to ensure patient safety. The frequency of co-prescribed drugs has increased lately as there is an increase in the number of elderly patients suffering from multiple comorbidities and also the frequent use of a cocktail of drugs to treat chronic diseases (Lea et al. 2013; O'Hare et al. 2006).

Conventionally, animal models are used for understanding drug-drug interactions, but it is not cost-effective and also need longer durations. Moreover, it is ethically not possible to perform interaction studies between all the available drugs using these animal models. Hence, one of the better approaches to understand drug-drug interactions is the use of computational modeling. Computational modeling uses various approaches to predict the toxicity due to drug-drug interaction, such as pharmacophore-based, machine learning-based, similarity-based, network-based, and molecular docking-based models. Apart from the network-based approach, the abovementioned approaches rely on 3D structures of drug molecules and negative examples of drug-drug interaction (Wu et al. 2018). Drug-drug interactions can be understood by identifying the commonality of drug targets or metabolic pathways, or pharmacological effects (Park et al. 2015). Attempts have also been made to develop computational methods which predict novel drug-drug interactions based on the structural similarities and side effects of known drug-drug interaction, based on the similarities between their molecular fingerprints, or based on their common targets (receptors or genes or pathways) (Vilar et al. 2013, 2014; Gottlieb et al. 2012).

The phenotypic, genomic, and therapeutic similarity between drug molecules can be used as descriptors for developing and evaluating machine learning models such as decision tree, random forest, support vector machines, k-nearest neighbours, and logistic regression (Cheng and Zhao 2014). Probabilistic approach considering known drug-drug interaction or protein-protein interaction or drug-enzyme interaction as input variables, novel drug-drug interactions, and their related adverse drug events can be predicted (Sridhar et al. 2016; Hunta et al. 2015). In addition, physicochemical properties and metabolic properties of drug molecules can also be considered input for developing machine learning models. While developing a

model for predicting novel drug-drug interaction, it is critical to consider the negative examples of drug pairs that do not interact. Models capable of predicting the severity of adverse drug reactions such as mild or severe are also important even if it cannot predict the exact adverse drug reaction because of drug-drug interaction (Herrero-Zazo et al. 2016).

Neural networks such as artificial neural networks have been used lately to develop models for predicting drug-drug interactions, which are of clinical significance. Various pharmacokinetic or pharmacodynamic, or drug-enzyme interaction properties were considered as input for the development of a model. Artificial neural network models can be built using a single-layer perceptron or multilayer perceptron for the best predictions of drug-drug interactions. Output and accuracy of the model majorly depend upon the dataset and the input variables considered for developing the model. And therefore, different models can be built using different datasets and input variables and finally selected based on the application of the study. For example, using drug-enzyme interaction properties as input variables, minor drug-drug interactions were best predicted, whereas, using pharmacokinetic or pharmacodynamic properties of drug molecules as input variables, major drug-drug interactions were best predicted (Herrero-Zazo et al. 2016).

Computational models using deep neural networks are also used for predicting drug-drug interaction by considering the structural information and chemical names of any two drugs in pair as input for the model, and the interaction between two drugs (synergism or antagonism) is predicted as output. Inputs are specified in the form of simplified molecular-input line-entry system (SMILES), whereas the output is given in the form of readable sentences such as “Drug 1 activity decreases when combined with Drug 2” or Risk or severity of “Drug 1 increases when combined with Drug 2” or vice versa. Output sentences can be generated from the predefined general sentences representing various types of interactions between drug molecules, as mentioned in DrugBank (Ryu et al. 2018).

Therefore, machine learning tools can gain information on novel drug-drug interactions and simplify the pharmacovigilance process for newly approved drugs by regulatory authorities.

22.4.3 Toxicity Due to Drug-Transporter Interaction

Several inward/outward-facing membrane proteins known as “Transporter” are known to facilitate the uptake/efflux of endogenous or drug substances across biological membranes (Kato et al. 2008). Drug regulatory agencies, including the US FDA and the European Medicines Agency (EMA), have recognized the clinical significance of transporters for drug safety. The human genome sequencing project has identified 850 genes encoding for transporters in establishing barrier function of cells, such as P-Glycoprotein (P-gp), multidrug resistance-associated proteins (MRP’s), and organic cation transporters (OCTs), and organic anion transporter proteins (OATPs). (Venter et al. 2001). Drug resistance is directly related to the expression of transporters in various organs, which limits the success of drug usage

for various diseases (Khuri and Deshmukh 2018). These transporters can cause toxicity when drug molecules act as a competitor to their endogenous or exogenous substrates (Gao et al. 2015; Taylor-Wells and Meredith 2014). Currently, the intracellular concentration of drugs is determined by understanding the equilibrium of influx and efflux transporters. The study of transporters in toxicology has gained much attention following the understanding of uptake of Cisplatin into kidney cells mediated by OCT2 transporter (Nigam 2015), specifically in the proximal tubule of the kidney and cochlea hair cells (Cridge 2018). A recent study explored the penetration of antimuscarinic agents (non-P-gp substrates) in the central nervous system (CNS), which are used in the treatment of overactive bladder (Muderrisoglu et al. 2019). Further, it was also established *in vitro* and *in vivo* that taurine transporter plays a crucial role in retinal toxicity caused due to accumulation of systemic vigabatrin (VGB) in the retina (Police et al. 2020). Many other studies also confirmed the crucial role of transporters in the accumulation of drugs at the non-target site. A study demonstrated alterations in transporter functions such as P-gp and OATP due to digoxin and high statin plasma levels, respectively (Ho and Kim 2005; Giacomini and Huang 2013; Fenner et al. 2009). It was mainly due to drug-drug interactions (DDI) or reduced transporter activity of variant OATPs for statins (Giacomini and Huang 2013).

Therefore, the role of transporters in drug absorption and clearance mechanism has to be understood to determine drug concentration at both target and non-target sites to predict the toxicity and pharmacokinetics of the drug. It can be better acknowledged if the interaction between drugs and transporters is studied based on their structural and physicochemical behavior. The significant time and cost requirement of experimental testing make AI an emerging area to build predictive computational models for determining the potential of substrate binding towards transporters (Diao et al. 2010; Moaddel et al. 2007). Many modeling approaches are being proposed to understand the specificity of transporters with various drugs in the human body.

Research is already advanced through *in silico* modeling to identify molecular fingerprints and predict new substrate-OCT interactions (Baidya et al. 2020). This may prognosticate to design better cationic drugs to minimize unwanted interactions with transporters and reduce toxicity. Using various computational techniques such as data mining, different descriptor calculators such as SMILE-based, graph-based, and a combination of both Monte Carlo optimization, Bayesian classification model, machine learning algorithms and associative neural network, and various classification models were developed to study the interaction of 111 FDA approved drugs with hOCT1 and hOCT2 transporter and found that 5 and 12 of these drugs may act as a substrate for hOCT1 and hOCT2 respectively (Baidya et al. 2020). Further, it was reported that 85% of newly tested substances screened through machine learning were confirmed as substrates for OCT1. Thereby, it can also help in understanding the molecular mechanisms of transporters (Jensen et al. 2021).

Machine learning algorithms such as kNN, SVM, XG-Boost, Random forest, and decision trees can be used for the development of models to predict the activity of drug molecules. Consensus machine learning models are built by a combination of

various machine learning algorithms to improve the accuracy and precision of final predictions. Usually, consensus models are built by selecting individual best models. Consensus models developed for hOCT1 and hOCT2 improved accuracy and sensitivity (Baidya et al. 2020). Using a combination of more than 10 different features, different machine learning models such as kNN, PLS, SVM, RF, and RNN were developed to predict inhibitors for hepatic drug transporters such as OATP1B1 and OATP1B3 (Khuri and Deshmukh 2018).

In silico predictions can guide researchers and industrialists to design and develop better drugs to avoid toxicity, dose-dependent adverse effects, and undesirable drug interactions with transporters. Using AI techniques, unique fingerprints of drug molecules can be identified, which helps to classify them into substrates or inhibitors for particular transporter. Drug-transporter interactions help us better understand the uptake and transport of drug molecules into cells.

22.5 Prediction of Toxicity in Different Organs by AI

22.5.1 Liver

The liver is the first-pass organ for the entire range of orally administered drugs, and thereby it is the recurrent site of xenobiotic toxicity. Hepatic toxicity may occur due to over-prescribed drugs or over-the-counter medication, which leads to drug-induced liver injury. It is one of the major reasons for the withdrawal of approved drugs from the market. Data from in vitro and in vivo studies fails to predict drug-induced liver injury in humans, which paves the path for AI-based computational models to arise and challenge the traditional in vitro and in vivo methods of screening drug molecules for their toxicity and efficacy. Several machine learning models, such as decision trees, random forest, support vector machine, Naïve Bayes, along with deep neural networks, are used by researchers and the pharmaceutical industry to predict the drug-induced liver injury of new drug molecules (Liu et al. 2011; Xu et al. 2015; Kotsampasakou et al. 2017).

Predicting the toxicity of drug molecules for the liver has advanced with deep learning machine models to predict the drug-induced liver injury of new test molecules based on the dataset containing positive and negative drugs causing liver injury as input variables. The model developed showed 87% accuracy, 83% sensitivity, and 93% specificity (Xu et al. 2015). To predict drug-induced liver injury Rank database and Tox21 database can be used to collect the list of hepatotoxic compounds to develop various machine learning models. Each model gives different accuracy, specificity, sensitivity, and AUC values. Classification models were developed using different machine learning algorithms for predicting the drug-induced liver toxicity of chemicals, of which support vector machines showed an accuracy of around 83% (Li et al. 2018). A random forest model was developed to predict hepatotoxicity according to various levels of hepatic adverse effects, which showed an accuracy between 67% and 78% (Liu et al. 2018). Many attempts are made to predict drug-induced liver toxicity by incorporating various types of input

variables, including the geometrical property of chemicals (available from the Tox21 dataset) which were used to develop a CNN model with a specificity and sensitivity of 52% and 79% respectively (Asilar et al. 2020).

Quantitative structure-activity relation-based models are also known to demonstrate good predictions for specific endpoints activity such as binding affinity and solubility of molecules; however, in the case of complex endpoint activity, this approach is less suitable due to various mechanisms of actions of drugs as seen in the liver (Hou and Wang 2008).

22.5.2 Heart

Drug-induced cardiotoxicity includes arrhythmia, Torsades de Pointes, mainly due to blockage of the human ether-a-go-go-related gene (hERG) potassium channel and other ion channels in the heart. In preclinical trials, drugs undergo a series of tests to identify drug effects on various organs, including the heart (Leishman et al. 2012; Vargas et al. 2015). Drugs are screened mainly for their interaction with ion channels in the heart, particularly hERG (Leishman et al. 2012). However, a number of drug molecules that can be screened using animal models is a major limitation for preclinical trials and also they do not mimic the actual physiologic conditions of humans (Lawrence et al. 2008). Consequently, reliable predictions of drug interaction with hERG in the initial stages of drug development is crucial to reduce the risk of drug-induced cardiotoxicity-related attenuation in the further developmental process. Thereby, several artificial intelligence-based models are developed to predict the drug-induced cardiotoxicity of a single type or multiple types. One approach to screen drug molecules which causes blocking of multiple ion channels has been simulated by ventricular myocyte models and the computed metrics of action potential and intracellular (Ca^{2+}) levels for the construction of classifiers which differentiates between the potential of drugs causing arrhythmogenic and non-arrhythmogenic effect. The developed classifiers were able to provide superior risk predictions, the influence of screened drugs on action potential and intracellular (Ca^{2+}) level, and also their interaction with cardiac ion channels (Lancaster and Sobie 2016).

Similarly, machine learning models have also been developed for multiple types of drug-induced cardiotoxicity using a large dataset of molecular and transcriptional profiles of drugs. The developed model produced 79% accuracy under the curve for safe drugs versus toxic drugs. In addition, it showed 66% accuracy for the unknown set of drug molecules. The model was also trained to predict the specific type of cardiotoxicity for an individual drug molecule which predicted signs and symptoms of the cardiac disorder for anti-inflammatory drugs with AUC of 80% and heart failures for anti-neoplastic drugs with 76% AUC (Mamoshina et al. 2020).

Neural network model was developed with a dataset of more than 2000 drug molecules, labeled as toxic and nontoxic based on their inhibitory concentration-50 value (concentration required to inhibit 50% of activity) to predict cardiotoxicity of molecules related to hERG with 90% accuracy. The developed model is accessible at

<http://ssbio.cau.ac.kr/CardPred>. The model can be used for high-throughput screening of new drug molecules to classify them as cardiotoxic or nontoxic molecules (Lee et al. 2019). Most of the models are developed using a single database which limits the scope and predictability of models. Hence, a novel approach of using multiple database can be used for the construction of the hERG classification model. An integrated database gives a collection of a huge number of molecules to develop a model. hERGCentral, PubChem, GOSTAR, and ChEMBL are a few of the available databases which used support vector machines for developing models to predict hERG-based cardiotoxicity (Ogura et al. 2019).

The quantitative structure-activity relationship model was also developed and evaluated by different machine learning and deep learning algorithms using more than 5000 hERG inhibitors in its dataset. The accuracy and AUC of the model was 86% and 90%, respectively (Choi et al. 2020).

A combinatorial approach involving machine learning and pharmacophore was used to develop a classification model to differentiate the drugs which are active or inactive in interacting with hERG. The recursive partitioning approach was used as an optimal ensemble of pharmacophore hypotheses to distinguish active and inactive hERG molecules, and later support vector machine and Bayesian classification were used to build classification models by assimilating significant pharmacophore hypotheses. Therefore, a combination of pharmacophore hypotheses with a machine learning model developed using a support vector machine algorithm proved to be more efficient in understanding multiple mechanisms of hERG blocker (Wang et al. 2016).

22.5.3 Eye and Skin

Skin and eyes are the primary superficial sensitized organs of mammals. Especially in the developing world, where cosmetics are used for daily purposes, understanding the sensitivity of skin to various chemicals is necessary. Moreover, skin irritants are considered to be also eye irritants (Verma and Matthews 2015). Eye and skin irritants are evaluated in animals using the Draize test, a standard testing method that classifies the chemicals and drugs as non-irritant, mild irritant, moderate irritant and highly irritant (Draize 1944). The Draize test is usually performed in rabbit's eyes, though human and rabbit eyes share similarities but do not mimic the true physiology of the human eye. Thereby, alternative *in vitro* methods have been developed to measure the ocular irritancy of chemicals along with various machine learning models for *in silico* predictions (Weil and Scala 1971; Curren and Harbell 2002; Cho et al. 2012).

Quantitative structure-activity relationship models were built using a small dataset of molecules causing ocular toxicity. K-nearest neighbor and random forest algorithms were utilized along with Dragon and Molecular Operating Environment descriptors. The developed individual model showed accuracy between 72% and 87%, which further improved upon building consensus model (based on prediction average of individual models) to 93% (Solimeo et al. 2012). Similarly, few more

quantitative structure-activity relationship models were built for predicting the ocular toxicity of compounds nonetheless the dataset used for their construction was small (Sugai et al. 1991; Cronin et al. 1994; Abraham et al. 1998). To overcome this problem, another approach of the machine learning model was applied where a diverse data of eye corrosive ($n = 2299$) and eye irritant ($n = 5220$) molecules was collected from various databases and literature. These molecules were represented with nine molecular fingerprints, and six machine learning algorithms were used to develop binary classification models with fivefold cross-validation to predict ocular toxicity. The sensitivity and specificity of the developed model for eye corrosive were 94.9% and 96.2%, respectively, whereas, for eye irritant molecules, it was found to be 96.9% and 82.7%. The high sensitivity and specificity of the developed model ensure the reliability and robustness of the model in predicting the activity of molecules causing ocular toxicity (Wang et al. 2017c).

22.5.4 Gastrointestinal

Gastrointestinal toxicity is the most common side effect of orally consumed medicines. These effects decrease patient compliance and cause physiological disturbances along with undesirable effects on the gut microflora. Microflora of the gastrointestinal tract plays a crucial role in maintaining the health conditions of individuals, including synthesis of vitamins, production of serotonin, and proper immune functioning (Oliphant and Allen-Vercoe 2019; Fung et al. 2019; Ghyselinck et al. 2020). Disturbance to normal gut microflora could lead to the cessation of health-promoting activities of microflora (Suez et al. 2014; Janssens et al. 2018; Kigerl et al. 2018). Various drugs, especially orally administered (antibiotics and other target-specific drugs), are known to alter gut microbiome composition and lead to gut dysbiosis (Dethlefsen et al. 2008; Maier et al. 2018).

Machine learning models were developed to predict if a drug retards the growth of gut bacteria. More than 18,000 drug-bacteria interactions were used to build 13 machine learning models were built including decision trees, ensemble models and artificial neural networks. With hyperparameter tuning and multi-metric evaluation, a principal model was selected based on its performance, measured by AUROC of 0.857, recall as 0.587 and precision as 0.8 (McCoubrey et al. 2021). Another interesting approach to predict the effect of drugs on gastrointestinal tract was made by collecting the freely available data, which included the list of drugs inducing a change in gene expression to develop small intestine epithelial cell metabolic models based on the specific drug. A multi-label support vector machine model was developed using a combination of local gut wall-specific metabolism and small intestine metabolism in producing the adverse effect. The predicted outcome was useful for screening the occurrence of drug toxicity in the gastrointestinal tract. Understanding the hidden resemblances of drugs based on their genetic and metabolic profile could lead to further classification of drugs apart from the indication-based classification of drugs (Ben Guebila and Thiele 2019). These models are of great importance to pharma and food companies in delivering drugs through the oral

route and prediction of drugs that impair the growth of microflora in the gastrointestinal tract.

22.5.5 Kidney

Irrespective of the dose and route of drug administration, all the drug molecules undergo the ADME phase, i.e., absorption, distribution, metabolism, and clearance from the body. Clearance of the drug from the body is one of the major concerns in any drug discovery process performed by pharmacokinetics. Kidneys are the primary organs for the clearance of the drug and its metabolites from the body. Therefore, it is crucial to understand the toxicity of drug molecules on the kidney and its associated tissue. Very few studies have been performed to build machine learning models and QSAR models to predict the renal toxicity of drug molecules (Antczak et al. 2010). It is partly because most of the toxicity in kidneys is related to either direct or indirect effects of drug molecules. Alterations in the blood flow, blood pressure, and damage to various regions of the kidney, including glomerular capillaries, Bowman's capsule, and proximal tubule, are considered as toxic effects of drug molecules. Apart from biological activity, gene expression data linked with physicochemical properties (descriptors) of drug molecules (88 compounds, out of which 22 compounds had the potential to cause degeneration of renal tubules) can also be used to develop a model and predict the toxicity of compounds (Antczak et al. 2010). It has also been suggested that data from any cytotoxic cell lines, irrespective of the organs, can be used commonly to predict the toxicity of drug molecules as they behave similarly (Lin and Will 2012).

Attempts are in progress to build a computational model for predicting the renal toxicity of drug molecules, a dataset consisting of molecules known to cause renal toxicity and nontoxic molecules was used to develop a classification model and also a Bayesian model, which showed a ROC value of 0.64. In contrast, the support vector machine model showed lower values than the Bayesian model (Lin and Will 2012). These studies have laid the foundation for predicting the toxicity of drug molecules in the kidney, which needs further attention in the drug discovery process and also to enhance the understanding regarding clearance of the drug and its metabolites from the body.

22.6 Conclusion

In the process of drug discovery, it is very crucial to understand the safety of a drug rather than just its efficacy. Many drugs are known to be efficacious, but they come at the cost of life-threatening side effects. Hence, a drug is approved in the market only when the benefit vs risk ratio of a drug is more. Chronic usage of drugs is usually not considered for approval of the drug, though pharmacovigilance continuously monitors the efficacy and safety of drugs in patients. Most of these approved drugs have been found to be causing one or other off-target side effects, which

becomes the major reason for the removal of drugs from the market even though they are highly efficacious. The withdrawal of drugs leads to a huge loss of money and time consumed for the discovery, development, and approval of any drug molecule. On the contrary, the field of artificial intelligence is widely spreading and has already conquered almost every aspect of human life, starting from a simple calculator to robotics and drug discovery. In developing and developed countries, technology is growing faster, and the pace of work has increased. In today's era, cost and time are two important factors that decide the profit and loss of any organization. Hence, the traditional methods of discovery and development of a drug, which usually take more than 15 years and a huge amount of money, are now been replaced by fast-growing computational techniques.

As the safety of drugs is the major concern for their usage, earlier prediction of their toxicity could lead to more advanced drug discovery. Drug toxicity could be due to their interaction with other drugs or endogenous molecules in the body leading to adverse effects, or could also be due to their accumulation in off-target sites, gaining entry by interacting with transporters. Machine learning models are developed to predict the abovementioned interactions of the drug with other drugs or transporter proteins which can help us to understand the safety mechanisms of the drug. Various artificial intelligence tools such as regression analysis, neural networks, and deep learning are being used continuously to develop better models for predicting the overall toxicity of drugs or specific toxicity related to a particular cell type, tissue, or organ. Machine learning models use the structural, physicochemical properties such as polar surface area, charge, hydrophobicity or hydrophilicity ($C \log P$ values), number of hydroxy or amine groups, and any other functional groups along with their biological activity as input data for constructing a model. Various models can be developed and ranked based on their performance measured by their accuracy, sensitivity, specificity, and ROC values. The predicted outcome from a model can be used in the determination of the activity of the drug both in terms of its efficacy and also toxicity. QSAR, which also involves the use of machine learning models, considers the structural along with physicochemical properties of drug molecules and relates them with their biological activity. QSAR approach is more valid in understanding the underlying mechanisms or targets of the drug molecule responsible for toxicity. Molecular docking is another approach for modeling where the structure of molecule plays a crucial role, i.e., they determine the interaction of two drug molecules or drug-transporter interaction based on their structural compatibility as seen in the lock-key model.

In silico predictions of drug toxicity has already been approved by regulatory authorities, obligated they follow the guidelines given by OECD and other regulatory bodies. Artificial intelligence-based machine learning models help to predict the toxicity of molecules even before the synthesis and production of drug molecules which can save all the efforts. Also, these techniques are proven to be reliable and reproducible, and therefore reduces the use of animals. Though alternatives have been proposed for in vivo studies such as in vitro cell line studies, organ culture and organ-on-chip, artificial intelligence-based machine learning models, deep learning,

and various neural networks help to screen thousands of drugs in a very short duration of time and are also cost-effective.

Therefore, for the future drug discovery process, it is very important to understand the role of artificial intelligence in predicting drug toxicity as it is the most crucial factor in deciding the fate of drug molecules. Also, the benefit vs risk ratio of drugs will be improved, increasing overall patient compliance. Though in vivo studies will continue to remain as the gold standard for testing the efficacy and safety of drugs in preclinical trials, the futuristic approach of drug discovery will also be highly dependent on computational techniques because of their high accuracy, reliability, and reproducibility.

Acknowledgments We would like to acknowledge University Grant of Commission, India for providing fellowship to Manisha Malani.

References

- Abadi M (2016) TensorFlow: learning functions at scale. In: Proceedings of the 21st ACM SIGPLAN international conference on functional programming
- Abadi M et al (2016) Tensorflow: large-scale machine learning on heterogeneous distributed systems. arXiv preprint arXiv:1603.04467
- Abdel-Ilah L et al (2017) Applications of QSAR study in drug design. *Int J Eng Res Technol (IJERT)* 6(6)
- Abiodun OI et al (2018) State-of-the-art in artificial neural network applications: a survey. *Heliyon* 4(11):e00938
- Abraham MH et al (1998) A quantitative structure–activity relationship (QSAR) for a Draize eye irritation database. *Toxicol In Vitro* 12(3):201–207
- Albanese D et al (2012) mply: Machine learning python. arXiv preprint arXiv:1202.6548
- Albawi S, Mohammed TA, Al-Zawi S (2017) Understanding of a convolutional neural network. In: 2017 International conference on engineering and technology (ICET). IEEE, Piscataway, NJ
- Alpaydin E (2020) Introduction to machine learning. MIT Press, Cambridge, MA
- Amin SA et al (2018) Exploring pyrazolo [3, 4-d] pyrimidine phosphodiesterase 1 (PDE1) inhibitors: a predictive approach combining comparative validated multiple molecular modelling techniques. *J Biomol Struct Dyn* 36(3):590–608
- Antczak P et al (2010) Mapping drug physico-chemical features to pathway activity reveals molecular networks linked to toxicity outcome. *PLoS One* 5(8):e12385
- Araque O et al (2017) Enhancing deep learning sentiment analysis with ensemble techniques in social applications. *Expert Syst Appl* 77:236–246
- Ashtawy HM, Mahapatra NR (2013) Molecular docking for drug discovery: machine-learning approaches for native pose prediction of protein–ligand complexes. In: International meeting on computational intelligence methods for bioinformatics and biostatistics. Springer, Cham
- Asilar E, Hemmerich J, Ecker GF (2020) Image based liver toxicity prediction. *J Chem Inf Model* 60(3):1111–1121
- Bahrapour S et al (2015) Comparative study of deep learning software frameworks. arXiv preprint arXiv:1511.06435
- Baidya AT et al (2020) In silico modelling, identification of crucial molecular fingerprints, and prediction of new possible substrates of human organic cationic transporters 1 and 2. *New J Chem* 44(10):4129–4143
- Barreca ML et al (2009) Induced-fit docking approach provides insight into the binding mode and mechanism of action of HIV-1 integrase inhibitors. *ChemMedChem* 4(9):1446–1456

- Basile AO, Yahi A, Tatonetti NP (2019) Artificial intelligence for drug toxicity and safety. *Trends Pharmacol Sci* 40(9):624–635
- Ben Guebila M, Thiele I (2019) Predicting gastrointestinal drug effects using contextualized metabolic models. *PLoS Comput Biol* 15(6):e1007100
- Böhm H-J (1992) LUDI: rule-based automatic design of new substituents for enzyme inhibitor leads. *J Comput Aided Mol Des* 6(6):593–606
- Boyacioglu MA, Kara Y, Baykan ÖK (2009) Predicting bank financial failures using neural networks, support vector machines and multivariate statistical methods: a comparative analysis in the sample of savings deposit insurance fund (SDIF) transferred banks in Turkey. *Expert Syst Appl* 36(2):3355–3366
- Chaudhary KK, Mishra N (2016) A review on molecular docking: novel tool for drug discovery. *Database* 3(4):1029
- Cheng F, Zhao Z (2014) Machine learning-based prediction of drug–drug interactions by integrating drug phenotypic, therapeutic, chemical, and genomic properties. *J Am Med Inform Assoc* 21(e2):e278–e286
- Cho S-A et al (2012) A new cell-based method for assessing the eye irritation potential of chemicals: an alternative to the Draize test. *Toxicol Lett* 212(2):198–204
- Choi K-E, Balupuri A, Kang NS (2020) The study on the hERG blocker prediction using chemical fingerprint analysis. *Molecules* 25(11):2615
- Ciemny M et al (2018) Protein–peptide docking: opportunities and challenges. *Drug Discov Today* 23(8):1530–1537
- Collobert R, Bengio S, Mariéthoz J (2002) Torch: a modular machine learning software library. *Idiap*
- Collobert R, Kavukcuoglu K, Farabet C (2011) Torch7: a Matlab-like environment for machine learning. In: *BigLearn, NIPS workshop*
- Costa E et al (2007) A review of performance evaluation measures for hierarchical classifiers. In: *Evaluation methods for machine learning II: papers from the AAAI-2007 workshop*
- Cridge B (2018) Drug transporters in toxicology. *Open Acc J Toxicol* 2(3):555588
- Cronin M, Basketter D, York M (1994) A quantitative structure-activity relationship (QSAR) investigation of a Draize eye irritation database. *Toxicol In Vitro* 8(1):21–28
- Curren RD, Harbell JW (2002) Ocular safety: a silent (in vitro) success story. *Altern Lab Anim* 30(2_Suppl):69–74
- da Silva Júnior APH, de Sousa Bezerra DG, Andrade YS (2020) Comparação de arquiteturas de deep Learning para segmentação de imagens dermatoscópicas de melanoma
- Dave VS, Dutta K (2014) Neural network-based models for software effort estimation: a review. *Artif Intell Rev* 42(2):295–307
- De Martino A, De Martino D (2018) An introduction to the maximum entropy approach and its application to inference problems in biology. *Heliyon* 4(4):e00596
- Dethlefsen L et al (2008) The pervasive effects of an antibiotic on the human gut microbiota, as revealed by deep 16S rRNA sequencing. *PLoS Biol* 6(11):e280
- Diao L, Ekins S, Polli JE (2010) Quantitative structure activity relationship for inhibition of human organic cation/carnitine transporter. *Mol Pharm* 7(6):2120–2131
- Donahue J et al (2014) Decaf: A deep convolutional activation feature for generic visual recognition. In: *International conference on machine learning*. PMLR
- Došilovic FK, Breic M, Hlupic N (2018) Explainable artificial intelligence: a survey. In: *2018 41st International convention on information and communication technology, electronics and micro-electronics (MIPRO)*, pp 0210–0215
- Draize JH (1944) Methods for the study of irritation and toxicity of substances applied topically to the skin and mucous membranes. *J Pharmacol Exp Ther* 82:377–390
- Dunteman GH (1989) Basic concepts of principal components analysis. SAGE Publications Ltd., London, pp 15–22
- Ekins S, Mestres J, Testa B (2007) In silico pharmacology for drug discovery: applications to targets and beyond. *Br J Pharmacol* 152(1):21–37

- Fenner K et al (2009) Drug–drug interactions mediated through P-glycoprotein: clinical relevance and in vitro–in vivo correlation using digoxin as a probe drug. *Clin Pharmacol Ther* 85(2): 173–181
- Fischer E (1894) Einfluss der configuration auf die wirkung der enzyme. *Ber Dtsch Chem Ges* 27(3):2985–2993
- Flood I, Kartam N (1994) Neural networks in civil engineering. I: principles and understanding. *J Comput Civ Eng* 8(2):131–148
- Forli S, Olson AJ (2012) A force field with discrete displaceable waters and desolvation entropy for hydrated ligand docking. *J Med Chem* 55(2):623–638
- Forli S et al (2016) Computational protein–ligand docking and virtual drug screening with the AutoDock suite. *Nat Protoc* 11(5):905–919
- Free SM, Wilson JW (1964) A mathematical contribution to structure-activity studies. *J Med Chem* 7(4):395–399
- Fung TC et al (2019) Intestinal serotonin and fluoxetine exposure modulate bacterial colonization in the gut. *Nat Microbiol* 4(12):2064–2073
- Gao B et al (2015) Differential cellular expression of organic anion transporting peptides OATP1A2 and OATP2B1 in the human retina and brain: implications for carrier-mediated transport of neuropeptides and neurosteroids in the CNS. *Pflugers Arch* 467(7):1481–1493
- Gertrudes J et al (2012) Machine learning techniques and drug design. *Curr Med Chem* 19(25): 4289–4297
- Ghyselinck J et al (2020) A 4-strain probiotic supplement influences gut microbiota composition and gut wall function in patients with ulcerative colitis. *Int J Pharm* 587:119648
- Giacomini K, Huang SM (2013) Transporters in drug development and clinical pharmacology. *Clin Pharmacol Ther* 94(1):3–9
- Goertzel B, Pennachin C (2007) Artificial general intelligence, vol 2. Springer, Berlin
- Gottlieb A et al (2012) INDI: a computational framework for inferring drug interactions and their associated recommendations. *Mol Syst Biol* 8(1):592
- Hansch C et al (1962) Correlation of biological activity of phenoxyacetic acids with Hammett substituent constants and partition coefficients. *Nature* 194(4824):178–180
- Hart TN, Read RJ (1992) A multiple-start Monte Carlo docking method. *Proteins* 13(3):206–222
- Hassan NM et al (2017) Protein–ligand blind docking using QuickVina-W with inter-process spatio-temporal integration. *Sci Rep* 7(1):1–13
- Haykin S, Network N (2004) A comprehensive foundation. *Neural Networks* 2004(2):41
- He H, Garcia EA (2009) Learning from imbalanced data. *IEEE Trans Knowl Data Eng* 21(9): 1263–1284
- Herrero-Zazo M, Lille M, Barlow DJ (2016) Application of machine learning in knowledge discovery for pharmaceutical drug–drug interactions. In: *KDWeb*
- Hertz J, Krogh A, Palmer RG (2018) Introduction to the theory of neural computation. CRC Press, Boca Raton, FL
- Ho RH, Kim RB (2005) Transporters and drug therapy: implications for drug disposition and disease. *Clin Pharmacol Ther* 78(3):260–277
- Hou T, Wang J (2008) Structure–ADME relationship: still a long way to go? *Expert Opin Drug Metab Toxicol* 4(6):759–770
- Hunta S, Aunsri N, Yooyativong T (2015) Drug–drug interactions prediction from enzyme action crossing through machine learning approaches. In: 2015 12th International conference on electrical engineering/electronics, computer, telecommunications and information technology (ECTI-CON). IEEE, Piscataway, NJ
- Hutter MC (2018) The current limits in virtual screening and property prediction. *Future Med Chem* 10(13):1623–1635
- Izeboudjen N, Larbes C, Farah A (2014) A new classification approach for neural networks hardware: from standards chips to embedded systems on a chip. *Artif Intell Rev* 41(4):491–534
- Jain AN (1996) Scoring noncovalent protein–ligand interactions: a continuous differentiable function tuned to compute binding affinities. *J Comput Aided Mol Des* 10(5):427–440

- Janssens Y et al (2018) Disbiome database: linking the microbiome to disease. *BMC Microbiol* 18(1):50
- Jayaram B et al (2012) Sanjeevini: a freely accessible web-server for target directed lead molecule discovery. *BMC Bioinformatics* 13:S7
- Jensen O, Brockmüller JR, Dücker C (2021) Identification of novel high-affinity substrates of OCT1 using machine learning-guided virtual screening and experimental validation. *J Med Chem* 64:2762
- Jia Y et al (2014) Caffe: convolutional architecture for fast feature embedding. In: Proceedings of the 22nd ACM international conference on multimedia
- Jiménez-Luna J et al (2020) A deep-learning approach toward rational molecular docking protocol selection. *Molecules* 25(11):2487
- Kato Y et al (2008) Involvement of multidrug resistance-associated protein 2 (Abcc2) in molecular weight-dependent biliary excretion of β -lactam antibiotics. *Drug Metab Dispos* 36(6):1088–1096
- Kennedy T (1997) Managing the drug discovery/development interface. *Drug Discov Today* 2(10):436–444
- Khamis MA, Gomaa W, Ahmed WF (2015) Machine learning in computational docking. *Artif Intell Med* 63(3):135–152
- Khuri N, Deshmukh S (2018) Machine learning for classification of inhibitors of hepatic drug transporters. In: 2018 17th IEEE international conference on machine learning and applications (ICMLA). IEEE, Piscataway, NJ
- Kigerl KA, Mostacada K, Popovich PG (2018) Gut microbiota are disease-modifying factors after traumatic spinal cord injury. *Neurotherapeutics* 15(1):60–67
- Kingston GB, Maier HR, Lambert MF (2005) Calibration and validation of neural networks to ensure physically plausible hydrological modelling. *J Hydrol* 314(1–4):158–176
- Kleandrova V et al (2015) In silico assessment of the acute toxicity of chemicals: recent advances and new model for multitasking prediction of toxic effect. *Mini Rev Med Chem* 15(8):677–686
- Kollman P (1993) Free energy calculations: applications to chemical and biochemical phenomena. *Chem Rev* 93(7):2395–2417
- Kong R et al (2019) CoDockPP: a multistage approach for global and site-specific protein–protein docking. *J Chem Inf Model* 59(8):3556–3564
- Koshland DE (1963) Correlation of structure and function in enzyme action. *Science* 142(3599):1533–1541
- Koshland DE Jr (1995) The key–lock theory and the induced fit theory. *Angew Chem Int Ed Engl* 33(23–24):2375–2378
- Kotsampasakou E, Montanari F, Ecker GF (2017) Predicting drug-induced liver injury: the importance of data curation. *Toxicology* 389:139–145
- Kuntz ID et al (1982) A geometric approach to macromolecule–ligand interactions. *J Mol Biol* 161(2):269–288
- Kuschewski JG, Hui S, Zak SH (1993) Application of feedforward neural networks to dynamical system identification and control. *IEEE Trans Control Syst Technol* 1(1):37–49
- Lancaster MC, Sobie E (2016) Improved prediction of drug-induced Torsades de Pointes through simulations of dynamics and machine learning algorithms. *Clin Pharmacol Ther* 100(4):371–379
- Lawrence C et al (2008) In vitro models of proarrhythmia. *Br J Pharmacol* 154(7):1516–1522
- Lea M et al (2013) Severity and management of drug–drug interactions in acute geriatric patients. *Drugs Aging* 30(9):721–727
- Lee HM et al (2019) Computational determination of hERG-related cardiotoxicity of drug candidates. *BMC Bioinformatics* 20(Suppl 10):250
- Leishman D et al (2012) Best practice in the conduct of key nonclinical cardiovascular assessments in drug development: current recommendations from the Safety Pharmacology Society. *J Pharmacol Toxicol Methods* 65(3):93–101

- Li X et al (2018) The development and application of in silico models for drug induced liver injury. *RSC Adv* 8(15):8101–8111
- Lin Z, Will Y (2012) Evaluation of drugs with specific organ toxicities in organ-specific cell lines. *Toxicol Sci* 126(1):114–127
- Liu Z et al (2011) Translating clinical findings into knowledge in drug safety evaluation-drug induced liver injury prediction system (DILiPs). *PLoS Comput Biol* 7(12):e1002310
- Liu L et al (2018) Three-level hepatotoxicity prediction system based on adverse hepatic effects. *Mol Pharm* 16(1):393–408
- Lo Y-C et al (2018) Machine learning in chemoinformatics and drug discovery. *Drug Discov Today* 23(8):1538–1546
- Maier L et al (2018) Extensive impact of non-antibiotic drugs on human gut bacteria. *Nature* 555(7698):623–628
- Malik JK, Soni H, Singhai A (2013) QSAR-application in drug design. *Int J Pharm Res Allied Sci* 2(1):1–13
- Mamoshina P, Bueno-Orovio A, Rodriguez B (2020) Dual transcriptomic and molecular machine learning predicts all major clinical forms of drug cardiotoxicity. *Front Pharmacol* 11:639
- Marengoni A, Onder G (2015) Guidelines, polypharmacy, and drug-drug interactions in patients with multimorbidity. *BMJ Br Med J* 350:h1059
- Mata J et al (2018) Artificial intelligence (AI) methods in optical networks: a comprehensive survey. *Opt Switch Netw* 28:43–57
- Mayr LM, Bojanic D (2009) Novel trends in high-throughput screening. *Curr Opin Pharmacol* 9(5):580–588
- McCoubrey LE et al (2021) Machine learning uncovers adverse drug effects on intestinal bacteria. *Pharmaceutics* 13(7):1026
- Mehta N, Ozick L, Gbadehan E (2010) Drug-induced hepatotoxicity. *State Univ NY Med J* 7:51–57
- Meng X-Y et al (2011) Molecular docking: a powerful approach for structure-based drug discovery. *Curr Comput Aided Drug Des* 7(2):146–157
- Minns A, Hall M (1996) Artificial neural networks as rainfall-runoff models. *Hydrol Sci J* 41(3):399–417
- Miranker A, Karplus M (1991) Functionality maps of binding sites: a multiple copy simultaneous search method. *Proteins* 11(1):29–34
- Moaddel R et al (2007) Pharmacophore modelling of stereoselective binding to the human organic cation transporter (hOCT1). *Br J Pharmacol* 151(8):1305–1314
- Morris GM et al (1998) Automated docking using a Lamarckian genetic algorithm and an empirical binding free energy function. *J Comput Chem* 19(14):1639–1662
- Mozaffari A, Emami M, Fathi A (2019) A comprehensive investigation into the performance, robustness, scalability and convergence of chaos-enhanced evolutionary algorithms with boundary constraints. *Artif Intell Rev* 52(4):2319–2380
- Muderrisoglu AE et al (2019) Cognitive and mood side effects of lower urinary tract medication. *Expert Opin Drug Saf* 18(10):915–923
- Müller AC, Guido S (2016) Introduction to machine learning with Python: a guide for data scientists. O'Reilly Media, Inc., Sebastopol, CA
- Murphy KP (2012) Machine learning: a probabilistic perspective. MIT Press, Cambridge, MA
- Narkhede S (2018a) Understanding confusion matrix. <https://towardsdatascience.com/understanding-confusion-matrix-a9ad42dcfd62>
- Narkhede S (2018b) Understanding AUC–ROC curve. <https://towardsdatascience.com/understanding-auc-roc-curve-68b2303cc9c5>
- Neves BJ et al (2018) QSAR-based virtual screening: advances and applications in drug discovery. *Front Pharmacol* 9:1275
- Nigam SK (2015) What do drug transporters really do? *Nat Rev Drug Discov* 14(1):29–44
- Norel R et al (1994) Molecular surface recognition by a computer vision-based technique. *Protein Eng Des Sel* 7(1):39–46

- O'Hare T, Corbin AS, Druker BJ (2006) Targeted CML therapy: controlling drug resistance, seeking cure. *Curr Opin Genet Dev* 16(1):92–99
- OECD (1994) OECD Guidelines for the Testing of Chemicals. OECD, Paris
- OECD (2022a) Organisation for Economic Co-operation and Development. OECD iLibrary. <https://www.oecd-ilibrary.org/oecd/about>
- OECD (2022b) OECD Guidelines for the Testing of Chemicals. https://www.oecd-ilibrary.org/environment/oecd-guidelines-for-the-testing-of-chemicals_72d77764-en?_ga=2.96179612.1235017736.1627133985-2063296582.1616570860
- OECD (2022c) OECD Guidelines for the Testing of Chemicals, Section 1. https://www.oecd-ilibrary.org/environment/oecd-guidelines-for-the-testing-of-chemicals-section-1-physical-chemical-properties_20745753?page=1
- OECD (2022d) OECD Guidelines for the Testing of Chemicals, Section 2. https://www.oecd-ilibrary.org/environment/oecd-guidelines-for-the-testing-of-chemicals-section-2-effects-on-biotic-systems_20745761
- OECD (2022e) OECD Guidelines for the Testing of Chemicals, Section 3. https://www.oecd-ilibrary.org/environment/oecd-guidelines-for-the-testing-of-chemicals-section-3-degradation-and-accumulation_2074577x
- OECD (2022f) OECD Guidelines for the Testing of Chemicals, Section 4. https://www.oecd-ilibrary.org/environment/oecd-guidelines-for-the-testing-of-chemicals-section-4-health-effects_20745788
- OECD (2022g) OECD Guidelines for the Testing of Chemicals, Section 5. https://www.oecd-ilibrary.org/environment/oecd-guidelines-for-the-testing-of-chemicals-section-5-other-test-guidelines_20745796
- Ogura K et al (2019) Support Vector Machine model for hERG inhibitory activities based on the integrated hERG database using descriptor selection by NSGA-II. *Sci Rep* 9(1):12220
- Ojha Lokendra K, Rachana S, Rani BM (2013) Modern drug design with advancement in QSAR: a review. *Int J Res Biosci* 2:1–12
- Oliphant K, Allen-Vercoe E (2019) Macronutrient metabolism by the human gut microbiome: major fermentation by-products and their impact on host health. *Microbiome* 7(1):91
- Park K et al (2015) Predicting pharmacodynamic drug-drug interactions through signaling propagation interference on protein-protein interaction networks. *PLoS One* 10(10):e0140816
- Patel HM et al (2014) Quantitative structure-activity relationship (QSAR) studies as strategic approach in drug discovery. *Med Chem Res* 23(12):4991–5007
- Pedregosa F et al (2011) Scikit-learn: machine learning in Python. *J Mach Learning Res* 12:2825–2830
- Pérez Santín E et al (2021) Toxicity prediction based on artificial intelligence: a multidisciplinary overview. *Wiley Interdiscip Rev Comput Mol Sci* 11:e1516
- Pirmohamed M, L'E Orme M (1998) In drug interactions of clinical importance. In: Davies DM, Ferner RE, de Glanville H (eds) *Davies's textbook of adverse drug reactions*. Chapman & Hall, London
- Plewczynski D (2009) Brainstorming: consensus learning in practice. arXiv preprint arXiv:0910.0949
- Police A, Shankar VK, Murthy SN (2020) Role of taurine transporter in the retinal uptake of vigabatrin. *AAPS PharmSciTech* 21(5):1–9
- Pu L et al (2019) eToxPred: a machine learning-based approach to estimate the toxicity of drug candidates. *BMC Pharmacol Toxicol* 20(1):2
- Rahmanifard H, Plaksina T (2019) Application of artificial intelligence techniques in the petroleum industry: a review. *Artif Intell Rev* 52(4):2295–2318
- Raies AB, Bajic VB (2016) In silico toxicology: computational methods for the prediction of chemical toxicity. *Wiley Interdiscip Rev Comput Mol Sci* 6(2):147–172
- Rarey M et al (1996) A fast flexible docking method using an incremental construction algorithm. *J Mol Biol* 261(3):470–489

- Roy K (2017) Advances in QSAR modeling. In: Applications in pharmaceutical, chemical, food, agricultural and environmental sciences, vol 555. Springer, Cham, p 39
- Roy K, Kar S, Das RN (2015) Understanding the basics of QSAR for applications in pharmaceutical sciences and risk assessment. Academic Press, Amsterdam
- Russell SJ, Norvig P (2016) Artificial intelligence: a modern approach. Malaysia. Pearson Education Limited, London
- Ryu JY, Kim HU, Lee SY (2018) Deep learning improves prediction of drug–drug and drug–food interactions. *Proc Natl Acad Sci* 115(18):E4304–E4311
- Shahlaei M (2013) Descriptor selection methods in quantitative structure-activity relationship studies: a review study. *Chem Rev* 113(10):8093–8103
- Sokolova M, Japkowicz N, Szpakowicz S (2006) Beyond accuracy, F-score and ROC: a family of discriminant measures for performance evaluation. In: Australasian joint conference on artificial intelligence. Springer, Berlin
- Solimeo R et al (2012) Predicting chemical ocular toxicity using a combinatorial QSAR approach. *Chem Res Toxicol* 25(12):2763–2769
- Sridhar D, Fakhraei S, Getoor L (2016) A probabilistic approach for collective similarity-based drug–drug interaction prediction. *Bioinformatics* 32(20):3175–3182
- Stanton DT (2012) QSAR and QSPR model interpretation using partial least squares (PLS) analysis. *Curr Comput Aided Drug Des* 8(2):107–127
- Suez J et al (2014) Artificial sweeteners induce glucose intolerance by altering the gut microbiota. *Nature* 514(7521):181–186
- Sugai S et al (1991) Studies on eye irritation caused by chemicals in rabbits: II. Structure-activity relationships and in vitro approach to primary eye irritation of salicylates in rabbits. *J Toxicol Sci* 16(3):111–130
- Sukumar N, Prabhu G, Saha P (2014) Applications of genetic algorithms in QSAR/QSPR modelling. In: Applications of metaheuristics in process engineering. Springer, Cham, pp 315–324
- Tan K-H, Lim BP (2018) The artificial intelligence renaissance: deep learning and the road to human-level machine intelligence. *APSIPA Trans Signal Inf Proc* 7:e6
- Tao X et al (2020) Recent developments in molecular docking technology applied in food science: a review. *Int J Food Sci Technol* 55(1):33–45
- Taylor-Wells J, Meredith D (2014) The signature sequence region of the human drug transporter organic anion transporting polypeptide 1B1 is important for protein surface expression. *J Drug Deliv* 2014:129849
- Team TTD et al (2016) Theano: a Python framework for fast computation of mathematical expressions. *arXiv preprint arXiv:1605.02688*
- Tokar AS, Johnson PA (1999) Rainfall-runoff modelling using artificial neural networks. *J Hydrol Eng* 4(3):232–239
- Trisciuzzi D et al (2018) Molecular docking for predictive toxicology. *Methods Mol Biol* 1800: 181–197
- Vargas HM et al (2015) Evaluation of drug-induced QT interval prolongation in animal and human studies: a literature review of concordance. *Br J Pharmacol* 172(16):4002–4011
- Vayer P et al (2009) Chemoinformatics and virtual screening of molecules for therapeutic use. *Med Sci M/S* 25(10):871–877
- Vedani A, Dobler M, Lill MA (2006) The challenge of predicting drug toxicity in silico. *Basic Clin Pharmacol Toxicol* 99(3):195–208
- Venter JC et al (2001) The sequence of the human genome. *Science* 291(5507):1304–1351
- Verma RP, Matthews EJ (2015) Estimation of the chemical-induced eye injury using a Weight-of-Evidence (WoE) battery of 21 artificial neural network (ANN) c-QSAR models (QSAR-21): Part II: corrosion potential. *Regul Toxicol Pharmacol* 71(2):331–336
- Verma J, Khedkar VM, Coutinho EC (2010) 3D-QSAR in drug design—a review. *Curr Top Med Chem* 10(1):95–115

- Vilar S et al (2013) Detection of drug-drug interactions by modeling interaction profile fingerprints. *PLoS One* 8(3):e58321
- Vilar S et al (2014) Similarity-based modeling in large-scale prediction of drug-drug interactions. *Nat Protoc* 9(9):2147–2163
- Vinardell Martínez-Hidalgo MP (2007) Alternativas a la experimentación animal en toxicología: situación actual. *Acta Bioethica* 13(1):41–52
- Wang S et al (2016) ADMET evaluation in drug discovery. 16. Predicting hERG blockers by combining multiple pharmacophores and machine learning approaches. *Mol Pharm* 13(8): 2855–2866
- Wang D, He H, Liu D (2017a) Intelligent optimal control with critic learning for a nonlinear overhead crane system. *IEEE Trans Ind Inform* 14(7):2932–2940
- Wang D, He H, Liu D (2017b) Adaptive critic nonlinear robust control: a survey. *IEEE Trans Cybernet* 47(10):3429–3451
- Wang Q et al (2017c) In silico prediction of serious eye irritation or corrosion potential of chemicals. *RSC Adv* 7(11):6697–6703
- Wang Z et al (2019) Various frameworks and libraries of machine learning and deep learning: a survey. *Arch Comput Methods Eng*:1–24. <https://doi.org/10.1007/s11831-018-09312-w>
- Weil CS, Scala RA (1971) Study of intra- and interlaboratory variability in the results of rabbit eye and skin irritation tests. *Toxicol Appl Pharmacol* 19(2):276–360
- Wexler P et al (2005) *Encyclopedia of toxicology*, vol 1. Academic Press, San Diego
- Wu Y, Wang G (2018) Machine learning based toxicity prediction: from chemical structural description to transcriptome analysis. *Int J Mol Sci* 19(8):2358
- Wu Z et al (2018) Network-based methods for prediction of drug-target interactions. *Front Pharmacol* 9:1134
- Xiang K et al (2016) Regularized Taylor echo state networks for predictive control of partially observed systems. *IEEE Access* 4:3300–3309
- Xing FZ, Cambria E, Welsch RE (2018) Natural language-based financial forecasting: a survey. *Artif Intell Rev* 50(1):49–73
- Xu Y et al (2015) Deep learning for drug-induced liver injury. *J Chem Inf Model* 55(10):2085–2093
- Yan C, Zou X (2017) Modeling protein flexibility in molecular docking
- Yan Y et al (2017) HDOCK: a web server for protein–protein and protein–DNA/RNA docking based on a hybrid strategy. *Nucleic Acids Res* 45(W1):W365–W373
- Zhou X et al (2017) Application of deep learning in object detection. In: 2017 IEEE/ACIS 16th International conference on computer and information science (ICIS). IEEE, Piscataway, NJ



Chemicals and Rodent Models for the Safety Study of Alzheimer's Disease **23**

Nimmi Varghese and Viji Vijayan

Animals have been used as model systems for research for a very long time. The use of animal model systems, particularly for research, dates to the era BC and references to the same can be found in the writings of many great thinkers and philosophers like Aristotle, Diocles, Praxagoras, and Herophilus (Ericsson et al. 2013). If one looks at research publications, the first publication about an experiment conducted on a mouse was published in 1902. It is very interesting to note that around 180 Nobel Prizes awarded to scientists in the category of Physiology and Medicine have employed rodent models for their research to capture a better understanding of nerve and epidermal growth factors, cell cycle checkpoint inhibitors, and innate immunity. The complete worthwhile history of the prolonged use of rodents for the safety evaluation of chemicals is beyond the scope of this chapter, but we will emphasize here how rodents especially mouse and rats have been employed as animal model systems for certain neurodegenerative disorders like Alzheimer's disease and how such models are created with gene manipulation, dietary components, and chemicals and used for screening other chemicals, compounds, and lead compounds for the disorder. But before we move onto those research aspects, the authors declare that although testing of drugs on rodents generates important data that will be useful in treating diseases in humans, we underscore the fact that animal experiments must be replaced wherever possible by other in vitro biological systems such as cell culture and methods such as mathematical modeling (Tannenbaum 1999). Therefore, an investigator who aspires to conduct an experiment on a rodent model system should refine the experiment and reduce the number of animals used or optimize the sample size just to obtain reliable data. To a large

N. Varghese · V. Vijayan (✉)

Neurobiology Lab, Department of Biochemistry, University of Kerala, Thiruvananthapuram, Kerala, India

e-mail: vijivijayan@keralauniversity.ac.in

© The Author(s), under exclusive license to Springer Nature Singapore Pte Ltd. 2023

P. V. Mohanan, S. Kappalli (eds.), *Biomedical Applications and Toxicity of Nanomaterials*, https://doi.org/10.1007/978-981-19-7834-0_23

637

extent, this can be done by performing a literature survey so that duplication of experiments can be avoided.

23.1 The Mouse as an Animal Model System

An animal model is a non-human species used in biomedical research because of its ability to mimic certain aspects of a disease found in humans. Animals as model systems provide the necessary information about an aspect of a disease enabling prevention of disease and therapeutic options for both animals and humans. More importantly, an animal model system enables researchers to carry out experiments that are ethically forbidden in human beings. Considering the many animals that have been used as models in research like guinea pigs, rabbits, monkeys, dogs, gerbils, hamsters, and rats, the mouse remains a convenient animal model system for researchers. The mouse or *Mus musculus* has had a long and matchless history as model system for research experiments. With the advent of the first inbred strain of mouse lines, there has been a significant rise in the breeding of these animals for research. This interest after that led to the development of genetically engineered models which were used for high throughput screening of drugs (Giacomotto and Segalat 2010).

A mouse is a feasible animal model for biomedical research studies for many reasons. The foremost reason is because of their similarities with humans in terms of anatomy and physiology. Mice and humans each have a genetic similarity. Mice also have economic advantages as these require comparatively lesser space. These animals develop into adults faster and have short gestation periods of 19–21 days, delivering a higher number of offspring and attaining sexual maturity by 5–6 weeks of age. With these advantages, mice are largely used by researchers to evaluate toxicity induced by a drug, determine the effectiveness of a drug, and design safer dosage schemes for humans in clinical trials. In understanding certain rare diseases where the patient numbers are lower, mouse model systems, despite not being a complete one, have enabled researchers to obtain functional information about the disease, comprehend the basis of rare diseases, and also develop therapeutic strategies for rare diseases. The laboratory mouse thus has made invaluable contributions to cardiovascular medicine, neural regeneration, wound healing, diabetes, transplantation, behavioral studies, and space motion sickness research. In this chapter, we look into how rodents and especially mice have enabled a greater understanding of Alzheimer's disease biology.

23.2 Mouse as an Animal Model System for Alzheimer's Disease (AD) Research

AD is a progressive neurodegenerative disorder and is a common form of dementia that affects adults. Clinically this disorder is characterized by extracellular beta-amyloid plaques and intracellular neurofibrillary tangles in specific regions of the

brain like the hippocampus and cerebral cortices, causing neuronal and synaptic loss, the main reason for loss of memory and development of confusion in AD patients (Alzheimer Association Report 2018). The etiology of AD is not completely known, so there is no cure for AD, just symptomatic relief. Here, the animal model system represents a beacon of hope for researchers and clinicians for deciphering the pathophysiology of AD. What is known is that the changes in the brain can develop many years before AD is manifested; what remains unknown are the underlying factors. The animal model can help a researcher comprehend the presymptomatic stage of AD so that therapeutic interventions can be designed accordingly.

23.2.1 The Amyloid Hypothesis

Although there are controversies today, the amyloid hypothesis is an important model system which researchers still believe. According to this hypothesis, the presence of plaque deposits in certain areas of the brain is the main feature of AD.

A description of the biochemistry of amyloid plaques is recorded by Blocq and Marnesco in the year 1892. These researchers described plaques as senile plaques, which are densely packed structures called “amyloid bodies.” The higher order fibrillar forms of amyloid-beta proteins are smooth and straight in appearance and about 10 nm in diameter. The monomeric forms of these structures were identified to be a 4 kDa protein called amyloid-beta.

Amyloid beta is, in fact, a “processed product” of a larger protein called APP or amyloid precursor protein (APP751 and APP770). It is believed that abnormal processing of APP is the reason for the formation of a form called amyloid beta42. This erroneously produced peptide of 42 amino acids has a greater tendency to misfold and aggregate oligomers and fibrils. Amyloid beta protein also exists in various isoforms, ranging between 39 and 43 amino acids (Hardy and Selkoe 2002; Skovronsky et al. 2006), predominant isoforms include amyloid-beta 40 and amyloid beta42. It is believed that the oligomeric forms of Abeta42 are toxic and cause extensive damage to the neurons (Kayed et al. 2003) (Fig. 23.1).

23.2.2 The Tau Hypothesis

According to the tau hypothesis, AD is a tauopathy characterized by abnormal hyperphosphorylation of a protein called tau, which eventually leads to the formation of neurofibrillary tangles. Tau has physiological relevance. Under normal conditions, tau is monomeric and unfolded cell membrane protein which acts as a scaffold for stabilizing microtubules and thereby aiding in the physiological function of a neuron (Duan et al. 2017). Under the influence of certain factors, tau undergoes posttranslational modification, viz., “hyperphosphorylation,” which influences the microtubule-stabilizing function of tau. Tau with the conformational changes imparted in it oligomerizes leading to the formation of paired helical filaments and neurofibrillary tangle formation (Chirita et al. 2005; Sahara et al. 2007;

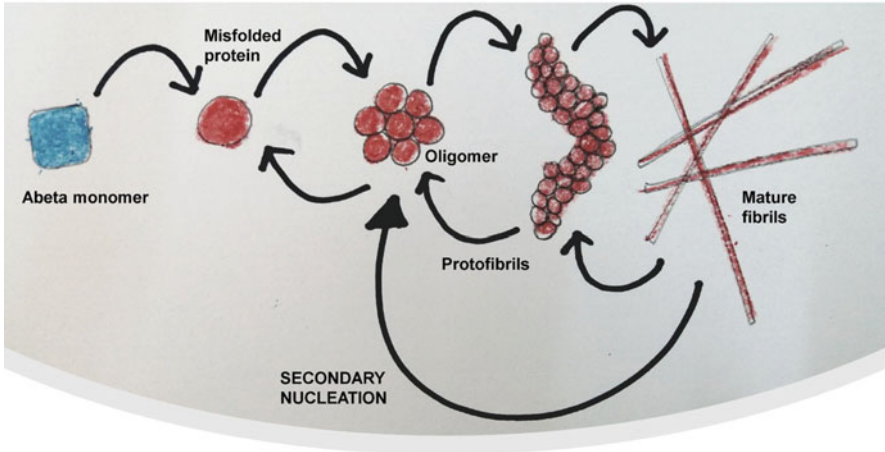


Fig. 23.1 Aggregation of Abeta. Misfolding of Abeta42 causes the peptide to oligomerize (toxic species) and thereafter aggregate to form protofibrils and higher order structures called fibrils

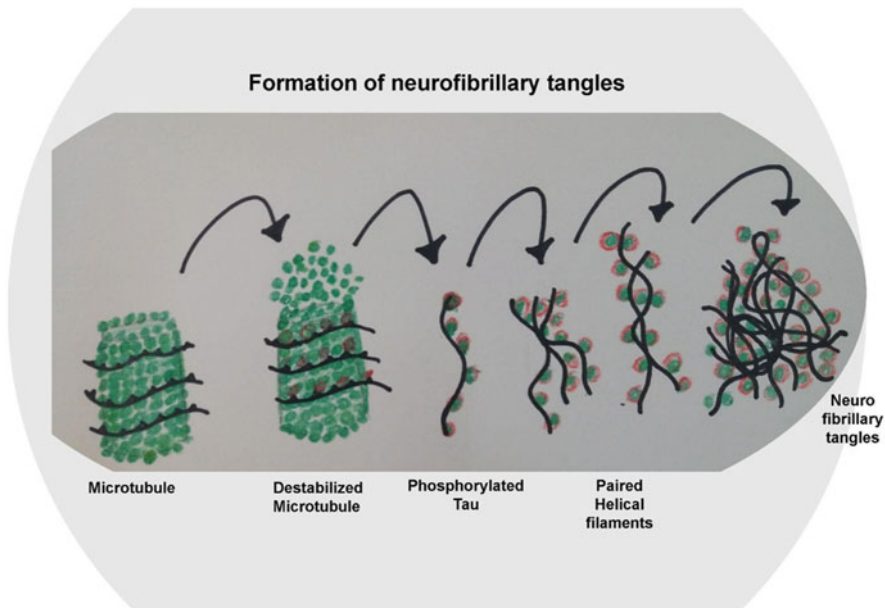


Fig. 23.2 Tau hypothesis. Hyperphosphorylation of tau and formation of paired helical filaments leading to the formation of neurofibrillary tangles

Mondragón-Rodríguez et al. 2008; Lasagna-Reeves et al. 2010; Patterson et al. 2011). The oligomeric forms are regarded as the toxic species that lead to neuronal

death and synaptic destruction (Guerrero-Muñoz et al. 2015; FÁ et al. 2016) (Fig. 23.2).

23.2.3 Cholinergic Hypothesis

This is one of the oldest hypotheses known to describe the factors that cause AD (Francis et al. 1999). It states that decreased production of neurotransmitters by neurons causes AD. Neurotransmitters like acetylcholine are required for the execution of numerous physiological activities like attention, learning, memory, stress response, wakefulness, and sleep, as well as sensory information, and the absence of these may cause AD (Hasselmo et al. 1992; Fine et al. 1997; Sarter and Bruno 1997; Miranda and Bermúdez-Rattoni 1999; Haam and Yakel 2017). The cholinergic hypothesis has been tested by researchers employing cholinesterase inhibitors which were then identified to be of use for AD treatment. Many inhibitors such as donepezil, galantamine, rivastigmine, and memantine have reached the market after numerous preclinical and clinical trials as a result of animal experiments (Brinkman and Gershon 1983; Summers et al. 1981) some of these have been withdrawn owing to side-effects (Fig. 23.3).

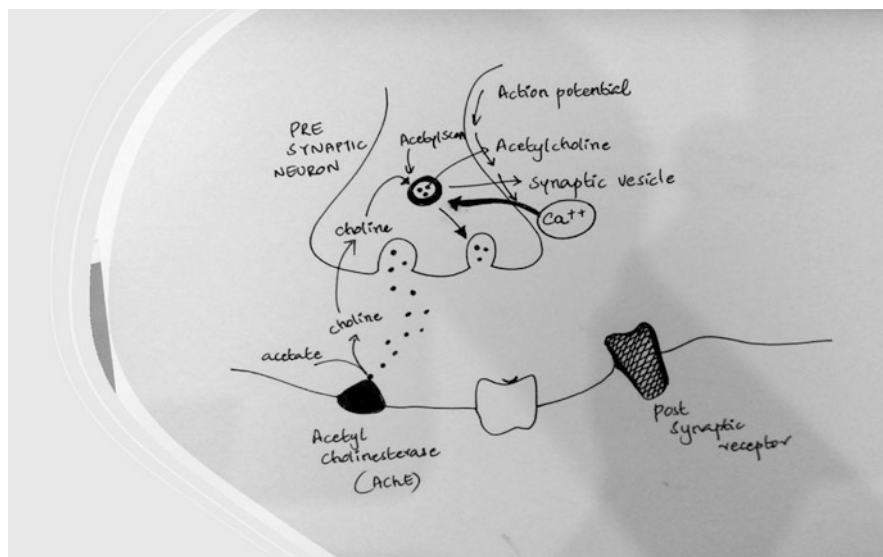


Fig. 23.3 Acetylcholine release and cholinergic hypothesis

23.3 Commonly Used Mouse Model Systems to Study AD

Many experimental studies on AD are currently conducted mostly on transgenic mouse model systems and chemically induced mouse model systems.

23.3.1 Transgenic Mouse Models of AD

Transgenic mouse model systems are genetically engineered mice with their genomes altered using genetic engineering techniques. Since AD is associated with misfolding of certain proteins like amyloid beta42 and tau (which later develops into higher order structures called amyloid plaques and neurofibrillary tangles, respectively), researchers have used mouse which harbors mutant genes like APP (amyloid precursor protein), beta and gamma-secretase, PS1, PS2, tau, ApoE, endothelial nitric oxide synthase-3, and alpha-macroglobulin (Chartier-Harlin et al. 1991; Rogaev et al. 1995; Levy-Lahad et al. 1995a, b; Goedert and Spillantini 2000; Neha et al. 2014; Liao et al. 1998; Dahiya et al. 1999). The widely used transgenic AD system is the mouse with mutant human APP gene or the TgAPP_{Swe} mice. The APP gene encodes a protein called amyloid precursor protein expressed in many tissues, including the brain and spinal cord. Mutation in APP shows the intracellular accumulation of Abeta and cognitive deficits without any plaque deposition. The model suggests that cognitive deficit in AD is not entirely dependent on plaque deposition, which is true because humans who had plaque deposition in the brain did not suffer AD, as evident from their postmortem samples. With an additional mutant, e.g., the Presenilin gene, TgAPP_{Swe} mice have been found to demonstrate abundant plaque deposition in significant regions of the brain like the neocortex, olfactory bulb, thalamus, and hypothalamus associated with glial activation (Braidy et al. 2012). Some of the other transgenic mouse models which are actively used by researchers include

1. PDAPP with human APP695 (Ind) and PDGF promoter shows the development of amyloid plaque deposits at 6–9 months of age but no neurofibrillary tangles and cognitive deficit at 6 months.
2. Tg2576 mice harbors human APP965 (Swe) and HamPrP promoter and shows extensive plaque deposition at 8 months and no neurofibrillary tangles.
3. APP23 with human APP751 (Swe) transgene and Thy-1 promoter shows an additional feature of vascular deposition of Abeta with Abeta42 deposition at 6 months and no neurofibrillary tangles (Games et al. 1995).

All these mouse models are in favor of the “amyloid cascade hypothesis,” which postulates that neurodegeneration in AD is caused by amyloid-beta accumulation in the brain and provides a platform for testing Abeta modifying compounds. A disadvantage of these models is that these mice do not showcase tau, another hallmark of AD, and it is now believed that multiple genes are involved in the development of AD. For this reason, researchers also worked with transgenic mice

that express human tau using various promoters. Since tau existed in several isoforms, different animal models had to be created to understand the pathophysiology of tau. The PrP-Tau mouse transgenic model with human Tau (P301L) transgenes and murine PrP promoter demonstrates tau expression in the brain at 6 months of age and display both behavioral and motor deficits (James et al. 1996; Allen et al. 2002; Forman et al. 2005; Higuchi et al. 2005; Ribé et al. 2005; Götz et al. 2001). In the GFAP-Tau model, a human Tau (P301L) with GFAP promoter is used that induces tau pathology in astrocytes with other traits like blood-brain barrier disruption and motor deficits (Forman et al. 2005). In the Thy-Tau22 mouse model that expresses 4-repeat human tau mutated at two sites of G272V and P301S and Thy1.2 promoter presence of neurofibrillary tangles in the hippocampus is seen alongside spatial memory loss, anxiety, and delayed learning but without motor deficits (Schindowski et al. 2006). All these models show tau aggregation and neuronal degeneration and mimic an important aspect of AD and are therefore a significant contribution to understanding the hyperphosphorylation of tau and tau aggregation, two important pathologies of AD.

To further understand whether the two important hallmarks of AD, viz., amyloid plaques and neurofibrillary tangles interact with each other, researchers put forth the APP-Tau double transgenic mice by crossing APP Tg2576 transgenic mice with VLW lines expressing human mutant tau, which demonstrate increased amyloid deposition and excessive neurofibrillary tangle formation in olfactory bulb and amygdala as compared to the tau transgenic mice alone (Götz et al. 2001; Lewis et al. 2001; Ribé et al. 2005). These results underpin the fact that the Abeta deposits promote NFT formation in AD. In the Thy1.2 promoter-driven P301L mice injected with A β 42 mice, a fivefold rise in neurofibrillary tangles at 18 days after the injection of Abeta into the amygdala (Götz et al. 2001). Both these model systems have helped researchers to a large extent to understand that Abeta interaction with tau is an important pathophysiology of AD and is an important target for AD therapy.

Researchers at the University of California worked on a triple-transgenic model (3xTg) AD mouse model harboring PS1(M146V), APP(Swe), and tau (P301L) transgenes to study the interaction between Abeta and tau and its effect on synaptic function. These mice were generated by microinjecting two transgenes into single-cell embryos from homozygous PS1(M146V) knockin mice to produce mice with the same genetic background. These mutant mice display a progressive development of amyloid plaques and neurofibrillary tangles and also showed synaptic dysfunction before the development of plaque and tangle pathology. Hence, drugs to evaluate potential anti-AD lead compounds against both plaque and tangle can be assessed using this model (Oddo et al. 2003).

To increase the formation of Abeta levels and plaque formation at a faster pace, researchers developed a model called the 5xFAD transgenic model that co-expressed 5 FAD mutant genes to bring about excessive Abeta, specifically the Abeta42 as compared to Abeta40 at the second month of age. The animal model demonstrated that FAD mutations, when present together, can produce an additive effect. Researchers also observed intraneuronal accumulation of Abeta42 within the neuronal soma and neurites at just 1.5 months of age, demonstrating that intracellular

deposition of A β is involved in neuronal health issues and degeneration. Other traits included high gliosis, reduced synaptic markers, and significant cognitive impairment without abnormal tau hyperphosphorylation. These results however are not in total favor of the amyloid hypothesis, warranting the need to look into the actual basis of AD initiation. A drawback of this model is that such a case of 5 familial mutations has not been reported in humans (Braidy et al. 2012).

When researchers and clinicians understood that the cause of AD is multifactorial, they started investigating pathophysiological problems in the body that may lead to AD. Many risk factors were identified, and a predominant one was seen to be diabetes. Both AD and diabetes share common features like brain atrophy, impaired insulin signaling, and increased tendency to develop metabolic disorders. In 2013, researchers at the University of Michigan showed that hyperglycemia or high sugar levels in the blood can induce tau modification during diabetes. This led to speculation about whether tau cleavage during diabetes and especially type 2 diabetes can increase the incidence of AD in diabetic patients (Kim et al. 2013). A β and hyperphosphorylated tau have been shown to induce dysfunction of pancreatic beta cells, reducing insulin sensitivity and glucose uptake by peripheral tissues like liver, skeletal muscle, and adipose tissue (Miklossy et al. 2010).

In this regard, many experiments were also carried out in a genetically diabetic db/db mouse model typically used to study type 2 diabetes and an associated disorder, viz., obesity. Here the diabetic obese db/db mouse carries a mutation in the leptin receptor gene and demonstrates many traits like obesity, chronic hyperglycemia, pancreatic beta-cell atrophy, and hypoinsulinemia. In the brain and specifically, the cortex and hippocampus region of db/db mice, increased cleavage of tau was seen as early as 8 weeks of age, implying that these models of a particular age group can be used to identify compounds to test compounds that inhibit tau dysregulation (Kim et al. 2009).

Apart from the transgenic mouse model systems, there are also some non-transgenic mouse model systems of diabetes that have been employed for studying AD. A time-consuming yet interesting mouse model is the high-fat diet-induced diabetic mice which demonstrate high cholesterol levels in both serum and brain. For the development of this diabetic mouse model, mice are fed a high-fat diet. The animals show the presence of amyloid-beta plaque deposits in the brain, and cognitive deficits but no signs of neurofibrillary tangles (Herculano et al. 2013). This model however can be used to investigate the modulatory role of dietary compounds in AD pathophysiology.

So far, we have discussed some of the transgenic and natural model systems that can be used to test compounds to develop a therapeutic modality for AD. Since no exact cause has been identified and multiple factors play a role in the development of AD, researchers have employed certain models to study the changes in neurotransmitter synthesis in AD pathophysiology. These models support the cholinergic hypothesis of AD which states that dysfunction of acetylcholine-containing neurons in the brain (an age-related issue) causes cognitive decline. To understand more about this hypothesis, mice are injected with chemical substances into specific regions of the body to create traits of AD. Important compounds used for this

purpose included Abeta, scopolamine, okadaic acid, sodium azide, L-methionine, heavy metals, and streptozotocin. Most of these substances induce dementia in mice by inhibiting neurotransmitter pathways. So conducting experiments in such animal models provides a unique way to study the effects of damage caused to specific neurotransmitter pathways as well as evaluate crucial lead compounds targeted at these pathways.

A very interesting study in this regard is that of Jean et al. reported in the Journal of Visualized Experiments (JoVE) in the year 2015. This method involves directly injecting certain forms of amyloid beta that are most toxic to neurons. The injection into certain areas of the brain is performed using an instrument called stereotaxy. This is generally a minimally invasive form of surgical intervention that employs a stereotactic planning system, including atlas, multimodality image matching tools, and coordinates system (to locate targets in brains and other organs) to perform various actions like injection, stimulation, ablation, biopsy, etc. It was found that injection of oligomeric forms of amyloid-beta (which are considered very toxic) into the dentate gyrus of the hippocampus demonstrated a significant amount of neuronal loss, increased cell death, and death of cholinergic neurons, showcasing this model of AD with a window period to test compounds for neuroprotection (Jean et al. 2015).

23.3.2 Chemical-Induced Models for Studying AD

Several chemicals have been employed to understand the etiology of AD and screen therapeutic agents for treating AD. Although many chemical-induced sporadic models like scopolamine, lipopolysaccharide (LPS), Abeta, sodium azide, etc., have some positive traits linked with AD and induce cognitive impairment in rodent models, there is no single model that retells the exact pathophysiology of AD. At the same time, each of these chemicals that induces signs of AD has been found to have its unique mechanism of action. The dosage of the chemical used for the development of each model is also different, and so is the time of action of these chemicals on the brain of the rodent model. A greater understanding of the events that happen in the biological system with the entry of these chemicals is very critical to achieving a better understanding of a complex disorder such as AD. Some of the chemicals that have been employed by researchers to study the pathophysiology of AD are detailed below:

23.3.2.1 Streptozotocin and AD Development

Streptozotocin (STZ), a chemical derived from glucosamine nitrosourea and seen in the strain of *Streptomyces achromogenes*, is a naturally occurring alkylating agent used in cancer treatment. Streptozotocin also possesses hypoglycemic effects. However, streptozotocin is highly toxic to beta cells of the pancreas in mammals and is therefore commonly used to create a type 1 diabetes system in rodents. Experimental studies have shown that when streptozotocin is administered ICV in rodents, a severe change in the brain's architecture and metabolism is noted like decreased

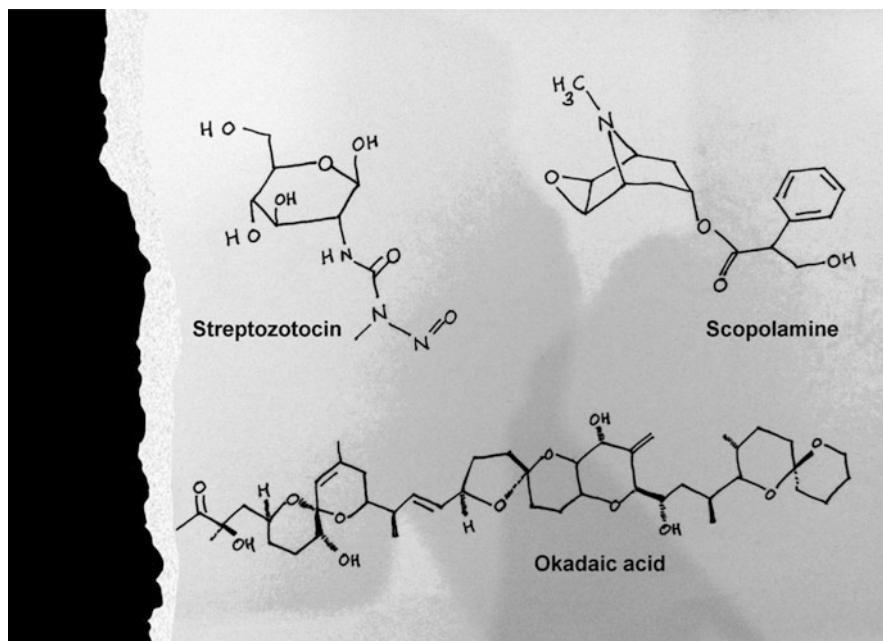


Fig. 23.4 Structure of streptozotocin, scopolamine, and okadaic acid

glucose uptake, reduced glycolysis and energy production, oxidative tissue stress, cholinergic differential, and cognitive abilities (Klinkenberg and Blokland 2010; Zhou et al. 2013; Neha et al. 2014) (Fig. 23.4).

A major reason identified for the reduced neuronal conductance with streptozotocin injection is the reduced acetyl CoA synthesis (Zhou et al. 2013). Other biochemical changes induced by streptozotocin include induction of neuronal damage and hyperphosphorylation of tau causing the release of reactive oxygen species (ROS) and reactive nitrogen species (RNS). Streptozotocin has also been shown to modify GSK alpha/beta, an enzyme involved in regulating amyloid-beta peptides in the brain and thereby activating the formation of Abeta aggregates (Yang et al. 2013). These features make streptozotocin-ICV an apt model to study sporadic AD. In 2012, a research group introduced streptozotocin into the mouse brain and evaluated the expression of amyloid-beta, choline acetyltransferase (ChAT), synapsin, axonal neurofilaments, and phosphorylated tau in the hippocampus region of the brain. These researchers, after introducing streptozotocin into the brain, found that within 2 weeks after injection of the chemical, AD markers studies were altered, most of these features were transient and did not last beyond 21 days of injection. Both short-term and long-term memory deficits were also seen on days 14 and 31 of streptozotocin injection (Ravelli et al. 2017). In a similar model used by Unsal et al. (2016), a synthetic drug molecule called Ebselen (which possesses antioxidant and anti-inflammatory activity) was found to markedly reduce the neuronal toxicity

induced by intracerebroventricular injection of streptozotocin (ICV-streptozotocin) at a dose of 3 mg per kg body weight. The authors showed that ebselen significantly reduced the streptozotocin-induced histopathological changes in frontal cortex tissue, which indicated how potential lead drug compounds like ebselen can be tested to determine therapeutic value for the treatment of AD.

23.3.2.2 Scopolamine and AD Development

Another very important chemical that is widely used by researchers to understand the pathophysiology of spontaneous AD is scopolamine. Scopolamine or hyoscyne is a natural or synthetically produced tropane alkaloid. Clinically scopolamine is used as an anticholinergic drug to treat motion sickness and postoperative nausea, vomiting, and sometimes memory deficits (Bubser et al. 2012). On the experimental side, researchers have identified that scopolamine nonselectively obstructs the adhesion site of acetylcholine muscarinic receptors in the cerebral cortex in a dose-related manner and reduces the synthesis of acetylcholine to induce learning and memory impairment in rodent model systems (Riedel et al. 2009; Pattipati and Singh 2016). Other studies have reported that scopolamine administration to the hippocampus inhibits long-term potentiation and interferes with spatial encoding (Blokland et al. 1992; Portero-Tresserra et al. 2014). When injected into the medial septum, scopolamine interferes with learning and decreases acetylcholine discharge into the hippocampus (Elvander et al. 2004). Very recent studies have shown that scopolamine promotes postoperative delirium. After surgery, mice injected with intraperitoneal scopolamine (2 mg/kg) showed significant changes in cognitive functions, learning and memory, and higher levels of anxiety alongside high pro-inflammatory cytokines and inflammasome components. These authors concluded that neuropsychiatric changes occur simultaneously with the neuroinflammatory response for the pathogenesis of delirium, a confused state seen in AD (Cheon et al. 2021).

23.3.2.3 Colchicine and AD Model

Biologists use colchicine to inhibit microtubule polymerization and assembly of the mitotic spindle and thus study cell cycle checkpoints. Colchicine is an alkaloid derived from the autumn crocus (*Colchicum autumnale*). Clinically colchicine is used to treat cancer in humans, it is commonly used to treat acute attacks of gout. However, the result of central colchicine administration is a state of progressive deterioration of learning and memory owing to neurotoxicity. Studies have shown that colchicine can induce hippocampal lesions and reduce the number of cholinergic neurons and decrease cholinergic renewal in the hippocampus (Evrard et al. 1998; Ganguly and Guha 2008). Colchicine can induce dementia by inhibiting cholinergic neurons. Cognitive impairment primarily arises due to decreased serotonin, dopamine, and norepinephrine within the caudate nucleus, hippocampus, and entire cerebral cortex. Colchicine has also been reported to increase the ratio of glutamate/GABA in the cortex and induce excitation of NMDA receptors which increases calcium influx and induces the expression of calcium-dependent enzymes like phospholipases A2, xanthine oxidase, proteases, cyclooxygenases, and protein kinases (Yu et al. 1997; Sharma and Singh 2010). Intracerebroventricular (ICV)

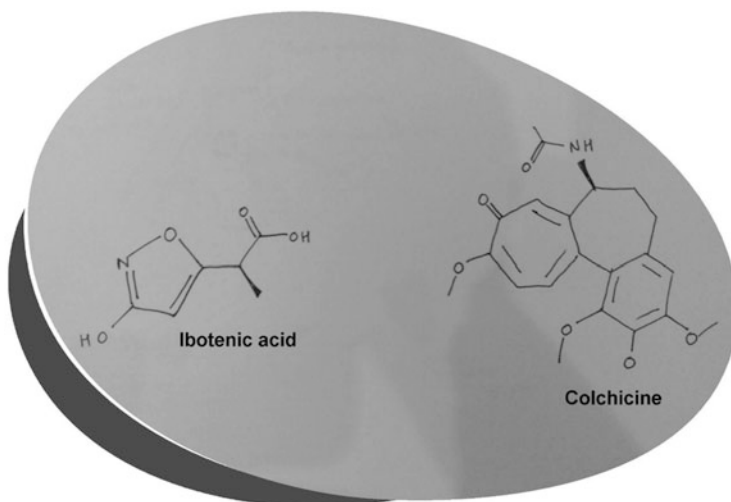


Fig. 23.5 Structure of ibotenic acid and colchicine

injections of colchicine at a dose of 3 g/mice produce spatial memory impairment (Tota et al. 2012). Colchicine-induced AD model system is therefore one of the important animal models to study sporadic AD (Fig. 23.5).

23.3.2.4 Okadaic Acid and AD Development

Okadaic acid is a potent polycyclic ether and a potent neurotoxin produced by the black dinoflagellate sponges. Molecular biologists employ okadaic acid as a chemical inhibitor to inhibit the expression of protein phosphatase 2A in cells. Experimental research has shown that okadaic acid triggers the production of reactive oxygen species in the hippocampus and produces mitochondrial abnormalities in the brain of rodents (Kamat et al. 2011). Infusion of okadaic acid into the hippocampus induces the expression of a glial marker glial fibrillary acidic protein, decreases the level of glutathione, and increases the level of oxidative stress (Costa et al. 2012). Okadaic acid-mediated memory decline in the rodent model system is also associated with uncontrolled pro-inflammatory cytokine and enzyme production in the hippocampus and cortex (Kamat et al. 2012). Researchers from the University of Queensland, Australia, injected 100 μM concentration of okadaic acid into the amygdala of mice and found that this chemical induces tau phosphorylation at the injected sites. Insoluble tau was found to increase in injected brains as early as day 7, indicating that tau phosphorylation is a primary response to an insult (Baker and Gotz 2016). The okadaic acid-induced mouse model system can therefore be used to study an important trait of AD such as tau phosphorylation and also evaluate lead compounds that can inhibit tau phosphorylation.

23.3.2.5 Sodium Azide-Induced AD Model

Sodium azide is a chemical inhibitor known to inhibit oxidative phosphorylation in the mitochondrial electron transport chain by inhibition of the final enzyme cytochrome oxidase in the respiratory chain. This results in rapid depletion of intracellular ATP. Such cytochrome oxidase inhibitors are also employed to create AD models. This is with regard to a hypothesis put forward by Swerdlow (2014), which states that defective mitochondrial enzymes cause AD development. As of now, it is understood that deficits in cytochrome oxidase cause AD (Gibson et al. 2009). Studies have shown that an altered structure of the cytochrome oxidase enzyme itself can cause AD (Parker and Parks 1995). Researchers have shown that selective cytochrome C complex inhibition using an intraperitoneal injection of sodium azide (6 or 12 mg/kg) into rodents slows their response to behavioral tests like the T maze test, water maze, and visual discrimination learning tasks as compared to their controls. Additionally, sodium azide administration causes oxidative damage and progressive loss of neurons in the cortical and hippocampal areas of the brain (Parker and Parks 1995).

23.3.2.6 Heavy Metal-Induced AD-Like Model

There are many environmental factors that are suspected to cause AD. An important environmental hazard is heavy metals which are known to induce neurotoxicity (100). Among the many heavy metals, aluminum, an industrial toxicant, is always suspected to cause toxicity to the biological systems like anemia, bone disorders, liver disorders, and brain disorders (Mujika et al. 2014; Nallagouni and Reddy 2017; Chiroma et al. 2018). Oral administration of aluminum at a dose of 300 mg/kg body weight induces oxidative stress, cholinergic deficit, cerebral gliosis, and accumulation of amyloid-beta and neurofibrillary tangles in the brain of rodents (Nallagouni and Reddy 2017). Chronic exposure to aluminum, i.e., for a year in the form of aluminum sulfate in drinking water of mice, has shown that this heavy metal can induce deposition of A β . Aluminum administration also reduces neuronal expression of GRP78 (a molecular chaperone located in the endoplasmic reticulum and involved in the assembly of proteins). These results indicate that aluminum can interfere with the functions of the endoplasmic reticulum in the brain, causing proteins to accumulate and deposit in the brain (Rodella et al. 2008).

23.3.2.7 Alcohol-Induced AD-Like Model

Dietary factors like alcohol have always been regarded as a contributory factor for the development of AD as it has been reported to induce many issues in humans like hyperactivity, learning and attention deficits, oxidative stress, language impairment, and motor dysfunction (Spinetta et al. 2008; Patil et al. 2015). Ethanol administration to the rodent model system has been found to induce damage in the hippocampus region of the brain and affect cholinergic neurons (Mailliard and Diamond 2004). Ethanol also induces an inflammatory response leading to the production of nitric oxide, another contributor to the impairment of learning and memory (Mailliard and Diamond 2004). Researchers have also identified that ethanol can increase adenosine that leads to memory impairment (Cui et al. 2015). In a transgenic mouse model

expressing APP, ethanol administration for 4 weeks increased the expression of APP and beta-site APP cleaving enzyme called BACE1 and elicited the production of amyloid-beta. The mice also showed increased deposition of amyloid-beta and plaque development alongside learning and memory impairments. Ethanol therefore exacerbated the AD phenotype in the APP transgenic mouse model system (Huang et al. 2018). Researchers investigated the effect of alcohol in the 3x transgenic mouse (3xTg) model system expressing human MAPT, APP, and PSEN-1 transgenes and identified that alcohol induces expression of phospho-tau in the hippocampus and inhibits Akt/mTOR signaling in the brain (Hoffman et al. 2019). These studies conducted on transgenic mouse model systems indicate that alcohol can increase the magnitude of AD-like pathology.

23.3.2.8 Ibotenic Acid-Induced AD Model System

Ibotenic acid (*S*)-2-amino-2-(3-hydroxyisoxazol-5-yl) acetic acid or ibotenate is a psychoactive drug from *Amanita muscaria* mushrooms. This chemical has structural similarity to glutamate, a neurotransmitter and therefore acts as an agonist for the glutamate receptor. This also makes ibotenic acid a potent neurotoxin capable of making lesions in the brains of animal model systems (Clark et al. 2012; Karthick et al. 2016). Experimental studies have shown that intrahippocampal administration of ibotenic acid (5 µg/µL PBS) induces memory impairment, increased acetylcholinesterase activity and malondialdehyde levels, and induces neuronal toxicity (Rattan and Tejwani 1992). In another study, ibotenic acid dissolved in phosphate buffered saline (PBS; pH 7.2) at a concentration of 5 µg/1 µL and infused into the hippocampus in a volume of 1.0 µL at a rate of 0.1 µL/min showed reduced hippocampal mRNA expression of acetylcholine receptors (alpha7-nAChR). Such events can happen with extended activation of glutamate receptors like *N*-methyl-D-aspartate receptor (NMDA) that triggers an increase in calcium influx (Karthick et al. 2016). Histological analysis of the brains of ibotenic acid-treated animals indicates a significant reduction in hippocampal pyramidal layer thickness and neurons. This model system has been used by researchers to identify whether plant polyphenols like resveratrol have any beneficial effect on reducing the deleterious effects of AD.

23.3.2.9 LPS-Induced AD Model System

Lipopolysaccharides or LPS are endotoxins consisting of a lipid and polysaccharide present in the outer membrane of gram-negative bacteria. LPS is renowned for its ability to induce the production of pro-inflammatory cytokines and create an inflammatory response, a critical factor associated with AD, although no direct links have been established (Maitra et al. 2012; Ghosh et al. 2015). Studies have shown that Gram-negative *E. coli* can form extracellular amyloids and that blood LPS levels are high in AD patients. Apart from blood, LPS is also seen co-localized with amyloid plaques, neurons, and glial cells in AD brains. Studies have shown that LPS acts on TLR-4/TLR-2 receptors to activate NF-kappaB to mediate cytokine production that increases Abeta42 levels. As Abeta42 is an agonist for TLR-4 receptors, this process creates an untoward forward cycle for the continuous progression towards AD. Therefore, agonists targeted towards dampening the LPS/TLR4-mediated

signalling or gram-negative bacteria may be regarded as potential drugs for treating sporadic AD (Zhan et al. 2018).

As mentioned in this chapter, the transgenic and chemical-induced rodent models of AD replicate many of the clinical symptoms associated with AD. However, there is no single model that mimics all the pathophysiological features of AD to test lead compounds/drugs for the treatment of AD. While transgenic mouse models demonstrate an increased deposition of amyloid plaques and neurofibrillary tangles, the chemical-induced sporadic rodent model lacks the presence of typical senile plaques and neurofibrillary tangles. Hence, both these models alone do not represent an apt model system for AD. At the same time, both these types of model systems are recommended to study the effect of a lead compound on various physiological and pathophysiological processes of AD-like senile plaque deposition, neurofibrillary tangle accumulation, lesions, neurotransmitter synthesis and other neurological symptoms, synaptic plasticity, glial activation, etc., as these processes biochemically replicate many of features of the human condition during AD. These model systems are therefore important for understanding AD and designing therapeutic modalities for curing AD.

References

- Allen B, Ingram E, Takao M, Smith MJ, Jakes R, Virdee K, Yoshida H, Holzer M, Craxton M, Emson PC et al (2002) Abundant tau filaments and nonapoptotic neurodegeneration in transgenic mice expressing human P301S tau protein. *J Neurosci* 22:9340–9351
- Alzheimer Association Report (2018) Alzheimer disease facts and figures. *Alzheimer's Dementia* 14:367
- Baker S, Gotz J (2016) A local insult of okadaic acid in wild-type mice induces tau phosphorylation and protein aggregation in anatomically distinct brain regions. *Toxicol Ind Health* 32:730–740
- Blokland A, Honig W, Raaijmakers WG (1992) Effects of intrahippocampal scopolamine injections in a repeated spatial acquisition task in the rat. *Psychopharmacology (Berl)* 109(3):373–376
- Braidy N, Muñoz P, Palacios AG, Castellano-Gonzalez G, Inestrosa NC, Chung RS, Sachdev P, Guillemin GJ (2012) Recent rodent models for Alzheimer's disease: clinical implications and basic research. *J Neural Transm* 119:173–195
- Brinkman SD, Gershon S (1983) Measurement of cholinergic drug effects on memory in Alzheimer's disease. *Neurobiol Aging* 4(2):139–145
- Bubser M, Byun N, Wood MR, Jones CK (2012) Muscarinic receptor pharmacology and circuitry for the modulation of cognition. *Handb Exp Pharmacol* 208:121–166
- Chartier-Harlin MC, Crawford F, Houlden H, Warren A, Hughes D, Fidani L, Goate A, Rossor M, Roques P, Hardy J, Mullan M (1991) Early-onset Alzheimer's disease caused by mutations at codon 717 of the beta-amyloid precursor protein gene. *Nature* 353:844–846
- Cheon SY, Koo BN, Kim SY et al (2021) Scopolamine promotes neuroinflammation and delirium-like neuropsychiatric disorder in mice. *Sci Rep* 11:8376
- Chirita CN, Congdon EE, Yin H, Kuret J (2005) Triggers of full-length tau aggregation: a role for partially folded intermediates. *Biochemistry* 44(15):5862–5872
- Chiroma SM, Moklas MAM, Taib CNM, Baharuldin MT, Amon Z (2018) D-Galactose and aluminium chloride induced rat model with cognitive impairments. *Biomed Pharmacother* 103:1602–1608
- Clark D, Tuor UI, Thompson R, Institoris A, Kulynych A, Zhang X et al (2012) Protection against recurrent stroke with resveratrol: endothelial protection. *PLoS One* 7(10):e47792

- Costa AP, Tramontina AC, Biasibetti R, Batassini C, Lopes MW, Wartchow KM et al (2012) Neuroglial alterations in rats submitted to the okadaic acid-induced model of dementia. *Behav Brain Res* 226(2):420–427
- Cui SQ, Wang Q, Zheng Y, Xiao B, Sun HW, Gu XL et al (2015) Puerarin protects against damage to spatial learning and memory ability in mice with chronic alcohol poisoning. *Braz J Med Biol Res* 48(6):515–522
- Dahiyat M, Cumming A, Harrington C, Wischik C, Xuereb J, Corrigan F, Breen G, Shaw D, St Clair D (1999) Association between Alzheimer's disease and the NOS3 gene. *Ann Neurol* 46:664–667
- Duan AR, Jonasson EM, Alberico EO, Li C, Scripture JP, Miller RA et al (2017) Interactions between tau and different conformations of tubulin: implications for tau function and mechanism. *J Mol Biol* 429(9):1424–1438
- Elvander E, Schött PA, Sandin J, Bjelke B, Kehr J, Yoshitake T et al (2004) Intraseptal muscarinic ligands and galanin: influence on hippocampal acetylcholine and cognition. *Neuroscience* 126(3):541–557
- Ericsson AC, Crim M, Franklin C (2013) A brief history of animal modelling. *Mol Med* 110:201–2015
- Evrard PA, Ragusi C, Boschi G, Verbeeck RK, Scherrmann JM (1998) Simultaneous microdialysis in brain and blood of the mouse: extracellular and intracellular brain colchicine disposition. *Brain Res* 786(1–2):122–127
- Fá M, Puzzo D, Piacentini R, Staniszewski A, Zhang H, Baltrons MA (2016) Extracellular tau oligomers produce an immediate impairment of LTP and memory. *Sci Rep* 6(1):19393
- Fine A, Hoyle C, Maclean CJ, Levatte TL, Baker HF, Ridley RM (1997) Learning impairments following injection of a selective cholinergic immunotoxin, ME20.4 IgG-saporin, into the basal nucleus of Meynert in monkeys. *Neuroscience* 81(2):331–343
- Forman MS, Lal D, Zhang B, Dabir DV, Swanson E, Lee VM, Trojanowski JQ (2005) Transgenic mouse model of tau pathology in astrocytes leading to nervous system degeneration. *J Neurosci* 25:3539–3550
- Francis PT, Palmer AM, Snape M, Wilcock GK (1999) The cholinergic hypothesis of Alzheimer's disease: a review of progress. *J Neurol Neurosurg Psychiatry* 66(2):137–147
- Games D, Adams D, Alessandrini R, Barbour R, Berthelette P, Blackwell C, Carr T, Clemens J, Donaldson T, Gillespie F et al (1995) Alzheimer-type neuropathology in transgenic mice overexpressing V717F beta-amyloid precursor protein. *Nature* 373:523–527
- Ganguly R, Guha D (2008) Alteration of brain monoamines & EEG wave pattern in rat model of Alzheimer's disease & protection by *Moringa oleifera*. *Indian J Med Res* 128(6):744–751
- Ghosh S, Lertwattanak R, Jde JG, Galeana JJ, Li J, Zamarripa F (2015) NMDA receptor is involved in neuroinflammation in intracerebroventricular colchicine-injected rats. *J Immunotoxicol* 13(4):474–489
- Giacomotto J, Segalat L (2010) High throughput screening and small animal models, where are we? *Br J Pharmacol* 160:204–216
- Gibson GE, Sheu KF, Blass JP (2009) Abnormalities of mitochondrial enzymes in Alzheimer's disease. *J Neural Transm (Vienna)* 105:855–870
- Goedert M, Spillantini MG (2000) Tau mutations in frontotemporal dementia FTDP-17 and their relevance for Alzheimer's disease. *Biochim Biophys Acta* 1502:110–121
- Götz J, Chen F, van Dorpe J, Nitsch RM (2001) Formation of neurofibrillary tangles in P301L tau transgenic mice induced by Aβ₄₂ fibrils. *Science* 293:1491–1495
- Guerrero-Muñoz MJ, Gerson J, Castillo-Carranza DL (2015) Tau oligomers: the toxic player at synapses in Alzheimer's disease. *Front Cell Neurosci* 9:464
- Haam J, Yakel JL (2017) Cholinergic modulation of the hippocampal region and memory function. *J Neurochem* 142:111–121
- Hardy J, Selkoe DJ (2002) The amyloid hypothesis of Alzheimer's disease: progress and problems on the road to therapeutics. *Science* 297(5580):353–356

- Hasselmo ME, Anderson BP, Bower JM (1992) Cholinergic modulation of cortical associative memory function. *J Neurophysiol* 67(5):1230–1246
- Herculano B, Tamura M, Ohba A, Shimatani M, Kutsuna N, Hisatsune T (2013) β -alanyl-L-histidine rescues cognitive deficits caused by feeding a high fat diet in a transgenic mouse model of Alzheimer's disease. *J Alzheimers Dis* 33:983–997
- Higuchi M, Zhang B, Forman MS, Yoshiyama Y, Trojanowski JQ, Lee VM (2005) Axonal degeneration induced by targeted expression of mutant human tau in oligodendrocytes of transgenic mice that model glial tauopathies. *J Neurosci* 25:9434–9443
- Hoffman JL, Faccidomo S, Kim M, Taylor SM, Agolia AE, May AM, Smith EN, Wong LC, Hodge CW (2019) Alcohol drinking exacerbates neural and behavioural pathology in the 3xTg AD mouse model of Alzheimer's disease. *Int Rev Neurobiol* 148:169–230
- Huang D, Yu M, Yang S, Lou D, Zhou W, Zheng L, Wang Z, Cai F, Zhou W, Li T, Song W (2018) Ethanol alters APP processing and aggravates Alzheimer associated phenotypes. *Mol Neurobiol* 55:5006–5018
- James ND, Davis DR, Sindon J, Hanger DP, Brion JP, Miller CC, Rosenberg MP, Anderton BH, Probst F (1996) Neurodegenerative changes including altered tau phosphorylation and neurofilament immunoreactivity in mice transgenic for the serine/threonine kinase Mos. *Neurobiol Aging* 17:235–241
- Jean YY, Baleriola J, Fa M, Henst U, Troy CM (2015) Stereotaxic infusion of oligomeric amyloid beta into the mouse hippocampus. *J Vis Exp* 17:e52805
- Kamat PK, Tota S, Shukla R, Ali S, Najmi AK, Nath C (2011) Mitochondrial dysfunction: a crucial event in okadaic acid (ICV) induced memory impairment and apoptotic cell death in rat brain. *Pharmacol Biochem Behav* 100(2):311–319
- Kamat PK, Tota S, Rai S, Swarnkar S, Shukla R, Nath C (2012) A study on neuroinflammatory marker in brain areas of okadaic acid (ICV) induced memory impaired rats. *Life Sci* 90(19–20): 713–720
- Karthick C, Periyasamy S, Jayachandran KS, Anusuyadevi M (2016) Intrahippocampal administration of ibotenic acid induced cholinergic dysfunction via NR2A/NR2B expression: implications of resveratrol against Alzheimer disease pathophysiology. *Front Mol Neurosci* 9(28):28
- Kayed R, Head E, Thompson JL, McIntire TM, Milton SC, Cotman CW et al (2003) Common structure of soluble amyloid oligomers implies common mechanism of pathogenesis. *Science* 300(5618):486–489
- Kim B, Backus C, Oh S, Hayes JM, Feldman EL (2009) Increased tau phosphorylation and cleavage in mouse models of type 1 and type 2 diabetes. *Endocrinology* 150:5294–5301
- Kim B, Backus C, Oh S, Feldman E (2013) Hyperglycemia induced tau cleavage in vitro and in vivo: a possible link between diabetes and Alzheimer's disease. *J Alzheimers Dis* 34:727–739
- Klinkenberg I, Blokland A (2010) The validity of scopolamine as a pharmacological model for cognitive impairment: a review of animal behavioural studies. *Neurosci Biobehav Rev* 34(8): 1307–1350
- Lasagna-Reeves CA, Castillo-Carranza DL, Guerrero-Muñoz MJ, Jackson GR, Kaye R (2010) Preparation and characterization of neurotoxic tau oligomers. *Biochemistry* 49(47): 10039–10041
- Levy-Lahad E, Lahad A, Wijsman EM, Bird TD, Schellenberg GD (1995a) Apolipoprotein E genotypes and age of onset in early-onset familial Alzheimer's disease. *Ann Neurol* 38:678–680
- Levy-Lahad E, Wijsman EM, Nemens E, Anderson L, Goddard KA, Weber JL, Bird TD, Schellenberg GD (1995b) A familial Alzheimer's disease locus on chromosome 1. *Science* 269:970–973
- Lewis J, Dickson DW, Lin WL, Chisholm L, Corral A, Jones G, Yen SH, Sahara N, Skipper L, Yager D (2001) Enhanced neuro-fibrillary degeneration in transgenic mice expressing mutant tau and APP. *Science* 293:1487–1491

- Liao A, Nitsch RM, Greenberg SM, Finckh U, Blacker D, Albert M, Rebeck GW, Gomez-Isla T, Clatworthy A, Binetti G et al (1998) Genetic association of an alpha2-macroglobulin (Val1000Ile) polymorphism and Alzheimer's disease. *Hum Mol Genet* 7:1953–1956
- Mailliard WS, Diamond I (2004) Recent advances in the neurobiology of alcoholism: the role of adenosine. *Pharmacol Ther* 101(1):39–46
- Maitra U, Deng H, Glaros T, Baker B, Capelluto DG, Li Z et al (2012) Molecular mechanisms responsible for the selective and low-grade induction of proinflammatory mediators in murine macrophages by lipopolysaccharide. *J Immunol* 189(2):1014–1023
- Miklossy J, Qing H, Radenovic A, Kis A, Vileno B, Laszlo F, Miller L, Martins RN, Waeber G, Mooser V, Bosman F, Khalil K, Darbinian N, McGeer PL (2010) Beta-amyloid and hyperphosphorylated tau deposits in the pancreas in type 2 diabetes. *Neurobiol Aging* 31:1503–1515
- Miranda MI, Bermúdez-Rattoni F (1999) Reversible inactivation of the nucleus basalis magnocellularis induces disruption of cortical acetylcholine release and acquisition, but not retrieval, of aversive memories. *Proc Natl Acad Sci U S A* 96(11):6478–6482
- Mondragón-Rodríguez S, Basurto-Islas G, Santa-Maria I, Mena R, Binder LI, Avila J (2008) Cleavage and conformational changes of tau protein follow phosphorylation during Alzheimer's disease. *Int J Exp Pathol* 89(2):81–90
- Mujika JI, Rezabal E, Mercero JM, Ruipérez F, Costa D, Ugalde JM et al (2014) Aluminium in biological environments: a computational approach. *Comput Struct Biotechnol J* 9(15):e201403002
- Nallagouni CS, Reddy KP (2017) Aluminium and fluoride impacts cortex, hippocampus and dentate gyrus structure in rats: protective effect of resveratrol. *Int J Appl Biol Pharm Technol* 8:89–97
- Neha RK, Sodhi RK, Jaggi AS, Singh N (2014) Animal models of dementia and cognitive dysfunction. *Life Sci* 109(2):73–86
- Oddo S, Caccamo A, Shepherd JD, Murphy MP, Golde TE, Kaye R, Metherate R, Mattson MP, Akbari Y, LaFerla FM (2003) Triple transgenic model of Alzheimer's disease with plaques and tangles: intracellular A β and synaptic dysfunction. *Neuron* 39:409–421
- Parker WD, Parks JK (1995) Cytochrome c oxidase in Alzheimer's disease brain: purification and characterization. *Neurology* 45(3 Pt 1):482–486
- Patil S, Tawari S, Mundhada D, Nadeem S (2015) Protective effect of berberine, an isoquinoline alkaloid ameliorates ethanol-induced oxidative stress and memory dysfunction in rats. *Pharmacol Biochem Behav* 136:13–20
- Patterson KR, Remmers C, Fu Y, Brooker S, Kanaan NM, Vana L et al (2011) Characterization of prefibrillar tau oligomers in vitro and in Alzheimer disease. *J Biol Chem* 286(26):23063–23076
- Pattipati KAS, Singh A (2016) Animal models in drug discovery of Alzheimer's disease: a mini review. *EC Pharmacol Toxicol* 2(1):60–79
- Portero-Tresserra M, Olmo ND, Martí-Nicolovius M, GuillazoBlanch G, Vale-Martínez A (2014) D-cycloserine prevents relational memory deficits and suppression of long-term potentiation induced by scopolamine in the hippocampus. *Eur Neuropsychopharmacol* 24(11):1798–1807
- Rattan AK, Tejwani GA (1992) The neurotoxic actions of ibotenic acid on cholinergic and opioid peptidergic systems in the central nervous system of the rat. *Brain Res* 571(2):298–305
- Ravelli K, Rosario B, Camarini R, Hernandes M, Britto L (2017) Intracerebroventricular streptozotocin as a model of Alzheimer's disease: neurochemical and behavioral characterization in mice. *Acta Neuropathol Commun* 4:32
- Ribé EM, Pérez M, Puig B, Gich I, Lim F, Cuadrado M, Sesma T, Catena S, Sánchez B, Nieto M et al (2005) Accelerated amyloid deposition, neurofibrillary degeneration and neuronal loss in double mutant APP/tau transgenic mice. *Neurobiol Dis* 20:814–822
- Riedel G, Kang SH, Choi DY, Platt B (2009) Scopolamine-induced deficits in social memory in mice: reversal by donepezil. *Behav Brain Res* 204(1):217–225

- Rodella LF, Ricci F, Borsani E, Stacchiotti A, Foglio E, FaveroG RR, Mariani C, Bianchi R (2008) Aluminium exposure induces Alzheimer's disease-like histopathological alterations in the mouse brain. *Histol Histopathol* 23:433–439
- Rogaev EI, Sherrington R, Rogaeva EA, Levesque G, Ikeda M, Liang Y, Chi H, Lin C, Holman K, Tsuda T et al (1995) Familial Alzheimer's disease in kindreds with missense mutations in a gene on chromosome 1 related to the Alzheimer's disease type 3 gene. *Nature* 376:775–778
- Sahara N, Maeda S, Murayama M, Suzuki T, Dohmae N, Yen SH et al (2007) Assembly of two distinct dimers and higher order oligomers from full-length tau. *Eur J Neurosci*. 25(10): 3020–3029
- Sarter M, Bruno JP (1997) Cognitive functions of cortical acetylcholine: toward a unifying hypothesis. *Brain Res Brain Res Rev* 23(1–2):28–46
- Schindowski K, Bretteville A, Leroy K, Bégard S, Brion JP, Hamdane M, Buée L (2006) Alzheimer's disease-like tau neuropathology leads to memory deficits, and loss of functional synapses in a novel mutated tau transgenic mouse without any motor deficits. *Am J Pathol* 169: 599–616
- Sharma B, Singh N (2010) Pitavastatin and 4'-hydroxy-3'- methoxyacetophenone (HMAP) reduce cognitive dysfunction in vascular dementia during experimental diabetes. *Curr Neurovasc Res* 7(3):180–191
- Skovronsky DM, Lee VM, Trojanowski JQ (2006) Neurodegenerative diseases: new concepts of pathogenesis and their therapeutic implications. *Annu Rev Pathol* 1(1):151–170
- Spinetta MJ, Woodlee MT, Feinberg LM, Stroud C, Schallert K, Cormack LK et al (2008) Alcohol-induced retrograde memory impairment in rats: prevention by caffeine. *Psychopharmacology* 201(3):361–371
- Summers WK, Viesselman JO, Marsh GM, Candelora K (1981) Use of THA in treatment of Alzheimer-like dementia: pilot study in twelve patients. *Biol Psychiatry* 16(2):145–153
- Swerdlow RH, Khan SM (2014) A “mitochondrial cascade hypothesis” for sporadic Alzheimer's disease. *Med Hypotheses* 63:8–20
- Tannenbaum J (1999) Ethics and pain research in animals. *ILAR J* 40:97–110
- Tota S, Nath C, Najmi AK, Shukla R, Hanif K (2012) Inhibition of central angiotensin converting enzyme ameliorates scopolamine induced memory impairment in mice: role of cholinergic neurotransmission, cerebral blood flow and brain energy metabolism. *Behav Brain Res* 232(1):66–76
- Unsal C, Oran M, Albayrak Y, Aktas C, Erboga M, Topcu B, Uygur R, Tulubas F, Yanartas O, Ates O, Ozen O (2016) Neuroprotective effect of ebselen against intracerebroventricular streptozotocin-induced neuronal apoptosis and oxidative stress in rats. *Toxicol Ind Health* 32: 730–740
- Yang S, Zhou G, Liu H, Zhang B, Li J, Cui R et al (2013) Protective effects of p38 MAPK inhibitor SB202190 against hippocampal apoptosis and spatial learning and memory deficits in a rat model of vascular dementia. *Biomed Res Int* 2013:215798
- Yu Z, Cheng G, Hu B (1997) Mechanism of colchicine impairment on learning and memory, and protective effect of CGP36742 in mice. *Brain Res* 750(1–2):53–58
- Zhan X, Stamova B, Sharp FR (2018) Lipopolysaccharide associates with amyloid plaques, neurons and oligodendrocytes in Alzheimer's disease brain: a review. *Front Aging Neurosci* 10:42
- Zhou S, Yu G, Chi L, Zhu J, Zhang W, Zhang Y et al (2013) Neuroprotective effects of edaravone on cognitive deficit, oxidative stress and tau hyperphosphorylation induced by intracerebroventricular streptozotocin in rats. *Neurotoxicology* 38:136–145



Mitochondria-Targeted Liposomal Delivery in Parkinson's Disease 24

Bipul Ray, Arehally M. Mahalakshmi, Mahendran Bhaskaran, Sunanda Tuladhar, A. H. Tousif, Musthafa Mohamed Essa, Byoung-Joon Song, and Saravana Babu Chidambaram

Abbreviations

α -syn	α -Synuclein
AD	Alzheimer disease
BBB	Blood–brain Barrier
DOPE	1,2-Dioleoyl-sn-glycero-3-phosphoethanolamine
DSPS	1,2-Distearoyl-sn-glycero-3-phosphatidylcholine
ETC	Electron transport chain

B. Ray · S. Tuladhar · A. H. Tousif · S. B. Chidambaram (✉)

Department of Pharmacology, JSS College of Pharmacy, JSS Academy of Higher Education and Research, Mysuru, India

Centre for Experimental Pharmacology and Toxicology, Central Animal Facility, JSS Academy of Higher Education and Research, Mysuru, India

e-mail: saravanababu.c@jssuni.edu.in

A. M. Mahalakshmi

Department of Pharmacology, JSS College of Pharmacy, JSS Academy of Higher Education and Research, Mysuru, India

M. Bhaskaran

Department of Pharmaceutics, JSS College of Pharmacy, JSS Academy of Higher Education and Research, Mysuru, India

M. M. Essa

Department of Food Science and Nutrition, CAMS, Sultan Qaboos University, Muscat, Oman

Aging and Dementia Research Group, Sultan Qaboos University, Muscat, Oman

Biomedical Sciences Department, University of Pacific, Sacramento, CA, USA

B.-J. Song

Section of Molecular Pharmacology and Toxicology, Laboratory of Membrane Biochemistry and Biophysics, National Institute on Alcohol Abuse and Alcoholism, Bethesda, MD, USA

IND	Investigational New Drug
MPTP	1-Methyl-4-phenyl-1,2,3,6 tetrahydropyridine
mtDNA	Mitochondrial DNA
NFs	Neurotrophic factors
NPs	Nanoparticles
PD	Parkinson's disease
SOD	Superoxide dismutase
STPP	Stearyl triphenylphosphonium
TPP	Triphenyl phosphonium
UTMD	Ultrasound-targeted microbubble destruction

24.1 Introduction

Mitochondrial dysfunction in Parkinson's Disease (PD) is implicated through both environmental exposure and genetic factors (Grünewald et al. 2016; Tzoulis et al. 2013; Flønes et al. 2018; Fonseca-Fonseca et al. 2021). The first evidence reported of mitochondrial dysfunction associated with PD was in 1983 when 1-methyl-4-phenyl-1,2,3,6-tetrahydropyridine (MPTP) exposure caused parkinsonian-like symptoms (Langston et al. 1983; Langston and Ballard 1983). Currently, there are limited approved drugs for the treatment of PD and these drugs only offer treatment for symptomatic purposes (Zhen and Chu 2020). However, as research advancements emerge in this field, organ-specific targeted therapies are receiving high priority as future therapeutic approaches hence nano-drug carriers like liposomes came into the valuable options for the treatment of PD. Around 30 years ago, researchers found a new way of delivering medicinal substances to specific areas of the brain—by injecting them into a certain part, in this case, the rat's striatum. Liposomes loaded with dopamine partially ameliorated the cognitive and motor deficits in a PD rat model, as well as demonstrated the importance of targeted delivery to the brain (During et al. 1992).

Doxil[®] was the first FDA-approved (in 1995) liposomal nano-drug for clinical purposes. Since then, technology has advanced, pioneering liposomal drug delivery systems with significant clinical implications. Artificial lipid vesicles called liposomes were discovered by hematologist Alec Bangham in 1961 (Bangham et al. 1965) for the first time, then it has been recognized for nano-drug delivery for various diseases treatment purposes including PD (Ahl et al. 1997; Davidson et al. 1998; Li et al. 1998; Meyer et al. 1998). Mackay et al. (2019) have reported the neuroprotection of dopamine-loaded liposomes in PD (Mackay et al. 2019). Liposome-based MITO-Porter was reported to deliver macromolecules into mitochondria in living cells (Yamada et al. 2008). The entry to the brain is protected by tight junctions of the cerebral capillary endothelium and the astrocytes through blood–brain barrier (BBB), resulting in reduced permeability thus restricting the delivery of drugs to the brain (Pardridge 2015; Rehman et al. 2017). BBB regulation

depends on the presence of different cellular components, like astrocytes, pericytes, and neurons (Abbott et al. 2010). The liposomal structure is similar to the cell membrane, represents biodegradable colloids, and are being used to deliver hydrophobic and hydrophilic drug molecules (Dimov et al. 2017), peptides (Gregori et al. 2017; Qu et al. 2018; You et al. 2018), proteins (Schwarze et al. 1999), and RNAs (Kim et al. 2009), protects them against degradation without altering the functions (Schnyder and Huwyler 2005). These are among the best-studied and clinically approved nanocarriers. They are also low in toxicity, have a long history, and can be used to transport both hydrophilic and lipophilic agents (Costantino et al. 2009). Nowadays, we have seen a number of different lipid compositions modified for targeted delivery to various parts of the brain. Ligands such as glucose (Xie et al. 2012), lactoferrin (Kuo and Tsao 2017), transferrin (Song et al. 2017), and specific peptides (Reijerkerk et al. 2014) are also loaded into the liposomes which can efficiently cross the BBB and deliver the contents to the targeted site. Liposomes crosslinked with functional groups in targeting mitochondria have shown promising results (Kuznetsova et al. 2019; Wagle et al. 2011; Yamada et al. 2008).

However, a faster rate of systemic elimination, high metabolic degradation of phospholipids, stability on long storage, difficulty in maintaining a continuous steady release, and efficiency in the encapsulation of lipophilic compounds are the major limitations of liposomes (Wong et al. 2012). In this chapter, we have discussed the recent advances of mitochondria-specific liposomal delivery in PD as well as regulatory challenges.

24.2 Mitochondrial Dysfunction and Parkinson's Disease

The mitochondrial electron transport chain (ETC) generates oxygen free radicals from complexes I and II during the process of oxidative phosphorylation (Ray et al. 2021a; Reeve et al. 2018). The reactive oxygen species (ROS) thus formed is neutralized by endogenous antioxidants like superoxide dismutase (SOD) and glutathione (GSH), and redox homeostasis is maintained (Indo et al. 2015). Mitochondrial dynamics is an integral part of the mitochondrial quality control pathway, allowing selective removal of damaged mitochondria through autophagy (Chen et al. 2021). Oxidative stress (Fig. 24.1) is shown to impair mitochondrial dynamics and autophagy which further aggravates PD (Akbar et al. 2016; Kataoka et al. 2020; Park et al. 2018). Unlike nuclear DNA, which is well-protected by the presence of histones, mitochondrial DNA (mtDNA) is more vulnerable to damage because it lacks histones (Akbar et al. 2016; Gureev et al. 2017). Since mtDNA encodes 13 essential proteins (Gustafsson et al. 2016), DNA mutations and deletions affect ETC and trigger oxidative stress that leads to neuronal death (Iannielli et al. 2018). Increased oxidative stress is linked to the neuronal accumulation of α -syn (Ray et al. 2021b; Scudamore and Ciossek 2018). The selective removal and subsequent catabolism of damaged mitochondria by autophagosomes is called mitophagy. Mitophagy plays important role in cellular health (Cai and Jeong 2020; Lee et al. 2021; Mani et al. 2021) and its impairment is associated with PD. Mutations in

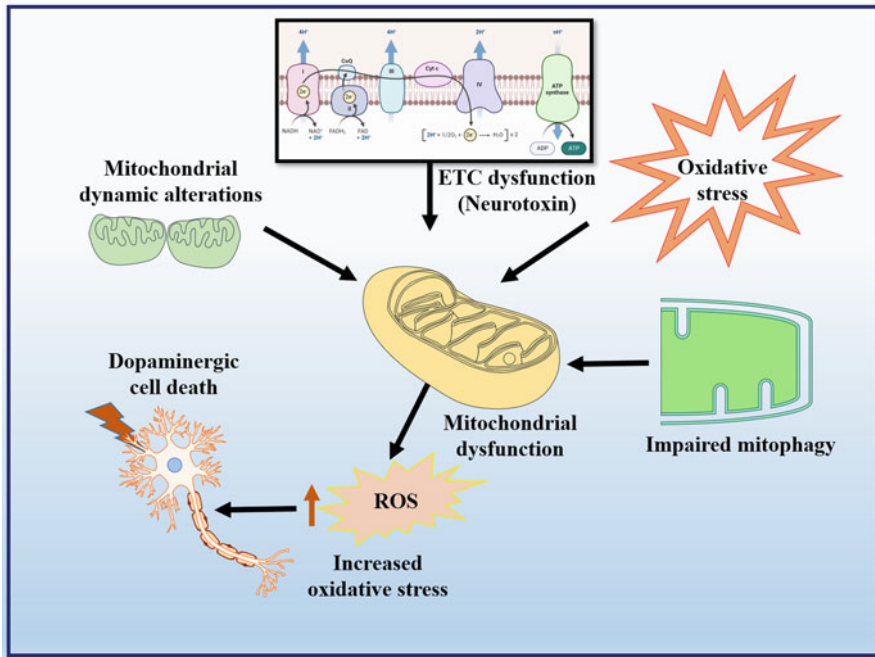


Fig. 24.1 Mitochondrial dysfunction in PD. This diagram depicts the key pathways that trigger mitochondrial dysfunction in PD. Altered fission-fusion dynamics, electron transport chain (ETC), and impaired mitophagy contribute to mitochondrial dysfunction. This in turn causes excessive production of free radicals and oxidative stress, which contributes to neuronal cell death and PD progression

mitochondria-specific genes are shown to impair mitophagy. PINK1 and PARKIN are two types of regulatory proteins in mitochondrial autophagy (Park and Koh 2020).

24.3 Liposomal Drug Delivery Across the BBB

Unfortunately, none of the therapeutic approaches have yet provided adequate support in preventing or slowing the development and progression of PD. The main hurdle to brain-targeted therapies is crossing the BBB (Torres-Ortega et al. 2019). Most of the drug targeting especially neurodegeneration fails to enter cross BBB. BBB consists of tight junction endothelial cells and astrocytes. Selective permeability through endothelial cells hinders the penetration of drug molecules into the brain (Abbott et al. 2010). To achieve this, the use of nano-drug delivery systems is being researched, capable of providing high bioavailability, minimizing adverse effects, and targeting specific tissues or subcellular organelles (Chidambaram et al. 2020; Patra et al. 2018; Peng et al. 2020). Quite a lot of nanoparticles have been

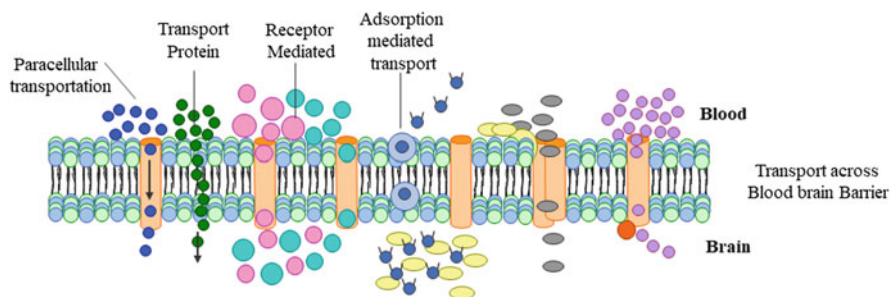


Fig. 24.2 Schematic representation of cerebrospinal fluid transport

engineered to efficiently transport drugs across the BBB without harming its function (Fig. 24.2). Several types of NPs, such as liposomes, micelles, carbon nanotubes, dendrimers, and metal particles cross BBB. Liposomes are becoming more widely used because of its nontoxic, biodegradable, and biocompatible properties. They show signs of potential in the clinical setting (Spuch and Navarro 2011). Liposomes are made of two layers of lipid and they act like cell membranes because they protect the inner parts while being insecure (Spuch and Navarro 2010). The brain-targeted liposomal delivery was reported in a mouse model of PD. A new delivery method, i.e., liposomal formulation of dopamine (DA) showed a good correlation between the amount of liposomal DA and improved behavior in mice who were also given amphetamine. These findings were discovered when the substances was delivered Intra-peritoneally (IP) (Kahana et al. 2021). In another report, Ultrasonic microbubble destruction (UTMD)-Liposome in conjunction with neurotrophic factor (NFs) gene delivery showed the ability to penetrate BBB and display neuroprotective activity against PD (Lin et al. 2020).

Initially, it was assumed that the liposomes crossed BBB extemporaneously by electrostatic interactions. This theory has since been superseded by the possible mechanism of active transporters by transcytosis or specific receptors, though (Spuch and Navarro 2011). Recent studies have shown that the more recent hypothesis is more consistent with scientific evidence. It is also been found that certain molecules bind to liposome surfaces, which makes them able to cross the BBB. That support helps account for why liposome transport finally succeeds (Noble et al. 2014). Therefore, nano delivery of drugs is acknowledged for increased safety, efficacy, and bioavailability as well as it is also associated with a reduction in dose necessities and adverse effects. Hence, NPs are receiving important consideration as therapeutic options (Chidambaram et al. 2020; Ray et al. 2021).

24.4 Mitochondria-Targeted Liposomal Formulations

The covalent bioconjugation strategy is most widely used to formulate prodrugs capable of self-assembling into liposomes (de la Fuente-Herrueruela et al. 2019; Wang et al. 2019; Zhang et al. 2020). Prodrugs are often composed of phospholipids

that are covalently linked to the drug with a reactive element that stimulates liposome breakdown, so the prodrug is metabolized and released (Signorell et al. 2018).

Liposomes can be further adorned with peptides or antibodies to the surface that can help reach the chosen target organelle. In recent years, the intracellular drug delivery system has developed rapidly with the main aim of specifically targeting sub-organelles like mitochondria, lysosomes, Golgi complexes, etc. (Sakhrani and Padh 2013). In early days organ-specific delivery carrying drug of interest to mitochondria was extremely challenging because mitochondria itself has several cellular structures through which the drug should pass, these include the plasma membrane, the intracellular cytoplasm, and membranes that surround the mitochondria. Few drug treatments can penetrate these barriers to access the mitochondria. However, many drugs require mitochondrial tropic conjugation to deliver the molecule. For example, when small water-soluble Szeto Schiller (SS) peptides were engineered to target and accumulate on the inner membrane of mitochondria. These peptides can cross cell membranes without involving any energy and they target mitochondria using a sequence motif. Furthermore, the SS peptides not only shield mitochondria from oxidative damage at a molecular level (Birk et al. 2013).

Surface modification of liposome with triphenylphosphonium (TPP) cations reported delivering to mitochondria (Boddapati et al. 2005) (Fig. 24.3). Boddapati et al. delivered a proapoptotic lipid molecule, ceramide functionalizing with stearyl triphenylphosphonium (STPP) to mitochondria (Boddapati et al. 2005). Many drugs need to be conjugated to mitochondria-specific molecules and MitoQ is one

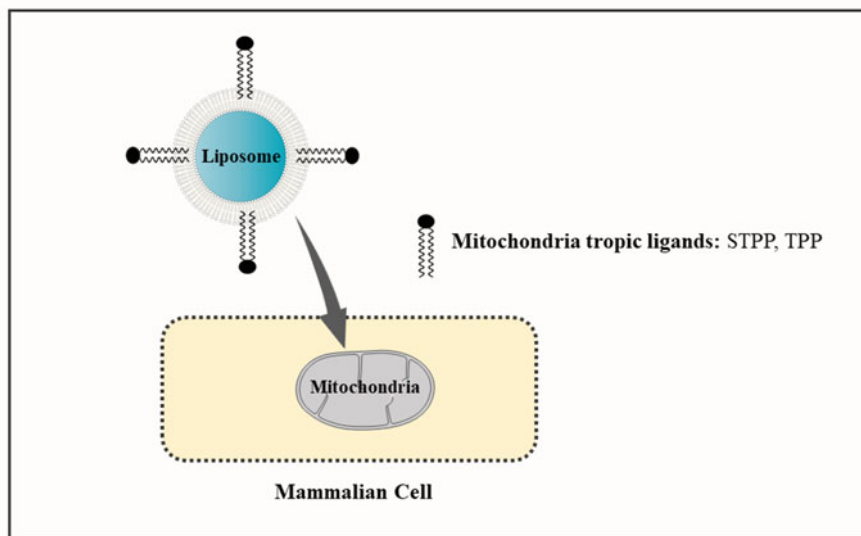


Fig. 24.3 Functionalized liposome targeting mitochondria in PD

example. MitoQ includes coenzyme Q, an antioxidant, coupled with TPP cation, a widely used lipophilic cation that is taken up and enriched by mitochondria (Smith and Murphy 2011; Yamada et al. 2007). MitoQ is used as a protective agent in many mitochondria-related health conditions such as stroke, Parkinson's disease, Alzheimer's, and multiple sclerosis (Mao et al. 2013; Miquel et al. 2014; Solesio et al. 2013). MitoQ is presently in clinical trials for PD (Smith and Murphy 2010; Snow et al. 2010). MITO-Porters are a type of liposome that deliver its macromolecular cargo to the inside of mitochondria via membrane fusion. They contain simulated octa-arginine coatings, which allow them to enter cells and enter unbroken into the mitochondria. The MITO-Porter help both its fusion with the mitochondrial membrane and intra-mitochondrial release of its cargo in living cells. Therefore, the MITO-Porter could be a great promise as an efficacious system to deliver a drug moiety into mitochondria (Yamada et al. 2008; Yamada and Harashima 2017).

24.5 Advantages and Challenges of Liposomal Delivery

24.5.1 Advantages of Liposomes

Liposomes are spherical vesicles with synthetic lipid with a bilayer membrane structure that can incorporate both hydrophilic and hydrophobic drugs. The use of a drug carrier system for medical purposes could protect the integrity of biologically active medications encapsulated in liposomes, suggesting that this is an effective way to transport drugs and other bioactive capsules in the targeted delivery (1) liposomes are biocompatible, completely biodegradable; (2) they have a unique ability to entrap hydrophilic and hydrophobic drugs; (3) they protect the encapsulated drug from the external environment or degradation; (4) liposomes are prepared from hydrogenated egg phosphatidylcholine, cholesterol, and the particle sizes are adjustable to about 50–100 nm; (5) by adding conjugates on its surface, the targeted delivery to the specific sites or organs can be modified (Boddapati et al. 2005) with peptides, proteins, and antibodies; (6) liposomes are generally considered to be pharmacologically active with minimal toxicity, as they tend to be composed of natural phospholipids (Sercombe et al. 2015).

24.5.2 Challenges of Liposomes

Liposomes are made up of mostly natural phospholipids and lipids, like 1,2-distearoyl-sn-glycero-3-phosphatidylcholine (DSPC), egg phosphatidylcholines and monosialoganglioside. Conventional liposomal formulations have encountered many challenges, one of them being unstable in plasma (Torchilin 2005). Many efforts have been made to overcome these challenges, specifically manipulation of the lipid membrane. Out of those, one attempted to manipulate the cholesterol in this membrane. The different types of micelles have different impacts on the plasma levels of the compound being delivered (Damen et al. 1981). The addition of

cholesterol decreases the rapid release rate and 1,2-dioleoyl-sn-glycero-3-phosphoethanolamine (DOPE) increases stability (Tran et al. 2009).

24.6 Regulatory Challenges for Liposomes

Since the approval of Doxil[®] in 1995, the first liposomal delivery system, liposomal delivery improvements in the past have led to better, more efficient delivery systems. For instance, by improving the physicochemical properties of such liposomes by using different polymer structures. Currently, Doxil[®] alone generates sales of over \$500 million per year (Zylberberg and Matosevic 2016). Presently, there are many liposome-based drugs approved for clinical use (Chang and Yeh 2012), with many more in the early stages of development. Although liposome-based drug delivery systems have been commercially successful, not enough attention has been given to their regulation.

As of 2015, most FDA-approved delivery vehicles are fully liposomal or PEGylated and none have addressed higher complex compositions like ethosomes or pharmacosomes, demonstrating the requirement of more data from the experiments to prove the efficacy of these formulations as required by the FDA. There are many ongoing initiatives related to clinical trials that will soon allow new versions of drugs based on nanotechnology to reach the market (Caster et al. 2017). When these nanomedicines are introduced into biological systems, it is important to consider the potential for the formation of aggregates and agglomerates. These aggregates do not reflect the properties of their individual particulate counterparts. This can generate different unexpected toxic effects depending on the nanoformulation (Wacker et al. 2016). Unfortunately, there is currently no established standard of protocols for the characterization of nanomedicines. This has prevented many researchers from evaluating the toxic effects of nanomedicines in the early stages of their development, leading to failures in late phase clinical trials. To streamline the approval process for new nanomedicines/drugs, it would be helpful if regulators worked together more closely (Lin et al. 2014; Ventola 2017). Due to the lack of regulation of nanomedicines and nano-drug delivery systems, their safety assessment is conducted with reference to guidelines used for conventional medicines. After obtaining investigational new drug status (Investigational New Drug, IND) from the FDA, nano-drugs are ready to begin their clinical trials to study their safety and efficacy when used in humans (Grossman et al. 2017; Sainz et al. 2015; Ventola 2017). FDA guidelines provide recommendations for meeting regulatory requirements. The FDA recommends designing new drug delivery systems just for these tests to validate bioequivalence through *in vivo* and *in vitro* studies. The FDA recommends the type and number of studies, the population to be studied, and the times of blood collection to be done. Analytes in the blood samples should also be mapped. Additionally, when developing new liposomal drug delivery systems, the composition and physicochemistry of the system are of major concern. It is crucial to assess the dose-dependent pharmacokinetic behavior and to ensure that equivalence is achieved, whereas for a validated bioanalytical method the

quantity must be reliably quantified. In these aspects, the governments of respective countries must come together to develop new harmonized protocols which must be precise and rigorous enough to meet the safety concerns guaranteeing the benefit of nanomedicine for patients.

24.7 Conclusion

Even though advantages and disadvantages are pointed out of liposomal delivery, it can be concluded that liposomal targeted delivery has strongly gained attention in the last decade. Although regulatory concerns about nanomedicine and safety/toxicity assessments will still require work in the future, nanomedicine has already revolutionized the way it is explored for biological systems, including clinical systems. Extensive research in this field over the past two decades has already led to the filing of more than 1500 patents and the performance of several dozen of clinical trials (Pandit and Zeugolis 2016). It remains to be proven whether active targeting mitochondria with drugs will be successful as a treatment for Alzheimer's, Parkinson's, and other neurodegenerative diseases. Multidisciplinary research is needed for the optimum liposomal formulation of a therapeutic agent and optimization of ligation strategy for a specific targeting ligand. With the breakthroughs in nanotechnology, it is now possible to diagnose diseases and even treat them simultaneously.

Acknowledgment Bipul Ray would like to acknowledge ICMR, New Delhi, GoI for providing Senior Research Fellowship. The authors would also like to thank JSS AHER for providing research facilities.

References

- Abbott NJ, Patabendige AAK, Dolman DEM, Yusof SR, Begley DJ (2010) Structure and function of the blood–brain barrier. *Neurobiol Dis* 37(1):13–25
- Ahl PL, Bhatia SK, Meers P et al (1997) Enhancement of the in vivo circulation lifetime of l- α -distearoylphosphatidylcholine liposomes: importance of liposomal aggregation versus complement opsonization. *Biochim Biophys Acta Biomembr* 1329(2):370–382
- Akbar M, Essa MM, Daradkeh G et al (2016) Mitochondrial dysfunction and cell death in neurodegenerative diseases through nitroxidative stress. *Brain Res* 1637:34–55
- Bangham AD, Standish MM, Watkins JC (1965) Diffusion of univalent ions across the lamellae of swollen phospholipids. *J Mol Biol* 13(1):238–252
- Birk AV, Liu S, Soong Y et al (2013) The mitochondrial-targeted compound SS-31 re-energizes ischemic mitochondria by interacting with cardiolipin. *J Am Soc Nephrol* 24(8):1250–1261
- Boddapati SV, Tongcharoensirikul P, Hanson RN, D'Souza GGM, Torchilin VP, Weissig V (2005) Mitochondriotropic liposomes. *J Liposome Res* 15(1–2):49–58
- Cai Q, Jeong YY (2020) Mitophagy in Alzheimer's disease and other age-related neurodegenerative diseases. *Cells* 9(1):150
- Caster JM, Patel AN, Zhang T, Wang A (2017) Investigational nanomedicines in 2016: a review of nanotherapeutics currently undergoing clinical trials. *WIREs Nanomed Nanobiotechnol* 9(1): e1416

- Chang H-I, Yeh M-K (2012) Clinical development of liposome-based drugs: formulation, characterization, and therapeutic efficacy. *Int J Nanomedicine* 7:49–60
- Chen N, Guo Z, Luo Z et al (2021) Drp1-mediated mitochondrial fission contributes to mitophagy in paraquat-induced neuronal cell damage. *Environ Pollut* 272:116413
- Chidambaram SB, Ray B, Bhat A et al (2020) Chapter 5—Mitochondria-targeted drug delivery in neurodegenerative diseases. In: Shegokar R (ed) *Delivery of drugs*. Elsevier, Amsterdam, pp 97–117
- Costantino L, Tosi G, Ruozi B, Bondioli L, Vandelli MA, Forni F (2009) Chapter 3—Colloidal systems for CNS drug delivery. In: Sharma HS (ed) *Progress in brain research*, vol 180. Elsevier, Amsterdam, pp 35–69
- Damen J, Regts J, Scherphof G (1981) Transfer and exchange of phospholipid between small unilamellar liposomes and rat plasma high density lipoproteins. Dependence on cholesterol content and phospholipid composition. *Biochim Biophys Acta* 665(3):538–545
- Davidson WS, Jonas A, Clayton DF, George JM (1998) Stabilization of α -synuclein secondary structure upon binding to synthetic membranes. *J Biol Chem* 273(16):9443–9449
- de la Fuente-Herreruela D, Monnappa AK, Muñoz-Úbeda M et al (2019) Lipid-peptide bioconjugation through pyridyl disulfide reaction chemistry and its application in cell targeting and drug delivery. *J Nanobiotechnol* 17(1):77
- Dimov N, Kastner E, Hussain M, Perrie Y, Szita N (2017) Formation and purification of tailored liposomes for drug delivery using a module-based micro continuous-flow system. *Sci Rep* 7(1):12045
- During MJ, Freese A, Deutch AY et al (1992) Biochemical and behavioral recovery in a rodent model of Parkinson's disease following stereotactic implantation of dopamine-containing liposomes. *Exp Neurol* 115(2):193–199
- Flønes IH, Fernandez-Vizarrá E, Lykouri M et al (2018) Neuronal complex I deficiency occurs throughout the Parkinson's disease brain, but is not associated with neurodegeneration or mitochondrial DNA damage. *Acta Neuropathol* 135(3):409–425
- Fonseca-Fonseca LA, da Silva VDA, Wong-Guerra M et al (2021) JM-20 protects against 6-hydroxydopamine-induced neurotoxicity in models of Parkinson's disease: mitochondrial protection and antioxidant properties. *Neurotoxicology* 82:89–98
- Gregori M, Taylor M, Salvati E et al (2017) Retro-inverso peptide inhibitor nanoparticles as potent inhibitors of aggregation of the Alzheimer's A β peptide. *Nanomedicine* 13(2):723–732
- Grossman JH, Crist RM, Clogston JD (2017) Early development challenges for drug products containing nanomaterials. *AAPS J* 19(1):92–102
- Gureev AP, Shaforostova EA, Starkov AA, Popov VN (2017) Simplified qPCR method for detecting excessive mtDNA damage induced by exogenous factors. *Toxicology* 382:67–74
- Gustafsson CM, Falkenberg M, Larsson N-G (2016) Maintenance and expression of mammalian mitochondrial DNA. *Annu Rev Biochem* 85(1):133–160
- Iannielli A, Bido S, Folladori L et al (2018) Pharmacological inhibition of necroptosis protects from dopaminergic neuronal cell death in Parkinson's disease models. *Cell Rep* 22(8):2066–2079
- Indo HP, Yen H-C, Nakanishi I et al (2015) A mitochondrial superoxide theory for oxidative stress diseases and aging. *J Clin Biochem Nutr* 56(1):1–7
- Kahana M, Weizman A, Gabay M et al (2021) Liposome-based targeting of dopamine to the brain: a novel approach for the treatment of Parkinson's disease. *Mol Psychiatry* 26:2626–2632
- Kataoka K, Bilkei-Gorzo A, Nozaki C et al (2020) Age-dependent alteration in mitochondrial dynamics and autophagy in hippocampal neuron of cannabinoid CB1 receptor-deficient mice. *Brain Res Bull* 160:40–49
- Kim B-K, Doh K-O, Nam JH et al (2009) Synthesis of novel cholesterol-based cationic lipids for gene delivery. *Bioorg Med Chem Lett* 19(11):2986–2989
- Kuo Y-C, Tsao C-W (2017) Neuroprotection against apoptosis of SK-N-MC cells using RMP-7- and lactoferrin-grafted liposomes carrying quercetin. *Int J Nanomedicine* 12:2857–2869
- Kuznetsova DA, Gaynanova GA, Vasileva LA et al (2019) Mitochondria-targeted cationic liposomes modified with alkyltriphenylphosphonium bromides loaded with hydrophilic drugs: preparation, cytotoxicity and colocalization assay. *J Mater Chem B* 7(46):7351–7362

- Langston JW, Ballard PA (1983) Parkinson's disease in a chemist working with 1-methyl-4-phenyl-1,2,5,6-tetrahydropyridine. *N Engl J Med* 309(5):310
- Langston JW, Ballard P, Tetrud JW, Irwin I (1983) Chronic Parkinsonism in humans due to a product of meperidine-analog synthesis. *Science (New York, N.Y.)* 219(4587):979–980
- Lee I-J, Chao C-Y, Yang Y-C et al (2021) Huang Lian Jie Du Tang attenuates paraquat-induced mitophagy in human SH-SY5Y cells: a traditional decoction with a novel therapeutic potential in treating Parkinson's disease. *Biomed Pharmacother* 134:111170
- Li X, Hirsh DJ, Cabral-Lilly D et al (1998) Doxorubicin physical state in solution and inside liposomes loaded via a pH gradient. *Biochim Biophys Acta Biomembr* 1415(1):23–40
- Lin P-C, Lin S, Wang PC, Sridhar R (2014) Techniques for physicochemical characterization of nanomaterials. *Biotechnol Adv* 32(4):711–726
- Lin C-Y, Lin Y-C, Huang C-Y, Wu S-R, Chen C-M, Liu H-L (2020) Ultrasound-responsive neurotrophic factor-loaded microbubble-liposome complex: preclinical investigation for Parkinson's disease treatment. *J Control Release* 321:519–528
- Mackay SM, Myint DMA, Easingwood RA et al (2019) Dynamic control of neurochemical release with ultrasonically-sensitive nanoshell-tethered liposomes. *Commun Chem* 2(1):1–10
- Mani S, Swargiary G, Chadha R (2021) Mitophagy impairment in neurodegenerative diseases: pathogenesis and therapeutic interventions. *Mitochondrion*. <https://doi.org/10.1016/j.mito.2021.01.001>
- Mao P, Manczak M, Shirendeb UP, Reddy PH (2013) MitoQ, a mitochondria-targeted antioxidant, delays disease progression and alleviates pathogenesis in an experimental autoimmune encephalomyelitis mouse model of multiple sclerosis. *Biochim Biophys Acta* 1832(12):2322–2331
- Meyer O, Kirpotin D, Hong K et al (1998) Cationic liposomes coated with polyethylene glycol as carriers for oligonucleotides. *J Biol Chem* 273(25):15621–15627
- Miquel E, Cassina A, Martínez-Palma L et al (2014) Neuroprotective effects of the mitochondria-targeted antioxidant MitoQ in a model of inherited amyotrophic lateral sclerosis. *Free Radic Biol Med* 70:204–213
- Pandit A, Zeugolis DI (2016) Twenty-five years of nano-bio-materials: have we revolutionized healthcare? *Nanomedicine* 11(9):985–987
- Pardridge WM (2015) Blood–brain barrier endogenous transporters as therapeutic targets: a new model for small molecule CNS drug discovery. *Expert Opin Ther Targets* 19(8):1059–1072
- Park SY, Koh HC (2020) FUNDC1 regulates receptor-mediated mitophagy independently of the PINK1/Parkin-dependent pathway in rotenone-treated SH-SY5Y cells. *Food Chem Toxicol* 137:111163
- Park J-S, Davis RL, Sue CM (2018) Mitochondrial dysfunction in Parkinson's disease: new mechanistic insights and therapeutic perspectives. *Curr Neurol Neurosci Rep* 18(5). <https://doi.org/10.1007/s11910-018-0829-3>
- Patra JK, Das G, Fraceto LF et al (2018) Nano based drug delivery systems: recent developments and future prospects. *J Nanobiotechnol* 16. <https://doi.org/10.1186/s12951-018-0392-8>
- Peng Y, Chen L, Ye S et al (2020) Research and development of drug delivery systems based on drug transporter and nano-formulation. *Asian J Pharm Sci*. <https://doi.org/10.1016/j.ajps.2020.02.004>
- Qu M, Lin Q, He S et al (2018) A brain targeting functionalized liposomes of the dopamine derivative N-3,4-bis(pivaloyloxy)-dopamine for treatment of Parkinson's disease. *J Control Release* 277:173–182
- Ray B, Bhat A, Mahalakshmi AM et al (2021a) Mitochondrial and organellar crosstalk in Parkinson's disease. *ASN Neuro* 13:175909142111028364
- Ray B, Mahalakshmi AM, Tuladhar S et al (2021b) “Janus-Faced” α -synuclein: role in Parkinson's disease. *Front Cell Dev Biol* 9:1175
- Reeve AK, Grady JP, Cosgrave EM et al (2018) Mitochondrial dysfunction within the synapses of substantia nigra neurons in Parkinson's disease. *Npj Parkinson's Dis* 4(1):9
- Rehman M, Madni A, Shi D et al (2017) Enhanced blood brain barrier permeability and glioblastoma cell targeting via thermoresponsive lipid nanoparticles. *Nanoscale* 9(40):15434–15440

- Reijkerk A, Appeldoorn CCM, Rip J, de Boer M, Gaillard PJ (2014) Systemic treatment with glutathione PEGylated liposomal methylprednisolone (2B3-201) improves therapeutic efficacy in a model of ocular inflammation. *Investig Ophthalmol Vis Sci* 55(4):2788–2794
- Sainz V, Connot J, Matos AI et al (2015) Regulatory aspects on nanomedicines. *Biochem Biophys Res Commun* 468(3):504–510
- Sakhrani NM, Padh H (2013) Organelle targeting: third level of drug targeting. *Drug Des Devel Ther* 7:585–599
- Schnyder A, Huwyler J (2005) Drug transport to brain with targeted liposomes. *NeuroRx* 2(1): 99–107
- Schwarze SR, Ho A, Vocero-Akbani A, Dowdy SF (1999) In vivo protein transduction: delivery of a biologically active protein into the mouse. *Science (New York, N.Y.)* 285(5433):1569–1572
- Scudamore O, Ciossek T (2018) Increased oxidative stress exacerbates α -synuclein aggregation in vivo. *J Neuropathol Exp Neurol* 77(6):443–453
- Sercombe L, Veerati T, Moheimani F, Wu SY, Sood AK, Hua S (2015) Advances and challenges of liposome assisted drug delivery. *Front Pharmacol* 6:286
- Signorell RD, Luciani P, Brambilla D, Leroux J-C (2018) Pharmacokinetics of lipid-drug conjugates loaded into liposomes. *Eur J Pharm Biopharm* 128:188–199
- Smith RAJ, Murphy MP (2010) Animal and human studies with the mitochondria-targeted antioxidant MitoQ. *Ann N Y Acad Sci* 1201:96–103
- Smith RAJ, Murphy MP (2011) Mitochondria-targeted antioxidants as therapies. *Discov Med* 11(57):106–114
- Snow BJ, Rolfe FL, Lockhart MM et al (2010) A double-blind, placebo-controlled study to assess the mitochondria-targeted antioxidant MitoQ as a disease-modifying therapy in Parkinson's disease. *Mov Disorders* 25(11):1670–1674
- Solesio ME, Prime TA, Logan A et al (2013) The mitochondria-targeted anti-oxidant MitoQ reduces aspects of mitochondrial fission in the 6-OHDA cell model of Parkinson's disease. *Biochim Biophys Acta* 1832(1):174–182
- Song X, Liu S, Jiang Y et al (2017) Targeting vincristine plus tetrandrine liposomes modified with DSPE-PEG2000-transferrin in treatment of brain glioma. *Eur J Pharm Sci* 96:129–140
- Spuch C, Navarro C (2010) The therapeutic potential of microencapsulate implants: patents and clinical trials. *Recent Patents Endocr Metab Immune Drug Discov* 4(1):59–68
- Spuch C, Navarro C (2011) Liposomes for targeted delivery of active agents against neurodegenerative diseases (Alzheimer's disease and Parkinson's disease). *J Drug Deliv* 2011:469679
- Torchilin VP (2005) Recent advances with liposomes as pharmaceutical carriers. *Nat Rev Drug Discov* 4(2):145–160
- Torres-Ortega PV, Saludas L, Hanafy AS, Garbayo E, Blanco-Prieto MJ (2019) Micro- and nanotechnology approaches to improve Parkinson's disease therapy. *J Control Release* 295: 201–213
- Tran MA, Watts RJ, Robertson GP (2009) Use of liposomes as drug delivery vehicles for treatment of melanoma. *Pigment Cell Melanoma Res* 22(4):388–399
- Ventola CL (2017) Progress in nanomedicine: approved and investigational nanodrugs. *Pharm Therap* 42(12):742–755
- Wacker MG, Proykova A, Santos GML (2016) Dealing with nanosafety around the globe—regulation vs. innovation. *Int J Pharm* 509(1):95–106
- Wagle MA, Martinville LE, D'Souza GGM (2011) The utility of an isolated mitochondrial fraction in the preparation of liposomes for the specific delivery of bioactives to mitochondria in live mammalian cells. *Pharm Res* 28(11):2790
- Wang Z, Ling L, Du Y, Yao C, Li X (2019) Reduction responsive liposomes based on paclitaxel-ss-lyso phospholipid with high drug loading for intracellular delivery. *Int J Pharm* 564:244–255
- Wong HL, Wu XY, Bendayan R (2012) Nanotechnological advances for the delivery of CNS therapeutics. *Adv Drug Deliv Rev* 64(7):686–700
- Xie F, Yao N, Qin Y et al (2012) Investigation of glucose-modified liposomes using polyethylene glycols with different chain lengths as the linkers for brain targeting. *Int J Nanomedicine* 7: 163–175

- Yamada Y, Harashima H (2017) MITO-porter for mitochondrial delivery and mitochondrial functional analysis. *Handb Exp Pharmacol* 240:457–472
- Yamada Y, Akita H, Kogure K, Kamiya H, Harashima H (2007) Mitochondrial drug delivery and mitochondrial disease therapy—an approach to liposome-based delivery targeted to mitochondria. *Mitochondrion* 7(1–2):63–71
- Yamada Y, Akita H, Kamiya H et al (2008) MITO-Porter: A liposome-based carrier system for delivery of macromolecules into mitochondria via membrane fusion. *Biochim Biophys Acta Biomembranes* 1778(2):423–432
- You L, Wang J, Liu T et al (2018) Targeted brain delivery of rabies virus glycoprotein 29-modified deferoxamine-loaded nanoparticles reverses functional deficits in Parkinsonian mice. *ACS Nano* 12(5):4123–4139
- Zhang Y, He W, Du Y et al (2020) Dimeric artesunate phospholipid-conjugated liposomes as promising anti-inflammatory therapy for rheumatoid arthritis. *Int J Pharm* 579:119178
- Zhen X, Chu H-Y (2020) Emerging novel approaches to drug research and diagnosis of Parkinson's disease. *Acta Pharmacol Sin* 41(4):439–441
- Zylberberg C, Matosevic S (2016) Pharmaceutical liposomal drug delivery: a review of new delivery systems and a look at the regulatory landscape. *Drug Deliv* 23(9):3319–3329



Routes of Nano-drug Administration and Nano-based Drug Delivery System and Toxicity

25

Boobalan Gopu, Ramajayan Pandian, Angayarkanni Sevel, and Sanket Shukla

25.1 Introduction: Importance of Nanoparticle-Based Drug Delivery

Nanotechnology employs nanostructures as different forms of nanoparticles such as nanocapsules, nanospheres, nanorobots in nanomedicine for in vivo and in vitro imaging and detection, and nano-based drug delivery. Large-sized conventional therapeutic molecules may have poor solubility, absorption, bioavailability, fluctuation in plasma concentration, and in vivo stability with potential adverse effects related to improper target-specific delivery (Martinho et al. 2011; Jahangirian et al. 2017). Therefore, targeted drug delivery at the required concentration is required to resolve these challenges.

Nanoparticles are small-sized (1–100 nm) with stable and robust ligand interaction, high carrier capacity, and miscible with hydrophilic and hydrophobic substances. Nanoparticles are commonly used for biosensors, drug delivery, and tissue engineering application (Joseph and Venkatraman 2017; Patra et al. 2018). They exhibit high oral bioavailability and penetrate the target site due to their small size. Further, nanoparticles offer negligible side effects due to reduced interaction with other receptors. Drugs with poor solubility, absorption, and high receptor interaction are encapsulated with metallic, inorganic, and polymeric nanostructures for drug delivery to target sites (Mirza and Siddiqui 2014). Encapsulation of the small drug molecules with nanoparticles could be precisely delivered to target areas

B. Gopu · R. Pandian (✉) · S. Shukla
Pharmacology Division, CSIR-Indian Institute of Integrative Medicine, Jammu, India
e-mail: boobalan.g@iiim.res.in; p.ramajayan@iiim.res.in; sanket.shukla@iiim.res.in

A. Sevel
National Institute of Siddha, Chennai, India

© The Author(s), under exclusive license to Springer Nature Singapore Pte Ltd. 2023

P. V. Mohanan, S. Kappalli (eds.), *Biomedical Applications and Toxicity of Nanomaterials*, https://doi.org/10.1007/978-981-19-7834-0_25

671

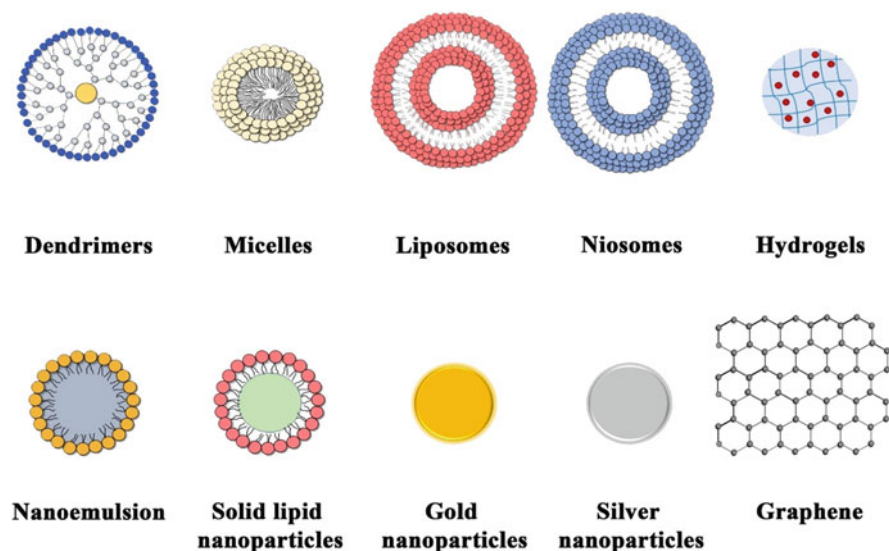


Fig. 25.1 Different types of nanocarriers

with controlled drug release administered by the convenient route (Lam et al. 2017; Patra et al. 2018).

Nanomaterials are classified into organic, inorganic, and carbon-based particles. The organic nanoparticles are further classified into polymer-based, lipid-based, and non-polymer. Polymeric nanoparticles (dendrimers, nanospheres, nanocapsules, and micelles) and lipid nanostructures (liposomes, niosomes, solid lipid nanoparticles, and nanoemulsions) are commonly used as targeted drug delivery systems (Watkins et al. 2015). Synthetic polymers, such as polylactic-*co*-glycolic acid (PLGA), polylactic acid (PLA), polyethylene glycol (PEG), and polyvinyl alcohol, as well as a natural polymers such as dextran, alginate, gelatine, agar, and chitosan, are extensively used in nanoparticles designing for targeted drug delivery (Watkins et al. 2015; Lombardo et al. 2019). Inorganic nanoparticles, mainly metals (gold and silver), silica, and quantum dots, are widely explored for diagnosis and treatment. Polymeric nanospheres, microspheres, liposomes, and nanoemulsion-based formulations significantly affected *in vivo* experimentations with long-acting potential. Some nano-based drug delivery systems were clinically approved by Food and Drug Administration, the USA, for cancer treatments (Fig. 25.1).

Nano-drug formulations are designed to reach the target site by two mechanisms: passive and self-delivery. Passive delivery implies that the drugs are incorporated within the hydrophobic cavities of the structures and are released at the particular target sites. The self-delivery represents the conjugation of the drug with the structures for fast delivery. However, the timing of the release may affect the bioactivity and efficacy as the drug may not reach the target site (Lu et al. 2016; Patra et al. 2018). Due to their small size, nanoparticles cross various biological

Table 25.1 Advantages and disadvantages of drug delivery system

Advantages of drug delivery systems	Disadvantages of drug delivery systems
Increase aqueous solubility and stability	Immune reaction against carrier systems
Improve bioavailability/residence time	Diffusion and redistribution of released drugs
Minimal drug degradation and loss	Requires sophisticated technology for formulation preparation
Produce a sustained release	Inexpensive
Reduced systemic toxicity with an increased therapeutic index	Requires skill for formulation preparation, storage, administration
Offer rapid formulation development	Possibility of skin irritation and damage at the site of application
Administration through all routes	Requirement of repeated patch application due to change in body temperature
Able to cross biological barriers	Poor in vivo and in vitro correlation
Avoidance of hepatic first-pass metabolism	
The dose is less compared to conventional drug delivery systems.	
Selective targeting to tumor cells only	
Reduction in frequency of dosing	
Prolonged duration of action	
More uniform plasma levels	
The flexibility of terminating dosing using the patch method	
Improved drug absorption	
Easy and self-administration, high patient compliance	

barriers and disrupt the typical cell environment (Khan et al. 2019). Further, the success of the treatment with a targeted delivery system depends on the physiological and biochemical properties of the selected therapeutic drugs. For efficient drug delivery, designing the nanoparticles with their characteristic physicochemical properties (size, viscosity, electric charge, and surface area) to improve safety with higher efficacy is required to enter into the gastrointestinal, respiratory, ocular, and integumentary systems (Table 25.1).

Numerous studies are still under investigation in developing efficient drug delivery systems to treat various diseases and successfully deliver drugs to target sites (Obeid et al. 2017). Most of the nano-drug-based delivery systems were intensively studied on the effective action of the drug in the cancer environment for severe cancer disease treatment. In recent years, nanomedicine has gained importance because nanostructures are used for drug delivery by encapsulating or attaching therapeutic agents to the target sites. Drug designing at the nanoscale is of greater interest due to the substantial potential to modify the drugs' bioavailability, solubility, immunogenicity, and diffusivity.

25.2 Routes of Nano-drug Delivery

Various drug delivery routes are employed for treating the diseases depending on the physiological and biochemical properties of the drug, usage in emergency conditions, and individual medical conditions (Fig. 25.2).

25.2.1 Oral Route of Drug Delivery

Oral ingestion is the most preferred and frequently used delivery method for nano-drug delivery. The advantages of the oral route are self-administration, flexibility in dosage regiment, convenience, and being devoid of sterile environments favors high compliance in chronic disease treatments. The gastrointestinal tract provides a considerable retention time, extensive surface area (300–400 m²), and blood supply for drug absorption (Kararli 1995; Ensign et al. 2012; Pridgen et al. 2015). However, many oral-based molecules have already been withdrawn in preclinical studies due to their poor efficacy, poor absorption, inter-/intra-subject variations in pharmacokinetic profile, and inadequate in vivo stability in gastric pH environments. Moreover, oral administration of hydrophobic and hydrophilic drugs also attributes to poor bioavailability due to their inadequate physicochemical and pharmaceutical properties. Recent studies have shown that encapsulation of drugs in nanoparticles improved oral bioavailability, resisting gastric enzymes and pH degradation and absorption of hydrophilic, hydrophobic, and biologic drugs (Kalepu et al. 2013; Pridgen et al. 2015). This section explains the effect of the nanoparticle formulations using nanocarriers such as polymers, dendrimers, and liposomes in the gastric, small intestinal, and colon environments.

25.2.1.1 Stomach Targeting Drug Delivery

Nanotechnology aids in target-based therapy and improves the absorption, bioavailability, and treatment of gastrointestinal tract (GIT) infections such as inflammatory bowel diseases, gastric cancer, gastric polyps, and *Helicobacter pylori* infections. Gastric retention of the administered nanoparticles depends on gastric/intestinal motility, the fed/fast state of the individuals, type of the ingested food, disease states, gastric pH, and mucus (Cone 2009; Gelberg 2014). For effective stomach targeting, nanoparticles should overcome these physiological barriers.

Polymers are linear in shape, biocompatible, biodegradable, and pH-responsive, comprised of *N*-vinylpyrrolidone, polyethylene glycol, and chitosan. Recent research on gastro-retentive delivery systems is focused on mucoadhesion and mucopenetration of nanoparticles in the stomach. Mucoadhesive formulations are designed to extend the drug residence time in the GIT, which allows sustained drug release and absorption. Chitosan is a mucoadhesive polymer complexed with polyanions to resist acidic pH and deliver the medications to mucosal surfaces. Chitosan is complexed with fucose, polyethylene glycol (PEG), gelatin, and epigallocatechin gallate (EGCG) to improve the gastric retention of EGCG in orthotopic gastric and Ehrlich Ascites tumor mouse models (Lin et al. 2015).

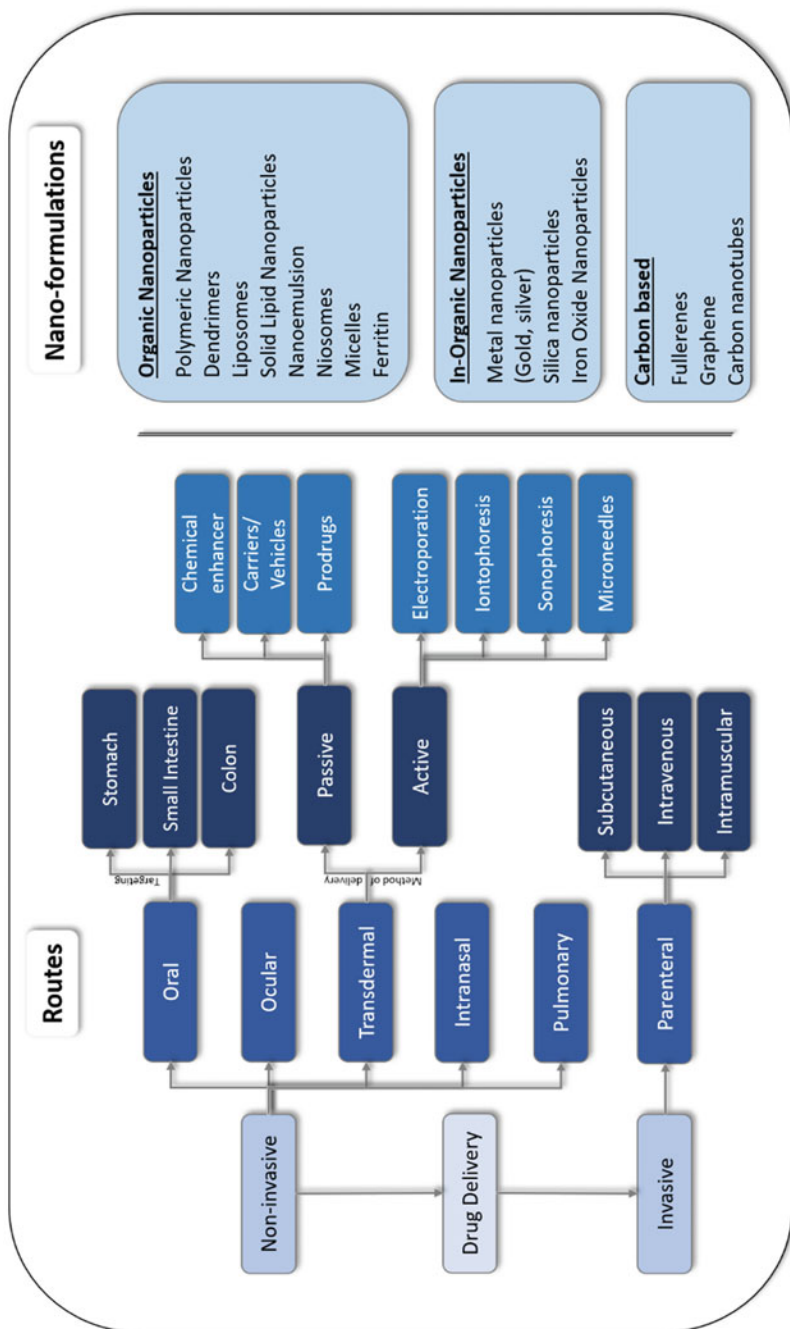


Fig. 25.2 Routes and formulations used for nano-drug delivery

However, continuous mucus production protects the gastric epithelium against luminal content acidity, xenobiotics, and drugs, including nanoparticles (Cone 2009; Ensign et al. 2012). Loosely adherent nanoparticles in the stomach lumen are washed off, resulting in less chance of interactions of nanoparticles with the mucosa. The success of eradicating *Helicobacter pylori* infections depends on the penetration and delivery of drugs through the mucus barrier as the bacteria are situated deep inside the gastric mucosa (Bardonnet et al. 2006). Preclinical studies are mainly targeted to achieve mucus penetrating formulations for improving gastric retention.

25.2.1.2 Small Intestine Targeting Drug Delivery

The small intestine consists of enterocytes, goblet cells, and microfold cells (M cells). M cells transport bacteria, viruses, and nanoparticles from Peyer's patches to subepithelial mucosa. Enterocytes are abundant and used for target drug delivery in the small intestine. Goblet cells produce mucus, a protective barrier that removes the adherent nanoparticles from reaching the cell surface. Nanoparticles coated with enteric polyanionic polymers are sensitive to acidic gastric pH and dissolve gradually in intestinal pH to release the drug into the small intestine (Yoshida et al. 2013). Nanoparticles coated with polyethylene glycol (PEG), enzymes (papain), thiols, and vitamin B12 are used to improve mucus penetration in the small intestine (Date et al. 2016). Insulin is sensitive to gastric pH, and degradation occurs within 5 min. Insulin coated with chitosan-tripolyphosphate resisted 10% degradation up to 30 min, whereas the insulin coated with chitosan-hydroxypropyl methylcellulose phthalate resisted 40% degradation up to 120 min. Insulin-loaded solid nanoparticles (SLN) with vitamin B12 conjugates decreased the blood glucose concentration and provided more oral bioavailability than the subcutaneous route in diabetic rats (He et al. 2015). A similar study employed calcium phosphate nanoparticles coated with sodium alginate and chitosan conjugated with/without vitamin B12. Previous studies showed that nanoparticles conjugated with Vit B12 increased insulin uptake and ileal location compared to unconjugated nanoparticles. Similarly, these conjugated nanoparticles produced comparable anti-glycemic activity to subcutaneous than oral route, demonstrating the potential effect of vitamin B12 in mediating insulin absorption (Verma et al. 2016).

25.2.1.3 Colon-Targeted Drug Delivery

Colorectal Disease, a significant health problem, is an uprising in more industrialized and developed nations. Colorectal disease involves the irritation and inflammation impacting the colon or rectum like inflammatory bowel diseases (IBD), colon cancer, diverticulitis, and polyps. Among these diseases, colorectal cancer causes the fourth largest cancer death and is expected to cause 1.1 million deaths by 2030 (Arnold et al. 2016). Targeting the colon to minimize metabolic degradation and absorption in GIT before reaching the colon improves the drug delivery to colorectal tissues. Nanoparticles resist various digestive enzymes and pH variations in the colon, allowing for effective drug release. pH-sensitive polymers are designed to release the drug molecules in the pH range of 6–7 to achieve colon-targeted drug

delivery systems. Intrarectal administration of glucocorticoids such as hydrocortisone, dexamethasone, and methylprednisolone are commonly prescribed for treating ulcerative colitis (Philip and Philip 2010).

Numerous efficacy studies have investigated the protective role of nanoparticles and polymers (pH, water, and enzyme sensitive) in the TNBS and DSS colitis model to increase drug delivery to the colon (Beloqui et al. 2014; Gugulothu et al. 2014). Drugs are encapsulated with polymers for sustained drug release and protection against the harsh GIT environment. Encapsulated nanoparticles are used as anti-tuberculosis drugs and promote insulin release in GIT (Pandey et al. 2003). Reactive oxygen species are found predominant in inflamed colon tissues during inflammatory bowel disease conditions. The administration of nanoparticles coated with ROS-sensitive materials can accurately deliver the drugs to the inflamed areas in the colon (Date et al. 2016).

The human colon harbors a diverse anaerobic bacterial population responsible for fermenting undigested food contents using galactosidase, glucuronidase, xylosidase, azoreductase, nitroreductase, urea hydroxylase, and deaminase (Cummings and Englyst 1987). Azoreductase cleaves the azo bond orally administered sulfasalazine to 5-aminosalicylic acid and sulfapyridine to treat inflammatory bowel disease. Azo compounds are administered as hydrogel carries for colon targeting. Oral-administered nanoparticles are coated with natural polysaccharide polymers (pectin, alginic acid, guar gum) or azo monomers to increase the bioavailability and reduce side effects in colon-targeted drug delivery systems (Zhang et al. 2016).

25.2.2 Nanocarriers in Oral Route

25.2.2.1 Dendrimers

Dendrimers, a three-dimensional symmetrical monodispersed polymer with a high branching rate, consist of a central nucleus, the repeated branch of units from the nucleus, and numerous terminal functional groups on the dendrimer surface (Madaan et al. 2014). Drugs incorporated into specific carriers (dendrimers) could increase oral bioavailability (permeation through the biological barriers) and decrease the adverse effects of therapy. Dendrimers are commonly used as nanocarriers because of their high bio-adhesive characteristics (drug retention in the intestine), resorption in the digestive tract, metabolic degradation resistance, and minimal interaction with the food and plasma proteins. Dendrimers have unique properties, as they possess functional groups on the surface for interaction with therapeutic drug molecules and retain the drug's efficacy and specificity at the target site (Santos et al. 2019). Dendrimers are most prescribed orally for treating hypolipidemic and anti-cancer activity.

25.2.2.2 Liposomes

Liposomes are spherical vesicles made up of lipid bilayers filled with water. Liposomes are used as carriers for transporting both lipophilic and hydrophilic drug molecules. Oral liposomal molecules are of interest to evaluate anti-cancer

activity because of their biocompatible, biodegradable, and nontoxic properties. Anti-cancer drugs such as doxorubicin, cisplatin, oxaliplatin, and carboplatin are encapsulated in liposomes for large biodistribution and delivery to the target site (Abraham et al. 2005). Disadvantages concerned with liposomes are poor permeability, slow release of the drug, and degradation by gastric acid and enzymes.

25.2.2.3 Others

Spirolactone, an aldosterone antagonist and potassium-sparing diuretic, shows poor absorption in patients due to its poor solubility and dissolution rate. However, the drug loaded with poly(ϵ -caprolactone) (PCL) showed improved solubility of the drug (Limayem Blouza et al. 2006).

Differences in gastrointestinal tract physiology between laboratory animals and humans such as gastric motility, enzymes, pH, fluid volume, bacterial populations, mucus secretion, location, and the number of Peyer's patches should also be considered while designing the nanoparticles (Kararli 1995). Other characteristics of the nanoparticles such as size, shape, surface charge, density, and materials affect mucus penetration and are also considered for designing nanoparticles (Mitchell et al. 2021).

25.2.3 The Transdermal Route of Drug Delivery

The transdermal drug delivery system delivers drugs through the skin surface into a systemic circulation system to produce sustained dose concentration at the target site. The transdermal drug delivery system helps dispense effective therapeutical doses to the targeted site of action, which could be utilized for localized treatment for specific tissues or generalized therapeutics of diseases. Transdermal delivery provides many benefits such as high patient compliance, inexpensive, self-administration, noninvasive/less painful than oral and hypodermic needle injection of therapeutic drugs (Prausnitz and Langer 2008; Palmer and DeLouise 2016). The pharmacological effects are equivalent to the intravenous route concerning bioavailability at the site of action. The transdermal route was preferred for drugs with poor solubility and absorption and bypass first-pass hepatic metabolism, standard in orally administered drugs. The advantage of the transdermal route of drug delivery compared to other parental routes of administration are administration with specialized equipment, sustained controllable release of the drugs for more extended periods with reduced toxicity, and frequency of administration (Samad et al. 2009). It is the preferred route of application for molecules that are easily affected by the gastric and intestinal fluids, which reduces the concentration, bioavailability, and alters the active pharmacological efficiency of the drug when administered through the oral route. It is also suitable for drugs possessing less molecular weight (<500 Da), exhibiting affinity in both lipophilic and hydrophilic states, shorter biological half-life, and non-irritant in nature (Chenthamara et al. 2019).

Only small molecular-sized and lipophilic-formulated topical medications permeate effectively through the skin barrier to treat local medical conditions with

decreased toxicity. Large molecules are not suitable for transdermal application as they cannot penetrate the outer layer of the skin (Prausnitz and Langer 2008). Other drawbacks of this route are not suitable for delivering ionic drugs. It generates lower blood concentration levels and inhibits drug formulation development and the chance of skin irritation and skin allergies due to long-term patch application in the skin. The development of transdermal delivery systems started with transdermal patches in clinical applications related to the conditions such as reproductive disorders, motion sickness, chronic pain, hypertension, Parkinson's disease, and dementia.

25.2.3.1 Anatomy of the Skin

Healthy skin provides a barrier to infection, protects it from ultraviolet, physical, chemical hazards, and regulates thermoregulation and trans-epidermal water loss. The largest organ, skin, consists of three distinct layers: the avascular epidermis, the vascular dermis (the site of systemic drug absorption due to abundant capillary vasculature), and hypodermis or subcutaneous contains fat and connective tissues (Wysocki 1999). The epidermal layer consists of five different epithelial cells. The stratum corneum is the outermost layer of the skin that appears in a brick-and-mortar structure. The brick shape is represented by a dead corneocyte containing non-linked keratin, whereas the latter represents the intercellular lipids in a bilayer formation (Wysocki 1999; Mojumdar et al. 2017). The structure of the stratum corneum and its lyophilic nature develops a barrier defense mechanism to prevent the entry of any foreign bodies into the system. This mechanism makes the transdermal mode of drug delivery difficult because few drugs have the physicochemical property to diffuse through the stratum corneum layer in sufficient concentration to achieve the therapeutic dose. The usage of some molecules is limited due to the poor stability, solubility, and diffusivity of the formulation through the thick stratum corneum lipid bilayers (Prausnitz and Langer 2008).

25.2.3.2 Drug Transportation Across the Skin

The mode of drug transportation occurs from the stratum corneum epidermal layer into the system through three different pathways, i.e., intercellular, intracellular or transcellular, and trans-appendageal pathways. Drug absorption occurs via the intercellular route via lipid particles found in the intercellular regions of the keratinocytes. In the intracellular or transcellular pathway, the transportation of the molecules occurs through the keratinocytes and lipid layers. The molecules diffuse through sebaceous glands, hair follicles, and sweat glands through trans appendageal routes (Desai et al. 2010).

The appendages of the skin are of significantly less quantity in the skin surface region and are never considered as the route of drug penetration. However, certain studies proved that more prolonged exposure of the molecules expressed better absorption through appendages. The drugs exhibiting lipophilic characteristics pass the stratum corneum through the lipid bilayer (intracellular pathways). In contrast, the drugs possessing a hydrophilic nature pass by penetrating through the stratum corneum epithelial layer (transcellular pathway). The hydrophilic and

lipophilic molecules diffuse the stratum corneum through the lipid head and tail regions, respectively (Gupta and Babu 2013).

25.2.4 Nanocarriers in Transdermal Route

Nanotechnology plays a significant role in enhancing the transportation of drugs that possess lower transdermal permeation characteristics with the help of different nanocarriers, which can be coupled with the drugs based on their appropriate chemical nature. The recent advancement in nanocarriers and new transdermal permeability enhancement technologies has increased research on transdermal drug delivery. Nanocarriers such as polymer nanoparticles, dendrimers, niosomes, ethosomes, transferosomes, nanoemulsions, and liposome applications are commonly used for transdermal delivery (Chenthamara et al. 2019).

Nano-based delivery improves skin permeability with the enhanced transportation of drugs and reduces damage to deeper areas (Prausnitz and Langer 2008). The factors influencing the bioavailability of molecules applied through the transdermal route are physiological factors that include the skin (age, hydration, and metabolism rate), blood flow in the surface, and the region in which the scaffolds are applied. Secondly, the formulation factors and suitability of nanocarrier, either liposomes, polymers, or nanoemulsion, are determined based on the nature of the molecules, i.e., the particle size and shapes, its physical stability, the required rate of drug release into the system, and appropriate permeation drug absorption enhancers. Thirdly, the drug and nanocarriers' physicochemical properties such as drug dose concentration, pH, molecular parameters (size and weight), and shape of the nanoparticle conjugated molecules. The pharmacokinetics of the drugs in the stratum corneum also affects the bioavailability, and determining the dermatopharmacokinetics helps assess the number of drugs required to achieve efficacy. Nanocarriers offer a better pharmacokinetic profile with a high surface area to volume ratio without causing toxicity. Drugs are formulated and loaded with nanoparticles to improve drug release at specified intervals and reduce drug dosing regimens and systemic effects (Samad et al. 2009).

Nevertheless, the problems associated with nano-drug delivery are reversible damage to the stratum corneum lipid bilayer, increased skin irritation, failure to transport large and hydrophilic molecules. Incidentally, disrupted skin favors enhanced nanoparticle penetration, as seen in inflammatory skin diseases like psoriasis and atopic dermatitis (Palmer and DeLouise 2016). Nanocarrier-based drugs such as tacrolimus are already approved for topical administration for psoriasis and atopic dermatitis. Tacrolimus, immunosuppressive calcineurin inhibitors offer greater dermal penetration when administered loaded with polymeric micelles, microemulsions systems, and liquid crystalline nanoparticles (Lapteva et al. 2014).

25.2.5 Methods of Transdermal Drug Delivery

The methods of transdermal drug delivery for effective skin permeation are classified into two enhancers: passive/chemical enhancer and active/physical enhancer. Effective concentration through topical, dermatological, and cosmetic applications is achieved by designing formulations with these chemical or mechanical enhancers (Prausnitz et al. 2004).

25.2.5.1 The Passive Method of Transdermal Delivery

The passive method refers to the diffusion of drugs through the stratum corneum with the help of chemical enhancers or nanocarriers, which increases the permeability in the outer layer for easy absorption and distribution of the compounds without affecting the integrity of skin structure.

25.2.5.1.1 Chemical Enhancers

Chemical enhancers are formulation-based, used to improve the thermodynamic activity of the drug in the formulation facilitating entry into the skin (Prausnitz and Langer 2008; Mathur et al. 2010). The chemical-based permeation enhancement occurs through different action modes like increasing the lipid layer's viscosity in the stratum corneum, intracellular protein interactions, and intracellular lipid removal. Also, chemical enhancers permeate the skin with the drugs improving the skin permeability, drug partitioning into the skin, and increasing drug solubilization. The commonly used chemical enhancers for improving penetration are alcohols, oils, terpenes, terpenoids, and fatty acids (Mathur et al. 2010). The main disadvantage of this method is the transport of low molecular weight drugs (<500 Da), reduced efficacy, and adverse effects like skin irritation and damage. These disadvantages are overcome with nanotechnology using nanocarriers such as liposomes, transferosome, and ethosome, which enhance the absorption, efficacy, and dose-dependent concentration into the system with minimal toxicity effect. Chemical enhancer combinations at specific compositions are developed to increase anti-cancer drugs' permeability and reduce damage to the deeper tissues. Kim et al. (2007b) studied magainin, a bacterial cell wall pore-forming peptide drug combined with surfactant chemical enhancers. *N*-lauroyl sarcosine (NLS), an anionic surfactant in 50% ethanol solution formulations, enhanced drug concentrations into stratum corneum and drug, increasing the permeability into the skin through reversible lipid disruption.

25.2.5.1.2 Prodrugs

Prodrugs are inactive, a bio-reversible chemical derivative of parent drugs in which the chemical groups are modified/added with promoiety. Prodrug methods employ the addition of side chains with cleavable linkers to one or more drugs. Prodrug under enzymatic or chemical reactions and elicit desired pharmacology effect of active drug molecules in the body. Prodrugs provide advantages such as increased solubility, stability against degradation, and effective penetration into the skin. The

facts associated with these methods are increased lipophilicity and molecular weight and decreased hydrophilicity and irritation (Sloan et al. 2006).

25.2.5.1.3 Carriers and Vehicles

Hydrogels

Hydrogels, a polymeric nanoparticle formulation applied to the wound as dressing materials for absorbing wound exudates and foreign bodies. Hydrogels treat dry and necrotic wounds and surgical, burns, and diabetic ulcer wounds (Kamoun et al. 2017). Poly (amidoamine) (PAMAM) dendrimers are spherical, tree-like branching with repetitive subunits of amide and amine and terminal groups on the surface. In recent years, PAMAM application is steadily increased in drug design and development and diagnostics due to inherent factors such as biodegradability, biocompatibility, nontoxicity, and multifunctionality. Effective skin permeation and topical drug delivery depend on the dendrimer size, generation, molecular weight, surface charge, and hydrophobicity. Dendrimers are promising transdermal nanocarriers developed for anti-cancer, antipsoriatic, NSAID drugs, and vitamins (Cheng et al. 2007).

Liposomes

Liposomes are spherical-shaped vesicles in a colloidal structure made up of phospholipid bilayers with nontoxic physiochemical and biochemical properties with better biocompatibility and efficiency to conjugate more load of drugs. Liposome application hydrates the skin contributing the lipids into the stratum corneum layer. Drugs are incorporated into the flexible liposomal formulations to reach the deepest layers of the skin and systemic circulation. The liposome has unique properties in that it can transport both hydrophilic drugs (within the core) and lipophilic drugs (between the lipid bilayer). Liposomal formulations penetrate the skin through passive diffusion and increase permeability through percutaneous absorption. Much investigational research attempts to prepare liposome-based drug combinations with anti-cancer properties such as daunorubicin, doxorubicin, paclitaxel, cisplatin, and vincristine. It is also combined with other drugs such as lornoxicam, sulfinamide, amphotericin B, chlorophyll, and vitamin A (Lombardo et al. 2016).

Vaccines

The nanocarrier-based vaccine preparation for transdermal application is part of research for developing booster-free or needle-free vaccination technologies. Transdermal delivery of the vaccines is designed to improve the immune response and bioavailability by targeting epidermal Langerhans and dermal dendritic cells. The nanocarriers like liposomes resist antigen degradation and promote the antigens uptake by the immune cells. The nanoformulations develop sustained antigen release into the tissue for better immunity to develop and avoid booster doses. Alternating painful hypodermic injection with patches application may expedite the vaccination in developing countries (Hansen and Lehr 2012).

Others

Transferosomes, niosomes, and ethosomes are lipid-based compounds developed to improve efficiency and penetration into the skin layer (Chenthamara et al. 2019). Cosmetic formulations such as nano-sized titanium dioxide and zinc oxide are developed as sunscreens against harmful ultraviolet radiation, whereas silica-based nanoparticles and fullerenes are used as desiccants or free radical scavengers (Smijs and Pavel 2011; Contado 2015).

25.2.5.2 The Active Method of Transdermal Delivery

The active method is the mechanical approach of improving skin permeability using physical enhancers such as electroporation, iontophoresis, sonophoresis, microneedles, laser, radio-frequency, and tape-stripping method for effective delivery of drugs and vaccines. The advantage of the active method is that the duration of action from the point of application to the targeted effect is relatively reduced compared to the passive method (Alkilani et al. 2015). Electroporation and iontophoresis imply electric current application to transport the drug into the skin and vary with the intensity and duration of the application.

25.2.5.2.1 Electroporation

Transdermal electroporation (electro-permeabilization) induces temporary perturbation of the skin by applications of high voltage pulses for a concise duration. Applying a high electric current to the lipid bilayers increases transmembrane transport (Denet et al. 2004; Ita 2016). Electroporation effectively transports ionic and non-ionic compounds, and it depends on the number, intensity, shape, and duration of the pulses and distance between electrodes. Short, high-voltage electric burst applied in transdermal electroporation is more effective than low constant voltage application of iontophoresis in transdermal delivery (Ita 2016). Electroporation effects are rapidly reversible. Denet et al. (2003) reported that the electrical application of pulses (electroporation protocol) to the stratum corneum increased five times the flux of timolol, a nonselective beta-adrenergic antagonist used to reduce intraocular pressure in the eye compared with passive diffusion. Also, the electrical resistance moves from the stratum corneum to the deeper tissues and induces pain and muscle stimulation in the skin. This method delivers small drugs, peptides, vaccines, and high molecular weight biopharmaceuticals through temporary aqueous pores into the skin (Denet et al. 2004).

25.2.5.2.2 Iontophoresis

In clinical applications, iontophoresis is the consistent application of moderate alternating electric current to enhance drug penetration through/into the skin. The applicability of the methods depends on the physicochemical properties and magnitude of the magnetic field related to the rate of drug delivery. Iontophoresis involves the movement of charged and uncharged drugs across the skin into systemic circulation (Ita 2015a). It involves two primary mechanisms, electromigration and electroosmosis. Iontophoresis transports large peptides and hormones such as insulin, calcitonin, vasopressin, thyrotropin-releasing hormone, and luteinizing

hormone-releasing hormone into the skin impossible through transdermal passive diffusion. Iontophoresis is applied for local anesthesia administration, treating hypo/hyper-drosis, and extracting interstitial fluid from the skin to monitor glucose (Kalia et al. 2004). Reverse iontophoresis mechanism is applied to transport the glucose from the interstitial fluid and the sensor implanted into the skin measures the glucose concentration (Koschinsky and Heinemann 2001).

25.2.5.2.3 Sonophoresis

Sonophoresis is an application of ultrasound for drug delivery classified into low, intermediate, and high frequency. These ultrasound-based pressure fields increase permeation through stratum corneum lipid structure (Ita 2015b). Non-cavitation ultrasound acts as a driving force to transport the drugs into the skin and increase permeability. Its advantages are limited due to the transport of only small and lipophilic compounds and the chance of tissue healing and damage. Cavitation ultrasound creates bubbles that oscillate and collapses at the skin surface and disrupts the stratum corneum lipid structure to improve the skin permeability. These transdermal drug delivery methods are developed to deliver insulin, heparin, lidocaine, and tetanus toxoids vaccines through the skin (Ogura et al. 2008). Phonophoresis, a physical therapy, employs topical administration of drugs and ultrasound for treating inflammation and pain in muscles, joints, and ligaments (Machet and Boucaud 2002).

25.2.5.2.4 Microneedles

Microneedles create micron-sized pathways into the dermal region to distribute the drug into systemic circulation. Microneedles are coated/encapsulated with the drug formulations for rapid/controlled release of macromolecules into the skin and increase skin permeability (Kim et al. 2012; Waghule et al. 2019). Advantages associated with microneedles are self-administration, controlled drug release, rapid onset of action, improved permeability, and efficacy. Solid microneedles are replaced with hollow and dissolving polymer-based to minimize the pain associated with the penetration into the skin and dissolving in the injection site minimizing medical waste (Prausnitz and Langer 2008; Ita 2015c). This system was applied to deliver insulin, vaccines, parathyroid, and oligonucleotide molecules using dip-coated microneedles (Gill and Prausnitz 2007). Preclinical studies established the effective delivery of live attenuated, inactivated virus, protein, and DNA units using solid and hollow vaccines using microneedles, especially influenza prophylaxis (Prausnitz and Langer 2008).

25.2.5.2.5 Others

Other methods of physical permeation, such as thermal ablation and microdermabrasion, employ alteration to the stratum corneum architecture. Thermal ablation explains heating the skin surface above the water boiling point for micro to milliseconds to induce a crater in the stratum corneum to deliver the drugs. Clinical trials proved the effectiveness of thermal ablation in the transport of growth hormones, insulin, and interferons. Microdermabrasion alters and damages the

skin structure to increase drug permeability, including lidocaine, 5-fluorouracil, and vaccines (Prausnitz and Langer 2008).

Transdermal drug delivery offers great potential to address low bioavailability, painful/invasive administration, and desired drug release. Advantages of this delivery include increased permeability targeted stratum corneum disruption at the expense of damage to the stratum corneum and deeper tissues. Scientific advances involve developing and applying epidermal patches, chemical and physical enhancers to deliver small macromolecules and vaccines. Effective delivery of hydrophilic drugs, large peptides, and macromolecules, including siRNA and DNA into/through the skin, still poses a vital challenge.

25.2.6 Ocular Route of Drug Delivery

Ocular drug delivery offers localized delivery of the drug into the eye. It is challenging to attain the desired therapeutic concentration for a more extended period concerning eye diseases. Localized administration of the drug to the target site avoids the drug dispersion to the surrounding tissues producing the maximum efficacy out of the dosing regimens and reducing the systemic toxic effects (Gaudana et al. 2010). Topical instillation of the drugs is most preferred due to its simplicity, compliance, safety, and noninvasiveness for anterior segment diseases. Most marketed ophthalmic developed as conventional eye drops are aimed to treat the anterior segment of the eye. The complexity of drug formulation and delivery to the eye is limited by tear dilution and turnover, reflex blinking, and nasolacrimal drainage. They possess significant challenges resulting in decreased penetration, bioavailability, and duration of the drug on the ocular surface (Gaudana et al. 2010; Joseph and Venkatraman 2017). Eye drops required high concentration and longer contact time in the precorneal area for passive diffusion to effectively corneal permeation. The unique anatomical architecture of the eye prevents the drugs from entering the eye allowing around 5% of administered drug into the eye. The drug delivery into the posterior segment is still the most challenging task for pharmacological scientists due to barriers. It is only achievable by intravitreal and periocular injections and systemic administration (Kim et al. 2007a; Bochot and Fattal 2012).

Conventional drugs are water-soluble drugs applied as solutions, suspensions, emulsions, lotions, and ointments, effective against eye anterior segment diseases. The small volume of these drugs is to be administered due to the capacity of the cul de sac, and it indirectly affects the absorption. The excess volume of the drug is removed by nasolacrimal or gravity-induced drainage within a few seconds after instillation (Gaudana et al. 2010). Conventional drug formulations are modified to include enhancers to increase the drug permeation and viscosity into the anterior segment of the eye. Various drug molecules are associated with nanocarriers, such as liposomes, hydrogel, solid nanoparticles, dendrimers, polymeric micelles, and inorganic nanoparticles, to cross the ocular barriers and achieve the desired concentration at the target site. These drugs are also encapsulated to resist the degradation to reach the target site (Weng et al. 2017; Joseph and Venkatraman 2017).

A clear understanding of the eye structure, its barriers, and the associated physicochemical properties of the drug provides a breakthrough for the ocular delivery system. This section explains the novel approaches to improve ocular drug delivery of drugs and the recent developments in nanomedicine for targeting ocular diseases.

25.2.6.1 Anatomy of the Eye

The human eye is made up of two chambers: anterior and posterior. The anterior segment includes the pupil, ciliary body, lens, cornea, and aqueous humor, whereas the latter consists of the retina, choroid, sclera, vitreous humor, and optic nerve. Numerous barriers impede the entry of the drug molecules/fluids into the retina, such as corneal and conjunctival epithelium, blood-aqueous, and blood-retinal barriers. The transparent corneal epithelium acts as a physical barrier for hydrophilic drugs and consists of multilayer epithelial cells with tight junctions. The anterior and posterior segments of the eye include the blood-aqueous and blood-retinal barriers, respectively. Both barriers are provided with tight junctions, which pose obstacles to the drugs' ocular delivery into the systemic circulation. The blood-aqueous barrier permits the permeation of small molecules into aqueous humor through capillaries in the ciliary process. A layer of retinal pigment epithelial cells and capillary endothelial cells forms the blood-retinal barriers. These cells forbid the entry of the molecules into the posterior segment and systemic circulation due to inheriting protective property (Cunha-Vaz 1979; Weng et al. 2017).

Intravitreal injections are commonly prescribed for treating posterior ocular diseases. They pose demerits such as repeated painful puncture of the vitreal humor and associate adverse effects such as hemorrhage, poor patient compliance, and retinal damage (Bochot and Fattal 2012). The periocular administration route with transscleral drug delivery has developed to deliver drugs to the posterior ocular tissues (Kim et al. 2007a). The significant advantages of conventional ocular drug delivery include needle-free application, self and painless medication of topical preparations. The poorly absorbed oral drug administered through ocular delivery undergoes no first-pass hepatic metabolism and gastric metabolism, which helps in accurate and reduced dosing. The disadvantages of this delivery are poor permeability and low bioavailability of drugs attributed to physical barriers, tear, and nasolacrimal drainage (Qamar et al. 2019).

25.2.7 Nanocarriers in Ocular Route

Nanocarriers such as liposomes, dendrimers, niosomes, solid lipid nanoparticles, and inorganic nanoparticles are encapsulated with drugs to improve the drug thermodynamic activity targeting ocular diseases (Qamar et al. 2019). The unique structure of liposomes with phospholipid bilayers with an aqueous phase helps transport both hydrophilic and hydrophobic drugs. Topical instillation of liposomal formulations consists of bioadhesive polymers that improve corneal adherence, penetration, and targeted distribution to the action site. Ocular drug delivery of liposomal

formulations is designed using liposome size and charge, and fluidity of lipid bilayers. Positively charged liposomes induced more corneal permeation than negative/no charged liposomes (Mishra et al. 2011). Various studies are performed with liposomes loaded with triamcinolone acetate, ibuprofen, and voriconazole to treat macular edema, anti-inflammatory, and fungal keratitis.

25.2.7.1 Niosomes

Like liposomes, niosomes, a primary lipid vesicle composed of nonionic surfactants, possess unique properties to hold hydrophilic and lipophilic compounds. However, niosomes are biodegradable, non-immunogenic, more stable, inexpensive with extended storage time at nonspecified conditions, and reduced side effects compared to liposomes as nanocarriers. Numerous factors affect the physicochemical properties of niosomes, such as surfactants, hydration temperature for preparation of niosomes, physicochemical properties of encapsulated drug, amount and type of surfactant, and cholesterol content and charge in niosomal formulation (Kazi et al. 2010). Niosomes formulations are beneficial in treating ocular infection, glaucoma, and ocular hypertension and can be used as carriers for drugs with poor absorption and penetration. Allam et al. (2019) developed a vancomycin niosomal formulation into a gel for treating methicillin-resistant *Staphylococcus aureus* (MRSA) infections in rabbits. Developed formulations provided increased residence time and about 180 times more antibacterial activity than vancomycin-free drugs. Niosomal-based drug delivery is gaining attention due to promising effects as anti-cancer and anti-leishmanial treatment.

25.2.7.2 Solid Lipid Nanoparticles

Solid Lipid Nanoparticles are small-sized (10 nm to 1 μ m) colloidal nanoparticles to encapsulate hydrophilic and hydrophobic compounds. The small size of the nanoparticles provides advantages in crossing the blood-aqueous barrier, blood-retinal barrier, and epithelial barrier, and enhanced absorption, bioavailability, and retention time are profound due to the sustained release of the drug (Mukherjee et al. 2009). These nanoparticles constitute natural/synthetic lipids such as steroids, fatty acids, and triglycerides to enhance drug delivery and reduce systemic toxic effects. The conventional drugs are loaded in solid nanoparticles to prepare the formulations using hot homogenization, micro-emulsification, and ultrasonication technique. Different solid nanoparticle formulations are developed by loading antitubercular (isoniazid), antibiotics (ofloxacin), and anti-fungal (natamycin) drugs using these methods.

25.2.7.3 Inorganic Nanoparticles

Inorganic nanoparticles are researched extensively for large surface area, stability, and catalytic property. These nanoparticles are prepared using gold, silver, silica, fullerenes, and carbon nanotubes. Inorganic-based drug delivery systems are effectively used against various disorders such as retinal infection, ocular inflammation, and cancer (Pandey and Dahiya 2016). Gold nanoparticles are commonly employed for treating cataracts, glaucoma, and cancer (Masse et al. 2019).

25.2.7.4 Others

Nanocarrier formulations such as nanosuspension, nanoemulsions, and hydrogels are novel drug delivery systems for treating ocular diseases. Nanosuspension can be employed for hydrophobic drugs and poor dissolution in lachrymal fluids. Mahboobian et al. (2019) loaded brinzolamide, a carbonic anhydrase inhibitor, in nanoemulsions to treat high intraocular pressure in glaucoma. Hydrogels are cross-linked polymeric structures with hydrophilic functional groups. Hydrogel's hydrophilicity is responsible for the faster liberation of the drugs from the formulations.

Though ocular nano-drug delivery offers more significant benefits in overcoming the low bioavailability and good penetration, developing these delivery systems takes substantial time and preparation.

25.2.8 Nasal Route of Drug Delivery

Nasal administration is highly preferred after the oral route and used as an alternative to various parenteral and other routes. Nasal administration has practical advantages, such as self, painless/noninvasive administration, and patient compliance. The nasal cavity possesses a rich vascular supply, large surface area, highly porous endothelial membrane, and epithelial microvilli resulting in good absorption, rapid onset of action, high therapeutic concentration, and enhanced bioavailability (Türker et al. 2004; Bahadur et al. 2020). It also offers high blood flow per cm^3 and delivery of the drugs through the olfactory nerves. The drugs are absorbed directly into the systemic circulation, circumventing first-pass hepatic metabolism and enzymatic degradation (Illum 2007; Pires et al. 2009).

Nasal delivery is an alternative promising drug delivery approach for drugs (decongestants, antibiotics, mucolytics) and vaccines (Illum 2007). Nasal delivery of liquid formulations such as aerosolized drugs provides wide distribution to the nasal cavity. Topically acting drugs such as antihistamines (chlorpheniramine maleate and diphenhydramine hydrochloride) and corticosteroids (fluticasone, mometasone, budesonide, and triamcinolone) are commonly used and prescribed for allergic rhinitis and nasal congestion. These drugs provide rapid onset with less systemic and CNS effects (Salib and Howarth 2003). Challenges associated with intranasal delivery are low membrane transport due to mucociliary clearance, hindering novel formulations development of new chemical entities. Mucociliary clearance involves profuse nasal secretion and ciliary movement and varies with individual health conditions (Kumar et al. 2014). Mucociliary clearance limits the residence time for absorption and sustained release of the drug.

Nevertheless, many aspects limit the absorption of polar or high molecular weight drugs (>1 kDa; peptides, proteins) from nasal mucosa for systemic delivery. It also includes poor permeability across the epithelium, and the small volume of the nasal cavity controls nasal administration. The nasal route of delivery is not possible in upper respiratory infections and allergic conditions. Low bioavailability of peptide and protein drugs is achieved compared to parenteral routes in these conditions

(Pires et al. 2009). Immense research approaches are required to overcome these limiting factors.

25.2.8.1 Nose to Brain Targeting

The intranasal route provides a better option for drug delivery to the brain since other routes are complicated in crossing the blood–brain barrier (Bahadur et al. 2020). The blood–brain barrier between the brain and systemic circulation prevents harmful particulates from entering the body. Intranasal administration aims to deliver therapeutic agents to bypass the blood–brain barrier to treat neurological conditions such as Alzheimer’s disease, Parkinson’s disease, cerebral ischemia, and all type of neurodegenerative diseases. Neurotrophins can protect the degeneration and promote the growth of the neurons in Alzheimer’s Disease. Nevertheless, the barrier limits CNS penetration, depending on the physicochemical properties of the drugs. Few small hydrophilic and lipophilic compounds, water, and gases (oxygen, carbon dioxide) can pass through the barrier to reach the brain (Pardridge 2005; Bahadur et al. 2020).

25.2.8.2 Mechanism of Transport to Brain

Olfactory and trigeminal nerves help to transport the drugs to the brain more effectively from the nasal cavity. Olfactory and Trigeminal nerves innervate nasal mucosa. Olfactory epithelium encloses olfactory neurons, and its axons pass through the cribriform plate of the ethmoid bone, which divides the cranial and nasal cavities to reach the olfactory bulb (Illum 2000; Ali et al. 2010; Bahadur et al. 2020). The olfactory region is responsible for direct communication with the environment to perceive a smell, and the drugs from the epithelium access the brain through nose-to-brain delivery. Drugs are transported from the nasal epithelium to the CNS via the olfactory bulb (Ali et al. 2010).

Possible transport mechanisms proposed for the delivery of the drugs along these nerves towards the CNS through the olfactory epithelium are intracellular and extracellular (paracellular and transcellular). In the intracellular pathway, the drugs bind with the surface receptor and are carried through intracellular axonal transfer into the olfactory bulb by receptor-mediated endocytosis and pinocytosis. The drugs are paracellularly transported via the leaky tight junctions between olfactory neurons of the nasal epithelium and sustentacular cells. The transcellular route involves drug absorption into the lamina propria via supportive (sustentacular) cells. Extracellular routes disperse drugs to the olfactory bulb, systemic circulation via local blood arteries, and deep cervical lymph nodes in the neck (Crowe et al. 2018; Keller et al. 2021).

25.2.9 Nanocarriers in Nasal Route

Mucoadhesive polymers such as hyaluronic acid, chitosan, and gelatin are commonly used in intranasal delivery. Drugs loaded with chitosan provided enhanced permeation and mucoadhesion for intranasal delivery to the brain.

Thymoquinone-loaded CS nanoparticles showed a 12-fold increase compared to free drugs from intranasal solution (Alam et al. 2012). The same type of study revealed that nonencapsulated rivastigmine showed higher brain concentrations through the intranasal route than intravenous, highlighting the importance of nasal-to-brain delivery. Rivastigmine, an acetylcholine enzyme inhibitor commonly used in Alzheimer's disease, reached a high blood-brain ratio by bypassing the BBB (Fazil et al. 2012).

Biodegradable nanoparticles are developed as nanocarriers or adjuvants in vaccines, in which the therapeutic drugs are dissolved, encapsulated, or chemically attached to the nanoparticles for formulation preparations (Pires et al. 2009). Nanoparticle-based adjuvants can increase antigenicity, sustained release of drugs, and may be used as an immunomodulator (Csaba et al. 2009). Numerous United States patents are filed against the stimulation of immune response using nanosuspension administration of vaccine by the intranasal route. Numerous intranasal-based formulations are developed to treat menopausal symptoms, osteoporosis, diabetes insipidus, prostate cancer, and endometriosis (Keller et al. 2021). Cyclodextrins carrier enhances the concentration and stability of dihydroergotamine for migraine headaches, absorption of female steroid hormones (estradiol and progesterone), and diffusivity of insulin across the nasal membrane. Delivery of the drug through the blood–brain barrier to target brain tumors is achieved through functionalized nanoparticles. Compared to doxorubicin alone, doxorubicin-loaded with polysorbate 80 and poly-butyl-cyanoacrylate nanoparticles may considerably penetrate the blood–brain barrier to enter the brain (Gulyaev et al. 1999).

25.2.10 Pulmonary Route of Drug Delivery

Pulmonary delivery is a noninvasive route commonly prescribed for administering active pharmaceutical ingredients to produce local and systemic effects. Localized drug delivery in inhalation therapy is focused on treating chronic obstructive pulmonary disease, asthma, pulmonary hypertension, cancer, and cystic fibrosis (Paranjpe and Müller-Goymann 2014). Lungs provide an effective rapid onset of action and absorption of drug molecules due to large surface area, high vascularization, and avoiding the hepatic first-pass effects for various therapeutic interventions (Sung et al. 2007). Considering these facts, several pharmaceutical companies are interested in developing aerosolized forms of insulin to control postprandial hyperglycemia.

25.2.10.1 Anatomy of Lungs

A clear understanding of formulation preparation, administration, pharmacokinetics, and pharmacodynamics is essential, and it is possible with a detailed knowledge of lung anatomy architecture and physiology. Lungs are involved in the gaseous exchange between the external environment and blood to maintain homeostasis (Patton and Byron 2007; Bailey and Berkland 2009). The lower respiratory tract consists of lungs and trachea, which bifurcates into the bronchi (primary, secondary,

and tertiary), smaller terminal bronchioles, and alveoli in the lungs. The bronchial airways are lined with serous fluid and mucus layers, which entrap pulmonary administered aerosolized particles. The tracheobronchial epithelium is responsible for mucociliary clearance, such as mucus secretion and rhythmic ciliary movement, removing the particles from entering the lung epithelium (Bustamante-Marin and Ostrowski 2017). The drug particles need to resist the thick mucus to reach the epithelial cells. The thickness of the epithelium narrows down from bronchi (3–5 mm) to bronchiolar (0.5–1 mm) and alveoli (0.1 mm). Also, the epithelium structure changes from ciliated columnar in proximal to cuboidal epithelium in distal airways (Weibel 1963).

Alveoli, a thin single-cell epithelium, are found approximately 300 million in the total lungs (Labiris and Dolovich 2003). The alveolar cells comprise two types of primary epithelial cells: Type I and Type II pneumocytes. Type I pneumocytes are attached to the pulmonary capillaries through the basement membrane. In contrast, type II pneumocytes secrete alveolar fluids and mucus containing phospholipid-based surfactant layer to prevent alveolar collapse. The surfactant proteins are responsible for optimal surface tension and are essential for breathing mechanisms by reducing friction in the lung tissues (Patton and Byron 2007; Beck-Broichsitter et al. 2011). Each alveolus lined with minute capillaries covers the vast network of the lungs and acts as a blood–gas barrier. However, a large surface area ($>100\text{ m}^2$) and thin distance (0.5 μm) between the alveoli and capillaries facilitate the intimate blood-gaseous exchange of inhaled particles by diffusion process (Courrier et al. 2002). The drugs encounter barriers such as mucus, enzymes (tracheobronchial region), and macrophages (alveoli region) to reach the target site. The small-sized drugs enter through the tight junctions and dissolve in the interstitial fluid before reaching systemic circulation through paracellular transport. Macrophages (15–22 μm) uptake particles of 1–3 μm in diameter, and macrophage phagocytosis depends on the particle size and composition of the nanoparticle coating. The large-sized and insoluble molecules, e.g., peptides, perform the above process slowly and are subject to phagocytosis by alveolar macrophages (Labiris and Dolovich 2003; Bailey and Berklund 2009). Despite these disadvantages, pulmonary administration of peptide and small protein therapeutics may be a feasible approach.

25.2.10.2 Mechanism of Drug Deposition in Lungs

The drug interaction in the lungs is based on the particle size of inhaled material. Particles are deposited in the different regions of the lungs by three distinct processes: inertial impaction, gravitational sedimentation, and Brownian diffusion (Yang et al. 2008; Tena and Clarà 2012; Paranjpe and Müller-Goymann 2014). The aerosolized drugs collide with the nasal mucosa and get deposited in the oropharynx regions. It is commonly observed in inhaler types of administration, such as metered-dose and dry powder inhalers containing more prominent drug molecules than 5 μm . The force of inspiration determines the deposition site of dry powder particles with bigger mass and inertial forces in the lungs. If the particles' diameter is between 1–5 μm , they are prone to sedimentation in bronchioles and smaller airways due to gravitation force. Sedimentation requires slow deposition of

the particles, and it is directly proportional to the slow breathing pattern of the individuals. Fine particles (0.5–1 μm diameter) are deposited in the deeper alveolar regions by diffusion based on the random movement of the molecules as per the Brownian effect (Labiris and Dolovich 2003; Yang et al. 2008). The particles less than 0.5 μm in diameter are more likely to reach the alveolar region, escape from the phagocytic activity, and are exhaled due to their smaller size. The particle deposition is influenced by aerosol particle morphology properties and anatomy of the upper and lower respiratory tract, and also physiological and environmental factors affecting ventilatory effects such as breathing pattern and breath-holding capacity, humidity, and air velocity (Labiris and Dolovich 2003; Yang et al. 2008).

25.2.11 Nanocarriers in Pulmonary Route

Nanoparticle formulations provide more advantages than conventional dosage forms, such as enhanced dissolution and stability through the pulmonary route. Nanocarriers are used to transport drugs via the lungs, resulting in a profound therapeutic effect. Inhaled nanoparticle coated drugs may raise serious toxicity concerns and should be thoroughly investigated for inherent toxic behavior. Numerous studies established the correlation between nanoparticles and their adverse effects on the lung and brain. Drug-nanoparticle formulations are developed to study the anti-asthma, anti-cancer, anti-tuberculosis, anti-hypertension, anti-oxidants, and surfactant therapy effects. Different active pharmaceutical ingredients are incorporated into nanoparticle systems such as lipid nanocarriers, solid lipid nanoparticles, polymeric nanoparticles, liposomes, and solid lipid microparticles in the pulmonary route formulations (Paranjpe and Müller-Goymann 2014).

25.2.11.1 Solid Lipid Nanoparticles

Solid lipid nanoparticles are aqueous suspensions made up of physiological components, phospholipids, and triglycerides. The use of solid nanoparticles in the formulations is extensively studied in pulmonary drug delivery owing to the reachability of the particles to deeper areas of the lung. Numerous researchers have investigated the mechanism and treatment of lung infection in the population. Solid nanoparticle loaded drugs such as quercetin, amikacin, and sildenafil are studied for efficacy in lung-related disorders (Paranjpe and Müller-Goymann 2014).

25.2.11.2 Polymeric Nanoparticles

Polymeric nanoparticles are prepared using different polymer bases. These drug delivery methods are gaining importance due to advantages such as biodegradable properties, high encapsulation, reduced degradation, and sustained release of drugs (Watkins et al. 2015; Lombardo et al. 2019). Polymer-based nanoparticle formulations are widely prescribed in cancer (methotrexate, paclitaxel), lung infections (voriconazole), blood coagulation (heparin), and anti-hypertension (sildenafil).

25.2.11.3 Others

Nano-suspension of budesonide, an insoluble water corticosteroid, was used to treat chronic obstructive pulmonary diseases and asthma. These formulations have a mean particle size of about 0.5 μm and are administered using metered dose inhaler or nebulizer (Jacobs and Müller 2002).

Nanoparticles-based formulations have numerous benefits over conventional aerosolized liquid and powder-based formulations in pulmonary drug delivery, particularly for poor hydrophilic drugs to improve bioavailability. The benefits of nanoparticle formulations link the nanotechnology and pulmonary delivery of drug aerosols. Nanoparticles are formulated to enhance dissolution, bioavailability, and delivery to deep lung tissues. Many alternative formulation techniques for medicines that employ a range of excipients to manufacture nanoparticles or nanoparticle complexes appropriate for pulmonary administration have been proposed in the literature. The new prospective nanomedicine may need to overcome practical encumbrances for pharmaceutical formulation processes to make the pulmonary route of drug delivery the preferred route for diagnostic and therapeutic reasons.

25.2.12 Parenteral Route of Drug Delivery

The parenteral route is preferred for drugs with limited absorption, stability, and bioavailability due to the destruction of the compounds by the gastrointestinal environment. The parenterally administered drugs undergo rapid and complete absorption (varies with routes), unlike oral drugs due to first-pass hepatic metabolism. The parenteral route provides desired therapeutic concentration with low dose and toxicity compared to oral or other routes. It also has other advantages such as continuous infusion and maintenance of steady-state concentration with a short half-life and possible administration to patients with clinical conditions such as coma, vomiting, and unconscious (Rowland 1972; Merisko-Liversidge and Liversidge 2011). This route usually exhibits rapid onset of action and biodistribution of the molecules into the system and sustained release based on the requirement of the targeted drug action. This section focuses on the commonly operated parenteral routes of administration for the effective delivery of drugs structured through nanotechnology.

Considering their advantages, the most commonly used parental administration for the drugs conjugated with nanoparticles is subcutaneous, intramuscular, and intravenous routes. The other forms of parental delivery of solution or suspension include the intra-arterial, epidural, and implantations under tissues which are implemented based on the pathophysiological condition of the diseases.

Subcutaneous/hypodermic administration is the better route of drug delivery into the subcutaneous tissues beneath the dermis for continuous release to the targeted tissues or cells from the site of accumulation or delivery. The particle size, encapsulation efficiency, zeta potential, biocompatibility, solubility, biodistribution, and long action helps to develop an appropriate formulation of nanoparticle-enriched molecules for effective dispersion by subcutaneous route (Jogala et al. 2015). The

subcutaneous route provides slow absorption due to relatively poor blood supply compared with other parental routes of administration. However, this route of administration is the most preferred route for the molecules with low bioavailability, larger molecular size, a more extended period of release, and which are more frequently degradable through the oral route of administration like protein molecules such as insulin and heparin. It is the most suitable route of drug delivery for diseases like diabetes and rheumatoid arthritis.

The intramuscular is the route of administration of the aqueous or oily, nonirritant solution, emulsion, and suspension into the suitable muscle tissues for the systemic release of the drug into the body. The drugs are diffusively absorbed from the injection site into the blood or lymphatic system through the surrounding tissues. The absorption rate varies with the site concentration of the drug and affects its half-life (Gutierrez and Munakomi 2020).

The intravenous route is the mode of administration of drug molecules directly into the venous blood vessels, and it is helpful in the passive method of delivery to inflammatory sites. The intravenous route is the most preferred route due to its advantages. It includes no absorption phase, rapid onset of action, continuous infusion of short half-life drugs, complete bioavailability, large administration volume, and compliance in emergency, coma, diarrhea, and vomiting conditions (Parker and Davey 1992; Merisko-Liversidge and Liversidge 2011). The intravenous route provides immediate response and allows precise control of the dose and administration rate of the drugs. It is also suitable for drugs that undergo hepatic/gastric metabolism or irritant drugs that cannot be injected into muscles, citing inflammation (Rowland 1972; Merisko-Liversidge and Liversidge 2011). The main advantage of this route is that even low-dose drug enters systemic circulation directly, resulting in 100% bioavailability of drugs.

Prominent drugs such as peptides and proteins are administered effectively to achieve the desired therapeutic concentration without pre-systemic degradation. The disadvantages are the danger of infection, expensive, invasive/painful procedures, requiring trained healthcare personnel, the chance of embolism and thrombophlebitis of the vein, and necrosis of adjoining tissues due to extravasation irritant drugs (Wong et al. 2008).

25.2.13 Nanocarriers in Parenteral Route

Nanotechnology has improved the solubility of molecules exhibiting poor solubility in water or solvent or surfactant and thereby enhanced its bioavailability and effective action specific to the organs, tissues, and cells to inhibit the mechanisms. Numerous disease indications are treated with analgesics, antibiotics, anti-inflammatory, anti-cancer, immune-modulatory/stimulatory, Alzheimer's diseases, and cardiovascular disorders, with therapeutic drugs encapsulated in nanoparticles (Kreuter 2014).

25.2.14 Nanocarriers in Subcutaneous Route

In the subcutaneous route, several nanoparticle-based insulin delivery approaches are used with natural and synthetic polymeric nanoparticles. Biocompatible nanomaterials are developed for insulin to prevent the premature degradation of the molecule. PLA and PEG was the common applicant in nanotechnology for increasing the encapsulation of the molecule and sustainable drug release for better efficacy of the drugs. The PLGA nanoparticle preparation for insulin significantly affected diabetic rats compared to the free insulin and insulin zinc suspension (Abdelkader et al. 2018). Similarly, PLGA nanoparticle co-encapsulated anti-tuberculosis drugs like rifampicin, isoniazid, and pyrazinamide expressed better bioavailability and reduced dose frequency in subcutaneous than other routes with prolonged delivery in the blood vessels and targeted organs like lungs and spleen (Pandey and Khuller 2004).

Low-molecular weight heparin has anti-coagulant activities to prevent and treat venous thromboembolism, therapy-related rheumatoid arthritis, and cancers. The shorter biological half-life, poor bioavailability, and reduced absorption in the intestinal epithelium are restraints in the oral administration of low molecular weight heparin. The nanoparticle-encapsulated heparin increased the bioavailability and sustainable release into the system without altering the integral structure of the drug when administered through the subcutaneous route (Jogala et al. 2015).

Nanotechnology has also provided a remarkable contribution to cancer biology in improving the efficiency, biodistribution, and stability of the molecules in the tumor environment for effective therapeutic purposes. The subcutaneous administration of chemotherapeutic drugs imposes drawbacks such as higher solubility rate of hydrophobic drugs, higher volume of injection, and engulfment of nanoparticle coated molecules by the macrophages through the phagocyte system involving the phagocyte system micropinocytosis resulting in reduced efficacy and nanotoxicity (Stack et al. 2021). The development of nanoparticles should be focused on the potential to inhibit the mechanism of micropinocytosis and increase the availability of the compounds to the targeted tissues by subcutaneous route. Latrunculin A coated polymeric micelles inhibited the uptake of drug molecules by the macrophage phagocytic system resulting in increased serum level and distribution of the drug through the subcutaneous method (Stack et al. 2021). The limitations in the conventional subcutaneous route of administration are drawn out by nanoparticle encapsulation, providing sufficient absorptive effects.

CUDC-101 is a novel potent anti-cancer molecule that possesses poor solubility in water. The hyaluronidase-conjugated nanoparticles have improved the stability, dose concentration, and solubility nature of the molecules. Concerning bioavailability and pharmacokinetics, polymer nanoparticle-coated molecules showed increased plasma levels and therapeutic effects compared to the standard uncoated substance when administered through the subcutaneous route (Soundararajan et al. 2020). Similarly, sustained and enhanced uptake of chemotherapeutic drug etoposide coated with nanoparticles by tumor cells was observed in subcutaneous routes compared with intravenous and intraperitoneal routes with slower and gradual

absorption from the injection site to tumor environment (Harivardhan Reddy et al. 2005).

25.2.15 Nanocarriers in Intramuscular Route

The challenges in intramuscular injection are the formulation of the drugs based on the mode of action, either slow or rapid action, and the selection of suitable vehicles for proper dissociation and absorption. The aqueous solution-based intramuscular preparations had substantial absorption of the drugs with rapid uptake depending upon the half-life. The compounds which are ionizable and possess poor solubility in water or higher dilution rate incur precipitation at the time of administration if proper pH is not maintained for the formulation. It may lead to irritation in the muscles and affect the rate of absorption, leading to the local toxicity effect (Ribeiro 2005). The nanoparticle-conjugated drug molecules overcome this limitation as the lipophilic or polymeric-based nanoparticles maintain the molecule's integrity in the aqueous solution. The drug-nanocrystal formulation improves the poor solubility of the drug with the required amount of dilution for intramuscular injection for rapid action.

The size and shape of the nanocarrier have to be considered in formulation for effective penetration or diffusion of particles into muscular tissues for entering into the systemic circulation. In addition, the combination of drugs with different physicochemical properties could be achieved with different combinations of nanocarriers for better bioavailability and efficacy. The lipid and polymer conjoined nanoparticles with polymeric region surrounded by lipid layer allow sheltering molecules of different properties for synergic effect. The lipid nanoparticle-based intramuscular administration of mRNA vaccine produced better absorption, stability, and immunogenicity in *in vivo* experimentation (Hassett et al. 2019).

25.2.16 Nanocarriers in Intravenous Route

Numerous drugs such as anti-cancer, antibiotic, anti-inflammatory, and immune system-based drugs are encapsulated in nanoparticles to achieve enhanced pharmacological effects and reduced toxicity (Kreuter 2014). Nanotechnology is effectively implied in cancer therapy to overcome drug accumulation, relapse of cancer, reduce toxicity, and prolong remissions from these diseases using controlled-release nanocarriers.

Nanoparticles are designed to circulate in the bloodstream to promote biodistribution, half-life, and reachability to solid tumors and inflammation sites. The FDA-approved Ambraxane®, a paclitaxel-nanoparticle formulation prepared without cremophor, reported good tolerability and efficacy in treating the tumors (Kalepu and Nekkanti 2015). A study proved that administration of radiolabeled paclitaxel oleate-coated cholesterol-rich nanoemulsion expressed high plasma half-life (14.51 vs 6.62 h) and AUC (2.49 vs 1.26 mg h/L) as compared to the

paclitaxel-cremophor combination in patients with gynecologic cancers (Dias et al. 2007).

25.3 Future Perspectives

This chapter explains the recent technological advances in route and nanocarrier-based delivery of therapeutic drugs to the target sites. This chapter provides only essential insights into the methodological delivery approach considering the vastness of the subject.

Nanofabricated drugs need to overcome anatomic and physiological barriers to achieve well-targeted drug delivery. Efficient delivery of drugs to targets with minimal side effects is necessary for nanoparticle formulations' success. Nanoparticles improve the stability of drugs inside the body by protecting the drug molecule inside systemic circulation. They also confine access to the drug to a specific site at a controlled and sustained rate. Designing the nanoparticles involves improving bioavailability, absorption and targeting the delivery sites to achieve favorable outcomes. Various forms of nano-drug carriers such as liposomes, dendrimers, cyclodextrins, solid lipid nanoparticles, and hydrogels can be used for effective therapeutic dosage regimens. Nanomedicine has tremendous potential to impact nano-drug delivery systems positively. The main concern of future research can be done in the preparation of nanoparticles that can further withstand the biological diversities and thus further improve drug stability in the biological environment. A clear understanding of the advantages and disadvantages of each route and the delivery system is the need of the hour for future drug development.

References

- Abdelkader DH, El-Gizawy SA, Faheem AM, McCarron PA, Osman MA (2018) Effect of process variables on formulation, in-vitro characterisation and subcutaneous delivery of insulin PLGA nanoparticles: an optimisation study. *J Drug Deliv Sci Technol* 43:160–171
- Abraham SA, Waterhouse DN, Mayer LD, Cullis PR, Madden TD, Bally MB (2005) The liposomal formulation of doxorubicin. In: *Methods in enzymology*. Elsevier, Amsterdam, pp 71–97
- Alam S, Khan ZI, Mustafa G, Kumar M, Islam F, Bhatnagar A, Ahmad FJ (2012) Development and evaluation of thymoquinone-encapsulated chitosan nanoparticles for nose-to-brain targeting: a pharmacoscintigraphic study. *Int J Nanomedicine* 7:5705–5718
- Ali J, Ali M, Baboota S, Kaur Sahni J, Ramassamy C, Dao L (2010) Bhavna: potential of nanoparticulate drug delivery systems by intranasal administration. *Curr Pharm Des* 16(14): 1644–1653
- Alkilani AZ, McCrudden MTC, Donnelly RF (2015) Transdermal drug delivery: Innovative pharmaceutical developments based on disruption of the barrier properties of the stratum corneum. *Pharmaceutics* 7(4):438–470
- Allam A, El-Mokhtar MA, Elsabahy M (2019) Vancomycin-loaded niosomes integrated within pH-sensitive in-situ forming gel for treatment of ocular infections while minimising drug irritation. *J Pharm Pharmacol* 71(8):1209–1221
- Arnold M, Sierra MS, Laversanne M, Soerjomataram I, Jemal A, Bray F (2016) Global patterns and trends in colorectal cancer incidence and mortality. *Gut* 66(4):683–691

- Bahadur S, Pardhi DM, Rautio J, Rosenholm JM, Pathak K (2020) Intranasal nanoemulsions for direct nose-to-brain delivery of actives for CNS disorders. *Pharmaceutics* 12(12):1230
- Bailey MM, Berkland CJ (2009) Nanoparticle formulations in pulmonary drug delivery. *Med Res Rev* 29(1):196–212
- Bardonnet PL, Faivre V, Pugh WJ, Piffaretti JC, Falson F (2006) Gastroretentive dosage forms: overview and special case of *Helicobacter pylori*. *J Control Release* 111(1–2):1–18
- Beck-Broichsitter M, Ruppert C, Schmehl T, Guenther A, Betz T, Bakowsky U, Seeger W, Kissel T, Gessler T (2011) Biophysical investigation of pulmonary surfactant surface properties upon contact with polymeric nanoparticles in vitro. *Nanomed Nanotechnol Biol Med* 7(3): 341–350
- Beloqui A, Coco R, Memvanga PB, Ucakar B, des Rieux A, Pr at V (2014) pH-sensitive nanoparticles for colonic delivery of curcumin in inflammatory bowel disease. *Int J Pharm* 473(1–2):203–212
- Bochot A, Fattal E (2012) Liposomes for intravitreal drug delivery: a state of the art. *J Control Release* 161(2):628–634
- Bustamante-Marin XM, Ostrowski LE (2017) Cilia and mucociliary clearance. *Cold Spring Harbour Perspect Biol* 9(4):a028241
- Cheng Y, Man N, Xu T, Fu R, Wang X, Wang X, Wen L (2007) Transdermal delivery of nonsteroidal anti-inflammatory drugs mediated by polyamidoamine (PAMAM) dendrimers. *J Pharm Sci* 96(3):595–602
- Chenthamara D, Subramaniam S, Ramakrishnan SG, Krishnaswamy S, Essa MM, Lin F-H, Qoronfleh MW (2019) Therapeutic efficacy of nanoparticles and routes of administration. *Biomater Res* 23:20–20
- Cone RA (2009) Barrier properties of mucus. *Adv Drug Deliv Rev* 61(2):75–85
- Contado C (2015) Nanomaterials in consumer products: a challenging analytical problem. *Front Chem* 3:48–48
- Courrier HM, Butz N, Vandamme TF (2002) Pulmonary drug delivery systems: recent developments and prospects. *Crit Rev Ther Drug Carrier Syst* 19(4–5):425–498
- Crowe TP, Greenlee MHW, Kanthasamy AG, Hsu WH (2018) Mechanism of intranasal drug delivery directly to the brain. *Life Sci* 195:44–52
- Csaba N, Garcia-Fuentes M, Alonso MJ (2009) Nanoparticles for nasal vaccination. *Adv Drug Deliv Rev* 61(2):140–157
- Cummings JH, Englyst HN (1987) Fermentation in the human large intestine and the available substrates. *Am J Clin Nutr* 45(5):1243–1255
- Cunha-Vaz J (1979) The blood-ocular barriers. *Surv Ophthalmol* 23(5):279–296
- Date AA, Hanes J, Ensign LM (2016) Nanoparticles for oral delivery: design, evaluation and state-of-the-art. *J Control Release* 240:504–526
- Denet A-R, Ucakar B, Pr at V (2003) Transdermal delivery of timolol and atenolol using electroporation and iontophoresis in combination: a mechanistic approach. *Pharm Res* 20(12): 1946–1951
- Denet A-R, Vanbever R, Pr at V (2004) Skin electroporation for transdermal and topical delivery. *Adv Drug Deliv Rev* 56(5):659–674
- Desai P, Patlolla RR, Singh M (2010) Interaction of nanoparticles and cell-penetrating peptides with skin for transdermal drug delivery. *Mol Membr Biol* 27(7):247–259
- Dias MLN, Carvalho JP, Rodrigues DG, Graziani SR, Maranh o RC (2007) Pharmacokinetics and tumor uptake of a derivatised form of paclitaxel associated to a cholesterol-rich nanoemulsion (LDE) in patients with gynecologic cancers. *Cancer Chemother Pharmacol* 59(1):105–111
- Ensign LM, Cone R, Hanes J (2012) Oral drug delivery with polymeric nanoparticles: the gastrointestinal mucus barriers. *Adv Drug Deliv Rev* 64(6):557–570
- Fazil M, Md S, Haque S, Kumar M, Baboota S, Sahni JK, Ali J (2012) Development and evaluation of rivastigmine loaded chitosan nanoparticles for brain targeting. *Eur J Pharm Sci* 47(1):6–15
- Gaudana R, Ananthula HK, Parenky A, Mitra AK (2010) Ocular drug delivery. *AAPS J* 12(3): 348–360

- Gelberg HB (2014) Comparative anatomy, physiology, and mechanisms of disease production of the esophagus, stomach, and small intestine. *Toxicol Pathol* 42(1):54–66
- Gill HS, Prausnitz MR (2007) Coated microneedles for transdermal delivery. *J Control Release* 117(2):227–237
- Gugulothu D, Kulkarni A, Patravale V, Dandekar P (2014) pH-sensitive nanoparticles of curcumin–celecoxib combination: evaluating drug synergy in ulcerative colitis model. *J Pharm Sci* 103(2): 687–696
- Gulyaev AE, Gelperina SE, Skidan IN, Antropov AS, Kivman GY, Kreuter J (1999) Significant transport of doxorubicin into the brain with polysorbate 80-coated nanoparticles. *Pharm Res* 16(10):1564–1569
- Gupta H, Babu RJ (2013) Transdermal delivery: product and patent update. *Recent Pat Drug Deliv Formul* 7(3):184–205
- Gutierrez JJP, Munakomi S (2020) Intramuscular injection. *StatPearls*
- Hansen S, Lehr C-M (2012) Nanoparticles for transcutaneous vaccination. *Microb Biotechnol* 5(2): 156–167
- Harivardhan Reddy L, Sharma RK, Chuttani K, Mishra AK, Murthy RSR (2005) Influence of administration route on tumor uptake and biodistribution of etoposide loaded solid lipid nanoparticles in Dalton's lymphoma tumor bearing mice. *J Control Release* 105(3):185–198
- Hassett KJ, Benenato KE, Jacquinet E, Lee A, Woods A, Yuzhakov O, Himansu S, Deterling J, Geilich BM, Ketova T et al (2019) Optimisation of lipid nanoparticles for intramuscular administration of mRNA vaccines. *Mol Ther Nucleic Acids* 15:1–11
- He H, Wang P, Cai C, Yang R, Tang X (2015) VB12-coated Gel-Core-SLN containing insulin: another way to improve oral absorption. *Int J Pharm* 493(1–2):451–459
- Illum L (2000) Transport of drugs from the nasal cavity to the central nervous system. *Eur J Pharm Sci* 11(1):1–18
- Illum L (2007) Nanoparticulate systems for nasal delivery of drugs: a real improvement over simple systems? *J Pharm Sci* 96(3):473–483
- Ita K (2015a) Transdermal iontophoretic drug delivery: advances and challenges. *J Drug Target* 24(5):386–391
- Ita K (2015b) Recent progress in transdermal sonophoresis. *Pharm Dev Technol* 22(4):458–466
- Ita K (2015c) Transdermal delivery of drugs with microneedles-potential and challenges. *Pharmaceutics* 7(3):90–105
- Ita K (2016) Perspectives on transdermal electroporation. *Pharmaceutics* 8(1):9
- Jacobs C, Müller RH (2002) Production and characterisation of a budesonide nanosuspension for pulmonary administration. *Pharm Res* 19(2):189–194
- Jahangirian H, Lemraski EG, Webster TJ, Rafiee-Moghaddam R, Abdollahi Y (2017) A review of drug delivery systems based on nanotechnology and green chemistry: green nanomedicine. *Int J Nanomedicine* 12:2957–2978
- Jogala S, Rachamalla SS, Aukunuru J (2015) Development of subcutaneous sustained release nanoparticles encapsulating low molecular weight heparin. *J Adv Pharm Technol Res* 6(2): 58–64
- Joseph RR, Venkatraman SS (2017) Drug delivery to the eye: what benefits do nanocarriers offer? *Nanomedicine* 12(6):683–702
- Kalepu S, Nekkanti V (2015) Insoluble drug delivery strategies: review of recent advances and business prospects. *Acta Pharm Sin B* 5(5):442–453
- Kalepu S, Manthina M, Padavala V (2013) Oral lipid-based drug delivery systems—an overview. *Acta Pharm Sin B* 3(6):361–372
- Kalia YN, Naik A, Garrison J, Guy RH (2004) Iontophoretic drug delivery. *Adv Drug Deliv Rev* 56(5):619–658
- Kamoun EA, Kenawy E-RS, Chen X (2017) A review on polymeric hydrogel membranes for wound dressing applications: PVA-based hydrogel dressings. *J Adv Res* 8(3):217–233
- Kararli TT (1995) Comparison of the gastrointestinal anatomy, physiology, and biochemistry of humans and commonly used laboratory animals. *Biopharm Drug Dispos* 16(5):351–380

- Kazi KM, Mandal AS, Biswas N, Guha A, Chatterjee S, Behera M, Kuotsu K (2010) Niosome: a future of targeted drug delivery systems. *J Adv Pharm Technol Res* 1(4):374–380
- Keller L-A, Merkel O, Popp A (2021) Intranasal drug delivery: opportunities and toxicologic challenges during drug development. *Drug Deliv Transl Res* 12:1–23
- Khan I, Saeed K, Khan I (2019) Nanoparticles: properties, applications and toxicities. *Arab J Chem* 12(7):908–931
- Kim SH, Lutz RJ, Wang NS, Robinson MR (2007a) Transport barriers in transscleral drug delivery for retinal diseases. *Ophthalmic Res* 39(5):244–254
- Kim Y-C, Ludovice PJ, Prausnitz MR (2007b) Transdermal delivery enhanced by magainin pore-forming peptide. *J Control Release* 122(3):375–383
- Kim Y-C, Park J-H, Prausnitz MR (2012) Microneedles for drug and vaccine delivery. *Adv Drug Deliv Rev* 64(14):1547–1568
- Koschinsky T, Heinemann L (2001) Sensors for glucose monitoring: technical and clinical aspects. *Diabetes Metab Res Rev* 17(2):113–123
- Kreuter J (2014) Drug delivery to the central nervous system by polymeric nanoparticles: what do we know? *Adv Drug Deliv Rev* 71:2–14
- Kumar A, Pandey AN, Jain SK (2014) Nasal-nanotechnology: revolution for efficient therapeutics delivery. *Drug Deliv* 23(3):671–683
- Labiris NR, Dolovich MB (2003) Pulmonary drug delivery. Part I: physiological factors affecting therapeutic effectiveness of aerosolised medications. *Br J Clin Pharmacol* 56(6):588–599
- Lam P-L, Wong W-Y, Bian Z, Chui C-H, Gambari R (2017) Recent advances in green nanoparticulate systems for drug delivery: efficient delivery and safety concern. *Nanomedicine* 12(4):357–385
- Lapteva M, Mondon K, Möller M, Gurny R, Kalia YN (2014) Polymeric micelle nanocarriers for the cutaneous delivery of tacrolimus: a targeted approach for the treatment of psoriasis. *Mol Pharm* 11(9):2989–3001
- Limayem Blouza I, Charcosset C, Sfar S, Fessi H (2006) Preparation and characterisation of spironolactone-loaded nanocapsules for paediatric use. *Int J Pharm* 325(1–2):124–131
- Lin Y-H, Chen Z-R, Lai C-H, Hsieh C-H, Feng C-L (2015) Active targeted nanoparticles for oral administration of gastric cancer therapy. *Biomacromolecules* 16(9):3021–3032
- Lombardo D, Calandra P, Barreca D, Magazù S, Kiselev MA (2016) Soft interaction in liposome nanocarriers for therapeutic drug delivery. *Nanomaterials (Basel)* 6(7):125
- Lombardo D, Kiselev MA, Caccamo MT (2019) Smart nanoparticles for drug delivery application: development of versatile nanocarrier platforms in biotechnology and nanomedicine. *J Nanomater* 2019:1–26
- Lu H, Wang J, Wang T, Zhong J, Bao Y, Hao H (2016) Recent progress on nanostructures for drug delivery applications. *J Nanomater* 2016:1–12
- Machet L, Boucaud A (2002) Phonophoresis: efficiency, mechanisms and skin tolerance. *Int J Pharm* 243(1–2):1–15
- Madaan K, Kumar S, Poonia N, Lather V, Pandita D (2014) Dendrimers in drug delivery and targeting: drug-dendrimer interactions and toxicity issues. *J Pharm Bioallied Sci* 6(3):139–150
- Mahboobian MM, Seyfoddin A, Aboofazeli R, Foroutan SM, Rupenthal ID (2019) Brinzolamide-loaded nanoemulsions: ex vivo transcorneal permeation, cell viability and ocular irritation tests. *Pharm Dev Technol* 24(5):600–606
- Martinho N, Damgé C, Reis CP (2011) Recent advances in drug delivery systems. *J Biomater Nanobiotechnol* 02(05):510–526
- Masse F, Ouellette M, Lamoureux G, Boisselier E (2019) Gold nanoparticles in ophthalmology. *Med Res Rev* 39(1):302–327
- Mathur V, Satrawala Y, Rajput M (2010) Physical and chemical penetration enhancers in transdermal drug delivery system. *Asian J Pharm* 4(3):173
- Merisko-Liversidge E, Liversidge GG (2011) Nanosizing for oral and parenteral drug delivery: a perspective on formulating poorly-water soluble compounds using wet media milling technology. *Adv Drug Deliv Rev* 63(6):427–440

- Mirza AZ, Siddiqui FA (2014) Nanomedicine and drug delivery: a mini review. *Int Nano Lett* 4(1): 94
- Mishra GP, Bagui M, Tamboli V, Mitra AK (2011) Recent applications of liposomes in ophthalmic drug delivery. *J Drug Deliv* 2011:863734
- Mitchell MJ, Billingsley MM, Haley RM, Wechsler ME, Peppas NA, Langer R (2021) Engineering precision nanoparticles for drug delivery. *Nat Rev Drug Discov* 20(2):101–124
- Mojumdar EH, Pham QD, Topgaard D, Sparr E (2017) Skin hydration: interplay between molecular dynamics, structure and water uptake in the stratum corneum. *Sci Rep* 7(1):15712
- Mukherjee S, Ray S, Thakur RS (2009) Solid lipid nanoparticles: a modern formulation approach in drug delivery system. *Indian J Pharm Sci* 71(4):349–358
- Obeid MA, Al Qaraghuli MM, Alsaadi M, Alzahrani AR, Niwasabutra K, Ferro VA (2017) Delivering natural products and biotherapeutics to improve drug efficacy. *Ther Deliv* 8(11): 947–956
- Ogura M, Paliwal S, Mitragotri S (2008) Low-frequency sonophoresis: current status and future prospects. *Adv Drug Deliv Rev* 60(10):1218–1223
- Palmer BC, DeLouise LA (2016) Nanoparticle-enabled transdermal drug delivery systems for enhanced dose control and tissue targeting. *Molecules* 21(12):1719
- Pandey P, Dahiya M (2016) A brief review on inorganic nanoparticles. *J Crit Rev* 3(3):18–26
- Pandey R, Khuller GK (2004) Subcutaneous nanoparticle-based antitubercular chemotherapy in an experimental model. *J Antimicrob Chemother* 54:266–268
- Pandey R, Zahoor A, Sharma S, Khuller GK (2003) Nanoparticle encapsulated antitubercular drugs as a potential oral drug delivery system against murine tuberculosis. *Tuberculosis* 83(6): 373–378
- Paranjpe M, Müller-Goymann CC (2014) Nanoparticle-mediated pulmonary drug delivery: a review. *Int J Mol Sci* 15(4):5852–5873
- Pardridge WM (2005) The blood-brain barrier: bottleneck in brain drug development. *NeuroRx* 2(1):3–14
- Parker SE, Davey PG (1992) Pharmacoeconomics of intravenous drug administration. *PharmacoEconomics* 1(2):103–115
- Patra JK, Das G, Fraceto LF, Campos EVR, Rodriguez-Torres MDP, Acosta-Torres LS, Diaz-Torres LA, Grillo R, Swamy MK, Sharma S et al (2018) Nano based drug delivery systems: recent developments and future prospects. *J Nanobiotechnol* 16(1):71–71
- Patton JS, Byron PR (2007) Inhaling medicines: delivering drugs to the body through the lungs. *Nat Rev Drug Discov* 6(1):67–74
- Philip AK, Philip B (2010) Colon targeted drug delivery systems: a review on primary and novel approaches. *Oman Med J* 25(2):79–87
- Pires A, Fortuna A, Alves G, Falcão A (2009) Intranasal drug delivery: how, why and what for? *J Pharm Pharmaceut Sci* 12(3):288–311
- Prausnitz MR, Langer R (2008) Transdermal drug delivery. *Nat Biotechnol* 26(11):1261–1268
- Prausnitz MR, Mitragotri S, Langer R (2004) Current status and future potential of transdermal drug delivery. *Nat Rev Drug Discov* 3(2):115–124
- Pridgen EM, Alexis F, Farokhzad OC (2015) Polymeric nanoparticle drug delivery technologies for oral delivery applications. *Expert Opin Drug Deliv* 12(9):1459–1473
- Qamar Z, Qizilbash FF, Iqbal MK, Ali A, Narang JK, Ali J, Baboota S (2019) Nano-based drug delivery system: recent strategies for the treatment of ocular disease and future perspective. *Recent Pat Drug Deliv Formul* 13(4):246–254
- Ribeiro CAF (2005) Influence of food and drugs on the bioavailability of antiepileptic drugs. In: *Antiepileptic drugs*. Cambridge University Press, Cambridge, pp 93–110
- Rowland M (1972) Influence of route of administration on drug availability. *J Pharm Sci* 61(1): 70–74
- Salib RJ, Howarth PH (2003) Safety and tolerability profiles of intranasal antihistamines and intranasal corticosteroids in the treatment of allergic rhinitis. *Drug Saf* 26(12):863–893

- Samad A, Ullah Z, Alam M, Wais M, Shams M (2009) Transdermal drug delivery system: patent reviews. *Recent Pat Drug Deliv Formul* 3(2):143–152
- Santos A, Veiga F, Figueiras A (2019) Dendrimers as pharmaceutical excipients: synthesis, properties, toxicity and biomedical applications. *Materials (Basel)* 13(1):65
- Sloan KB, Wasdo SC, Rautio J (2006) Design for optimised topical delivery: prodrugs and a paradigm change. *Pharm Res* 23(12):2729–2747
- Smijs TG, Pavel S (2011) Titanium dioxide and zinc oxide nanoparticles in sunscreens: focus on their safety and effectiveness. *Nanotechnol Sci Appl* 4:95–112
- Soundararajan R, Wang G, Petkova A, Uchegbu IF, Schätzlein AG (2020) Hyaluronidase coated molecular envelope technology nanoparticles enhance drug absorption via the subcutaneous route. *Mol Pharm* 17(7):2599–2611
- Stack T, Liu Y, Frey M, Bobbala S, Vincent M, Scott E (2021) Enhancing subcutaneous injection and target tissue accumulation of nanoparticles via co-administration with macropinocytosis inhibitory nanoparticles (MiNP). *Nanoscale Horizons* 6(5):393–400
- Sung JC, Pulliam BL, Edwards DA (2007) Nanoparticles for drug delivery to the lungs. *Trends Biotechnol* 25(12):563–570
- Tena AF, Clarà PC (2012) Deposition of inhaled particles in the lungs. *Arch Bronconeumol (Engl Ed)* 48(7):240–246
- Türker S, Onur E, Ózer Y (2004) Nasal route and drug delivery systems. *Pharm World Sci* 26(3):137–142
- Verma A, Sharma S, Gupta PK, Singh A, Teja BV, Dwivedi P, Gupta GK, Trivedi R, Mishra PR (2016) Vitamin B12 functionalised layer by layer calcium phosphate nanoparticles: a mucoadhesive and pH responsive carrier for improved oral delivery of insulin. *Acta Biomater* 31:288–300
- Waghule T, Singhvi G, Dubey SK, Pandey MM, Gupta G, Singh M, Dua K (2019) Microneedles: a smart approach and increasing potential for transdermal drug delivery system. *Biomed Pharmacother* 109:1249–1258
- Watkins R, Wu L, Zhang C, Davis RM, Xu B (2015) Natural product-based nanomedicine: recent advances and issues. *Int J Nanomedicine* 10:6055–6074
- Weibel ER (1963) Principles and methods of morphometry. In: *Morphometry of the human lung*. Elsevier, Academic Press, pp 9–39
- Weng Y, Liu J, Jin S, Guo W, Liang X, Hu Z (2017) Nanotechnology-based strategies for treatment of ocular disease. *Acta Pharm Sin B* 7(3):281–291
- Wong J, Brugger A, Khare A, Chaubal M, Papadopoulos P, Rabinow B, Kipp J, Ning J (2008) Suspensions for intravenous (IV) injection: a review of development, preclinical and clinical aspects. *Adv Drug Deliv Rev* 60(8):939–954
- Wysocki AB (1999) Skin anatomy, physiology, and pathophysiology. *Nurs Clin N Am* 34(4):777–797
- Yang W, Peters JJ, Williams RO (2008) Inhaled nanoparticles—a current review. *Int J Pharm* 356(1–2):239–247
- Yoshida T, Lai TC, Kwon GS, Sako K (2013) pH- and ion-sensitive polymers for drug delivery. *Expert Opin Drug Deliv* 10(11):1497–1513
- Zhang L, Sang Y, Feng J, Li Z, Zhao A (2016) Polysaccharide-based micro/nanocarriers for oral colon-targeted drug delivery. *J Drug Target* 24(7):579–589



Green Synthesized Silver Nanoparticles Phytotoxicity and Applications in Agriculture: An Overview

26

R. Santhoshkumar, A. Hima Parvathy, and E. V. Soniya

26.1 Introduction

In the twenty-first century, nanotechnology significantly affects the global economy, technology, and daily needs (Gruère et al. 2011). Nanotechnology is the branch of science concerned with studying materials in the nanoscale, which ranges from 1 to 100 nm. It has a great potential to enhance life quality through its applications in various fields such as agriculture, therapeutics, drug delivery, cosmetics, and biosensors (Rafique et al. 2017). Nanotechnology has many significant applications in optics, electronics, biomedical science, mechanics, chemical industry, optoelectronic devices, nonlinear optical devices, catalysis, space industries, energy science, and photo-electrochemical technologies (Singh et al. 2019a). Because of the significance and wide range of applications, the researchers are interested in synthesizing silver nanoparticles even for cancer detection and therapy, which have proven helpful (Ahmed et al. 2016).

Different methods used for nanoparticle synthesis, such as physical and chemical ones, are pretty expensive and potentially hazardous as they can create environmental toxicity responsible for various biological risks. The biological synthesis of nanoparticles is evolving as a safe alternative for these techniques in the field of nanotechnology (Ahmed et al. 2016). For the synthesis of NPs, two different techniques are used: “top-down” and “bottom-up” (Fig. 26.1). Size reduction processes such as grinding, milling, sputtering, thermal/laser ablation, and others are employed in the top-to-bottom approach (physical method) to break down acceptable bulk material into smaller fine particles. In a top-down approach, the most common procedure for synthesizing metal NPs is evaporation and condensation. The

R. Santhoshkumar · A. Hima Parvathy · E. V. Soniya (✉)
Transdisciplinary Biology, Rajiv Gandhi Centre for Biotechnology, Thiruvananthapuram, Kerala,
India
e-mail: evsoniya@rgcb.res.in

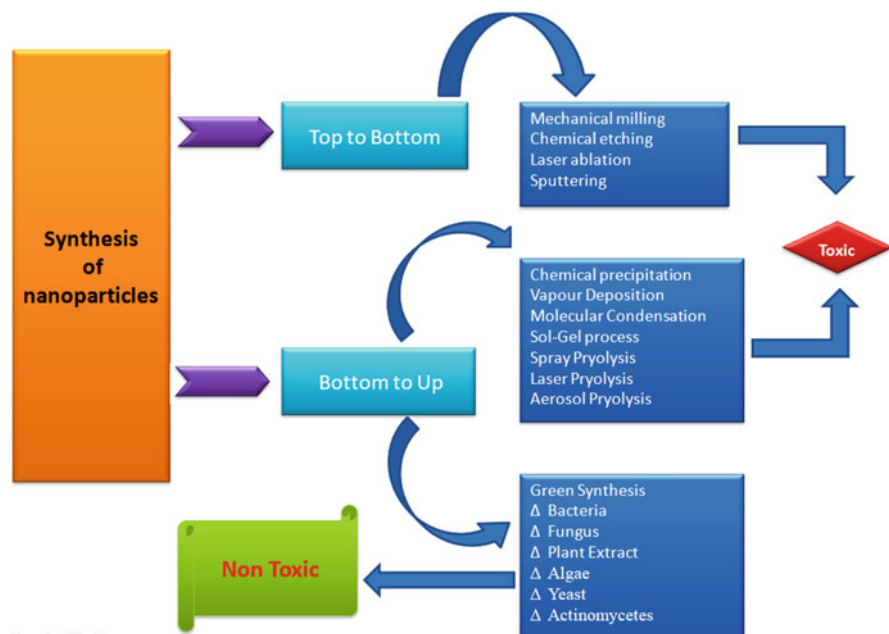


Fig. 26.1 Different methods of metal nanoparticles synthesis

foundation material is placed in the center of a furnace and vaporized into a carrier gas in this procedure. The existence of flaws in the product's surface structure, which influences the physical characteristics of NPs, is one of the most significant drawbacks of this approach.

Nanoparticles are synthesized using two different methods like chemical and biological in the bottom-to-top approach, including chemical reduction, electrochemical methods, and so no decomposition by self-assembly of atoms to new nuclei, which grow into nanosize particles (Mathur et al. 2018). Chemical reduction with organic and inorganic reducing chemicals is the most frequent method for producing silver NPs. For the reduction of silver ions (Ag^+) in aqueous or nonaqueous solutions, several organic solvents such as sodium citrate, ascorbate, sodium borohydride (NaBH_4), elemental hydrogen, polyol process, Tollens reagent, *N,N*-dimethylformamide (DMF), and poly(ethylene glycol)-block copolymers are utilized. These reducing chemicals decrease Ag^+ and cause metallic silver (Ag^0) to form, agglomerated into oligomeric clusters (Iravani et al. 2014). The techniques described above have a high yield, but they also have drawbacks such as the use of hazardous chemicals and a high functional cost and energy requirement. Alternative cost-effective approaches employing plant extracts, microbes, and natural polymers have been used to circumvent the constraints of physical and chemical approaches for the biosynthesis of AgNPs. The range of cytogenetically and physiologically compatible metallic NPs has been expanded because of the combination of green chemistry and nanotechnology (Tarannum and Gautam 2019).

The chemicals used in these types of synthesis are harmful, resulting in non-environmentally friendly by-products. This might be the reason for the green biosynthesis of NPs without toxic chemicals, which is proving to be an increasing desire to upgrade environmentally friendly processes. As a result, green nanoparticle synthesis is becoming more critical in nanotechnology; using biological systems such as microorganisms, plant extracts, or plant biomass for nanoparticle synthesis might be a more environmentally friendly alternative to chemical and physical processes (Reddy et al. 2012). Green synthesis is ecologically safe, valuable, and simple to scale up to large-scale NP synthesis since it does not require high temperatures, energy, stress, or harmful chemicals. Chemically produced nanomaterials, on the other hand, are regarded to be more dangerous. Hence, green nanotechnology-based alternatives are becoming more popular (Prasad et al. 2017b).

26.2 Capping Agents in Nanotechnology

Capping agents are new therapeutics that work in tandem with the biocompatible nanoparticles to which they have been attached to show environmental benefits. The steric barrier created by the covalent interaction between the chains of capping ligands and the nanoparticles' surface provides ultimate stability to the nanocomposite. Capping agents are often used to render the sizes of the nanoparticles. One of the most significant benefits of this process is that it can produce many nanoparticles in a short period. Concerns about nanoparticles' safety and long-term toxicity in biological systems are growing, and they must be addressed. Biocapping nanoparticles using aqueous plant extracts is an excellent approach to achieve regulated nanoparticle development with little toxicity. However, because surface modification of nanocrystals is required to get monodisperse nanoparticles, polydispersion and purification from by-products are barriers to its use on a large scale (Javed et al. 2020).

Different kinds of reducing agents, such as surfactants, small ligands, polymers, dendrimers, cyclodextrins, and polysaccharides, were employed to produce nanoparticles. All of these have been effectively used as capping agents capable of inducing modest modifications in nanoparticles, evidencing a huge medicinal and environmental cleaning impact (Radini et al. 2018). Green synthesis is the process of making nanoparticles utilizing plant extracts as possible capping and reducing agents. The extracts from plant leaves, fruit, roots, and seeds may affect the characteristics of the nanoparticles formed by ideally improving their functioning for biological applications (Javed et al. 2020).

Many previous works on the biological synthesis methods of silver nanoparticles employing plants, bacteria, and fungi were reported; antioxidants or reducing characteristics typically reducing for metallic substances in their respective nanoparticles. The most recent previous findings are listed in Table 26.1.

Table 26.1 Biologically synthesized silver nanoparticles using different sources and the biological activities

Plant part	Biological sources used for AgNPs synthesis	Anti-bacterial and anti-fungal activity and other biological activities against organisms	References
Leaves	<i>Justicia spicigera</i>	<i>Bacillus cereus</i> , <i>Klebsiella pneumoniae</i> , and <i>Macrophomina phaseolina</i> , <i>Alternaria alternate</i> , <i>Colletotrichum</i> sp., <i>Fusarium solani</i>	Bernardo-Mazariegos et al. (2019)
	<i>Eucalyptus citriodora</i>	Multi-drug resistant <i>Acinetobacter baumannii</i>	Wintachai et al. (2019)
	<i>Capparis zeylanica</i>	<i>Staphylococcus epidermis</i> , <i>Enterococcus faecalis</i> , <i>Salmonella paratyphi</i> , <i>Salmonella dysenteriae</i> , <i>Candida albicans</i> , <i>Aspergillus niger</i>	Nilavukkarasi et al. (2020)
	<i>Phyllanthus niruri</i>	<i>Aeromonas hydrophila</i>	Amalorpavamary et al. (2019)
	<i>Bryophyllum pinnatum</i>	<i>Agrobacterium tumefaciens</i> , <i>Salmonella setubal</i> , <i>Enterobacter aerogenes</i>	Noor (2020)
	<i>Premna serratifolia</i> L.	<i>Staphylococcus aureus</i> , <i>Enterococcus faecalis</i> , <i>Shigella dysenteriae</i> , <i>Shigella flexneri</i> , and <i>Vibrio parahaemolyticus</i>	Singh et al. (2019b)
	<i>Aloe vera</i>	<i>Staphylococcus aureus</i> , <i>Escherichia coli</i> , <i>Pseudomonas aeruginosa</i> , <i>Enterobacter</i> spp.	Anju et al. (2021)
	<i>Acanthospermum hispidum</i>	<i>Streptococcus pyogenes</i> , <i>Candida albicans</i> , <i>Aspergillus niger</i>	Ghotekar et al. (2019)
	<i>Melaleuca alternifolia</i>	<i>Staphylococcus aureus</i> , methicillin-resistant <i>Staphylococcus epidermidis</i> , <i>Staphylococcus pyogenes</i> , <i>Klebsiella pneumoniae</i> , <i>Pseudomonas aeruginosa</i>	Ramadan et al. (2020)
	<i>Abutilon indicum</i>	<i>Bacillus</i> sp. and <i>Streptococcus</i> sp.	Chandirika and Annadurai (2018)
	<i>Berberis vulgaris</i>	<i>Escherichia coli</i> and <i>Staphylococcus aureus</i>	Behravan et al. (2019)
	<i>Elephantopus scaber</i>	<i>Bacillus subtilis</i> , <i>Lactococcus lactis</i> , <i>Aspergillus penicillioides</i> , <i>Aspergillus flavus</i>	Francis et al. (2018)
	<i>Salvia leritifolia</i>	<i>Pseudomonas aeruginosa</i> , <i>Klebsiella pneumonia</i> , <i>Staphylococcus coagulase</i> , <i>Acinetobacter baumannii</i> , and <i>Streptococcus pneumonia</i>	Baghayeri et al. (2018)
	<i>Aesculus hippocastanum</i>	<i>Staphylococcus aureus</i> , <i>Staphylococcus epidermidis</i> , <i>Listeria monocytogenes</i> , <i>Corynebacterium renale</i> , <i>Micrococcus luteus</i> , <i>Bacillus subtilis</i> , <i>Bacillus cereus</i> , <i>Pseudomonas aeruginosa</i> , <i>Pseudomonas quorescens</i> , <i>Escherichia coli</i>	Küp et al. (2020)

(continued)

Table 26.1 (continued)

Plant part	Biological sources used for AgNPs synthesis	Anti-bacterial and anti-fungal activity and other biological activities against organisms	References
	<i>Caesalpinia pulcherrima</i>	<i>Bacillus cereus</i> , <i>Bacillus subtilis</i> , <i>Staphylococcus aureus</i> , <i>Escherichia coli</i> , <i>Pseudomonas aeruginosa</i> , <i>Salmonella typhimurium</i> , <i>Klebsiella pneumoniae</i> , <i>Candida albicans</i> , <i>Candida glabrata</i> , <i>Candida neoformans</i>	Moteriya and Chanda (2020)
	<i>Capparis zeylanica</i>	<i>Staphylococcus epidermis</i> , <i>Enterococcus faecalis</i> , <i>Shigella dysenteriae</i> , <i>Candida albicans</i> , <i>Aspergillus niger</i>	Nilavukkarasi et al. (2020)
	<i>Catharanthus roseus</i>	<i>Shigella dysenteriae</i> , <i>Klebsiella pneumoniae</i> , <i>Bacillus anthracis</i> , <i>Staphylococcus aureus</i> , and <i>Pseudomonas aeruginosa</i>	Ahmad et al. (2019)
Seeds	<i>Alpinia katsumadai</i>	<i>Escherichia coli</i> , <i>Pseudomonas aeruginosa</i>	He et al. (2017)
	<i>Nelumbo nucifera</i>	<i>Escherichia coli</i> , <i>Bacillus subtilis</i> , <i>Salmonella typhi</i> , and <i>Vibrio cholerae</i>	He et al. (2018)
	<i>Tectona grandis</i>	<i>Staphylococcus aureus</i> , <i>Bacillus cereus</i>	Rautela et al. (2019)
	<i>Phoenix dactylifera</i>	<i>Staphylococcus aureus</i>	Ansari and Alzohairy (2018)
	<i>Mangifera indica</i>	<i>Pseudomonas aeruginosa</i> , <i>Salmonella typhimurium</i> , <i>Cryptococcus neoformans</i> , <i>Candida albicans</i>	Donga and Chanda (2021)
	<i>Persea americana</i>	<i>Escherichia coli</i>	Girón-Vázquez et al. (2019)
	<i>Avicennia marina</i>	<i>Klebsiella pneumoniae</i> , <i>Escherichia coli</i> , <i>Enterococcus faecalis</i> , <i>Enterococcus faecalis</i>	Naidu et al. (2019)
	<i>Moringa oleifera</i>	<i>Enterococcus faecalis</i> , <i>Pseudomonas aeruginosa</i> , <i>Klebsiella pneumoniae</i>	Moodley et al. (2018)
	<i>Trigonella foenum-graecum</i> L.	<i>Staphylococcus aureus</i> , <i>Aspergillus flavus</i> , <i>Trichophyton rubrum</i> , and <i>Trichoderma viridiae</i>	Varghese et al. (2019)
	<i>Carum copticum</i>	<i>Pseudomonas aeruginosa</i> , <i>Serratia marcescens</i> , <i>Chromobacterium violaceum</i>	Qais et al. (2020)
Flower	<i>Malva sylvestris</i>	<i>Staphylococcus aureus</i> , <i>Streptococcus pyogenes</i> , <i>Escherichia coli</i>	Esfanddarani et al. (2017)
	<i>Abelmoschus esculentus</i>	<i>Bacillus subtilis</i> , <i>Staphylococcus aureus</i> , <i>Staphylococcus epidermidis</i> , and <i>Streptococcus pyogenes</i>	Devanesan and AlSalhi (2021)
	<i>Zingiber officinale</i>	<i>Vibrio anguillarum</i> , <i>Vibrio alginolyticus</i> , <i>Aeromonas punctata</i> ,	Yang et al. (2017)

(continued)

Table 26.1 (continued)

Plant part	Biological sources used for AgNPs synthesis	Anti-bacterial and anti-fungal activity and other biological activities against organisms	References
		<i>Vibrio parahaemolyticus</i> , <i>Vibrio splendidus</i> , and <i>Vibrio harveyi</i>	
	<i>Solanum mammosum</i>	<i>Aedes aegypti</i>	Pilaquinga et al. (2019)
	<i>Turbinaria ornata</i>	<i>Anopheles stephensi</i> and <i>Culex quinquefasciatus</i>	Deepak et al. (2017)
	<i>Moringa oleifera</i>	<i>Klebsiella pneumoniae</i> , <i>Staphylococcus aureus</i>	Bindhu et al. (2020)
	<i>Datura innoxia</i>	Cytotoxicity effect	Gajendran et al. (2019)
	<i>Syzygium aromaticum</i>	<i>Staphylococcus</i> spp., <i>Escherichia coli</i> , <i>Pseudomonas</i> spp., <i>Bacillus</i> spp., <i>Penicillium</i> spp.	Ajitha et al. (2019)
Fruits	<i>Phyllanthus emblica</i>	<i>Aspergillus oryzae</i>	Renuka et al. (2020)
	<i>Abelmoschus esculentus</i>	<i>Bacillus subtilis</i>	Mollick et al. (2019)
	<i>Myristica fragrans</i>	<i>Escherichia coli</i> , <i>Pseudomonas aeruginosa</i> , <i>Staphylococcus aureus</i> , <i>Bacillus subtilis</i>	Sasidharan et al. (2020)
	<i>Aegle marmelos</i>	<i>Escherichia coli</i> , <i>Pseudomonas aeruginosa</i> , <i>Salmonella typhi</i> , <i>Shigella dysenteriae</i> , <i>Yersinia pestis</i>	Devi et al. (2020)
	<i>Cordia obliqua</i>	<i>Escherichia coli</i> , <i>Bacillus circulans</i> , <i>Pseudomonas aeruginosa</i> , and <i>Staphylococcus aureus</i>	Saidu et al. (2019)
	<i>Nauclea latifolia</i>	<i>Escherichia coli</i> , <i>Candida albicans</i> , <i>Rhizopus</i> sp., <i>Aspergillus niger</i> , <i>Citrobacter freundii</i> , <i>Staphylococcus aureus</i> , <i>Staphylococcus</i> sp., <i>Klebsiella</i> sp.	Odeniyi et al. (2020)
Root	<i>Berberis asiatica</i>	<i>Escherichia coli</i> , <i>Staphylococcus aureus</i>	Dangi et al. (2020)
	<i>Astragalus tribuloides</i>	<i>Staphylococcus aureus</i> , <i>Shigella flexneri</i> , <i>Escherichia coli</i>	Sharifi-Rad et al. (2020)
	<i>Lysiloma acapulcensis</i>	<i>Escherichia coli</i> , <i>Pseudomonas aeruginosa</i> , <i>Staphylococcus aureus</i> , <i>Candida albicans</i>	Garibo et al. (2020).
	<i>Diospyros assimilis</i>	<i>Bacillus pumilis</i> , <i>Bacillus subtilis</i> , <i>Staphylococcus aureus</i> , <i>Streptococcus pyogenes</i> , <i>Klebsiella pneumoniae</i> , <i>Escherichia coli</i> , <i>Pseudomonas aeruginosa</i> , <i>Aspergillus niger</i> , <i>Candida albicans</i>	Kantipudi et al. (2018)

(continued)

Table 26.1 (continued)

Plant part	Biological sources used for AgNPs synthesis	Anti-bacterial and anti-fungal activity and other biological activities against organisms	References
Bacteria	<i>Novosphingobium</i> sp. HG-C3)	<i>Staphylococcus aureus</i> , <i>Candida tropicalis</i> , <i>Pseudomonas aeruginosa</i> , <i>Escherichia coli</i> , <i>Vibrio parahaemolyticus</i>	Du et al. (2017)
	<i>Kinneretia</i> THG-SQ14	<i>Candida albicans</i> , <i>Candida tropicalis</i> , <i>Bacillus cereus</i> , <i>Bacillus subtilis</i> , <i>Staphylococcus aureus</i>	Singh et al. (2016)
	<i>Bacillus methylotrophicus</i>	<i>Candida albicans</i> , <i>Salmonella enterica</i> , <i>Escherichia coli</i> , and <i>Vibrio parahaemolyticus</i>	Wang et al. (2016)
	<i>Phenerochaete chrysosporium</i>	<i>Pseudomonas aeruginosa</i> , <i>Klebsiella pneumoniae</i> , <i>Staphylococcus aureus</i>	Saravanan et al. (2018b)
	<i>Bacillus endophyticus</i>	<i>Candida albicans</i> , <i>Escherichia coli</i> , <i>Salmonella typhi</i>	Gan et al. (2018)
	<i>Acinetobacter baumannii</i>	<i>Escherichia coli</i> , <i>Pseudomonas aeruginosa</i> , and <i>Klebsiella pneumoniae</i>	Shaker and Shaaban (2017)
	<i>Weissella oryzae</i>	<i>Bacillus anthracis</i> , <i>Staphylococcus aureus</i> , <i>Escherichia coli</i> , and <i>Candida albicans</i>	Singh et al. (2016)
	<i>Bacillus thuringiensis</i>	<i>Trichoplusiani</i> (Hübner), <i>grotisipsilon</i> (Hufnagel)	Sayed et al. (2017)
	<i>Pseudomonas deceptionensis</i>	<i>Staphylococcus aureus</i> , <i>Staphylococcus enterica</i> , <i>Vibrio parahaemolyticus</i> , <i>Candida albicans</i> , and <i>Bacillus anthracis</i>	Jo et al. (2016)
	<i>Bacillus brevis</i>	<i>Salmonella typhi</i> and <i>Staphylococcus aureus</i>	Saravanan et al. (2018a)
	<i>Bacillus siamensis</i>	<i>Xanthomonas oryzae</i> pv. <i>oryzae</i> (Xoo), <i>Acidovorax oryzae</i> (Ao)	Ibrahim et al. (2019)
Fungi	<i>Penicillium citreonigrum</i> , <i>Scopulariopsis brumptii</i>	<i>Staphylococcus aureus</i>	Hamad (2019)
	<i>Alternaria</i> sp.	<i>Bacillus subtilis</i> , <i>Staphylococcus aureus</i> , <i>Escherichia coli</i> , and <i>Serratia marcescens</i>	Singh et al. (2017a, b)
	<i>Penicillium polonicum</i>	<i>Salmonella enterica</i> , serovar <i>Typhimurium</i>	Neethu et al. (2018)
	<i>Aspergillus versicolor</i>	<i>Sclerotinia sclerotiorum</i> and <i>Botrytis cinerea</i>	Elgorban et al. (2016)
	<i>Penicillium aculeatum</i>	<i>Escherichia coli</i> , <i>Pseudomonas aeruginosa</i> , <i>Staphylococcus aureus</i> , <i>Bacillus subtilis</i> , and <i>Candida albicans</i>	Ma et al. (2017)
	<i>Trichoderma harzianum</i>	<i>Sclerotinia sclerotiorum</i>	Guilger et al. (2017)

(continued)

Table 26.1 (continued)

Plant part	Biological sources used for AgNPs synthesis	Anti-bacterial and anti-fungal activity and other biological activities against organisms	References
	<i>Penicillium italicum</i>	Multidrug-resistant <i>Staphylococcus aureus</i> , <i>Shewanella putrefaciens</i> , and <i>Candida albicans</i>	Nayak et al. (2018)
	<i>Fusarium verticillioides</i>	<i>Staphylococcus aureus</i> and <i>Escherichia coli</i>	Mekkawy et al. (2017)
	<i>Aspergillus terreus</i>	<i>Salmonella typhi</i> , <i>Staphylococcus aureus</i> , and <i>Escherichia coli</i>	Rani et al. (2017)
	<i>Trichoderma harzianum</i> SYA.F4	<i>Helmintho sporium</i> sp., <i>Alternaria alternata</i> , <i>Phytophthora arenaria</i> , and <i>Botrytis</i> sp.	El-Moslamy et al. (2017)
	<i>Beauveria bassiana</i>	<i>Lipaphiserysimi</i>	Kamil et al. (2017)
Algae	<i>Ulva compressa</i> , <i>Cladophora glomerata</i>	<i>Klebsiella pneumoniae</i> , <i>Pseudomonas aeruginosa</i> , <i>Escherichia coli</i> , <i>Enterococcus faecium</i> , and <i>Staphylococcus aureus</i>	Minhas et al. (2018)
	<i>Caulerpa serrulata</i>	<i>Staphylococcus aureus</i> , <i>Pseudomonas aeruginosa</i> , <i>Shigella</i> sp., <i>Salmonella typhi</i> , and <i>Escherichia coli</i>	Aboelfetoh et al. (2017)
	<i>Enteromorpha compressa</i>	<i>Escherichia coli</i> , <i>Klebsiella pneumoniae</i> , <i>Pseudomonas</i> sp., <i>Staphylococcus aureus</i> , and <i>Salmonella paratyphi</i>	Ramkumar et al. (2017)
	<i>Spatoglossum asperum</i>	<i>Klebsiella pneumoniae</i>	Ravichandran et al. (2018)
	<i>Saccharina japonica</i>	<i>Pseudomonas aeruginosa</i> , <i>Salmonella typhimurium</i> , <i>Escherichia coli</i> , <i>Staphylococcus aureus</i> , <i>Listeria monocytogenes</i> , <i>Aspergillus brasiliensis</i> , and <i>Candida albicans</i>	Sivagnanam et al. (2017)
	<i>Gelidium amansii</i>	<i>Staphylococcus aureus</i> , <i>Bacillus pumilus</i> , <i>Escherichia coli</i> , <i>Pseudomonas aeruginosa</i> , <i>Vibrio parahaemolyticus</i> , <i>Aeromonas hydrophila</i>	Pugazhendhi et al. (2018)
	<i>Padina</i> sp.	<i>Staphylococcus aureus</i> and <i>Pseudomonas aeruginosa</i>	Bhuyar et al. (2020)
	<i>Caulerpa racemosa</i>	<i>Staphylococcus aureus</i> and <i>Proteus mirabilis</i>	Kathiraven et al. (2015)
	<i>Chlorella vulgaris</i>	<i>Salmonella enterica</i> subsp. <i>enterica</i> serovar <i>typhimurium</i> , and <i>Staphylococcus aureus</i>	Torabfam and Yüce (2020)
	<i>Gracilaria birdiae</i>	<i>Escherichia coli</i> and <i>Staphylococcus aureus</i>	de Aragao et al. (2019)

26.3 Silver Nanoparticles

Silver and its salts have been utilized as an antimicrobial agent from ancient times, though their utilization was discontinued because of its side effects (Singh et al. 2015). In recent years, silver nanoparticles have made a remarkable comeback due to their unique properties—silver nanoparticles range from 1 to 100 nm and are one of the widely studied nanoparticles. Different sizes and shapes can be considered and modified for different types of applications. AgNPs are safe to use because they are of low toxicity as silver does not interact with the organisms during the preparation (Navarro et al. 2008). Silver nanoparticles are commonly used in a spherical shape, but octagonal and thin plate AgNPs are also famous for their uses. The distinct properties of AgNPs make them a tool for investigating through research and evaluating their potential efficacy and harm. Various forms of AgNPs were synthesized upon application request. AgNPs have broad-spectrum antimicrobial properties to be used in the biomedical field, medical devices, textiles (Toh et al. 2017), water purifiers, cosmetics, and the food industry, in wound healing treatment, and in pharmaceuticals (Zhang et al. 2012).

26.4 Importance of Biosynthesis of AgNPs

Using abundant and sustainable plant resources, biosynthesis of silver nanoparticles is a viable option for meeting the high demand for “biocompatible and green synthesized nanoparticles,” particularly for biomedical and environmental applications. Chemical and physical synthesis processes are both costly and hazardous, whereas biosynthesis provides a viable alternative. Physical techniques are challenging to scale up, and the NPs generated have a minimal shelf life, necessitating the inclusion of a capping agent, as well as shallow heat stability (Rajoriya et al. 2021).

Silver is the most efficient against a broad spectrum of diseases, among other metallic nanoparticles. Numerous attempts have been undertaken in the recent decade to create green synthesis processes that prevent harmful consequences. Different chemicals and physical methods for synthesizing silver nanoparticles using harmful chemicals and sophisticated procedures have been developed that need high energy levels and pollute the environment. These disadvantages require a new solution that is favorable for the environment, cheap, and industrially feasible. An appropriate and practical strategy has developed from the current unconventional approaches for AgNPs syntheses such as microorganisms and plant extracts (Gautam et al. 2020).

Plant extract substitutes for all harmful substances, such as trisodium and sodium borohydrides (NaBH₄). The plant extract helps well in the biosynthesis of silver nanoparticles, as iron agents and terpenoids are formed stabilized by leaf broth, while polyol and water-soluble heterocyclic components are used for reducing the silver ions of leaf broth. The productivity of plants may be enhanced by connecting nanotechnology-based smart plant sensors with electronic actuators to optimize and

automate the allocation of water and agrochemical products and allow the chemical phenotyping of high-distance plants. AgNPs are used to preserve plant nutrition and disease, whereas pesticides can be used in plants to enhance agricultural crop productivity. Therapeutic compounds have been extensively used as anti-bacterial, antimicrobial, and antiviral agents (Tarannum and Gautam 2019).

26.5 Role of Plants in Green Synthesis of Nanoparticles

Various plant extracts utilized to synthesize silver nanoparticles are gaining popularity owing to several benefits, including being environmentally friendly, efficient, non-pathogenicity, and cost-effective. Many biomolecules in plant extracts, such as amino acids, proteins, enzymes, alkaloids, saponins, terpenoids, phenolics, tannins, and vitamins, decrease and stabilize silver ions. Plant extracts convert AgNO₃ to AgO ions, which may be detected using a UV-Visible spectrophotometer (Roy 2017). The ecologically recognized “green chemistry” technique, which incorporates bacteria, fungi, plants, actinomycetes, and other species, is being used in the biosynthesis of nanoparticles to create safe and ecologically acceptable nanoparticles (Pal et al. 2019).

Aqueous or alcoholic plant extracts to synthesize silver nanoparticles offer several benefits over other biological entities, mainly because it does not need cell cultures. Even though there are multiple literature publications on the green production of silver nanoparticles, plant extracts are being investigated as prospective candidates for silver nanoparticle biosynthesis. Plant-mediated biosynthesis is a simple and effective way of producing nanoparticles on a large scale without contamination (Kaur et al. 2016). The plant portion that will be used to make nanoparticles is washed and boiled in purified water. After pressing, filtering, and adding the appropriate solutions for the nanoparticles we want to synthesize, the color of the solution begins to change, revealing the formation of nanoparticles, which we can then separate (Fig. 26.2). A green technique has efficiently synthesized several nanoparticles, including gold, silver, zinc oxide, and iron. Phyto compounds reduce metallic ions in plant extracts such as polyols, terpenoids, and polyphenols (Ovais et al. 2018).

The leaf broth’s flavanone and terpenoid components are thought to stabilize the synthesis of AgNPs, whereas the polyol and water-soluble heterocyclic components are responsible for silver ion reduction. It is also widely known that AgNPs made from plant extract have a reddish hue in aqueous solutions owing to surface plasmon vibration stimulation. Two extracts may be utilized to produce AgNPs from the plants indicated above: aqueous or alcoholic, and in most situations, aqueous plant extracts are chosen since the synthesized AgNPs will be employed in medicinal or biological applications (Sorescu et al. 2016).

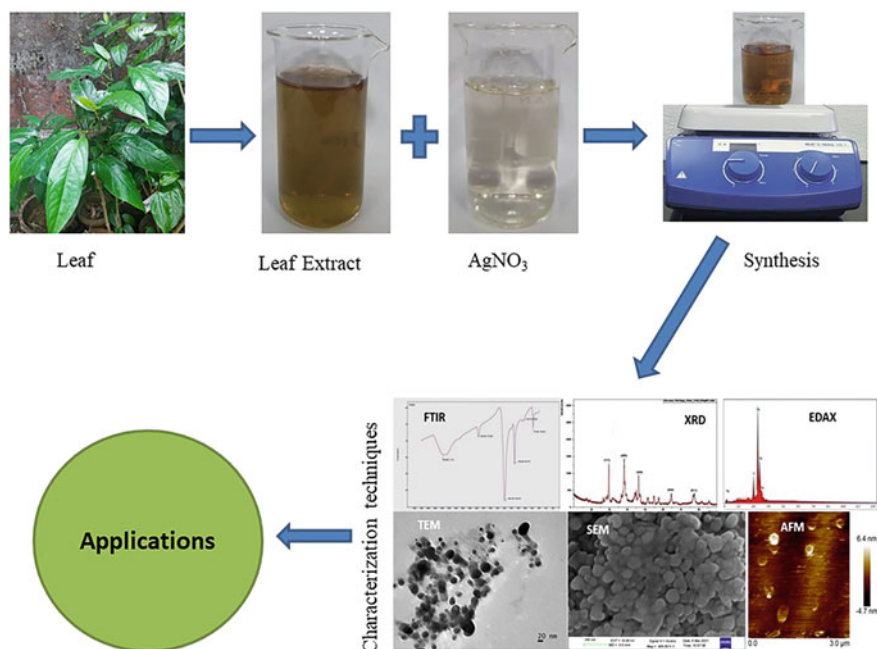


Fig. 26.2 Green synthesis of silver nanoparticle using leaf extract

26.6 Phytotoxicity Effect

The impacts on plant growth and development of nanoparticles are known to be favorable and unfavorable. One of the most severe issues concerning the usage of AgNPs in agriculture is their toxicity. According to Shams et al. (2013), foliar application of AgNPs promotes cucumber growth and production. Under AgNPs treatment, the activity of superoxide dismutase (SOD), catalase (CAT), and peroxidase (POD) enzymes increased in the *Spirodela polyrhiza* plant (Jiang et al. 2014). The phytotoxicity of nanoparticles of silver formed biologically using extract *Veronica officinalis* was assessed by Dobrucka et al. (2019) who found that biosynthesized silver nanoparticles did not have a damaging effect on concentrations of 0.0009–0.0675 in *Linum flavum* and *Lepidium sativum* seeds.

Plant-mediated silver nanoparticles have been shown to have lesser influence and a capacity to scavenge ROS, making them potential antioxidants. In particular, Ag plant-mediated NP has demonstrated significant inhibition effects for microbial growth, including bacteria such as *Pseudomonas nitroreduens*, *Escherichia coli*, *Staphylococcus aureus*, *Enterococcus*, *Acinetobacter baumannii*, *Proteus mirabilis*, *Pseudomonas*, *Klebsiella*, *Bacillus cereus*, *Aspergillus flavus*, *Pseudomonas aeruginosa*, and fungus. Given the potent inhibition of pathogens, plant-mediated

AgNPs are ideal candidates for nano-pesticides. Because of the robust pathogen's inhibition, plant-medicated silver nanoparticles are suitable candidates for agricultural nano-pesticides (Zhang et al. 2021).

The effects of AgNPs on three plant species, namely watermelon, maize, and zucchini, were investigated, and it was discovered that their germination rates increased in response to AgNPs. Much research has been conducted to determine the impact of AgNPs on plant development and yield. AgNPs have been demonstrated to inhibit the development of *Pisum sativum* (Tripathi et al. 2017) and *Oryza sativa* (Nair and Chung 2014) plants, as well as to cause oxidative stress in the medicinal plant *Portulaca oleracea* (Zare et al. 2020).

Mehta et al. (2016) showed improved seed germination and increased germination and biomass when nanoparticles were used. The application of AgNPs enhances the generation of root exudates, which may enable plant-microbe interactions and aid plant development. When AgNPs were treated with Fenugreek, Jasim et al. (2017) showed an increase in growth metrics (*Trigonella foenum-graecum* L.). Upregulation of these genes altered the levels of ABA and IAA. Gruyer et al. (2013) also found that AgNPs had a favorable effect on plant development in greenhouse produced radish and lettuce, with the impact varying depending on the species. The biosynthesized AgNPs can boost *T. aestivum* growth both singly and in combination with bacterial inoculation. Bacterial AgNPs is exploited as silver ion extractors and increase plant development (Wagi and Ahmed 2019).

The use of AgNPs as an exogenous interference enhanced seed germination and early growth parameters. *T. foenum-graecum*, *Z. mays*, and *A. cepa* seed germination percentages were more significant in the biosynthesized AgNPs-treated plants than in the controls (Soliman et al. 2020). In *Spirodela polyrrhiza*, nanoparticle toxicity has been exposed, including seed germination impairment and root and shoots growth suppression. Plant development is harmed by AgNPs, which cause biomass loss in Cucurbita pepo, cytotoxic damage in *Allium cepa* root tip cells, and degradation of nitrogen content and photosystem II efficiency in *Spirodela polyrrhiza*. In *Solanum lycopersicum*, AgNPs reduce chlorophyll concentration while increasing superoxide dismutase (SOD) activity (Syu et al. 2014).

Although AgNPs have been demonstrated to have adverse effects on various vegetative growths regularly, earlier research has revealed that AgNPs have a phytostimulatory impact. The application of AgNP, for example, promotes *Brassica juncea* root growth (Sharma et al. 2012). AgNP may improve root growth in *Crocus sativus* by blocking ethylene (ET) signaling during flooding (Rezvani et al. 2012). The morphological and physiological growth and development of *Maerua oblongifolia* grown in vitro were considerably enhanced by the biosynthesized AgNPs (Shaikhaldein et al. 2020). The impact of NPs on higher plants is a relatively new study. Krishnaraj et al. (2012) discovered that biosynthesized AgNPs substantially influenced seed germination and promoted protein and carbohydrate synthesis on *Bacopa monnieri* growth metabolism a few years ago. Also, AgNPs enhanced the growth profile (shoot and root length), chlorophyll, carbohydrate and protein contents, and antioxidant enzymes of *Brassica juncea*, common bean, and maize (Salama 2012). The majority of documented research shows that NPs have favorable

effects on plant development, with a few isolated research showing that they have deleterious effects (Hojjat and Hojjat 2015).

The harmful level of nanoparticles may be responsible for the loss in shoot length, and fresh and dry weight of wheat plants at higher dosages. AgNPs efficiently promote photosynthesis and are associated with changes in nitrogen metabolism, according to Farghaly and Nafady (2015). In comparison to the control, *M. indica* at 20 and 40 ppm caused considerable increases. However, at 60 ppm, AgNPs resulted in a considerable drop in protein content. These findings corroborate those of prior research (Najafi et al. 2014), which found that silver nanoparticles increased the protein rate of *Phaseolus vulgaris* seedlings. Mirmoeini et al. (2021) investigated the effect of different ratios of AgNPs produced using *camelina* plant extract on camelina growth and physiological features. The findings revealed that adding AgNPs inhibited *camelina* growth in a concentration-dependent manner (height and biomass).

26.7 Applications of Silver Nanoparticles in Agriculture

In most countries, agriculture is the backbone of development, and most people depend on agricultural products. Scientists are attempting to find a way to feed the rapidly increasing world population, which currently stands at over 7 billion people. Nanoculture is currently focused on specific cultivation with nanoscale particles that have unique biochemical properties to increase productivity. The nanoparticles included target specification, autonomic and multifunctional capabilities. Nanotechnology is a rapidly advanced science nowadays with both scientific and industrial applications. Scientists are trying to discover their potential applications in drug delivery and cancer treatment, and agriculture (Gu et al. 2011).

The aim of phyto-nanotechnology focused on developing “smart crops.” In the agriculture system, nanotechnology has a demand for pest protection and nutritional enrichment. As a result, chemical fertilizers are utilized less frequently in conventional farming. The scope of nanoparticles in agriculture is shown in Fig. 26.3. AgNPs have many pesticide applications due to their high efficacy against phytopathogens and low toxicity. It is effective towards site-targeted delivery of important agricultural substances and diagnostics devices in the event of plant disease identification in advance. Silver nanoparticles have the potential to enhance food safety, global food supply, plant health, disease prevention and regulation, plant growth tracking, and pest control for “sustainable agricultural development” due to their broad spectrum of antimicrobial properties (Prasad et al. 2017a).

Size, surface charge, and other factors play a vital role in revealing the AgNPs unique properties. AgNPs with a spherical form are now widely used. Because of its enormous surface area, it can synchronize a large number of ligands. The antioxidant, anti-bacterial, anti-fungal, antiviral, and anti-inflammatory properties of AgNPs are well-known. This nanotechnology plays a critical role in processing agricultural products by regulating nutrients.



Fig. 26.3 Silver nanoparticle application in agriculture

26.8 Plant Disease Management and Protection

AgNPs are used as antimicrobial agents because of their broad-spectrum function and various inhibitory mechanisms against pathogens. Colloidal AgNPs that are well spread and stabilized adhere better to bacterial and fungal cell surfaces, making them more effective bactericides and fungicides. Several research groups have documented plant disease management with AgNPs. Disease control of food crops and fruits is crucial for the economy. Ocoy et al. (2013) analyzed the anti-bacterial action of DNA-directed silver NPs grown on graphene oxide against *Xanthomonas perforans*, the causative agent of tomato bacterial spots. In a greenhouse experiment, they discovered that applying 100 ppm DNA-directed AgNPs grown on graphene oxide to Tomato transplants significantly decreased the incidence of bacterial spot disease relative to untreated plants.

Ouda (2014) showed that AgNPs inhibited the development of two plant pathogens, *Alternaria alternata* and *Botrytis cinerea*, at various concentrations in the growth medium. Secondary metabolites such as tannin, saponin, and glycosides responsible for plant extract are antimicrobial function (Polash et al. 2017). Elamawi et al. (2018) also tested the anti-fungal activity of AgNPs produced by *Trichoderma longibrachiatum* against nine different fungal isolates, including *Aspergillus alternate*, *Fusarium verticillioides*, *Fusarium moniliforme*, *Aspergillus flavus*, *Aspergillus heteromorphus*, *Penicillium glabrum*, *Penicillium brevicompactum*, *Helminthospororyzae*, and *Pyricularia grisea*.

26.9 Nanofertilizers

Nanotechnology can enable sustainable development applications by establishing innovative delivery systems using nanofertilizers, pesticides, and herbicides. Nanofertilizers containing AgNP were developed to synchronize nutrient delivery with plant uptake. It inhibits nutrient loss and soil and groundwater contamination by chemical interactions with water, soil, and microorganisms, making them ineffective or unnecessary (Castillo-Henríquez et al. 2020). Large quantities of commercial fertilizers are being utilized in urea and nitrates. However, these chemical fertilizers are hazardous to plants and important microflora. They are also harmful to the environment. Due to their high surface areas compared to traditional ones, they allow for gradual releases of fertilizers and pesticides. The nano-silver promotes nutrient absorption from the soil over the bulk silver. As a result, it can be used in crop improvement as well as crop protection. They have the potential to be employed as nanofertilizers. Silver nanoparticles have been suggested as a way to improve seed germination in a variety of plants. Nanofertilizers aid in the gradual and efficient release of nutrients, decreasing nutrient losses. The use of nanofertilizers can help plants absorb more nutrients from the soil (Anand and Bhagat 2019).

Silver nanoparticles were highly stable, biocompatible, and had a delayed agro-chemical release. Therefore, it may be employed for the gradual and enhanced distribution of agricultural chemicals, herbicides, and fertilizers—the nano-bio fertilizer made from onion extract by Gosavi et al. (2020). The developed nanofertilizer is suitable for brinjal and tomato plants, but it has to be tested in the field. The use of nano-bio fertilizers like these can help minimize environmental pollution and the overuse of chemical fertilizers in the field and farm management expenses. Kang et al. (2016) reported using a 5 mg/L silver nanoparticle fertilizer suspension three times per day at 14-day intervals to red ginseng shoots. After harvesting, the nanofertiliser was reported to enhance the amount of ginsenoside.

26.10 Pest Management

Silver nanoparticles have been tested as insecticides to control insect infestations in crops. It requires pest control and nutritional supplementation. Chemical fertilizers are used less frequently in conventional farming as a result of this. It can eliminate undesirable bacteria from soils and hydroponics systems. The anti-bacterial capabilities of aqueous silver solution, which is used to treat plants, have been demonstrated to be effective against pathogenic bacteria that cause powdery mildew or downy mildew. It also promotes physiological activity and growth in plants and disease and stress resistance (Yokesh Babu et al. 2014). Nano-silver is an efficient, nontoxic, safe, and improved pest control agent and a high dosage pesticide based on silver nano products also supply the target plants with a high dosage of pesticides. Because the biological agents utilized in the green technique of making silver nanoparticles may be microbes or plants, and the flavonoids contained in the plants are shown to be harmful to the plants, the pesticide activity of silver nanoparticles can assist a lot in the management of pests (Kale et al. 2021).

AgNPs have been used in the management of insect pests. Goswami et al. (2010) investigated the utilization of agricultural nanoparticles to prevent rice weevil and grasserie disease. Even after 2 months of treatment with AgNPs, stored rice remained uninfected, so it is suggested that AgNPs can also be used as an efficient method for seed protecting agents. Smaller AgNPs were found to be the most effective against the tested phytopathogenic fungi. Indeed, several experiments have shown that AgNP behavior is highly influenced by nanoparticle size (Rahimi et al. 2016).

26.11 Conclusion

Developing a reliable and environmentally acceptable method for silver nanoparticle production is a critical requirement in nanotechnology. Nanoparticles are regarded as essential components of nanotechnology. Because of their fascinating physicochemical characteristics, silver nanoparticles play a significant role in biology and biomedical research. Green synthesis has an advantage over chemical and physical processes since it is less expensive, more environmentally friendly, and more easily scaled up for large-scale synthesis. Nature has beautiful and imaginative ways of creating the most capable tiny valuable materials. The motivation to create eco-friendly approaches arose from a growing knowledge of green chemistry and green routes to manufacture metal NPs, particularly AgNPs. Green-synthesized AgNPs have essential features of nanotechnology across a range of applications.

AgNPs provide various cardiovascular, dental, medical, therapeutic, biosensor, farming, and more applications. Instead of utilizing commercially available synthetic pesticides, which have higher toxicity to people, biosynthesized nanoparticles might be utilized to protect various agricultural plants and their products from plant phytopathogens. As a result, all nanoparticles have no discernible detrimental influence on seed germination, root-shoot ratio, or soil microbiota, while some are

helpful to plants and, as a result, to farmers. As a result, the use of green-produced silver nanoparticles in plant disease management, nanofertilizers, nanopesticides, pesticide treatment, and plant pathogen detection is concluded in this chapter.

Nanotechnology is a fortunate technique that can drastically alter agricultural processes. AgNPs have distinguished themselves in the agricultural field by demonstrating unique characteristics. They have been shown to increase crop production, protect crops from bacterial and fungal infections/diseases, and protect crops from insect attack/infestation. Ag NPs are often used in “nano-packages” to extend the shelf life of fresh agricultural products such as fruits and vegetables. Future research should examine the function of plant metabolites in AgNP synthesis and synthesis using distilled single metabolites rather than crude extracts and process and physicochemical state control to achieve shapes other than circular, such as triangle, square, and hexagon. Other than commercial processing and the use of agricultural applications, research must concentrate on assessing the effect of AgNPs on biotic and abiotic factors in the ecosystem and human health.

References

- Aboelfetoh EF, El-Shenody RA, Ghobara MM (2017) Eco-friendly synthesis of silver nanoparticles using green algae (*Caulerpa serrulata*): reaction optimisation, catalytic and anti-bacterial activities. *Environ Monit Assess* 189(7):1–15
- Ahmad S, Tauseef I, Haleem KS, Khan K, Shahzad M, Ali M, Sultan F (2019) Synthesis of silver nanoparticles using leaves of *Catharanthus roseus* and their antimicrobial activity. *Appl Nanosci*:1–6. <https://doi.org/10.1007/s13204-019-01221-z>
- Ahmed S, Ahmad M, Swami BL, Ikram S (2016) A review on plants extract mediated synthesis of silver nanoparticles for antimicrobial applications: a green expertise. *J Adv Res* 7(1):17–28
- Ajitha B, Reddy YAK, Lee Y, Kim MJ, Ahn CW (2019) Biomimetic synthesis of silver nanoparticles using *Syzygium aromaticum* (clove) extract: catalytic and antimicrobial effects. *Appl Organomet Chem* 33(5):e4867
- Amalorpavamary G, Dineshkumar G, Jayaseelan K (2019) Ecofriendly synthesis of silver nanoparticles from leaves extract of *Phyllanthus niruri* (L.) and their anti-bacterial properties. *J Drug Deliv Therap* 9(1-S):196–200
- Anand R, Bhagat M (2019) Silver nanoparticles (AgNPs): As nanopesticides and nanofertilizers. *MOJ Biol Med* 4:19–20. <https://doi.org/10.15406/mojbm.2019.04.00107>
- Anju TR, Parvathy S, Veetil MV, Rosemary J, Ansalna TH, Shahzabanu MM, Devika S (2021) Green synthesis of silver nanoparticles from Aloe vera leaf extract and its antimicrobial activity. *Mater Today Proc* 43:3956–3960
- Ansari MA, Alzohairy MA (2018) One-pot facile green synthesis of silver nanoparticles using seed extract of *Phoenix dactylifera* and their bactericidal potential against MRSA. *Evid Based Complement Alternat Med* 2018:1860280
- Baghayeri M, Mahdavi B, Abadi ZH-M, Farhadi S (2018) Green synthesis of silver nanoparticles using water extract of *Salvia leriifolia*: anti-bacterial studies and applications as catalysts in the electrochemical detection of nitrite. *Appl Organomet Chem* 32(2):e4057
- Behravan M, Panahi AH, Naghizadeh A, Ziaee M, Mahdavi R, Mirzapour A (2019) Facile green synthesis of silver nanoparticles using *Berberis vulgaris* leaf and root aqueous extract and its anti-bacterial activity. *Int J Biol Macromol* 124:148–154
- Bernardo-Mazariegos E, Valdez-Salas B, González-Mendoza D, Abdelmoteleb A, Camacho OT, Duran CC, Gutiérrez-Miceli F (2019) Silver nanoparticles from *Justicia spicigera* and their

- antimicrobial potentialities in the biocontrol of foodborne bacteria and phytopathogenic fungi. *Rev Argent Microbiol* 51(2):103–109
- Bhuyar P, Rahim MHA, Sundararaju S, Ramaraj R, Maniam GP, Govindan N (2020) Synthesis of silver nanoparticles using marine macroalgae *Padina* sp. and its anti-bacterial activity towards pathogenic bacteria. *Beni-Suef Univ J Basic Appl Sci* 9(1):1–15
- Bindhu MR, Umadevi M, Esmail GA, Al-Dhabi NA, Arasu MV (2020) Green synthesis and characterisation of silver nanoparticles from *Moringa oleifera* flower and assessment of antimicrobial and sensing properties. *J Photochem Photobiol B Biol* 205:111836
- Castillo-Henríguez L, Alfaro-Aguilar K, Ugalde-Álvarez J, Vega-Fernández L, de Oca-Vásquez GM, Vega-Baudrit JR (2020) Green synthesis of gold and silver nanoparticles from plant extracts and their possible applications as antimicrobial agents in the agricultural Area. *Nanomaterials* 10(9):1763
- Chandirika JU, Annadurai G (2018) Biosynthesis and characterisation of silver nanoparticles using leaf extract *Abutilon indicum*. *Glob J Biotechnol Biochem* 13(1):7–11
- Dangi S, Gupta A, Gupta DK, Singh S, Parajuli N (2020) Green synthesis of silver nanoparticles using aqueous root extract of *Berberis asiatica* and evaluation of their anti-bacterial activity. *Chem Data Collect* 28:100411
- de Aragao AP, de Oliveira TM, Quelemes PV, Perfeito MLG, Araujo MC, de Araújo Sousa Santiago J, Cardoso VS, Quaresma P, de Souza de Almeida JR, da Silva DA (2019) Green synthesis of silver nanoparticles using the seaweed *Gracilariabirdiae* and their antibacterial activity. *Arab J Chem* 12(8):4182–4188
- Deepak P, Sowmiya R, Ramkumar R, Balasubramani G, Aiswarya D, Perumal P (2017) Structural characterisation and evaluation of mosquito-larvicidal property of silver nanoparticles synthesised from the seaweed, *Turbinariaornata* (Turner) J. Agardh 1848. *Artif Cells Nanomed Biotechnol* 45(5):990–998
- Devanesan S, AlSalhi MS (2021) Green synthesis of silver nanoparticles using the flower extract of *abelmoschus esculentus* for cytotoxicity and antimicrobial studies. *Int J Nanomedicine* 16:3343
- Devi M, Devi S, Sharma V, Rana N, Bhatia RK, Bhatt AK (2020) Green synthesis of silver nanoparticles using methanolic fruit extract of *Aegle marmelos* and their antimicrobial potential against human bacterial pathogens. *J Tradit Complement Med* 10(2):158–165
- Dobrucka R, Szymanski M, Przekop R (2019) The study of toxicity effects of biosynthesised silver nanoparticles using *Veronica officinalis* extract. *Int J Environ Sci Technol* 16(12):8517–8526
- Donga S, Chanda S (2021) Facile green synthesis of silver nanoparticles using *Mangifera indica* seed aqueous extract and its antimicrobial, antioxidant and cytotoxic potential (3-in-1 system). *Artif Cells Nanomed Biotechnol* 49(1):292–302
- Du J, Singh H, Yi T-H (2017) Biosynthesis of silver nanoparticles by *Novosphingobium* sp. THG-C3 and their antimicrobial potential. *Artif Cells Nanomed Biotechnol* 45(2):211–217
- Elamawi RM, Al-Harbi RE, Hendi AA (2018) Biosynthesis and characterisation of silver nanoparticles using *Trichoderma longibrachiatum* and their effect on phytopathogenic fungi. *Egypt J Biol Pest Control* 28(1):1–11
- Elgorban AM, Aref SM, Seham SM, Elhindi KM, Bahkali AH, Sayed SR, Manal MA (2016) Extracellular synthesis of silver nanoparticles using *Aspergillus versicolor* and evaluation of their activity on plant pathogenic fungi. *Mycosphere* 7(6):844–852
- El-Moslamy SH, Elkady MF, Rezk AH, Abdel-Fattah YR (2017) Applying Taguchi design and large-scale strategy for mycosynthesis of nano-silver from endophytic *Trichoderma harzianum* SYA. F4 and its application against phytopathogens. *Sci Rep* 7(1):1–22
- Esfanddarani HM, Kajani AA, Bordbar A-K (2017) Green synthesis of silver nanoparticles using flower extract of *Malva sylvestris* and investigation of their anti-bacterial activity. *IET Nanobiotechnol* 12(4):412–416
- Farghaly FA, Nafady NA (2015) Green synthesis of silver nanoparticles using leaf extract of *Rosmarinus officinalis* and its effect on tomato and wheat plants. *J Agric Sci* 7(11):277

- Francis S, Joseph S, Koshy EP, Mathew B (2018) Microwave-assisted green synthesis of silver nanoparticles using leaf extract of *Elephantopus scaber* and its environmental and biological applications. *Artif Cells Nanomed Biotechnol* 46(4):795–804
- Gajendran B, Durai P, Varier KM, Liu W, Li Y, Rajendran S, Nagarathnam R, Chinnasamy A (2019) Green synthesis of silver nanoparticle from *Datura innoxia* flower extract and its cytotoxic activity. *BioNanoScience* 9(3):564–572
- Gan L, Zhang S, Zhang Y, He S, Tian Y (2018) Biosynthesis, characterisation and antimicrobial activity of silver nanoparticles by a halotolerant *Bacillus endophyticus* SCU-L. *Prep Biochem Biotechnol* 48(7):582–588
- Garibo D, Borbón-Núñez HA, Jorge N, de León D, Mendoza EG, Estrada I, Toledano-Magaña Y, Tiznado H et al (2020) Green synthesis of silver nanoparticles using *Lysilomaacapulcensis* exhibit high-antimicrobial activity. *Sci Rep* 10(1):1–11
- Gautam N, Salaria N, Thakur K, Kukreja S, Yadav N, Yadav R, Goutam U (2020) Green silver nanoparticles for phytopathogen control. *Proc Natl Acad Sci India B Biol Sci* 90(2):439–446
- Ghotekar S, Pansambal S, Pawar SP, Pagar T, Oza R, SachinBangale. (2019) Biological activities of biogenically synthesised fluorescent silver nanoparticles using *Acanthospermum hispidum* leaves extract. *SN Appl Sci* 1(11):1–12
- Girón-Vázquez NG, Gómez-Gutiérrez CM, Soto-Robles CA, Nava O, Lugo-Medina E, Castrejón-Sánchez VH, Vilchis-Nestor AR, Luque PA (2019) Study of the effect of *Persea americana* seed in the green synthesis of silver nanoparticles and their antimicrobial properties. *Results Phys* 13: 102142
- Gosavi VC, Daspute AA, Patil A, Gangurde A, Wagh SG, Sherkhane A, Deshmukh VA (2020) Synthesis of green nanobiofertilizer using silver nanoparticles of *Allium cepa* extract short title: green nanofertilizer from *Allium cepa*. *IJCS* 8(4):1690–1694
- Goswami A, Roy I, Sengupta S, Debnath N (2010) Novel applications of solid and liquid formulations of nanoparticles against insect pests and pathogens. *Thin Solid Films* 519(3): 1252–1257
- Grùere G, Narrod C, Abbott L (2011) *Agricultural, food, and water nanotechnologies for the poor*. International Food Policy Research Institute, Washington, DC
- Gruyer N, Dorais M, Bastien C, Dassylva N, Triffault-Bouchet G (2013) Interaction between silver nanoparticles and plant growth. In: *International symposium on new technologies for environment control, energy-saving and crop production in greenhouse and plant*, vol 1037, pp 795–800
- Gu Z, Biswas A, Zhao M, Tang Y (2011) Tailoring nanocarriers for intracellular protein delivery. *Chem Soc Rev* 40(7):3638–3655
- Guilger M, Pasquoto-Stigliani T, Bilesky-Jose N, Grillo R, Abhilash PC, Fraceto LF, De Lima R (2017) Biogenic silver nanoparticles based on *Trichoderma harzianum*: synthesis, characterisation, toxicity evaluation and biological activity. *Sci Rep* 7(1):1–13
- Hamad MT (2019) Biosynthesis of silver nanoparticles by fungi and their anti-bacterial activity. *Int J Environ Sci Technol* 16(2):1015–1024
- He Y, Wei F, Ma Z, Zhang H, Yang Q, Yao B, Huang Z, Li J, Zeng C, Zhang Q (2017) Green synthesis of silver nanoparticles using seed extract of *Alpinia katsumadai*, and their antioxidant, cytotoxicity, and anti-bacterial activities. *RSC Adv* 7(63):39842–39851
- He Y, Li X, Zheng Y, Wang Z, Ma Z, Yang Q, Yao B, Zhao Y, Zhang H (2018) A green approach for synthesising silver nanoparticles, and their anti-bacterial and cytotoxic activities. *New J Chem* 42(4):2882–2888
- Hojjat SS, Hojjat H (2015) Effect of nanosilver on seed germination and seedling growth in fenugreek seed. *Int J Food Eng* 1(2):106–110
- Ibrahim E, Fouad H, Zhang M, Zhang Y, Qiu W, Yan C, Li B, Mo J, Chen J (2019) Biosynthesis of silver nanoparticles using endophytic bacteria and their role in inhibition of rice pathogenic bacteria and plant growth promotion. *RSC Adv* 9(50):29293–29299
- Iravani S, Korbekandi H, Mirmohammadi SV, Zolfaghari B (2014) Synthesis of silver nanoparticles: chemical, physical and biological methods. *Res Pharm Sci* 9(6):385

- Jasim B, Thomas R, Mathew J, Radhakrishnan EK (2017) Plant growth and diosgenin enhancement effect of silver nanoparticles in Fenugreek (*Trigonella foenum-graecum* L.). *Saudi Pharm J* 25(3):443–447
- Javed R, Zia M, Naz S, Aisida SO, Ain N u, Ao Q (2020) Role of capping agents in the application of nanoparticles in biomedicine and environmental remediation: recent trends and future prospects. *J Nanobiotechnol* 18(1):1–15
- Jiang H-S, Qiu X-N, Li G-B, Li W, Yin L-Y (2014) Silver nanoparticles induced accumulation of reactive oxygen species and alteration of antioxidant systems in the aquatic plant *Spirodela polyrrhiza*. *Environ Toxicol Chem* 33(6):1398–1405
- Jo JH, Singh P, Kim YJ, Wang C, Mathiyalagan R, Jin C-G, Yang DC (2016) *Pseudomonas deceptionensis* DC5-mediated synthesis of extracellular silver nanoparticles. *Artif Cells Nanomed Biotechnol* 44(6):1576–1581
- Kale SK, Parishwad GV, Husainy ASN, Patil AS (2021) Emerging agriculture applications of silver nanoparticles. *ES Food Agroforest* 3:17–22
- Kamil D, Prameeladevi T, Ganesh S, Prabhakaran N, Nareshkumar R, Thomas SP (2017) Green synthesis of silver nanoparticles by entomopathogenic fungus *Beauveria bassiana* and their bioefficacy against mustard aphid (*Lipaphis erysimi* Kalt.). *Indian J Exp Biol* 55:555–561
- Kang H, Hwang Y-G, Lee T-G, Jin C-R, Cho CH, Jeong H-Y, Kim D-O (2016) Use of gold nanoparticle fertiliser enhances the ginsenoside contents and anti-inflammatory effects of red ginseng. *J Microbiol Biotechnol* 26(10):1668–1674
- Kantipudi S, Pethakamsetty L, Kollana SM, Sunkara JR, Kollu P, Parine NR, Rallabhandi M, Pammi SVN (2018) *Diospyros* assimilis root extract assisted biosynthesised silver nanoparticles and their evaluation of antimicrobial activity. *IET Nanobiotechnol* 12(2):133–137
- Kathiraven T, Sundaramanickam A, Shanmugam N, Balasubramanian T (2015) Green synthesis of silver nanoparticles using marine algae *Caulerpa racemosa* and their anti-bacterial activity against some human pathogens. *Appl Nanosci* 5(4):499–504
- Kaur N, Sharma I, Kirat K, Pati PK (2016) Detection of reactive oxygen species in *Oryza sativa* L. (rice). *Bio-protocol* 6(24):e2061
- Krishnaraj C, Jagan EG, Ramachandran R, Abirami SM, Mohan N, Kalaichelvan PT (2012) Effect of biologically synthesised silver nanoparticles on *Bacopa monnieri* (Linn.) Wettst. plant growth metabolism. *Process Biochem* 47(4):651–658
- Küp FÖ, Çoşkunçay S, Duman F (2020) Biosynthesis of silver nanoparticles using leaf extract of *Aesculus hippocastanum* (horse chestnut): evaluation of their anti-bacterial, antioxidant and drug release system activities. *Mater Sci Eng C* 107:110207
- Ma L, Wei S, Liu J-X, Zeng X-X, Huang Z, Li W, Liu Z-C, Tang J-X (2017) Optimisation for extracellular biosynthesis of silver nanoparticles by *Penicillium aculeatum* Su1 and their antimicrobial activity and cytotoxic effect compared with silver ions. *Mater Sci Eng C* 77: 963–971
- Mathur P, Jha S, Ramteke S, Jain NK (2018) Pharmaceutical aspects of silver nanoparticles. *Artif Cells Nanomed Biotechnol* 46(Suppl 1):115–126
- Mehta CM, Srivastava R, Arora S, Sharma AK (2016) Impact assessment of silver nanoparticles on plant growth and soil bacterial diversity. *3 Biotech* 6(2):1–10
- Mekkawy AI, El-Mokhtar MA, Nafady NA, Yousef N, Hamad MA, El-Shanawany SM, Ibrahim EH, Elsabahy M (2017) In vitro and in vivo evaluation of biologically synthesised silver nanoparticles for topical applications: effect of surface coating and loading into hydrogels. *Int J Nanomedicine* 12:759
- Minhas FT, Arslan G, Gubbuk IH, Akkoz C, Ozturk BY, Asikkutlu B, Arslan U, Ersoz M (2018) Evaluation of anti-bacterial properties on polysulfone composite membranes using synthesised biogenic silver nanoparticles with *Ulva compressa* (L.) Kütz. and *Cladophora glomerata* (L.) Kütz. extracts. *Int J Biol Macromol* 107:157–165
- Mirmoeini T, Pishkar L, Kahrizi D, Barzin G, Karimi N (2021) Phytotoxicity of green synthesised silver nanoparticles on *Camelina sativa* L. *Physiol Mol Biol Plants* 27(2):417–427

- Mollick MMR, Rana D, Dash SK, Chattopadhyay S, Bhowmick B, Maity D, Mondal D et al (2019) Studies on green synthesised silver nanoparticles using *Abelmoschus esculentus* (L.) pulp extract having anticancer (in vitro) and antimicrobial applications. *Arab J Chem* 12(8): 2572–2584
- Moodley JS, Krishna SBN, Pillay K, Govender P (2018) Green synthesis of silver nanoparticles from *Moringa oleifera* leaf extracts and its antimicrobial potential. *Adv Nat Sci Nanosci Nanotechnol* 9(1):015011
- Moteriya P, Chanda S (2020) Green synthesis of silver nanoparticles from *Caesalpinia pulcherrima* leaf extract and evaluation of their antimicrobial, cytotoxic and genotoxic potential (3-in-1 system). *J Inorg Organomet Polym Mater* 30(10):3920–3932
- Naidu KSB, Murugan N, Adam JK (2019) Biogenic synthesis of silver nanoparticles from *Avicennia marina* seed extract and its anti-bacterial potential. *Bionanoscience* 9(2):266–273
- Nair PMG, Chung IM (2014) Physiological and molecular level effects of silver nanoparticles exposure in rice (*Oryza sativa* L.) seedlings. *Chemosphere* 112:105–113
- Najafi S, Heidari R, Jamei R (2014) Photosynthetic characteristics, membrane lipid levels and protein content in the *Phaseolus vulgaris* L. (cv. Sadri) exposed to magnetic field and silver nanoparticles. *Bull Environ Pharmacol Life Sci* 3:72–76
- Navarro E, Baun A, Behra R, Hartmann NB, Filser J, Miao A-J, Quigg A, Santschi PH, Sigg L (2008) Environmental behavior and ecotoxicity of engineered nanoparticles to algae, plants, and fungi. *Ecotoxicology* 17(5):372–386
- Nayak BK, Nanda A, Prabhakar V (2018) Biogenic synthesis of silver nanoparticle from wasp nest soil fungus, *Penicillium italicum* and its analysis against multidrug resistance pathogens. *Biocatal Agric Biotechnol* 16:412–418
- Neethu S, Midhun SJ, Radhakrishnan EK, Jyothis M (2018) Green synthesised silver nanoparticles by marine endophytic fungus *Penicillium polonicum* and its anti-bacterial efficacy against biofilm forming, multidrug-resistant *Acinetobacter baumannii*. *Microb Pathog* 116:263–272
- Nilavukkarasi M, Vijayakumar S, Prathip Kumar S (2020) Biological synthesis and characterisation of silver nanoparticles with *Capparis zeylanica* L. leaf extract for potent antimicrobial and anti-proliferation efficiency. *Mater Sci Energy Technol* 3:371–376
- Noor H (2020) Therapeutic evaluation of silver nanoparticles synthesized using *Bryophyllum pinnatum* plant extract. PhD diss., Capital University
- Ocsoy I, Paret ML, Ocsoy MA, Kunwar S, Chen T, You M, Tan W (2013) Nanotechnology in plant disease management: DNA-directed silver nanoparticles on graphene oxide as an anti-bacterial against *Xanthomonas perforans*. *ACS Nano* 7(10):8972–8980
- Odeniyi MA, Okumah VC, Adebayo-Tayo BC, Odeniyi OA (2020) Green synthesis and cream formulations of silver nanoparticles of *Nauclea latifolia* (African peach) fruit extracts and evaluation of antimicrobial and antioxidant activities. *Sustain Chem Pharm* 15:100197
- Ouda SM (2014) Anti-fungal activity of silver and copper nanoparticles on two plant pathogens, *Alternaria alternata* and *Botrytis cinerea*. *Res J Microbiol* 9(1):34
- Ovais M, Khalil AT, Islam NU, Ahmad I, Ayaz M, Saravanan M, Shinwari ZK, Mukherjee S (2018) Role of plant phytochemicals and microbial enzymes in biosynthesis of metallic nanoparticles. *Appl Microbiol Biotechnol* 102(16):6799–6814
- Pal G, Rai P, Pandey A (2019) Green synthesis of nanoparticles: a greener approach for a cleaner future. In: *Green synthesis, characterisation and applications of nanoparticles*. Elsevier, Amsterdam, pp 1–26
- Pilaquinga F, Morejón B, Ganchala D, Morey J, Piña N, Debut A, Neira M (2019) Green synthesis of silver nanoparticles using *Solanum mammosum* L. (Solanaceae) fruit extract and their larvicidal activity against *Aedes aegypti* L. (Diptera: Culicidae). *PLoS One* 14(10):e0224109
- Polash SA, Saha T, Hossain MS, Sarker SR (2017) Investigation of the phytochemicals, antioxidant, and antimicrobial activity of the *Andrographis paniculata* leaf and stem extracts. *Adv Biosci Biotechnol* 8(5):149
- Prasad R, Bhattacharyya A, Nguyen QD (2017a) Nanotechnology in sustainable agriculture: recent developments, challenges, and perspectives. *Front Microbiol* 8:1014

- Prasad R, Gupta N, Kumar M, Kumar V, Wang S, Abd-Elsalam KA (2017b) Nanomaterials act as plant defense mechanism. In: Nanotechnology. Springer, Singapore, pp 253–269
- Pugazhendhi A, Prabakar D, Jacob JM, Karuppusamy I, Saratale RG (2018) Synthesis and characterisation of silver nanoparticles using *Gelidiummamsanii* and its antimicrobial property against various pathogenic bacteria. *Microb Pathog* 114:41–45
- Qais FA, Shafiq A, Ahmad I, Husain FM, Khan RA, Hassan I (2020) Green synthesis of silver nanoparticles using *Carum copticum*: assessment of its quorum sensing and biofilm inhibitory potential against gram negative bacterial pathogens. *Microb Pathog* 144:104172
- Radini IA, Hasan N, Malik MA, Khan Z (2018) Biosynthesis of iron nanoparticles using *Trigonella foenum-graecum* seed extract for photocatalytic methyl orange dye degradation and anti-bacterial applications. *J Photochem Photobiol B Biol* 183:154–163
- Rafique M, Iqra Sadaf M, Rafique S, Bilal Tahir M (2017) A review on green synthesis of silver nanoparticles and their applications. *Artif Cells Nanomed Biotechnol* 45(7):1272–1291
- Rahimi G, Alizadeh F, Khodavandi A (2016) Mycosynthesis of silver nanoparticles from *Candida albicans* and its anti-bacterial activity against *Escherichia coli* and *Staphylococcus aureus*. *Trop J Pharm Res* 15(2):371–375
- Rajoriya P, Barcelos MCS, Ferreira DCM, Misra P, Molina G, Pelissari FM, Shukla PK, Ramteke PW (2021) Green silver nanoparticles: recent trends and technological developments. *J Polym Environ* 29:1–27
- Ramadan MA, Shawkey AE, Rabeh MA, Abdellatif AO (2020) Promising antimicrobial activities of oil and silver nanoparticles obtained from *Melaleuca alternifolia* leaves against selected skin-infecting pathogens. *J Herb Med* 20:100289
- Ramkumar VS, Pugazhendhi A, Gopalakrishnan K, Sivagurunathan P, Saratale GD, Dung TNB, Kannapiran E (2017) Biofabrication and characterisation of silver nanoparticles using aqueous extract of seaweed *Enteromorpha compressa* and its biomedical properties. *Biotechnol Rep* 14: 1–7
- Rani R, Sharma D, Chaturvedi M, Yadav JP (2017) Green synthesis, characterisation and anti-bacterial activity of silver nanoparticles of endophytic fungi *Aspergillus terreus*. *J Nanomed Nanotechnol* 8(4):1000457
- Rautela A, Rani J, Das MD (2019) Green synthesis of silver nanoparticles from *Tectona grandis* seeds extract: characterisation and mechanism of antimicrobial action on different microorganisms. *J Anal Sci Technol* 10(1):1–10
- Ravichandran A, Subramanian P, Manoharan V, Muthu T, Periyannan R, Thangapandi M, Ponnuchamy K, Pandi B, Marimuthu PN (2018) Phyto-mediated synthesis of silver nanoparticles using fucoidan isolated from *Spatoglossum asperum* and assessment of anti-bacterial activities. *J Photochem Photobiol B Biol* 185:117–125
- Reddy GAK, Joy JM, Mitra T, Shabnam S, Shilpa T (2012) Nanosilver—a review. *Int J Adv Pharm* 2(1):9–15
- Renuka R, Renuka Devi K, Sivakami M, Thilagavathi T, Uthrakumar R, Kaviyarasu K (2020) Biosynthesis of silver nanoparticles using *Phyllanthus emblica* fruit extract for antimicrobial application. *Biocatal Agric Biotechnology* 24:101567
- Rezvani N, Sorooshzadeh A, Farhadi N (2012) Effect of nano-silver on growth of saffron in flooding stress. *World Acad Sci Eng Technol* 6(1):517–522
- Roy A (2017) Synthesis of silver nanoparticles from medicinal plants and its biological application: a review. *Res Rev Biosci* 12(4):138
- Saidu FK, Mathew A, Parveen A, Valiyathra V, Thomas GV (2019) Novel green synthesis of silver nanoparticles using clammy cherry (*Cordia obliqua* Willd) fruit extract and investigation on its catalytic and antimicrobial properties. *SN Appl Sci* 1(11):1–13
- Salama HMH (2012) Effects of silver nanoparticles in some crop plants, common bean (*Phaseolus vulgaris* L.) and corn (*Zea mays* L.). *Int Res J Biotechnol* 3(10):190–197
- Saravanan M, Barik SK, Ali DM, Prakash P, Pugazhendhi A (2018a) Synthesis of silver nanoparticles from *Bacillus brevis* (NCIM 2533) and their anti-bacterial activity against pathogenic bacteria. *Microb Pathog* 116:221–226

- Saravanan M, Arokiyaraj S, Lakshmi T, Pugazhendhi A (2018b) Synthesis of silver nanoparticles from *Phenocrhaete chrysosporium* (MTCC-787) and their anti-bacterial activity against human pathogenic bacteria. *Microb Pathog* 117:68–72
- Sasidharan D, Namitha TR, Johnson SP, Jose V, Mathew P (2020) Synthesis of silver and copper oxide nanoparticles using *Myristica fragrans* fruit extract: antimicrobial and catalytic applications. *Sustain Chem Pharm* 16:100255
- Sayed AMM, Kim S, Behle RW (2017) Characterisation of silver nanoparticles synthesised by *Bacillus thuringiensis* as a nanobiopesticide for insect pest control. *Biocontrol Sci Technol* 27(11):1308–1326
- Shaikhhaldein HO, Al-Qurainy F, Nadeem M, Khan S, Tarroum M, Salih AM (2020) Biosynthesis and characterisation of silver nanoparticles using *Ochradenusarabicus* and their physiological effect on *Maeruaoblongifolia* raised in vitro. *Sci Rep* 10(1):1–8
- Shaker MA, Shaaban MI (2017) Synthesis of silver nanoparticles with antimicrobial and anti-adherence activities against multidrug-resistant isolates from *Acinetobacter baumannii*. *J Taibah Univ Med Sci* 12(4):291–297
- Shams G, Ranjbar M, Amiri A (2013) Effect of silver nanoparticles on concentration of silver heavy element and growth indexes in cucumber (*Cucumis sativus* L. negeen). *J Nanopart Res* 15(5): 1–12
- Sharifi-Rad M, Pohl P, Epifano F, Álvarez-Suarez JM (2020) Green synthesis of silver nanoparticles using *Astragalus tribuloides* Delile. Root extract: characterisation, antioxidant, antibacterial, and anti-inflammatory activities. *Nanomaterials* 10(12):2383
- Sharma P, Bhatt D, Zaidi MGH, Saradhi PP, Khanna PK, Arora S (2012) Silver nanoparticle-mediated enhancement in growth and antioxidant status of *Brassica juncea*. *Appl Biochem Biotechnol* 167(8):2225–2233
- Singh R, Shedbalkar UU, Wadhvani SA, Chopade BA (2015) Bacteriogenic silver nanoparticles: synthesis, mechanism, and applications. *Appl Microbiol Biotechnol* 99(11):4579–4593
- Singh P, Kim YJ, Wang C, Mathiyalagan R, Yang DC (2016) *Weissella* DC6-facilitated green synthesis of silver nanoparticles and their antimicrobial potential. *Artif Cells Nanomed Biotechnol* 44(6):1569–1575
- Singh H, Juan D, Yi T-H (2017a) *Kinneretia* THG-SQ14 mediated biosynthesis of silver nanoparticles and its antimicrobial efficacy. *Artif Cells Nanomed Biotechnol* 45(3):602–608
- Singh T, Jyoti K, Patnaik A, Singh A, Chauhan R, Chandel SS (2017b) Biosynthesis, characterisation and anti-bacterial activity of silver nanoparticles using an endophytic fungal supernatant of *Raphanus sativus*. *J Genet Eng Biotechnol* 15(1):31–39
- Singh T, Singh A, Wang W, Yadav D, Kumar A, Singh PK (2019a) Biosynthesized nanoparticles and its implications in agriculture. In: *Biological synthesis of nanoparticles and their applications*. CRC Press, Boca Raton, p 257
- Singh C, Kumar J, Kumar P, Chauhan BS, Tiwari KN, Mishra SK, Srikrishna S, Saini R, Nath G, Singh J (2019b) Green synthesis of silver nanoparticles using aqueous leaf extract of *Premna integrifolia* (L.) rich in polyphenols and evaluation of their antioxidant, anti-bacterial and cytotoxic activity. *Biotechnol Equip* 33(1):359–371
- Sivagnanam SP, Getachew AT, Choi JH, Park YB, Woo HC, Chun BS (2017) Green synthesis of silver nanoparticles from deoiled brown algal extract via Box-Behnken based design and their antimicrobial and sensing properties. *Green Process Synth* 6(2):147–160
- Soliman M, Qari SH, Abu-Elsaoud A, El-Esawi M, Alhaithloul H, Elkesh A (2020) Rapid green synthesis of silver nanoparticles from blue gum augment growth and performance of maize, fenugreek, and onion by modulating plants cellular antioxidant machinery and genes expression. *Acta Physiol Plant* 42(9):1–16
- Sorescu A-A, Nuță A, Rodica M, Bunghez I (2016) Green synthesis of silver nanoparticles using plant extracts. In: *The 4th international virtual conference on advanced scientific results*, pp 10–16

- Syu Y-Y, Hung J-H, Chen J-C, Chuang H-W (2014) Impacts of size and shape of silver nanoparticles on Arabidopsis plant growth and gene expression. *Plant Physiol Biochem* 83: 57–64
- Tarannum N, Gautam YK (2019) Facile green synthesis and applications of silver nanoparticles: a state-of-the-art review. *RSC Adv* 9(60):34926–34948
- Toh HS, Faure RL, Amin LBM, Hay CYF, George S (2017) A light-assisted in situ embedments of silver nanoparticles to prepare functionalised fabrics. *Nanotechnol Sci Appl* 10:147
- Torabfam M, Yüce M (2020) Microwave-assisted green synthesis of silver nanoparticles using dried extracts of *Chlorella vulgaris* and anti-bacterial activity studies. *Green Process Synth* 9(1): 283–293
- Tripathi DK, Singh S, Singh S, Srivastava PK, Singh VP, Singh S, Prasad SM et al (2017) Nitric oxide alleviates silver nanoparticles (AgNPs)-induced phytotoxicity in *Pisum sativum* seedlings. *Plant Physiol Biochem* 110:167–177
- Varghese R, Almalki MA, Ilavenil S, Rebecca J, Choi KC (2019) Silver nanoparticles synthesised using the seed extract of *Trigonella foenum-graecum* L. and their antimicrobial mechanism and anticancer properties. *Saudi J Biol Sci* 26(1):148–154
- Wagi S, Ahmed A (2019) Green production of AgNPs and their phytostimulatory impact. *Green Process Synth* 8(1):885–894
- Wang C, Kim YJ, Singh P, Mathiyalagan R, Jin Y, Yang DC (2016) Green synthesis of silver nanoparticles by *Bacillus methylotrophicus*, and their antimicrobial activity. *Artif Cells Nanomed Biotechnol* 44(4):1127–1132
- Wintachai P, Paosen S, Yupunqui CT, Voravuthikunchai SP (2019) Silver nanoparticles synthesised with *Eucalyptus critriodora* ethanol leaf extract stimulate anti-bacterial activity against clinically multidrug-resistant *Acinetobacter baumannii* isolated from pneumonia patients. *Microb Pathog* 126:245–257
- Yang N, Li F, Jian T, Liu C, Sun H, Wang L, Hui X (2017) Biogenic synthesis of silver nanoparticles using ginger (*Zingiber officinale*) extract and their anti-bacterial properties against aquatic pathogens. *Acta Oceanol Sin* 36(12):95–100
- Yokesh Babu M, Janaki Devi V, Ramakritinan CM, Umarani R, Taredahalli N, Kumaraguru AK (2014) Application of biosynthesised silver nanoparticles in agricultural and marine pest control. *Curr Nanosci* 10(3):374–381
- Zare Z, Pishkar L, Iranbakhsh A, Talei D (2020) Physiological and molecular effects of silver nanoparticles exposure on purslane (*Portulaca oleracea* L.). *Russ J Plant Physiol* 67:521–528
- Zhang H, Ji Z, Xia T, Meng H, Low-Kam C, Liu R, Pokhrel S et al (2012) Use of metal oxide nanoparticle band gap to develop a predictive paradigm for oxidative stress and acute pulmonary inflammation. *ACS Nano* 6(5):4349–4368
- Zhang H, Chen S, Jia X, Huang Y, Ji R, Zhao L (2021) Comparison of the phytotoxicity between chemically and green synthesised silver nanoparticles. *Sci Total Environ* 752:142264



Status of Safety Concerns of Microplastic Detection Strategies

27

Deepika Sharma, Virender Sharma, and Gurjot Kaur

27.1 Introduction

The ever-increasing plastic usage in marketed products is causing an alarming increase in microplastics worldwide. Microplastics are smaller particles of size up to 5 mm produced by either plastic degradation or used in the processing of consumer products. Microplastics are already known as a health risk to birds and marine organisms (Kelkar et al. 2019). They are persistent in the environment and when ingested by marine organisms. Consequently, they enter the food chain and bioaccumulate in organisms (Mato et al. 2001; Cole et al. 2011; Besseling et al. 2013; Van Cauwenberghe and Janssen 2014). Oral exposure to microplastics causes various effects in marine animals, i.e., digestive tract clogging, slowed growth, hepatic damage, inflammation, and slower mobility (Setälä et al. 2016; Wright et al. 2013). Also, organic pollutants get adsorbed on microplastics and are prone to environmental release and exposure upon microplastic aging (Wang et al. 2016; Bakir et al. 2012; Engler 2012; Rios et al. 2007; Teuten et al. 2009; Rochman et al. 2013).

Interestingly, the human health effects of microplastics are not yet established. Humans are exposed to microplastics both through water and diet (fish), but the effect of dietary seafood and bioaccumulation is not entirely established (Carbery et al. 2018). A report in 2017 discussed the presence of plastic microfibers in lung tissue in biopsies and while one report in 2019 showed respiratory irritation due to inhalation in industrial workers (Wright and Kelly 2017; Koelmans et al. 2019). In addition, as plastics such as polyethylene and polypropylene are being used widely in various consumer products, microplastic exposure to human organs such as skin and gastrointestinal tract is likely taking place. Some lesser reported microplastic

D. Sharma · V. Sharma · G. Kaur (✉)
School of Pharmaceutical Sciences, Shoolini University, Solan, India

© The Author(s), under exclusive license to Springer Nature Singapore Pte Ltd. 2023

P. V. Mohanan, S. Kappalli (eds.), *Biomedical Applications and Toxicity of Nanomaterials*, https://doi.org/10.1007/978-981-19-7834-0_27

727

human exposure cases link them to estrogen-mimicking and reproductive health changes in women, even in breast cancer (Sharma and Chatterjee 2017; Anderson et al. 2015). As numerous reports have now established the presence of microplastics in world waters, including surface waters, a need to have accurate and efficient detection methods has arisen. It seems that it is difficult to assess the sources of microplastic pollution as there are many, but mostly, they are added into sewage water from factories, previous sedimentations, as well as household objects. Microplastics are released in sewage from various sources such as assembling plants, urban overspill, and sediment bioturbation (Eerkes-Medrano et al. 2015). Plastics in consumer products, cosmetics, textiles, medicines, transport materials, and industrial abrasives are all sources of microplastics (Browne et al. 2011; Rochman et al. 2019). Although wastewater treatment and recycling plants can remove microplastics, these methods are only partially efficient, and no current methods exist for the complete and specific removal of microplastics (Talvitie et al. 2015; Tofa et al. 2019). Unfortunately, detection methods currently in use are restricted by the incomplete understanding of the physiochemical properties. In addition, no sample contains only one type of microplastics, and, therefore, the detection is also limited by the variable size distribution of microplastics in a sample coupled to changing microplastic properties. WHO has shown concern about the microplastic contamination of the environment in recent years and required characterization of microplastic physiochemical properties as well as newer microplastic-specific detection methods.

This chapter provides an in-depth examination of the physiochemical properties, existing detection methods, and their advantages and pitfalls. In addition, a classification to categorize microplastics is given. Newer detection methods to improve the current detection are also briefly discussed.

27.2 Microplastics

Microplastics are widely defined as synthetic plastic polymers with an upper size limit of 5 mm and without a specified lower limit (Thompson et al. 2009; Browne et al. 2015; Sharma and Chatterjee 2017). The first evidence of microplastics in the earth's natural environment was provided in the 1970s by Carpenter and Smith by detection of micro-sized plastics in sea surface water and characterizing them using density, shape, physical and chemical behavior, and concentration while performing electron micrography of wax particles obtained from pine needles (Carpenter and Smith 1972). The term "microplastic" was coined much later by Thompson and coworkers in 2004 after they detected microplastics in the seawater using FTIR spectroscopy (Thompson et al. 2004). Microplastics are either produced industrially or are degraded from larger plastics with time. The synthesized microplastics are called primary microplastics, while the latter are named secondary microplastics as they are produced indirectly after degradation. In both cases, they are extremely persistent contaminants with very long half-lives which could be potentially harmful to organisms as well as ecosystems (Cole et al. 2011; Prata et al. 2019).

27.2.1 Types

Microplastics are divided into two main classes owing to their source (Fig. 27.1). Primary microplastics include polystyrene, polypropylene, and polyethylene polymer particles that are manufactured for industrial and domestic applications for use in cosmetics: facewashes, facial cleansers, toothpaste, peeling, shower/bath gels, scrubs, mascara, shaving cream, eye shadow, deodorant, blush powders, makeup foundation, baby products, hair coloring products, nail polish, pest repellents, sunscreens (Cole et al. 2011; Castañeda et al. 2014; Costa et al. 2010; Duis and Coors 2016), synthetic clothing, abrasives in cleaning products, drilling fluids, and air-blasting media (Alomar et al. 2016; Auta et al. 2017). Other primary microplastics are obtained by spillage of plastic resin powders and the production of plastic materials used for air blasting and feedstocks (Kelkar et al. 2019). They can be transported by rivers when discharged from water treatment plants and wind and surface overflows (Gall and Thompson 2015).

The secondary microplastics are obtained after the breakdown of large-sized plastic particles during environmental degradation. The physical, chemical, and biological processes may decrease the structural integrity of the microplastic debris and induce the breakdown of the plastic material (Cole et al. 2011). Also, a combination of environmental factors, i.e., temperature, humidity, and sunlight, and polymer properties such as density, size, and shape may impact the disintegration process (Auta et al. 2017). Sources of Secondary microplastics include

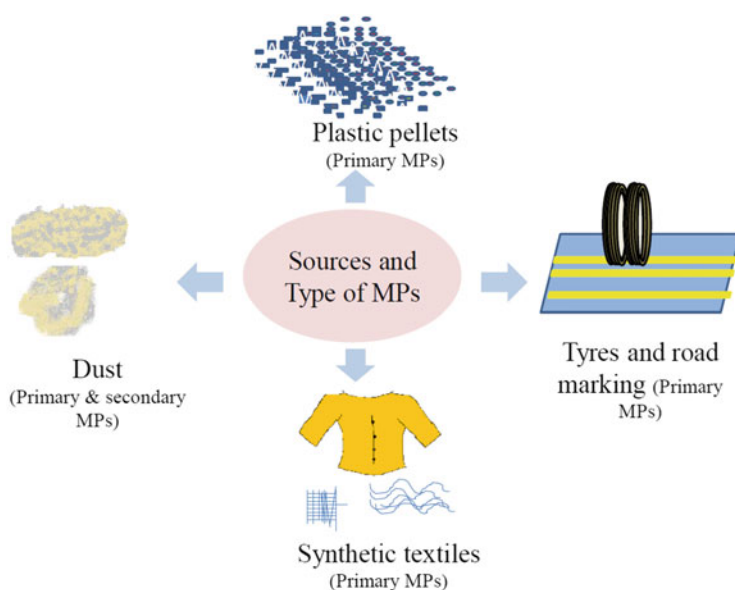


Fig. 27.1 Sources and types of microplastics

microplastic fibers produced during washing polyester, acrylic, and polyamide fabrics (Kelkar et al. 2019).

27.2.1.1 Sources

Many sources (other than those listed above) have been identified for primary and secondary microplastics (Fig. 27.1).

27.2.1.1.1 Dust

Due to the usage of plastics in many household items and construction materials, city dust is a significant source of microplastics. Microplastic dust is generated by the usage and cleaning of plastic cooking utensils, house varnishing, and abrasives in metropolitan cities worldwide (Magnusson et al. 2016). The increasing utilization of plastic items in households prompts microplastic shedding and accumulation of indoor dust (Magnusson et al. 2016). Both primary and secondary microplastics have been observed in the dust.

27.2.1.1.2 Plastic Pellets

Microplastics have been used in the industry as plastic pellets during manufacturing, processing, recycling, and transport. These pellets can enter the environment. As they have sizes between 2 and 5 mm, they are classified as primary microplastics and may be the source of smaller sized microplastics (Essel et al. 2015).

27.2.1.1.3 Synthetic Textiles

Nowadays, clothing and everyday household items are also manufactured from synthetic textiles which can cause microplastic fibers shedding (Browne et al. 2011; Magnusson et al. 2016). Cloth washing is a known method of primary microplastic production (Browne et al. 2011).

27.2.1.1.4 Tires and Road Markings

Continuous wear and tear of tires result in the production and release of primary microplastic fibers. Tires are usually made up of synthetic plastic polymers like styrene-butadiene rubber that are shown to be present in sea samples (Essel et al. 2015; Sundt et al. 2014). Unfortunately, the country's economics and road infrastructure, paint, and polymer-based road markings and maintenance play a major role in the microplastic production from tires and road markings.

27.2.2 Physicochemical Properties

Many physicochemical properties have been essential for identifying and detecting microplastics from various simple and complex matrices. These properties are particle size, surface chemistry, and particle shape (Fig. 27.2).

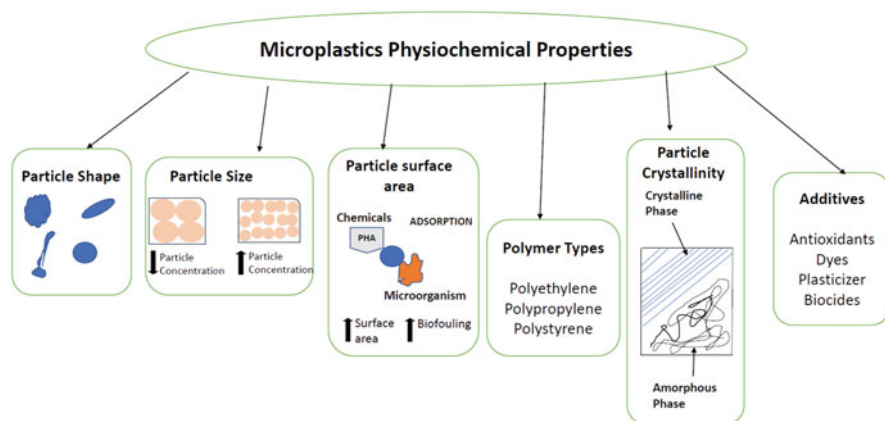


Fig. 27.2 Physicochemical properties of microplastics

27.2.2.1 Particle Size

Particle size is an important property for microplastics when considering how small particles interact with biological systems. Many recent studies that showed adverse effects on individual organisms after microplastic exposure utilized microplastics of uniform submicron or nano size (reviewed in Lambert et al. 2017). The size can be categorized as $<100\ \mu\text{m}$ (62–100 μm), 100–500, 500–1000, or $>1000\ \mu\text{m}$ (1000–5000 μm). According to some reports (Cole et al. 2013; Lee et al. 2013; Jeong et al. 2016), small microplastics (0.05–1.7 μm) that tend to get entrapped between GIT have a higher chance of ingestion than larger particles. As a result, they show comparatively higher toxicity and produce deleterious effects on reproduction time, feeding behavior, and survival rate of marine organisms. The particle size distribution of weathered microplastics is usually polydispersed, i.e., increase in concentration is observed with decreasing size. This function can be used to assess the levels of larger plastic particles and the possibility of forming smaller microplastics after the breakdown. Therefore, a high probability of exposure to a mixed-sized microplastic sample in biological systems can be predicted (Lambert and Wagner 2016).

27.2.2.1.1 Surface Chemistry

Surface chemistry plays a vital role in influencing the interactions between microplastics and biological systems. Processes such as ultraviolet irradiation, freezing, photo, and oxidative degradation modify the plastic surface. The reactions usually create new functional groups with hydroxyl radicals, oxygen, nitrogen oxides, and other photo-generated radicals. The new surface structure leads to enhanced surface erosion and rougher surface morphologies, in turn, changing polymer hydrophobicity (Hossain et al. 2019). These processes may weaken the plastic surface, causing the further release of microplastics. In aqueous environments, the surfaces of eroded microplastics adsorb organic and inorganic

molecules, an ideal environment for bacterial colonization. Microplastics with comparatively smooth and inert surface morphologies are more hydrophobic and less colonized by bacteria, while rougher and charged surfaces are hydrophilic and promote colonization (Fotopoulou and Karapanagioti 2012).

27.2.2.1.2 Particle Shape

Microplastics are present in a variety of shapes. They range from fibers to irregular fragments as well as spherical and rod-like structures. Microplastic shapes can be categorized as beads, fibers, fragments, foams, and films. Particle shape may potentiate adverse effects upon microplastic exposure to living organisms (Wright et al. 2013). According to a study, higher toxicity of polypropylene fibers was observed on the freshwater amphipod, *Hyalella azteca*, than with polyethylene beads (Au et al. 2015). The zinc oxide nano sticks demonstrated more toxicity (measured as mortality rate and growth rate inhibition) as compared to other nanoparticles (nanospheres and cuboidal submicron particles) in zebrafish embryos (Hua et al. 2014). It has been hypothesized that particles having an irregular shape or needlelike shape may have a higher affinity for intracellular and extracellular living cell surfaces and thus are more toxic (Lambert et al. 2017).

27.2.2.1.3 Surface Area

Surface area is a well-known parameter for determining the toxicity of tested particles, and an inverse relationship between particle size and surface area has been already described in the literature. The surface area may affect the concentrations of adsorbed chemicals. An increase in surface area due to change in polymer's fractal structure, i.e., voids, has been directly associated with the bio-fouling rate of the particle (Chubarenko et al. 2016). As the particle size decreases, its surface area increases. According to one report, nano-sized microplastics showed more significant toxicity due to their large surface area (Van Hoecke et al. 2008). In studies where primary microbeads have been used, the surface area has been calculated based on spherical equivalent diameter. However, this approach may lead to overestimation for irregularly shaped secondary microplastics as confirmed in nanoscale soot particles (spheres or spheroids) where the surface area was calculated using geometrical estimates. Surface area was estimated to be 24 times lesser than that of a sphere of equivalent size and a particle shape factor had to be applied for corrections (Lambert et al. 2017; La Rocca et al. 2016).

27.2.2.1.4 Polymer Crystallinity

A polymer crystal consists of chains linked to a tight structure and is a critical polymer property. Crystallinity affects the physical properties, such as density and permeability, that are dependent on the hydration and swelling behavior. Upon polymer erosion, crystallinity is affected by the generation of crystallized oligomers and monomers, as well as the behavior of the partially crystalline polymer. Faster erosion of the amorphous region of polymer results in a change in microplastic crystallinity (Göpferich 1996; Chen et al. 2000). As the microplastics decreases in

size, crystallinity increases and the formation of crystallites takes place, resulting in differing toxicities for microplastics of different sizes. Changes in crystallinity will influence physical properties such as surface area, particle shape, particle size, density, and chemical properties such as additives leaching and pollutant adsorption. As a result, changes in the ingestion rates and effects of microplastics with living organisms will also vary (Lambert et al. 2017).

27.2.2.1.5 Polymer Additives

Polymer additives are the chemicals used in the manufacturing process of polymer to improve the performance of a material. The additives, i.e., residual monomers, solvents, catalysts, and additives (e.g., antioxidants, dyes, biocides, plasticizers), are incorporated within the porous structure of the polymer (Lambert et al. 2014). Toxicity associated with microplastics may be caused by the leaching of these chemicals (Andrady 2015). The leaching rate of the additives in the environment depends upon the additive's pore diameter and molecular size and on how a particular chemical is compounded within the polymer matrix (Göpferich 1996; Lambert et al. 2014). For example, low molecular weight additives in a polymer matrix will weakly embed and freely migrate, while high molecular weight will show the opposite behavior (Kim et al. 2006). Overall, the potential adverse effects of microplastics will depend on the concentration of the chemicals or additives that were present in the parent plastics, their partitioning coefficient, degradation time, and the aging and degradation of the polymer. Aged microplastics may demonstrate reduced leaching due to changes in their crystallinity (Lambert et al. 2017).

27.2.2.1.6 Polymer Types

Microplastics associated toxicity also depends on the type of plastic polymers used. All polymers tested till now show variable toxicity. The toxicological profiles of plastic monomers used in producing different types of plastic are well-known (Lambert et al. 2017). Some well-known examples of polymer toxicities are given below:

1. Plasticized polyvinyl chloride (PVC) is considered the most hazardous plastic because of its high chlorine and additive content and is known to result in dioxin formation during manufacturing and incineration processes (Rossi and Lent 2006).
2. Polycarbonate, manufactured from bisphenol A, is a known endocrine disruptor (Lambert et al. 2017).
3. Polyacrylonitriles and acrylonitrile, butadiene styrene monomers are labeled as carcinogenic and mutagenic based on classifications (Carcinogenicity 1B (V) and Skin Sensitizing 1 (IV)) within the European Union classification, labeling, and packaging regulation (Lithner et al. 2011).
4. Monomers of Polystyrene are suspected carcinogens (Rossi and Lent 2006; Lithner et al. 2011). In addition, styrene oligomers are shown to leach into ambient water and sediments (Kwon et al. 2015).

5. Both polyurethanes (Carcinogenicity 1B (V)) and epoxy resins (Skin Sensitizing 1 (IV)) are labeled as mutagens and carcinogens based on their monomer classifications within the European Union CLP regulation (Lithner et al. 2011).
6. Polyethylene terephthalate or PET is suspected to leach endocrine-disrupting chemicals into the water and is banned from being used in plastic bottles (Wagner and Oehlmann 2009, 2011).

27.3 Separation Methods for Microplastics

Currently, many plastic polymer types with varying properties exist. Although some approaches have been partially successful in detecting MPs and limited removal from water, these general approaches have their pitfalls, as demonstrated below:

27.3.1 Density-Based Approaches

In general, plastic polymers, therefore MPs, are less dense with higher hydrophobicity than biopolymers (Nguyen et al. 2019). The process of density-based separation or flotation can be used for MPs by manipulating their densities. The method involves using brine solutions (salts) with different densities, i.e., water, sodium chloride, and sodium bromide having low density while sodium iodide and zinc bromide have high density, to render the plastic buoyant. The separation of the MPs is based on the density of the particles and allows the floating of the light particles while the heavier particles sink (Quinn et al. 2017). The salt used is a significant factor in MP separation from the sample as denser salt solutions can themselves be toxic to the environment (Quinn et al. 2017). Although the efficiency of MP removal may depend heavily on plastic polymer type, high-density sodium iodide solution has been used to extract polyvinylchloride MPs with very high efficiency (Claessens et al. 2013).

In this approach, elutriation can assist MPs separation. Ethanol (96%) provides a relatively good density separation medium to separate plastic from the vegetable-rich samples without visible toxic effects other than hydrogen peroxide (Herrera et al. 2018). Flotation can separate millimeter-sized MPs and is not optimum for smaller MPs with low floating strength and fluctuating molecule thickness because of surface fouling. The presence of soap bubbles may result in the transport of denser particles to the air-liquid interface, mixing MPs and resulting in inaccurate separation (Nguyen et al. 2019).

27.3.2 Hydrophobicity-Based Approaches

This approach is based on the hydrophobicity of plastics that enhances MPs adsorption onto the surface of bubbles, aided by foam buoyancy, and hence carries MPs to the air-liquid interface. Adjusting surface tension is performed either by modifying

hydrophobicity or chemically changing the MPs surface (Imhof et al. 2012). Approximately 55% of MPs per sample have been separated using hydrophobicity-based approaches (Imhof et al. 2012). An oil-extraction protocol could recover 1 mm-sized MPs with an efficiency of 96% (Crichton et al. 2017). Recently, 92% of 15 μm -sized MPs could be separated using hydrophobic iron nanoparticles coupled with salinization. Also, approximately 92% of 10–20 μm polyethylene and polystyrene beads and 93% of >1 mm MPs could be separated by this procedure (Nguyen et al. 2019). However, hydrophobicity-based approaches may not be appropriate for the analytical separation of MPs due to particle loss after contact with the surface bubbles. Unfortunately, attempts at hydrophobic partitioning MPs from natural matrices have been unsuccessful until now (Nguyen et al. 2019).

27.3.3 Size-Based Approaches

An approach utilizing separations based on MPs size is performed using crossflow ultrafilters. These ultrafilters are a bundle of hollow fiber membranes with an inner diameter of 200 μm . Samples are pumped through the crossflow ultrafilter at a constant flow rate and overpressure, resulting in the accumulation of particles on the filter (Mintenig et al. 2018). Size-based separation can be achieved by sequential filtration (Hernandez et al. 2017). As the approach is filter-based, clogging of pores is a limiting factor. Consecutive filtration utilizing progressively smaller pore sizes can diminish this filter clogging. Usually, MPs not trapped in dense solid phases can be easily separated. This methodology is used for the qualitative detection of nano-sized MPs in the sample. However, loss of nano-sized MPs due to the attachment of the particles with the filters may occur and is a perceived pitfall (Nguyen et al. 2019).

27.3.4 Approaches for Nanoparticle Separation

Last decade, there has been considerable research on nanoplastics, including their synthesis and purification, and thus many strategies for their separation exist. These strategies incorporate magnetic field-flow fractionation, gel electrophoresis, and size-exclusion chromatography (Robertson et al. 2016).

Magnetic field-flow fractionation is a method based on the differences between the magnetic behaviors of nanoparticles. In this method, a magnetic force acts on a particle, and this force is opposed by diffusion back into the flow stream. Hydrodynamic forces then act perpendicularly to the applied field and separate the components according to their magnetic charge. In this way, charged nanoparticles, moving through a capillary channel, are partitioned by the magnetic field. Nanoparticles with thick layers interact weakly with the magnetic field and are eluted in a shorter period, and particles with small thicknesses are eluted comparatively later. Although this technique shows great potential for MPs separation,

charging the MPs surface may be restricted due to the requirement of large scaling in MPs-based detection methods (Latham et al. 2005).

Gel electrophoresis, a well-known research method, has also been employed for nanoparticle separation. It is based on the migration behavior of analytes in gel under an electric field and uses pores with sizes of usually a few nanometers for separation. The speed of the molecule is dependent on its size and charge. The pore sizes are the main restriction for the separation of MPs with a comparatively larger size. Changes in gel coloring after sample penetration has been used for successful separation of NPs and may be used for MPs separation. Nanoparticle distribution in the different gel regions has been analyzed by transmission electron microscopy (Liu et al. 2012). Although performing gel electrophoresis on pure MPs samples may result in high-resolution separation of MPs, the technique is not MPs-specific and may need a further removal of MPs for any assessment. Therefore, it is not adequate for the detection of MPs from a complex sample. The method may be developed as a laboratory technique for MP identification and separation (Nguyen et al. 2019).

Size-exclusion chromatography allows the separation of nanoparticles according to their sizes. It utilizes the introduction of a suspension through a size-exclusion column and separation based on the hydrodynamic sizes. The important factors for a proper separation include column medium, particle size, gel porosity, and eluent composition. In this method, the nanoparticles are trapped, and elution is performed by exchanging the eluent (Flavel et al. 2013). Unfortunately, this technique is also not plastic-specific and thus is currently limited to pure MPs samples. We perceive that it may still be used in combination with another method for the early separation of MPs from an ecological sample (Nguyen et al. 2019).

27.4 Methods for Microplastics Detection

After initial morphology and size characterization, microplastics can be studied in detail with more sophisticated techniques. As more sophisticated equipment is needed, these techniques are usually expensive, and, thus, specialized facilities are needed. This can be considered as a major drawback, especially when samples need to be transported and may degrade in the process. Given below are the main methods as classified according to major principles (Fig. 27.3).

27.4.1 Spectroscopy-Based Detection Methods

27.4.1.1 Raman Spectroscopy

Raman spectroscopy is used to measure the length and width of micrometer-sized particles and quantify different types of plastics in sediments (Van Cauwenberghé et al. 2013; Imhof et al. 2012, 2013). It is used for analytical and structural polymer studies for microplastics with sizes between 1 and 20 μm , regardless of particle shape and thickness. The Raman signal can be modified by dyes, microbiological, organic, and inorganic chemicals. An advantage of this technique is using a complete

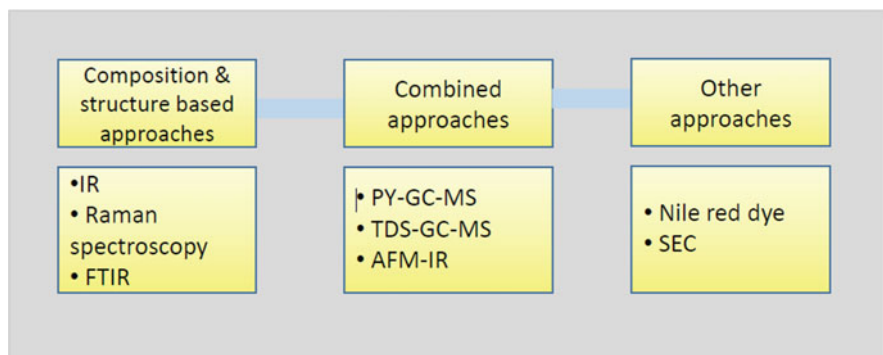


Fig. 27.3 Various detection approaches for microplastics

wavelength range and even detecting amorphous carbon (Imhof et al. 2012; Nguyen et al. 2019; Cole et al. 2013). During the process, the sample is irradiated with a monochromatic laser source. Laser wavelength lies between 500 and 800 nm, and the beam excites the sample. Microplastics sample is pumped in, and reflection is performed on a filter through the flow cell. The beam width is set to 1 mm to avoid repeated detection. The interaction between laser light and microplastics causes changes in the frequency of the backscattered light when compared to the irradiated laser frequency. For detecting spectra of single microplastics in a streaming medium, the most favorable integration time of the spectrometer depends on the particle speed flow, excitation time, cross-sectional area of the flow cell, height of the beam, and pump rate (Löder and Gerdts 2015; Kniggendorf et al. 2019). One disadvantage of this technique is the excitation of the fluorescent samples by the laser (e.g., residues of biological origin in samples) that prevents accurate detection due to the generation of uninterpretable Raman spectra (Löder and Gerdts 2015).

27.4.1.2 Infrared (IR) Spectroscopy

IR Spectroscopy, similar to Raman spectroscopy, offers an increased probability of identification of plastic polymer particles (Thompson et al. 2004; Ng and Obbard 2006; Harrison et al. 2012; Frias et al. 2010). The results of an unknown plastic sample can be compared with the spectra of known polymers. Microplastics can be studied based on molecular vibrations emitted in an IR spectrum. When infrared radiations interact with the sample, it excites molecular vibrations. The excitation of molecular vibrations depends on the microplastics' specific wavelength, arrangement, and atomic structure (Löder and Gerdts 2015). Spectroscopy is a highly reliable method for the identification as well as chemical composition analysis of microplastics. Plastic polymers have different IR spectra, an ideal method for distinguishing microplastics (Hidalgo-Ruz et al. 2012).

27.4.1.3 Fourier Transform Infrared Spectroscopy (FTIR)

FTIR spectroscopy can provide information about the surface oxidation of weathered microplastics. Surface oxidation of microplastics is seen as absorption peaks for oxidized species in FTIR spectra (Corcoran et al. 2009). FTIR spectroscopy provides information on the specific chemical bonds of particles. It can give the polymer composition and abundance of microplastics, and, thus, the origin and sample source (Shim et al. 2016). For the characterization of the microplastics, FTIR contains two measuring modes: reflectance mode and transmittance mode. The transmittance mode needs IR transparent filters (e.g., aluminum oxide) for the total absorption concerning the thickness of the microplastic sample. However, the use of micro-ATR (attenuated total reflectance) with microscopy enables the direct measurement of the sample filter without the need for manual handling of microplastics. Transmittance measurements with micro-ATR show the total absorption of microplastics <500 μm collected on filters (Löder and Gerdts 2015). The signal depends on the change in the permanent dipole moment of a chemical bond, making it helpful in distinguishing polymers using their polar functional groups. FTIR microscopes have spatial resolutions of 5 μm and are useful for measuring microplastics larger than 20 μm (Mallikarjunachari and Ghosh 2016). However, FTIR requires a minimum sample thickness of 150 nm (Nguyen et al. 2019). Reflectance mode does not require the sample preparation step for dense microplastics. However, generation of spectral distortion in irregularly shaped microplastics due to refractive error may occur (Harrison et al. 2012).

27.4.2 Microscopy-Based Detection Methods

27.4.2.1 Scanning Electron Microscopy (SEM)

SEM gives detailed information about the microplastic size and shape and the presence of inorganic plastic additives on microplastics (Hanvey et al. 2017). This method can provide clear and high-magnification images of the surface of plastic particles, and, thus, microplastics obtained from the organic particles can be differentiated (Shim et al. 2017). Microplastics are transferred onto a conductive and adhesive carbon tape mounted on an aluminum SEM sample holder. The microplastics' chemical and morphological characterization is performed by scanning electron microscope (SEM) equipped with an energy-dispersive X-ray micro-analyzer. A combination of SEM analysis with energy-dispersive X-ray spectroscopy (EDS) is useful to determine the elemental composition of the particles. These compositions are used for the identification of carbon-dominant microplastics from inorganic materials. EDX analysis can be performed in the "low vacuum" mode with a high voltage thus avoiding any electrical charge effects and the need for further sample preparation (Fries et al. 2013; Shim et al. 2017). SEM-EDS is however an expensive and time-consuming method, and a large number of samples will incur huge costs. The microplastic color cannot be differentiated in SEM (Shim et al. 2017).

27.4.3 Mass Spectrometry (MS)-Based Detection Methods

Mass spectrometry is based on the investigation of microplastics using their mass. Microplastics can be detected and measured quantitatively in mixture samples, and the detection does not depend on the surface differences of microplastics (Nguyen et al. 2019). Many advanced techniques using mass spectrometry are now used as given below:

27.4.3.1 Pyrolysis-Gas Chromatography-Mass Chromatography (Py-GC-MS)

Py-GC-MS combines gas chromatography and mass spectrometry for efficient separation of the sample. MS can obtain structural information about the sample through analysis of degradation products (Fries et al. 2013). Py-GC-MS involves the decomposition of a sample at high temperatures. It is used after extraction and a visual separation of microplastics from sediments. The results depend on sample preparation and type of pyrolysis (Nguyen et al. 2019; Löder and Gerdt 2015). Briefly, the particle is placed in a pyrolysis tube and preconditioned at 40 °C for 60 min to remove absorbed contaminants. In order to trap the compounds at this stage, the initial temperature is around –50 °C. The temperature is increased to 350 °C to allow thermal desorption. Once the first chromatogram is obtained after thermal desorption, the sample is pyrolyzed at 700 °C for 60 s. To separate and detect pyrolysis products, the thermal desorption system is attached to a gas chromatograph coupled with a mass-selective detector. Mass spectra of organic plastic additives and pyrolysis products are obtained with a mass range between 10 and 600 amu (Fries et al. 2013; Nuelle et al. 2014). The polymer origin is identified by comparing between pyrograms of the sample and standard polymer pyrograms (Fries et al. 2013). A disadvantage associated with this technique is that only one particle can be analyzed per run and cannot be used for large sample quantities (Löder and Gerdt 2015). Py-GC-MS offers accurate results for microplastics having sizes less than 50 µm. This method is useful for the identification of microplastics in drinking water and in environmental samples where plastics are attached to other materials (Nguyen et al. 2019).

27.4.3.2 Thermal Desorption Coupled with Gas Chromatography: Mass Spectrometry (TDS-GC-MS/TED-GC-MS)

TDS-GC-MS is an analytical technique for determining microplastics and organic residues in environmental samples. Microplastics can be identified and quantified in samples by a combination of thermal extraction with thermo-gravimetric analysis (TGA) on solid-phase adsorbers and analysis of these adsorbers with thermal desorption gas chromatography-mass spectrometry (TDS-GC-MS). This combination (TGA-solid-phase extraction, TDS-GC-MS) is called TED-GC-MS (Dümichen et al. 2014, 2015b). The sample is kept onto a thermo-gravimetric balance and heated up under a nitrogen atmosphere to 600 °C. Degraded products are adsorbed onto the surface. To collect the degradation products, a thermal desorption tube is placed in TGA, and the temperature is brought to 300 °C at a heating rate of 5 °C/min for

separation. For all measurements, a carrier gas flow (Helium) is added (Dümichen et al. 2014, 2015a, 2017). TDS-GC-MS is a procedure appropriate for tests with generally high quantities (up to 100 mg) but is limited to qualitative analysis (Nguyen et al. 2019). The biological origin of the organic compounds is assessed by comparison to known spectral libraries (Dümichen et al. 2014, 2017).

27.4.4 Chromatography-Based Detection Methods

27.4.4.1 Size-Exclusion Chromatography (SEC)

The microplastics testing by SEC requires first solubilization based on polymer solubility in a solvent, heating to 45 °C, and finally filtration to separate dissolved analytes according to their hydrodynamic volume. SEC is used for microplastic detection when changes in the molecular mass of microplastics are expected. Microplastics are estimated with a liquid chromatography pump equipped with a refractive index detector using an eluent with a specific flow rate. The average value of the molar mass distribution is calculated. Different types of polymers with different molar masses are used as calibration standards for microplastic detection. The quantification is performed on reversed-phase systems for hydrophobic microplastics detection (Elert et al. 2017).

27.4.5 Composition-Based Analysis

27.4.5.1 Density Separation with Subsequent C:H:N Analysis

Morét-Ferguson et al. (2010) utilized the bulk chemistry of the particles to differentiate the polymer source of microplastics (Morét-Ferguson et al. 2010). Briefly, the sample is added to distilled water under agitation to remove air bubbles from the sample surface. Ethanol or concentrated calcium or strontium chloride is added into the sample depending on the particle density until all the particles are similarly buoyant. There should be no air bubbles in the sample to maintain the buoyancy. The density of the particles can be determined by weighing the volume of the sample (Löder and Gerdts 2015). Carbon, hydrogen, and nitrogen (C:H:N) analysis is used to differentiate between polymer types of different compositions, identifying the origin of plastic particles. It is possible to evaluate whether the sample is plastic and its types by correlating the densities and C:H:N proportions of the polymer. However, this technique may not yield complete chemical composition (Morét-Ferguson et al. 2010). Furthermore, this technique is time-consuming, needs sample combustion, and cannot be used for particles having sizes less than 0.41 mm (Löder and Gerdts 2015; Morét-Ferguson et al. 2010).

27.4.6 Novel Detection-Based Methods

27.4.6.1 Atomic Force Microscopy (AFM) Coupled to IR or Raman Spectroscopy

Atomic force microscopy joined with either IR or Raman spectroscopy is a potential applicant for nano-sized microplastics detection. AFM can give results at a nanometer scale and can be worked in both contact and non-contact mode with objects. IR or Raman spectroscopy joined with AFM can differentiate between chemical compositions of microplastics in a sample. Thermal expansion of the test sample by IR offers the movement of the AFM beam whose ring-down patterns are detected by Fourier change. This permits the extraction of the frequencies and amplitudes of the oscillations. AFM-IR can obtain IR spectra with absorption images in the range of 50–100 nm. It is difficult and tedious to investigate a nano-sized single molecule by AFM-IR in an unknown sample. However, particles can be measured according to their volume. The particles are spread in the form of mist onto a glass slide with the help of high air pressure. Therefore, microplastics can be detected individually (Shim et al. 2016).

27.4.6.2 Dyes

Microplastics can be visualized under a microscope in surface water samples using a lipophilic dye such as Nile red (Andrady 2011). It is strongly fluorescent in a hydrophobic environment and can be used to detect fluorescently labeled microplastics. The dye is dissolved either in acetone or methanol, although methanol is preferred as it is plastic resistant. The fluorescence of Nile red is inversely proportional to its concentration, i.e., ideal range lies between 0.1 and 2 µg/mL of the tested sample. Higher concentrations may cause quenching. The dye is used to distinguish microplastics with sizes between 20 µm and 1 mm. This dye cannot be used to assess the chemical identity of plastic particles (Erni-Cassola et al. 2017). According to a report, Nile red can be used to detect irregularly shaped microplastics and colored plastic particulates (Cole 2016). However, Nile red is not plastic-specific and can only be used in relatively clean samples (Nguyen et al. 2019). As it can also stain neutral lipids in biological samples, removing organic material is essential (Shim et al. 2016, 2017).

27.5 Factors Affecting MP Detection

Besides physiochemical properties (discussed in a previous section), sampling, size, and morphology are important factors affecting MPs detection. As MPs detection is not plastic-specific and utilizes methods based on hydrophobicity, size, or density, these factors may affect detection from complex samples.

27.5.1 Sampling

Most of the efforts for MPs detection have been attempted on water samples as part of studies on marine life and ocean contamination. In general, water sampling for MPs can be categorized into freshwater sampling and seawater sampling, depending on the source of the water sample.

Freshwater sampling includes potable and sewage water sampling, while seawater sampling includes beach and sediment sampling. As MPs distribution in water depends upon physicochemical properties (particle thickness, adsorption, shape, size, and surface properties) and environmental conditions (wind flow, water thickness, waves, and hydrodynamic profile), the number of MPs depend heavily on the sampling location. The density of the seawater and freshwater are 1.03 and 1.00 g cm³, respectively, which affect the distribution of the MPs, i.e., MPs will be found deeper in the water column in freshwater systems. Therefore, adjusting the depth and location of sampling is needed based on the salinity, densities, and location. The sampling can be done by using sieves, nets, or water pumps dependent on the volume of water to be sampled. A flow meter can be attached to the nets to estimate the final sampled water volume (Prata et al. 2019). A disadvantage associated with nets is the blockage of pores with organic and mineral material in suspension. This limits the volume of sampled water. Water samples can be collected in glass bottles and then processed further in the lab.

According to a recent study, a pump-based closed filter was designed to investigate MP contamination in surface and sub-surface water, although difficulty in sampling MPs having a size below 300 µm was observed (Lenz and Labrenz 2018). In another study, 100 mL of the sample was collected from surface water. Due to the small sample volume, the sampling was inefficient as it did not collect the plastic fiber fragments resulting in the observed variability and inhomogeneous separation of the MPs (Dubaihash and Liebezeit 2013). The erroneous MPs detection can also be caused by nylon and plastic in the pump systems. The use of glass and metal bottles avoids this risk of contamination in the sampling. However, these plastic-free materials are limited to processing limited water volumes, leading to inaccurate extrapolation (Prata et al. 2019). Furthermore, due to low MPs concentration in environmental samples, a large volume of water is needed during sampling. The measured MPs retained on the sieve depend upon the mesh size and may range between 50 and 3000 µm (Hidalgo-Ruz et al. 2012). A large sampling of water requires the usage of nets. The filtering volume is affected by the area of the net that acts as a filter. Nets usually have a 300 µm mesh size and are 3–4.5 m long and do not sample MPs below 300 µm. A recent study showed a technique that used fractionated pressure to filter large (>1 m³) volumes of water through the filter. This technique allowed the sampling of MPs having a size <10 µm (Löder and Gerdtz 2015).

In seawater sampling, sampling approaches depend on the sampling location (high tide line, intertidal areas, transects) and require selective sampling and, in most cases, bulk volume sampling (Hidalgo-Ruz et al. 2012; Prata et al. 2019). For example, sediment sampling can be done directly from beaches. This MPs sampling

from the beaches is a simple method and requires nonplastic tools for sampling, a frame to indicate the area, and a container to collect the sample. The sample quantity can vary between 0.15 and 10 kg (Hidalgo-Ruz et al. 2012). The less-dense MPs are most abundant and deposited at downwind sites, and dense particles are less abundant where the tide meets the stream (Browne et al. 2010). Another criterion for sampling is depth since some areas may contain higher concentrations of MPs. If box corers (marine geological sampling tool for soft sediments in lakes or oceans) are used, MPs can be sampled at different depth layers. The use of box corers enables sampling to a water depth of 5000 m and more (Van Cauwenberghes et al. 2013). Large MPs (1–5 mm) and small MPs (20 μm –1 mm) can be detected. Small MPs should be sampled with a metal spoon by combining several scoops at arm's length in an arc-shaped area. Large MPs should be sampled from the top 5 cm and by sieving over a 1 mm sieve directly at the beach (Löder and Gerdtts 2015). Subtidal coastal habitats are dynamic systems due to continuous and seasonal erosion of sediments and may consist of uneven covering of MPs of the sediments (Hidalgo-Ruz et al. 2012).

For the accurate sampling of subtidal sediments, the sample should be collected at a 1–5 cm depth as it contains higher MPs concentrations than the top 10 cm. Sediment samples are prone to temperature-dependent degradation and should be stored at frozen or dried temperature and kept in a dark area until further analysis (Löder and Gerdtts 2015). National Oceanic and Atmospheric Administration (NOAA) specifies the utilization of 400 g (w/w) per duplicate sample. At the same time, the Marine Strategy Framework Directive (MSFD) specialized subgroup suggests using five replicates of sediments at 5 cm depth for the accuracy of the results (Prata et al. 2019). Subtidal sediments are collected using a ship-based apparatus. Grabs can perform bulk sampling (a sampler used to sample sediment in oceans), but this may result in a disturbance in the sediment layer. Small sampling that collects samples from small areas is used to obtain samples in a relatively undisturbed state. Volume measurements of the above samples can allow the determination of MPs concentration in the known sediment volume. MSFD and NOAA highly recommend a density-based method for separating MPs from organics in beach sediments (Lusher et al. 2017).

27.5.2 Size and morphology

Visual characterization is an inexpensive technique based on the morphological and physical characteristics of MPs. It is the initial step to screening MPs in environment samples. MPs are generally classified by morphological characteristics such as shape, color, and size (Lusher et al. 2017). MPs with sizes greater than 500 μm can be seen with the naked eye (Rocha-Santos and Duarte 2015), but MPs with sizes less than 500 μm need a stereomicroscope (Löder and Gerdtts 2015). Color can be used for easy separation of MPs when MPs are present in large amounts in debris. Plastic particles with high color intensity can be isolated comparatively easier than

less intense MPs (Hidalgo-Ruz et al. 2012). However, color differentiation is subjective, and MPs cannot be detected by color alone (Lusher et al. 2017).

MPs can be visualized by the use of staining dyes such as Nile Red and Rose-Bengal. Rose-Bengal allows a 92% coloration of 25 μm MPs, while Nile Red can detect MPs but is not plastic-specific (Nguyen et al. 2019; Prata et al. 2019). However, the dyes are size-specific and cannot detect MPs having a size greater than 25 μm . They can be used to detect MPs between 1 mm and 25 μm sizes (Prata et al. 2019; Erni-Cassola et al. 2017). We concluded that visual identification should not be applied to particles having sizes $<500 \mu\text{m}$ as erroneous reporting may occur, as shown in a study (Löder and Gerdt 2015). According to another study, the MPs having sizes $>1 \text{ mm}$ may still be distinguished using multiple parameters such as particle clarity, absence of organic and cellular structures, particle thickness, and particle turbidity under a high-resolution microscope (Hidalgo-Ruz et al. 2012). For advanced morphological characterization, different types of detection methods such as SEM (scanning electron microscopy), TEM (transmission electron microscopy), and AFM (Atomic Force Microscope) can be used as discussed above (Safarova et al. 2007).

27.6 Conclusion

Microplastics are turning out to be one of the major contaminants of our environment in the modern era. Unfortunately, the current detection strategies are yet not refined to study the health effects on humans, although humans are exposed through water and diet. Further, all techniques that do provide accurate information on microplastics are expensive, and any detection on a large scale for environmental protection would require the development of cheaper alternatives. Detection of microplastics in humans would require techniques that can process complex samples such as blood. Finally, as microplastic contamination of both humans and the environment is a worldwide concern, the development of simple and cheap detection methods must precede all other research questions for an optimum human risk assessment.

Acknowledgment Gurjot Kaur conceptualized this chapter. Virender Sharma prepared Fig. 27.2. Deepika Sharma wrote the first draft and prepared Figs. 27.1 and 27.3. Gurjot Kaur edited and refined the final draft. This work is partially funded by the Society of Toxicology Undergraduate research fund.

References

- Alomar C, Estarellas F, Deudero S (2016) Microplastics in the Mediterranean Sea: deposition in coastal shallow sediments, spatial variation and preferential grain size. *Mar Environ Res* 115:1–10

- Anderson A, Andrady A, Arthur C, Baker J, Bouwman H, Gall S, Hildalgo-Ruz V, Köhler A, Lavender Law K, Leslie HA (2015) Sources, fate and effects of microplastics in the environment: a global assessment. GESAMP reports and studies series 90
- Andrady AL (2011) Microplastics in the marine environment. *Mar Pollut Bull* 62(8):1596–1605
- Andrady AL (2015) Plastics and health impacts. In: *Plastics and environmental sustainability*. Wiley, Hoboken, NJ, pp 227–254
- Au SY, Bruce TF, Bridges WC, Klaine SJ (2015) Responses of *Hyalella azteca* to acute and chronic microplastic exposures. *Environ Toxicol Chem* 34(11):2564–2572
- Auta HS, Emenike CU, Fauziah SH (2017) Distribution and importance of microplastics in the marine environment: a review of the sources, fate, effects, and potential solutions. *Environ Int* 102:165–176
- Bakir A, Rowland SJ, Thompson RC (2012) Competitive sorption of persistent organic pollutants onto microplastics in the marine environment. *Mar Pollut Bull* 64(12):2782–2789
- Besseling E, Wegner A, Foekema EM, Van Den Heuvel-Greve MJ, Koelmans AA (2013) Effects of microplastic on fitness and PCB bioaccumulation by the lugworm *Arenicola marina* (L.). *Environ Sci Technol* 47(1):593–600
- Browne MA, Galloway TS, Thompson RC (2010) Spatial patterns of plastic debris along estuarine shorelines. *Environ Sci Technol* 44(9):3404–3409
- Browne MA, Crump P, Niven SJ, Teuten E, Tonkin A, Galloway T, Thompson R (2011) Accumulation of microplastic on shorelines worldwide: sources and sinks. *Environ Sci Technol* 45(21):9175–9179
- Browne MA, Underwood AJ, Chapman MG, Williams R, Thompson RC, van Franeker JA (2015) Linking effects of anthropogenic debris to ecological impacts. *Proc R Soc B Biol Sci* 282(1807):20142929
- Carbery M, O'Connor W, Palanisami T (2018) Trophic transfer of microplastics and mixed contaminants in the marine food web and implications for human health. *Environ Int* 115:400–409
- Carpenter EJ, Smith KL (1972) Plastics on the Sargasso Sea surface. *Science* 175(4027):1240–1241
- Castañeda RA, Suncica Avlijas M, Simard A, Ricciardi A (2014) Microplastic pollution in St. Lawrence river sediments. *Can J Fish Aquat Sci* 71(12):1767–1771
- Cauwenberghe V, Lisbeth AV, Mees J, Janssen CR (2013) Microplastic pollution in deep-sea sediments. *Environ Pollut* 182:495–499
- Chen DR, Bei JZ, Wang SG (2000) Polycaprolactone microparticles and their biodegradation. *Polym Degrad Stab* 67(3):455–459
- Chubarenko I, Bagaev A, Zobkov M, Esiukova E (2016) On some physical and dynamical properties of microplastic particles in marine environment. *Mar Pollut Bull* 108(1–2):105–112
- Claessens M, Van Cauwenberghe L, Vandegehuchte MB, Janssen CR (2013) New techniques for the detection of microplastics in sediments and field collected organisms. *Mar Pollut Bull* 70(1–2):227–233
- Cole M (2016) A novel method for preparing microplastic fibers. *Sci Rep* 6:34519
- Cole M, Lindeque P, Halsband C, Galloway TS (2011) Microplastics as contaminants in the marine environment: a review. *Mar Pollut Bull* 62(12):2588–2597
- Cole M, Lindeque P, Fileman E, Halsband C, Goodhead R, Moger J, Galloway TS (2013) Microplastic ingestion by zooplankton. *Environ Sci Technol* 47(12):6646–6655
- Corcoran PL, Biesinger MC, Grifi M (2009) Plastics and beaches: a degrading relationship. *Mar Pollut Bull* 58(1):80–84
- Costa MF, Ivar Do Sul JA, Silva-Cavalcanti JS, Araújo MCB, Spengler Â, Tourinho PS (2010) On the importance of size of plastic fragments and pellets on the strandline: a snapshot of a Brazilian beach. *Environ Monit Assess* 168(1–4):299–304
- Crichton EM, Noël M, Gies EA, Ross PS (2017) A novel, density-independent and FTIR-compatible approach for the rapid extraction of microplastics from aquatic sediments. *Anal Methods* 9(9):1419–1428

- Dubaish F, Liebezeit G (2013) Suspended microplastics and black carbon particles in the Jade system, southern North Sea. *Water Air Soil Pollut* 224(2):1352
- Duis K, Coors A (2016) Microplastics in the aquatic and terrestrial environment: sources (with a specific focus on personal care products), fate and effects. *Environ Sci Eur* 28(1):2
- Dümichen E, Ulrike Braun R, Senz GF, Sturm H (2014) Assessment of a new method for the analysis of decomposition gases of polymers by a combining thermogravimetric solid-phase extraction and thermal desorption gas chromatography mass spectrometry. *J Chromatogr A* 1354:117–128
- Dümichen E, Barthel A-K, Braun U, Bannick CG, Brand K, Jekel M, Senz R (2015a) Analysis of polyethylene microplastics in environmental samples, using a thermal decomposition method. *Water Res* 85:451–457
- Dümichen E, Javdanitehran M, Erdmann M, Trappe V, Sturm H, Braun U, Ziegmann G (2015b) Analyzing the network formation and curing kinetics of epoxy resins by in situ near-infrared measurements with variable heating rates. *Thermochim Acta* 616:49–60
- Dümichen E, Eisentraut P, Bannick CG, Barthel A-K, Senz R, Braun U (2017) Fast identification of microplastics in complex environmental samples by a thermal degradation method. *Chemosphere* 174:572–584
- Eerkes-Medrano D, Thompson RC, Aldridge DC (2015) Microplastics in freshwater systems: a review of the emerging threats, identification of knowledge gaps and prioritisation of research needs. *Water Res* 75:63–82
- Elert AM, Becker R, Duemichen E, Eisentraut P, Falkenhagen J, Sturm H, Braun U (2017) Comparison of different methods for MP detection: what can we learn from them, and why asking the right question before measurements matters? *Environ Pollut* 231:1256–1264
- Engler RE (2012) The complex interaction between marine debris and toxic chemicals in the ocean. *Environ Sci Technol* 46(22):12302–12315
- Erni-Cassola G, Gibson MI, Thompson RC, Christie-Oleza JA (2017) Lost, but found with Nile Red: a novel method for detecting and quantifying small microplastics (1 mm to 20 µm) in environmental samples. *Environ Sci Technol* 51(23):13641–13648
- Essel R, Engel L, Carus M, Ahrens RH (2015) Sources of microplastics relevant to marine protection in Germany. *Texte* 64:2015
- Flavel BS, Kappes MM, Krupke R, Frank %J Acs Nano Hennrich. (2013) Separation of single-walled carbon nanotubes by 1-dodecanol-mediated size-exclusion chromatography. *ACS Nano* 7(4):3557–3564
- Fotopoulou KN, Karapanagioti HK (2012) Surface properties of beached plastic pellets. *Mar Environ Res* 81:70–77
- Frias JPGL, Sobral P, Ferreira AM (2010) Organic pollutants in microplastics from two beaches of the Portuguese coast. *Mar Pollut Bull* 60(11):1988–1992
- Fries E, Dekiff JH, Willmeyer J, Nuelle M-T, Ebert M, Remy D (2013) Identification of polymer types and additives in marine microplastic particles using pyrolysis-GC/MS and scanning electron microscopy. *Environ Sci Processes Impacts* 15(10):1949–1956
- Gall SC, Thompson RC (2015) The impact of debris on marine life. *Mar Pollut Bull* 92(1-2): 170–179
- Göpferich A (1996) Mechanisms of polymer degradation and erosion. *Biomaterials* 17(2):103–114
- Hanvey JS, Lewis PJ, Lavers JL, Crosbie ND, Pozo K, Clarke BO (2017) A review of analytical techniques for quantifying microplastics in sediments. *Anal Methods* 9(9):1369–1383
- Harrison JP, Ojeda JJ, Romero-González ME (2012) The applicability of reflectance micro-Fourier-transform infrared spectroscopy for the detection of synthetic microplastics in marine sediments. *Sci Total Environ* 416:455–463
- Hernandez LM, Yousefi N, Tufenkji N (2017) Are there nanoplastics in your personal care products? *Environ Sci Technol Lett* 4(7):280–285
- Herrera A, Garrido-Amador P, Martínez I, Samper MD, López-Martínez J, Gómez M, Packard TT (2018) Novel methodology to isolate microplastics from vegetal-rich samples. *Mar Pollut Bull* 129(1):61–69

- Hidalgo-Ruz V, Gutow L, Thompson RC, Thiel M (2012) Microplastics in the marine environment: a review of the methods used for identification and quantification. *Environ Sci Technol* 46(6): 3060–3075
- Hossain MR, Jiang M, Wei QH, Leff LG (2019) Microplastic surface properties affect bacterial colonization in freshwater. *J Basic Microbiol* 59(1):54–61
- Hua J, Vijver MG, Richardson MK, Ahmad F, Peijnenburg WJ (2014) Particle-specific toxic effects of differently shaped zinc oxide nanoparticles to zebrafish embryos (*Danio rerio*). *Environ Toxicol Chem* 33(12):2859–2868
- Imhof HK, Schmid J, Niessner R, Ivleva NP, Laforsch C (2012) A novel, highly efficient method for the separation and quantification of plastic particles in sediments of aquatic environments. *Limnol Oceanogr Methods* 10(7):524–537
- Imhof HK, Ivleva NP, Schmid J, Niessner R, Laforsch C (2013) Contamination of beach sediments of a subalpine lake with microplastic particles. *Curr Biol* 23(19):R867–R868
- Jeong C-B, Won E-J, Kang H-M, Lee M-C, Hwang D-S, Hwang U-K, Zhou B, Souissi S, Lee S-J, Lee J-S (2016) Microplastic size-dependent toxicity, oxidative stress induction, and p-JNK and p-p38 activation in the monogonont rotifer (*Brachionus koreanus*). *Environ Sci Technol* 50(16): 8849–8857
- Kelkar VP, Rolsky CB, Pant A, Green MD, Tongay S, Halden RU (2019) Chemical and physical changes of microplastics during sterilization by chlorination. *Water Res* 163:114871. <https://doi.org/10.1016/j.watres.2019.114871>
- Kim Y-J, Osako M, Sakai S-i (2006) Leaching characteristics of polybrominated diphenyl ethers (PBDEs) from flame-retardant plastics. *Chemosphere* 65(3):506–513
- Kniggendorf A-K, Wetzel C, Roth B (2019) Microplastics detection in streaming tap water with Raman spectroscopy. *Sensors* 19(8):1839
- Koelmans B, Phal S, Backhaus T, Bessa F, van Calster G, Contzen N, Cronin R, Galloway T, Hart A, Hendersen L (2019) A scientific perspective on microplastics in nature and society. SAPEA, Berlin
- Kwon BG, Koizumi K, Chung S-Y, Kodera Y, Kim J-O, Saido K (2015) Global styrene oligomers monitoring as new chemical contamination from polystyrene plastic marine pollution. *J Hazard Mater* 300:359–367
- La Rocca A, Campbell J, Fay MW, Orhan O (2016) Soot-in-oil 3D volume reconstruction through the use of electron tomography: an introductory study. *Tribol Lett* 61(1):8
- Lambert S, Wagner M (2016) Characterisation of nanoplastics during the degradation of polystyrene. *Chemosphere* 145:265–268
- Lambert S, Sinclair C, Boxall A (2014) Occurrence, degradation, and effect of polymer-based materials in the environment. *Rev Environ Contam Toxicol* 227:1–53
- Lambert S, Scherer C, Wagner M (2017) Ecotoxicity testing of microplastics: Considering the heterogeneity of physicochemical properties. *Integr Environ Assess Manag* 13(3):470–475
- Latham AH, Freitas RS, Schiffer P, Williams ME (2005) Capillary magnetic field flow fractionation and analysis of magnetic nanoparticles. *Anal Chem* 77(15):5055–5062
- Lee K-W, Shim WJ, Kwon OY, Kang J-H (2013) Size-dependent effects of micro polystyrene particles in the marine copepod *Tigriopus japonicus*. *Environ Sci Technol* 47(19):11278–11283
- Lenz R, Labrenz M (2018) Small microplastic sampling in water: development of an encapsulated filtration device. *Water* 10(8):1055
- Lithner D, Larsson Å, Dave G (2011) Environmental and health hazard ranking and assessment of plastic polymers based on chemical composition. *Sci Total Environ* 409(18):3309–3324
- Liu J-f, Su-juan Y, Yin Y-g, Chao J-b (2012) Methods for separation, identification, characterization and quantification of silver nanoparticles. *TrAC Trends Anal Chem* 33:95–106
- Löder MGJ, Gerdtz G (2015) Methodology used for the detection and identification of microplastics—a critical appraisal. In: *Marine anthropogenic litter*. Springer, Cham, pp 201–227
- Lusher A, Hollman P, Mendoza-Hill J (2017) Microplastics in fisheries and aquaculture. FAO fisheries aquaculture technical paper eng no. 615

- Magnusson K, Eliasson K, Fråne A, Haikonen K, Hultén J, Olshammar M, Stadmark J, Voisin A (2016) Swedish sources and pathways for microplastics to the marine environment. A review of existing data. *IVL, C* 183
- Mallikarjunachari G, Ghosh P (2016) Analysis of strength and response of polymer nano thin film interfaces applying nanoindentation and nanoscratch techniques. *Polymer* 90:53–66
- Mato Y, Isobe T, Takada H, Kanehiro H, Ohtake C, Kaminuma T (2001) Plastic resin pellets as a transport medium for toxic chemicals in the marine environment. *Environ Sci Technol* 35(2): 318–324
- Mintinig SM, Bäuerlein PS, Koelmans AA, Dekker SC, Van Wezel AP (2018) Closing the gap between small and smaller: towards a framework to analyse nano- and microplastics in aqueous environmental samples. *Environ Sci Nano* 5(7):1640–1649
- Morét-Ferguson S, Law KL, Proskurowski G, Murphy EK, Peacock EE, Reddy CM (2010) The size, mass, and composition of plastic debris in the western North Atlantic Ocean. *Mar Pollut Bull* 60(10):1873–1878
- Ng KL, Obbard JP (2006) Prevalence of microplastics in Singapore's coastal marine environment. *Mar Pollut Bull* 52(7):761–767
- Nguyen B, Claveau-Mallet D, Hernandez LM, Elvis Genbo X, Farner JM, Tufenkji N (2019) Separation and analysis of microplastics and nanoplastics in complex environmental samples. *Acc Chem Res* 52(4):858–866
- Nuelle M-T, Dekiff JH, Remy D, Fries E (2014) A new analytical approach for monitoring microplastics in marine sediments. *Environ Pollut* 184:161–169
- Prata JC, da Costa JP, Duarte AC, Rocha-Santos T (2019) Methods for sampling and detection of microplastics in water and sediment: a critical review. *TrAC Trends Anal Chem* 110:150–159
- Quinn B, Murphy F, Ewins C (2017) Validation of density separation for the rapid recovery of microplastics from sediment. *Anal Methods* 9(9):1491–1498
- Rios LM, Moore C, Jones PR (2007) Persistent organic pollutants carried by synthetic polymers in the ocean environment. *Mar Pollut Bull* 54(8):1230–1237
- Robertson JD, Rizzello L, Avila-Olias M, Gaitzsch J, Contini C, Magoñ MS, Renshaw SA, Battaglia G (2016) Purification of nanoparticles by size and shape. *Sci Rep* 6(1):1–9
- Rocha-Santos T, Duarte AC (2015) A critical overview of the analytical approaches to the occurrence, the fate and the behaviour of microplastics in the environment. *TrAC Trends Anal Chem* 65:47–53
- Rochman CM, Hoh E, Kurobe T, Teh SJ (2013) Ingested plastic transfers hazardous chemicals to fish and induces hepatic stress. *Sci Rep* 3:3263
- Rochman CM, Brookson C, Bikker J, Djuric N, Earn A, Bucci K, Athey S, Huntington A, McIlwraith H, Munno K (2019) Rethinking microplastics as a diverse contaminant suite. *Environ Toxicol Chem* 38(4):703–711
- Rossi M, Lent T (2006) Creating safe and healthy spaces: selecting materials that support healing. *Designing the 21st Century Hospital* 55
- Safarova K, Dvorak A, Kubinek R, Vujtek M, Rek A (2007) Usage of AFM, SEM and TEM for the research of carbon nanotubes. *Modern Res Educ Topics Microsc* 2:513–519
- Setälä O, Norkko J, Lehtiniemi M (2016) Feeding type affects microplastic ingestion in a coastal invertebrate community. *Mar Pollut Bull* 102(1):95–101
- Sharma S, Chatterjee S (2017) Microplastic pollution, a threat to marine ecosystem and human health: a short review. *Environ Sci Pollut Res* 24(27):21530–21547
- Shim WJ, Song YK, Hong SH, Jang M (2016) Identification and quantification of microplastics using Nile Red staining. *Mar Pollut Bull* 113(1–2):469–476
- Shim WJ, Hong SH, Eo SE (2017) Identification methods in microplastic analysis: a review. *Anal Methods* 9(9):1384–1391
- Sundt P, Schulze PE, Syversen F (2014) Sources of microplastic-pollution to the marine environment (MEPEX) [www.miljodirektoratet.no. Documents/publikasjoner M 321](http://www.miljodirektoratet.no/Documents/publikasjoner/M_321)

- Talvitie J, Heinonen M, Pääkkönen J-P, Vahtera E, Mikola A, Setälä O, Vahala R (2015) Do wastewater treatment plants act as a potential point source of microplastics? Preliminary study in the coastal Gulf of Finland, Baltic Sea. *Water Sci Technol* 72(9):1495–1504
- Teuten EL, Saquing JM, Knappe DRU, Barlaz MA, Jonsson S, Björn A, Rowland SJ, Thompson RC, Galloway TS, Yamashita R (2009) Transport and release of chemicals from plastics to the environment and to wildlife. *Philos Trans R Soc B Biol Sci* 364(1526):2027–2045
- Thompson RC, Olsen Y, Mitchell RP, Davis A, Rowland SJ, John AWG, McGonigle D, Russell AE (2004) Lost at sea: where is all the plastic? *Science* 304(5672):838–838
- Thompson RC, Moore CJ, Vom Saal FS, Swan SH (2009) Plastics, the environment and human health: current consensus and future trends. *Philos Trans R Soc B Biol Sci* 364(1526): 2153–2166
- Tofa TS, Kunjali KL, Paul S, Dutta J (2019) Visible light photocatalytic degradation of microplastic residues with zinc oxide nanorods. *Environ Chem Lett* 17(3):1341–1346
- Van Cauwenberghe L, Janssen CR (2014) Microplastics in bivalves cultured for human consumption. *Environ Pollut* 193:65–70
- Van Hoecke K, De Schamphelaere KAC, Van der Meeren P, Lucas S, Janssen CR (2008) Ecotoxicity of silica nanoparticles to the green alga *Pseudokirchneriella subcapitata*: importance of surface area. *Environ Toxicol Chem Int J* 27(9):1948–1957
- Wagner M, Oehlmann J (2009) Endocrine disruptors in bottled mineral water: total estrogenic burden and migration from plastic bottles. *Environ Sci Pollut Res* 16(3):278–286
- Wagner M, Oehlmann J (2011) Endocrine disruptors in bottled mineral water: estrogenic activity in the E-Screen. *J Steroid Biochem Mol Biol* 127(1–2):128–135
- Wang J, Tan Z, Peng J, Qiu Q, Li M (2016) The behaviors of microplastics in the marine environment. *Mar Environ Res* 113:7–17
- Wright SL, Kelly FJ (2017) Plastic and human health: a micro issue? *Environ Sci Technol* 51(12): 6634–6647
- Wright SL, Thompson RC, Galloway TS (2013) The physical impacts of microplastics on marine organisms: a review. *Environ Pollut* 178:483–492



Impact of Insecticides on Man and Environment

28

C. A. Jayaprakas, Joseph Tom, and S. Sreejith

28.1 Introduction

Archaeological evidence reveals that modern man existed on this planet roughly 200,000–300,000 years ago, but no supporting documentation is available for structured farming between 15,000 and 20,000 BCE. Agriculture might be emerged during the Neolithic Era, before 9000 BCE with the onset of developing polished stone tools at the end of the ice age. Origin of agriculture is believed to be in the Fertile Crescent of Mesopotamia, a hemispherical region in the Middle East once considered the “Cradle of Civilization.” This region roughly corresponds to most of today’s Iraq, Syria, Lebanon, Palestine, Israel, Jordan, and Egypt, together with the southeastern region of Turkey and the western fringes of Iran (Unsworth 2010). Aboriginal Australians who settled here had practiced fire-stick farming and forest gardening for thousands of years. Further, they started large-scale farming of wheat, barley, peas, lentils, chickpeas, bitter vetch, and flax were cultivated (Kislev et al. 2004).

The World Population Prospects 2019 published by the Population Division of the UN Department of Economic and Social Affairs estimates the global population will reach 11 billion by the end of the twenty-first century. Agriculture at the international level faces multifaceted challenges to boost food and fiber production to cater to the burgeoning population’s needs and ensure food security. By reviewing 57 global food security projections, van Dijk et al. (2021) concluded that the total global food demand is expected to increase by 35–56% between 2010 and 2050. Together with the global community, the world’s biosphere is facing an unprecedented challenge to plant health by the invasion of pests under the scenario of

C. A. Jayaprakas (✉) · J. Tom · S. Sreejith
Biopesticide Laboratory, Division of Crop Protection, ICAR-Central Tuber Crops Research Institute, Thiruvananthapuram, Kerala, India

climate change due to anthropogenic activities. Increased market globalization coupled with rising temperatures led to a situation favorable to pest infestation. Canton and Helen (2021) estimates that annually up to 40% of global crop production is lost to pests, and each year the global economy suffers over \$220 billion to pathogens and at least \$70 billion to pests. Tudi et al. (2021) reported that the application of pesticides produces about one-third of agricultural products, or else there would be a loss of 78% loss of fruit production, 54% of vegetable production, and 32% loss of cereal production. Food production since the 1940s amplified tremendously due to the increased use of synthetic pesticides (Bernardes et al. 2015).

Insect pest management through chemical measures might consider as one of the most beneficial developments of civilization (Klassen and Schwartz 1985). FAO defines pesticides are any substance or mixture of substances of chemical or biological ingredients intended for repelling, destroying, or controlling any pest or for regulating plant growth. Pesticides play an essential role in the farming system to lessen the losses of agricultural products and improve the affordable yield and quality of food (Fenik et al. 2011; Strassemeyer et al. 2017); nevertheless, their deleterious role in environmental pollution can never be ignored. Since the dawn of the Green Revolution, there has been a tremendous increase in using a diversified form of pesticides in agriculture and horticulture to combat biotic factors. Like many other agrochemicals, the requirement for pesticides increases in the current crop production system to increase the yield. The current consumption of pesticides on a global basis is 2 million tons/year, and the share of the utilization of herbicides, insecticides, and fungicides are 47.5%, 29.5%, and 17.5%, respectively (De et al. 2014). Sharma et al. (2019) reported the share of the utilization of herbicides, insecticides, and fungicides as 50%, 30%, and 18%, respectively. The production of plant protection chemicals increased from 0.2 million tons in the 1950s to more than 5 million tons by 2000, at a rate of almost 11% per year (Carvalho 2017).

The FAO reports that globally, 4.1 million tons of chemical pesticides were applied in 2015, 35% greater than in 2001 (Maggi et al. 2019). Environmental modeling with the global database of pesticide applications indicates that over 60% of global agricultural land (~24.5 million km²) is at risk of pesticide pollution by more than one active ingredient (Tang et al. 2021). While spraying pesticides, only a small quantity is reaching the target, and the remaining pesticides reach non-target organisms, water bodies, and the environment (Bernardes et al. 2015). Given the grave concern of insecticides as a major pollutant, mainly when farming is over-reliant on chemical pesticides and fertilizers, the UN's Global Environment Outlook (GEO) in 2019 called for reducing pesticide use.

28.2 History of Insecticide

The history of pesticide use is classified into three periods of time. During the 1870s, various natural compounds such as sulfur, heavy metals, salt of sulfur, and heavy metals were used against pests and pathogens. National Academy of Science (1969)

has reported that sulfur compounds were used to control insects in Asia Minor way back in 1000 BCE and by Sumerians about 4500 years ago against insects and mites. Chinese used mercury and arsenical compounds to control body lice about 3500 years ago (Unsworth 2010). Ancient Romans used Salts, ashes, and bitters for controlling weeds. The smoke produced by burning straw, chaff, dung, fish, or other animal products was also used to eliminate pathogens that cause blight or mildew in the orchard and vineyard (Unsworth 2010; National Research Council 2000). Prior to the entry of synthetic pesticides, readily available sources like chaff, hedge clippings, crabs, fish, dung, or other animal products were used as the source of fumes, and the malodorous spread throughout the orchard protects the crops from blight or mildew (Unsworth 2010). Pyrethrins, extracted from the seed cases of *Chrysanthemum cinerariaefolium*, were the economically most important natural neurotoxic pesticide used against a wide range of insect pests (Yang et al. 2014). French soldiers used pyrethrins to control fleas and body lice during the Napoleonic wars (1804–1815). The first record of the pyrethrum was when China's Chou Dynasty in the first century AD to kill insects. In Iran, crushed chrysanthemum flowers were used to produce Persian Powder, a green eco-friendly insecticide to mitigate household insects, garden pests, and agricultural pests for centuries.

Insecticides claimed to be the forerunner in the twentieth-century's agricultural productivity (van Emden et al. 2004) are chemicals or biological ingredients intended to kill or repel insect pests in agriculture and industry. During the second phase between 1870 and 1945, inorganic and synthetic materials were used to manage pests. Copper and sulfur compounds were used by farmers in Sweden in the 1800s against fungal attacks in fruit and potatoes (Sheail 1991). The third phase of pesticides came into being with the advent of synthetic insect ices like DDT, BHC, aldrin, dieldrin, endrin, chlordane, parathion, captan, and 2,4-D (Zhang et al. 2011). New pesticide molecules such as triazolopyrimidine, triketone, and isoxazole herbicides, strobilurin and azolone fungicides, chloronicotinyl, spinosyn, fiprole diacylhydrazine, and organophosphate insecticides, were introduced to the market between 1970 and 1990.

28.3 Classification of Insecticide

They have been classified mostly based on their chemical composition, mode of action, and targeted pest species (Drum 1980).

28.3.1 Classification Based on Chemical Composition

Pesticides are generally classified into two broad categories: synthetic and biopesticides. Based on the nature of the chemical composition, insecticides are classified into organic and inorganic insecticides.

28.3.1.1 Inorganic Pesticide

Compounds of heavy metals like arsenic (As), copper (Cu), lead (Pb), and sulfur (S) in varying formulations were popular among farmers from the mid-1800 to mid-1900 to control pests of cultivated crops, as these are generally less expensive, very effective, highly persistent, and easy to formulate. The use of lead arsenate (PbHAsO_4) as an insecticide was first recorded in 1982 against the gypsy moth, *Lymandriya dispar*, in Massachusetts. Later it was used to control codling moths in apple, plum, and peach orchards (Klassen and Schwartz 1985; Peryea 1998).

Arsenical insecticides in the form of lead (PbAsO_4), calcium (CaAsO_4), magnesium (MgAsO_4), zinc (ZnAsO_4), and Paris green [$\text{Cu}(\text{C}_2\text{H}_3\text{O}_2)_2 \cdot 3\text{Cu}(\text{AsO}_2)_2$] were used in agriculture for centuries. As ant bait, arsenic sulfides were used in China as early as AD 900 and arsenic oxide in Europe in 1699 (Shepard 1939). Control of Colorado potato beetle, *Leptinotarsa decemlineata* (Say), using the Paris green (copper acetoarsenate) in the USA in 1867 was the first example of the large-scale chemical control of an insect pest; subsequently, fruit growers used it for the control of codling moth *Laspeyresia pomonella* (Linnaeus) on fruit trees (Klassen and Schwartz 1985). Due to its efficacy in controlling gypsy moths, lead arsenate was replaced with Paris green in New England in 1892. Paris green was internationally used by applying it directly to water bodies as a powder or mixed with moist sand for the abatement of mosquitoes. Lime sulfur prepared by reacting calcium hydroxide with elemental sulfur was used to manage lice. Similarly, sulfur dioxide that formed by burning elemental sulfur was used as a fumigant against mealy bugs.

28.3.1.2 Synthetic Insecticides

There are four main synthetic insecticide categories: organochlorines, organophosphorus, carbamates, and pyrethrin and pyrethroids (Buchel 1983) (Fig. 28.1).

28.3.1.2.1 Organochlorides

Chlorinated hydrocarbons are the first major synthetic class of insecticides developed during the 1930s and 1940s in agriculture and public health. The compound contains five or more chlorine atoms, and their half-life varies from 3 to 20 years. Besides the long-term residual effects due to the resistance to most chemical and microbial degradations, they have exceptional qualities like high stability, insecticidal potency, relatively low mammalian toxicity, and low cost. Some commonly used organochloride insecticides are aldrin, chlordane, dichloro-diphenyl trichloroethane, dieldrin, endrin, heptachlor, lindane, and toxaphene, but most of them are designated as persistent organic pollutants and even endocrine-disrupting chemicals.

Dichloro-diphenyl-trichloroethane (DDT), the synthetic insecticide synthesized by the Austrian chemist Othmar Zeidler in 1874, was the first modern synthetic insecticide ever developed. However, its insecticidal property was discovered by the Swiss chemist Paul Hermann Müller in 1939, and this discovery led to the award of the Nobel Prize in 1948. During the second half of World War II, DDT was widely used to prevent the spread of malaria, typhus, body lice, and bubonic plague (WHO 1979), and the cases of malaria fell drastically from 400,000 in 1946 to

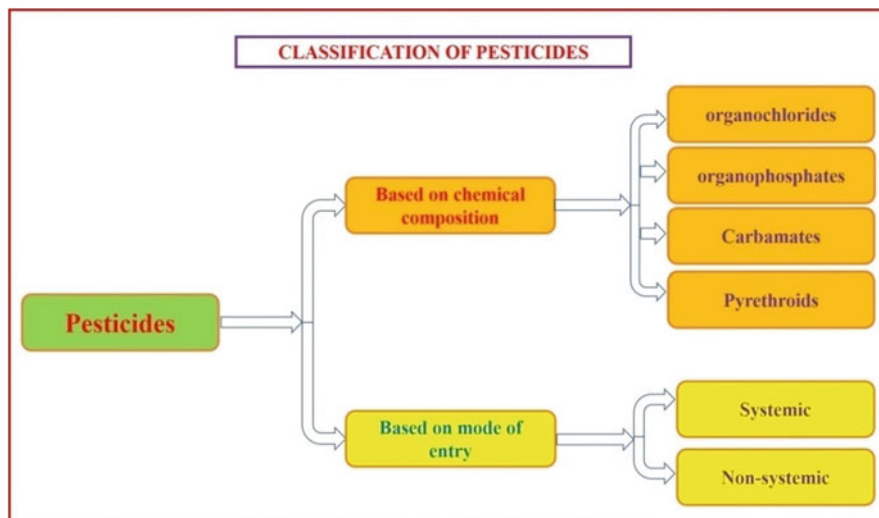


Fig. 28.1 Classification of pesticide

virtually none in 1950 (Casida and Quistad 1995). DDT was made available in 1945 to control insect pests in crops (WHO 1979).

Hexachlorocyclohexane (HCH), also known as benzene hexachloride (BHC), a cyclic, saturated, chlorinated hydrocarbon, was first produced by the English scientist Michael Faraday in 1825, but its property as an insecticide was not identified until 1944. Extensive use of this pesticide has brought enormous benefits to humanity by protecting crops from the menace of pests and eradicating certain vector-borne diseases (Li 2020; Vijgen et al. 2006). Lindane (γ -HCH) is the most predominant isomer used as an insecticide for fruit, vegetables, and animals.

28.3.1.2.2 Organophosphates

These are the first group of insecticides used on a large scale to replace chlorinated hydrocarbons, are used to control a wide range of pests, and are considered one of the broad-spectrum pesticides. Unlike organochloride insecticides, organophosphates are easily degradable, least stored in the human body, and inflict minimum environmental pollution. They were used as war gases also (Barr and Needham 2002).

28.3.1.2.3 Carbamates

They are the derivative of carbamic acid, are structurally similar to organophosphates, and degrade quickly in the natural environment with minimal environmental pollution. Like organophosphates, carbamates act as contact insecticides, and to a certain extent, as a stomach poison. They do not accumulate in the fatty tissues of mammals or the environment.

28.3.1.2.4 Pyrethrins

The natural pyrethrins used as an insecticide originated from the plant *Chrysanthemum cinerariaefolium*. Its bioactive principles are a mixture of six lipophilic compounds of pyrethrin I–VI, which is highly photodegradable and has a short knockdown effect. Of these six compounds, pyrethrin I and II are the most active. The compounds in natural pyrethrins decompose rapidly in the presence of light, but their synthetic products are relatively more stable with longer residual effects (Sheail 1991). The earliest mention of the *Chrysanthemum* flowers as a source of pyrethrins was from early Chinese history, where it is believed that the flower passed into Europe along the silk roads (Glynn-Jones 2001). Dried and powdered flower heads of the white-flowered *Chrysanthemum* is termed as “pyrethrum.” The insecticidal property of the pyrethrum was recognized by an American named Junticoff in the middle of the nineteenth century, who observed that many Caucuses tribes used it to control body lice (Glynn-Jones 2001). The earliest cultivation of pyrethrum (*Chrysanthemum* or *Tanacetum*) for the extraction of insecticidal compounds, which is called Persian pyrethrum (Persian powder or Persian pellitory), was in the region of the Caucuses extending into Northern Persia (Bhat 1995). In 1917, the US military extracted the active principle of pyrethrum by percolating the ground flower heads with kerosene, which was used against house flies and mosquitoes. As the pyrethrins are highly photosensitive, derivatives of pyrethrins were synthesized as pyrethroids to resist photodegradation. The advantages of pyrethrins and pyrethroids are that they are highly lipophilic, have short half-life in the environment, have low toxicity to terrestrial vertebrates, and do not biomagnify like organochlorine insecticides.

28.3.1.2.5 Neonicotinoids

These are a relatively new class of insecticides launched in 1991 and are chemically related to nicotine, the tobacco toxin. Neonicotinoids were designed to be more persistent, as nicotine degrades very fast. The “new nicotine-like insecticides” are much more toxic to invertebrates than they are to mammals, birds, and other higher organisms. Neonicotinoids are further classified into compounds of Chloronicotiny, Thionicotiny, Furanicotiny, and pyridine carboxamide. Although several different kinds of neonicotinoid insecticides are available, imidacloprid was the first to reach the market in Europe and Japan in 1991, followed by nitenpyram and acetamiprid in 1995, thiamethoxam in 1997, thiacloprid in 1999, and clothianidin in 2002 (Jeschke et al. 2011). Imidacloprid is one of the fastest growing insecticides used on more than 140 crops in more than 120 countries (PAN Germany 2012). Neonicotinoids have extensively been used to manage insect pests of potato-like the Colorado potato beetle, leafhoppers, psyllids, aphids, and flea beetles. Now neonicotinoids are the most common insecticide worldwide, accounting for 24% of the global insecticide market (Popp et al. 2013). Large-scale deployment of neonicotinoids in the seed treatments of maize, sunflower, and cotton to control a wide range of pests has received a rapid increase in use worldwide (Douglas and Tooker 2015). The seven critical neonicotinoids are Acetamiprid, clothianidin, dinotefuran, imidacloprid, nitenpyram, thiacloprid, and thiamethoxam, widely used against insect pests.

28.3.1.2.6 Biopesticides

According to the Environmental Protection Agency, biopesticides are agents derived from natural materials such as animals, plants, bacteria, and certain minerals. The use of botanicals as insecticides is as old as agricultural practice; nonetheless, their use was curtailed considerably with the advent of synthetic insecticides. Biopesticides are eco-friendly, and while promising in controlling yield loss without compromising the quality of the product, it leaves the least genetic modification in the plants (Kumar et al. 2021). Unlike synthetic insecticides, biopesticides ensure little chance of pesticide resistance in pests. As there is public awareness of the ill effect of the injudicious use of synthetic insecticides, the requirement for biopesticide is on its uphill; accordingly, there is a rise in the demand for biopesticide in the international market (Essiedu et al. 2020). Pyrethrin, essential oils, and organic pesticides have common features like fast degradation in sunlight, air and moisture, and selectivity to non-target insects. Fipronil is a broad-spectrum insecticide that belongs to the phenylpyrazole family widely used in agriculture to fight against insect pests in sugarcane, rice, cotton, potato, corn, and soybean crops in veterinary medicine to control ectoparasites (Mohamed and Hogg 2004).

Quinazoline derivatives are a class of heterocyclic derivatives used as insecticides or acaricides (Wu et al. 2014) that inhibit or block the synthesis of chitin in the larval stages of insects. Fenazaquin, a derivative of Quinazoline, available commercially, is a contact acaricide, particularly against tetranychid and eriophyid mites in apples, pears, and citrus fruits (Dreikorn et al. 1991; Shanker et al. 2001).

28.3.2 Mode of Entry

28.3.2.1 Systemic Pesticides

When applied in the field, systemic insecticide plants absorb it and transfer it to other areas like leaves, stems, or roots through vascular bundles. Mortality of the pest happens when it feeds the treated plant. Systemic insecticides are directly applied in flowable solutions or granules to the crop, soil, and seedlings using foliar applications. The movement of pesticides in the plant may be unidirectional, either up or down, or multidirectional. Systemic insecticides are readily taken up by the roots and leaves of the plant, and when the pests come to eat them ingest a lethal dose and die (Fig. 28.2). Sap feeders like sucking insects are fatally exposed to systemic insecticides, as sap carries the most concentrated fraction of the poisonous chemicals. Systemic insecticides contaminate all plant tissues, from the roots to leaves and flowers, where active residues can be found for up to 45–90 days (Lue et al. 1984; Meher et al. 2010), lasting as long as in soil. Pollination is highly affected as systemic insecticides contaminate pollen and guttation. Because these insecticides are incorporated in the flesh of fruits, application of such insecticides is prohibited in many countries, as it has caused human poisoning. Systemic insecticides successfully control sucking pests and burrowing larvae in many crops, being their advantage of translocation to all treated plant tissues. Although systemic insecticides are commonly used, they are not advisable for many food crops because the insecticide

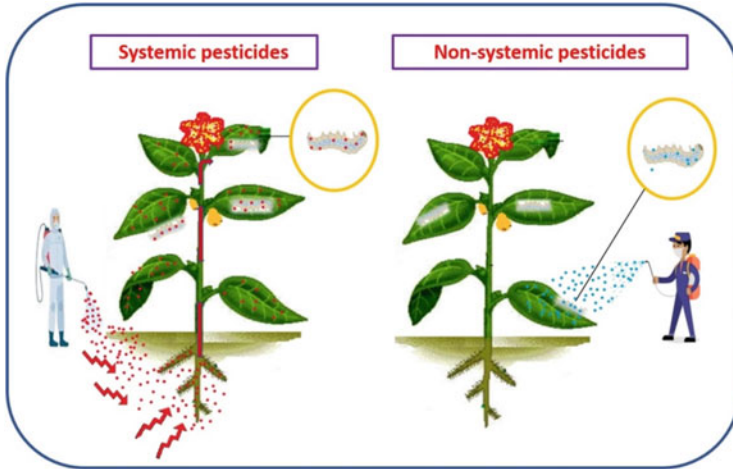


Fig. 28.2 Pesticide classification based on the mode of entry

remains in the food after harvest. Systemic insecticides are also used in animals to control ectoparasites like warble grubs, lice, or fleas or by including it in the diets of domestic animals to protect them from internal parasites like cattle grubs and other botflies.

28.3.2.2 Contact Pesticides

A contact pesticide that can be natural, inorganic, or even organic products is harmful, damaging, or lethal to the target insect when the pesticide is absorbed through direct contact (Fig. 28.2).

Most contact pesticides come in the form of aerosols or foggers.

28.3.2.3 Fumigants

Fumigants are volatile chemicals used to kill insects, particularly the stored product pests, nematodes, and other animals or plants that damage seeds, human dwellings, clothing, and nursery stock. They can get through inaccessible areas such as cracks, crevices, woods, and tightly packed areas than conventional contact and residual insecticides. High vapor pressure Fumigants, such as methyl bromide, ethylene oxide, hydrogen cyanide, and hydrogen phosphide, can easily penetrate, and hence they are used to treat sealed storage areas or materials enclosed in gas-proof sheets, whereas low-pressure compounds such as ethylene dibromide and ethylene dichloride diffuse more slowly; therefore, they are preferred to use more open storage areas and as soil fumigants. Common fumigants used to treat stored products or nursery stock includes hydrogen cyanide, naphthalene, nicotine, and methyl bromide. Soil fumigants are used to control nematodes, and the common soil fumigants are methyl bromide, dichloropropane, propylene oxide, dibromochloropropane, organophosphate insecticides, and chloropicrin.

28.3.3 Mode of Action

Organochlorine pesticides mainly act on neurons by causing a sodium-potassium imbalance that prevents standard transmission of nerve impulses. By disrupting the ionic balance, organochlorine pesticide causes fire to the nerve axons repetitively, causing tremors, convulsions, and eventually death. This group of insecticide also prevent the GABA (γ -aminobutyric acid) receptor may also occur which inhibits the entry of chloride ions from the neurons, causing a hyperexcitable state characterized by tremors and convulsions.

Organophosphorus and carbamates inhibit cholinesterase (ChE), and the enzyme is phosphorylated, as in the case of organophosphorus or carbamylated in carbamates. This inactivates the essential enzyme in the nervous system of humans and other animal species (Krieger 2001); but, reactivation of the carbamylated enzyme by hydrolysis is a faster-phosphorylated enzyme (Jokanović 2009). Inhibition of the enzyme hastens the accumulation of acetylcholine (ACh) at the neuromuscular junctions or synapses, causing rapid twitching of voluntary muscles and, finally, paralysis. Pyrethroids exert the exact mechanism of action in insects and mammals. Both pyrethrins and pyrethroids have insecticidal potential as they disrupt the muscular system and alter the normal functioning of voltage-dependent sodium channels. It binds to the α -subunit of the sodium channel that leads to increased membrane permeability for a longer time. The specific interaction of pyrethroids with the sodium channel shows both the activation and inactivation properties of the sodium channel convert the cell to hyperexcitation (Ray and Fry 2006). The toxicodynamics of pyrethroids may also include other mechanisms such as antagonism of gamma-aminobutyric acid (GABA), stimulation of chloride channels by the modulation of protein kinase, modulation of nicotinic cholinergic transmission, increased release of noradrenaline, and deregulation of calcium homeostasis. Benzimidazoles, an introductory class of pesticides commonly used as veterinary medicines (anthelmintics) and pesticides, inhibit microtubule formation when they bind to free β -tubulin monomers at the colchicine-binding site (Ermler et al. 2013). Fipronil, the broad-spectrum insecticide of the phenylpyrazole group, targets two families of nicotinic acetylcholine receptors and gamma-aminobutyric acid receptors and blocks glutamate-activated chloride. Its inhibition of the mitochondrial electron transport at the NADH-CoQ reductase site leads to the disruption of ATP formation. Quinazoline derivatives of insecticide or acaricide inhibit or block the synthesis of chitin in the larval stages of insects. Fenazaquin, a derivative of Quinazoline, inhibits electron transport at complex I of the mitochondrial respiratory chain (Hollingworth et al. 1994).

The mode of action of botanicals varies in a variety of ways depending on their active principles. Pyrethrins and pyrethroids act similarly; both affect the central and peripheral nervous systems and alter the function of voltage-gated sodium channels in insect neuronal membranes. This leads to the disruption of electrical signaling in the nervous system and causes paralysis followed by the insect's death. Nicotine interacts with acetylcholine (ACh) receptors in the central nervous ganglia, causing

twitching, convulsions, and death. After forming a complex with NADH dehydrogenase, Rotenone inhibits NADH oxidation to NAD.

28.4 Environmental Impact of Insecticides

Insecticides play a pivotal role in increasing agricultural production; nevertheless, they have a major role in contaminating soil and water bodies. They are omnipresent and persistent, causing havoc to humankind due to their bioaccumulation properties and high toxicity (Annex C 2008). Bioaccumulation and biomagnification of pesticides eventually cause high risk for humans and other living organisms (Willis and McDowell 1982; Jardim and Caldas 2012; Lozowicka et al. 2014; Skretteberg et al. 2015; Liu et al. 2016) (Fig. 28.3). Imprudent use of pesticides pollutes the environment and negatively impacts human health (Bernardes et al. 2015). The use of DDT in the US was banned in 1972 as it is deleteriously affecting non-target plants and animals and accumulating in tissues (Barnhoorn et al. 2009). Pesticides tend to persist in the environment for a long time, and their accumulation leads to ecological imbalances resulting in economic, social, and esthetic losses (Parween and Jan 2019). Pesticides also incur heavy losses to pollinators, predators, and other beneficial and useful organisms (Pimentel et al. 1993). Development of pest resistance, groundwater contamination, and harm to pets, livestock, and public health are the other hidden impact of pesticides on man and the environment. Depleting the population of earthworms and other beneficial organisms can also be attributed to the leaching of organophosphates and carbamate pesticides into the soil (Edwards 1993). Off-target loss to a tune of 50–70% due to the contamination of the pesticide was also reported by Pimentel and Burgess (2014). Through the phenomenon of

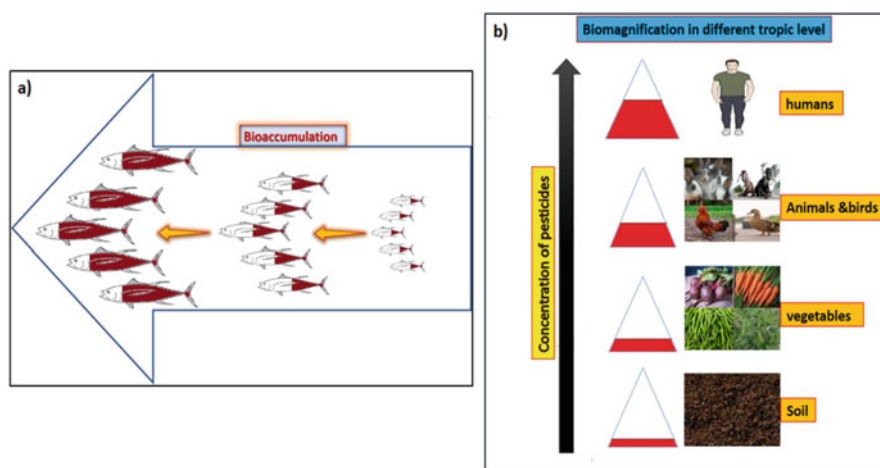


Fig. 28.3 Pesticide transport mechanism in the ecosystem (a) bioaccumulation and (b) biomagnification

biomagnifications, pesticides pass from trophic to different trophic levels through food chains, and it remains in higher animals for an extended period (Fig. 28.3b) (Bagheri et al. 2019; Li 2020). Improper disposal of obsolete pesticides often pollutes the agricultural and surrounding soil.

Persistent organic pollutants (POPs) are organic compounds resistant to environmental degradation through chemical, biological, and photolytic processes and adversely affect human health and the environment around the world (Ritter 1998). POPs can drift from the place of origin to distant places by wind or water. Of the applied pesticides, all the fractions may not degrade chemically or biologically, and that leaves residues in the atmosphere, soil and water (European Food Safety Authority 2017), foods, and even in a remote region like the Antarctic (Tatton and Ruzicka 1967) and these residues become hazards to the ecosystem.

Fumigants to manage pests in the warehouse are highly volatile, and 80–90% of this biofumigants escape out within a few days of application. Subsequently, the volatile pesticides reach back to the land through rainfall and affect the non-target organisms, air, water, and soil (Abong'o et al. 2014). Pesticides entering into the soil, groundwater, streams, rivers, sea, and other water bodies often pollute the ecosystem and raise a threat to untargeted species. Leaching pesticides into groundwater poses grave concerns (Rasmussen et al. 2015). Pesticides entering into the soil, groundwater, streams, rivers, sea, and other water bodies often pollute the ecosystem and raise a threat to untargeted species. Groundwater resources are highly vulnerable to pollution by insecticides, mainly due to the infiltration through riverbeds and riverbanks and leaching through the soil and unsaturated zone (Reichenberger et al. 2007; Arias-Estévez et al. 2008).

DDT is a persistent hygroscopic pesticide that stays longer in the aquatic environment due to its higher half-life of 150 years (as listed by the National Pesticide Information Center) and causes toxicity to birds, fishes, and amphibians like frogs, toads, and salamanders (Barr and Needham 2002; Ellenhorn and Barceloun 1988). Thinning of eggshells, death of the embryo, and deleterious effects on heart and brain of certain aquatic animals were also reported due to exposure of DDT (Barr and Needham 2002). DDE and DDD, the breakdown products of DDT, are also persistent and have similar properties. The Stockholm Convention on Persistence convened in 2001 under the auspices of the United Nations Environment Program, has enacted a global ban on POP following the WHO recommendations and guidelines. Accordingly, DDT was listed in Annex B with its production and use that restricted disease vector control. The book, *Silent Spring*, published by Carson (2002), a marine biologist and conservationist in 1962, resulted in an enormous public outcry raising the issues of environmental and health impacts of DDT due to its use in agriculture in the United States. Eventually, the outrage led to a ban on DDT's agricultural use in the United States. Given the long persistence and adverse effect on the environment, the Environmental Protection Agency (EPA) issued a cancellation order for DDT in 1972.

Many of the prohibited pesticides under POP category are still detected in the soil and water due to their persistence in the environment. Samples collected from the Wangyanggou River in Shijiazhuang City, China, had 14 organochlorine

insecticides with a dominance of DDT in the surface water, sediments, and soils (Xi et al. 2016).

Organophosphorus pesticides (OPs) pose an increasing threat to human health and wildlife as they are the most frequently detected pesticides in contaminated soils (Colorado et al. 2016). Pan et al. (2018) reported that 93% of soil samples collected from the agricultural soils collected from the Yangtze River Delta of China were contained by OPs. Anticholinesterase pesticides like organophosphates and carbamates are the most common globally polluting pesticides (Huang et al. 2015; Lim et al. 2015).

28.5 Impact of Insecticides on Human Health

Pesticide poisoning has ever been a perennial public health problem. The Human Rights Council of the UN has reported that pesticides are responsible for an estimated 200,000 acute poisoning deaths each year, of which 99% in developing countries where there is a laxity in observing environmental regulations. Contaminated food or water, inhalation of vapor, and absorption through the skin are the routes of insecticides that usually reach the human body (Snedeker 2001) (Fig. 28.4).

Pesticides are the main cause of death by suicide, particularly in middle-income countries, but WHO (2019) reported that this could be mostly preventable through better pesticide regulation. Dandona and Gunnell (2021) reported a decline in suicide in countries where pesticides are banned. Mew et al. (2017) recorded a fall in deaths due to pesticide poisonings in the past two decades from around 260,000 a

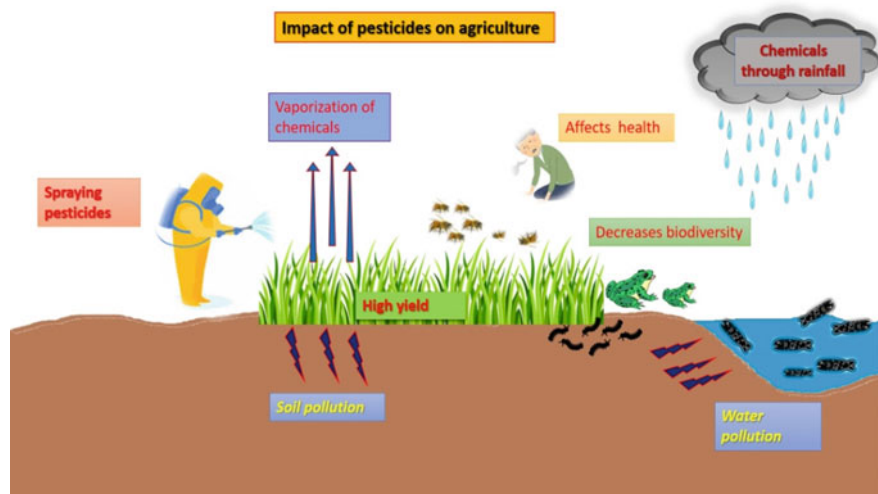


Fig. 28.4 Impact of pesticides on the environment

year to 160,000 a year; nevertheless, over 150,000 people die each year from deliberate ingestion of pesticides.

Organochlorine insecticides persist long in the human body due to their high solubility in fat and the environment (Barr 2002). Lipid solvents increase dermal penetration of organochlorine insecticide and increase the risk of toxicity when workers apply insecticides without proper protective equipment (Ellenhorn and Barceloun 1988). Cancer, asthma, diabetes, and growth disorders are fatal diseases linked with organochlorine insecticides in children (Lee and Jacobs 2006).

Neurotoxicity, including developmental neurotoxicity (DNT), is a significant adverse effect in mammals due to exposure to organophosphorus insecticide. Crude pyrethrum is a dermal and respiratory allergen and has been reported contact dermatitis, allergic respiratory reactions, and asthma in humans (Roberts and Reigart 2013). Diagnosis can be difficult because acute pyrethroid poisoning can be mistaken for organophosphorus insecticide. Pyrethroid toxicity leads to tremors, spasms, prostration, drooling, irregular limbs, convulsions, and hypersensitivity. Insecticides at concentrations below the safety limit can have developmental and behavioral neurological effects (Costa et al. 2008) and cause impairment of the endocrine system (de Sousa et al. 2014).

28.6 Alternative to Synthetic Insecticides

Despite the mounting usage of pesticides, crop loss due to the invasion by pests is on the rise; nonetheless, the realization of the challenges posed by synthetic chemicals, globally there is a shift from the use of synthetic pesticides to more reliable, sustainable, and environmentally friendly approach in pest management strategy. Biopesticides are biomolecules usually derived from plants or microbes as potential substitutes for synthetic pesticides to manage agricultural pests.

During ancient times, Indian and Egyptian farmers used to mix ashes with stored grains against insect invasion (Bhargava and Kumawat 2010). In India, farmers use neem plant extracts and other secondary metabolites derived from plants to regulate the storage of insect pests (Sharon et al. 2014).

Biopesticides, the environment-friendly largest group of broad-spectrum biopesticides derived from microorganisms, including bacteria, fungi, and viruses can be classified into different categories based on the extraction sources and the type of molecule/compound used for their preparation (Ruiu 2018). The successful use of *Bacillus thuringiensis* (Bt) and some other microbial species led to many new microbial species and strains. Among the most widely used microorganisms against insect pests is Bt, which is used against a broad spectrum of pests, including lepidopterans, coleopterans, and dipterans (Gill et al. 1992). Major entomopathogenic bacterial species are *Pseudomonas*, *Yersinia*, and *Chromobacterium*, while fungi are the *Beauveria*, *Metarhizium*, *Verticillium*, *Lecanicillium*, *Hirsutella*, and *Paecilomyces* (Chang et al. 2003; Kumar et al. 2021).

28.7 Conclusion

It is imperative to increase food production to meet the demand for food for the burgeoning population. Pesticides play a crucial role in increasing productivity in agriculture through the control of pests. If pesticide application is not proper, it will indeed affect the equilibrium of the environment, and its outcome will be adverse. One of the most severe problems is the destruction of non-target organisms like natural predators, beneficial microbes, earthworms, pollinators, including humans. It also causes soil, water, and air pollution, which affects organisms at each tropic level, leading to biodiversity loss. Even though pesticide helps increase the yield, the imbalance in the environment caused by pesticide will make it a huge loss. The consequent effect of pesticides on the agricultural system and other organisms has to be understood in detail. Considering the harmful effects of chemical pesticides, authorities must design and implement rules and regulations for the safe usage of pesticides by minimizing their application or replacing it with relatively cheaper biopesticides. Farmers must take proper precautions while handling pesticides by wearing masks and gloves.

References

- Abong'o D, Wandiga S, Jumba I, Madadi V, Kylin H (2014) Impacts of pesticides on human health and environment in the River Nyando catchment, Kenya. *Int J Human Arts Med Sci* 2(3):1–14
- Annex C (2008) Stockholm convention on persistent organic pollutants. United Nations Environmental Programme, Geneva, 29
- Arias-Estévez M, López-Periágo E, Martínez-Carballo E, Simal-Gándara J, Mejuto J-C, García-Río L (2008) The mobility and degradation of pesticides in soils and the pollution of groundwater resources. *Agric Ecosyst Environ* 123(4):247–260
- Bagheri M, Al-Jabery K, Wunsch DC, Burken JG (2019) A deeper look at plant uptake of environmental contaminants using intelligent approaches. *Sci Total Environ* 651:561–569
- Barnhoorn IEJ, Bornman MS, Van Rensburg CJ, Bouwman H (2009) DDT residues in water, sediment, domestic and indigenous biota from a currently DDT-sprayed area. *Chemosphere* 77(9):1236–1241
- Barr DB, Needham LL (2002) Analytical methods for biological monitoring of exposure to pesticides: a review. *J Chromatogr B* 778(1-2):5–29
- Bernardes MFF, Pazin M, Pereira LC, Dorta DJ (2015) Impact of pesticides on environmental and human health. In: *Toxicology studies—cells, drugs and environment*. IntechOpen, London, pp 195–233
- Bhargava MC, Kumawat KC (2010) *Pests of stored grains and their management*. New India Publishing, New Delhi
- Bhat BK (1995) Breeding methodologies applicable to pyrethrum. In: Casida JE, Quistad GB (eds) *Pyrethrum flowers: production, chemistry, toxicology and uses*. Oxford University Press, New York, pp 67–94
- Buchel KH (1983) *Chemistry of pesticides*. No. 668.65 B82
- Canton H (2021) Food and Agriculture Organization of the United Nations—FAO. In: *The Europa Directory of International Organizations 2021*. Routledge, pp 297–305
- Carson R (2002) *Silent spring*. Houghton Mifflin Harcourt, Boston
- Carvalho FP (2017) Pesticides, environment, and food safety. *Food Energy Security* 6(2):48–60

- Casida JE, Quistad GB (1995) Pyrethrum flowers: production, chemistry, toxicology, and uses. In: International symposium on pyrethrum flowers: production, chemistry, toxicology and uses, Honolulu, Hawaii, USA, 1992. Oxford University Press
- Chang JH, Choi JY, Jin BR, Roh JY, Olszewski JA, Seo SJ, O'Reilly DR, Je YH (2003) An improved baculovirus insecticide producing occlusion bodies that contain *Bacillus thuringiensis* insect toxin. *J Invertebr Pathol* 84(1):30–37
- Colorado BE, Jaramillo ABT, Ballestas IT (2016) Organophosphorus pesticides degrading bacteria present in contaminated soils. *Revista Ciencias Técnicas Agropecuarias* 25(3):13–22
- Costa LG, Giordano G, Guizzetti M, Vitalone A (2008) Neurotoxicity of pesticides: a brief review. *Front Biosci* 13(4):1240–1249
- Dandona R, Gunnell D (2021) Pesticide surveillance and deaths by suicide. *Lancet Glob Health* 9(6):e738–e739
- de Sousa G, Nawaz A, Cravedi J-P, Rahmani R (2014) A concentration addition model to assess activation of the pregnane X receptor (PXR) by pesticide mixtures found in the French diet. *Toxicol Sci* 141(1):234–243
- De A, Bose R, Kumar A, Mozumdar S (2014) Targeted delivery of pesticides using biodegradable polymeric nanoparticles. Springer, New Delhi
- Douglas MR, Tooker JF (2015) Large-scale deployment of seed treatments has driven rapid increase in use of neonicotinoid insecticides and preemptive pest management in U.S. field crops. *Environ Sci Technol* 49(8):5088–5097
- Dreikorn BA, Thompson GD, Suhr RG, Worden TV, Davis NL (1991) The discovery and development of fenazaquin (EL-436), a new broad spectrum acaricide. In: Proceedings of seventh international congress on pesticide chemistry, vol 1
- Drum C (1980) Soil chemistry of pesticides. PPG Industries Inc, Pittsburgh, PA
- Edwards CA (1993) The impact of pesticides on the environment. In: The pesticide question. Springer, Boston, MA, pp 13–46
- Ellenhorn MJ, Barceloun DG (1988) Medical toxicology diagnosis and treatment of human poisoning. Elsevier, New York
- Ermiler S, Scholze M, Kortenkamp A (2013) Seven benzimidazole pesticides combined at sub-threshold levels induce micronuclei in vitro. *Mutagenesis* 28:417–426
- Essiedu JA, Adepoju FO, Ivantsova MN (2020) Benefits and limitations in using biopesticides: a review. In: AIP conference proceedings, vol 2313(1). AIP Publishing LLC, Melville, NY, p 080002
- European Food Safety Authority (2017) The 2015 European Union report on pesticide residues in food. *EFSA J* 15(4):e04791
- Fenik J, Tankiewicz M, Biziuk M (2011) Properties and determination of pesticides in fruits and vegetables. *TrAC Trends Anal Chem* 30(6):814–826
- Gill SS, Cowles EA, Pietrantonio PV (1992) The mode of action of *Bacillus thuringiensis* endotoxins. *Annu Rev Entomol* 37(1):615–634
- Glynn-Jones A (2001) Pyrethrum. *Pesticide Outlook* 12(5):195–198
- Hollingworth RM, Ahammadsahib KI, Gadelhak G, McLaughlin JL (1994) New inhibitors of complex I of the mitochondrial electron transport chain with activity as pesticides. *Biochem Soc Trans* 22(1):230–233
- Huang H-S, Hsu C-C, Weng S-F, Lin H-J, Wang J-J, Shih-Bin S, Huang C-C, Guo H-R (2015) Acute anticholinesterase pesticide poisoning caused a long-term mortality increase: a nationwide population-based cohort study. *Medicine* 94(30):e1222
- Jardim ANO, Caldas ED (2012) Brazilian monitoring programs for pesticide residues in food—results from 2001 to 2010. *Food Control* 25(2):607–616
- Jeschke P, Nauen R, Schindler M, Elbert A (2011) Overview of the status and global strategy for neonicotinoids. *J Agric Food Chem* 59(7):2897–2908
- Jokanović M (2009) Medical treatment of acute poisoning with organophosphorus and carbamate pesticides. *Toxicol Lett* 190(2):107–115

- Kislev ME, Weiss E, Hartmann A (2004) Impetus for sowing and the beginning of agriculture: ground collecting of wild cereals. *Proc Natl Acad Sci* 101(9):2692–2695
- Klassen W, Schwartz PH Jr (1985) ARS research program in chemical insect control. In: Beltsville symposia in agricultural research, Beltsville, MA (USA), 16–19 Mar 1983. Rowman and Allanheld, Lanham, MD
- Krieger R (ed) (2001) *Handbook of pesticide toxicology: principles and agents*. Academic Press, San Diego
- Kumar J, Ramlal A, Mallick D, Mishra V (2021) An overview of some biopesticides and their importance in plant protection for commercial acceptance. *Plants* 10(6):1185
- Lee D-H, Jacobs DR Jr (2006) Association between serum concentrations of persistent organic pollutants and γ glutamyltransferase: results from the national health and examination survey 1999–2002. *Clin Chem* 52(9):1825–1827
- Li Z (2020) Spatiotemporal pattern models for bioaccumulation of pesticides in herbivores: an approximation theory for North American white-tailed deer. *Sci Total Environ* 737:140271
- Lim Y-P, Lin C-L, Hung D-Z, Ma W-C, Lin Y-N, Kao C-H (2015) Increased risk of deep vein thrombosis and pulmonary thromboembolism in patients with organophosphate intoxication: a nationwide prospective cohort study. *Medicine* 94(1):e341
- Liu Y, Li S, Ni Z, Qu M, Zhong D, Ye C, Tang F (2016) Pesticides in persimmons, jujubes and soil from China: residue levels, risk assessment and relationship between fruits and soils. *Sci Total Environ* 542:620–628
- Lozowicka B, Kaczynski P, Paritova AE, Kuzembekova GB, Abzhaliyeva AB, Sarsembayeva NB, Alihan K (2014) Pesticide residues in grain from Kazakhstan and potential health risks associated with exposure to detected pesticides. *Food Chem Toxicol* 64:238–248
- Lue LP, Lewis CC, Melchor VE (1984) The effect of aldicarb on nematode population and its persistence in carrots, soil and hydroponic solution. *J Environ Sci Health B* 19(3):343–354
- Maggi F, Tang FHM, la Cecilia D, McBratney A (2019) PEST-CHEMGRIDS, global gridded maps of the top 20 crop-specific pesticide application rates from 2015 to 2025. *Sci Data* 6(1):1–20
- Meher HC, Gajbhiye VT, Singh G, Kamra A, Chawla G (2010) Persistence and nematicidal efficacy of carbosulfan, cadusafos, phorate, and triazophos in soil and uptake by chickpea and tomato crops under tropical conditions. *J Agric Food Chem* 58(3):1815–1822
- Mew EJ, Padmanathan P, Konradsen F, Eddleston M, Chang S-S, Phillips MR, Gunnell D (2017) The global burden of fatal self-poisoning with pesticides 2006–15: systematic review. *J Affect Disord* 219:93–104
- Mohamed AMA, Hogg DB (2004) The attachment and stylostome of *Trombidium newelli* (Acari: Trombididae), an ectoparasitic mite on adults of alfalfa weevil, *Hyperapostica* (Coleoptera: Curculionidae). *Exp Appl Acarol* 34(3):323–333
- National Academy of Science (1969) *Insecticides*. In: *Insect pest management control principles and animal pest control*, vol 3. National Academy of Science, Washington, DC, pp 360–446. Publ. 1695
- National Research Council (2000) *The future role of pesticides in U.S. agriculture*. National Academies Press, Washington, DC
- PAN Germany (2012) *Pesticides and health hazards facts and figures*. PAN Germany—Pestizid Aktions-Netzwerk eV, Hamburg
- Pan L, Sun J, Zhiheng Li Y, Zhan SX, Zhu L (2018) Organophosphate pesticide in agricultural soils from the Yangtze River Delta of China: concentration, distribution, and risk assessment. *Environ Sci Pollut Res* 25(1):4–11
- Parween T, Jan S (2019) *Ecophysiology of pesticides: interface between pesticide chemistry and plant physiology*. Academic Press, London
- Peryea FJ (1998) Historical use of lead arsenate insecticides, resulting soil contamination and implications for soil remediation. In: 16th World congress of soil science, Montpellier, France, pp 20–26
- Pimentel D, Burgess M (2014) Environmental and economic costs of the application of pesticides primarily in the United States. In: *Integrated pest management*. Springer, Dordrecht, pp 47–71

- Pimentel D, McLaughlin L, Zepp A, Lakitan B, Kraus T, Kleinman P, Vancini F et al (1993) Environmental and economic impacts of reducing U.S. agricultural pesticide use. In: *The pesticide question*. Springer, Boston, MA, pp 223–278
- Popp J, Pető K, Nagy J (2013) Pesticide productivity and food security. A review. *Agron Sustain Dev* 33(1):243–255
- Rasmussen JJ, Wiberg-Larsen P, Baattrup-Pedersen A, Cedergreen N, McKnight US, Kreuger J, Jacobsen D, Kristensen EA, Friberg N (2015) The legacy of pesticide pollution: an overlooked factor in current risk assessments of freshwater systems. *Water Res* 84:25–32
- Ray DE, Fry JR (2006) A reassessment of the neurotoxicity of pyrethroid insecticides. *Pharmacol Ther* 111(1):174–193
- Reichenberger S, Bach M, Skitschak A, Frede H-G (2007) Mitigation strategies to reduce pesticide inputs into ground-and surface water and their effectiveness; a review. *Sci Total Environ* 384(1–3):1–35
- Ritter L (1998) Persistent organic pollutants. International Programme on Chemical Safety (IPCS) within the framework of the Inter-Organization Programme for the Sound Management of Chemicals (IOMC), 1998
- Roberts JR, Reigart JR (2013) Recognition and management of pesticide poisonings. US Environmental Protection Agency, Washington, DC
- Ruii L (2018) Microbial biopesticides in agroecosystems. *Agronomy* 8(11):235
- Shanker A, Jasrotia P, Kumar A, Jaggi S, Kumar V, Sood C (2001) Bioefficacy of new miticide: fenazaquin. *Pestology* 15(6):57–60
- Sharma A, Kumar V, Shahzad B, Tanveer M, Sidhu GPS, Handa N, Kohli SK et al (2019) Worldwide pesticide usage and its impacts on ecosystem. *SN Appl Sci* 1(11):1–16
- Sharon M, Abirami CV, Alagusundaram K (2014) Grain storage management in India. *J Postharvest Technol* 2(1):12–24
- Sheail J (1991) *The regulation of pesticide use: an historical perspective*
- Shepard HH (1939) *The chemistry and toxicology of insecticides*. Burgess Publishing Co., Minneapolis, MN, 383 pp
- Skretteberg LG, Lyrån B, Holen B, Jansson A, Fohgelberg P, Siivinen K, Andersen JH, Jensen BH (2015) Pesticide residues in food of plant origin from Southeast Asia—a Nordic project. *Food Control* 51:225–235
- Snedeker SM (2001) Pesticides and breast cancer risk: a review of DDT, DDE, and dieldrin. *Environ Health Perspect* 109(Suppl 1):35–47
- Strassemeyer J, Daehmlow D, Dominic AR, Lorenz S, Golla B (2017) SYNOPSIS-WEB, an online tool for environmental risk assessment to evaluate pesticide strategies on field level. *Crop Prot* 97:28–44
- Tang FHM, Lenzen M, McBratney A, Maggi F (2021) Risk of pesticide pollution at the global scale. *Nat Geosci* 14(4):206–210
- Tatton JOG, Ruzicka JHA (1967) Organochlorine pesticides in Antarctica. *Nature* 215(5099):346–348
- Tudi M, Ruan HD, Wang L, Lyu J, Sadler R, Connell D, Chu C, Phung DT (2021) Agriculture development, pesticide application and its impact on the environment. *Int J Environ Res Public Health* 18(3):1112
- Unsworth J (2010) *History of pesticide use*. International Union of Pure and Applied Chemistry, Research Triangle Park
- Van Emden HF (2004) *Pest and vector control*. Cambridge University Press
- van Dijk M, Morley T, Rau ML, Saghai Y (2021) A meta-analysis of projected global food demand and population at risk of hunger for the period 2010–2050. *Nat Food* 2(7):494–501
- Vijgen L, ElsKeyaerts PL, Maes P, Van Reeth K, Nauwyncck H, Pensaert M, Van Ranst M (2006) Evolutionary history of the closely related group 2 coronaviruses: porcine hemagglutinating encephalomyelitis virus, bovine coronavirus, and human coronavirus OC43. *J Virol* 80(14):7270–7274

- Willis GH, McDowell LL (1982) Pesticides in agricultural runoff and their effects on downstream water quality. *Environ Toxicol Chem Int J* 1(4):267–279
- World Health Organization (1979) WHO handbook for reporting results of cancer treatment. World Health Organization, Geneva
- World Health Organization (2019) WHO global report on traditional and complementary medicine 2019. World Health Organization
- Wu J, Bai S, Yue M, Luo L-J, Shi Q-C, Ma J, Xian-Li D, Kang S-H, Deyu H, Yang S (2014) Synthesis and insecticidal activity of 6, 8-dichloro-quinazoline derivatives containing a sulfide substructure. *Chem Pap* 68(7):969–975
- Xi BD, Yu MD, Zhang Y, Gao R, Zhang H, Li D, Tan WB, Hou HB, Yu H (2016) Residues and health risk assessments of organochlorine pesticides in a typical wastewater irrigation area of North China. *Asian J Ecotoxicol* 11:453–464
- Yang X, Wang F, Meng L, Zhang W, Fan L, Geissen V, Ritsema CJ (2014) Farmer and retailer knowledge and awareness of the risks from pesticide use: a case study in the Wei River catchment, China. *Sci Total Environ* 497:172–179
- Zhang WJ, Jiang FB, Jian Feng O (2011) Global pesticide consumption and pollution: with China as a focus. *Proc Int Acad Ecol Environ Sci* 1(2):125